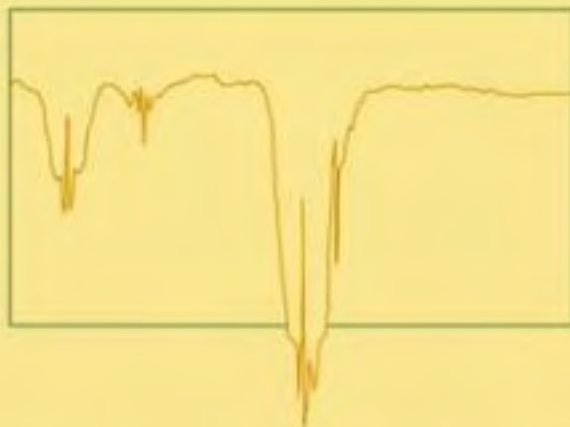


INTERPRETING
INFRARED, RAMAN, AND
NUCLEAR MAGNETIC
RESONANCE SPECTRA

VOLUME **1**

*Variables in Data Interpretation of
Infrared and Raman Spectra*



RICHARD ALLEN NYQUIST



ELSEVIER

*Building Insights.
Breaking Boundaries*

[Home](#) | [Site map](#) | [Elsevier websites](#) | [Alerts](#)

INTERPRETING INFRARED, RAMAN, AND NUCLEAR MAGNETIC RESONANCE SPECTRA

To order this title, and for more information, click [here](#)

By

Richard Nyquist, Nyquist Associates, Midland, Michigan, U.S.A.

Description

This book teaches the analyst why it is advantageous to obtain vibrational data under different physical phases. Molecular vibrations are affected by change in physical phase, and knowledge of how certain molecular vibrations are affected by change in the chemical environment improves the analyst's ability to solve complex chemical problems. This book is invaluable for students and scientists engaged in analytical and organic chemistry, since application of IR and Raman spectroscopy is essential in identifying and verifying molecular structure. This reference provides analysts with information that enables them to acquire the maximum amount of information when sampling molecular vibrations via IR and Raman spectroscopy.

Audience

Spectroscopists, analytical and organic chemists, chemical physicists, both in academia and especially industry.

Contents

Volume 1: Theory of Vibrational Spectroscopy Experimental Alkyl Carbon-Hydrogen Vibrations Alkenes and Other Compounds Containing C=C Double Bonds Alkynes and Compounds Containing C≡C Groups Carboxamides, Ureas, Thioureas, Imidazolidinones, Caffeine, Isocaffeine, Uracils, Imides, Hydantoins, and s-Triazine (1H, 3H, 5H)- Triones Aldehydes Ketones Carboxylic Acid Esters Organic Carbonates, Thiol Carbonates, Chloroformates, Thiol Chloroformates, Acetyl Chloride, Benzoyl Chloride, Carbamates, and an Overview of Solute-Solvent Effects Upon Carbonyl Stretching Frequencies **Volume 2:** Epoxides and Ethers Nitriles, Isonitriles, and Dialkyl Cyanamides Azines, Isocyanates, Isothiocyanates, and Carbodiimides Thiols, Sulfides and Disulfides, Alkanethiols, and Alkanedithiols (S--H stretching) Sulfoxides, Sulfones, Sulfates, Monothiosulfates, Sulfonyl Halides, Sulfites, Sulfonamides, Sulfonates, and N-Sulfinyl Anilines Halogenated Hydrocarbons Nitroalkanes, Nitrobenzenes, Alkyl Nitrates, Alkyl Nitrites, and Nitrosamines Phosphorus Compounds Benzene and Its Derivatives The Nyquist Vibrational Group Frequency Rule Infrared Raman and Nuclear Magnetic Resonance (NMR) Spectra-Structure Correlations for Organic Compounds

Bibliographic & ordering Information

Hardbound, 1068 pages, publication date: APR-2001

ISBN-13: 978-0-12-523475-7

ISBN-10: 0-12-523475-9

Imprint: ACADEMIC PRESS

Price: [Order form](#)

GBP 435

USD 755

EUR 630

Books and book related electronic products are priced in US dollars (USD), euro (EUR), and Great Britain Pounds (GBP). USD prices apply to the Americas and Asia Pacific. EUR prices apply in Europe and the

ACKNOWLEDGMENTS

I thank the management of The Dow Chemical Company for providing me with a rewarding career in chemistry for over 41 years. I also thank the management of Sadtler Research Laboratories, a Division of Bio-Rad, for the opportunity to serve as an editorial consultant for several of their spectral collections of IR and Raman spectra.

I thank Marcia Blackson for typing the book manuscript. Her cooperation and editorial comments are appreciated.

NYQUIST'S BIOGRAPHY

In 1985, Richard A. Nyquist received the Williams-Wright Award from the Coblenz Society for his contributions to industrial IR spectroscopy. He was subsequently named an honorary member of the Coblenz Society for his contributions to vibrational spectroscopy, and in 1989, he was a national tour speaker for the Society of Applied Spectroscopy. The Association of Analytical Chemists honored Dr. Nyquist with the ANACHEM Award in 1993 for his contributions to analytical chemistry. He is listed in Who's Who in Science and Engineering, Who's Who in America, and Who's Who in the World. The Dow Chemical Company, from which Dr. Nyquist retired in 1994, honored him with the V.A. Stenger Award in 1981, and the Walter Graf European Award in 1994 for excellence in analytical chemistry. He has also been a member of ASTM, and received the ASTM Award of Appreciation for his contributions to the Practice of Qualitative Infrared Analysis. In 2000, Dr. Nyquist was awarded honorary membership to the Society of Applied Spectroscopy for his exceptional contributions to spectroscopy and to the Society. Dr. Nyquist received his B.A. in chemistry from Augustana College, Rock Island, Illinois, his M.S. from Oklahoma State University, and his Ph.D. from Utrecht University, The Netherlands. He joined The Dow Chemical Company in 1953. He is currently president of Nyquist Associates, and is the author or coauthor of more than 160 scientific articles including books, book chapters, and patents. Nyquist has served as a consultant for Sadtler Research Laboratories for over 15 years. In 1997 Michigan Molecular Institute, Midland, Michigan selected him as their consultant in vibrational spectroscopy.

PREFACE

My intention in compiling this book is to integrate IR, Raman, and NMR data in order to aid analysts in the interpretation of spectral data into chemical information useful in the solution of problems arising in the real world.

There is an enormous amount of IR and Raman data available in the literature, but in my opinion there has not been enough emphasis on the effects of the physical environment of chemicals upon their molecular vibrations. Manipulation of the physical phase of chemicals by various experiments aids in the interpretation of molecular structure. Physical phase comprises solid, liquid, vapor, and solution phases.

In the solid crystalline phase, observed molecular vibrations of chemicals are affected by the number of molecules in the unit cell, and the space group of the unit cell. In the liquid phase, molecular vibrations of chemicals are affected by temperature, the presence of rotational conformers, and physical interaction between molecules such as hydrogen bonding and/or dipolar interaction. In the vapor phase, especially at elevated temperature, molecules are usually not intermolecularly hydrogen bonded and are free from dipolar interaction between like molecules. However, the rotational levels of the molecules are affected by both temperature and pressure. Induced high pressure (using an inert gas such as nitrogen or argon) will hinder the molecular rotation of molecules in the vapor phase. Thus, the rotational-vibrational band collapses into a band comparable to that observed in a condensed phase. Higher temperature will cause higher rotational levels to be observed in the vibrational-rotational bands observed in the vapor phase.

In solution, the frequencies of molecular vibrations of a chemical are affected by dipolar interaction and/or hydrogen bonding between solute and solvent. In addition, solute-solvent interaction also affects the concentration of rotational conformers of a solute in a solvent.

The number of intermolecular hydrogen-bonded molecules existing in a chain in solution depends upon the solute concentration. In addition, the number of molecules of a solute in solution existing in a cluster in the absence of intermolecular hydrogen bonding also depends upon solute concentration.

INTRODUCTION

Infrared (IR) and Raman (R) spectroscopy are essential tools for the study and elucidation of the molecular structures of organic and inorganic materials. There are many useful books covering both IR and R spectroscopy (1–14). However, none of these books emphasize the significance of changes in the molecular vibrations caused by changes in the physical state or environment of the chemical substance. One goal of this book is to show how changes in the physical environment of a compound aid in both the elucidation of molecular structure and in the identification of unknown chemical compositions. Studies of a variety of chemicals in various physical states have led to the development of the Nyquist Rule. The Nyquist Rule denotes how the in-phase- and out-of-phase- or symmetric and antisymmetric molecular vibrations (often called characteristic group frequencies) differ with changes to their physical environment. These group frequency shift differences aid the analyst in interpreting the data into useful chemical information. Another goal of this book is to gather information on the nature of solute-solvent interaction, solute concentration, and the effect of temperature. This knowledge also aids the analyst in interpretation of the vibrational data. Another goal of this work was to compile many of the authors' and coauthors' vibrational studies into one compendium.

INTRODUCTION

Infrared (IR), Raman (R), and Nuclear Magnetic Resonance (NMR) spectroscopy are essential tools for the study and elucidation of the molecular structures of organic and inorganic materials. There are many useful books covering both IR and R spectroscopy (1–14). However, none of these books emphasize the significance of changes in the molecular vibrations caused by changes in the physical state or environment of the chemical substance. One goal of this book is to show how changes in the physical environment of a compound aid in both the elucidation of molecular structure and in the identification of unknown chemical compositions. Studies of a variety of chemicals in various physical states have led to the development of the Nyquist Rule. The Nyquist Rule denotes how the in-phase- and out-of-phase- or symmetric and antisymmetric molecular vibrations (often called characteristic group frequencies) differ with changes to their physical environment. These group frequency shift differences aid the analyst in interpreting the data into useful chemical information. Another goal of this book is to gather information on the nature of solute-solvent interaction, solute concentration, and the effect of temperature. This knowledge also aids the analyst in interpretation of the vibrational data. Another goal of this work was to compile many of the authors' and coauthors' vibrational studies into one compendium.

REFERENCES

1. Herzberg, G. (1945). *Molecular Spectra and Molecular Structure II. Infrared and Raman Spectra of Polyatomic Molecules*, New Jersey: D. Van Nostrand Company, Inc.
2. Wilson, E.B. Jr., Decius, J.C., and Cross, P.C. (1955). *Molecular Vibrations*, New York: McGraw-Hill Book Company, Inc.
3. Colthup, N.B., Daly, L.H., and Wiberley, S.E. (1990). *Introduction to Infrared and Raman Spectroscopy*, 3rd ed., New York: Academic Press.
4. Potts, W.J., Jr. (1963). *Chemical Infrared Spectroscopy*, New York: John Wiley & Sons, Inc.
5. Nyquist, R.A. (1984). *The Interpretation of Vapor-Phase Infrared Spectra: Group Frequency Data*, Philadelphia: Sadtler Research Laboratories, A Division of Bio-Rad.
6. Nyquist, R.A. (1989). *The Infrared Spectra Building Blocks of Polymers*, Philadelphia: Sadtler Research Laboratories, A Division of Bio-Rad.
7. Nyquist, R.A. (1986). *IR and NMR Spectral Data-Structure Correlations for the Carbonyl Group*, Philadelphia: Sadtler Research Laboratories, A Division of Bio-Rad.
8. Griffiths, P.R. and de Haseth, J.A. (1986). Fourier Transform Infrared Spectrometry, *Chemical Analysis*, vol. 83, New York: John Wiley & Sons.
9. Socrates, G. (1994). *Infrared Characteristic Group Frequencies Tables and Charts*, 2nd ed., New York: John Wiley & Sons.
10. Lin-Vien, D., Colthup, N.B., Fateley, W.G., and Grasselli, J.G. (1991). *The Handbook of Infrared and Raman Characteristic Frequencies of Organic Molecules*, San Diego, CA: Academic Press.
11. Nyquist, R.A., Putzig, C.L. and Leugers, M.A. (1997). *Infrared and Raman Spectral Atlas of Inorganic and Organic Salts*, vols. 1–3, San Diego, CA: Academic Press.
12. Nyquist, R.A., and Kagel, R.O. (1997). *Infrared Spectra of Inorganic Compounds*, vol. 4, San Diego, CA: Academic Press.
13. Nakamoto, K. (1997). *Infrared and Raman Spectra of Inorganic and Coordination Compounds, Part A: Theory and Applications in Inorganic Chemistry*, New York: John Wiley & Sons.
14. Nakamoto, K. (1997). *Infrared and Raman Spectra of Inorganic and Coordination Compounds, Part B, Applications in Coordination, Organometallic, and Bioinorganic Chemistry*, New York: John Wiley & Sons.

Theory of Vibrational Spectroscopy

I. Theory	1
II. Examples of Molecular Structure	2
A. Linear molecules: $I_A = 0, I_B = I_C$	2
B. Spherical Top Molecules: $I_A = I_B = I_C$	4
C. Symmetric Top Molecules	4
1. Prolate: $I_A < I_B = I_C$	4
2. Oblate Top: $I_A = I_B < I_C$	5
D. Asymmetric Top Molecules: $I_A \neq I_B \neq I_C$ (where $I_A < I_B < I_C$, and the rotational constants are ordered $A > B > C$)	6
III. Pressure Effect	6
IV. Temperature Effect	6
V. Vapor-Phase vs Condensed IR Spectra	7
VI. Fermi Resonance (FR.) and Other Factors	7
References	8

Figures

Figure 1-1	9 (3)	Figure 1-9	17 (4)
Figure 1-2	10 (3)	Figure 1-10	18 (4)
Figure 1-3	11 (3)	Figure 1-11	19 (4)
Figure 1-4	12 (3)	Figure 1-12	20 (4)
Figure 1-5	13 (3)	Figure 1-13	21 (5)
Figure 1-6	14 (3)	Figure 1-14	22 (5)
Figure 1-7	15 (3)	Figure 1-15	23 (5)
Figure 1-8	16 (4)	Figure 1-16	24 (6)

*Numbers in parentheses indicate in-text page reference.

I. THEORY

For detailed discussion on the theoretical treatment of vibrational data (IR and Raman) the reader is referred to the following References (1–4). Extensive interpretation of IR vapor-phase

spectra have been presented in Reference (5). The infrared and Raman methods are based on the fact that within any molecule the atoms vibrate within a few definite, sharply defined frequencies characteristic of the molecule. These vibrational frequencies occur in the region of the electromagnetic spectrum 13333 cm^{-1} to 50 cm^{-1} and beyond. Only those molecular vibrations producing a dipole-moment change are IR active, allowed in the IR, and only those molecular vibrations producing polarization of the electron cloud are Raman active, allowed in the Raman. In the vapor-phase, molecules are free to rotate in three-dimensional (3D) space. The molecular rotational moments of inertia are governed by molecular geometry, and the atomic mass of each atom in the molecule together with their relative spatial positions within the molecule. Therefore, in the vapor-phase, molecules undergo transitions between quantized rotation states as well as quantized vibrational transitions. The result is that a transition between the ground state and the first excited state of a normal mode is accompanied by a manifold of rotational transitions. This leads to a complex rotation-vibration band for every IR active molecular vibration. Overtones are also IR active for molecules without a center of symmetry, and they result from transitions between the ground state and the second excited state of a normal vibration. Combination tones result from simultaneous transitions from the ground state to the first excited state of two or more normal vibrations. Both combination tones and overtones are also accompanied by manifold rotational transitions. In the liquid or solution phase, rotation of the molecule in space is restricted. Therefore, the rotation-vibration bands are "pressure broadened," and do not exhibit the sharp manifold rotational translational lines.

The number of molecular vibrations allowed in the IR or R for a given molecule is governed by the number of atoms in the molecule together with its molecular geometry. For nonlinear molecules, the total number of normal vibrations is determined by the equation $3N-6$, where N is the number of atoms in the molecule. Because the molecules are free to vibrate, rotate, and translate in 3D space, N is multiplied by 3. The number 6 is subtracted because the number of possible molecular vibrations is not determined by rotation and translation of the molecule. For linear molecules, the total number of normal vibrations is determined by equation $3N-5$.

In order to determine the active IR and Raman normal vibrations for any molecule, one has to apply a method known as Group Theory (1-4). Application of Group Theory also allows the determination of which overtones and combination tones are active in either the IR or Raman.

Pure molecular rotation transitions are also IR active, and they occur in the IR spectrum in the region below 600 cm^{-1} for small molecules having a permanent dipole, such as H_2O , NH_3 , PH_3 , etc.

In the vapor-phase, interpretation of the rotation-vibration band contour is helpful in the elucidation of molecular structure. Band contours result from a combination of molecular symmetry and the moments of inertia I_A , I_B , and I_C about three mutually perpendicular axes.

II. EXAMPLES OF MOLECULAR STRUCTURE

A. LINEAR MOLECULES: $I_A = 0$, $I_B = I_C$

Examples of these are:

Hydrogen halides, HX ;
Carbon monoxide, CO ;

Nitrogen oxide, NO;
Carbon dioxide, O=C=O;
Carbon disulfide, S=C=S; and
Acetylene, H-C≡C-H.

In the case of linear molecules, I_A is the moment of inertia along the molecular axis, and I_B and I_C are mutually perpendicular axes. The infrared active stretching vibrations produce a dipole-moment change along the molecular symmetry axis, and the resulting rotation-vibration band contour is called a parallel band. In this case, the P and R branches are predominate with no center Q branch.

Figure 1.1 shows the IR vapor-phase spectrum of hydrogen bromide. The P branch of HBr occurs in the region $2300\text{--}2550\text{ cm}^{-1}$ and the R branch occurs in the region $2500\text{--}2725\text{ cm}^{-1}$. Figure 1.2 shows the IR vapor-phase spectrum of hydrogen chloride. The P branch of HCl occurs in the region $2600\text{--}2880\text{ cm}^{-1}$ and the R branch occurs in the region $2900\text{--}3080\text{ cm}^{-1}$. The rotational subband spacings are closer together for HBr than those for HCl, and this is because the individual rotation subbands in the P and R branches are dependent upon the moments of inertia, and become more closely spaced as I_B and I_C become larger. Neither HBr nor HCl exhibits a central Q branch for the hydrogen-halogen stretching vibration.

Figure 1.3 shows an IR vapor-phase spectrum for carbon monoxide in the region $1950\text{--}2300\text{ cm}^{-1}$. In this case the P branch occurs in the region $2000\text{--}2150\text{ cm}^{-1}$, and the R branch occurs in the region $2150\text{--}2250\text{ cm}^{-1}$. Both the P and R branches exhibit closely spaced rotation subbands of the CO stretching vibration, producing essentially a solid continuum of absorption lines.

Figure 1.4 shows an IR vapor-phase spectrum of nitrogen oxide. The NO stretching vibration is assigned to the parallel band occurring in the region $1760\text{--}1970\text{ cm}^{-1}$. However, it should be noted that this is an exceptional case for linear molecules, because a central Q branch is observed near 1872 cm^{-1} . This exception results from the presence of an unpaired electron in nitrogen oxide causing a resultant electronic angular momentum about the molecular axis, which gives rise to a Q branch in the parallel band (1). The P branch subbands occur below 1872 cm^{-1} , and the R branch subbands occur above 1872 cm^{-1} . Otherwise, a band with this contour for linear molecules would be called a perpendicular band.

Figure 1.5 is a vapor-phase IR spectrum of carbon dioxide. The perpendicular band for CO_2 exhibits its Q branch near 670 cm^{-1} with a P branch near 656 cm^{-1} and an R branch near 680 cm^{-1} . This CO_2 bending vibration is doubly degenerate. The parallel band for the antisymmetric CO_2 stretching vibration occurs in the region $2300\text{--}2400\text{ cm}^{-1}$. The P branch occurs near 2350 cm^{-1} and the R branch occurs near 2360 cm^{-1} .

Figure 1.6 is an IR vapor-phase spectrum of carbon disulfide. The P branch of the parallel band occurs near 1560 cm^{-1} and the R branch of the parallel band occurs near 1540 cm^{-1} for this antisymmetric CS_2 stretching vibration.

Figure 1.7 is an IR vapor-phase spectrum for acetylene. The perpendicular band occurring in the region $650\text{--}820\text{ cm}^{-1}$ is assigned to the in-phase $(\equiv\text{C-H})_2$ bending vibration, which is doubly degenerate. The Q branch occurs near 730 cm^{-1} , the P branch in the region $650\text{--}720\text{ cm}^{-1}$, and the R branch in the region $735\text{--}820\text{ cm}^{-1}$. Rotational subbands are noted in both the P and R branches of this linear molecule.

Acetylene, carbon dioxide, and carbon disulfide have a center of symmetry; therefore, some vibrations are only IR active and some vibrations are only Raman active. Raman active vibrations

for acetylene are the in-phase $(\equiv\text{C}-\text{H})_2$ stretching vibration, the $\text{C}\equiv\text{C}$ stretching vibration, and the out-of-phase $(\equiv\text{C}-\text{H})_2$ bending vibration. A Raman active fundamental for CO_2 and CS_2 is the symmetric $\overline{\text{CO}_2}$ and $\overline{\text{CS}_2}$ stretching vibration. Comparison of the frequency separation between the subbands of the P and R branches shows that it is less for CS_2 than for CO_2 , and this is a result of a larger $I_B = I_C$ for CS_2 compared to CO_2 .

B. SPHERICAL TOP MOLECULES: $I_A = I_B = I_C$

Molecules in this class have T_d symmetry, and examples are methane and symmetrically substituted carbon tetrahalides. In this case IR active fundamentals exhibit P, Q and R branches in the vapor-phase comparable to that exhibited by perpendicular vibrations in linear molecules.

Figure 1.8 is an IR vapor-phase spectrum for methane. The antisymmetric CH_4 stretching vibration is triply degenerate, the perpendicular band exhibits the Q branch near 3020 cm^{-1} , the P branch in the region $2850\text{--}3000\text{ cm}^{-1}$, and the R branch in the region $3040\text{--}3180\text{ cm}^{-1}$. The triply degenerate antisymmetric CH_4 bending vibration also appears as a perpendicular band. The Q branch occurs near 1303 cm^{-1} , the P branch in the region $1200\text{--}1290\text{ cm}^{-1}$, and the R branch in the region $1310\text{--}1380\text{ cm}^{-1}$. Numerous subbands are noted in the P and R branches of both vibrations. The symmetric CH_4 stretching vibration is only active in the Raman (2914 cm^{-1}), and the symmetric CH_4 bending vibration, triply degenerate, is only Raman active (1306 cm^{-1}). The antisymmetric CH_4 stretching vibration, triply degenerate, and the symmetric CH_4 bending vibration, doubly degenerate, are both IR and Raman active.

Figure 1.9 shows an IR vapor-phase spectrum of carbon tetrafluoride. The antisymmetric CF_4 stretching vibration is triply degenerate, and its Q branch is noted near 1269 cm^{-1} . The antisymmetric CF_4 bending vibration is triply degenerate. Its Q branch is noted near 630 cm^{-1} , and the P and R branches are noted near 619 cm^{-1} and 650 cm^{-1} , respectively. Because the moments of inertia are large, the subbands of the P and R branches are so narrowly spaced that the P and R branches appear as a continuum.

C. SYMMETRIC TOP MOLECULES

1. Prolate: $I_A < I_B = I_C$ (essentially rod shaped)

Molecules in this class have C_{3v} symmetry. Examples include the methyl halides, propyne, and 1-halopropynes.

Prolate symmetric top molecules exhibit both parallel and perpendicular bands in the vapor phase. Molecular vibrations mutually perpendicular to the highest symmetry axis exhibit perpendicular bands and molecular vibrations symmetric with respect to the highest symmetry axis exhibit parallel bands.

Figures 1.10, 1.11, and 1.12 are IR vapor-phase spectra of methyl chloride, methyl bromide, and methyl iodide, respectively.

The P and R branches of the parallel bands for these methyl halides are given here:

<i>Branch</i>	CH ₃ Cl cm ⁻¹	CH ₃ Br cm ⁻¹	CH ₃ I cm ⁻¹	Assignment
P	2952	2980	2980	symmetric CH ₃ stretching
R	2981	2985	2958	
P	1346	1293	1261	symmetric CH ₃ bending
R	1366	1319	1235	
P	713	598	518	C–X stretching
R	748	622	540	

The parallel bands are nondegenerate.

The P, Q, and R branches of the perpendicular bands for these methyl halides are given here:

<i>Branch</i>	CH ₃ Cl cm ⁻¹	CH ₃ Br cm ⁻¹	CH ₃ I cm ⁻¹	Assignment
P	~3000–3150	~3020–3140	~3020–3140	antisymmetric CH ₃ stretching
Q	~1325–1600	~1300–1600	~1300–1600	
R	~940–1120	~850–1050	~770–1000	CH ₃ rocking

The perpendicular modes are doubly degenerate.

Figures 1.13 and 1.14 are IR vapor-phase spectra of 1-bromopropyne and 1-iodopropyne, respectively. Detailed assignments for these two compounds are given in Reference (6).

2. Oblate Top: $I_A = I_B < I_C$ (essentially disc shaped)

Molecules in this class have D_{6h} symmetry, and molecules with this symmetry include benzene, benzene-d₆, and the hexahalobenzenes, which contain only F₆, Cl₆, Br₆, or I₆. Oblate symmetric top molecules exhibit both parallel and perpendicular bands. Planar molecular vibrations exhibit parallel bands, and out-of-plane vibrations exhibit perpendicular bands. These complex molecules exhibit relatively simple IR vapor-phase IR spectra, because these molecules have a center of symmetry, and only a few normal modes are IR active.

Figure 1.15 is an IR vapor-phase spectrum of benzene. The type C perpendicular band with a Q branch at ~ 670 cm⁻¹, with P and R branches near ~ 651 and ~ 686 cm⁻¹, respectively, is assigned to the in-phase-out-of plane 6 hydrogen deformation. Benzene exhibits a type A band with P, Q, and R branches near 1019, 1039, and 1051 cm⁻¹, respectively. Both the type A and type C bands show P, Q, and R branches, but the spacings between P and R branches for type A bands for benzene are less than the spacings between the P and R branches of type C bands.

D. ASYMMETRIC TOP MOLECULES: $I_A \neq I_B \neq I_C$ (WHERE $I_A < I_B < I_C$, AND THE ROTATIONAL CONSTANTS ARE ORDERED $A > B > C$)

Molecules in this class will exhibit type A, B, and C bands providing the dipole moment change during the normal vibration is parallel to the a, b, or c axis, respectively. Mixed band contours described as type AB are exhibited by molecules where the dipole moment change during the normal vibration is not exactly parallel to the a or b symmetry axis.

Figure 1.16 is a vapor-phase IR spectrum of ethylene oxide. Type B bands exhibit no central peak, and classic type B bands are noted near 1269 and 875 cm^{-1} . For the 1269 cm^{-1} band the P and R branches are assigned near 1247 and 1292 cm^{-1} , respectively, and the Q^I and Q^{II} branches are assigned near 1263 and 1274 cm^{-1} , respectively. For the 875 cm^{-1} band, the P and R branches are assigned near 848 and 894 cm^{-1} , respectively, and the Q^I and Q^{II} branches are assigned near 869 and 881 cm^{-1} , respectively. The 1269 cm^{-1} band is assigned to ring breathing, the 875 cm^{-1} band to a ring deformation. The weak type C band with a Q branch near 820 cm^{-1} is assigned to CH₂ rocking (7).

III. PRESSURE EFFECT

With increasing pressure there are more frequent collisions of like molecules, or between a molecule and a diluent gas such as nitrogen or helium, and this has the effect of broadening the vapor-phase IR band contours resulting from molecular rotation-vibration. This effect is termed pressure broadening. The individual subbands (or lines) become increasingly broad due to restricted rotation in the vapor phase due to frequent molecular collisions. Under high pressure, the subbands are completely broadened so that the molecular vibrations with highly restricted molecular rotation produce IR band shapes with no apparent subbands. Thus, these pressure broadened vapor-phase IR bands for various molecular structures have shapes comparable to their IR band shapes observed in their neat liquid or solution phases. This is so because, in the neat liquid or solution phases, there are frequent collisions between like molecules or molecular collisions between solute molecules and between solute and solvent molecules for molecules in solution, which restrict molecular rotation of these molecules.

In order to measure the intensities of the IR vibrational bands for ethane and ethane-d₆ in the vapor-phase, the samples were pressurized up to 50 atm to broaden the bands (8).

IV. TEMPERATURE EFFECT

In the vapor-phase temperature can cause change in the band contours. The individual lines or subbands in the P and R branches are due to the relative population of the rotational states. An increase in temperature will change the population of rotation states, hence the change in IR band contour. Secondly, increased temperature in a closed volume cell increases the pressure, which induces the pressure broadening effect.

Hot bands are also temperature dependent, and change in temperature causes change in IR band intensity (3).

When molecules exist as rotational conformers (rotamers), they are also affected by changes in temperature, because the concentration of the different rotamers is dependent upon temperature. Therefore, it is essential to record IR spectra at different temperatures in cases where molecules exist as rotamers in order to determine which bands result from the same rotamer.

V. VAPOR-PHASE VS CONDENSED IR SPECTRA

The IR group frequencies of molecules are dependent upon physical phase. These frequency differences result from solute-solvent interaction via dipolar interaction or from weak intermolecular hydrogen bonding. Large frequency differences, as large as 400 cm^{-1} , result from strong intermolecular hydrogen bonding between molecules or between solute and solvent. These effects are absent in the vapor phase, especially at temperatures above 180°C at ordinary pressure. The vibrational frequency changes will be extensively discussed in later chapters.

VI. FERMI RESONANCE (F.R.) AND OTHER FACTORS

Some molecules exhibit two or more bands in a region where only one fundamental vibration is expected, excluding the presence of rotational conformers. In this case Fermi resonance between a fundamental and an overtone or combination tone of the same symmetry species interacts. The combination or overtone gains intensity at the expense of the intensity of the fundamental. The result is that one band occurs at a higher frequency and one band occurs at a lower frequency than expected due to this resonance interaction between the two modes. Langseth and Lord (9) have developed a method to correct for F.R. (10).¹ This equation is presented here:

$$W_o = \frac{W_a + W_b}{2} \pm \frac{W_a - W_b}{2} \cdot \frac{I_a - I_b}{I_a + I_b}$$

where, W_a and W_b are the observed vibrational frequencies, I_a and I_b their band intensities, and the two values of W_o calculated by the equation will be approximately the unperturbed frequencies. The amount of F.R. is dependent upon the unperturbed frequencies of the fundamental and the combination or overtone. If two bands of equal intensity are observed, each band results from an equal contribution from the fundamental vibration and an equal contribution from the combination tone or overtone. The combination or overtone may occur above or below the fundamental frequency. In the case in which the bands are of unequal intensity, both bands are still a mixture of both vibrations but the stronger band has more contribution from the fundamental than the weaker band. Correction for F.R. is necessary in

¹Reference (10) also includes the same equation developed for the correction of two bands in Fermi resonance (8). In addition, the newer reference shows the development for the correction of Fermi resonance for cases where three vibrations are in Fermi resonance.

cases where one needs to perform a normal coordinate analysis, or when comparing IR data of certain classes of compounds where not all of the compounds show evidence for FR.

Parameters such as bond force constants, bond lengths, bond angles, field effects, inductive effects, and resonance effects are independent of physical phase and these parameters are useful in the elucidation of molecular structure via IR spectra-structure interpretation.

REFERENCES

1. Herzberg, G. (1945). *Molecular Spectra and Molecular Structure II. Infrared and Raman Spectra of Polyatomic Molecules*, New Jersey: D. Van Nostrand Company, Inc.
2. Wilson, E. B. Jr., Decius, J. C., and Cross, P. C. (1955). *Molecular Vibrations*, New York: McGraw-Hill Book Company, Inc.
3. Potts, W. J. Jr. (1963). *Chemical Infrared Spectroscopy*, New York: John Wiley & Sons, Inc.
4. Colthup, N. B., Daly, L. H., and Wiberley, S. E. (1990). *Introduction to Infrared and Raman Spectroscopy*, 3rd ed., Boston: Academic Press.
5. Nyquist, R. A. (1984). *The Interpretation of Vapor-Phase Infrared Spectra: Group Frequency Data*, vol. 1, Philadelphia: Sadlter Research Laboratories, Division of Bio-Rad Laboratories.
6. Nyquist, R. A. (1965). *Spectrochim Acta*, **21**, 1245.
7. Lord, R. C. and Nolin, B. (1956). *J. Chem. Phys.*, **24**, 656.
8. Nyquist, I. M., Mills, I. M., Person, W. B., and Crawford, B. Jr. (1957). *J. Chem. Phys.*, **26**, 552.
9. Langseth, A. and Lord, R. C. (1948). *Kgl. Danske Videnskab Selskab Mat-fys. Medd*, **16**, 6.
10. Nyquist, R. A., Fouchea, H. A., Hoffman, G. A., and Hasha, D. L. (1991). *Appl. Spectrosc.*, **45**, 860.

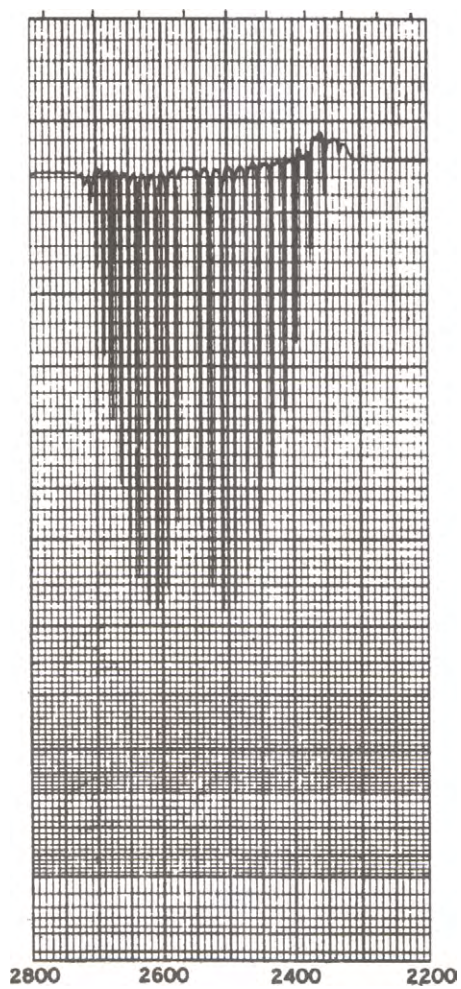


FIGURE 1.1 Infrared vapor-phase spectrum for hydrogen bromide (5-cm glass cell with KBr windows: 600 mm Hg HBr).

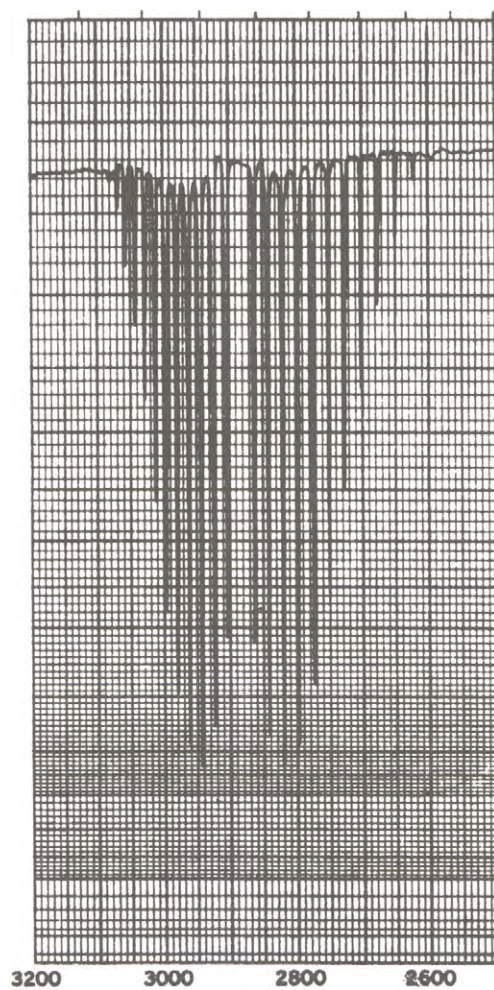


FIGURE 1.2 Infrared vapor-phase spectrum for hydrogen chloride (5-cm glass cell with KBr windows: 200 mm Hg HCl, total pressure 600 mm Hg with N₂).

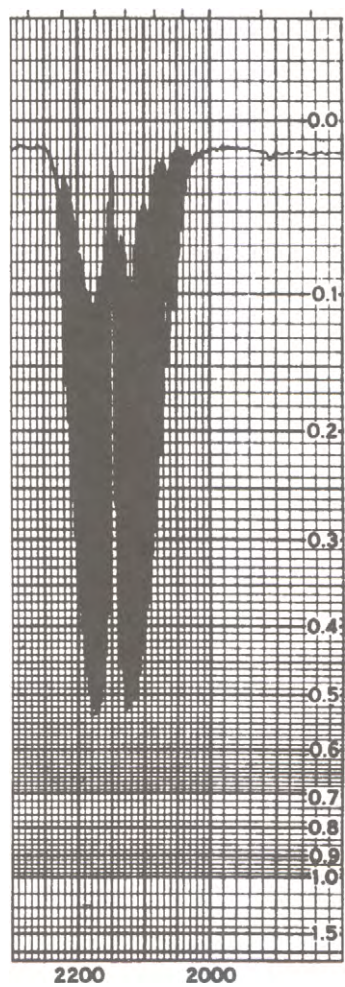


FIGURE 1.3 Infrared vapor-phase spectrum for carbon monoxide (5-cm glass cell with KBr windows: 400 mm Hg CO, total pressure 600 mm Hg with N₂).

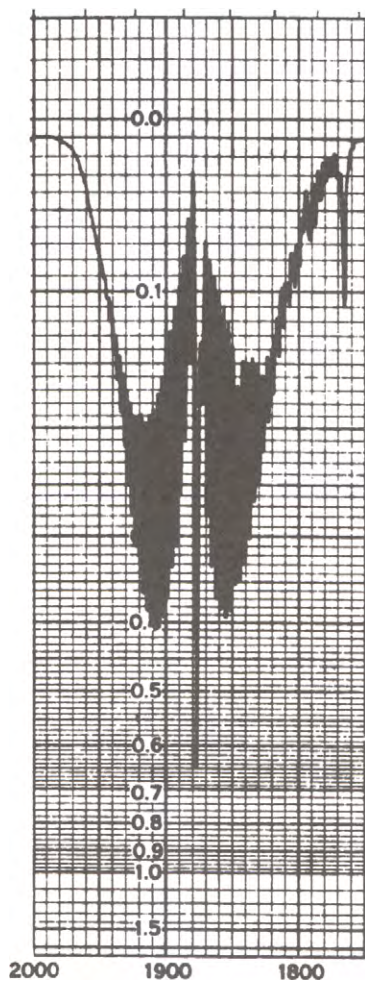


FIGURE 1.4 Infrared vapor-phase spectrum for nitrogen oxide, NO.

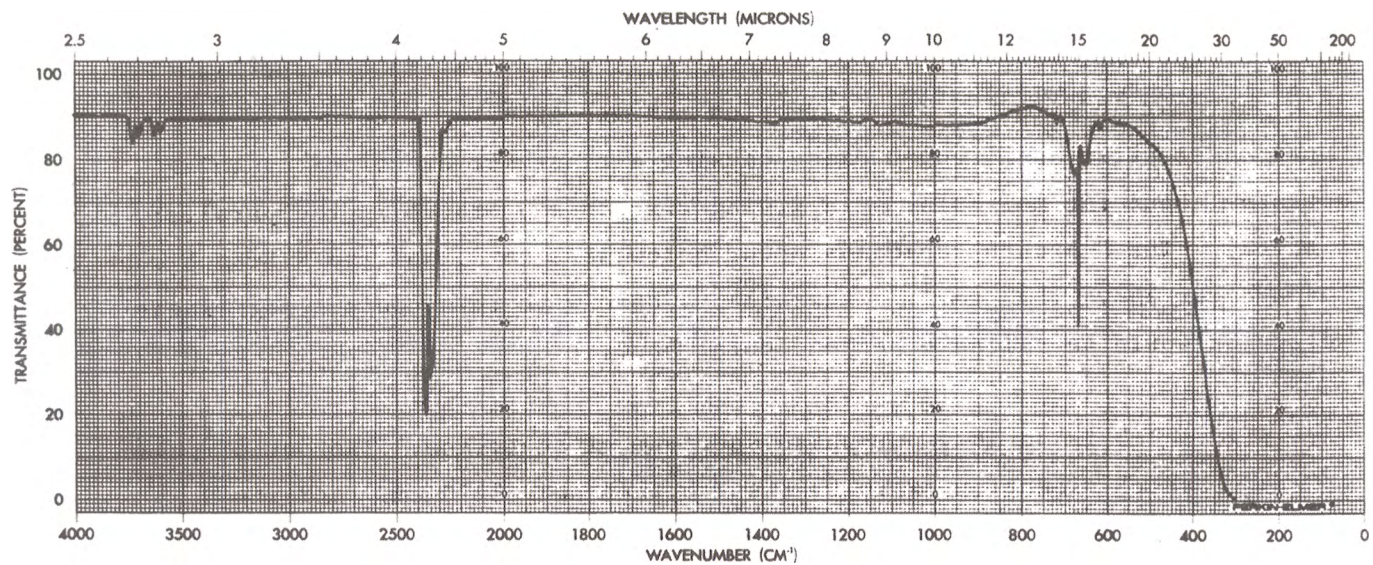


FIGURE 1.5 Infrared vapor-phase spectrum for carbon dioxide (5-cm glass cell with KBr windows: 50 and 200 mm Hg CO₂, total pressure 600 mm with N₂).

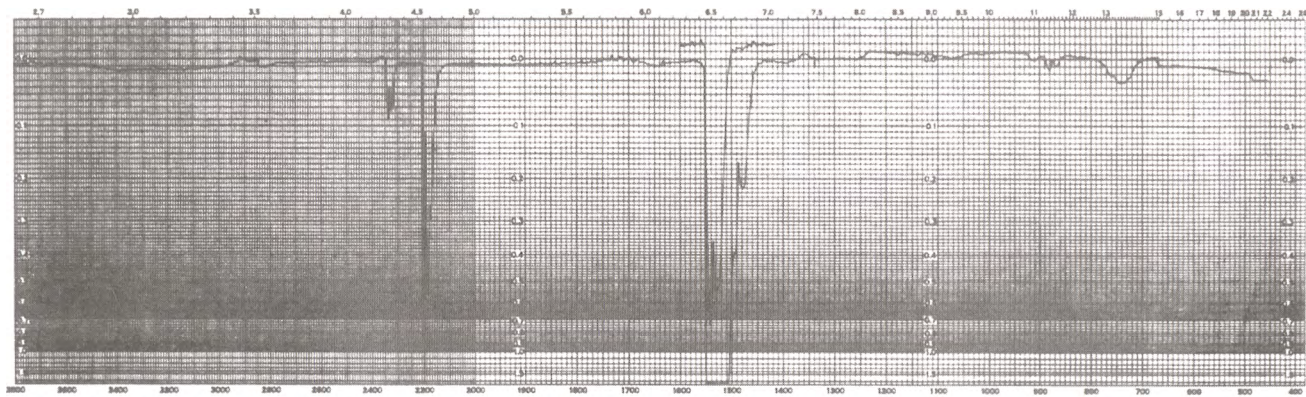


FIGURE 1.6 Infrared vapor-phase spectrum for carbon disulfide (5-cm glass cell with KBr windows: 2 and 100 mm Hg CS₂, total pressure 600 mm Hg with N₂).

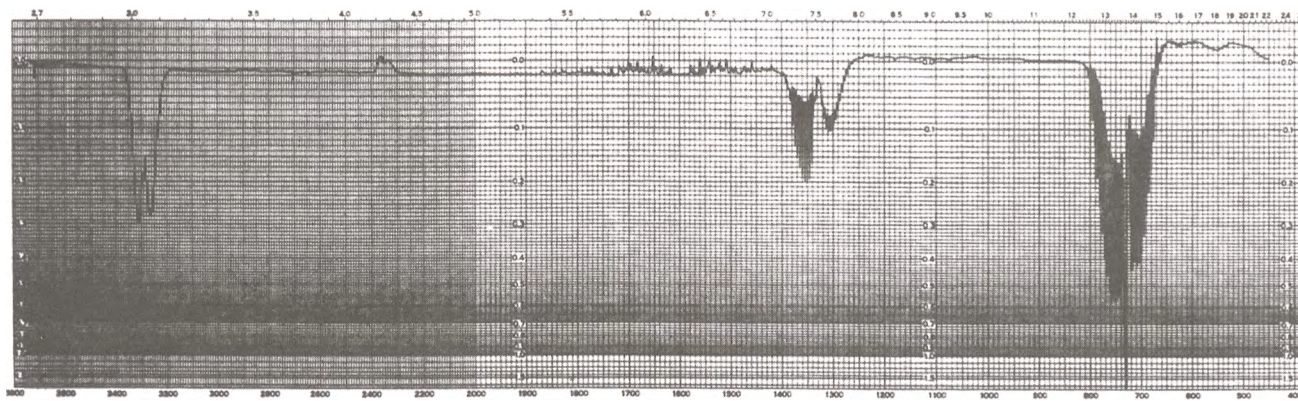


FIGURE 1.7 Infrared vapor-phase spectrum for acetylene (5-cm glass cell with KBr windows: 50 mm Hg C_2H_2 , total pressure 600 mm Hg with N_2).

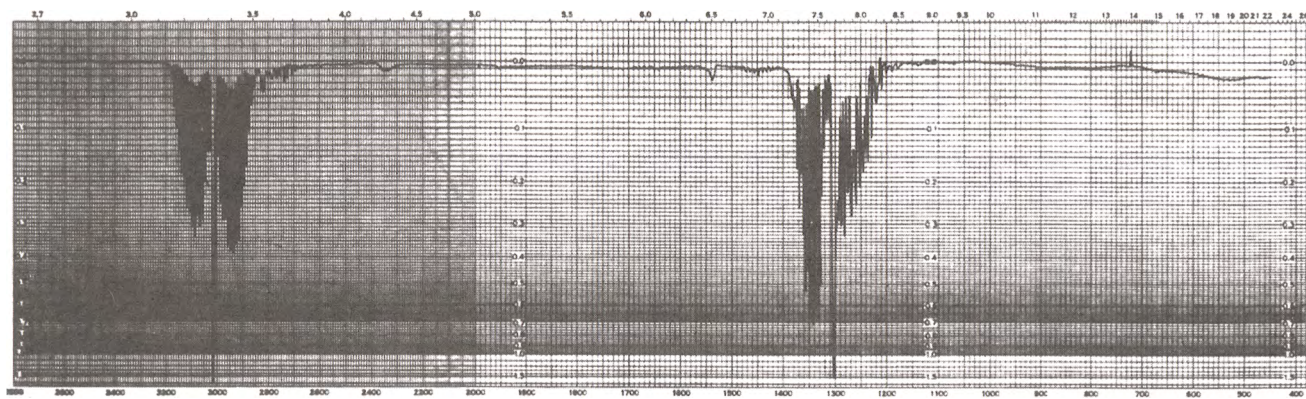


FIGURE 1.8 Infrared vapor-phase spectrum for methane (5-cm glass cell with KBr windows: 150 mm Hg CH₄, total pressure 600 mm Hg with N₂).

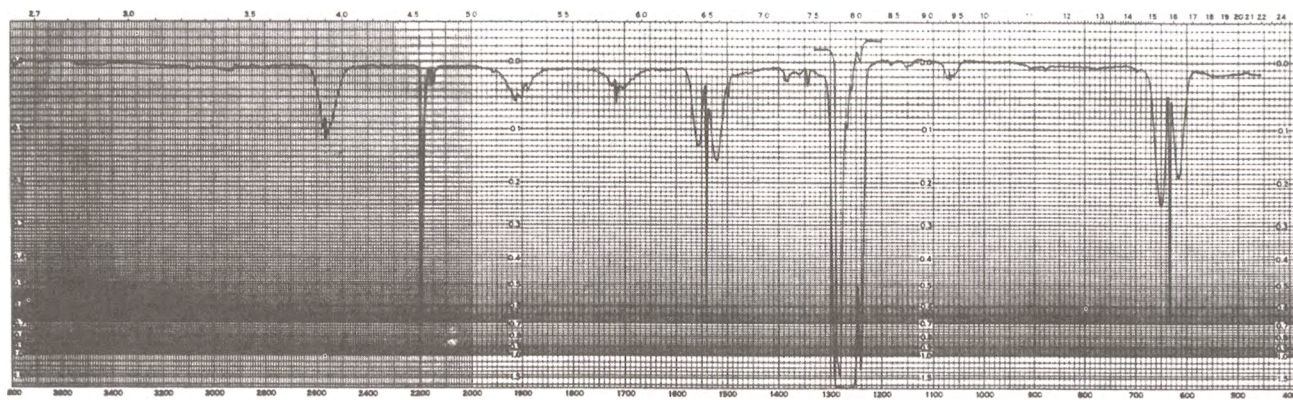


FIGURE 1.9 Infrared vapor-phase spectrum for carbon tetrafluoride (5-cm glass cell with KBr windows: 100 mm Hg CF₄, total pressure 600 mm Hg with N₂).

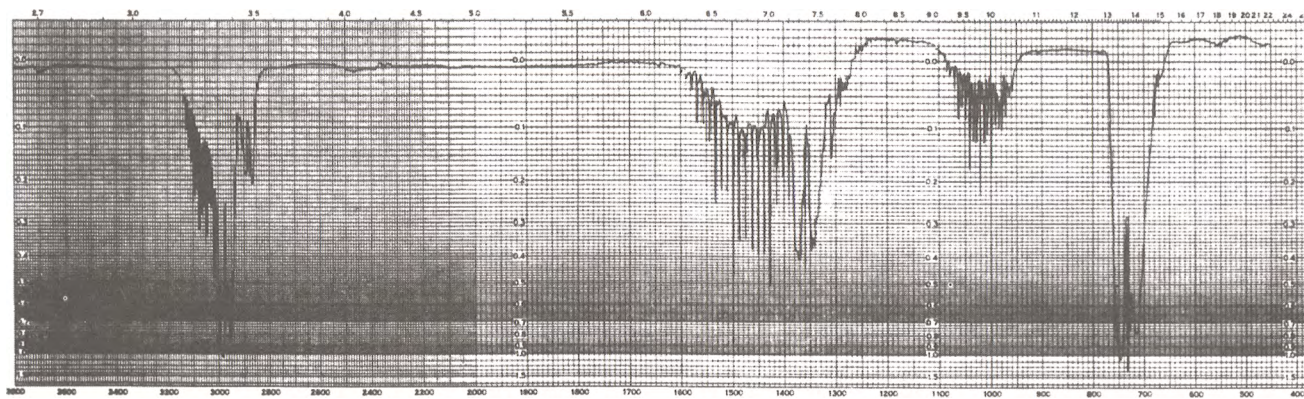


FIGURE 1.10 Infrared vapor-phase spectrum for methyl chloride (5-cm glass cell with windows: 200 mm Hg CH₃, Cl, total pressure 600 mm Hg with N₂).

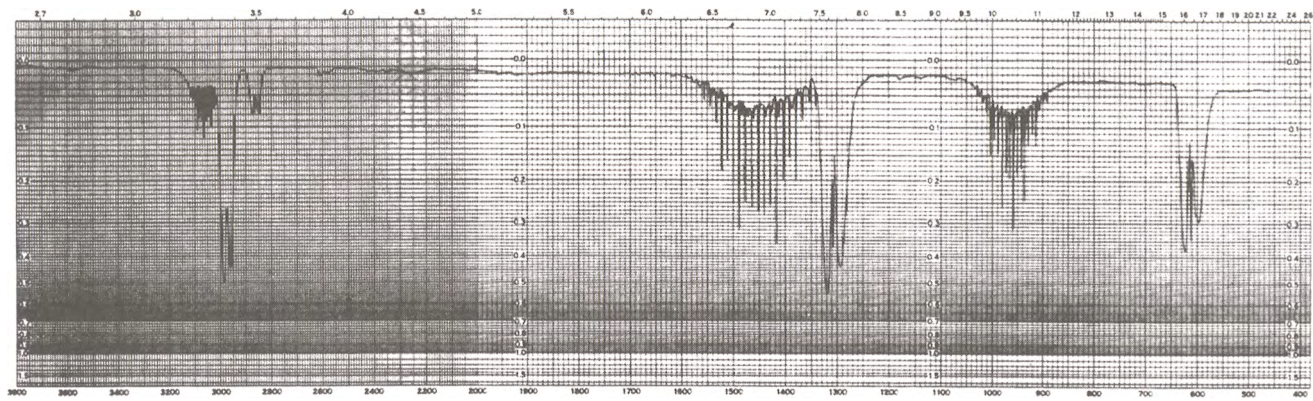


FIGURE 1.11 Infrared vapor-phase spectrum for methyl bromide (5-cm glass cell with KBr windows: 100 mm Hg CH₃Br, total pressure 600 mm Hg with N₂).

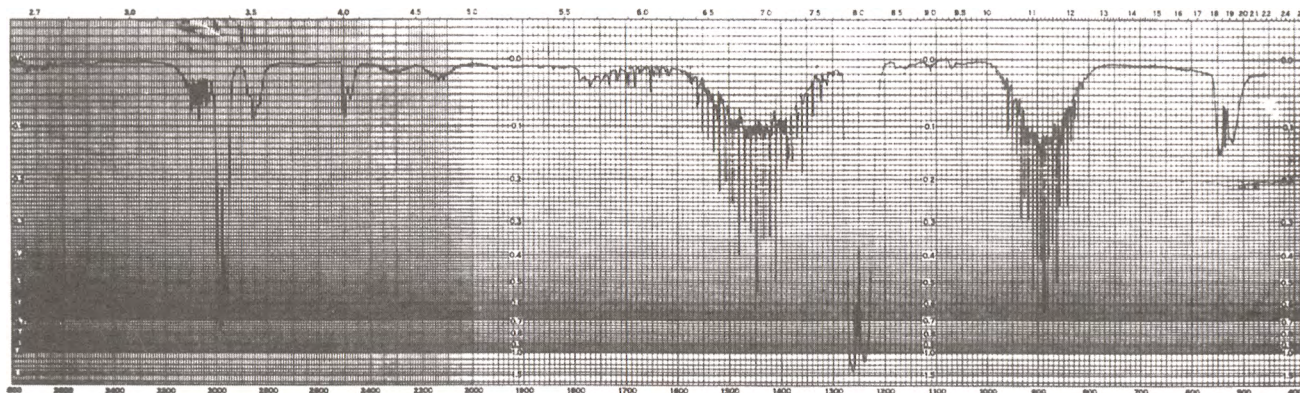


FIGURE 1.12 Infrared vapor-phase spectrum for methyl iodide (5-cm glass cell with KBr windows: 200 mm Hg CH₃I, total pressure 600 mm Hg with N₂).

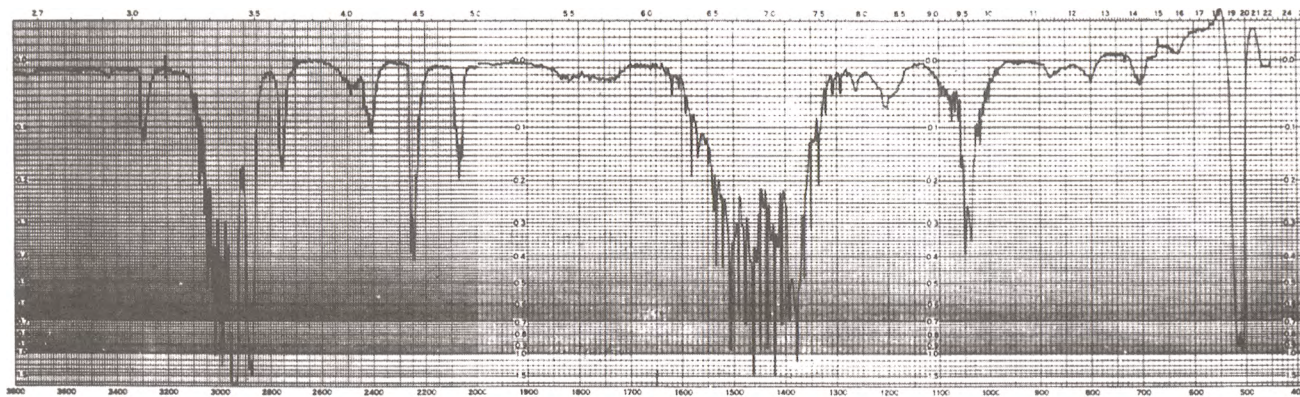


FIGURE 1.13 Infrared vapor-phase spectrum for 1-bromopropyne, C_3H_3Br .

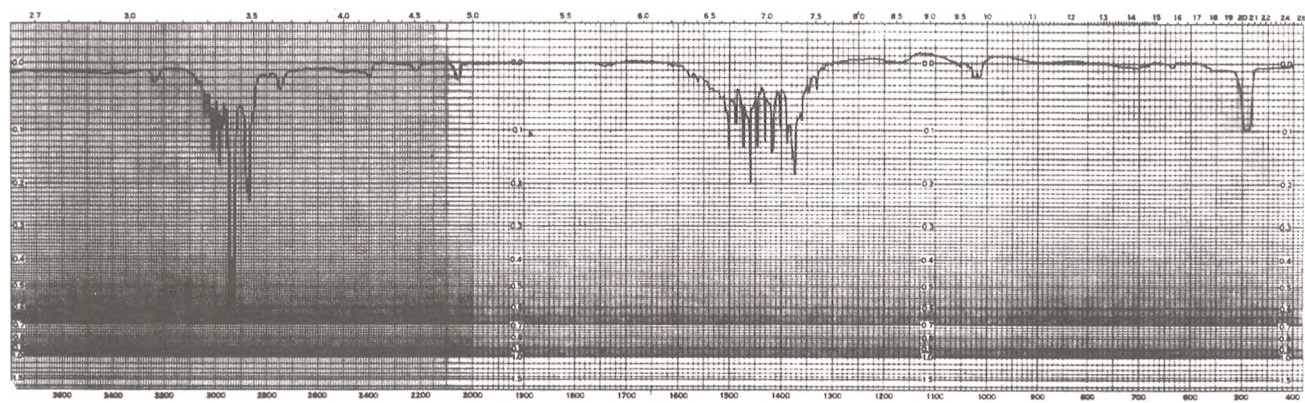


FIGURE 1.14 Infrared vapor-phase spectrum for 1-iodopropyne, C₃H₃I.

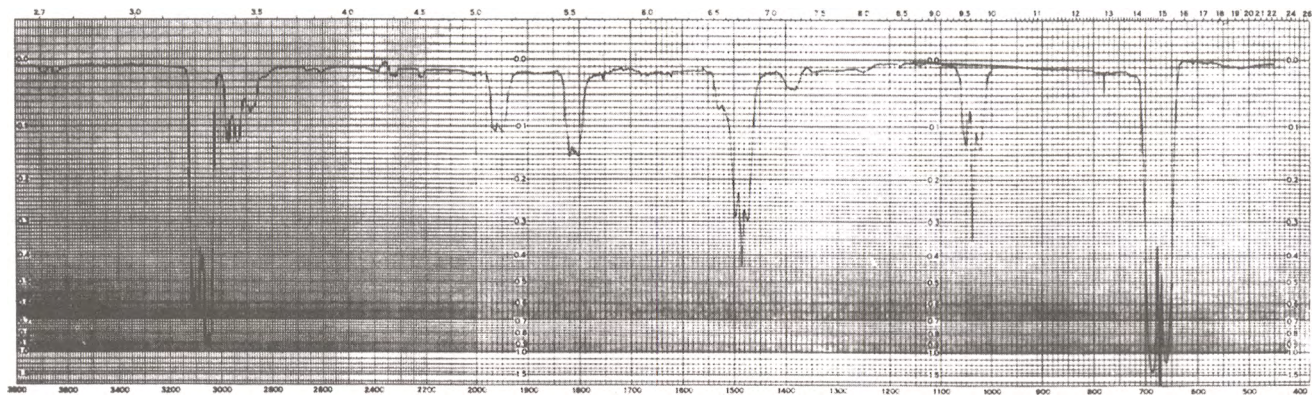


FIGURE 1.15 Infrared vapor-phase spectrum for benzene (5-cm glass cell with KBr windows: 40 mm Hg with C_6H_6 , total pressure 600 mm Hg with N_2).

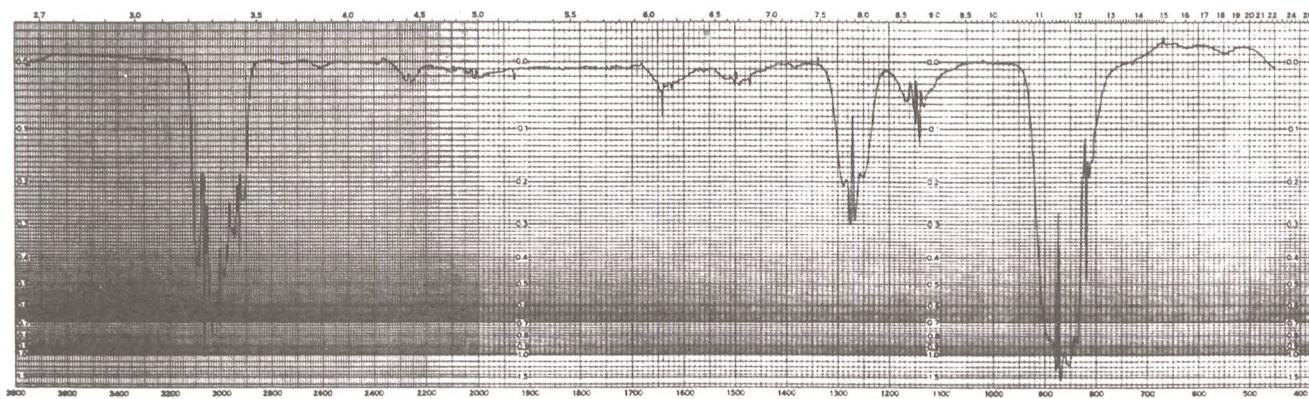


FIGURE 1.16 Infrared vapor-phase spectrum for ethylene oxide (5-cm glass cell with KBr windows: 50 mm Hg C_2H_2O , total pressure 600 mm Hg with N_2).

Experimental

I. Solids (Excluding Single Crystals)	25
A. Mull Technique	26
B. Potassium Bromide (KBr) Disk Techniques	26
C. Solutions (Solids, Liquids, and Gases)	27
II. Liquid Films (See the Forementioned I–C for Liquids in Solution) and Cast Polymer Films	27
III. Vapors and Gases	28
References	30

Sample preparation is a very important part of the IR technique. Because chemicals can exist in the solid, liquid, vapor, or solution phases, different methods of preparation are required in order to be able to record their IR spectra. This chapter is not intended to include all methods of obtaining IR spectra. It includes only the methods used to acquire the data included in this book.

I. SOLIDS (EXCLUDING SINGLE CRYSTALS)

Solid samples are usually prepared as mulls or as KBr pellets. Both techniques require that the particle size be smaller than $2.5\ \mu$. Larger particles scatter IR radiation via Rayleigh scattering in the IR region of interest. For example, if particles are present in decreasing concentration from 2.5 through $25\ \mu$, the baseline of the spectrum will slope upward in the region 2.5 to $25\ \mu$ (4000 – $400\ \text{cm}^{-1}$, the region most commonly examined by chemists).

Thus, solid samples must be ground using a mortar and pestle (or a wiggle bug) to meet the preceding requirements. The closer one gets to a virtual horizontal baseline, the better the quality of the IR spectrum. The bands of the chemical solid start absorbing IR radiation at the point of the baseline where their vibrational frequencies occur in this region of the spectrum.

There is another factor that causes distortion of IR absorption bands. If the refractive index of solid particles and the surrounding medium differ appreciably, the Christiansen effect is encountered (1). The Christiansen effect develops because the refractive index of a chemical is a function of frequency that has a discontinuity in each frequency region of a strong absorption band. The refractive index falls rapidly on the high frequency side of the absorption

maximum and on the low frequency side the refractive index falls rapidly from a high value to its value of no absorption. This effect causes peculiar absorption band distortion when there are many large particles present due to inadequate sample preparation. The Christiansen effect is minimized by a reduction of as many particles as possible smaller than $2\ \mu$ in size. However, the effect is never completely eliminated when recording spectra of powdered crystalline materials.

A. MULL TECHNIQUE

After the sample has been properly ground, Nujol oil or Fluorolube is added and mixed in order to suspend the particles in the mulling agent. However, it is preferable to grind the solid in the presence of the mulling agent to help in the grinding process. The mulling agents suspend the solid particles, which helps to produce a closer match of the refractive index between these particles and the surrounding medium. Nujol is useful for recording IR spectra in the region $1333\text{--}400\ \text{cm}^{-1}$, and Fluorolube is useful for recording IR spectra in the region $4000\text{--}1333\ \text{cm}^{-1}$. In order to place these mull suspensions in the IR sample compartment, sodium chloride and/or potassium bromide plates are required. A Fluorolube mull paste is then placed between two sodium chloride plates or two potassium bromide plates using pressure to obtain the proper thickness of this paste in order to obtain a quality IR spectrum in the region $4000\text{--}1333\ \text{cm}^{-1}$ that is essentially void of significant Fluorolube absorption bands. In the region $1333\text{--}400\ \text{cm}^{-1}$ the process is repeated using the Nujol mull suspension between potassium bromide plates, which minimizes absorption from Nujol oil.

B. POTASSIUM BROMIDE (KBr) DISK TECHNIQUE

After grinding the solid to proper particle size, KBr is mixed with the solid particles. A ratio somewhere between 50 to 100 KBr : 1 of solid sample usually produces a quality IR spectrum. The KBr and ground particles are then thoroughly mixed to produce a uniform mixture. Further grinding of the mixture should be avoided because this additional grinding will usually induce water into the mixture. The proper amount of this KBr preparation is placed in a special die, and a disk is pressed using approximately 9600 Kg pressure. The disk is placed in a holder and placed then in the sample compartment of the IR spectrometer.

Both the mull and KBr pressed disk technique can cause changes to the sample. Grinding or increased pressure upon the sample can cause changes in crystalline form of the sample. In addition, the pressed KBr disk can cause chemical reactions to occur between KBr and the sample (e.g., $\text{R-NH}_3^+\text{Cl}^- + \text{KBr} \rightarrow \text{R-NH}_3^+\text{Br}^- + \text{KCl}$). In the mull technique ion exchange can also occur between the window and the suspended sample (e.g., $\text{R-NH}_3^+\text{F}^- + \text{KBr} \rightarrow \text{R-NH}_3^+\text{Br}^-$). This latter reaction occurs when pressure between the plates together with plate rotation causes solid state interaction between the plates and the sample. Thus, one should be aware that the chemist can inadvertently alter the original sample during preparation, thereby causing problems in the solution of the chemical problem at hand.

The IR spectra of solids obtained after evaporating water solutions to dryness can also be recorded using the mull or KBr disk technique.

C. SOLUTIONS (SOLIDS, LIQUIDS, AND GASES)

Solids, liquids, and gases are often soluble in solvents such as carbon tetrachloride and carbon disulfide. Other solvents such as chloroform, methylene chloride, or dimethyl sulfoxide (DMSO) can also be used depending upon the particular problem. Since like dissolves like, the more polar solvents are used to dissolve the more polar compounds. Carbon tetrachloride and carbon disulfide are used to dissolve the less polar compounds.

Carbon tetrachloride is a useful solvent in the region $4000\text{--}1333\text{ cm}^{-1}$ and carbon disulfide is a useful solvent in the region $1333\text{--}400\text{ cm}^{-1}$. This is because these solvents have the least absorption in these regions. Quality IR spectra can be recorded using samples prepared at 10% by weight in each of these solvents, and placing the solutions in 0.1-mm sodium chloride cell ($4000\text{--}1333\text{ cm}^{-1}$ for CCl_4 solutions) and 0.1-mm potassium bromide cell ($1333\text{--}400\text{ cm}^{-1}$ for CS_2 solutions). Comparable IR spectra will be recorded using 1% by weight using 1.0-mm cells; however, absorption from the solvent will be increased by a factor of 10. Variation of concentration and cell path length can be used to record the spectrum most useful in obtaining useful chemical information. For example, changing the concentration of a chemical, in say CCl_4 , can help to distinguish between inter- and intramolecular hydrogen bonding. The OH or NH stretching frequencies remain essentially unchanged upon dilution, in the case of intramolecular hydrogen bonding, but increase markedly in frequency upon dilution in the case of intermolecular hydrogen bonding.

Solution spectra are very useful in performing quantitative analysis when both the sample concentration and cell path length are known, providing the absorbance of a band due to the presence of the critical analyte can be directly measured. In the worst case, interference from the presence of another analyte may have to be subtracted before the analysis can be performed on the critical analyte in question.

A solvent such as CS_2 is also useful for extracting some chemicals from water. After thorough shaking with water, the sample can be concentrated by partial solvent evaporation in a well-ventilated hood containing no source of ignition. The sample is then salted using dry NaCl powder in order to remove water. The CS_2 is then placed in a suitable KBr cell before the solution spectrum is recorded. This same solvent can be used to extract certain additives from polymer compositions.

II. LIQUID FILMS (SEE THE FOREMENTIONED I–C FOR LIQUIDS IN SOLUTION) AND CAST POLYMER FILMS

a. Liquid films between KBr plates are easily prepared by placing a drop or more on one plate and then placing the second plate on top with enough pressure to form the desired film thickness. Very volatile liquids are better prepared as solutions.

b. IR spectra of polymers are often recorded of freestanding film or of films cast on a suitable IR plate. Freestanding films are prepared by heating polymeric material above its melting point between heated plates in a suitable press. The film is allowed to cool to ambient temperature before removing it from the metal plates. The freestanding film is then placed in the IR spectrometer.

c. IR spectra are often recorded of polymeric substances cast from boiling solution onto a preheated KBr plate, often under a nitrogen atmosphere in order to avoid oxidation of the polymer. After the solvent has evaporated, the plate and film are allowed to cool to ambient temperature before placing in the IR sample compartment. Failure to preheat the KBr plate will cause it to shatter when first in contact with the hot solution. Moreover, removal of the heated cast film after solvent evaporation to a ambient environment without prior cooling will also cause the KBr plate to shatter. Organic solvents such as 1,2-dichlorobenzene, toluene, and dimethyl formamide are often used to cast polymer films. The solvent used is dependent upon the particular polymer or copolymer, and its solubility in that solvent.

Silver chloride plates are often used as the substrate for casting films of water-soluble polymers. The water is removed by heat after first placing the water solution onto the AgCl plate placed under an IR heat lamp. It is essential that AgCl plates be stored in the dark to prevent darkening of the plates due to the formation of silver oxide upon exposure to light.

It is essential that all plates be cleaned after being used in these experiments. The polymer film can be removed from the plates using the same solvents used to cast the films. It is again necessary to avoid sudden temperature change to the plates during the cleaning operation in order to avoid plate shattering in cases such as KBr, NaCl, CaF₂, etc.

III. VAPORS AND GASES

Quality IR spectra can be recorded using partial pressures and appropriate cell lengths equipped, say, with potassium bromide windows. It should be noted that certain inorganic compounds react with KBr and form other inorganic salts on the surface of the KBr plate. Their reactions are readily detected because their reaction products can not be removed when the sample is evacuated under vacuum from the cell.

The IR spectra of chemicals with low vapor pressure can be recorded using a variable long path length vapor cell either at ambient temperature or at elevated temperature. It is best if these variable path length cell walls are coated with a substance such as poly (tetrafluoroethylene) to help prevent adsorption of the chemical on the surface of the metallic cell body. It is sometimes necessary to heat the cell body under vacuum to remove adsorbed chemical molecules. Another method to clean out adsorbed molecules present in the cell is to flush the cell with nitrogen or dry air.

It is also possible to perform quantitative analysis of compounds whose IR spectra have been recorded in the vapor phase. An often-used method is to record the partial pressure of the chemical in the vapor, and then bring the total pressure up to 600-mm Hg using dry nitrogen. The constant total pressure of 600-mm Hg helps eliminate the effects of pressure broadening on the absorption bands.¹ This requires of course that the appropriate vacuum line and dry nitrogen be available to the chemist. A longer path length setting is required as vapor pressure of a chemical falls. Of course, some chemicals react with the mirrors, and this will limit this application for these particular compounds.

It is possible to detect low parts per million of chemicals in air using the variable long path cells. The interpretable regions of the IR spectrum are significantly improved by spectral

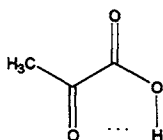
¹ The windows (KBr, NaCl, etc) of most glass-bodied cells are adhered to the glass body by a material such as paraffin wax. Pressures higher than 760-mm Hg will blow the windows from the glass body. Thus, 600-mm Hg sample pressure is a reasonable total pressure to safely achieve in these laboratory experiments.

subtraction of absorption due to the presence of H_2O and CO_2 . This can be done electronically or by dual cells placed in separate beams of a double beam spectrometer. In the case of FT-IR spectrometers, it is an easy task to remove these absorption bands due to the presence of air. In a case where there is no IR radiation being transmitted in a particular region of the IR spectrum, detection of a compound present in air (or in any phase) is not possible in these spectral regions, because the spectrometer is “dead” in these regions. Spectral subtraction will not change the “dead” regions of the spectrum.

A simple method of obtaining IR vapor spectra of chemicals with high vapor pressure is to connect the sample container using a rubber stoppered hose to a 0.1-mm (or 0.2-mm, etc.) liquid cell. The stopper is opened and the chemical vapor is allowed to flush out the 0.1-mm cell. The exit port of the cell is then stoppered, the sample connection is closed and removed, and the entrance part of the cell is also stoppered. The cell is now filled with the sample in the vapor phase at ambient temperature and pressure. Of course, this operation should be performed in a well-ventilated hood.

Gas chromatography has been coupled to infrared spectroscopy (GC/FT-IR) to form a powerful analytical technique capable of solving many real world problems. This technique requires that the chromatographed vapors pass sequentially through a gold-coated light pipe heated to a temperature of over 200°C . The light pipe path-length must be short enough so that only one chromatographed component is in the light pipe at one time. This technique has a major pitfall in that not all chemical compounds are stable at the high temperatures encountered utilizing this technique. For example, phthalic acid present as one component in a mixture would not be detected as one of the chromatographed fractions. This is because at these elevated temperatures, water splits out of phthalic acid to form phthalic anhydride, which is the compound detected using this technique. Other types of chemical reactions can occur if the chemicals contact hot metal surfaces (excluding gold) during their path through the GC/FT-IR system.

In order to identify unequivocally a vapor-phase IR spectrum of a chemical, an IR vapor-phase standard spectrum of this compound recorded under comparable conditions must be available for comparison. The reasons for this are presented here. A compound such as acetic acid exists as a hydrogen-bonded cyclic dimer in the condensed phase and in the vapor-phase at temperatures 150°C and below. At elevated temperature, acetic acid exists as isolated $\text{CH}_3\text{CO}_2\text{H}$ molecules. In this monomeric state, the OH stretching frequency exhibits a weak-medium sharp band near 3580 cm^{-1} in the vapor phase, and the $\text{C}=\text{O}$ stretching frequency exhibits a strong band near 1791 cm^{-1} . These features are uniquely different from the condensed phase IR spectra of acetic acid. This monomeric situation is even more complicated in situations where intramolecular hydrogen bonding can occur between the proton of the carboxylic acid group and a basic site in the molecule. For example, pyruvic acid (2-oxo-propionic acid) exhibits two bands in the vapor phase at 95°C (2). A weak band near 3580 cm^{-1} is assigned to an unassociated OH group of CO_2H . The weak-medium band near 3465 cm^{-1} results from the intramolecular hydrogen bond OH group to the free pair of electrons on the ketone carbonyl group to form a 5-membered cyclic ring as illustrated here:



Other situations occur where molecules that are intermolecularly hydrogen bonded in the condensed phase form intramolecular hydrogen bonds in the vapor phase. In addition, the regions for group frequencies in the condensed or solution phases have shifted from those in the vapor phase. Therefore, one must have at hand a collection of vapor-phase group frequency data, available to enable one to interpret these GC/FT-IR spectra by spectra-structure correlations (3). A compilation of the vapor-phase group frequency data has been developed from editorial work performed by Nyquist on the 10,000 vapor-phase spectra published by Sadtler Research Laboratories, G. Division of Bio-Rad Laboratories, Inc. The collection of these Sadtler spectra are a valuable asset for those employing the GC/FT-IR technique to solve real world problems.

Raman spectra of solids and liquids are routinely recorded utilizing dispersive or Fourier transform systems.

For example, Raman spectra of liquid ethynyl benzene and ethynyl benzene-d were recorded utilizing a Hylger spectrometer and 4358 Å radiation (7 Å/mm) filtered through rhodamine/nitrite filters. Depolarization measurements were made (4). These depolarization measurements aid in distinguishing between in-plane vibrational modes and out-of-plane vibrational modes in the case of ethynyl benzene. The in-plane modes are polarized and the out-of-plane modes are depolarized.

More recently, Raman spectra of inorganics in water solution have been recorded utilizing the Dilor XY Raman triple spectrograph operating in the double subtractive mode and fitted with 1200 g/mm gratings. The detector is a 3-stage Peltier-cooled EG&G silicon CCD model 15305 equipped with a Thomson 1024 × 256 chip, operated at -60 °C (5).

Sample fluorescence limits the application of the Raman technique because fluorescence is a first-order phenomenon, and the Raman effect is a second-order phenomenon. This fluorescence problem has been overcome recently by the development of FT/Raman. In this case, near-IR is used as the source of excitation of the molecules. Coleyshaw *et al.* reported on the quality of FT-Raman spectra as related to the color of the minerals. They report that white-, gray-, yellow-, pink-, orange-, and red-colored minerals yield good FT-Raman spectra, but they had little success with blue-, green-, or dark-colored minerals (6). This is because these colors absorb red light.

A Nicolet model 800 FT-IR spectrometer/Nicolet FT-Raman accessory equipped with a CaF₂ beamsplitter, Ge detector, and a CVI model C-95 Nd/YAG laser can be used successfully in recording the Raman spectra of many organic and inorganic compounds. The beauty of this combination device is that it can be used to record either IR or Raman spectra. Other manufacturers also produce FT-Raman systems.

REFERENCES

1. Potts, W. J. Jr. (1963). *Chemical Infrared Spectroscopy*, New York: John Wiley & Sons, Inc.
2. Welti, D. (1970). *Infrared Vapor Spectra*, New York: Hyden & Son Ltd.
3. Nyquist, R. A. (1984). *The Interpretation of Vapor-Phase Infrared Spectra: Group Frequency Data*, vols. 1 and 2, Philadelphia: Sadtler Research Laboratories, Division of Bio-Rad Laboratories.
4. Evans, J. C. and Nyquist, R. A. (1960). *Spectrochim. Acta*, **16**, 918.
5. Nyquist, R. A., Putzig, C. L., and Leugers, M. A. (1997). *Infrared and Raman Spectral Atlas of Inorganic Compounds and Organic Salts*, vol. 1, Boston: Academic Press.
6. Coleyshaw, E. E., Griffith, W. P., and Bowell, R. J. (1994). *Spectrochim. Acta*, **50A**, 1909.

Alkyl Carbon–Hydrogen Vibrations

Summary	32
Other <i>n</i> -Alkane Vibrations	34
1,2-Epoxyalkanes	34
Sodium Dimethylphosphonate (CH ₃) ₂ P(O) ₂ Na	34
Methylthiomethyl Mercury, Dimethylmercury (4), and Methylthiochloroformate (5)	35
Cycloalkanes	35
References	35

Figures

Figure 3-1	36 (31)
Figure 3-2	37 (31)
Figure 3-3	38 (32)
Figure 3-4	39 (32)
Figure 3-5	39 (32)
Figure 3-6	40 (32)
Figure 3-7	40 (32)

Tables

Table 3-1	41 (31)
Table 3-2	42 (32)
Table 3-2a	43 (32)
Table 3-3	44 (32)
Table 3-4	45 (32)
Table 3-5	45 (34)
Table 3-6	46 (34)
Table 3-7	47 (34)
Table 3-8	47 (35)
Table 3-9	48 (35)
Table 3-10	49 (35)
Table 3-11	50 (35)
Table 3-12	52 (35)
Table 3-13	53 (35)

*Numbers in parentheses indicate in-text page reference.

This chapter discusses alkyl carbon–hydrogen molecular vibrations and, in some cases, looks at how these molecular vibrations are affected by their surrounding chemical environment. However, in some cases the alkyl carbon–hydrogen vibrations will be included in the section that discusses their most distinguishing molecular vibrations.

The series of *n*-alkanes, C_{*n*}H_{2*n*+2} were prepared as 0.5 wt. % solutions in CCl₄, CDCl₃, and 54.6 mol % CHCl₃/CCl₄. Table 3.1 lists the IR frequency data for the *vasym.* CH₃ and *vsym.* CH₃ stretching frequencies for C₅H₁₂ to C₁₈H₃₈ (1). Figure 3.1 shows plots of *vasym.* CH₃ vs the molecular weight (M.W.) of each *n*-alkane and Fig. 3.2 shows plots of *vsym.* CH₃ vs M.W. of each *n*-alkane. A study of the IR data and figures show that *vasym.* CH₃ generally decreases as the number of carbon atoms increases in the order C₅H₁₂ to C₁₈H₃₈ by 0.11 to 0.22 cm⁻¹ in going from solution in CCl₄ to solution in CDCl₃.

The $\nu_{\text{sym. CH}_3}$ mode for this series of *n*-alkanes shows that it generally decreases by approximately 0.8 cm^{-1} in CCl_4 solution and approximately 1.2 cm^{-1} in CDCl_3 solution progressing in the series C_5H_{12} to $\text{C}_{18}\text{H}_{38}$ in going from solution in CCl_4 to solution in CDCl_3 .

Table 3.2 lists the IR absorbance data for C_5H_{12} to $\text{C}_{18}\text{H}_{38}$ for the $\nu_{\text{asym. CH}_3}$ and $\nu_{\text{sym. CH}_3}$ modes, Fig. 3.3 shows a plot of $(\nu_{\text{asym. CH}_3})/(\nu_{\text{asym. CH}_2})$ vs $A(\nu_{\text{sym. CH}_3})/A(\nu_{\text{sym. CH}_2})$ in CCl_4 solution for C_5H_{12} to $\text{C}_{18}\text{H}_{38}$, and Fig. 3.4 shows a plot of $(\nu_{\text{sym. CH}_3})/(\nu_{\text{sym. CH}_2})$ vs $A(\nu_{\text{asym. CH}_3})/A(\nu_{\text{asym. CH}_2})$ in CCl_4 solution for C_5H_{12} to $\text{C}_{18}\text{H}_{38}$. Both plots show an essentially linear relationship. The slight deviation from linearity is most likely due to overlapping interferences in the measurement of these peak height absorbances.

Table 3.2a lists absorbance ratios; all of these absorbance ratios for the νCH_3 and νCH_2 modes generally decrease progressing in the series C_5H_{12} to $\text{C}_{18}\text{H}_{38}$.

Table 3.3 lists IR data for $\nu_{\text{asym. CH}_2}$ and $\nu_{\text{sym. CH}_2}$ for the *n*-alkane at 0.5 wt. % in CCl_4 , CDCl_3 , and 54.6 mol % $\text{CDCl}_3/\text{CCl}_4$ solutions. Figure 3.5 shows plots of $\nu_{\text{asym. CH}_2}$ vs $\nu_{\text{sym. CH}_2}$ in each of the solvent systems, and Fig. 3.6 shows plots of $\nu_{\text{asym. CH}_3}$ vs $\nu_{\text{sym. CH}_3}$ in all three solvent systems. These plots show that these relationships are not linear over the entire *n*-alkane series. The plots do point out in general that as $\nu_{\text{asym. CH}_2}$ decreases in frequency, $\nu_{\text{sym. CH}_2}$ also decreases in frequency progressing in the series C_5H_{12} to $\text{C}_{18}\text{H}_{38}$, and that the $\nu_{\text{asym. CH}_3}$ and $\nu_{\text{sym. CH}_3}$ frequencies show the same trend.

A study of Tables 3.1 and 3.3 show some interesting trends in CCl_4 , CDCl_3 , or 54.6 mol % solutions progressing in the series C_5H_{12} to $\text{C}_{18}\text{H}_{38}$. The $\nu_{\text{asym. CH}_3}$ frequency decrease in going from solution in CCl_4 to solution in CDCl_3 is small ($\sim 0.1\text{ cm}^{-1}$) while for $\nu_{\text{sym. CH}_3}$ the frequency decrease is more in CDCl_3 solution (1.2 cm^{-1}) than in CCl_4 solution (0.7 cm^{-1}). In addition, the frequency difference for $\nu_{\text{asym. CH}_3}$ in CCl_4 and in CDCl_3 increases from 0.11 to 0.22 cm^{-1} and for $\nu_{\text{sym. CH}_2}$ in CCl_4 and in CDCl_3 decreases from 0.45 to 0.85 progressing in the series C_5H_{12} to $\text{C}_{18}\text{H}_{38}$. The $\nu_{\text{asym. CH}_2}$ frequency decrease in going from solution in CCl_4 to solution is small (0.1 cm^{-1}) while for $\nu_{\text{sym. CH}_2}$ the frequency decrease is larger in going from solution in CCl_4 to a solution in CDCl_3 (0.6 cm^{-1}) progressing in the series C_5H_{12} to $\text{C}_{18}\text{H}_{38}$. Moreover, these data show that the $\nu_{\text{sym. CH}_2}$ mode changes in frequency by a factor of approximately 5 times more than $\nu_{\text{asym. CH}_2}$, $\nu_{\text{asym. CH}_3}$, and $\nu_{\text{sym. CH}_3}$. In addition, the $\nu_{\text{asym. CH}_2}$ frequency increases in frequency while the $\nu_{\text{sym. CH}_2}$ frequency decreases in frequency in going from solution in CCl_4 to CDCl_3 . In general these last two trends generally decrease progressing in the series C_5H_{12} to $\text{C}_{18}\text{H}_{38}$.

Table 3.4 lists the frequency difference between $\nu_{\text{asym. CH}_3}$ and $\nu_{\text{sym. CH}_3}$ and between $\nu_{\text{asym. CH}_2}$ and $\nu_{\text{sym. CH}_2}$ in the three solvent systems. These data show that the frequency separation is much larger for the two νCH_3 vibrations ($\sim 85^{-1}$) than for the two νCH_2 vibrations ($\sim 69\text{ cm}^{-1}$). Figure 3.7 shows plots of $\nu_{\text{asym. CH}_3} - \nu_{\text{sym. CH}_3}$ vs $\nu_{\text{asym. CH}_2} - \nu_{\text{sym. CH}_2}$, which clearly shows the behavior of the frequency separation of the νCH_3 and νCH_2 vibrations in the three solvent systems.

SUMMARY

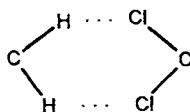
For *n*-alkanes, $\text{C}_{5-18}\text{H}_{12-38}$, the $\nu_{\text{asym. CH}_3}$ occurs in the region $2957.26\text{--}2959.55\text{ cm}^{-1}$ in CCl_4 and in the region $2957.48\text{--}2959.66\text{ cm}^{-1}$ in CDCl_3 , and $\nu_{\text{sym. CH}_3}$ occurs in the region $2872.35\text{--}2873.12\text{ cm}^{-1}$ in CCl_4 and in the region $2871.50\text{--}2872.67\text{ cm}^{-1}$ in CDCl_3 . Moreover,

vasym. CH_2 occurs in the region $2926.61\text{--}2927.73\text{ cm}^{-1}$ in CCl_4 and in the region $2926.92\text{--}2928.14\text{ cm}^{-1}$ in CDCl_3 , and vsym. CH_2 occurs in the region $2854.59\text{--}2861.82\text{ cm}^{-1}$ in CCl_4 and in the region $2854.55\text{--}2861.21\text{ cm}^{-1}$ in CDCl_3 . In addition, these four vibrations decrease in frequency progressing in the series C_5H_{12} through $\text{C}_{18}\text{H}_{38}$.

The *n*-alkanes are nonpolar molecules, and one would expect that there would be minimal solute-solvent interaction between *n*-alkane molecules and solvent molecules such as CCl_4 and CDCl_3 . The *n*-alkanes in going from solution CCl_4 to solution in CDCl_3 solution show a frequency increase of 0.11 to 0.22 cm^{-1} for vasym. CH_3 and for vsym. CH_3 it decreases by -0.45 to -0.85 cm^{-1} , with decreases for vsym. CH_3 progressing in the order C_5H_{12} to $\text{C}_{18}\text{H}_{38}$. In addition, the vasym. CH_2 frequency difference is 0.41 to 0.23 cm^{-1} and for vsym. CH_2 is -0.61 to -0.04 cm^{-1} . Again the vasym. CH_2 mode increases in frequency and the vsym. CH_2 mode decreases in frequency in going from solution in CCl_4 to solution in CDCl_3 . Thus, both vasym. CH_3 and vsym. CH_2 increase in frequency and both vsym. CH_3 and vsym. CH_2 decrease in frequency in going from solution in CCl_4 to solution in CDCl_3 at 0.5 wt. \% solutions. These data confirm that the effects of these solvents are minor in these four molecular stretching vibrations. It is noteworthy that the vsym. CH_2 vibration shifts progressively to lower frequency in the order C_5H_{12} to $\text{C}_{18}\text{H}_{38}$, and that it decreases in frequency by a factor of at least 7 times more than the vsym. CH_3 vibration.

Apparently, the *n*-alkane protons form weak intermolecular hydrogen bonds with the free pair of electrons on the Cl atoms of the CCl_4 and/or CDCl_3 solvent system, and an explanation is needed to determine the frequency behavior of these four molecular vibrations in going from solution in CCl_4 to solution in CDCl_3 . As these vasym. CH_3 , vasym. CH_2 , vsym. CH_3 , and vsym. CH_2 modes vibrate, the protons obtain a weak positive charge and the carbon atom obtains a weak negative charge. This is the so-called dipole moment change during these molecular vibrations. Therefore, the *n*-alkane protons would form weak intermolecular hydrogen bonds with the free pair of electrons on the Cl atoms of the CCl_4 and/or CDCl_3 solvent system. The Cl atoms of CCl_4 would be expected to be more basic than those for CDCl_3 due to the fact that the D atom attracts electrons from the Cl atoms. In addition, there is intermolecular bonding between D and Cl such as $\text{CCl}_3\text{D}:\text{ClCCl}_2\text{D}:\text{ClCCl}_3$. Therefore, one would expect a stronger C–H : Cl bond to be formed between the protons in *n*-alkanes and the Cl atoms in CCl_4 than for Cl atoms in CDCl_3 . Hydrogen bonding also weakens the O–H or C–H bond, and the vibration $\nu\text{OH}:\text{X}$ or $\nu\text{C–H}:\text{X}$ is expected to decrease in frequency—this is what we noted in the vsym. CH_3 and vsym. CH_2 modes. However, the opposite was observed for vasym. CH_3 and vasym. CH_2 , where both modes increased in frequency in going from solution in CCl_4 to solution in CDCl_3 . This frequency increase for the vasym. modes needs an explanation. Because the vasym. CH_3 and vasym. CH_2 modes increase in frequency, it requires more energy for these two modes to vibrate in going from solution in CCl_4 to solution in CDCl_3 . The two CH_3 groups are isolated by $(\text{CH}_2)_n$ groups, and as the Cl atoms in CDCl_3 are weaker bases than the Cl atoms in CCl_4 a weaker C–H...ClCDCl₂ bond is expected. Consequently, the vasym. CH_3 and vasym. CH_2 increases in frequency when CCl_4 is replaced by CDCl_3 .

On the other hand there are $(\text{CH}_2)_n$ units present in the n -alkane series which are capable of forming n units of



in either CCl_4 or CDCl_3 solution. It is noted that $\nu_{\text{sym. CH}_3}$ increasingly decreases in frequency progressing in the series C_5H_{12} to $\text{C}_{18}\text{H}_{38}$ in going from solution in CCl_4 to solution in CDCl_3 . This indicates that the $\text{C-H}:\text{ClCDCl}_3$ bond strength is increased as n is increased for $\text{CH}_3(\text{CH}_2)_n\text{CH}_3$. The inductive effect of additional CH_2 groups apparently weakens the CH_3 bonds, causing $\nu_{\text{sym. CH}_2}$ to decrease in frequency as the number of CH_2 groups are increased in the n -alkane. As the number of CH_2 groups are increased, the decrease in $\nu_{\text{sym. CH}_2}$ for n -alkanes decreases progressing in the series C_5H_{12} to $\text{C}_{10}\text{H}_{22}$ and is relatively constant from C_9H_{20} to $\text{C}_{18}\text{H}_{38}$. This suggests that the effect of the number of CH_2 groups forming intermolecule hydrogen bonds with a CDCl_3 chain is minimized after eight CH_2 groups are present in that the effect of the number of $(\text{CH}_2)\text{ClCDCl}_3$ intermolecular hydrogen bonds formed between the n -alkane and CDCl_3 is minimized in the series $\text{C}_{11}\text{H}_{24}$ to $\text{C}_{18}\text{H}_{38}$. It is also possible that the Cl atoms in CDCl_3 are closer in space to the C-H bonds compared to that for CCl_4 , and this fact would also contribute to lower $\nu_{\text{sym. CH}_2}$ frequencies.

In the series C_5H_{12} to $\text{C}_{18}\text{H}_{38}$ there is a comparatively large change in the $\nu_{\text{sym. (CH}_2)_n}$ mode. There is a decrease of 7.23 cm^{-1} in CCl_4 and 6.66 cm^{-1} in CDCl_3 . This is attributed to the increasing number of CH_2 groups stretching in-phase progressing in the n -alkane series.

The smooth correlation of the absorbance values of the CH_2 and CH_3 groups as the ratio of the CH_3 groups to CH_2 groups decreases is just what is predicted. There is apparently no significant difference in the dipole moments of either CH_2 or CH_3 stretches progressing in the n -alkane series.

OTHER n -ALKANE VIBRATIONS

The CH_2 bend asym. CH_3 bend, and the sym. CH_3 bend occurs near 1467 , 1458 , and 1378.5 cm^{-1} in CCl_4 solution (Table 3.5).

1,2-EPOXYALKANES

Table 3.6 lists IR vapor-phase data for the alkyl (R) vibrations of 1,2-epoxyalkanes (2). The $\nu_{\text{asym. CH}_3}$ mode occurs in the region 2953 – 2972 cm^{-1} , the $\nu_{\text{asym. CH}_2}$ mode in the region 2920 – 2935 cm^{-1} , the $\nu_{\text{sym. CH}_2}$ mode in the region 2870 – 2932 cm^{-1} , and the $\nu_{\text{sym. CH}_3}$ bending mode in the region 1363 – 1388 cm^{-1} .

SODIUM DIMETHYLPHOSPHONATE $(\text{CH}_3)_2\text{P}(\text{O})_2\text{Na}$

The IR and Raman dating for sodium dimethylphosphonate are listed in Table 3.7 (3). The $\nu_{\text{asym. CH}_3}$ and $\nu_{\text{sym. CH}_3}$ modes are assigned at 2985 and 2919 cm^{-1} , respectively. The asym.

$(\text{CH}_3)_2$ bending modes are assigned at 1428 and 1413 cm^{-1} and the sym. $(\text{CH}_3)_2$ bending modes are assigned at 1293 and 1284 cm^{-1} .

METHYLTHIOMETHYL MERCURY, DIMETHYLMERCURY (4), AND METHYLTHIOCHLOROFORMATE (5)

Table 3.8 lists assignments for the $\text{CH}_3\text{-Hg}$ and $\text{CH}_3\text{-S}$ groups for the preceding 3 compounds. These assignments should aid the reader in assigning vibrations for these CH_3 groups in other compounds.

CYCLOALKANES

Table 3.9 lists IR vapor-phase data for cycloalkanes (6). Raman data for the ring breathing and ring deformation modes are also presented for cyclobutane and cyclopentane. The *vasym.* CH_2 mode occurs in the region 2930–3100 cm^{-1} . The *vsym.* CH_2 mode occurs in the region 2880–3020 cm^{-1} . Both νCH_2 vibrations decrease in frequency as the ring becomes larger. This is the result of lesser ring strain with increasing ring size. The CH_2 bend, CH_2 wag, CH_2 twist, CH_2 rock, ring breathing, and ring deformation vibration assignment are also presented.

MISCELLANEOUS ALKYL AND CYCLOALKYL COMPOUND

Vibrational assignments for cycloalkyl groups are presented in Table 3.10, for alkyl groups of monomers and polymers in Table 3.11, for cyclopropane derivatives in Table 3.12, and for octadecane, octadecane- D_{38} , tetracosane, and tetracosane- D_{50} in Table 3.13.

REFERENCES

1. Nyquist, R. A. and Fiedler, S. L. (1993). *Appl. Spectrosc.*, **47**, 1670.
2. Nyquist, R. A. (1986). *Appl. Spectrosc.*, **40**, 275.
3. Nyquist, R. A. (1968). *J. Mol. Struct.*, **2**, 111.
4. Nyquist, R. A. and Mann, J. R. (1972). *Spectrochim. Acta*, **28A**, 511.
5. Nyquist, R. A. (1967–68). *J. Mol. Struct.*, **1**, 1.
6. Nyquist, R. A. (1984). *The Interpretation of Vapor-Phase Infrared Spectra: Group Frequency Data*, Philadelphia: Sadtler Research Laboratories, A Division of Bio-Rad.

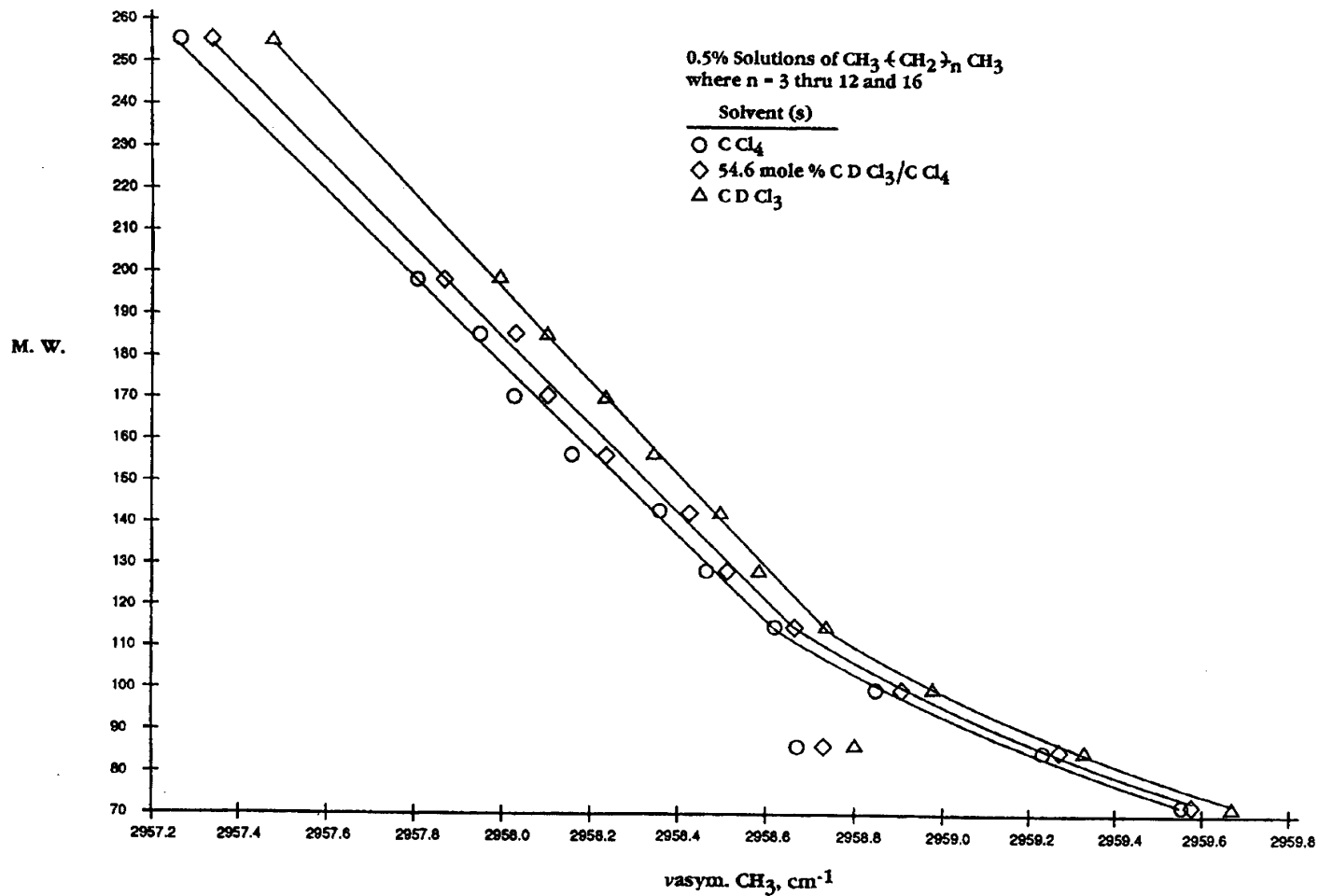
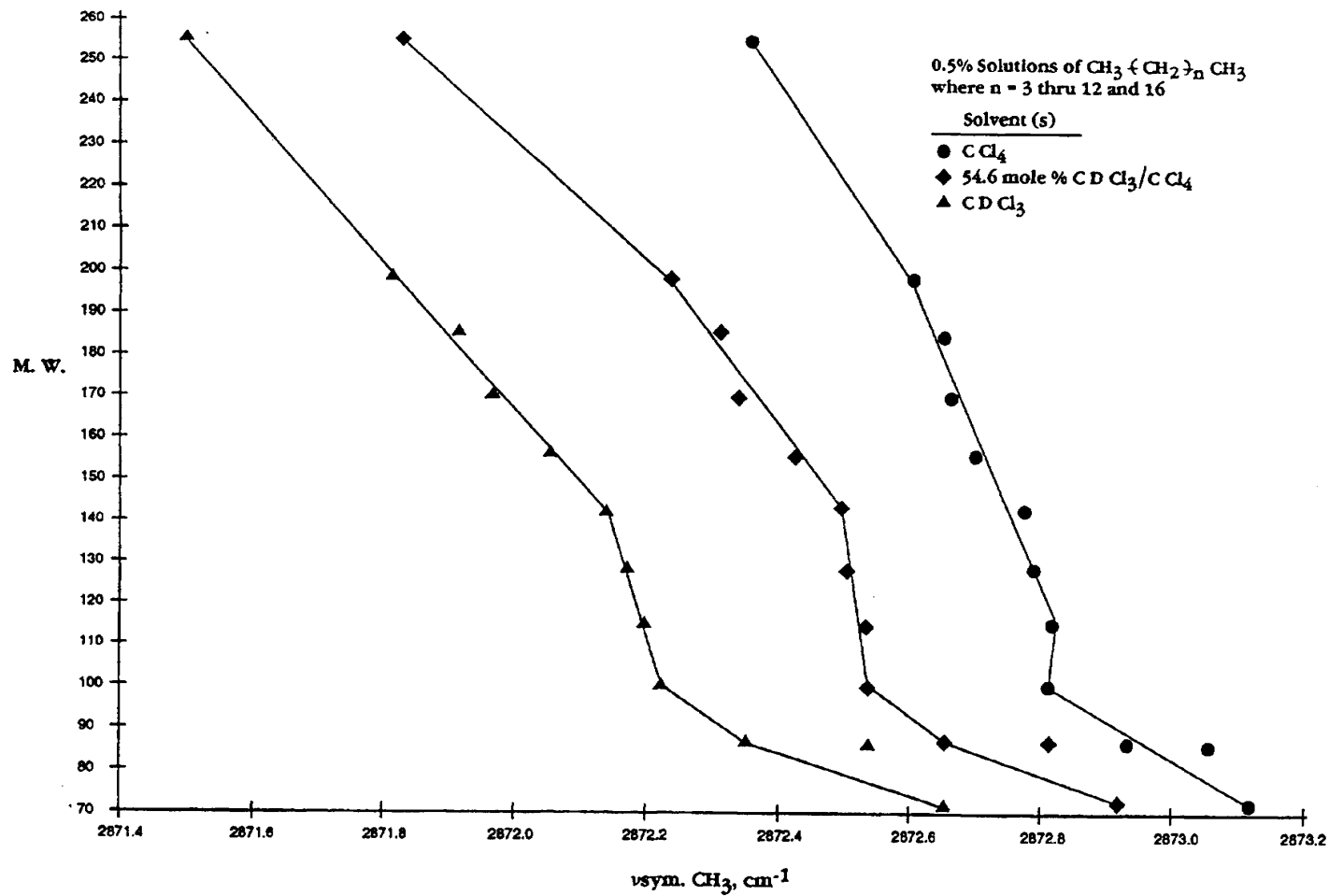


FIGURE 3.1 Plots of $\nu_{\text{asym. CH}_3}$ vs the molecular weight of each n -alkane.

FIGURE 3.2 Plots of $\nu_{\text{sym. CH}_3}$ vs the molecular weight of each n -alkane.

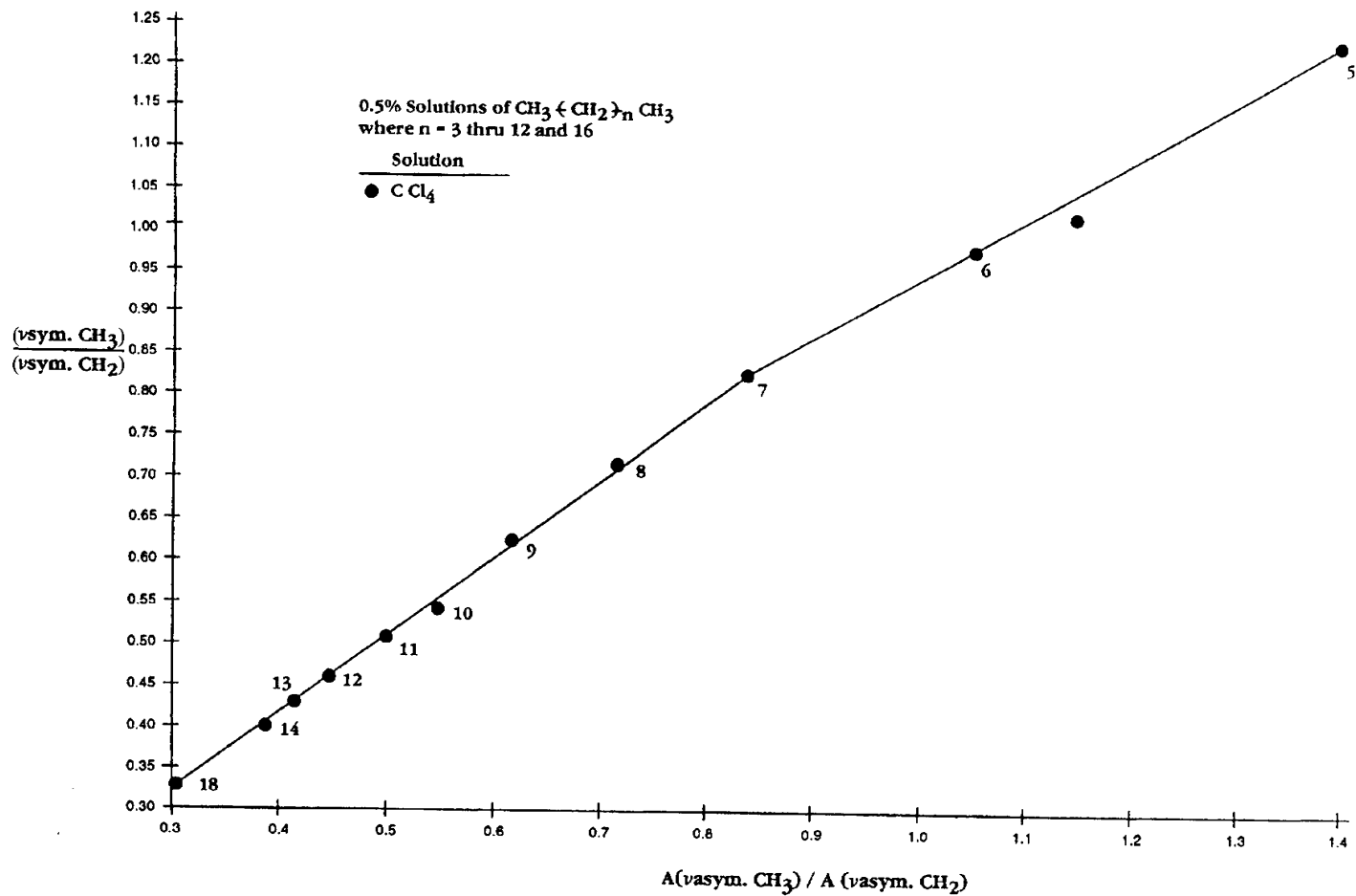


FIGURE 3.3 A plot of the absorbance ratio $A(\nu_{\text{sym. CH}_3})/A(\nu_{\text{sym. CH}_2})$ vs the absorbance ratio $A(\nu_{\text{sym. CH}_3})/A(\nu_{\text{sym. CH}_2})$ in CCl_4 solution for C_5H_{12} to $\text{C}_{18}\text{H}_{38}$.

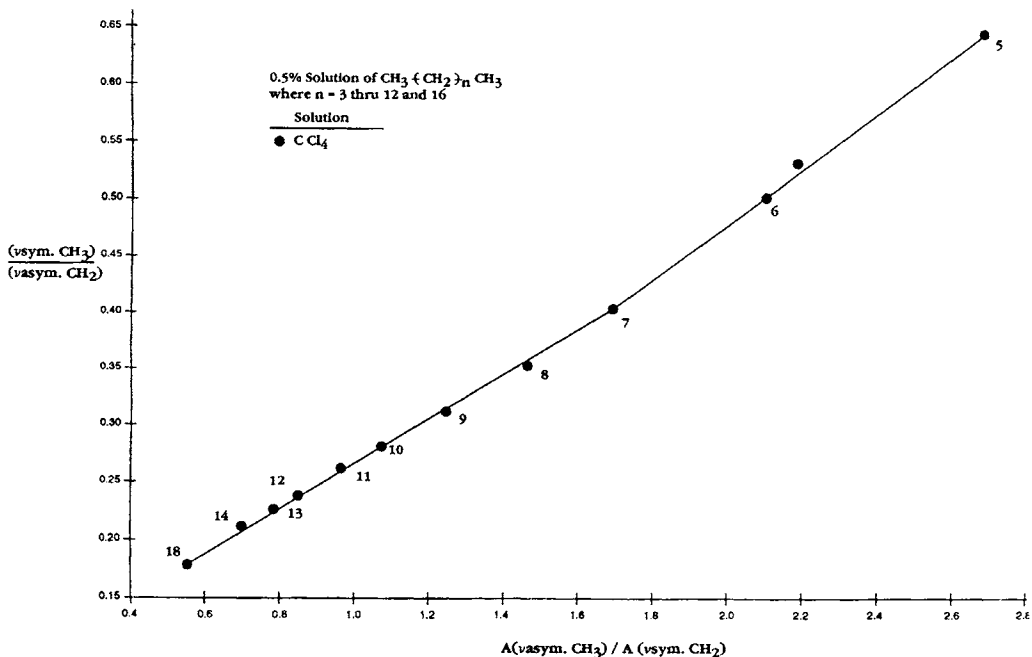


FIGURE 3.4 A plot of the absorbance ratio $A(\text{vsym. CH}_3)/A(\text{vsym. CH}_2)$ vs the absorbance ratio $A(\text{vsym. CH}_3)/A(\text{vsym. CH}_2)$ in CCl_4 solution for C_5H_{12} to $\text{C}_{18}\text{H}_{38}$.

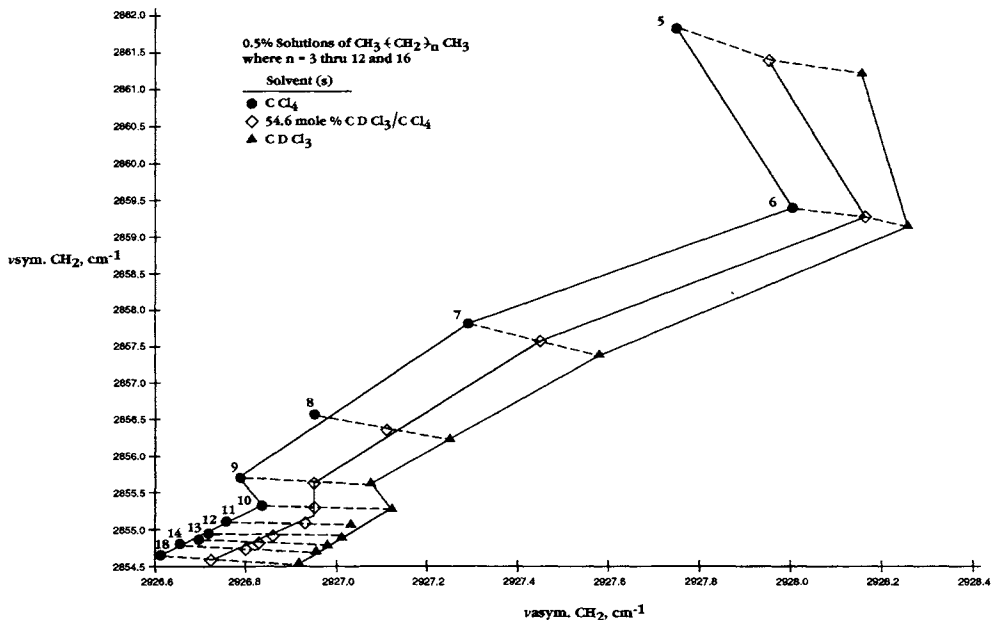


FIGURE 3.5 Plots of vsym. CH_2 vs vsym. CH_2 in CCl_4 , 54.6 mol % $\text{CDCl}_3/\text{CCL}_4$, and CDCl_3 solutions.

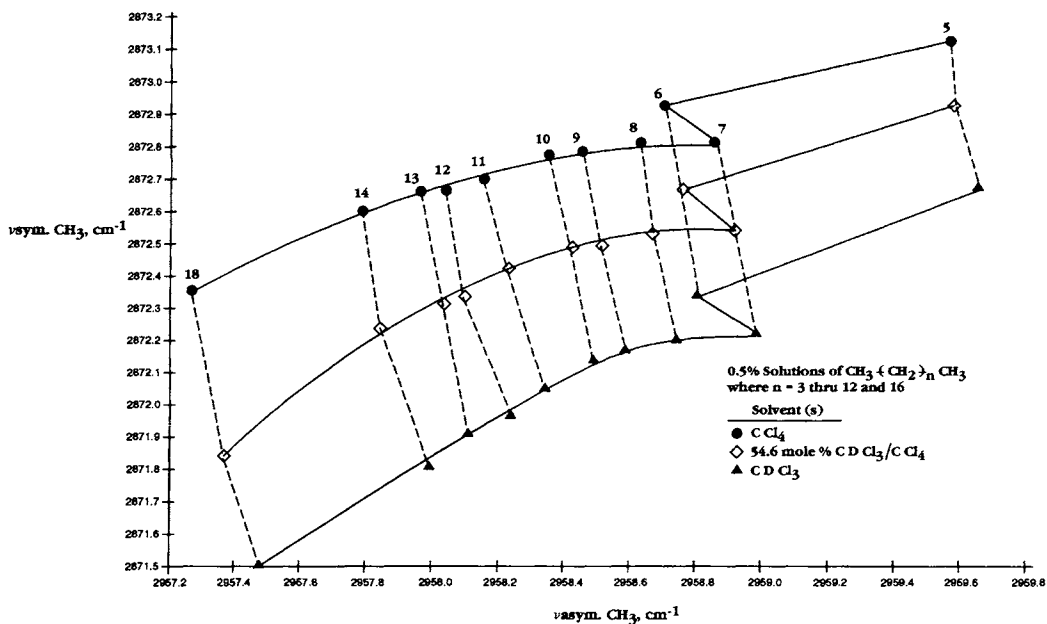


FIGURE 3.6 Plots of $\nu_{\text{asym. CH}_3}$ vs $\nu_{\text{sym. CH}_3}$ in CCl_4 , 54.6 mol % $\text{CDCl}_3/\text{CCl}_4$, and CDCl_3 solutions.

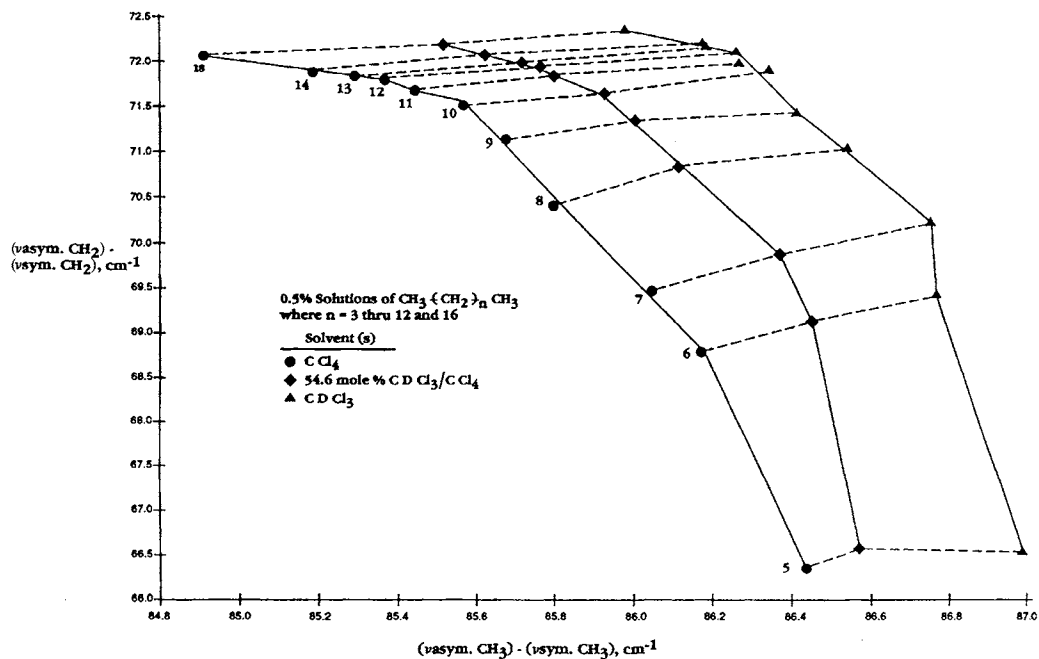


FIGURE 3.7 Plots of the frequency separation ($\nu_{\text{asym. CH}_3} - \nu_{\text{sym. CH}_3}$) vs the frequency separation ($\nu_{\text{asym. CH}_2} - \nu_{\text{sym. CH}_2}$) for each n -alkane in CCl_4 , 54.6 mol % $\text{CDCl}_3/\text{CCl}_4$, and CDCl_3 solutions.

TABLE 3.1 IR data for a. and s.CH₃ stretching for *n*-alkanes in 0.5 mol % solutions in CCl₄, 54.6 mol % CHCl₃/CCl₄

Compound	a.CH ₃ str. CCl ₄ cm ⁻¹	a.CH ₃ str. 54.6 mol % CDCl ₃ /CCl ₄ cm ⁻¹	a.CH ₃ str. CDCl ₃ cm ⁻¹	s.CH ₃ str. CCl ₄ cm ⁻¹	s.CH ₃ str. 54.6 mol % CDCl ₃ /CCl ₄ cm ⁻¹	s.CH ₃ str. CDCl ₃ cm ⁻¹
Pentane	2959.6	2959.6	2959.7	2873.1	2872.9	2872.7
Hexane	2958.7	2958.7	2958.8	2872.9	2872.7	2872.3
Hexane	2959.2	2959.3	2959.3	2873.1	2872.8	2872.5
Heptane	2958.9	2958.9	2959	2872.8	2872.5	2872.2
Octane	2958.6	2958.7	2958.7	2872.8	2872.5	2872.2
Nonane	2958.5	2958.5	2958.6	2872.8	2872.5	2872.2
Decane	2958.4	2958.4	2958.5	2872.8	2872.5	2872.1
Undecane	2958.1	2958.2	2958.3	2872.7	2872.4	2872.1
Dodecane	2958	2958.1	2958.2	2872.7	2872.3	2872
Tridecane	2957.9	2958	2958.1	2872.7	2872.3	2871.9
Tetradecane	2957.8	2957.9	2858	2872.6	2872.2	2871.8
Octadecane	2957.3	2957.3	2957.5	2872.4	2871.8	2871.5
delta cm ⁻¹	-2.3	-2.3	-2.2	-0.7	-1.1	-1.2

	a.CH ₃ str. [CCl ₄]- [54.6 mol % CDCl ₃ /CCl ₄] cm ⁻¹	a.CH ₃ str. [CCl ₄]- [CDCl ₃] cm ⁻¹	s.CH ₃ str. [CCl ₄]- [54.6 mol % CDCl ₃ /CCl ₄] cm ⁻¹	s.CH ₃ str. [CCl ₄]- [CDCl ₃] cm ⁻¹
Pentane	0.02	0.11	-0.2	-0.45
Hexane	0.03	0.08	-0.24	-0.51
Heptane	0.05	0.12	-0.27	-0.58
Octane	0.04	0.11	-0.29	-0.62
Nonane	0.04	0.12	-0.29	-0.62
Decane	0.06	0.14	-0.29	-0.64
Undecane	0.08	0.19	-0.28	-0.65
Dodecane	0.16	0.2	-0.33	-0.7
Tridecane	0.08	0.16	-0.34	-0.74
Tetradecane	0.06	0.2	-0.36	-0.79
Octane	0.08	0.22	-0.52	-0.85

TABLE 3.2 IR absorbance data for *n*-alkanes: a. and s.CH₂ and CH₃ stretching and CH₂ bending

Compound	A[a.CH ₃ str.]	A[a.CH ₂ str.]	A[s.CH ₃ str.]	A[s.CH ₂ str.]
Pentane	1.09	0.78	0.502	0.407
Hexane	0.879	0.759	0.408	0.402
Hexane	0.903	0.86	0.419	0.43
Heptane	0.769	0.925	0.372	0.45
Octane	0.67	0.938	0.329	0.458
Nonane	0.637	1.027	0.319	0.512
Decane	0.563	1.028	0.287	0.527
Undecane	0.538	1.083	0.283	0.558
Dodecane	0.478	1.073	0.256	0.56
Tridecane	0.496	1.197	0.271	0.632
Tetradecane	0.473	1.23	0.263	0.66
Octadecane	0.374	1.234	0.221	0.672

	A[CH ₂ bend] CCl ₄	A[CH ₂ bend] 54.6 mol % CDCl ₃ /CCl ₄	A[CH ₂ bend] CDCl ₃
Pentane	0.137	0.141	0.105
Hexane	0.127	0.115	0.082
Hexane	0.152	0.123	0.09
Heptane	0.147	0.111	0.084
Octane	0.128	0.096	0.073
Nonane	0.143	0.103	0.063
Decane	0.136	0.092	0.06
Undecane	0.134	0.093	0.057
Dodecane	0.132	0.084	0.05
Tridecane	0.141	0.081	0.051
Tetradecane	0.141	0.081	0.047
Octadecane	0.132	0.08	0.037

TABLE 3.2A Absorbance ratios for CH₃ and CH₂ groups for *n*-alkanes

Compound	A[a.CH ₃ str.] /A[s.CH ₃ str.]	A[a.CH ₂ str.] /A[s.CH ₂ str.]	A[a.CH ₃ str.] /A[a.CH ₂ str.]	A[s.CH ₃ str.] /A[s.CH ₂ str.]
Pentane	2.171	1.916	1.397	1.233
Hexane	2.154	1.912	1.143	1.015
Hexane	2.155	2	1.05	0.974
Heptane	2.067	2.064	0.831	0.827
Octane	2.036	2.048	0.714	0.718
Nonane	1.997	2.006	0.62	0.623
Decane	1.962	1.951	0.548	0.545
Undecane	1.901	1.941	0.497	0.507
Dodecane	1.867	1.916	0.445	0.457
Tridecane	1.83	1.894	0.414	0.428
Tetradecane	1.798	1.864	0.385	0.398
Octadecane	1.692	1.836	0.303	0.329

	A[a.CH ₃ str.] /A[s.CH ₂ str.]	A[s.CH ₃ str.] /A[a.CH ₂ str.]	A[s.CH ₃ str.] /A[CH ₂ bend]
Pentane	2.678	0.644	4.781
Hexane	2.187	0.531	4.976
Hexane	2.1	0.5	4.656
Heptane	1.689	0.402	4.429
Octane	1.463	0.351	4.507
Nonane	1.244	0.311	5.063
Decane	1.068	0.279	4.783
Undecane	0.964	0.261	4.965
Dodecane	0.854	0.238	5.12
Tridecane	0.785	0.226	5.313
Tetradecane	0.717	0.214	5.596
Octadecane	0.557	0.179	5.972

TABLE 3.3 IR data for a. and s.CH₂ stretching for *n*-alkanes in 0.5% solutions in CCl₄, 54.6 mol % CDCl₃/CCl₄, and CDCl₃

Compound	a.CH ₂ str.	a.CH ₂ str.	a.CH ₂ str.	s.CH ₂ str.	s.CH ₂ str.	s.CH ₂ str.
	CCl ₄ cm ⁻¹	54.6 mol % CDCl ₃ /CCl ₄ cm ⁻¹	CDCl ₃ cm ⁻¹	CCl ₄ cm ⁻¹	54.6 mol % CDCl ₃ /CCl ₄ cm ⁻¹	CDCl ₃ cm ⁻¹
Pentane	2927.7	2928	2928.1	2861.8	2861.4	2861.2
Hexane	2928	2928.2	2928.3	2959.4	2859.3	2859.1
Hexane	2927.9	2928	2928.1	2859.1	2859	2858.7
Heptane	2927.3	2927.5	2927.6	2857.8	2857.6	2857.4
Octane	2927	2927.1	2927.3	2856.6	2856.3	2856.2
Nonane	2926.8	2927	2927.1	2855.7	2855.6	2855.6
Decane	2926.8	2927	2927.1	2855.3	2855.3	2855.3
Undecane	2926.8	2926.9	2927	2855.1	2855.1	2855.1
Dodecane	2926.7	2926.9	2927	2854.9	2854.9	2854.9
Tridecane	2926.7	2926.8	2927	2854.8	2854.8	2854.8
Tetradecane	2926.7	2926.8	2927	2854.8	2854.7	2854.7
Octadecane	2926.6	2926.7	2926.9	2854.6	2854.6	2854.6
delta cm ⁻¹	-1.1	-1.3	-1.2	-7.2	-6.8	-6.6

	a.CH ₂ str.	a.CH ₂ str.	s.CH ₂ str.	s.CH ₂ str.
	[CCl ₄]- [mol % CDCl ₃ /CCl ₄] cm ⁻¹	[CCl ₄]- [CDCl ₃] cm ⁻¹	{CCl ₄ }- [mol % CDCl ₃ /CCl ₄] cm ⁻¹	{CCl ₄ }- [CDCl ₃] cm ⁻¹
Pentane	0.22	0.41	-0.41	-0.61
Hexane	0.16	0.25	-0.08	-0.26
Hexane	0.15	0.23	-0.17	-0.38
Heptane	0.16	0.29	-0.25	-0.44
Octane	0.16	0.31	-0.21	-0.33
Nonane	0.16	0.28	-0.09	-0.1
Decane	0.12	0.3	-0.04	-0.06
Undecane	0.17	0.27	-0.02	-0.04
Dodecane	0.14	0.29	-0.02	-0.04
Tridecane	0.13	0.28	-0.01	-0.04
Tetradecane	0.14	0.3	-0.03	-0.06
Octadecane	0.12	0.31	-0.01	-0.06

TABLE 3.4 The frequency separation between the a. and s.CH₃ and the a. and s.CH₂ stretching vibrations for n-alkanes in CCl₄, CDCl₃/CCl₄, and CDCl₃ solutions

Compound	[a.CH ₃ str.] - [s.CH ₃ str.]	[a.CH ₃ str.] - [s.CH ₃ str.]	[a.CH ₃ str.] - [s.CH ₃ str.]	[a.CH ₂ str.] - [s.CH ₂ str.]	[a.CH ₂ str.] - [s.CH ₂ str.]	[a.CH ₂ str.] - [s.CH ₂ str.]
	CCl ₄ cm ⁻¹	54.6 mol % CDCl ₃ /CCl ₄ cm ⁻¹	CDCl ₃ cm ⁻¹	CCl ₄ cm ⁻¹	CDCl ₃ /CCl ₄ cm ⁻¹	CDCl ₃ cm ⁻¹
Pentane	86.43	86.55	86.99	66.32	66.54	66.52
Hexane	86.18	86.45	86.77	66.6	68.84	69.11
Heptane	86.05	86.37	86.75	69.48	69.89	70.21
Octane	85.8	86.13	86.53	70.4	70.77	71.04
Nonane	85.67	86	86.41	71.11	71.36	71.42
Decane	85.57	85.92	86.35	71.52	71.68	71.88
Undecane	85.44	85.8	86.28	71.67	71.86	71.98
Dodecane	85.37	85.76	86.27	71.8	71.96	72.13
Tridecane	85.29	85.71	86.19	71.87	72.01	72.19
Tetradecane	85.19	85.61	86.18	71.89	72.06	72.25
Octadecane	84.91	85.51	85.98	72.02	72.15	72.34
delta cm ⁻¹	-1.52	-1.04	-1.01	5.7	5.61	5.82

TABLE 3.5 The CH₃ and CH₂ bending frequencies and frequency separations for n-alkanes

Compound	CH ₂ bend cm ⁻¹	a.CH ₃ bend cm ⁻¹	s.CH ₃ bend cm ⁻¹	[CH ₂ bend] - [s.CH ₃ bend]	[a.CH ₃ bend] - [s.CH ₃ bend]
	cm ⁻¹	cm ⁻¹	cm ⁻¹	cm ⁻¹	cm ⁻¹
Pentane	1467.55	1458	1379.23	88.32	78.77
Hexane	1467.22	1458.37	1378.48	88.74	79.89
Hexane	1467.35	1458.29	1378.59	88.76	79.7
Heptane	1467.39	1458.08	1378.66	88.73	79.42
Octane	1467.36	1458.85	1378.62	88.74	80.23
Nonane	1467.33	1458.27	1378.57	88.76	79.7
Decane	1467.39	1458.56	1378.39	89	80.17
Undecane	1467.63	1458.27	1378.6	88.76	79.67
Dodecane	1467.39	1458.27	1378.62	88.77	79.65
Tridecane	1467.36	1458.27	1378.64	88.72	79.63
Tetradecane	1467.35	1458.56	1378.61	88.74	79.95
Octadecane	1467.33	1457.97	1378.64	88.69	79.33

TABLE 3.6 IR vapor-phase data for the alkyl group of 1,2-epoxyalkanes

1,2-epoxyalkane R	a.CH ₃ str. cm ⁻¹	A	s.CH ₂ str. cm ⁻¹	A	a.CH ₂ str. cm ⁻¹	A	a.CH ₃ bending cm ⁻¹	A	s.CH ₃ bending cm ⁻¹	A
CH ₃	2969	0.835	2930	0.594			1457 1445	0.368 0.353	1370	0.25
C ₂ H ₅	2972	1.568	2932	0.804	2920	0.769	1465	0.595	1379	0.158
C ₃ H ₇	2965	~ 1.8	2920	0.6	2934	1.37	1467	0.473	1381	0.226
iso-C ₄ H ₉	2970	~ 1.8	2920	0.729	2935	1.158	1469	0.672	1388* ¹ 1371* ²	0.428 0.415
iso-C ₃ H ₇	2970	~ 1.7	2881	0.533			1470	0.574	1382* ¹ 1366* ²	0.205 0.32
t-C ₄ H ₉	2965	~ 1.8	2870	0.561			1467	0.435	1381* ¹ 1366* ²	0.168 0.783
C ₈ H ₁₇	2960	0.649	2870	0.49	2930	0.88	1467	0.28	1378	0.087
C ₉ H ₁₉	2959	0.52	2870	0.37	2929	0.87	1465	0.238	1378	0.07
C ₁₂ H ₂₅	2958	0.546	2878	0.435	2930	0.847	1468	0.302	1377	0.07
C ₁₄ H ₂₉	2958	0.482	2870	0.386	2920	0.842	1465	0.295	1374	0.07
C ₁₆ H ₃₃	2953	0.47			2920	0.82	1462	0.27	1372	0.052
Range	2953–2972		2870–2932		2920–2935		1445–1470		1363–1388	

*¹ [in-phase].*² [out-of-phase].

TABLE 3.7 IR and Raman data for $(\text{CH}_3)_2\text{PO}_2\text{Na}$ in water and in the solid phase

$(\text{CH}_3)_2\text{P}(\text{O})_2\text{Na}$ Assignments	IR	IR	Raman	5 a1	4 a2	4 b1	5 b2
	solid phase cm^{-1}	H_2O soln. cm^{-1}	H_2O soln. cm^{-1}				
a. $[(\text{CH}_3)_2 \text{ str.}]$	2985		2988	1	1	1	1
s. $[(\text{CH}_3)_2 \text{ str.}]$	2919		2921	1			1
a. $[(\text{CH}_3)_2 \text{ bend}]$	1428	1429	1422	1	1	1	1
	1413	~ 1412	1413				
s. $[(\text{CH}_3)_2 \text{ bend}]$	1293	1309		1			1
	1284	1301					
	912		915	1			
	860sh						
$(\text{CH}_3)_2 \text{ rock}$	851	878			1	1	1
	839sh						
$(\text{CH}_3)_2 \text{ torsion}$?	?			1	1	

TABLE 3.8 IR data and assignments for $\text{CH}_3\text{HgSCH}_3$, $\text{CH}_3\text{SC}(\text{C}=\text{O})\text{Cl}$, and $(\text{CH}_3)_2\text{Hg}$

$\text{CH}_3\text{-Hg-S-CH}_3$ cm^{-1}	$\text{CH}_3\text{-S-C(=O)Cl}$ cm^{-1}	$\text{CH}_3\text{-S-P(=O)Cl}_2$ cm^{-1}	$(\text{CH}_3)_2\text{Hg}$ cm^{-1}	Assignment
[$\text{CH}_3\text{-Hg group}$]			[$\text{CH}_3\text{-Hg group}$]	
2984			2970	a. $\text{CH}_3 \text{ str.}$
2919			2910	a. $\text{CH}_3 \text{ str.}$
1408			1397 or 1443	a. $\text{CH}_3 \text{ bend}$
1177			1182	s. $\text{CH}_3 \text{ bend}$
763			700, 788	$\text{CH}_3 \text{ rock}$
?			?	$\text{CH}_3 \text{ torsion}$
[$\text{CH}_3\text{-S group}$]	[$\text{CH}_3\text{-S group}$]	[$\text{CH}_3\text{-S group}$]		
2984	3025	3011		a. $\text{CH}_3 \text{ str.}$
2919	2940	2938		s. $\text{CH}_3 \text{ str.}$
1432	1430	1431		a. $\text{CH}_3 \text{ bend}$
1309	1320	1321		s. $\text{CH}_3 \text{ bend}$
956	976	972		$\text{CH}_3 \text{ rock}$
?	?	?		$\text{CH}_3 \text{ torsion}$
533				Hg-C str.
333				Hg-S str.
190				Hg-S-C bend
120				$\text{Hg-S-CH}_3 \text{ torsion ?}$

? not observed.

TABLE 3.9 IR vapor-phase data for cycloalkanes

Compound	a.CH ₂ str.	s.CH ₂ str.	CH ₂ bend	CH ₂ wag	CH ₂ twist	CH ₂ rock	Ring breathing	Ring def.	(A)s.CH ₂ str. /(A)a.CH ₂ str.
Cyclopropane	3130 (0.200) 3100 (1.250)	3035 (0.480) 3020 (0.570) 2998 (0.325)	1439 (0.022) 1430 (0.018) 1414 (0.020)	1050 (0.175) 1024 (0.325) 1000 (0.160)			[1188]	899 (0.206) 862 (0.512) 832 (0.162)	0.46
Cyclobutane	[2974, vs] [2965, vs]	[2945, s]	[1443, m]	[1260, s]	[1224, m]		[1005, vs, R]	[926, s, R] [901, w, R]	
Cyclopentane	2988 (0.850) 2960 (1.250) 2945 (0.500)	2885 (0.400)	1479 (0.050) 1460 (0.061) 1445 (0.050)				[889, stg, R]	914 (0.020) 895 (0.040) 870 (0.020)	0.32
Cyclohexane	2945 (0.950) 2935 (1.250)	2875 (0.352) 2860 (0.619) 2850 (0.340)	1475 (0.074) 1459 (0.180) 1444 (0.076)	1271 (0.015) 1261 (0.019) 1245 (0.012)	1041 (0.020)		879 (0.010) 861 (0.020) 842 (0.012)	910 (0.020) 900 (0.020)	0.49
Cycloheptane	2935 (1.250)	2860 (0.230)	1464 (0.060)	1354 (0.005)	950 (0.005)	730 (0.001)	812 (0.011)		0.18
Cyclooctane	2930 (1.250)	2862 (0.619)	1460 (0.143)	1355 (0.044)	1042 (0.020)	767 (0.020)	852 (0.020)	952 (0.010)	0.49
Cyclodecane	2930 (1.250)	2880 (0.370) 2865 (0.340)	1486 (0.110) 1454 (0.120)	1354 (0.040)	1286 (0.040)	720 (0.040)			0.29 0.29
Cyclododecane	2940 (1.250)	2870 (0.520)	1471 (0.120) 1453 (0.115)	1350 (0.041)	1310 (0.020)	718 (0.060)	1030 (0.020)	1080 (0.011)	0.42
Cyclododecane-D ₂₄	a.CD ₂ str. 2202 (1.250)	s.CD ₂ str. 2102 (0.610)	CD ₂ bend 1160 (0.040)	CD ₂ wag 1160 (0.040)	CD ₂ twist 1118 (0.050)	CD ₂ rock 550 (0.042)	983 (0.085)	1095 (0.180)	(A)s.CD ₂ str. /(A)a.CD ₂ str. 0.49
Cyclododecane /cyclododecane-D ₂₄	1.335	1.365	1.268 1.253	1.164	1.172	1.305	1.048	0.986	

TABLE 3.10 Raman and IR data for compounds containing cycloalkyl groups

Compound	Raman neat a.CH ₂ str.	Raman neat s.CH ₂ str.	Raman neat s.CH ₂ str. in FR.	Raman neat CH ₂ bend	IR v.p. a.CH ₂ str.	IR v.p. s.CH ₂ str.
Cyclopropane (vap.)		3039 (83, p)	3020 (37, p)	1452 (2, p)	3100	3020
Cyclopropane carboxylic acid		3020 (37, p)		1458 (5, p)	3102	3032
Chlorocyclobutane	2985 (26, p)	2955 (44, p)		1433 (4, p)		
Cyclobutane carboxylic acid					2995	2890
Cyclopentane	2943 (43, p)	2868 (45, p)		1446 (6, p)	2960	2880
Chlorocyclopentane	2971 (46, p)	2919 (33, p)	2876 (21, p)	1446 (6, p)	2980	2890
Bromocyclopentane	2967 (43, p)	2915 (29, p)		1448 (5, p)	2970	2890
Cyclopentanecarbonitrile ¹	2970 (40, p)	2875 (29, p)		1446 (6, p)		
Cyclopentane carboxylic acid	2967 (41, p)	2875 (29, p)		1449 (8, p)	2970	2890
Cyclopentyl alcohol	2962 (84, p)	2875 (45, p)		1448 (9, p)		
Cyclohexane	2924 (40)	2852 (52)		1446 (10)	2935	2860
Chlorocyclohexane					2948	2870
Bromocyclohexane					2942	2865
Cyclohexyl alcohol	2940 (42, p)	2855 (45, p)		1440 (7, p)	2940	2864
Cyclohexyl amine	2937 (71, p)	2855 (76, p)		1440 (10, p)	2938	2862
	2920 (59, p)					
1,2,4-Trivinylcyclohexane	2932 (4)	2852 (4)		1443 (1)		
Cycloheptane	2927 (42, p)	2853 (37, p)		1441 (8, p)		
Cyclodecane	2914 (84, p)			1442 (10, p)	2930	2880

¹[CN str., 2234 (40, p)].

TABLE 3.11 Raman data for the CH stretching and bending modes of the alkyl group, and C–C–C=O skeletal bending for monomers and polymers

Compound	a.CH ₃ O str.	a.CH ₃ str.	s.CH ₃ str.	a.CH ₂ str.	s.CH ₂ str.	s.CH ₃ str.	CH ₂ bend	a.CH ₃ bend	s.CH ₃ bend	CC=O bend
Methyl acrylate			2957 (4)	2924 (2)		2858 (4)	1443 (1)			
Poly(methyl methacrylate)	3001 (4)		2952 (9)			2844 (1)		1451 (1)	1391 (0)	601 (4)
Ethyl methacrylate								1455 (6)	1392 (0)	602 (4)
Propyl acrylate			2941 (7)		2882 (5)			1453 (3)		
Propyl methacrylate		2963 (4)	2931 (9)		2882 (5)			1452 (5)		604 (4)
Poly(propyl acrylate)			2938 (9)		2881 (5)			1453 (4)		
Poly(propyl methacrylate)			2938 (9)		2881 (5)			1452 (5)		602 (3)
Dibutyl phosphonate		2965 (5)	2938 (8)	2913 (9)	2876 (9)			1452 (3)		[2434 (1) P–H str.]
Dibutyl fumarate		2964 (5)	2939 (7)	2914 (8)	2877 (7)			1451 (3)		
Dibutyl phthalate			2938 (7)	2914 (7)	2876 (6)			1450 (3)		
Poly(butyl acrylate)			2937 (9)	2919 (9)	2875 (7)			1451 (4)		
Poly(butyl methacrylate)		2963 (9)		2915 (8)	2876 (6)					603 (3)
Hexyl methacrylate		2961 (4)	2930 (9)	2901 (7)	2876 (6)			1441 (3)		604 (2)
Bis(isooctyl) fumarate		2963 (8)		2909 (8)	2878 (9)			1450 (4)		
Vinyl(isooctyl ether)			2933 (7)	2913 (7)	2874 (9)			1450 (3)		
Poly(isodecyl methacrylate)		2959 (7)	2932 (9)		2875 (9)					605 (1)
Undecyl acrylate				2900 (8)	2854 (8)			1439 (4)		
Undecyl methacrylate			2928 (9)		2854 (8)			1439 (5)		604 (2)
Vinyl undecyl ether				2900 (8)	2854 (8)			1439 (4)		
Dodecyl acrylate				2897 (8)	2853 (9)			1440 (4)		
Dodecyl methacrylate			2929 (9)	2896 (9)	2853 (9)			1439 (4)		605 (1)
Poly(dodecyl methacrylate)			2929 (8)	2804 (9)	2853 (9)			1440 (4)		
Vinyl dodecyl ether				2895 (8)	2853 (9)			1439 (3)		
					2874 (8)					
Strontium stearate			2923 (3)	2884 (9)	2852 (5)			1447 (4)		
Zinc stearate				2882 (9)	2849 (5)			1440 (3)		
Poly(vinyl stearate)				2882 (9)	2848 (8)			1438 (3)		
Vinyl octadecyl ether				2890 (7)	2852 (9)			1439 (3)		
Poly(octadecyl acrylate)				2862 (9)	2847 (7)			1438 (3)		
Octadecyl methacrylate			2928 (7)	2894 (8)	2852 (9)			1439 (4)		605 (1)
Poly(octadecyl methacrylate)			2928 (7)	2892 (8)	2852 (9)			1440 (4)		605 (0)
		2964 (8)	2939 (9)	2922 (8)	2875 (9)			1453 (4)		
Isobutyl methacrylate		2965 (7)	2931 (9)	2901 (7)	2877 (9)			1453 (4)		603 (3)
Poly(isobutyl methacrylate)		2964 (9)	2937 (9)		2875 (9)			1452 (6)		602 (3)
Vinyl isobutyl ether		2962 (5)	2943 (4)	2911 (6)	2876 (9)			1464 (2)		
Poly(vinyl isobutyl ether)		2957 (6)		2913 (8)	2872 (9)			1462 (3)		

2-Ethylhexyl acrylate	2963 (5)	2939 (9)	2877 (9)	1451 (3)	
2-Ethylhexyl methacrylate	2983 (5)	2931 (9)	2900 (7)	2877 (7)	1450 (4)
3,3,5-Trimethylhexyl methacrylate	2960 (7)	2930 (9)			
Ethylene dimethacrylate	2962 (5)	2931 (8)		1380 (2)	603 (3)
Cyclohexyl acrylate			2954 (9)	2861 (8)	1447 (4)
3,5,5-Trimethylcyclohexyl acrylate	2956 (9)	2931 (9)	2904 (9)	2873 (9)	1463 (4)
					1450 (4)
1,1,1-Trimethylolethane tri-acrylate	2966 (2)		2902 (1)		1464 (1)
Trimethylolpropane triethoxyacrylate	2951 (4)			2885 (4)	
Poly(2-Hydroxyethyl methacrylate)	2944 (9)				1455 (9)
					604 (9)
2-Hydroxypropyl acrylate	2940 (4)			2885 (2)	1458 (2)
Poly(2-Hydroxypropyl methacrylate)	2939 (9)				1455 (8)
					604 (5)
Propargyl acrylate			2953 (1)		1439 (1)
Propargyl methacrylate		2933 (1)			1439 (1)
1,1H,1H,3H-terafluoropropyl methacrylate	2971 (5)	2937 (7)			[2132 (9) CC str.]
					[2132 (9) CC str.]
2,2,2-Trifluoromethyl methacrylate	2978 (5)	2937 (7)			1453 (2)
					603 (3)
2,2,2-Trichloroethyl acrylate	2980 (2)				1455 (0)
Trichloromethyl methacrylate		2929 (0)			
Tribromoneopentyl acrylate			2921 (2)	2883 (1)	1465 (2)
					1434 (2)
Tribromoneopentyl methacrylate	2969 (5)	2928 (2)			
N,N-dimethylaminoethyl methacrylate	2954 (9)	2931 (9)			1467 (4)
					1447 (4)
Trimethylammonium methosulfate methacrylate	2963 (2)				1460 (3)
					606 (3)
3-Sulfopropyl potassium salt methacrylate	2983 (3)	2933 (5)			612 (1)
					[1063 (9) s.S03 str.]
					601 (1)
					619 (1)
Poly(phenyl methacrylate)					1448 (3)
					615 (2) i.p. ring

TABLE 3.12 IR vapor-phase data for cyclopropane derivatives

Compound	a.CH ₂ str.	s.CH ₂ str.	CH ₂ bend	CH ₂ wag	Ring Breathing	CH ₂ twist	CH ₂ rock	Ring Deformation				
Cyclopropane	3130 (0.200)3035 (0.480) 3100 (1.250)	1439 (0.022) 3020 (0.570) 2998 (0.325)	1050 (0.175) 1430 (0.018) 1024 (0.325) 1414 (0.020) 1000 (0.160)		[1188]		899 (0.206)	862 (0.512) 832 (0.162)				
Bromocyclopropane	3110 (0.170) 3101 (0.210) 3090 (0.220)	3030 (0.280) 3020 (0.300) 3010 (0.250)	1045 (0.329) 1446 (0.172) 1025 (0.240)	1279 (1.240) 1035 (0.430) 1271 (1.040) 1260 (1.140)		1191 (0.035)	868 (0.100) 800 (0.180)	811 (0.160) 550 (0.240) 544 (0.220)	C-Br str.			
Cyclopropane-carbonitrile	3125 (0.210) 3118 (0.279) 3105 (0.210)	3050 (0.355) 3040 (0.430) 3030 (0.410)	1445 (0.210) 1440 (0.155) 1434 (0.171)	1074 (0.490) 1060 (0.630) 1050 (0.620)	950 (1.103) 940 (1.115) 930 (1.215)	1205 (0.080) 1199 (0.060) 1186 (0.089)	735 (0.255) 722 (0.290) 711 (0.180)	824 (0.375) 814 (0.435) 805 (0.415)	CN. str.			
1-Phenylcyclopropane-carbonitrile	3100 (0.250)	3038 (0.400)	1447 (0.220)	1030 (0.282)	942 (0.310)	1191 (0.010)	masked	860 (0.068)	2235 (0.250)	Phenyl o.p. ip. H5 def.	o.p. Phenyl def.	
Cyclopropane-carboxylic acid	3108 (0.040)	3035 (0.090)	1425 (0.330) 1413 (0.360) 1405 (0.320)	1060 (0.080) 1035 (0.160) 1018 (0.100)	938 (0.110) 929 (0.150) 919 (0.140)	1181 (0.160)	755 (0.100)	825 (0.165)	O-H str. 3590 (0.291) 3580 (0.340) 3575 (0.260)	C=O str. 1779 (0.950) 1772 (1.250) 1768 (1.050)	C-O str. 1135 (1.150) 1130 (1.250) 1125 (1.125)	⁷ C=O 585 (0.355) 570 (0.290) 562 (0.290)
Methyl cyclopropane-carboxylate	3102 (0.052) [a.CH ₃ str.] [2960 (0.200)]	3024 (0.169) [s.CH ₃ str.] [2910 (0.050)]		1035 (0.100)	905 (0.172)			827 (0.100)	1751 (0.945)	1179 (1.240)	3490 (0.015) 1091 (0.295)	
Cyclopropylbenzene	masked Phenyl CH str. 3084 (1.050)	3035 (1.250) & Phenyl CH str.	1465 (0.130)	1028 (0.340)	898 (0.270)	1178 (0.015)	masked	812 (0.130)	Phenyl o.p. ip. H5 def. 750 (0.730)	o.p. Phenyl def. 695 (1.030)		

TABLE 3.13 IR data for octadecane, octadecane-D₃₈, tetracosane, and tetracosane-D₅₀

Compound	a.CH ₃ str.	a.CH ₂ str.	s.CH ₃ str.	s.CH ₂ str.	a.CH ₃ bend	CH ₂ bend	s.CH ₃ bend	CH ₂ wag	CH ₂ twist	CH ₃ rock?	CH ₂ rock
Octadecane	2970 (0.471)	2930 (1.250)		2863 (0.621)	1465 (0.120)		1385 (0.030)	1354 (0.042)	1310 (0.1030)	1105 (0.010)	720 (0.021)
	a.CD ₃ str.	a.CD ₂ str.	s.CD ₃ str.	s.CD ₂ str.	a.CD ₃ bend	CD ₂ bend	s.CD ₃ bend	CD ₂ wag	CD ₂ twist	CD ₃ rock?	CD ₂ rock
Octadecane-D ₃₈	2215 (0.650)	2199 (1.250)		2100 (0.590)	1085 (0.111)		1060 (0.050)	975 (0.020)	960 (0.020)	865 (0.015)	530 (0.020)
Octadecane /octadecane-D ₃₈	1.341	1.332		1.363	1.349		1.316	1.389	1.365	1.277	1.358
	a.CH ₃ str.	a.CH ₂ str.	s.CH ₃ str.	s.CH ₂ str.	a.CH ₃ bend	CH ₂ bend	s.CH ₃ bend	CH ₂ wag	CH ₂ twist	CH ₃ rock?	CH ₂ rock
Tetracosane	2970 (0.241)	2930 (1.250)		2860 (0.435)	1460 (0.077)		1385 (0.015)	1351 (0.020)	1300 (0.015)		715 (0.012)
	a.CD ₃ str.	a.CD ₂ str.	s.CD ₃ str.	s.CD ₂ str.	a.CD ₃ bend	CD ₂ bend	s.CD ₃ bend	CD ₂ wag	CD ₂ twist	CD ₃ rock?	CD ₂ rock
Tetracosane-D ₅₀		2200 (1.250)		2100 (0.470)	1085 (0.101)		1053 (0.040)	985 (0.020)	960 (0.020)	875 (0.010)	530 (0.020)
Tetracosane /Tetracosane-D ₅₀		1.332		1.362	1.346		1.315	1.371	1.354		1.349

Alkenes and Other Compounds Containing C=C Double Bonds

In-Plane Vibrations	56
Out-of-Plane Vibrations	56
Band Absorbance Ratios and Frequency Separations for Vinyl Twist, Vinyl C=CH ₂ , and Vinyl CH=CH ₂ Wag	57
Raman Data for X-CH=CH ₂ Compounds	58
Conjugated Vinyl Groups	58
Rotational Conformers or Fermi Resonance (F.R.)	58
1-Alkene (CH=CH ₂) CH and CH ₂ Stretching Vibrations	60
C=CH ₂ Wag Frequencies vs (sigma σ -sigma')	60
CH=CH ₂ Twist Frequencies vs σ^1 and pK _a of G for G-CH ₂ CO ₂ H	60
Allyl Halides	61
Cycloalkenes and Cycloalkadienes	61
Alkyl Acrylates and Alkyl Methacrylates	62
Trans-Alkenes	63
Alkylcinnamates	64
Cinnamyl Esters	65
1,1-Disubstituted Ethylenes	64
Styrenes and α -Methyl Styrenes	65
Butadienes, Propadienes, Conjugated Cyclic Dienes	66
Alkyl Groups of 1-Alkenes and Vinyl Alkyl Ethers	67
References	67

Figures

Figure 4-1	68 (61)	Figure 4-4	70 (65)
Figure 4-2	69 (64)	Figure 4-5	71 (65)
Figure 4-3	70 (65)		

Tables

Table 4-1	72 (56, 57)	Table 4-5	78 (61)
Table 4-2	73 (56)	Table 4-5a	78 (62)
Table 4-2a	74 (57)	Table 4-6	79 (62)
Table 4-2b	75 (57, 58, 60)	Table 4-6a	80 (62)
Table 4-2c	76 (59)	Table 4-7	81 (63, 64)
Table 4-3	77 (60)	Table 4-8	82 (64)
Table 4-3a	77 (60)	Table 4-9	82 (64)
Table 4-4	78 (60)	Table 4-10	83 (64)

Tables

Table 4-11	84 (64)	Table 4-15	88 (65)
Table 4-11a	85 (64)	Table 4-16	89
Table 4-12	85 (65)	Table 4-17	90
Table 4-13	86 (65)	Table 4-18	91
Table 4-14	87 (65)		

*Numbers in parentheses indicate in-text page reference.

The IR spectra of a variety of chemicals containing carbon-carbon double bonds (C=C) together with spectra-structure correlations are readily available in book form to aid chemists in the identification of these important polymer building blocks (1). Chapter 4 contains IR and Raman data for these compounds in different environments. Discussions of both chemical and physical effects upon group frequencies associated with carbon-carbon double bonds are included.

Table 4.1 lists vibrational assignments for C=C stretching ($\nu_{\text{C=C}}$), vinyl twist, vinyl CH₂ wag, vinyl CH=CH₂ wag, and the first overtone of vinyl CH₂ wag in the vapor-phase (2). The $\nu_{\text{C=C}}$ mode for 1-alkenes (R-CH=CH₂) occur in the region 1641–1650 cm⁻¹. The vinyl twist mode occurs in the region 991–1008 cm⁻¹. Branching in the 3-carbon atom increases the vinyl twist frequency. The vinyl C=CH₂ wag occurs in the region 910–918 cm⁻¹ and its first overtone occurs in the region 1829–1835 cm⁻¹. The vinyl wag vibration occurs in the region 572–685 cm⁻¹. This vibration increases in frequency with increased substitution on the 3-carbon atom (e.g., R-CH₂-CH=CH₂, 572–627 cm⁻¹; R₂CH-CH=CH₂, 653–678 cm⁻¹, and R₃C-CH=CH₂, 681–685 cm⁻¹).

Absorbance ratios and frequency separations are also presented for some vibrational bands.

IN-PLANE VIBRATIONS

Table 4.2 lists IR vapor-phase frequencies and assignments for a variety of compounds containing C=C double bonds. Acrylonitrile and divinylsulfone exhibit $\nu_{\text{C=C}}$ at 1613 and 1620 cm⁻¹, respectively. The allyl derivatives exhibit $\nu_{\text{C=C}}$ in the region 1641–1653 cm⁻¹. It is apparent that CN and SO₂ groups joined to the vinyl group have the effect of lowering the C=C stretching frequency (3).

The *vsym.* CH₂=, *vsym.* CH₂=, and CH₂= bending modes occur in the regions 3082–3122, 2995–3045, and 1389–1430 cm⁻¹, respectively. The CN and SO₂ groups raise the *vsym.* CH₂= frequencies. Compare acrylonitrile (3122 cm⁻¹) and divinylsulfone (3110 cm⁻¹) vs those for 3-butenic acid and the allyl derivatives (3082–3100 cm⁻¹).

OUT-OF-PLANE VIBRATIONS

The CH=CH₂ twist frequencies for these compounds are assigned in the region 962–997 cm⁻¹. The lowest frequency, 962 cm⁻¹, is exhibited by divinylsulfone, and the two vinyl groups are

joined to the sulfur atom of the SO_2 group. All of the other compounds exhibit $\text{CH}=\text{CH}_2$ twist in the region $970\text{--}997\text{ cm}^{-1}$, and in these cases the vinyl group is joined to a carbon atom.

The $\text{C}=\text{CH}_2$ wag vibration and its first overtone occur in the regions $911\text{--}971\text{ cm}^{-1}$ and $1835\text{--}1942\text{ cm}^{-1}$, respectively. The CN and SO_2 groups cause the $\text{C}=\text{CH}_2$ wag mode to occur at higher frequency than the other vinyl compounds, which exhibit this molecular vibration in the region $911\text{--}934\text{ cm}^{-1}$.

As noted here, the $\text{CH}=\text{CH}_2$ wag mode for vinyl groups joined to $\text{R}-\text{CH}_2$, $(\text{R}-)_2\text{CH}$, and $\text{R}-_3\text{C}$ groups for 1-alkenes occur in the regions $572\text{--}627$, $653\text{--}678$, and $681\text{--}685\text{ cm}^{-1}$, respectively. With the exceptions of allyl formate (638 cm^{-1}), allyl benzene (648 cm^{-1}) and allyl naphthalene (655 cm^{-1}), $\text{CH}=\text{CH}_2$ wag occurs in the region $551\text{--}558\text{ cm}^{-1}$. Acrylonitrile and divinylsulfone exhibit $\text{CH}=\text{CH}_2$ wag at 680 and 715 cm^{-1} , respectively, and occur at higher frequency than for compounds of form $(\text{R}-)_3\text{CCH}=\text{CH}_2$. On the other hand, allylbenzene and allylnaphthalene exhibit $\text{CH}=\text{CH}_2$ wag at 648 and 655 cm^{-1} , respectively, and occur at higher frequency than for 1-alkenes of form $\text{R}-\text{CH}_2-\text{CH}=\text{CH}_2$ ($572\text{--}627\text{ cm}^{-1}$). The reason for the $\text{CH}=\text{CH}_2$ wag frequency behavior with chemical structure is as follows: The $\text{CH}=\text{CH}_2$ wag includes bending of the $\text{C}-\text{C}=\text{C}$ bonds, and as the $\text{C}(-)_2$ becomes increasingly branched it becomes more difficult for the $\text{C}-\text{C}=\text{C}$ group to bend out-of-plane together with the three hydrogen atoms joined to vinyl group bending out-of-plane in the same direction as the 3-carbon atom. Therefore, $\text{CH}=\text{CH}_2$ wag increases in frequency as the 3-carbon atom is increasingly branched. Apparently, in the case of acrylonitrile and divinylsulfone, it is more difficult for the $\text{C}=\text{C}-\text{CN}$ and $\text{C}=\text{C}-\text{S}$ bonds to bend than for $(\text{R}-)_3\text{C}-\text{C}=\text{C}$ bond bending in the complex $\text{CH}=\text{CH}_2$ wag vibration.

BAND ABSORBANCE RATIOS AND FREQUENCY SEPARATIONS FOR VINYL TWIST, VINYL $\text{C}=\text{CH}_2$, AND VINYL $\text{CH}=\text{CH}_2$ WAG

Table 4.2a and Table 4.1 list the numbers and frequencies for the normal vibrations listed in this section (3). For 1-alkenes the ratio of the absorbances (A) for (A) $\text{CH}=\text{CH}_2$ twist/(A) $\text{C}=\text{CH}_2$ wag is in the range $0.341\text{--}0.617$. This shows that the $\text{C}=\text{CH}_2$ wag mode has more intensity than the $\text{CH}=\text{CH}_2$ twist mode. Table 4.2a shows the same trend except for acrylonitrile and allyl alcohol where these two modes have essentially identical intensity.

In Table 4.1 it is noted that the frequency separation between $\text{CH}=\text{CH}_2$ twist and $\text{C}=\text{CH}_2$ wag varies between 80 and 94 cm^{-1} , and in Table 4.2a it varies between 41 and 80 cm^{-1} with the exception of 19 and 9 cm^{-1} for acetonitrile and divinylsulfone, respectively.

The frequency separation between $\text{CH}=\text{CH}_2$ twist and $\text{CH}=\text{CH}_2$ wag varies between 319 and 419 cm^{-1} and with most compounds it varies between 319 and 344 cm^{-1} . These latter 1-alkenes are substituted in the 3-position with a methyl group (see Table 4.1). For the 1-alkenes not substituted in the 3-position, this frequency separation, varies between 370 and 419 cm^{-1} . In contrast, the frequency separation between $\text{CH}=\text{CH}_2$ twist and $\text{CH}=\text{CH}_2$ wag is 290 and 247 cm^{-1} for acrylonitrile and divinylsulfone, respectively. Other compounds studied extend this frequency separation to include 339 to 437 cm^{-1} for allyl naphthalene and allyl carbamate, respectively.

In the case of the frequency separation between $C=CH_2$ wag and $CH=CH_2$ wag it varies between 226 and 339 cm^{-1} for 1-alkenes (see Table 4.1). The frequency separation for the 1-alkenes not substituted in the 3-position varies between 286 and 239 cm^{-1} , while for those substituted in the 3-position it varies between 226 and 257 cm^{-1} (see Table 4.2a).

RAMAN DATA FOR $X-CH=CH_2$ COMPOUNDS

Table 4.2b contains Raman data and assignments for $X-CH=CH_2$ compounds and for cis- and trans-crotonitrile. The numbers in parentheses are for the relative Raman band intensities. They vary between 0 and 9, nine being the most intense band in the spectrum, and 0 being the least intense band in the spectrum. As these are whole numbers, it does not differentiate between the variances in intensity for bands whose intensities lie between any of the whole numbers (4).

In the case of cis- and trans-crotonitrile the $\nu C=C$ modes occur at 1639 and 1629 cm^{-1} , respectively, and the Raman band is stronger in the case of the trans isomer than for the cis isomer (the trans to cis ratio is 5:4). Thus, the polarization of the electron cloud during the $\nu C=C$ vibration is larger for the trans isomer than it is for the cis isomer.

Comparison of the Raman data for 1-octene and 1-decene shows that $\nu C=C$ occurs at 1642 cm^{-1} ; however, it is noted that the band intensity is 8 for 1-octene and 5 for 1-decene. The empirical structure for 1-octene is $CH_3-(CH_2)_5-CH=CH_2$ and for 1-decene is $CH_3-(CH_2)_7-CH=CH_2$. The CH_2 groups are in a 5:7 in this case while the band intensity is in an 8:5 for $\nu C=C$. This is what is expected, because the more CH_2 groups present in 1-alkenes the stronger the relative intensity for $\nu C=C$. Perhaps the ratios would be exactly 5:7 and 7:5 if the exact band intensities were measured.

CONJUGATED VINYL GROUPS

Vinyl-containing compound where the vinyl group is joined directly to a carbon atom of an aromatic ring exhibits $\nu C=C$ in the region $1629-1633\text{ cm}^{-1}$ (Table 4.2b) while 1-alkenes exhibit $\nu C=C$ at higher frequency ($1641-1653\text{ cm}^{-1}$). This decrease in frequency is attributed to resonance of the $C=C$ group with the aromatic ring. Resonance weakens the strength of the $C=C$ bond, which causes $\nu C=C$ to vibrate at lower frequency.

Table 4.2b show that the lowest $\nu C=C$ frequencies are for those compounds containing the $Si-CH=CH_2$ group ($\nu C=C$, $1590-1603\text{ cm}^{-1}$). The Raman band intensities for $\nu C=C$ are relatively in the weak-medium class. The $\nu C=C$ frequency for vinyl phenyl sulfone is also low (1607 cm^{-1}) where the vinyl group is joined to sulfur (3).

ROTATIONAL CONFORMERS OR FERMI RESONANCE (F.R.)

Table 4.2b shows that the vinyl ethers of form $R-O-CH=CH_2$ exhibit a Raman band in the region $1626-1639\text{ cm}^{-1}$ and a Raman band in the region $1610-1620\text{ cm}^{-1}$. In the case of vinyl phenyl ether, Raman bands are observed at 1644 and 1593 cm^{-1} . The 1593 cm^{-1} most likely results from an in-plane bend stretching mode of the phenyl group. In all cases of $R-O-CH=CH_2$, the Raman band in the region $1610-1620\text{ cm}^{-1}$ has more intensity than the

Raman band in the region $1626\text{--}1639\text{ cm}^{-1}$. In the IR, two (or sometimes three) bands are observed in the $\nu\text{C}=\text{C}$ stretching region of the spectrum (5). An explanation is required to explain the existence of two bands in this region when only one $\text{O}-\text{CH}=\text{CH}_2$ group is present in these molecules. There are two possibilities for this observation (presuming the spectra represent pure materials), and these are for the presence of rotational conformers or from band splitting due to Fermi resonance (FR.) of $\nu\text{C}=\text{C}$ with the first overtone of a lower lying fundamental of the $\text{CH}=\text{CH}_2$ group. Criteria for FR. to occur between a fundamental and a combination or overtone of a lower lying fundamental or two lower lying fundamentals are presented in what follows (4).

The combination or overtone must be of the same symmetry species as the $\nu\text{C}=\text{C}$ vibration and the combination or overtone must involve molecular motion within the $\text{CH}=\text{CH}_2$ group. In addition, $\nu\text{C}=\text{C}$ and the combination or overtone must occur at similar frequencies in order for a significant amount of FR. to occur between $\nu\text{C}=\text{C}$ and its combination or overtone. It does not matter if the combination or overtone occurs above or below the unperturbed $\nu\text{C}=\text{C}$ vibration. If the combination or overtone is identical in frequency to the unperturbed $\nu\text{C}=\text{C}$ frequency, both Raman or IR bands will have equal intensity. In other words, in this case both bands result from an equal contribution of $\nu\text{C}=\text{C}$ and an equal amount of the combination or overtone. Because combination or overtones usually have intensities at least an order of magnitude less than most fundamental vibrations, an explanation is required for the often two strong bands or a strong and medium band in the event of FR. This occurs because the fundamental contributes intensity to the combination or overtone, which causes the perturbed fundamental to be weaker than its unperturbed intensity and the perturbed combination or perturbed overtone to be more intense than its unperturbed intensity. It is usual practice to assign the most intense band of the Fermi doublet and the weaker band to the combination or overtone. However, the truth of the matter is that both bands are in FR., and both modes contribute to both the band frequencies and the intensities. The stronger of the bands has more contribution from the unperturbed fundamental and the weaker of the bands has the least contribution from the fundamental and the most contribution from the unperturbed combination or overtone.

It so happens that $\text{C}=\text{CH}_2$ wag for vinyl phenyl ether is assigned at 850 cm^{-1} , and its first overtone would be expected to occur above 1700 cm^{-1} . This is due to the fact that $\text{C}=\text{CH}_2$ wag exhibits negative anharmonicity (occurs at higher frequency than twice the fundamental frequency) (5). A very weak band is noted at 1710 cm^{-1} in the case of vinyl phenyl ether, and it is reasonably assigned as $2(\text{C}=\text{CH}_2\text{ wag})$. The Raman band at 1644 cm^{-1} and the strong 1643 IR band are assigned to a $\nu\text{C}=\text{C}$ mode. A weak-medium IR band is noted at 1615 cm^{-1} . Obviously, from both the intensities and frequencies of these two IR bands neither fits the criteria for FR. On this basis we assign the 1643 cm^{-1} band to $\nu\text{C}=\text{C}$ for the gauche conformer and the 1615 cm^{-1} band to the cis conformer for vinyl phenyl ether (5,6). Therefore, the vinyl alkyl ethers exhibit gauche $\nu\text{C}=\text{C}$ in the region $1636\text{--}1639\text{ cm}^{-1}$ and cis $\nu\text{C}=\text{C}$ in the region $1610\text{--}1620\text{ cm}^{-1}$.

Table 4.2c lists IR vapor-phase data for vinyl alkyl ether (3). The gauche $\nu\text{C}=\text{C}$ conformer is assigned in the region $1630\text{--}1648\text{ cm}^{-1}$ and the cis $\nu\text{C}=\text{C}$ conformer in the region $1611\text{--}1628\text{ cm}^{-1}$. Comparison of the vapor-phase IR data vs the Raman liquid phase data for vinyl isobutyl ether [gauche $\nu\text{C}=\text{C}$, VP(1645) vs liquid (1638 cm^{-1}) and cis $\nu\text{C}=\text{C}$, vP(1618 cm^{-1}) vs liquid (1612 cm^{-1})], and for vinyl octadecyl ether [gauche $\nu\text{C}=\text{C}$, vP(1641 cm^{-1})] cis $\nu\text{C}=\text{C}$, vP(1613 cm^{-1}) vs liquid (1610 cm^{-1})] indicates that both gauche $\nu\text{C}=\text{C}$ and cis $\nu\text{C}=\text{C}$ occur at higher frequency in the vapor-phase (3).

In the vapor-phase, *vasym.* $\text{CH}_2=$ for vinyl alkyl ethers occur in the region ($3122\text{--}3135\text{ cm}^{-1}$), $\nu\text{CH}=\text{C}$ occurs in the region ($3060\text{--}3070\text{ cm}^{-1}$), *vsym.* $\text{CH}_2=$ in the region ($2984\text{--}3015\text{ cm}^{-1}$), $\text{CH}_2=$ bend in the region ($1400\text{--}1418\text{ cm}^{-1}$), $\text{CH}=\text{C}$ rock in the region ($1311\text{--}1321\text{ cm}^{-1}$), $\text{CH}=\text{CH}_2$ twist in the region ($961\text{--}965\text{ cm}^{-1}$), $\text{C}=\text{CH}_2$ wag in the region ($812\text{--}825\text{ cm}^{-1}$), *cis*- $\text{CH}=\text{CH}_2$ wag in the region ($687\text{--}701\text{ cm}^{-1}$), *vasym.* $\text{C}=\text{C}-\text{O}-\text{C}$ in the region ($1203\text{--}1220\text{ cm}^{-1}$), and *vsym.* $\text{C}=\text{C}-\text{O}-\text{C}$ in the region ($837\text{--}888\text{ cm}^{-1}$).

1-ALKENE ($\text{CH}=\text{CH}_2$) CH AND CH_2 STRETCHING VIBRATIONS

The carbon hydrogen stretching frequencies for 1-alkenes all take place within the plane of the $\text{C}=\text{C}$ group (Table 4.2b).

The Raman band in the region $3120\text{--}3122\text{ cm}^{-1}$ with the relative intensity between 0 and 2 is assigned to *vasym.* $\text{CH}_2=$, the Raman band in the region $3043\text{--}3046\text{ cm}^{-1}$ with the relative bond intensity between 1 and 4 is assigned to $\nu\text{CH}=\text{C}$, the Raman band in the region $3022\text{--}3023\text{ cm}^{-1}$ with a relative intensity between 1 and 2 is assigned to *vsym.* $\text{CH}_2=$, and the Raman band in the region $1320\text{--}1329\text{ cm}^{-1}$ with a relative intensity between 2 and 9 is assigned $\text{CH}=\text{C}$ in-plane rocking. The $\text{CH}=\text{C}$ in-plane rocking mode for vinyl phenyl ether is assigned at 1311 cm^{-1} .

$\text{C}=\text{CH}_2$ WAG FREQUENCIES VS ($\text{SIGMA } \rho\text{-SIGMA}'$)

The term ($\text{sigma } \rho\text{-sigma}'$) defines the inductive effect of G for $\text{G}-\text{CH}=\text{CH}_2$. Table 4.3 lists the $\text{C}=\text{CH}_2$ wag frequencies and the inductive value of group G. The positive values withdraw sigma electrons from the vinyl group, the negative values contribute sigma electrons to the vinyl group. A plot of the $\text{C}=\text{CH}_2$ wag frequencies vs $\sigma\rho-\sigma'$ shows a smooth relationship (5).

$\text{CH}=\text{CH}_2$ TWIST FREQUENCIES VS σ' AND pK_a OF G FOR $\text{G}-\text{CH}_2\text{CO}_2\text{H}$

Table 4.3a lists IR CS_2 solution and IR vapor-phase data for $\text{CH}=\text{CH}_2$ twist frequencies, pK_a of $\text{G}-\text{CH}_2-\text{CO}_2\text{H}$ and σ' of G. Table 4.3b shows that in general the $\text{CH}=\text{CH}_2$ twist mode decreases in frequency as the pK_a value of $\text{G}-\text{CH}_2\text{CO}_2\text{H}$ decreases in value. The σ' values of G do not correlate as well with $\text{CH}=\text{CH}_2$ twist as do the pK_a values. These parameters are useful in assigning $\text{CH}=\text{CH}_2$ twist vibrations in unknown materials containing this group (5). It should be noted that the vapor-phase $\text{CH}=\text{CH}_2$ twist frequencies occur at higher frequency than they do in CS_2 solution.

ALLYL HALIDES

Table 4.4 lists the IR data and assignments for the *cis* and *gauche* conformers of the allyl halides. In all cases, *cis* $\nu_{C=C}$ ($1645\text{--}1652\text{ cm}^{-1}$) occurs at higher frequency than *gauche* $\nu_{C=C}$ ($1630\text{--}1643\text{ cm}^{-1}$) (7). However, the frequency separation for *gauche* $\text{CH}=\text{CH}_2$ twist and *gauche* $\text{C}=\text{CH}_2$ wag is nearly constant ($48.2\text{--}48.9\text{ cm}^{-1}$). An interesting correlation exists for the frequency separation between *gauche* $\text{CH}=\text{CH}_2$ twist and *gauche* $\text{CH}=\text{CH}_2$ wag in that it increases in the order F(347 cm^{-1}), Cl(395.2 cm^{-1}), Br(446.2 cm^{-1}), and I(489.7 cm^{-1}). The frequency separation between *gauche* $\text{C}=\text{CH}_2$ wag and *gauche* $\text{CH}=\text{CH}_2$ wag increases in the same order: F(292.7 cm^{-1}), Cl(347 cm^{-1}), Br(397.3 cm^{-1}), and I(440.8 cm^{-1}). The *gauche* $\text{CH}=\text{CH}_2$ wag frequency is the most affected progressing in the order F through I for these allyl halides, because the frequency separation between F and Cl is 52.3 cm^{-1} , Cl and Br is 52.3 cm^{-1} , and Br and I is 46.5 cm^{-1} . In this case the inductive effect of the halogen atoms decreases in the order F to I while the mass increases in the same order. The $\text{C}\text{--}\text{C}=\text{C}$ bond strength decreases in the order F to I due to the decreasing inductive effect of the halogen atoms, which causes $\text{CH}=\text{CH}_2$ wag to occur at a lower frequency because the $\text{C}\text{--}\text{C}=\text{C}$ bond is more easily bent during this complex $\text{CH}=\text{CH}_2$ wag fundamental.

CYCLOALKENES AND CYCLOALKADIENES

Table 4.5 lists IR data and $\text{C}=\text{C}$ or $(\text{C}=\text{C})_2$ stretching assignments for cyclopentene, cyclohexene, 1,4-cyclohexadiene, and 1,3-cyclohexadiene in mole % $\text{CHCl}_3/\text{CCl}_4$ solutions (8). Only three data points are listed in the table, but 20 data points were taken in the original experiment. Figure 4.1 shows the plot of the $\nu_{C=C}$ or $\nu_{(\text{C}=\text{C})_2}$ modes vs mole % CDCl_3 /or CHCl_3 /solvent system.

The $\nu_{C=C}$ mode for cyclopentene (1613.9 to 1611.2 cm^{-1}) and cyclohexene (1652.8 to 1650.9) decreases in frequency as the mole % CHCl_3 increases. These data suggest that the strength of the intermolecular proton bond formed between the $\text{C}=\text{C}$ π system and the H or D atom of CHCl_3 or CDCl_3 increases as the mole % CHCl_3 or CDCl_3 increases. In addition the slopes of the plots for cyclopentene and cyclohexene are essentially identical. The relatively large frequency difference between that for cyclopentene and cyclohexene does not represent the basicity of the $\text{C}=\text{C}$ bond. The major factor in determining the $\nu_{C=C}$ frequency is the bond angles of the carbon atoms joined to *cis* $\text{C}=\text{C}$ (9). The $\nu_{C=C}$ frequency changes randomly in the order cyclopropene (1656 cm^{-1}), cyclobutene (1566 cm^{-1}), cyclopentene (1613.9 cm^{-1}), and cyclohexene (1652.8 cm^{-1}) (9,10).

Both 1,4- and 1,3-cyclohexadienes contain two $\text{C}=\text{C}$ double bonds, and in each case the $\text{C}=\text{C}$ bonds couple and split into out-of-phase $(\text{C}=\text{C})_2$ stretching and in-phase stretching (8).

In the case of 1,3-cyclohexadiene $\nu_{i_p}(\text{C}=\text{C})_2$ occurs at 1577.9 cm^{-1} and $\nu_{o_p}(\text{C}=\text{C})_2$ at 1603.3 cm^{-1} in the neat phase, while in solution with CDCl_3 $\nu_{i_p}(\text{C}=\text{C})_2$ occurs at 1577.1 cm^{-1} and $\nu_{o_p}(\text{C}=\text{C})_2$ occurs at 1608 cm^{-1} . In this case, $\nu_{i_p}(\text{C}=\text{C})_2$ decreases in frequency by 0.8 cm^{-1} while $\nu_{o_p}(\text{C}=\text{C})_2$ increases in frequency by 4.7 cm^{-1} in going from the neat phase to solution in CDCl_3 . In the case of 1,4-cyclohexadiene, the $\nu_{i_p}(\text{C}=\text{C})_2$ frequency occurs at 1672.3 cm^{-1} and $\nu_{o_p}(\text{C}=\text{C})_2$ occurs at 1676.8 cm^{-1} in the neat phase, while in CHCl_3 solution

ν_{ip} occurs at 1676.8 cm^{-1} and $\nu_{op}(\text{C}=\text{C})_2$ occurs at 1637.9 cm^{-1} . In this case, it is the $\nu_{ip}(\text{C}=\text{C})_2$ frequency that increases 4.5 cm^{-1} while the $\nu_{op}(\text{C}=\text{C})$ frequency decreases 1.3 cm^{-1} . However, Figure 4.1 shows that the higher frequency band in each set increases in frequency while the lower frequency band in each set decreases in frequency going from the neat phase to decreasing concentration in CHCl_3 or CDCl_3 solutions (8).

In the case of 1,3-cyclohexadiene, the two C=C groups are conjugated $\text{CH}=\text{CH}-\text{CH}=\text{CH}_2$ while in the case of 1,4-cyclohexadiene the two C=C groups are not conjugated. For the sake of comparison, the $\nu_{ip}(\text{C}=\text{C})_2$ and $\nu_{op}(\text{C}=\text{C})_2$ modes for *s*-trans-butadiene in the liquid phase occur at 1638 and 1592 cm^{-1} , respectively (10). The compound, *cis* 2-tert-butylbutadiene, exhibits $\nu_{ip}(\text{C}=\text{C})_2$ and $\nu_{op}(\text{C}=\text{C})_2$ at 1610 and 1645 cm^{-1} , respectively. Therefore, the $\nu_{ip}(\text{C}=\text{C})_2$ and $\nu_{op}(\text{C}=\text{C})_2$ frequency order is the same for 1,3-cyclohexadiene and *cis* tert-butylbutadiene. In this case, the two C=C groups have to be in a *cis*-*cis* configuration due to ring restraint, and this is in good agreement with the *cis* configuration assignment for *cis*-tert-butylbutadiene.

Table 4.5a lists IR vapor-phase data for *cis*-cycloalkene derivatives. Cyclopentene exhibits $\nu\text{C}=\text{C}$ at 1621 cm^{-1} in the vapor phase and 1614 cm^{-1} in CCl_4 solution, and cyclohexene exhibits $\nu\text{C}=\text{C}$ at 1651 cm^{-1} in the vapor phase and 1653 cm^{-1} in CCl_4 solution. In this case the $\nu\text{C}=\text{C}$ mode for the solution-phase data read directly from the computer are considered more accurate than the manually read vapor-phase data. If these data are valid, the correlation of $\nu\text{C}=\text{C}$ occurring at higher frequency in the vapor than in solution is an exception in the case of cyclohexene.

A study of Table 4.5a shows that $\nu\text{C}=\text{C}$ for the 5-membered rings occur at the lower frequency than those for the 6-membered rings as already discussed here. Comparison of the $\nu\text{C}=\text{C}$ vibrations for 2-cyclopentene-1-one and 2-cyclohexene-1-one (1600 cm^{-1} vs 1624 cm^{-1}) shows that $\nu\text{C}=\text{C}$ for the 5-membered ring still occurs at lower frequency than it does for the 6-membered ring. However, both $\nu\text{C}=\text{C}$ modes are lower in frequency than for cyclopentene (lower by 21 cm^{-1}) and for cyclohexene (lower by 27 cm^{-1}). The reason for this is that the C=C and C=O bonds are conjugated, which causes both bonds to become weaker and the connecting C-C bond to become stronger. Therefore, $\nu\text{C}=\text{O}$ also occurs at lower frequency in the case of 2-cyclopentene-1-one (1745 cm^{-1}) vs (1765 cm^{-1}) for cyclopentanone in the vapor phase and 2-cyclohexene-1-one (1710 cm^{-1}) vs (1732 cm^{-1}) for cyclohexanone in the vapor phase. In the $\nu\text{C}=\text{O}$ cases, they are lower by 20 and 22 cm^{-1} for the 5- and 6-membered rings, respectively. Therefore, conjugation of C=C with C=O decreases both modes in the same order of magnitude.

An IR band in the region $699-750\text{ cm}^{-1}$ is assigned to *cis* CH=CH wag in the six *cis* compounds studied. Another band is noted in the region $635-658\text{ cm}^{-1}$. It is not certain whether these bands result from a different vibrational mode or from *cis* CH=CH wag of another conformer.

ALKYL ACRYLATES AND ALKYL METHACRYLATES

It is relatively easy to distinguish between alkyl acrylates and alkyl methacrylates by studying the $\nu\text{C}=\text{C}$ and $\nu\text{C}=\text{O}$ frequencies. The acrylates exhibit two bands in the $\nu\text{C}=\text{C}$ region of the spectrum, and it has been suggested that they result from *cis* and *trans* conformers (10,11). Table 4.6 lists IR data and assignments for alkyl acrylates in CHCl_3 and CCl_4 solutions (11). In CCl_4

solution, cis $\nu\text{C}=\text{C}$ is assigned in the region $1619.2\text{--}1620.4\text{ cm}^{-1}$, and in CHCl_3 solution, in the region $1618.5\text{--}1619.9\text{ cm}^{-1}$. In CCl_4 solution, trans $\nu\text{C}=\text{C}$ occurs in the region $1635.3\text{--}1637.2\text{ cm}^{-1}$, and in CHCl_3 solution in the region $1635.1\text{--}1636.6\text{ cm}^{-1}$. In all cases cis $\nu\text{C}=\text{C}$ occurs at lower frequency than trans $\nu\text{C}=\text{C}$, and both cis and trans $\nu\text{C}=\text{C}$ occur at lower frequency in CHCl_3 than in CCl_4 solution.

Table 4.6a lists IR data and assignments for alkyl methacrylates in CCl_4 and CHCl_3 solution (11). In CCl_4 solution $\nu\text{C}=\text{C}$ for the alkyl methacrylates occurs in the region $1635.7\text{--}1637.3\text{ cm}^{-1}$, in CHCl_3 solution, $\nu\text{C}=\text{C}$ occurs in the region $1635.7\text{--}1637.3\text{ cm}^{-1}$, and in CHCl_3 solution, $\nu\text{C}=\text{C}$ occurs in the region $1635.8\text{--}1637.3\text{ cm}^{-1}$. In all cases $\nu\text{C}=\text{C}$ occurs at lower frequency in CHCl_3 than in CCl_4 solution by 0.8 to 2.3 cm^{-1} .

The $\nu\text{C}=\text{O}$ frequencies for the alkyl methacrylates occur in the region $1719.5\text{--}1726\text{ cm}^{-1}$ (in CCl_4) and $1709.5\text{--}1718\text{ cm}^{-1}$ (in CHCl_3). Thus, $\nu\text{C}=\text{O}$ occurs at lower frequency by 8 to 10.6 cm^{-1} in going from CCl_4 to CHCl_3 solution. The $\nu\text{C}=\text{O}$ frequencies for alkyl acrylates occur in the region $1722.9\text{--}1734.1\text{ cm}^{-1}$ (in CCl_4) and in the region $1713.8\text{--}1724.5\text{ cm}^{-1}$ (in CHCl_3). Thus, the $\nu\text{C}=\text{O}$ occurs at lower frequency by $3.4\text{--}10.8\text{ cm}^{-1}$ in going from CCl_4 to CHCl_3 solution (11). In the vapor phase $\nu\text{C}=\text{O}$ for methyl methacrylate and methyl acrylate occur at 1741 and 1751 cm^{-1} , respectively (2). These data show that the $\nu\text{C}=\text{O}$ frequencies occur at higher frequency in the vapor phase than in solution.

It should be noted from the preceding $\nu\text{C}=\text{O}$ for the methacrylates occur at lower frequency than for the acrylates. This shift to lower frequency is attributed to the inductive contribution of the CH_3 group to the carbonyl group, which weakens the $\text{C}=\text{O}$ bond.

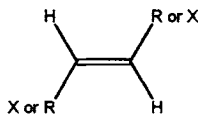
It should be also noted that the alkyl group also causes a shift in the $\nu\text{C}=\text{O}$ frequency. For example, in the case of alkyl acrylates in CCl_4 solution, $\nu\text{C}=\text{O}$ occurs at 1734.1 , 1727.3 , 1727.1 , and 1722.9 cm^{-1} for the methyl, butyl, 2-ethylhexyl, and tert-butyl analogs, respectively. In the case of the same series of alkyl methacrylates in CCl_4 solution, $\nu\text{C}=\text{O}$ occurs at 1718 , 1710.5 , and 1709.5 , respectively. These $\nu\text{C}=\text{O}$ frequency decreases also are attributed to the increased inductive contribution of the alkyl group progressing in the series methyl to tert-butyl.

In the case of alkyl acrylates, the $\text{CH}_2=\text{C}$ bend occurs in the region $1401.6\text{--}1407.2\text{ cm}^{-1}$ (in CCl_4) and in the region $1404\text{--}1410.3\text{ cm}^{-1}$ (in CHCl_3). Thus $\text{CH}_2=\text{C}$ bend increases in frequency by 2.4 to 3.4 cm^{-1} on going from CCl_4 to CHCl_3 solution.

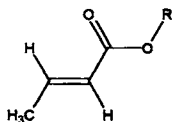
Alkyl acrylates exhibit $\text{CH}_2=\text{CH}$ twist in the region $982.6\text{--}984.9\text{ cm}^{-1}$ (in CCl_4) and $983.4\text{--}985\text{ cm}^{-1}$ (in CHCl_3). The $\text{C}=\text{CH}_2$ wag frequencies occur in the region $966.3\text{--}968.4\text{ cm}^{-1}$ (in CCl_4) and $966.5\text{--}970.3\text{ cm}^{-1}$ (in CHCl_3).

TRANS-ALKENES

Table 4.7 lists IR vapor-phase frequency data for trans-alkenes and compounds containing a trans carbon-carbon double bond (3). Compounds containing a trans carbon-carbon double bond have the following configuration:



When the R groups or X groups are identical the $\nu_{\text{C}=\text{C}}$ is not allowed in the IR, because these compounds have a center of symmetry. Therefore, there is no dipole moment change during a cycle of $\nu_{\text{C}=\text{C}}$. However, in this case the $\nu_{\text{C}=\text{C}}$ mode is Raman active. However, even in the case where the trans-alkenes do not have a center of symmetry, the dipole moment change during a cycle of trans $\nu_{\text{C}=\text{C}}$ is small, and the IR band is very weak. Raman spectroscopy is required to readily detect the C=C in trans-alkenes.



Alkyl crotonates exist in a trans configuration, and in the vapor phase trans $\nu_{\text{C}=\text{C}}$ occurs near 1664 cm^{-1} . A weak band at 1649 cm^{-1} and a weak-medium band is noted at 1621 cm^{-1} in the vapor-phase spectrum of cinnamionitrile, suggesting that both the cis and trans isomers are present.

The trans CH=CH twist is assigned in the region $961\text{--}972\text{ cm}^{-1}$ for most of these compounds included in Table 4.7. Halogen atoms joined to C=C lowers the trans CH=CH twist mode. For example, it occurs at 897 cm^{-1} for trans-1,2-dichloroethylene and at 930 cm^{-1} for 1,3-dichloropropene; Table 4.8 lists data for a variety of trans disubstituted ethylenes in CS_2 solution in most cases (5). The trans CH=CH twist mode occurs in the region $896\text{--}975\text{ cm}^{-1}$.

ALKYLCINNAMATES

Table 4.9 lists IR vapor-phase data for alkyl cinnamates (3). The $\nu_{\text{C}=\text{C}}$ vibration occurs in the region $1640\text{--}1642\text{ cm}^{-1}$ in the vapor-phase, and it has medium band intensity. The CH=CH twist occurs in the region $972\text{--}982\text{ cm}^{-1}$, and its intensity is always less than that exhibited by $\nu_{\text{C}=\text{C}}$ as demonstrated by the absorbance ratio $[(A)_{\text{HC-CH twist}}]/[(A)_{\nu_{\text{C}=\text{C}}}]$ in the range 0.42–0.67. The $\nu_{\text{C}=\text{O}}$ mode for these alkyl cinnamates will be discussed in Chapter 15.

CINNAMYL ESTERS

Table 4.10 lists IR vapor-phase data for cinnamyl esters (3). In this case, $\nu_{\text{C}=\text{C}}$ occurs in the region $1652\text{--}1660\text{ cm}^{-1}$, and it occurs at higher frequency than in the case of alkyl cinnamates (compare with data in Table 4.10). In the case of alkyl cinnamate, $\phi\text{-CH}=\text{CH-C}(=\text{O})\text{-O-R}$, the C=O and C=C groups are conjugated causing both $\nu_{\text{C}=\text{C}}$ and $\nu_{\text{C}=\text{O}}$ to occur at lower frequency than those for cinnamyl esters, $\phi\text{-CH}=\text{CH-CH}_2\text{-O-(=O)-R}$. In the case of the cinnamyl esters the absorbance ratio $[(A)_{\text{CH}=\text{CH}}]/[(A)_{\nu_{\text{C}=\text{C}}}]$ is in the range 6.9–20.5, and this is the reverse of that exhibited by the alkyl cinnamates. Chapter 15 discusses $\nu_{\text{C}=\text{O}}$ for these cinnamyl esters.

Table 4.10 also lists vibrational data and assignment for the R-C=O-O- portion of these esters.

1,1-DISUBSTITUTED ETHYLENES

Table 4.11 lists IR data for $C=CH_2$ wag and its first overtone for 1,1-disubstituted ethylenes (5). The fundamental is recorded in CS_2 solution and its overtone in CCl_4 solution. The $C=CH_2$ wag mode occurs in the region $711\text{--}1004\text{ cm}^{-1}$, and its first overtone occurs in the region $1400\text{--}2020\text{ cm}^{-1}$. The $C=CH_2$ wag frequency exhibits negative anharmonicity because the first overtone occurs at more than twice the $C=CH_2$ wag frequency.

Infrared and Raman spectra for 1-bromo-1-chloroethylene are shown in Figure 4.2, and these data were used to assign its 12 fundamental vibrations (13). Comparison of these data with those for 1,1-dichloroethylene (14,15) and 1,1-dibromoethylene (16) show that 9 fundamentals decrease in the order Cl_2 , $ClBr$, and Br_2 , and this trend is often observed in other halogenated analogs (see Table 4.11a).

Table 4.12 lists Raman data and assignments for the vinyl esters of carboxylic acids in the neat phase (4). With the exception of vinyl cinnamate ($\nu C=C$ at 1636 cm^{-1}) all of the other vinyl esters exhibit $\nu C=C$ in the region $1644\text{--}1648\text{ cm}^{-1}$. In all cases where the aliphatic group of the ester is saturated the $\nu C=C$ mode has much higher relative intensity (RI) than the (RI) for $\nu C=O$. The ratio $[(RI)\nu C=O]/[(RI)\nu C=C]$ is in the range 0.11–0.29. In cases where the carboxylate portion of the ester is conjugated with the $C=C$ group this RI ratio varies from 0.22 to 2.

The frequency separation between $\nu C=C$ and $\nu C=O$ varies between 98 and 110 cm^{-1} for compounds of form $R-C(=O)-O-CH=CH_2$, and between 84 and 92 cm^{-1} in cases where the $C=O$ is conjugated with $C=C$ or an unsaturated ring. This difference in the lower frequency separation is attributed to resonance between the $C=C$ and $C=O$ groups ($C=C-C=O$).

STYRENES AND α -METHYL STYRENES

Table 4.13 lists Raman data and assignments for styrene, α -methyl styrene monomers in the condensed phase (4). The $\nu C=C$ vibration occurs in the region $1624\text{--}1635\text{ cm}^{-1}$. The α -methylstyrene ($\nu C=C$, 1631 cm^{-1}) and 1,3-di(α -methyl) styrene (1631 cm^{-1}) exhibit $\nu C=C$ frequencies comparable to styrene. However, $\nu C=C$ of these compounds occur lower in frequency than for 1-octene (1642 cm^{-1}), and this is the result of conjugation between $\nu C=C$ and the phenyl group. Other Raman bands listed in this table are assigned to in-plane phenyl ring vibrations.

Table 4.14 lists IR group frequency data and assignments for styrene and ring-substituted styrenes (12). Only data for styrenes that had corresponding ring-substituted phenols whose pK_a values were included were taken from Reference 12. Figure 4.3 gives the $C=CH_2$ wag frequencies plotted against the pK_a value of the corresponding ring-substituted phenol. Examination of Fig. 4.3 shows that styrenes substituted with atoms or groups in at least the 2,6-positions correlate in a manner different from styrenes not substituted in the 2,6-positions. The pK_a values are affected by contributions from both inductive and resonance effects of substituent atoms or groups joined to the phenyl ring. In the case of 2,6-disubstituted styrenes, the vinyl and 2,6-disubstituted phenyl group are not coplanar; therefore it is not possible for the resonance effects of the 2,6-atoms or groups to affect the $C=CH_2$ wag frequencies. Thus, it is the

inductive effects of the atoms or groups substituted in the 2,6-positions that are affecting the C=CH₂ wag frequencies (assuming that the effects of intramolecular forces between atoms or groups in the 2,6-positions and the vinyl group are negligible). The C=CH₂ wag frequencies are affected by both inductive and resonance effects in cases where styrenes are not substituted in the 2,6-positions.

Figure 4.4 is a plot of the frequency separation between CH=CH₂ twist and C=CH₂ wag for styrene and ring-substituted styrenes vs the same pK_a values. Again, separate correlations exist for the planar and nonplanar styrenes with the exception of 2,4,6-trimethyl styrene, where the frequency separation between CH=CH₂ twist and C=CH₂ wag is less than for the corresponding 2,6-disubstituted phenols whose pK_a values are lower than ~7.2.

Table 4.15 lists IR data for α -halostyrenes, α -alkylstyrenes, and related compounds (12). Figure 4.5 shows a plot of the CH₂ wag frequencies for styrene and ring-substituted styrenes vs the C=CH₂ wag frequency for α -methylstyrene and correspondingly ring-substituted α -methylstyrenes. This plot suggests that the factors affecting C=CH₂ wag for both styrenes and α -methylstyrenes are comparable. However, the CH₂ wag frequencies for α -methyl styrene occur at lower frequency than the correspondingly substituted styrenes by 10–18 cm⁻¹. The α -methylstyrenes are not planar for those substituted with Cl or CH₃ in the 2-position, while for styrenes it takes substitution in the 2,6-positions in order to sterically prevent the vinyl and phenyl groups from being coplanar.

BUTADIENES, PROPADIENES, CONJUGATED CYCLIC DIENES

Table 4.16 lists IR vapor-phase data and assignments for butadienes and propadienes (3,17). Compounds containing the 1,3-butadiene structure are of form C=C–C=C, and the two C=C bonds couple during their $\nu(\text{C}=\text{C})_2$ vibrations into in-phase $\nu(\text{C}=\text{C})_2$ and out-of-phase $\nu(\text{C}=\text{C})_2$. In the cases of 1,3-butadiene and 2-methyl-1,3-butadiene ip $\nu(\text{C}=\text{C})_2$ occur at 1684 and 1649 cm⁻¹, respectively, while op $\nu(\text{C}=\text{C})_2$ occur at 1594 and 1602 cm⁻¹, respectively. Other vibrational assignments are presented for these two molecules.

Propadienes have the basic skeletal structure C=C=C, and exhibit ip $\nu(\text{C}=\text{C})_2$ and op $\nu(\text{C}=\text{C})_2$ vibrational mode. In the case of propadiene, the ip $\nu(\text{C}=\text{C})_2$ is not IR active due to its molecular symmetry. With substitution of an atom or group in the 1-position of propadiene, these molecules have only a plane of symmetry, and ip $\nu(\text{C}=\text{C})$ occurs in their region 1072–1101 cm⁻¹ progressing in frequency in the order CH₃, I, Br, and Cl. The op $\nu(\text{C}=\text{C})$ mode is allowed in IR for propadiene, and its monosubstituted derivatives, and it occurs in the region 1953–1663 cm⁻¹ (18).

The compound 2,5-norbornadiene has the following basic structure:



In this case, the C=C bonds are each in a fused 5-membered ring and they are conjugated. Therefore, 2,5-norbornadiene and related compounds exhibit ip and op $\nu(\text{C}=\text{C})_2$ modes. The compounds 2,5-norbornadiene and 2,5-norbornadiene-yl acetate exhibit ip $\nu(\text{C}=\text{C})_2$ at 1639 and 1651 cm⁻¹, respectively, and op $\nu(\text{C}=\text{C})$ at 1546 and 1543 cm⁻¹, respectively. In the case of

1,3-cyclohexadiene the ring is larger than in the case of the 2,5-norbornadienes. The 6-membered ring is not fused in this case, but the two C=C groups are conjugated. The ip $\nu(\text{C}=\text{C})_2$ and op modes are assigned at 1600 and 1701 cm^{-1} , respectively. The order of ip and op $\nu(\text{C}=\text{C})_2$ is reversed when comparing it to those for the 2,5-norbornadienes.

The ip and op cis $(\text{CH}=\text{CH})_2$ wag occur at 748 and 658 cm^{-1} for 1,3-cyclohexadiene, respectively. In the case of the 1,5-norbornadienes ip and op cis $(\text{CH}=\text{CH})$ wag occur at 654 and 728–735 cm^{-1} , respectively. Again the ip and op cis $(\text{CH}=\text{CH})$ wag mode assignments are in the reverse order for these two sets of compounds.

ALKYL GROUPS OF 1-ALKENES AND VINYL ALKYL ETHERS

Table 4.17 contains the IR vapor-phase data and assignments for the carbon hydrogen vibrations for the 1-alkenes (also see Table 4.1). These assignments are given here rather than in Chapter 3 for the convenience of those interested in the vibrational spectra of 1-alkenes.

Table 4.18 contains the IR vapor-phase data and assignments for the alkyl group of vinyl alkyl ethers (also see Table 4.2b). The assignments are placed here rather than in Chapter 3 for the convenience of those interested in the vibrational spectra of vinyl alkyl ethers.

REFERENCES

1. Nyquist, R. A. (1989). *The Infrared Spectra, Building Blocks of Polymers*, Philadelphia: Sadtler Research Laboratories, A Division of Bio-Rad.
2. Nyquist, R. A. (1984). *The Interpretation of Vapor-Phase Infrared Spectra: Group Frequency Data*, Philadelphia: Sadtler Research Laboratories, A Division of Bio-Rad.
3. Nyquist, R. A. (ed.) (1984). *A Collection of 9200 Spectra*, Philadelphia: Sadtler Standard Infrared Vapor Phase Spectra, Sadtler Research Laboratories, A Division of Bio-Rad.
4. (1987). *Sadtler Standard Raman Spectra*, Philadelphia: Sadtler Research Laboratories, A Division of Bio-Rad.
5. Potts, W. J. and Nyquist, R. A. (1959). *Spectrochim. Acta*, **15**, 679.
6. Owen, N. L. and Sheppard, N. (1964). *Trans, Faraday Soc.*, **60**, 634.
7. McLachlan, R. D. and Nyquist, R. A. (1968). *Spectrochim. Acta*, **24A**, 103.
8. Nyquist, R. A. (1992). *Appl. Spectrosc.*, **47**, 560.
9. Colthup, N. B., Daly, L. H., and Wiberley, S. E. (1990). *Introduction to Infrared and Raman Spectroscopy*, 3rd ed., New York: Academic Press.
10. Lin-Vien, D., Colthup, N. B., Fateley, W. G., and Grasselli, J. G. (1991). *The Handbook of Infrared and Raman Frequencies of Organic Molecules*, Boston: Academic Press, Inc.
11. Nyquist, R. A. and Streck, R. (1994). *Vib. Spectrosc.*, **8**, 71.
12. Nyquist, R. A. (1986). *Appl. Spectrosc.*, **40**, 196.
13. Nyquist, R. A. and Thompson, J. W. (1977). *Spectrochim. Acta*, **33A**, 63.
14. Winter, R. (1970). *Z. Naturforsch.*, **25A**, 1912.
15. Joyner, P. and Slockler, G. (1952). *J. Chem. Phys.*, **20**, 302.
16. Scherer, J. R. and Overend, J. (1960). *J. Chem. Phys.*, **32**, 1720.
17. Nyquist, R. A., Lo, Y.-S., and Evans, J. C. (1964). *Spectrochim. Acta*, **20**, 619.
18. Nyquist, R. A., Lo, Y.-S., and Evans, J. C. (1964). *Spectrochim. Acta*, **20**, 619.

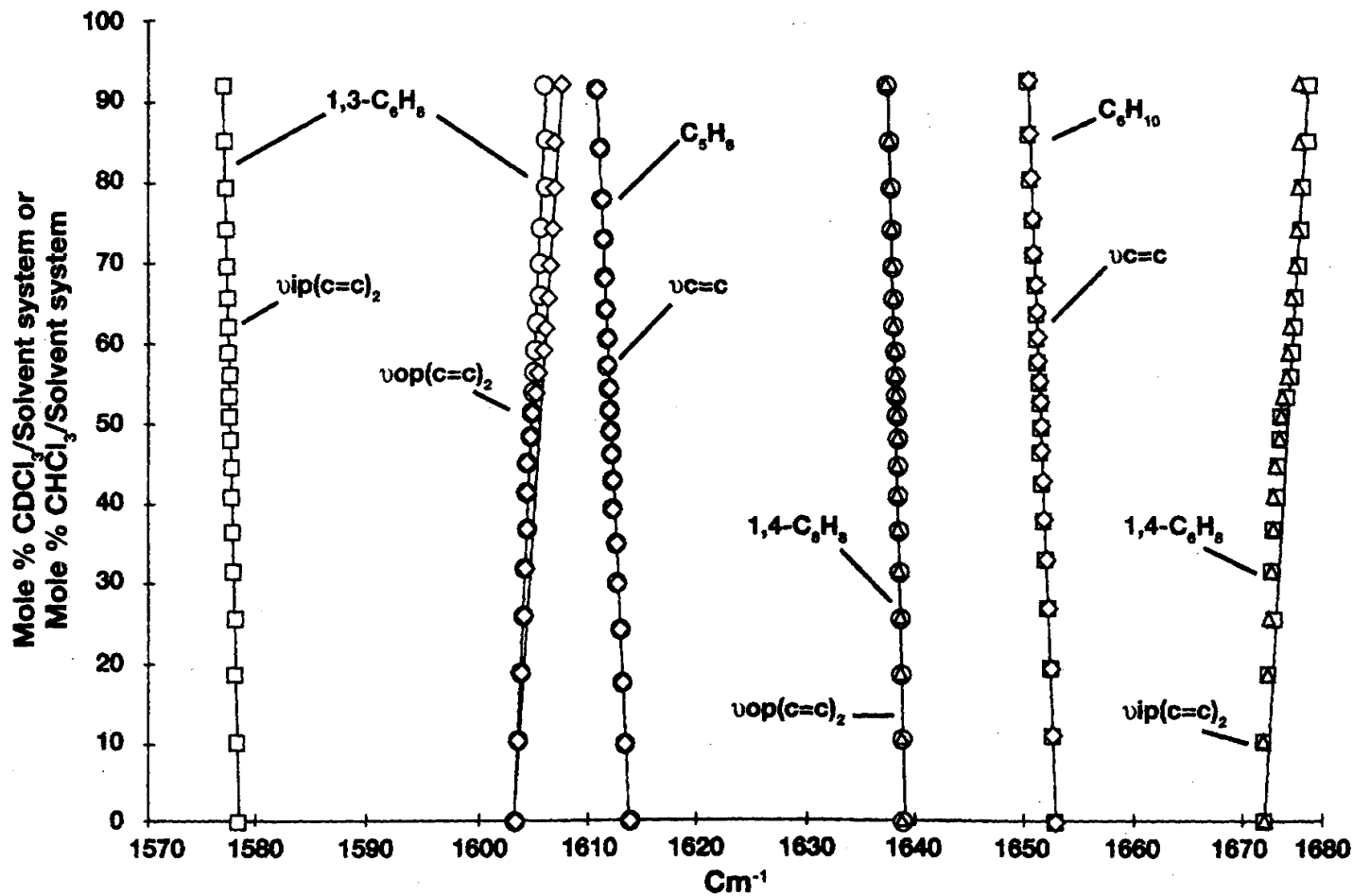
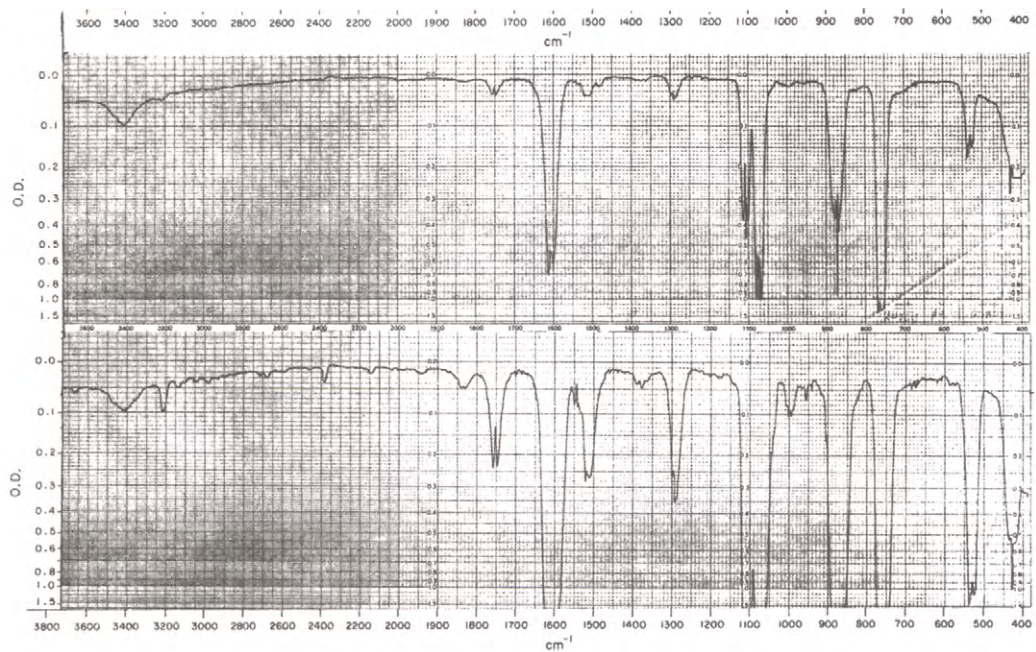
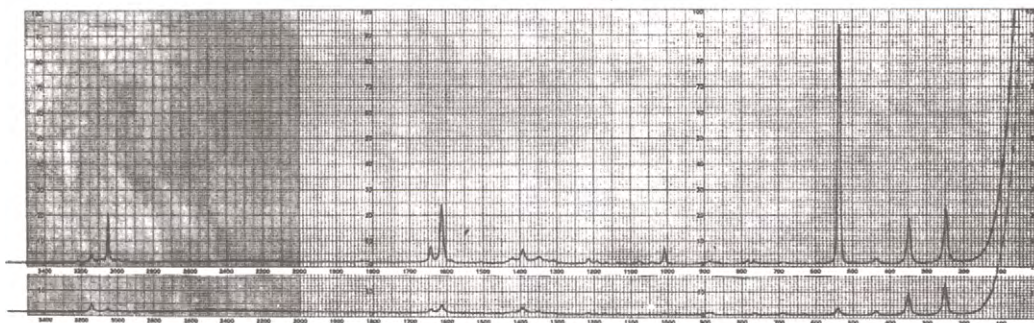


FIGURE 4.1 Shows plots of the $\nu\text{C}=\text{C}$ or $\nu(\text{C}=\text{C})_2$ modes for 1,3-cyclohexadienes, 1,4-cyclohexadienes, cyclopentene, and cyclohexene vs mole % CDCl_3 /or CHCl_3 /solvent system.



Upper: Infrared vapor-phase spectrum of $\text{CH}_2=\text{CBrCl}$ in the region $3800\text{--}400\text{ cm}^{-1}$ using a 10-cm KBr cell. The vapor pressure is 10 mm Hg. Lower: Same as upper spectrum except the vapor pressure is 100 mm Hg.



Raman liquid-phase spectrum of CH_2CBrCl . Upper: Parallel polarization. Lower: Perpendicular polarization.

FIGURE 4.2 Infrared and Raman spectra for 1-bromo-1-chloroethylene.

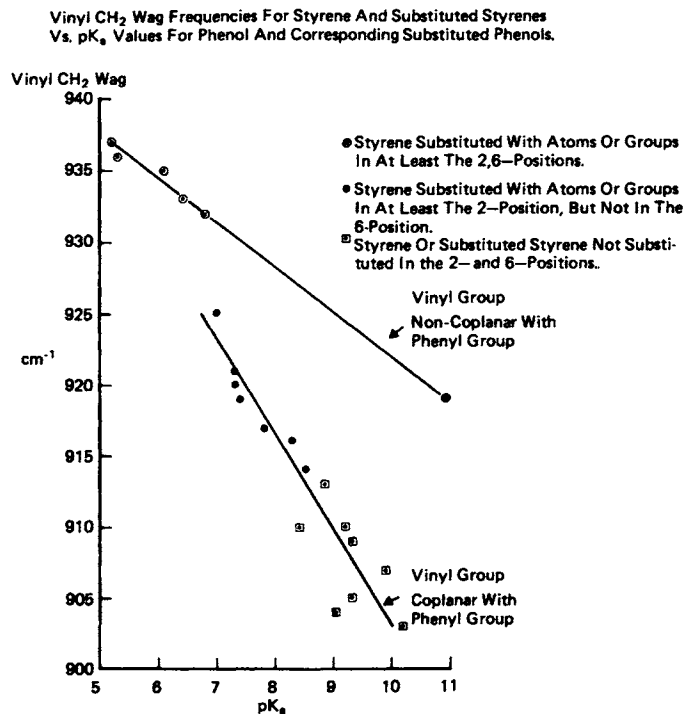


FIGURE 4.3 Plots of the C=CH₂ wag frequencies for styrenes and ring substituted styrenes vs the pK_a values for correspondingly substituted phenols.

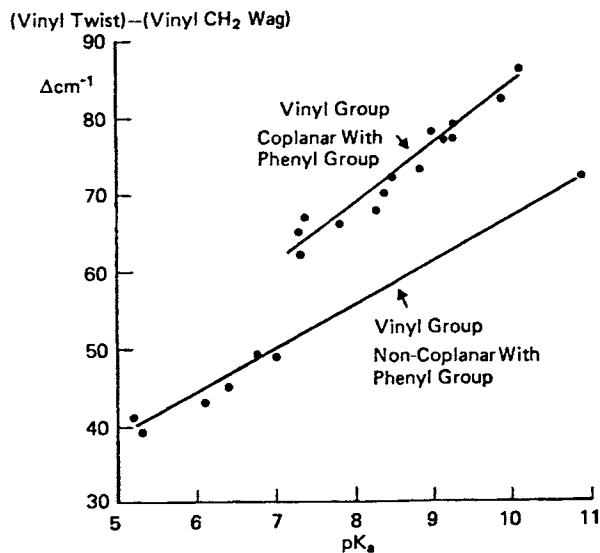


FIGURE 4.4 A plot of the frequency separation between CH=CH₂ twist and C=CH₂ wag for styrene and ring-substituted styrenes.

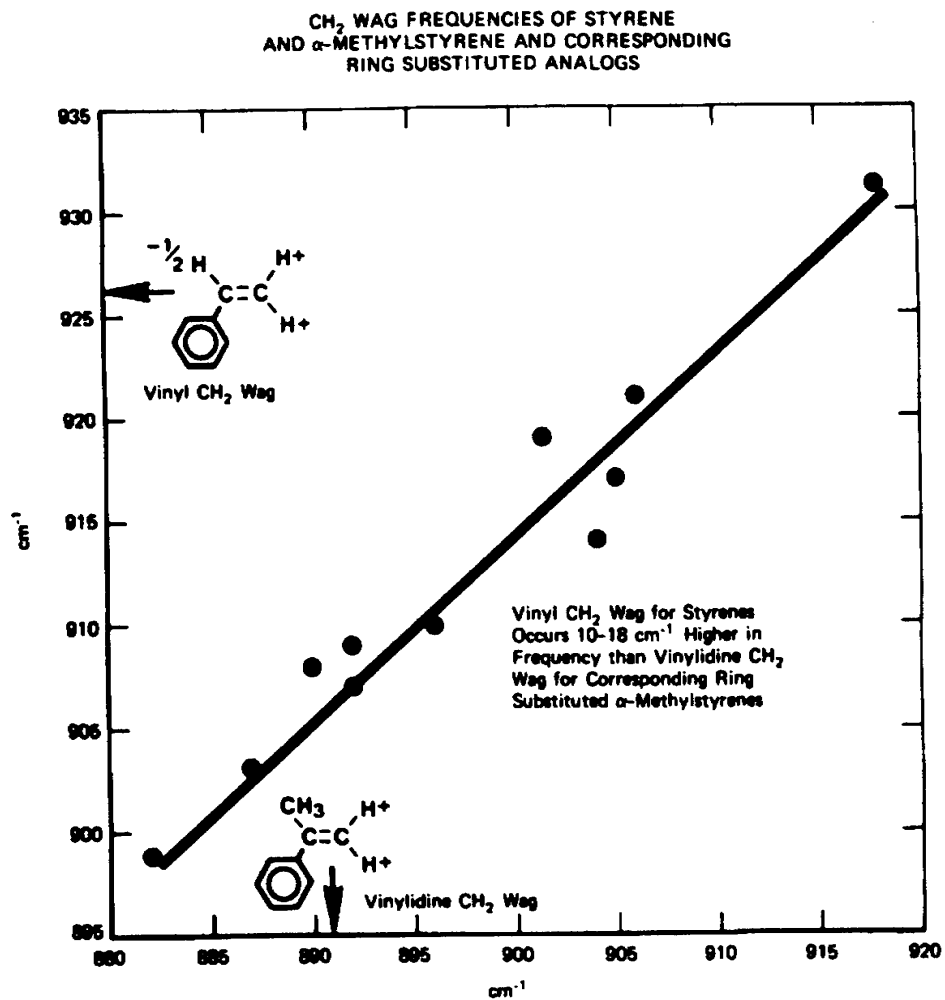


FIGURE 4.5 A plot of the C=CH₂ wag frequencies for styrene and ring-substituted styrenes vs the C=CH₂ wag frequency for α -methyl- α -methylstyrenes.

TABLE 4.1 IR vapor-phase data and assignments for 1-alkenes

Compound	Empirical structure	2(CH ₂ wag)	C=C str.	CH=CH ₂ twist	C=CH ₂ wag	CH=CH ₂ wag	[(A)CH=CH ₂ twist] / [(A)C=CH ₂ wag]	[CH=CH ₂ twist]- [C=CH ₂ wag]	[CH=CH ₂ twist]- [CH=CH ₂ wag]
Propene	CH ₃ CH=CH ₂	1830 (0.122)	1650 (0.123)	991 (0.245)	911 (1.250)	572 (0.100)		80	419
1-Butene	CH ₃ CH ₂ CH=CH ₂	1834 (0.029)	1648 (0.118)	995 (0.150)	911 (0.440)	625 (0.058)	0.341	84	370
4-Methyl-1-pentene	(CH ₃) ₂ CHCH ₂ CH=CH ₂	1835 (0.040)	1645 (0.130)	998 (0.161)	918 (0.350)	627 (0.050)	0.461	80	371
3-Methyl-1-butene	(CH ₃) ₂ CHCH=CH ₂	1830 (0.028)	1643 (0.070)	997 (0.140)	910 (0.285)	660 (0.059)	0.491*	87*	337*
3-Methyl-1-pentene	CH ₃ CH ₂ (CH ₃)CHCH=CH ₂ *	1829 (0.040)	1641 (0.140)	1000 (0.230)	914 (0.389)	671 (0.071)	0.591*	86*	329*
3,4-Dimethyl-1-pentene	(CH ₃) ₂ CH(CH ₃)CHCH=CH ₂ *	1831 (0.021)	1643 (0.068)	1000 (0.110)	916 (0.245)	671 (0.035)	0.449*	84*	329*
3,7-Dimethyl-1-octene	(CH ₃) ₂ CH(CH ₂) ₃ (CH ₃)CHCH=CH ₂	1830 (0.020)	1643 (0.080)	998 (0.095)	914 (0.225)	678 (0.040)	0.422	84	320
3,3-Dimethyl-1-butene	(CH ₃) ₃ CH=CH ₂	1833 (0.020)	1648 (0.091)	1001 (0.096)	915 (0.150)	682 (0.061)	0.641	86	319
3,3-Dimethyl-1-pentene	CH ₃ CH ₂ (CH ₃) ₂ CCH=CH ₂	1831 (0.020)	1648 (0.080)	1008 (0.117)	915 (0.270)	681 (0.050)	0.433	93	327
3,3-Dimethyl-1-hexene	CH ₃ (CH ₂) ₂ (CH ₃) ₂ CH=CH ₂	1830 (0.022)	1643 (0.061)	1005 (0.090)	911 (0.200)	685 (0.050)	0.451	94	320
Vinylcyclohexane	C ₅ H ₁₀ CHCH=CH ₂ *	1830 (0.020)	1641 (0.071)	997 (0.087)	911 (0.141)	653 (0.025)	0.617*	86*	344*
							[(A)CH=CH ₂ twist] / [(A)CH=CH ₂ wag]	[(A)C=CH ₂ wag] / [(A)CH=CH ₂ wag]	[C=CH ₂ wag]- [CH=CH ₂ wag]
Propene	CH ₃ C=CH ₂						2.45	12.5	339
1-Butene	CH ₃ CH ₂ CH=CH ₂						2.59	7.59	286
4-Methyl-1-pentene	(CH ₃) ₂ CHCH ₂ CH=CH ₂						3.22	7.01	291
3-Methyl-1-butene	(CH ₃) ₂ CHC=CH ₂ *						2.37*	4.83*	250*
3-Methyl-1-pentene	CH ₃ CH ₂ (CH ₃)CHC=CH ₂ *						3.24*	5.48*	243*
3,4-Dimethyl-1-pentene	(CH ₃) ₂ (CH ₃)CHCH=CH ₂ *						3.14*	4.83*	245*
3,7-Dimethyl-1-octene	(CH ₃) ₂ CH(CH ₂) ₃ (CH ₃)CHCH=CH ₂						2.38	5.63	236
3,3-Dimethyl-1-butene	(CH ₃) ₃ CCH=CH ₂						1.57	7.01	234
3,3-Dimethyl-1-pentene	CH ₃ CH ₂ (CH ₃) ₂ CH=CH ₂						2.34	5.41	234
3,3-Dimethyl-1-hexene	CH ₃ (CH ₂) ₂ (CH ₃) ₂ CH=CH ₂						1.8	4.01	226
Vinylcyclohexane	C ₅ H ₁₀ CHCH=CH ₂ *						3.48*	5.64*	257*

* New data assigned from Sadtler Collection of IR Vapor Phase Spectra.

TABLE 4.2 The IR vapor-phase frequencies and assignments for the X-CH=CH₂ group

Compounds	a.CH ₂ = str.	s.CH ₂ = str.	CH ₂ = bend	2(C=CH ₂ wag)	C=C str.	CH=CH ₂ twist	C=CH ₂ wag	CH=CH ₂ wag
Acrylonitrile	3135 (0.060)	3055 (0.060)	1425 (0.131)	1918 (0.112)	1626 (0.101)			700 (0.119)
	3122 (0.040)	3045 (0.038)	1411 (0.090)	1911 (0.089)	1613 (0.070)	970 (1.250)	951 (1.250)	680 (0.320)
	3015 (0.059)	3035 (0.040)	1401 (0.124)	1898 (0.101)	1601 (0.078)			659 (0.148)
Divinylsulfone	3110 (0.040)	3035 (0.060)	1389 (0.250)	1942 (0.032)	1620 (0.020)	962 (0.420)	971 (0.565)	715 (0.270)
Allyl alcohol	3082 (0.265)	3002 (0.300)	1415 (0.340)	1855 (0.059)	1652 (0.070)	985 (0.850)	918 (0.875)	552 (0.095)
					1645 (0.077)			
Allyl amine	3082 (0.211)	3002 (0.221)	1414 (0.135)	1841 (0.045)	masked	997 (0.270)	919 (0.620)	551 (0.085)
Allyl cyanide	3099 (0.210)	3040 (0.130)	1421 (0.375)	1870 (0.051)	1650 (0.210)	989 (0.582)	931 (1.250)	558 (0.250)
3-Butenoic acid	3094 (0.064)	2995 (0.154)	1420 (0.080)		1653 (0.106)	970 (0.110)	929 (0.150)	555 (0.201)
Allyl carbamate	3099 (0.051)	3030 (0.030)			1650 (0.052)	992 (0.100)	928 (0.151)	555 (0.079)
Allyl formate	3100 (0.071)		1430 (0.080)	1865 (0.028)	1643 (0.045)	990 (0.151)	934 (0.268)	638 (0.081)
Allyl benzene				1835 (0.061)	1641 (0.239)	991 (0.290)	911 (0.835)	648 (0.211)
Allyl naphthalene				1835 (0.035)	1641 (0.110)	994 (0.100)	915 (0.225)	655 (0.050)
Acrylonitrile	[CN str.]	[a.CH ₂ str.]						
	2240 (0.018)	2942 (0.039)						
Divinylsulfone	[a.SO ₂ str.]	[s.SO ₂ str.]	[a.CSC str.]	[s.CSC str.]	[SO ₂ bend]	[SO ₂ wag]		
	1354 (1.250)	1149 (0.970)	770 (1.040)	715 (0.270)	589 (0.145)	485 (0.185)		
Allyl alcohol	H-O str.	C-O str.						
	3662 (0.285)	1021 (1.250)						
Allyl amine	[a.NH ₂ str.]	[s.NH ₂ str.]	[NH ₂ bend]	[NH ₂ wag]	[a.CH ₂ str.]	[s.CH ₂ str.]	[CH ₂ bend]	
	3420 (0.005)	3355 (0.011)	1635 (0.230)	780 (1.220)	2920 (0.340)	2862 (0.300)	1438 (0.122)	
Allyl cyanide	[CN str.]	[a.CH ₂ str.]	[s.CH ₂ str.]	[CH ₂ bend]	[CH= rock]			
	2262 (0.021)	2941 (0.133)	2840 (0.020)	1439 (0.285)	1290 (0.069)			
3-Butenoic acid	[H-O str.]	[C=O str.]	[COH bend]	[gamma C=O]	[a.CH ₂ str.]			
	3580 (0.390)	1785 (1.040)	1362 (0.230)	640 (0.270)	2940 (0.044)			
Allyl carbamate	[a.NH ₂ str.]	[s.NH ₂ str.]	[C=O str.]	[NH ₂ bend]	[a.NCO str.]	[s.NCO str.]	[C-O str.]	
	3582 (0.111)	3462 (0.119)	1772 (1.139)	1589 (0.410)	1322 (1.245)	1108 (0.300)	1058 (0.481)	
Allyl formate	[C-O str.]	[C-O str.]	[a.CH ₂ str.]					
	1750 (1.240)	1168 (1.250)	2928 (0.290)					
Allyl benzene	[a.CH ₂ str.]	[s.CH ₂ str.]	[CH ₂ bend]	[i.p. o.p. 5H Ring def.]	[o.p. Ring def.]			
	2920 (0.320)	2858 (0.090)	1449 (0.097)	739 (0.770)	698 (1.240)			
1-Allyl naphthalene				[i.p. o.p. 3H Ring def.]	[i.p. o.p.4H Ring def.]			
	2925 (0.110)	2862 (0.040)	1447 (0.060)	785 (0.590)	775 (1.245)			

TABLE 4.2A IR absorbance ratio and assignments for X-CH=CH₂ compounds

Compound	$\frac{[(A)HC=CH \text{ twist}]}{[(A)C=CH_2 \text{ wag}]}$	$\frac{[(A)HC=CH \text{ twist}]}{[(A)CH=CH_2 \text{ wag}]}$	$\frac{[(A)C=CH_2 \text{ wag}]}{[(A)CH=CH_2 \text{ wag}]}$	$\frac{[HC=CH \text{ twist}]-}{[C=CH_2 \text{ wag}]}$	$\frac{[HC=CH \text{ twist}]-}{[CH=CH_2 \text{ wag}]}$	$\frac{[C=CH_2 \text{ wag}]}{[CH=CH_2 \text{ wag}]}$
Acrylonitrile	1	3.91	3.91	19	290	271
Divinylsulfone	0.74	1.56	2.09	9	247	256
Allyl alcohol	0.97	8.94*	9.21*	67	433	366
Allyl cyanide	0.47	2.33	5.01	58	431	373
3-Butenoic acid	0.73	0.55	0.75	41	415	374
Allyl carbamate	0.66	1.27	1.91	64	437	373
Allyl formate	0.56	1.86	3.31	56	352	296
Allyl benzene	0.35	1.37	3.96	80	343	263
Allyl naphthalene	0.44	2	4.51	79	339	260

*exceptionally high value.

TABLE 4.2B Raman data and assignments for X-CH=CH₂ compounds

Compound	C=C str. cm ⁻¹ (A)	a.CH ₂ = str. cm ⁻¹ (A)						
1- Octene	1642 (8)	3081 (1)						
1-Decene	1642 (5)	3081 (1)						
1,2,4-Trivinyl cyclohexane	1641 (9)	3081 (2)						
cis-Crotononitrile	1639 (4)							
trans-Crotononitrile	1629 (5)							
4-Vinyl benzoic acid	1629 (9)							
4-Vinyl benzene sulfonic acid, Na salt	1631 (9)							
2-Vinyl naphthalene	1632 (6)							
4-(Vinyl) phenylacetonitrile	1633 (9)							
2-Vinyl-4,6-diamino-S-triazine	1640 (9)							
Vinyl trimethoxysilane	1603 (3)							
Vinyl tris(betamethoxy ethoxy) silane	1600 (4)							
Divinyl diphenyl silane	1590 (2)							
	C=C str.	C=C str. cis cm ⁻¹ (A)	a.CH ₂ = str. cm ⁻¹ (A)	CH= str. cm ⁻¹ (A)	s.CH ₂ = str. cm ⁻¹ (A)	CH= rock cm ⁻¹ (A)	delta C=C str. cm ⁻¹	(A)C=C str. /(A)C=C str. cis
Vinyl isobutyl ether	1638 (2)	1612 (3)	3122 (1)	3046 (3)	3023 (2)	1322 (7)	26	0.67
Vinyl isoocetyl ether	1638 (1)	1611 (2)	3121 (0)	3046 (2)	3022 (1)	1320 (4)	27	0.5
Vinyl decyl ether	1637 (1)	1611 (2)	3121 (0)	3046 (2)	3022 (1)	1321 (5)	26	0.5
Vinyl dodecyl ether	1638 (0)	1610 (1)	3121 (0)	3046 (2)	3022 (1)	1320 (4)	28	0.5
Vinyl octadecyl ether wk		1610 (0)		3046 (1)		1321 (2)		
Diethyleneglycol divinyl ether	1639 (3)	1620 (4)	3120 (2)	3045 (4)		1323 (9)	19	0.75
1,4-butandiol divinyl ether	1639 (3)	1616 (4)	3120 (1)	3044 (4)	3022 (2)	1322 (9)	23	0.75
Triethylene glycol divinyl ether	1636 (3)	1620 (4)	3120 (2)	3044 (4)		1329 (9)	19	0.75
Vinyl 2-(2-ethoxyethyl) ether	1639 (1)	1620 (2)	3120 (1)	3045 (2)		1323 (4)	19	0.5
Vinyl 4-hydroxybutyl ether	1639 (3)	1617 (4)	3120 (0)	3043 (2)		1322 (9)	22	0.75
Vinyl phenyl ether	1644 (3)	1593 (2)				1311 (2)	51	1.5
Vinyl phenyl sulfone	1607 (2)							
1,3-Diisopropenyl benzene	1631 (8)							

TABLE 4.2C IR vapor-phase data for vinyl alkyl ethers

Vinyl ether	a.CH ₂ str.	CH= str.	s.CH ₂ = str.	C=C str. gauche	C=C str. cis	CH ₂ = bend	CH= rock	CH=CH ₂ twist	C=CH ₂ wag	CH=CH ₂ wag	CH=CH ₂ wag cis	a.C=C-O-C str.	s.C=C-O-C str.	C-O-C bend
Methyl	3139 (0.075)		3023 (0.140)	1655 (0.490)			1335 (0.180)		836 (0.210)			1231 (1.090)	900 (0.180)	600 (0.020)
	3129 (0.080)	3070 (0.055)	3015 (0.171)	1630 (0.890)	1614 (0.640)	1400 (0.040)	1321 (0.240)	962 (0.191)	811 (0.350)	728 (0.035)	701 (0.025)	1220 (1.245)	888 (0.170)	585 (0.015)
	3119 (0.080)		2998 (0.190)		1602 (0.510)		1310 (0.190)	940 (0.115)				1205 (0.944)	874 (0.190)	575 (0.018)
	3139 (0.075)		2997 (0.434)				1330 (0.309)	976 (0.193)	830 (0.279)		700 (0.031)			
	3135 (0.070)	3070 (0.060)	2984 (0.370)	1648 (0.632)	1625 (0.746)		1321 (0.329)	963 (0.245)	812 (0.353)			695 (0.028)	1204 (1.240)	
Ethyl	3129 (0.081)				01611 (0.580)		1311 (0.359)	955 (0.225)			685 (0.031)			
	3125 (0.070)	3060 (0.059)		1640 (0.580)	1620 (0.612)		1321 (0.294)	965 (0.179)	818 (0.229)					
Octadecyl	3124 (0.015)			1641 (0.080)	1613 (0.090)		1323 (0.051)	962 (0.021)	812 (0.038)			1209 (0.140)		
Isobutyl	3125 (0.092)	3061 (0.050)		1645 (0.570)	1618 (0.650)		1320 (0.270)	964 (0.175)	814 (0.245)		700 (0.020)	1209 (1.245)		
2-Ethylhexyl	3130 (0.090)	3060 (0.070)	3015 (0.070)	1640 (0.572)	1612 (0.743)	1417 (0.060)	1321 (0.310)	965 (0.160)	815 (0.250)		700 (0.020)	1204 (1.250)	837 (0.250)	
2-Methoxyethyl	3122 (0.084)	3060 (0.062)		1637 (0.683)	1621 (0.699)		1319 (0.410)	962 (0.280)	824 (0.270)		695 (0.020)	1203 (1.250)		
2-Chloroethyl	3130 (0.041)	3070 (0.021)		1642 (0.520)	1628 (0.629)		1319 (0.231)	961 (0.165)	825 (0.186)		687 (0.082)	1204 (1.230)		
Bis[2-(vinyloxy)ethyl]ether	3130 (0.062)	3060 (0.030)		1640 (0.590)	1618 (0.605)	1418 (0.060)	1320 (0.320)	965 (0.180)	820 (0.210)		698 (0.020)	1205 (1.240)		

TABLE 4.3 CH₂= wag frequencies vs (sigma ρ -sigma') for group G

Group G	C=CH ₂ wag	
	CS ₂ soln.	(sigma ρ -sigma')
CO ₂ H	970	
CF ₃	965	0.14
(C=O)OCH ₃	964	
(C=O)NH ₂	964	
(C=O)OC ₂ H ₅	961	0.2
CN	960	0.07
(C=O)CH ₃	960	0.25
Si(CH ₃) ₃	949	0.11
CHCl ₂	937	
CH ₂ Cl	929	0.01
R	908	-0.13
I	905	-0.1
Br	898	-0.22
Cl	894	-0.24
CH ₃ (C=O)O	873	
F	863	-0.44
C ₆ H ₅ O	851	-0.41
CH ₃ O	813	-0.5

TABLE 4.3A IR carbon disulfide solution data for the CH=CH twist frequency for compounds of form G-CH₂CO₂H vs σ' of G and pK_a of G-CH₂CO₂H

Group G	twist CS ₂ soln. cm ⁻¹	HC=CH ₂ twist		σ' of G
		vapor phase cm ⁻¹	pK _a of G-CH ₂ CO ₂ H	
(CH ₃) ₃	1009			-0.12
(CH ₃) ₃ C	999			-0.07
(CH ₃) ₂ CH	996		4.78	-0.056
(CH ₃)CH ₂	990		4.82	-0.052
CH ₃	986		4.88	-0.045
C ₆ H ₅	989		4.26	0.101
4-Cl-C ₆ H ₄	983		4.19	
ClCH ₂ [gauche conformer]	983	[995.5; 987.7]	4.08	0.17
ClCH ₂ [cis conformer]		982.6		
ICH ₂ [gauche conformer]	982	[990.6; 980.6]	4.06	
BrCH ₂ [gauche conformer]	981	987.5	4.01	
R(C=O)NH	972		3.65	
CH ₃ O	963		3.53	0.23
CN	960	970	2.44	0.58
C ₆ H ₅ O	944		3.13	0.38
I	943		3.15	0.38
Br	936	941	2.87	0.45
Cl	938	941	2.86	0.47
F	~925	929	2.68	0.5

TABLE 4.4 IR data and assignments for the *cis* and *gauche* conformers of allyl halides

Allyl fluoride	Allyl chloride	Allyl bromide	Allyl iodide	Assignment
1630	1642.7	1638.4	1631.8	<i>gauche</i> C=C str.
1651.7	1649	1647	1645	<i>cis</i> C=C str.
989.3	985.2	983.9	980.9	<i>gauche</i> CH=CH ₂ twist
935	937	935	932	<i>gauche</i> C=CH ₂ wag
925				<i>cis</i> C=CH ₂ wag
642.3	590	537.7	491.2	<i>gauche</i> CH=CH ₂ wag
552.1	549.4		540	<i>cis</i> CH=CH ₂ wag
48.3	48.2	48.9	48.9	[<i>gauche</i> CH=CH ₂ twist]- [<i>gauche</i> C=CH ₂ wag]
347	395.2	446.2	489.7	[<i>gauche</i> CH=CH ₂ twist]- [<i>gauche</i> CH=CH ₂ wag]
292.7	347	397.3	440.8	[<i>gauche</i> C=CH ₂ wag]- [<i>gauche</i> CH=CH ₂ wag]

TABLE 4.5 IR data and assignments for cyclopentene, cyclohexene, 1,4-cyclohexadiene, and 1,3-cyclohexadiene [C=C and (C=C)₂ stretching]

Mole % CHCl ₃ /C ₅ H ₈	C=C str.	Mole % CHCl ₃ /C ₆ H ₁₀	C=C str.	Mole % CHCl ₃ /1,4-C ₆ H ₈	i.p. C=C str.	o.p. C=C str.	Mole % CDCl ₃ /1,3-C ₆ H ₈	o.p. C=C str.	i.p. C=C str.
0	1613.9	0	1652.8	0	1672.3	1639.2	0	1603.3	1577.9
51.6	1612.2	52.5	1651.9	50.8	1674.3	1638.6	50.7	1605.4	1577.5
91.4	1611.2	92.5	1650.9	91.9	1676.8	1637.9	92	1608	1577.1
[delta cm ⁻¹]	[-2.7]		[-1.9]		[4.5]	[-1.3]		[4.7]	[-0.8]

TABLE 4.5A IR vapor-phase data and assignments for *cis*-cycloalkene derivatives

Compound	a.CH ₂ = str.	a.CH ₂ str.	a.CH ₂ str.	s.CH ₂ str.	C=C str.	CH ₂ bend	<i>cis</i> HC=CH wag	<i>cis</i> HC=CH wag
Cyclopentene	3070 (0.320)	2964 (0.950)	2920 (0.800)	2864 (0.620)	1621 (0.048)	1449 (0.050)	720 (0.179) 699 (0.595) 678 (0.199)	649 (0.095)
5-Norbornene-2- carbonitrile	3042 (0.110)		[CN str.] 2245 (0.050)		1635 (0.020)	1454 (0.050)	721 (0.445)	
Cyclohexene	3032 (0.410)	2935 (1.250)		2865 (0.550)	1651 (0.050)	1463 (0.191)	732 (0.065) 719 (0.200) 701 (0.060)	657 (0.160) 635 (0.244) 615 (0.095)
4-Methylcyclo- hexene	3035 (0.400)				1651 (0.045)		728 (0.050)	658 (0.240)
2-Cyclopentene- 1-one	3075 (0.041)	2980 (0.060)	2940 (0.120)	2875 (0.030)	1600 (0.030)	1440 (0.041)	750 (0.230)	1745 (1.230)
2-Cyclohexene- 1-one	3042 (0.110)	2942 (0.439)		2890 (0.150)	1624 (0.030)	1430 (0.100)	730 (0.160)	1710 (1.230)

TABLE 4.6 IR C=O stretching frequency data for alkyl acrylates [CHCl₃ and CCl₄ solutions]

Mole % CHCl ₃ /CCl ₄	Methyl acrylate C=O str.	2-Hydroxy- butyl acrylate C=O str.	Allyl acrylate C=O str.	2- Hydroxy- propyl acrylate C=O str.	Butyl acrylate C=O str.	2-Ethyl- hexyl acrylate C=O str.	tert-Butyl acrylate C=O str.
[vapor]	1751				1741		
0	1734.1	1730.6	1730.5	1729.4	1727.3	1727.1	1722.9
100	1724.5	1721.6	1727.1	1721.3	1716.7	1716.3	1713.8
[delta cm ⁻¹]	16.9; 26.5; 9.6	9	3.4	8.1	13.8; 24.3; 10.6	10.8	9.1
	s-trans C=C str.	s-trans C=C str.	s-trans C=C str.	s-trans C=C str.	s-trans C=C str.	s-trans C=C str.	s-trans C=C str.
0	1635.3	1636.5	1635.4	1637	1637.2	1635.7	1635.6
100	1635.1	1636.1	1635.4	1636.6	1635.8	1636.3	1635.8
[delta cm ⁻¹]	-0.2	-0.4	0	-0.4	-1.4	0.6	0.2
	s-cis	s-cis	s-cis	s-cis	s-cis	s-cis	s-cis
0	1620.4	1619.3			1619.7		1619.2
100	1619.9				1619.2		1618.5
[delta cm ⁻¹]	-0.5				-0.5		-0.7
	CH ₂ = bend	CH ₂ = bend	CH ₂ = bend	CH ₂ = bend	CH ₂ = bend	CH ₂ = bend	CH ₂ = bend
0		1406.4	1404.6	1406.6	1407.2	1406.5	1401.6
100		1409.4	1407	1409.5	1410.3	1409.9	1404
[delta cm ⁻¹]		3	2.4	2.9	3.1	3.4	2.4
	HC=CH twist	CH=CH twist	CH=CH twist	CH=CH twist	CH=CH twist	CH=CH twist	CH=CH twist
0	984.9	982.6	984.7	983.3	983.5	983.6	984.5
100	985	983.4	984.4	983.9	984.3	984.5	985.6
[delta cm ⁻¹]	0.1	0.8	-0.3	0.6	0.8	0.9	1.1
	C=CH ₂ wag	C=CH ₂ wag	C=CH ₂ wag	C=CH ₂ wag	C=CH ₂ wag	C=CH ₂ wag	C=CH ₂ wag
0	968.1	982.6			968.4		966.3
100	970.3	983.4			969		966.5
[delta cm ⁻¹]	2.2	0.8			0.6		0.2

TABLE 4.7 IR vapor-phase data for trans-alkenes

trans Alkenes	CH=CH str.	a.CH ₂ str.	a.CH ₂ str.	s.CH ₃ str.	s.CH ₂ str.	C=C str.	a.CH ₃ def.	s.CH ₃ def.	HC=CH twist	(A)[a.CH ₃ def.] / (A)[HC=CH twist]	(A)[C=C str.] / (A)[CH=CH twist]
2-Butane	3035 (0.310)	2981 (0.600)	2942 (1.250)	2982 (0.325)	2982 (0.325)	inactive	1447 (0.150)	1392 (0.080)	961 (0.455)	0.33	0
2-Pentene	3030 (0.283)	2997 (1.235)	2942 (0.440)	2980 (0.568)		?	1460 (0.210)	1390 (0.070)	961 (0.375)	0.56	0
2-Hexene	3021 (0.179)	2965 (1.240)	2940 (1.040)	2890 (0.440)	2880 (0.540)	?	1460 (0.169)	1390 (0.330)	965 (0.330)	0.51	0
3-Hexene	3035 (0.095)	2970 (1.240)	2950 (0.530)	2910 (0.332)	2890 (0.362)	inactive	1461 (0.080)	1385 (0.031)	969 (0.220)	0.36	0
4-Octene	3020 (0.160)	2965 (1.250)	2935 (1.150)	2880 (0.600)	2880 (0.600)	inactive	1460 (0.150)	1385 (0.080)	964 (0.250)	0.61	0
5-Decene	3020 (0.120)	2968 (1.115)	2940 (1.245)	2880 (0.512)	2865 (0.512)	1635 (0.025)?	1466 (0.151)	1385 (0.070)	969 (0.211)	0.72	0.12?
2,2-Dimethyl-3-hexene	3030 (0.090)	2975 (1.245)	2920 (0.315)	2888 (0.275)	2888 (0.275)		1478 (0.120)	1370 (0.100)	971 (0.110)	0.93	0
2,2-Dimethyl-3-heptene	3030 (0.093)	2970 (1.240)	2940 (0.566)	2880 (0.365)	2880 (0.365)		1476 (0.130)	1390 (0.046) 1370 (0.134)	972 (0.158)	0.82	0
2-Butene-1-ol	3030 (0.275) [H-O str.] 3670 (0.130)	2982 (0.630) [C-O str.] 1004 (1.240)	2940 (0.850)	2982 (0.630)	2982 (0.630)	1675 (0.085)	1476 (0.270)	1385 (0.750)	970 (0.975)	2.08	0.09
[Crotonate]						[C=O str.] 1754 (1.229)					
methyl						1750 (1.219) 1741 (1.229) 1745 (1.050)	1663 (0.299)		970 (0.210)		1.42
ethyl						1745 (0.950) 1740 (1.050) [C.T.]	1665 (0.271)		971 (0.244)		1.1
1,2-Dichloroethylene	3080 (0.210)					1661 (0.092) 1654 (0.081) 1641 (0.110)	inactive 815 (1.250)		910 (0.255) 897 (0.450) 880 (0.290)		0
1,3-Dichloropropene						1631 (0.510)	[=C-Cl str.] 775 (1.245)	[C-Cl str.] 691 (0.570)	930 (0.356)		1.43
beta-Bromostyrene						1668 (0.060)	[=C-Br str.] 740 (1.245)		938 (0.442)		0.14
Cinnamionitrile	1265 (0.071)	1201 (0.092)	i.p. o.p. 5H Ring def. 741 (1.240)	[o.p. Ring def.] 689 (0.640)	[CN str.] 2224 (0.335)	1621 (0.379) 1649 (0.050)			960 (0.862)		0.44 0.06
beta-Bromostyrene		1220 (0.271)	732 (0.910)	690 (0.452)							

? not observed.

TABLE 4.8 IR data for the CH=CH twist frequency for trans disubstituted ethylenes

trans disubstituted ethylene XCH=CY X, Y	CH=CH twist cm ⁻¹
R,R'	962-966
O, CH ₃	959
C ₆ H ₅ , C ₆ H ₅	958
CH ₃ , (CH ₃)CH-O-	964-967
CH ₂ X', CH ₂ X'	960-965
C ₆ H ₅ , CH ₂ -O-	964-966
C ₆ H ₅ , CN	964-967
CH ₃ , CN	953
C ₆ H ₅ , CN	962
Cl, CH ₃	926
Cl, CH ₂ Cl	931
Br, CH ₂ Br	935
Cl, CH ₂ -O-	925-932
Cl, C ₆ H ₅	930-942
Cl, CN	920
Cl, B(OH) ₂	960
CH ₃ O, CH(OCH ₃) ₂	929
Cl, Cl	892
Br, Br	896
CH ₃ , (C=O)H	964
CH ₃ , (C=O)CCH	967
CH ₃ , CO ₂ H	966
CH ₃ , (C=O)OC ₂ H ₅	968
CH ₃ , (C=O)N(CH ₃) ₂	966
C ₆ H ₅ , (C=O)CH ₃	972
C ₆ H ₅ , (C=O)C ₆ H ₅	975
C ₆ H ₅ , (C=O)H	972
C ₆ H ₅ , CO ₂ H	976
C ₆ H ₅ , (C=O)OR	976
RO(C=O), (C=O)OR	976
4-ClC ₆ H ₄ , CO ₂ H	975

TABLE 4.9 IR data for the =CH₂ wag and its overtone for 1,1-disubstituted ethylenes

Cinnamate	C=O str.	C=C str.	[(A)C=C] / [(A)C=O]	HC=CH twist	[(A)HC=CH twist] / [(A)C=C str.]	[(A)C=CH twist] / [(A)C=O str.]
Methyl	1740 (1.141)	1640 (0.431)	0.38	975 (0.181)	0.42	0.16
Ethyl	1735 (1.050)	1640 (0.370)	0.35	975 (0.169)	0.46	0.16
Butyl	1731 (1.141)	1641 (0.379)	0.33	978 (0.205)	0.54	0.18
Isobutyl	1735 (0.806)	1641 (0.310)	0.38	975 (0.130)	0.42	0.16
Isopentyl	1737 (0.830)	1642 (0.282)	0.34	980 (0.171)	0.61	0.21
Isopropyl	1731 (1.250)	1641 (0.500)	0.41	982 (0.310)	0.62	0.25
Tert-butyl	1727 (1.030)	1640 (0.370)	0.36	972 (0.247)	0.67	0.24
Cyclohexyl	1731 (0.654)	1642 (0.214)	0.33	980 (0.129)	0.6	0.2
Benzyl	1739 (0.959)	1640 (0.371)	0.39	980 (0.246)	0.66	0.26

TABLE 4.10 A comparison of the fundamentals for 1,1-dihaloethylenes

Cinnamyl	C=O str.	C=C str.	CCO str.	COC str.	HC=CH twist			
Acetate	1763 (0.740)	1652 (0.035)	1229 (1.240)	1026 (0.295)	962 (0.240)			
Butyrate	1754 (0.950)	1660 (0.011)	1170 (1.240)		968 (0.225)			
Isobutyrate	1753 (1.042)	1655 (0.020)	1155 (1.230)		968 (0.292)			
	[a.CH ₃ str.]	[s.CH ₃ str.]	[a.CH ₃ def.]	[s.CH ₃ def.]	[i.p. o.p. 5H def.]	[op. Ring def.]	[a.CH ₂ str.]	[s. CH ₂ str.]
Acetate	2955 (0.080)	2895 (0.025)	1451 (0.082)	1366 (0.235)	740 (0.140)	689 (0.130)		
Butyrate	2975 (0.210)	2885 (0.085)	1451 (0.080)	1380 (0.075)	740 (0.100)	690 (0.095)	2945 (0.195)	2885 (0.085)
Isobutyrate	2982 (0.330)	2890 (0.080)	1475 (0.130)	1391 (0.100)	742 (0.130)	691 (0.120)	2958 (0.159)	2890 (0.080)
							[CH ₂ bend]	
							1453 (0.092)	
	[(A)C=C str.] /[(A)C=O str.]	[(A)HC=CH twist] /[(A)C=C str.]	[(A)HC=CH twist] /[(A)C=O str.]	[C=O str.]- [CCO str.]	[(A)C=O str.] /[(A)CCO str.]	[C=C str.]- [HC=CH twist]		
Acetate	0.05	6.9	0.32	534	0.59	690		
Butyrate	0.01	20.5	0.24	584	0.77	692		
Isobutyrate	0.02	14.6	0.28	598	0.85	687		

TABLE 4.11 IR vapor-phase data and assignments for alkyl cinnamates [C=C stretching, CH=CH twisting, and C=O stretching]

1,1-Substituted ethylene XYC=CH ₂ X, Y	C=CH ₂ wag CS ₂ soln. cm ⁻¹	2(C=CH ₂ wag) CCl ₄ soln. cm ⁻¹
R, R'	885-890	1785-1795
CH ₃ , C ₆ H ₅	885-890	1785-1805
CH ₃ , 2,3-Cl ₂ -C ₆ H ₃	905	1820
CH ₃ , CH ₂ Cl	902	1820
C ₆ H ₅ , CH ₂ Cl	907	1820
CH ₃ , CH ₂ OH	893	1792
CH ₃ , CH(OH)CN	914	1840
CH ₃ , Cl	875	1765
C ₆ H ₅ , Cl	877	1768
Cl, Cl	867	1744
Br, Br	877	1765
F, F	804 v.p.	1613 v.p.
Cl, CH ₂ Cl	891	1788
Br, CH ₂ Br	896	1802
Cl, CH ₂ OC ₆ H ₅	887	
Cl, N=C=N	897	1811
Br, CF ₃	929	
CH ₃ , O(C=O)CH ₃	869	
CH ₃ , OCH ₃	795	1600
C ₂ H ₅ O, OC ₂ H ₅	711	
CH ₃ , (C=O)OR	939	1882
C ₅ H ₁₁ , (C=O)OCH ₃	939	1888
CH ₃ , (C=O)OH	947	1905
C ₅ H ₁₁ , (C=O)OH	947	1898
CH ₃ , (C=O)R	930	1865
C ₂ H ₅ , (C=O)CH ₃	931	1870
Cl, CO ₂ H	933	1878
Cl, (C=O)OR	925	1860
CH ₃ , CN	930	1878
Cl, CN	916	1843
CN, CN	985	1970
C ₂ H ₅ SO ₂ , C ₂ H ₅ SO ₂	1004	2020

TABLE 4.11A IR vapor-phase data and assignments for cinnamyl esters

CH ₂ =CCl ₂ cm ⁻¹	CH ₂ =CBrCl cm ⁻¹	CH ₂ =CBr ₂ cm ⁻¹	Assignment cm ⁻¹
3130	3140	3112	asym. CH ₂ = str.
3035	3046	3027	sym. CH ₂ = str.
1616	1609	1601	C=C str.
1391	1383	1364	CH ₂ = bend
1088	1074	1070	CH ₂ = rock
788	765	698	asym. CX ₂ = str.
601	531	474	sym. CX ₂ = str.
375	336	324	CX ₂ = rock
299	240	182	CX ₂ = bend
874	872	[881] (*1)	CH ₂ = wag
686	684	[675] (*2)	CH ₂ = twist
458	427	[404] (*2)	CX ₂ = wag

*¹ Unpublished Dow Chemical Company data.*² Reference 5.

TABLE 4.12 Raman data and assignments for vinyl esters of carboxylic acids

Vinyl	C=O str.		C=C str.		C=O str.- C=C str.	
	RI	RI	RI	RI	RI C=O str. /RI C=C str.	RI C=O str. /RI C=C str.
Propionate	1756	1	1648	9	108	0.11
Butyrate	1758	1	1648	4	110	0.25
Deconate	1759	1	1648	6	111	0.17
2-Ethylhexanoate	1753	2	1647	9	108	0.22
Neodecanoate	1748	2	1647	8	101	0.13
tert-Nonanoate	1744	2	1646	9	98	0.22
Pivalate	1749	2	1647	7	102	0.29
Adipate, di	1752	2	1648	9	104	0.22
Sebacate, di	1755	2	1648	9	107	0.22
Acrylate	1740	4	1648	5	92	0.81
2-Butenoate	1734	2	1644	9	90	0.22
2-Furoate	1734	2	1648	1	86	2
Cinnamate	1720	0.5	1636	9	84	0.06
Benzoate	1732	3	1647	2	85	1.5

TABLE 4.14 IR group frequency data for styrene and substituted styrenes

Compound	2(C=CH ₂ wag) cm ⁻¹	C=C str. cm ⁻¹	CH=CH twist CS ₂ soln. cm ⁻¹	C=CH ₂ wag CS ₂ soln. cm ⁻¹	CH=CH twist minus C=CH ₂ cm ⁻¹	pK _a of corresponding sub. phenol
Styrene	1821	1632	989	907	82	9.9
Styrene sub.						
4-Methyl	1812	1631	987	903	84	10.35
4-Bromo	1826	1631	986	909	77	9.34
4-Chloro	1815	1628	982	904	78	9.2
4-fluoro	1825 [vp]	1638 [vp]	990 [vp]	911 [vp]	79	9.95
4-Cyano	1833 [CS ₂]	1627 [CS ₂]	982	917	65	
3-Chloro	1831	1631	986	913	73	8.93
3-Hydroxy	1815	1629	984	905	79	9.33
3-Chloromethyl	1832	1637	987	909	78	
3-Acetyl	1828	1637	987	910	77	9.18
3,4-Dichloro	1824	1626	980	910	70	8.4
3,4-Dimethyl	1817	1628	989	903	86	10.17
3,5-Dimethyl	1808	1626	984	903	81	10.1
2,4-Dimethyl	1821	1626	987	907	80	10.49
2-Chloro	1833	1629	986	914	72	8.5
2-Bromo	1835	1629	984	916	68	8.43
2-Methyl	1832 [vp]	1630 [vp]	989 [vp]	914 [vp]	75	10.28
2,3-Dichloro	1842	1626	986	919	67	7.4
2,4-Dichloro	1832	1623	983	917	66	7.8
2,5-Dichloro	1842	1624	986	921	65	7.3
2,6-Dichloro	1872	1637	981	932	49	6.8
2,3,6-Trichloro	1876	1631	978	935	43	6.1
2,4,5-Trichloro	1876	1631	978	933	45	6.4
2,3,4,5-Tetrachloro	1858	1627	974	925	49	7
2,3,4,6-Tetrachloro	1883	1633	978	937	41	5.22
2,3,4,5,6-Pentachloro	1883	1631	975	936	39	4.77
2,4,6-Trimethyl	1843	1632	991	919	72	10.83

TABLE 4.15 IR group frequency data for α -halostyrenes, α -methylstyrenes, and related compounds

Compound	2(CH ₂ wag) CCl ₄ soln. cm ⁻¹	C=C str. CCl ₄ soln. cm ⁻¹	CH ₂ = wag CS ₂ soln. cm ⁻¹
Styrene			
alpha-(X)			
X			
Chloro	1760	1626	877
Bromo	1775	1617	882
Propyl	1801	1629	897
Phenyl	1809	1616	896
2-Hydroxyethyl	1799	1627	897
α -Methylstyrene	1797	1629	892
Sub.			
4-Chloro	1790	1627	890
4-Bromo	1789	1623	892
4-Hydroxy	1772	1630	882
4-Acetyl	1795	1626	897
4-Methyl	1783	1629	887
3,4-Dichloro	1802	1634	896
3,5-Dichloro	1810	1629	899
4-Chloro, 3-methyl	1790	1631	892
2-Hydroxy	1822	1632	911
2-Chloro	1810	1642	904
2,3-Dichloro	1805	1640	902
2,4-Dichloro	1819	1642	905
2-Chloro, 5-methyl	1814	1642	902
2-Nitro	1822	1643	902
2,4,5-Trimethyl	1803	1642	899
2,3,4,5,6-Pentafluoro	1830	1645	918
1-Isopropenylnaphthalene	1815	1634	904
1-Isopropenylpyridine	1815	1634	904

TABLE 4.16 IR vapor-phase data for butadienes and propadienes

Compound	a.CH ₂ str.	CH= str.	a.CH ₂ = str.	2(CH ₂ wag)	i.p. (C=C) ₂ str.	o.p. (C=C) ₂ str.	CH ₂ = bend	Compound	i.p. and o.p. CH=CH ₂ twist	C=CH ₂ wag	RC=CH ₂ wag	CH=CH ₂ wag	RC=CH ₂ wag	
1,3- Butadiene	3102 (0.130)	3030 (0.100)	3000 (0.120)	1830 (0.110) 1822 (0.060) 1810 (0.090)	1648 (0.010)	1604 (0.190) 1594 (0.130) 1585 (0.165)	1390 (0.032) 1379 (0.028) 1369 (0.035)	1,3-Butadiene	1011 (0.240) 995 (0.200)	908 (1.250)		518 (0.060)		
2-Methyl- 1,3-butadiene or Isoprene	3099 (0.380)	3030 (0.185)	2990 (0.430)	1802 (0.120)	1649 (0.060)	1602 (0.420)	1375 (0.100)	2- Methyl- 1,3- butadiene	990 (0.371)	907 (1.130)	895 (1.240)		758 (0.020)	
Propadiene or Allene	3100 (0.030) perpendicular		3020 (0.090) 3010 (0.060) 2995 (0.070)	1700 (0.098) 1690 (0.087) 1681 (0.097)	IR inactive al	1972 (1.250) 1953 (0.590) 1942 (0.860)	1409 (0.080) 1397 (0.060) 1378 (0.100)	Propadiene	1040 (0.060) perpen- dicular v9 (e)	845 (0.690) perpen- dicular v10 (e)				
	v8 (e)		parallel, vb (b2)	parallel		parallel, v6 (b2)	parallel, v7 (b2)							
1,2-Butadiene or 1-Methyl- propadiene	3080 (0.231)	3010 (0.690)		1802 (0.120)	1081 (0.091) 1072 (0.082) 1063 (0.100)	1970 (0.590) 1962 (0.540) 1959 (0.550)		1,2-Butadiene	910 (0.256)	859 (1.240) 849 (0.935) 839 (0.949)	-1175 (0.020)	[CH= bend] [CH ₃ C=C bend]?	560 (0.182) 552 (0.160) 544 (0.200) C=C=C bend (a')	C=C=C bend (a)
1-Chloro-propadiene*	3079	3079?	3009		1101	1963	1435	1-Chloro- propadiene	999	875	822	767	548	
1-Bromo-propadiene*	3080	3008?	3005		1078	1961	1432	1-Bromo- propadiene	1000	862	813	681	519	
1-Iodo-propadiene*	3070	3070?	3004		1076	1953	1425	1-Iodo- propadiene	995	854	807	609	485	
	C=C-X str.	C=C=C bend (a')	C=C=C bend (a)	C=C-X bend (a')	C=C-X (a)									
1-Chloro-propadiene	767	592	548	494	184*1									
1-Bromo-propadiene	681	603	519	423*2	169*1									
1-Iodo-propadiene	609	625	485	387*1	154*1									
	o.p. cis (HC=CH) ₂ str.	i.p. cis (HC=CH) ₂ str.	i.p. (C=C) ₂ str.	o.p. (C=C) ₂ str.	cis (HC=CH) ₂ i.p. wag	cis (CH=CH) ₂ o.p. wag	C=O str.							
2,5-Norbormadiene	3130 (0.115)	3080 (0.285)	1641 (0.020) 1639 (0.010) 1630 (0.010)	1559 (0.100) 1546 (0.160) 1535 (0.090)	666 (0.225) 654 (0.570) 643 (0.285)	740 (0.370) 728 (1.110) 711 (0.330)								
2,5- Norbor- nadiene-7-yl acetate	3080 (0.111)		1651 (0.040)	1543 (0.154)	654 (0.090)	735 (0.265)	1759 (0.750)							
1,3-Cyclohexadiene	3080 (0.790)		1600 (0.030)	1701 (0.040)	748 (0.190)	658 (1.240)								

* Reference 18.

TABLE 4.17 IR vapor-phase data for carbon hydrogen stretching vibrations and other vibrations for 1-alkenes

Compound	2(C=CH ₂ wag) + s.CH ₃ bend	a.CH ₂ = str.	s.CH ₂ = str.	a.CH ₃ str.	a.CH ₂ str.	s.CH ₃ str.	s.CH ₂ str.	a.CH ₃ bend (A)	Compound	a.CH ₃ bend (A')	CH ₂ bend	CH ₂ = bend	s.CH ₃ bend	s.CH ₃ bend	C-C str.?	CH ₂ wag	CH ₂ rock
Propene		3080 (0.170)	3000 (0.320)	2960 (0.580)		2920 (0.300)		1475 (0.110)	Propene	1443 (0.220)			1399 (0.079)				
1-Butene	3182 (0.005)	3085 (0.211)		2975 (1.245)		2900 (0.420)	2880 (0.300)	1462 (0.129)	1-Butene	1432 (0.129)			1380 (0.090)			1307 (0.109)	800 (0.020)
3-Methyl-1-butene	3190 (0.010)	3084 (0.180)		2964 (1.245)	2930 (0.300)		2890 (0.300)	14865 (0.111)	3-Methyl-1-butene				1380 (0.096)			1305 (0.050)	
3-Methyl-1-pentene	3180 (0.020)	3084 (0.275)		2970 (1.240)	2930 (0.871)		2885 (0.585)	1461 (0.200)	3-Methyl-1-pentene			1421 (0.090)	1387 (0.140)			1290 (0.050)	782 (0.020)
3,4-Dimethyl-1-pentene	3190 (0.010)	3082 (0.150)		2965 (1.245)	2940 (0.370)		2882 (0.464)	1463 (0.140)	3,4-Dimethyl-1-pentene			1422 (0.040)	1380 (0.131)				
3,7-Dimethyl-1-octene	3199 (0.010)	3090 (0.131)		2970 (1.235)	2940 (0.835)		2882 (0.452)	1469 (0.240)	3,7-Dimethyl-1-octene			1423 (0.040)	1385 (0.110)		1170 (0.020)		734 (0.011)
3,3-Dimethyl-1-butene		3100 (0.142)		2970 (1.250)			2890 (0.250)	1472 (0.110)	3,3-Dimethyl-1-butene			1421 (0.070)	1380 (0.119)	1370 (0.173)	1214 (0.080)		
3,3-Dimethyl-1-pentene	3200 (0.005)	3095 (0.149)	3009 (0.061)	2980 (1.245)			2892 (0.200)	1470 (0.115)	3,3-Dimethyl-1-pentene			1420 (0.068)	1381 (0.103)	1369 (0.098)	1185 (0.032)		
3,3-Dimethyl-1-hexene	3205 (0.005)	3095(0.110)	3008 (0.080)	2970 (1.245)	2940 (0.440)	2905 (0.290)	2885 (0.340)	1470 (0.110)	3,3-Dimethyl-1-hexene			1420 (0.050)	1380 (0.071)	1370 (0.080)	1200 (0.030)		
Vinylcyclohexane* ¹		3082 (0.091)	3000 (0.080)		2935 (1.250)		2862 (0.460)				1454 (0.121)	1415 (0.030)					

*¹ [Ring breathing, 840 (0.012)].

TABLE 4.18 IR data and assignments for the alkyl group of vinyl alkyl ethers

Vinyl alkyl ether	a.CH ₃ str.	s.CH ₃ str.	a.CH ₃ bend	CH ₃ rock									
Methyl		2870 (0.100)		1145 (0.260)	1024 (0.186)								
		2958 (0.310)	2860 (0.095)	1460 (0.152)	1136 (0.190)	1011 (0.175)							
		2930 (0.240)	2850 (0.110)		1127 (0.210)	997 (0.171)							
		a.CH ₃ str.	a.CH ₂ str.	s.CH ₃ str.	s.CH ₂ str.	a.CH ₃ bend	s.CH ₃ bend	CH ₂ wag and or C—C str.	CH ₂ twist	CH ₃ rock and or C—C str.	CH ₂ rock	C—Cl str.	C—Cl str.
						1319 (0.225)							
Ethyl	2997 (0.434)	2940 (0.270)	2900 (0.260)	1476 (0.087)	1388 (0.200)	1128 (0.481)	1079 (0.226)	1059 (0.271)					
Butyl	2984 (0.370)				1377 (0.210)								
	2971 (0.790)	2950 (0.690)	2894 (0.410)	1476 (0.135)	1379 (0.190)	1135 (0.249)	1083 (0.270)	1030 (0.177)					
Isobutyl	2965 (0.840)	2925 (0.392)	2897 (0.376)	1475 (0.200)	1388 (0.195)	1145 (0.232)	1080 (0.280)	1019 (0.310)					
2-Ethylhexyl	2970 (1.245)	2938 (1.245)	2882 (0.640)	1470 (0.250)	1380 (0.180)		1079 (0.266)	1015 (0.164)	735 (0.035)				
2-Methoxyethyl	2995 (0.322)	2930 (0.902)	2890 (0.555)	2830 (0.327)	1462 (0.185)	1360 (0.185)	1135 (1.150)	1095 (0.560)	1039 (0.250)				
									1013 (0.145)				
2-Chloroethyl		2980 (0.105)		2895 (0.065)	1466 (0.060)	1377 (0.100)		1086 (0.240)	1010 (0.138)	764 (0.170)	687 (0.082)?		
									1001 (0.142)	and CH=CH ₂ wag?			
Bis[2-(vinyloxy) ethyl]ether		2938 (0.291)		2880 (0.256)	1460 (0.090)	1359 (0.140)	1140 (0.970)	1092 (0.350)	1010 (0.165)				
									980 (0.200)				

Alkynes and Compounds Containing $C\equiv C$ Groups

Terminal $C\equiv CH$	93
1-Halopropynes	95
Phenylacetylene in Various Solutions	96
1,4-Diphenylbutadiyne	97
Propargyl Alcohol vs Propargyl Fluoride	98
1,3-Dihalopropynes	98
Phenylacetylene and Phenylacetylene-1d	99
References	99

Figures

Figure 5-1	100 (95)
Figure 5-2	101 (96)
Figure 5-3	101 (97)
Figure 5-4	102 (97)
Figure 5-5	102 (97)
Figure 5-6	103 (98)
Figure 5-7	104 (98)
Figure 5-8	105 (99)

Tables

Table 8-1	106 (93)
Table 5-2	107 (94)
Table 5-3	108 (94)
Table 5-4	109 (95)
Table 5-4a	109 (95)
Table 5-5	109 (97)
Table 5-6	110 (97, 98)
Table 5-7	111 (98)
Table 5-8	112 (98)
Table 5-9	113 (99)

*Numbers in parentheses indicate in-text page reference.

TERMINAL $C\equiv CH$

Table 5.1 lists IR data and assignments for compounds containing the terminal acetylenic group (1). The $\nu\equiv C-H$ mode occurs near 3300 cm^{-1} with a weak shoulder on the low frequency side of the strong IR band. This weak shoulder has been attributed to a Fermi resonance interaction with $\nu\equiv C-H$ and the combination tone $\nu C\equiv C + 2[C\equiv C-H$ bending] (1).

All of these compounds exhibit $\nu C\equiv C$ in the region $2100-2148\text{ cm}^{-1}$, and this band is weak in most cases. Compounds where the halogen atom or a carbonyl group is joined to the terminal acetylenic group exhibit strong IR $\nu c\equiv c$ absorption bands.

A weak IR band in the region $897-961\text{ cm}^{-1}$ is assigned to $\nu C-C$. The $\equiv C-H$ bending mode is not split in the case of 1-alkynes, and occurs in the region $628-633\text{ cm}^{-1}$. Substitution of a

halogen atom on the 3-carbon atom splits the degeneracy and both in-plane and out-of-plane $\equiv\text{C}-\text{H}$ bending modes are observed in the IR. With the exception of 3-iodopropyne the in-plane bending mode occurs at a higher frequency than the out-of-plane bending modes. For example, 3-iodopropyne exhibits the C-H bending modes at 637 cm^{-1} , while the Cl, Br, and F analogs exhibit the in-plane bending mode at 652 , 649 , and 674 cm^{-1} , respectively, and the out-of-plane bending mode occurs at 637 , 639 , and 636 cm^{-1} , respectively (2).

Substitution of deuterium for hydrogen $\equiv\text{C}-\text{H}$ to $\equiv\text{C}-\text{D}$ helps in establishing the fundamental vibrations that result from this portion of the molecule. In the case of 3-chloropropyne-1-d

and 3-bromopropyne-1-d the $\nu\equiv\text{C}-\text{D}$ modes occur at 2618 and 2607 cm^{-1} , respectively (see Table 5.2). In the case of $\equiv\text{C}-\text{D}$ bending, the Cl and Br analogs exhibit the in-plane mode at 516 and 512 cm^{-1} , respectively, while the out-of-plane mode occurs at 502 and 503 cm^{-1} , respectively.

The 3-chloropropyne-1-d, 3-bromopropyne-1-d, and phenylacetylene-1-d are interesting because their $\nu\equiv\text{C}-\text{D}$ and $\nu\text{C}\equiv\text{C}$ modes couple. The $\nu\text{C}\equiv\text{C}$ mode shifts from 2147 to 2000 , 2138 to 2006 , and 2119 to 1989 cm^{-1} for 3-Cl, Br, and 2-phenyl $\text{C}\equiv\text{C}-\text{H}$ and D analogs, respectively. On the other hand, the $\nu\equiv\text{C}-\text{H}$ mode and $\nu\equiv\text{C}-\text{D}$ modes are (3325 and 2618), (3315 and 2607), and (3315 and 2596 cm^{-1}) for the 3-Cl, 3-Br and 2-phenyl $\text{C}\equiv\text{C}-\text{H}$ and D analogs, respectively. The ratio of $\nu\equiv\text{C}-\text{H}/\nu\equiv\text{C}-\text{D}$ is 1.27, 1.28, and 1.28, respectively, and, if $\nu\equiv\text{C}-\text{D}$ were a pure vibration it would be expected to occur at 2340 cm^{-1} . Because $\nu\text{C}\equiv\text{C}$ shifts to lower frequency upon D substitution together with the behavior of $\nu\text{C}-\text{D}$, their frequency behavior is expected when the two modes are coupled. As $\nu\text{C}\equiv\text{C}$ and $\nu\equiv\text{C}-\text{H}$ occur approximately 1170 cm^{-1} apart, the amount of coupling between these two modes is most likely negligible (3-5).

Terminal acetylenic compounds often exhibit the first overtone of $\equiv\text{C}-\text{H}$ bending in the region $1219-1265\text{ cm}^{-1}$, and for the D analogs near $1000-1043\text{ cm}^{-1}$. In addition, the $\text{C}-\text{C}\equiv\text{C}$ bending mode is observed in the region $300-353\text{ cm}^{-1}$ (1).

Table 5.2 lists the 15 vibrational assignments for 3-halopropynes using both IR and Raman data (2,4,5). The $\nu\text{C}-\text{H}$ and $\nu\text{C}-\text{D}$ and $\nu\text{C}\equiv\text{C}$ modes have been previously discussed. The vibrations most affected by change in the halogen atom for the CH_2X group are $\nu\text{C}-\text{X}$ skeletal bending, CH_2 wagging, CH_2 twisting, and CH_2 rocking. In most cases these fundamentals decrease in frequency progressing in the series F to I. These molecules have a plane of symmetry, and the 10 vibrations that occur within the plane are designated as a' fundamentals and the 5 vibrations that occur out-of-the plane are designated as a'' fundamentals. These molecules have C_s symmetry.

Table 5.3 lists IR vapor phase data and assignments for 1-alkynes (3). Most of these assignments are for the alkyl group of these 1-alkynes. The numbers in parenthesis are the measured absorbances, and study of these numbers shows the intensities relative to one another in each spectrum. It is of interest to note that the ratio $[(A)\text{CCH bend}/(A)\text{vasym. CH}_2]$ decreases as the number of $(\text{CH}_2)_n$ increases from 2 to 10. This indicates that the intensity for CCH bending is essentially constant and the intensity for $\text{vasym. (CH}_2)_n$ becomes more intense as n becomes larger. It should be noted that $\text{vasym. (CH}_2)_n$ shifts to lower frequency by 17 cm^{-1} as n is increased from 2 to 10. Most likely the dipole moment change during vasym. CH_2 changes slightly with this small shift in its frequency.

Figure 5.1 shows a plot of absorbance ratios for the 1-alkynes vs the number of carbon atoms in the 1-alkynes (3). Correlations such as these help in spectra-structure identification of unknown samples.

1-HALOPROPYNES

1-Halopropynes have C_{3v} symmetry, and the 15 fundamentals are distributed: $5a_1$, and $5e$ (The e fundamentals are doubly degenerate). The a_1 modes should yield parallel IR vapor bands and polarized Raman bands while the e modes should yield perpendicular IR vapor bands and depolarized Raman bands. Vibrational assignments in Table 5.4 were made using these criteria (7).

It has already been noted that $\nu\equiv C-D$ and $\nu C\equiv C$ coupled considerably in the case of the 1-halopropynes. During a cycle of $\nu C\equiv C$, both the $C-C$ and $C-X$ bonds must expand and contract.



Therefore, this complex $\nu C\equiv C$ mode must include contribution from both $\nu C-C$ and $\nu C-X$. A comparison of these modes vs those for propyne are presented here:

1-halopropyne	$\nu C\equiv C$ cm^{-1}	$\nu C-C$ cm^{-1}	$\nu C-X$ or $\nu C-H$ cm^{-1}
Br	2239	1037	465
I	2210	1013	403
propyne	2130	930	3320

It is noted that $\nu C\equiv C$ for 1-halopropynes occurs approximately 95 cm^{-1} higher in frequency than it occurs for propyne. In addition, $\nu C-C$ for 1-halopropynes occurs approximately 90 cm^{-1} higher in frequency than it occurs for propyne. The $\nu C-X$ mode occurs at lower frequency than the other two vibrations while $\nu C-H$ occurs at higher frequency. Moreover, the force constant for Br is higher than it is for I. All of these facts suggest that the $\nu C\equiv C$ mode for 1-halopropyne is complex and involves a stretching motion of the two adjacent groups.

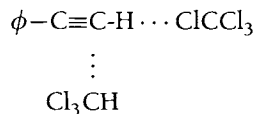
Table 5.4a lists the Coriolis coupling constants for 1-halopropyne (7,8), propyne (9) and propyne-1-d (10). These Coriolis constant coupling coefficients are included so that the reader has better knowledge about interpreting spectral data. Lord and Merrifield (11) have stated that the physical meaning of the minus sign to the Coriolis constant is that the angular momentum of vibration, which is so related to that of the rotation, produces an increase angular velocity of rotation of the vibrating molecular dipole moment about the molecular axis. The plus sign means that the velocity of rotation of the vibrating dipole moment is less than it would be if no angular momentum of vibration were present. In terms of normal vibrations, this means that

there is only a slight decrease in the velocity of rotation during the asym. CH₃ stretching vibration (ν_6) in these molecules relative to what the velocity would be for the nonvibrating molecule. A significant increase is noted in the velocity of rotation during the asymmetric CH₃ deformation (ν_7), because all Coriolis coupling constants are negative (between -0.33 and -0.39). These results are what is expected if the CH₃ group were considered to be a symmetrical 3-armed flywheel rotating about a fixed axis. The velocity of rotation would be increased if one or more of the arms were bent toward the fixed axis; in the case of ν_7 there is an alternating bending of two hydrogen atoms with one hydrogen atom toward and away from the molecular axis. Perhaps this can be more clearly demonstrated in $\nu_{10}(e)$, which is essentially C–X bend in the case of 1-halopropyne; a shift of such a heavy atom off of the molecular axis would most certainly slow down the velocity of the molecular rotation relative to that of the fixed rigid rotating molecule. The order of magnitude of the Coriolis coupling coefficients has significance in the interpretation of the IR spectra of these compounds. The larger the value the closer the Q peaks are spaced in the subband. Consequently, a value of approximately one might appear to be nearly one broad absorption band with little or no fine structure due to unresolved closely spaced Q peaks in the subband. It is significant to note that the perpendicular (e) modes in solution or in the liquid phases appear to be as broad as they are in the vapor phase. They differ only in that the fine structure (Q peaks) are not observed. This suggests that in the condensed phases the molecules are still rotating, but not as freely as in the vapor phase (7).

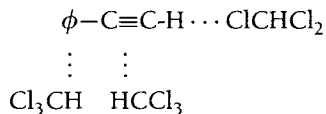
PHENYLACETYLENE IN VARIOUS SOLUTIONS

Phenylacetylene in 0 to 100 mol % CHCl₃/CCl₄ solutions has been studied utilizing FT-IR spectroscopy (14) (see Table 5.5). Figure 5.2 shows a plot of $\nu_{\equiv C-H}$ for phenylacetylene vs mole % CHCl₃/CCl₄. Figure 5.2 shows that the $\nu_{\equiv C-H}$ decreases in frequency as the mole % CHCl₃/CCl₄ increases. Breaks in the plot near 10 and 45–55 mol % CHCl₃/CCl₄ suggest that different complexes are being formed as the mole % CHCl₃/CCl₄ changes.

In the case of phenylacetylene in solution, a complex such as $\phi-C\equiv C-H \cdots ClCCl_3$ is suggested, in intermediate solutions of CHCl₃/CCl₄ a complex such as



and in CHCl₃ a complex such as



are suggested to explain the changes in both the $\nu_{\equiv C-H}$ and $\nu_{C\equiv C}$ frequency changes with change in the solvent system. Bulk dielectric effects of the solvents also contribute to the group frequency shifts as the mole % change from 0–100.

Figure 5.3 shows a plot of $\nu\text{C}\equiv\text{C}$ vs mole % $\text{CHCl}_3/\text{CCl}_4$. This plot shows that $\nu\text{C}\equiv\text{C}$ decreases in frequency as the mole % $\text{CHCl}_3/\text{CCl}_4$ is increased. Figure 5.4 shows a plot of the in-plane $\equiv\text{C}-\text{H}$ bending mode $\delta_{\text{ip}} \equiv\text{C}-\text{H}$ vs mole % $\text{CHCl}_3/\text{CCl}_4$. The plot stops near 60 mol% $\text{CHCl}_3/\text{CCl}_4$. The plot stops near 60 mol% CH_3/CCl_4 , because absorbance from CHCl_3 masks the absorbance of $\delta_{\text{ip}} \equiv\text{C}-\text{H}$. This plot shows that $\delta_{\text{ip}} \equiv\text{C}-\text{H}$ increases in frequency as the mole % $\text{CHCl}_3/\text{CCl}_4$ is increased. Figure 5.5 shows a plot of the out-of-plane $\equiv\text{C}-\text{H}$ mode, $\gamma_{\text{op}} \equiv\text{C}-\text{H}$ vs mole % $\text{CHCl}_3/\text{CCl}_4$ for phenylacetylene, and it shows that it increases in frequency as the mole % $\text{CHCl}_3/\text{CCl}_4$ is increased. The breaks in Figs. 5.2 and 5.5 indicate that different complexes are forming in these mole % $\text{CHCl}_3/\text{CCl}_4$ segments of the plots.

Table 5.5 lists IR data for phenylacetylene in 2% wt/vol solutions in mole % $\text{CHCl}_3/\text{CCl}_4$ solutions (14). Two IR bands are noted near 3300 cm^{-1} in the neat phase and in solution in various solvents. For example, in hexane solution, the strongest band in this set occurs at 3322.91 cm^{-1} and the shoulder occurs at 3311.27 cm^{-1} while in the neat liquid the strongest band in this set occurs at 3291.17 cm^{-1} and the shoulder occurs at 3305.08 cm^{-1} . The changes in both frequency and the intensity ratio of this band set is proof that these two bands are in Fermi resonance (FR.), and these two bands have been corrected for FR. The corrected frequencies vary between 3297.2 and 3318.1 cm^{-1} for $\nu\equiv\text{C}-\text{H}$ and between 3299.2 and 3316.1 cm^{-1} for the combination tone. The highest $\nu\equiv\text{C}-\text{H}$ frequency exhibited by phenylacetylene is when it is in solution with hexane and the lowest when in the neat liquid phase.

A plot of $\gamma_{\text{op}} \equiv\text{C}-\text{H}\text{ cm}^{-1}$ vs $\delta_{\text{ip}} \equiv\text{C}-\text{H}\text{ cm}^{-1}$ for phenylacetylene (recorded in solvents that were not masked by the solvents used in this study and that for the neat liquid phase show a linear relationship). This indicates that both modes are affected equally in a particular solvent, but differently in each solvent in the neat liquid phase (14). These data do not correlate well with the solvent acceptor number (AN), and this may be due to the fact that the AN values do not reflect the intermolecular hydrogen bonding capabilities of solvents such as CH_2Cl_2 and CHCl_3 .

1,4-DIPHENYLBUTADIENE

In the solid state 1,4-diphenylbutadiene has a monoclinic crystal structure with two molecules in the unit cell. The two molecules in the unit cell have a center of symmetry (12). The space group for 1,4-diphenylbutadiene is $\text{P}2_1/\text{C}$, which is isomorphous with the $\text{C}_{2\text{h}}$ point group. Thus, the $\nu_{\text{ip}}(\text{C}\equiv\text{C})_2$, Ag mode should be only Raman active and the $\nu_{\text{op}}(\text{C}\equiv\text{C})_2$, Bu mode should be only IR active.

Table 5.6 lists IR data and assignments for 1,4-diphenylbutadiene in $\sim 10\%$ wt/vol $\text{CHCl}_3/\text{CCl}_4$ solutions (13). Raman data for this compound in the solid state and in CHCl_3 and CCl_4 solutions are also included. A Raman band at 2218.9 (in CCl_4), at 2217.8 (in CHCl_3), and at 2214.4 cm^{-1} in the solid phase is assigned to $\nu_{\text{ip}}(\text{C}\equiv\text{C})_2$. The IR band at 2150 cm^{-1} in the solid state is assigned to $\nu_{\text{op}}(\text{C}\equiv\text{C})_2$. The $\nu_{\text{ip}}(\text{C}\equiv\text{C})_2$ mode in the solid state occurs 64.4 cm^{-1} higher in frequency than the $\nu_{\text{op}}(\text{C}\equiv\text{C})_2$ mode in the solid state. There is no evidence for $\nu_{\text{op}}(\text{C}\equiv\text{C})_2$ in the Raman spectrum in either of the solution or solid phases. The solid phase data and assignments for 1,4-diphenylbutadiene support the x-ray data (12).

In CCl_4 solution $\nu_{\text{ip}}(\text{C}\equiv\text{C})_2$ is assigned at 2250.51 cm^{-1} and in CHCl_3 solution at 2219.45 cm^{-1} , a decrease in frequency of 1.06 cm^{-1} . In CCl_4 solution $\nu_{\text{op}}(\text{C}\equiv\text{C})_2$ is assigned

at 2152.23 cm^{-1} and in CHCl_3 solution at 2150.22 cm^{-1} , a decrease in frequency of 2.01 cm^{-1} (see Table 5.6). In the IR, the absorbance ratio $[(A)v_{\text{ip}}(\text{C}\equiv\text{C})_2]/[(A)v_{\text{op}}(\text{C}\equiv\text{C})_2]$ generally increases as the mole % $\text{CHCl}_3/\text{CCl}_4$ increases. As $v_{\text{ip}}(\text{C}\equiv\text{C})_2$ is observed in the IR when 1,4-butadiyne is in solution, this indicates that in solution the two phenyl groups are not coplanar as they are in the solid phase (13).

PROPARGYL ALCOHOL VS PROPARGYL FLUORIDE

Table 5.7 list vibrational data and assignments for propargyl alcohol, its $-\text{OD}$ and 1-d and O-D analogs and propargyl fluoride (3-fluoropropyne). It is helpful to compare the frequency assignments of a fluoro analog to the corresponding OH analog, because the C-F and C-O modes occur at similar frequency, and the F analog contains 3 less fundamental vibrations. The OH analog has an additional 3 fundamental vibrations. They are νOH , δOH , and τOH (or OH torsion in the vapor phase). The assignments for the propargyl alcohol and its deuterium analogs are included to show the reader the value of using the vibrational assignment for corresponding R-F vs R-OH or R-O analogs. The same will be shown to be of value in the vibrational assignments for Aryl analogs and phosphorus analogs.

The interesting feature in the study of propargyl alcohol is that in the liquid phase it does not have a plane of symmetry because CH_2 twist couples with OH bending and CH_2 wag, indicating that these fundamentals all belong to the same species. With C_s symmetry, CH_2 twisting belongs to the a'''' symmetry species, and δOH and CH_2 wag belong to the a' species (15).

1,3-DIHALOPROPYNES

Vapor- and solution-phase infrared spectra of 1,3-dichloropropyne are presented in Figures 5.6 and 5.7, respectively. Complete vibrational assignments have been made for both 1,3-dichloropropyne and its 1,3- Br_2 analog (16). Vibrational assignments based on both IR and Raman data for the 15 fundamentals of each analog are presented in Table 5.8. The a' and a'' fundamentals are due to in-plane and out-of-plane vibrations, respectively. The a' modes should yield type A/B IR vapor bands and polarized Raman bands while a'' modes should yield type C IR vapor bands and depolarized Raman bands.

The band at 2261 cm^{-1} is assigned to primarily $\nu\text{C}\equiv\text{C}$ in the case of 1,3-dichloropropyne. The band at 2224 cm^{-1} is assigned to a combination tone ($\nu_5 + \nu_{10}$). The two bands are in Fermi resonance (FR.) and these two frequencies have not been corrected for FR. The FR. correction would lower the unperturbed $\nu\text{C}\equiv\text{C}$ frequency and raise the combination tone frequency.

Assignments in Table 5.8 are simplified because the $\text{X-C-C}\equiv\text{C-X}$ stretching modes are expected to be complex as discussed for the 1-haloalkynes.

In the case of the 1,3-dihaloalkynes it appears as though the $\nu\text{C}\equiv\text{C}$ mode is even more complex than it is in the case of 1-haloalkyne. The $\text{C-C}\equiv\text{C-X}$ atoms are all on the molecular axis, and the other X atom is in the plane of molecular symmetry. Therefore, when the $\text{C}\equiv\text{C}$ group expands and contracts during a cycle of $\nu\text{C}\equiv\text{C}$, the C-C of the group, $\text{C-C}\equiv$, and the $\equiv\text{C-X}$ groups must compress and expand. In addition the $\text{X-C-C}\equiv$ bond angle most likely decreases to a small degree in the case of 3-bromopropyne. Comparison of these vibrations for 1,3-dibromopropyne and 1-bromopropyne show that these modes occur at similar frequencies.

Compound	$\nu\text{C}\equiv\text{C}$ cm^{-1}	$\nu\text{C}-\text{C}\equiv$ cm^{-1}	$\nu\equiv\text{C}-\text{X}$ cm^{-1}
1,3-dibromopropyne	2226	1064	512
1-bromopropyne	2239	1037	464
3-bromopropyne	2138	961	3335

The $\nu\text{C}-\text{C}\equiv$ and $\nu\equiv\text{C}-\text{X}$ modes for 1,3-dibromopropyne occur at higher frequency than the corresponding modes for 1-bromopropyne. Moreover, the $\nu\text{C}\equiv\text{C}$ and $\nu\text{C}-\text{C}\equiv$ modes are higher than those exhibited by the 3-halopropynes. These data indicate that $\nu\text{C}\equiv\text{C}$ is a more complex mode than just stretching of the $\text{C}\equiv\text{C}$ bond. Nevertheless, $\nu\text{C}\equiv\text{C}$ is considered to be a good group frequency in identifying this group in unknown samples.

Figure 5.8 shows the expected normal vibrations of 1-halopropynes, 3-halopropynes, and 1,3-dihalopropynes (16) and their frequency assignments. These normal modes are most likely oversimplified.

PHENYLACETYLENE AND PHENYLACETYLENE-1D

Table 5.9 lists vibrational data for phenylacetylene and phenylacetylene-1d. The in-plane $\text{CC}-\text{H}$ and $\text{CC}-\text{D}$ bending frequencies are assigned at 648 and 482 cm^{-1} , respectively. The out-of-plane $\text{CC}-\text{H}$ and $\text{CC}-\text{D}$ bending frequencies are assigned at 612 and 482 cm^{-1} , respectively. Again, the $\nu\text{C}\equiv\text{C}$ mode for the H and D analogs occur at 2119 and 1989 cm^{-1} , respectively, and this is attributed to coupling between $\nu\text{C}\equiv\text{C}$ and $\nu\text{C}-\text{D}$ (17).

Assignment of the ring modes will be discussed later.

REFERENCES

1. Nyquist, R. A. and Potts, W. J. (1960). *Spectrochim. Acta*, **16**, 419.
2. Evans, J. C. and Nyquist, R. A. (1963). *Spectrochim. Acta*, **19**, 1153.
3. Nyquist, R. A. (1985). *Appl. Spectrosc.*, **39**, 1088.
4. Nyquist, R. A., Reder, T. L., Ward, G. R., and Kallos, G. J. (1971). *Spectrochim. Acta*, **27A**, 541.
5. Nyquist, R. A., Reder, T. L., Stec, F. F., and Kallos, G. J. (1971). *Spectrochim. Acta*, **27A**, 897.
6. Evans, J. C. and Nyquist, R. A. (1960). *Spectrochim. Acta*, **16**, 918.
7. Nyquist, R. A. (1965). *Spectrochim. Acta*, **7**, 1245.
8. Davidson, D. W., Sundaram, S., and Cleveland, F. F. (1962). *J. Chem. Phys.*, **37**, 1087.
9. Boyd, D. R. J. and Thompson, H. W. (1952). *Trans. Faraday Soc.*, **48**, 493.
10. Grisenthwaite, H. A. J. and Thompson, H. W. (1954). *Trans. Faraday Soc.*, **50**, 212.
11. Lord, R. C. and Merrifield, R. E. (1952). *J. Chem. Phys.*, **20**, 1348.
12. Wiebenga, E. H. (1940). *Z. Kristallogr.*, **102**, 93.
13. Nyquist, R. A. and Putzig, C. L. (1992). *Vib. Spectrosc.*, **4**, 35.
14. Nyquist, R. A. and Fiedler, S. (1994). *Vib. Spectrosc.*, **7**, 149.
15. Nyquist, R. A. (1971). *Spectrochim. Acta*, **27A**, 2513.
16. Nyquist, R. A., Johnson, A. L., and Lo, Y.-S. (1965). *Spectrochim. Acta*, **21**, 77.
17. Evans, J. C. and Nyquist, R. A. (1960). *Spectrochim. Acta*, **16**, 918.

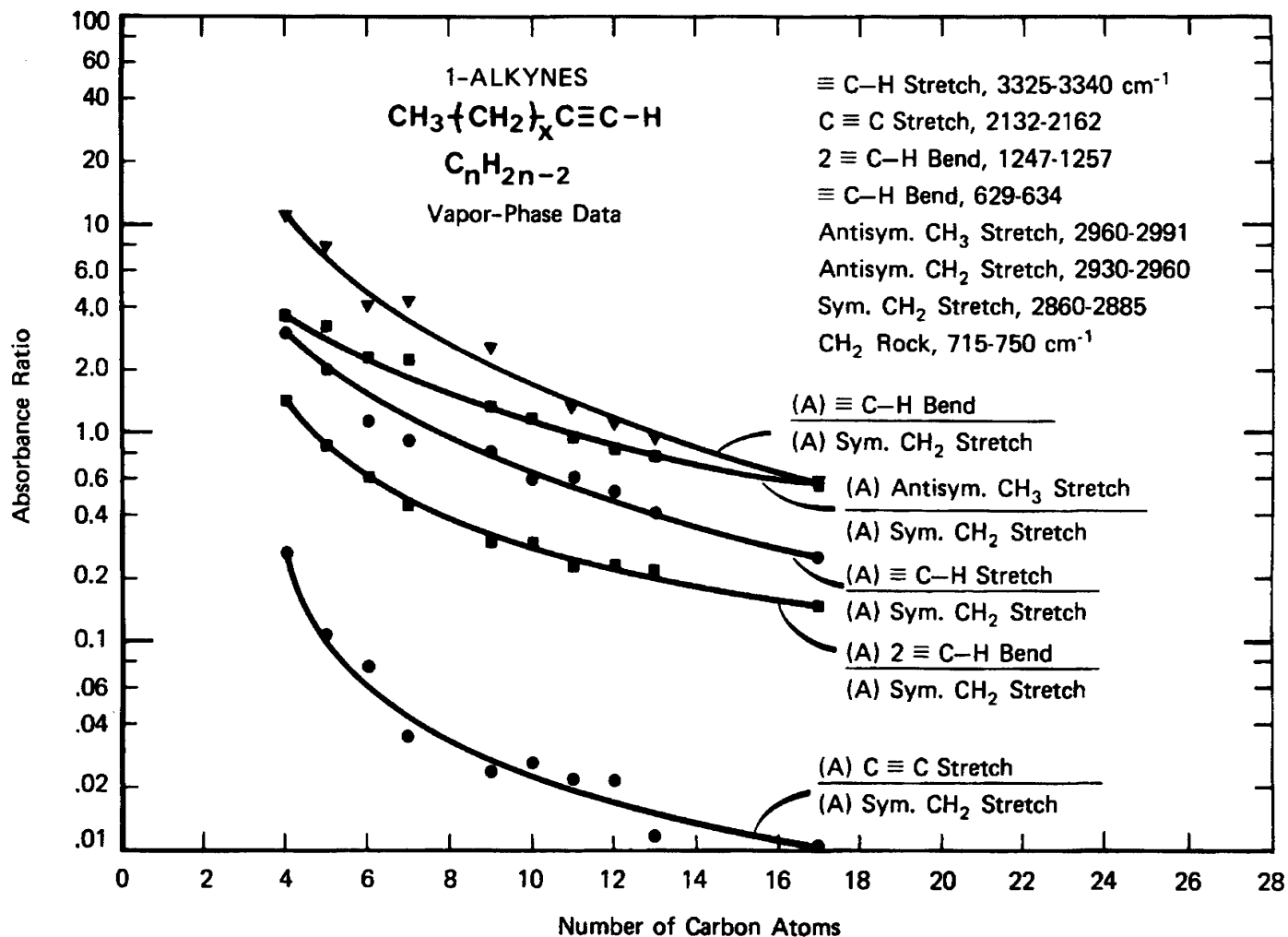
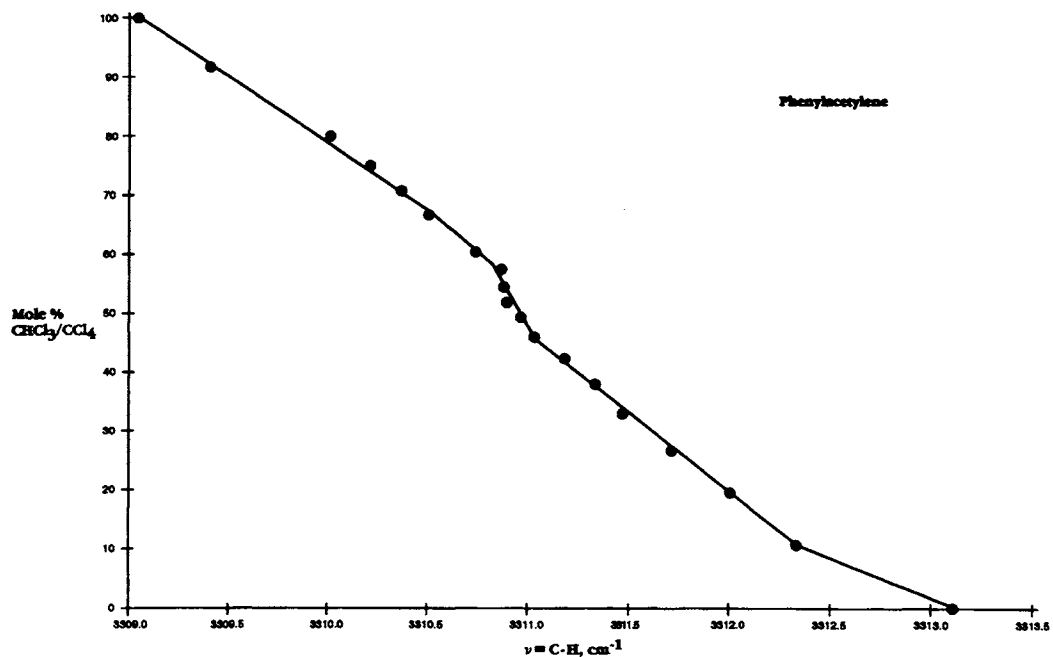
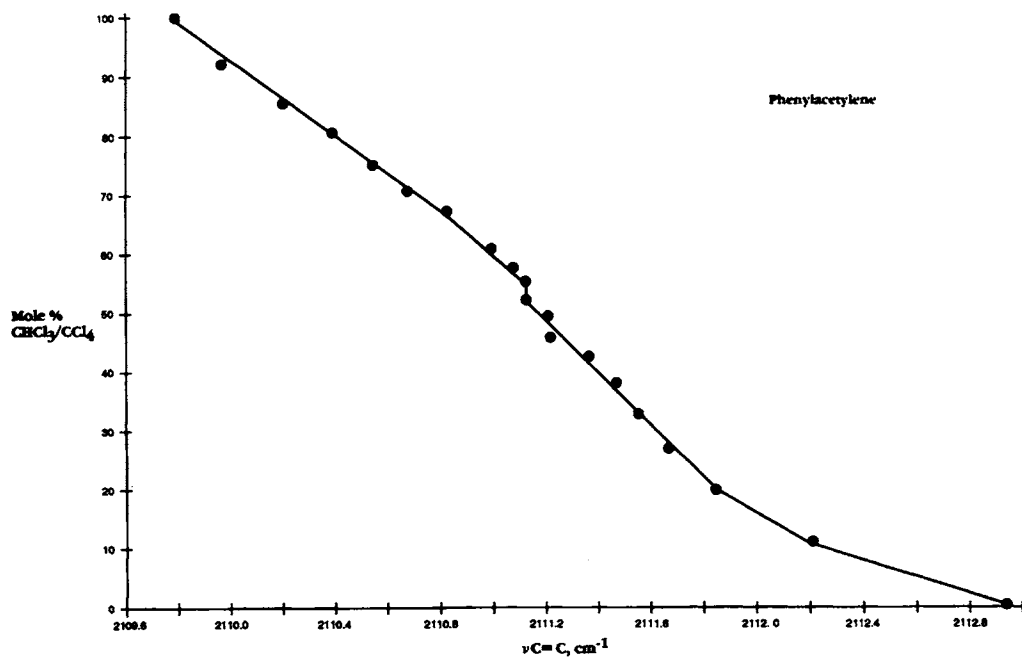


FIGURE 5.1 A plot of absorbance ratios for the 1-alkynes vs the number of carbon atoms in the 1-alkynes.

FIGURE 5.2 A plot of $\nu_{\text{C-H}}$ for phenylacetylene vs mole % $\text{CHCl}_3/\text{CCl}_4$.FIGURE 5.3 A plot of $\nu_{\text{C}\equiv\text{C}}$ for phenyl acetylene vs mole % $\text{CHCl}_3/\text{CCl}_4$.

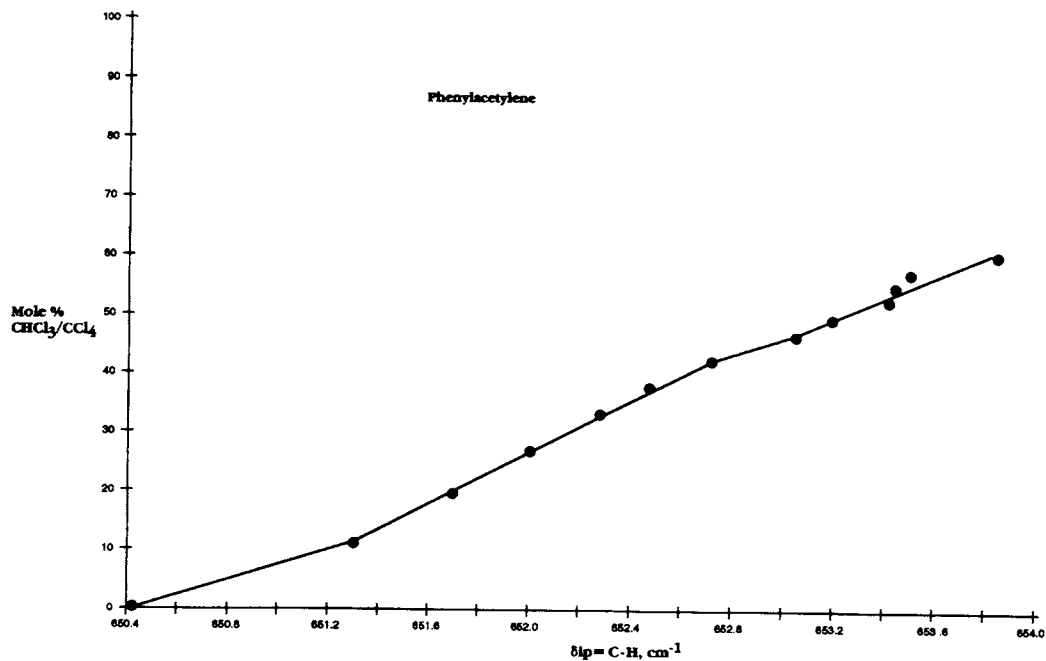


FIGURE 5.4 A plot of the in-plane $\equiv\text{C-H}$ mode vs mole % $\text{CHCl}_3/\text{CCl}_4$.

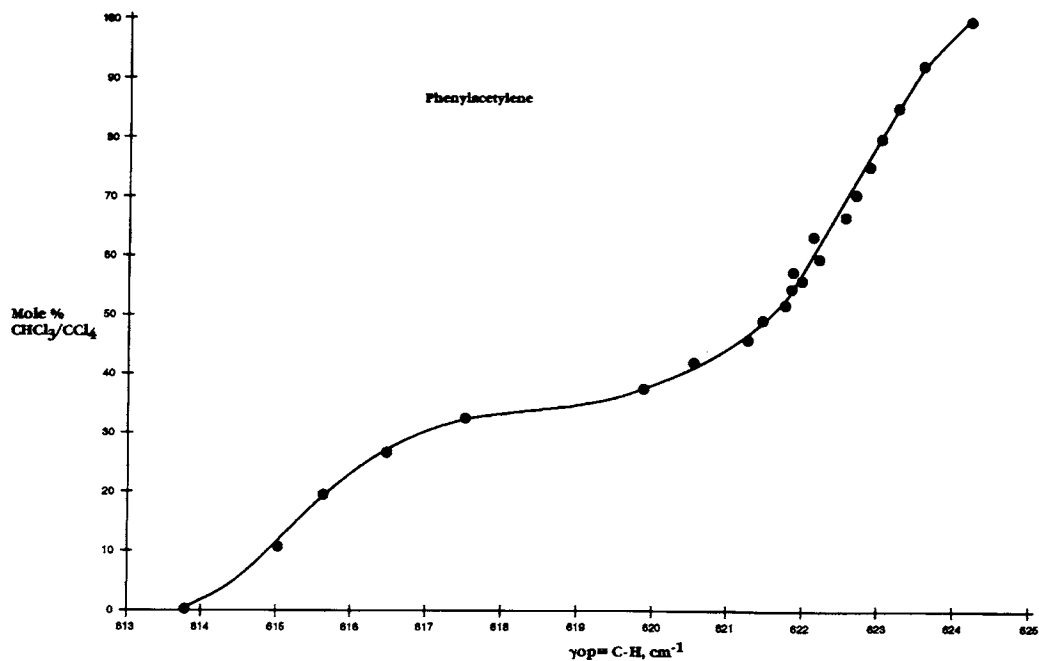


FIGURE 5.5 A plot of out-of-plane $\equiv\text{C-H}$ mode vs the in-plane $\equiv\text{C-H}$ bending mode.

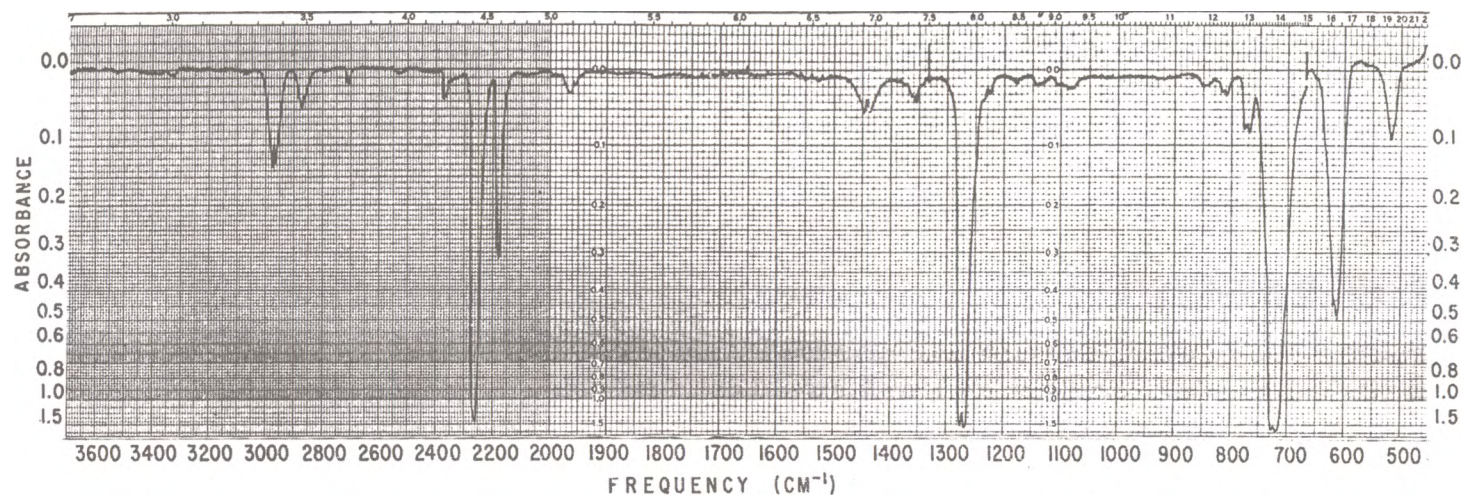


FIGURE 5.6 Vapor- and solution-phase infrared spectra of 1,3-dichloropropyne.

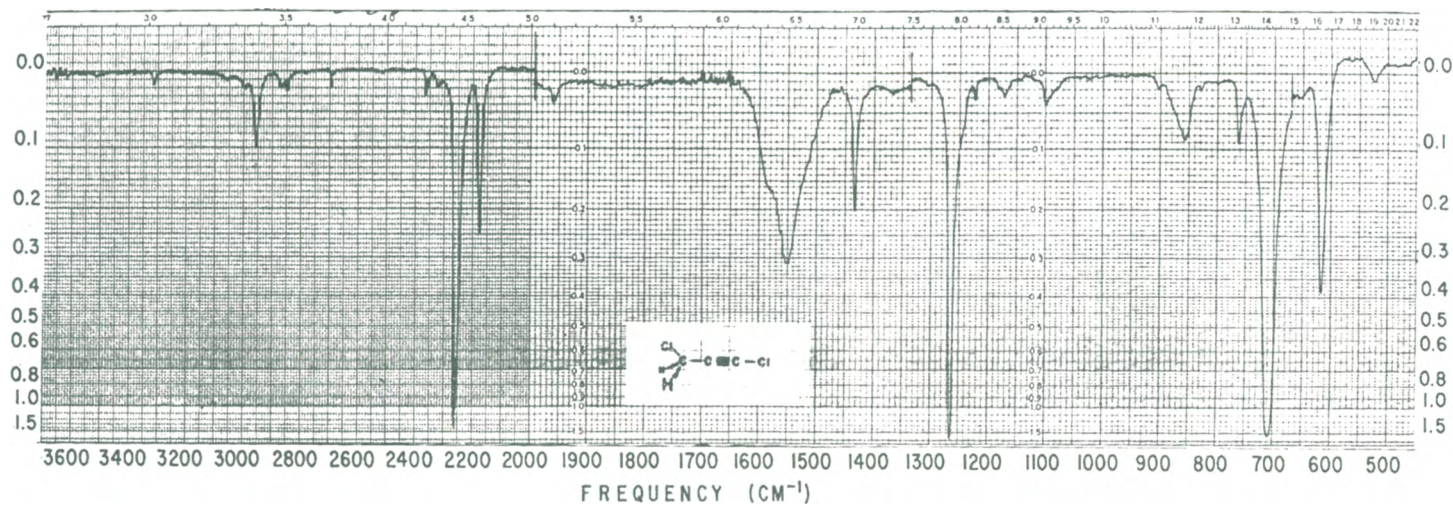
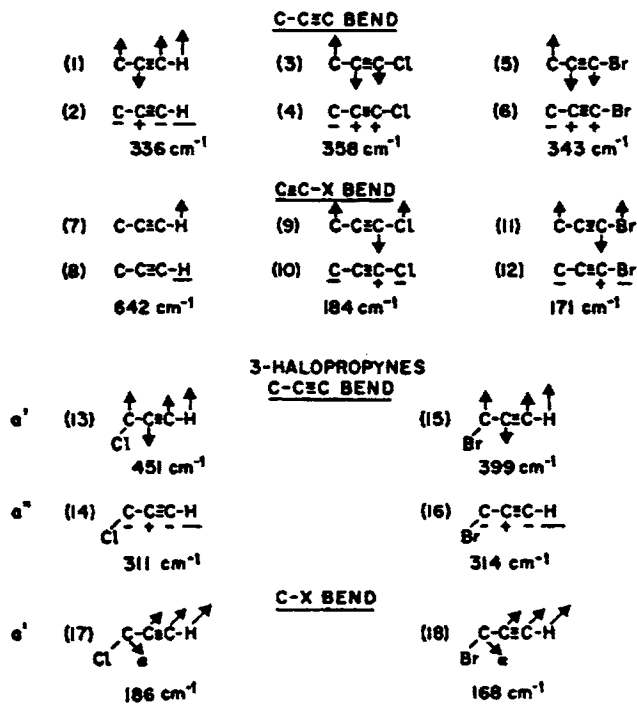


FIGURE 5.7 Vapor- and solution-phase infrared spectra of 1,3-dichloropropyne.

**APPROXIMATE NORMAL MODES
PROPYLENE AND 1-HALOPROPYNES**



1,3-DIHALOPROPYNES

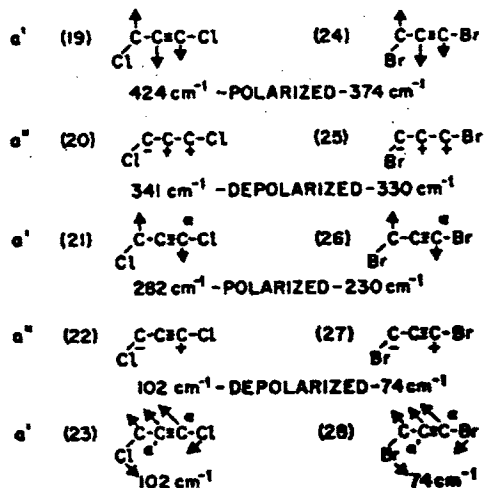


FIGURE 5.8 The expected normal modes of 1-halopropynes, 3-halopropynes, and 1,3-dihalopropynes.

TABLE 5.1 IR data and assignments for terminal acetylenic compounds

Compound type	C-H str.	CC str.	C-C str.	C-H bend	2(C-H bend)	C-CC bend
CH ₃ -CC-H	3320 3300sh	2130	930	630	1249	
R-CH ₂ -CC-H	3320 3299sh	2121	924-959	628-633	1242-1249	335
C ₆ H ₅ -CC-H [vapor]	3340 3320sh	2120		642 and 613	1219	
C ₆ H ₅ -CC-H [soln]	3316 3305sh	2115		648 and 611	1219	353?
ICH ₂ -CC-H	3315 3298sh	2109sh 2148sh	961	637	1263	
BrCH ₂ -CC-H	3315 3300sh	2126 2121sh	959	649 and 639	1265	313?
BrCH ₂ -CC-D	2599, CD str. 2582sh	1994	943	512 and 503	1000	301
ClCH ₂ -CC-H	3315 3299sh	2131 2126sh	959	652 and 637		310?
ClCH ₂ -CC-D	2618, CD str. 2589sh	2000	943	516 and 502	1043	300
FCH ₂ -CC-H	3322 3310sh	2148		674 and 636		
HOCH ₂ -CC-H	3316 3296sh	2120	902	650 and 629	1268?	
HOCH ₂ C(-R) ₂ -CC-H	3314-3316 3294-3300sh	2102-2115		649-655 620-630		
CH ₃ O-CC-H	3317 3296sh	2119 2104sh	932	663 and 625		
ROC(-R) ₂ -CC-H	3312-3314 3292-3296sh	2103-2111	908-938	651-660 627-630		
C ₆ H ₅ OCH ₂ -CC-H	3312-3320 3292-3301sh	2121-2131 2139sh		665-671 628-663		
C ₆ H ₅ CH ₂ SCH ₂ -CC-H	3317 3299sh	2120 2100sh	949	634	1248?	325?
C ₆ H ₅ SCH ₂ -CC-H	3318 3300sh	2122 2100sh	950	635		320?
(R) ₂ NCH ₂ -CC-H	3311-3316 3295-3300sh	~ 2100	897-925	647-653 622-624		~ 330?

?tentative assignment.

TABLE 5.2 IR and Raman data and assignments for 3-halopropynes

Species	3-fluoro-propyne	3-chloro-propyne	3-chloro-propyne-1-d	3-bromo-propyne	3-bromo-propyne-1-d	3-iodo-propyne	Assignment
a'	3328	3335	2618	3335	2607	3335	CH or CD str.
	2955	2968	2969	2976	2978	2958	s. CH ₂ str.
	2150	2147	2000	2138	2006	2130	CC str.
	1465	1441	1442	1431	1436	1423	CH ₂ bend
	1381	1271	1265	1218	1215	1160	CH ₂ wag
	940	960	943	961	945	959	C-C str.
	1039	725	723	621	634	570	C-X str.
	675	650	516	652	512	640	C-H or C-D bend
	539	451	438	399	386	364	skeletal bend
	211	186	165	168	163	157	skeletal bend
a''	2972	3002	2992	3006	3008	3008	a.CH ₂ str.
	1242	1179	1176	1152	1151	1116	CH ₂ twist
	1018	908	908	866	866	810	CH ₂ rock
	635	637	502	637	501	640	CH or CD bend
	310	311	294	314	296	314	skeletal bend

TABLE 5.3 IR vapor-phase data and assignments for 1-alkynes

Compound	CC-H str.	C.T.	a.CH ₃ str.	a.CH ₂ str.	s.CH ₃ str.	s.CH ₂ str.	CC str.	CH ₂ bend	s.CH ₃ bend	2(CCH bend)	CH ₂ rock	CCH bend	RI(A) CCH bend/RI(A) a.CH ₂ str.
1-Pentyne	3330 (0.310)		2978 (0.390)	2952 (0.290)		2890 (0.110)	2135 (0.020)	1460 (0.059)	1390 (0.020)	1250 (0.125)		630 (1.240)	4.28
1-Hexyne	3330 (0.388)		2970 (0.877)	2948 (0.750)	2900 (0.318)	2880 (0.323)	2120 (0.056)	1455 (0.101)	1385 (0.048)	1249 (0.199)	740 (0.020)	630 (1.250)	1.67
1-Heptyne	3330 (0.273)		2970 (0.661)	2945 (0.990)		2980 (0.296)	2125 (0.034)	1460 (0.090)	1380 (0.035)	1250 (0.131)	740 (0.020)	631 (1.230)	1.24
1-Nonyne	3338 (0.305)		2970 (0.491)	2940 (1.240)		2870 (0.385)	2130 (0.030)	1467 (0.084)	1386 (0.025)	1249 (0.120)	725 (0.010)	630 (0.950)	0.77
1-Decyne	3338 (0.259)	3320 (0.106)	2970 (0.540)	2940 (1.143)		2875 (0.490)	2124 (0.024)	1465 (0.100)	1385 (0.049)	1250 (0.139)	724 (0.010)	632 (0.700)	0.61
1-Undecyne	3338 (0.250)	3318 (0.060)	2970 (0.420)	2940 (1.250)		2868 (0.440)	2124 (0.034)	1466 (0.090)	1385 (0.030)	1250 (0.100)	722 (0.030)	630 (0.604)	0.48
1-Dodecyne	3328 (0.270)	3320 (0.070)	2970 (0.440)	2935 (1.240)		2864 (0.420)	2122 (0.025)	1465 (0.100)	1380 (0.022)	1248 (0.119)	719 (0.011)	630 (0.590)	0.47
1-Tridecyne	3330 (0.169)	3310 (0.056)	2970 (0.319)	2935 (1.250)		2860 (0.430)	2121 (0.015)	1465 (0.048)	1385 (0.030)	1246 (0.089)	720 (0.020)	631 (0.409)	0.32

TABLE 5.4 IR data and assignments for 1-chloropropyne and 1-bromopropyne

Species	1-Bromopropyne	1-Iodopropyne	Assignment
a ₁	2922	2922	s.CH ₃ str.
	2239	2210	CC str.
	1368	1364	s.CH ₃ bend
	1037	1013	C—C str.
	465	403*1	C—X str.
e	2965	2965	a.CH ₃ str.
	1442	1439	a.CH ₃ bend
	1027	1021	CH ₃ rock
	343*1	343	skeletal bend
	171*1	163*1	G—X bend

*¹ [liquid].

TABLE 5.4A Coriolis coupling constants for 1-chloropropyne and 1-bromopropyne

Assignment	1-Chloropropyne	1-Bromopropyne	1-Iodopropyne	Propyne	Propyne-1-d
a.CH ₃ , e [stretch]	0.042	0.051	0.072	0.074	0.071
a.CH ₃ , e [bend]	-0.357	-0.347	-0.336	-0.39	-0.37
a.CH ₃ , e [rock]	0.4	0.393	0.383	0.387	0.4
skeletal bend, e	0.90 less than 1	0.95 less than 1	0.94 less than 1	0.96 less than 1	0.92 less than 1
C—X bend, e	0.90 less than 1	0.95 less than 1	0.94 less than 1	0.96 less than 1	0.92 less than 1

TABLE 5.5 IR data for phenylacetylene in CHCl₃/CCl₄ solutions

Phenyl- acetylene Mole % CHCl ₃ /CCl ₄	C—H str.		i.p. CC—H	o.p. CC—H	v32 (b2)	v34 (b2)	v24 (b1)
	cm ⁻¹	cm ⁻¹	bend cm ⁻¹	bend cm ⁻¹	ring def. cm ⁻¹	sk. def. cm ⁻¹	sk. def. cm ⁻¹
0	3313.1	2113	650.4	613.8	690.4	530	513.6
26.53	3311.7	2111.7	652	616.5	690.6	530.2	513.5
52	3310.9	2111.1	653.4	621.7	690.9	530.3	513.4
75.06	3310.2	2110.5		622.9	691.2	530.4	513.4
100	3309.1	2109.8		624.2	691.8	530.5	513.4
delta cm ⁻¹	-4	-3.2	3	10.4	1.4	0.5	-0.2

TABLE 5.6 IR data and assignments for 1,4-diphenylbutadiyne in CHCl₃/CCl₄ solutions

1,4-Diphenyl- butadiyne							Raman	Raman		
IR	i.p. (CC) ₂ str.	o.p. (CC) ₂ str.	[i.p. (CC) ₂ str]-	A[i.p. (CC) ₂ str.]	A[o.p. (CC) ₂ str.]	A[i.p. (CC) ₂ str.] /A[o.p. (CC) ₂ str.]	i.p. (CC) ₂ str.	i.p. (CC) ₂ str.	[i.p. (CC) ₂ str]-	[o.p. (CC) ₂ str.]
Mole % CHCl ₃ /CCl ₄	cm ⁻¹	cm ⁻¹	[o.p. (CC) ₂ str.]	A[i.p. (CC) ₂ str.]	A[o.p. (CC) ₂ str.]	cm ⁻¹	cm ⁻¹	cm ⁻¹	[solid]	[o.p. (CC) ₂ str.]
0	2220.51	2152.23	68.28	0.215	0.32	0.67	2150	2218.9	2214.4	64.4
10.8	2220.34	2151.93	68.41							
10.8	2220.2	2152.15	68.05	0.26	0.36	0.55				
26.7	2220.11	2151.57	68.54							
26.7	2220.13	2151.61	68.52	0.293	0.369	0.79				
37.7	2219.99	2151.29	68.7	0.365	0.422	0.86				
45.9	2119.89	2151.12	68.6	0.414	0.464	0.89				
52.2	2219.83	2150.99	68.84	0.432	0.481	0.9				
63.4	2219.72	2150.79	68.9	0.476	0.518	0.92				
70.8	2219.65	2150.63	69.02	0.516	0.561	0.92				
80.2	2219.55	2150.45	69.1	0.575	0.617	0.93				
92.4	2219.41	2150.25	69.16	0.618	0.65	0.95				
100	2219.45	2150.22	69.23	0.649	0.697	0.93	[CHCl ₃] 2217.8			67.58
delta cm ⁻¹	1.06	2.01	0.95					1.1		

TABLE 5.7 Vibrational assignments for propargyl alcohol, propargyl alcohol-od, propargyl alcohol-ld, od, and propargyl fluoride

H-CC-CH ₂ -OH cm ⁻¹	H-CC-CH ₂ -OD cm ⁻¹	D-CC-CH ₂ -OD cm ⁻¹	H-CC-CH ₂ -F cm ⁻¹	Assignments and approximate descriptions [OH or OD analogs are all assigned to the a species]
3319	3319	2597	3320	C-H str., a' or C-D str. coupled with CC str.
2950	2950	2960	2980	a.CH ₂ str., a''
2925	2930	2937	2957	s.CH ₂ str. a'
2138	2133	1987	2146	CC str. or CC str. coupled with C-D str.
1452	1456	1457	1457	CH ₂ bend, a''
1382	1362	1366	1375	CH ₂ wag, a'
1227 [H-bonded]	1220	1165	1240	CH ₂ twist, a''
1197 [unassociated]				
1032	1030	1035	1020	C-F str., a' or C-O str.
972	971	981	1018	CH ₂ rock, a''
907	907	938	943	C-C str., a'
955	656	519 or 493	675	C-H bend, a' or C-D bend
629	629	493 or 519	637	C-H bend, a'' or C-D bend
551	553	562	544	C-C-F bend, a' or C-C-O bend
312	313	304	310	C-CC bend, a''
235	~ 230	211	211	C-CC bend, a'
3663 [vapor] and 3625 [soln.]		2706 [vapor]		O-H or O-D str. [unassociated]
~ 3500bd [soln.]	2678 [soln.]	2640 [liquid]		O-H or O-D str. [bonded]
1298 [vapor]				C-O-H or C-O-D bend [unassociated]
1420 [liquid]				C-O-H or C-O-D bend [bonded]
192 [soln.]		~ 150 [soln.]		C-O-H or C-O-D torsion

TABLE 5.8 Vibrational data for 1,3-dichloropropyne and 1,3-dibromopropyne

1,3-Dichloropropyne cm ⁻¹	1,3-Dibromopropyne cm ⁻¹	Assignment
		a' species
2957	2959	CH ₂ str.
2261	2226	CC str.
1433	1423	CH ₂ bend
1264	1205	CH ₂ wag
1098	1064	C-C str.
709	613	C-X str.
617	512	CC-X str.
424	374	C-CC bend
282	230	skeletal bend
102	74	CC-X bend
		a' species
2994	3004	CH ₂ str.
1172	1140	CH ₂ twist
904	857	CH ₂ rock
341	330	C-CC bend
102	74	CC-X bend

TABLE 5.9 Vibrational data and assignments for phenylacetylene and phenylacetylene-1d

Phenylacetylene cm ⁻¹	Phenylacetylene-1d cm ⁻¹	Assignment	Description
		a1	
3315		v1	CC-H str.
	2596	v1	CC-D str.
3065	3068	v2	
3058	3059	v3	
3035	3037	v4	
2119		v5	CC str.
	1989	v5	CC str.
1597	1596	v6	
1490	1489	v7	
1192	1189	v8	
1178	1174	v9	
1028	1023	v10	
1000	998	v11	
763	759	v12	
467	462	v13	
		b1	
3101	3101	v14	
3083	3085	v15	
1573	1572	v16	
1446	1443	v17	
1332	1328	v18	
1285	1279	v19	
1158	1157	v20	
1071	1069	v21	
648		v22	CC-H bend
	482	v22	CC-D bend
610	623	v23	
515	529	v24	
351	344	v25	
		a2	
967	968	v26	
842	840	v27	
418	418	v28	
		b2	
983	982	v29	
917	914	v30	
754	754	v31	
688	688	v32	
612		v33	o.p. CC-H bend
	482	v33	op. CC-D bend
529	529	v34	
351	344	v35	
165	152	v36	

1-Halopropadienes and 1-Bromopropadiene-1d

References	116
Figures	Table
Figure 6-1	118 (115)
Figure 6-2	118 (115)
Figure 6-3	119 (115)
Figure 6-3a	119
Figure 6-4	120 (115, 116)
Figure 6-5	121 (116)
Figure 6-6	122 (116)
	Table 6-1
	123 (115)

*Numbers in parentheses indicate in-text page reference.

Propadienes were discussed in Chapter 4, and assignments were presented in Table 4.16. Chapter 6 is presented separately from previous discussion of propadienes because these compounds are formed from the rearrangement of 3-halopropynes. By study of the rearrangement of 3-bromopropyne-1d, it was possible to determine the rearrangement mechanism.

Assignments of these propadienes were based upon both IR and Raman data. Table 6.1 lists the frequencies and assignments for these 1-halopropadienes and 1-bromopropadiene-1d (1,2). Infrared solution and vapor-phase spectra of 3-bromopropyne-1d impure with 3-bromopropyne are shown in Fig. 6.1 and the Raman spectra are shown in Fig. 6.2. Figure 6.3 shows IR solution and vapor-phase spectra and Fig. 6.3a shows the Raman spectrum of 1-bromopropadiene-1d impure with 1-bromopropadiene (2).

The exchange between $C\equiv C-H$ and $O-D$ to form $C\equiv C-D$ is known to occur under basic conditions, and it was used to prepare phenylacetylene-1d (3). The method for deuterium change utilizes a basic column packing. The sample of 3-bromopropyne-1d was passed through a preparative gas-liquid chromatography column packed with chromosorb w(30-60 mesh) coated with 15% E20M and 10% KOH that had been pretreated with D_2O (4). The sample of 1-bromopropadiene-1d was prepared using a method developed at The Dow Chemical Company (5). Using 2 ml of the ~90% sample of 3-bromopropyne-1d as starting material, in solution in 20 ml of dimethylformamide in the presence of 50 mg of NaBr under atmospheric pressure and 100 °C for 5 h, the sample of 1-bromopropadiene-1d was synthesized. The solution was then passed through a preparative liquid-gas chromatographic column, and the sample collected in a

trap. The sample of 1-bromopropadiene-1d contained about 10% 1-bromopropadiene as an impurity.

The halopropadienes have C_s symmetry, and the 15 normal modes are distributed as: $10a'$ and $5a''$. The a' modes are symmetrical and the a'' modes antisymmetrical with respect to the plane of symmetry. The a' modes should yield type A/B IR vapor bands and polarized Raman bands, while a'' modes should yield type C IR vapor bands and depolarized Raman bands. The question to be answered is whether the product formed is $HDC=C=CHBr$ or $CH_2=C=CDBr$. In other words, did the deuterium atom or the bromine atom move in the chemical rearrangement?

IR vapor-phase spectra for 1-chloro-, 1-bromo-, and 1-iodopropadiene are shown in Figs. 6.4, 6.5, and 6.6, respectively. IR vapor-phase type A/B bands are noted at $(888/868\text{ cm}^{-1})$, $(873/852\text{ cm}^{-1})$, and $(860/848\text{ cm}^{-1})$ for the Cl, Br, and I analogs, respectively. In addition, a type A/B band is noted at $(872/865\text{ cm}^{-1})$ in the case of the deuterated propadiene analog. Each of these compounds exhibits a type A/B band at $(1758/1745\text{ cm}^{-1})$, $(1743/1732\text{ cm}^{-1})$, $(1717/1707\text{ cm}^{-1})$, and $(1735/1725\text{ cm}^{-1})$ for the Cl, Br, I, and BrD analogs, respectively. The calculated first overtone of the type A/B bands reported here are: $(1776/1736\text{ cm}^{-1})$, $(1746, 1704\text{ cm}^{-1})$, $(1720/1696\text{ cm}^{-1})$, and $1744/1730\text{ cm}^{-1}$ for the Cl, Br, I, and BrD analogs, respectively. Assignment of the type A/B bands in the region $848\text{--}888\text{ cm}^{-1}$ to $CH_2 = \text{wag}$, and the type A/B bands in the region $1725\text{--}1758\text{ cm}^{-1}$ as $2(CH_2 = \text{wag})$ is correct, because the $CH_2 = \text{wag}$ mode always exhibits negative anharmonicity (occurs at higher frequency than the calculated $2(CH_2 = \text{wag})$ (6).

A vapor-phase type C band is observed at $822, 812, \text{ and } 807\text{ cm}^{-1}$ in the IR spectra of 1-chloro-, 1-bromo-, and 1-iodopropadiene, and a type C band is observed at 681 cm^{-1} in the case of the BrD analog. The ratio $812\text{ cm}^{-1}/681\text{ cm}^{-1}$ is equal to 1.19. The bands in the region $807\text{--}882\text{ cm}^{-1}$ are assigned to the out-of-plane $=C-H$ bending vibration for the Cl, Br, and I propadiene analogs, respectively. In the case of the BrD analog the out-of-plane $C-D$ bending mode is assigned at 681 cm^{-1} . The out-of-plane $C=C=C$ bending mode for 1-bromopropadiene is assigned at 519 cm^{-1} and for the BrD analog it is assigned at 501 cm^{-1} . It is most likely that the out-of-plane bending mode and the out-of-plane $C-D$ bending modes are coupled, as the out-of-plane mode occurs at higher frequency than predicted ($\sim 574\text{ cm}^{-1}$) and the out-of-plane $C=C=C$ bending mode occurs 18 cm^{-1} lower than it does for 1-bromopropadiene. Thus, this rearrangement involves migration of the halogen atom rather than the proton or deuterium atoms in a bimolecular reaction (2).

Plots of the fundamental vibrations and some combination and overtones for the 1-halopropadienes vs Pauling electronegativity values have been published (7). The dashed portion of these plots is where these vibrations would be predicted in the case of 1-fluoropropadiene. In our studies of 1-halopropynes, no evidence was observed for the presence of 1-fluoropropadiene. This may not seem surprising, as the strength of the $C-X$ bond decreases in the order F to I. As already noted, it is the halogen atom that is involved in the bi-molecular rearrangement, and the activation energy required to break the $C-F$ bond in this rearrangement is apparently larger than it is for the Cl, Br, and I analogs.

REFERENCES

1. Nyquist, R. A., Lo, Y-S, and Evans, J. C. (1964). *Spectrochim. Acta*, 20, 619.
2. Nyquist, R. A., Reder, T. L., Stec, F. E., and Kallos, G. J. (1991). *Spectrochim. Acta*, 27A, 897.

3. Evans, J. C. and Nyquist, R. A. (1960). *Spectrochim. Acta*, **16**.
4. Kallos, G. J. and Westover, L. B. (1967). *Tetrahedron Lett.*, 1223.
5. Pawloski, C. E. and Stewart, R. L. (1960). Method for the synthesis of 1-bromopropadiene. The Dow Chemical Company, Midland, MI.
6. Potts, W. J. and Nyquist, R. A. (1959). *Spectrochim. Acta*, **15**, 679.
7. Pauling, L. (1948). *The Nature of the Chemical Bond*, Ithaca, New York: Cornell University Press.



FIGURE 6.1 Infrared solution and vapor-phase spectra of 3-bromopropyne-1d impure with 3-bromopropyne.

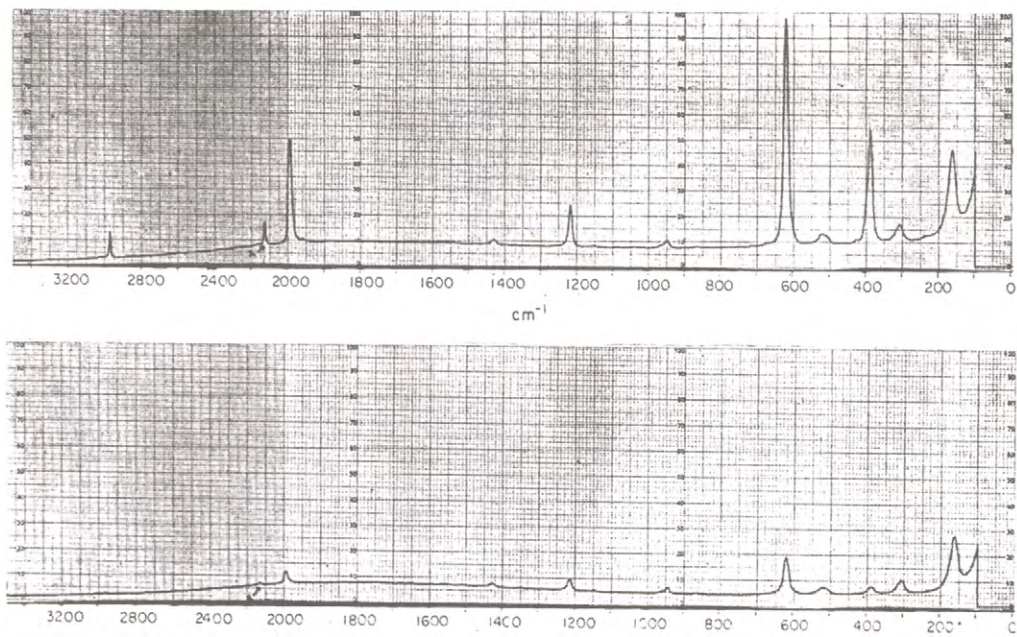


FIGURE 6.2 Raman spectra of 3-bromopropyne-1d impure with 3-bromopropyne.

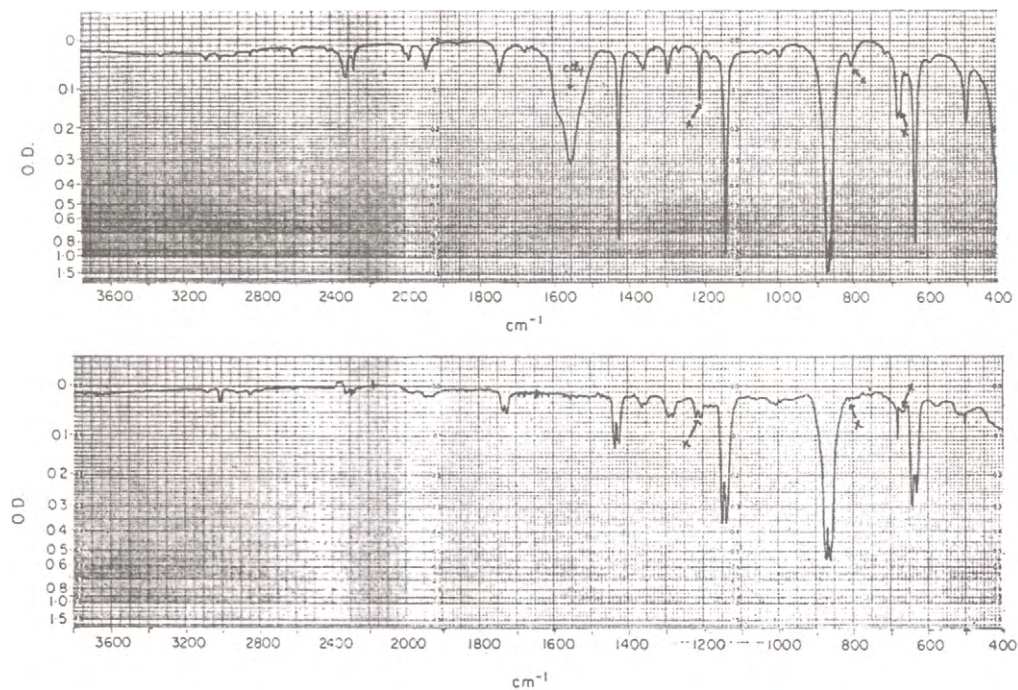


FIGURE 6.3 IR solution and vapor-phase spectra of 1-bromopropadiene-1d impure with 1-bromopropadiene.

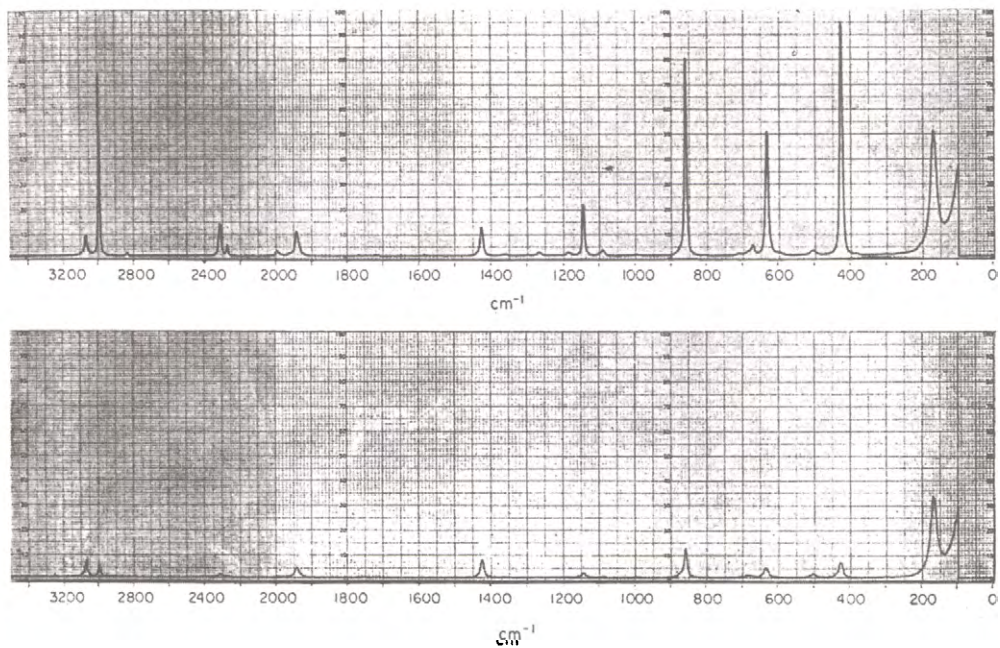


FIGURE 6.3A Raman spectrum of 1-bromopropadiene-1d impure with 1-bromopropadiene.

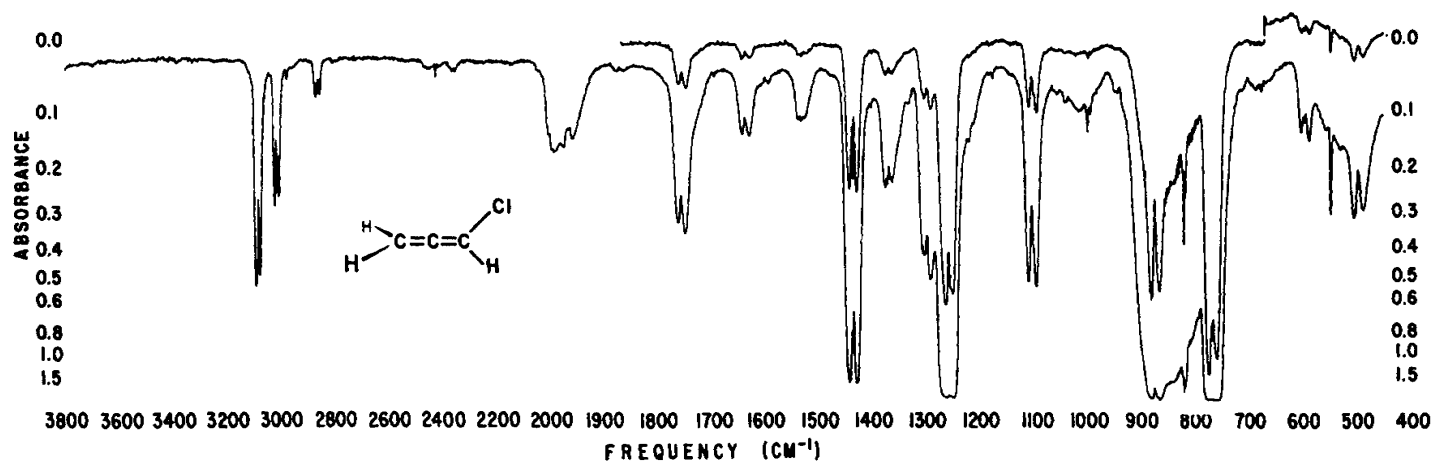


FIGURE 6.4 IR vapor-phase spectra of 1-chloropropadiene.

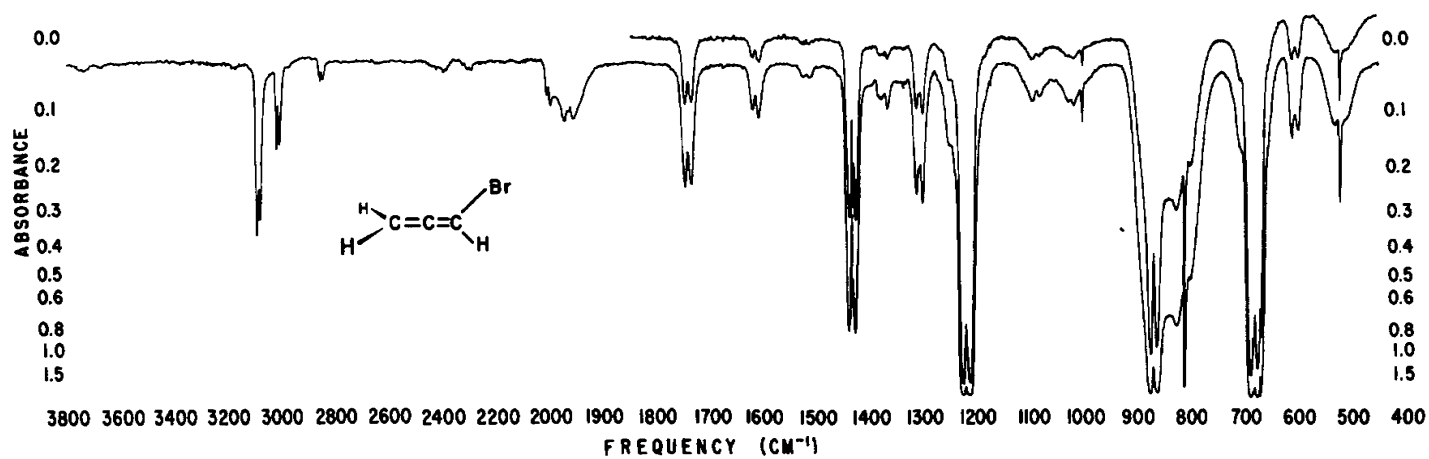


FIGURE 6.5 IR vapor-phase spectra of 1-bromopropadiene.

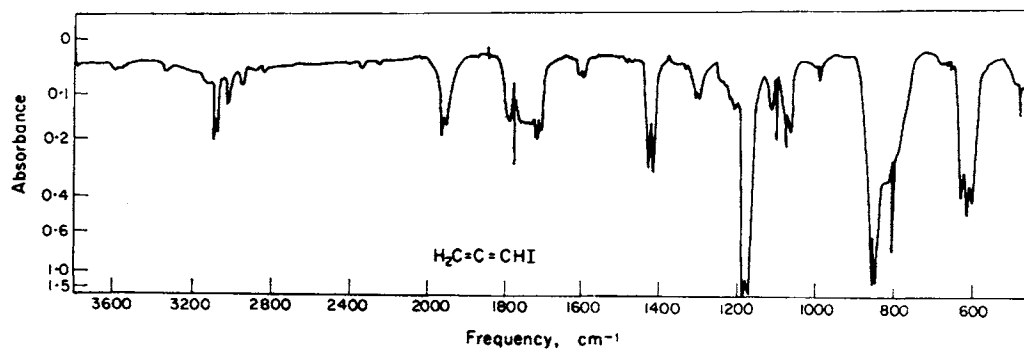


FIGURE 6.6 IR vapor-phase spectra of 1-iodopropadiene.

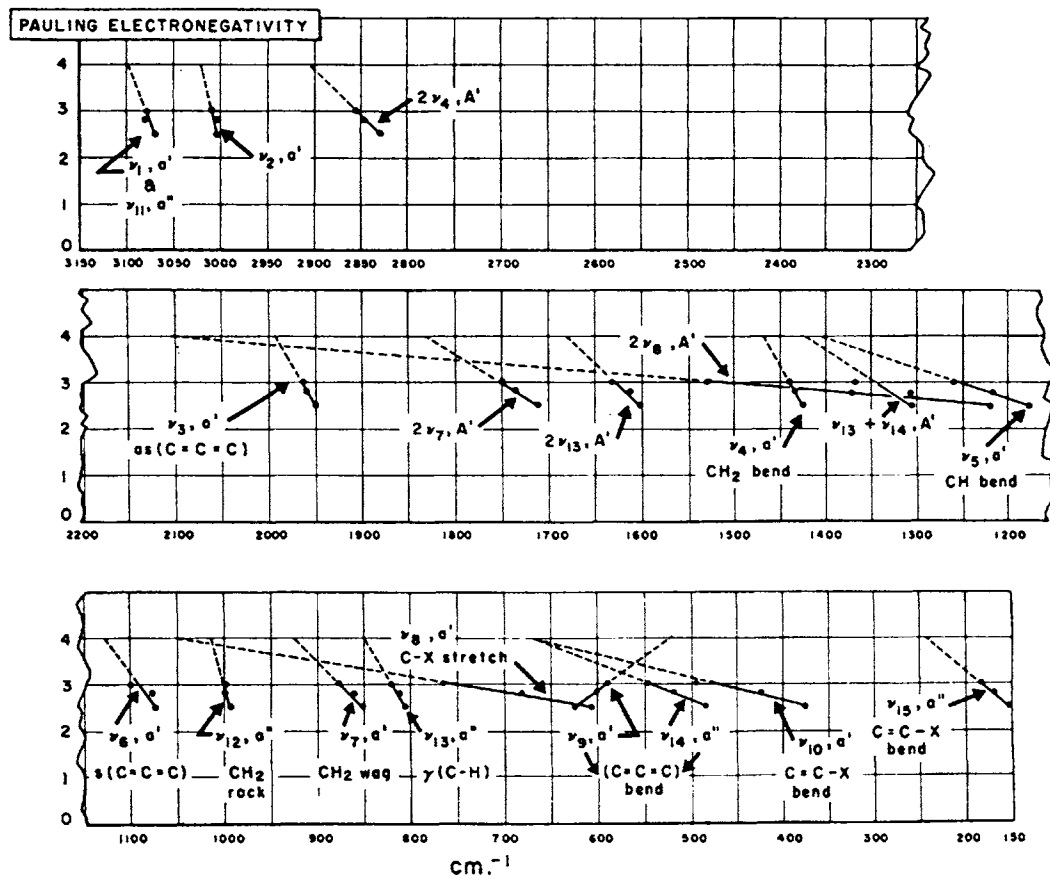


FIGURE 6.7 Plots of the fifteen fundamentals, certain first overtones, and one combination band vs. Pauling electronegativity. The solid lines represent observed data, and the dashed extension is the extrapolation used to predict the partial spectrum of fluoropropadiene (see text).

TABLE 6.1 IR and Raman data and assignments for 1-halopropadienes and 1-bromopropadiene-1d

Species	Chloro-propadiene	Bromo-propadiene	1-Bromo-propadiene-1d	Iodo-propadiene	Assignment
a'	3079	3080	2316	3070	CH str. or CD str.
	3009	3005	3005	3004	CH ₂ str.
	1963	1961	1936	1953	a.C=C=C str.
	1435	1432	1426	1425	CH ₂ bend
	1256	1217	858	1178	CH bend or CD bend
	1101	1078	1141	1076	s.C=C=C str.
	875	862	867	854	CH ₂ wag
	767	681	636	609	C-X str.
	592	603	576	625	C=C=C bend
	494	423 ^{*1}	426	387 ^{*2}	C=C-X
a''	3079	2080	3075	3070	CH ₂ str.
	999	1000	994	995	CH ₂ rock
	822	812	681	807	CH bend or CD bend
	548	519	501	485	C=C=C bend
	184 ^{*2}	169 ^{*2}	170	154 ^{*2}	C=C-X bend

^{*1} [liquid]^{*2} [CS₂ soln.]

Alcohols and Phenols

OH Stretching for Alcohols	125
Alcohol C–O Stretching	127
Primary Alcohols and Cycloalkanols (carbon-hydrogen vibrations)	127
Phenols	127
OH Stretching	127
Phenyl-oxygen Stretching and OH Bending	128
Intramolecular $\nu\text{OH} \cdots \text{X}$ Frequencies in the Vapor and CCl_4 Solution Phases	130
Weak Intramolecularly Hydrogen-Bonded Phenols	131
Temperature Effects	131
References	131

Figures

Figure 7-1	132 (128)
Figure 7-2	133 (129)
Figure 7-3	132 (130)
Figure 7-4	132 (131)

Tables

Table 7-1	133 (125)
Table 7-2	135
Table 7-3	136 (128)
Table 7-4	137 (128)
Table 7-5	138 (128, 129)

*Numbers in parentheses indicate in-text page reference.

Both alcohols and phenols are widely used for their unique properties, or as intermediates in the manufacture of other chemicals.

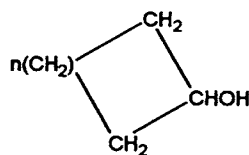
OH STRETCHING FOR ALCOHOLS

Table 7.1 lists IR vapor-phase data for alcohols (1). Primary alcohols, $\text{R}-\text{CH}_2-\text{OH}$, exhibit the OH stretching frequency in the region $3670\text{--}3680\text{ cm}^{-1}$, secondary alcohols, $(\text{R})_2\text{CH}-\text{OH}$, $3650\text{--}3660\text{ cm}^{-1}$, and tertiary alcohols, $(\text{R})_3\text{C}-\text{OH}$, $3640\text{--}3648\text{ cm}^{-1}$. This decrease in νOH frequency progressing in the series primary, secondary, tertiary alcohols is attributed to the increasing inductive effect of the alkyl groups, which weaken the OH bond (1). In dilute CCl_4 solution, the primary, secondary, and tertiary alcohols occur in the regions $3630\text{--}3634$, $3620\text{--}3635$, and $3600\text{--}3620\text{ cm}^{-1}$, respectively (2). The νOH frequencies occur at lower frequency in CCl_4 solution as a result of intermolecular hydrogen bonding between the OH proton and the Cl atom of CCl_4 (e.g., $\text{O}-\text{H} \cdots \text{Cl}-\text{C Cl}_3$)(3). In the vapor phase and in dilute solution the νOH band is sharp, and has relatively weak intensity. This is in contrast to intermolecular hydrogen-bonded $\text{OH}:\text{OH}$ frequencies, which occur at lower frequency, $3200\text{--}3400\text{ cm}^{-1}$, and have very strong broad band intensities.

Cycloalkanols are also secondary alcohols and their νOH frequencies in dilute CCl_4 solution occur in the region $3621.4\text{--}3627.7\text{ cm}^{-1}$. These νOH frequencies decrease progressively in the order C_4 through C_8 (3). It is interesting to compare the νOH frequencies in the vapor and in dilute CCl_4 solution.

	Vapor cm^{-1} (1)	CCl_4 solution cm^{-1} (3)	Vapor- CCl_4 cm^{-1}
cyclopentanol	3660	3625.5	34.5
cyclohexanol	3659	3623.9	35.1
cycloheptanol	3655	3621.7	34.3
cyclooctanol	3650	3621.4	28.6
$\Delta\text{ cm}^{-1}$	10	4.1	5.9

In the vapor phase and in CCl_4 solution νOH decreases 10 and 4.1 cm^{-1} progressing in the series C_5 to C_8 for these cyclic secondary alcohols. In CCl_4 solution the OH is intermolecularly bonded to a Cl atom such as $\text{OH}\cdots\text{ClCCl}_3$. This intermolecular hydrogen bond weakens the OH bond; consequently, νOH occurs at lower frequency in CCl_4 solution than it occurs in the vapor phase. In addition, the increasing inductive contribution of $(\text{CH}_2)_3$ to $(\text{CH}_2)_7$ to CHOH is the reason the νOH frequency shifts to lower frequency as the series progresses from C_5 to C_8 . Perhaps the reason that νOH does not shift as much to lower frequency in CCl_4 solution as it does in the vapor phase is that the α -bond



angle increases as n increases from 2 to 5. With the increasing α -bond angle, the α -carbon atoms prevent the OH and CCl_4 Cl atoms from coming as close in space to form the $\text{OH}\cdots\text{Cl}$ bond. In other words the intermolecular $\text{OH}\cdots\text{Cl}$ bond distance increases as $(\text{CH}_2)_n$ increases due to the increase in the α -bond angle, which increases the steric factor of the two adjacent CH_2 groups.

All alcohols form intermolecular hydrogen bonds in the condensed phase, if steric factors are not present. These intermolecular hydrogen bonds are formed between $(\text{OH}:\text{OH})_n$ groups. In the case of the alcohols, the OH group is the most basic site as indicated. In the vapor phase, OH group for ordinary alcohols do not form intermolecular hydrogen bonds at elevated temperature. However, in the vapor phase at elevated temperature alcohols do form intramolecular hydrogen bonds with other available basic sites within the molecule to form 5-, 6-, 7-, or 8-membered intramolecular $\text{OH}\cdots\text{X}$ bonds. Examples are presented in what follows (1).

The compound 2-methoxyethanol in the vapor phase exhibits a weak shoulder at 3680 cm^{-1} assigned as νOH , and the 3640 cm^{-1} band is assigned to the intramolecular hydrogen bonded $\text{OH}\cdots\text{O}$ group forming a 5-membered group (1). In the case of 2-(2-methoxyethoxy) ethanol, the unassociated νOH is assigned at 3678 cm^{-1} , and the IR bands at 3639 and 3540 cm^{-1} are assigned to intramolecular hydrogen bond $\text{OH}:\text{O}$ groups forming 5- and 8-membered rings, respectively. In both the 5- and 8-membered rings the OH group is bonded to an ether oxygen atom and both have comparable basicity. The 8-membered $\nu\text{OH}\cdots\text{O}$ group occurs at lower frequency than that for the 5-membered ring, because the $\text{OH}\cdots\text{O}$ groups are closer in space and

form a stronger intramolecular hydrogen bond. Numerous examples of intramolecular hydrogen bonds for primary, secondary, and tertiary alcohols with OH, R–O–R, S, halogen, C=C, phenyl, and C=O groups are presented in Reference (1). Those engaged in GC/FT-IR experiments would benefit from information available in this text.

ALCOHOL C–O STRETCHING

The C–O stretching frequency, $\nu_{\text{C-O}}$, in the vapor phase occurs in the region 1031–1060 cm^{-1} , 1135–1147 cm^{-1} , and 1141–1180 cm^{-1} for the primary, secondary, and tertiary alcohols, respectively (1). The absorbance (A) for $\nu_{\text{C-O}}$ for the primary alcohols generally decreases in intensity progressing in the series ethanol through 1-decanol, and it is attributed to an increase in the number of (CH_2) groups. The $\nu_{\text{C-O}}$ frequency increase progressing in the series primary, secondary, tertiary alcohol is attributed to increased branching on the C–O–H carbon atom, and $\nu_{\text{C-O}}$ in these cases includes some stretching of the C–C bonds.

PRIMARY ALCOHOLS AND CYCLOALKANOLS (CARBON-HYDROGEN VIBRATIONS)

The $\nu_{\text{asym. CH}_3}$ and $\nu_{\text{sym. CH}_3}$ modes occur in the region 2950–2980 cm^{-1} and 2899–2920 cm^{-1} , respectively. The $\nu_{\text{asym. CH}_2}$ and $\nu_{\text{sym. CH}_2}$ modes occur in the region 2930–2940 cm^{-1} and 2865–2910 cm^{-1} , respectively. The CH_2 bending and sym. CH_3 bending modes occur in the region 1452–1469 cm^{-1} and 1384–1392 cm^{-1} , respectively. The CH_2 rocking mode occurs in the region 720–778 cm^{-1} .

PHENOLS

In the solid phase (Nujol mull) phenols, which are not intramolecular, exhibit intermolecular hydrogen-bonded hydroxyl groups, $\nu(\text{OH}\cdots\text{OH})_n$ in the range 3180–3400 cm^{-1} . The 2-alkyl-phenols exhibit $\nu(\text{OH}\cdots\text{OH})_n$ in the range 3438–3535 cm^{-1} , and the frequency increases with the increasing steric factor of the alkyl group [CH_3 to $\text{C}(\text{CH}_3)_3$] (12). The increasing steric factor increases the bond distance between $(\text{OH}\cdots\text{OH})_n$ group. Table 7.2 lists IR vapor-phase data for ν_{OH} , $\nu_{\text{OH}\cdots\text{X}}$, in-plane OH bending, and phenyl oxygen stretching.

OH STRETCHING

Unassociated ν_{OH} for these phenols is assigned in the region 3642–3660 cm^{-1} . In cases where the OH group is in the cis spatial configuration to a tert.-butyl group, the ν_{OH} frequency occurs at higher frequency in the region 3670–3680 cm^{-1} . The higher frequency is attributed to repulsion between the OH proton and the protons on the tert.-butyl group. In cases where only one 2-tert.-butyl group is present, a ν_{OH} band will occur in each of these regions of the spectrum, and when 2,6-di-tert.-butyl groups are present only one band will occur in the lower region. The phenol $\nu_{\text{OH}}:\text{X}$ frequencies occur in the region 3278–3630 cm^{-1} depending upon which atom or groups are in the 2- or 6-positions. The frequency is dependent upon both the basicity of the X group, the acidity of the OH proton, and the spatial distance between OH and X in the cyclic intramolecular hydrogen bond.

PHENYL-OXYGEN STRETCHING AND OH BENDING

Phenols show a strong band in the region $1209\text{--}1295\text{ cm}^{-1}$ assigned to a complex in-plane ring mode, which includes stretching of the phenyl-O bond, $\nu\phi\text{--O}$ (1). A band in the region $1152\text{--}1224\text{ cm}^{-1}$ is attributed to in-plane OH bending.

INTRAMOLECULAR $\nu\text{OH}\cdots\text{X}$ FREQUENCIES IN THE VAPOR AND CCl_4 SOLUTION PHASES

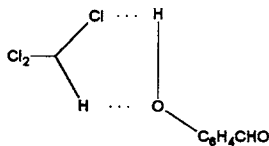
Table 7.3 compares the νOH , trans νOH , and $\nu\text{OH}\cdots\text{X}$ frequencies in the vapor and CCl_4 solution phases.

In the case of phenol, νOH (3650 cm^{-1}) in the vapor decreases 40 cm^{-1} in CCl_4 solution (3610 cm^{-1}). The decrease in the νOH frequency is attributed to the formation of an intermolecular hydrogen bond of form $\text{OH}\cdots\text{Cl}$ with CCl_4 molecules when phenol is in dilute solution in CCl_4 . The $\nu\text{OH}:\text{X}$ frequencies listed occur in region ($3202\text{--}3595\text{ cm}^{-1}$) in the vapor and occur at lower frequency by $17\text{--}35\text{ cm}^{-1}$ in CCl_4 solution ($3185\text{--}3560\text{ cm}^{-1}$). This decrease in frequency we attribute to the formation of $\text{X}\cdots\text{H}\text{--}\text{O}$ which further weakens the OH bond.



Table 7.4 lists the νOH frequencies for 1% wt./vol. 4-hydroxybenzaldehyde in 0–100 mol % $\text{CHCl}_3/\text{CCl}_4$ (4). In this case νOH for 4-hydroxybenzaldehyde decreases 12.4 cm^{-1} in going from solution in CCl_4 to solution in CHCl_3 . Moreover, νOH decreases continually as the mole % $\text{CHCl}_3/\text{CCl}_4$ is increased (see Fig. 7.1). This decrease in frequency results from an increase in the Solvent Field effect as the mole % $\text{CHCl}_3/\text{CCl}_4$ is increased.

One would expect that the Cl atoms of CCl_4 would be more basic than the Cl atoms of CHCl_3 and that the $\nu\text{OH}:\text{Cl}$ in the case of CCl_4 would occur at a lower frequency than in CHCl_3 , and the opposite is observed in the case of 4-hydroxybenzaldehyde. Apparently, the situation is much more complex in the case of $\text{CHCl}_3/\text{Cl}_4$ solutions. There is, of course, intermolecular bonding such as $(\text{Cl}_3\text{CH}\cdots\text{ClCCl}_3)_n$ in the mixed solvent system. The Cl_3CH proton would also bond intermolecularly with the $\text{C}=\text{O}$ group ($\text{C}=\text{O}\cdots\text{HCCl}_3$), both sides of the π system of the phenyl group, and to the OH group such as



All of these intermolecular hydrogen bonding sites filled with CHCl_3 would weaken the OH bond because it would be more acidic. Consequently, the $\nu\text{OH}:\text{X}$ mode would occur at lower frequency than that exhibited by the much simpler case of CCl_4 solution. Apparently, the hydrogen bonding equilibrium shifts as the mole % $\text{CHCl}_3/\text{CCl}_4$ changes.

Table 7.5 lists IR data for phenol and intramolecular hydrogen-bonded phenols 10% wt./vol. in CCl_4 solution in the region $3800\text{--}1333\text{ cm}^{-1}$ and in CS_2 solution in the region 1333--

400 cm^{-1} using 0.1-mn cells and 10 and 2% wt./vol. in 2,2,4-trimethylpentane in the region $450\text{--}280\text{ cm}^{-1}$ using a 0.4-mn cell unless otherwise indicated (5).

In the case of phenol, νOH occurs at 3610 cm^{-1} and OH torsion occurs at 300 cm^{-1} (6). In this case the OH group turns about the phenyl-O bond in a circle in and out of the plane of the phenyl group. However, in the case of the intramolecular hydrogen-bonded phenols the OH proton is in the plane of the phenyl ring and the 2-X group. Thus, its out-of-plane OH deformation is best described as γOH or as $\gamma\text{OH}\cdots\text{X}$. The maximum peak of absorption for $\nu\text{OH}\cdots\text{X}$ occurs in the region $3598\text{--}3180\text{ cm}^{-1}$ for most of the compounds listed in Table 7.5. However, compounds considered to exist in resonance forms such as

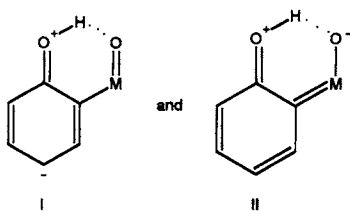


exhibit very broad νOH bands (2500 to 3500 cm^{-1} with a maximum near 3050 cm^{-1} in the case of the 2-hydroxyacetophenones), for 2,4-dibenzoyl resorcinol (very broad in this region $2200\text{--}3600\text{ cm}^{-1}$ with the maximum near 3000 cm^{-1}), and for 2-hydroxybenzophenone (very broad in the region $2200\text{--}3600\text{ cm}^{-1}$ with the maximum near 3100 cm^{-1}). The γOH or $\gamma\text{OH}\cdots\text{X}$ frequencies occur in the region $366\text{--}858\text{ cm}^{-1}$. The $\gamma\text{OH}\cdots\text{X}$ frequencies increase in frequency as the $\nu\text{OH}\cdots\text{X}$ frequencies decrease in frequency as demonstrated in Fig. 7.2. It is usually easy to detect $\gamma\text{OH}\cdots\text{X}$ due to the following: (a) its absorption band is always uniquely broad, and it is easily distinguished from other fundamental absorption bands occurring in this region of the spectrum; (b) the -OD analogs exhibit $\nu\text{OD}\cdots\text{X}$ lower in frequency than $\gamma\text{OH}\cdots\text{X}$ by a factor of ~ 1.35 , and this indicates that $\gamma\text{OH}\cdots\text{X}$ is essentially motion of the proton (or deuteron) alone; and (c) as the $\nu\text{OH}\cdots\text{X}$ bond becomes stronger its frequency decreases, and with a stronger hydrogen bond it becomes more difficult to twist the OH proton out of the plane causing $\gamma\text{OH}\cdots\text{X}$ to shift to higher frequency.

One can perform a simple experiment utilizing IR to determine whether a phenol is inter- or intra-molecularly hydrogen bonded.

When IR spectra of phenolic compounds are recorded in the solid, condensed, or say, 10% wt./vol. in CCl_4 and CS_2 , the OH group forms polymeric $(\text{OH}\cdots\text{OH})_n$ bonds which appear as broad bands centered near $3200\text{--}3400\text{ cm}^{-1}$. This happens even in cases when the OH is intramolecularly hydrogen bonded if the OH oxygen atom is more basic than the atom or group substituted in the 2-position. Examination of the sample in dilute CCl_4 or CS_2 solution using 01.0-mm cell in all cases shows only an unassociated phenolic νOH band or an intramolecular $\nu\text{OH}\cdots\text{X}$ band for compounds containing only 2-x groups (which is not very basic). When the 2-x group is very basic or in the case of compounds such as 2-hydroxybenzophenone, the intramolecular hydrogen bond does not shift significantly or change in intensity. In all classes of OH containing compounds, the inter- or intra-molecularly hydrogen-bonded OH group has much more intensity than the same OH group existing in an unassociated state, or say, intermolecularly hydrogen bonded to CCl_4 or CS_2 .

WEAK INTRAMOLECULARLY HYDROGEN-BONDED PHENOLS

The weak intramolecularly hydrogen-bonded phenols exhibit $\gamma\text{OH}\cdots\text{X}$ frequencies in the range 366–400 cm^{-1} and $\nu\text{OH}\cdots\text{X}$ frequencies above 3500 cm^{-1} . The $\gamma\text{OH}\cdots\text{X}$ frequencies for 2-F, 2-I, 2-Br, and 2-Cl phenol occur at 366, 379, 394, and 359 cm^{-1} , respectively, and their pK_a values (7) are 9.37, 9.04, 9.01, and 8.99, respectively. The halogen atoms increase in size in the order F, Cl, Br, and I, and the data show that the size of the halogen atom does not correlate with $\gamma\text{OH}\cdots\text{X}$, but it does correlate with the pK_a values.

Compounds such as 2-(methylthio) phenol and 2-(methoxy) phenol exhibit their $\nu\text{OH}\cdots\text{X}$ and $\gamma\text{OH}\cdots\text{X}$ frequencies at (3415 and 537 cm^{-1}) and (3560 and 428 cm^{-1}), respectively. In this case, the sulfur atom is larger than the oxygen atom. Consequently, the $\text{S}\cdots\text{HO}$ spatial distance of the intramolecular hydrogen bond is shorter than the $\text{O}\cdots\text{HO}$ spatial distance of the intramolecular hydrogen bond. Thus, a stronger intramolecular hydrogen bond is formed in the case of 2-(methylthio) phenol than in the case of 2-(methoxy) phenol.

In the case of 2-phenylphenol the two rings are not coplanar, and the OH group intramolecularly hydrogen bonds to the π electron system of the 2-phenyl group (8). In this case, $\nu\text{OH}\cdots\pi\phi$ and $\gamma\text{OH}\cdots\pi\phi$ occur at 3570 and 386 cm^{-1} , respectively.

The 2-hydroxy acetophenones form very strong intramolecular hydrogen bonds, and as already noted here, produce a very broad multi peaked absorption band extending over the range 2500–3500 cm^{-1} with a maximum near 3050 cm^{-1} . This is caused by the resonance forms I and II shown on page 127 and this affects both the $\nu\text{OH}\cdots\text{O}=\text{C}$ and $\gamma\text{OH}\cdots\text{O}=\text{C}$ frequencies as discussed here. Enhancement of structure I would elongate the OH bond, thus making the proton more acidic. Enhancement of structure II would tend to increase the carbonyl group. Both of these effects would lower $\nu\text{OH}\cdots\text{O}=\text{C}$, and raise $\gamma\text{OH}\cdots\text{O}=\text{C}$ frequencies, because the intramolecular hydrogen bond would be stronger. In addition, these resonance effects would induce more double bond character into the C–O bond, which would also contribute to an increase in the $\gamma\text{OH}\cdots\text{O}=\text{C}$ frequency, as the $\nu\text{OH}\cdots\text{O}=\text{C}$ bond would be stronger. In addition, these resonance effects would induce more double bond character into the C–O bond, which would also contribute to an increase in $\gamma\text{OH}\cdots\text{O}=\text{C}$. Because the $\nu\text{OH}\cdots\text{O}=\text{C}$ band is so broad, it is difficult to correlate $\nu\text{OH}\cdots\text{O}=\text{C}$ with Tafts $(\sigma_\rho - \sigma')$ and $(\sigma_m - \sigma')$ values. Tafts $(\sigma_\rho - \sigma')$ and $\sigma_m - \sigma'$ are measures of the resonance effects of the 5-substituent upon the OH and COCH_3 groups (9,10). Figure 7.3 shows a plot of $(\sigma_\rho - \sigma') + (\sigma_m - \sigma')$ vs the $\gamma\text{OH}\cdots\text{O}=\text{C}$ frequencies. The sum of the Taft values is expected to yield a parameter with which to compare the $\gamma\text{OH}\cdots\text{O}=\text{C}$ frequencies for 2-hydroxy-5-X- acetophenones. Similar curves are obtained by plotting $\gamma\text{OH}\cdots\text{O}=\text{C}$ vs $(\sigma_\rho - \sigma')$ or $(\sigma_m - \sigma')$ alone. In Fig. 7.3, the plot is continued with the dashed line representation through the two solid points that one would predict from the $(\sigma_\rho - \sigma')$ and $(\sigma_m - \sigma')$ values for acetyl and nitro, respectively. The x points are values previously obtained for phenols (10), and the agreement is quite good. A similar plot of $\gamma\text{OH}\cdots\text{O}=\text{C}$ vs $(\sigma_\rho - \sigma')$ for these compounds when extrapolated as a straight line to higher values allows one to predict $(\sigma_\rho - \sigma')$ values for the acetyl group (+0.48) and the nitro group (+0.62), and the values obtained are +0.60 and +0.64 for acetyl and nitro, respectively (10). In the case of 2-methylsulfonylphenol, $\nu\text{OH}\cdots\text{O}_2\text{S}$ occurs at 3330 and $\nu\text{OD}\cdots\text{O}_2\text{S}$ at 2475 cm^{-1} . The $\nu\text{OH}/\nu\text{OD}$ ratio is ~ 1.35 , and the $\gamma\text{OH}\cdots\text{O}_2\text{S}/\gamma\text{OD}\cdots\text{O}_2\text{S}$ frequency ratio

$645\text{ cm}^{-1}/529\text{ cm}^{-1}$ is equal to ~ 1.22 . The 529 cm^{-1} band is the only broad band in this region of the spectrum. An SO_2 deformation has been assigned in this region of the spectrum (11), and it is suggested that the reason $\gamma\text{OH}\cdots\text{O}_2\text{S}$ occurs at higher frequency is because it is coupled with an SO_2 deformation.

TEMPERATURE EFFECTS

Figure 7.4 shows plots of the intramolecular hydrogen-bonded OH : Cl stretching frequencies for 2-chlorophenol, 2,4,5-trichlorophenol and 2,6-dichlorophenol in CS_2 solution vs temperature in $^\circ\text{C}$. These plots show that the $\nu\text{OH} : \text{Cl}$ frequencies decrease in frequency in a linear manner as temperature is decreased (13). As the temperature is decreased the CS_2 volume contracts, and the Field effect of CS_2 increases. This then causes the $\nu\text{OH} : \text{Cl}$ frequencies to decrease as the temperature is lowered.

REFERENCES

1. Nyquist, R. A. (1984). *The Interpretation of Vapor-phase Infrared Spectra: Group Frequency Data*, Philadelphia: Sadtler Research Laboratories, Div. of Bio-Rad.
2. Bellamy, L. J. (1975). *The Infrared Spectra of Complex Molecules*, vol. 1, 3rd ed., London: Chapman and Hall; New York: John Wiley & Sons, Inc. p. 108.
3. van der Maas, J. H. and Lutz, E. T. G. (1974). *Spectrochim. Acta*, **30A**, 2005.
4. Nyquist, R. A., Settineri, S. E., and Luoma, D. A. (1992). *Appl. Spectrosc.*, **46**, 293.
5. Nyquist, R. A. (1963). *Spectrochim. Acta*, **19**, 1655.
6. Evans, J. C. (1960). *Spectrochim. Acta*, **16**, 1382.
7. Bennett, G. M., Brooks, G. L., and Glasstone, S. (1935). *J. Chem. Soc.*, 1821.
8. Baker, A. W. and Shulgin, A. T. (1958). *J. Am. Chem. Soc.*, **80**, 5358.
9. Taft, R. W. Jr. (1956). *Steric Effects in Organic Chemistry*, Chap. 13, New York: J. Wiley.
10. Taft, R. W. Jr., Deno, N. C., and Skell, P. S. (1958). *Ann. Rev. Phys. Chem.*, **9**, 287.
11. Simon, A., Kriegsman, H., and Dutz, H. (1956). *Chem. Ber.*, **89**, 2378.
12. Lin-Vien, D., Colthup, N. B., Fateley, W. G., and Grasselli, J. G. (1991). *The Handbook of Infrared and Raman Characteristic Frequencies of Organic Molecule*, San Diego: Academic Press.
13. Nyquist, R. A. (1986). *Appl. Spectrosc.*, **40**, 79.

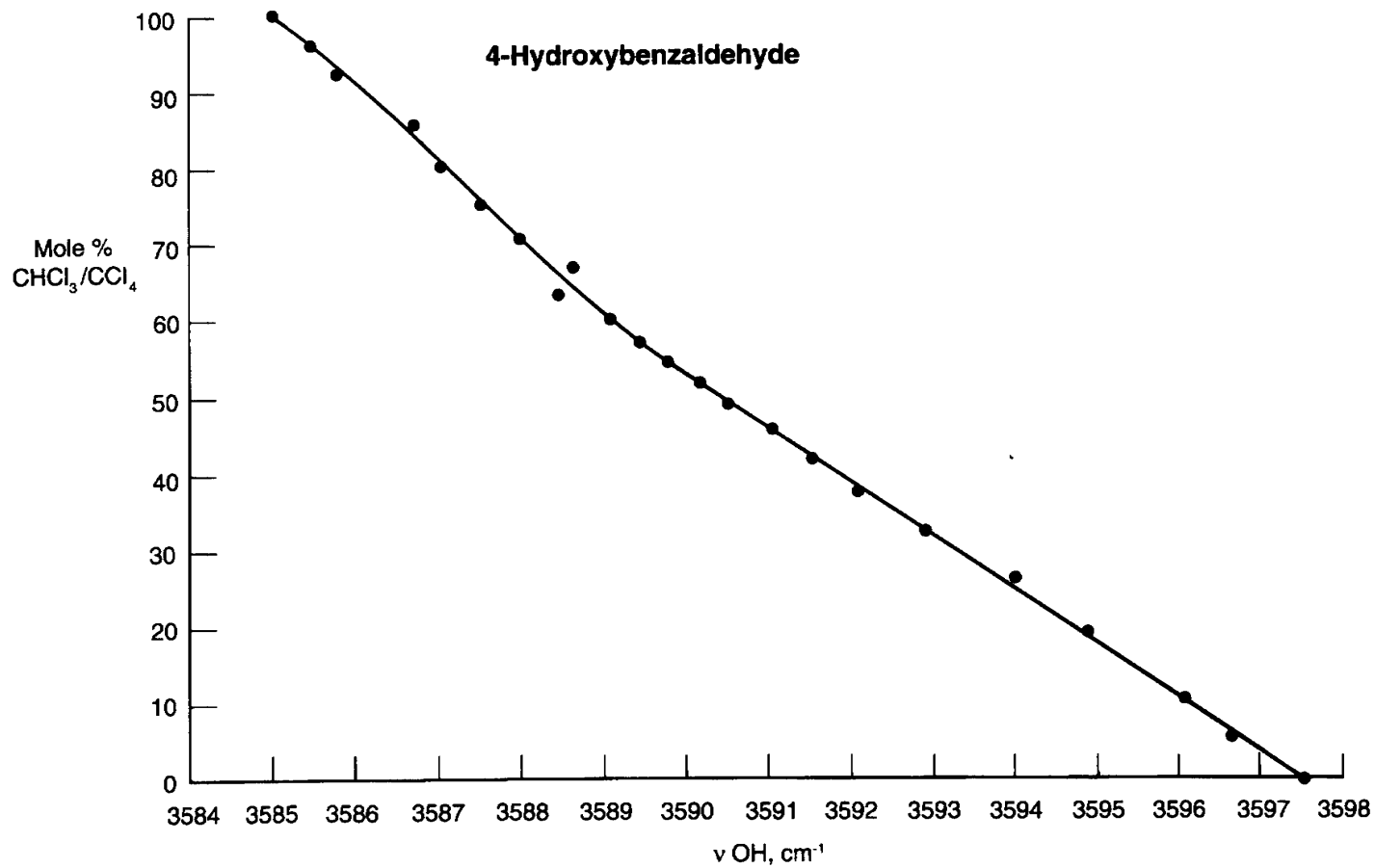


FIGURE 7.1 A plot of νOH for 4-hydroxybenzaldehyde vs mole % $\text{CHCl}_3/\text{CCl}_4$.

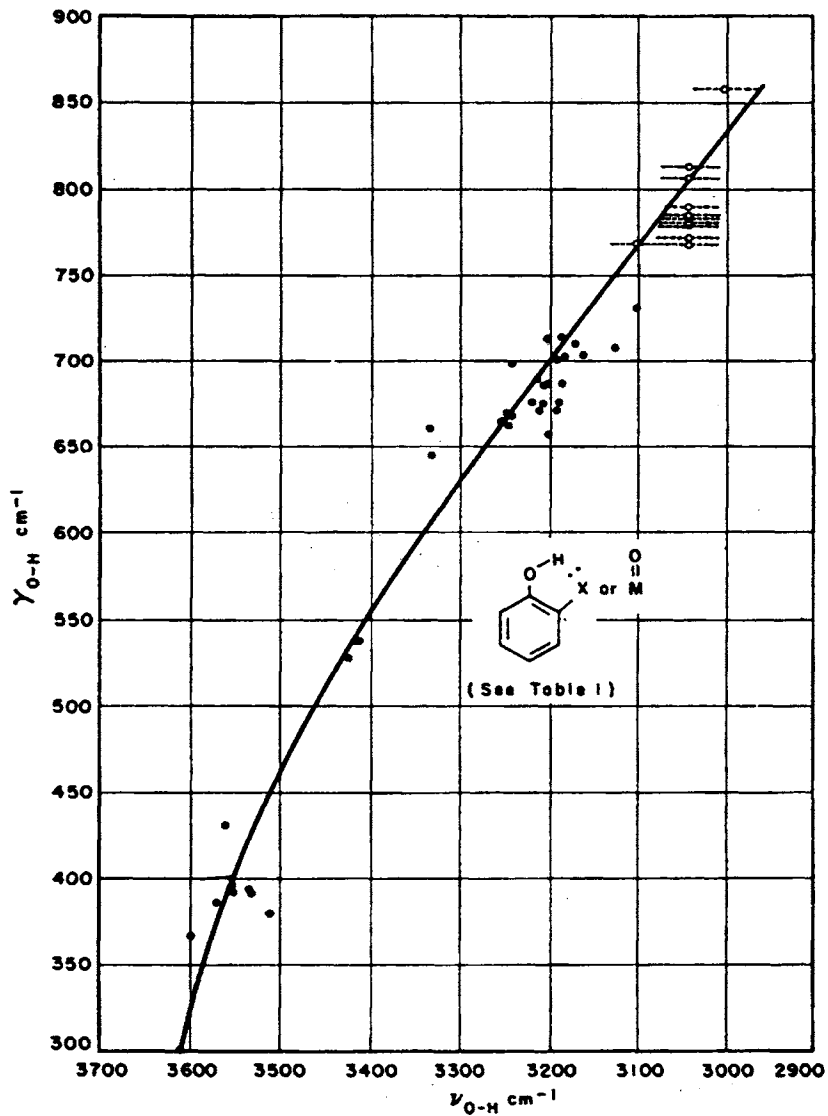


FIGURE 7.2 A plot of the $\gamma_{O-H} \cdots X$ frequencies vs the $\nu_{O-H} \cdots X$ frequencies for 2-X-substituted phenols.

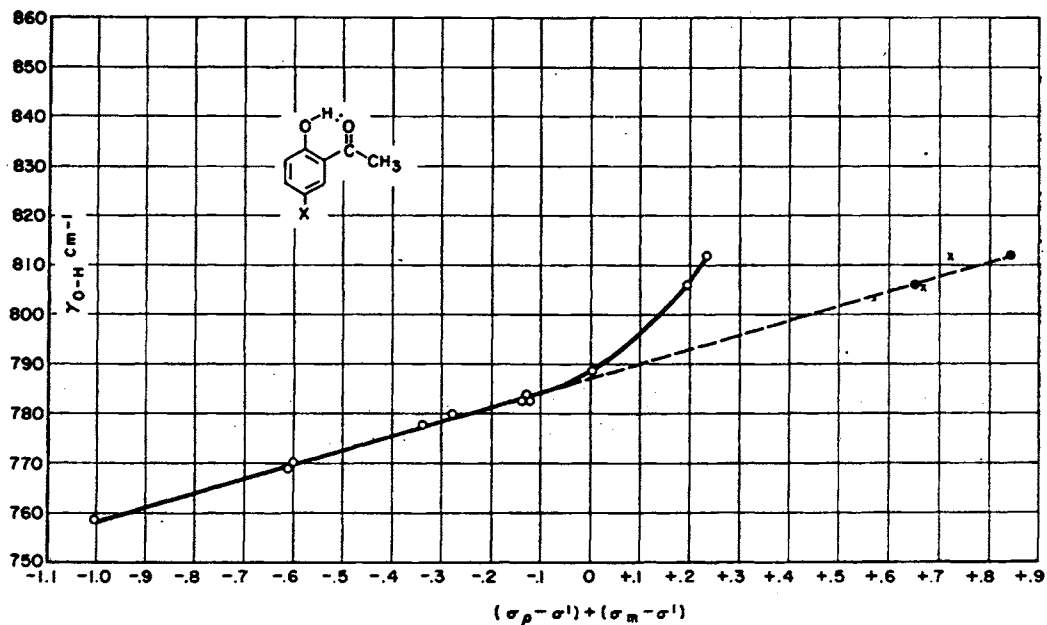


FIGURE 7.3 A plot of Tafts $(\sigma_p - \sigma') + (\sigma_m - \sigma')$ vs $\gamma_{OH \cdots OC}$ frequencies.

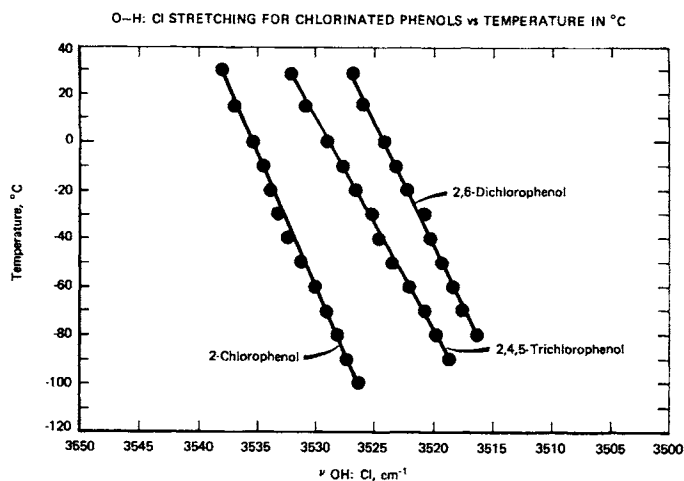


FIGURE 7.4 Plots of intramolecular hydrogen-bonded OH:Cl stretching frequencies for chlorinated phenols in CS_2 solution vs temperature in $^{\circ}\text{C}$.

TABLE 7.1 IR vapor-phase data and assignments for alcohols

Compound	OH str.	C-O str.	a.CH ₃ str.	a.CH ₂ str.	2 (a.CH ₃ bend)		s.CH ₂ str.	a.CH ₃ bend	CH ₂ bend	s.CH ₃ bend	CH ₂ rock
					in FR.	s.CH ₃ str.					
Methanol	3680 (0.150)	1031 (1.150)	2980 (0.620)		2920 (0.600)	2820 (0.370)		1458 (0.129)			
Ethanol	3679 (0.240)	1060 (1.230)	2975 (1.150)				2910 (1.150)		1452 (0.150)	1392 (0.460)	800 (0.030)
Propanol	3675 (0.160)	1065 (0.840)	2965 (1.230)	2940 (1.150)	2900 (0.700)		2890 (0.495)		1461 (0.140)	1390 (0.190)	740 (0.020)
1-Butanol	3670 (0.161)	1041 (0.572)	2950 (1.230)				2890 (0.820)		1466 (0.151)	1389 (0.1510)	749 (0.035)
1-Hexanol	3675 (0.111)	1053 (0.400)	2970 (0.850)	2940 (1.230)	2899 (0.590)		2880 (0.600)		1467 (0.133)	1389 (0.130)	728 (0.020)
1-Heptanol	3670 (0.111)	1050 (0.341)	2970 (0.750)	2935 (1.250)			2878 (0.651)		1464 (0.130)	1389 (0.130)	722 (0.022)
1-Octanol	3675 (0.081)	1050 (0.320)	2970 (0.700)	2935 (1.250)			2870 (0.680)		1464 (0.141)	1388 (0.122)	723 (0.020)
1-Nonanol	3670 (0.070)	1052 (0.251)	2970 (0.640)	2935 (1.250)			2865 (0.475)		1464 (0.130)	1388 (0.130)	720 (0.005)
1-Decanol	3679 (0.055)	1052 (0.188)	2970 (0.500)	2935 (1.250)			2865 (0.551)		1464 (0.102)	1385 (0.079)	
1-Dodecanol	3670 (0.060)	1050 (0.211)	2970 (0.555)	2935 (1.252)			2865 (0.770)		1460 (0.150)	1384 (0.090)	725 (0.022)
Cyclopentanol	3660 (0.160)	1004 (0.380)		2970 (1.250)			2900 (0.540)		1452 (0.100)		
Cyclohexanol	3659 (0.050)	1070 (0.250)		2940 (1.250)			2864 (0.330)		1458 (0.100)		
Cycloheptanol	3655 (0.053)	1034 (0.245)		2940 (1.230)			2870 (0.330)		1461 (0.110)		
Cyclooctanol	3650 (0.040)	1054 (0.135)		2930 (1.230)			2864 (0.290)		1456 (0.109)		

(continued)

TABLE 7.2 IR vapor-phase data for substituted phenols

X-Phenol	OH str. cm ⁻¹	Phenyl-O str. cm ⁻¹	delta OH cm ⁻¹	OH str. cis[t.-C ₄ H ₉] cm ⁻¹	OH : X str. cm ⁻¹
	4-X				
H	3650	1260	1182		
CH ₃	3655	1255	1171		
isoC ₃ H ₇	3655	1257	1172		
tert.-C ₄ H ₉	3658	1260	1172		
F	3660	1230	1178		
Cl	3658	1255	1172		
Br	3655	1256	1171		
OH	3658	1243	1170		
CH ₃ O	3655	1239	1174		
C ₆ H ₅ O	3655	1255	1171		
NO ₂	3645	1270	1190		
CN	33645	1270	1178		
	3-X				
CH ₃	3650	1278	1158		
tert.-C ₄ H ₉	3655	1285	1160		
Cl	3658	1289	1180		
Br	3655	1291	1181		
I	3642	1288	1179		
CH ₃ O	3659	1295	1150		
CN	3650	1285	1152		
	2,4-X ₂				
CH ₃ ,CH ₃	3658	1262	1191		
2-t-C ₄ H ₉ ,4-CH ₃	3642	1241	1177	3670	
2,4-Di-t.-C ₄ H ₉	3646	1248	1178	3678	
2-NO ₂ ,4-CH ₃		1250	1185		3278
2,4-Di-Cl ₂	3660	1275	1192		3580
2,4-Di-Br ₂	3655	1278	1188		3562
2-Br,4-t.-C ₄ H ₉	3655	1281	1183		3560
	2,5-X ₂				
2,5-Di-t.-C ₄ H ₉	3645	1200	1149	3678	
2-Br,5-OH	3655	12114	1149		3559
	2,6-Di-X ₂				
2,6-Di-CH ₃	3655	1269	1192		
2-CH ₃ ,6-t.C ₄ H ₉	3644	1270	1200	3670	
2,6-Di-isoC ₃ H ₇	3650	1263	1201		
2-t.-C ₄ H ₉ ,6-isoC ₃ H ₇	3645	1263	1201	3670	
2,6-Di-CH ₂ CH=CH ₂	3650	1258	1200		3585
2,6-Di-CH ₃ O		1285	1220		3580
2-CH ₃ ,6-NO ₂		1250	1159		3222
2,6-Di-NO ₂		1271	1170		3230
2,6-Di-Cl ₂		1240	1175		3570
2,6-Di-Br ₂		1231	1172		3545
	2,4,6-Tri-X ₃				
2,4,6-Tri-CH ₃	3658	1233	1198		
2,4-Di-CH ₃ ,6-t.-C ₄ H ₉	3650	1224	1178	3680	
4-CH ₃ ,2,6-Di-t.-C ₄ H ₉		1230	1161	3675	
2,4-Di-Cl,6-NO ₂		1245	1152		3560[Cl] 3240[NO ₂]

(continued)

TABLE 7.2 (continued)

X-Phenol 4-X	OH str. cm ⁻¹	Phenyl-O str. cm ⁻¹	delta OH cm ⁻¹	OH str. cis[t.-C ₆ H ₅] cm ⁻¹	OH : X str. cm ⁻¹
2,4-Di-Br,6-NO ₂		1248	1160		3545[Br] 3230[NO ₂]
2,4,6-Tri-Cl		1221	1166		3578
2,4,6-Tri-Br		1228	1160		3544
2,3,6-Tri-Cl		1298	1167		3562
2,3,4,6-Tetra-Cl		1285	1200		3564
2,3,5,6-Tetra-Cl		1290	1218		3558
2,3,4,5,6-Penta-F		1209	1224		3630

TABLE 7.3 A comparison of OH:X stretching frequencies in the vapor and CCl₄ solution phases

2-X-phenol X	OH : X str. vapor cm ⁻¹	OH : X str. CCl ₄ soln. cm ⁻¹	[vapor]-CCl ₄ soln.] cm ⁻¹	OH str, or trans vapor cm ⁻¹	OH str. CCl ₄ soln. cm ⁻¹
H				3650	3610
Cl	3580	3553	27	3650	
Br,4-Br	3562	3534	28	3655	
CH ₃ O	3595	3560	35	3655	
CH ₃ S	3445	3415	30	3650	
NO ₂	3270	3245	25	3520	
CH(=O)	3202	3185	17		
NO ₂ ,4-NO ₂	3238	3215	23		
Cl,4-Cl,6-NO ₂	3560(Cl) 3240(NO ₂)	3209	31		

TABLE 7.4 The OH stretching frequency for 4-hydroxybenzaldehyde in 0 to 100 mol % $\text{CHCl}_3/\text{CCl}_4$ solutions

4-Hydroxybenzaldehyde 1%(wt./vol.) Mole %	
$\text{CHCl}_3/\text{CCl}_4$	O-H str.
0	3597.5
5.68	3596.7
10.74	3596.1
19.4	3594.9
26.53	3594.1
32.5	3592.9
37.57	3592.1
41.93	3591.5
45.73	3591.1
49.06	3590.5
52	3590.2
54.62	3589.8
57.22	3589.4
60.07	3589.1
63.28	3588.5
66.74	3588.6
70.65	3587.9
75.06	3587.5
80.05	3587.1
85.75	3586.7
92.33	3585.8
96.01	3585.4
100	3585.1
delta O-H str.	[-12.4]

TABLE 7.5 The OH stretching frequencies for phenol and intramolecular hydrogen-bonded phenols and the OH torsion frequency for phenol and the out-of-plane OH:X deformation frequencies for intramolecular hydrogen-bonded phenols

Compound Phenol* ¹	O-H str. 3610	O-H torsion 300 gamma O-H	O-D str.	gamma O-D	see text
2-phenyl	3570	386* ²			
2-fluoro	3598* ¹	366* ¹			
	3587				
2-iodo	3511* ¹	379* ¹			
	3507				
2-bromo	3534* ¹	394* ¹			
2,4-dibromo	3533* ¹	392* ¹			
	3534				
2-chloro	3553* ¹	395* ¹	2622* ²	298* ²	
	3553	400* ²			
2,4,5-trichloro	3553* ¹	395* ¹			
	3535				
2-methoxy	3560	433* ²			
		428* ³			
2-methylthio	3415	537	2540	not recorded	0
2-ethylthio	3413	537			
4-methyl-2-methylthio	3422	528			-0.3
2-methylsulfonyl	3330	645	2475	529	
4-chloro-isopropyl-6-nitro	3200	687			-0.24
4-chloro-2-s.-butyl-6-nitro	3205	686			-0.24
2-t-butyl-4,6-dinitro	~3100	731			0.15
2,4-di-t-butyl-6-nitro	~3125	698			-0.13
4,6-dinitro-2methyl	3170	710			0.15
4-chloro-6-nitro-2-methyl	3212	679			-0.24
2-bromo-4,6-dinitro	3159	700 or 706			0.15
2-bromo-3,4-dichloro-6-nitro	3185	786			-0.34
2-chloro-4,6-dinitro	3159	708			0.15
2-chloro-4-cyclohexyl-6-nitro	3219	676			-0.13
2-chloro-4-bromo-6-nitro	3205	675			-0.22
2,4-dichloro-6-nitro	3209	671			-0.24
4-t-butyl-2,6-dinitro	3186	678			-0.13
4-chloro-2,6-dinitro	3190	672			-0.24
4-fluoro-2,6-dinitro	3200	657			-0.44
2,4-dinitro	3215	680			0.15
2-nitro	3245	669			0.15
5-bromo-2-nitro	3220	668			-0.06
4-chloro-2-nitro	3252	664			-0.24
4,5-dichloro-2-nitro	3245	662			-0.34
Salicylate					
p-chlorophenylthio	3190	701			
methyl	3200	713			
phenyl	3240	698			
chloride	3331	660			
Aldehyde					
salicyl	3185	713	2360* ⁴	520* ⁴	0

(continued)

TABLE 7.5 (continued)

Compound Phenol* ¹ Phenol	O-H str. 3610	O-H torsion 300 gamma O-H	O-D str.	gamma O-D	see text
5-chlorosalicyl	3180	700			-0.34
2-Hydroxyacetophenone	* ⁵	789	2361sh 2294 2138sh		0
5-nitro		812			0.23
5-acetyl		806			0.19
4-phenyl		784			-0.13
5-iodo		783			-0.13
5-methyl		783			-0.14
5-bromo		780			-0.28
5-chloro		778			-0.34
5-fluoro		770			-0.6
5-methoxy		769			-0.61
5-amino		758			-1.01
2,4-dibenzoyl resorcinol			~2255 broad	635	
2-hydroxybenzophenone		~768			

*¹ [2,2,4-trimethyl-pentane soln.]*² [CCl₄ soln.]*³ & *⁴ [CS₂ soln.]

Aliphatic Amines

NH ₂ Stretching Frequencies for Aliphatic Amines	143
NH ₂ Wag Frequencies for Aliphatic Amines	144
NH ₂ Bending for Alkylamines	145
Raman Data for Primary Amines	145
Chemical Reactions of Alkylamines Containing NH ₂ or NH Groups	145
Secondary Aliphatic Amines	146
References	146

Tables

Table 8-1	147 (144)
Table 8-2	148 (145)

*Numbers in parentheses indicate in-text page reference.

In the discussion of aliphatic amines it is necessary to coin symbols for each type of amine, and this was established in Reference (1).

The symbols P, S, and T are used first to denote primary, secondary, and tertiary amines (NH₂, NH, and N), respectively. The symbols P', S', and T' are used second to denote the structure of the alkyl portion of the amine [RCH₂-, (R)₂CH, and (R)₃C] for the primary, secondary, and tertiary, respectively. For example, dimethylamine would be denoted as SP'P', diisopropylamine as SS'S', methylamine as PP', and tert-butylamine as PT'.

NH₂ STRETCHING FREQUENCIES FOR ALIPHATIC AMINES

In the vapor phase, *vasym.* NH₂ and *vsym.* NH₂ have weak IR band intensity, and often the *vasym.* NH₂ mode is not observed. The *vasym.* NH₂ mode is assigned in the region 3404–3422 cm⁻¹ and *vsym.* NH₂ in the region 3340–3361 cm⁻¹. In most cases, *vsym.* NH₂ has more intensity than *vasym.* NH₂ (1).

However, the situation is reversed in the 2-alkoxyethylamine series, but is normal in the 3-alkoxypropylamine series. Thus, this intensity reversal results from weak intramolecular hydrogen bonding between an N–H proton and the free pair of electrons on the 2-alkoxy oxygen atom.

Primary aliphatic amines with PS' structure exhibit $\nu_{\text{sym. NH}_2}$ in the region $\sim 3330\text{--}3340\text{ cm}^{-1}$, and this IR band is weak. When observed, $\nu_{\text{asym. NH}_2}$ is assigned in the region $\sim 3400\text{--}3422\text{ cm}^{-1}$.

Primary aliphatic amines with PT' structure exhibit $\nu_{\text{sym. NH}_2}$ in the region $3322\text{--}3335\text{ cm}^{-1}$, and $\nu_{\text{asym. NH}_2}$ when observed in the region $3395\text{--}3400\text{ cm}^{-1}$. Both IR bands are weak. In summary, the ν_{NH_2} frequency progressing in the order PP', PS', and PT' is shown here (1):

Structure	$\nu_{\text{asym. NH}_2}\text{ cm}^{-1}$	$\nu_{\text{sym. NH}_2}\text{ cm}^{-1}$	Type
R-CH ₂ -NH ₂	3404-3422	3340-3361	PP'
(R-)CH-NH ₂	$\sim 3400\text{--}3422$	3330-3340	PS'
(R-)C(-NH ₂)	3395-3400	3322-3335	PT'
HO-CH ₂ -CH ₂ -NH ₂	3465	3342	PP'
HO-CH ₂ -CHCH ₃ -NH ₂	3414	3348	PS'
HO-CH ₂ -C(CH ₃) ₂ -NH ₂	3400	3335	PT'

NH₂ WAG FREQUENCIES FOR ALIPHATIC AMINES

Table 8.1 lists IR vapor-phase data and assignments for primary alkylamines. The compounds with PP' structure exhibit a strong relatively broad band in the region $764\text{--}780\text{ cm}^{-1}$. The absorbance (A) ratios: (A) [NH₂ wag]/(A) [$\nu_{\text{sym. CH}_2}$] and (A) [NH₂ wag]/(A) [CH₂ bend] show that the values decrease progressing in the order C₂ to C₁₉. This presumably indicates that (A) for NH₂ wag is relatively constant, and that (A) for $\nu_{\text{sym. CH}_2}$ and (A) for CH₂ bend increase as the number of (CH₂)_n increases. Correlations such as these are valuable in spectra-structure identification of unknown aliphatic amines.

The cycloalkylamines with the structure PS' exhibit NH₂ wag in the region $755\text{--}785\text{ cm}^{-1}$, and with the exception of cyclohexylamine increase in frequency as the cycloalkyl ring increases in size from C₃ to C₈. The absorbance (A) ratios for NH₂ wag/ $\nu_{\text{sym. CH}_2}$ and NH₂ wag/CH₂ bend also decrease in value as the number of CH₂ groups increase from 3 to 8.

The NH₂ wag for alkylamines is also affected by the structure of the alkyl group. For example, PP', PS', and PT' exhibit NH₂ wag in the regions $760\text{--}780\text{ cm}^{-1}$, $779\text{--}799\text{ cm}^{-1}$, and $800\text{--}813\text{ cm}^{-1}$, respectively. In addition, a weak band assigned to $\nu_{\text{C-N}}$ is also affected by the nature of the alkyl group. For example, $\nu_{\text{C-N}}$ for PP', PS', and PT' occur in the regions $1043\text{--}1085\text{ cm}^{-1}$, $1111\text{--}1170\text{ cm}^{-1}$, and $1185\text{--}1265\text{ cm}^{-1}$, respectively. Both NH₂ wag and $\nu_{\text{C-N}}$ increase in frequency with increased branching on the α -carbon atom of the alkyl group. As already noted here, $\nu_{\text{sym. NH}_2}$ decreased in frequency with increased branching on the alkyl α -carbon atom. The apparent reason for the decrease in frequency of $\nu_{\text{sym. NH}_2}$ is that with increased branching on the α -carbon atom more electrons are released to the C-N group (inductive effect). This causes the N atom to become more basic; consequently, the NH₂ bonds are weakened causing the ν_{NH_2} modes to vibrate at lower frequencies. Also, the inductive effect increases in the order P', S', and T', and this causes the C-N bond strength to increase in the same order. Consequently, $\nu_{\text{C-N}}$ increases in frequency as the strength of the hydrogen bond increases. In addition, the NH₂ wag increases in frequency in the order P', S', and T'. This is because it takes more energy for the two relatively charged NH₂ protons to wag about the relatively negative free pair of electrons in the C-N plane as the protons and the nitrogen atom have increasingly relative opposite electrical charges. A similar explanation was presented for the ν_{OH} , $\nu_{\text{C-O}}$, OH torsion for alkanols (see Chapter 6).

NH₂ BENDING FOR ALKYLAMINES

The NH₂ bending mode for the alkylamines with PP' structure occurs in the region 1599–1629 cm⁻¹, with PS' in the region 1612–1621 cm⁻¹, and with PT' in the region 1610–1616 cm⁻¹, and has weak to weak-medium IR band intensity in the vapor phase. Therefore, the NH₂ bending mode frequencies are not useful for distinguishing between alkylamines with PP', PS', and PT' structures. In the liquid it is assigned in the region 1590–1627 cm⁻¹ with medium intensity (3). In contrast, NH₂ bend for arylamines (anilines) occurs at higher frequency with strong IR band intensity (3). (See the next chapter.)

RAMAN DATA FOR PRIMARY AMINES

Table 8.2 lists Raman data and assignments for the neat phase for primary amines.

In the neat phase, *vasym.* NH₂ and *vsym.* NH₂ occur in the region 3367–3379 cm⁻¹ and 3307–3322 cm⁻¹, respectively. In all cases, the *vsym.* NH₂ mode has more relative band intensity than the *vasym.* NH₂ modes as indicated by the number in parenthesis (2).

It is interesting to compare the *vasym.* NH₂ and *vsym.* NH₂ frequencies obtained for butylamine (1-aminobutane) in the vapor and liquid phases: *vasym.* NH₂ (3411 cm⁻¹, vap. and 3376 cm⁻¹, liq.) and *vsym.* NH₂ (3345 cm⁻¹, vap. and 3322 cm⁻¹, liquid). This comparison shows that *vasym.* NH₂ and *vsym.* NH₂ occur at lower frequency in the liquid phase by 35 and 23 cm⁻¹, respectively.

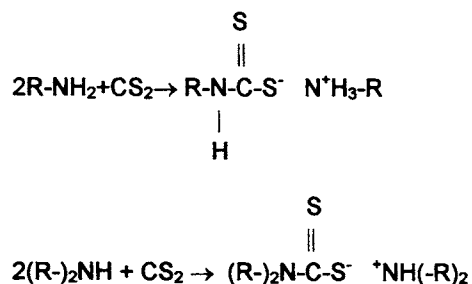
Two of the examples given in Table 8.2 contain a 4-aminocyclohexyl group, and both exhibit a very strong Raman band at 784 cm⁻¹, which is assigned to the cyclohexyl breathing mode.

CHEMICAL REACTIONS OF ALKYLAMINES CONTAINING NH₂ OR NH GROUPS

This section is brought to the reader's attention for matters of safety and because it can cause confusion when interpreting spectral data.

From experience it has been noted that heat generated from the chemical reaction of aliphatic primary or secondary amines with CS₂ can cause the entire content of the volumetric flask to blow out of its mouth. This can cause an injury, or possibly a fire, because CS₂ has a low flashpoint.

These chemical reactions occur as follows:



As well, if exposed to air for a period of time these same alkylamines can undergo comparable reactions with CO_2 (replace CS_2 with CO_2). In addition, alkylamines can react slowly with solvents such as CCl_4 , CHCl_3 , and CH_2Cl_2 , and this can cause problems in specifically identifying the original sample.

SECONDARY ALIPHATIC AMINES

The N–H stretching band for compounds of form $(\text{R}-)_2\text{NH}$ is weak, and is not readily detected in compounds whose IR spectra have been recorded in the vapor phase (1). However, N–H wag has strong IR band intensity with half bandwidths varying between 50 and 100 cm^{-1} and occurs in the region $686\text{--}750\text{ cm}^{-1}$ in the vapor phase. Thus, it occurs at lower frequency than NH_2 wag. In the liquid, the weak IR band occurs in the region $3320\text{--}3280\text{ cm}^{-1}$ and in dilute solution in the region $3310\text{--}3360\text{ cm}^{-1}$ (3).

Dialkylamines with $\text{SP}'\text{P}'$ structure exhibit NH wag in the region $699\text{--}715\text{ cm}^{-1}$, with $\text{SP}'\text{S}'$ structure near $\sim 686\text{ cm}^{-1}$. These data suggest that NH wag decreases in frequency in the order $\text{SS}'\text{S}'$, $\text{SP}'\text{S}'$, and $\text{SP}'\text{P}'$, which is the opposite order for the primary alkylamines (see the preceding materials here).

In the dialkyl amine series with $\text{SP}'\text{P}'$ structure a band assigned as $\nu\text{N}(\text{--C})_2$ occurs in the region $1132\text{--}1151\text{ cm}^{-1}$ (1).

REFERENCES

1. Nyquist, R. A. (1984). *The Interpretation of Vapor-Phase Infrared Spectra: Group Frequency Data*, Philadelphia: Sadtler Research Laboratories, Division of Bio-Rad Laboratories, Inc.
2. *Raman Data from the Sadtler Research Laboratories*, Philadelphia: Division of Bio-Rad Laboratories, Inc.
3. Lin-Vien, D., Colthup, N. B., Fateley, W. G., and Grasselli, J. G. (1991). *The Handbook of Infrared and Raman Characteristic Frequencies of Organic Molecules*, San Diego: Academic Press.

TABLE 8.1 IR vapor-phase data and assignments for primary amines

Amine	a.CH ₃ str.	a.CH ₂ str.	s.CH ₃ str.	s.CH ₂ str.	CH ₂ bend	s.CH ₃ bend	NH ₂ wag	(A)[NH ₂ wag] (A)[s.CH ₂ str.]	(A)[NH ₂ wag] (A)[CH ₂ bend]
Methyl	2960 (0.640)		2898 (0.600)				778 (0.784)		
Ethyl		2965 (1.240)	2922 (0.940)	2870 (0.640)	1456 (0.164)	1398 (0.280)	772 (1.087)	1.69	6.63
Propyl		2978 (1.230)		2880 (0.679)	1465 (0.135)	1387 (0.129)	764 (0.630)	0.93	4.67
Butyl		2940 (1.250)		2880 (0.621)	1465 (0.120)	1387 (0.111)	779 (0.664)	1.07	5.53
Heptyl	2970 (0.700)	2940 (1.250)		2868 (0.510)	1468 (0.130)	1377 (0.080)	770 (0.248)	0.49	1.9
Octyl	2970 (0.462)	2930 (1.250)		2964 (0.510)	1465 (0.091)	1385 (0.050)	771 (0.190)	0.37	2.09
Nonyl	2970 (0.460)	2930 (1.250)		2864 (0.530)	1466 (0.100)	1388 (0.066)	775 (0.189)	0.36	1.89
Decyl	2970 (0.290)	2935 (1.250)		2864 (0.380)	1466 (0.080)	1385 (0.035)	780 (0.120)	0.32	1.51
Undecyl	2970 (0.410)	2935 (1.210)		2864 (0.570)	1465 (0.100)	1385 (0.050)	775 (0.131)	0.23	1.11
Tridecyl		2935 (1.250)		2864 (0.310)	1460 (0.050)	1389 (0.020)	775 (0.050)	0.16	1.01
Tetradecyl		2938 (1.250)		2864 (0.310)	1460 (0.058)	1385 (0.050)	770 (0.060)	0.19	1.11
Pentadecyl		2930 (1.250)		2860 (0.310)	1460 (0.059)	1385 (0.011)	770 (0.040)	0.13	0.68
Octadecyl	2970 (0.040)	2935 (1.250)		2962 (0.310)	1465 (0.045)	1385 (0.005)	775 (0.035)	0.11	0.77
Nonadecyl		2930 (1.250)		2860 (0.400)	1460 (0.089)	1385 (0.005)	775 (0.044)	0.11	0.49
Cyclopropyl		3100 (0.220)		3010 (0.250)	1455 (0.140)		755 (1.230)	4.03	8.79
Cyclopentyl		2968 (1.250)		2884 (0.420)	1459 (0.061)		779 (0.223)	0.53	3.66
		2935 (1.250)		2864 (0.420)	1458 (0.130)		770 (0.170)	0.41	1.42
Cycloheptyl		2930 (1.250)		2860 (0.320)	1460 (0.100)		784 (0.151)	0.47	1.51
Cyclooctyl		2932 (1.150)		2868 (0.199)	1459 (0.069)		785 (0.060)	0.31	0.87

TABLE 8.2 Raman data and assignments for primary amines

1-Amino-butane	bis-(4-Amino-cyclohexyl) methane	Ethoxyethyl amine	Hexa-methylene diamine	2-Aminoethyl methyl ether	3-Methoxy-propyl amine	4,4'-bis(p-Amino-cyclo-hexyl) methane	Assignment
3376(1)		3379(1)	3367(1)	3379(1)	3377(2)	3367(0)	a.NH ₂
3322(3)	3311(1)	3322(3)	3307(3)	3322(3)	3319(5)	3312(1)	s.NH ₂
2963(5)		2977(5)		2985(5)			a.CH ₃ str.
2938(7)		2934(9)		2950(6)	2929(7)	2931(2)	a.CH ₂ str.
			2899(1)				a.CH ₂ str.
2875(4)		2870(5)			2868(4)		s.CH ₂ str.
			2853(2)	2823(4)	2826(6)	2846(3)	s.CH ₂ str.
					2811(5)		C.T.
		2797(2)		2723(2)	2755(3)		C.T.
			1640(1)	1597(1)			NH ₂ bend
1444(7)	1441(5)	1459(6)	1440(9)	1453(9)	1450(9)	1441(5)	CH ₂ bend
	784(9)					784(9)	Ring breathing

Arylamines (Anilines), Azines, and Oximes

NH ₂ Stretching Frequencies vs Temperature	150
Azines	151
Oximes	152
References	153

Figures

Figure 9-1	155 (149)
Figure 9-2	155 (149, 150)
Figure 9-3	156 (149)
Figure 9-4	156 (150)
Figure 9-5	157 (150)

Tables

Table 9-1	158 (149)
Table 9-2	159 (149)
Table 9-3	160 (149, 150)
Table 9-3a	161 (150)
Table 9-4	162 (150)
Table 9-5	163 (151)
Table 9-6	162 (152)

*Numbers in parentheses indicate in-text page reference.

Table 9.1 lists IR data for the *vasym.* NH₂ and *vsym.* NH₂ frequencies for 3-X and 4-X-anilines in the vapor phase, and in (0.5% wt./vol. or less) n-hexane, CCl₄, and CHCl₃ solutions (1). The IR vapor-phase data for arylamines are also given in Reference (2).

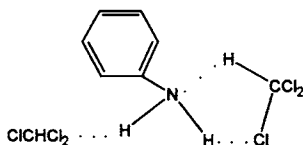
Califano and Moccia (3) have shown that the *vasym.* NH₂ and *vsym.* NH₂ frequencies and intensities recorded in CCl₄ solution correlate with Hammett σ values. The ranges for *vasym.* NH₂ and *vsym.* NH₂ in each of the solvents are given in Table 9.1. In general, the *vasym.* NH₂ and *vsym.* NH₂ IR vapor-phase frequencies correlate with Hammett σ values as shown previously (3) (see Fig. 9.1 and 9.2 for plots of the CCl₄ solution data). In all cases these modes occur at the highest frequency in the vapor phase.

Figure 9.3 shows a plot of *vasym.* NH₂ vs *vsym.* NH₂ frequencies for 3-X and 4-X anilines in each solvent. Three of the plots are essentially linear, and the plot of the lower frequency bands observed in the case of the CHCl₃ solutions is nonlinear. In each case where the *vasym.* NH₂ and *vsym.* NH₂ frequencies have been recorded in both hexane and CCl₄ solutions, the *vasym.* NH₂ mode occurs from 0.36 to 7.51 cm⁻¹ lower in frequency in CCl₄ than in hexane, while the *vsym.* NH₂ mode occurs at higher frequency by 2.05 cm⁻¹ to 3.45 cm⁻¹ in CCl₄ than in hexane (1).

The *vasym.* NH₂ mode for 4-X and 3-X anilines occurs from 1.04 to 9.19 cm⁻¹ higher in frequency in CHCl₃ solution than in CCl₄, while *vsym.* NH₂ occurs from 0.33 to 7.34 cm⁻¹ higher in frequency in CHCl₃ than in CCl₄.

The *vasym.* NH₂ and *vsym.* NH₂ frequency decreases in going from solution in hexane to solution in CCl₄ because the NH₂ protons intermolecularly bond to the Cl electron pairs of CCl₄

(1). The same explanation can be used to support the analogous behavior of one plot in CHCl_3 solution. The second plot in the case of CHCl_3 solution most likely is the result of:



Interaction of the CCl_3H proton with the N atom would cause the NH_2 modes to weaken further, and both $\nu_{\text{asym.}} \text{NH}_2$ and $\nu_{\text{sym.}} \text{NH}_2$ would shift to even lower frequency as observed. Of course, the CHCl_3 proton also intermolecularly bonds with other basic sites such as the phenyl ring, $\text{C}=\text{C}$, and $\text{C}=\text{O}$ groups (see the chapters that follow).

Linnett (4) has developed equations to calculate the NH_2 bond angles of 3-X and 4-X anilines, and there are:

$$4\pi^2 \nu_{\text{asym.}} \text{NH}_2 = k[1/{}^m\text{H} + (1 + \cos\theta)/{}^m\text{N}]$$

$$4\pi^2 \nu_{\text{sym.}} \text{NH}_2 = k[1/{}^m\text{H} + (1 + \cos\theta)/{}^m\text{N}]$$

In these equations ${}^m\text{H}$ is the mass of hydrogen, and ${}^m\text{N}$ is the mass of nitrogen used to determine the bond angles of the NH_2 group. The $\nu_{\text{asym.}} \text{NH}_2$ and $\nu_{\text{sym.}} \text{NH}_2$ frequencies recorded in each of the solvents were utilized in the calculations. Figure 9.4 shows a plot of σ_m and σ_p vs the calculated NH_2 bond angles (Table 9.2). This plot shows that the NH_2 bond angles for these anilines increase as the Hammett σ values increase, and this result is in agreement with Krueger's conclusion (5). However, this does not exclude some change in the NH_2 bond lengths with change in the inductive effect as discussed for alkylamines in Chapter 8. Both of these factors would lower the ν_{NH_2} frequencies.

The frequency separation between $\nu_{\text{asym.}} \text{NH}_2$ and $\nu_{\text{sym.}} \text{NH}_2$ changes in each solvent system (see Table 9.3 and 9.3a). In solution, these separations are larger in the cases of CCl_4 and CHCl_3 solution than in hexane solution, and it is less in the other complex existing in CHCl_3 solution. In addition, these separations generally appear to increase in CCl_4 and CHCl_3 solutions as the σ values increase.

NH_2 STRETCHING FREQUENCIES VS TEMPERATURE

Table 9.4 lists $\nu_{\text{asym.}} \text{NH}_2$ and $\nu_{\text{sym.}} \text{NH}_2$ frequencies recorded in CS_2 solution over the range $+27$ to -60 $^\circ\text{C}$ for both aniline and 4-chloroaniline. In both compounds the $\nu_{\text{asym.}} \text{NH}_2$ and $\nu_{\text{sym.}} \text{NH}_2$ decrease in frequency with a decrease in temperature. In addition, because the $\nu_{\text{sym.}} \text{NH}_2$ mode decreases more in frequency than the $\nu_{\text{asym.}} \text{NH}_2$ mode, there is a small increase in the frequency separation as the temperature decreases. Figure 9.5 shows plots of both ν_{NH_2} modes for aniline and 4-chloroaniline vs $^\circ\text{C}$, and within experimental error the plots are linear. These data are included to demonstrate to the reader that vibrational modes are also temperature dependent. These ν_{NH_2} modes most likely decrease in solution with a decrease in temperature, because the CS_2 volume contracts with a decrease in temperature forcing the NH_2 bonds closer

to CS₂ molecules. Thus, the weak hydrogen bonds formed between S=C=S bonds are somewhat stronger, causing the νNH_2 modes to decrease in frequency (6).

AZINES

Table 9.5 lists infrared and Raman data and assignments for azines. Azines are formed by the reaction of hydrazine with either an aldehyde or a ketone. These compounds have the following empirical structures:

- A. (H₂C=N-)₂
- B. (RCH=N-)
- C. $\phi\text{CH=N-}$ ₂
- D. [(R)₂C=N-]₂
- E. [(ϕ)₂C=N-]₂

These compounds are reported to exist in either *s-trans*, *s-cis*, and/or *gauche* isomers depending upon their physical state. In the solid state, formaldazine, empirical structure A, is reported to exist in the *s-trans* configuration, and in the liquid phase, a small amount of the *gauche* isomer is also present. In the *s-trans* configuration *vasym.* (C=N-)₂ is IR active and only *vsym.* (C=N-)₂ is Raman active because these molecules have a center of symmetry located between the N-N bond. Thus, for formaldazine the medium IR band at 1637 cm⁻¹ and the strong Raman band at 1612 cm⁻¹ are assigned to the *vasym.* (C=N-)₂ and *vsym.* (C=N-)₂ modes, respectively (8).

In studies of aldazines and ketazines, *vasym.* (C=N-)₂ was assigned to a strong IR band in the region 1636–1663 cm⁻¹ and *vsym.* (C=N-)₂ was assigned to a strong Raman band in the region 1608–1625 cm⁻¹ (9–12). King *et al.* (13) have assigned *vasym.* (C=N-)₂ to the strong IR band at 1747 cm⁻¹ and the strong Raman band at 1758 cm⁻¹ to *vsym.* (C=N-)₂, for (CF₂=N-)₂. In this latter case, the (C=N-)₂ modes are reversed when compared to those already reported here.

The arylaldehyde azines reported in Table 9.5 were assigned on the same basis as reported in the foregoing. These compounds were all recorded in the solid phase. In making these assignments both their IR and Raman spectra were recorded, and the IR data were also compared to the IR data for the correspondingly substituted benzaldehydes. The *vasym.* (C=N-)₂ mode was assigned to the IR band in the region 1606–1632 cm⁻¹ and *vsym.* (C=N-)₂ was assigned to the Raman band in the region 1539–1563 cm⁻¹.

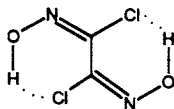
In all the aldehyde azines studied, *vsym.* (C=N-)₂ was assigned to the most intense Raman band in the region 1539–1587 cm⁻¹. In the case of nitrobenzenes, the *vsym.* NO₂ mode has very strong intensity. The argument for assigning *vsym.* (C=N-)₂ to the region 1539–1587 cm⁻¹ is that they exhibit the most intense bands in the Raman spectra, and that the 1560 cm⁻¹ Raman band for 2-nitrobenzaldehyde azine is twice as strong as the 1348 cm⁻¹ Raman band assigned as *vsym.* NO₂ (7). In the case of the 2,6-dichloro isomer, it is not possible for the phenyl group and the C=N groups to be coplanar. As *vsym.* (C=N-)₂ for the 2,6-dichlorophenyl isomer occurs 24–48 cm⁻¹ higher in frequency than the other benzaldehyde azines, this indicates that there is no conjugation between the phenyl and C=N groups (ϕ - C=N-) groups. In the case of the 2,6-

dichlorophenyl isomer the reason why $\nu_{\text{sym.}}(\text{C}=\text{N}-)_2$ occur at lower frequency for other benzaldehyde azines is that the phenyl and $\text{C}=\text{N}$ groups are conjugated. Further support for this conclusion is that $\nu_{\text{sym.}}(\text{C}=\text{N}-)_2$ occurs at 1587 cm^{-1} for the 2,6- Cl_2 analog, which is intermediate between those assigned to the other benzaldehyde azines ($1539\text{--}1563\text{ cm}^{-1}$) and those for the alkylaldehyde azines ($1608\text{--}1625\text{ cm}^{-1}$) (7). In conclusion, the benzaldehyde azines exist in an s-trans configuration in the solid state (7).

OXIMES

In the vapor phase aliphatic aldehyde and ketone oximes exhibit $\nu_{\text{C}=\text{N}}$ in the range $1650\text{--}1665\text{ cm}^{-1}$, and in the liquid and solid phase in the range $1649\text{--}1670\text{ cm}^{-1}$ (2, 18). In the vapor phase ν_{OH} occurs in the range $3642\text{--}3654$ (2), and in CCl_4 solution in the range $3580\text{--}3600\text{ cm}^{-1}$ (18). In CCl_4 solution, the decrease in frequency in going from the vapor to CCl_4 solution is attributed to intermolecular hydrogen bonding of form $(\text{OH}\cdots\text{ClCCl}_3)$. In dilute CCl_4 solution, the ν_{OH} frequencies form a linear plot when plotted vs Hammett σ values (19). In the neat or solid phase $\nu(\text{OH}\cdots\text{HO})_n$ occurs in the range $3100\text{--}3330\text{ cm}^{-1}$, and is comparable to that which is exhibited by alcohols and phenols. In the vapor phase $\nu_{\text{N}=\text{O}}$ for both aliphatic and aromatic oximes are reported to occur in the range $910\text{--}980\text{ cm}^{-1}$ (2), and in the liquid or solid phase for a larger number of oximes in the range $870\text{--}1030\text{ cm}^{-1}$ (19).

Table 9.6 lists IR and Raman data for glyoximes in the solid state. Glyoximes have the following empirical structure: $\text{HO}-\text{N}=\text{CX}-\text{CY}=\text{N}-\text{OH}$. These compounds contain two $\text{C}=\text{N}$ groups and two hydroxyl groups, and it would be expected that the hydroxyl groups would be hydrogen bonded either inter- or intramolecularly. An intramolecular hydrogen bond between the OH group and Cl $(\text{OH}\cdots\text{Cl})_2$ is possible in the case of the dichloro analog, and as shown here:



this structure has a center of symmetry at the midpoint of the $\text{C}-\text{C}$ bond.

With a center of symmetry, a mode such as $\nu_{\text{sym.}}(\text{N}=\text{C}-)_2$ would be only Raman active and $\nu_{\text{asym.}}(\text{N}=\text{C}-\text{H})_2$ would be only IR active. Dichloroglyoxime is reported to have a very strong Raman band at 1588 cm^{-1} , and a very weak IR band at $\sim 1620\text{ cm}^{-1}$. Moreover, the $\sim 1620\text{ cm}^{-1}$ IR band is not observed in the Raman spectrum, nor is the 1588 cm^{-1} band observed in the IR spectrum. These data support that dichloroglyoxime has a center of symmetry. In the case of the CN, CN analog, there is also the possibility that intramolecular hydrogen bonding can take place between OH and CN. If so, the two $\nu(\text{N}=\text{C}-)_2$ modes are reversed from those exhibited by the Cl, Cl analog because the very strong Raman band (1593 cm^{-1}) occurs at a higher frequency than the weak IR band (1582 cm^{-1}). Thus, $\nu_{\text{sym.}}(\text{N}=\text{C}-)_2$ would be assigned at 1593 cm^{-1} and $\nu_{\text{asym.}}(\text{N}=\text{C}-)_2$ at 1582 cm^{-1} .

In the case of glyoxime the intramolecular molecular hydrogen-bonded structure would not exist. However, $\nu_{\text{sym.}}(\text{N}=\text{C}-)_2$ is observed as a strong band in the Raman at 1636 cm^{-1} and $\nu_{\text{asym.}}(\text{N}=\text{C}-)_2$ is observed as a weak band in the IR at 1610 cm^{-1} . Thus, glyoxime apparently also has a center of symmetry.

The glyoxime analogs, such as (H and CH₃) and (H and NO₂), do not have a center of symmetry. Therefore, both *vasym.* (N=C-)₂ and *vsym.* (N=C-)₂ are allowed in both the IR and Raman spectra. They are also allowed in *cis* and *gauche* structures. In the Raman, the symmetric modes usually have stronger intensity than the antisymmetric modes, and vice versa in the IR. In the case of the (H and CH₃) analog, strong Raman bands are reported at 1630 and 1516 cm⁻¹, and in the case of the (H and NO₂) analog, strong Raman bands are noted at 1650 and 1608 cm⁻¹. A medium IR band is observed at 1650 and 1608 cm⁻¹ for the (H and NO₂) analog. Based on intensity arguments, the medium IR band at 1650 cm⁻¹ and the weak IR band at 1608 cm⁻¹ would be assigned as *vasym.* (N=C-)₂ and *vsym.* (N=C-)₂, respectively. On the other hand, the assignments would be reversed in the case of the (CH₃ and CH₃) analog: *vsym.* (N=C-H)₂ at 1650 cm⁻¹ and *vasym.* (N=C)₂ at ~1512 cm⁻¹, because the 1650 cm⁻¹ Raman band is stronger than the ~1512 Raman band. However, the *vasym.* (N=C-)₂ mode is forbidden in the case of the (CH₃ and CH₃) analog with a center of symmetry. Therefore, the (CH₃ and CH₃) analog does not have a plane of symmetry.

In Table 9.6 the higher $\nu(\text{N}=\text{C}-)_2$ frequencies are listed in the third (IR) and fourth (Raman) columns, and the fifth (IR) and sixth (Raman) columns list the lower frequencies. It has been suggested that the frequencies in columns 3 and 4 are in all cases attributed to *vsym.* (N=C-)₂, and the frequencies in columns 5 and 6 are assigned to *vasym.* (N=C-)₂ (18), but the foregoing discussion does not support all of these assignments. Raman bands in the regions 1627–1650 cm⁻¹ and ~1495–1608 cm⁻¹ do appear to be characteristic for these glyoximes. Comparison of CH₃, CH₃ glyoxime $\nu(\text{CN}=\text{C}-)_2$ frequencies (Raman: 1650, ~1512 cm⁻¹) vs C₆H₅, C₆H₅ glyoxime (Raman: 1627, 1495 cm⁻¹) suggests that conjugation plays a role in decreasing $\nu(\text{N}=\text{C}-)_2$ frequencies just as in the case of azines.

REFERENCES

1. Nyquist, R. A., Luoma, D. A., and Puehl, C. W. (1992). *Appl. Spectrosc.*, **46**, 1273.
2. Nyquist, R. A. (1984). *The Interpretation of Vapor-Phase Infrared Spectra: Group Frequency Data*, Philadelphia: Sadtler Research Laboratories, Division of Bio-Rad Laboratories.
3. Califano, S. and Moccia, R. (1956). *Gazz. Chem.*, **86**, 1014.
4. Linnett, I. W. (1945). *Trans. Farad. Soc.*, **41**, 223.
5. Krueger, P. J. (1962). *Nature*, **194**, 1077.
6. Nyquist, R. A. (1986). *Appl. Spectrosc.*, **40**, 79.
7. Nyquist, R. A., Peters, T. L., and Budde, P. B. (1978). *Spectrochim. Acta*, **34A**, 503.
8. Bondybey, V. E. and Nibbler, J. W. (1973). *Spectrochim. Acta*, **29A**, 645.
9. Kirrman, A. (1943). *Compt. Rend.*, **217**, 148.
10. West, W. and Killingsworth, R. B. (1938). *J. Chem. Phys.*, **6**, 1.
11. Kitaev, Yu. P., Nivorozhkin, L. E., Plegontov, S. A., Raevskii, O. A., and Titova, S. Z. (1968). *Dokl. Acad. Sci. USSR*, **178**, 1328.
12. Ogilvie, J. F. and Cole, K. C. (1971). *Spectrochim. Acta*, **27A**, 877.
13. King, S. T., Overend, J., Mitsch, R. A., and Ogden, P. H. (1970). *Spectrochim. Acta*, **26A**, 2253.
14. Bardet, L. and Alain, M. (1970). *C. R. Acad. Sc., Paris*, **217A**, 710.
15. Cherskaya, N. O., Raktin, O. A., and Shlyapochnikov, V. A. (1987). *Acad. Sci., USSR, Div. Chem. Sci.*, **53**, 2150.

16. (1976). *Sadtler Standard Raman Spectra*, Philadelphia: Sadtler Research Laboratories, Division of Bio-Rad Laboratories.
17. Kahovec, L. and Kohlrausch, K. W. (1952). *Monatsch. Chem.*, **83**, 614.
18. Lin-Vien, D., Colthup, N. B., Fateley, W. G., and Grasselli, J. G. (1991). *The Handbook of Infrared and Raman Characteristic Frequencies of Organic Molecules*, San Diego: Academic Press, Inc.
19. Bellamy, L. J. (1968). *Advances in Infrared Group Frequencies*, Bungay, Suffolk, England: Chaucer Press.

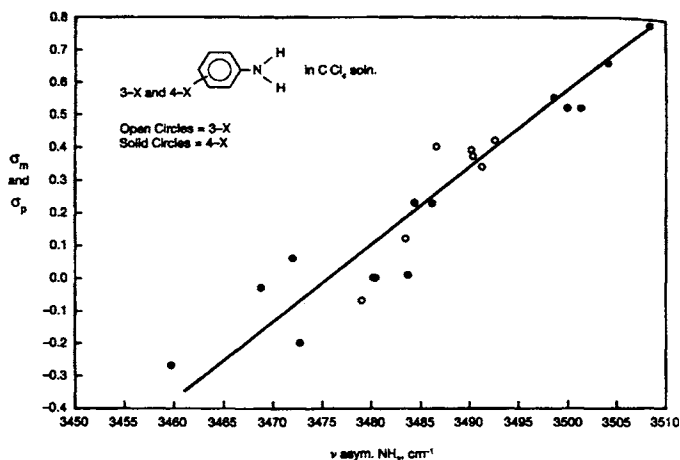


FIGURE 9.1 A plot of $\nu_{\text{asym. NH}_2}$ for 3-X and 4-X anilines in CCl_4 solutions vs Hammett σ_m and σ_p values for the 3-X and 4-X atoms or groups. The open circles are for 3-X anilines and the closed circles are for 4-X anilines.

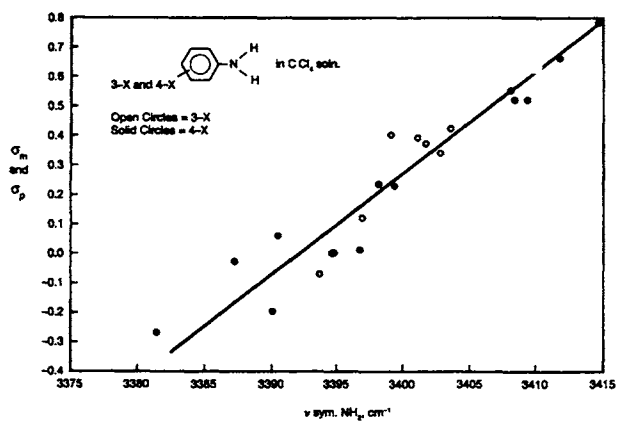


FIGURE 9.2 A plot of $\nu_{\text{sym. NH}_2}$ for 3-X and 4-X anilines in CCl_4 solutions vs Hammett σ_m and σ_p values for the 3-X and 4-X atoms or groups. The open circles are for 3-X anilines and the closed circles are for 4-X anilines.

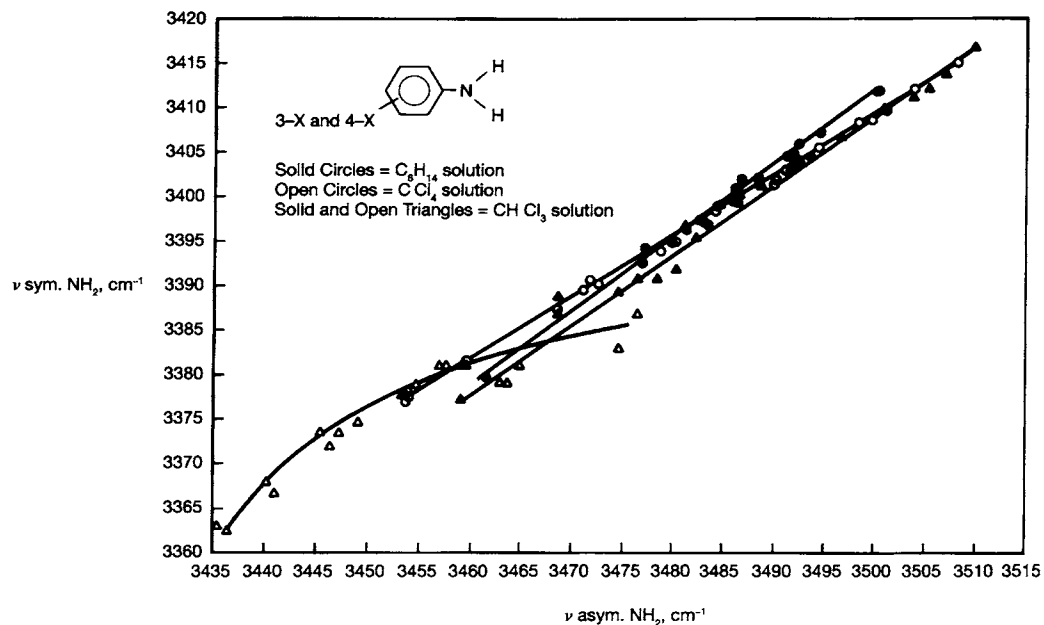


FIGURE 9.3 A plot of $\nu_{asym. NH_2}$ vs $\nu_{sym. NH_2}$ for 3-X and 4-X anilines in solution with C_6H_{14} , CCl_4 , and $CHCl_3$.

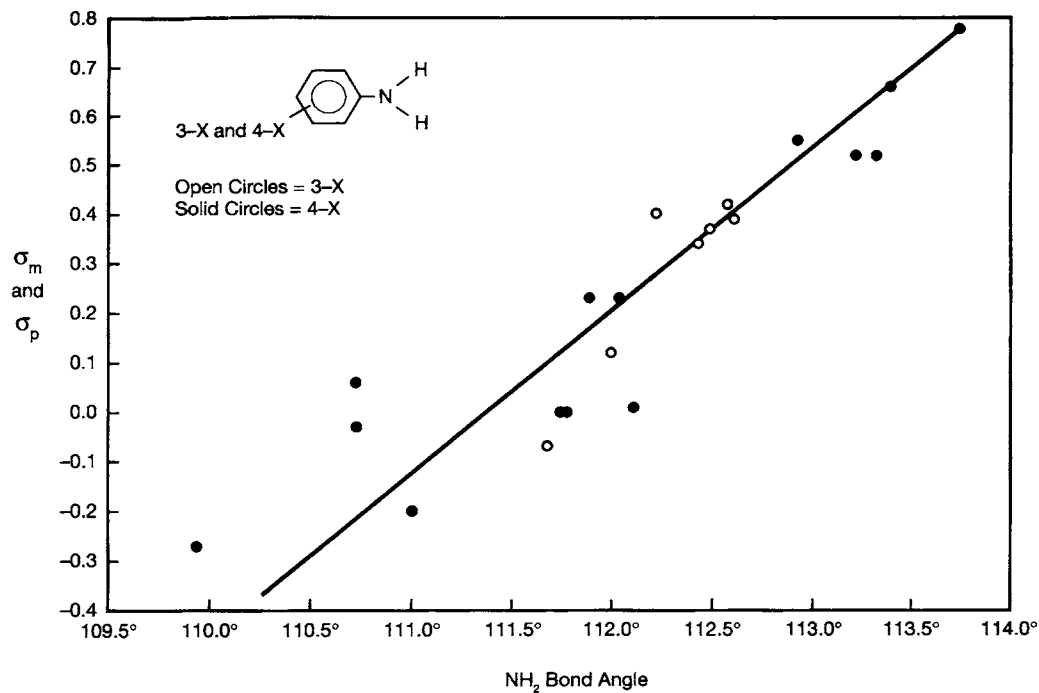


FIGURE 9.4 A plot of σ_m and σ_p vs the calculated NH_2 bond angles for the *m*- and *p*-substituted anilines.

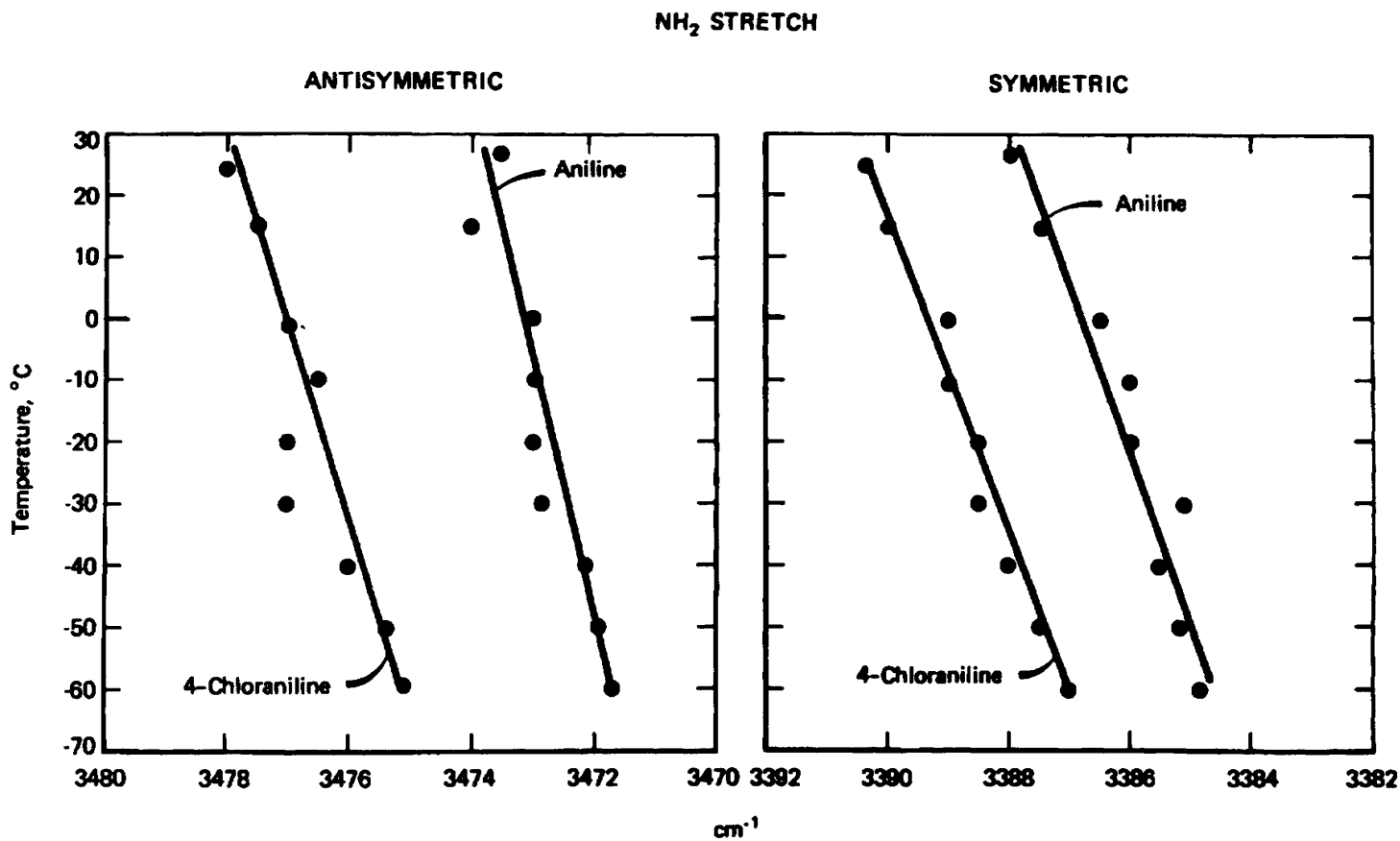
FIGURE 9.5 A plot of both ν NH₂ frequencies for aniline and 4-chloroaniline in CS₂ solution vs °C.

TABLE 9.1 IR data for the a. and s. NH₂ stretching frequencies of 3-X and 4-X-anilines in the vapor-phase, and in *n*-C₆H₁₄, CCl₄, and CHCl₃ solutions

4-X-aniline X	vapor phase a.NH ₂ str. cm ⁻¹	Hexane a.NH ₂ str. cm ⁻¹	CCl ₄ a.NH ₂ str. cm ⁻¹	CHCl ₃ a.NH ₂ str. cm ⁻¹	CHCl ₃ a.NH ₂ : HCCL ₃ str. cm ⁻¹	vapor phase s.NH ₂ str. cm ⁻¹	Hexane s.NH ₂ str. cm ⁻¹	CCl ₄ s.NH ₂ str. cm ⁻¹	CHCl ₃ s.NH ₂ str.	CHCl ₃ s.NH ₂ : HCCL ₃	σ p
OH	3481			3468.9	3440.31	3402			3386.8	3367.89	-0.36
OCH ₃	3480		3459.71	3468.9	3441.09	3400		3381.41	3388.75	3366.62	-0.27
N(CH ₃) ₂		3461.63	3454.12	3459.13	3435.4			3377.35	3377.02	3362.96	
NH ₂	3480	3453.81			3436.41	3400	3379.54	3376.79	3388.75	3362.43	
OC ₆ H ₅			3468.78	3474.77	3445.62			3387.3	3389.28	3373.49	-0.03
F	3498	3477.02	3472.02	3476.72	3449.2	3415	3394.23	3390.56	3390.71	3374.57	0.06
Cl	3500	3486.41	3484.52	3486.89	3457.74	3418	3400.84	3398.35	3400.11	3380.93	0.23
Br	3502	3488.72	3486.23	3488.96	3459.32	3422	3402.06	3399.48	3401.15	3380.93	0.23
H	3500	3482.98	3480.29	3481.75	3453.95	3400	3397.36	3394.77	3396.43	3378.03	0
H	3500	3482.99	3480.53	3481.57	3453.78	3400	3397.35	3394.88	3396.75	3377.76	0
C ₂ H ₅		3477.22	3471.32	3478.68	3446.47			3392.48	3389.44	3390.77	
C(CH ₃) ₃	3500	3477.18	3472.72	3480.63	3447.29	3418	3392.52	3390.13	3391.79	3373.36	-0.2
C ₆ H ₅	3500	3484.73	3483.8	3486.75	3454.79	3417	3398.89	3396.84	3399.33	3378.79	0.01
C(=O)OC ₂ H ₅		3500.82	3500.08	3504.25	3478.68			3411.85	3408.59	3411.06	0.52
CN	3510		3504.31	3507.43		3422	3414.42	3412.05	3413.73		0.66
CF ₃	3510	3500.65	3498.73	3501.31	3476.7	3420	3411.8	3408.35	3409.82	3386.8	0.55
C(=O)CH ₃	3502		3501.51	3505.77		3421		3409.6	3412.09		0.52
NO ₂	3518		3508.61	3510.27		3430		3414.96	3416.69		0.78
3-X-aniline											
X											
OCH ₃	3500	3485.02	3483.54	3485.08	3457.05	3420	3399.2	3397.02	3399.07	3380.93	0.12
F	3501	3492.7	3491.35	3492.65	3464.99	3420	3405.86	3402.99	3404.1	3380.93	0.34
Cl	3502	3492.17	3490.49	3492.02	3464.99	3420	3404.82	3401.94	3403.23	3380.93	0.37
Br	3500	3491.55	3490.31	3491.94	3463.79	3420	3404.5	3401.31	3403.05	3378.98	0.39
CH ₃	3500	3481.7	3479.05	3482.59	3453.48	3420	3396.27	3393.8	3395.42	3377.62	-0.07
C(=O)OC ₂ H ₅	3491	3487.08	3486.72	3488.89	3459.56	3410	3401.9	3399.26	3401.39	3380.93	0.4
CN			3494.7	3496.96				3405.49	3406.75	3382.89	
CF ₃	3510	3494.9	3492.74	3493.9	3463.04	3424	3407.14	3403.81	3404.53	3378.98	0.42
Range	3480– 3518	3461.63– 3500.82	3453.81– 3508.61	3459.13– 3510.27	3435.40– 3478.72		3379.54– 3414.42	3376.79– 3414.96	3377.02– 3416.69	3362.43– 3386.8	

TABLE 9.2 The calculated NH₂ bond angles for 3-X and 4-X anilines in *n*-C₆H₁₄, CHCl₃, and CCl₄ solutions

4-X-aniline 4-X	degree NH ₂ C ₆ H ₁₄	degree NH ₂ CCl ₄	degree NH ₂ CHCl ₃	degree NH ₂ NH ₂ : HCCl ₃
OH			110.9	108.48
OCH ₃		109.94	110.36	109.02
N(CH ₃) ₂	110.94	109.56	110.97	108.51
NH ₂		109.63		108.91
OC ₆ H ₅		110.73	111.78	108.37
F	111.15	110.73	111.91	109.01
Cl	111.72	111.9	112.05	109.55
Br	111	112.04	112.31	109.96
H	111.76	111.75	111.69	109.33
H	111.76	111.78	111.56	109.36
C ₂ H ₅	111.56	110.83	112.41	109.01
C(CH ₃) ₃	111.54	111.01	112.65	108.84
C ₆ H ₅	111.81	112.12	113.86	109.35
C(=O)OC ₂ H ₅	112.54	113.23	113.67	
CN		113.41	113.78	
CF ₃	112.51	112.94	113.23	112.97
C(=O)CH ₃		113.34	113.79	
NO ₂		113.76	113.73	
3-X-aniline				
3-X				
OCH ₃	111.8	112	111.85	109.37
F	112.02	112.44	112.49	111.46
Cl	112.17	112.5	112.56	111.46
Br	112.09	112.63	112.58	111.67
CH ₃	111.72	111.69	112.18	109.32
C(=O)OC ₂ H ₅	111.61	112.23	112.23	110.03
CN		112.65	112.91	113.52
CF ₃	112.26	112.59	112.7	111.47

TABLE 9.3 IR data for the frequency separation between a.NH₂ and s.NH₂ stretching in the vapor, and in *n*-C₆H₁₄, Cl and CHCl₃ solutions for 3-X and 4-X-anilines

	[a.NH ₂ str.] [s.NH ₂ str.] Vapor phase delta cm ⁻¹	[a.NH ₂ str.] [s.NH ₂ str.] Hexane delta cm ⁻¹	[a.NH ₂ str.] [s.NH ₂ str.] CCl ₄ delta cm ⁻¹	[a.NH ₂ str.] [s.NH ₂ str.] CHCl ₃ delta cm ⁻¹	[a.NH ₂ :HCCL ₃ str.] [s.NH ₂ :HCCL ₃ str.] CHCl ₃ delta cm ⁻¹
OH	79			82.11	72.42
OCH ₃	80		78.3	80.15	74.47
N(CH ₃) ₂		82.09	76.77	82.08	72.44
NH ₂	80		77.02		73.98
OC ₆ H ₅			81.48	85.49	72.13
F	83	83.23	81.31	86.01	
Cl	82	85.57	86.17	86.78	76.81
Br	80	86.68	86.75	87.81	78.39
H	100	85.62	85.52	85.32	75.92
H	100	85.64	85.65	84.82	76.02
C ₂ H ₅		84.74	81.88	80.55	74.56
C(CH ₃) ₃	82	84.96	82.59	88.84	73.93
C ₆ H ₅	83	85.84	86.96	87.42	76
C(=O)OC ₂ H ₅		88.97	91.49	93.19	
CN	88		92.26	93.7	
CF ₃	90	88.85	90.38	92.11	89.92
C(=O)CH ₃	81		91.91	93.68	
NO ₂	88		93.65	93.58	
3-X-aniline					
X					
OCH ₃	80	85.82	86.52	86.01	76.12
F	81	86.84	88.36	88.55	84.06
Cl	82	87.35	88.55	88.79	84.06
Br	80	87.05	89	88.89	84.81
CH ₃	80	85.43	85.25	87.17	75.86
C(=O)OC ₂ H ₅	81	85.18	87.46	87.5	78.63
CN			89.21	90.21	91.88
CF ₃	86	87.76	88.93	89.37	84.06
Range		82.08–88.85	76.77–93.65	80.15–93.70	72.42–91.88

TABLE 9.3A. IR data for the frequency separation between a. and s.NH₂ bending for 3-X and 4R-X-anilines in the vapor-phase and in solutions with *n*-C₆H₁₄, CCl₄, and CHCl₃

4-X-aniline 4-X	[Vapor]- [Hexane] delta a.NH ₂ str. cm ⁻¹	[Vapor]- [Hexane] delta s.NH ₂ str. cm ⁻¹	[Hexane]- [CCl ₄] delta a.NH ₂ str. cm ⁻¹	[Hexane]- [CCl ₄] delta s.NH ₂ str. cm ⁻¹	[CHCl ₃]- [CCl ₄] delta a.NH ₂ str. cm ⁻¹	[CHCl ₃]- [CCl ₄] delta s.NH ₂ str. cm ⁻¹
OH						
OCH ₃					9.19	7.34
N(CH ₃) ₂			7.51	2.19	5.01	[-0.33]
NH ₂	26.14	20.46				
OC ₆ H ₅					5.99	1.98
F	20.98	20.77	5	3.67	4.7	0.15
Cl	13.59	17.16	1.89	2.49*	2.37	1.76
Br	13.28	19.94	2.49	2.58*	2.73	1.67
H	17.02	2.64	2.69	2.59	1.46	1.66*
H	17.01		2.46	2.47*	1.104	1.87*
C ₂ H ₅			5.9	3.04	7.63	1.33
C(CH ₃) ₃	22.82	25.48	4.46	2.39	7.91	1.66
C ₆ H ₅	15.27	18.11	0.93	2.05*	2.95	2.49
C(=O)OC ₂ H ₅			0.74	3.26*	4.17	2.47
CN				2.37	3.12	1.68
CF ₃	9.35	8.2	1.92	3.45*	2.58	1.47
C(=O)CH ₃					4.26	2.49
NO ₂					1.66	1.73*
3-X						
OCH ₃	14.98	20.8	1.48	2.18*	1.54	2.05*
F	8.3	15.14	1.35	2.87*	1.3	1.11
Cl	9.83	15.18	1.68	2.88*	1.53	1.29
Br	8.45	15.5	1.24	3.19*	1.64	1.73*
CH ₃	18.3	23.73	2.65	2.47	3.54	1.62
C(=O)OC ₂ H ₅	3.92	8.1	0.36	2.64*	2.17	2.13
CN					2.26	1.26
CF ₃	15.1	16.86	2.16	3.33*	1.16	0.72

*delta s.NH₂ str is larger than delta a.NH₂ str.

TABLE 9.4 IR data for the NH₂ stretching frequencies of aniline and 4-chloroaniline in CS₂ solution in the temperature between 27 and 60°C

°C	Aniline a.NH ₂ str. [CS ₂] cm ⁻¹	Aniline s.NH ₂ str. [CS ₂] cm ⁻¹	[a.NH ₂ str.]- s.NH ₂ str.] cm ⁻¹	°C	4-Chloroaniline a.NH ₂ str. [CCS ₂] cm ⁻¹	4-Chloroaniline s.NH ₂ str. [CS ₂] cm ⁻¹	[a.NH ₂ str.]- [s.NH ₂ str.] cm ⁻¹
27	3473.5	3388	85.5	25	3478	3390.8	87.2
15	3474	3387.5	86.5	15	3477.5	3390	87.5
0	3473	3386.5	86.5	0	3477	3389	88
-10	3473	3386	87	-10	3476.5	3389	87.5
-20	3473	3386	87	-20	3477	3388.5	88.5
-30	3472.8	3385.1	87.7	-30	3477	3388.5	88.5
-40	3472.1	3385.5	86.6	-40	3476	3388	88
-50	3471.9	3385.2	86.7	-50	3475.8	3387.5	88.3
-60	3471.7	3384.8	86.9	-60	3475.3	3387	88.3
delta C [-87]	delta a.NH ₂ str. [-1.8]	delta s.NH ₂ str. [-3.2]	delta cm ⁻¹ [1.4]	delta C [-85]	delta a.NH ₂ str. [-2.7]	delta s.NH ₂ str. [-3.8]	delta cm ⁻¹ [1.1]

TABLE 9.5 IR and Raman data and assignments for azines

Compound	IR a.(C=N) ₂ str.	Raman s.(C=N-) ₂ str.	IR a.(C=N-) ₂ str.	IR vapor cm ⁻¹ (A)	IR vapor cm ⁻¹ (A)
Benzaldehyde	solid	solid	vapor		
Azine	cm ⁻¹	cm ⁻¹	cm ⁻¹ (A)		
4-dimethylamino	1608	1539			
4-methoxy	1606	1553			
4-methyl	1623	1553			
4-hydrogen	1628	1556	1630(1.240)		
4-fluoro	1633	1561			
4-chloro	1627	1547			
4-acetoxy	1631	1562			
4-trifluoromethyl	1631	1561			
4-cyano	1624	1541			
3-nitro	1629	1551			
2-methoxy	1619	1552			
2-chloro	1618	*1			
2-hydroxy	1630	1555			
2-nitro	1627	1560			
2,4-dihydroxy	1632	1563			
2,4-dimethoxy	1617	1546			
3,4-dimethoxy	1626	1557			
2-hydroxy-4-methoxy	1630	1554			
3-methoxy-4-hydroxy	1629	1558			
2,6-dichloro	1629	1587*2			
Range	1606-1632	1539-1563 1587*2			o.p.Ring
2-furaldehyde			1630(0.940)	745(1.221)	
Azine					o.p.Ring
Acetophenone			1630(1.240)	756(0.730)	690(1.130)
azine					
Azine				a.CH2 str.	s.CH2 str.
Cyclooctanone			1627(0.120)	2935(1.200)	2864(0.210)
Azine					
(CF2=N-) ₂ *3	1747	1758			
(RCH=N-) ₂					
and					
(RR'C=N-) ₂					
Range	1636-1663	1608-1625			

*1 not recorded.

*2 reference 7, (C=N-)₂ not planar of 2,6-Cl₂C₆H₃ rings.

*3 reference 13.

TABLE 9.6 IR and Raman data for glyoximes in the solid state [(NC-)₂ stretching vibrations]

Atom or Group X	Atom or Group X	(N=C-) ₂ str.		(N=C-) ₂ str.		References
		IR cm ⁻¹	Raman cm ⁻¹	IR cm ⁻¹	Raman cm ⁻¹	
H	H	[-----]	1636 stg.	1610 vwk	[-----]	14,15
CH ₃	CH ₃	[-----]	1650 stg.	[-----]	~1512 m	15-17
C ₆ H ₅	C ₆ H ₅	[-----]	1627 stg.	1495 m ?	1495 m ?	15,16
Cl	Cl	~1620 vw	[-----]	[-----]	1588 vstg	
CN	CN	[-----]	1593 vstg	1582 vw	[-----]	15
H	CH ₃	[-----]	1630 stg.	[-----]	1516 stg	17
H	NO ₂	1650 m	1650 stg.	1608 w	1608 stg	15

?tentative assignment.

Carboxylic Acids

4-X-Benzoic Acids	170
Half Salts of Carboxylic Acids	172
References	173

Figures

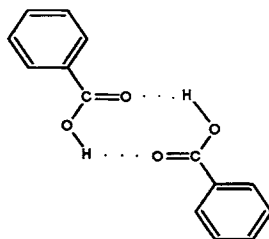
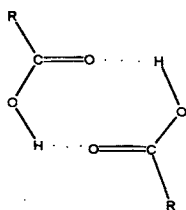
Figure 10-1	175 (166)
Figure 10-2	176 (166)
Figure 10-3	177 (166)
Figure 10-4	178 (167)
Figure 10-5	179 (168, 169)
Figure 10-6	180 (168, 169)
Figure 10-7	181 (168, 169)
Figure 10-8	182 (168, 169)
Figure 10-9	183 (168, 169)
Figure 10-10	184 (169)
Figure 10-11	185 (169)
Figure 10-12	186 (169)
Figure 10-13	187 (169)
Figure 10-14	188 (169)
Figure 10-15	189 (170)
Figure 10-16	190 (170)
Figure 10-17	191 (170)
Figure 10-18	192 (170, 171)
Figure 10-19	193

Tables

Table 10-1	194
Table 10-2	195 (167)
Table 10-3	196 (167)
Table 10-4	197 (170)
Table 10-4a	198 (170)
Table 10-5	199 (171)
Table 10-6	200 (172)
Table 10-7	201 (172)
Table 10-8	202 (172)
Table 10-9	203 (172)

*Numbers in parentheses indicate in-text page reference.

In the condensed phase or in concentrated solution carboxylic acids exist as a double hydrogen bonded dimer as illustrated here:

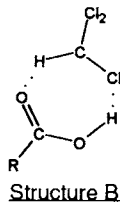


Structure A

Thus, these dimers have a center of symmetry, and only the out-of-phase $(\text{C}=\text{O})_2$ stretching mode is IR active, and only the in-phase $(\text{C}=\text{O})_2$ stretching mode is Raman active. However, in the vapor phase at elevated temperatures carboxylic acids exist in the monomeric form ($\text{R}-\text{CO}_2\text{H}$ or $\phi-\text{CO}_2\text{H}$).

The *vasym.* $(\text{OH}\cdots\text{O}=\text{C})_2$ mode for structure A is very broad over the range 2500–3000 with subsidiary maxima, which are due to combination and overtones in Fermi resonance with *vasym.* $(\text{OH}\cdots\text{O}=\text{C})_2$. The $\nu_{\text{ip}}(\text{C}=\text{O})_2$ occurs in the region 1625–1687 cm^{-1} in the Raman, in-plane $(\text{C}-\text{OH})_2$ bend in the region 1395–1445 cm^{-1} , and $\gamma(\text{OH})_2$ in the range 875–960 cm^{-1} .

Table 10.1 lists IR vapor-phase data, and CCl_4 and CHCl_3 solution-phase data for aliphatic carboxylic acids (1,2). The monomeric νOH frequency for the aliphatic carboxylic acid occurs near 3580, 3534, and 3519 cm^{-1} in the vapor, CCl_4 , and CHCl_3 phases, respectively. In CCl_4 solution the decrease in the νOH frequency is due to intermolecular hydrogen bonding between the acid proton and the Cl atom of CCl_4 ($\text{CO}_2\text{H}\cdots\text{ClCCl}_3$). The Cl atoms are less basic in CHCl_3 than they are in CCl_4 ; however, the νOH still occurs at lower frequency in CHCl_3 than in CCl_4 solution. This is attributed to the following doubly hydrogen-bonded complex in CHCl_3 , which causes νOH to shift to a lower frequency than in CCl_4 solution (2).



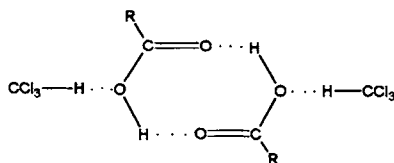
The $\nu\text{C}=\text{O}$ frequencies for these aliphatic carboxylic acids decrease in frequency in the order for vapor (1789–1769 cm^{-1}), CCl_4 (1767.3–1750.3 cm^{-1}), and CHCl_3 (1756.3–1769 cm^{-1}), and in the order of increased branching on the α -carbon atom [CH_3 to $\text{C}(\text{CH}_3)_3$] within each physical phase.

Figure 10.1 shows plots of $\nu\text{C}=\text{O}$ for aliphatic carboxylic acids in CCl_4 solution and in CHCl_3 solution vs the number of protons on the acid α -carbon atom (2). The numbers 1–5 on each curve in Figs. 1–4 are for acetic acid, propionic acid, butyric acid, isobutyric acid, and trimethylacetic acid, respectively. Similar curves were obtained plotting $\nu\text{C}=\text{O}$ vs σ^* and $\nu\text{C}=\text{O}$ vs E_s . The σ^* values are a measure of the inductive contribution of the alkyl group and E_s is a measure of the steric factor of the alkyl group (3). Thus, it appears that both inductive and steric factors affect $\nu\text{C}=\text{O}$ frequencies as well as the intermolecular hydrogen-bonded complex formed, as discussed previously.

The out-of-phase $(\text{C}=\text{O})_2$ stretching, $\nu_{\text{op}}(\text{C}=\text{O})_2$, modes occur in the range 1702.2–1714.6 cm^{-1} and 1699.6–1712.5 cm^{-1} in CCl_4 and CHCl_3 solutions, respectively, and within each solvent the frequencies decrease as σ^* and E_s increase. In the case of $\nu_{\text{ip}}(\text{C}=\text{O})_2$, it is not IR active.

Figures 10.2 and 10.3 show, respectively, plots of $\nu\text{C}=\text{O}$ vs mole % $\text{CHCl}_3/\text{CCl}_4$ and $\nu_{\text{op}}(\text{C}=\text{O})_2$ vs mole % $\text{CHCl}_3/\text{CCl}_4$ for aliphatic carboxylic acids. In CCl_4 solution $\nu\text{C}=\text{O}$ occur at the highest frequency, and then decrease in frequency as the mole % $\text{CHCl}_3/\text{CCl}_4$ is increased from ~10 to 100. On the other hand, $\nu_{\text{op}}(\text{C}=\text{O})_2$ decreases linearly as the mole % $\text{CHCl}_3/\text{CCl}_4$ is increased from 0 to 100. The essentially linear decrease in both $\nu\text{C}=\text{O}$ and $\nu_{\text{op}}(\text{C}=\text{O})_2$ after the

initial intermolecular hydrogen bond formation in the case of $\nu\text{C}=\text{O}$ is attributed to the reaction field of the solvent system. The reaction field is defined as follows: $[\text{R}] = (\epsilon - 1)/(2\epsilon + n^2)$ where ϵ is the dielectric constant and n is the refractive index of the solvent system (4). It has been shown that there is a linear relationship between the mole % $\text{CHCl}_3/\text{CCl}_4$ and the reaction field (3). The reaction field increases as the mole % $\text{CHCl}_3/\text{CCl}_4$ increases and this is a result of an increasing dielectric contribution of the solvent system accompanied by a decrease in the refractive index of the solvent system. The decrease in the $\nu_{\text{op}}(\text{C}=\text{O})_2$ frequency in going from solution in CCl_4 to solution in CHCl_3 is attributed to the following intermolecularly hydrogen-bonded structure (2):



Structure C

The gradual decrease in frequency is attributed to the increase in the reaction field as the mole % $\text{CHCl}_3/\text{CCl}_4$ is increased.

Figure 10.4 show plots of $A(\nu\text{C}=\text{O})/A[\nu_{\text{op}}(\text{C}=\text{O})_2]$ vs mole % $\text{CHCl}_3/\text{CCl}_4$. These plots indicate that as this ratio increases, as the mole % $\text{CHCl}_3/\text{CCl}_4$ increases, the concentration of molecules existing as Structure B increases while compounds existing as Structure A decrease with a subsequent increase in Structure C.

IR vapor-phase bands in the range $1105\text{--}1178\text{ cm}^{-1}$ are assigned to $\nu\text{C}-\text{C}-\text{O}$ and IR vapor-phase bands in the range $571\text{--}580\text{ cm}^{-1}$ are assigned to $\gamma\text{C}=\text{O}$ (1). The frequency separation between these two modes in the vapor phase varies between 520 and 598 cm^{-1} .

Table 10.2 lists Raman data and assignments for $\nu(\text{C}=\text{O})_2$ and $\nu\text{C}=\text{C}$ for carboxylic acids (6).

Four of the acids listed in Table 10.2 exhibit a Raman band, which can be assigned as $\nu_{\text{op}}(\text{C}=\text{O})_2$ in the range $1712\text{--}1730\text{ cm}^{-1}$. Apparently these four hydrogen-bonded carboxylic acids do not have a center of symmetry in the neat phase. The $\nu_{\text{ip}}(\text{C}=\text{O})_2$ has weak to strong relative Raman band intensity and occurs in the range $1630\text{--}1694\text{ cm}^{-1}$. The lowest frequency is exhibited by 3-(4-hydroxy-3-methoxyphenyl)-2-propionic acid, and the highest frequency is exhibited by polymethacrylic acid.

The $\nu\text{C}=\text{C}$ mode occurs as low as 1557 cm^{-1} in the case of trichloroacrylic acid to as high as 1690 cm^{-1} in the case of itaconic acid (6).

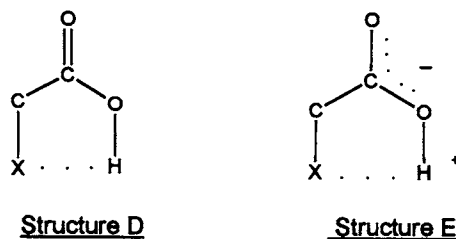
Table 10.3 lists IR group frequency data for acetic acid and its derivatives in the vapor and solution phases (1,7). The $\nu\text{OH}\cdots\text{ClCCl}_3$ frequency occurs in the region $3534.3\text{--}3500.5\text{ cm}^{-1}$ in CCl_4 solution, and for $\nu\text{OH}\cdots\text{HClCCl}_2$ in the range $3521.0\text{--}3479.6\text{ cm}^{-1}$. The lower frequencies in CHCl_3 solution are attributed to the double hydrogen bond complexed as previously discussed here. The lowest νOH frequency is exhibited by trifluoroacetic acid and the highest νOH frequency is exhibited by trimethylacetic acid. The lowest Taft σ^* value is for trimethylacetic acid $[-0.300]$ and the highest Taft σ^* value is for trifluoroacetic acid $[2.778]$ (3). Moreover, the highest pK_a value is for trimethylacetic acid $[5.03]$ and the lowest pK_a value is for

trifluoroacetic acid [0.05] (8). These data show that as the OH proton becomes more acidic the ν_{OH} mode decreases in frequency in both CCl_4 and CHCl_3 solutions. Moreover, in general the frequency separation between CCl_4 and CHCl_3 solution becomes larger as the OH proton becomes more acidic due to the formation of stronger $\text{OH}\cdots\text{Cl}$ bonds.

Figure 10.5 is a schematic of the number of possible rotational conformers for the tri-, di-, and haloacetic acid monomers (14). X is one halogen atom, 2X is two halogen atoms, 3X is three halogen atoms. The following symbols are used: E(X) indicates that the carbonyl group is eclipsed by X; E(H) indicates that the carbonyl group is eclipsed by H; A(X) indicates that X is anti to the carbonyl group; and A(H) indicates that H is anti to the carbonyl group.

Taft σ values have been correlated with the $\nu_{\text{C=O}}$ and absorbance values for acetic acid and its derivatives (9). There does not appear to be a linear relationship between $\nu_{\text{C=O}}$ and Taft σ^* values. For example, Cl acetic ($\nu_{\text{C=O}}$, 1791 vs 1.05), Cl_2 acetic ($\nu_{\text{C=O}}$, 1784 vs 1.94), and Cl_3 acetic ($\nu_{\text{C=O}}$, 1789 vs 2.65) in CCl_4 solution. On the other hand the $\nu_{\text{op}}(\text{C=O})_2$ frequencies for the mono-, di-, and trichloroacetic acids increase in frequency as the Taft σ^* constants increase in value (Cl acetic acid, 1737 cm^{-1} vs 1.05; Cl_2 acetic acid, 1744 cm^{-1} vs 1.94; and Cl_3 acetic acid, 1752 cm^{-1} vs 2.65). Therefore, factors other than Taft's inductive effect must affect $\nu_{\text{C=O}}$ and $\nu_{\text{op}}(\text{C=O})_2$. Intermolecular hydrogen bonding between C=O and $(\text{C=O})_2$, as discussed previously, is one factor that affects these stretching modes. The other factor has been reported to be the existence of rotational conformers (7).

The α -halogenated acetic acids existing in rotational forms $1\text{X}-\text{A}(\text{X})$, $2\text{X}-\text{A}(\text{X})$, and $3\text{X}-\text{A}(\text{X})\text{X}$ can form intramolecular hydrogen bonds with the α -halo atom as depicted in Structure D. The intramolecular hydrogen bond would be expected to lower the $\nu_{\text{C=O}}$ frequency, because the C=O bond would be weakened due to the induced contribution for Structure E.



Therefore, the polar A(X) forms would be expected to exhibit the lowest $\nu_{\text{C=O}}$ frequencies within each halo series. Compounds such as 2-methoxyacetic acid and pyruvic acid in the vapor phase also exist in structures such as (D) and (E). In these cases the acid proton is intramolecularly bonding to the oxygen atom of the CH_3O or $\text{CH}_3\text{C=O}$ group, respectively (1,13).

Figures 10.6–10.9 show that in either CCl_4 or CHCl_3 solution, the $\nu_{\text{C=O}}$ mode decreases in frequency within each series ($\text{X}_3\text{CO}_2\text{H}$, $\text{X}_2\text{CHCO}_2\text{H}$, $\text{XCH}_2\text{CO}_2\text{H}$, and RCO_2H) as the pK_a increases or as the acid becomes less acidic (e.g., see F, Cl, Br, and I). Figures 10.10–10.13 (14) show that in either CCl_4 or CHCl_3 solution the $\nu_{\text{C=O}}$ or $\nu_{\text{op}}(\text{C=O})_2$ mode increases in frequency within each of the four series as σ^* values increase (e.g., see Br_2 , Cl_2 , and F_2). Thus, as more sigma (σ) electrons are donated to the acid carbonyl group, the $\nu_{\text{C=O}}$ or $\nu_{\text{op}}(\text{C=O})_2$ mode

decreases in frequency due to σ electrons being donated to the carbonyl group, and as more σ electrons are withdrawn from the acid $\text{C}=\text{O}$ or $(\text{C}=\text{O})_2$ groups, the $\nu\text{C}=\text{O}$ or $\nu_{\text{op}}(\text{C}=\text{O})_2$ increase in frequency. This agrees with what was discussed previously here. However, the opposite or an erratic behavior is noted in Fig. 10.6, Br_3 to Br , Cl_3 to Cl , F_3 to F ; Fig. 10.7, Br_3 to Br , Cl_3 to Cl ; Fig. 10.8, Br to Br_3 , Cl to Cl_3 , F to F_3 ; Figs. 10.9 and 10.10, Br to Br_3 , Cl to Cl_3 , F to F_3 ; Fig. 10.11, Br to Br_3 , Cl to Cl_3 ; and Fig. 10.12, Br to Br_3 . In these cases the $\nu\text{C}=\text{O}$ or $\nu_{\text{op}}(\text{C}=\text{O})_2$ mode decreases in frequency as the pK_a value is increased or that the $\nu\text{C}=\text{O}$ or $\nu_{\text{op}}(\text{C}=\text{O})_2$ does not increase in frequency as the Taft σ^* value increases. This erratic behavior is attributed to the existence of rotational conformers, the result of rotation of the XCH_2 , X_2CH , and CX_3 groups about the $\text{C}-\text{C}=\text{O}$ bond as depicted in Fig. 10.5.

Figure 10.13 shows plots of $\nu\text{C}=\text{O}$ for the haloacetic acids vs mole % $\text{CHCl}_3/\text{CCl}_4$ solutions. In Fig. 10.13, two plots are noted for iodoacetic acid (14). The IR band near 1769 cm^{-1} is assigned to the rotational conformer $\text{II}-\text{E}(\text{I})$ and the IR band near 1736 cm^{-1} is assigned to rotational conformer $\text{II}-\text{E}(\text{H})$. In the case of chloroacetic acid, two rotational conformers are noted at high mole % $\text{CHCl}_3/\text{CCl}_4$. The lower frequency $\nu\text{C}=\text{O}$ band is assigned to the rotational conformer $\text{1Cl}-\text{E}(\text{H})$ and the higher frequency IR band to rotational conformer $\text{1Cl}-\text{E}(\text{Cl})$. In the case of fluoroacetic acid at low mole % $\text{CHCl}_3/\text{CCl}_4$ solutions, the low frequency IR band is assigned to rotational conformer $\text{1F}-\text{E}(\text{H})$, the higher frequency IR band is assigned to rotational conformer $\text{1F}-\text{E}(\text{F})$. The other 1-haloacetic acids exist in the form of rotational conformer $\text{1X}-\text{E}(\text{X})$. The dihalogenated acid $\nu\text{C}=\text{O}$ frequencies are assigned to the $\text{2X}-\text{A}(\text{X})$ rotational conformers. Dibromoacetic acid exhibits a band in the region $1797.4-1799.3\text{ cm}^{-1}$ in going from CCl_4 solution to CHCl_3 solution, and this IR band is assigned to rotational conformer $\text{2Br}-\text{E}(\text{Br})$. The trihaloacetic acid $\nu(\text{C}=\text{O})$ IR band frequencies (14) are assigned to rotational conformer $\text{3X}-\text{A}(\text{X})$.

Figure 10.14 shows plots of $\nu_{\text{op}}(\text{C}=\text{O})_2$ vs mole % $\text{CHCl}_3/\text{CCl}_4$ solutions. In Fig. 10.14, the plot for trifluoroacetic acid shows that $\nu_{\text{op}}(\text{C}=\text{O})_2$ increases in frequency as the mole % $\text{CHCl}_3/\text{CCl}_4$ increases (14). This noted exception in this series of plots is attributed to the following—the two CF_3 groups in the intermolecularly hydrogen-bonded dimer are rotating to the more polar form as the mole % $\text{CHCl}_3/\text{CCl}_4$ is increased. The most polar form is where the CF_3 groups are in rotational conformer $\text{3F}-\text{E}(\text{F})$. The field effect of the eclipsed F atom apparently overrides the field effect of the solvent system, and the intermolecular hydrogen bonding between CHCl_3 protons and the carbonyl groups, because $\nu_{\text{op}}(\text{C}=\text{O})_2$ increases rather than decreases in frequency as the mole % $\text{CHCl}_3/\text{CCl}_4$ is increased. The $\text{3F}-\text{E}(\text{F})$ rotational conformer for $\nu_{\text{op}}(\text{C}=\text{O})_2$ is reasonable, because the OH protons in this case are intramolecularly hydrogen-bonded with the two $\text{C}=\text{O}$ groups, whereas in the case of the monomer, the $\text{3X}-\text{A}$ rotational conformer is stabilized by intramolecular hydrogen bonding via $(\text{X} \cdots \text{HO})$.

In conclusion, these halogenated acetic acids exist as rotational isomers. Within a series the highest $\nu\text{C}=\text{O}$ frequency results from the conformer where the halogen atom eclipses the carbonyl oxygen atom denoted as $\text{E}(\text{X})$. The lowest $\nu\text{C}=\text{O}$ frequency is where the halogen atom is anti with the carbonyl oxygen atom denoted as $\text{A}(\text{X})$. In the anti configuration the acid proton bonds intramolecularly with the anti halogen atom, causing a weakening of the $\text{C}=\text{O}$ bond. The inductive effect of the halogen atom(s) is (are) independent of molecular geometry, but the field effect is dependent upon molecular geometry. Thus, the field effect upon the $\text{C}=\text{O}$ group is responsible for the relatively high $\nu\text{C}=\text{O}$ frequency with rotational conformers with $\text{E}(\text{X})$ structure, but not with $\text{A}(\text{X})$ structure (14).

It has been found that the type of carboxylic acid of form RCO_2H had to be identified before its approximate pK_a value could be calculated from $\nu\text{C}=\text{O}$ and $\nu_{\text{op}}(\text{C}=\text{O})_2$ frequencies recorded in CCl_4 solution (10). The $\nu\text{C}=\text{O}$ and $\nu_{\text{op}}(\text{C}=\text{O})_2$ frequencies recorded in CCl_4 solution have been reported to correlate in a linear manner with pK_a values (11). It has been reported that $\nu_{\text{op}}(\text{C}=\text{O})_2$ band intensities for aromatic carboxylic acids are higher than those for aliphatic carboxylic acids (12). In the vapor-phase at temperatures above 150°C , carboxylic acids exist only in the monomeric state. At lower temperature both the monomer and dimer carboxylic acid can exist in equilibrium. With increase in temperature the equilibrium shifts toward the monomeric species (1,13).

4-X-BENZOIC ACIDS

Table 10.4 lists IR data and assignments for 4-X-benzoic acids in the vapor, CCl_4 and/or CHCl_3 solution phases. The OH, C=O, and $(\text{C}=\text{O})_2$ frequency ranges and assignments are compared here:

	vapor, cm^{-1} (1)	CCl_4 , cm^{-1} (14)	CHCl_3 , cm^{-1} (14)
range	νOH 3582–3595	$\nu\text{OH}\cdots\text{ClCCl}_3$ 3529–3544	$\nu\text{OH}\cdots\text{ClHCCl}_2$ 3519–3528
range	$\nu\text{C}=\text{O}$ 1758–1768	$\nu\text{C}=\text{O}$ 1735–1751	$\nu\text{C}=\text{O}\cdots\text{HCCl}_3$ 1719–1744
range	$\nu_{\text{op}}(\text{C}=\text{O})_2$ -----	$\nu_{\text{op}}(\text{C}=\text{O})_2$ 1689–1707	$\nu_{\text{op}}(\text{C}=\text{O})_2\cdots(\text{HCCl}_3)_2$ 1687–1707

This comparison shows that the νOH , $\nu\text{C}=\text{O}$, and $\nu_{\text{asym.}}(\text{C}=\text{O})_2$ decrease in frequency progressing in the order vapor, CCl_4 , and CHCl_3 solutions. In the case of $\nu_{\text{op}}(\text{C}=\text{O})_2$, the frequency change in going from CCl_4 and CHCl_3 is small due to the fact that in the dimer form each O–H group is already hydrogen bonded to each of the C=O groups, and the O–H oxygen atom is much less basic; therefore, the CHCCl_3 proton will not form a strong intermolecular hydrogen bond as in the case of $\nu\text{C}=\text{O}\cdots\text{HCCl}_3$. See Table 10.4a for the factors that affect the CO_2H and $(\text{CO}_2)_2$ groups for 4X-benzoic acids in CHCl_3 and CCl_4 solutions.

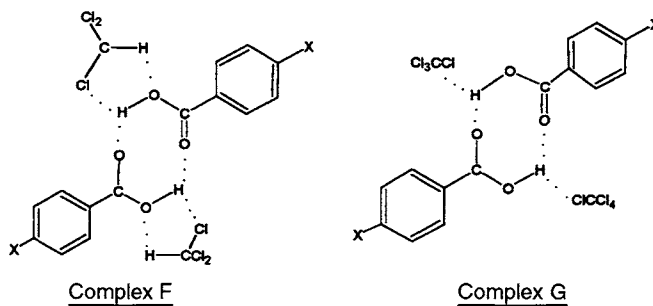
Figure 10.15 shows plots of νOH for 4-X-benzoic acids vs Hammett's σ_p values. These plots show a relationship with the Hammett σ_p values, but many of the points fall off the linear line.

Figure 10.16 shows plots of $\nu\text{C}=\text{O}$ for 4-X-benzoic acids vs Hammett's σ_p values. Linear relationships are apparent except for the 4-tert-butyl and 4-methoxy analogs for CHCl_3 solution (14).

Figure 10.17 shows plots of $\nu_{\text{op}}(\text{C}=\text{O})_2$ for 4-X-benzoic acids vs Hammett's σ_p values. The plots for both CCl_4 and CHCl_3 solutions are linear in three different segments (14).

Figure 10.18 shows plots of $\nu_{\text{op}}(\text{C}=\text{O})_2$ for 4-X-benzoic acids vs mole % $\text{CHCl}_3/\text{CCl}_4$. The Cl, Br, H, CH_3 , tert-butyl, and methoxy analogs all decrease essentially linearly in going from CCl_4 to CHCl_3 solutions. In addition, the frequency separation between these linear plots decreases as Hammett's σ_p values increase in value. However, in the case of the 4-nitro and 4-cyano analogs the $\nu_{\text{op}}(\text{C}=\text{O})_2$ frequencies actually increase in going from CCl_4 to CHCl_3 solution.

In CCl_4 solution, the 4-nitro analog would have the most acidic OH proton and the most basic C–O oxygen atoms. Therefore, a complex such as (F) would cause the C=O bond to be

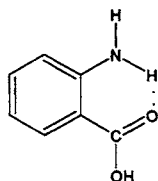


strengthened. Therefore, the $\nu_{\text{op}}(\text{C}=\text{O})_2$ mode would vibrate at a higher frequency than in a case such as Complex G. In addition, the NO_2 group of aryl NO_2 has been shown to form intermolecular hydrogen bonds with CHCl_3 (15), and between $\text{Cl}_3\text{CH}\cdots\text{NC}$ for benzonitrile (16). Intermolecular hydrogen bonding of the CHCl_3 proton with the 4- NO_2 or 4-cyano group would also cause an increase of $\nu_{\text{op}}(\text{C}=\text{O})_2$ in these $(\text{Cl}_3\text{C}-\text{HClCCl}_3)_n$ complex solutions. Moreover, intermolecular hydrogen complexes involving the CH_3Cl_3 proton with the π system on one or both sides of the planar phenyl group would also cause $\nu\text{C}=\text{O}$ to increase in frequency. These $\nu_{\text{op}}(\text{C}=\text{O})_2$ shifts are 0.27 and 0.65 cm^{-1} for the NO_2 and CH_3O analogs, respectively. For the Cl, Br, H, CH_3 , $(\text{CH}_3)_2\text{C}$, and CH_3O these shifts are -1.01, -1.10, -1.33, -2.34, -2.27, and -2.52, respectively.

Figure 10.18 shows plots of $\nu\text{C}=\text{O}$ for 4-X-benzoic acids vs mole % $\text{CHCl}_3/\text{CCl}_4$. In CCl_4 solution, the Br analog occurs at a higher frequency than the Cl analog, and in CHCl_3 solution the CN analog occurs at a higher frequency than the NO_2 analog. These cases are exceptions to the correlation of $\nu\text{C}=\text{O}$ vs Hammett σ_p values.

The 4-*tert*-butylbenzoic exhibits two $\nu\text{C}=\text{O}$ bands. The lower frequency band frequencies listed by the computer are in the range 1721.55–1718.0 cm^{-1} . The $\nu\text{C}=\text{O}$ for the 1721.55–1718.0 cm^{-1} IR band is in good agreement with the $\nu\text{C}=\text{O}$ vs Hammett σ_p values. The higher $\nu\text{C}=\text{O}$ frequency band for 4-*tert*-butylbenzoic increases in frequency as the mole % $\text{CHCl}_3/\text{CCl}_4$ is increased while none of the other 4-X-benzoic acids show this opposite trend. A possible explanation for this $\nu\text{C}=\text{O}$ frequency behavior is that the *tert*-butyl group is hyperconjugated, and that the $\text{Cl}_3\text{C}-\text{H}$ proton is hydrogen bonded to the phenyl π system while the positively charged tertiary carbon atom is associated with the Cl_3CH chlorine atom. Such an interaction would cause the $\nu\text{C}=\text{O}$ mode to increase in frequency as observed. Because 4-*tert*-butylbenzoic acid exhibits two $\nu\text{C}=\text{O}$ frequencies it is apparent that it exists as clusters in CHCl_3 solutions. All of the 4-X-benzoic acids show breaks in the plots in the range 10–30 mol % $\text{CHCl}_3/\text{CCl}_4$ solution, which indicates that other $\text{CHCl}_3/\text{CCl}_4$ complexes of $(\text{Cl}_3\text{C}-\text{H}\cdots\text{ClCCl}_3)_n$ with the 4-X-benzoic are also present.

Table 10.5 lists IR vapor-phase data and assignments for anthranilic acids. These acids have the following basic structure:



The $\nu\text{O-H}$ stretching frequencies occur in the range $3484\text{--}3494\text{ cm}^{-1}$. The *vasym.* NH_2 mode occurs in the range $3518\text{--}3525\text{ cm}^{-1}$ and *vsym.* NH_2 in the range $3382\text{--}3395\text{ cm}^{-1}$. The frequency separation of $123\text{--}141\text{ cm}^{-1}$ indicates that the N-H proton is intramolecularly hydrogen bonded to the C=O group as was illustrated here. A weak band in the region $3430\text{--}3436\text{ cm}^{-1}$ is assigned to $\nu\text{OH}\cdots\text{N}$. The $\nu\text{C=O}$ mode is in the range $1724\text{--}1732\text{ cm}^{-1}$. The NH_2 bending mode is exhibited in the range $1613\text{--}1625\text{ cm}^{-1}$. A medium-strong band in the range $1155\text{--}1180\text{ cm}^{-1}$ is attributed to O=C stretch.

N-methyl anthranilic acid and N-phenyl anthranilic acid exhibit $\nu\text{N-H}\cdots\text{O=C}$ at 3392 and 3348 cm^{-1} , respectively. The N-H \cdots O=C intramolecular hydrogen bond is stronger in the case of the N-phenyl analog due to the inductive effect of the phenyl group compared to that for the N-methyl group.

The $\nu\text{C=O}\cdots\text{H-N}$ frequencies occur near 1719 cm^{-1} for N-methyl and N-phenyl anthranilic acid compared to $1724\text{--}1732\text{ cm}^{-1}$ for the other anthranilic acids studied.

Table 10.6 lists infrared data for acrylic acid and methacrylic acid in 0 to 100 mol % $\text{CHCl}_3/\text{CCl}_4$ solutions. The *sym.* CH_3 bending mode for methacrylic acid increases steadily from 1375.5 to 1377.8 cm^{-1} as the mole % $\text{CHCl}_3/\text{CCl}_4$ is increased from 0 to 100, while the $\text{CH}_2=\text{wag}$ mode for methacrylic acid increases *wag* only 0.5 cm^{-1} , from 948.7 to 949.2 cm^{-1} . In the case of acrylic acid, the $\text{CH}_2=\text{bending}$ mode decreases steadily from 1433.1 to 1429.9 cm^{-1} as the mole % $\text{CHCl}_3/\text{CCl}_4$ increases from 0 to 100, while the vinyl twist mode varies from 983.9 to 983.6 to 984 cm^{-1} .

Table 10.7 lists Raman data for carboxylic acid salts (6). In some cases *vasym.* CO_2 is observed in the Raman, and its intensity is always less than the Raman intensity for *vsym.* CO_2 . The Raman bands in the region $1383\text{--}1468\text{ cm}^{-1}$ are assigned to *vsym.* CO_2 .

Frequency assignments for *vasym.* CO_2 and *vsym.* CO_2 are summarized in Table 10.8. Study of this table suggests that the inductive effect causes *vasym.* CO_2 for the dichloroacetate ion to occur at higher frequency than the other carboxylate ions.

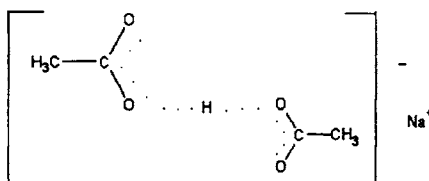
Table 10.9 lists IR data for carboxylic acid salts. This table demonstrates as well that the inductive effect also increases the *vasym.* CO_2 frequency as it increases from 1585 cm^{-1} for sodium acetate to 1640 cm^{-1} for sodium difluoroacetate. It appears that a divalent cation such as calcium (Ca) lowers the *vasym.* CO_2 frequency compared to a monovalent cation such as lithium (Li) or sodium (Na). Compare lithium and calcium formate (1604 vs 1596 cm^{-1}) and sodium and calcium 2-ethylhexanoate (1555 vs 1545 cm^{-1}) while the opposite effect is noted for *vsym.* CO_2 (1382 vs 1400 cm^{-1}) and (1415 and 1424 cm^{-1}) for the formate and 2-ethylhexanoates, respectively.

HALF SALTS OF CARBOXYLIC ACIDS

Sodium hydrogen diacetate is an example of a transmission anomaly observed within broad absorption bands of solids. This anomaly indicates that there are perturbations between overlapping energy levels in the solid state.

Sodium hydrogen diacetate is classified as a type A acid salt with a centrosymmetric anion:

Sodium hydrogen diacetate has 24 molecules per unit cell in its crystal structure (18). The broad intense absorption is determined by coupling between two or more vibrating $(-\text{O}\cdots\text{H}\cdots\text{O}-)_n$ groups (19).



There are two C–C stretch modes in the centrosymmetric anion, a vsym. $(C-C)_2$ and vasm., $(C-C)_2$. The vasm. $(C-C)_2$ mode yields a strong Raman band at 920 cm^{-1} , and it is this mode that interacts, causing the transmission window in the broadband at 920 cm^{-1} (see Fig. 10.19a). Figure 10.19b is that for the $(CD_3)_2$ analog, and in this case the vasm. C–C mode has shifted to 874 cm^{-1} exhibiting the transmission anomaly at this frequency. Another anomaly near 840 cm^{-1} results from the CD_3 rocking mode at this frequency (20).

Application of the perturbation theory redistributes both energy levels and absorption intensity. Near E_1° the interaction is greatest and the resulting shift of the levels leads to a fall in energy-level density. The loss in absorption intensity in this region appears as a gain in the other regions and the perturbation involves all the E_1° and E_2° levels. The intensity may be redistributed over a relatively large frequency range. This yields within the broadband a narrow region of increased transmission, with some regions of increased absorption nearby; the latter might not be easily noted in the spectrum (20).

Because Evans was the first to explain these peculiar effects that appear sometimes in the solid state IR spectra, it is now referred to as the “Evans Transmission Hole” or “Evans Hole.”

REFERENCES

1. Nyquist, R. A. (1984). *The Interpretation of Vapor-phase Infrared Spectra: Group Frequency Data*. Philadelphia: Sadtler Research Laboratories, Division of Bio-Rad.
2. Nyquist, R. A., Clark, T. D., and Streck, R. (1994). *Vib. Spectrosc.*, 7, 275.
3. Taft, R. W. Jr. (1956). In *Steric Effects in Organic Chemistry*, M. S. Newman (ed.), Chap. 3, New York: Wiley.
4. Buckingham, A. D. (1960). *Can. J. Chem.*, 308, 300.
5. Nyquist, R. A., Putzig, C. L., and Hasha, D. L. (1989). *Appl. Spectrosc.*, 1049.
6. (1984). *Sadtler Standard Raman Spectra*, Philadelphia: Sadtler Research Laboratories, Division of Bio-Rad Laboratories.
7. Nyquist, R. A. and Clark, T. D. (1996). *Vib. Spectrosc.*, 10, 203.
8. Christensen, J. J., Hansen, L. D., and Isatt, R. M. (1976). *Handbook of Proton Ionization and Related-Thermodynamic Quantities*, New York: Wiley Interscience.
9. Bellanato, J. and Baraceló, J. R. (1960). *Spectrochim. Acta*, 16, 1333.
10. Golden, J. D. S. (1954). *Spectrochim. Acta*, 6, 129.
11. St. Fleet, M. (1962). *Spectrochim. Acta*, 18, 1537.
12. Brooks, C. J. W., Eglinton, G., and Moran, J. F. (1961). *J. Chem. Soc.*, 106.
13. Welti, D. (1970). *Infrared Vapor Spectra*, London: Heyden, in cooperation with Sadtler Research Laboratories, Philadelphia, PA.
14. Nyquist, R. A. and Clark, T. D. (1995). *Vib. Spectrosc.*, 8, 387.
15. Nyquist, R. A. and Settineri, S. E. (1990). *Appl. Spectrosc.*, 44, 1552.
16. Nyquist, R. A. (1990). *Appl. Spectrosc.*, 44, 1405.

17. Nyquist, R. A., Putzig, C. L., and Leugers, M. Anne (1997). *Infrared and Raman Spectral Atlas of Inorganic Compounds and Organic Salts*, vol. 1, p. 72. Academic Press, Boston.
18. Splakman, J. C. and Mills, H. H. (1961). *J. Chem. Soc.*, 1164.
19. Albert, N. and Badger, R. M. (1958). *J. Chem. Phys.*, **29**, 1193.
20. Evans, J. C. (1962). *Spectrochim. Acta*, **18**, 507.

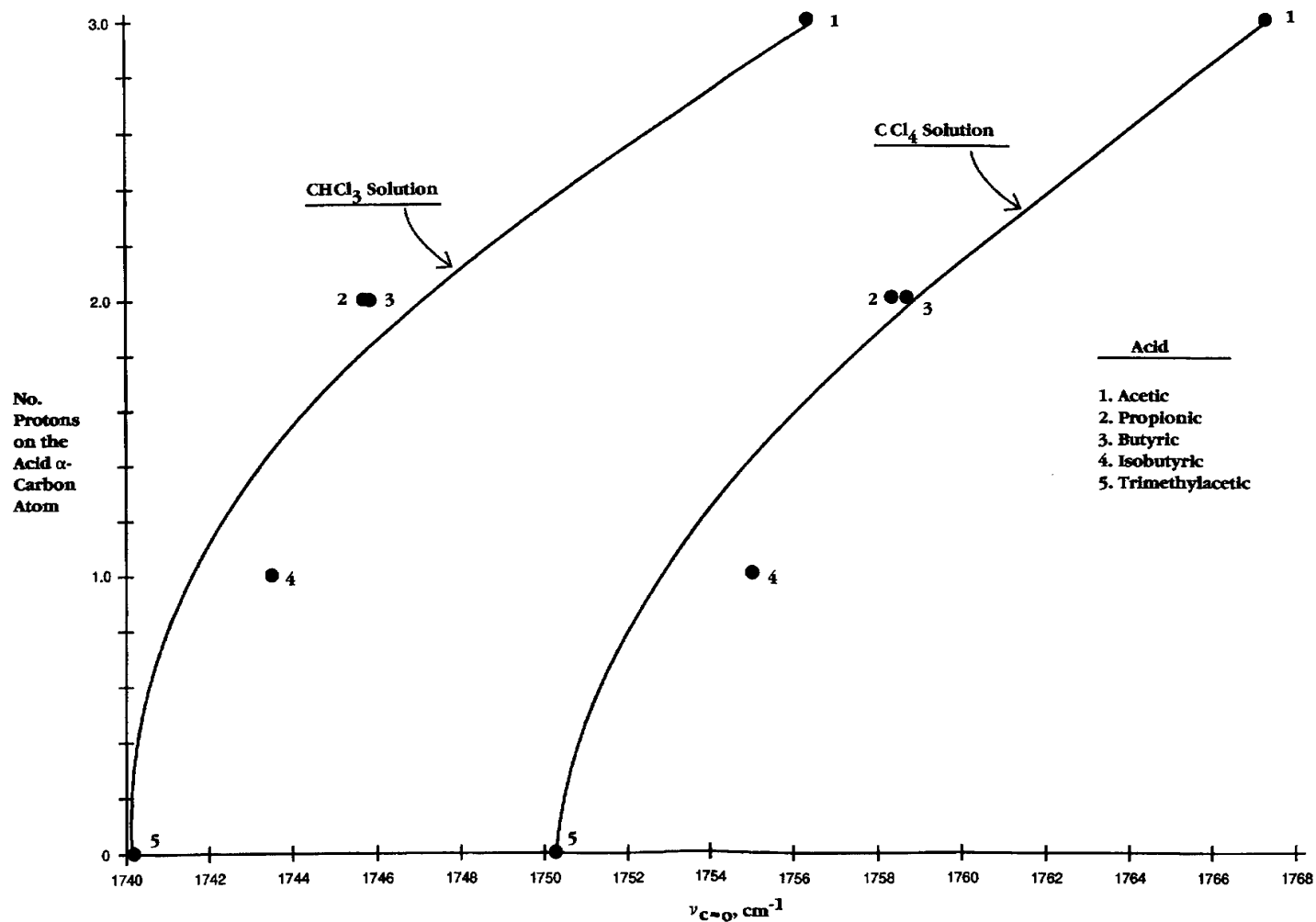


FIGURE 10.1 Plots of the number of protons on the acid α -carbon atom of the carboxylic acid vs $\nu_{C=O}$ for alkyl carboxylic acids in 2% wt./vol. in CCl_4 and in 2% wt./vol. CHCl_3 solutions.

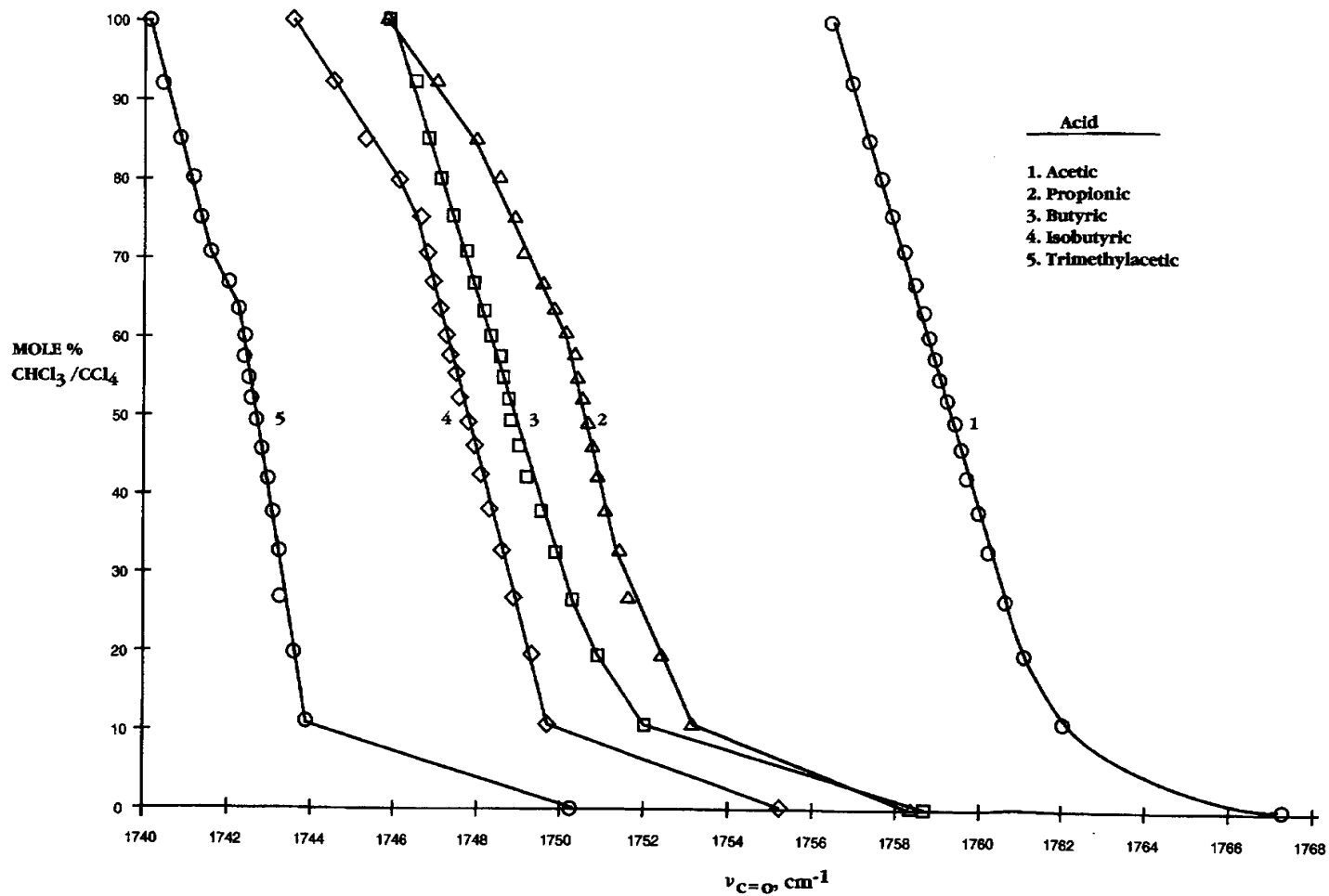


FIGURE 10.2 Plots of the mol % CHCl₃/CCl₄ vs $\nu_{C=O}$ for alkyl carboxylic acids in 2% wt./vol. CHCl₃ and/or CCl₄ solutions.

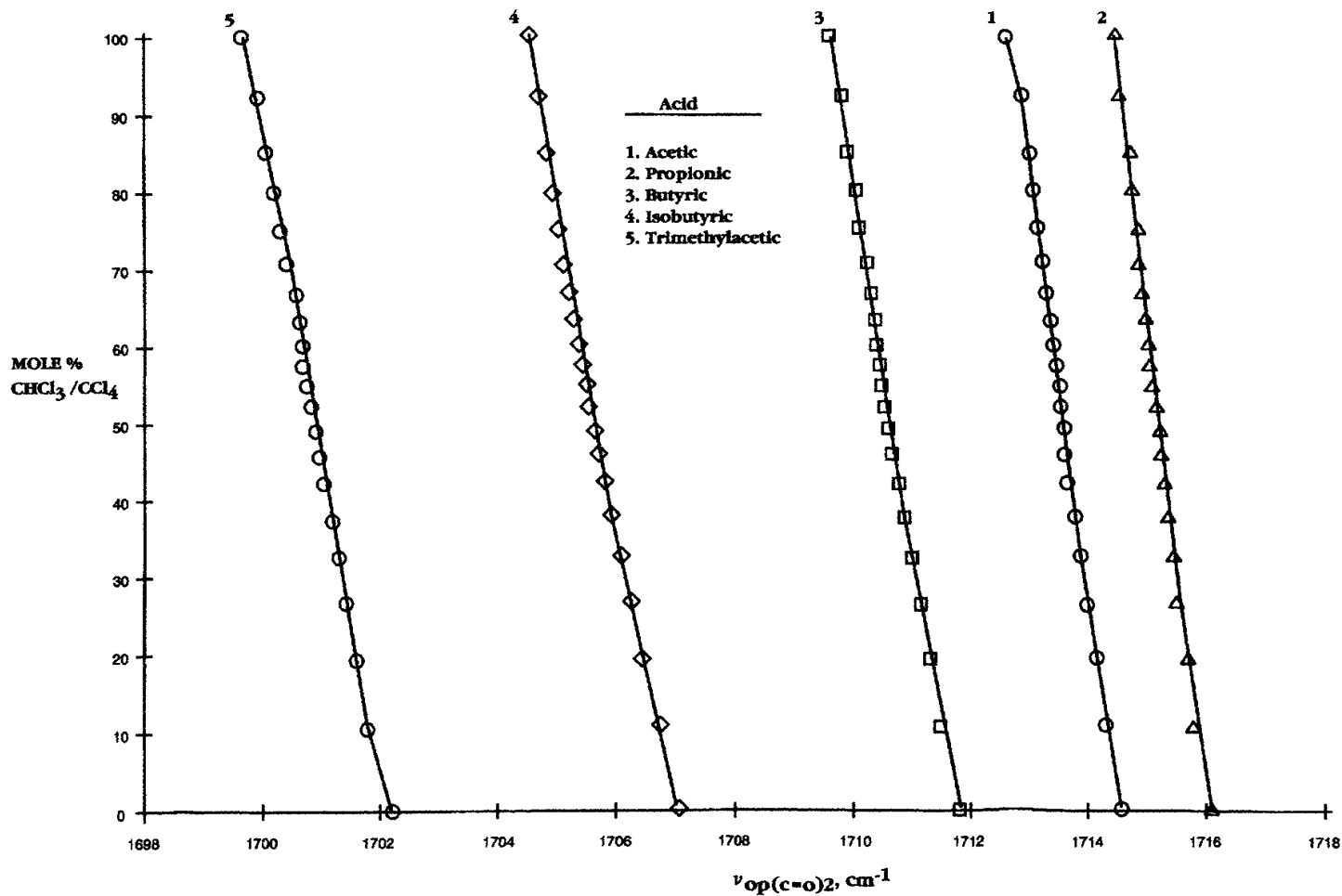


FIGURE 10.3 Plots of the mole % CHCl₃/CCl₄ vs $\nu_{op}(C=O)_2$ for alkyl carboxylic acids in 2% wt./vol. CHCl₃ and/or CCl₄ solutions.

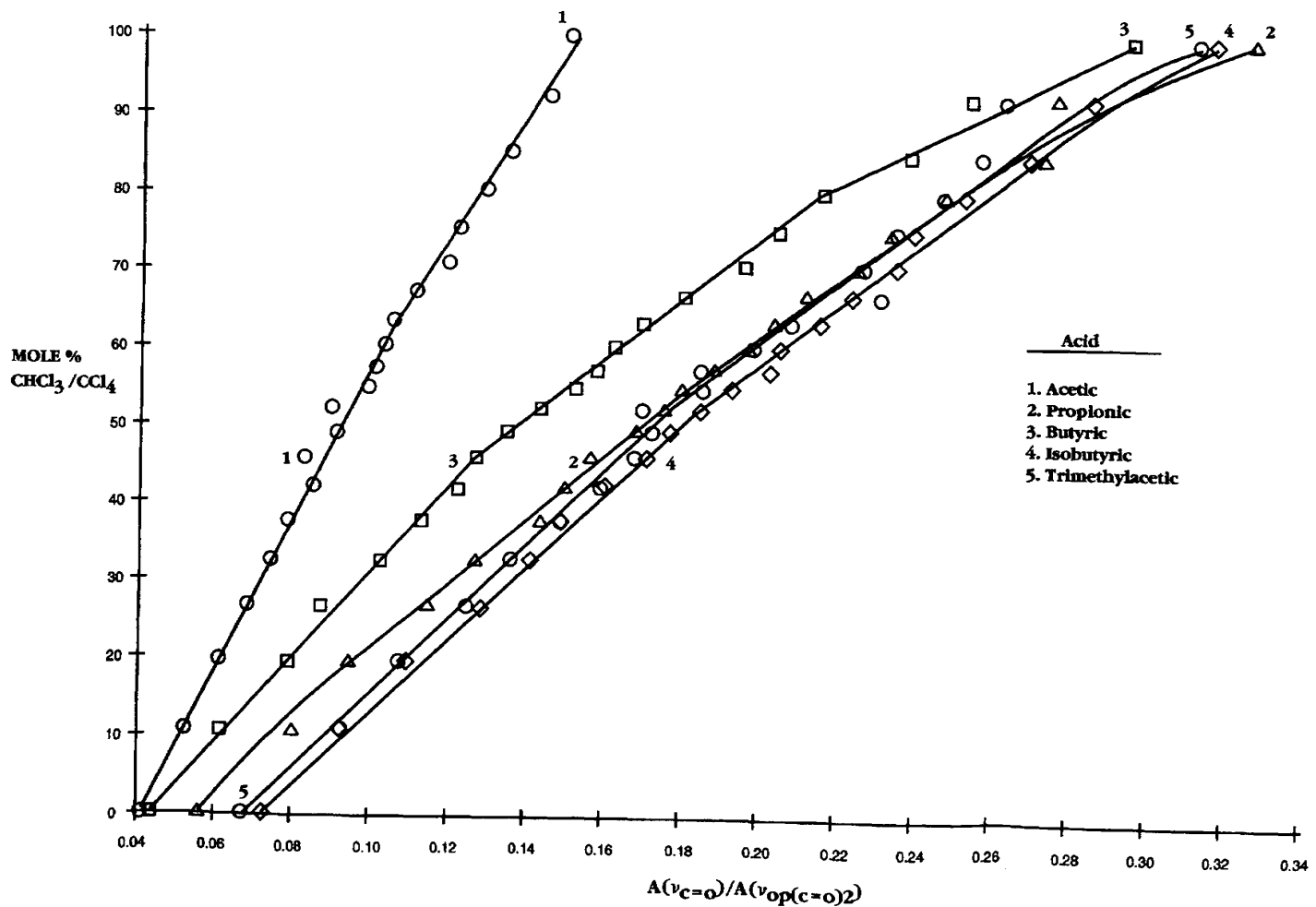


FIGURE 10.4 Plots of the mole % CHCl₃/CCl₄ vs absorbance $[\nu(C=O)]/absorbance [\nu_{op}(C=O)_2]$ for the alkyl carboxylic acids in 2% wt./vol. CHCl₃ and/or CCl₄ solutions.

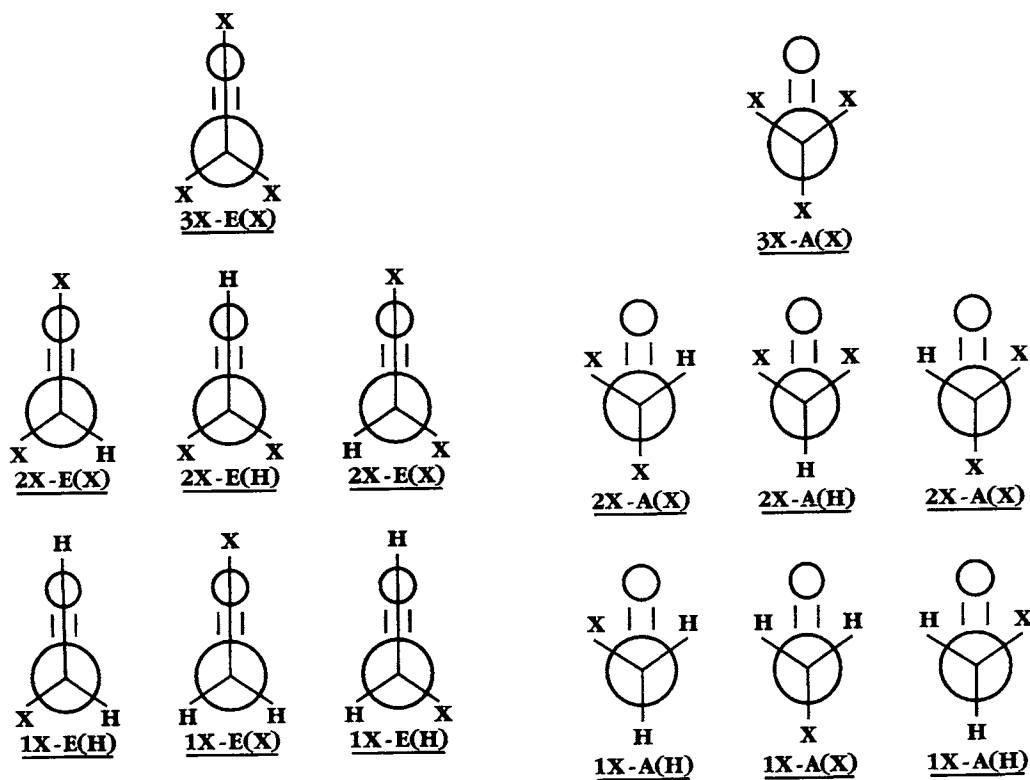


FIGURE 10.5 A schematic of the number of possible rotational isomers for the tri-, di-, and haloacetic acids not in the form of intermolecular hydrogen-bonded dimers. X is a halogen atom, 2X is two halogen atoms, 3X is three halogen atoms.

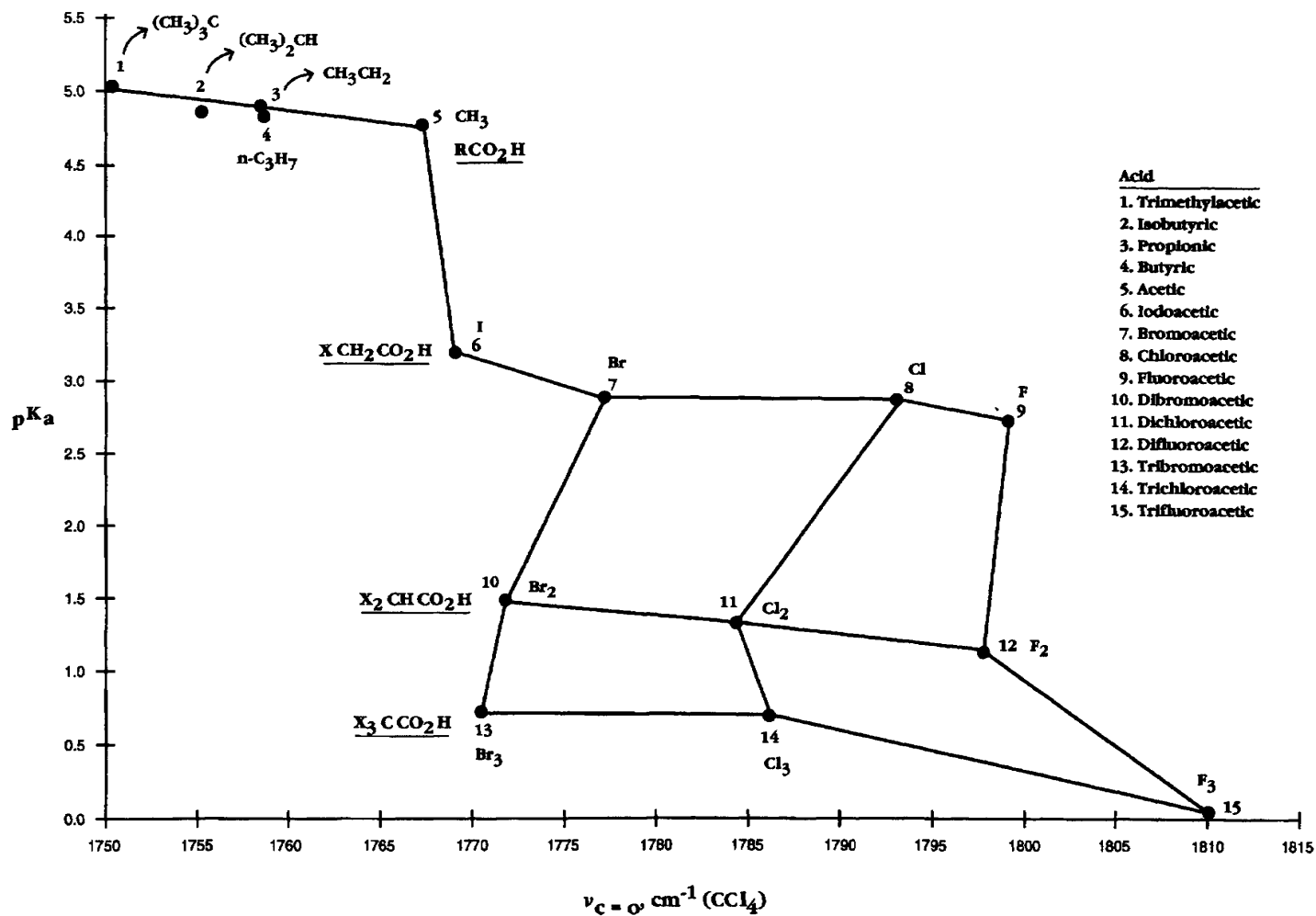


FIGURE 10.6 Plots of $\nu_{C=O}$ for each carboxylic acid in CCl_4 solution vs the pK_a value for each carboxylic acid.

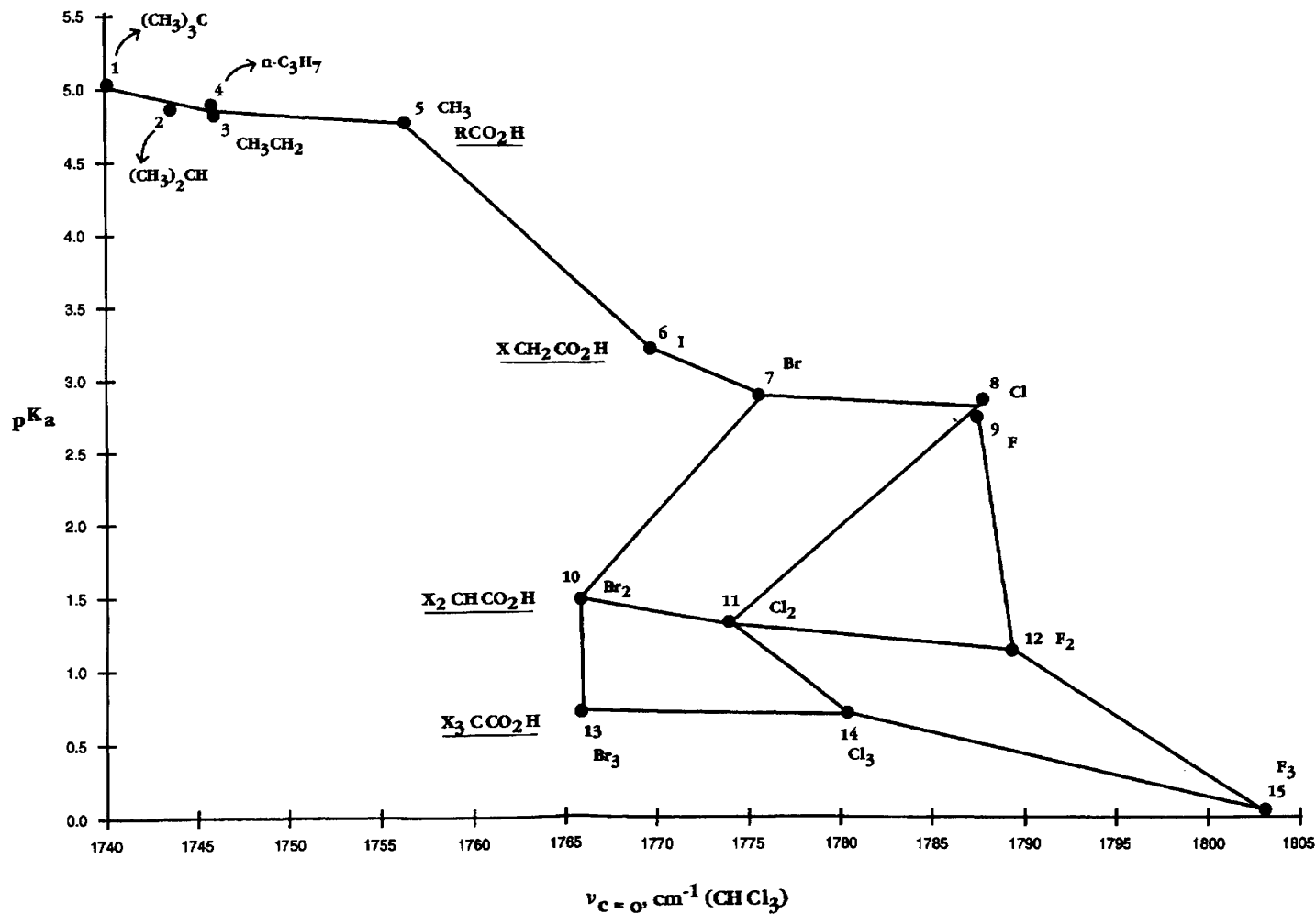


FIGURE 10.7 Plots of $\nu_{C=O}$ for each carboxylic acid in CHCl_3 solution vs the pK_a value for each carboxylic acid.

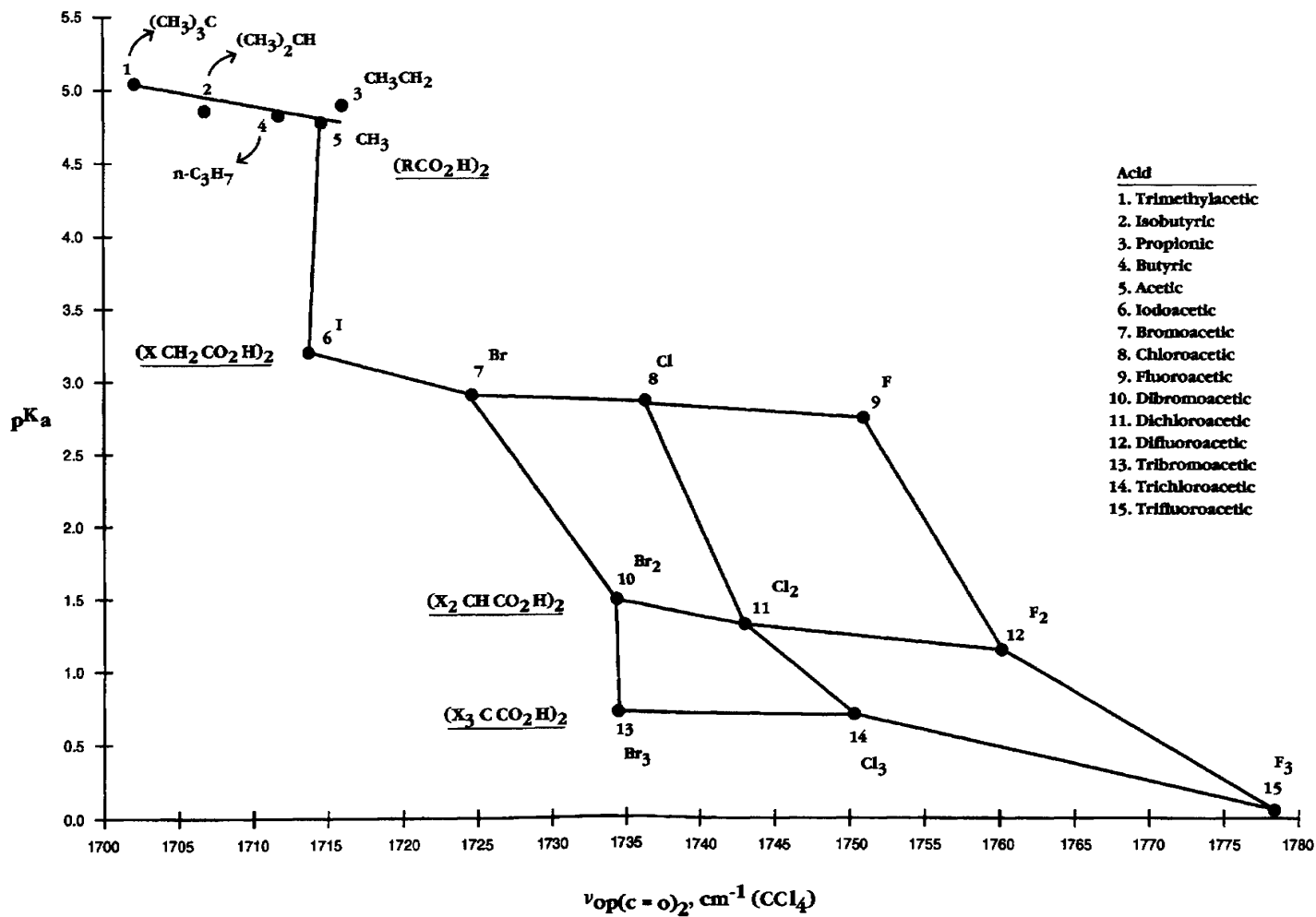


FIGURE 10.8 Plots of $\nu_{op}(C=O)_2$ for each carboxylic acid in CCl_4 solution vs the pK_a value for each carboxylic acid.

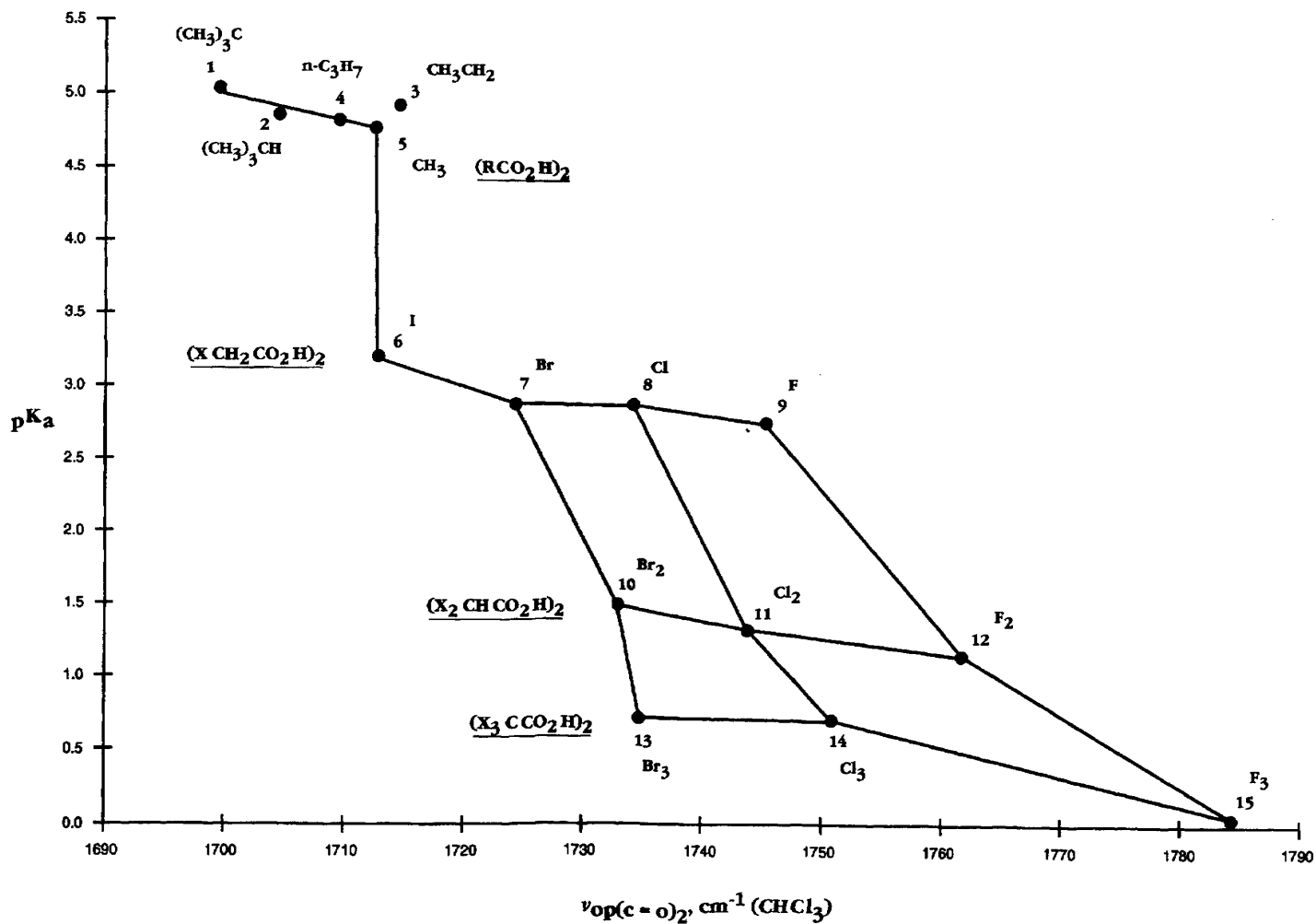


FIGURE 10.9 Plots of $\nu_{op}(\text{C}=\text{O})_2$ for each carboxylic acid in CHCl_3 solution vs the pK_a value for each carboxylic acid.

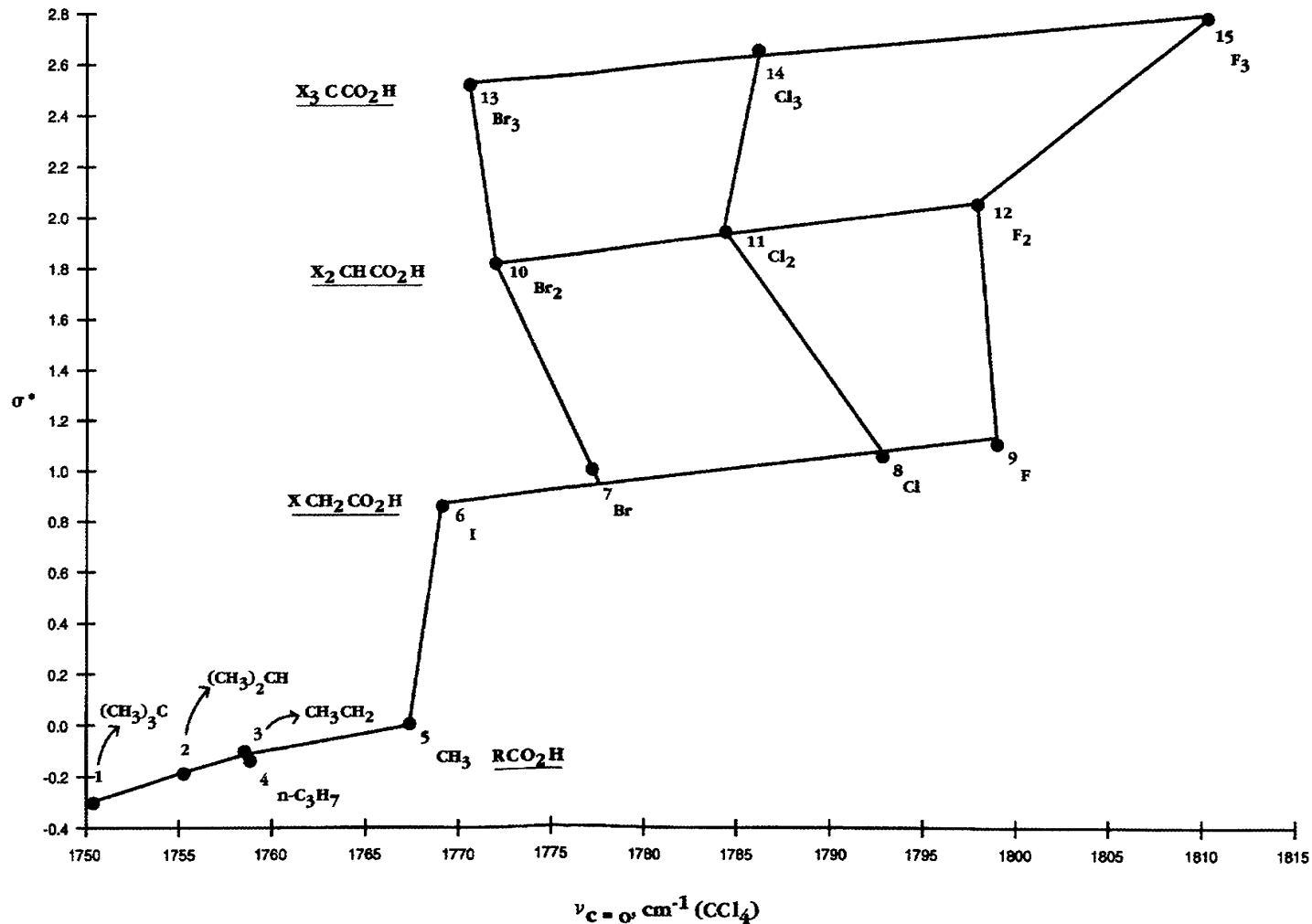


FIGURE 10.10 Plots of $\nu_{C=O}$ for each carboxylic acid in CCl_4 solution vs the σ^* value for each carboxylic acid.

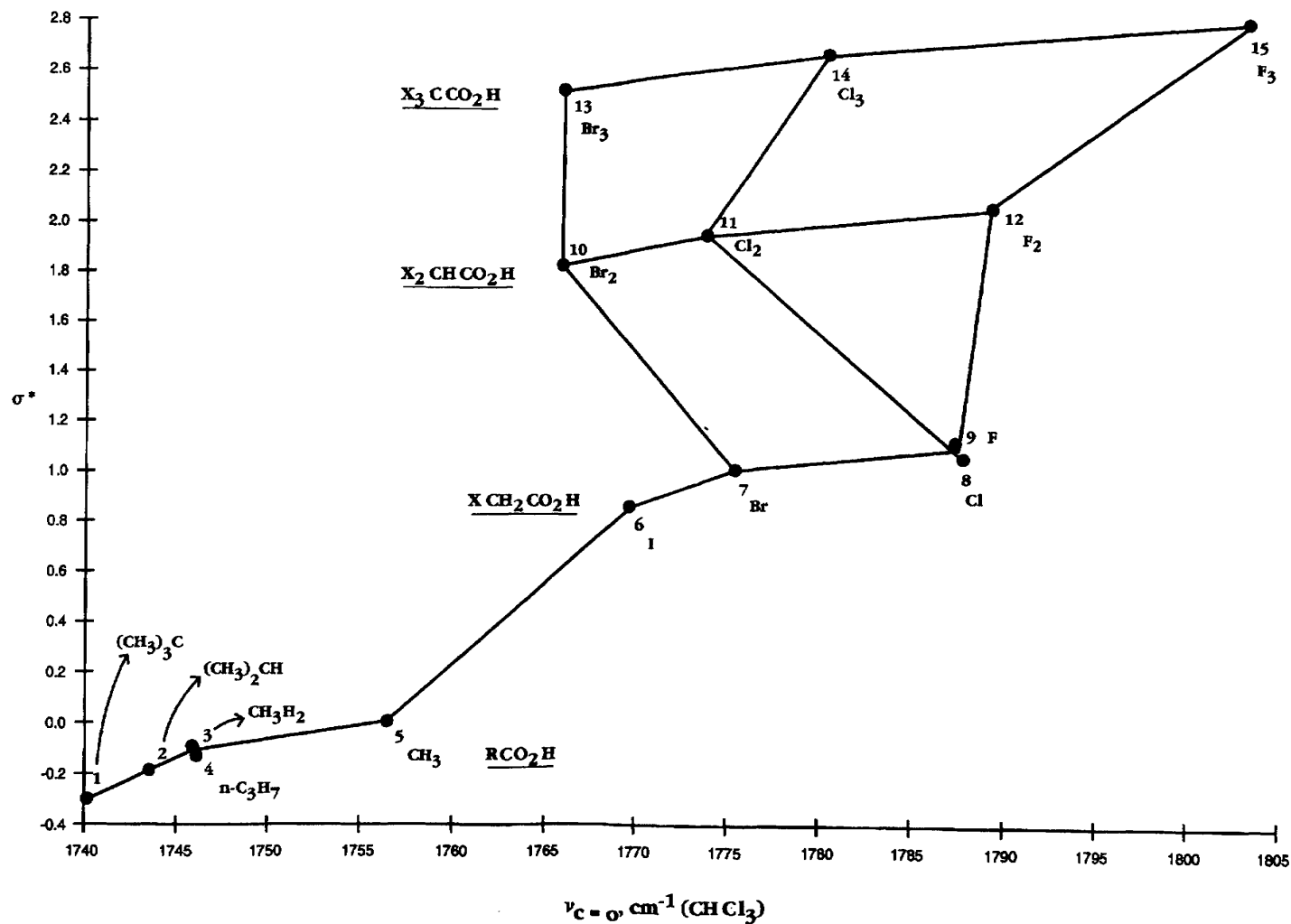


FIGURE 10.11 Plots of $\nu(\text{C}=\text{O})$ for each carboxylic acid in CHCl_3 solution vs the σ^* value for each carboxylic acid.

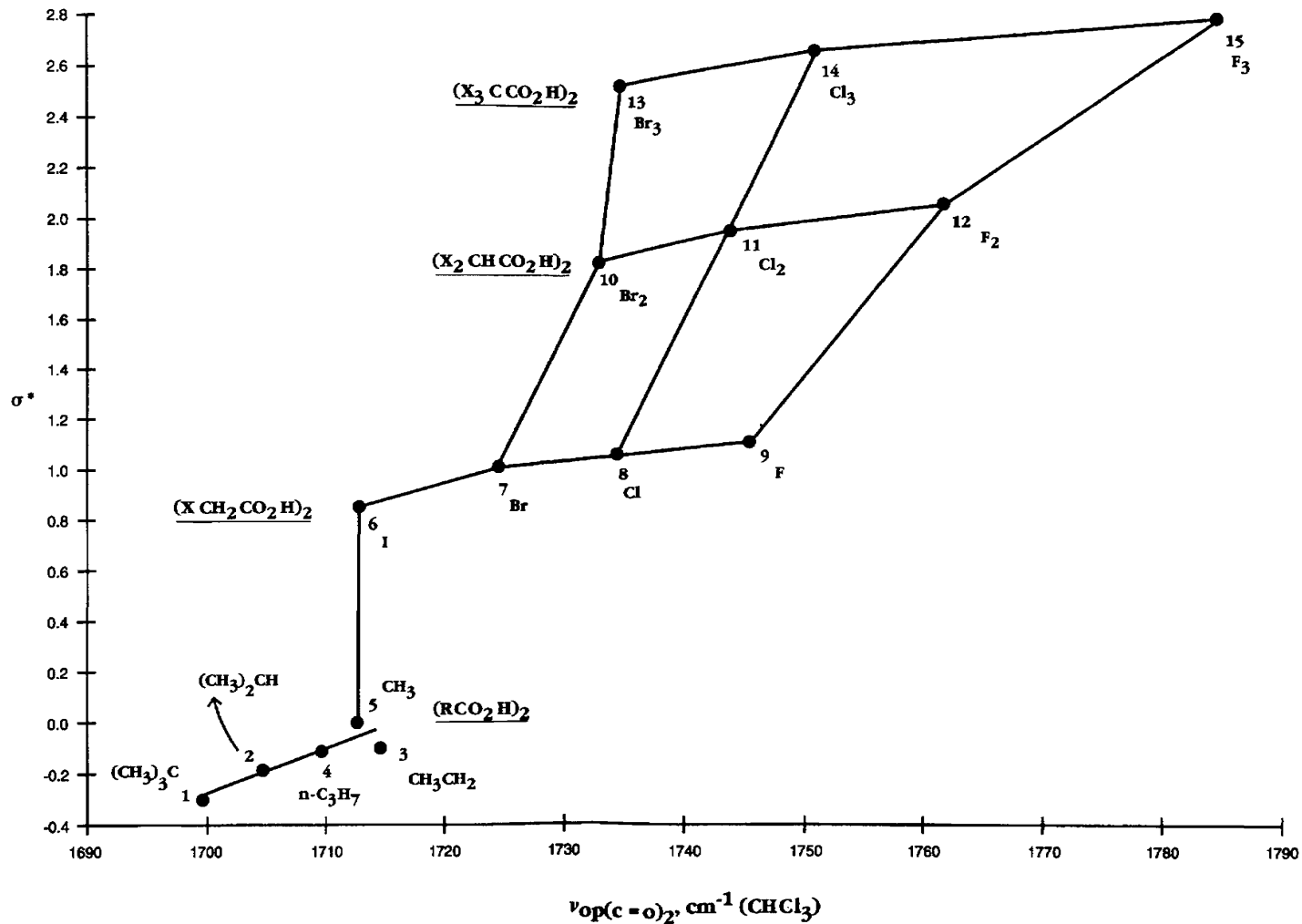


FIGURE 10.12 Plots of $\nu_{op}(C=O)_2$ for each carboxylic acid in CHCl_3 solutions vs the σ^* value for each carboxylic acid.

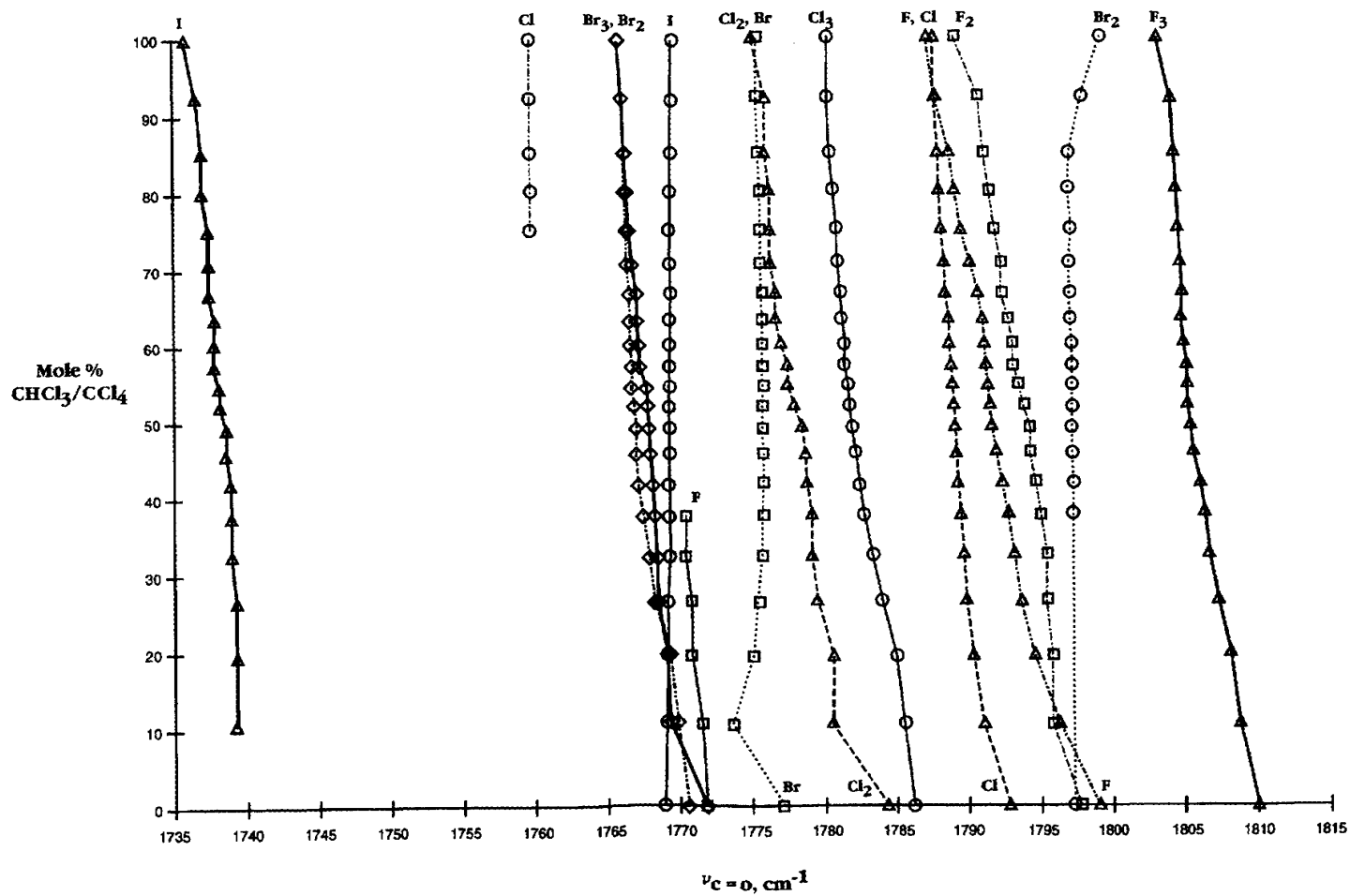


FIGURE 10.13 Plots of $\nu(\text{C}=\text{O})_2$ for trihalo, dihalo, and haloacetic acids vs mole % $\text{CHCl}_3/\text{CCl}_4$.

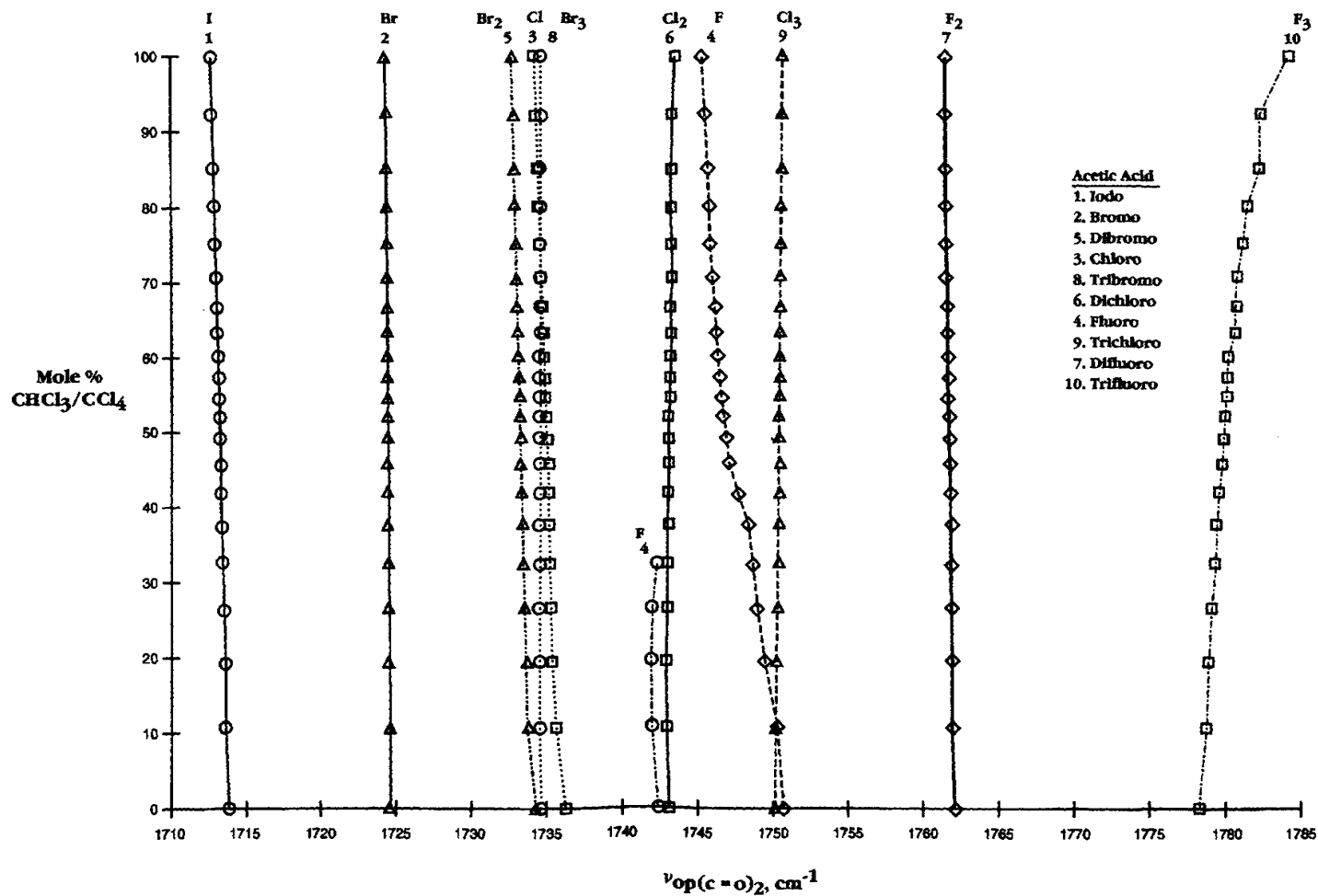


FIGURE 10.14 Plots of $\nu_{op}(\text{C}=\text{O})_2$ for trihalo, dihalo, and haloacetic acids vs mole % $\text{CHCl}_3/\text{CCl}_4$.

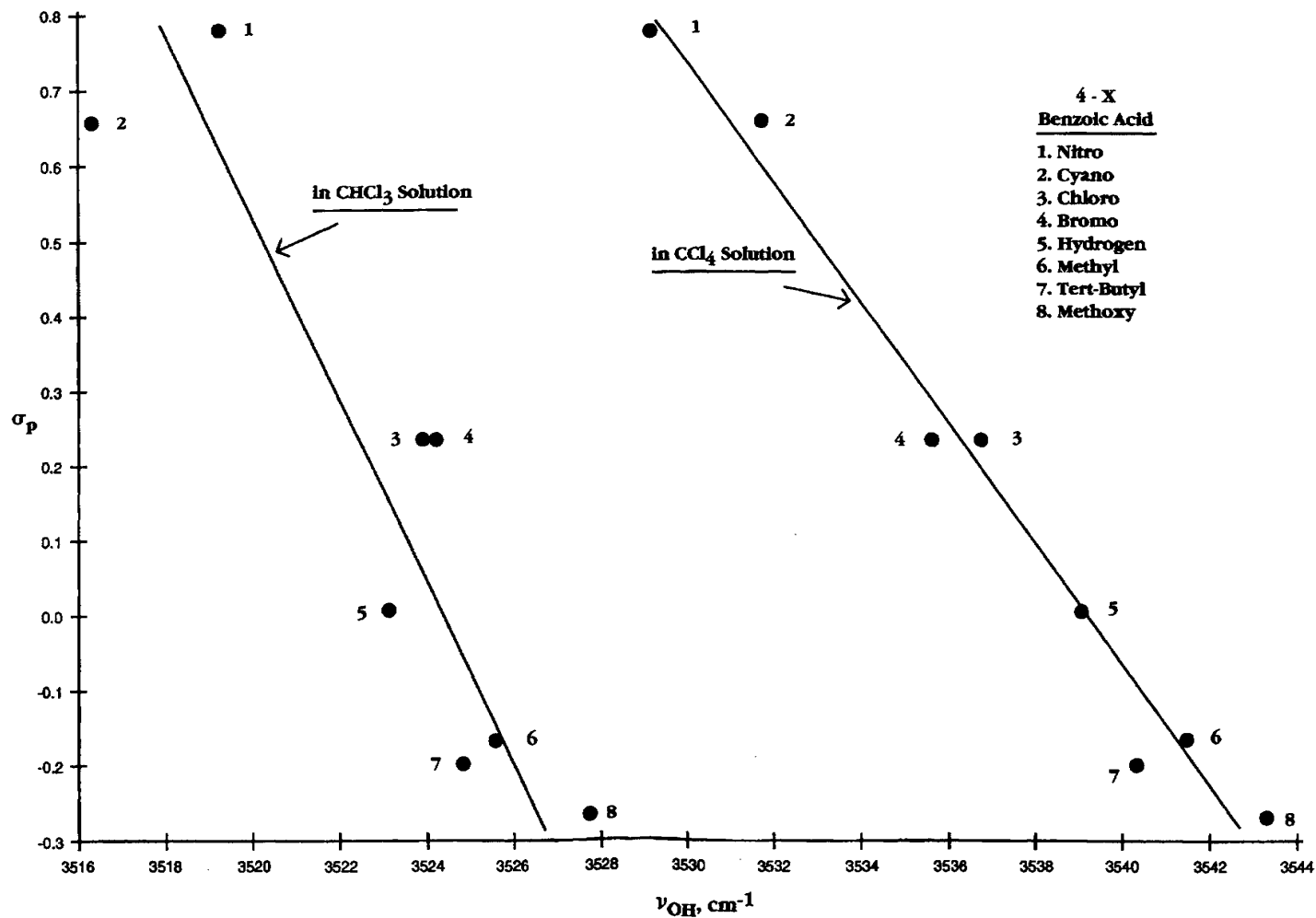


FIGURE 10.15 Plots of ν_{OH} mode for 4-X-benzoic acids in CCl_4 solution and in $CHCl_3$ solution vs σ_p values for the 4-X atom or group.

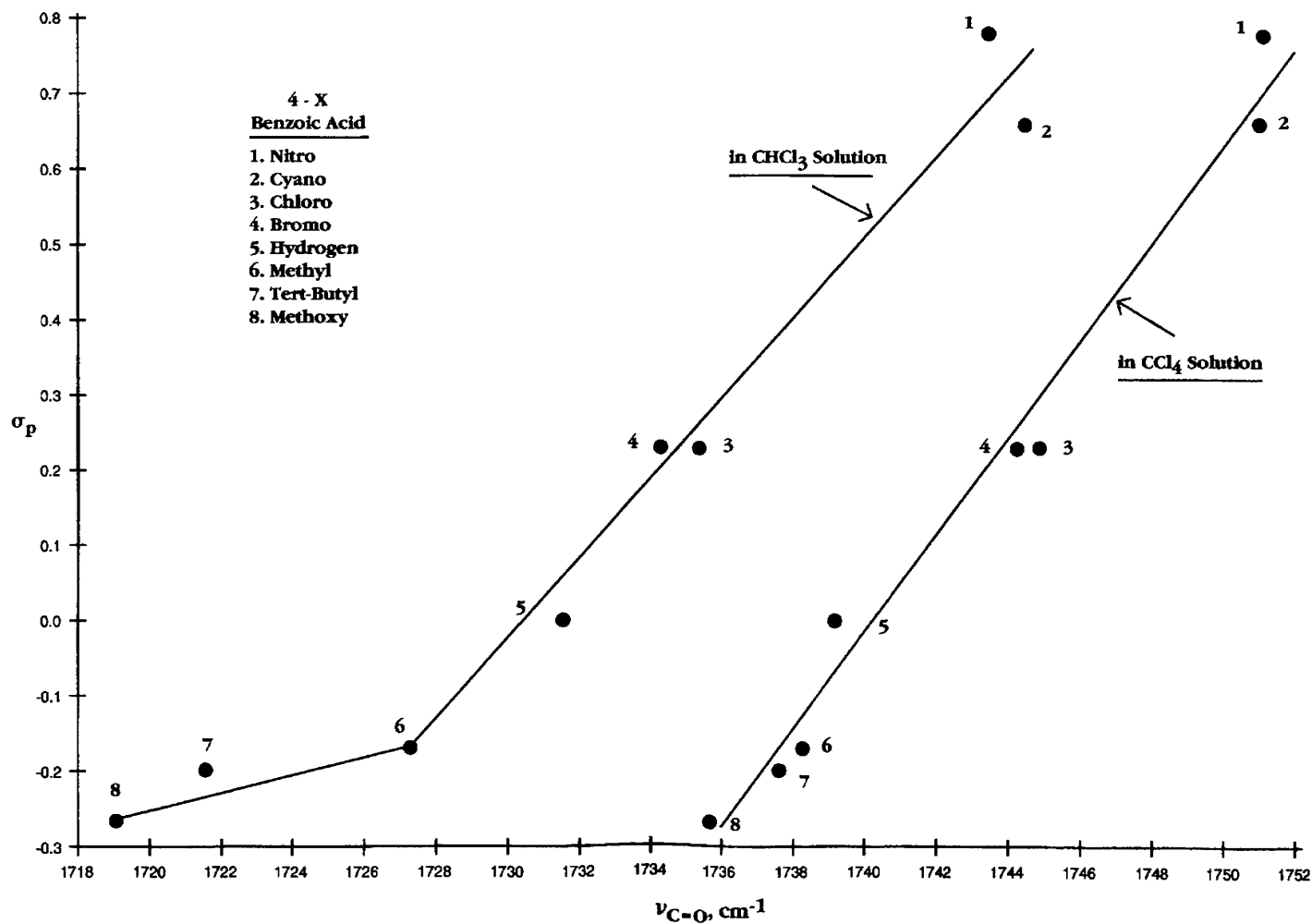


FIGURE 10.16 Plots of $\nu(\text{C=O})$ mode for 4-X-benzoic acids in CCl_4 solution and in CHCl_3 solution vs σ_p values for the 4-X atom or group.

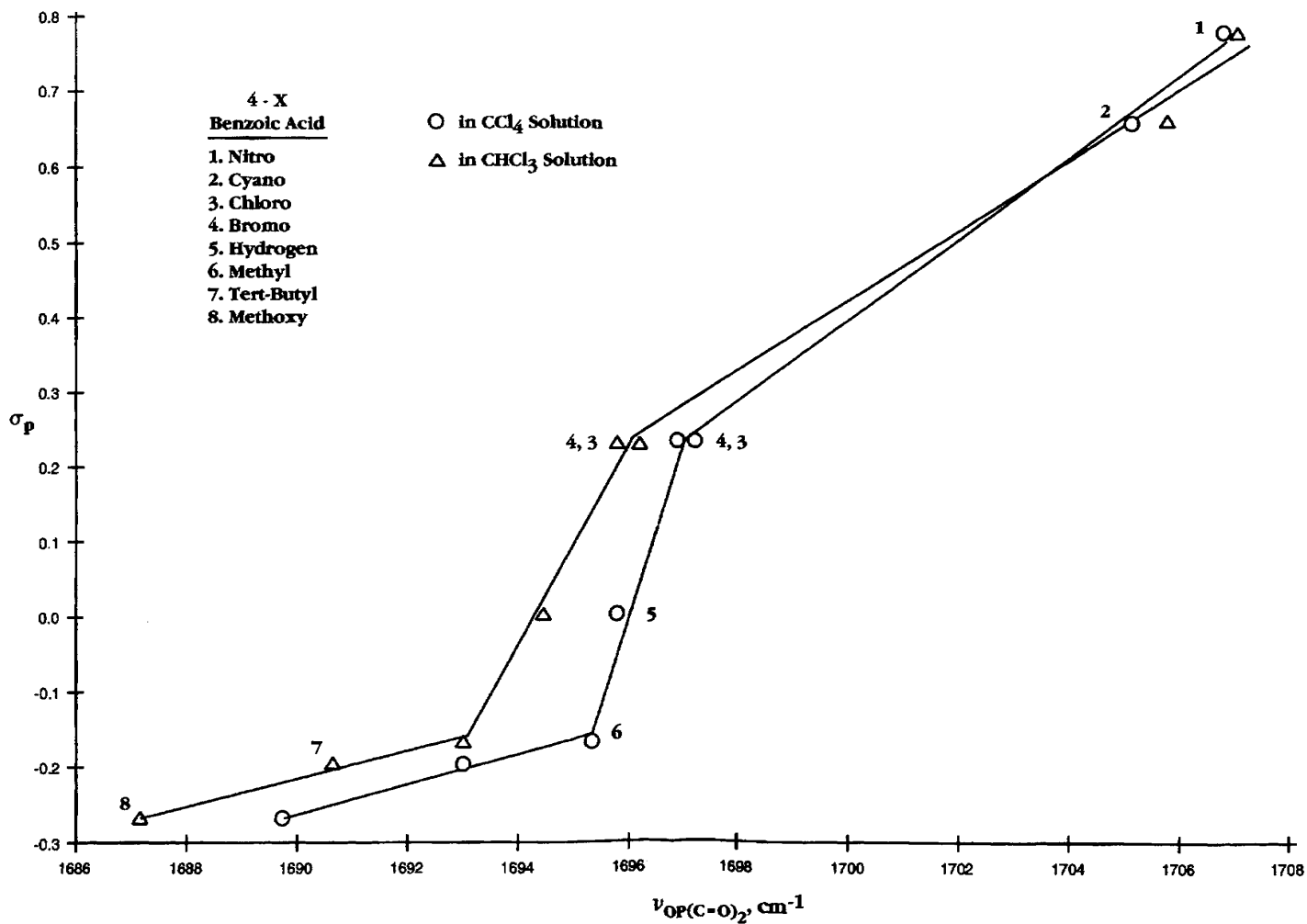


FIGURE 10.17 Plots of $\nu_{\text{op}(\text{C}=\text{O})_2}$ frequencies for 4-X-benzoic acids in CCl₄ solution and CHCl₃ solution vs σ_p values for the 4-X atom or group.

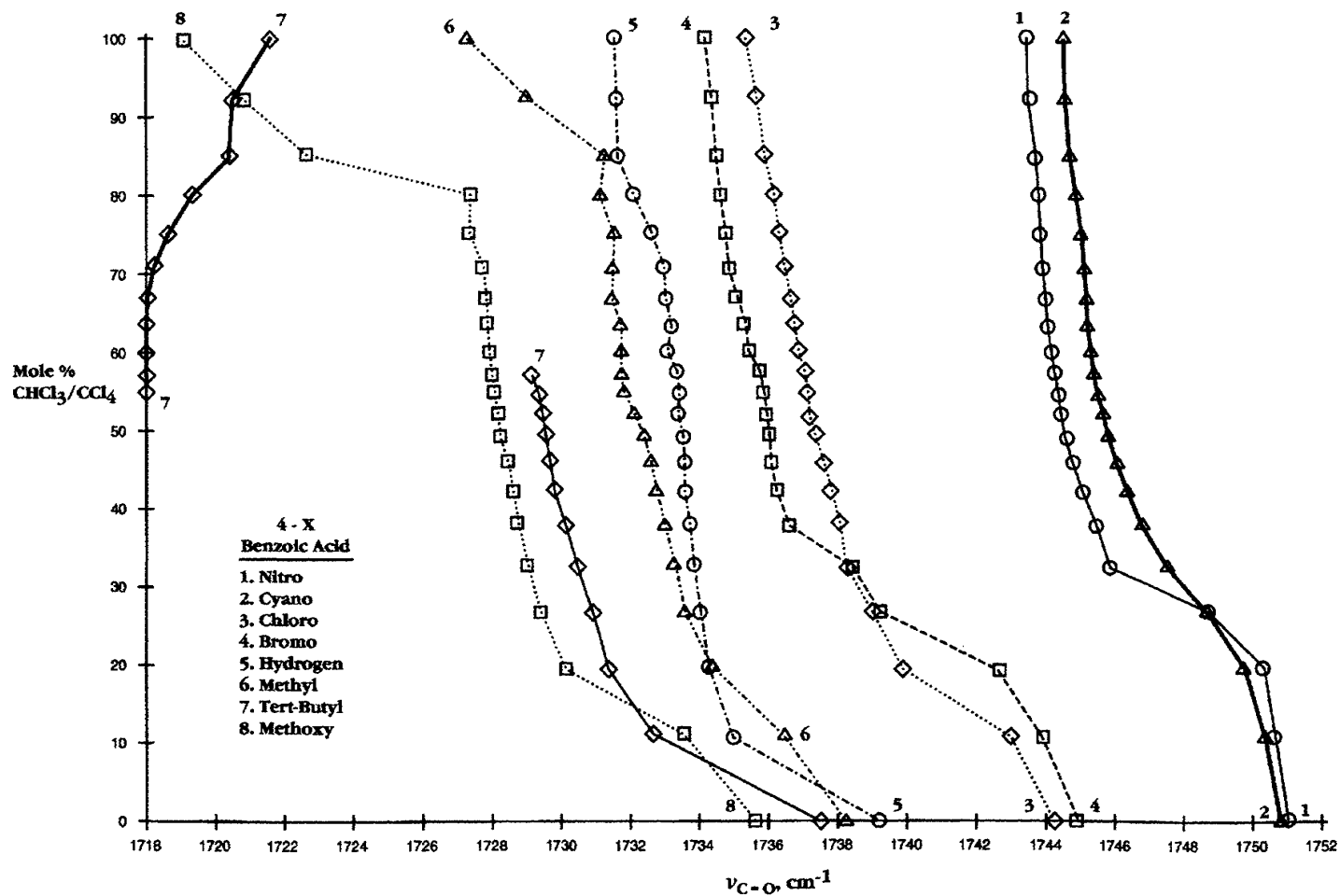


FIGURE 10.18 Plots of $\nu_{C=O}$ frequencies for 4-X-benzoic acids vs mole % $\text{CHCl}_3/\text{CCl}_4$.

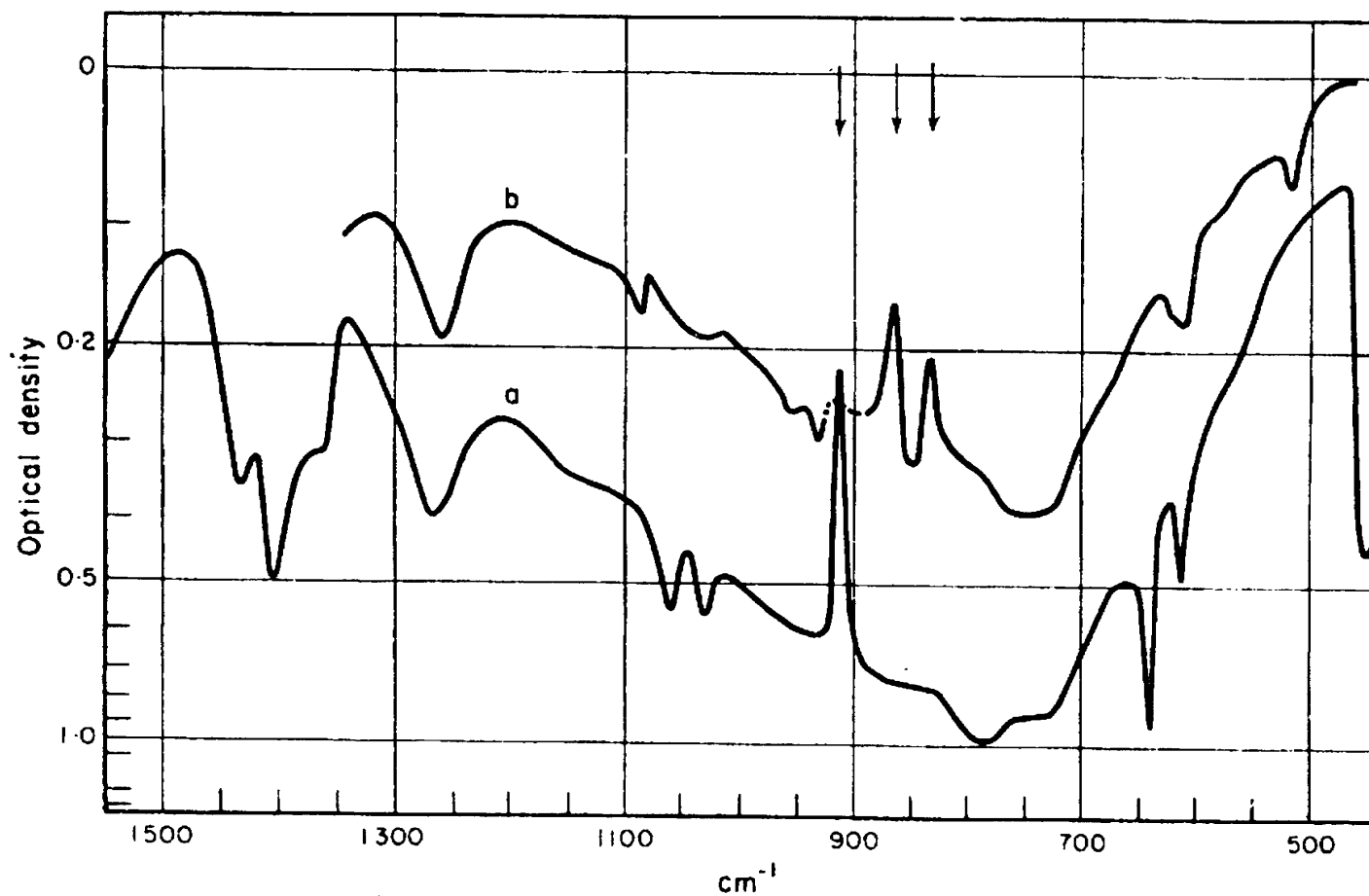


FIGURE 10.19 (a) Parts of the infrared spectrum of mulls containing sodium hydrogen diacetate; above 1330 cm^{-1} Fluorolube was used and below 1330 cm^{-1} , Nujol. (b) A Nujol mull spectrum of $\text{NaH}(\text{CD}_3\text{COO})_2$.

TABLE 10.1 IR vapor-phase data, CCl₄ and CHCl₃ solution-phase data, and assignments for aliphatic carboxylic acids

Acid	O-H str. vapor	O-H str. CCl ₄ soln.	O-H str. CHCl ₃ soln.	[vapor]- [CCl ₄ soln.]	[vapor]- [CHCl ₃ soln.]	[CCl ₄ soln.] - [CHCl ₃ soln.]
Acetic	3580(0.310)	3335.0(0.007)	3518.4(0.016)	45	61.6	16.6
Propionic	3579(0.460)	3535.7(0.015)	3520.7(0.032)	43.3	58.3	15
Butyric	3579(0.291)	3533.9(0.015)	3518.9(0.024)	45.1	60.1	10
Isobutyric	3579(0.411)	3534.1(0.012)	3518.6(0.026)	44.9	60.4	15.5
Trimethyl-acetic	3579(0.291)	3534.3(0.011)	3521.0(0.028)	44.7	58	13.3
	C=O str. vapor	C=O str. Cl ₄ soln.	C=O str. CHCl ₃ soln.			
Acetic	1789(1.230)	1767.3(0.056)	1756.3(0.110)	21.7	32.7	11
Propionic	1780(1.150)	1758.4(0.052)	1745.8(0.180)	21.6	34.2	12.6
Butyric	1780(1.250)	1758.7(0.037)	1745.9(0.116)	21.3	34.1	12.8
Isobutyric	1778(1.242)	1755.2(0.043)	1743.6(0.153)	22.8	34.4	11.6
Trimethyl-acetic	1769(1.142)	1750.3(0.047)	1740.1(0.174)	18.7	28.9	10.2
	o.p.(C=O) ₂ str. vapor	o.p.(C=O) ₂ str. CCl ₄ soln.	o.p.(C=O) ₂ str. CHCl ₃ soln.			
Acetic		1714.6(1.343)	1712.5(0.735)			2.1
Propionic		1716.1(0.927)	1714.4(0.552)			1.7
Butyric		1711.8(0.839)	1709.5(0.393)			2.3
Isobutyric		1707.0(0.598)	1704.5(0.484)			2.5
Trimethyl-acetic		1702.2(0.696)	1699.6(0.556)			2.6
	C-C-O str. vapor	gamma C=O vapor		[vp-vp]		
Acetic	1178(9.744)	580(0.268)		598		
Propionic	1145(0.858)	588(0.250)		557		
Butyric	1150(0.667)	590(0.189)		560		
Isobutyric	1105(0.755)	585(0.353)		520		
Trimethyl-acetic	1115(1.245)	571(0.311)		544		

TABLE 10.2 Raman data and assignments for out-of-phase and in-phase (C=O)₂ stretching modes and C=C stretching modes for carboxylic acids

ACID	o.p.(C=O) ₂ str.	i.p.(C=O) ₂ str.	C=C str.	Acid	o.p.(C=O) ₂ str.	i.p.(C=O) ₂ str.
Acrylic	1727(2)	1661(2)	1638(9)	Acetic*	1718(sh)	1668(7)
Methacrylic		1660(3)	1640(4)	Dichloroacetic*		1680(9)
2-Chloroacrylic		1656(2)	1614(1)	Iodoacetic*		1664(6)
Trichloroacrylic		1650(1)	1557(9)	4-Methoxy Benzoic*		1688(m)
Itaconic	1712(1)	1655(7)	1690(9)			
cis-Aconitic	1730(2)	1671(8)				
trans-Aconitic		1668(9)				
Tiglic		1653(9)	1625(1)			
2,6-Naphthalene-dicarboxylic		1639(5)				
Benzoic		1635(1)				
Terephthalic		1632(4)				
Isophthalic		1638(3)				
1,3,5-Tricarboxy benzene		1654(4)				
Succinic		1657(2)				
Thioglycolic		1687(20)				
Thiopropionic		1646(2)				
3-(4-Hydroxy-3-methoxyphenyl)		1630(5)				
2-Propionic						
Polyacrylic		1678(3)				
Polymethacrylic		1694(1)				

* Reference 6.

TABLE 10.3 IR group frequency data for acetic acid and its derivatives in the vapor and solution phases

Acetic acid	sigma*	pK _a 25°C	C=O str. vapor	C=O str. CCl ₄ soln.	C=O str. CHCl ₃ soln.	C=O str. CCl ₄ soln. (9)	o.p.(C= number of O) ₂ str. CCl ₄ soln.	o.p.(C=O) ₂ str. CHCl ₃ soln.	o.p.(C=O) ₂ str. CCl ₄ soln. (9)	[vapor]- [CCl ₄ soln.]	[vapor]- [CHCl ₃ soln.]	[CCl ₄ soln.] [CHCl ₃ soln.]	
Trimethyl	[-0.300]	[5.03]	1769(1.142)	1750.30(0.047)	1740.1(0.174)		1702.2(0.696)	1699.6(0.556)		18.7	28.9	10.2	
Dimethyl	[-0.190]	[4.85]	1788(1.242)	1755.2(0.043)	1743.6(0.153)		1707.0(0.595)	1704.5(0.484)		22.8	34.4	11.6	
Methyl	[-0.100]	[4.88]	1780(1.150)	1758.4(0.053)	1745.8(0.180)		1716.1(0.927)	1714.4(0.552)		21.6	34.2	12.6	
Hydrogen	[0.00]	[4.76]	1789(1.230)	1767.3(0.056)	1756.3(0.110)	1771			1714	21.7	32.7	11	
Iodo	[0.85]	[3.19]	1781(1.240)	1769.1(0.020)	1769.6(0.045)	1739.2(0.029)* ²	1772	1713.8(0.491)	1712.7(0.377)	1713	11.9	11.4	
Bromo	[1.00]	[2.87]		1777.1(0.020)	1775.5(0.061)		1772	1724.5(0.457)	1724.3(0.419)	1726	1.6		
Chloro	[1.05]	[2.85]	1815(0.585)	1792.8(0.030)	1787.7(0.071)	1759.7(0.100)* ³	1791	1736.3(0.629)	1734.2(0.576)	1737	22.2	27.3	5.1
Chloro			1797(1.240)							4.2	9.3		
Fluoro	[1.10]	[2.72]		1798.9(0.034)	1787.3(0.488)	1771.8(0.023)* ⁴	1797	1750.8(0.123)	1745.3(1.168)	1743			11.6
Dibromo	[1.82]	[1.48]	1804(0.540)										
Dibromo			1784(1.240)										
Dichloro	[1.94]	[1.30]		1784.3(0.027)	1775.1(0.098)		1784	1743.1(0.482)	1743.7(0.408)	1744			9.2
Difluoro	[2.05]	[1.13]		1797.7(0.073)	1789.2(0.197)		1794	1762.0(0.524)	1761.6(0.670)	1764			8.5
Tribromo	[2.52]	[0.72]		1770.5(0.039)	1765.9(0.094)		1772	1734.5(0.309)	1734.6(0.174)	1735			4.6
Trichloro	[2.65]	[0.70]		1786.1(0.066)	1780.3(0.149)		1789	1750.2(0.537)	1750.7(0.354)	1752			5.8
Trifluoro	[2.78]	[0.05]		1810.1(0.116)	1803.1(0.168)		1813	1778.3(0.462)	1784.3(0.288)	1780			7
			O-H str. CCl ₄ soln.	O-H str. CHCl ₃ soln.	{CCl ₄ soln.}- [CHCl ₃ soln.]	CCO str. vapor	gamma C=O vapor					{CCl ₄ soln.}- [CHCl ₃ soln.]	
Trimethyl			3534.3(0.011)	3521.0(0.028)	13.3	1115(1.245)	571(0.311)						
Dimethyl			3534.1(0.012)	3518.6(0.026)	15.5	1105(0.755)	585(0.353)						
Methyl			3535.5(0.015)	3520.7(0.032)	14.8	1145(0.858)	588(0.250)						
Hydrogen			3535.0(0.007)	3518.4(0.016)	17	1178(0.744)	580(0.268)						
Iodo			3527.0(0.006)	3507.9(0.014)	19.1	1189(0.487)	598(0.598)						
Bromo			3524.4(0.008)	3504.2(0.017)	20.2								
Chloro			3524.7(0.008)	3503.7(0.022)	21	1120(0.810)	616(0.290)						
Fluoro			3529.1(0.014)	3510.6(0.086)	18.5								
Dibromo			3517.1(0.007)	3497.7(0.0150)	19.4	1155(0.580)	599(0.415)						
Dichloro			3508.0(0.019)	3492.4(0.023)	15.6								
Difluoro			3508.6(0.032)	3485.8(0.045)	22.8								
Tribromo			3506.1(0.008)	3481.4(0.020)	24.7								
Trichloro			3505.0(0.013)	3484.8(0.025)	20.2								
Trifluoro			3500.5(0.023)	3479.6(0.023)	20.9								

*² is for 19.4 mole % CHCl₃/CCl₄ and is assigned to the 11-A(I) · HCCl₃ rotational conformer.

*³ is for 75.6 mole % CHCl₃/CCl₄ and is assigned to the 1Cl-A(Cl) · HCCl₃ rotational conformer.

*⁴ is also for CCl₄ solution and is assigned to the 1F-A(F) rotational conformer.

TABLE 10.4 IR data and assignments for 4-X-benzoic acids in the vapor and solution phases

4-X-Benzoic Acid	O-H str. vapor	O-H str. CCl ₄ soln.	O-H str. CHCl ₃ soln.	[vapor]-[CCl ₄ soln.]	[vapor]-[CHCl ₃ soln.]	[CCl ₄ soln.]-[CHCl ₃ soln.]	sigma p
Nitro	3582	3529.2(0006)	3519.2(0.048)	52.8	62.8	10	0.78
Cyano	3584(0.4950)	3531.7(0.006)	3516.3(0.081)	52.3	67.7	15.4	0.66
Chloro	3585(0.290)	3536.7(0.016)	3523.9(0.044)	48.3	61.1	12.8	0.23
Bromo		3535.6(0.011)	3524.2(0.033)			11.4	0.23
Hydrogen	3585(0.350)	3539.1(0.014)	3523.1(0.035)	45.9	61.9	16	0
Methyl	3590(0.450)	3541.5(0.007)	3525.6(0.018)	48.5	64.4	15.9	-0.17
tert-Butyl	3582(0.300)	3540.3(0.012)	3524.8(0.027)	57.2	57.2	15.5	-0.2
Methoxy	3595(0.292)	3543.3(0.002)	3527.7(0.021)	51.7	67.3	15.6	-0.27
	C=O str. vapor	C=O str. CCl ₄ soln.	C=O str. CHCl ₃ soln.				
Nitro	1768	1751.0(0.029)	1743.4(0.406)	17	24.6	7.6	
Cyano	1768(1.230)	1750.9(0.026)	1744.4(0.485)	17.1	23.6	6.5	
Chloro	1762(1.243)	1744.1(0.074)	1735.3(0.333)	17.9	26.7	8.8	
Bromo		1744.8(0.056)	1734.2(0.250)			10.6	
Hydrogen	1762(1.250)	1739.2(0.073)	1731.5(0.188)	22.8	30.5	8	
Methyl	1760(1.231)	1738.2(0.020)	1727.3(0.092)	21.8	32.7	10.9	
tert-Butyl	1758(1.250)	1737.6(0.050)	1729.1(0.117)* ¹	20.4	28.9	8.5	
			1718.0(0.120)*		40		
			1721.6(0.157)		36.4		
Methoxy	1760(1.243)	1735.6(0.023)	1719.1(0.120)	24.4	40.9	16.5	
[57.2 mol % CHCl ₃ /CCl ₄] ⁺¹	[60.1 mol % CHCl ₃ /CCl ₄] ⁺²						
	o.p.(C=O)2 str. vapor	o.p.(C=O) ₂ str. CCl ₄ soln.	o.p.(C=O) str. CHCl ₃ soln.				
Nitro		1706.7(0.015)	1707.0(0.355)			-0.3	
Cyano		1705.0(0.040)	1705.7(1.832)			-0.3	
Chloro		1697.2(0.429)	1696.2(0.768)			1	
Bromo		1696.9(0.204)	1695.8(0.366)			1.1	
Hydrogen		1695.8(1.536)	1694.5(1.206)			1.3	
Methyl		1695.3(0.705)	1693.0(0.462)			2.3	
tert-Butyl		1693.0(1.442)	1690.7(0.901)			-0.7	
Methoxy		1689.7(0.260)	1687.2(0.559)			2.5	
	Ring-C=O str. vapor	gamma C=O vapor					
Nitro	1180	565					
Cyano	1172(0.530)	532(0.230)					
Chloro	1177(0.355)	570(0.060)					
Hydrogen	1180(0.590)	571(0.060)					
Methyl	1170(0.680)	582(0.239)					
tert-Butyl	1178(0.450)	568(0.115)					
Methoxy	1166(0.742)	593(0.187)					

⁺¹ Two bands are present at 572 mol % CHCl₃/CCl₄ (14).

TABLE 10.4A Factors affecting the CO₂H and (CO₂)₂ groups for 4-X-benzoic acids in CHCl₃ and/or CCl₄ solutions

Factor Hammett σ_p	O-H str. cm ⁻¹	C=O str. cm ⁻¹	op(C=O) str. cm ⁻¹
NO ₂ (0.78) to CH ₃ O (-0.27)	increase	decrease	decrease
CCl ₄ solution	3529.2–3543.3	1751.0–1735.6	1706.7–1689.7
CHCl ₃ solution	3519.2–3527.7	1743.4–1719.1	1707.0–1687.2
CH ₃ O (-0.27) to NO ₂ (0.78)	decrease	increase	increase
CCl ₄ solution	3543.3–3529.3	1735.6–1751.0	1689.7–1706.7
CHCl ₃ solution	3527.7–3519.2	1719.1–1735.6	1687.2–1707.0
pKa values			
NO ₂ (3.42) to CH ₃ O (4.47)	increase	decrease	decrease
CCl ₄ solution			
CHCl ₃ solution			
CH ₃ O (4.47) to NO ₂ (3.42)	decrease	increase	increase
intermolecular hydrogen bond to 4-X group			
NO ₂ , CN, CH ₃ O	increase	increase	increase
OH : π system of phenyl group			
CH ₃ is 0	increase	increase	increase
(CH ₃) ₃ C is -1.54	decrease	decrease	decrease

TABLE 10.5 IR vapor-phase data and assignments for anthranilic acids

Compound	O—H str.	a.NH ₂ str.	s.NH ₂ str.	OH : N str.	C=O str.	NH ₂ bending	O—C= str.	A[a.NH ₂ str.]/ A[s.NH ₂ str.]	a.NH ₂ str.-s.NH ₂ str.	gamma C=O
Anthranilic acid	3584(0.256)	3520(0.082)	3395(0.141)	3436(0.020)	1729(1.237)	1613(0.580)	1180(0.380)	0.58	125	561(0.152)
3-Methyl	3584(0.465)	3520(0.165)	3382(0.240)	3430(0.031)	1724(1.230)	1620(0.570)	1168(0.560)	0.69	138	564(0.260)
3-Ethyl	3584(0.505)	3521(0.180)	3382(0.260)	3435(0.030)	1725(1.230)	1620(0.620)	1155(0.560)	0.69	139	548(0.200)
5-Methyl	3584(0.320)	3519(0.098)	3395(0.170)	3435(0.020)	1726(1.240)	1625(0.290)	1162(0.922)	0.58	124	570(0.210)
5-Methoxy	3584(0.250)	3518(0.070)	3395(0.120)	3435(0.020)	1730(1.230)	1604(0.341)	1165(0.720)	0.58	123	580(0.120)
3,4-Dimethyl	3594(0.330)	3525(0.080)	3384(0.155)		1724(1.230)	1613(0.750)	1177(0.335)	0.52	141	570(0.150)
5-Chloro-3-methyl	3584(0.340)	3520(0.100)	3385(0.169)	3430(0.030)	1725(1.220)	1621(0.343)	1161(0.631)	0.59	135	571(0.170)
3,5-Dichloro	3584(0.360)	3515(0.160)	3395(0.200)	3430(0.050)	1732(1.230)	1618(0.380)	1178(1.110)	0.79	120	574(0.130)
N-Methyl	3584(0.357)	3392(0.212)		N—H str. OH : N str.	1718(1.240)	1520(0.470)	1162(0.730)			559(0.210)
N-Phenyl	3584(0.235)	3348(0.150)		OH : N str.	1720(1.209)	1518(0.650)	1162(0.641)			568(0.122)

TABLE 10.6 Infrared data for methacrylic acid and acrylic acid in CHCl_3 and/or CCl_4 solutions

Mole % CHCl_3 / CCl_4	Methacrylic acid s. CH_3 bending cm^{-1}	Methacrylic acid $\text{CH}_2=$ wag cm^{-1}	Acrylic acid $\text{CH}_2=$ bending cm^{-1}	Acrylic acid vinyl twist cm^{-1}
0	1375.5	948.7	1433.1	983.9
10.74	1375.6	948.8	1433	983.8
19.4	1375.7	948.9	1432.8	983.8
26.53	1375.8	949	1432.6	983.7
32.5	1375.9	949	1432.4	983.65
37.57	1376.1	949	1432.3	983.6
41.93	1376.2	949.1	1432.15	983.6
45.73	1376.3	949.1	1432	983.6
49.06	1376.4	949.2	1431.9	983.6
52	1376.5	949.2	1431.8	983.6
54.62	1376.6	949.2	1431.7	983.7
57.22	1376.7	949.2	1431.6	983.7
60.07	1376.8	949.2	1431.5	983.7
63.28	1376.9	949.2	1431.4	983.7
66.73	1377	949.2	1431.2	983.7
70.65	1377.1	949.2	1431	983.7
75.06	1377.2	949.2	1430.9	983.8
80.06	1377.3	949.2	1430.8	983.8
85.05	1377.4	949.2	1430.6	983.9
92.33	1377.8	949.2	1430.3	983.9
100		949.2	1429.9	984
delta cm^{-1}	2.3	0.5	-3.2	0.1

TABLE 10.7 Raman data and assignments for carboxylic acid salts

Compound	a.CO ₂ str.	s.CO ₂ str.	a.CH ₂ str.	s.CH ₃ str.	s.CH ₂ str.	CH ₂ bend	i.p.CH ₂ twist	cis CH s. rock	C-C str.			
Strontium stearate		1468(3)	2923(3)	2884(9)	2852(5)	1447(4)	1296(3)		1062(1)			
Zinc stearate		1460(2)		2882(9)	2849(5)	1440(3)	1296(3)		1064(2)			
Stannous oleate		1435(5)		2897(9)	2853(9)		1302(3)	1267(2)				
K dichloroacetate*	1646(7)	1383(14)										
			a.CH ₂ = str.	CH= str.	CH= str.	s.CH ₂ = str.	C=C str.		CH ₂ = bend	CH= bend	s.C-CO ₂ str.	
Lithium acrylate							1649(6)			1280(9)	904(3)	
Sodium acrylate	1565(1)	1459(7)										
Zinc diacrylate	1603(1)?	1445(5)	3107(1)	3056(2)	3029(3)	2997(1)	1640(9)		138(1)	1280(5)	915(3)	
Lead acrylate		1445(4)					1639(9)			1278(8)	920(2)	
			s.C-CO ₂ str.	CCO ₂ bend								
Barium methacrylate		1423(9)	853(6)	606(3)			1648(6)					
Lead methacrylate		1426(7)	866(9)	604(0)								
Zirconium methacrylate		1422(4)	857(4)	58610			1645(9)					
Zinc dimethacrylate	1600(0)?	1445(5)					1640(9)					

* Unpublished data from the Dow chemical company.

TABLE 10.8 The asymmetric and symmetric CO₂ stretching frequencies for carboxylic acid salts

Carboxylate ion	asym.CO ₂ str. cm ⁻¹	sym.CO ₂ str. cm ⁻¹
Formate	1538–1604	1342–1400
Acetate	1543–1585	1404–1457
Dichloroacetate	1646	1383
Propionate	1550	1415
Butyrate	1563–1578	1420–1430
Valerate	1561–1565	near 1437
Stearate	1539–1558	1438–1468
Cyanoacetate	1605	near 1390
Malonate	1570	1420
Succinate	1569	1437
Tartrate	1571–1600	1386–1455
Citrate	1575–1620	1390–1430
Acrylate	1565–1603	1445–1459
Methacrylate	1603	1422–1445
Benzoate	1515–1559	1392–1431
Salicylate	1540–1598	1365–1409
Phthalate	1565	1384
Cinnamate	1549	1424

TABLE 10.9 IR data for carboxylic acid salts

Compound Formate	asym.CO ₂ str. cm ⁻¹	sym.CO ₂ str. cm ⁻¹	a.-s. delta cm ⁻¹
lithium	1604	1382	222
calcium	1596	1400	196
Acetate			
sodium	1585	1445	140
sodium iodo-	1586	1398	190
sodium fluoro-	1616	1449	167
sodium difluoro-	1640	1449	191
sodium mercapto-	1585	1400	185
sodium N,N-diethylamino-	1590	1400	190
Propionate			
cadmium	1550	1415	135
sodium 2-hydroxy	1590	1410	180
sodium 2,3-dichloro-2methyl-	1609	1395	214
Hexanoate			
sodium 2-ethyl	1555	1415	140
calcium 2-ethyl	1545	1424	121
Laurate			
sodium	1555	1421	134
Benzoate			
sodium	1545	1410	135
sodium 3-amino-	1559	1410	149
sodium 4-amino-	1545	1405	140
sodium 2-hydroxy	1582	1378	204
sodium 4-hydroxy-	1544	1415	129

Anhydrides

Phthalic Anhydride	206
Maleic Anhydride	207
References	208

Figure		Tables	
Figure 11-1	209 (206)	Table 11-1	210 (205)
		Table 11-2	210 (206)
		Table 11-3	211 (207)
		Table 11-4	212 (207)

*Numbers in parentheses indicate in-text page reference.

Carboxylic acid anhydrides exhibit symmetrical and asymmetric $(\text{C}=\text{O})_2$ stretching vibration [$\nu_{\text{ip}}(\text{C}=\text{O})_2$ and $\nu_{\text{op}}(\text{C}=\text{O})_2$], respectively. Open chain saturated aliphatic anhydrides exhibit $\nu_{\text{ip}}(\text{C}=\text{O})_2$ in the range $1815\text{--}1825\text{ cm}^{-1}$ and $\nu_{\text{op}}(\text{C}=\text{O})_2$ in the range $1745\text{--}1755\text{ cm}^{-1}$. The $\nu_{\text{ip}}(\text{C}=\text{O})_2$ mode has stronger IR band intensity than $\nu_{\text{op}}(\text{C}=\text{O})_2$. Conjugation lowers both modes. The strong band in the range $1770\text{--}1780\text{ cm}^{-1}$ is assigned to $\nu_{\text{ip}}(\text{C}=\text{O})_2$, and the weaker IR band in the region $1715\text{--}1725\text{ cm}^{-1}$ is assigned to $\nu_{\text{op}}(\text{C}=\text{O})_2$. In the case of unconjugated 5-membered ring anhydrides the IR bands occurring in the range $1845\text{--}1870\text{ cm}^{-1}$ have relatively weak intensity and the IR bands in the range $1775\text{--}1800\text{ cm}^{-1}$ have strong intensity. These bands are assigned as $\nu_{\text{ip}}(\text{C}=\text{O})_2$ and $\nu_{\text{op}}(\text{C}=\text{O})_2$, respectively. Conjugated 5-membered anhydrides exhibit the weak IR band in the range $1850\text{--}1860\text{ cm}^{-1}$ and the strong IR band in the region $1760\text{--}1780\text{ cm}^{-1}$, which are assigned to $\nu_{\text{ip}}(\text{C}=\text{O})_2$ and $\nu_{\text{op}}(\text{C}=\text{O})_2$, respectively (1,2).

It was found helpful in the discussions of the $\nu(\text{C}=\text{O})_2$ modes of anhydrides to give letters and numbers to classify each type. For example, an open chain anhydride such as acetic is labeled (OC), succinic anhydride whose cyclic structure includes a 5-membered saturated ring (5SR), glutaric anhydride whose cyclic structure include a 6-membered saturated ring (6SR), maleic and phthalic anhydrides whose cyclic structures include a 5-membered unsaturated ring (5UR), naphthalic anhydride whose cyclic structure includes a 6-membered unsaturated ring (6UR), and 2,2-biphenyldicarboxylic anhydride whose cyclic structure includes a 7-membered unsaturated ring (7UR), (3).

Table 11.1 lists IR vapor phase and Raman data in the neat phase for anhydrides.

Ring strain and conjugation play a role in the $\nu(\text{C}=\text{O})_2$ modes for anhydrides. The frequency separation between $\nu_{\text{ip}}(\text{C}=\text{O})_2$ and $\nu_{\text{op}}(\text{C}=\text{O})_2$ together with their band intensity ratio also can be used to classify anhydrides.

The inductive effect also affects the $\nu(\text{C}=\text{O})_2$ modes for OC anhydrides. For example, $\nu_{\text{ip}}(\text{C}=\text{O})_2$ decreases in the order 1830, 1825, 1824, and 1822 cm^{-1} and $\nu_{\text{op}}(\text{C}=\text{O})_2$ decrease in the order 1775, 1769, 1761, and 1759 cm^{-1} for acetic, propionic, isobutyric and 2-ethylbutyric anhydrides, respectively. Moreover, when the inductive effect causes electrons to be withdrawn from the $(\text{C}=\text{O})_2$ bonds such as in the case of trifluoroacetic anhydride, $\nu_{\text{ip}}(\text{C}=\text{O})_2$ and $\nu_{\text{op}}(\text{C}=\text{O})_2$ occur at the relatively high frequencies of 1881 and 1817, respectively (3).

Table 11.2 lists Raman data and assignments for carboxylic acid anhydrides. In the Raman, the $\nu_{\text{ip}}(\text{C}=\text{O})_2$ mode is always more intense than $\nu_{\text{op}}(\text{C}=\text{O})_2$. The OCU compounds exhibit $\nu_{\text{ip}}(\text{C}=\text{O})_2$ and $\nu_{\text{op}}(\text{C}=\text{O})_2$ in the range 1771–1788 cm^{-1} and 1715–1725 cm^{-1} , respectively, and occur at lower frequency than the OC anhydrides due to the effects of conjugation of the $\text{C}=\text{O}$ and $\text{C}=\text{C}$ groups.

PHTHALIC ANHYDRIDE

Figure 11.1 shows the IR spectra of phthalic anhydride in the region 2000–1600 cm^{-1} . The spectrum on the left is that for a saturated solution of phthalic anhydride in CCl_4 solution, the center spectrum is that for a saturated solution of phthalic anhydride in a 23.1% vol. $\text{CHCl}_3/\text{CCl}_4$ solution, and the spectrum on the right is that for a saturated solution of phthalic anhydride in CHCl_3 solution. All spectra were recorded using 0.2-mm KBr cells. The spectrum is more intense in going from left to right due to the increased solubility in CHCl_3 . What is important in this case is to note that the 1789 cm^{-1} band is more intense than the 1776 cm^{-1} band in CCl_4 solution, in 23.1% vol. in $\text{CHCl}_3/\text{CCl}_4$ solution the two bands have equal intensity, and in CHCl_3 solution the 1775 cm^{-1} band has more intensity than the 1788 cm^{-1} band. Whereas phthalic anhydride is a planar molecule with C_{2v} symmetry, changes in the band intensity ratio can not be attributed to the presence of rotational conformers because solvent techniques are also used to determine which bands in each set of band results from which rotational conformer. In the case of phthalic anhydride, the doublet near 1789 cm^{-1} and 1776 cm^{-1} is the result of $\nu_{\text{op}}(\text{C}=\text{O})_2$ in Fermi resonance with a combination tone. It is common practice (but not correct) to assign as the fundamental the band in the doublet with the most intensity; in this case it is $\nu_{\text{op}}(\text{C}=\text{O})_2$. The dilemma in this situation is apparent in the middle spectrum where both bands have equal intensity and only one $\nu_{\text{op}}(\text{C}=\text{O})_2$ mode. The answer is that both bands are in Fermi resonance, and each band is a mixture of $\nu_{\text{op}}(\text{C}=\text{O})_2$ and the combination tone. After correction for Fermi resonance, $\nu_{\text{op}}(\text{C}=\text{O})_2$ shows a steady decrease in frequency in CCl_4 solution (1784.6 cm^{-1}) to (1779.4 cm^{-1}) in CHCl_3 solution. This is a decrease of 5.2 cm^{-1} for $\nu_{\text{op}}(\text{C}=\text{O})_2$ going from CCl_4 to CHCl_3 solution, and this is reasonable from study of the other carbonyl-containing compounds included in this book. It is important to note that $\nu_{\text{ip}}(\text{C}=\text{O})_2$ decreased only 3 cm^{-1} in going from CCl_4 solution (1856 cm^{-1}) to (1853 cm^{-1}) in CHCl_3 solution. The behavior of $\nu_{\text{op}}(\text{C}=\text{O})_2$ and $\nu_{\text{ip}}(\text{C}=\text{O})_2$ in solvents such as CCl_4 and CHCl_3 will be discussed in Volume 2 of the book. The general decrease in frequency of $\nu_{\text{op}}(\text{C}=\text{O})_2$ and $\nu_{\text{ip}}(\text{C}=\text{O})_2$ is attributed to the field effect of the solvent. Hydrogen bonding

between the Cl_3CH protons and the two carbonyl groups plays a role in lowering both $\nu(\text{C}=\text{O})_2$ frequencies compared to where they occur in CCl_4 solution.

The lowest $\nu_{\text{ip}}(\text{C}=\text{O})_2$, $\nu_{\text{op}}(\text{C}=\text{O})_2$ and CT frequencies for phthalic anhydride are observed for solutions in dimethyl sulfoxide. These are 1850 cm^{-1} , 1788 cm^{-1} , and 1772 cm^{-1} , respectively. After correction for FR, the unperturbed $\nu_{\text{op}}(\text{C}=\text{O})_2$ is determined to be 1780.5 and CT at 1788.9 cm^{-1} (4).

MALEIC ANHYDRIDE

Vibrational assignments have been made for maleic anhydride (5). The combination tone (560 cm^{-1} , B, $+1235\text{ cm}^{-1}$, A, $=1795\text{ cm}^{-1}$, B.) was ruled out as the possibility of being in Fermi resonance with $\nu_{\text{op}}(\text{C}=\text{O})_2$, because it was noted that there is a strong dependence of the band intensity ratio on the nature of the solvent while the frequencies remain practically constant (6). Phthalic anhydride reported on in the preceding showed the same phenomena, but $\nu_{\text{op}}(\text{C}=\text{O})_2$ was shown to be in Fermi resonance.

Table 11.3 lists IR data for maleic anhydride in $n\text{-C}_6\text{H}_{14}/\text{CHCl}_3$, $\text{CHCl}_3/\text{CCl}_4$, and $n\text{-C}_6\text{H}_{14}/\text{CCl}_4$ mole % solutions. Maleic anhydride is of the type 5UR (3). The $\nu(\text{C}=\text{O})_2$ frequencies for the 5% UR structure might be expected to be lower than those for 5SR structure due to conjugation of the $\text{C}=\text{C}$ group with the two $\text{C}=\text{O}$ groups. However, the ring strain is more in the case of maleic anhydride than in the case of succinic anhydride, as the $\text{C}=\text{C}$ bond distance is less than the $\text{C}-\text{C}$ bond distance. Therefore, the two opposing effects essentially cancel each other in the case of maleic anhydride.

Maleic anhydride is a planar structure with C_{2v} symmetry. The $\nu_{\text{ip}}(\text{C}=\text{O})_2$ mode belongs to the A_1 symmetry species while $\nu_{\text{op}}(\text{C}=\text{O})_2$ belongs to the B_1 symmetry species. Therefore, $\nu_{\text{op}}(\text{C}=\text{O})_2$ can only be in Fermi resonance with a combination tone belonging to the B_1 symmetry species. It can not be in Fermi resonance with an overtone because any overtone is assigned to the A_1 symmetry species. A study of Table 11.3 shows that two bands occur in the range 1770 and 1793 cm^{-1} in each of the solvent systems, and in all cases the higher frequency band has more intensity than the lower frequency band. As in the case of phthalic anhydride, the $\nu_{\text{op}}(\text{C}=\text{O})_2$ mode is in Fermi resonance with the B_1 combination tone. The experimental data has been corrected for Fermi resonance, and unperturbed $\nu_{\text{op}}(\text{C}=\text{O})$ is determined to be between 1789.8 and 1790 cm^{-1} in $n\text{-C}_6\text{H}_{14}$ solution, $1787.1\text{--}1787.5\text{ cm}^{-1}$ in CCl_4 solution, $1785\text{--}1785.4\text{ cm}^{-1}$ in CHCl_3 solution, and 1778.9 cm^{-1} in $60.19\text{ mol } \% (\text{CH}_3)_2\text{SO}/\text{CCl}_4$. These $\nu_{\text{op}}(\text{C}=\text{O})_2$ frequencies decrease in the order of increasing polarity of the solvent, and also decrease in frequency as the reaction field of the solvent is increased.

Table 11.4 lists the in-phase and out-of-phase $(\text{C}=\text{O})_2$ stretching vibrations for hexahydrophthalic, tetrachlorophthalic, tetrabromophthalic, dichloromaleic (7), phthalic (4), and maleic anhydrides in different physical phases (6). In all cases the $\nu_{\text{op}}(\text{C}=\text{O})_2$ modes have been corrected for Fermi resonance. These data show that both $\nu_{\text{ip}}(\text{C}=\text{O})_2$ and $\nu_{\text{op}}(\text{C}=\text{O})_2$ decrease progressively in the order: vapor, and C_6H_{14} , CCl_4 , CHCl_3 and $(\text{CH}_3)_2\text{SO}$ solution phases. In all cases the $\nu_{\text{op}}(\text{C}=\text{O})_2$ mode decreases more in frequency in each solvent pair than does the $\nu_{\text{ip}}(\text{C}=\text{O})_2$ mode.

In the case of styrene-maleic anhydride copolymer, the anhydride has a 5SR structure, and in CH_2Cl_2 solution $\nu_{\text{ip}}(\text{C}=\text{O})_2$ and $\nu_{\text{op}}(\text{C}=\text{O})$ occur at 1856.6 and 1779.7 cm^{-1} , respectively, and

in CHCl_3 solution at 1856.5 and 1778 cm^{-1} , respectively. In this case, $\nu_{\text{ip}}(\text{C}=\text{O})_2$ decreases 0.1 cm^{-1} , and $\nu_{\text{op}}(\text{C}=\text{O})$ decreases 1 cm^{-1} , a factor of 10 (7); this type of frequency difference was noted in the study of the other anhydride in different solvent systems.

REFERENCES

1. Dauben, W. S. and Epstein, W. W. (1959). *J. Org. Chem.*, **24**, 1595.
2. Bellamy, L. J., Connelly, B. J., Phillips, A. R., and Williams, A. L. (1960). *Z. Electrochem.*, **64**, 563.
3. Nyquist, R. A. (1984). *The Interpretation of Vapor-phase Infrared Spectra: Group Frequency Data*, Vol. 1, Philadelphia: Sadtler Research Laboratories, Division of Bio-Rad.
4. Nyquist, R. A. (1989). *Appl. Spectrosc.*, **43**, 1374.
5. Mirone, P. and Chiorboli, P. (1962). *Spectrochim. Acta*, **18**, 1425.
6. Nyquist, R. A. (1990). *Appl. Spectrosc.*, **44**, 438.
7. Nyquist, R. A. (1990). *Appl. Spectrosc.*, **44**, 783.
8. Schrader, B. (1989). *Raman/Infrared Atlas of Organic Compounds*, 2nd edition, Germany, VCH.

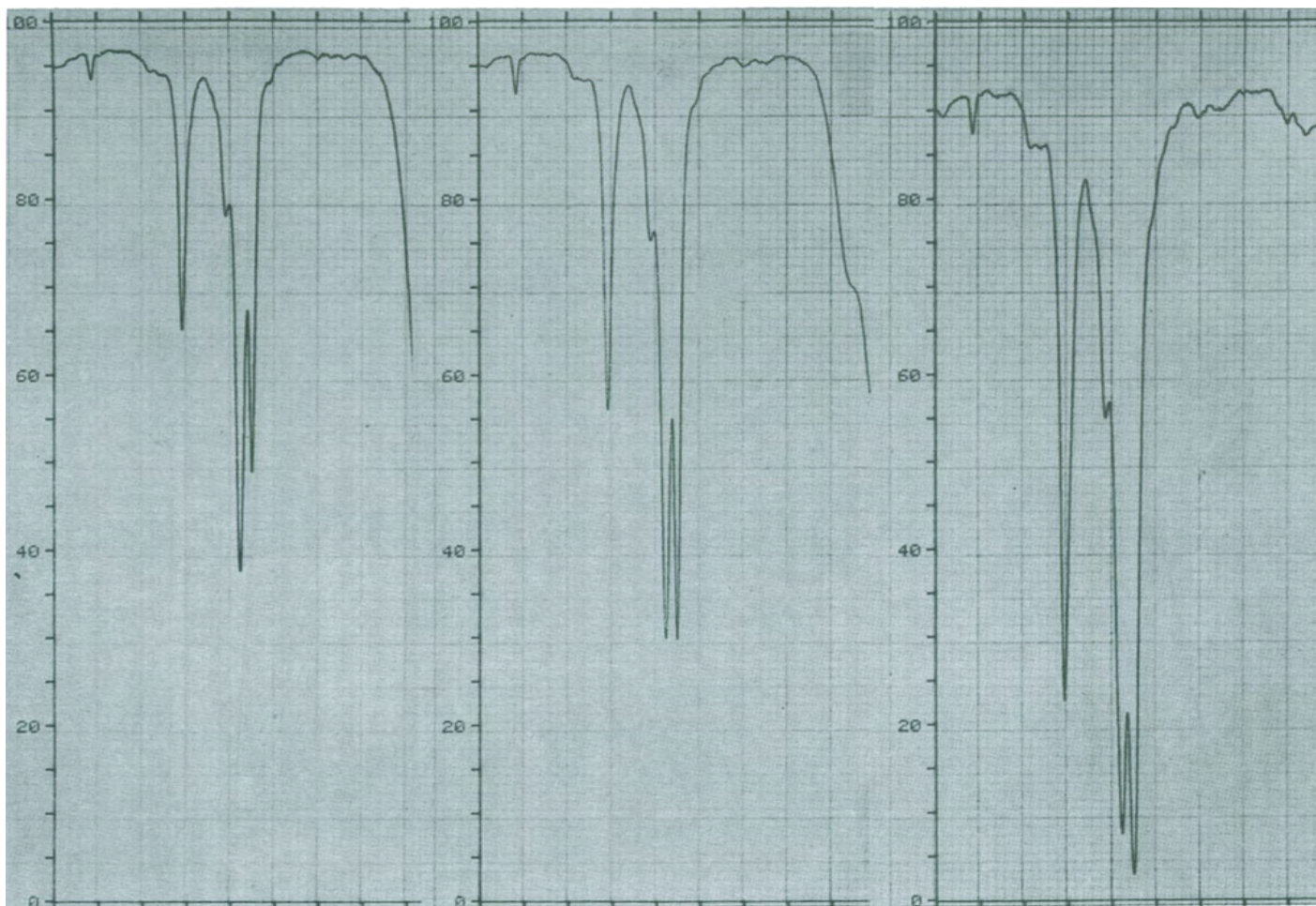


FIGURE 11.1 IR spectra of phthalic anhydride in the region $2000\text{--}1600\text{ cm}^{-1}$. The spectrum on the left is for a saturated solution CCl_4 , the center spectrum is for a saturated solution for in a 23.1% vol. $\text{CHCl}_3/\text{CCl}_4$, and the spectrum on the right is for a saturated solution in CHCl_3 .

TABLE 11.1 IR vapor-phase data and Raman data in the neat phase for anhydrides

Anhydride type	sym.(C=O) ₂ str. cm ⁻¹	asym.(C=O) ₂ str. cm ⁻¹	(A)sym.(C=O) ₂ str. (A)asym.(C=O) ₂ str.	Frequency separation cm ⁻¹
OC	1822-1830	1759-1775	0.96-1.31	55-63
OCU	[1771-1788]	[1715-1725]		[39-58]
5SR	1861-1880	1802-1812	0.11-0.23	59-72
6SR	1820-1830	1782-1790	0.35-0.51	36-40
5UR	1855-1880	1785-1813	0.07-0.35	51-85
6UR	1802	1768	0.72	34
7UR	1800	1772	0.66	28

[Raman data]

TABLE 11.2 Raman data and assignments for carboxylic anhydrides

Anhydride	ip(C=O) ₂ cm ⁻¹	op(C=O) ₂ cm ⁻¹	Type	Frequency separation cm ⁻¹	C=C str. cm ⁻¹	Ring breathing cm ⁻¹
Allylsuccinic	1853(3)	1782(0)	5SR	71	1644(8)	
Acrylic	1788(3)	1730(2)	OCU	58	1630(9)	
Methacrylic	1782(3)	1725(2)	OCU	57	1639(9)	
Crotonic*	1771(27,p)	1732(vwk)	OCU	39	1648(80,p)	
Benzoic*	1771(32)	1715(13)	OCU	56		
Citraconic	1841(6)	1770(1)	5UR	71	1652(3)	
Propionic*	1812(7,p)	1743(3,p)	OC	69		
Butyric*	1813(7,p)	1751(3,p)	OC	62		
Trifluoroacetic*	1877(28,p)	1810(9,p)	OC	67		
4-Cyclohexene- 1,2-dicarboxylic*	1834(2)	1729(1)	5SR	105	1629(3)	
Glutaric*	1780(18)	1755(vwk)	6SR	25		
Phthalic	1840(45)	1760(37)	5UR	80		1005(44)

* Reference 8.

TABLE 11.3 IR data for maleic anhydride in $n\text{-C}_6\text{H}_{14}/\text{CHCl}_3$, $\text{CHCl}_3/\text{CCl}_4$, and $n\text{-C}_6\text{H}_{14}/\text{CCl}_4$ solutions

Maleic anhydride mole % $n\text{-C}_6\text{H}_{14}/\text{CHCl}_3$	o.p.(C=O) ₂ str. in FR cm ⁻¹	Bl comb. tone in FR cm ⁻¹	a[o.p.(C=O) ₂ str. in FR]	A[Bl comb. tone in FR]	o.p.(C=O) ₂ str. corrected for FR cm ⁻¹	Bl comb. tone corrected for FR cm ⁻¹	i.p.(C=O) ₂ str. cm ⁻¹	A[i.p.(C=O) ₂ str.]
0	1781.4	1792.5	0.603	0.286	1785	1788.9	1851.7	0.069
23.57	1782.5	1793.2	0.493	0.324	1786.7	1789	1852.6	0.054
50.68	1782.7	1793.5	0.413	0.353	1787.7	1788.5	1853.3	0.044
75.51	1782.6	1783.8	0.381	0.332	1788.4	1787.9	1852.7	0.038
100	1793.7	1781.2	0.411	0.168	1789.8	1785.1	1852.6	0.025
delta cm ⁻¹	12.3	-11.3			4.8	-3.8	0.9	
mole % $\text{CHCl}_3/\text{CCl}_4$								
0	1792.5	1781.4	0.521	0.489	1787.1	1786.8	1851.7	0.079
26.7	1781.7	1792.8	0.539	0.41	1786.5	1788	1852	0.08
52.2	1781.8	1792.9	0.553	0.354	1786.2	1788.6	1851.9	0.077
75.2	1781.9	1792.6	0.564	0.325	1785.8	1788.7	1851.9	0.079
100	1781.9	1792.6	0.573	0.274	1785.4	1789.1	1851.7	0.077
delta cm ⁻¹	-10.6	11.2			-1.7	2.3	0	
Mole % $n\text{-C}_6\text{H}_{14}/\text{CCl}_4$								
0	1792.6	1781.8	0.546	0.497	1787.5	1787	1851.6	0.081
26.99	1793.1	1781.5	0.505	0.363	1788.3	1786.4	1852.4	0.055
51.37	1793.4	1781.5	0.479	0.302	1788.8	1786.1	1852.7	0.042
71.14	1793.7	1781.5	0.462	0.266	1789.2	1785.9	1852.9	0.037
100	1794	1781.2	0.3394	0.176	1790	1785.1	1852.6	0.027
delta cm ⁻¹	1.4	-0.6			2.5	-1.9	1	
Mole % $(\text{CH}_3)_2\text{SO}/\text{CCl}_4$								
0	1792.5	1781.4	0.569	0.52	1787.2	1786.7	1851.7	0.084
28.99	1778.3	~1791.4	0.568	0.15	1781.1	1788.7	1847	0.099
48.78	1777.3	~1791.4	0.571	0.11	1779.6	1785.2	1847.6	0.102
60.19	1776.7	~1791.4	0.588	0.105	1778.9	1789.2	1847.3	0.105
100	1772.3		0.587		1772.3* ¹		1845.8	0.093
delta cm ⁻¹	-20.2	10			[-14.9* ¹]		-5.9	
Mole % $(\text{CH}_3)_2\text{SO}/\text{CHCl}_3$								
0	17811.4	1792.5	0.603	0.286	1785	1788.9	1851.6	0.07
25.4	1780.5	~1791.4	0.545	0.183	1783.3	1788.7	1849.9	0.085
50.53	1779.1	~1791.4	0.5	0.121	1782.2	1789.2	1848.3	0.088
73.94	1776.6	~1791.4	0.466	0.07	1778.2	1789.5	1847.5	0.079
100	1772.3		0.449		1772.3* ¹		1845.8	0.076
delta cm ⁻¹	-9.1	-1.1			[-12.7* ¹]		-5.8	

*¹ not corrected for Fermi resonance.

TABLE 11.4 The in-phase and out-of-phase (C=O)₂ stretching vibrations for carboxylic anhydrides in the vapor phase and in various solution phases

Anhydride	i.p.(C=O) ₂ str. [vapor]	i.p.(C=O) ₂ str. [n-C ₆ H ₁₄]	i.p.(C=O) ₂ str. [CCl ₄]	i.p.(C=O) ₂ str. [CHCl ₃]	i.p.(C=O) ₂ str. [(CH ₃) ₂ SO]	
Hexahydrophthalic		1864.5	1861.4	1859.1	1852.3	
Phthalic	1865	1858	1856	1853	1850	
Tetrachlorophthalic	1859		1845.9*	1845.5*		
Tetrabromophthalic			1867.2*	1863.4*		
Maleic		1852.6	1851.74	1851.68	1845.8	
Dichloromaleic		1877.9*	1876.7*	1876.2*		
	o.p.(C=O) ₂ str. [vapor]	o.p.(C=O) ₂ str. [n-C ₆ H ₁₄]	o.p.(C=O) ₂ str. [CCl ₄]	o.p.(C=O) ₂ str. [CHCl ₃]	o.p.(C=O) ₂ str. [(CH ₃) ₂ SO]	
Hexahydrophthalic		1798.9	1792.7	1787.5	1781.4	
Phthalic	1802	1789.7*	1784.6*	1779.4*	1771.1*	
Tetrachlorophthalic	1809		1790.7*	1786.8*		
Tetrabromophthalic			1795.6*	1790.3*		
Maleic		1790.0*	1787.1*	1785.4*	1772.3	
Dichloromaleic		1801.7*	1799.0*	1796.4*		
	i.p.(C=O) ₂ str. [CCl ₄]-[CHCl ₃]	o.p.(C=O) ₂ str. [CCl ₄]-[CHCl ₃]	i.p.(C=O) ₂ str. [C ₆ H ₁₄]-[CCl ₄]	o.p.(C=O) ₂ str. [C ₆ H ₁₄]-[CCl ₄]	i.p.(C=O) ₂ str. [CCl ₄]-[(CH ₃) ₂ SO]	o.p.(C=O) ₂ str. [CCl ₄]-[(CH ₃) ₂ SO]
Hexahydrophthalic	2.3	5.2	3.1	6.2	9.2	11.3
Phthalic	3	5.2	2	5.1	6	13.5
Tetrachlorophthalic	0.4	3.9				
Tetrabromophthalic	3.8	5.3				
Maleic	0.1	1.7	0.9	2.9	5.9	14.8
Dichloromaleic	0.5	2.6	1.2	2.7		

* corrected for Fermi resonance

Carboxamides, Ureas, Thioureas, Imidazolidinones, Caffeine, Isocaffeine, Uracils, Imides, Hydantoins, and s-Triazine(1H,3H,5H)-Triones

Dilution Studies of N-alkylacetamide and N-alkylchloroacetamide	216
Trans and/or Cis Secondary Amides	217
N-H Intensity	219
Acetanilides	222
N-alkyl Benzamides	223
N-alkyl Methyl Carbanates	223
N,N'-Dialkyl Oxamides and N,N'-Diaryl Oxamide	223
Dimethylacetamide and Tetraalkylurea	224
1,1,3,3-Tetramethylurea vs 1,3-Dimethyl-2-imidazolidinone	225
Caffeine, Isocaffeine, 1,3,5-Trimethyluracil, 1,3,6-Trimethyluracil, and 1,3-dimethyl-2,4-(1H,3H) quinazolinedione	226
Imides	227
4-Bromobutylphthalimide in Solution	229
Hydantoins	229
Triallyl-1,3,5-triazine-2,4,6-(1H,3H5H) trione	229
References	230

Figures

Figure 12-1	232 (216)	Figure 12-7	238 (226)
Figure 12-2	233 (217)	Figure 12-8	239 (230)
Figure 12-3	234 (222)	Figure 12-9	239 (230)
Figure 12-4	235 (224)	Figure 12-10	239 (230)
Figure 12-5	236 (226)	Figure 12-11	240 (228)
Figure 12-6	237 (226)		

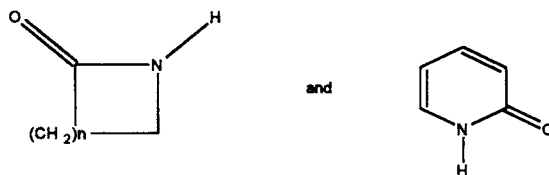
Tables

Table 12-1	241 (215, 217)	Table 12-1c	243 (217)
Table 12-1a	242 (216)	Table 12-2	244 (217, 219)
Table 12-1b	242 (216)	Table 12-2a	246 (219)

Table 12-3	248 (220)	Table 12-11	257 (225)
Table 12-4	249 (220)	Table 12-12	258 (225)
Table 12-4a	249 (220)	Table 12-13	259 (226)
Table 12-5	250 (221)	Table 12-14	260 (226)
Table 12-5a	251 (221)	Table 12-15	261 (227)
Table 12-6	252 (221)	Table 12-16	262 (227)
Table 12-7	253 (222)	Table 12-17	264 (229)
Table 12-8	254 (223)	Table 12-18	265 (229)
Table 12-9	255 (223)	Table 12-19	266 (229)
Table 12-10	256 (224)	Table 12-20	266 (230)

*Numbers in parentheses indicate in-text page reference.

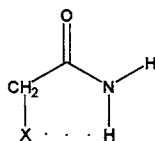
There are several forms of carboxamides, and they are separated into three classes: primary, secondary, and tertiary. Primary carboxamides also exist in three forms: $\text{H}(\text{C}=\text{O})\text{NH}_2$, $\text{R}(\text{C}=\text{O})\text{NH}_2$, and $\phi(\text{C}=\text{O})\text{NH}_2$. Secondary carboxamides exist in the following forms: $\text{H}(\text{C}=\text{O})\text{NHR}$, $\text{R}(\text{C}=\text{O})\text{NHR}'$, $\text{R}(\text{C}=\text{O})\text{NH}\phi$, $\phi(\text{C}=\text{O})\text{NHR}$, $\phi(\text{C}=\text{O})\text{NH}\phi$,



Tertiary carboxamides can have the basic structures as denoted for the secondary carboxamides with the replacement of the NH proton with R or ϕ . Each of these forms yields its own characteristic group frequencies, and each will be discussed in what follows.

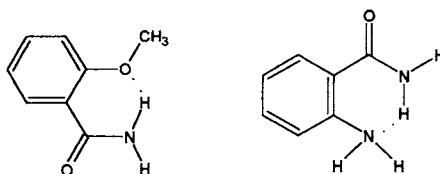
Table 12.1 shows a comparison of primary, secondary, and tertiary amides in various physical phases.

In the case of the primary amides the $\nu_{\text{asym. NH}_2}$, $\nu_{\text{sym. NH}_2}$, and $\nu_{\text{C}=\text{O}}$ modes occur at higher frequency in the vapor phase than in the neat phase. It is noteworthy that $\nu_{\text{C}=\text{O}}$ for $\phi(\text{C}=\text{O})\text{NH}_2$ ($1719\text{--}1731\text{ cm}^{-1}$) occurs at lower frequency than $\nu_{\text{C}=\text{O}}$ for $\text{R}(\text{C}=\text{O})\text{NH}_2$ ($1732\text{--}1780\text{ cm}^{-1}$) due to conjugation of the carbonyl group with the π system of the phenyl group (1). In the case of $\text{R}(\text{C}=\text{O})\text{NH}_2$, the high frequency $\nu_{\text{C}=\text{O}}$ mode at 1780 cm^{-1} is the result of the inductive effect of the CF_3 group for $\text{CF}_3(\text{C}=\text{O})\text{NH}_2$, and the low frequency is the result of the inductive effect of the alkyl group ($\text{C}_{13}\text{H}_{26}$) for $\text{R}(\text{C}=\text{O})\text{NH}_2$ (1). Evidence is also presented that in the vapor phase the $\alpha\text{-X}$ analogs are in an intramolecularly hydrogen-bonded trans configuration (1).



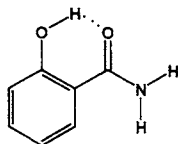
For example, in the vapor phase $\nu\text{C}=\text{O}$ occurs at 1740, 1749, and 1780 cm^{-1} for acetamide, fluoroacetamide, and trifluoroacetamide, respectively, while $\nu_{\text{asym. NH}_2}$ occurs at 3565, 3552, and 3560 cm^{-1} , and $\nu_{\text{sym. NH}_2}$ occurs at 3442, 3444, and 3439 cm^{-1} , respectively (1). Substitution of the first F atom on the α -carbon atom raises $\nu\text{C}=\text{O}$ by 9 cm^{-1} while substitution of three F atoms raises $\nu\text{C}=\text{O}$ by 40 cm^{-1} . Therefore, $\nu\text{C}=\text{O}$ is raised 31 cm^{-1} for the substitution of the second and third F atoms, or 15.5 cm^{-1} per F atom. These data indicate that the addition of the first α -fluorine atom on the α -carbon atom of acetamide forms an intramolecular hydrogen atom as depicted here, and lowers $\nu\text{C}=\text{O}$ by $\sim 6.5\text{ cm}^{-1}$. This intramolecular N-H \cdots F bond is present in the F, F₂ and F₃ analogs, or otherwise each $\nu\text{C}=\text{O}$ mode would be $\sim 6.5\text{ cm}^{-1}$ higher in frequency (1).

Compounds such as 2-aminobenzamide and 2-methoxybenzamide in the vapor phase exhibit $\nu\text{C}=\text{O}$ at 1698 and 1709 cm^{-1} , respectively, while benzamide and 3-X and 4-X benzamides exhibit $\nu\text{C}=\text{O}$ in the range $1719\text{--}1731\text{ cm}^{-1}$. In the case of 2-aminobenzamide and 2-methoxybenzamide, the amide NH₂ proton is intramolecularly hydrogen bonded to the oxygen atom of the CH₃O group or the nitrogen atom of the amino NH₂ group.



In the case of the 2-amino analog, the $\nu_{\text{asym. NH}_2}$ and $\nu_{\text{sym. NH}_2}$ for the amino NH₂ group occur at 3511 and $\nu 3370\text{ cm}^{-1}$, respectively. The frequency separation of 141 cm^{-1} is evidence that an aniline type NH₂ group is intramolecularly hydrogen bonded (1). In the case of the 2-methoxy analog, $\nu_{\text{asym. NH}_2}$ and $\nu_{\text{sym. NH}_2}$ for the amide group are assigned at 3540 and 3420 cm^{-1} , which is lower than other members in the other benzamides studied in the vapor phase.

The 2-hydroxybenzamide in the vapor phase is a special case in that the OH proton is intramolecularly hydrogen bonded to the carbonyl group.



In this case $\nu\text{C}=\text{O}\cdots\text{HO}$ occurs at 1679 cm^{-1} , and $\nu\text{OH}\cdots\text{N}$ at 3270 cm^{-1} (1).

In the vapor phase, another unique case is 2,6-dichlorobenzamide, because $\nu\text{C}=\text{O}$ occurs at 1735 cm^{-1} . The high $\nu\text{C}=\text{O}$ frequency (1731 cm^{-1}) listed in Table 12.1 is for 3,5-dinitrobenzamide. In the case of the 2,6-Cl₂ analog, the phenyl and (C=O)NH₂ groups are not coplanar, and the reason that $\nu\text{C}=\text{O}$ occurs at such a relatively high frequency is that these two groups are no longer in resonance. The two groups are coplanar in the case of 3,5-dinitrobenzamide, but the high Hammett σ_m value for the two NO₂ groups contributes to the relatively high $\nu\text{C}=\text{O}$ frequency.

Methylmethacrylamide ($\nu_{\text{C=O}}$, 1721 cm^{-1} , vapor) exhibits $\nu_{\text{C=O}}$ at lower frequency than acrylamide ($\nu_{\text{C=O}}$, 1731 cm^{-1} , vapor) due to the inductive electron donation of the methyl group to the C=O group (1).

DILUTION STUDIES OF N-ALKYLACETAMIDE AND N-ALKYLCHLOROACETAMIDE

Table 12.1a lists the N-H stretching frequencies for $\text{N-methyl acetamide}$ in mol/l concentrations ranging from 1.37×10^{-3} to 1.37. The ν_{NH} mode decreases from 3476 to 3471 cm^{-1} , and the absorbance increases from 0.2 to 8.9. At 1.37×10^{-3} mol/l no intermolecular association is noted between $\text{C=O} \cdots \text{HN}$. However, the % $\nu_{\text{N-H} \cdots \text{C=O}}$ increases steadily to $\sim 95\%$ at 1.37 mol/l. In the case of $\text{N-methyl chloroacetamide}$ in mole/liter concentrations ranging from 9.21×10^{-3} to 9.21, the $\nu_{\text{N-H}}$ frequency range of from 3450 – 3448 cm^{-1} in a decreasing order with increasing concentration while absorbance increases from 0.2 to 5. In this case, the intermolecular hydrogen bonding between $\text{N-H} \cdots \text{O=C}$ varies from 1–64% (5). It has been shown that the $\text{N-alkyl chloroacetamide}$ and α -halo-*p-x*-acetanilides in dilute solution exist in an intramolecular hydrogen bonded-form (6,7).

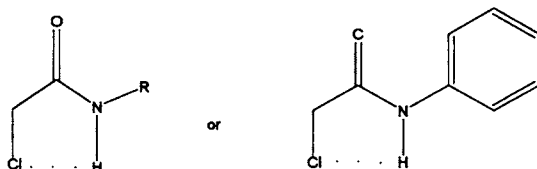


Figure 12.1 shows plots of the concentration vs the absorption maxima at each of the $\nu_{\text{N-H} \cdots \text{O=C}}$ frequencies shown in Table 12.1a. At low concentrations (below 0.01 M for $\text{N-methyl acetamide}$ and below 0.2 M for $\text{N-methyl chloroacetamide}$) the frequency of absorption maximum of the intermolecular $\nu_{\text{N-H} \cdots \text{O=C}}$ band is independent of concentration, indicating that in addition to a monomer only one $\text{N-H} \cdots \text{O=C}$ intermolecular species is present, presumably a dimer (5). At higher concentrations the frequency of absorption decreases rapidly with increasing concentration. In the case of $\text{N-methyl acetamide}$ at concentration above $\sim 0.3\text{ M}$ the $\nu_{\text{N-H} \cdots \text{O=C}}$ frequency is independent of concentration and the average size of the intermolecular $(\text{N-H} \cdots \text{O=C})_n$ complex is about seven or more. The $\text{N-methyl chloroacetamide}$ is different, because in saturated CCl_4 solution only one-third of the molecules exist in an intermolecular hydrogen-bonded form $(\text{N-H} \cdots \text{O=C})_n$. At concentrations of less than 0.2 M, $\text{N-methyl chloroacetamide}$ molecules exist in the intramolecular hydrogen-bonded form $(\text{NH} \cdots \text{Cl})$ (5).

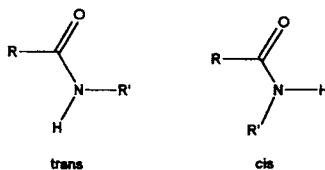
Table 12.1b lists amide I, II, and III frequencies for $\text{N-methyl acetamide}$ in various mole/liter in Br_3CH solution. Bromoform was used in this case instead of chloroform in order to measure the amide II frequencies. The data show that as the concentration increases $\nu_{\text{N-H}}$ increases from 3456 to 3457 cm^{-1} while amide II (or N-H bending) increases from 1531 to 1537 cm^{-1} in 0.685 mol/l. At 0.685 mol/l concentration $\nu_{\text{N-H} \cdots \text{O=C}}$ bonding is observed at 3325 cm^{-1} and amide II is noted at 1560 cm^{-1} . With increasing concentration (2.74 mol/l) amide II is observed at 1563 cm^{-1} , $\nu_{\text{N-H}(\text{O=C})}$ at 3305 cm^{-1} . With increasing concentration (2.74 mol/l) $\nu_{\text{N-H}}$ is observed at 1563 cm^{-1} and $\nu_{\text{N-H} \cdots \text{O=C}}$ at 3305 cm^{-1} . As the $\nu_{\text{C=O}}$ and $\nu_{\text{C=O} \cdots \text{HN}}$

frequencies decrease from 1668–1649 cm^{-1} the amide II (or N–H bending) frequencies increase from 1531–1563 cm^{-1} with increasing concentration. The amide III mode is apparently independent of concentration, as it occurs near 1278–1279 cm^{-1} .

Table 12.1c lists IR data for the first overtone of amide II for N-methyl acetamide and N-methyl chloroacetamide in varying mole/liter concentrations in CCl_4 solution. These data show that the band intensity of the first overtone of amide II (or N–H bending) increases as the mole/liter concentration is increased (0.6 to 28×10^8 for N-methyl acetamide and 1.7 to 15×10^8 for N-methyl chloroacetamide). As the $\nu\text{N-H} \cdots \text{O}=\text{C}$ frequencies decrease the amide II frequency increases with an increase in concentration. Thus, the first overtone of amide II should increase in frequency with an increase in the mole/liter concentration, and the $\nu\text{N-H} \cdots \text{O}=\text{C}$ frequency shows decreases in frequency. Thus, the amount of Fermi resonance interaction between these two modes shows decrease, because the two modes are moving in opposite directions. As a consequence of this behavior, this absorption has no significant intensity in those amides, which are only slightly associated. Of the compounds studied, only Cl, Br, and CF_3 N-alkyl acetamide exhibited significant absorption in this region of the spectrum (5).

TRANS AND/OR CIS SECONDARY AMIDES

In the case of 4-, 5-, 6-, and 7-membered lactams the N–H group is cis to the carbonyl group. Table 12.1 shows that $\nu\text{N-H}$ for the 5-, 6-, 7-membered lactams occurs at 3478, 3438, and 3442 cm^{-1} , respectively. It has been reported that a compound such as N-methyl acetamide exists 95% in the trans form and 5% in the cis form.



Moreover, N-tert-butyl phenylacetamide was reported to exist as 30% in the trans form and 70% in the cis form. The possibility of Fermi resonance between $\nu\text{N-H}$ and the first overtone of $\nu\text{C}=\text{O}$ was excluded on the grounds that the anharmonicity factor would be much too negative (8,9).

Figure 12.2 shows IR spectra of N-methyl acetamide, N-ethyl acetamide, N-isopropyl acetamide, N-tert-butyl acetamide, and acetanilide in CCl_4 solution in the region 3800–3300 cm^{-1} . In these cases, the $\nu\text{N-H}$ stretch mode decreases in frequency in the order 3479, 3462, 3451, 3453, and 3449 cm^{-1} , respectively, and the $\nu\text{C}=\text{O}$ frequency increases in the order: 1686, 1686, 1687, 1686, and 1708 cm^{-1} , respectively. The weak bands in the range 3350–3400 cm^{-1} are readily assigned as $2(\nu\text{C}=\text{O})$ (6). The difference between the N-methyl acetamide $\nu\text{N-H}$ frequency and those for the N-ethyl, N-isopropyl, N-tert-butyl, and N-phenyl analogs is 17, 28, 26, and 30 cm^{-1} , respectively. In addition, there is no other band present to indicate the presence of another rotational conformer, and the $\nu\text{N-H}$ frequency decrease follows closely the inductive contribution of the N-alkyl group to the carbonyl group. Therefore, it was concluded that the N-alkyl acetamides exist in the trans configuration in dilute CCl_4 solution. There is no positive evidence for the existence of the cis conformer (6).

Table 12.2 lists IR data and assignments for N-alkyl acetamides and N-alkyl- α -substituted acetamides.

The data on the N-alkyl acetamides showed that ν -H is sensitive to the nature of the N-alkyl group. Thus, when comparing data for N-alkyl α -haloacetamides vs those for N-alkyl acetamides it is necessary to compare data for the same N-alkyl analogs.

Comparison of the ν N-H frequencies for N-butyl acetamide (3460 cm^{-1}) vs N-butyl α -chloroacetamide (3433 cm^{-1}), N-isopropyl acetamide (3451 cm^{-1}) vs N-isopropyl α -chloroacetamide (3429 cm^{-1}), and N-tert-butyl acetamide (3453 cm^{-1}) vs N-tert-butyl α -chloroacetamide (3421 cm^{-1}) shows that ν N-H occurs at lower frequency by $22\text{--}32\text{ cm}^{-1}$ in the case of the α -chloro analog. Comparison of the ν C=O frequencies for N-butyl acetamide (1688 cm^{-1}) vs N-butyl α -chloroacetamide (1684 cm^{-1}), N-isopropyl acetamide (1687 cm^{-1}) vs N-isopropyl α -chloroacetamide (1682 cm^{-1}), and N-tert-butyl acetamide (1688 cm^{-1}) vs N-tert-butyl α -chloroacetamide (1684 cm^{-1}) shows that ν C=O decreases in frequency by 4 to 5 cm^{-1} .

Comparison of the ν N-H frequencies for N-butyl α -chloroacetamide (3433 cm^{-1}) vs N-butyl α,α -dichloroacetamide (3439 cm^{-1}), isopropyl α -chloroacetamide (3430 cm^{-1}) vs isopropyl α,α -dichloroacetamide (3439 cm^{-1}), and tert-butyl α -chloroacetamide (3421 cm^{-1}) vs N-tert-butyl α,α -dichloroacetamide (3435 cm^{-1}) shows that ν N-H increases in frequency by 6 to 14 cm^{-1} with the addition of the second α -chloro atom.

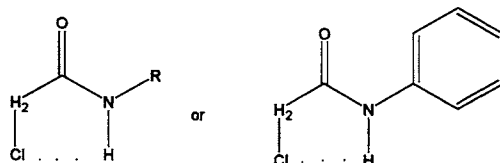
Comparison of the ν C=O frequencies for N-butyl chloroacetamide (1684 cm^{-1}) vs N-butyl α,α -dichloroacetamide (1705 cm^{-1}), N-isopropyl α -chloroacetamide (1682 cm^{-1}) vs N-isopropyl α,α -dichloroacetamide (1703 cm^{-1}), and N-tert-butyl α -chloroacetamide (1684 cm^{-1}) vs N-tert-butyl α,α -dichloroacetamide (1702 cm^{-1}) shows that ν C=O increases in frequency by $18\text{--}22\text{ cm}^{-1}$ with the addition of the second chlorine atom.

Comparison of the ν N-H frequencies for N-butyl α,α -dichloroacetamide (3439 cm^{-1}) vs N-butyl α,α,α -trichloroacetamide (3445 cm^{-1}), N-isopropyl α,α -dichloroacetamide (3430 cm^{-1}) vs N-isopropyl α,α,α -trichloroacetamide (3439 cm^{-1}), and N-tert-butyl α,α -dichloroacetamide (3427 cm^{-1}) vs N-tert-butyl α,α,α -trichloroacetamide (3435 cm^{-1}) shows that ν N-H increases in frequency by another 6 to 9 cm^{-1} with the addition of the third chlorine atom.

Comparison of the ν C=O frequencies for N-butyl α,α -dichloroacetamide (1705 cm^{-1}) vs N-butyl α,α,α -trichloroacetamide (1726 cm^{-1}), N-isopropyl α,α -dichloroacetamide (1703 cm^{-1}) vs N-isopropyl α,α,α -trichloroacetamide (1725 cm^{-1}), and N-tert-butyl α,α -dichloroacetamide (1702 cm^{-1}) vs N-tert-butyl α,α,α -trichloroacetamide (1725 cm^{-1}) shows that ν C=O increases in frequency by another 21 to 23 cm^{-1} with the addition of the third chlorine atom.

These comparisons show that with the addition of the first α -chlorine atom on N-alkyl acetamide the ν N-H frequencies decrease by $22\text{--}32\text{ cm}^{-1}$ and the ν C=O frequencies increase by 4 to 5 cm^{-1} . With the addition of the second α -chlorine atom the ν N-H frequencies increase by 6 to 14 cm^{-1} and the ν C=O frequencies increase by $18\text{--}22\text{ cm}^{-1}$. With the addition of the third α -chlorine atom ν N-H increase by another $6\text{--}9\text{ cm}^{-1}$ and ν C=O increase by another $21\text{--}23\text{ cm}^{-1}$.

There is only one explanation for the behavior of the ν N-H and ν C=O data for the N-alkyl chloroacetamide analogs. Upon addition of the first α -chlorine atom an intramolecular hydrogen bond is formed between the N-H proton and the α -chloroatom as depicted here:



The formation of the $\text{Cl} \cdots \text{HN}$ bond causes $\nu\text{N-H}$ to decrease in frequency while the $\nu\text{C=O}$ mode is only increased by 4 to 5 cm^{-1} . With the addition of the second and third chlorine atoms the $\nu\text{N-H}$ frequencies increase progressively by 6 to 14 cm^{-1} and 6 to 9 cm^{-1} while the $\nu\text{C=O}$ frequencies increase progressively by 18 to 22 cm^{-1} and 21 to 23 cm^{-1} . The $\nu\text{N-H}$ frequency increases with the addition of the second and third α -chlorine atoms and is the result of the inductive effect. In the case of the $\nu\text{C=O}$ frequencies substitution of the second and third chlorine atoms is a combination of the inductive effect and the field effect between the carbonyl oxygen atom and the two gauche chlorine atoms (6).

Comparison of the vapor and CCl_4 solution data for N-isopropyl acetamide (3460 vs 3451 cm^{-1} and 1714 vs 1687 cm^{-1}) and N-tert-butyl α,α,α -trichloroacetamide (3444 vs 3435 cm^{-1} and 1743 vs 1725 cm^{-1}) shows that both $\nu\text{N-H}$ and $\nu\text{C=O}$ occur at higher frequency in the vapor. This most likely reflects the effect of $\text{N-H} \cdots \text{ClCCl}_3$ interaction in the solution phase.

The $\nu\text{N-H}$ vibration occurs at the lowest frequency for the N-phenyl analogs of the forementioned four series of acetamides. The N-phenyl analogs of these series exhibit $\nu\text{N-H}$ at the lowest frequency in the order: CH_3 (3449 cm^{-1}), ClCH_2 (3409 cm^{-1}), Cl_2CH (3419 cm^{-1}), and Cl_3C (3425 cm^{-1}), and exhibit $\nu\text{C=O}$ at the highest frequency in the order: CH_3 (1708 cm^{-1}), ClCH_2 (1692 cm^{-1}), Cl_2CH (1713 cm^{-1}), and CCl_3 (1731 cm^{-1}). The inductive effect of the phenyl group tightens the C=O bond, thereby raising its $\nu\text{C=O}$ frequency, and the N-H group becomes more acidic, causing it to form a stronger intramolecular $\text{N-H} \cdots \text{Cl}$ bond. The $\nu\text{N-H}$ and $\nu\text{C=O}$ frequency behavior with α -chloro substitution is comparable to that exhibited by the N-alkyl α -chlorinated analogs.

N-H INTENSITY

A study of Table 12.2 shows that the apparent intrinsic integrated absorption ($B \times 10^8$)* for the N-H stretching vibration is significantly raised by the intramolecular $\text{N-H} \cdots \text{X}$ bond, while the intensity is influenced only to a relatively small extent by the inductive effect.

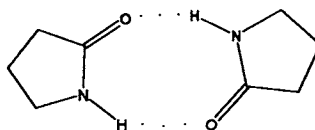
In saturations of 10% or $< 10\%$, CCl_4 solutions bonded $\nu\text{N-H} \cdots \text{O=C}$ occur in the region $3280\text{--}3400 \text{ cm}^{-1}$ (see Table 12.2a). For those compounds that exhibited significant "amide II" overtone absorption, both the observed frequencies and frequencies corrected for Fermi resonance with the "amide II" overtone are listed.

The frequency separation between the $\nu\text{N-H}$ frequency and the intermolecular $\nu\text{N-H} \cdots \text{O=C}$ frequency varies between 60 and 195 cm^{-1} . The intramolecularly hydrogen-bonded secondary amides exhibit less intermolecular H-bonding than the simple N-alkyl acetamides, and exhibit higher bonded $\nu\text{N-H}$ frequencies.

In contrast, pyrrolidone is a cyclic secondary amide whose N-H group is cis with the C=O group. In this case, the $\nu\text{N-H}$ frequency is nearly independent of concentration, ranging from

* $B \times 10^8$ [Intensity $B = (1/\text{Cl}) \ln (I_0/I) dv$ in $\text{CM}^2 \text{ molecule}^{-1} \text{ s}^{-1}$, and represents the apparent intrinsic absorption for $\nu\text{N-H}$].

3207–3219 cm^{-1} at concentrations ranging from 0.01–1.0 M in CCl_4 solution. This indicates that only one bonded species is present: the cis dimer (10).

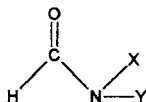


pyrrolidone cis intermolecular hydrogen bonded dimer

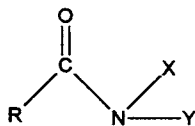
Table 12.3 lists IR data for N-alkyl α -substituted acetamides in 10% wt./vol. and 0.002 M CCl_4 solutions. In all cases, except for tert-butyl phenoxy-acetamide and tert-butyl trichloroacetamide, the $\nu\text{C}=\text{O}$ or "Amide I" mode occurs at higher frequency in dilute solution. Within each series, the tert-butyl analogs show the least frequency shift in going from 10% wt./vol. to 0.002 M in CCl_4 solution; and this is most likely due to the steric effect of the tert-butyl group, which prevents the N–H proton of another amide molecule from forming as strong an intermolecular hydrogen bond as in the case of the other N-alkyl analogs, or prevents intermolecular hydrogen bonding as in the case of tert-butyl trichloroacetamide.

Table 12.4 shows a comparison of primary and secondary amides in the solid phase. In this case, the $\nu_{\text{asym.}} \text{NH}_2$ frequencies occur in the range 3310–3380 cm^{-1} and $\nu_{\text{sym.}} \text{NH}_2$ frequencies occur in the range 3150–3195 cm^{-1} while $\nu\text{N}-\text{H}$ for the secondary amides occur in the range 3242–3340 cm^{-1} . The primary amides exhibit NH_2 bending in the region 1620–1652 cm^{-1} while the secondary amides exhibit N–H bending in the region 1525–1550 cm^{-1} . Inductive and resonance effects upon the $\nu\text{C}=\text{O}$ frequency are also apparent in the solid phase.

Table 12.4a lists IR data for the $\nu\text{C}=\text{O}$ frequencies for tertiary amides in the neat or solid phase. Formamides have the basic structure:



In the neat phase, when X and Y are C_2H_5 groups, $\nu\text{C}=\text{O}$ occurs at 1665 cm^{-1} . When X is C_2H_5 and Y is C_6H_5 , $\nu\text{C}=\text{O}$ occurs at 1670 cm^{-1} . When X is C_6H_5 and Y is C_6H_5 , $\nu\text{C}=\text{O}$ occurs at 1690 cm^{-1} . The increase in the $\nu\text{C}=\text{O}$ frequency when C_6H_5 is substituted for C_2H_5 is attributed to the larger inductive effect of C_6H_5 vs C_2H_5 . Tertiary amides have the following basic structure:



The tertiary acetamides exhibit $\nu\text{C}=\text{O}$ in the region 1650–1670 cm^{-1} , and the inductive effect of the X or Y alkyl and phenyl groups is also apparent. In the vapor phase, $\nu\text{C}=\text{O}$ for tertiary amides occur $40 \pm 5 \text{ cm}^{-1}$ higher in frequency than they occur in the neat or solid phase. The lower

$\nu\text{C}=\text{O}$ frequencies in the condensed phases most likely result from dipolar interaction between molecules such as the one illustrated here; this interaction weakens the $\text{C}=\text{O}$ bond.

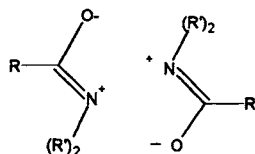


Table 12.5 shows a comparison of Raman data and assignments for acrylamide, methacrylamide, and their polymers. Study of Table 12.5 indicates that as the average molecular weight of polyacrylamide increases, the $\nu\text{C}=\text{O}$ frequency increases from 1658 to 1668 cm^{-1} , while the Raman relative band intensity decreases. The N-alkyl acrylamides exhibit a weak Raman band in the region $1657\text{--}1659\text{ cm}^{-1}$ and a strong Raman band in the region $1627\text{--}1629\text{ cm}^{-1}$, which are assigned to $\nu\text{C}=\text{O}$ and $\nu\text{C}=\text{C}$, respectively. The N,N-dialkyl or N-alkyl, N-vinyl acrylamides exhibit a weak to strong Raman band in the region $1648\text{--}1666\text{ cm}^{-1}$ and a strong Raman band in the region $1609\text{--}1625\text{ cm}^{-1}$, which are assigned to $\nu\text{C}=\text{O}$ and $\nu\text{C}=\text{C}$, respectively. The inductive effect of the N-vinyl group apparently affects both the frequency and Raman band intensity of $\nu\text{C}=\text{O}$.

Methacrylamide exhibits a weak Raman band at 1673 cm^{-1} , which is 9 cm^{-1} lower in frequency than $\nu\text{C}=\text{O}$ for acrylamide. This decrease in the $\nu\text{C}=\text{O}$ frequency is attributed to the inductive effect of the α -methyl group. The medium-strong Raman band at 1647 cm^{-1} is assigned as $\nu\text{C}=\text{C}$ for methacrylamide while the strong Raman band at 1639 cm^{-1} is assigned as $\nu\text{C}=\text{C}$ for acrylamide. Apparently the inductive effect of the α -methyl group in polymethacrylamide causes $\nu\text{C}=\text{O}$ to occur at lower frequency than $\nu\text{C}=\text{O}$ for polyacrylamide.

Table 12.5a lists Raman data for N-alkyl or N-aryl acrylamides and methacrylamides in the neat phase. The most distinguishing features between the N-alkyl or N-aryl acrylamides and the N-alkyl or N-aryl methacrylamides is the relative Raman band intensities of $\nu\text{C}=\text{O}/\nu\text{C}=\text{C}$. In the case of the acrylamides it varies between 0.06 and 0.8 and in the case of the methacrylamides it varies between 0.11 and 3. Moreover, the frequency separation between $\nu\text{C}=\text{O}$ and $\nu\text{C}=\text{C}$ varies between $29\text{--}35\text{ cm}^{-1}$ for the acrylamides and varies between $35\text{--}39\text{ cm}^{-1}$ for the methacrylamides.

A strong Raman band in the range $875\text{--}881\text{ cm}^{-1}$ most likely results from a symmetric $\text{C}-\text{C}-\text{C}$ skeletal stretching vibration of the group for the methacrylamide while a medium-strong Raman band in the range $1236\text{--}1256\text{ cm}^{-1}$ results from a skeletal vibration of the $=\text{C}-\text{C}(=\text{O})-\text{N}$ group for the acrylamides.

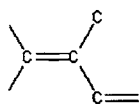
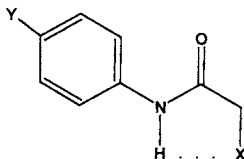


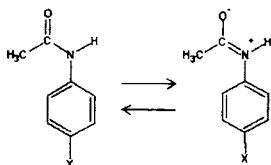
Table 12.6 lists IR data for p-x-acetanilides and p-x, α -haloacetanilides. Study of Table 12.6 shows that in general all $\nu\text{C}=\text{O}$ modes occur at lower frequency in CHCl_3 solution than in CCl_4 solution. Part of the $\nu\text{C}=\text{O}$ frequency decrease is the result of intermolecular hydrogen bonding ($\text{C}=\text{O} \cdots \text{HCCl}_3$). It should be noted that the $\nu\text{C}=\text{O}$ frequencies increase in the order α -bromo-p-x-acetanilide, p-x-acetanilide, and α,α,α -trichloro-p-x-acetanilide. The α -bromo analogs and the

α,α,α -trichloro analogs in dilute solution exist in the intramolecular hydrogen bonded form as depicted here:



As discussed previously, substitution of the first α -halogen atom on the α -carbon atom decreases the $\nu\text{C}=\text{O}$ frequency. Addition of the second and third halogen atoms on the α -carbon atom additively increases the $\nu\text{C}=\text{O}$ frequency due to both inductive and field effects (7).

Figure 12.3 shows plots of the $\nu\text{C}=\text{O}$ frequencies of α -bromo-*p*-*x*-acetanilide, *p*-*x*-acetanilide, and α,α,α -trichloro-*p*-*x*-acetanilide in 0.002 M solutions or less in CCl_4 and CHCl_3 vs the Hammett σ_p values. All six plots show that the $\nu\text{C}=\text{O}$ mode increases linearly in frequency as the σ_p value increases. This is the result of the greater tendency of the para substituent to attract electrons (higher σ_p values), the smaller the nitrogen nonbonding electron pair. The carbonyl stretching frequency decreases as the electron density on the nitrogen atom increases as a result of an increased tendency toward shifting the mesomeric equilibrium:



For example, the higher the nitrogen electron density, the greater the tendency to impart double-bond character to the C–N bond at the expense of double-bond character of the C=O bond, thus reducing the C=O force constant (7).

ACETANILIDES

It has been shown that the IR $\nu\text{C}=\text{O}$ band intensities for *p*- and *m*-substituted acetanilides are a function of Hammett σ_p and σ_m values (11). The higher the σ_p or σ_m values the lower the $\nu\text{C}=\text{O}$ IR band intensities. Examples given here are from Reference (7):

<i>p</i> - <i>x</i>	<i>p</i> - <i>x</i> -acetanilide	α -bromo- <i>p</i> - <i>x</i> -acetanilide	α,α,α -trichloro- <i>p</i> - <i>x</i> -acetanilide
CH_3O	14.4	15.10	13.42
Cl	12.56	14.41	12.93
NO_2	9.40	11.15	11.55

These absorbance values are $\times 10^7 \text{ cm}^2 \text{ molecule}^{-1} \text{ s}^{-1}$

Table 12.7 lists IR data for the N–H stretching frequencies for *p*-*x*-acetanilides and *p*-*x*, α -haloacetanilides and their absorbance values ($\times 10^7 \text{ cm}^2 \text{ molecule}^{-1} \text{ s}^{-1}$) obtained in CHCl_3 solution. The αN –H frequencies generally occur at lower frequency in CHCl_3 solution than in

CCl_4 solution. The $\nu\text{N-H}$ frequencies in CCl_4 solution decrease in the order p-x-acetanilide ($3436\text{--}3445\text{ cm}^{-1}$), α,α,α -trichloro-p-x-acetanilide ($3415\text{--}3422\text{ cm}^{-1}$), and α -bromo-p-x-acetanilide ($3391\text{--}3405$). In CHCl_3 solution they occur in the same order, $3429\text{--}3440\text{ cm}^{-1}$, $3406\text{--}3415\text{ cm}^{-1}$, and $3387\text{--}3395\text{ cm}^{-1}$.

Study of the absorbance values shows that in general they increase progressing in the order p-x-acetanilide, α -bromo-p-x-acetanilide, and α,α,α -p-x-acetanilide. There is a general but not systematic increase in the absorbance values as the σ_p values increase. These data support that an intramolecular hydrogen bond is formed between $\text{N-H}\cdots\text{X}$ as already depicted here. In the case of the α -Br analog, the Br atom is larger than say a Cl atom, and the $\text{H}\cdots\text{Br}$ distance would be shorter than the $\text{H}\cdots\text{Cl}$ distance. A stronger intramolecular hydrogen bond would be formed as the distance is decreased, causing $\nu\text{N-H}\cdots\text{Br}$ to decrease in frequency by approximately 40 cm^{-1} . These data show that as the N-H proton becomes more acidic, the $\nu\text{N-H}$ frequency decreases (7).

N-ALKYL BENZAMIDES

Table 12.8 lists the NH and C=O stretching frequencies for N-alkyl p-methoxybenzamide, N-alkyl p-chlorobenzamide, and N-alkyl methyl carbamate in CCl_4 solutions (6). The absorbance values are $\times 10^8\text{ cm}^2\text{ molecule}^{-1}\text{ s}^{-1}$ for the NH group.

The N-alkyl p-x-benzamides are also affected by the nature of the N-alkyl group. The $\nu\text{N-H}$ frequencies generally decrease with branching on the N-alkyl α -carbon atom.

The $\nu\text{C=O}$ frequencies for the N-alkyl p-methoxybenzamides occur in the range $1670\text{--}1676\text{ cm}^{-1}$ and for N-alkyl p-chlorobenzamides in the range $1671\text{--}1681\text{ cm}^{-1}$. Closer examination shows that in all cases $\nu\text{C=O}$ for n-alkyl p-methoxybenzamide occurs at a lower frequency than that for the comparable N-alkyl p-chloro-benzamide (N-methyl vs N-methyl, etc.). This is the result of Hammett σ_p values. The σ_p values also appear to affect the band intensities, because a higher σ_p value increases the band intensity.

N-ALKYL METHYL CARBANATES

The N-alkyl methyl carbanates exhibit $\nu\text{N-H}$ in the region $3449\text{--}3478\text{ cm}^{-1}$; and the frequencies tend to decrease with branching on the α -carbon atom. The N-phenyl analog exhibits νNH at 3450 cm^{-1} . The $\nu\text{C=O}$ frequencies for the N-alkyl analogs occur in the range $1730\text{--}1738\text{ cm}^{-1}$ while $\nu\text{C=O}$ for the N-phenyl analog occurs at 1748 cm^{-1} due to the inductive effect of the phenyl ring (6).

N,N'-DIALKYL OXAMIDES AND N,N'-DIARYL OXAMIDE

Table 12.9 lists IR and Raman data for both N,N'-dialkyl oxamides and N,N'-diaryl oxamides (12). In the case of IR, the samples were prepared as either split mulls or KBr pellets. Raman spectra were recorded of the solid samples. The out-of-phase (N-H)₂ stretching vibration (a B_{1u} mode) is IR active and in the case of the N,N'-dialkyl analogs occurs in the range 3279--

3311 cm^{-1} while for the $\text{N,N}'$ -diaryl analogs it occurs in the range 3295–3358 cm^{-1} . The in-phase $(\text{N-H})_2$ stretching vibration (an A_g mode) is Raman active and in the case of the $\text{N,N}'$ -dialkyl analogs it occurs in the range 3302–3325 cm^{-1} while for the $\text{N,N}'$ -diaryl analogs it occurs in the range 3320–3349 cm^{-1} . The IR band occurring in the range 1643–1660 cm^{-1} for $\text{N,N}'$ -dialkyl oxamides is assigned to the amide I mode (in this case, out-of-phase $(\text{C=O})_2$ stretching) while for the $\text{N,N}'$ -diaryl analog it occurs in the range 1662–1719 cm^{-1} . In the solid state, a weak shoulder appears in the region 1628–1638 cm^{-1} of the IR spectrum. It is the result of crystal splitting, as it is not present in solution phase or vapor-phase spectra (12). The in-phase $(\text{C=O})_2$ stretching A_g mode is assigned to the Raman band occurring in the range 1686–1695 cm^{-1} in the case of the $\text{N,N}'$ -dialkyl analogs while in the case of the $\text{N,N}'$ -diaryl analogs it occurs in the range 1682–1741 cm^{-1} .

The Amide II mode—the out-of-phase $(\text{N-H})_2$ bending (B_{1u}) mode and the in-phase $(\text{N-H})_2$ bending (A_{1g}) mode—occur in the range 1508–1541 cm^{-1} and 1547–1567 cm^{-1} for the $\text{N,N}'$ -dialkyl oxamides, respectively, while for the $\text{N,N}'$ -diaryl analogs they occur in the range 1484–1520 cm^{-1} and 1537–1550 cm^{-1} , respectively. In all cases discussed here the A_g modes occur at higher frequency than the corresponding B_{1u} mode. These IR and Raman data indicate that the $\text{N,N}'$ -diaryl oxamide exist in an intermolecularly hydrogen-bonded trans configuration in the solid state where each oxamide group can be viewed as having C_{2h} symmetry (12). In the vapor phase $\text{N,N}'$ -dimethyloxamide also exists in the trans configuration (12).

The $\text{N,N}'$ -dialkyloxamide exhibits B_{1u} modes in the range 1223–1251 cm^{-1} (Amide III), 725–782 cm^{-1} (Amide IV), 532–619 cm^{-1} (Amide VI), and A_g modes in the region 1298–1315 cm^{-1} (Amide III), and 1130–1210 cm^{-1} ($(\text{C-N})_2$ stretching) (12).

DIMETHYLACETAMIDE AND TETRAALKYLUREA

Table 12.10 lists IR data and assignments for dimethylacetamide and tetraalkylurea in different physical phases (13,14). These data show that the C=O stretching frequency of dimethylacetamide or tetraalkylurea is sensitive to the physical phase, and that in $n\text{-C}_6\text{H}_{14}/\text{CHCl}_3$ solutions clusters of tetramethylurea exist that exhibit $\nu\text{C=O}$ at 1650.9 and 1635.4 cm^{-1} in 14 mol % $n\text{-C}_6\text{H}_{14}/\text{CHCl}_3$ and at 1640.2 and 1629.5 cm^{-1} in 80.6 mol % $n\text{-C}_6\text{H}_{14}/\text{CHCl}_3$ solutions.

In CCl_4 and/or CHCl_3 solutions, the behavior of the C=O stretching mode is explained on the basis of hydrogen-bonded complexes between solvent-solvent and solute-solvent and the bulk dielectric effects of the solvents. Figure 12.4 shows plots of $\nu\text{C=O}$ for 1 wt % solutions of acetone, dimethylacetamide, and tetramethylurea vs mole % $\text{CHCl}_3/\text{CCl}_4$. The plots become more complex proceeding in the series acetone, dimethylacetamide, and tetramethylurea. In the case of acetone, the nonlinear segment is attributed to the complex $(\text{CH}_3)_2\text{C=O}\cdots\text{HCCl}_3$, and the first nonlinear segments in the other two plots are attributed to $\text{C=O}\cdots\text{HCCl}_3$ complexes with dimethylacetamide and tetraalkylurea. The second break in the case of dimethylacetamide is attributed to intermolecular hydrogen bonding between both $\text{Cl}_3\text{CH}\cdots\text{O=C-N}(\cdots\text{HCCl}_3)$. The third break may be due to a complex such as $(\text{Cl}_3\text{CH}\cdots)_2\text{O=C-N}\cdots\text{HCCl}_3$ and/or $\text{Cl}_3\text{CH}\cdots\text{O=C-N}(\cdots\text{HCCl}_3)_2$. The additional break in $\text{N,N,N}',\text{N}'$ -tetramethylurea is attributed to the additional $-\text{N}$ -group, which also is capable of forming a $\text{Cl}_3\text{CH}\cdots\text{N}$ bond.

It is interesting to compare the $\nu\text{C=O}$ frequencies of tetramethylurea (TMU), tetraethylurea (TEU), and tetrabutyl urea (TBU) in CCl_4 solution (1652.9, 1646.2, and 1643.2 cm^{-1} ,

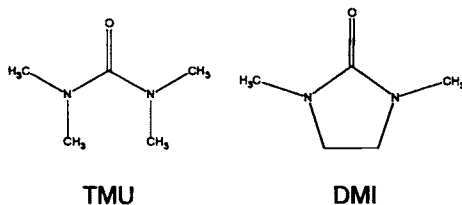
respectively, and in CHCl_3 solution (1627.3, 1620.1, and 1616.1 cm^{-1} , respectively). The frequency difference between these two solvents increases in the order 25.6, 26.1, and 27.0 cm^{-1} for TMU, TEU, and TBU, respectively. In addition, it is noted that the $\text{C}=\text{O}$ stretching frequency decreases in the order TMU, TEU, and TBU. These data show that as the alkyl groups contribute more of an inductive contribution to the $\text{C}=\text{O}$ group the $\nu\text{C}=\text{O}$ mode decreases in frequency and the strength of the $\text{C}=\text{O} \cdots \text{HCCl}_3$ bond increases (14).

Table 12.11 lists IR vapor-phase data for urea, thiourea, and guanidine derivatives. These data show that the 1,1,3,3-tetraalkylureas exhibit a weak IR band in the range 3338–3358 cm^{-1} , which results from the first overtone of $\text{C}=\text{O}$ stretching. As $2\nu\text{C}=\text{O}$ occurs at lower frequency than the calculated $2\nu\text{C}=\text{O}$ frequency in each case, the $2\nu\text{C}=\text{O}$ mode exhibits positive anharmonicity.

The 1,1,3,3-tetraethylthiourea exhibits a band at approximately 1085 cm^{-1} that is assigned to $\text{C}=\text{S}$ stretching, $\nu\text{C}=\text{S}$. The 1619 cm^{-1} band for 1,1,3,3-tetramethylguanidine is assigned to $\text{C}=\text{N}$ stretching, $\nu\text{C}=\text{N}$. All of the compounds listed in Table 12.11 exhibit a band in the range 1239–1334 cm^{-1} , which most likely results from an antisymmetric NCN stretching mode.

1,1,3,3-TETRAMETHYLUREA VS 1,3-DIMETHYL-2-IMIDAZOLIDINONE

Table 12.12 lists IR data for 1,1,3,3-tetramethylurea and 1,3-dimethyl-2-imidazolidinone in various solvents at 1% wt./vol. (14–16). These two compounds have the following empirical structures:



In all solvents, the $\nu\text{C}=\text{O}$ mode for DMI occurs at higher frequency than $\nu\text{C}=\text{O}$ for TMU. The only chemical difference between TMU and DMI is that a $(\text{CH}_2)_2$ group has been substituted for two CH_3 groups, and the chemical difference is minimal. The $\text{C}=\text{O}$ group occurs at a significantly higher frequency in the case of DMI due to geometric restrictions of the 5-membered ring, which makes it more difficult for the carbonyl carbon atom to move in and out of the ring during a cycle of $\nu\text{C}=\text{O}$. (This is often referred to as ring strain. In any $\nu\text{C}=\text{O}$ mode, the bond angle must change to some degree, and the smaller the $\text{X}-\text{C}-\text{Y}$ angle the more difficult it is for the $\text{C}=\text{O}$ bond to vibrate.)



In Table 12.12 under the solvent heading, the neat phase is listed as 1, hexane 2, sequentially to methyl alcohol as 20. These numbers are used to show for which solvent or next phase the particular data were recorded or the data difference was determined.

Figure 12.5 shows plots of $\nu_{\text{C=O}}$ of DMI and TMU in the neat phase or in 1 of the 19 solvents vs $\nu_{\text{C=O}}$ (hexane) minus $\nu_{\text{C=O}}$ (solvent). These two plots are linear, and any set of numbers treated in the same mathematical way will yield a linear relationship. The important point to note in these two plots is that the number in each plot is not in the identical sequence. These differences suggest that the solute-solvent interaction is not comparable in all cases (16). This suggests that the steric factor of the $(\text{CH}_3)_2$ or $(\text{CH}_3)_4$ and $(\text{CH}_2)_2$ groups alters the spatial distance between solute and solvent.

Figure 12.6 shows plots of $\nu_{\text{C=O}}$ for TMU and DMI vs the solvent acceptor number (AN). The numbers 17' through 20' are for the $\nu_{\text{C=O}} \cdots \text{HOR}$ frequencies for these compounds in tertiary butyl alcohol, isopropyl alcohol, ethyl alcohol, and methyl alcohol, respectively. The numbers 17 through 20 are for $\nu_{\text{C=O}}$ in these same alcohols, but where the C=O groups are not intermolecularly hydrogen bonded. This indicates that intermolecularly bonded alkyl alcohols (R-OH) can cluster in surrounding TMU or DMI without forming intermolecular hydrogen bonds with the solute. Projection of these points by dashed lines onto the lower lines indicates that the AN values for the alcohols are much lower than the values determined by NMR (17). These projected AN values for the alcohols are comparable to the AN values for alkyl ethers.

Figure 12.7 shows plots of $\nu_{\text{C=O}}$ for DMI and TMU vs mole % $\text{CHCl}_3/\text{CCl}_4$. Both plots show similar a, b, c, and d segments. It has been suggested that the concentration of DMI or TMU molecules are in equilibrium with the concentration of CHCl_3 and/or CCl_4 molecules in regions (a) through (d). In addition, as the mole % $\text{CHCl}_3/\text{CCl}_4$ is increased from 0 to 100, the $(\text{CHCl}_3)_x$ one, two, three or four complexes are replaced by $(\text{CCl}_3\text{H}:\text{ClCl}_2\text{CH})_x$ complexes:

- Region (a) DMI or TMU $\cdots (\text{HCCl}_3)_1$
- Region (b) DMI or TMU $\cdots (\text{HCCl}_3)_2$
- Region (c) DMI or TMU $\cdots (\text{HCCl}_3)_3$
- Region (d) DMI or TMU $\cdots (\text{HCCl}_3)_4$

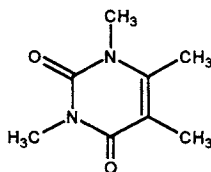
Complexes between CCl_4 and TMU or DMI would also decrease the $\nu_{\text{C=O}}$ frequencies.

Different complexes are reported to be formed between DMI or TMU and mole % n- $\text{C}_6\text{H}_{14}/\text{CCl}_4$ or mole % n- $\text{C}_6\text{H}_{14}/\text{CHCl}_3$ solutions (15,16). Data in Table 12.13 show that in mole % $\text{CHCl}_3/\text{CCl}_4$ solutions only one $\nu_{\text{C=O}}$ frequency is observed, in mole % $\text{CCl}_4/\text{n-C}_6\text{H}_{14}$ solutions two $\nu_{\text{C=O}}$ frequencies are observed, and in mole % $\text{CHCl}_3/\text{n-C}_6\text{H}_{14}$ solutions three $\nu_{\text{C=O}}$ frequencies are observed. These are due to the presence of different DMI clusters in these various complex solution mixtures.

CAFFEINE, ISOCAFFEINE, 1,3,5-TRIMETHYLURACIL, 1,3,6-TRIMETHYLURACIL, AND 1,3-DIMETHYL-2,4- (1H, 3H) QUINAZOLINEDIONE

Table 12.14 lists the in-phase and out-of-phase $(\text{C=O})_2$ stretching frequencies for caffeine, isocaffeine, 1,3,5-trimethyluracil, 1,3,6-trimethyluracil, and 1,3-dimethyl-2,4-(1H,3H) quinazo-

linedione in CCl_4 and CHCl_3 solutions (18). All of these compounds contain the dimethyl cyclic 6-membered ring as shown here.



The two $\text{C}=\text{O}$ stretching modes couple into in-phase $(\text{C}=\text{O})_2$, $\nu_{\text{ip}}(\text{C}=\text{O})_2$, and out-of-phase $(\text{C}=\text{O})_2$ stretching, $\nu_{\text{op}}(\text{C}=\text{O})_2$.

The $\nu_{\text{ip}}(\text{C}=\text{O})$ mode for caffeine occurs at 1721 cm^{-1} in the vapor phase, at 1710.6 cm^{-1} in CCl_4 solution, and at 1708.9 cm^{-1} in CHCl_3 solution while the $\nu_{\text{op}}(\text{C}=\text{O})_2$ mode occurs at 1685 cm^{-1} in the vapor phase, 1667.5 cm^{-1} in CCl_4 solution, and at 1658.4 cm^{-1} in CHCl_3 solution. With change in phase, the $\nu_{\text{op}}(\text{C}=\text{O})_2$ mode shifts more in frequency than the $\nu_{\text{ip}}(\text{C}=\text{O})_2$ mode (17.5 , 26.6 , and 9.1 cm^{-1}) vs (10.4 , 12.1 , and 1.7 cm^{-1}).

In CCl_4 solution, caffeine, isocaffeine, 1,3,5-trimethyl uracil, 1,3,6-trimethyluracil, and 1,3-dimethyl-2,4-(1H,3H)-quinazolinone exhibit $\nu_{\text{ip}}(\text{C}=\text{O})_2$ in the range $1706.6\text{--}1716.3\text{ cm}^{-1}$, and in CHCl_3 solution in the range $1700\text{--}1711.3\text{ cm}^{-1}$.

The $\nu_{\text{op}}(\text{C}=\text{O})_2$ mode for 1,3,5-trimethyluracil and 1,3-dimethyl-2,4-(1H,3H)-quinazolinone is in Fermi resonance with a combination or overtone, and in these two cases $\nu_{\text{op}}(\text{C}=\text{O})_2$ was corrected for FR. Therefore, for these five compounds $\nu_{\text{op}}(\text{C}=\text{O})_2$ occurs in the range $1663.4\text{--}1669\text{ cm}^{-1}$ in CCl_4 solution and in the range $1652.4\text{--}1664\text{ cm}^{-1}$ in CHCl_3 solution (18).

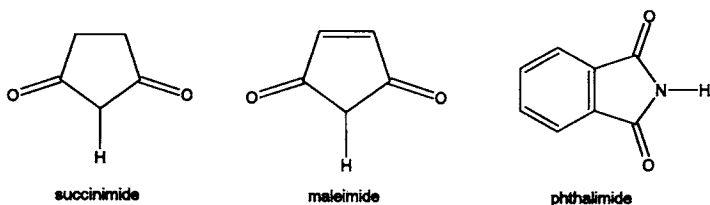
Table 12.15 lists IR data for uracils in the solid phase. In the solid phase, the uracils not substituted in the 1,3-position (contain two N-H groups) exhibit $\nu_{\text{ip}}(\text{C}=\text{O})_2$ in the range $1704\text{--}1750\text{ cm}^{-1}$ and $\nu_{\text{op}}(\text{C}=\text{O})_2$ in the range $1661\text{--}1704\text{ cm}^{-1}$. The 1,3,5-trimethyl and 1,3,6-trimethyl analogs exhibit both $\nu_{\text{ip}}(\text{C}=\text{O})_2$ and $\nu_{\text{op}}(\text{C}=\text{O})_2$ at lower frequency in the solid phase than in either CCl_4 or CHCl_3 solution. The frequency separation between $\nu_{\text{ip}}(\text{C}=\text{O})_2$ and $\nu_{\text{op}}(\text{C}=\text{O})_2$ varies between 23 and 80 cm^{-1} in the solid phase.

IMIDES

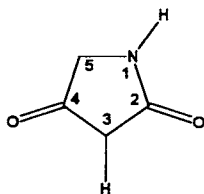
Table 12.16 lists IR vapor-phase data and assignments for imides (1).

The imides exhibit an in-phase [$\nu_{\text{ip}}(\text{C}=\text{O})_2$] and out-of-phase [$\nu_{\text{op}}(\text{C}=\text{O})_2$] stretching vibrations. The $\nu_{\text{ip}}(\text{C}=\text{O})_2$ mode has weaker absorbance than the absorbance for $\nu_{\text{op}}(\text{C}=\text{O})_2$. On this basis $\nu_{\text{ip}}(\text{C}=\text{O})$, and $\nu_{\text{op}}(\text{C}=\text{O})_2$ for diacetamide, $[\text{CH}_3\text{C}(\text{O})]_2\text{NH}$, are assigned at 1738 and 1749 cm^{-1} , respectively, in the vapor phase. All of the other imides included in Table 12.16 exhibit $\nu_{\text{ip}}(\text{C}=\text{O})$, at higher frequency than $\nu_{\text{op}}(\text{C}=\text{O})_2$. For example, N-phenyldibenzamide, $\text{C}_6\text{H}_5(\text{C}=\text{O})_2\text{NC}_6\text{H}_5$, exhibit $\nu_{\text{ip}}(\text{C}=\text{O})_2$ and $\nu_{\text{op}}(\text{C}=\text{O})_2$ at 1801 and 1702 cm^{-1} , respectively.

Succinimides, maleimides, and phthalimides contain 5-membered rings:



hydantoin also contains a similar type imide structure:



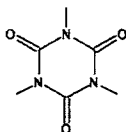
Succinimide exhibits $\nu_{ip}(\text{C}=\text{O})_2$ and $\nu_{op}(\text{C}=\text{O})_2$ at 1820 and 1772 cm^{-1} , respectively, while its N-(2,6-xylyl) analog exhibits $\nu_{ip}(\text{C}=\text{O})_2$ and $\nu_{op}(\text{C}=\text{O})_2$ at 1790 and 1741 cm^{-1} , respectively. In this case, the 2,6-xylyl group can not be coplanar with the $\text{N}(\text{C}=\text{O})_2$ group due to the steric factor of the 2,6-dimethyl groups. The N-alkylmaleimides and N-arylmaleimides exhibit $\nu_{ip}(\text{C}=\text{O})_2$ and $\nu_{op}(\text{C}=\text{O})_2$ in the range 1780–1820 cm^{-1} and 1730–1745 cm^{-1} , respectively.

Phthalimide exhibits $\nu_{ip}(\text{C}=\text{O})_2$ and $\nu_{op}(\text{C}=\text{O})_2$ at 1795 and 1766 cm^{-1} in the vapor phase, respectively. Substitution of a 3-or-4-nitro group raises both $\nu(\text{C}=\text{O})_2$ modes, which most likely is the result of the σ_p and σ_m effect. Substitution of a 3-amino group lowers both modes significantly, and this most likely is the combined effect of intramolecular hydrogen bonding $\text{HNH}\cdots\text{O}=\text{C}$ and the σ_m effect.

N-alkylphthalimides exhibit $\nu_{ip}(\text{C}=\text{O})_2$ and $\nu_{op}(\text{C}=\text{O})_2$ in the range 1771–1789 cm^{-1} and 1734–1740 cm^{-1} , respectively, while the N-aryl analogs exhibit $\nu_{ip}(\text{C}=\text{O})_2$ and $\nu_{op}(\text{C}=\text{O})_2$ in the range 1795–1800 cm^{-1} and 1735–1746 cm^{-1} , respectively.

Hydantoin in the vapor phase exhibits $\nu_{ip}(\text{C}=\text{O})_2$ and $\nu_{op}(\text{C}=\text{O})_2$ at 1826 and 1785 cm^{-1} , respectively. The 5,5-dimethylhydantoin exhibits $\nu_{ip}(\text{C}=\text{O})_2$ at 1811 cm^{-1} and $\nu_{op}(\text{C}=\text{O})_2$ at 1775 cm^{-1} in the vapor phase; however, in the solid phase $\nu_{ip}(\text{C}=\text{O})_2$ occurs at 1779 cm^{-1} , and $\nu_{op}(\text{C}=\text{O})_2$ occurs as a doublet (1744 and 1716 cm^{-1}). Apparently in the solid phase the $\nu_{op}(\text{C}=\text{O})_2$ mode is split by crystalline effects.

The s-triazine (1H,3H,5H)-triones have the basic structure:



and the substituent groups are joined to the N atoms (hydrogen, aliphatic or aromatic groups). For the three compounds recorded in the vapor phase, $\nu_{op}(\text{C}=\text{O})_2$ occurs in the range 1710–1720 cm^{-1} . The $\nu_{ip}(\text{C}=\text{O})_2$ mode for the 1,3-diphenyl-5-octyl analog occurs at 1766 cm^{-1} .

All of these imide type compounds exhibit a weak band in the range 3470–3570 cm^{-1} , which is assigned to the combination tone $\nu_{\text{ip}}(\text{C}=\text{O})_2 + \nu_{\text{op}}(\text{C}=\text{O})_2$. In the vapor phase, imides that contain N–H exhibit a weak band in the range 3415–3455 cm^{-1} assigned to $\nu\text{N}-\text{H}$. In the case of hydantoins, $\nu\text{N}-\text{H}$ occurs in the range 3482–3490 cm^{-1} in the vapor phase, and in the range 3205–3215 cm^{-1} in the solid phase. Of course in the solid phase hydantoins exist in an intermolecular hydrogen-bonded state.

4-BROMOBUTYLPHTHALIMIDE IN SOLUTION

Table 12.17 lists IR data for 4-bromobutylphthalimide in CCl_4 and/or CHCl_3 solutions (19). These data show that as the mole % $\text{CHCl}_3/\text{CCl}_4$ is increased from 0 to 100 both $\nu_{\text{ip}}(\text{C}=\text{O})_2$ and $\nu_{\text{op}}(\text{C}=\text{O})_2$ decrease in frequency. In addition, the $\nu_{\text{op}}(\text{C}=\text{O})_2$ mode decreases more than $\nu_{\text{ip}}(\text{C}=\text{O})_2$ by a factor of ~ 3.5 .

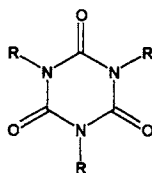
HYDANTOINS

Table 12.18 lists IR data and assignments for hydantoins in the vapor and solid phases. The $\nu\text{N}-\text{H}$ frequencies occur in the range 3485–3495 cm^{-1} in the vapor and in the range 3150–3330 cm^{-1} in the solid phase.

In the vapor phase, $\nu_{\text{ip}}(\text{C}=\text{O})_2$ occurs in the range 1808–1825 cm^{-1} and in the range 1755–1783 cm^{-1} in the solid phase while $\nu_{\text{op}}(\text{C}=\text{O})_2$ occurs in the range 1774–1785 cm^{-1} in the vapor phase and in the range 1702–1744 cm^{-1} in the solid phase. In the four cases where the same hydantoin was studied in both the vapor and solid phases, the frequency separation between $\nu_{\text{ip}}(\text{C}=\text{O})_2$ and $\nu_{\text{op}}(\text{C}=\text{O})_2$ is much less in the vapor phase (34–40 cm^{-1}) than it is in the solid phase (54–66 cm^{-1}).

TRIALLYL-1,3,5-TRIAZINE-2,4,6-(1H,3H,5H) TRIONE

Table 12.19 lists IR data and assignments for triallyl-1,3,5-triazine-2,4,6-(1H,3H,5H) trione in CHCl_3 and/or CCl_4 solutions (20). The empirical structure of this compound is



where R is allyl, and for simplicity we will name this compound T_3one . T_3one has been determined to have D_{3h} symmetry, the $\nu_{\text{ip}}(\text{C}=\text{O})_3$ mode belongs to the E' species, and the $\nu_{\text{ip}}(\text{C}=\text{O})_3$ mode belongs to the A' species. The $\nu_{\text{op}}(\text{C}=\text{O})_3$ mode is doubly degenerate, and is IR active while $\nu_{\text{ip}}(\text{C}=\text{O})_3$ is Raman active. T_3one in 1% wt./vol. CCl_4 solution exhibits a strong Raman band at 1761.2 cm^{-1} , at 5% wt./vol. CCl_4 solution at 1762.3 cm^{-1} , and at 10% wt./vol.

CCl_4 solution at 1763.0 cm^{-1} . In CHCl_3 solutions at the same % wt./vol. concentrations, strong Raman bands occur at 1758.3 , 1760.5 , and 1761.4 cm^{-1} , respectively. Therefore, in both CCl_4 and CHCl_3 solution the Raman band increases in frequency with an increase in the % wt./vol. T_3one . A corresponding IR band is not observed, and this Raman band is assigned as $\nu_{\text{ip}}(\text{C}=\text{O})_3$.

In the case of $\nu_{\text{op}}(\text{C}=\text{O})_3$ for T_3one , 1 and 5% vol./wt. solutions in CCl_4 show that it decreases in frequency from 1698.6 cm^{-1} to 1698.5 cm^{-1} while at these same concentrations in CHCl_3 it decreases from 1695.7 cm^{-1} to 1695.5 cm^{-1} .

The $\nu_{\text{op}}(\text{C}=\text{O})_3$ mode for T_3one decreases in a nonlinear manner as the mole % $\text{CHCl}_3/\text{CCl}_4$ is increased from 0 to 100 as shown in Figure 12.8. These data indicate that different $\text{T}_3\text{one} \cdots (\text{HCCl}_3)_n$ complexes are formed as the mole % $\text{CHCl}_3/\text{CCl}_4$ is increased, and that in general the $\nu_{\text{op}}(\text{C}=\text{O})_3$ frequency decreases with increase in the mole % $\text{CHCl}_3/\text{CCl}_4$ are due to the dielectric effect of each particular solvent system.

A strong IR band assigned to $\nu_{\text{op}}(\text{C}_3\text{N}_3)$ is assigned in the region $1455.2\text{--}1458.6\text{ cm}^{-1}$. This mode increases in frequency in almost a linear manner as the mole % $\text{CHCl}_3/\text{CCl}_4$ is increased (see Figure 12.9).

The allyl groups in T_3one exhibit three characteristic frequencies. The $\nu\text{C}=\text{C}$ mode is not affected by change in the solvent system, as it occurs at 1645.4 cm^{-1} . On the other hand, the $\text{C}=\text{CH}_2$ wag mode decreases in frequency in a nonlinear manner as the mole % $\text{CHCl}_3/\text{CCl}_4$ is increased (see Figure 12.10).

Table 12.20 lists IR data and assignments for T_3one in 1% wt./vol. solutions in various solvents (20). In these 18 solvents, $\nu_{\text{op}}(\text{C}=\text{O})_3$ ranges from 1703.2 cm^{-1} in hexane to 1693.3 cm^{-1} in dimethyl sulfoxide. In the case of the four alcohols, $\nu_{\text{op}}(\text{C}=\text{O})_3$ exhibits both $\nu_{\text{op}}(\text{C}=\text{O})_3$ and $\nu_{\text{op}}(\text{C}=\text{O})_3 \cdots \text{HOR}$. The former occurs in the range $1701.5\text{--}1703.5\text{ cm}^{-1}$ and the latter in the range $1688\text{--}1690.6\text{ cm}^{-1}$. Figure 12.11 shows a plot of the $\nu_{\text{op}}(\text{C}=\text{O})_3$ frequency for T_3one vs the solvent acceptor number (AN). The solid triangles show the data points for the $\text{T}_3\text{one} \cdots \text{HOR}$ molecules; the solid squares show the data points for T_3one molecules not intermolecularly hydrogen bonded in solution surrounded by intermolecularly hydrogen-bonded alcohol molecules. Projecting these points onto the broad linear line shows that the AN values for the alcohols when not hydrogen bonded to solvent molecules are very similar to the AN values for alkyl ethers. The AN values are not a precise measure of the solute-solvent interaction, as they do not accurately account for steric effects between solute and solvent, or do not distinguish between molecules that are or are not intermolecularly hydrogen bonded (20).

REFERENCES

1. Nyquist, R.A. (1984). *The Interpretation of Vapor-phase Infrared Spectra: Group Frequency Data*, Philadelphia: Sadtler Research Laboratories, Division of Bio-Rad Inc.
2. Richards, R.E. and Thompson, H.W. (1947). *J. Chem. Soc. London*, 1248.
3. Brown, T.L., Regan, J.E., Scheutz, D.R., and Sternberg, J. (1959). *J. Phys. Chem.*, **63**, 1324.
4. Lin-Vien, D., Cotthrup, N.B., Fateley, W.G., and Grasselli, J.G. (1991). *The Handbook of Infrared and Raman Characteristic Frequencies of Organic Molecule*, San Diego: Academic Press, Inc.
5. McLachlan, R.D. and Nyquist, R.A. (1964). *Spectrochim. Acta*, **20**, 1397.
6. Nyquist, R.A. (1963). *Spectrochim. Acta*, **19**, 509.

7. Nyquist, R.A. (1963). *Spectrochim. Acta*, **19**, 1595.
8. Russell, R.A. and Thompson, H.W. (1956). *Spectrochim. Acta*, **8**, 138.
9. Moccia, R. and Thompson, H.W. (1957). *Spectrochim. Acta*, **10**, 240.
10. Klemperer, W., Cronyn, M., Maki, A., and Pimentel, G. (1954). *J. Am. Chem. Soc.*, **76**, 5846.
11. Thompson, H.W. and Jameson, D.A. (1958). *Spectrochim. Acta*, **13**, 236.
12. Nyquist, R.A., Chrisman, R.W., Putzig, C.L., Woodward, R.W., and Loy, B.R. (1979). *Spectrochim. Acta*, **35A**, 91.
13. Nyquist, R.A. and Luoma, D.A. (1991). *Appl. Spectrosc.*, **45**, 1501.
14. Nyquist, R.A. and Luoma, D.A. (1991). *Appl. Spectrosc.*, **45**, 1491.
15. Nyquist, R.A. and Luoma, D.A. (1991). *Appl. Spectrosc.*, **45**, 1497.
16. Nyquist, R.A., Putzig, C.L., and Clark, T.D. (1996). *Vib. Spectrosc.*, **12**, 81.
17. Gutmann, V. (1978). *The Donor-acceptor Approach to Molecular Interactions*, p. 29, New York: Plenum Press.
18. Nyquist, R.A. and Fiedler, S.L. (1995). *Vib. Spectrosc.*, **8**, 365.
19. Nyquist, R.A. (1990). *Appl. Spectrosc.*, **44**, 215.
20. Nyquist, R.A., Puehl, C.W., and Putzig, C.L. (1993). *Vib. Spectrosc.*, **4**, 193.

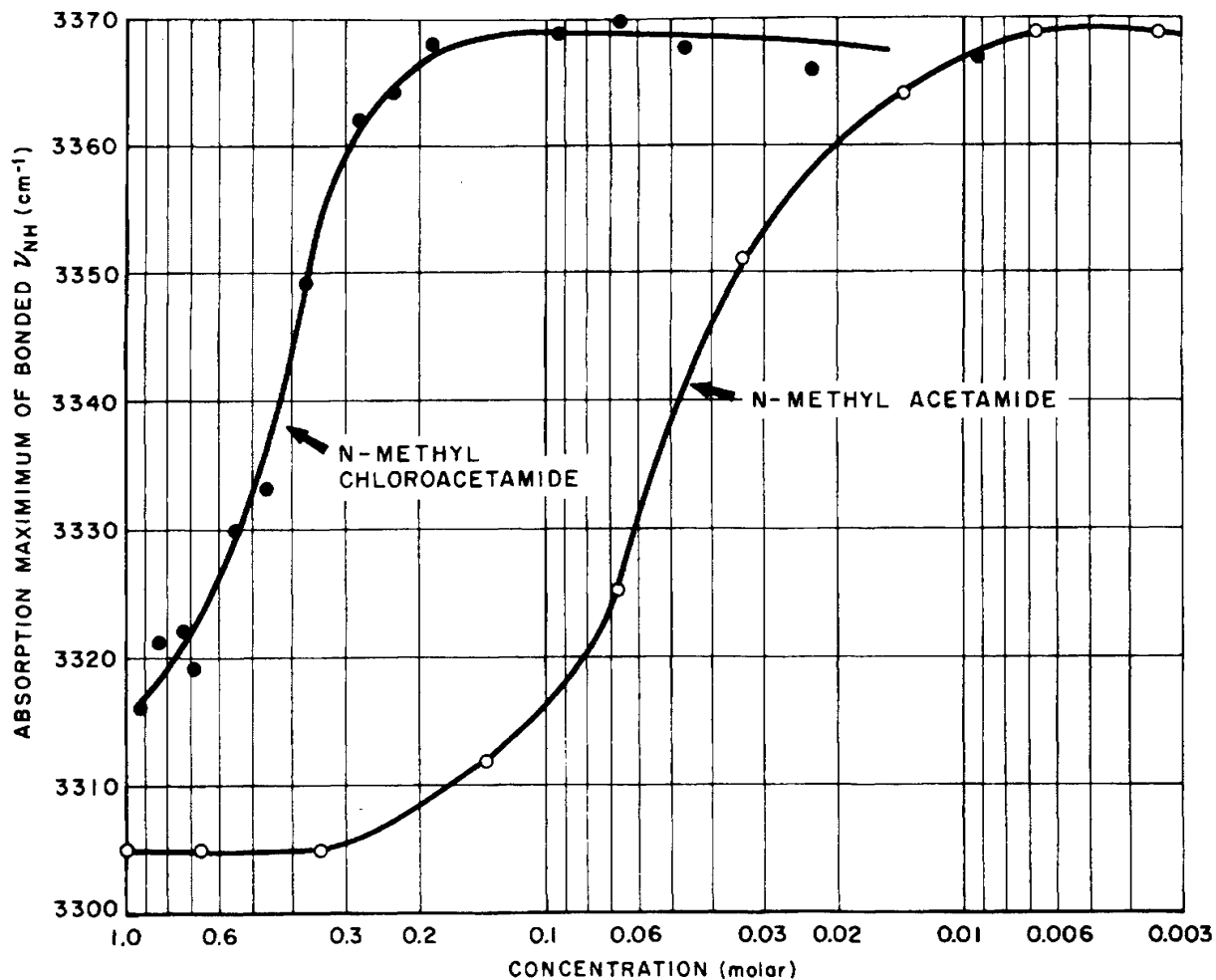


FIGURE 12.1 Plots of the $\nu_{N-H \cdots O=C}$ frequencies for N-methylacetamide and N-methyl chloroacetamide vs the absorption maximum at each of the $\nu \cdots O=C$ frequencies.

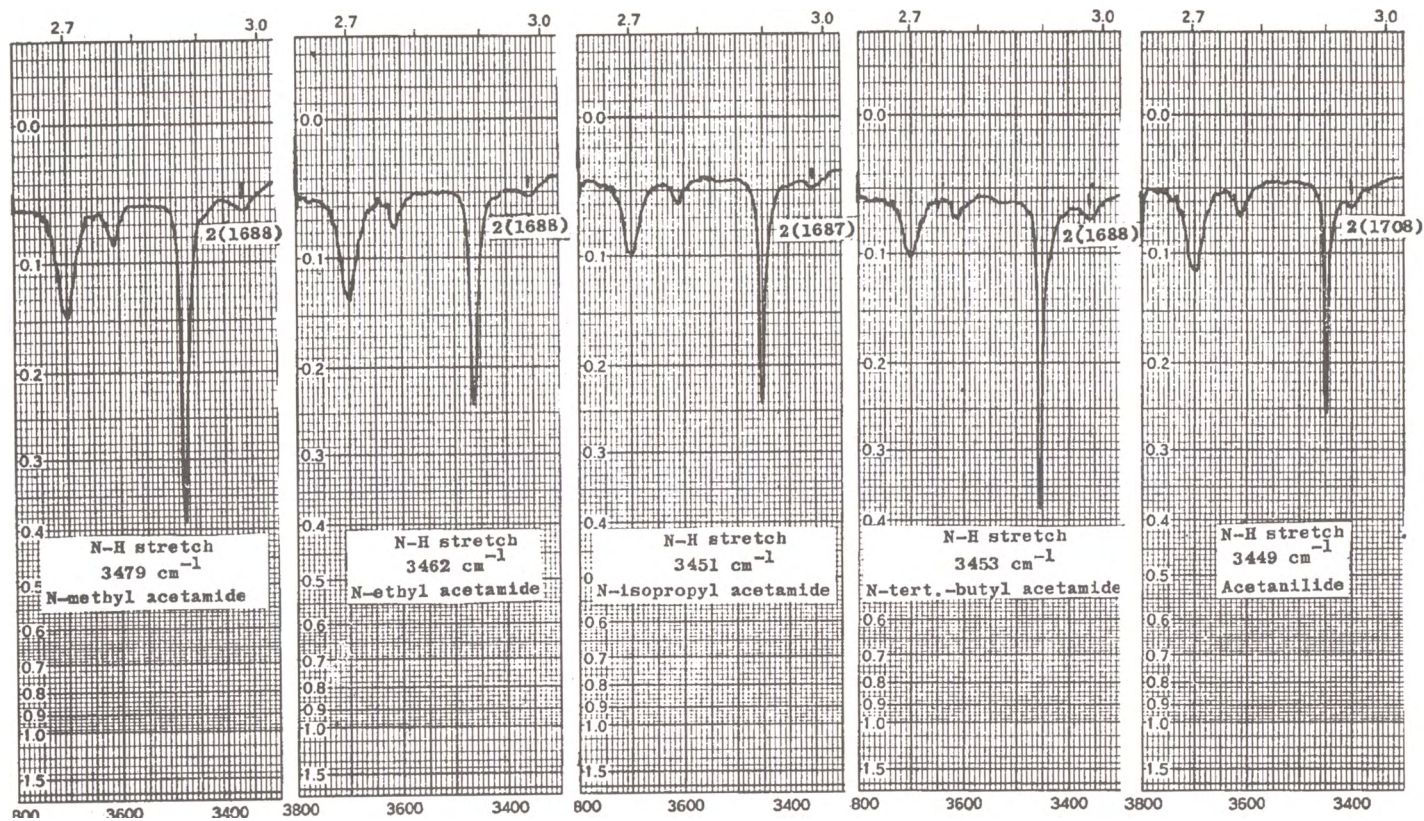


FIGURE 12.2 IR spectra of N-methyl acetamide, N-ethyl acetamide, N-isopropyl acetamide, N-tert-butyl acetamide, and acetanilide in CCl_4 solution in the region $3800\text{--}3300 \text{ cm}^{-1}$.

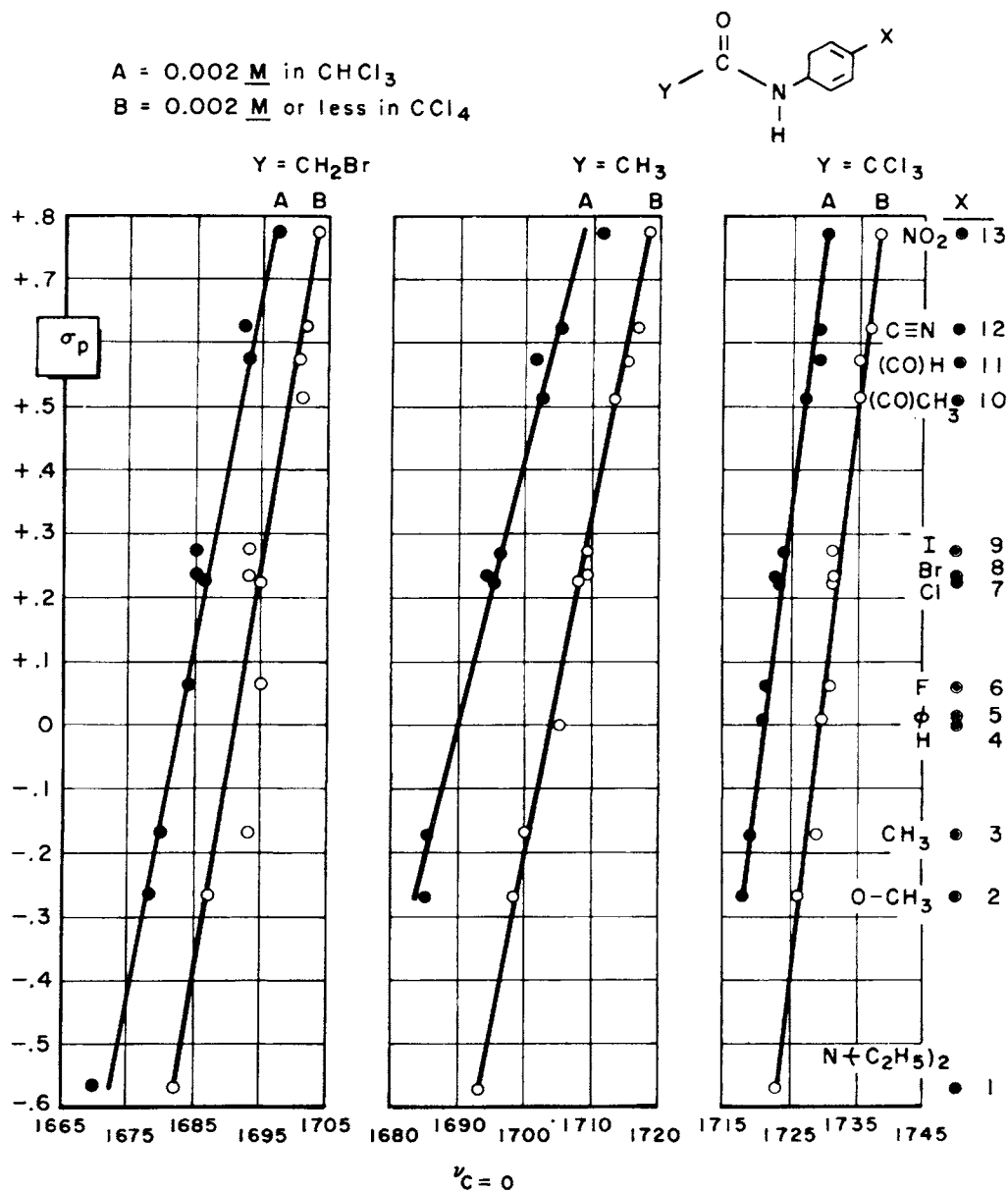


FIGURE 12.3 Plots of the $\nu_{\text{C}=\text{O}}$ frequencies for α -bromo-*p*-x-acetanilide, *p*-x-acetanilide, and α,α,α -trichloro-*p*-x-acetanilide in 0.002 M solutions or less in CCl_4 and CHCl_3 vs Hammett σ_p values.

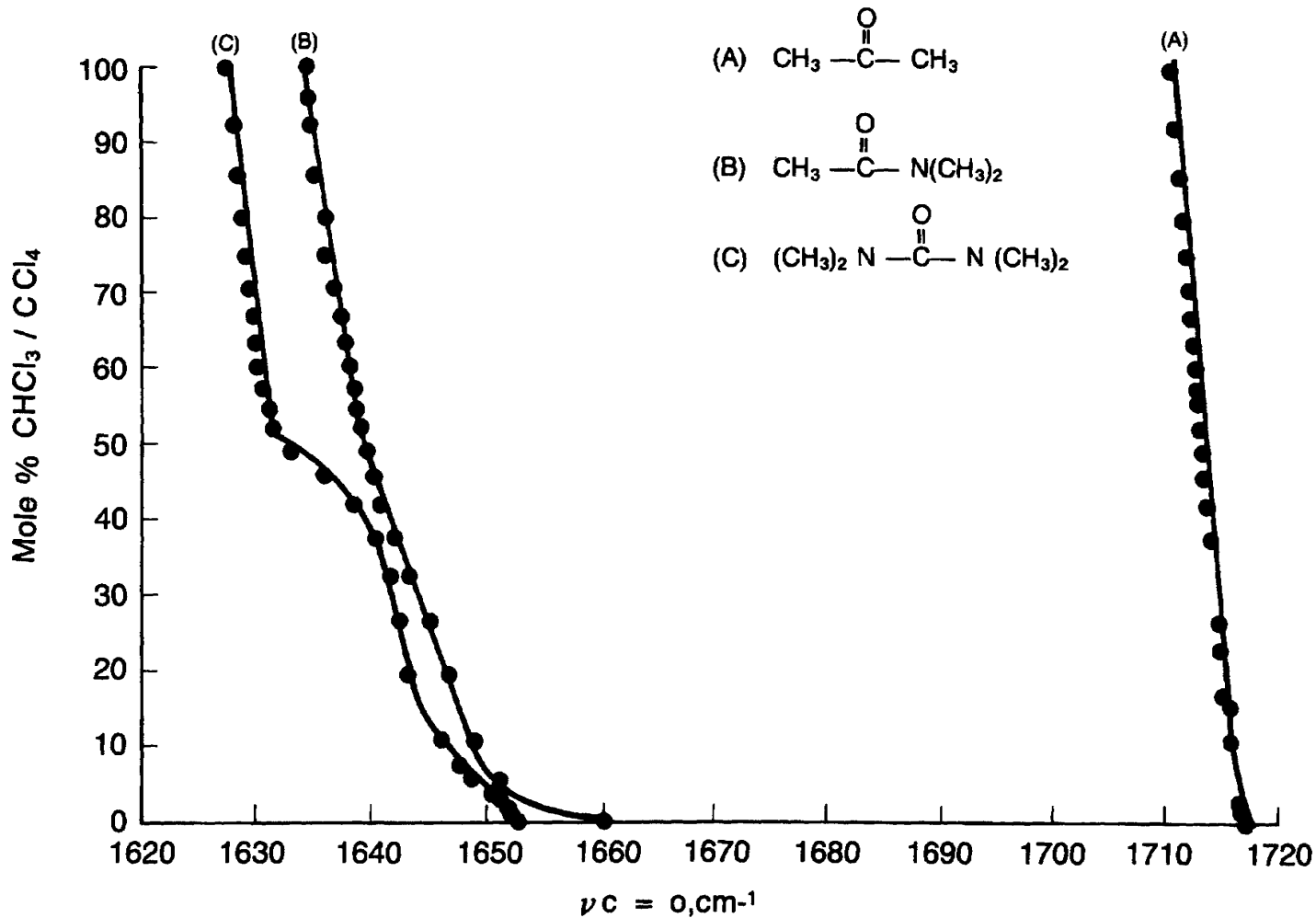


FIGURE 12.4 Plots of $\nu_{\text{C}=\text{O}}$ for 1% wt./vol. solutions of acetone, dimethylacetamide, and tetramethylurea vs mole % $\text{CHCl}_3/\text{CCl}_4$.

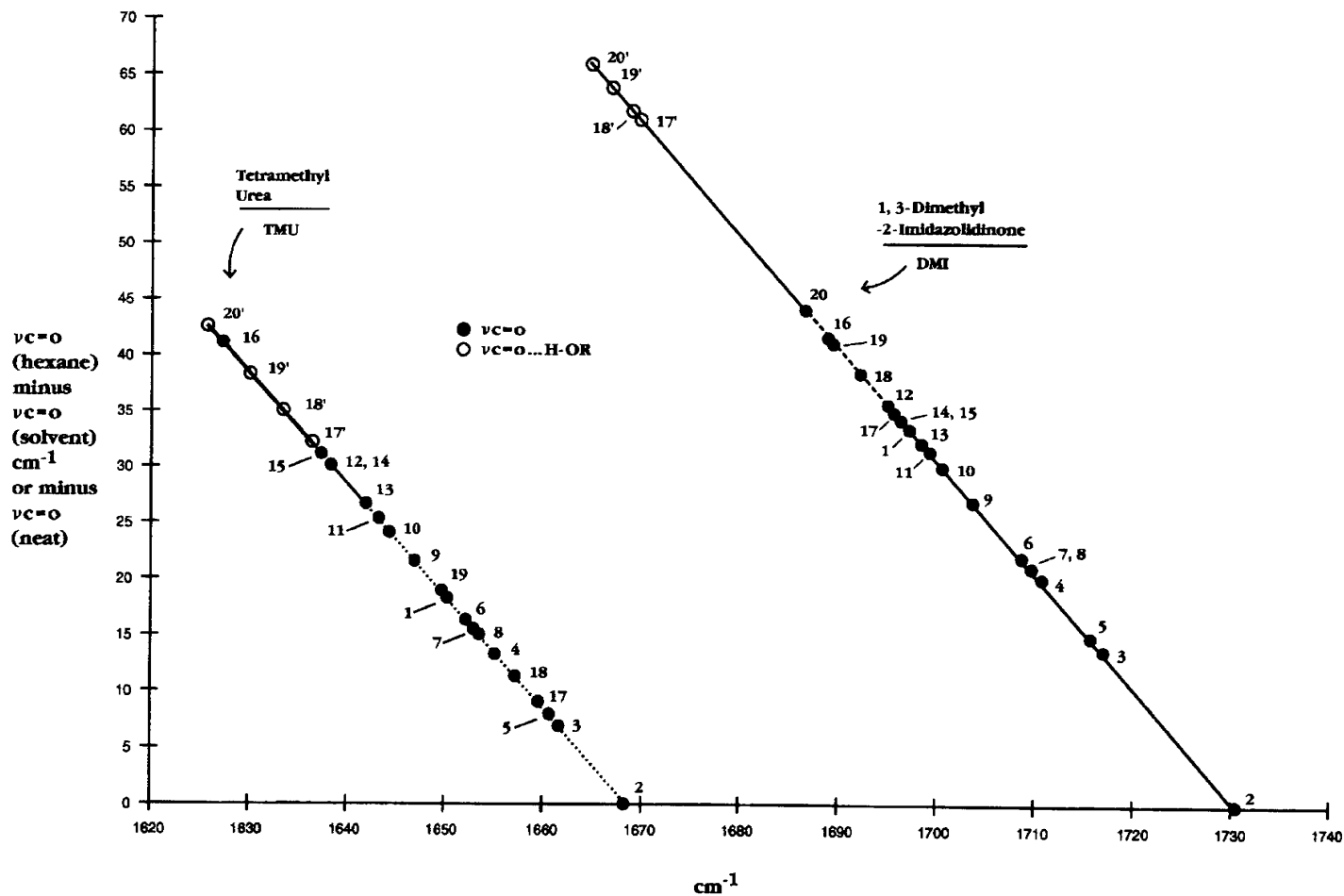


FIGURE 12.5 Plots of $\nu_{C=O}$ of 1,3-dimethyl-2-imidazolidinone (DMI) and 1,1,3-tetramethylurea (TMU) in the neat phase or in 1 of the 19 solvents vs $\nu_{C=O}(\text{hexane}) - \nu_{C=O}(\text{solvent})$.

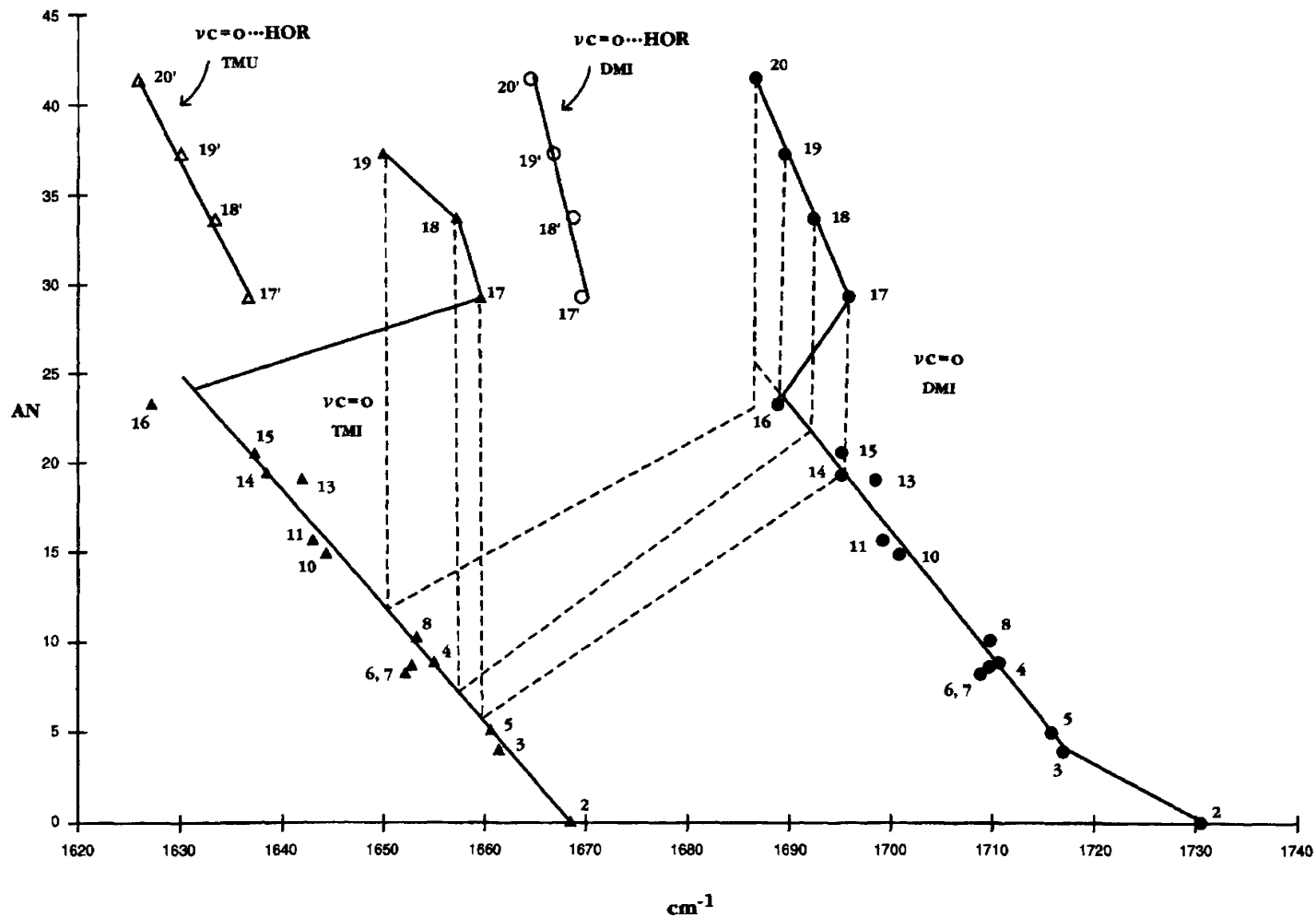
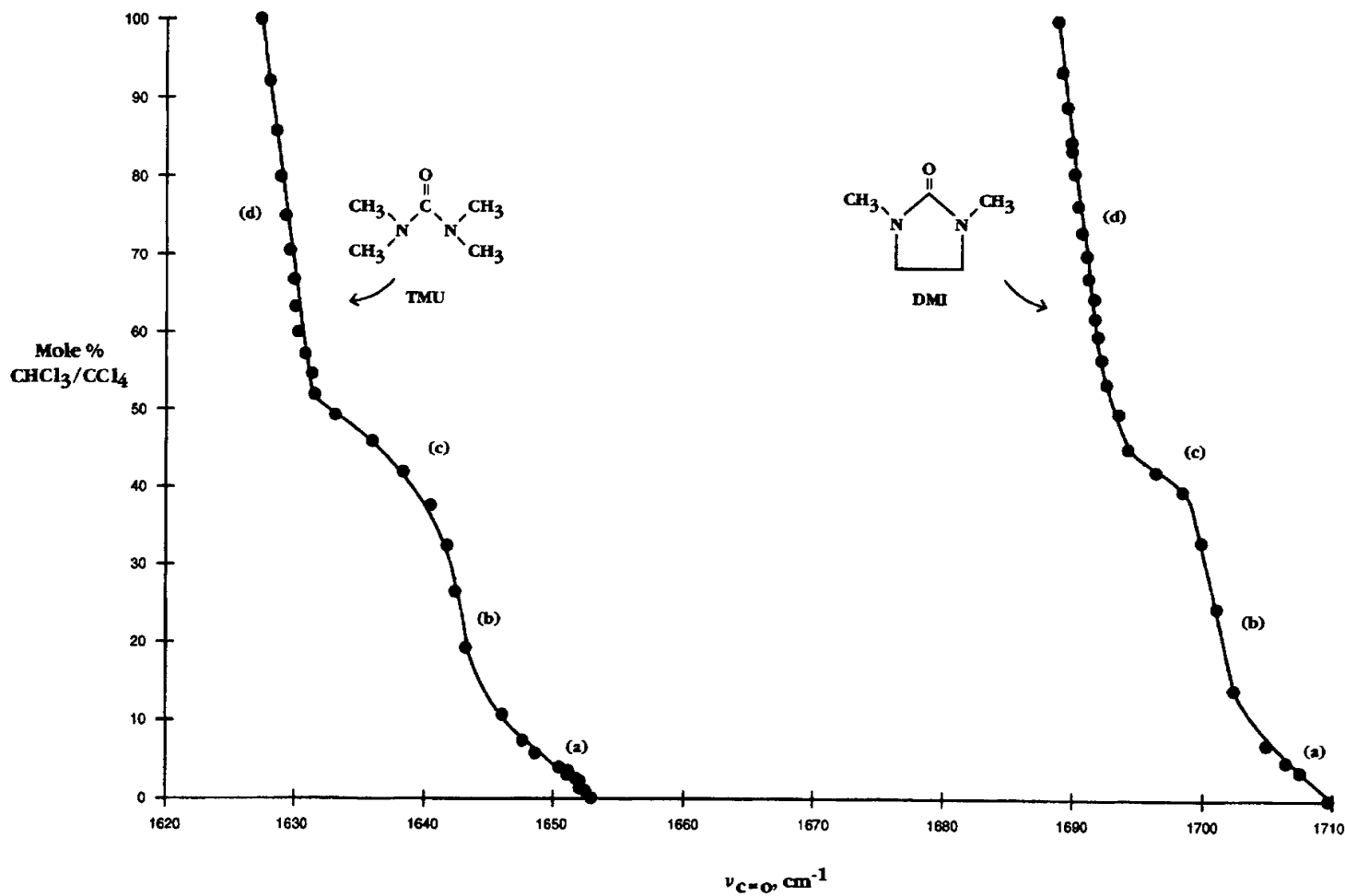


FIGURE 12.6 Plots of $\nu_{\text{C=O}}$ for 1,1,3,3-tetramethylurea (TMU) and 1,3-dimethyl-2-imidazolidinone (DMI) vs the solvent acceptor number (AN).

FIGURE 12.7 Plots of $\nu_{\text{C=O}}$ for 1,1,3,3-tetramethylurea (TMU) and 1,3-dimethyl-2-imidazolidinone (DMI) vs mole % CHCl₃/CCl₄.

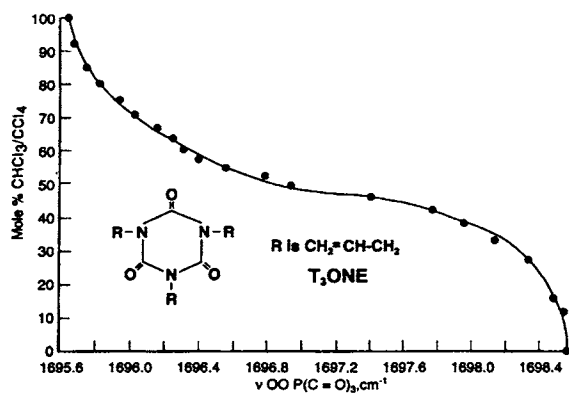


FIGURE 12.8 A plot of $\nu_{op}(C=O)_3$ for triallyl-1,3,5-triazine-2,4,6-(1H,3H,5H) trione (T_3 one) vs mole % $\text{CHCl}_3/\text{CCl}_4$.

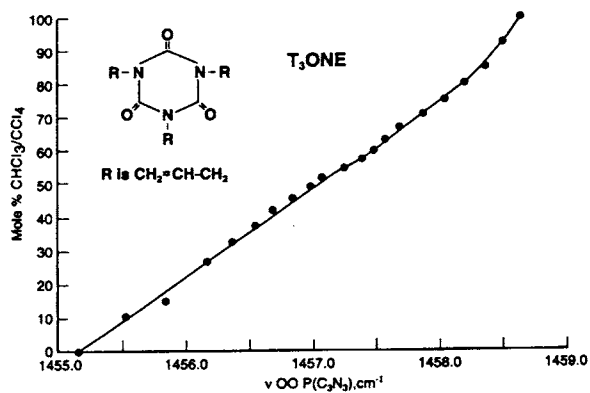


FIGURE 12.9 A plot of $\nu_{op}(C_3N_3)$ for triallyl-1,3,5-triazine-2,4,6-(1H,3H,5H) trione (T_3 one) vs mole % $\text{CHCl}_3/\text{CCl}_4$.

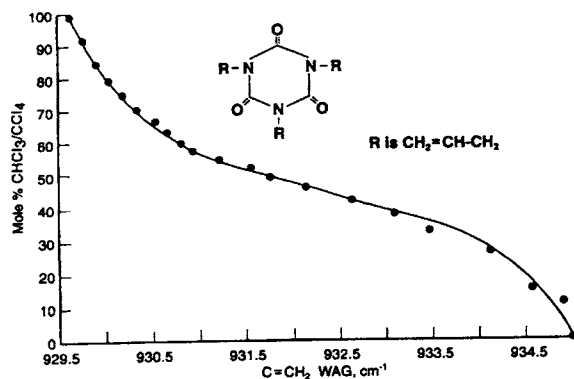


FIGURE 12.10 A plot of $\text{C}=\text{CH}_2$ wag for triallyl-1,3,5-triazine-2,4,6-(1H,3H,5H) trione (T_3 one) vs mole % $\text{CHCl}_3/\text{CCl}_4$.

TABLE 12.1 A comparison of primary, secondary, and tertiary amides in various physical phases

Primary amide assignments	Vapor phase [Ref. 1] R-(C=O)NH ₂ cm ⁻¹	Vapor phase [Ref. 1] C ₆ H ₅ -(C=O)NH ₂ cm ⁻¹	Neat phase nonbonded [Refs. 2,3,4] cm ⁻¹	Intermolecular H-bonded [Refs. 2,3,4] cm ⁻¹
asym.NH ₂ str.	3548–3565	3556–3540	ca.3520	3350–3475
sym.NH ₂ str.	3430–3444	3435–3448	ca.3400	3160–3385
C=O str.	1732–1780	1719–1731* ¹	1675–1715	1640–1680
NH ₂ bending	1576–1600	1586–1600	1585–1620	1620–1640
C–N str.	1308–1400	1341–1355	1390–1430	1390–1430
NH ₂ rock			1100–1150	1100–1150
NH ₂ wag				600–750* ²
N–C=O in-plane bend			550–600	550–600
Secondary amide assignments	Vapor phase* ³		Neat phase nonbonded cm ⁻¹	H-bonded cm ⁻¹
NH str.,trans	3416–3419		3400–3490	3300
cis			3200	
[5 M.R.]* ⁴	3478			
[6 M.R.]	3438			
[7 M.R.]	3442			
C=O str.	1698–1720		1650–1700	1630–1680
C=O str.[4 M.R.]				1730–1780
C=O str.[5 M.R.]	1759			1700–1750
C=O str. [6 M.R.]	1715			
C= str. [7 M.R.]	1711			
CNH str.-bend,trans			1500–1550	1510–1570
,cis			ca. 1450	1400–1490
CNH str.-open,trans			1200–1250	1250–1310
,cis			ca.1350	1310–1350
Tertiary amide assignments				
C=O str.	1671–1731		1630–1680	

*¹ See text.*² Broad.*³ See text.*⁴ M.R. = membered ring or lactam.

TABLE 12.1A The NH stretching frequencies and absorbance data for N-methyl acetamide in concentration ranging from 1.37×10^{-3} to 1.37 mol/liter in CCl_4 solution

Concentration mole/liter N-methylacetamide	N-H str.	A	Band halfwidth	% Bonded	Apparent intensity $B' \times 10(7)$
0.00137	3476	0.199	6.8	0	3.6
0.00342	3475	0.426	7	11	3.2
0.00685	3475	0.81	7.1	15	3
0.0137	3475	1.48	7.1	19	2.9
0.0342	3475	2.87	7.4	27	2.2
0.685	3474	3.99	7.3	56	1.6
0.137	3474	4.93	7.4	73	0.96
0.342	3472	6.63	7.4	86	0.52
0.685	3472	7.1	7.1	92	0.28
1.027	3471	8.1	7.4	94	0.21
1.37	3471	8.88	7.4	95	0.17
N-methyl chloroacetamide					
0.00921	3450	0.197	6.4	1	4.9
0.023	3450	0.479	6.4	4	4.8
0.046	3450	0.897	6.4	10	4.5
0.0681	3451	1.28	6.5	12	4.4
0.0921	3450	1.63	6.9	12	4.4
0.184	3450	2.6	7.2	26	3.7
0.23	3450	3.04	7.5	28	3.6
0.276	3449	3.41	7.5	33	3.3
0.368	3449	3.86	8	39	3.6
0.46	3449	3.97	8.2	50	2.5
0.553	3449	4.31	8.5	52	2.4
0.691	3448	4.37	9.1	58	2.1
0.727	3448	4.65	9.1	58	2.1
0.829	3447	4.89	9.2	61	2
0.921	3448	4.95	9.3	64	1.8

TABLE 12.1B The NH stretching, C=O stretching, amide II, and amide III frequencies for N-methyl acetamide in CHBr_3 solutions

Concentration mole/liter [CHBr_3] N-methylacetamide	N-H str.	N-H str. bonded	C=O str.	Amide II	Amide III
0.00685	3456		1668	1531	1278
0.027	3456		1668	1531	1279
0.137	3457		1668	1532	1278
0.685	3457	3325	1660	1537,1560	1279
2.05	3454	3320	1656	1561	1279
2.74	3451	3305	1649	1563	1279

TABLE 12.1C The overtone for amide II of N-methyl acetamide and N-methyl chloroacetamide in varying concentrations in CCl₄ solutions

Concentration mole/liter [CCl ₄]	2(amide II)	A	Band halfwidth	Intensity B×10(8)
N-methyl acetamide				
0.342		0.02	30	0.6
0.0685	3102	0.059	28	9
0.137	3103	0.206	30	16
0.342	3104	0.775	30	25
0.685	3105	1.65	31	26
1.027	3104	2.76	30	29
1.37	3105	3.55	30	28
N-methyl chloroacetamide				
0.276	3098	0.049	26	1.7
0.46	3098	0.33	26	6.7
0.553	3098	0.46	26	7.8
0.727	3098	0.82	27	10.5
0.829	3099	0.93	27	11
0.921	3099	1.38	28	15

TABLE 12.2 IR data and assignments for N-alkyl acetamides, and N-alkyl α -substituted acetamides in dilute solutes

Compound acetamide	N-H str.	A* ¹	C=O str.	2(C=O str.) or cis N-H str.	N-H bending	CCN str.
N-methyl	3478	21.5	1688	3365		
N-ethyl	3462	16.2	1688	3360		
N-propyl	3461	18.5	1690	3360		
N-n-butyl	3460	18.1	1688	3360		
N-isobutyl	3471	21.7	1689	3365		
N-isopropyl [vapor]	3460(0.051)		1714(1.240)	3420(0.020)	1490(0.803)	1244(0.372)
N-isopropyl	3451	18.9	1687	3360		
N-s-butyl	3450	23.2	1685	3360		
N-t-butyl	3453	25.4	1688	3360		
N-phenyl	3449	34.6	1708	3400		
α -chloro-acetamide						
N-n-butyl	3433	30.9	1684	3348		
N-isopropyl	3429		1682	3345		
N-s-butyl	3422		1680	3335		
N-t-butyl	3421	38.5	1684	3350		
N-phenyl	3409	56	1692	3350		
α,α -dichloroacetamide						
N-ethyl	3441	47.8	1707	3383		
N-propyl	3439	39.9	1706	3382		
N-n-butyl	3439	43.4	1705	3395		
N-isopropyl	3430	40.8	1703	3385		
N-t-butyl	3427	31.6	1702	3365		
N-phenyl	3419	51.3	1713	3400		
α,α,α -trichloroacetamide						
N-methyl	3462	58.9	1728			
N-ethyl	3449	45.4	1725			
N-propyl	3448	45.5	1724			
N-butyl	3445	41.6	1726			
n-isobutyl	3451	44.2	1725			
N-isopropyl	3439	39.3	1725			
N-s-butyl	3438	36	1724			
N-t-butyl[vapor]	3444(0.190)		1743(1.230)		1505(1.230)	1244(0.451)
N-t-butyl	3435	39.9	1725			
N-phenyl	3425	51.8	1731			
α -bromo-acetamide						
N-ethyl	3435	29.8	1680			
N-propyl	3432	30.9	1680			
N-n-butyl	3432	31.2	1681			
N-isobutyl	3433	32	1680			
N-isopropyl	3422	30.2	1679			
N-s-butyl	3420	30.6	1679			
N-t-butyl	3419	26.2	1680			

(continued)

TABLE 12.2 (continued)

Compound acetamide	N-H str.	A* ¹	C=O str.	2(C=O str.) or cis N-H str.	N-H bending	CCN str.
<i>α,α</i> -dibromo-acetamide						
N-methyl	3450	35.8	1701			
N-ethyl	3439	32.7	1700			
N-propyl	3438	30.5	1700			
N-n-butyl	3437	303.4	1700			
N-isobutyl	3440	30.2	1700			
N-isopropyl	3427	26.8	1699			
N-s-butyl	3422	26.8	1698			
N-t-butyl	3425	25.5	1701			
<i>α,α,α</i> -tribromoacetamide						
N-ethyl	3441	35.4	1712			
N-isopropyl	3430	28.2	1710			
N-t-butyl	3429	27.4	1717			
<i>α,α,α</i> -trifluoroacetamide						
N-methyl	3470	51.6	1741			
N-ethyl	3454	49.5	1736			
N-propyl	3456	46.6	1738			
N-n-butyl	3454	44.9	1736			
N-isobutyl	3456	56	1738			
N-isopropyl	3447	43.2	1735			
N-s-butyl	3443	38	1733			
N-t-butyl	3446	37.4	1736			
<i>α</i> -methoxy-acetamide						
N-ethyl	3438	30.7	1689			
N-propyl	3439	28.7	1690			
N-isobutyl	3440	38.3	1690			
N-isopropyl	3427	32	1687			
N-s-butyl	3422	31.1	1685			
N-t-butyl						
<i>α</i> -phenoxy acetamide						
N-ethyl	3446	35.5	1691			
N-propyl	3447	35.6	1692			
N-n-butyl	3446	32.9	1691			
N-isobutyl	3449	35.2	1692			
N-isopropyl	3430	32.7	1688			
N-s-butyl	3430	29.4	1688			
N-t-butyl	3428	28.4	1689			

TABLE 12.2A The NH stretching frequencies for N-alkyl acetamides, N-alkyl X-halo, X,X-dihalo-, X,X,X-trihaloacetamides, and N-alkyl methoxyacetamide in CCl₄ solutions

Compound [10%(wt./vol.) or saturated*] or [2%* ¹] [CCl ₄]	N-H str.	N-H str. H-bonded	N-H str [corrected for ER.]	delta N-H str.	A (bonded)/ A (unbonded)
Acetamide N-alkyl					
ethyl*	3460	3300	3285	175	2.2
isobutyl*	3460	3288	3265	195	11
isopropyl*	3434	3280	3264	175	2.4
t-butyl*	3450	3303	3277	173	5.7
Bromoacetamide N-alkyl					
ethyl	3433	3299	3280	153	3.2
propyl	3430	3291	3268	162	4
butyl	3430	3294	3270	160	2.9
isopropyl	3420	3290	3269	151	2.7
t-butyl	3420	3272	148	148	0.7
Trifluoroacetamide N-alkyl					
methyl	3460	3325	3311	149	4.3
ethyl	3446	3310	3297	149	3.7
propyl	3451	3315	3305	146	3.5
isobutyl	3451	3320	3307	144	2.8
isopropyl	3440	3311	3295	148	2.3
s-butyl	3439	3310	3296	143	2.4
t-butyl	3438	3340	3313	125	0.6
Trichloroacetamide N-alkyl					
methyl*	3459	3390		69	0.15
ethyl	3443	3360		83	0.3
propyl	3442	3358		84	0.3
butyl	3447	3360		87	0.27
isobutyl	3448	3369		79	0.18
isopropyl	3437	3360		77	0.14
s-butyl	3430	3352		78	0.1
t-butyl	3433	3370		63	0.01
Dibromoacetamide N-alkyl					
ethyl* ¹	3439	3354		85	0.17
propyl* ¹	3437	3355		82	0.2
butyl* ¹	3433	3355		78	0.17
isobutyl* ¹	3440	3368		72	0.14
isopropyl*	3420	3360		60	0.04
s-butyl* ¹	3419	3343		76	0.17
Methoxyacetamide N-alkyl					
ethyl	3433	3345		88	0.3

(continued)

TABLE 12.2A (continued)

Compound [10%(wt./vol.) or saturated*] or [2%* ¹] [CCl ₄]	N-H str.	N-H str. H-bonded	N-H str [corrected for ER.]	delta N-H str.	A (bonded)/ A (unbonded)
propyl	3431	3345		86	0.35
butyl	3438	3351		87	0.31
isobutyl	3439	3351		88	0.27
isopropyl	3421	3335		86	0.19
s-butyl	3422	3335		86	0.18
t-butyl	3418	3352		66	0.07
Phenoxyacetamide N-alkyl					
ethyl	3441	3349		92	0.3
propyl	3445	3354		91	0.3
isobutyl	3444	3356		88	0.24
isopropyl	3439	3352		87	0.21
s-butyl	3430	3340		90	0.2
t-butyl	3430	3355		75	0.05

*saturated at 2% in CCl₄.

TABLE 12.3 IR data for N-alkyl α -substituted acetamides in 10% wt./vol. CCl₄ and 0.002 M CCl₄ solutions

Compound	C=O str. 10% (wt./vol.) [CCl ₄]	c=O str. (0.002 M) [CCl ₄]	delta C=O str.	Amide II	2(amide II)
Bromoacetamide N-alkyl					
ethyl	1668	1680	12	1525,1555	3090
propyl	1666	1680	14	1545	3087
butyl	1666	1681	15	1540	3086
isopropyl	1664	1680	16	1521,1552	3081
t-butyl	1674	1680	6	1522,1550	3071
Trifluoroacetamide N-alkyl					
ethyl	1724	1741	17	1564	3120
ethyl	1716	1736	20	1553	3100
propyl	1720	1738	18	1555	3109
isobutyl	1720	1738	18	1554	3108
isopropyl	1716	1735	19	1548	3094
s-butyl	1715	1733	18	1550	3099
t-butyl	1722	1736	14	1530	3076
Trichloroacetamide N-alkyl					
ethyl	1712	1725	13	1518	
propyl	1712	1724	12	1518	
butyl	1713	1726	13	1520	
isobutyl	1717	1725	8	1520	
isopropyl	1714	1721	7	1512	
s-butyl	1715	1724	9	1512	
t-butyl	1725	1725	0	1509	
Methoxyacetamide N-alkyl					
ethyl	1678	1689	11	1532	
propyl	1678	1690	12	1530	
isobutyl	1682	1690	8	1531	
isopropyl	1675	1687	12	1522	
s-butyl	1680	1685	5	1524	
t-butyl	1685	1690	5	1523	
Phenoxyacetamide N-alkyl					
ethyl	1683	1691	8	1531	
propyl	1684	1692	8	1531	
isobutyl	1688	1692	4	1533	
isopropyl	1686	1688	2	1527	
s-butyl	1684	1688	4	1524	
t-butyl	1690	1689	-1	1527	

TABLE 12.4 A comparison of primary and secondary amides in the solid phase

Compound solid [KBr pellet]	asym.NH ₂ str. cm ⁻¹	sym.NH ₂ str. cm ⁻¹	C=O str. cm ⁻¹	NH ₂ bending cm ⁻¹	Gama NH ₂ cm ⁻¹
H ₂ N-C=OCH ₃	3310	3160	1686	1652	720
H ₂ N-C=OCH ₂ Cl	3380	3180	1650	1620	645
H ₂ N-C=OCHCl ₂	3320	3150	1670	1625	?
H ₂ N-C=OCH ₂ -OCH ₃	3380	3195	1635	1645	725
H ₂ N-C=OC ₆ H ₅	3362	3170	1659	1625	650
H ₂ N-C=OC ₆ H ₄ (2-OH)	3398	3185	1661	1629	615
	NH:O=C cm ⁻¹	c=O:HN cm ⁻¹	N-H bending cm ⁻¹		
4-CH ₃ C ₆ H ₄ -NH-C=OCH ₃	3295	1660	1530		
C ₆ H ₅ -NH-C=OC ₂ H ₅	3242	1660	1546		
C ₆ H ₅ -NH-C=OC ₃ H ₇ -iso	3300	1664	1550		
C ₆ H ₅ -NH-C=OC ₆ H ₅	3339	1648	1525		
CH ₃ -NH-C=OC ₆ H ₅	3340	1635	1546		

TABLE 12.4A A comparison of IR data for tertiary amides in the neat or solid phase

Compound	Phase	C=O str. cm ⁻¹
(C ₂ H ₅) ₂ N-C=OH	neat	1665
(C ₂ H ₅)(C ₆ H ₅)N-C=OH	neat	1670
(C ₆ H ₅) ₂ N-C=OH	KBr pellet	1690
(C ₆ H ₅)(CH ₃)N-C=OCH ₃	KBr pellet	1659
(C ₆ H ₅)(C ₂ H ₅)-C=OCH ₃	KBr pellet	1650
(C ₆ H ₅) ₂ N-C=OCH ₃	film	1670
(C ₆ H ₅)N-C=O(CH ₂) ₃	melt	1685*
(C ₄ H ₉) ₂ N-C=OCH ₃	neat	1640
(C ₂ H ₅) ₂ N-C=OC ₂ H ₅	neat	1636
(C ₄ H ₉) ₂ N-C=OC ₂ H ₅	neat	1635
(CH ₃) ₂ N-C=OC ₃ H ₇	neat	1634
(C ₂ H ₅) ₂ N-C=OC ₃ H ₇	neat	1634
(CH ₃) ₂ N-C=OC ₁₁ H ₂₃	neat	1650
1,2-C ₆ H ₄ (C=O-N(C ₂ H ₅) ₂) ₂	neat	1625

* 5-Membered ring.

TABLE 12.5 A comparison of Raman data and assignments for acrylamide, methacrylamide, and their polymers

Compound	A.M.W.	C=O str.	C=O str. monomer C=O str. polymer	C=C str.	C=O str. C=C str.	RI C=O str./ RI C=C str.	C=O str. Acrylamide C=O str. N-alkyl or N,N-dialkyl- acrylamide	Acrylamide C=O str. Methacrylamide C=O str. and for their polymers
Acrylamide		1682(2)		1639(9)	43	0.22	0	9
Polyacrylamide	18,000,000	1668(2)	14					15
		1665(3)	17					13
	6,000,000	1660(3)					7	
		1659(3)	23					6
	5,000,000	1658(4)	24				5	
Acrylamide								
N-methyl		1659(1)		1628(9)	31	0.11	23	
N-ethyl		1657(2)		1628(9)	29	0.22	25	
N-tert-butyl		1659(1)		1629(9)	30	0.11		
N-(1,1-dimethyl-3-oxybutyl)		1658(3)		1627(9)	31	0.33		
Acrylamide								
N,N'-dimethyl		1648(1)		1612(9)	36	0.11	34	
N,N'-diethyl		1649(2)		1609(9)	40	0.22	33	
N-methyl		1666(8)		1625(7)	41	1.1	16	
N'-vinyl								
Methacrylamide		1673(1)		1647(5)				
Polymethacrylamide		1653(1)	20					

TABLE 12.5A Raman data and assignments for N-alkyl or N-aryl acrylamides and methacrylamides

N-alkyl or N-aryl acrylamide	C=O str.	C=C str.	[C=C-N str.]	C=O str. C=C str.	RI C=O str./ RI C=C str.	N-alkyl or N-aryl methacryl- amide	C=O str.	C=C str.	CH ₂ = bend	s.C-C-C str.	C=O str.- C=C str.	RI C=O str./ RI C=C str.
N'-methyl- lene-bis	1663(1)	1632(9)	1252(5)	31	0.11	N'-methyl- lene-bis	1661(9)	1622(3)	1421(6)	879(8)	39	3
methyl	1659(1)	1628(9)	1252(5)	31	0.11							
ethyl	1657(2)	1628(9)	1250(6)	29	0.22	ethyl	1656(9)	1621(5)		875(8)	35	1.8
trimethylene-bis	1651(4)	1617(5)	1245(9)	34	0.8							
butyl	1657(2)	1628(9)	1248(6)	29	0.22							
isopropyl	1656(2)	1622(9)	1248(6)	34	0.22							
cyclohexyl	1656(3)	1624(9)	1247(5)	32	0.33							
octadecyl		1625(2)										
tert-octyl	1660(2)	1625(7)		35	0.29	tert-butyl	1658(4)	1620(4)		881(9)	38	1
benzyl	1652(2)				1	benzyl	1653(4)					
N'-hexamethyl- lene-bis	1654(5)	1620(9)	1240(9)	34	0.56							
isobutoxymethyl	1669(1)	1631(9)	1239(2)	38	0.11	isobutoxy- methyl	1664(7)	1620(4)			36	1.8
hydroxymethyl	1665(0.5)	1632(9)	1236(3)	33	0.06							
						2-hydroxy- propyl	1652(9)	1620(4)				
						butoxy	1671(1)	1632(9)			39	0.11
phenyl		1638(6)	1256(9)			phenyl	1657(3)	1620(3)			37	1
				29-35							35-39	

TABLE 12.6 IR C=O stretching frequencies for p-x-acetanilides and p-x, α -haloacetanilides in CCl₄ and CHCl₃ solutions

p-x group X	Sigma p	Acetanilide p-x C=O str. [CCl ₄]	Acetanilide p-x C=O str. [CHCl ₃]	α -Bromo-p-x acetanilide C=O str. [CCl ₄]	α -Bromo-p-x acetanilide C=O str. [CHCl ₃]	α,α,α -Trichloro- p-x-acetanilide C=O str. [CCl ₄]	α,α,α -Trichloro- p-x-acetanilide C=O str. [CHCl ₃]
N(C ₂ H ₅) ₂	-0.57	1693		1682	1670	1723	
OCH ₃	-0.268	1698.5	1685	1687	1678	1726	1718
CH ₃	-0.17	1700	1700	1693	1680	1729	1719
H	0	1705					
C ₆ H ₅	0.01					1729.5	1721
F	0.062			1695	1684	1731	1721
Cl	0.227	1708	1695	1695	1686	1731	1723
Br	0.323	1709	1694	1693	1685	1731	1723
I	0.276	1709	1696	1693	1685	1731	1724
COCH ₃	0.516	1713	1702	1701	1686	1736	1727
CHO	0.575	1715	1701*	1701	1693*	1735	1729
CN	0.628	1716.5	1705	1701.5	1692	1737	1729
NO ₂	0.778	1718	1711	1703	1697	1738	1730
N(C ₂ H ₅) ₂ :HCl	?						1730
p-x group							
COCH ₃		1685.5	1688	1687	1681	1689	1681
CHO		1701	1701	1700.5	1693	1706	1702

* not resolved from $\nu_{C=O}$ for the H-C=O group.

TABLE 12.7 The NH stretching frequencies for p-x-acetanilides and p-x, α -haloacetanilides in CCl₄ and CHCl₃ solutions

p-x Group	Sigma p	p-x-acetanilide	p-x-acetanilide	α -Bromo-p-x acetanilide	α -Bromo-p-acetanilide	α,α,α -Trichloro-p-x-acetanilide	α,α,α -Trichloro-p-x-acetanilide
		N-H str. [CCl ₄]	N-H str. [CHCl ₃]	N-H str. [CCl ₄]	N-H str. [CHCl ₃]	N-H str. [CCl ₄]	N-H str. [CHCl ₃]
N(C ₂ H ₅) ₂	-0.57	3443		3405	3395	3422	
OCH ₃	-0.268	3445	3440	3403	3395	3421	3415
CH ₃	-0.17	3443	3435	3402	3395	3422	3414
H	0	3441					
C ₆ H ₅	0.01					3421	3409
F	0.062			3401	3393	3422	3413
Cl	0.227	3441	3435	3402	3392	3420	3413
Br	0.232	3441	3436	3400	3393	3420	3411
I	0.276	3442	3437	3399	3392	3419	3413
COCH ₃	0.515	3436	3431	3303	3388	3416	3409
CHO	0.575* ¹	3439	3442	3399	3390	3415	3407
CN	0.628	3437	3431	3393	3388	3416	3409
NO ₂	0.778	3438	3430	3391	3387	3415	3406
N(C ₂ H ₅) ₂ :HCl	?		3429				
N(C ₂ H ₅) ₂			A* ¹		A* ¹		A* ¹
OCH ₃			2.89		4.12		4.55
CH ₃			2.66		4.1		4.41
C ₆ H ₅							
F							4.81
Cl					4.68		5.12
Br			2.68		4.47		5.06
I			3.17		4.8		5.09
COCH ₃			2.84		5.14		4.92
CHO			3.12				4.75
CN			3.16		4.82		
NO ₂			3.09		5.37		5.27
			3.66		5.3		5.36

*¹ Based on reading in Figure 12.3. See text.

TABLE 12.8 The NH and C=O stretching frequencies for N-alkyl p-methoxybenzamide, N-alkyl p-chlorobenzamide, and N-alkylmethyl carbamate in CCl₄ solutions

Compound [CCl ₄ solutions]	N-H str. cm ⁻¹	A* ¹	C=O str. cm ⁻¹
p-Methoxybenzamide			
N-methyl	3481		1676
N-ethyl	3463	22.1	1669
N-propyl	3464	20.5	1670
N-n-butyl	3464		1671
N-isobutyl	3469	20	1671
N-isopropyl	3456	18.3	1665
N-s-butyl	3451	18.4	1668
N-t-butyl	3452	15.9	1672
p-Chlorobenzamide			
N-methyl	3481	24.7	1681
N-ethyl	3460	22.3	1675
N-propyl	3463	22.3	1675
N-n-butyl	3463	21.9	1677
N-isobutyl	3469	23.7	1679
N-isopropyl	3450	17.9	1671
N-s-butyl	3451	21.5	1674
N-t-butyl	3451	17.2	1676
Methyl Carbamate			
N-methyl	3478	41.6	1738
N-propyl	3464	32.3	1736
N-n-butyl	3461		1735
N-isobutyl	3467	27.9	1735
N-isopropyl	3452	28.2	1732
N-s-butyl	3449	28.5	1730
N-t-butyl	3455	30.5	1738
N-phenyl	3450	47.2	1748

*¹ Times 10⁸ cm² molecule⁻¹ sec⁻¹

TABLE 12.9 IR and Raman data for N,N'-dialkyl oxamide and N,N'-diaryl oxamide

Oxamide N,N'-dialkyl	o.p.(N-H) ₂ str. IR	i.p.(N-H) ₂ str. Raman	Amide I	Bu	Amide I Ag	Amide II Bu	Amide II Ag	Amide IV Bu
Methyl	3309	3325	1659	1639sh	1692	1533	1567	761
Butyl	3299	3315	1651	1632sh	1688	1532	1560	760
Octyl	3299	3314	1645	1629sh	1690	1508	1551	725
Dodecyl	3311	3325	1645	1628sh	1689	1512	1555	725
Hexadecyl	3304	3320	1645	1629sh	1690	1508	1554	725
Octadecyl	3304	3321	1643	1628sh	1690	1509	1554	752
2-Chloroethyl	3290	3310	1654	1636sh	1695	1536	1562	769
3-Chloropropyl	3306	3320	1654	1633sh	1689	1528	1559	782
2-Hydroxyethyl	3292	3308	1653		1691	1541	1557	764
3-Hydroxypropyl	3308	3324	1655	1635sh	1691	1538	1560	767
2-Methylallyl	3295	3305	1660	1634sh	1686	1524	1559	777
Benzyl	3279	3302	1653	1634sh	1689	1524	1557	781
o-Methylbenzyl	3302		1653	1631sh		1514		750
Range	(3279–3311)	(3302–3325)	(1643–1660)	(1628–1638)	(1686–1695)	(1508–1541)	(1547–1567)	(725–782)
N-(2-Chloroethyl)	3295	3314	1653		1691	1536	1562	764
N'-(3-Hydroxypropyl)								
N-2-(Chloroethyl)	3299	3311	1657		1690	1535	1560	761
N'-(Allyl)								
N,N'-diaryl								
Phenyl	3298	3320	1662 1688sh	1682 1697	1520 1509sh	1550	730	
3-Chlorophenyl	3308	3320	1669	1701 1690	1518	1547	717	
3,4-Dichlorophenyl	3358 3230sh	3335	1686	1704 1690	1508 1514sh	1545	693	
3,6-Dichloro-2-pyridyl	3325	3338	1711	1727	1488	1536	627	
3,5-(Trifluoromethyl)- 2-pyridyl	3323	3349	1719	1741	1484	1537	638	
2,6-(Trifluoromethyl)- 4-pyridyl	3290	3325	1692	1723	1510	1549	660	
Range	(3295–3358)	(3320–3349)	(16620–1719)	(1682–1741)	(1484–1520)	(1537–1550)	(628–750)	

TABLE 12.10 IR data and assignments for dimethylacetamide and tetraalkylurea in the vapor, neat and solution phases

Compound	C=O str. [vapor]	C=O str. [n-C ₆ H ₁₄]	C=O str. [CCl ₄]	C=O str. CHCl ₃	C=O str. 14.0 mol % [n-C ₆ H ₁₄ /CHCl ₃]	C=O str. 80.6 mol % [n-C ₆ H ₆ /CHCl ₃]	C=O str. neat
Dimethylacetamide	1690(1.250)		1660.5	1634.2			
Urea							
Tetramethyl	1685(1.240)	1668.4(1.491)	1653.2 1652.9	1627.3	1650.9; 1635.4	1640.2; 1629.5	1649.6
Tetraethyl	1674(1.232)		1646.2	1620.1			1644
Tetrabutyl	1669(0.840)		1643.2	1616.1			
	[vapor]-[n-C ₆ H ₁₄]	[vapor]-[CCl ₄]	[vapor]-[CHCl ₃]	[CCl ₄]-[CHCl ₃]	[vapor]-[neat]		
Dimethylacetamide		29.5	55.8	26.3			
Urea							
Tetramethyl	16.6	31.9	57.7	25.8	35.4		
Tetraethyl		27.8	53.9	26.1			
Tetrabutyl		25.8	52.9	27.1	25		

TABLE 12.11 IR vapor-phase data and assignments for urea, thiourea, and guanidine derivatives

Urea	N-H str.	2(C=O str.)	C=O str.	a.NCN?	N-H bending
1,1,3,3-Tetramethyl		3358(0.011)	1685(1.240)	1239(0.210)	
1,1,3,3-Tetraethyl		3338(0.006)	1674(1.240)	1261(1.240)	
1,1,3,3-Tetrabutyl			1669(0.790)	1255(0.159)	
1,3-Diethyl-1,3-diphenyl		3340(0.005)	1680(1.240)	1273(0.610)	
			1741(1.243)		
1,3-Dimethyl	3480(0.073)		1732(1.043)	1334(0.460)	1522(1.149)
			1726(1.143)		
Thiourea			C=S str.		
1,1,3,3-Tetraethyl			~1085(0.280)	1261(1.230)	
Guanidine			C=N str.		
1,1,3,3-Tetramethyl	3358(0.015)		1619(1.245)	1249(0.190)	

TABLE 12.12 IR data and assignments for tetramethylurea and 1,3-dimethyl-2-imidazolidinone in various solvents

Solvent	DMI		[DMI C=O str.] [TMU C=O str.]	TMU C=O str.	TMU	TMU	TMU	DMI	DMI	AN	
	C=O str. cm ⁻¹	A			C=O str. [Hexane]		C=O str. [Hexane]				
[Neat]	1697.1		47.4	1649.6				33.5			
Hexane	1730.6	0.922	62.2	1668.4			0	0		0	
Diethyl ether	1716.8	0.974	55.3	1661.5			6.9	13.7		3.9	
Tetrahydrofuran	1710.6	1.128	55.4	1660.7			13.2	20		8.8	
Methyl t-butyl ether	1715.6	0.993	55	1660.7			7.7	14.9		5	
Benzene	1708.7	1.091	56.6	1652.1			16.3	21.9		8.2	
Carbon tetrachloride	1709.6	1.017	56.8	1652.9			15.5	21		8.6	
Carbon disulfide	1709.6	1.321	56.2	1653.4			15	21		10.1	
1,2-Dichlorobenzene	1703.6	1.267	56.6	1646.9			21.5	27			
Nitrobenzene	1700.6	0.935	56.2	1644.4			24	30		14.8	
Benzonitrile	1699	1.017	55.9	1643.2			25.2	31.5		15.5	
Nitromethane	1696.3	0.905	57.9	1638.4			30	34.3			
Acetonitrile	1698.3	1.04	56.4	1641.9			26.5	32.2		18.9	
Dimethyl sulfoxide	1695.1	1.09	56.7	1638.4			30	35.5		19.3	
Methylene chloride	1695	0.939	57.6	1637.4			31	35.6		20.4	
Chloroform	1688.8	0.927	61.5	1627.3			41	41.7		23.1	
t-Butyl alcohol	1695.6	0.901	1669.5	33	1659.5	1636.5	8.9	31.9	35	61.1	29.1
Isopropyl alcohol	1692.2	0.782	1668.7	35.3	1657.1	1633.4	11.3	35	38.4	61.9	33.5
Ethyl alcohol	1689.3	0.783	1666.8	39.2	1650.1	1630.1	18.3	38.3	41.3	63.8	37.1
Methyl alcohol	1686.5	0.599	1664.7	38.9		1625.8		43	44.1	65.9	41.3

TABLE 12.13 IR data and assignments for 1,3-dimethyl-2-imidazolidinone 1% wt./vol. in various solutions

Imidazolidinone [1% wt./vol.] Mole % CHCl ₃ /CCl ₄	1,3-Dimethyl-2- imidazolidinone [1% wt./vol.] Mole % CCl ₄ /n-C ₆ H ₁₄					1,3-Dimethyl-2- imidazolidinone [1% wt./vol.] Mole % CHCl ₃ /n-C ₆ H ₁₄							
	C=O str. cm ⁻¹		C=O str. cm ⁻¹	A	C=O str. cm ⁻¹	A	C=O str. cm ⁻¹	A	C=O str. cm ⁻¹	A	C=O str. cm ⁻¹	A	
0	1709.6	0	1730.6					0	1730.6	0.855	1725.2	0.735	
3.51	1707.5	2.98	1729.8	0.826	1723	0.77	7.01	1727.9	0.309	1710.2	0.92	1698	0.397
4.67	1706.5	5.97	1729.4	0.774	1722.4	0.767	14.02	1728.3	0.193	1709.4	0.87	1697	0.57
7.01	1704.8	11.93	1729	0.748	1720.9	0.798	24.59	1728.7	0.154	1708.4	0.799	1696.3	0.699
14.02	1702.4	19.33	1728.7	0.675	1719.2	0.835	32.85	1729.5	0.122	1707.2	0.712	1695.3	0.79
24.59	1700.9	28.9	1728.6	0.621	1718.3	0.864	39.48	1729.1	0.092	1706.2	0.667	1694.6	0.84
32.85	1699.7	35.04	1728.3	0.602	1717.4	0.892	44.92	1729.5	0.085	1705.7	0.635	1694	0.865
39.48	1698.3	40.38	1727.9	0.595	1716.8	0.902	49.46	1729.5	0.085	1704.9	0.608	1693.7	0.886
42.2	1696.1	44.84	1727.5	0.592	1716.2	0.923	53.3	1729.1	0.08	1704.1	0.587	1693.2	0.912
44.92	1694.1	48.68	1727.5	0.475	1715.7	0.925	56.61	1729.1	0.074	1703.7	0.579	1692.9	0.928
49.46	1693.6	52.01	1727.5		1715.4		59.48	1729.1	0.06	1703.3	0.555	1692.6	0.883
53.3	1692.5	54.94	1727.1		1715		61.99					1692.4	0.925
56.61	1692.1	57.27			1714.8		64.4					1692.3	0.929
59.48	1691.9	60.09			1714.4		67.09					1692	0.932
61.99	1691.7	62.87			1714		69.97					1691.7	0.94
64.44	1691.5	65.93			1713.8		73.1					1691.5	0.95
67.09	1691.1	69.31			1713.4		78.53					1691.2	0.952
69.97	1690.0	73.04			1712.9		80.58					1690.8	0.963
73.1	1690.6	77.2			1712.4		84.69					1690.4	0.967
76.53	1690.4	81.87			1711.7		89.05					1690	0.974
80.58	1690.1	87.14			1711.3		93.52					1689.4	0.955
84.69	1689.8	93.13			1710.5		100					1688.7	0.985
89.05	1689.6	100			1709.5								
93.52	1689.2												
100	1688.8												
delta cm ⁻¹	20.8		-3.5		-13.5				-1.5		-21.9		-9.3

TABLE 12.14 The in-phase and out-of-phase (C=O)₂ stretching frequencies for caffeine, isocaffeine, 1,3,5- trimethyluracil, 1,3,6-trimethyluracil, and 1,3-dimethyl-2,4-(1H,3H) 2, quinazolidinedione in CCl₄ and CHCl₃ solutions

Compound [vapor]	i.p.(C=O) ₂ str.+ +o.p.(C=O) ₂ str.	i.p.(C=O) ₂ str.	o.p.(C=O) ₂ str.	[vapor]-[CCl ₄]	[vapor]-[CHCl ₃]	[CCl ₄]-[CHCl ₃]
Caffeine	3395(0.005)	1721(0.731)	1685(1.250)			
[solution]				i.p.(C=O) ₂ str.	i.p.(C=O) ₂ str.	i.p.(C=O) ₂ str.
Caffeine				o.p.(C=O) ₂ str.	o.p.(C=O) ₂ str.	o.p.(C=O) ₂ str.
[CCl ₄]		1710.6(0.193)	1667.5(0.298)	10.4	12.1	1.7
[CHCl ₃]		1708.9(0.204)	1658.4(0.210)	17.5	26.6	9.1
[solution]						
Isocaffeine]						
[CCl ₄]/[CHCl ₃]						
10.74 mol %		1716.7	1673.2			i.p.(C=O) ₂ str.
19.4 mol %		1716.3(0.016)	1669.0(0.019)			0.4*
[CHCl ₃]		1711.3(0.487)	1664.0(0.487)			5.4*
						o.p.(C=O) ₂ str.
						4.2*
						9.2*
[solution]						
Uracil				Corrected		i.p.(C=O) ₂ str.
1,3,5-Trimethyl				Fermi Res.		o.p.(C=O) ₂ str.
[CCl ₄]		1706.6(0.128)	1663.4			6.6
[CHCl ₃]		1700.0(0.124)	1652.4			11
Uracil						
1,3,6-Trimethyl						
[CCl ₄]		1710.8(0.160)	1668.3			8.8
[CHCl ₃]		1702.0(0.126)	1658.2			10.1
[solution]						
1,3-Dimethyl-2,4- (1H,3H)-quinazolidinedione				Corrected		i.p.(C=O) ₂ str.
				Fermi Res.		o.p.(C=O) ₂ str.
[CCl ₄]		1711.6(0.155)	1667			7.9
[CHCl ₃]		1703.7(0.105)	1657.4			9.6

* differences from 10.74 and 19.4 mol% CHCl₃/CCl₄ from CHCl₃ solution.

TABLE 12.15 IR data for uracils in the solid phase

Uracil [solid phase]	i.p.(C=O) ₂ str.	o.p.(C=O) ₂ str.	[i.p.(C=O) ₂ str.]-[o.p.(C=O) ₂ str.]
5-Fluoro	1710	1661	49
5-Amino	1750	1670	80
5-Methyl	1745	1675	70
5-Bromo	1704	1680	24
5-Chloro	1718	1695	23
5-Nitro	1719	1695	24
5-Acetyl	1730	1704	26
6-Methyl	1720	1685	35
1,3-Dimethyl*	1733	1699	34
1,3-Dimethyl	1710	1658	52
1,3-Dimethyl-5- (morpholine carbonyl)	1709	1659	50
1,3-Dimethyl-5-nitro	1720	1668	52
1,6-Dimethyl-3-(p-chlorophenyl)-5-bromo	1700	1648	52
1,3-bis(2-Amino-ethyl-2HCl)	1701	1659	42
1,3,5-Trimethyl	1701	1667	34
1,3,6-Trimethyl	1689	1652	37
Range	1689–1750	1652–1704	23–80

* Vapor phase

TABLE 12.16 IR vapor-phase data and assignments for imides

Compound	i.p.(C=O) ₂ str.+ +o.p.(C=O) ₂ str.	A	N-H str.	A	i.p.(C=O) ₂ str.	A	o.p.(C=O) ₂ str.	A	A{i.p.(C=O) ₂ }/ A{o.p.(C=O) ₂ }
Diacetamide			3438	0.031	1738	0.941	1749	1.24	0.76
N-phenyldibenzamide	3485	0.011			1801	0.101	1702	0.84	0.08
Succinimide			3458	0.055	1820	0.089	1772	1.24	0.07
N-(2,6-xylyl)succinimide	3522	0.011			1790	0.041	1741	1.24	0.03
4-Cyclohexene-1,2-di-carboximide			3455	0.101	1799	0.201	1759	1.25	0.16
4-Methyl-N-(3',3'-trifluoromethyl-phenyl)- 4-cyclohexene-1,2-dicarboximide	3518	0.011			1795	0.051	1735	1.25	0.04
Maleimide			3490	0.135			1755	1.24	
N-ethylmaleimide	3499	0.011			1820	0.019	1735	1.23	0.02
N-benzylmaleimide	3500	0.011			1810	0.021	1735	1.23	0.02
N-phenylmaleimide	3510	0.015					1739	1.23	
N-(4-iodophenyl)maleimide	3502	0.011			1795	0.091	1738	1.22	0.07
N-(3-chloro-4-methyl)phenylmaleimide	3504	0.011			1795	0.011	1738	1.23	0.01
N-(4-metoxyphenyl)maleimide	3504	0.011					1737	1.23	
N-(p-tolyl)maleimide	3510	0.011					1740	1.23	
N-(4-isopropylphenyl)maleimide	3504	0.011			1790	0.031	1735	1.24	0.03
N-(1-naphthyl)maleimide	3509	0.011			1790	0.031	1740	1.24	0.03
N-(2-chlorophenyl)maleimide	3518	0.011					1742	1.24	
N-(3,4-dimethoxyphenethyl)maleimide	3495	0.011			~1780	0.011	1730	1.23	0.01
N-[bis(3,5-trifluoromethyl)phenyl]maleimide	3510	0.005					1743	0.731	
N,N'-m-phenyldimaleimide	3504	0.011			1795	0.031	1739	1.24	0.03
N-[-(dimethylamino)-o-tolyl]maleimide	3502	0.011			1880	0.026	1738	1.23	0.2
N-[(4-Chloro-2-trifluoromethyl)maleimide	3520	0.011			1785	0.101	1745	1.22	0.08
N-4-(dimethylamino)phenyl]maleimide	3508	0.011			1798	0.031	1739	1.23	0.03
N-(2,6-diisopropylphenyl)maleimide	3498	0.011					1731	1.24	
3,3-dimethylglutarimide			3415	0.093			1745	1.24	
Phthalimide			3479	0.111	1795	0.169	1766	1.23	0.14
4-Nitrophthalimide	3558	0.011	3470	0.281	1800	0.401	1769	1.23	0.33
3-Nitrophthalimide	3550	0.011	3470	0.205	1798	0.295	1768	1.23	0.24
3-Aminophthalimide			3450	0.141	1785	0.365	1745	1.24	0.29
	[a.NH ₂ str.]	[A]	[s.NH ₂ str.]	[A]					
	[3520]	[0.049]	[3402]	[0.075]					
N-methylphthalimide	3510	0.011			1785	0.111	1739	1.22	0.09
N-[(dimethylamino)methyl]phthalimide	3475	0.111			1771	0.201	1735	1.24	0.16
N-(2-bromoethyl)phthalimide	3509	0.021			1789	0.281	1739	1.23	0.23

N-(2-chloroethyl)phthalimide	3510	0.011			1787	0.162	1740	1.222	0.13
N-(3-bromopropyl)phthalimide	3502	0.011			1788	0.171	1734	1.24	0.14
N-(3-chloro-2-hydroxypropyl)Phthalimide	3510	0.011			1785	0.151	1735	1.24	0.12
N-(2,5-dichlorophenyl)phthalimide	3524	0.011			1800	0.151	1746	1.22	0.12
N-(3-chloro-o-tolyl)phthalimide	3518	0.011			1795	0.121	1735	1.22	0.11
N-[[[(3,4-methylenedioxy)benzylidene]amino]-phthalimide	3522	0.011			1791	0.111	1740	1.21	0.09
N-(2,6-dimethylphenyl)phthalimide	3502	0.011			1761	0.129	1745	1.22	0.11
N-[(5-bromo-2-hydroxybenzylidene)amino]phthalimide	3539	0.011			1789	0.201	1759	1.22	0.16
	[OH:N=C]	[A]							
	[3475]	[0.101]							
2-Phthalimidoglututaric anhydride	3478	0.011			masked		1745	0.245	
					[Anhydride]	[A]	[Anhydride]	[A]	
					[1871]	[0.135]	[1799]	[1.23]	
N-2-propynylphthalimide	3510	0.011			1789	0.162	1741	1.24	0.13
	[CC-H str.]	[A]	[a',CCH bend]	[[A]	a'',CCH bend	[A]			
	[3330]	[0.111]	[669]	[0.152]	[629]	[0.138]			
	[3310]	0.031							
Hydantoin			3495(0.074)		1826(0.133)		1785(1.245)		
1-Methylhydantoin	3564	0.011	3482	0.085	1815	0.221	1775	1.24	0.18
5,5-Dimethylhydantoin			3490	0.121	1811	0.231	1775	1.24	0.19
5,5-Dimethylhydantoin (solid phase)			3210(0.312)		1779(0.540)		1744(1.460)		
							1716(1.460)		
5-Methyl-5-propylhydantoin	3570	0.011	3490	0.241	1806	0.611	1775	1.21	0.55
5-Methyl-5-propylhydantoin (solid phase)			3215(0.271)		1761(0.415)		1707(1.170)		
5-Methyl-5-isopropylhydantoin	3570	0.011	3490	0.241	1805	0.682	1771	1.23	0.55
5-Methyl-5-isopropylhydantoin (solid phase)			3205(0.530)		1770(0.873)		1712(1.300)		
N-[(4,4-dimethyl-2,5-dioximidazolidinyl)-methyl]anthranilic acid, methyl ester	[N-H:O=O str.]	[A]	3482	0.081	1810	0.201	1779	1.25	0.16
	[3395]	0.075							
	[1719 ester]	0.501							
1,3-Diphenyl-5-octyl-s-triazine-(1H,3H,5H)-trione	3459	0.011			1766	0.161	1720	1.21	0.13
1-Benzyl-3,5-diallyl-s-triazine-2,4,6-(1H,3H,5H)-trione	3470	0.05					1711	1.24	
Triallyl-s-triazine-2,4,6-(1H,3H,5H)-trione	3470	0.05					1710	1.24	

TABLE 12.17 IR data for the in-phase and out-of-phase stretching frequencies of 4-bromobutyl phthalimide in $\text{CHCl}_3/\text{CCl}_4$ solutions

N-(4-bromobutyl)phthalimide [1% solutions] Mole % $\text{CHCl}_3/\text{CCl}_4$	i.p.(C=O) ₂ str. cm^{-1}	o.p.(C=O) ₂ str. cm^{-1}	[i.p.(C=O) ₂ str.]-[o.p.(C=O) ₂ str.] cm^{-1}
0	1773.8	1718.7	55.2
26.53	1773.1	1716.9	56.2
52	1772.5	1715.6	56.9
70.65	1772.3	1714.2	58.1
100	1772.2	1713	59.2
delta cm^{-1}	-1.6	-5.7	4

TABLE 12.18 IR data and assignments for hydantoins in the vapor and solid phases

Hydantoin	NH str. cm ⁻¹	A [NH str.]	i.p.(C=O) ₂ str. cm ⁻¹	o.p.(C=O) ₂ str. cm ⁻¹	A[i.p.(C=O) ₂ str.]	A[o.p.(C=O) ₂ str.]	A[i.p.(C=O) ₂ str.] /A[o.p.(C=O) ₂ str.]	{i.p.(C=O) ₂ str.}- [o.p.(C=O) ₂ str.] cm ⁻¹
1,3,5,5-H,H,H,H	[3495]	{0.082}	[1825]	{1785}	{0.13}	[1.27]	[0.10]	[40]
H,H,H,H	3262	0.25	1783	1717	0.705	1.25	0.56	66
	3150	0.26						
H,H,CH ₃ ,CH ₃	3210	0.31	1779	1744	0.54	1.46	0.37	35
				1716		1.46		63
H,H,C ₃ H ₇ ,C ₃ H ₇	3200	0.312	1766	1717	0.622	1.3	0.48	49
H,H,C ₆ H ₁₁ ,C ₆ H ₁₁	3180	0.2	1755	1702	0.4	1.07	0.37	53
H,H,CH ₃ ,C ₃ H ₇	3215	0.271	1761	1707	0.415	1.17	0.35	54
H,H,CH ₃ ,C ₃ H ₇	[3485]	[0.234]	{1809}	[1774]	[0.613]	[1.24]	[0.49]	[35]
H,H,CH ₃ ,iso-C ₃ H ₇	3205	0.53	1770	1712	0.873	1.3	0.67	59
H,H,CH ₃ ,iso-C ₃ H ₇	[3485]	[0.224]	[1808]	[1774]	[0.690]	[1.26]	[0.58]	[34]
H,H,CH ₃ ,iso-C ₄ H ₉	3180	0.345	1780	1718	0.65	1.25	0.52	62
H,H,CH ₃ ,iso-C ₄ H ₉	[3485]	[0.210]	[1809]	[1774]	[0.55]	[1.25]	[0.44]	[35]
H,H,CH ₃ ,C ₆ H ₅	3270	0.47	1758	1720	0.64	1.24	0.52	38
	3200	0.52		1709		0.96	0.67	49
H,H,CH ₃ ,p-ClC ₆ H ₄	3250	0.13	1777	1727	0.3	0.9	0.33	50
	3185	0.15		1720		0.8	0.38	57
H,H,C ₃ H ₅ *,C ₃ H ₅ *	3300	0.16	1781	1720	0.19	1.14	0.17	61
	3165	0.08	1761	0.15			0.13	41
C ₆ H ₅ ,C ₆ H ₅ ,H,H			1782	1720	0.23	0.86	0.27	62
C ₂ H ₅ ,CH ₃ ,C ₆ H ₅ ,C ₆ H ₅			1778	1721	0.2	0.95	0.21	57
			1771		0.21	0.22		50
iso-C ₃ H ₇ ,CH ₃ ,C ₆ H ₅ ,C ₆ H ₅			1770	1711	0.49	1	0.49	59
iso-C ₄ H ₉ ,CH ₃ ,C ₆ H ₅ ,C ₆ H ₅			1774	1720	0.39	1.05	0.37	54
iso-C ₇ H ₁₁ ,CH ₃ ,C ₆ H ₅ ,C ₆ H ₅			1779	1723	0.37	1.19	0.31	56
Range	3150-3300		1755-1783	1702-1744				35-66
	[3485-3495]		[1808-1825]	[1774-1785]				[34-40]
	[] Sadtler vp at 280 °C							

* = allyl.

TABLE 12.19 IR data and assignments for tri-allyl-1,3,5-triazine-2,4,6-(1H,3H,5H) trione in CHCl₃/CCl₄ solutions

Triallyl-1,3,5-triazine-2,4,6-(1H,3H,5H) trione Mole % CHCl ₃ /CCl ₄	o.p.(C=O) ₃ str. cm ⁻¹	o.p.(CN) ₃ str. cm ⁻¹	C=C str. cm ⁻¹	CH=CH ₂ twist cm ⁻¹	CH=CH ₂ wag cm ⁻¹
0	1698.6	1455.2	1645.4	992	935
10.74	1698.6	1455.5	1645.4	991.8	934.9
15.07	1698.5	1455.8	1645.4	991.7	934.6
26.53	1698.3	1456.2	1645.4	991.7	934.1
52	1696.8	1457.1	1645.4	991.6	931.6
70.65	1696	1457.9	1645.4	991.7	930.4
85.05	1695.8	1458.4	1645.4	991.8	929.9
100	1695.7	1458.6	1645.4	991.8	929.7
delta cm ⁻¹	-2.9	3.4			-5.3

TABLE 12.20 IR data and assignments for tri-allyl-1,3,5-triazine-2,4,6-(1H,3H,5H) trione in various solvents

Triallyl-1,3,5-triazine-2,4,6-(1H,3H,5H) trione 1 wt./vol. % solutions	o.p.(C=O) ₃ str. cm ⁻¹	o.p.(C=O) ₃ :HO str. cm ⁻¹	AN
Hexane	1703.2		0
Diethyl ether	1702.3		3.9
Methyl t-butyl ether	1701.6		
Toluene	1698.7		
Carbon tetrachloride	1698.6		8.6
Carbon disulfide	1698.2		
1,2-Dichlorobenzene	1697.1		8.2
Acetonitrile	1695.5		
Nitrobenzene	1696		14.8
Benzonitrile	1694.5		
Methylene chloride	1696.2		20.4
Nitromethane	1695.9		
t-Butyl alcohol	1703.5	1690.1	29.1
Chloroform	1695.7		23.1
Dimethyl sulfoxide	1693.3		19.3
Isopropyl alcohol	1702.2	1690.4	33.5
Ethyl alcohol	1702.4	1690.6	37.1
Methyl alcohol	1701.5	1688	41.3

Aldehydes

References 270

Figures		Tables	
Figure 13-1	271 (268)	Table 13-1	282 (267)
Figure 13-2	272 (268)	Table 13-1a	282 (268)
Figure 13-3	273 (268)	Table 13-2	282 (268)
Figure 13-4	274 (269)	Table 13-3	283 (269)
Figure 13-5	275 (269)	Table 13-4	284 (269)
Figure 13-6	276 (269)	Table 13-5	285 (270)
Figure 13-7	277 (270)	Table 13-6	286 (270)
Figure 13-8	278 (270)		
Figure 13-9	279 (270)		
Figure 13-10	280 (270)		
Figure 13-11	281 (270)		

*Numbers in parentheses indicate in-text page reference.

Aldehydes are easily oxidized to the corresponding carboxylic acid. Therefore, the reader is cautioned to look for the presence of carboxylic acid impurities when interpreting the IR or Raman spectra of aldehydes. Several published spectra of aldehydes contain acid impurity, and the impurity is not marked on the IR spectrum.

Aldehydes contain the $\text{O}=\text{C}-\text{H}$ group; the empirical structure for the aliphatic forms is $\text{R}-\text{C}(=\text{O})\text{H}$, for the conjugated form it is $\text{C}=\text{C}-\text{C}(=\text{O})\text{H}$, and for the aromatic form it is $\text{C}_6\text{H}_5\text{C}(=\text{O})\text{H}$. Characteristic vibrations of the aldehyde group are:

- $\text{C}=\text{O}$ stretching (IR, strong);
- the first overtone of $\text{C}=\text{O}$ stretching (IR very weak);
- $\text{C}-\text{H}$ bending (IR, medium); and
- $\text{C}-\text{H}$ stretching in Fermi resonance with $\text{C}-\text{H}$ bending (IR, weak-medium bands).

Table 13.1 compares IR data and assignments for some nonconjugated aldehydes recorded in different physical phases. In all cases the $\nu\text{C}=\text{O}$ frequency occurs at higher frequency in the vapor than in solution or neat phase. In the neat phase $\nu\text{C}=\text{O}$ for the compounds of form $\text{R}-\text{C}(=\text{O})\text{H}$ exhibit $\nu\text{C}=\text{O}$ in the range $1715\text{--}1731\text{ cm}^{-1}$. Substitution of halogen atoms raises the $\nu\text{C}=\text{O}$ frequencies. For example, in CCl_4 solution $\nu\text{C}=\text{O}$ occurs at 1730, 1748, and 1768 cm^{-1} for the Cl , Cl_2 , and Cl_3 analogs of acetaldehyde, respectively (1). In the vapor phase, $\nu\text{C}=\text{O}$ occurs at 1760, 1778, and 1788 cm^{-1} for the Br_3 , Cl_3 and CF_3 analogs of acetaldehyde, respectively (2,3). Therefore, these data show that $\nu\text{C}=\text{O}$ for aldehydes increases

in the order of Br, Cl, and F substitution. The inductive power of the halogen atom also increases in this same order.

The aldehydic in-plane ($\text{O}=\text{C}-\text{H}$ plane) bending mode occurs in the region $1350-1400\text{ cm}^{-1}$, and its first overtone ($2\delta\text{CH}$) in Fermi resonance with $\nu\text{C}-\text{H}$ occurs in the regions $2800-2860\text{ cm}^{-1}$ and $2680-2722\text{ cm}^{-1}$. Usually the higher frequency band has more intensity than the lower frequency band in the Fermi resonance doublet. However, sometimes the two bands have nearly equal or equal intensity. Where both bands of the Fermi doublet have equal intensity, both bands result from equal mixtures of $\nu\text{C}-\text{H}$ and $2\delta\text{C}-\text{H}$. It is not theoretically correct to assign the stronger of the two bands to only the $\nu\text{C}-\text{H}$ fundamental.

Trichloroacetaldehyde does form a hydrate, and in its hydrate form it is no longer an aldehyde. It exists as a dihydroxide, $\text{CCl}_3\text{CH}(\text{OH})_2$.

Table 13.1a list Raman data and assignments for several aldehydes. The Raman data were taken from Reference (4), and the assignments were made by Nyquist. Data in the parentheses indicate the relative Raman band intensities and p is polarized. These data show that the relative Raman band intensity for $\nu\text{C}=\text{O}$ is less than that for the band intensities for $\nu\text{C}-\text{H}$ and $2\delta\text{CH}$ in Fermi resonance.

Acrolein is a conjugated aldehyde, $\text{CH}_2=\text{CH}-\text{C}(=\text{O})\text{H}$ and the Raman bands at 1688 cm^{-1} and 1618 cm^{-1} are assigned to $\nu\text{C}=\text{O}$ and $\nu\text{C}=\text{C}$, respectively. Benzaldehyde, $\text{C}_6\text{H}_5\text{C}(=\text{O})\text{H}$, is also conjugated, and its $\nu\text{C}=\text{O}$ mode occurs at 1701 cm^{-1} in the condensed phase. In the case of salicylaldehyde, or 2-hydroxybenzaldehyde, the OH group is intramolecularly hydrogen bonded to the $\text{C}=\text{O}$ group, and its $\nu\text{C}=\text{O}$ mode occurs at 1633 cm^{-1} in the condensed phase.

Table 13.2 lists IR data for 4-X-benzaldehydes in the vapor, CCl_4 , and CHCl_3 solution phases (5). Many of the $\nu\text{C}=\text{O}$ frequencies have been corrected for Fermi resonance ($\nu\text{C}=\text{O}$ in Fermi resonance with $2\gamma\text{C}-\text{H}$). As shown in Fig. 13.1, the $\nu\text{C}=\text{O}$ frequencies generally decrease as the Hammett σ_p values decrease. This figure shows plots of $\nu\text{C}=\text{O}$ for 4-X-benzaldehydes vs Hammett's σ_p value for the 4-X atom or group. The points on each line correspond to $\nu\text{C}=\text{O}$ frequencies assigned for the 0-100 mol % $\text{CHCl}_3/\text{CCl}_4$ solutions (5). Figure 13.2 shows plots of $\nu\text{C}=\text{O}$ for 4-X-benzaldehydes corrected for Fermi resonance in CCl_4 solution vs the frequency difference between $\nu\text{C}=\text{O}$ corrected for Fermi resonance in CCl_4 solution minus $\nu\text{C}=\text{O}$ corrected for FR for each of the mole % $\text{CHCl}_3/\text{CCl}_4$ solutions for each of the 4-X-benzaldehydes (5). These plots again demonstrate the effect of the 4-X substituent upon $\nu\text{C}=\text{O}$ as well as the effect of the solvent system. The mathematical treatment of the experimental data presented here always yields a linear relationship.

Figure 13.3 shows plots of $\nu\text{C}=\text{O}$ and an overtone in Fermi resonance and their corrected frequencies vs mole % $\text{CHCl}_3/\text{CCl}_4$ for 4-(trifluoromethyl) benzaldehyde. After correction for FR, it can be readily seen that the corrected $\nu\text{C}=\text{O}$ and OT frequencies are closer in frequency than their uncorrected observed frequencies. Figure 13.4 shows plots of $\nu\text{C}=\text{O}$ and OT in Fermi resonance and their corrected frequencies vs mole % $\text{CHCl}_3/\text{CCl}_4$ for 4-bromobenzaldehyde. In this case it is noted that the corrected $\nu\text{C}=\text{O}$ and OT frequencies converge at ~ 45 mol % $\text{CHCl}_3/\text{CCl}_4$. Below this point corrected $\nu\text{C}=\text{O}$ occurs at higher frequency than corrected OT and above this point corrected $\nu\text{C}=\text{O}$ occurs at lower frequency than corrected OT. Without correction for FR, the uncorrected $\nu\text{C}=\text{O}$ mode occurs at higher frequency than uncorrected OT. Without correction for FR, both observed bands are some combination of $\nu\text{C}=\text{O}$ and OT, which changes as the mole % $\text{CHCl}_3/\text{CCl}_4$ changes. Other examples of both types as just discussed are presented by Nyquist *et al.* (5). The general decrease in frequency in these plots is attributed to

the bulk dielectric effect of the solvent system together with intermolecular hydrogen bonding of form $C=O \cdots HCCl_3$.

Table 13.3 lists the unperturbed $\nu_{C=O}$ frequencies of 4-X-benzaldehydes in various solvent systems (6). The 4-X-benzaldehydes designated with an asterisk (*) list the $\nu_{C=O}$ frequency corrected for Fermi resonance. The overall $\nu_{C=O}$ frequency range for 4-X-benzaldehydes is $1664.4\text{--}1718.1\text{ cm}^{-1}$. The highest $\nu_{C=O}$ frequency is exhibited by 4-nitrobenzaldehyde in hexane and the lowest $\nu_{C=O}$ frequency is exhibited by 4-(dimethylamino) benzaldehyde in solution in methyl alcohol.

Figure 13.4 shows plots of the $\nu_{C=O}$ frequency for each of the 4-X-benzaldehydes in a solvent vs the $\nu_{C=O}$ frequency difference between the $\nu_{C=O}$ frequency in hexane solution and each of the other solvents. These plots are similar to the plots shown in Fig. 13.2.

Figure 13.5 shows a plot of $\nu_{C=O}$ for each of the 4-X-benzaldehydes in dimethyl sulfoxide solution vs Hammett's σ_p values. Other plots of $\nu_{C=O}$ for each of the 4-X-benzaldehydes in each of the other solvents show similar plots with 4-OH, 4- CH_3 -O, and 4- CH_3 S analogs not correlating as well as the other 4-X analogs.

Figure 13.6 shows a plot of $\nu_{C=O}$ for 4-(dimethylamino) benzaldehyde vs the solvent acceptor number (AN) for each of the solvents. Solvents are listed sequentially 1 through 17 starting with hexane as 1 and 17 for methyl alcohol. Two essentially linear relationships are noted in this figure. The plot 12, 15, 16, and 17 represents $\nu_{C=O} \cdots HOR$ frequencies for tert-butyl alcohol, isopropyl alcohol, ethyl alcohol, and methyl alcohol, respectively. The 4-(dimethylamino) benzaldehyde would be expected to form the strongest $C=O \cdots HOR$ bond, because the $(CH_3)_2N$ group is the most basic and the weakest is the case of the 4- NO_2 analog. The lower linear relationship is for $\nu_{C=O}$ frequencies. Other 4-X-benzaldehydes in these same solvents show similar plots with somewhat more scattered data points (see (6) for other plots). This led to the conclusion that the solute/solvent interactions are complex because the solvent also interacts with certain 4-X groups as well as with the π system of the phenyl group. The AN values give a rough prediction of $\nu_{C=O}$ and $\nu_{asym NO_2}$, but do not take into account all of the solute/solvent interactions (e.g., steric factors, relative basic sites in the solute, intermolecular hydrogen bonding between solvent molecules vs between solute and solvent molecules).

In general, the Hammett σ_p values for the 4-X atom or group for 4-X-benzaldehydes appear to correlate with the $\nu_{C=O}$ frequencies. However, due to scattering of the data points in the plots in each of the other solvent systems (6), these values do not appear to take into account intermolecular hydrogen bonding, the relative basicity of the $C=O$ group, and the interaction of the solvent with other sites in the 4-X-benzaldehydes.

The molecular geometry of both solvent and solute molecules, the basic and/or acidic sites in both solute and solvent molecules, the dipolar interactions between solute and solvent molecules, the steric factor of solute molecules, and the concentration of the solute most likely determine the overall solute/solvent interaction. Therefore, parameters such as AN values and Hammett σ_p values can not be expected to exhibit universal linear relationships between IR or Raman group frequencies. However, they do help in predicting the direction of frequency shifts within a class of compounds (6).

Table 13.4 lists the aldehydic C-H in-plane bending mode for 4-X-benzaldehydes in the CCl_4 and $CHCl_3$ solution and in the vapor phase (7). In CCl_4 solution, δ_{C-H} occurs in the range $1381.3\text{--}1392.1\text{ cm}^{-1}$ and in $CHCl_3$ solution in the range $1382.9\text{--}1394.3\text{ cm}^{-1}$ for the 4-X-benzaldehydes. The δ_{C-H} frequencies are higher by 1.5 to 4.1 cm^{-1} in $CHCl_3$ solution. It is well

known that the aldehydic CH stretching mode, νCH , and the first overtone of the aldehydic CH in-plane bending mode, $2\delta\text{CH}$, are in Fermi resonance (8–12). Because δCH frequencies are dependent upon the solvent system, one might expect that the amount of Fermi resonance interaction between $\nu\text{C}-\text{H}$ and $2\delta\text{CH}$ would also be dependent upon the solvent system. Table 13.5 lists the δCH , calculated $2\delta\text{CH}$, and $2\delta\text{CH}$ frequencies corrected for Fermi resonance in both CCl_4 and CHCl_3 solutions. The agreement between the calculated and corrected $2\delta\text{CH}$ frequencies varies between ~ 0.4 to 15 cm^{-1} .

Table 13.6 lists IR data and assignments for the perturbed and unperturbed $\nu\text{C}-\text{H}$ frequencies for the 4-X-benzaldehydes (7). The unperturbed $\nu\text{C}-\text{H}$ frequencies for 4-X-benzaldehydes in CCl_4 solution occur in the range $2768.7\text{--}2789.7\text{ cm}^{-1}$ and in CHCl_3 solution in the range $2776.6\text{--}2808.9\text{ cm}^{-1}$.

Figure 13.7 shows plots of half of the Fermi doublet for each of the 4-X-benzaldehydes in the range $2726\text{--}2746\text{ cm}^{-1}$ vs mole % $\text{CHCl}_3/\text{CCl}_4$ and Figure 13.8 show plots of half of the Fermi doublet in the range $2805\text{--}2845\text{ cm}^{-1}$ vs mole % $\text{CHCl}_3/\text{CCl}_4$. Figure 13.9 shows plots of unperturbed νCH for each of the 4-X-benzaldehydes vs mole % $\text{CHCl}_3/\text{CCl}_4$. These plots show that the Fermi doublet and the unperturbed νCH frequencies increase in frequency as the mole % $\text{CHCl}_3/\text{CCl}_4$ is increased. However, the $\nu\text{C}-\text{H}$ or $2\delta\text{CH}$ frequencies apparently do not correlate with Hammett σ_p values because the plots show that the frequencies do not increase or decrease in the order 1 through 13.

Submaxima are also noted for 4-X-benzaldehydes in the range $2726\text{--}2816\text{ cm}^{-1}$, and these bands are assigned to combination tones.

Benzaldehyde and 4-phenylbenzaldehyde are examples of how the unperturbed νCH and unperturbed $2\delta\text{CH}$ cross over with change in the mole % $\text{CHCl}_3/\text{CCl}_4$. In the case of benzaldehyde the crossover is at $\sim 55\text{ mol \% CHCl}_3/\text{CCl}_4$ and for 4-phenylbenzaldehyde the crossover is at $\sim 35\text{ mol \% CHCl}_3/\text{CCl}_4$ (see Figures 13.10 and 13.11).

REFERENCES

1. Bellamy, L. J. and Williams, R. L. (1958). *J. Chem. Soc. London*, 3645.
2. Nyquist, R. A. (1984). *The Interpretation of Vapor-Phase Infrared Spectra: Group Frequency Data*, Philadelphia: Sadtler Research Laboratories, Div. of Bio-Rad Inc.
3. Lin-Vien, D., Colthup, N. B., Fately, W. G., and Grasselli, J. G. (1991). *The Handbook of Infrared and Raman Characteristic Frequencies of Organic Molecules*, Boston: Academic Press, Inc.
4. Schrader, B. (1989). *Raman/Infrared Atlas of Organic Compounds*, 2nd ed., Weinheim, Germany: VCH.
5. Nyquist, R. A., Settineri, S. E., and Luoma, D. A. (1991). *Appl. Spectrosc.*, **45**, 1641.
6. Nyquist, R. A. (1992). *Appl. Spectrosc.*, **46**, 306.
7. Nyquist, R. A. (1992). *Appl. Spectrosc.*, **46**, 293.
8. Pozefsky, A. and Coggeshall, N. D. (1951). *Anal. Chem.*, **23**, 1611.
9. Pinchas, S. (1955). *Anal. Chem.*, **27**, 2.
10. Saier, E. L., Coussins, L. R., and Basillia, M. R. (1962). *J. Phys. Chem.*, **66**, 232.
11. Saier, E. L., Cousins, L. R., and Basillia, M. R. (1962). *Anal. Chem.*, **34**, 824.
12. Rock, S. L. and Hammaker, R. M. (1971). *Spectrochim. Acta*, **27**, 1899.

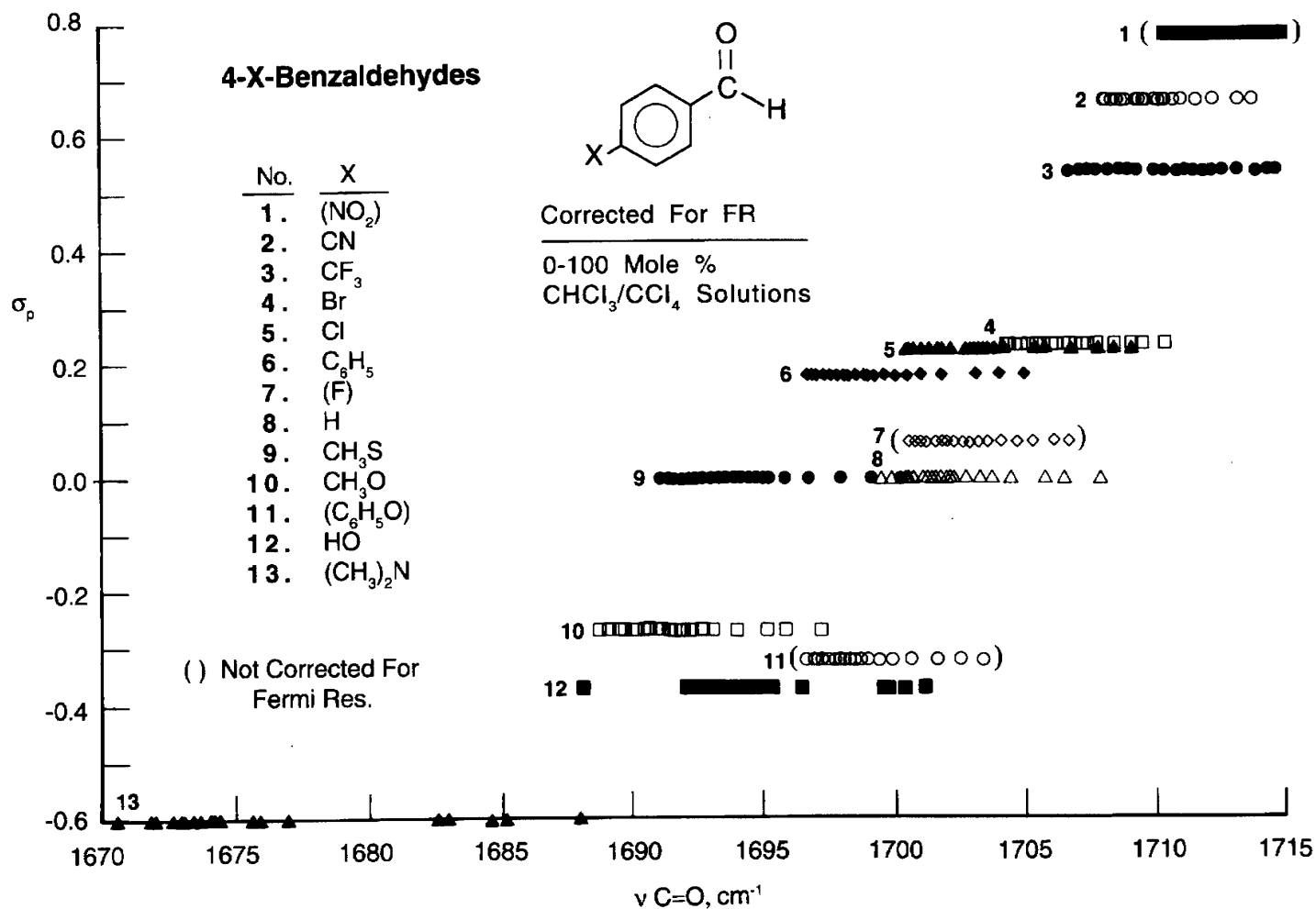


FIGURE 13.1 Plots of ν C=O corrected for Fermi resonance for each of the 4-X-benzaldehydes vs σ_p for the 4-X atom or group. The points on each line correspond to ν C=O frequencies for 0–100% CHCl₃/CCl₄ solutions.

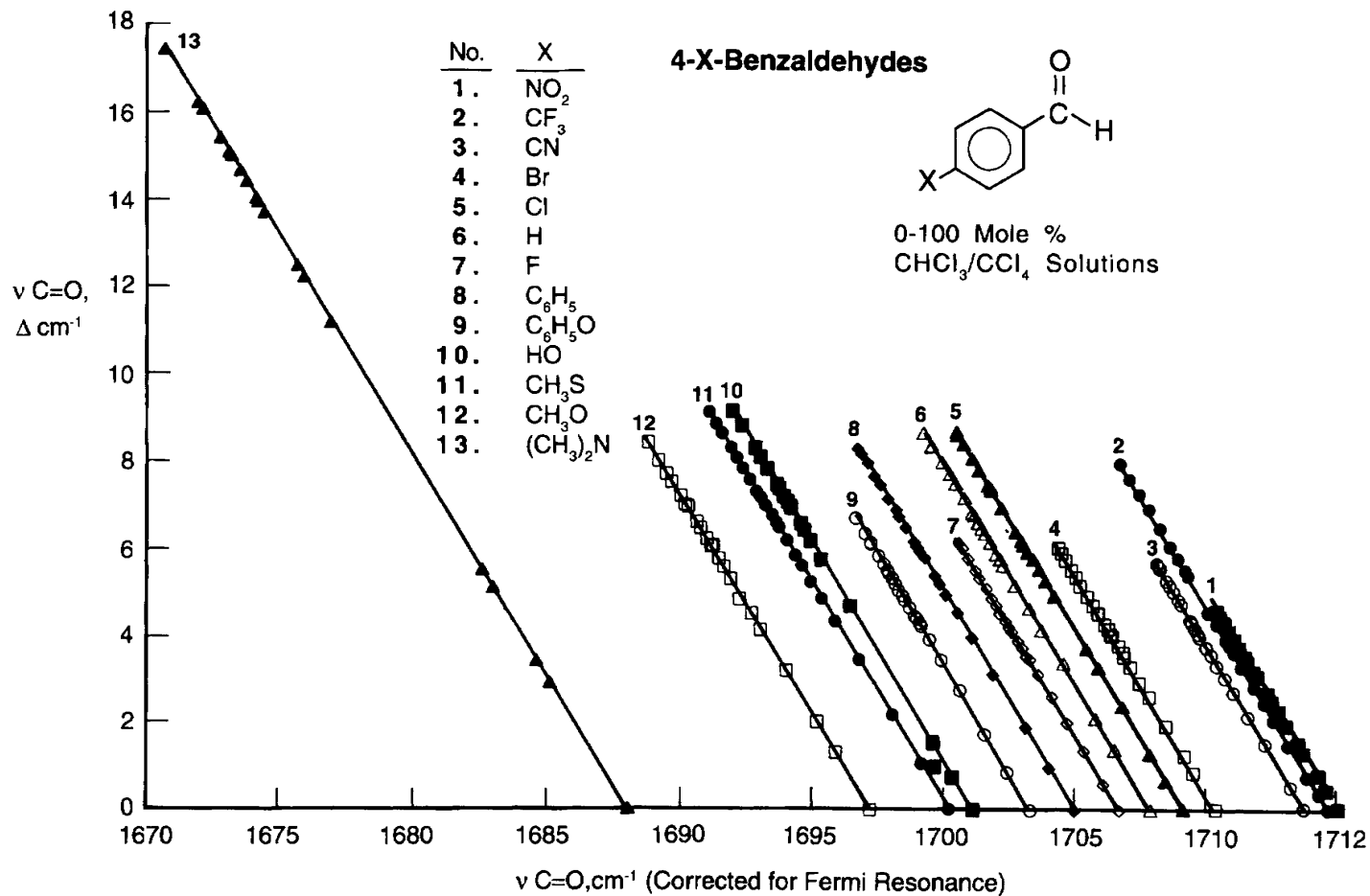


FIGURE 13.2 Plots of $\nu_{\text{C=O}}$ corrected for Fermi resonance in CCl₄ solution vs the frequency difference between ($\nu_{\text{C=O}}$ corrected for FR in CCl₄ solution minus $\nu_{\text{C=O}}$ corrected for FR for each of the mole % CHCl₃/CCl₄ solutions) for each of the 4-X-benzaldehydes.

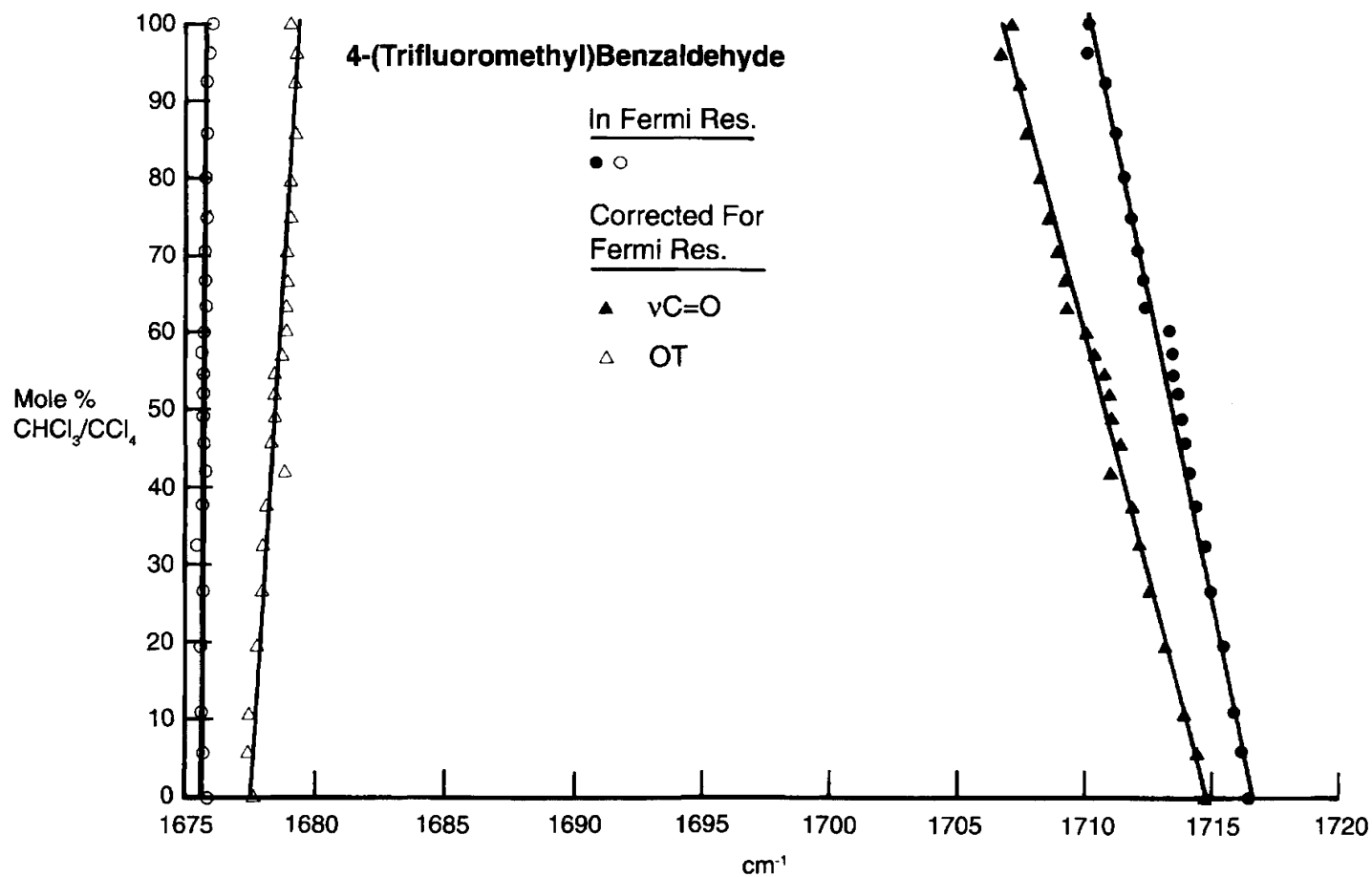


FIGURE 13.3 Plots of $\nu\text{C}=\text{O}$ and an overtone in Fermi resonance and their corrected frequencies vs mole % $\text{CHCl}_3/\text{CCl}_4$ for 4-(trifluoromethyl) benzaldehyde.

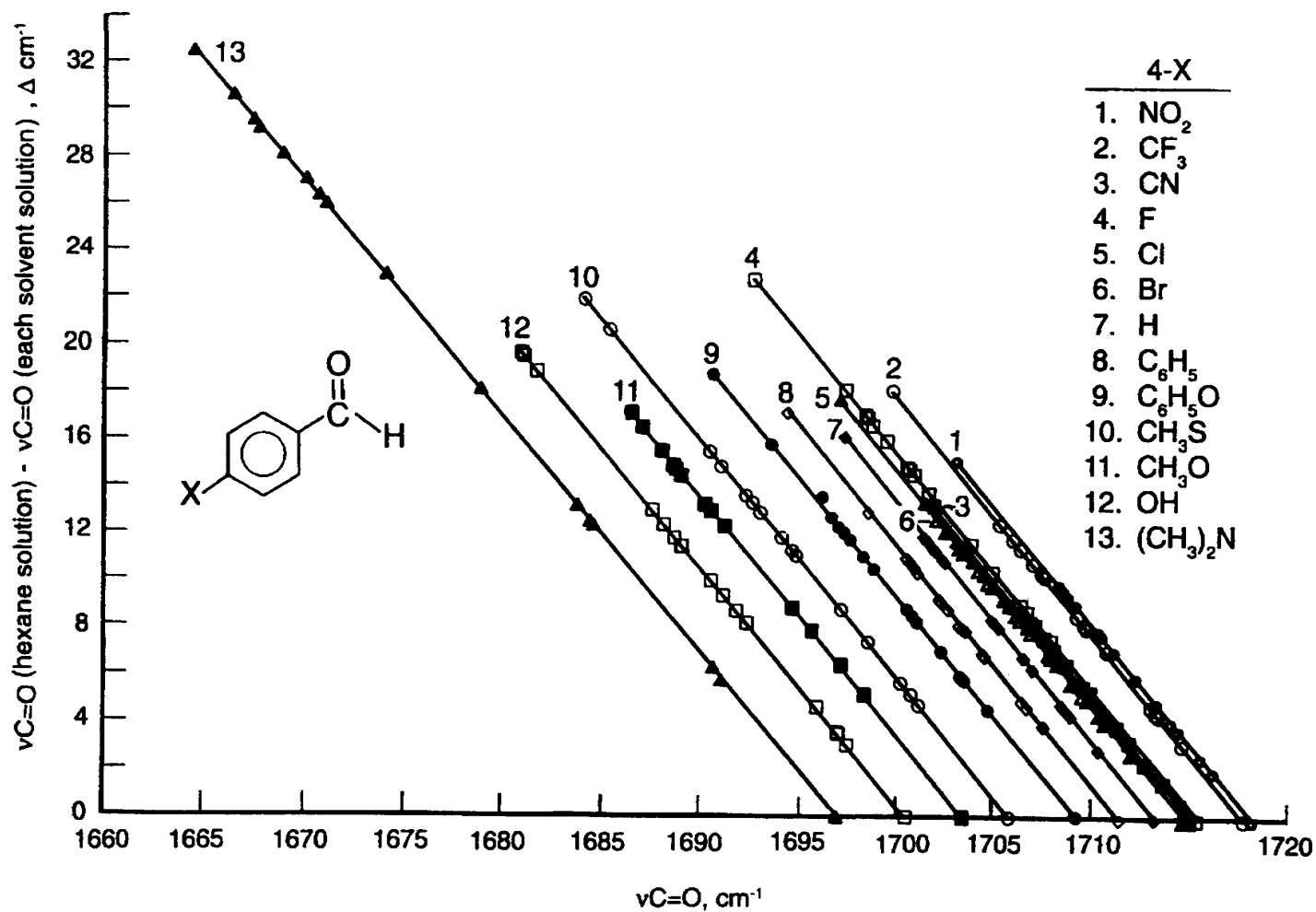
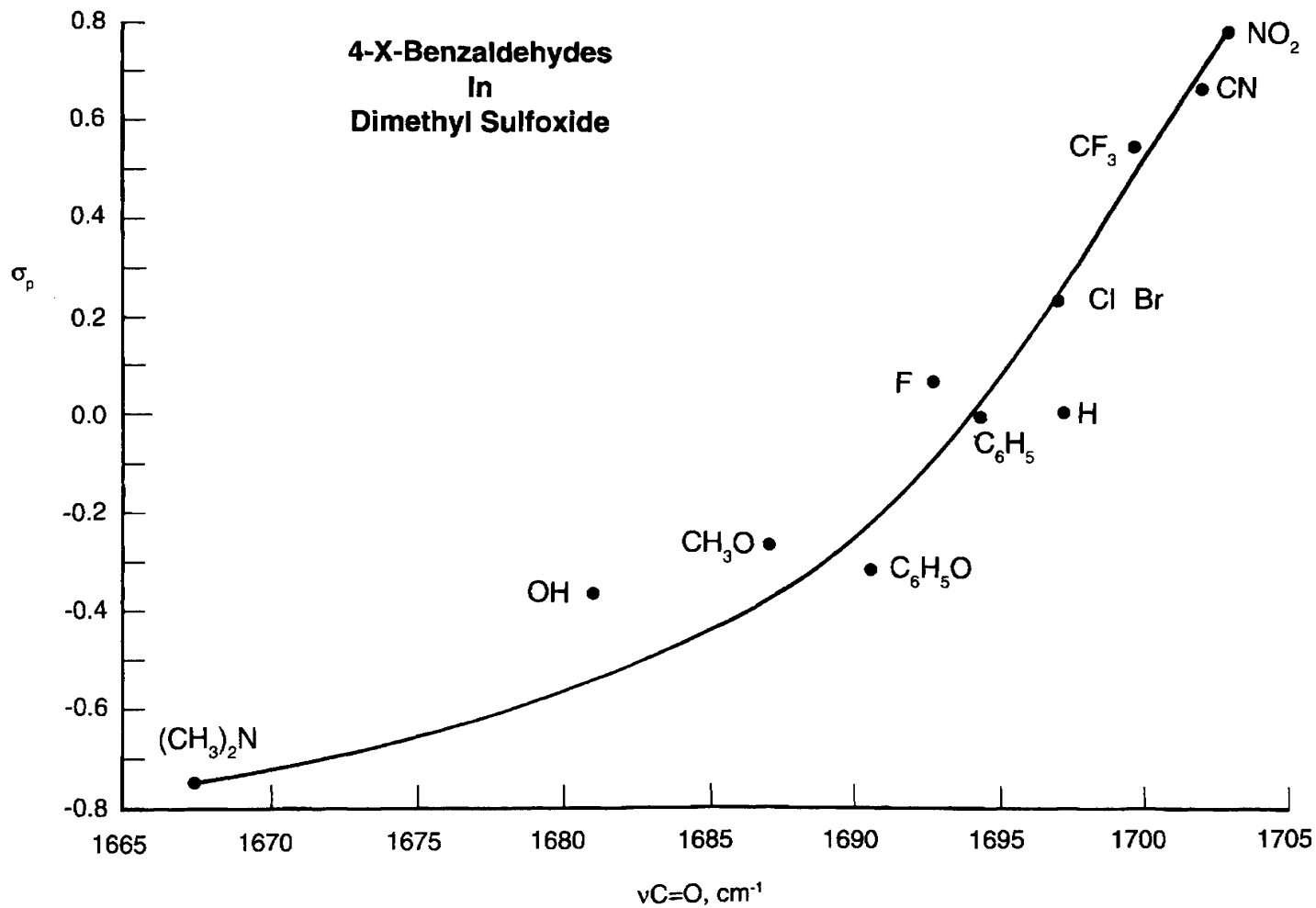


FIGURE 13.4 Plots of the $\nu_{\text{C=O}}$ frequency for each of the 4-X-benzaldehydes in a solvent vs the $\nu_{\text{C=O}}$ frequency difference between the $\nu_{\text{C=O}}$ frequency in hexane solution and the $\nu_{\text{C=O}}$ frequency in each of the other solvents used in the study.



Variables in Data Interpretation

FIGURE 13.5 A plot of $\nu_{\text{C=O}}$ vs Hammett σ_p for each of the 4-X-benzaldehydes in dimethyl sulfoxide solution.

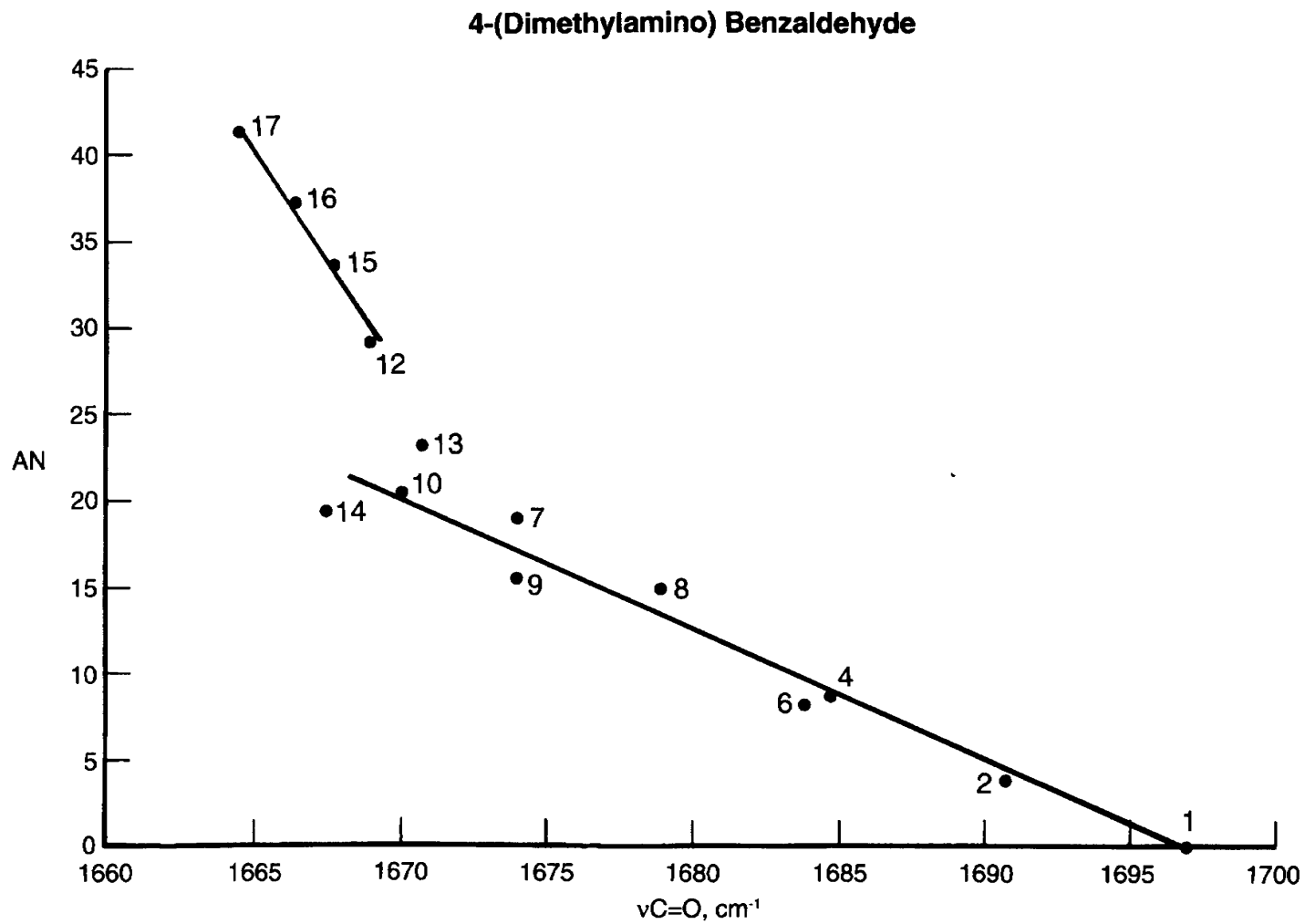


FIGURE 13.6 A plot of $\nu\text{C}=\text{O}$ for 4-(dimethylamino) benzaldehyde vs the solvent acceptor number (AN) for each of the solvents.

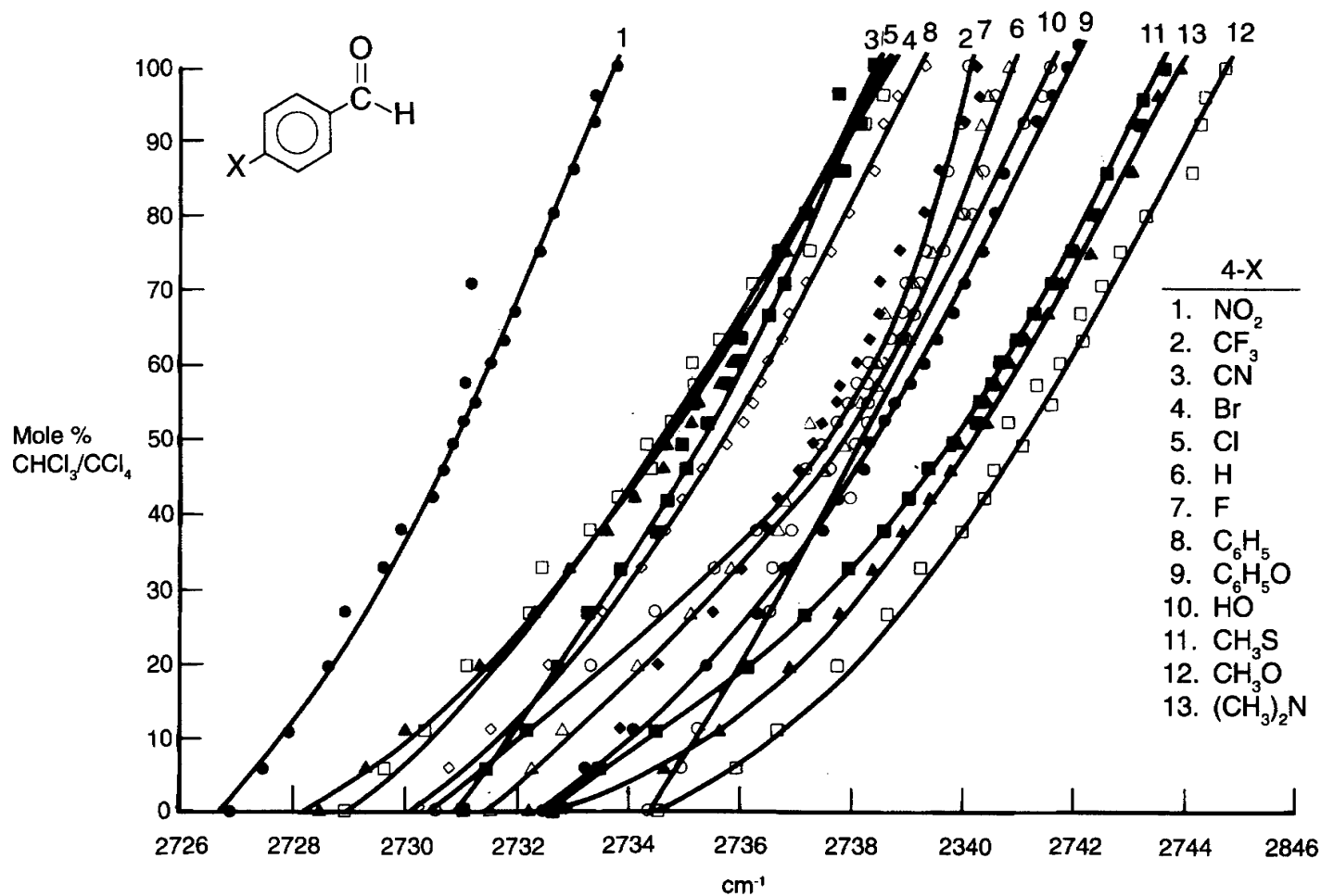


FIGURE 13.7 Plots of half of the Fermi doublet for each of the 4-X-benzaldehydes in the range 2726–2746 cm^{-1} vs mol % $\text{CHCl}_3/\text{CCl}_4$.

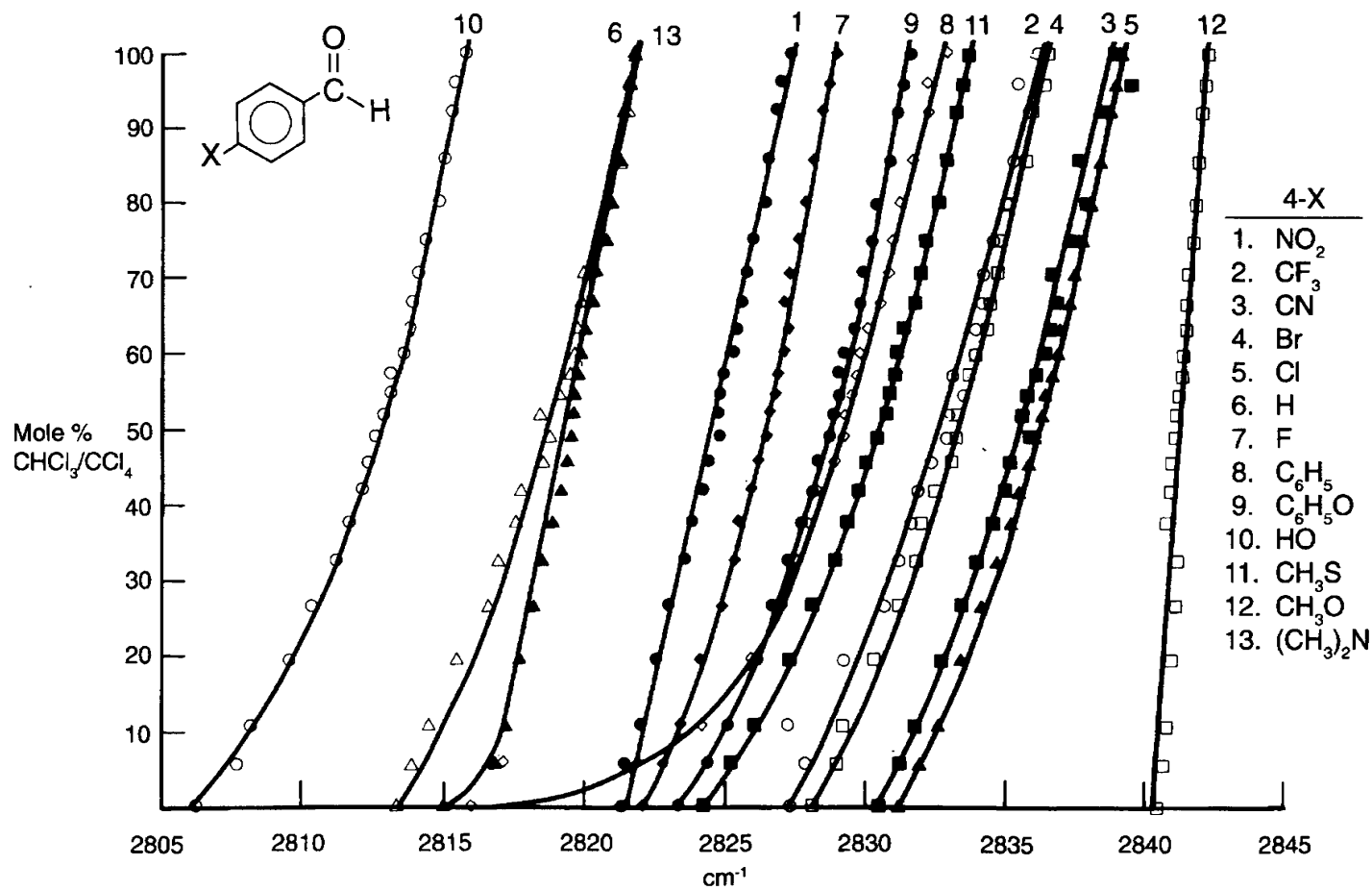


FIGURE 13.8 Plots of half of the Fermi doublet for each of the 4-X-benzaldehydes in the range 2805–2845 cm⁻¹ vs mole % CHCl₃/CCl₄.

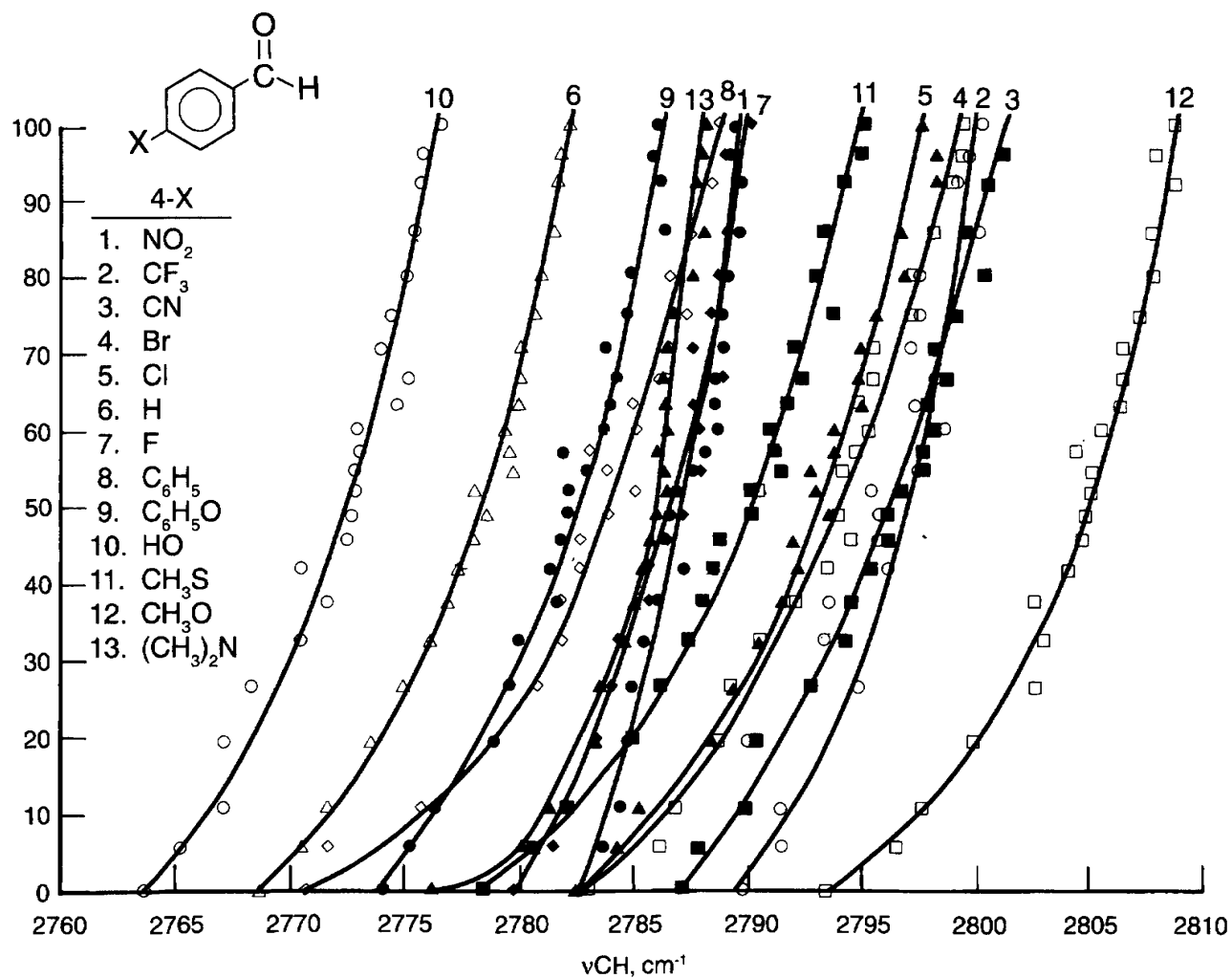


FIGURE 13.9 Plots of unperturbed ν_{CH} for each of the 4-X-benzaldehydes vs mole % $\text{CHCl}_3/\text{CCl}_4$.

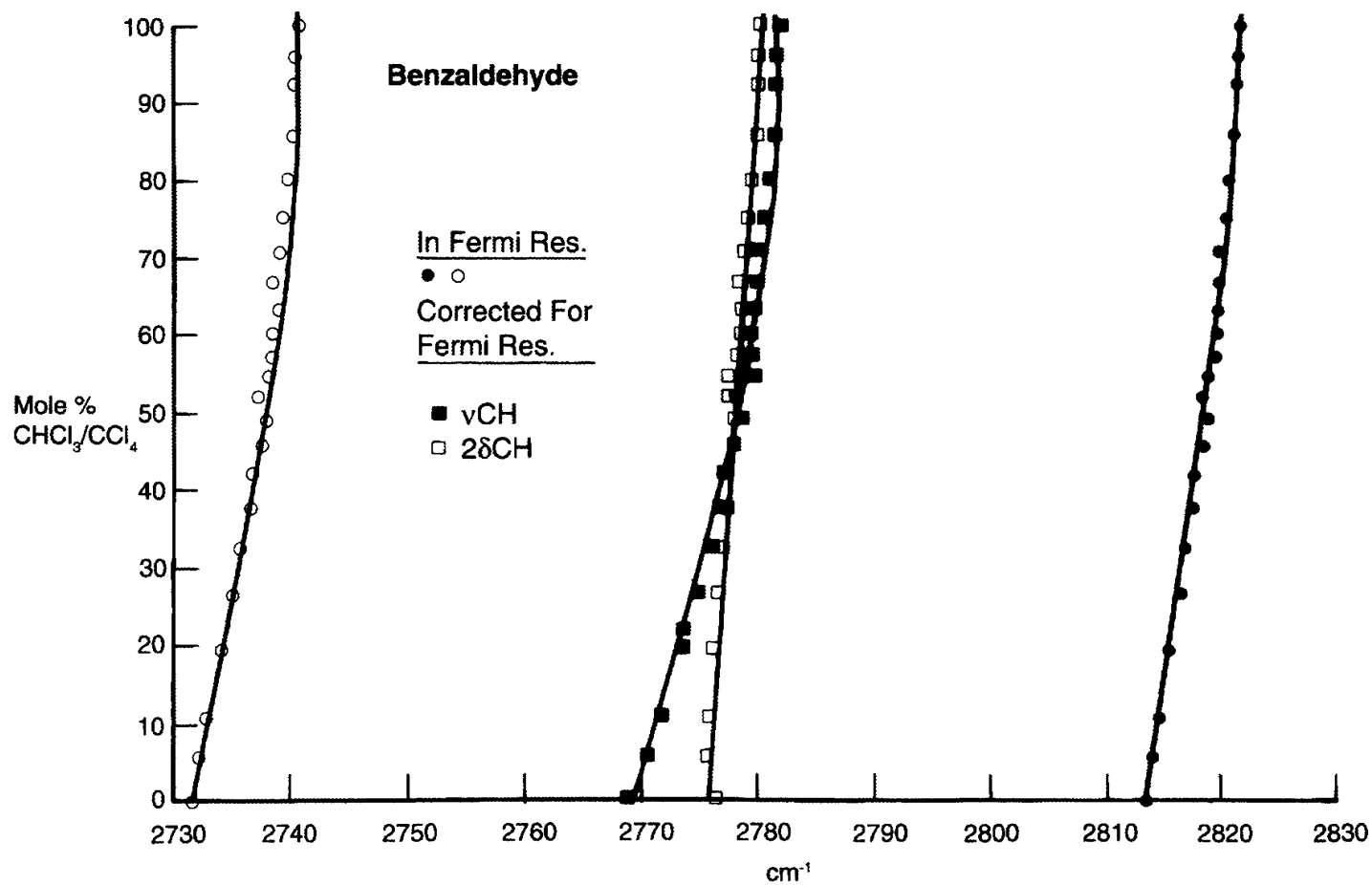


FIGURE 13.10 Plots of νCH and $2\delta\text{CH}$ in Fermi resonance and νCH and δCH corrected for FR for benzaldehyde vs mole % $\text{CHCl}_3/\text{CCl}_4$.

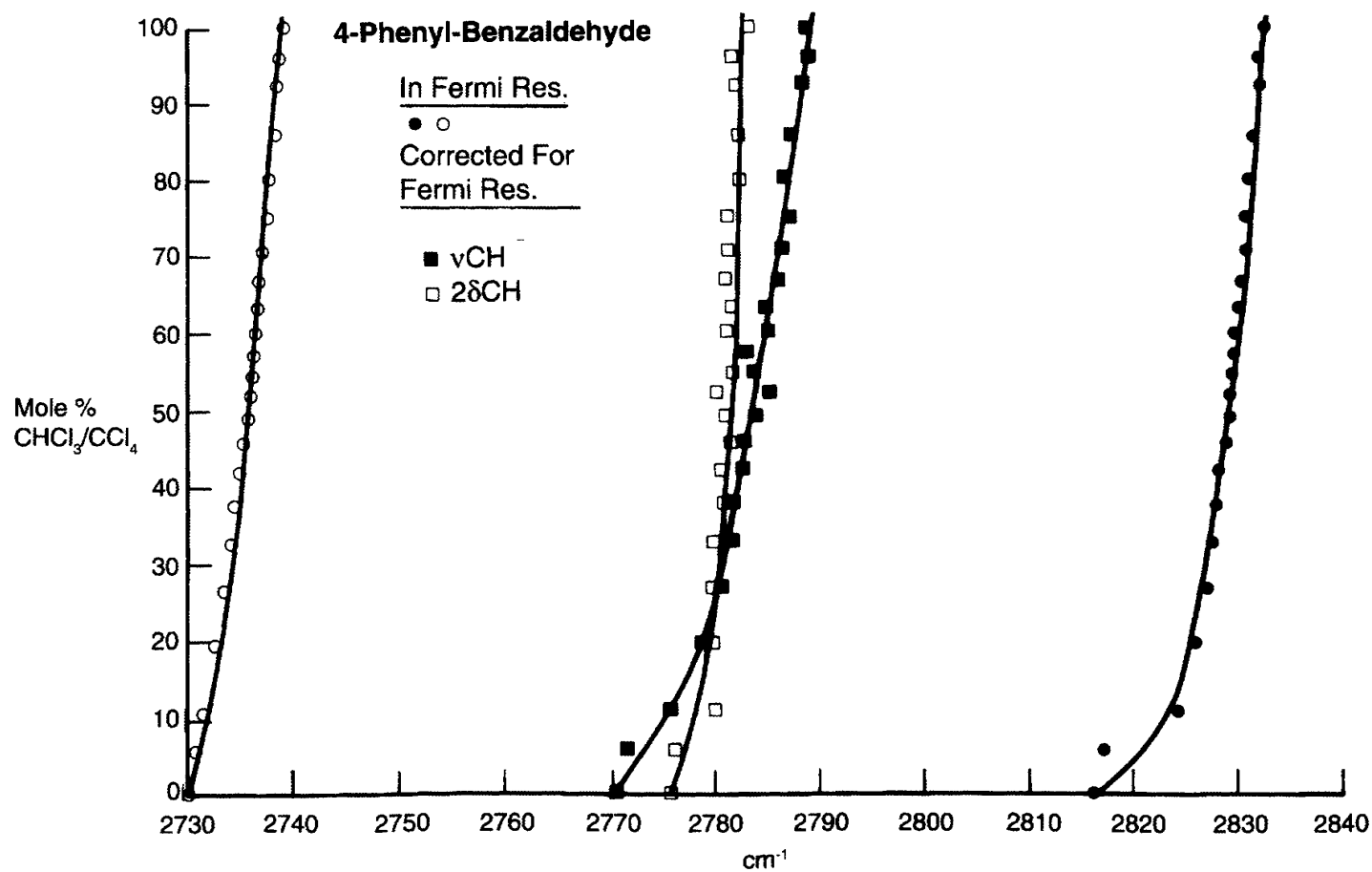
FIGURE 13.11 Plots of νCH and $2\delta\text{CH}$ in Fermi resonance and νCH and δCH corrected for FR for 4-phenylbenzaldehyde vs mole % $\text{CHCl}_3/\text{CCl}_4$.

TABLE 13.1 A comparison of IR data of nonconjugated aldehydes in different phases

Aldehyde	2(C=O str.) vapor cm ⁻¹	C=O str. vapor cm ⁻¹	C=O str. CCl ₄ soln. cm ⁻¹	2(C=O str.) neat cm ⁻¹	C=O str. neat cm ⁻¹	CH str. in FR. neat cm ⁻¹	2(CH bend) in FR. neat cm ⁻¹	CH bend neat cm ⁻¹
Butyr				3430	1721	2820	2720	1390
Isobutyr				3430	1721	2810	2710	1397
3-Cyclohexenyl	3462	1741		3420	1731	2830	2700	1392
Phenethyl	3452	1743		3410	1715	2810	2722	1400
Chloroacet			1730* ¹					
Dichloroacet			1748* ¹			vapor	vapor	vapor
Trifluoroacet		1788						
Trichloroacet		1778	1768* ¹			2859	2700	1365
Tribromoacet	3501	1760				2841	2680	1352

*¹ See Reference 1.

TABLE 13.1A Raman data and assignments for aldehydes

Aldehyde	C=O str.	C-H str. in FR.	2(delta-C-H) in FR.	delta-C-H	gama-C-H	C=C str.
Propion*	1723(7,p)	2830(9,p)	2718(9,p)	1337(1,p)	849(11,p)	
Isobutyr*	1730(5,p)	2813(5,p)	2722(9,p)		798(14,p)	
Hexanal*	1723(10,p)		2723(15,p)	1303(7)	891(7,p)	
Heptanal*	1723(9,p)		2723(14,p)	1303(7)	895(5,p)	
Bromal	1744(10,p)	2850(7,p)		1353(2,p)	785(9,p)	
Acrolein*	1688(42,p)	2812(3,p)		1359(32,p)		1618(22,p)
Benz*	1701	2815	2732			
Salicyl*	1633(22,P)					

*Reference 4.

TABLE 13.2 IR data and assignments for 4-X-benzaldehydes in the vapor and CHCl₃ and CCl₄ solution

4-X-Benzaldehyde x-Group	C=O str. [vapor] cm ⁻¹ (A)	C=O str. [CCl ₄] cm ⁻¹ (A)	C=O str. [CHCl ₃] cm ⁻¹ (A)	[vapor]- [CCl ₄] cm ⁻¹	[vapor]- [CHCl ₃] cm ⁻¹	[CCl ₄]- [CHCl ₃] cm ⁻¹
NO ₂	1728(1.289)	1715.0(0.261)	1710.4(0.417)	13	17.6	5.4
CN		1713.7*	1708.1*			
CF ₃		1714.6*	1707.1*			
Br	1720(1.250)	1710.4	1704.3*	19.6	15.7	6.1
Cl	1722(1.250)	1709.1*	1700.5*	12.9	21.5	8.6
C ₆ H ₅		1705.0*	1696.7*			
F	1719(1.230)	1706.7(0.862)	1700.6(0.808)	12.3	18.4	6.1
H		1707.9*	1699.2*			
CH ₃ S		1700.2*	1691.1*			
CH ₃ O	1717(1.240)	1697.2*	1688.8*	19.8	28.2	8.4
HO	1715(1.250)	1701.1*	1688.2*	13.9	26.8	12.9
(CH ₃) ₂ N	1711(1.042)	1688.1*	1671.8*	22.9	39.2	16.3

* Corrected for Fermi Res.

TABLE 13.3 The C=O stretching frequency for 4-X-benzaldehydes in various solvents

Solvent	4-NO ₂ cm ⁻¹	4-CF ₃ *† cm ⁻¹	4-CN*† cm ⁻¹	4-F cm ⁻¹	4-Cl cm ⁻¹	4-Br*† cm ⁻¹	4-H cm ⁻¹
Hexane	1718.1	1717.8	1715.2	1715.7*	1714.8	1714.8	1713.3
Diethyl ether	1714.1	1713.3	1711.9	1709.7	1710.4	1709.6	1709.1
Methyl t-butyl ether	1713.3	1713.4	1711.3	1706.4	1709.7	1708.1	1708.8
Carbon tetrachloride	1714.4	1714.6	1713.7	1706.7	1710.7	1710.4	1708.5
Carbon disulfide	1712.2	1713.1	1712.8	1705.1	1708.2	1709.5	1706.6
Benzene	1711.1	1710.7	1709.6	1703.9	1706.7	1707.8	1705.2
Acetonitrile	1709.2	1707.6	1707.6	1701.6	1703.9	1703.6	1702.5
Nitrobenzene	1708.6	1705.4	1707.1	1700.9	1703.1	1704.8	1702.1
Benzonitrile	1708.4	1707.6	1706.9	1700.7	1701.4	1703.3	1701.8
Methylene chloride	1710.3	1707.5	1708.7	1698.7*	1703.6	1704.3	1702.4
Nitromethane	1708.5	1706.4	1707.1	1698.5*	1702.6	1702.1	1701.5
t-Butyl alcohol	1716.2	1709.6	1707.9	1697.3*	1712.1	1706.2	1710.4
Chloroform	1710.4	1717.1	1708.1	1700.6	1703.4	1704.3	1701.9
Dimethyl sulfoxide	1703.1	1699.7	1702.1	1697.7	1697.1	1697.1	1697.2
Isopropyl alcohol	1716.2	1709.7	1709.9	1698.4*	1709.1	1706.9	1708.6
Ethyl alcohol	1715.6	1709.3	1708.7	1699.4*	1705.6	1706.4	1707.1
Methyl alcohol	1708.8	1706.1	1707.2	1697.5*	1704.6	1705.1	1705.1
Tetrahydrofuran	1709.9	1710.4	1704.8	1704.8	1705.8	1707.4	1705.1
1,2-Dichlorobenzene	1703.7	1708.8	1702.7	1702.7	1705.8	1705.4	1703.9
Range	(1718.2–1803.1)	(1717.8–1699.7)	(1715.2–1702.1)	(1715.4–1692.7)	(1714.8–1697.1)	(1714.8–1697.1)	(1713.3–1697.2)
	4-C ₆ H ₅	4-C ₆ H ₄ O	4-CH ₃ S	4-CH ₃ O*†	4-OH	4-N(CH ₃) ₂ *†	
Hexane	1711.4	1709.3	1705.9	1703.5		1696.9	
Diethyl ether	1707.6	1704.7	1700.8	1698.3	1696.9	1690.7	
Methyl t-butyl ether	1706.7	1703.5	1701.2	1697.1	1697.4	1691.1	
Carbon tetrachloride	1706.5	1703.4	1700.2	1695.6	1700.5	1684.6	
Carbon disulfide	1704.6	1701.1	1698.5	1694.7	1697.1	1684.4	
Benzene	1703.5	1700.7		1691.2	1695.9	1683.8	
Acetonitrile	1701.1	1697.5	1694.1	1690.6	1689.1	1674.1	
Nitrobenzene	1700.8	1697.3	1692.6	1690.6	1689.1	1678.9	
Benzonitrile	1700.8	1697.3	1692.3	1690.4	1688.2	1674.1	
Methylene chloride	1701.1	1697.1	1693.1	1690.3	1689.1	1670.1	
Nitromethane	1700.8	1696.2	1694.7	1689.1	1688.8	1671.1	
t-Butyl alcohol	1698.6	1693.5	1685.3	1686.4	1681.7	1668.9	
Chloroform	1700.5	1696.6	1691.1	1688.8	1687.6	1670.6	
Dimethyl sulfoxide	1694.3	1690.6		1687.1	1681.1	1667.4	
Isopropyl alcohol	1702.4	1702.3	1685.3	1688.1	1680.9	1667.7	
Ethyl alcohol	1704.5	1701.1	1684.1	1688.6	1692.3	1666.4	
Methyl alcohol	1702.6	1698.3	1690.5	1687.1	1690.6	1664.4	
Tetrahydrofuran	1703.4	1700.6	1697.2	1697.8	1691.9	1685.4	
1,2-Dichlorobenzene	1702.3	1696.8	1694.8	1694.4	1691.2	1681.3	
Range	(1711.4–1694.3)	(1709.3–1690.6)	(1705.9–1684.1)	(1703.5–1686.4)	(1696.9–1680.9)	(1696.9–1666.4)	
Overall Range in all solvents	(1718.1–1664.4)						
Delta C=O	53.7						

† See the explanatory text on page 269 for discussion of material designated by an asterisk.

TABLE 13.4 The CH bending vibration for 4-X-benzaldehydes in CCl₄ and CHCl₃ solutions and in the vapor phase

4-X-Benzaldehyde X	Vapor cm ⁻¹	1%(wt./vol.) PCCl ₄ cm ⁻¹	1%(wt./vol.) [CHCl ₃] cm ⁻¹	[CHCl ₃]-[CCl ₄] cm ⁻¹	[vapor]-[CHCl ₃] cm ⁻¹
NO ₂		1382.92	1384.79	1.87	
CF ₃		1386.36	1388.61	2.25	
CN		1381.28	1382.89	1.61	
Br	1387	1383.12			
Cl	1381	1383.6	1385.8	2.23	-4.8
O		1387.35	1390.11	2.76	
F	1386	1385.91	1388.39	2.48	-2.4
C ₆ H ₅		1383.96	1385.45	1.49	
C ₆ H ₅ O		1386.52	1388.98	2.46	
OH		1393.46			
CH ₃ S		1387.34	1390.03	2.69	
CH ₃ O		1390.2	1394.31	4.11	
(CH ₃) ₂ N	1385	1392.07	1394.28	2.21	-9.3
Range		(1381.28-1392.07)	(1382.89-1394.28)	(1.49-4.11)	

TABLE 13.5 The overtone of CH bending in Fermi resonance with =CH stretching for 4-X-benzaldehydes corrected for Fermi resonance

4-X-benzaldehydes 1%(wt./vol.)	4-NO ₂ CH bend cm ⁻¹	4-CF ₃ CH bend cm ⁻¹	R-CN CH bend cm ⁻¹	4-Br CH bend cm ⁻¹	4-Cl CH bend cm ⁻¹	4-H CH bend cm ⁻¹	4-F CH bend cm ⁻¹	C ₆ H ₅ CH bend cm ⁻¹	C ₆ H ₅ O CH bend cm ⁻¹	OH CH bend cm ⁻¹	CH ₃ S CH bend cm ⁻¹	CH ₃ O CH bend cm ⁻¹	4-N(CH ₃) ₂ CH bend cm ⁻¹
CCl ₄	1382.92	1386.36	1381.28		1383.61	1387.35	1385.91		1386.52		1387.34	1390.2	1392.07
CHCl ₃	1384.79	1388.61	1382.89		1385.84	1390.11	1388.39		1388.98		1390.03	1394.31	1394.28
delta-CH bend	1.87	2.25	1.61		2.23	2.76	2.48		2.46		2.69	4.11	2.21
[calculated 2(CH bend)]													
CCl ₄	2765.84	2772.72	2762.56	2766.24	2767.22	2774.7	2771.82		2773.04		2774.68	2780.4	2784.14
CHCl ₃	2769.58	2777.22	2765.78		2771.68	2780.22	2776.78		2777.96		2780.06	2788.62	2788.56
delta-2(CH bend)	3.74	4.5	3.22		4.46	5.52	4.96		4.92		5.38	8.22	4.42
2(CH bend) corrected for Fermi Res.													
CCl ₄	2765.47	2771.99	2774.31	2774.08	2782.93	2779.82	2775.08	2775.57	2781.68	2773.1	2778.39	2781.58	2770.98
CHCl ₃	2771.7	2775.96	2777.44	2775.53	2788.78	2788.78	2779.13	2783.4	2787.33	2780.74	2782.08	2778.21	2777.53
delta-CH bend													
CCl ₄	6.23	3.97	3.13	7.84	5.85	8.96	4.05	7.83	5.65	7.64	3.69	-3.37	6.55
CHCl ₃													

TABLE 13.6 IR data and assignments for the observed and corrected for Fermi resonance CH stretching frequencies for 4-X-benzaldehydes in CCl₄ and CHCl₃ solutions

4-X-Benzaldehydes 1% solutions X	obs. =CH str.	obs. =CH str.	[=CH str. corrected for FR.]	[=CH str. corrected for FR.]	obs. =CH str.	cor. FR.	[obs.]	[obs.]
	CCl ₄ cm ⁻¹	CHCl ₃ cm ⁻¹	CCl ₄ cm ⁻¹	CHCl ₃ cm ⁻¹	[CHCl ₃]-[CCl ₄] cm ⁻¹	[CHCl ₃]-[CCl ₄] cm ⁻¹	CCl ₄ cm ⁻¹	CHCl ₃ cm ⁻¹
NO ₂	2821.3	2827.3	2782.7	2789.4	6	6.7	38.6	37.9
CF ₃	2827.3	2836.2	2789.7	2800.3	8.9	10.6	37.6	35.9
CN	2830.4	2838.9	2787.1	2799.9	8.5	12.8	43.3	39
F	2822.1	2829	2779.8	2790.1	6.9	10.3	42.3	38.9
Cl	2828.1	2836.6	2782.9	2799.5	8.5	16.6	45.2	37.1
H	2813.3	2821.8	2768.7	2782.2	8.5	13.5	44.6	39.6
C ₆ H ₅	2815.9	2832.8	2770.6	2788.8	16.9	18.2	45.3	44
OH	2806.2	2815.7	2763.6	2776.6	9.5	13	42.6	39.1
C ₆ H ₅ O	2823.3	2831.6	2774	2786.1	8.3	12.1	49.3	45.5
CH ₃ S	2824.2	2833.6	2778.4	2795.2	9.4	16.8	45.8	38.4
CH ₃ O	2840.5	2842.3	2793.4	2808.9	1.8	15.5	47.1	33.4
(CH ₃) ₂ N	2814.9	2821.8	2776.1	2788.2	6.9	12.1	38.8	33.6

Ketones

Solvent-Induced Frequency Shifts	288
Solute-Solvent Interaction Affected by Steric Factors	289
Inductive, Resonance, and Temperature Effects	290
Other Chemical and Physical Effects	291
Other Conjugated Carbonyl Containing Compounds	291
Chalcones	294
Intramolecular Hydrogen Bonding	294
Cycloalkanones	295
Substituted 1,4-Benzoquinones	297
Concentration Effects	299
References	299

Figures

Figure 14-1	301 (288)
Figure 14-2	302 (290)
Figure 14-3	303 (290)
Figure 14-4	303 (291)
Figure 14-5	304 (295)
Figure 14-6	305 (296)
Figure 14-7	306 (296)
Figure 14-8	307 (296)
Figure 14-9	308 (297)
Figure 14-10	308 (297)
Figure 14-11	309 (297)
Figure 14-12	309 (298)
Figure 14-13	310 (298)

Tables

Table 14-1	311 (288)
Table 14-2	312 (288)
Table 14-2a	313 (288)
Table 14-3	314 (288)
Table 14-3a	315 (289)
Table 14-3b	315 (290)
Table 14-3c	316 (290)
Table 14-4	316 (290)
Table 14-5	317 (290)
Table 14-6	318 (291)
Table 14-7	319 (294)
Table 14-7a	320 (294)
Table 14-8	321 (294)
Table 14-9	322 (295)
Table 14-10	323 (295)
Table 14-11	324 (296)
Table 14-12	325 (298)
Table 14-13	326 (298)
Table 14-14	327 (298)
Table 14-15	328 (298)
Table 14-16	328 (298)
Table 14-17	329 (298)
Table 14-18	329 (298)
Table 14-19	330 (299)

*Numbers in parentheses indicate in-text page reference.

Acetone is the simplest member of the ketone series. Its empirical structure is $\text{CH}_3\text{-C(=O)-CH}_3$. Table 14.1 lists IR and Raman data for acetone and acetone- d_6 (1,2). The CD_3 frequencies and assignments are listed directly under those for the CH_3 frequencies and assignments. The frequency ratios for CH_3/CD_3 vary between 1.11 and 1.38. The B_1 and B_2 CH_3 rocking mode to CD_3 rocking mode frequency ratios are 1.132 and 1.108, respectively, and this indicates that these two modes are coupled with B_1 and B_2 modes, respectively. These data illustrate that both IR and Raman data and deuterated analogs are required to make detailed assignments of molecular compounds.

SOLVENT-INDUCED FREQUENCY SHIFTS

Hallam has reviewed the literature concerning attempts to develop an accurate quantitative and physical meaningful explanation of solvent-induced stretching frequencies (3). Kirkwood *et al.* (4) and Bauer and Magot (5) related the observed frequency shifts and the dielectric constant ϵ of the solvent. The (K)irkwood (B)auer (M)agot work resulted in the KBM equation:

$$(\nu_{\text{vapor}} - \nu_{\text{solution}})/\nu_{\text{vapor}} = \Delta\nu/\nu = C[(\epsilon - 1)/(2\epsilon + 1)]$$

Josien and Fuson refined the equation to include a term based on the index of refraction of the solvent (6). Bellamy *et al.* found that $\Delta\nu/\nu$ for any solute plotted vs $(\Delta\nu/\nu)$ for any other solvent within a class of compounds produced a linear curve (7). They therefore predicted that group frequency shifts were local association effects between solute and solvent and not dielectric effects. Bellamy *et al.* proposed that ν hexane should be substituted for ν vapor in the KBM equation in order to negate the effects of phase change (7). Table 14.2 illustrates the application of the KBM equation using IR data for acetone $\nu\text{C=O}$ frequencies in various solvents. Table 14.2 shows that the KBM equation predicts the $\nu\text{C=O}$ mode within -2.1 to $+14.3 \text{ cm}^{-1}$. The best fit is for acetone in solution with acetonitrile and the worst fit is for acetone in water. In the case of CHCl_3 and the four alcohols, the $\nu\text{C=O}$ frequency differences between the calculated and observed range are between 4.3 and 7.7 cm^{-1} . The larger differences here compared to the other solvents are most likely the result of intermolecular hydrogen bonding ($\text{C=O}\cdots\text{HCCl}_3$ or $\text{C=O}\cdots\text{HOR}$).

Table 14.2a contains the calculated values for $A - 1/2A + 1$ and $X - Y/X$ where A and Y are equal to 0 to 85 and X equals 85 (see the KBM equation). These two sets of data are plotted in Fig. 14.1. These data show that any set of numbers using the equivalent of the KBM equation or Bellamy's proposal yields a mathematical curve. In particular, the linear plot $X - Y$ vs Y is thus meaningless in predicting $\nu\text{C=O}$ frequencies (8). Intermolecular hydrogen bonding and dipolar interaction between solute and solvent as well as dielectric effects must play a role in the $\nu\text{C=O}$ frequencies of carbonyl containing compounds. Steric factors, which also play a role between solute-solvent interaction, must also be considered in predicting $\nu\text{C=O}$ frequencies in any particular physical phase (see in what follows).

Table 14.3 lists the C=O stretching frequencies for aliphatic ketones in the vapor phase and in 1% wt./vol. in various solvents (9).

In this series of ketones (dimethyl ketone through di-*tert*-butyl ketone) the steric factor of the alkyl group(s) and the basicity of the carbonyl group both increase. As the steric factor of the alkyl group increases the intermolecular distance between the carbonyl group and a solvent

molecule increases. In the case of intermolecular hydrogen bonding between a solvent and a proton and a carbonyl group, the strength of the hydrogen bond depends upon at least four factors. These are, the basicity of the carbonyl group, the acidity of the solvent proton, the steric factor of the dialkyl groups of the dialkyl ketone, and the steric factor of the atoms or groups of the solvent molecules not involved directly with the intermolecular hydrogen bond.

All of the aliphatic ketones exhibit their $\nu\text{C}=\text{O}$ mode at its highest frequency in the vapor phase ($1699\text{--}1742\text{ cm}^{-1}$). In solution, the highest $\nu\text{C}=\text{O}$ frequencies are exhibited in hexane solution ($1690.3\text{--}1727.2\text{ cm}^{-1}$). With the exception of dimethyl ketone (acetone) in hexane, the $\nu\text{C}=\text{O}$ frequency for the other dialkyl ketones decreases in frequency with increasing negative values for both σ^* (increasing electron release to the carbonyl group) and E_s (an increasing steric factor of the alkyl group) and the summation of σ^* times the summation of $E_s \cdot 10^{-2}$.

In the case of dimethyl ketone, its $\nu\text{C}=\text{O}$ mode occurs at a higher frequency than $\nu\text{C}=\text{O}$ for methyl ethyl ketone only in the following solvents, tert-butyl alcohol, chloroform, isopropyl alcohol, ethyl alcohol, and methyl alcohol. In these solvents there is intermolecular hydrogen bonding between solute and solvent ($\text{C}=\text{O}\cdots\text{HOR}$ and $\text{C}=\text{O}\cdots\text{HCCl}_3$). Moreover, in these protic solvents the $\nu\text{C}=\text{O}$ frequency order for methyl ethyl ketone and diethyl ketone is reversed from the sequence that they exhibit when these dialkyl ketones are in the other solvents.

SOLUTE-SOLVENT INTERACTION AFFECTED BY STERIC FACTORS

Table 14.3a shows a comparison of the carbonyl stretching frequency difference for ketones in hexane solution and in each of the other solvents (9). The strength of an intermolecular hydrogen bond ($\text{C}=\text{O}\cdots\text{HOR}$ or $\text{C}=\text{O}\cdots\text{HCCl}_3$) is proportional to this frequency difference. The larger this frequency difference, the stronger the intermolecular hydrogen bond. Or, in other words, the stronger the intermolecular hydrogen bond between the ketone solute and the protic solvent, the more $\nu\text{C}=\text{O}$ shifts to lower frequency when compared to $\nu\text{C}=\text{O}$ for the same ketone in n-hexane solution. The most acid proton for the alcohol series is that for methyl alcohol, and the least acidic proton is that for tert-butyl alcohol. In addition, the steric factor is the largest for tert-butyl alcohol, and the least for methyl alcohol. The most basic ketone carbonyl group is in the case of di-tert-butyl ketone and the least basic carbonyl group is in the case of dimethyl ketone. Neglecting steric factors, these facts would predict that the strongest intermolecular hydrogen bonds would be formed between methyl alcohol and di-tert-butyl ketone, and the weakest between tert-butyl alcohol, and dimethyl ketone. Study of Table 14.3a shows that the strongest intermolecular hydrogen is actually formed between methyl alcohol and diisopropyl ketone, and the strength of the intermolecular hydrogen bond with diisopropyl ketone decreases in the order methyl alcohol, ethyl alcohol, isopropyl alcohol, and tert-butyl alcohol. The strength of the intermolecular hydrogen bond formed between diisopropyl ketone and chloroform falls between that for tert-butyl alcohol and isopropyl alcohol. In the alcohol series, the strength of the intermolecular hydrogen is also stronger between diisopropyl ketone than between di-tert-butyl ketone. The strength of the intermolecular hydrogen bond is less in the case of ethyl isopropyl ketone compared to diisopropyl ketone, but it also is stronger than in the case of di-tert-butyl ketone. These data show that steric factors increase the $\text{C}=\text{O}\cdots\text{H}$ intermolecular

hydrogen bond distance, thus weakening the possible strength of this intermolecular hydrogen bond.

The ketone $\nu_{\text{C=O}}$ frequency shifts in nonprotic solvents are also less in the case of di-tert-butyl ketone vs the other dialkyl ketones. Therefore, steric factors of the alkyl groups also play a role in the dielectric effects of the solvent upon the carbonyl group.

Table 14.3b shows a comparison of the carbonyl stretching frequency difference for dialkyl ketones in methyl alcohol and other protic solvents (9). In this case, the strength of the intermolecular hydrogen bond ($\text{C=O} \cdots \text{H}$) decreases as the number increases. This comparison shows that steric factors also affect the strength of the intermolecular hydrogen bond.

Table 14.3c shows a comparison of the differences in the carbonyl stretching frequencies of dialkyl ketones in hexane solution and in alcohol solution for solute molecules not intermolecularly hydrogen bonded (9). These data show that the frequency difference decreases for these ketones in alcohol solution, progressing in the series methyl alcohol through tert-butyl alcohol. With increased branching on the α -carbon atom of the C–OH group, the intermolecular polar effect due to the alcohol oxygen atom is decreased; thus, there is a lesser polar effect upon dialkyl ketone carbonyl groups surrounded by intermolecularly hydrogen-bonded alcohol molecules progressing in the series methyl alcohol through tert-butyl alcohol. The $\nu_{\text{C=O}}$ mode decreases in frequency as the polarity of the solvent increases.

Table 14.4 lists data for the C=O stretching frequencies for n-butyrophenone and tert-butyrophenone in 0–100 mol% $\text{CHCl}_3/\text{CCl}_4$ solutions (2% wt./vol.). The $\nu_{\text{C=O}}$ mode for both n-butyrophenone (1691–1682.6 cm^{-1}) and tert-butyrophenone (1678.4–1674.1 cm^{-1}) decreases in frequency as the mole % $\text{CHCl}_3/\text{CCl}_4$ is increased from 0–100 cm^{-1} . However, it is noted that the $\nu_{\text{C=O}}$ frequency for n-tert-butyrophenone decreases in frequency by only one-half as much as that for n-butyrophenone ($4.3 \text{ cm}^{-1}/9 \text{ cm}^{-1} = 0.48$) in going from solution in CCl_4 to solution in CHCl_3 . The C=O group for the tert-butyro analog is more basic than the n-butyro analog, and on this basis one would expect a stronger intermolecular hydrogen bond to be formed between $\text{C=O} \cdots \text{HCCl}_3$ for the tert-butyro analog than for the n-butyro analog, and it is noted that this is not the case. The reason for this is that the steric effect of the tert-butyro group prevents the Cl_3CH proton from coming as close in space to the C=O oxygen atom in the case of tert-butyrophenone, which prevents it from forming as strong a $\text{C=O} \cdots \text{HCCl}_3$ bond as in the case of the n-butyro analog where the n-butyro group has a lesser steric factor.

Figure 14.2 show a plot of the $\nu_{\text{C=O}}$ frequency for tert-butyrophenone vs the mole % $\text{CHCl}_3/\text{CCl}_4$. The resulting curve is nonlinear due to the formation of $\text{C=O} \cdots \text{HCCl}_3$ hydrogen bonds. The general decrease in frequency is due to the dielectric effects of the solvent system. The carbonyl stretching frequencies for n-tert-butyrophenone occur at lower frequencies (1678.4–1674.1 cm^{-1}) compared to those for di-tert-butyl ketone (1685.9–1680.7 cm^{-1}) in 0–100 mol% $\text{CHCl}_3/\text{CCl}_4$ due to conjugation of the phenyl group with the carbonyl group, which weakens the C=O bond (10).

INDUCTIVE, RESONANCE, AND TEMPERATURE EFFECTS

Table 14.5 list IR data for acetone, α -chloroacetone, acetophenone, and benzophenone in CS_2 solution between ~ 29 and -100°C (11). Figure 14.3 shows plots of the carbonyl stretching frequencies for these four compounds vs the temperature of the CS_2 solution in $^\circ\text{C}$. These plots

show that all of the $\nu_{\text{C=O}}$ modes decrease in frequency as the temperature is lowered from room temperature. Two $\nu_{\text{C=O}}$ frequencies are noted in the case of α -chloroacetone, and both occur at a higher frequency than $\nu_{\text{C=O}}$ for acetone. The inductive effect of an α -Cl atom increases the $\nu_{\text{C=O}}$ frequency, and the inductive effect is independent of spatial orientation. There is a field effect of a Cl atom near in space to the carbonyl oxygen atom, and it also causes the $\nu_{\text{C=O}}$ mode to increase in frequency. Thus, rotational conformer I is assigned to the higher frequency $\nu_{\text{C=O}}$ band, while rotational conformer II is assigned to the lower frequency $\nu_{\text{C=O}}$ band in the case of α -chloroacetone. The concentration of rotational conformer I increases while the concentration of rotational conformer II decreases with decrease in temperature (11).

Substitution of one or two phenyl groups for one or two methyl groups of acetone yields acetophenone ($\nu_{\text{C=O}}$, 1689.4 cm^{-1}) and benzophenone ($\nu_{\text{C=O}}$, 1663.3 cm^{-1}), respectively. Thus, the first phenyl group causes $\nu_{\text{C=O}}$ to decrease in frequency by 28.1 cm^{-1} while the second phenyl group causes $\nu_{\text{C=O}}$ to decrease in frequency by an additional 26.1 cm^{-1} . The phenyl group(s) is (are) conjugated with the carbonyl group, and it weakens the C=O bond, which causes its $\nu_{\text{C=O}}$ mode to vibrate at lower frequency.

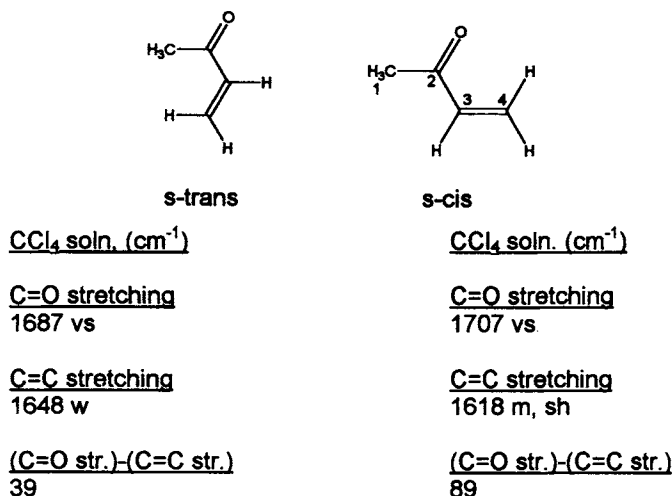
OTHER CHEMICAL AND PHYSICAL EFFECTS

Table 14.6 shows a comparison of the $\nu_{\text{C=O}}$ frequencies for 2% wt./vol. ketone in 0–100 mol% $(\text{CH}_3)_2\text{SO}/\text{CCl}_4$ solutions. Figure 14.4 shows plots of $\nu_{\text{C=O}}$ vs mole % $(\text{CH}_3)_2\text{SO}/\text{CCl}_4$ for the same six ketones as shown in Table 14.6. All six curves decrease in frequency in a linear manner as mole % $(\text{CH}_3)_2\text{SO}/\text{CCl}_4$ is increased from ~ 30 to 100 mol% $(\text{CH}_3)_2\text{SO}/\text{CCl}_4$. This is in the order of the increasing polarity of the solvent system. All six ketones appear to be affected in the same manner because the linear portion of the curves is parallel. The $\nu_{\text{C=O}}$ frequencies decrease in the order acetone, 2,4,6-trimethylacetophenone, 4-nitroacetophenone, acetophenone, 4-methoxyacetophenone, and benzophenone. The effect of conjugation was discussed previously. In the case of 2,4,6-trimethylacetophenone, the carbonyl group and the phenyl group are not coplanar; therefore, the C=O group is not conjugated with the phenyl group. Thus, the C=O group is higher in frequency than that exhibited by acetophenone by 13 cm^{-1} , but lower in frequency than acetone by 14 cm^{-1} . Hammett σ_p values for 4-nitro and 4-methoxy benzophenone cause the $\nu_{\text{C=O}}$ mode to be higher and lower in frequency, respectively, than $\nu_{\text{C=O}}$ for acetophenone.

OTHER CONJUGATED CARBONYL CONTAINING COMPOUNDS

It is interesting to consider the possible molecular configurations of conjugated carbonyl containing compounds. Lin-Vien *et al.* (13) have reviewed the published studies of these compounds (14), and they report that a planar compound such as 3-buten-2-one exists in s-trans

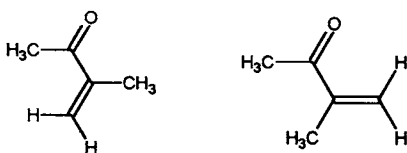
and s-cis configurations in CCl_4 solution. These two conformers for 3-buten-2-one are illustrated here:



These two conformers result from 180° rotation of the $\text{C}=\text{C}$ group about the C^2-C^3 single bond. This notation adequately describes the molecular configurations in the forementioned case (13–15).

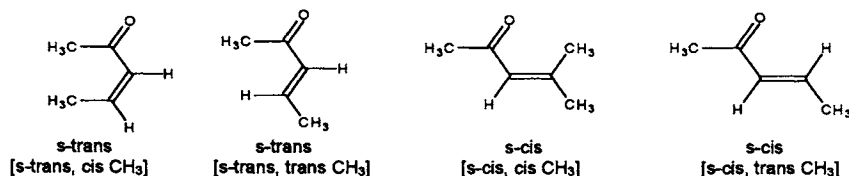
In the vapor phase the $\text{C}=\text{O}$ str. and $\text{C}=\text{C}$ str. frequencies are assigned at 1715 and 1627 cm^{-1} , respectively (16). The frequency separation between these two modes is 88 cm^{-1} . Corresponding modes for the s-trans isomer are not detected in the vapor phase at elevated temperature. Therefore, 3-buten-2-one exists only as the s-cis conformer at elevated temperature in the vapor phase. The IR bands at 986 and 951 cm^{-1} confirm the presence of the $\text{CH}=\text{CH}_2$ group.

Similarly, a compound such as 3-methyl-3-buten-2-one can also be adequately defined as s-trans and s-cis conformers as illustrated here:



In the vapor phase at elevated temperature the IR bands at 1700 cm^{-1} and 1639 cm^{-1} are assigned to $\text{C}=\text{O}$ stretching and $\text{C}=\text{C}$ stretching, respectively (16). The frequency separation between these two modes is 61 cm^{-1} . Therefore, 3-methyl-3-buten-2-one exists only as the s-cis conformer in the vapor-phase at elevated temperature. The IR band at 929 cm^{-1} confirms the presence of the $\text{C}=\text{CH}_2$ group.

Let us now consider the number of possible conformers for 4-methyl-3-buten-2-one:



Here we note that *s-trans* and *s-cis* do not define the spatial position of the CH_3 group. Therefore, the additional term *trans* CH_3 and *cis* CH_3 must be used to adequately specify each of the four possible conformers for 4-methyl-3-buten-2-one as shown in brackets in the conformers shown here.

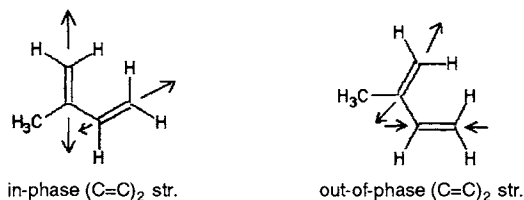
The $\text{C}=\text{O}$ and $\text{C}=\text{C}$ stretching frequencies for 4-methyl-3-buten-2-one in CCl_4 solution are given here:

<u>s-trans conformer (cm^{-1})</u>		<u>($\text{C}=\text{O}$ str.)-($\text{C}=\text{C}$ str.) (cm^{-1})</u>
<u>$\text{C}=\text{O}$ str. (vs)</u>	<u>$\text{C}=\text{C}$ str. (m,sh)</u>	
1674	1654	29
<u>s-cis conformer (cm^{-1})</u>		
<u>$\text{C}=\text{O}$ str. (s)</u>	<u>$\text{C}=\text{C}$ str. (s)</u>	
1692	1632	60

These data support only the presence of the *s-cis* or *s-trans* part of the conformer. NMR data are needed to help establish the presence of a *cis* or *trans* CH_3 group, and these data were not available. Similar compounds containing the *trans* $\text{CH}=\text{CH}$ group exhibit a weak-medium band in the region $974\text{--}980\text{ cm}^{-1}$.

As already shown, the $\text{C}=\text{C}$ and $\text{C}=\text{O}$ stretching frequencies for *s-cis* and *s-trans* conformers are very different. The question to answer is why they are different. It is possible that in one case the $\text{C}=\text{C}$ and $\text{C}=\text{O}$ stretching vibrations couple into in-phase and out-of-phase stretching modes in one conformer and not in the case of the other conformer.

In the case of 3-methyl-1,3-pentadiene the two $\text{C}=\text{OC}=\text{C}$ groups are coupled into an in-phase ($\text{C}=\text{C}$)₂ vibration and an out-of-phase ($\text{C}=\text{C}$)₂ vibration as depicted here:



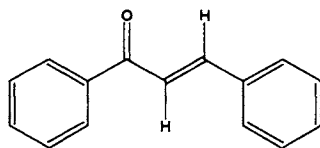
In the case of 3-methyl-1,3-pentadiene, the in-phase str. mode occurs at 1650 cm^{-1} and the out-of-phase str. mode occurs at 1610 cm^{-1} in the vapor phase. In cases such as 2-methyl-2-pentene and 2,4,4-trimethyl-2-pentene the $\text{C}=\text{C}$ bond is not conjugated and the $\text{C}=\text{C}$ stretching mode occurs at 1665 and 1658 cm^{-1} , respectively. Therefore, it appears that the in-phase ($\text{C}=\text{C}$)₂ stretching vibration occurs near that expected for isolated $\text{C}=\text{C}$ stretching vibrations while the out-of-phase ($\text{C}=\text{C}$)₂ stretching vibrations occur considerably lower than isolated $\text{C}=\text{C}$ stretching vibrations.

The same behavior for the C=O and C=C stretching modes was already noted here for the *s-cis* conformers. The C=O str. mode occurred at a frequency expected for a conjugated carbonyl containing compound, while the C=C str. mode occurred at a lower frequency than expected for an isolated C=C double bond. On the other hand, the *s-trans* conformers exhibited frequencies for C=O and C=C stretching expected for conjugated carbonyl containing compounds while the C=C stretching frequency occurred at frequencies comparable to those exhibited by compounds containing isolated trans CH=CH groups. On this basis, we believe that these modes are best described as in-phase and out-of-phase C=C–C=O stretching vibrations in the case of the *s-cis* conformers, and as C=O and C=C stretching modes in the case of the *s-trans* conformers. Compounds such as 3-methyl-4-phenyl-3-buten-2-one and α -hexylcinnamaldehyde contain the C=CH group, and we are only able to establish that they are in the *s-cis* configuration. The cis [H, CH₃] and cis [H, C₆H₁₁] are one of the two possibilities for these two compounds. The bands in the region 867–870 cm⁻¹ support the presence of the C=CH group.

Table 14.7 also lists IR vapor-phase data for chalcone and its derivatives. The IR data is recorded at elevated temperature, and all of the data indicate that these compounds exist only as the *s-cis*, trans CH=CH conformer.

CHALCONES

Chalcones have the following empirical planar structure:



The phenyl group of the styryl group is numbered 2 through 6, and the phenyl group of the benzoyl group is numbered 2' through 6'. Substitution in the 2,6-positions with Cl₂ or (CH₃)₂ would sterically prevent the styryl phenyl group from being coplanar with the rest of the molecule. Moreover, substitution of Cl₂ or (CH₃)₂ in the $\alpha,2$ -positions on the styryl group would also sterically prevent the styryl phenyl group from being coplanar with the rest of the molecule. Substitution of Cl₂ or (CH₃)₂ in the 2',6' -positions would sterically prevent the phenyl group of the benzoyl group from being coplanar with the rest of the molecule. The six chalcones studied, (see Table 14.6) exhibit ν C=O in the region 1670–1684 cm⁻¹, and exhibit ν C=C in the region 1605–1620 cm⁻¹. The frequency separation between ν C=O and ν C=C varies between 59 and 73 cm⁻¹ (16). These data indicate that these chalcones exist in planar *s-cis* configurations. Noncoplanar chalcones were not available for study.

Table 14.7a lists some fundamental vibrations for the conjugated ketones studied. These group frequencies aid in identifying these compounds by additional spectra-structure identification.

INTRAMOLECULAR HYDROGEN BONDING

Table 14.8 lists IR data for 2-hydroxy-5-X-acetophenone in CCl₄ solution (3800–1333 cm⁻¹) and CS₂ solution (1333–400 cm⁻¹). The intramolecular ν OH··O=C and γ OH··O=C vibrations for 2-hydroxy-5-X-acetophenone were presented in Chapter 7.

The $\nu\text{C}=\text{O}\cdots\text{HO}$ frequencies for 2-hydroxy-5-X-acetophenones occur in the range 1641–1658 cm^{-1} (17). These compounds exhibit $\nu\text{C}=\text{O}\cdots\text{HO}$ at lower frequency by $40 \pm 10 \text{ cm}^{-1}$ compared to nonhydrogen bonded acetophenones due to the strength of the $\text{C}=\text{O}\cdots\text{HO}$ bond. In the solid phase (Nujol mull) the $\nu\text{C}=\text{O}\cdots\text{HO}$ mode occurs 13 to 17 cm^{-1} lower in frequency than in CCl_4 solution.

The 2-hydroxy-5-X-acetophenones exhibit characteristic vibrations in the range 954–973 cm^{-1} [$\text{C}-\text{C}(=\text{O})-\text{C}$ stretching], 1283–1380 cm^{-1} [phenyl-0 stretching], and 1359–1380 cm^{-1} [symmetric CH_3 bending].

CYCLOALKANONES

In the vapor phase cycloalkanones exhibit $\nu\text{C}=\text{O}$ frequencies in the range 1719–1816 cm^{-1} (2). The frequencies decrease as the number of carbon atoms in the cycloalkanone ring increase from 4 to 8 and 10 (1816, 1765, 1732, 1721, 1720, and 1719 cm^{-1} , respectively). The behavior of the $\nu\text{C}=\text{O}$ frequency is attributed to changes in the $\text{C}-\text{C}(=\text{O})-\text{C}$ bond angle. During a cycle of $\text{C}=\text{O}$ stretching, more or less energy is required to move the carbonyl carbon atom as the $\text{C}-\text{C}(=\text{O})-\text{C}$ bond angle becomes smaller or larger than the normal $\text{C}-\text{C}(=\text{O})-\text{C}$ bond angle for an open chain ketone such as dimethyl ketone (acetone). This is because during a cycle of $\text{C}=\text{O}$ stretching, the $\text{C}-\text{C}(=\text{O})-\text{C}$ angle must increase, and as the size of the cycloalkanone $\text{C}-\text{C}(=\text{O})-\text{C}$ angle decreases from normal bond angles (cyclohexanone for example), the more difficult it is for a normal $\text{C}=\text{O}$ vibration to occur. Conversely, in cases where the bond angle is larger than normal, the easier it is for the $\nu\text{C}=\text{O}$ vibration to occur.

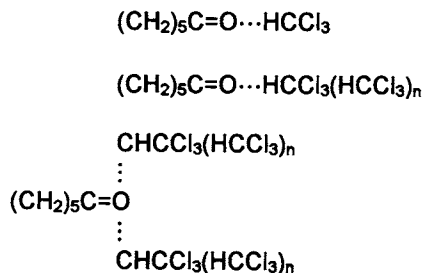
Table 14.9 lists IR vapor-phase data and assignments for cyclobutanone and cyclopentanone. The $\nu\text{C}=\text{O}$ frequencies were already discussed here. It should be noted that $\nu_{\text{asym. CH}_2}$, $\nu_{\text{sym. CH}_2}$, CH_2 twisting, the ring deformation, and the first overtone of $\nu\text{C}=\text{O}$ also decrease in frequency while the CH_2 bending mode increases in frequency as the ring size is increased from four to five carbon atoms.

Table 14.10 lists the $\text{C}=\text{O}$ stretching frequencies for cyclopentanone and cyclohexanone in the vapor, neat, and solution phases (18).

Cyclopentanone exhibits $\nu\text{C}=\text{O}$ at 1765 (vapor) and 1739.2 cm^{-1} in neat phase after correction for Fermi resonance (18). In all solutions, $\nu\text{C}=\text{O}$ has been corrected for Fermi resonance. Cyclopentanone exhibits $\nu\text{C}=\text{O}$ at 1750.6 cm^{-1} in n-hexane solution and at 1728.8 cm^{-1} in water solution. Cyclohexanone exhibits $\nu\text{C}=\text{O}$ at 1723 cm^{-1} in n-hexane solution and at 1701 cm^{-1} in ethyl alcohol solution. After correction for Fermi resonance, $\nu\text{C}=\text{O}$ for cyclopentanone decreases in frequency by approximately 17.1 cm^{-1} progressing in the series of solvents hexane through methyl alcohol (18). Progressing in the same series of solvents, $\nu\text{C}=\text{O}$ for cyclohexanone decreases in frequency by approximately 22 cm^{-1} . The $\text{C}=\text{O}$ group for cyclohexanone is more basic than the $\text{C}=\text{O}$ group for cyclopentanone, and this is given as the reason that there is more of a solute-solvent interaction in the case of cyclohexanone than in the case of cyclopentanone (18). The $\nu\text{C}=\text{O}$ frequencies for these two cycloalkanones do not correlate well with the solvent acceptor numbers (AN), and this is attributed to steric factors of the solvents that hinder solute-solvent interaction.

Figure 14.5 shows a plot of $\nu\text{C}=\text{O}$ for cyclohexanone vs mole % $\text{CHCl}_3/\text{n-C}_6\text{H}_{14}$. Definite breaks in the plot are noted at ~ 2.5 to 1, ~ 6 to 1, ~ 50 to 1, and ~ 62.1 to 1 mol of CHCl_3 to 1 mol cyclohexanone. The cause of these $\nu\text{C}=\text{O}$ frequency shifts is most likely a result of

different hydrogen bonding complexes between C=O and CHCl₃ which changes with increasing CHCl₃ concentration, that is,

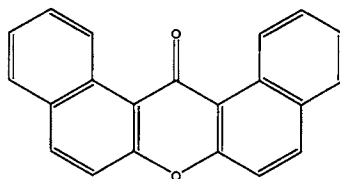


The general decrease in the $\nu\text{C}=\text{O}$ frequency most likely is the result of continual change in solvent dielectric effect. Figure 14.6 shows a plot of $\nu\text{C}=\text{O}$ for cyclohexanone vs mole % CCl₄/n-C₆H₁₄. This linear plot decreases in frequency as the mole % CCl₄/n-C₆H₁₄ increases. The dielectric effect of this solvent mixture increases as the mole % CCl₄/n-C₆H₁₄ increases, causing $\nu\text{C}=\text{O}$ to occur at lower frequency in a linear manner. Unlike CHCl₃, there are no different CCl₄ solute complexes as noted.

Figure 14.7 show a plot of $\nu\text{C}=\text{O}$ for 0.345 mol% acetone in CHCl₃/CCl₄ solution vs the mole % CHCl₃/CCl₄ (19). This plot shows that it is linear over the mole % CHCl₃/CCl₄ range of ~17–100%. Extrapolation of the linear plot to zero mol% CHCl₃ indicates that the $\nu\text{C}=\text{O}$ frequency for acetone in the range 0–17% ratio CHCl₃/CCl₄ varies from linearity by ~1 cm⁻¹. The mole fraction of CHCl₃ is in excess of the 0.345 mol% acetone present, even at the 1.49 mol% ratio CHCl₃/CCl₄ where the CHCl₃ protons forms weak hydrogen bonds between Cl atoms of other CHCl₃ molecules and CCl₄ molecules as well as with the carbonyl oxygen atom (19).

Figure 14.8 shows a plot of the $\nu\text{C}=\text{O}$ frequency for acetone vs the reaction field for each of the mole % CHCl₃/CCl₄ solutions. Comparison of Fig. 14.7 with Fig. 14.8 shows that the curves are identical. The reaction field $|R| = \frac{(e-1)}{2e+n^2}$, with e the dielectric constant of each solvent, and n the refractive index of each solvent. A plot of mole % CHCl₃/CCl₄ vs the reaction field yields a linear curve (19). Therefore, it appears as though the refractive index of the solvent as well as the dielectric value of the solvent system together with intermolecular hydrogen bonding with C=O of the solute affects the induced frequency shift of $\nu\text{C}=\text{O}$ in solution with CHCl₃/CCl₄. In summary, the frequency behavior of the solvent-induced ketone carbonyl stretching vibration, $\nu\text{C}=\text{O}$, is affected by the reaction field, inductive effects, and solute-solvent intermolecular hydrogen bonding (29).

Table 14.11 lists IR data for 14H-dibenzo[a, j]xanthen-14-one in CHCl₃/CCl₄ and in various solvents (20). This ketone has the following empirical structure:



For simplicity, this compound is given the name DX-14-O. The maximum symmetry for DX-14-O is C_{2v} . The $\nu C=O$ mode belongs to the A_1 species if it has C_{2v} symmetry. The DX-14-O has two significant IR bands in the region expected for $\nu C=O$, and a solution study in $CHCl_3/CCl_4$ solution was used to help explain the presence of these two IR bands. In order for $\nu C=O$ to be in Fermi resonance in the case of DX-14-O both the combination (CT) or overtone (OT) and $\nu C=O$ must belong to the A_1 symmetry species. In addition, the CT or OT would have to occur in the range expected for $\nu C=O$. It is obvious from the ketone structure given here that the IR doublet could not be due to the presence of rotational isomers.

Figure 14.9 shows IR spectra of DX-14-O in the region 1550–1800 cm^{-1} . Spectrum (A) is for a saturated solution in hexane, spectrum (B) is for a saturated solution in carbon tetrachloride, and spectrum (C) is for a 0.5% solution in chloroform. In hexane the IR bands occur at 1651.9 and 1636.8 cm^{-1} , in carbon tetrachloride the bands occur at 1648.9 and 1634.9 cm^{-1} , and in chloroform the bands occur at 1645.4 and 1633.1 cm^{-1} . Inspection of their IR spectra shows that the absorbance ratio of the low frequency band to the high frequency band increases in the solvent order $n-C_6H_{14}$, CCl_4 , $CHCl_3$. Figure 14.10 shows a plot of $\nu C=O$ and the OT or CT in Fermi resonance, and $\nu C=O$ and OT or CT corrected for Fermi resonance. The corrected data show that unperturbed $\nu C=O$ occurs at higher frequency than unperturbed OT or CT at mole % $CHCl_3/CCl_4$ below $\sim 28\%$; at mole % $CHCl_3/CCl_4$ above $\sim 28\%$ unperturbed $\nu C=O$ occurs at a lower frequency than unperturbed OT or CT. Without FR correction, each IR band results from some combination of $\nu C=O$ and the OT or CT. At the ~ 28 mol% $CHCl_3/CCl_4$, both IR bands result from equal contributions of $\nu C=O$ or OT or CT.

Figure 14.11 shows plots of $\nu C=O$ and OT or CT and their corrected frequencies vs the solvent acceptor number (AN) for each of the eight solvents, numbered 1–8, and listed sequentially. These plots show that in general the two modes in Fermi resonance and unperturbed $\nu C=O$ decrease in frequency as the AN of the solvent is increased. The scattering of data points suggests that the AN values do not take into account the steric factor of the solvent, which causes variance in the solute-solvent interaction. It should be noted that unperturbed $\nu C=O$ occurs at lower frequency than the OC or OT in only chloroform and benzonitrile solutions.

SUBSTITUTED 1,4-BENZOQUINONES

The ketone 1,4-benzoquinone has the following planar structure:



It has two $C=O$ groups, and these couple into an in-phase $(C=O)_2$ stretching vibration, $\nu_{ip}(C=O)_2$, and an out-of-phase $(C=O)_2$ stretching vibration, $\nu_{op}(C=O)_2$. In CCl_4 solution, 1,4-benzoquinone exhibits a strong IR band at 1670 cm^{-1} and a medium strong band at 1656 cm^{-1} . Without consideration of the molecular symmetry of 1,4-benzoquinone, it would seem reasonable to assign the 1670 cm^{-1} band to $\nu_{op}(C=O)_2$ and the 1656 cm^{-1} band to $\nu_{ip}(C=O)_2$. However, 1,4-benzoquinone has a center of symmetry and it has V_h symmetry. The 30 fundamentals are distributed as $6A_g$, $1B_{1g}$, $3B_{2g}$, $5B_{1u}$, 5_{2u} , and $3B_u$. Only the u classes are IR

active, and only the g classes are Raman active. The $\nu_{\text{op}}(\text{C}=\text{O})_2$ mode belongs to the b_{1u} species, and the $\nu_{\text{ip}}(\text{C}=\text{O})_2$ mode belong to the A_g species. Of course, 1,4-benzoquinone can not have rotational conformers. Therefore, one of the forementioned IR bands either results from the presence of an impurity, or else it must result from a B_{1u} combination tone in Fermi resonance with the $\nu_{\text{op}}(\text{C}=\text{O})_2$, b_{1u} fundamental. It could not be in Fermi resonance from an overtone of a lower lying fundamental, because a first overtone would belong to the A_g species. The Raman band at 1661.4 cm^{-1} in CCl_4 solution is assigned to the $\nu_{\text{ip}}(\text{C}=\text{O})_2$, A_g mode.

Figure 14.12 shows plots of $\nu_{\text{op}}(\text{C}=\text{O})$, b_{1u} and the CT B_{1u} modes in Fermi resonance, and their unperturbed frequencies after correction for Fermi resonance for 1,4-benzoquinone in 0.5% wt./vol. or less in 0–100 mol% $\text{CHCl}_3/\text{CCl}_4$. The two observed IR band frequencies in Fermi resonance in this case increase in frequency as the mole % $\text{CHCl}_3/\text{CCl}_4$ is increased. However, unperturbed $\nu_{\text{op}}(\text{C}=\text{O})_2$ decreases in frequency as the mole % $\text{CHCl}_3/\text{CCl}_4$ increases, and this is always the case for other carbonyl containing compounds as the mole % $\text{CHCl}_3/\text{CCl}_4$ is increased. It is noted that the unperturbed $\text{CT}b_{1u}$ mode increases in frequency as the mole % $\text{CHCl}_3/\text{CCl}_4$ is increased from 0–100%. In this case, at ~ 25 mol% $\text{CHCl}_3/\text{CCl}_4$ both IR bands result from equal contributions from $\nu_{\text{op}}(\text{C}=\text{O})_2$ and the CT b_{1u} mode.

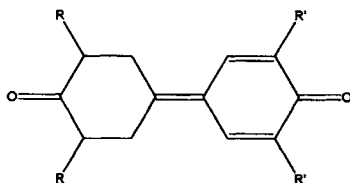
Table 14.12 lists IR and Raman data for several 1,4-benzoquinones in CCl_4 and CHCl_3 solutions (at 0.5% wt./vol. or less due to saturation). The point group pertaining to their molecular symmetry is given for each of these ketones. None of the other 1,4-benzoquinones show IR evidence for the $\nu_{\text{op}}(\text{C}=\text{O})_2$ mode being in Fermi resonance. The $\nu_{\text{op}}(\text{C}=\text{O})_2$ mode for these 1,4-benzoquinones occurs in the range $1657\text{--}1702.7\text{ cm}^{-1}$ in CCl_4 solution and at slightly lower frequency in CHCl_3 solution. In CHCl_3 solution, $\nu_{\text{ip}}(\text{C}=\text{O})_2$ occurs in the range $1666.9\text{--}1697.7\text{ cm}^{-1}$. The increasing inductive effect of the halogen atoms (progressing in the order Br, Cl, F) together with their field effect increase both $\nu_{\text{op}}(\text{C}=\text{O})_2$ and $\nu_{\text{ip}}(\text{C}=\text{O})_2$ frequencies (22).

Tables 14.13–14.17 list IR data for tetrafluoro-1,4-benzoquinone, tetrachloro-1,4-benzoquinone, tetrabromo-1,4-benzoquinone, chloro-1,4-benzoquinone, and 2,5-dichlorobenzoquinone in three different solvent systems.

In the IR, tetrafluoro-1,4-benzoquinone exhibits strong IR bands at 1702.7 and 1667.6 cm^{-1} in CCl_4 solution and at 1701.4 and 1668.4 cm^{-1} in CHCl_3 solution. In all cases the higher frequency band has more intensity than the lower frequency band. These two IR are assigned to $\nu_{\text{op}}(\text{C}=\text{O})_2$ and $\nu_{\text{op}}(\text{C}=\text{C})_2$, respectively. Figure 14.13 shows plots of $\nu_{\text{op}}(\text{C}=\text{O})_2$ and $\nu_{\text{op}}(\text{C}=\text{C})_2$ for 1,4-tetrafluorobenzoquinone vs mole% $\text{CHCl}_3/\text{CCl}_4$. The $\nu_{\text{op}}(\text{C}=\text{O})_2$ mode decreases in frequency as expected as the mole% $\text{CHCl}_3/\text{CCl}_4$ is increased. The $\nu_{\text{op}}(\text{C}=\text{C})_2$ ring mode increases in frequency as the mole% $\text{CHCl}_3/\text{CCl}_4$ is increased.

The frequency behavior of the other substituted 1,4-benzophenones is discussed in detail in Reference 21, and the reader is referred to this paper for further information on these interesting solute-solvent interactions.

Table 14.18 lists IR data for 3,3',5,5'-tetraalkyl-1,4-diphenoquinones in CHCl_3 solution and in the solid phase (22). The 3,3',5,5'-tetraalkyl-1,4-diphenoquinones have the following empirical structure:



When the 3,3',5,5' positions are substituted with identical atoms or groups, the compounds have D_{2h} symmetry (22). These molecules have a center of symmetry, and only the $\nu_{op}(C=O)$, B_{3u} fundamental is IR active. The $\nu_{op}(C=O)_2$, A_g fundamental is only Raman active. The $\nu_{op}(C=O)_2$ mode for the 3,3',5,5'-tetraalkyl-1,4-diphenquinones occurs in the range 1586–1602 cm^{-1} in the solid phase and in the range 1588–1599 cm^{-1} in $CHCl_3$ solution. The compound 3,3'-dimethyl, 5,5'-di-tert-butyl-1,4-diphenquinone has C_{2v} symmetry, and in this case both $\nu_{ip}(C=O)_2$ are IR active as well as Raman active. In this case the IR band at 1603 cm^{-1} is assigned to both $\nu_{op}(C=O)_2$ and $\nu_{ip}(C=O)_2$. The frequencies in brackets in Table 14.18 are calculated. All of these five 3,3',5,5'-tetraalkyl-1,4-diphenquinones exhibit a weak IR band in the range 3168–3204 cm^{-1} in the solid phase and in the range 3175–3200 cm^{-1} in $CHCl_3$ solution. These bands are assigned to the combination tone $\nu_{op}(C=O)_2 + \nu_{ip}(C=O)_2$. Using the observed $\nu_{op}(C=O)_2$ and combination tone frequencies for these compounds, the $\nu_{ip}(C=O)_2$ frequencies are calculated to occur in the range 1579–1601 cm^{-1} in the solid phase and in the range 1583–1602 cm^{-1} $CHCl_3$ solution (22). These data confirm a previous conclusion that diphenquinones exhibit a strong IR band near 1600 cm^{-1} , which must include stretching of the C=O bond (23). Thus, it is possible to distinguish between 4,4'-diphenquinones and 1,4-benzoquinones, since the latter compounds exhibit carbonyl stretching modes 30 to 80 cm^{-1} higher in frequency (21).

CONCENTRATION EFFECTS

Table 14.19 lists data that show the dependence of the $\nu_{C=O}$ frequency of dialkyl ketones upon the wt./vol.% ketone in solution with CCl_4 or $CHCl_3$ (10). In CCl_4 solution, the $\nu_{C=O}$ mode for diisopropyl ketone decreases more in frequency in going from ~0.8% to 5.25% than it does for di-tert-butyl ketone at comparable wt./vol. ketone in CCl_4 solution (–0.19 to –0.08 cm^{-1} at 5.25% wt./vol.). In $CHCl_3$ solution, the shift of $\nu_{C=O}$ is in the opposite direction to that noted for CCl_4 solutions. At 5.89% wt./vol. in $CHCl_3$ solution, $\nu_{C=O}$ increase 0.38 cm^{-1} for diisopropyl ketone and at 5.78 wt./vol. in $CHCl_3$ for di-tert-butyl ketone the increase is 0.1 cm^{-1} . The smaller $\nu_{C=O}$ frequency shifts in the case of the di-tert-butyl analog compared to the diisopropyl analog is attributed to steric factors of the alkyl group. The steric factor of the tert-butyl groups does not allow as much solute-solvent interaction between C=O and the solvent as it does in the case of the diisopropyl analog. With increase in the wt./vol. of ketone/ $CHCl_3$ $\nu_{C=O}$ increases in frequency, indicating that the strength of the $C=O \cdots HCCl_2 Cl \cdots (HCCl_2 Cl)_n$ intermolecular hydrogen bond becomes weaker as n becomes smaller.

REFERENCES

1. Schrader, B. (1989). *Raman/Infrared Atlas of Organic Compounds*, 2nd ed., Weinheim, Germany: VCH.
2. Nyquist, R. A. (1984). *The Interpretation of Vapor-Phase Infrared Spectra: Group Frequency Data*, Philadelphia: Sadtler Research Laboratories, a Division of Bio-Rad Laboratories, Inc.
3. Hallam, H. E. (1963). *Infra-Red Spectroscopy and Molecular Structure*, p. 420, M. Davies, ed., New York: Elsevier.
4. Kirkwood, J. G., West, W., and Edwards, R. T. (1937). *J. Chem. Phys.*, 5, 14.
5. Bauer E. and Magot, M. (1938). *J. Phys. Radium*, 9, 319.

6. Josien M. L. and Fuson, N. (1954). *J. Chem. Phys.*, **22**, 1264.
7. Bellamy, L. J., Hallam, H. E., and Williams, R. L. (1959). *Trans. Farad. Soc.*, **55**, 1677.
8. Nyquist, R. A. (1989). *Appl. Spectrosc.*, **43**, 1208.
9. Nyquist, R. A. (1994). *Vib. Spectrosc.*, **7**, 1.
10. Nyquist, R. A., Putzig, C.L., and Yurga, L. (1989). *Appl. Spectrosc.*, **43**, 983.
11. Nyquist, R. A. (1986). *Appl. Spectrosc.*, **40**, 79.
12. Nyquist, R. A., Chrzan, V., and Houck, J. (1989). *Appl. Spectrosc.*, **43**, 981.
13. Lin-Vien, D., Colthup, N. B., Fateley, W. G., and Grasselli, J. G. (1991). *The Handbook of Infrared and Raman Characteristic Group Frequencies of Organic Molecules*, San Diego: Academic Press, Inc.
14. Bowles, A. J., George, W. O., and Maddams, W. F. (1969) *J. Chem. Soc.*, B, 810.
15. Cottee, F. H., Straugham, B. P., Timmons, C. J., Forbes, W. F., and Shilton, R. (1967). *J. Chem. Soc.*, B, 1146.
16. (1982) *Sadtler Standard Infrared Vapor phase Spectra*, Philadelphia: Sadtler Research Laboratories, a Division of Bio-Rad, Inc.
17. Nyquist, R. A. (1963). *Spectrochim. Acta*, **19**, 1655.
18. Nyquist, R. A. (1990). *Appl. Spectrosc.*, **44**, 426.
19. Nyquist, R. A., Putzig, C. L., and Hasha, D. L. (1989). *Appl. Spectrosc.*, **43**, 1049.
20. Nyquist, R. A., Luoma, D. A., and Wilkening, D., (1991). *Vib. Spectrosc.*, **2**, 61.
21. Nyquist, R. A., Luoma, D. A., and Putzig, C. L. (1992). *Vib. Spectrosc.*, **3**, 181.
22. Nyquist, R. A. (1982). *Appl. Spectrosc.*, **36**, 533.
23. Gordon J. M. and Forbes, J. W. (1968). *Appl. Spectrosc.*, **15**, 19.

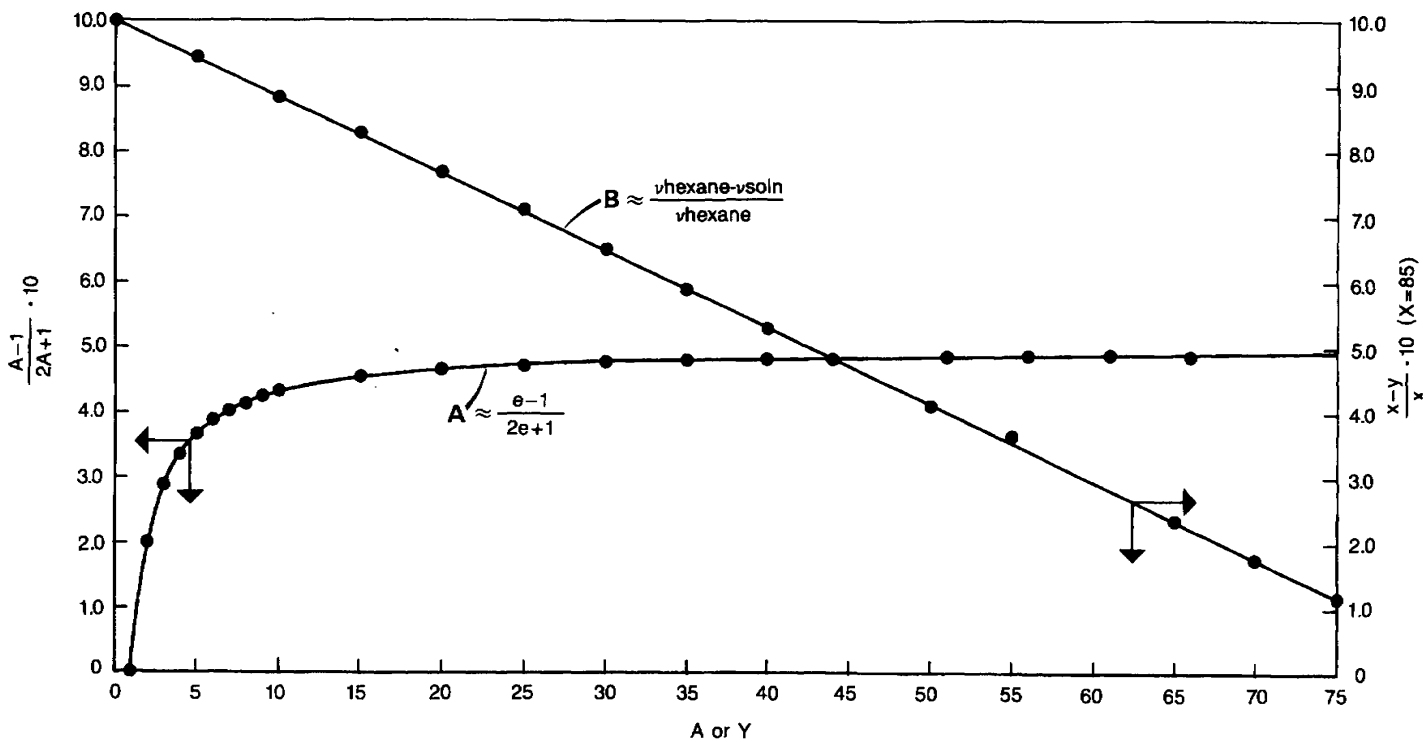


FIGURE 14.1 Plots of the number for A or Y vs the corresponding calculated value multiplied by a factor of 10 (see Table 14.2a).

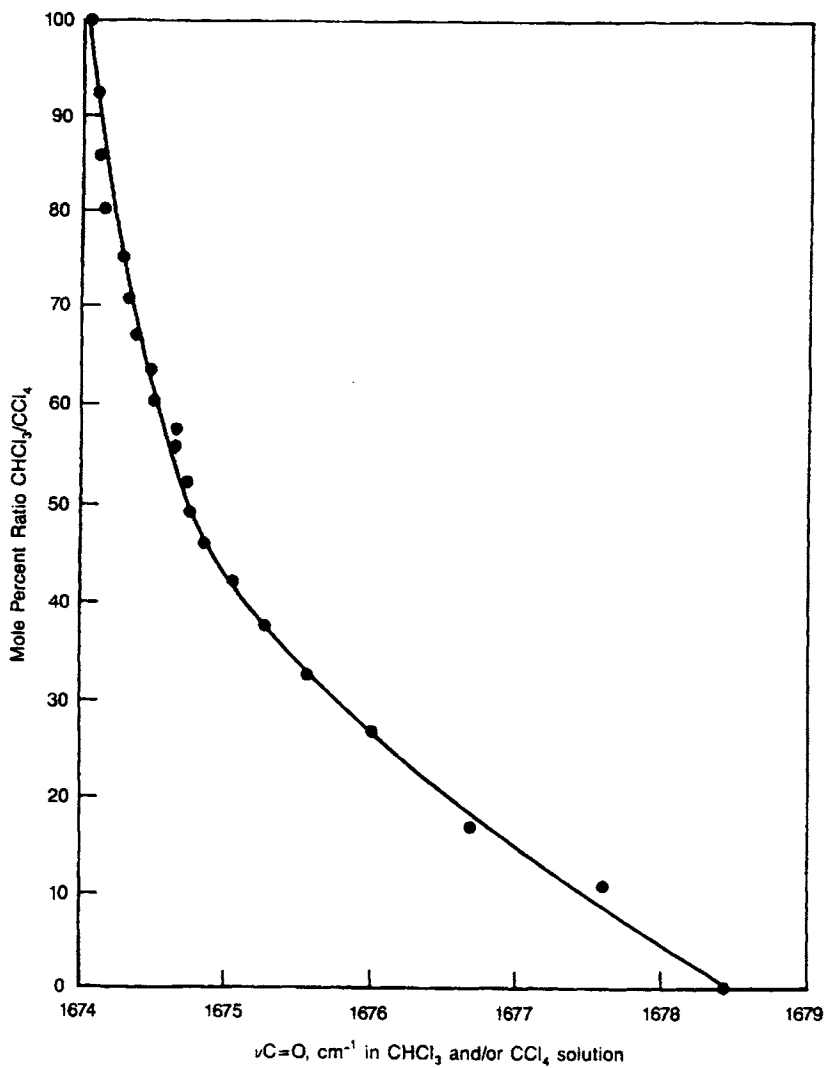


FIGURE 14.2 A plot of $\nu_{C=O}$ for tert-butylphenone (phenyl tert-butyl ketone) vs mol % $\text{CHCl}_3/\text{CCl}_4$.

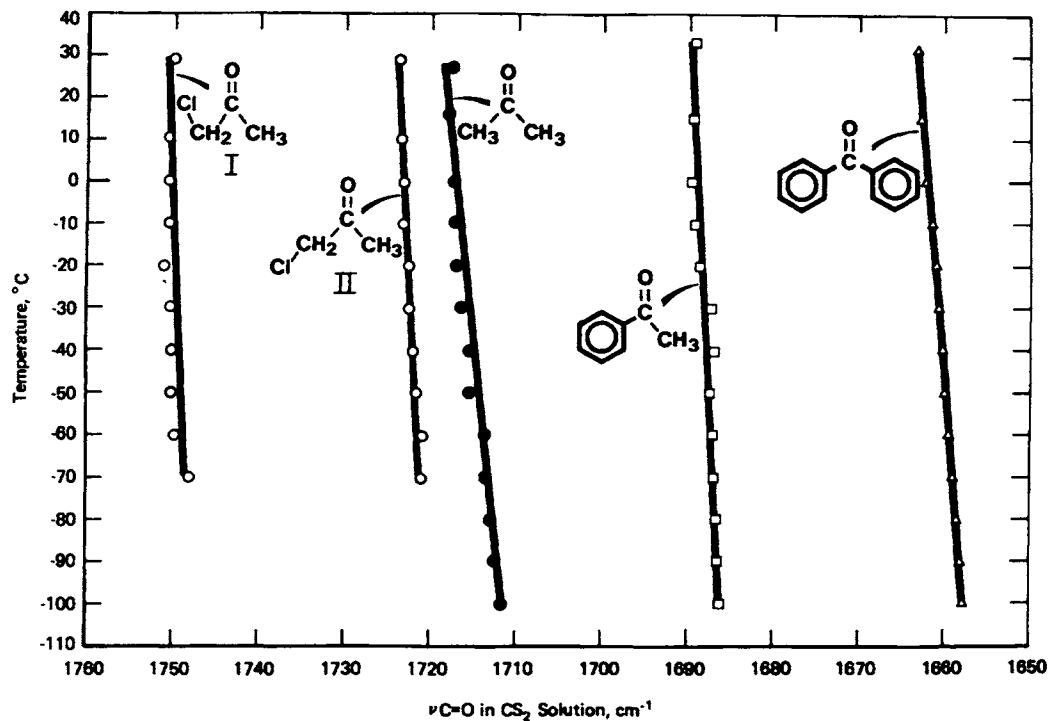


FIGURE 14.3 Plots of the $\nu_{C=O}$ frequencies for acetone, α -chloroacetone, acetophenone, and benzophenone in CS_2 solution between ~ 29 and $-100^\circ C$.

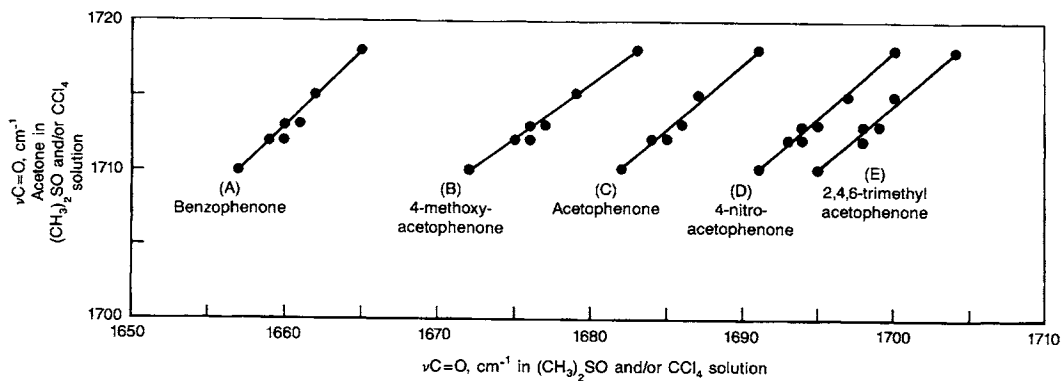


FIGURE 14.4 Plots of $\nu_{C=O}$ for 2% wt./vol. solutions of (A) benzophenone, (B) 4-methoxyacetophenone, (C) acetophenone, (D) 4-nitroacetophenone, (E) 2,4,6-trimethylacetophenone, and (F) acetone in mole % $(CH_3)_2SO/CCl_4$ solutions.

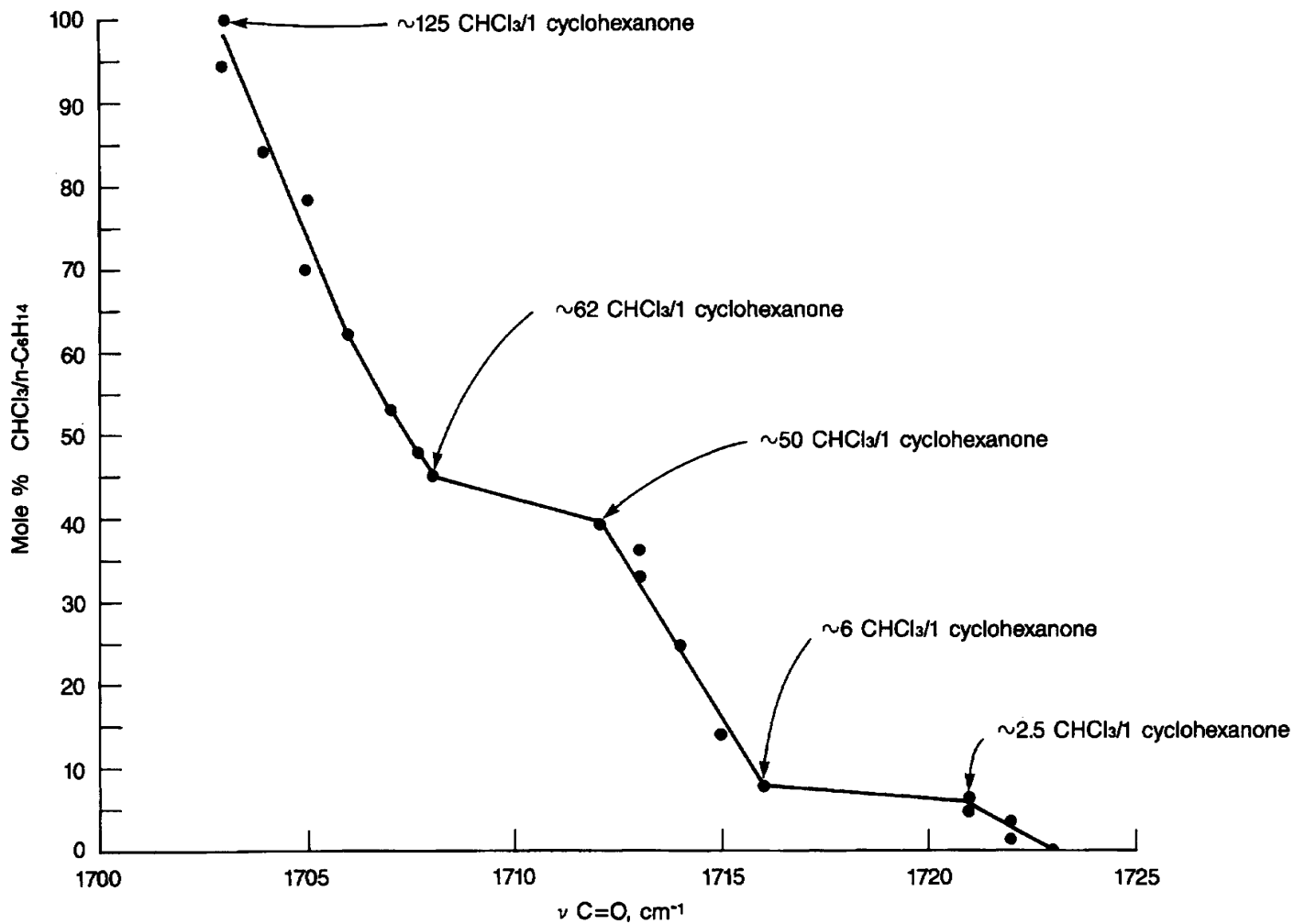
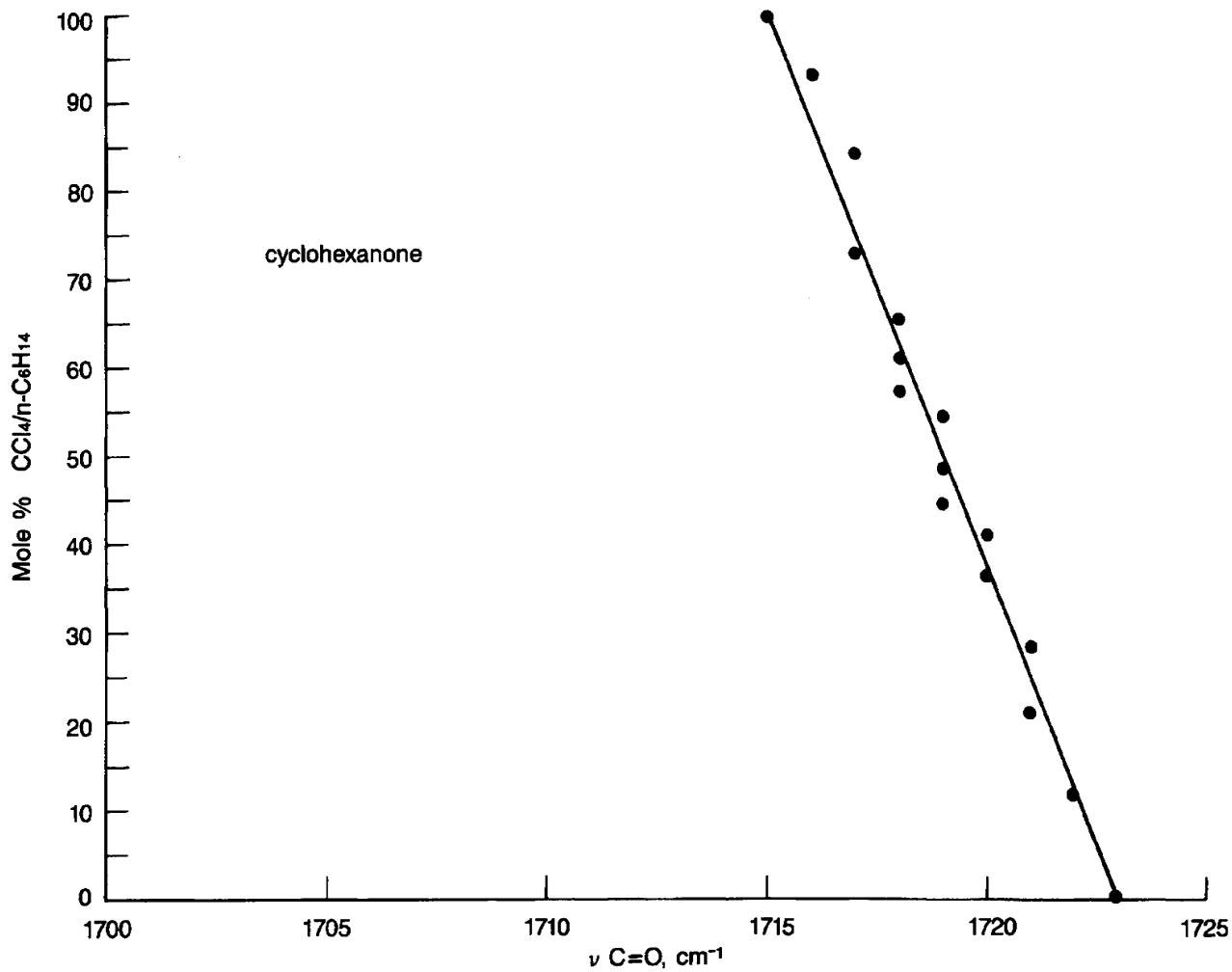


FIGURE 14.5 A plot of $\nu\text{C}=\text{O}$ for 1% wt./vol. cyclohexanone vs mole % $\text{CHCl}_3/n\text{-C}_6\text{H}_{14}$ solutions.

FIGURE 14.6 A plot of $\nu\text{C=O}$ for 1% wt./vol. cyclohexanone vs mole % $\text{CCl}_4/n\text{-C}_6\text{H}_{14}$.

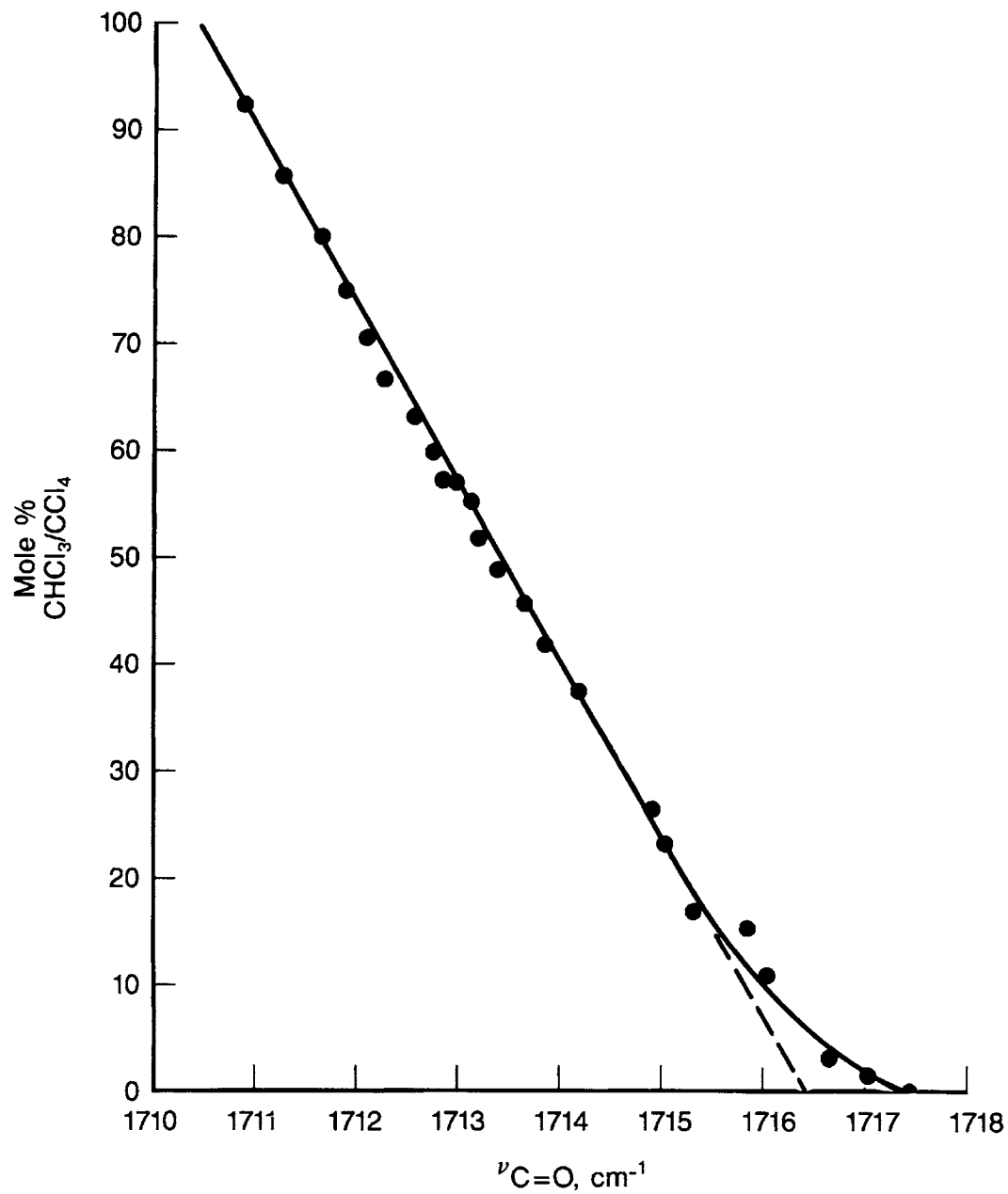


FIGURE 14.7 A plot of $\nu_{\text{C=O}}$ for 0.345 mole % acetone vs mol % $\text{CHCl}_3/\text{CCl}_4$ solutions.

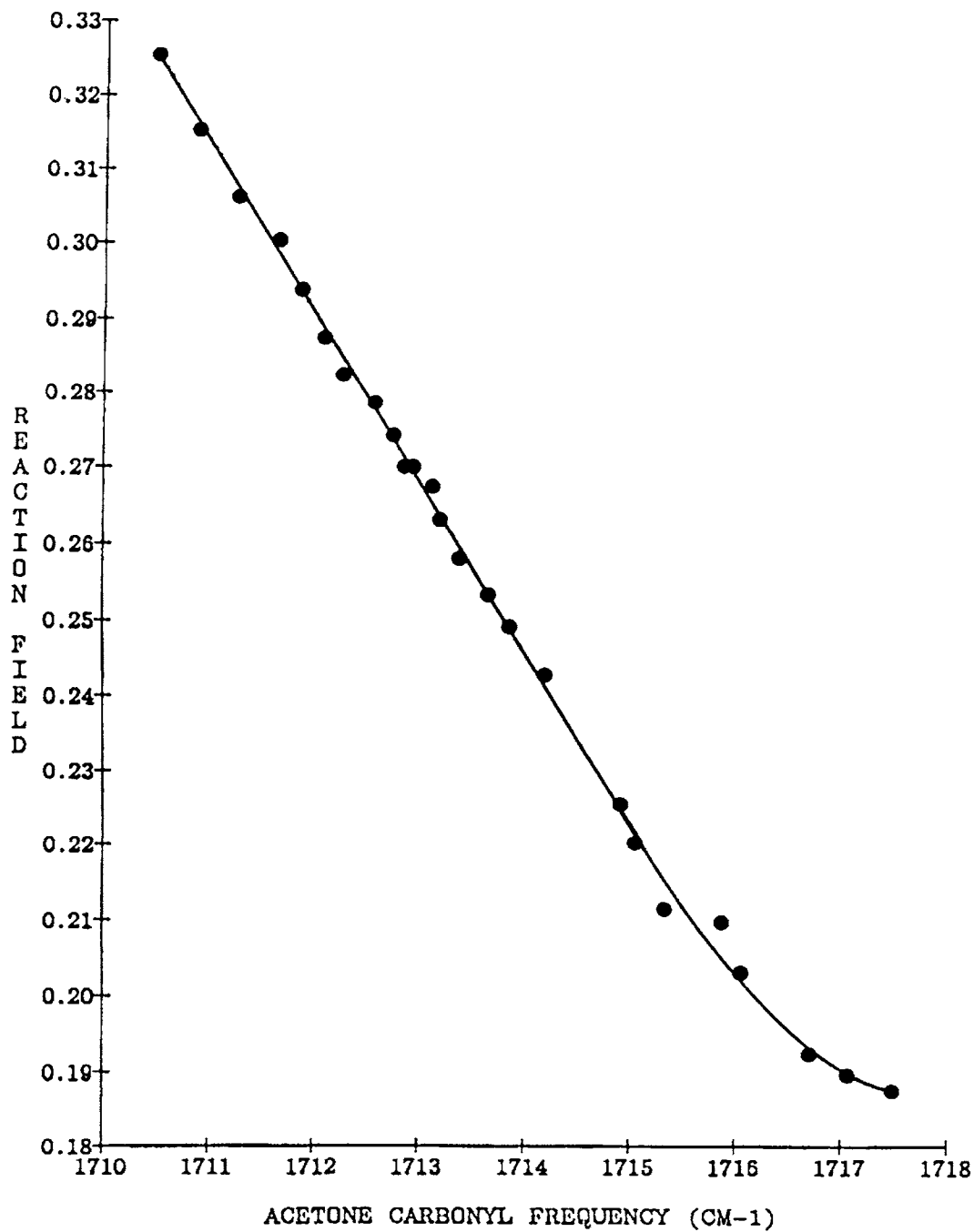


FIGURE 14.8 A plot of the reaction field vs $\nu_{\text{C=O}}$ for 0.345 mole % acetone in $\text{CHCl}_3/\text{CCl}_4$ solutions.

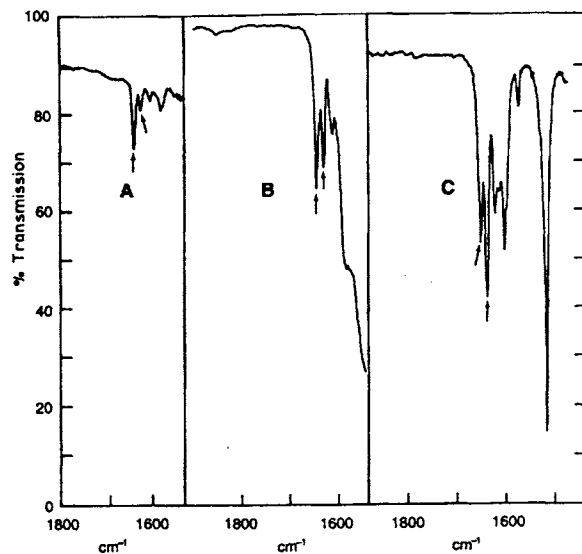


FIGURE 14.9 IR spectra for 14H-dibenzo [a,j] X anthen-14-one. (A) Saturated solution in hexane; (B) saturated solution in carbon tetrachloride; (C) 0.5% wt./vol. solution in chloroform.

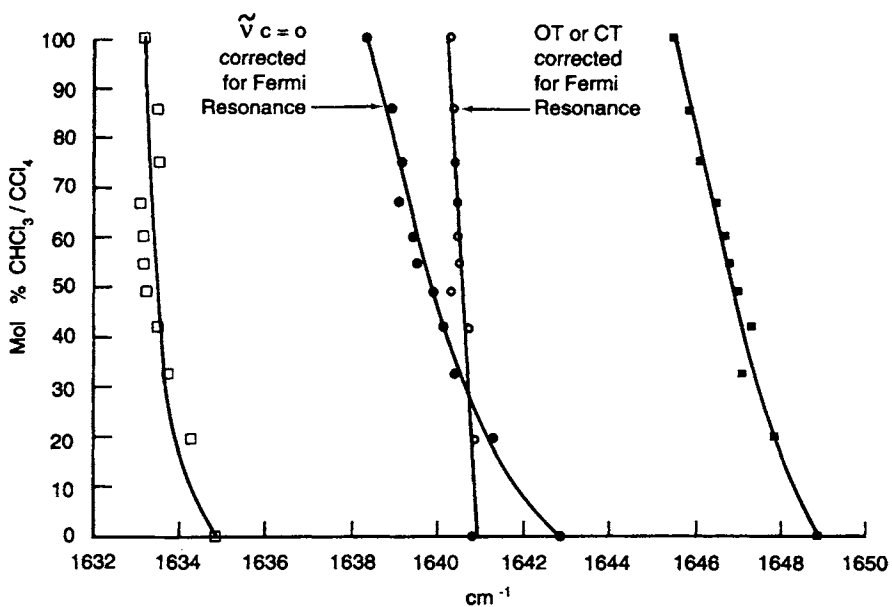


FIGURE 14.10 Plots of $\nu_{C=O}$ and OT or CT in Fermi resonance and their corrected unperturbed frequencies for 14H-dibenzo [a,j] xanthen-14-one vs mole % $CHCl_3/CCl_4$. The solid squares and open squares represent uncorrected frequency data, the solid circle represents $\nu_{C=O}$ corrected for Fermi resonance and the open circles represent OT or CT corrected for Fermi resonance.

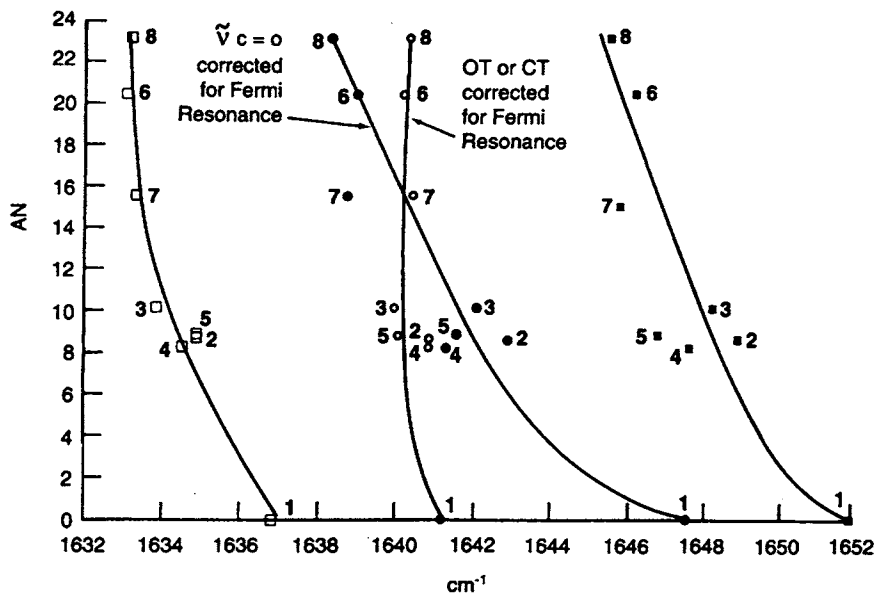


FIGURE 14.11 Plots of $\nu_{C=O}$ and OT or CT uncorrected and corrected for Fermi resonance for 14H-dibenzo [a,j]-xanthen-14-one vs the solvent acceptor number (A) for (1) hexane; (2) carbon tetrachloride; (3) carbon disulfide; (4) benzene; (5) tetrahydrofuran; (6) methylene chloride; (7) nitrobenzene; and (8) chloroform.

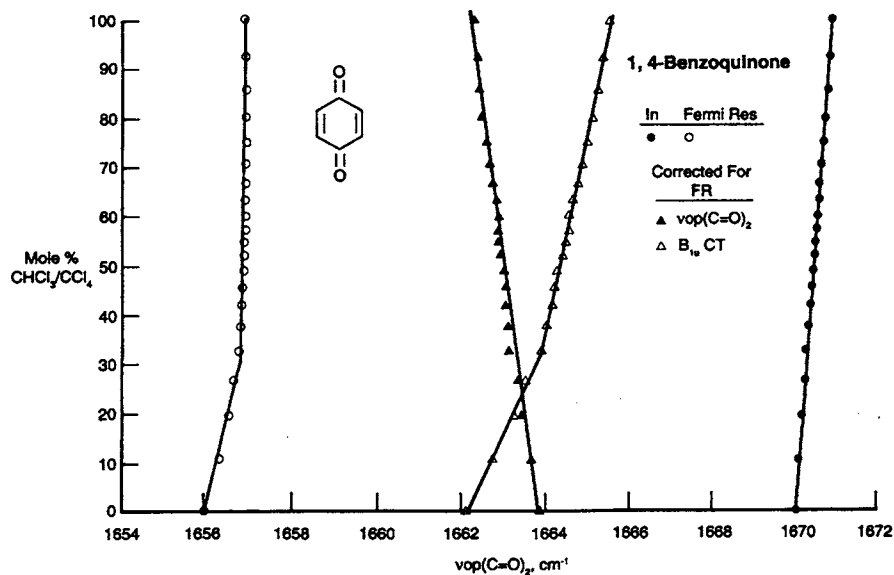


FIGURE 14.12 Plots of $\nu_{op}(C=O)_2$ and B_{1u} CT in Fermi resonance and their unperturbed frequencies after correction for Fermi resonance for 1,4-benzoquinone vs mole % CHCl₃/CCl₄.

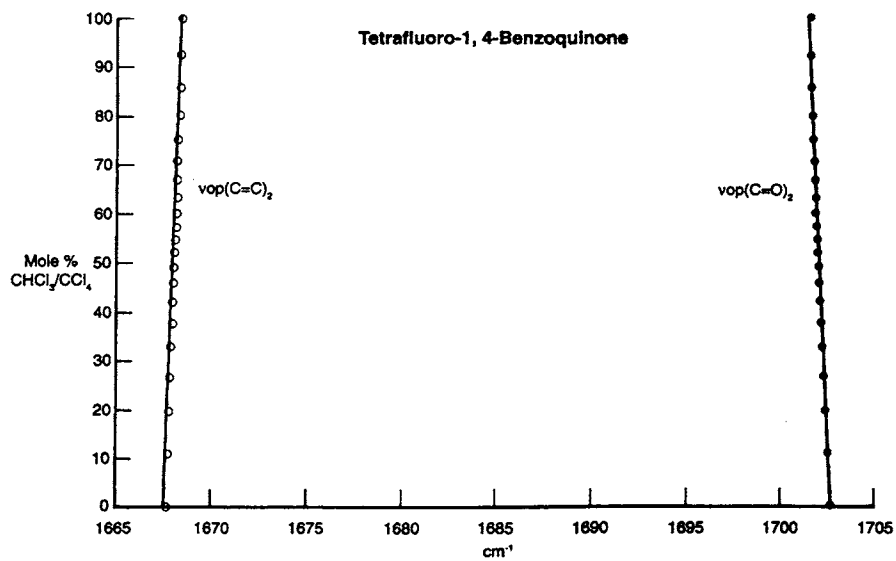


FIGURE 14.13 Plots of $v_{\text{op}}(\text{C}=\text{O})_2$ and $v_{\text{op}}(\text{C}=\text{C})_2$ for tetrafluoro-1, 4-benzoquinone vs mole % $\text{CHCl}_3/\text{CCl}_4$.

TABLE 14.1 IR vapor phase and Raman data for acetone and acetone-d₆

Compound	2(C=O str.) cm ⁻¹ (A)	a.CH ₃ str. cm ⁻¹ (A)	s.CH ₃ str. cm ⁻¹ (A)	C=O str. cm ⁻¹ (A)	? cm ⁻¹ (A)	a.CH ₃ bend cm ⁻¹ (A)	s.CH ₃ bend cm ⁻¹ (A)	a.CCC str. cm ⁻¹ (A)	CH ₃ rock B2 cm ⁻¹ (A)	CH ₃ rock B1 cm ⁻¹ (A)	delta C=O cm ⁻¹	s.CCC str. Raman* ¹ liquid cm ⁻¹	delta C=O Raman* ¹ liquid cm ⁻¹	gamma C=O Raman* ¹ liquid cm ⁻¹	gamma C=O IR2 vapor cm ⁻¹	CCC bend IR* ² vapor
Acetone	3460 (0.03)	3000 (0.120) 2970 (0.150)	2941 (0.090)	1748 (1.110) 1735 (1.250) 1721 (1.050) 1745 (1.240)	1550 (0.050)	1435 (0.140)	1378 (0.500) 1362 (0.620) 1353 (0.550) 1070 (0.090)	1228 (0.530) 1212 (0.650)	1092 (0.040)	900 (0.050)	538 (0.080) 525 (0.135) 510 (0.120) 485 (0.110)	786.5 stg.,pol.	530 med.,pol.?	493 wk.,depol.	484 wk.type C	385 wk. type B
Acetone-db	3450 (0.030)	2250 (0.074)	2220 (0.090)	1738 (1.210) 1729 (1.240)	1415 (0.060)	1140 (0.060)	1050 (0.140) 1027 (0.090)	1239 (1.130)	986 (0.050)	795 (0.020)	472 (0.140) 458 (0.150)	695.5 stg.,pol.	478 wk.,depol.	393 wk.,depol.	405 wk.type C	321 wk. type B
Acetone/Acetone-db	1.003	1.32	1.325	0.998	1.095	1.38	1.297	0.978	1.108	1.132	1.112	1.131	1.109	1.254	1.195	1.199

*¹Reference 1.*²Reference 2.

TABLE 14.2 Application of the KBM equation using IR data for acetone C=O stretching frequencies in various solvents

Solvent	For acetone [C=O(hexane)-C=O(soln.)] / $\times 10(3)$ [C=O(hexane)]	Calculated C=O cm ⁻¹	delta C=O(obs.)-C=O(calc.) cm ⁻¹
Hexane			
Diethyl ether	2.322	1715.9	-2.1
Benzene	4.645	1717.9	3.9
Toluene	2.904	1717.8	3.8
Carbon tetrachloride	2.322		
Pyridene	5.226	1714.2	1.2
Nitrobenzene	5.226	1713.7	0.7
Acetonitrile	5.226	1713.5	0.5
Dimethyl sulfoxide	6.969	1713.4	3.4
Methylene chloride	5.388	1714.5	2.5
Chloroform	6.388	1715.6	4.6
t-Butyl alcohol	6.969	1714.3	4.3
Isopropyl alcohol	7.549	1713.7	4.9
Ethyl alcohol	8.13	1713.7	5.7
Methyl alcohol	8.711	1814.7	7.7
Water	13.36	1713.3	14.3

TABLE 14.2A The calculated values for $A-1/2A+1$ and $X-Y/X$ where A and Y equal 0 to 85 and X equals 85 [the KBM equation]

A or Y	$A - 1/2A + 1$	$X-Y/X$ [X=85]
0	-1	1
1	0	0.988
2	0.22	0.976
3	0.286	0.964
4	0.333	0.953
5	0.364	0.941
6	0.385	0.929
7	0.4	0.918
8	0.412	0.906
9	0.421	0.894
10	0.428	0.882
15	0.452	0.824
20	0.463	0.765
25	0.47	0.706
30	0.475	0.647
35	0.478	0.588
40	0.481	0.529
45	0.483	0.471
50	0.485	0.412
55	0.486	0.353
60	0.488	0.294
65	0.489	0.235
70	0.4894	0.176
75	0.49	0.118
80	491	0.058
85	0.4912	0

TABLE 14.3 The C=O stretching frequencies for aliphatic ketones in the vapor phase and various solvents

Solvent	Dimethyl ketone cm ⁻¹	Methyl ethyl ketone cm ⁻¹	Diethyl ketone cm ⁻¹	Ethyl isopropyl ketone cm ⁻¹	Disopropyl ketone cm ⁻¹	Di-t-butyl ketone cm ⁻¹	AN
[Vapor]	1735	1742	1731	1730	1726	1699	0
Hexane	1722.4	1727.2	1725.1	1721.4	1720.3	1690.3	3.9
Diethyl ether	1719.6	1723	1721.4	1718.2	1717.8	1687.7	8.6
Carbon tetrachloride	1717.7	1721.3	1719.6	1716.5	1716	1685.9	
Carbon disulfide	1716.3	1720.1	1718.3	1715.2	1714.5	1684.9	18.9
Benzene	1715.8	1718.6	1717.4	1714	1713.5	1684.5	18.9
Acetonitrile	1713.3	1714	1713.7	1710.6	1707.8	1681.6	14.8
Nitrobenzene	1712.8	1714.3	1713.8	1710.6	1707.6	1681.7	15.5
Benzonitrile	1712.7	1713.9	1713.2	1710.2	1706.8	1682.2	20.4
Methyl chloride	1712	1712.6	1712.5	1709.6	1706.4	1680.5	
Nitromethane	1712.2	1712.4	1712.4	1709.5	1706.3	1680.6	
t-Butyl alcohol	1711.8	1711.2	1711.8	1709.2	1705.6	1678.5	29.1
t-Butyl alcohol* ¹		1722sh* ²	1722.5sh	1718.8sh	1718sh	1687.0sh	39.1
Chloroform	1710.6	1710.2	1710.7	1708.2	1705.3	1680.8	23.1
Dimethyl sulfoxide	1709.2	1709.7	1710.1	1707.4	1704.6	1680.1	19.3
Isopropyl alcohol	1710.3	1709.8	1710.3	1707.7	1704.2	1677.9	33.5
Isopropyl alcohol* ¹		1720.5sh	1720.5sh	1716.2sh	1717sh	1687sh	33.5
Ethyl alcohol	1709	1708.5	1710.1	1706.1	1703.1	1676.8	37.1
Ethyl alcohol* ¹	1717sh	1719.4sh	1717.8sh	1715.4sh	1716sh	1686.4sh	37.1
Methyl alcohol	1708	1707.5	1707.7	1704.8	1701.1	1675.2	41.3
Methyl alcohol* ¹	1716.2sh	1718.6sh	1717.0sh	1715sh	1715sh	1684.8sh	41.3
$\Sigma 6^* \cdot \Sigma \alpha \cdot 10^{-2}$	0	0.7	2.8	15.7	35.7	184.8	
$\Sigma 6^*$	0	-0.1	-0.2	-0.29	-0.38	-0.6	
$\Sigma \alpha$	0	-0.07	-0.14	-0.54	-0.94	-3.08	

*¹C=O not H bonded.*²sh = shoulder.

TABLE 14.3A A comparison of the carbonyl stretching frequency difference ($\Delta \text{C}=\text{O}$ str. in cm^{-1}) for dialkyl ketones in hexane and each of the other solvents

Solvent	Dimethyl ketone cm^{-1}	Methyl ethyl ketone cm^{-1}	Diethyl ketone cm^{-1}	Ethyl isopropyl ketone cm^{-1}	Diisopropyl ketone cm^{-1}	Di-t-butyl ketone cm^{-1}
Hexane	0	0	0	0	0	0
Diethyl ether	2.8	4.2	3.6	3.2	2.5	[2.6]
Carbon tetrachloride	4.7	5.9	5.4	4.9	4.3	[4.4]
Carbon disulfide	6.1	7.1	6.7	6.2	5.8	5.35
Benzene	6.5	8.6	7.65	7.4	6.8	5.8
Acetonitrile	9	13.25	11.4	10.8	[12.5]	8.7
Nitrobenzene	9.6	12.9	11.2	10.8	[12.7]	8.6
Benzonitrile	9.7	13.3	11.8	11.2	[13.5]	8.1
Methyl chloride	10.3	14.6	12.6	11.8	[13.9]	9.8
Nitromethane	10.15	14.8	12.7	11.9	[14.0]	9.7
t-Butyl alcohol	10.5	16	13.25	12.2	[14.7]	11.8
t-Butyl alcohol		5.2	2.6	2.6	2.3	[3.3]
Chloroform	11.75	17	14.35	13.2	[15.0]	9.5
Dimethyl sulfoxide	13.1	17.5	14.9	14	[15.7]	10.2
Isopropyl alcohol	12	17.4	14.7	13.7	[16.1]	12.4
Isopropyl alcohol		6.7	4.5	5.2	3.3	3.3
Ethyl alcohol	13.3	18.7	14.9	[15.3]	[17.2]	13.5
Ethyl alcohol	5.35	7.8	7.3	6	4.3	3.9
Methyl alcohol	14.3	19.7	17.4	16.6	[19.2]	15.1
Methyl alcohol	6.15	8.6	8.05	6.4	5.3	[5.5]
	0	0.7	2.8	15.7	35.7	184.8

TABLE 14.3B A comparison of the carbonyl stretching frequency difference ($\Delta \text{C}=\text{O}$ str. in cm^{-1}) for dialkyl ketones in methyl alcohol and the other protic solvents

Protic solvent	Dimethyl ketone cm^{-1}	Methyl ethyl ketone cm^{-1}	Diethyl ketone cm^{-1}	Ethyl isopropyl ketone cm^{-1}	Diisopropyl ketone cm^{-1}	Di-t-butyl ketone cm^{-1}
Chloroform	2.6	2.7	3	3.4	4.2	5.7
t-Butyl alcohol	3.8	3.7	4.1	4.4	4.5	3.3
Isopropyl alcohol	2.3	2.3	2.7	2.9	3.1	2.7
Ethyl alcohol	1	1	2.5	1.3	2	1.7
Methyl alcohol	0	0	0	0	0	0

TABLE 14.3C A comparison of the differences in the carbonyl stretching frequencies (Δ C=O str. in cm^{-1}) of dialkyl ketones in hexane solution and in alcohol solution [non-H-bonded C=O]

Alcohol	Dimethyl ketone cm^{-1}	Methyl ethyl ketone cm^{-1}	Diethyl ketone cm^{-1}	Ethyl isopropyl ketone cm^{-1}	Diisopropyl ketone cm^{-1}	Di-t-Butyl ketone cm^{-1}
Methyl	6.15	8.6	8.05	6.4	5.3	5.5
Ethyl	5.35	7.8	7.3	6	4.3	3.9
Isopropyl		6.7	4.5	5.2	3.3	3.3
t-Butyl		5.2	2.6	2.6	2.3	3.3

TABLE 14.4 The C=O stretching frequencies for *n*-butyrophenone and *tert*-butyrophenone in 0 to 100 mol % $\text{CHCl}_3/\text{CCl}_4$ solutions

Mole % $\text{CHCl}_3/\text{CCl}_4$	<i>n</i> -Butyro-phenone C=O str.	<i>t</i> -Butyro-phenone C=O str.	Δ C=O
0	1691	1678.43	12.6
10.8	1689	1677.6	11.4
16.9	1687	1676.7	10.3
26.7	1687	1676	11
32.6	1686	1675.6	10.4
37.7	1686	1675.3	10.7
42.1	1685	1675.1	10.9
45.9	1685	1674.9	10.1
49.2	1685	1674.8	10.2
52.2	1685	1674.7	10.3
55.7	1685	1674.7	10.3
57.4	1685	1674.7	10.3
60.2	1685	1674.5	10.5
63.4	1685	1674.5	10.5
66.89	1684	1674.4	9.6
70.8	1684	1674.3	9.7
75.2	1684	1674.3	9.7
80.2	1684	1674.2	9.8
85.8	1684	1674.1	9.9
92.4	1683	1674.1	8.89
100	1682	1674.1	7.9

TABLE 14.5 IR data for acetone, α -chloroacetone, acetophenone, and benzophenone in CS₂ solution between ~ 29 and -100°C

$^\circ\text{C}$	Acetone	$^\circ\text{C}$	α -Chloro-acetone	α -Chloro-acetone	[conformer 1]– [conformer 2]	$^\circ\text{C}$	Acetophenone	$^\circ\text{C}$	Benzophenone
	C=O str. [CS ₂] cm ⁻¹		conformer 1 C=O str. [CS ₂] cm ⁻¹	conformer 2 C=O str. [CS ₂] cm ⁻¹			C=O str. [CS ₂] cm ⁻¹		C=O str. [CS ₂] cm ⁻¹
27	1717.5	29	1750.2	1723.7	26.5	32	1689.4	31	1663.3
15	1717.3	11	1750.7	1723.7	27	15	1689.5	15	1662.7
0	1717.5	0	1750.5	1723.3	27.2	0	1689.7	0	1662.2
-10	1717.3	-10	1750.5	1723.3	27.2	-10	1689.2	-10	1661.5
-20	1717	-20	1751	1722.9	28.1	-20	1688.7	-20	1661
-30	1716.4	-30	1750.2	1722.4	27.8	-30	1687.4	-30	1660.7
-40	1715.4	-40	1749.9	1722	27.9	-40	1687	-40	1660.3
-50	1715.4	-50	1750	1721.6	28.4	-50	1687.4	-50	1660
-60	1713.6	-60	1749	1720.7	28.3	-60	1687.1	-60	1659.6
-70	1713.6	-70	1747.9	1721	26.9	-70	1687	-70	1659
-80	1713					-80	1686.5	-80	1658.5
-90	1712.7					-90	1686.4	-90	1658
-100	1711.7					-100	1686.2	-100	1657.8
delta C [-127]	delta C=O str. [-5.8]	delta C [-99]	delta str. C=O [-2.3]	delta C=O str. [-2.7]		delta C [-132]	delta C=O str. [-3.2]	delta C [-131]	delta C=O str. [-5.5]

TABLE 14.6 A comparison of carbonyl stretching frequencies for 2% wt./vol. ketone in dimethyl sulfoxide and/or carbon tetrachloride solution

Mole % (CH ₃) ₂ SO/CCl ₄	Acetone cm ⁻¹	Aceto-phenone 2,4,6-Tri-methyl- cm ⁻¹	Aceto-phenone 4-nitro- cm ⁻¹	Aceto-phenone cm ⁻¹	Aceto-phenone 4-methoxy- cm ⁻¹	Aceto-phenone cm ⁻¹
0	1718	1704	1700	1691	1683	1665
11.87	1715	1700	1697	1687	1679	1662
29.48	1713	1699	1695	1686	1677	1661
40.48	1713	1698	1694	1686	1676	1660
48.78	1712	1698	1694	1685	1676	1660
57.63	1712	1698	1693	1684	1675	1659
100	1710	1695	1691	1682	1672	1657

TABLE 14.7 IR vapor-phase data for conjugated ketones

Compound and Conformer	2(C=O str.)*	C=O str.* (see text)*	C=C, str. (see text)*	CH=CH twist	[C=O str.]– [C=C str.]*	[(A)C=C str.]/ [(A)C=O str.]*	[C=C str.]– [HC=CH twist]	[(A)CH=CH twist]/ [(A)C=C str.]*	C=CH ₂ wag	CH=CH ₂ wag
s-cis,trans CH=CH										
Chalcone	3358(0.005)	1680(0.690)	1620(1.230)	980(0.129)	60	1.78	640	0.11		
4,4'-Difluoro-		1680(0.372)	1619(0.614)	980(0.090)	61	1.65	639	0.15		
4'-Fluoro-methoxy	3350(0.005)	1678(0.365)	1605(1.220)	979(0.131)	73	3.34	626	0.11		
3,4-Dichloro-4'-methyl	3350(0.005)	1675(0.491)	1612(1.240)	979(0.180)	63	2.53	633	0.15		
2-Chloro-2',4'-dimethyl	3330(0.005)	1670(1.230)	1611(0.225)	979(0.225)	59	0.68	632	0.27		
4-Nitro-	3360(0.005)	1684(0.385)	1619(0.393)	978(0.130)	65	1.02	641	0.33		
s-cis										
3-Buten-2-one	3400(0.011)	1715(1.245)	1627(0.120)	986(0.250)	88	0.09	641	2.08	951(0.400)	760(0.030)
		1695(1.239)	1616(0.112)	[C=CH ₂ wag] 951(0.400)				[(A)C=CH ₂ wag]/	[CH=CH twist]-	
s-cis										
3-Methyl-3-buten-2-one	3388(0.030)	1700(1.240)	1639(0.210)	929(0.520)	61	0.17	710	[(A)C=C str.] 2.48	[C=CH ₂ wag] 35	
s-cis 1-Penten-3-one	3399(0.020)	1712(1.240)	1624(0.210)	987(0.400)	88	0.17	637	1.9		
s-cis,trans HC=CH										
1-Phenyl-1-hepten-3-one	3395(0.010)	1690(0.920)	1620(1.210)	974(0.370)	70	1.32	646	0.31		
								[(A)o.p.=C–H def.]/		
s-cis,cis(H,CH ₃)										
Methyl 2-methyl-1-propenyl ketone	3400(0.011)	1710(1.140) 1705(0.940) 1699(1.150)	1634(1.240)	821(0.091)	71	1.32	813	[(A)C=C str.] 0.07		
s-cis,cis(H,CH ₃)?										
3-Methyl-4-phenyl-3-buten-2-one	3358(0.005)	1690(1.250)	1627(0.160)	860(0.030)	63	0.13	767	0.19		[(A)o.p.=C–H def.]/

TABLE 14.7A Other fundamental vibrations for conjugated ketones

Compound	trans=C-H s. rock and a.CCC str.	i.p. Ring	i.p.o.p. 5H def.	o.p. Ring def.			
Chalcone	1320(0.600)	1015(0.500)	746(0.440) [o.p.2H def]	691(0.381)			
4, 4'-Difluoro-	1320(0.261)	1015(0.285)	821(0.285)				
4'-Fluoro-4-methoxy	1320(0.295)	1015(0.385)	821(0.300)				
3,4-Dichloro-4'-methyl	1322(0.370)	1030(0.600)	801(0.400) [o.p.H def.]	[o.p.2H def.]	[o.p.4H def]		
2-chloro-2',4'-dimethyl	1310(0.490)	1009(0.360)	873(0.445) [o.p.2H def.]	817(0.180) [a.NO ₂ str.]	752(0.440) [s.NO ₂ str.]		
4-Nitro-	1318(0.470) [CH ₂ =bend]	1011(0.390) [s.CH ₃ bend]	851(0.232)	1538(0.542)	1348(1.230)		
3-Buten-2-one	1410(0.310) a.CH ₂ =str.]	1380(0.359) [a.CH ₃ str.]	1240(0.365) [s.CH ₃ str.]	1175(0.390) [s.CH ₃ str.]	760(0.030) [a.CH ₃ bend]	[s.CH ₃ bend]	[CCC str.]
3-Methyl-3-buten-2-one	3100(0.172)	2988(0.540)	2938(0.680)	2880(0.285)	1450(0.399) [CH ₂ =twist ?] 700(0.070)	[gamma C=O] 561(0.140)	1145(1.030)
1-Penten-3-one	[a.CH ₂ =str.] 3102(0.103) [CH=str.]	[CH ₂ =bend] 1410(0.530) [a.CH ₃ str.]	[s.CH ₃ str.]	{CCC str. ?} 1196(0.300) [a.CH ₃ bend]	[a.CH ₃ bend] 1460(0.191) [s.CH ₄ bend]	[s.CH ₃ bend]	
Methyl-2-methyl-1-propenyl ketone	3020(0.190)	2980(0.270)	2870(0.140)	1448(0.235)	1390(0.370)	1367(0.520)	
1-Phenyl-1-hepten-3-one	[a.CH ₃ str.] 2970(0.940) [CCC str.] 1325(0.430)	[a.CH ₂ str.] 2940(0.790)	[s.CH ₂ str.] 2885(0.400)	[CH ₂ bend] 1451(0.280)	[s.CH ₃ bend] 1385(0.100) [i.p.o.p.5H def.] 745(0.360)	[o.p. Ring def.] 690(0.320)	
3-Methyl-4-phenyl-3-buten-2-one				see text 770(0.068)	see text 726(0.104)	695(0.146)	
Cinnamaldehyde	[OC-H str. in FR.] 2805(0.116)	[s(OC-H bend) in FR.] 2737(0.109)	[OC-H bend] 1395(0.005)		[i.p.o.p.5H def.] 741(0.157)	[o.p. Ring def.] 688(0.111)	
alpha-Hexyl cinnamaldehyde	2828(0.1180)	2705(0.115)	1400(0.035)		745(0.082)	695(0.131)	

TABLE 14.8 Infrared data for 2-hydroxy-5-X-acetophenone in CCl₄ and CS₂ solutions

2-Hydroxy-5-X- acetophenones	C=O: H=O cm ⁻¹ CCl ₄ soln.	C=O: H=O cm ⁻¹ NM	C=O: H=O cm ⁻¹ CHCl ₃	C=OCH ₃ cm ⁻¹ CCl ₄ soln.	delta cm ⁻¹	C-C(=)-C str. cm ⁻¹ CS ₂ soln.	C ₆ H ₅ -C(=)str. cm ⁻¹ CS ₂ soln.	C ₆ H ₅ -O str, cm ⁻¹ CS ₂ soln.	sym. CH ₃ bend cm ⁻¹ CCl ₄ soln.
NO ₂	1658	1645			13	973	1295	1192	1360* ¹
C=OCH ₃	1650			1687	37	968,958	1302	1212	1370;1359
H	1646.2		1642.3		3.9	957	1303	1212	1369
C ₆ H ₅	1650					958	1301	1212	1368
I	1641					954	1283	1190	1365
CH ₃	1654					960	1297	1213	1369
Br	1649					959	1318	1207	1363
Cl	1650					959	1321	1208	1367
F	1655					963	1322	1211	1371
CH ₃ O	1652					960	1370	1205	1370
NH ₂	1648	1641			7	961	1380	1211	1380
NH ₂						[969 solid]		[1218 solid]	
NH ₂	NH ₂ bend cm ⁻¹ 1636								

*¹and sym. NO₂ str.

TABLE 14.9 IR vapor-phase data and assignments for cyclobutanone and cyclopentanone

Compound	a.CH ₂ str. cm ⁻¹ (A)	s.CH ₂ str. cm ⁻¹ (A)	CH ₂ bend cm ⁻¹ (A)	CH ₂ wag cm ⁻¹ (A)	CH ₂ twist cm ⁻¹ (A)	CH ₂ rock cm ⁻¹ (A)	Ring def. cm ⁻¹ (A) breathing	Ring cm ⁻¹ (A)	2(C=O) str. cm ⁻¹ (A)	C=O str. cm ⁻¹ (A)
Cyclobutanone			1402 (0.070)		1223 (0.050)					1828 (1.041)
	3004 (0.240)	2930 (0.105)	1404 (0.060)	1254 (0.025)	1210 (0.040)	845 (0.010)	1072 (0.290)	945 (0.010)	3602 (0.021)	1815 (1.240)
	2980 (0.170)		1396 (0.070)		1195 (0.030)		1060 (0.232)			1800 (1.141)
		2904 (0.241)								
Cyclopentanone	2979 (0.841)	2895 (0.321)	1419 (0.175)	1275 (0.063)	1142		964		3510 (0.040)	1767 (1.250)
	2965 (0.690)									

TABLE 14.10 The C=O stretching frequencies for cyclopentanone and cyclohexanone in the vapor, neat, and solution phases

Cyclopentanone solvent	Corrected for fermi res. C=O str. 1 % (wt./vol.) cm ⁻¹	Corrected for fermi res. C.T cm ⁻¹	AN	delta C=O [Hexane]-[soln.] cm ⁻¹	Cyclohexanone	C=O str. 1 % (wt./vol.) cm ⁻¹	delta C=O str. [vap.]-[soln.] cm ⁻¹	delta C=O [Hexane]-C=O str. [soln.] cm ⁻¹
{Vapor}	1765					1732		
{Neat}	1739.2	1736.8						
Hexane	1750.6	1727.4	0			1723	0	27.6
Methyl t-Butyl ether	1745.8	1731.2		5.3		1718	5	27.3
Diethyl ether	1744.5	1730.5	3.9	6.1		1718	5	26.5
Carbon tetrachloride	1742.9	1731.1	8.6	7.7		1715	8	28.9
Benzene	1740.8	1731.2	8.2	9.8		1713	10	27.8
Carbon disulfide	1741.7	1727.3		8.9		1714	9	27.7
Benzonitrile	1736.9	1735.1	15.5	13.7		1706	10	30.9
Nitrobenzene	1736.1	1734.6	14.8	14.5		1707	18	29.8
Acetonitrile	1736.3	1736.7	18.9	14.3		1707	16	29.3
Methyl dichloride	1734.9	1735.1	20.4	15.7		1705	18	29.9
Nitromethane	1734.8	1737.2		15.8		1705	18	29.8
Dimethyl sulfoxide	1731.6	1735.4	19.3	19		1703(wet)	20	28.6
Chloroform						1703	20	30.6
Chloroform (4.0%)	1733.6	1735.4	23.1	17				
Chloroform (0.1%)	1733	1735	23.1	17.6				
Chloroform-d	1733.4	1735.6	23.1	17.2				
t-Butyl alcohol	1734.9	1737.1	29.1	15.7				
Isopropyl alcohol	1735.8	1738.2	33.5	14.8				
Ethyl alcohol	1735.2	1737.7	37.1	15.4		1702	21	33.2
Methyl alcohol	1733.5	1738.5	41.3	17.1		1701	22	32.5
Water	1728.8	1734.7	54.8	22.8				

TABLE 14.11 IR data for 14H-dibenzo[a,j] xanthen-14-one in CHCl₃/CCl₄ and various solvents

14H-dibenzo[a,j] xanthen-14-one Mole % CHCl ₃ /CCl ₄	C=O str. in FR [1] cm ⁻¹	C=O str. [2] in FR cm ⁻¹	A[1]	A[2]	A[1]/A[2]	C=O str. corrected for FR cm ⁻¹	OT or CT corrected for FR cm ⁻¹	
0	1648.85	1634.85	0.148	0.11	1.345	1642.9	1640.8	
54.62	1648.78	1633.14	0.094	0.108	0.87	1639.5	1640.3	
100	1645.4	1633.08	0.197	0.273	0.721	1638.2	1640.2	
Solvent								AN* ¹
Hexane	1651.89	1636.83	0.076	0.031	2.45	1647.5	1641.2	0
Carbon tetrachloride	1648.85	1634.85	0.148	0.031	1.345	1642.9	1640.8	8.6
Carbon disulfide	1648.18	1633.8	0.482	0.359	1.34	1642	1639.9	[10.1]
Benzene	1647.59	1634.49	0.178	0.166	1.07	1641.3	1640.8	8.2
Tetrahydrofuran	1646.74	1634.82	0.384	0.299	1.28	1641.5	1640	[8.8]
Methylene chloride	1646.06	1632.98	0.224	0.27	0.83	1638.9	1640.1	20.4
Benzonitrile	1645.79	1633.28	0.357	0.47	0.76	1638.7	1640.4	15.5
Chloroform	1645.4	1633.08	0.197	0.273	0.72	1638.2	1640.2	23.1

*¹AN = acceptor number.

TABLE 14.12 IR and Raman data for 1,4-benzoquinones in CCl₄ and CHCl₃ solutions

Substituted 1,4-benzoquinone	Point group	Species	IR data	IR data	[CCl ₄ soln.]–	Species	Raman data	Raman data	[CCl ₄ soln.]–
			o.p.(C=O) ₂ str. [CCl ₄ soln.] cm ⁻¹	o.p.(C=O) ₂ str. [CHCl ₃ soln.] cm ⁻¹	[CHCl ₃ soln.] cm ⁻¹		i.p.(C=O) ₂ str. [CCl ₄ soln.] cm ⁻¹	i.p.(C=O) ₂ str. [CHCl ₃ soln.]	[CHCl ₃ soln.]
Tetrafluoro	Vh	B _{1u}	1702.71	1701.42	-1.29	A _g	1696.8	1697.7	0.9
Tetrachloro	Vh	B _{1u}	1694.68	1693.37	-1.31	A _g		1685.1	
Trichloro	Cs	A'	[1694]* ¹			A'	[1675]		
Tetrabromo	Vh	B _{1u}	1687.48	1685.37	-2.11	A _g			
2,5-Dichloro	C2h	B _u	1682.18	1681.25	-0.09	A _g	1672.5	1673.6	1.1
Chloro	Cs	A'	1681.89	1680.95	-0.94	A'	1659.3	1659.3	0
Unsubstituted	Vh	B _{1u}	1663.51* ²	1662	-1.51	A _g	1661.4	1661.8	0.4
Methyl	Cs	A'	1662.47	1659.57	-2.9	A'	1665.7	1665.9	0.2
2,6-Dimethyl	C2v	A ₁	1657			A ₁		1666.9	2.5

*¹CS₂ soln.*²Corrected for FR.

TABLE 14.13 IR data for tetrafluoro-1,4-benzoquinone in CCl₄, CHCl₃, and C₆H₁₄ solutions

Tetrafluoro- 1,4-benzoquinone	o.p.(C=O) ₂ str. cm ⁻¹	o.p.(C=C) ₂ str. cm ⁻¹	A[1]	A[2]
Mole % CHCl ₃ /CCl ₄				
0	1702.71	1667.63	1.279	1.164
26.53	1702.27	1667.88	1.308	1.157
52	1701.91	1668.05	1.506	1.314
75.06	1701.66	1668.21	1.614	1.416
100	1701.42	1668.35	1.805	1.525
delta cm ⁻¹	-1.29	0.72		
Mole % CHCl ₃ /C ₆ H ₁₄				
0	1705.03	1667.67	0.443	0.388
24.49	1704.07	1668.04	0.451	0.413
53.16	1702.82	1668.31	0.551	0.511
76.43	1702.09	1668.52	0.703	0.639
100	1701.21	1668.05	0.911	0.813
delta cm ⁻¹	-3.82	0.38		
Mole % CCl ₄ /C ₆ H ₁₄				
0	1705.06	1667.67	0.466	0.408
28.26	1704.48	1667.72	0.495	0.439
51.96	1703.88	1667.78	0.539	0.49
73.01	1703.28	1667.79	0.563	0.517
100	1702.83	1667.79	0.78	0.713
delta cm ⁻¹	-2.23	0.12		

TABLE 14.14 IR data for tetrachloro-1,4-benzoquinone in $\text{CHCl}_3/n\text{-C}_6\text{H}_{14}$, $\text{CCl}_4/n\text{-C}_6\text{H}_{14}$, and $\text{CHCl}_3/\text{CCl}_4$ solutions

Tetrachloro- 1,4-benzoquinone	o.p.(C=O) ₂ str. cm ⁻¹	A
Mole % $\text{CHCl}_3/n\text{-C}_6\text{H}_{14}$		
0	1696.3	0.222
24.29	1695.27	0.267
53.16	1694.86	0.539
76.43	1693.76	0.726
100	1693.27	1.024
delta cm ⁻¹	-3.03	
Mole % $\text{CCl}_4/n\text{-C}_6\text{H}_{14}$		
0	1696.4	0.217
28.26	1695.73	0.255
51.96	1695.19	0.32
73.01	1695.51	0.406
100	1694.66	0.593
delta cm ⁻¹	-1.74	
Mole % $\text{CHCl}_3/\text{CCl}_4$		
0	1694.68	
26.563	1693.97	
52	1693.4	
75.06	1693.09	
100	1693.37	
delta cm ⁻¹	-1.31	

TABLE 14.15 IR data for tetrabromo-1,4-benzoquinone in $\text{CCl}_4/\text{C}_6\text{H}_{14}$, $\text{CHCl}_3/\text{C}_6\text{H}_{14}$, and $\text{CHCl}_3/\text{CCl}_4$ solutions

Tetrabromo- 1,4-benzoquinone	o.p.(C=O) ₂ str. cm ⁻¹	CT cm ⁻¹
Mole % $\text{CCl}_4/\text{C}_6\text{H}_{14}$		
0	1689.87	
28.26	1688.52	1676.44
51.96	1688.11	1672.04
73.01	1687.52	1670.82
73.01	1687.52	1670.82
100	1687.59	1669.38
delta cm ⁻¹	-2.28	
Mole % $\text{CHCl}_3/\text{C}_6\text{H}_{14}$		
0	1689.54	
24.49	1688.33	1670.82
49.31	1687.82	1670.02
72.99	1686.76	1669.45
100	1685.39	1669.33
delta cm ⁻¹	-4.15	
Mole % $\text{CHCl}_3/\text{CCl}_4$		
0	1687.48	
26.53	1686.89	1669.88
52	1686.41	1669.84
75.06	1685.78	1669.9
100	1685.37	
delta cm ⁻¹	-2.11	

TABLE 14.16 IR data for chloro-1,4-benzoquinone in $\text{CHCl}_3/n\text{-C}_6\text{H}_{14}$, $\text{CCl}_4/n\text{-C}_6\text{H}_{14}$, and $\text{CHCl}_3/\text{CCl}_4$ solutions

Chloro-1,4-benzoquinone	o.p.(C=O) ₂ str.n cm ⁻¹	i.p.(C=O) ₂ str. cm ⁻¹	A[1]	A[2]
Mole % $\text{CHCl}_3/n\text{-C}_6\text{H}_{14}$				
0	1683.76	1662.23	0.595	0.252
24.49	1683.32	1661.56	0.485	0.234
49.31	1682.23	1660.96	0.517	0.272
74.71	1681.85	1660.37	0.675	0.379
100	1680.9	1660.32	0.616	0.361
delta cm ⁻¹	-2.86	-1.92		
Mole % $\text{CCl}_4/n\text{-C}_6\text{H}_{14}$				
0	1683.73	1662.19	0.599	0.256
28.26	1683.87	1661.71	0.526	0.235
51.96	1683.36	1661.33	0.565	0.254
77.17	1682.64	1660.86	0.613	0.288
100	1681.87	1660.37	0.689	0.34
delta cm ⁻¹	-1.86	-1.82		
Mole % $\text{CHCl}_3/\text{CCl}_4$				
0	1681.89	1660.36	0.709	0.348
26.53	1682.01	1660.82	0.733	0.385
52	1681.59	1660.62	0.707	0.389
75.06	1681.31	1660.49	0.656	0.375
100	1680.95	1660.35	0.798	0.411
delta cm ⁻¹	-0.94	-0.01		

TABLE 14.17 IR data for 2,5-dichlorobenzoquinone in $\text{CHCl}_3/n\text{-C}_6\text{H}_{14}$, $\text{CCl}_4/n\text{-C}_6\text{H}_{14}$, and $\text{CHCl}_3/\text{CCl}_4$ solutions

2,5-Dichloro-1,4-benzoquinone	$\text{o.p.}(\text{C}=\text{O})_2$ cm^{-1}
Mole % $\text{CHCl}_3/n\text{-C}_6\text{H}_{14}$	
0	1684.86
24.29	1683.25
53.16	1682.76
76.43	1681.59
100	1681.59
delta cm^{-1}	-3.48
Mole % $\text{CCl}_4/n\text{-C}_6\text{H}_{14}$	
0	1684.74
28.26	1683.9
51.96	1683.2
73.01	1683.33
100	1682.15
delta cm^{-1}	-2.59
Mole % $\text{CHCl}_3/\text{CCl}_4$	
0	1682.18
26.53	1681.64
52	1681.87
75.06	1681.57
100	1681.25
delta cm^{-1}	-0.83

TABLE 14.18 IR data for 3,3',5,5'-tetraalkyl-1,4-diphenylquinone in CHCl_3 solution and in the solid phase

3, 3', 5, 5'-Tetraalkyl-1,4-diphenylquinone	Symmetry	$\text{o.p.}(\text{C}=\text{O})_2$ str. solid cm^{-1}	$\text{o.p.}(\text{C}=\text{O})_2$ str. CHCl_3 cm^{-1}	$\text{i.p.}(\text{C}=\text{O})_2$ str. solid cm^{-1}	$\text{i.p.}(\text{C}=\text{O})_2$ str. CHCl_3 cm^{-1}	$\text{o.p.}(\text{C}=\text{O})_2$ str.+ $\text{i.p.}(\text{C}=\text{O})_2$ str. solid cm^{-1}	$\text{o.p.}(\text{C}=\text{O})_2$ str.+ $\text{i.p.}(\text{C}=\text{O})_2$ str. CHCl_3 cm^{-1}
$(\text{CH}_3)_4$	D_{2h}	1589	1595	[1589]	[1597]	3178	3192
(iso C_4H_9) ₄	D_{2h}	1589	1592	[1579]	[1583]	3168	3175
(tert C_4H_9) ₄	D_{2h}	1602	1597	[1602]	[1583]	3204	3180
(cyclo C_5H_{11}) ₄	D_{2h}	1598	1598	[1601]	[1602]	3199	3200
3,3'-(CH_3) ₂ -5,5'	C_{2v}	1586	1588	[1582]	[1592]	3168	3180
(tert. C_4H_9) ₂		1588	1589	1603	1603	3189	3195
						[3191]	[3192]

TABLE 14.19 The dependence of the C=O stretching frequency upon solute concentration of dialkyl ketones in CCl₄/CHCl₃ solutions

wt./vol. % solute [CCl ₄]	Diisopropyl ketone C=O str.	wt./vol. % solute [CCl ₄]	Di-t-butyl ketone C=O str.
0.75	1715.91	0.8	1685.9
1.5	1715.87	1.2	1685.88
2.63	1715.8	1.8	1685.86
3.75	1715.75	2.62	1685.87
5.25	1715.72	3.94	1685.83
7.5	1715.67	5.25	1685.82
		6.26	1685.81
delta C=O str. [CHCl ₃]	-0.24	[CHCl ₃]	-0.09
0.22	1704.94	0.4	1680.71
0.43	1704.95	0.8	1680.99
1.08	1704	1.2	1680.73
2.16	1705.05	1.6	1680.73
4.04	1705.2	2.3	1680.73
5.89	1705.32	3.47	1680.78
7.29	1705.38	4.63	1680.79
8.62	1705.47	5.78	1680.81
delta C=O str.	0.53		0.1

Carboxylic Acid Esters

Conjugation Effect	332
Inductive Effect	332
Intramolecular Hydrogen Bonding	333
Diesters	333
Vapor vs Solution Phases	333
Rotational Conformers	335
Methods to Confirm the Presence of Rotational Conformers	337
Lactones	337
Alkyl Benzoates	341
Salicylates and 2-Hydroxyacetophenone (a Ketone)	341
Phthalates	342
Acrylates and Methacrylates	343
Cinnamates	345
Phenoxarsine Derivatives	346
Thiol Esters	347
Thiol Acids	349
Thiol Acid Anhydrides	349
Other Ester Vibrations	350
References	351

Figures

Figure 15-1	352 (333)	Figure 15-14	360 (340)
Figure 15-2	353 (334)	Figure 15-15	361 (340)
Figure 15-3	354 (334)	Figure 15-16	362 (341)
Figure 15-4	355 (334)	Figure 15-17	363 (341)
Figure 15-5	356 (335)	Figure 15-18	364 (341)
Figure 15-6	356 (335)	Figure 15-19	365 (341)
Figure 15-7	357 (337)	Figure 15-20	366 (342)
Figure 15-8	357 (339)	Figure 15-21	367 (342)
Figure 15-9	358 (339)	Figure 15-22	367 (343)
Figure 15-10	358 (339)	Figure 15-23	368 (344)
Figure 15-11	359 (339)	Figure 15-24	369 (347)
Figure 15-12	359 (339)	Figure 15-25	370 (349)
Figure 15-13	360 (340)		

Tables

Table 15-1	371 (332)	Table 15-3	373 (334)
Table 15-2	372 (333)	Table 15-4	373 (335)

Table 15-5	373 (335)	Table 15-15	383 (345)
Table 15-5a	374 (335)	Table 15-15a	383 (346)
Table 15-6	374 (337, 338)	Table 15-15b	384 (346)
Table 15-7	375 (339)	Table 15-16	385 (346)
Table 15-8	375 (340)	Table 15-17	386 (348)
Table 15-9	376 (340)	Table 15-17a	386 (348)
Table 15-10	377 (341)	Table 15-17b	387 (348)
Table 15-11	378 (341)	Table 15-17c	387 (349)
Table 15-12	378 (342)	Table 15-18	388 (350)
Table 15-13	379 (343)	Table 15-19	389 (350)
Table 15-13a	380 (343)	Table 15-20	390 (350)
Table 15-14	381 (343)		

*Numbers in parentheses indicate in-text page reference.

Table 15.1 lists IR data for the carbonyl stretching frequencies, $\nu_{\text{C=O}}$, for some carboxylic acid esters. This table also shows how the $\nu_{\text{C=O}}$ frequencies change or shift with change of phase or with change in the molecular structure (1).

In all cases, $\nu_{\text{C=O}}$ occurs at higher frequency in the vapor phase than in the liquid or condensed phase. In the liquid phase the dipolar interaction of esters (dielectric effect) causes the C=O bond to weaken and occur at lower frequency. In any series of esters, the methyl analog will occur at the highest frequency, and the frequencies decrease with increased branching on the α -carbon atom. This is attributed to the inductive effect of the alkyl group, because the electron donation of the alkyl group increases with increased branching on the α -carbon atom, which causes $\nu_{\text{C=O}}$ to weaken and vibrate at lower frequency.

The vinyl or phenyl esters of any series always occur at higher frequencies than their corresponding alkyl esters, and this is also due to the inductive effect. The vinyl or phenyl groups withdraw electrons, and this strengthens the C=O bond, which causes $\nu_{\text{C=O}}$ to vibrate at higher frequency. For example, alkyl acetates exhibit $\nu_{\text{C=O}}$ in the range 1755–1769 cm^{-1} , and $\nu_{\text{C=O}}$ for vinyl acetate and phenyl acetates occur in the range 1781–1786 cm^{-1} in the vapor phase.

CONJUGATION EFFECT

Conjugation of C=O with a vinyl or phenyl group ($\text{C}=\text{C}-\text{C}=\text{O}$ or $\text{C}_6\text{H}_5-\omega\text{C}=\text{O}$) causes $\nu_{\text{C=O}}$ to decrease in frequency. For example, alkyl propionates exhibit $\nu_{\text{C=O}}$ in the range 1751–1762 cm^{-1} and alkyl acrylates exhibit $\nu_{\text{C=O}}$ in the range 1746–1751 cm^{-1} in the vapor phase.

INDUCTIVE EFFECT

The inductive effect of the phenyl group also causes $\nu_{\text{C=O}}$ for phenyl benzoate to occur at higher frequency (1760 cm^{-1}) than $\nu_{\text{C=O}}$ for alkyl benzoates (1737–1749 cm^{-1}). The $\nu_{\text{C=O}}$ frequencies for dialkyl isophthalates, and dialkyl terephthalates occur in the range 1739–1753 cm^{-1} , and are essentially identical to those exhibited by the alkyl benzoates in the vapor phase.

INTRAMOLECULAR HYDROGEN BONDING

In the vapor phase at high temperature alkyl salicylates exhibit $\nu_{\text{C=O}}$ in the range 1740–1755 and $\nu(\text{C=O})\cdots\text{H-O}$ in the range 1687–1698 cm^{-1} , and phenyl salicylates exhibit $\nu_{\text{C=O}}$ in the range 1750–1762 and $\nu(\text{C=O})\cdots\text{H-O}$ in the range 1695–1706 cm^{-1} . The higher frequency $\nu_{\text{C=O}}$ mode is attributed to C=O groups not intramolecularly hydrogen bonded and the lower frequency $\nu(\text{C=O})\cdots\text{H-O}$ mode is attributed to intramolecularly hydrogen-bonded C=O groups.

DIESTERS

It should be noted that dialkyl malonates, dialkyl succinates, and dialkyl adipates which contain two ester groups exhibit $\nu_{\text{C=O}}$ frequencies similar to those exhibited by the esters containing only one ester group in the vapor phase at elevated temperature.

VAPOR VS SOLUTION PHASES

Table 15.2 compares the $\nu_{\text{C=O}}$ frequencies for alkyl alkanoates in the vapor phase and in various solvents at 0.5 % wt./vol. Here MA is methyl acetate, MP is methyl propionate, MIB is methyl isobutyrate, MTMA is methyl trimethylacetate, EA is ethyl acetate, EP is ethyl propionate, EIB is ethyl isobutyrate, and ETMA is ethyl trimethyl acetate (2).

A study of Table 15.2 shows that $\nu_{\text{C=O}}$ for each of these esters occur at the highest frequency in the vapor phase, and in solution occur at the highest frequency in solution with n-hexane, a nonpolar solvent. In addition the $\nu_{\text{C=O}}$ mode decreases in frequency as the branching is increased on the acetate α -carbon atom and as methyl is replaced by ethyl. From other studies, the $\nu_{\text{C=O}}$ for the isopropyl and tert-butyl esters in each series would be expected to occur at subsequently lower frequency due to the increased inductive contribution of the isopropyl and tert-butyl groups.

It is interesting to compare the $\nu_{\text{C=O}}$ frequency differences for these alkyl alkanoates in solution in n-hexane and in the neat phase. These frequency differences are 10.2, 9.1, 7.1, and 6.2 cm^{-1} and 8.3, 7.8, 6.3 and 6.1 cm^{-1} for the methyl and ethyl analogs of acetate, propionate, isobutyrate, and trimethyl isobutyrate, respectively. Moreover, the differences between the $\nu_{\text{C=O}}$ frequencies of the methyl and ethyl analogs are 1.9, 1.3, 0.8 and 0.1 cm^{-1} progressing in the series acetate, propionate, isobutyrate, and trimethylacetate. These data indicate that as the steric factor of the R-C=O and O-R' groups for R-C(=O)-OR' is increased there is less dipolar interaction between ester molecules in the neat phase; thus, there is less of a frequency difference between the $\nu_{\text{C=O}}$ frequencies in n-hexane solution than in the neat phase (2).

Figure 15.1 shows plots of $\nu_{\text{C=O}}$ (solvent or neat) vs $\nu_{\text{C=O}}$ (hexane) minus $\nu_{\text{C=O}}$ (solvent or neat) for the alkyl alkanoates. These plots do not show data for the $\nu(\text{C=O})\cdots\text{H-O}$ frequencies noted when in solution with the four alcohols included in this study. Methyl trimethylacetate exhibits two bands, and this is attributed to Fermi resonance (2). The plots demonstrate that the frequencies decrease in a progressive manner, as was discussed here. There is no theoretical significance to these linear plots because any set of data (numbers) treated mathematically in this manner yields a linear relationship.

Figure 15.2 shows plots of $\nu(\text{C}=\text{O}) \cdots \text{HO}(\text{ROH})$ vs $\nu\text{C}=\text{O}$ (hexane) minus $\nu(\text{C}=\text{O}) \cdots \text{HO}(\text{ROH})$ for alkyl alkanoates. These plots show that the $\nu(\text{C}=\text{O}) \cdots \text{HO}$ frequencies decrease in each series in the order tert-butyl alcohol through methyl alcohol, and this is the order of progressive decreasing ROH acidity and progressive refractive index of these four alcohols. However, the dielectric constant of each alcohol increases progressively in the solvent order tert-butyl alcohol through methyl alcohol. Using these data to calculate the reaction field $[(R) = (e - 1)/(2e + n^2)]$, where e is the dielectric constant and n is the refractive index (3,4) shows that the reaction field increases in the order of butyl alcohol through methyl alcohol. Therefore, the reaction field is responsible for lowering the $\nu\text{C}=\text{O}$ frequencies in alkyl alkanoates in alkyl alcohols. The $\nu(\text{C}=\text{O}) \cdots \text{HOR}$ frequencies for these alkyl alkanoates are also progressively lowered in frequency by the increasing reaction field plus the additional lowering of the $\nu\text{C}=\text{O}$ mode due to intermolecular hydrogen bonding between the ROH proton and the carbonyl oxygen atom. Therefore, a quantitative measure of the strength of the intermolecular hydrogen bonds formed between $\text{C}=\text{O} \cdots \text{HOR}$ is the difference between the $\nu\text{C}=\text{O}$ and $\nu\text{C}=\text{O} \cdots \text{HOR}$ frequencies for each compound in each of the four alcohols. The larger the number, the stronger the intermolecular hydrogen bond. The strength of an intermolecular hydrogen bond between $\text{C}=\text{O} \cdots \text{HOR}$ is dependent upon three factors: 1) the acidity of the OH proton; 2) the basicity of the $\text{C}=\text{O}$ groups; and 3) the steric factors of both the alkyl group of each alcohol and the alkyl groups in each alkyl alkanoate. The larger their steric factors the larger the $\text{C}=\text{O} \cdots \text{HOR}$ bond distance. The strength of the hydrogen bond decreases as this $\text{C}=\text{O} \cdots \text{HOR}$ bond distance increases, and causes the frequency separation between $\nu\text{C}=\text{O}$ and $\nu\text{C}=\text{O} \cdots \text{HOR}$ to decrease. The steric factor of the alkyl groups prevents the strongest intermolecular hydrogen bonds from being formed between the most acid OH proton (tert-butyl alcohol in this case) and the most basic carbonyl group (ethyl trimethylacetate in this case). The frequency differences between $\nu\text{C}=\text{O}$ and $\nu\text{C}=\text{O} \cdots \text{HOR}$ in the alkyl alcohol solution of ethyl trimethylacetate should be less than exhibited by methyl trimethylacetate. Table 15.3 lists the frequency difference between $\nu\text{C}=\text{O}$ and $\nu\text{C}=\text{O} \cdots \text{HOR}$ for the alkyl alkanoates. The data shows that the strongest intermolecular hydrogen bonds are formed between the carbonyl oxygen atom and the alcohol OH protons with minor exception in the case of methanol. With the exception of isopropyl alcohol, the strength of the intermolecular hydrogen bond formed is also greater in the case of methyl trimethylacetate than in the case of ethyl trimethyl acetate. These data support the supposition that steric factors of these molecules do affect the molecular association between solute and solvent. In addition, steric factors must then play a role in the dielectric or dipolar interaction between solute and solvent.

Figure 15.3 shows plots of $\nu\text{C}=\text{O}$ for alkyl alkanoates vs AN for the solvent or neat alkyl alkanoate(s). AN is the solvent acceptor number (6). These plots show that AN values are not a precise measure of solute-solvent interaction due to steric factors if the alkyl groups and basicity of the carbonyl group (2).

Figure 15.4 shows plots of $\nu\text{C}=\text{O} \cdots \text{HO}(\text{ROH})$ vs AN for alkyl alkanoates in alkyl alcohols. With the exception of ethyl acetate in methyl alcohol, the $\nu\text{C}=\text{O} \cdots \text{OH}$ frequencies decrease in essentially a linear manner as the acidity of the OH proton decreases in the order tert-butyl alcohol through methyl alcohol. Reversal of that order of $\nu\text{C}=\text{O} \cdots \text{HOR}$ frequency decrease with decreasing strength of the intermolecular hydrogen bond indicates that dielectric properties of the solvent play a major role in affecting molecular vibrations.

Figure 15.5 shows plots of $\nu_{\text{C=O}} \cdots \text{HOR}$ for methyl acetate, ethyl acetate, isopropyl acetate, and tert-butyl acetate vs the solvent acceptor number (AN) for tert-butyl alcohol, isopropyl alcohol, ethyl alcohol, and methyl alcohol, numbered in solvent order 14–17 (5).

These alkyl acetates exhibit two bands in the carbonyl region of the IR spectrum in each of these four alkyl alcohols. Plots (A) through (D) are for the alkyl acetates in alcohol solution, but the carbonyl oxygen atoms are not intermolecularly hydrogen bonded. The lower frequency plots marked (A') through (D') are for the alkyl acetates in these alcohol solutions where the carbonyl oxygen atom is intermolecularly hydrogen bonded ($\text{C=O} \cdots \text{HOR}$). Plots (A') through (D') show a relationship with the AN values of both the nonprotic and protic solvents, and this indicates that the AN values include a value for the intermolecular hydrogen bond to a basic site in a solute molecule. This is understandable when considering how these AN values were determined. Since $(\text{C}_2\text{H}_5)_3\text{P=O}$ was used as the solute molecule to determine the AN values of solvents by application of NMR(6), it is reasonable that in the case of the alkyl alcohols an intermolecular hydrogen bond was also formed between the P=O oxygen atom and the alcohol OH proton ($\text{P=O} \cdots \text{HOR}$).

Table 15.4 lists the frequency difference between $\nu_{\text{C=O}}$ and $\nu_{\text{C=O}} \cdots \text{HO}$ for alkyl acetates in solution with alkyl alcohols (5). In this case the basicity of the carbonyl group increases in the order methyl through tert-butyl acetate. With the exception of isopropyl acetate in solution in methanol, the strongest intermolecular hydrogen bonds are formed between the carbonyl oxygen atom of tert-butyl acetate and the OH proton of each of the four alcohols. Thus, the strongest intermolecular hydrogen bonds are formed in the molecule with the most basic carbonyl group. It then follows that branching on the $\text{O-R}\alpha$ -carbon atom does not have as much effect on intermolecular hydrogen bonding as does branching on the acetate α -carbon atom. This is reasonable, because the alkyl group joined to an acetate α -carbon atom is much closer in space to the carbonyl oxygen atom than are the alkyl groups joined to the $\text{O-R}\alpha$ -carbon atom.

Again it should be noted that both $\nu_{\text{C=O}}$ and $\nu_{\text{C=O}} \cdots \text{HOR}$ decrease in frequency as the acidity of the OH proton decreases, which is the opposite of what one might predict. The overriding factor is that the reaction field increases in the order tert-butyl alcohol through methyl alcohol, and this causes a general decrease in both vibrational modes. In other words there is more dipolar interaction between the solute and solvent as the reaction field increases, which subsequently weakens the C=O bond. As previously discussed, steric factors also must affect dipolar interaction between solute and solvent. It is reasonable to assume that the AN values of the $\nu_{\text{C=O}}$ frequencies for alkyl acetates in these alkyl alcohols which are not intermolecularly hydrogen bonded are comparable to those AN values for dialkyl ethers, because these are the values predicted by projection of these frequencies onto the (A') through (D') curves.

ROTATIONAL CONFORMERS

Table 15.5 lists the $\nu_{\text{C=O}}$ frequencies for alkyl 2,2-dichloroacetates and alkyl acetates in the vapor or neat phases (1,7). The alkyl dichloroacetates in the vapor and neat phases exhibit rotational conformers 1 and 2, and both rotational conformer $\nu_{\text{C=O}}$ modes occur at lower frequency in the neat phase than the vapor phase by $11\text{--}16\text{ cm}^{-1}$. The $\nu_{\text{C=O}}$ for rotational

conformer 1 is 21–25 cm^{-1} higher in frequency than $\nu\text{C}=\text{O}$ for conformer 2, and the corresponding alkyl analogs of alkyl acetate and conformer 2 of alkyl 2,2-dichloroacetates exhibit $\nu\text{C}=\text{O}$ within $\pm 4 \text{ cm}^{-1}$ of each other. The inductive effect of the Cl atoms upon the $\text{C}=\text{O}$ bond is independent of molecular orientation; therefore, another factor is needed to explain the relatively low frequency exhibited by $\nu\text{C}=\text{O}$ of conformer 2 for alkyl dichloroacetates.

Comparison of the $\nu\text{C}=\text{O}$ vapor-phase data for the methyl, ethyl, and butyl esters of 2-chloroacetates vs the corresponding alkyl acetates: (1770 vs 1769 cm^{-1}), (1764 vs 1761 cm^{-1}), and (1759 vs 1761 cm^{-1}), respectively, shows that substitution of a chlorine atom in the α -carbon atom has very little effect upon the $\nu\text{C}=\text{O}$ mode. These vapor-phase data are recorded at high temperature. At ambient temperature in CCl_4 solution methyl chloroacetate exhibits $\nu\text{C}=\text{O}$ for rotational conformer 1 at 1772 cm^{-1} and rotational conformer 2 at 1747 cm^{-1} (1). These data indicate that in the vapor phase at elevated temperature methyl chloroacetate exists in the form of rotational conformer 2 where the Cl atom is not cis of gauche with the carbonyl oxygen atom. It is suggested that the Cl atom is in a configuration in which the Cl atom is trans to the carbonyl oxygen atom.

In the case of the alkyl dichloroacetates, possible molecular rotational conformers are:

- a. 2 Cl atoms gauche to the carbonyl oxygen atom;
- b. 1 Cl atom cis and one Cl atom gauche to the carbonyl oxygen atom; and
- c. 1 Cl atom trans and one Cl atom gauche to the carbonyl oxygen atom.

In a rotational conformer where one Cl atom is trans and one Cl atom is gauche to the carbonyl oxygen atom, the $\text{O}-\text{C}(=\text{O})-\text{C}$ bond angle is most likely increased due to electrostatic repulsion between the trans Cl atom and the $\text{R}-\text{O}$ oxygen atom. The increase in the $\text{O}-\text{C}(=\text{O})-\text{C}$ bond angle would lower the $\nu\text{C}=\text{O}$ frequency for rotational conformer 2, and this factor then offsets the inductive effect of the Cl atoms which raise the $\nu\text{C}=\text{O}$ frequency. This would account for the fact that $\nu\text{C}=\text{O}$ for conformer 2 for alkyl 2-chloroacetate and $\nu\text{C}=\text{O}$ for comparable alkyl acetates vibrate at comparable frequency.

Even though $\nu\text{C}=\text{O}$ frequencies are always observed at lower frequency in the neat liquid phase than in CCl_4 or CS_2 solution, it is of interest to compare the following data, which data illustrate the inductive effect. The IR data for ethyl 2-chloroacetate is for CS_2 solution data, and for ethyl 2,2-dichloroacetate is for liquid phase data (7,8):

	$\nu\text{C}=\text{O}$ (cm^{-1}) rotation conformer	$\nu\text{C}=\text{O}$ (cm^{-1}) rotation conformer 2
ethyl 2-chloroacetate (CS_2)	1765.0	1740.5
ethyl 2,2-dichloroacetate (neat)	1771	1750
ethyl acetate (CS_2)		1740.8

The $\nu\text{C}=\text{O}$ frequency for rotational conformer 2 increases with the addition of the second Cl atom when comparing data for ethyl 2-chloroacetate and ethyl 2,2-dichloroacetate (Cl, 1740.5 cm^{-1} vs 2 Cl, 1750 cm^{-1}) while $\nu\text{C}=\text{O}$ for rotational conformer 1 also increases with the addition of the second Cl atom (Cl, 1765.0 cm^{-1} , Cl_2 , 1771 cm^{-1}). The addition of the second Cl atom shows the additional inductive effect attributed by the second Cl atom. The

inductive effect of the first Cl atom is offset by the change in the O–C(=O)–C bond angle as already discussed here.

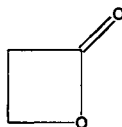
METHODS TO CONFIRM THE PRESENCE OF ROTATIONAL CONFORMERS

One method is to record IR spectra of a compound in CS₂ solution over a temperature range of 27°C to approximately –100°C (8). The data in Table 15.5a is plotted in Fig. 15.6. The left plot shows ν C=O rotational conformers 1 and 2 for ethyl 2-chloroacetate and ν C=O for ethyl acetate in CS₂ solutions vs temperature in °C. The right figure shows a plot of the absorbance ratio for ν C=O conformer 1/ ν C=O conformer 2 vs temperature in °C. These plots show that all of the ν C=O modes decrease in frequency in a linear manner as the temperature of the CS₂ solution is lowered. In addition, the concentration of rotational conformer 1 increases while the concentration of rotational conformer 2 decreases with decrease in temperature.

Another method for determining the presence of rotational isomers is to record IR spectra of a compound in different solvents or mixtures of two solvents (8). Figure 15.7 illustrates this technique for methyl 2,4-dichlorophenoxyacetate in carbon tetrachloride and/or dimethyl sulfoxide solution. This figure shows a plot of the ν C=O frequencies for rotational conformer 1 vs ν C=O for rotational conformer 2 with change in the CCl₄ to (CH₃)₂SO ratio. These data show that both frequencies decrease in a linear manner with change in the ratio of CCl₄ to (CH₃)₂SO. What it does not show is that both ν C=O frequencies decrease in frequency as the concentration of CCl₄ is decreased or concentration of (CH₃)₂SO is increased. This figure also shows that the absorbance ratio for (A) ν C=O conformer 2/(A) ν C=O conformer 1 decreases as the ratio of CCl₄ to (CH₃)₂SO is decreased. Thus, the most polar isomer for methyl 2,4-dichlorophenoxyacetate is for rotational conformer 1. Rotational conformer 1 is where the phenoxy oxygen atom is near in space (cis or gauche) to the phenoxy oxygen atom, and rotational isomer 2 is where the phenoxy oxygen atom is away in space (trans or gauche) from the carbonyl oxygen atom (8).

LACTONES

Table 15.6 lists IR data for β -propiolactone in various solvents (1% wt./vol.) (9). Figure 15.8 shows IR spectra of β -propiolactone in CCl₄ solution (left) 52 mole % CHCl₃/CCl₄ solution (middle), and CHCl₃ solution (right). The β -propiolactone has the following empirical structure:



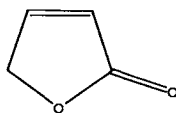
This structure is designated 4SR (4-membered saturated ring).

The C–C(=)–C bond angle is very small ($\sim 90^\circ$), and one would expect ν C=O to occur at a very high frequency. Inspection of Fig. 15.8 shows that the two lower frequency bands increase

in intensity while the higher frequency band decreases in intensity in progressing in the solvent series: CCl_4 , 52 mol % $\text{CHCl}_3/\text{CCl}_4$, and CHCl_3 . These bands are the result of $\nu\text{C}=\text{O}$ A' being in Fermi resonance with the combination $\nu_6 + \nu_{13}$, A' and the first overtone $2\nu_{10}$, A' (9). In this study of β -propiolactone an approximate correction for Fermi resonance based on perturbation theory for cases involving three modes was developed (9) (also see Chapter 1).

The data in Table 15.6 show that after correction for Fermi resonance, $\nu\text{C}=\text{O}$ for β -propiolactone occurs as high as 1850.2 cm^{-1} in *n*-hexane and as low as 1830.7 in methyl alcohol. Presumably the 1830.7 cm^{-1} band is for $\nu\text{C}=\text{O}\cdots\text{HOCH}_3$. The solvent acceptor numbers (AN) do not correlate with observed or unperturbed $\nu\text{C}=\text{O}$ β -propiolactone frequencies (9).

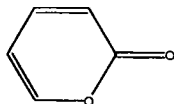
It is helpful to classify lactones as to the type of ring comprising the lactone group. For examples:



4 SR (see preceding text for β -propiolactone)

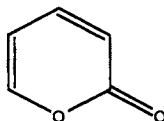
5 UR - 2,3(5-membered unsaturated ring where C=C group is in the 2,3-positions.

6 UR-2,3,4,5 (6-membered unsaturated ring where the C=C groups are in the 2,3- and 4,5-positions. The α -pyrone and coumarin are examples containing this group.)



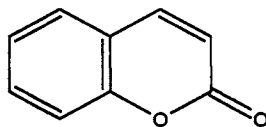
Lactones with 5 UR-2,3 structures are affected by alkyl substitution in the 4-position (1,10). In CCl_4 solution perturbed frequencies occur at 1785.4 and 1742 cm^{-1} for 4-H, 4-H analog, at 1782 and 1765 cm^{-1} for the 4-H, 4- CH_3 analog, and at 1776 and 1764 cm^{-1} for the 4- CH_3 , 4- HC_3 analog (10) after correction for Fermi resonance, $\nu\text{C}=\text{O}$ occurs at 1781.4 , 1776.2 , and 1769.9 cm^{-1} for the 4H, 4H analog, the 4-H, 4- HC_3 analog, and the 4- HC_3 , 4- HC_3 analog, respectively. The inductive effect of the CH_3 groups lowers the $\nu\text{C}=\text{O}$ frequencies. In addition, the $\nu\text{C}=\text{O}$ frequencies are lower in the case of 5 UR-2,3 compared to 5 SR lactones (1796 and 1784 cm^{-1} in CCl_4 solution and $\nu\text{C}=\text{O}$ is 1789.1 cm^{-1} after correction for Fermi resonance) due to conjugation of the $\text{C}=\text{C}-\text{C}=\text{O}$ groups, which weakens the $\text{C}=\text{O}$ bond and thus causes it to vibrate at a lower frequency (3).

The α -Pyrone has the following empirical structure:



In CCl_4 solution, IR bands are noted at 1752 and 1716 cm^{-1} , and after correction for Fermi resonance unperturbed $\nu\text{C}=\text{O}$ is 1749.4 cm^{-1} (10).

Coumarin has the following empirical structure:

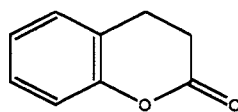


In CCl_4 solution at 1% wt./vol. coumarin exhibits IR bands at 1754.8 and 1741.3 cm^{-1} , and after correction for Fermi resonance $\nu\text{C}=\text{O}$ is calculated to be 1747.2 cm^{-1} . In CHCl_3 solution at 1% wt./vol., coumarin exhibits IR bands at 1729.9 and 1754.9 cm^{-1} , and after correction for Fermi resonance $\nu\text{C}=\text{O}$ is calculated to be 1734.9 cm^{-1} (10). Figure 15.9 shows a plot of the unperturbed $\nu\text{C}=\text{O}$ frequencies (corrected for FR.) for coumarin vs the mole % $\text{CHCl}_3/\text{CCl}_4$. This plot is essentially linear over the mole % ~ 10 – 95 % $\text{CHCl}_3/\text{CCl}_4$ range. Deviation from linearity below 10 mole % $\text{CHCl}_3/\text{CCl}_4$ is caused by $\text{C}=\text{O} \cdots \text{HCCl}_3$.

Figure 15.10 shows a plot of unperturbed $\nu\text{C}=\text{O}$ (corrected for FR.) for coumarin vs the mole % $(\text{CH}_3)_2\text{SO}/\text{CCl}_4$ and Fig. 15.7 shows a plot of unperturbed $\nu\text{C}=\text{O}$ (corrected for FR.) for coumarin vs the mole % $(\text{CH}_3)_2\text{SO}/\text{CHCl}_3$ (10). In Fig. 15.10 the plot is essentially linear over the ~ 10 – 95 % $(\text{CH}_3)_2\text{SO}/\text{CCl}_4$ range. In only CCl_4 or $(\text{CH}_3)_2\text{SO}$ solution, there is deviation from linearity (10). In Fig. 15.11 the plot is unique, as the $\nu\text{C}=\text{O}$ frequencies increase up to ~ 35 mol % $(\text{CH}_3)_2\text{SO}/\text{CHCl}_3$ stays relatively constant in the 40–50 mol % range, and decrease in frequency in the ~ 55 – 100 mol % range. The unique plot in Fig. 15.11 most likely is the result of intermolecular hydrogen bonding between the CHCl_3 proton and the coumarin carbonyl group and between the CHCl_3 proton and the oxygen atom of dimethyl sulfoxide. In the case of $\text{CHCl}_3/\text{CCl}_4$ solutions, the strength of the intermolecular hydrogen bonding between $\text{Cl}_3\text{CH} \cdots \text{ClCCl}_3$ is much weaker than in the case of $\text{Cl}_3\text{CH} \cdots \text{OS}(\text{CH}_3)_2$. Therefore, in $\text{CHCl}_3/\text{CCl}_4$ solution formation between $\text{C}=\text{O} \cdots \text{HCCl}_3$ is apparent only after the first formation of $(\text{CH}_3)_2\text{SO} \cdots \text{HCCl}_3$ (10).

Figure 15.12 shows a plot of the unperturbed $\nu\text{C}=\text{O}$ frequencies for coumarin (corrected for FR.) vs the reaction field of the $\text{CHCl}_3/\text{CCl}_4$ solvent system (10). The reaction field is $(R) = (e - 1)/2e + n^2$, where e is the solvent dielectric constant and n is the refractive index of the solvent, and this equation is derived from bulk dielectric theory (3,4). Bulk dielectric theory predicts a single band ($\nu\text{C}=\text{O}$, for example) which shifts in frequency according to the composition of the solvent mixture. Figure 15.12 shows deviation from linearity, which is attributed to the formation of intermolecular hydrogen bonding between the CHCl_3 proton and the coumarin carbonyl group (10).

Table 15.7 lists IR group frequency data for coumarin and derivatives in the vapor and solution phases (1,10). Coumarin exhibits $\nu\text{C}=\text{O}$ at 1776 cm^{-1} in the vapor phase, which is higher than it occurs in any of the solvent systems. Substitution of a 3-Cl or 6- CH_3 group apparently does not affect the $\nu\text{C}=\text{O}$ frequency, as $\nu\text{C}=\text{O}$ is observed at 1775 cm^{-1} in both cases (1). On the other hand, there is a noticeable increase in the $\nu\text{C}=\text{O}$ frequency in the case of 3,4-dihydrocoumarin,



6UR-5, 6

In this case, the lactone has 6 UR-5,6 structure, and the C=O bond is not conjugated as it is in the case of coumarin; therefore, $\nu\text{C}=\text{O}$ occurs at a higher frequency (1802 cm^{-1} vs 1776 cm^{-1} in the vapor phase (1)).

In summary, the unperturbed $\nu\text{C}=\text{O}$ frequencies for lactones in CCl_4 solution occur at or in the range:

1748.0-1749.4 cm^{-1} with 6 UR-2,3,4,5 structure

1769.9-1781.4 cm^{-1} with 5 UR-2,3 structure

1789.1-1792.7 cm^{-1} with 5 SR structure

1841.8 cm^{-1} with 4 SR structure

Figure 15.13 shows plots of unperturbed $\nu\text{C}=\text{O}$ for coumarin 1% wt./vol. In various solvents vs the solvent acceptor number (AN). The solvents are numbered sequentially 1–16 as they are listed in Table 15.6. Two linear plots are noted. Solvent 13–16 are for the four alcohols. In this case the OH group is intermolecularly hydrogen bonded with the coumarin carbonyl oxygen atom. Steric factors of solute and solvent cause variations in solute-solvent interaction, plus intermolecular hydrogen bonding prevent the AN values to be a precise predictor of $\nu\text{C}=\text{O}$ values. However, they are useful in predicting approximate $\nu\text{C}=\text{O}$ frequencies in many cases (10).

Table 15.8 lists IR data for 1% wt./vol. phenyl acetate in $\text{CHCl}_3/\text{CCl}_4$ solutions (11). In the case of phenyl acetate, the $\nu\text{C}=\text{O}$ mode is in Fermi resonance with a combination tone (CT). Plots of the uncorrected and corrected $\nu\text{C}=\text{O}$ and CT frequencies are shown in Fig. 15.14. After correction for Fermi resonance, the $\nu\text{C}=\text{O}$ and CT frequencies converge as the mole % $\text{CHCl}_3/\text{CCl}_4$ increases. The $\nu\text{C}=\text{O}$ mode decreases in frequency while the CT increases in frequency. It is apparent from these plots that intermolecularly hydrogen bonding occurs between the CHCl_3 proton and the phenyl acetate carbonyl oxygen atom at low mole % $\text{CHCl}_3/\text{CCl}_4$ concentration. Identical plots are obtained plotting the same IR data for phenyl acetate vs the reaction field (R) [see preceding text]. Therefore, $\nu\text{C}=\text{O}$ is affected by bulk dielectric effects and refractive index of the solvent system as well as intramolecular hydrogen bonding (11).

Table 15.9 lists IR data for phenyl acetate 1% wt./vol. In various solvents, and Fig. 15.15 shows plots of the CT and $\nu\text{C}=\text{O}$ modes in Fermi resonance and the $\nu\text{C}=\text{O}$ and CT modes corrected for FR. vs the solvent acceptor number (AN) (11). The observed uncorrected C=O and CT modes converge for solvents 1–11, 14, and 15 and diverge for solvents 12, 13, 16, 17. After correction for F.R., $\nu\text{C}=\text{O}$ and CT converge for solvents 1–11, 14, 15, cross-over in the case of solvent 12, tert-butyl alcohol, and diverge even more for solvents 13, 16, 17, the other three alcohols in order of increasing acidity of the OH proton. Steric factors of the solvent and solute and intermolecular hydrogen bonding prevent a simple precise correlation to be developed between $\nu\text{C}=\text{O}$ for any given compound in a particular solvent using its AN value (11).

ALKYL BENZOATES

Table 15.10 lists IR data for alkyl benzoates in CS_2 solution between 29 and -10°C (11). In each case, the $\nu\text{C}=\text{O}$ mode(s) decreases in frequency as the temperature is decreased from ambient temperature to 90 or 100°C . Both methyl 2-bromobenzoate and methyl 2-methoxybenzoate exhibit two $\nu\text{C}=\text{O}$ IR bands. In each case, the lower frequency $\nu\text{C}=\text{O}$ mode decreases more in frequency than the higher frequency $\nu\text{C}=\text{O}$ mode. These two $\nu\text{C}=\text{O}$ modes result from the presence of rotational conformers. The higher frequency $\nu\text{C}=\text{O}$ band is assigned to conformer 1 and the lower frequency $\nu\text{C}=\text{O}$ band is assigned to conformer 2. Conformer 1 is assigned to the structure where the Br atom or methoxy oxygen atom is near in space to the carbonyl oxygen atom while conformer 2 is assigned to the structure where the Br atom or methoxy oxygen atom is near in space to the methyl ester oxygen atom. Methyl 2-methoxybenzoate exhibits two linear segments above and below $\sim 50^\circ\text{C}$. The other five plots are all linear (see Fig. 15.16). The break in the plots for methyl 2-methoxybenzoate is attributed to change in the rotational configuration of the 2-methoxy group (rotation of the 2-methoxy group about the aryl-oxygen bond).

Figure 15.17 shows plots of the absorbance ratios $A(\nu\text{C}=\text{O} \text{ conformer 1})/A(\nu\text{C}=\text{O} \text{ conformer 2})$. These plots show that conformer 1 increases and conformer 2 decreases in concentration as the temperature is lowered (11).

SALICYLATES AND 2-HYDROXYACETOPHENONE (A KETONE)

Table 15.11 lists IR data for methyl salicylate, phenyl salicylate, and 2-hydroxyacetophenone in various solvents at 1% wt./vol. The 19 solvents used in study this study are presented 1–19 in descending order (12). Figure 15.18 shows plots of these data vs the solvent acceptor number (AN) for each of the 19 solvents (12). These compounds are intramolecularly hydrogen bonded as shown in this figure. Linear relationships are noted for $\nu\text{C}=\text{O} \cdots \text{HO}$ vs (AN) for each of these compounds in solution with the alkyl alcohols (solvents 14, 17–19). However, a linear relationship is not observed for $\nu\text{C}=\text{O} \cdots \text{HO}$ for vs (AN) for the other 14 solvents. However, there is a general increase in frequency as the (AN) value becomes larger. This behavior is attributed to steric factors of both the solute and solvent, which prevents the AN values from being precise predictors of vibrational frequencies.

Figure 15.19 shows plots of $\nu\text{C}=\text{O} \cdots \text{HO}$ frequencies for 2-hydroxyacetophenone, methyl salicylate, and phenyl salicylate vs the frequency difference between $\nu\text{C}=\text{O} \cdots \text{HO}$ (hexane) and $\nu\text{C}=\text{O} \cdots \text{HO}$ (solvent) for each of the other solvents. These linear plots are due to the mathematical treatment of the data. However, they do show that the number sequence in each of the three plots is not the same, showing that the (AN) values of these solvents are not precise predictors of vibrational frequencies.

It is noted that the $\nu\text{C}=\text{O} \cdots \text{HO}$ frequency for methyl salicylate and phenyl salicylate occur at 1680.4 and 1693.0 cm^{-1} in CS_2 solution, respectively, while $\nu\text{C}=\text{O}$ for methyl benzoate at ambient temperature in CS_2 solution occurs at 1727 cm^{-1} . The 46.6 cm^{-1} decrease in frequency between the $\nu\text{C}=\text{O}$ frequency for methyl benzoate and methyl salicylate is due to more than just

intramolecular hydrogen bonding. The resonance effect of the OH group would weaken the C=O bond, causing a decrease in the frequency. This latter effect may be offset by the field effect between the hydroxyl oxygen atom and the carbonyl oxygen atom. The larger inductive effect of the phenyl group vs the methyl group causes $\nu\text{C}=\text{O}\cdots\text{HO}$ for phenyl salicylate to occur at a higher frequency than $\nu\text{C}=\text{O}\cdots\text{HO}$ for methyl benzoate.

In going from solution in CCl_4 to solution in CHCl_3 the $\nu\text{C}=\text{O}\cdots\text{HO}$ frequency decreases by 4.3 and 4.8 cm^{-1} for methyl salicylate and phenyl salicylate, respectively. In the case of phenyl benzoate, the $\nu\text{C}=\text{O}$ frequency decrease is 9 cm^{-1} in going from solution in CCl_4 to solution in CHCl_3 . In going from solution in CCl_4 to solution in $(\text{CH}_3)_2\text{SO}$, the $\nu\text{C}=\text{O}\cdots\text{OH}$ or $\nu\text{C}=\text{O}$ frequency decrease is 7.2, 6.3, and 10 cm^{-1} for methyl salicylate, phenyl salicylate, and phenyl benzoate, respectively. It is thus readily apparent that the $\nu\text{C}=\text{O}\cdots\text{HO}$ modes are not altered as much in frequency as $\nu\text{C}=\text{O}$ modes in going from solution in CCl_4 to solution in CHCl_3 or $(\text{CH}_3)_2\text{SO}$. This is because the OH proton essentially neutralizes the basicity of the C=O oxygen atom and also acts as a site for $\text{OH}\cdots\text{ClCCl}_3$ or $\text{OH}\cdots\text{ClCHCl}_2$ interaction.

Figure 15.20 shows a plot of $\nu\text{C}=\text{O}\cdots\text{HO}$ for phenyl salicylate vs mole % $\text{CHCl}_3/\text{CCl}_4$ (12). This plot shows essentially three linear segments with breaks at ~ 23 and 69 mol % $\text{CHCl}_3/\text{CCl}_4$. The mole ratio of solvent to solute is 22.1 : 1 in CCl_4 solution and 26.7 : 1 in CHCl_3 solution. The mole ratio CHCl_3 to solute 6.1 : 18.4 at ~ 23 and 69 mol % $\text{CHCl}_3/\text{CCl}_4$, respectively. These data indicate that different complexes are formed between phenyl salicylate and the $\text{CHCl}_3/\text{CCl}_4$ solvent system in the mole % $\text{CHCl}_3/\text{CCl}_4$ ranges 0–23, 23–69 and 69–100.

PHTHALATES

Table 15.12 shows Raman group frequency data for dialkyl phthalates in the neat phase. The relative intensity (RI) values are normalized to the strongest Raman band in the spectrum occurring near 1045 cm^{-1} . The abbreviation denotes depolarization ratio. Figure 15.21 gives bar graphs of the Raman group frequencies for 21 dialkyl phthalates. The upper graph represents both the frequency ranges and intensities for each of the 12 group frequencies. The intensities are proportional to $(45\alpha')^2 + (4\beta')^2$ (α' and β' are the derivative of the mean polarizability and anisotropy, respectively, with respect to the normal coordinate of the polarizability tensor). The horizontal lines across the range of frequencies indicate minimum band intensity relative to the ~ 1045 cm^{-1} group frequency. The lower graph of these Raman group frequencies is proportional to $(3\beta')^2$.

The Raman phthalate $\nu\text{C}=\text{O}$ mode occurs in the range 1728–1738 cm^{-1} , whose relative intensity has a value in the range 40–51. The strongest Raman band occurs in the range 1042–1047 cm^{-1} and is assigned to the ortho phenylene ring breathing mode. It occurs at a slightly higher frequency than the breathing mode of the phenyl group for mono-substituted benzenes. Phthalates show a Raman band in the range 1277–1294 cm^{-1} having a relative intensity value in the range 24–40, and it is polarized. This band is assigned to a complex skeletal mode of the aryl $[-\text{C}(=\text{O})-\text{R}]_2$ groups. The other Raman group frequencies have been correlated with in-plane ring mode of 1,2-dichlorobenzene (13).

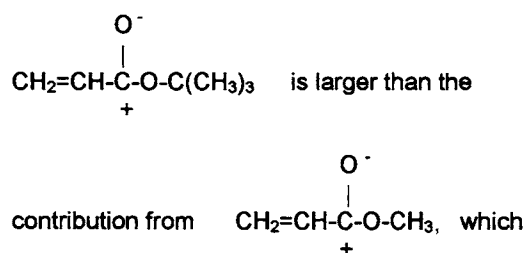
ACRYLATES AND METHACRYLATES

Table 15.13 lists Raman data for the $\nu\text{C}=\text{O}$ and $\nu\text{C}=\text{C}$ stretching vibrations for acrylates (14). The $\nu\text{C}=\text{O}$ mode occurs in the range $1717\text{--}1774\text{ cm}^{-1}$. The alkyl acrylates exhibit $\nu\text{C}=\text{O}$ in range $1717\text{--}1740\text{ cm}^{-1}$ and aryl acrylates exhibit $\nu\text{C}=\text{O}$ in the range $1731\text{--}1774\text{ cm}^{-1}$. Variations in frequency within each class can be attributed to the inductive effect of the alkyl or haloalkyl groups and branching on the $\text{O}-\text{R}\alpha$ -carbon atom.

The *s-trans* $\nu\text{C}=\text{C}$ mode for alkyl and aryl acrylates occurs in the range $1623\text{--}1640\text{ cm}^{-1}$ in the neat phase. The relative Raman band intensity (RI) for *s-trans* $\nu\text{C}=\text{C}$ is higher than it is for *s-cis* $\nu\text{C}=\text{C}$, and *s-cis* $\nu\text{C}=\text{C}$ occurs at lower frequency than *s-trans* $\nu\text{C}=\text{C}$ by $\sim 14\text{--}16\text{ cm}^{-1}$. With the exceptions of hexafluoroisopropyl acrylate, pentabromophenyl acrylate, 1-naphthyl acrylate, and bis-phenol-A diacrylate, the ratio (RI) $\nu\text{C}=\text{O}/(\text{RI})$ *s-trans* $\text{C}=\text{C}$ is in the range 0.25 through 0.83.

Table 15.13a lists IR data for alkyl acrylates in CHCl_3 and/or CCl_4 solutions (1% wt./vol. Of solute). In CCl_4 solution and in CHCl_3 solution, $\nu\text{C}=\text{O}$ occurs in the range $1722.9\text{--}1734.1\text{ cm}^{-1}$ and $1713.8\text{--}1724.5\text{ cm}^{-1}$, respectively (15,16). In CCl_4 solution and in CHCl_3 solution, *s-trans* $\nu\text{C}=\text{C}$ occurs in the range $1635.3\text{--}1637.0\text{ cm}^{-1}$ and $1635.3\text{--}1637.9\text{ cm}^{-1}$ respectively. In CCl_4 solution and in CHCl_3 solution, *s-cis* $\nu\text{C}=\text{C}$ occurs in the range $1619.2\text{--}1620.4\text{ cm}^{-1}$ and $1618.5\text{--}1619.9\text{ cm}^{-1}$, respectively. The $\text{CH}=\text{CH}_2$ twist and $\text{C}=\text{CH}_2$ wag modes occur in the range $982.6\text{--}985.6\text{ cm}^{-1}$ and $966.3\text{--}983.4\text{ cm}^{-1}$, respectively (15).

Figure 15.22 shows plots of $\nu\text{C}=\text{O}$ for seven alkyl acrylates vs mole % $\text{CHCl}_3/\text{CCl}_4$ (1% wt./vol.). The $\nu\text{C}=\text{O}$ mode for all of these acrylates decreases in frequency as the mole % $\text{CHCl}_3/\text{CCl}_4$ is increased. There is a distinct difference between the rate of $\nu\text{C}=\text{O}$ frequency in the $0\text{--}35$ mol % $\text{CHCl}_3/\text{CCl}_4$ range than at higher mole % $\text{CHCl}_3/\text{CCl}_4$. At the lower mole % $\text{CHCl}_3/\text{CCl}_4$ range, the faster rate of $\nu\text{C}=\text{O}$ frequency decrease is attributed to the formation of $\text{C}=\text{O}\cdots\text{HCCl}_3$ bonds, $(\text{Cl}_3\text{CH}\cdots\text{ClCCl}_3)_x$ and $(\text{ClCl}_2\text{CH}\cdots)_n$. The general gradual linear decrease with change in the mole % $\text{CHCl}_3/\text{CCl}_4$ is attributed to an increasing value of the solvent reaction field (R). In the case of *tert*-butyl acrylate vs methyl acrylate the inductive contribution



causes $\nu\text{C}=\text{O}$ mode for the *tert*-butyl analog to occur at lower frequency than for the methyl analog (15).

Table 15.14 shows Raman data for alkyl and aryl methacrylates in the neat phase, and a summary of the IR CCl_4 and CHCl_3 solution data for $\nu\text{C}=\text{O}$ and $\nu\text{C}=\text{C}$ (14). In the neat phase, alkyl methacrylates exhibit Raman bands in the range $1732\text{--}1762\text{ cm}^{-1}$ (the alkyl analogs in the range $1713\text{--}1742\text{ cm}^{-1}$, and the aryl analogs in the range $1735\text{--}1762\text{ cm}^{-1}$). These bands are assigned to the $\nu\text{C}=\text{O}$ mode. In all cases, the Raman band assigned as $\nu\text{C}=\text{C}$ occurs in the range $1635\text{--}1642\text{ cm}^{-1}$, and with the exceptions of 2-phenoxyethyl methacrylate, 2-methyl metha-

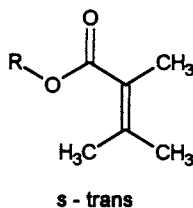
crylate, and pentachlorophenyl methacrylate the Raman band intensity ratio (RI) $\nu\text{C}=\text{O}/(\text{RI})\nu\text{C}=\text{C}$ is always < 1 . In cases where the Raman spectra were recorded of the same alkyl or phenyl acrylates and methacrylates, the $\nu\text{C}=\text{O}$ mode always occurs at lower frequency in the case of the methacrylates than for that of the acrylates. The lower $\nu\text{C}=\text{O}$ mode frequencies in the case of the methacrylate analogs are due to the inductive contribution of the α -methyl group to the $\text{C}=\text{O}$ group. Moreover, with the exception of pentafluorophenyl methacrylate, the $\nu\text{C}=\text{C}$ mode occurs at higher frequency than both *s-trans* $\nu\text{C}=\text{C}$ and *s-cis* $\nu\text{C}=\text{C}$ for corresponding alkyl or aryl acrylates.

Figure 15.23 shows plots of $\nu\text{C}=\text{O}$ for corresponding alkyl acrylate and alkyl methacrylate analogs vs mole % $\text{CHCl}_3/\text{CCl}_4$ (15). The plots for the methacrylate and acrylate analogs appear to be comparable at ~ 40 mol % $\text{CHCl}_3/\text{CCl}_4$ and above, and are different below ~ 40 mol % $\text{CHCl}_3/\text{CCl}_4$. That there are differences between the plots of these acrylate and methacrylate analogs warrants further discussion. In the case of the methacrylates the $\text{C}=\text{O}$ group is more basic than the $\text{C}=\text{O}$ group for the acrylates due to the inductive contribution of the α -methyl carbon atom to the $\text{C}=\text{O}$ bond. Thus, a stronger intermolecular hydrogen bond would be expected to be formed between $\text{C}=\text{O}\cdots\text{HCCl}_3$ for methacrylates than in the case of the corresponding alkyl acrylates. However, it is noted that the $\nu\text{C}=\text{O}$ frequency decrease for the allyl, butyl, and 2-ethylhexyl methacrylates in going from solution in CCl_4 to solution in CHCl_3 is 8.63, 9.43, and 9.99 cm^{-1} , respectively, while for the corresponding acrylate analogs the $\nu\text{C}=\text{O}$ frequency decrease is 9.43, 10.58, and 10.82 cm^{-1} , respectively. In both cases, the $\nu\text{C}=\text{O}$ frequency decreases in the order of increasing inductive contribution of the $\text{O}-\text{R}$ alkyl group to the $\text{C}=\text{O}$ group. However, the decrease in the $\nu\text{C}=\text{O}$ frequency is larger in each case of the acrylates than in the case of the methacrylates. Thus, the $\text{C}=\text{O}\cdots\text{HCCl}_3$ intermolecular hydrogen bond appears to be stronger in the case of alkyl acrylates than for alkyl methacrylates. However, the contribution of hydrogen bonding of the CHCl_3 proton to $\text{C}=\text{O}$ group ($\text{C}=\text{O}\cdots\text{HCCl}_3$) can not be separated from the contribution of the reaction field (R) for acrylates and methacrylates in $\text{CHCl}_3/\text{CCl}_4$ solution merely by subtracting the $\nu\text{C}=\text{O}$ frequencies in CCl_4 solution from those in CHCl_3 solution. As the reaction field (R) is a linear function of mole % $\text{CHCl}_3/\text{CCl}_4$ it is reasonable to extrapolate the linear portion of each plot to 0 mol % $\text{CHCl}_3/\text{CCl}_4$ to obtain the $\Delta\nu\text{C}=\text{O}$ frequency decrease attributed to the $\text{C}=\text{O}\cdots\text{HCCl}_3$ intermolecular hydrogen bond. This $\Delta\nu\text{C}=\text{O}$ frequency decrease divided by the total $\nu\text{C}=\text{O}$ frequency decrease between $\nu\text{C}=\text{O}(\text{CCl}_4)$ minus $\nu\text{C}=\text{O}(\text{CHCl}_3)$ multiplied by 100 yields the percentage of the $\nu\text{C}=\text{O}$ frequency decrease attributed to the intermolecular hydrogen bond. The results are as follows:

	acrylate	methacrylate
allyl	37.4%	45.1%
butyl	42.2%	49.4%
2-ethylhexyl	47.8%	54.6%

These calculations indicate that the percentage of $\nu\text{C}=\text{O}$ frequency decrease is larger in the case of the alkyl methacrylates than in the case of the alkyl acrylates. Thus, the reaction field (R) contributes more to the $\nu\text{C}=\text{O}$ frequency decrease in the case of alkyl acrylate than for alkyl

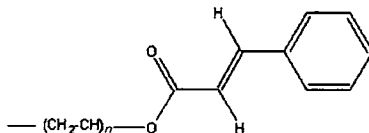
methacrylates. The most reasonable explanation for the preceding data is that the alkyl methacrylate exist in the *s-trans* configuration. By analogy



with the alkyl α -methyl branched acetates discussed previously, the α -methyl group in alkyl methacrylates would affect the spatial distance between the carbonyl carbon atom and the solvent system ($\text{CHCl}_3/\text{CCl}_4$). Thus, the reaction field would be less in the case of alkyl methacrylates in the *s-trans* configuration than for the alkyl acrylates in either the *s-cis* or *s-trans* configurations. The methacrylate $\text{C}=\text{O}$ group is more basic than the acrylate $\text{C}=\text{O}$ group, and apparently a stronger $\text{C}=\text{O} \cdots \text{HCCl}_3$ bond is formed in the case of the methacrylates even though the spatial distance between the carbonyl oxygen atom and the CHCl_3 proton is greater in the case of alkyl methacrylates.

CINNAMATES

Poly (vinyl cinnamate) has the following empirical structure:



The Raman spectrum for poly (vinyl cinnamate) exhibits bands at 1701 and 1638 cm^{-1} whose relative band intensity ratio (RI) is 1:9 and these bands are assigned to $\nu\text{C}=\text{O}$ and $\nu\text{C}=\text{C}$, respectively. Phenyl in-plane ring modes are assigned at 1601 , 1030 , 1002 , and 620 cm^{-1} whose (RI) ratios are 6:9, 1:9, 4:9, and 1:9, respectively. In most cases the phenyl breathing mode for monosubstituted benzenes has the highest Raman band intensity. In this case it occurs at 1002 cm^{-1} with an (RI) of 4 compared to an (RI) of 9 for $\nu\text{C}=\text{C}$. Thus, the Raman band intensity of $\nu\text{C}=\text{C}$ for this polymer is very strong. The Raman bands for other alkyl cinnamates are expected to occur at similar frequencies.

Table 15.15 lists IR vapor-phase data and assignments for alkyl cinnamates (1). In the vapor phase the alkyl cinnamates exhibit $\nu\text{C}=\text{O}$ in the range 1727 – 1740 cm^{-1} . The highest and lowest $\nu\text{C}=\text{O}$ frequencies are exhibited by the methyl and tert-butyl cinnamates, respectively. Again the $\nu\text{C}=\text{O}$ frequencies decrease in the order of the increasing inductive contribution of the O–R alkyl group to the $\text{C}=\text{O}$ bond. The $\nu\text{C}=\text{C}$ mode occurs in the range 1649 – 1642 cm^{-1} . The IR band intensity ratio $(A)\nu\text{C}=\text{C}/(A)\nu\text{C}=\text{O}$ varies between 0.33 and 0.41.

As noted in the empirical structure for poly (vinyl cinnamate), the $\text{CH}=\text{CH}$ is presented in the *trans* configuration. In the IR, the band in the range 972 – 980 cm^{-1} results from the *trans*

CH=CH twisting vibration, and confirms the trans configuration for the C=C bond. The IR band intensity ratio (A) CH=CH twist/(A) ν C=C varies between 0.42 and 0.67.

Table 15.15a lists IR vapor-phase data for alkyl cinnamates (1). In-plane phenyl ring modes are presented in columns [1] through [3] and these group frequencies occur in the ranges 1304–1314, 1245–1276 cm^{-1} , and 1198–1200 cm^{-1} , respectively. The phenyl ring in-phase out-of-plane 5-hydrogen deformation and the out-of-plane phenyl ring deformation occur in the range 750–765 and 685–696 cm^{-1} , respectively.

With the exception of the isopropyl analog, the strongest IR band for the alkyl cinnamates occurs in the range 1154–1171 cm^{-1} , it is attributed to a C–C(=O) stretching mode, and its intensity is used to normalize the 3 in-plane ring modes.

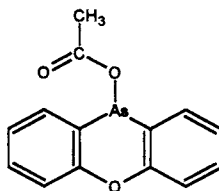
The ratio (A)[6]/(A)[7] is larger for the alkyl cinnamates than for benzyl cinnamate by a factor of 2 or more. The reason for this is that the comparable modes for the benzyl group are also absorbing at these frequencies. The ratio (A) ν C=C/(A) [4] shows that the ν C=C mode has much less IR absorbance than the absorbance for ν C–C(=O).

Table 15.15b lists IR data for the alkyl and phenyl groups of cinnamates.

The first overtone, 2ν C=O, occurs in the range 3435–3470 cm^{-1} . Phenyl ring carbon-hydrogen stretching modes occur in the ranges 3065–3075 cm^{-1} and 3030–3040 cm^{-1} . The *vasym.* CH₃ and *vsym.* CH₃ modes occur in the range 2961–2985 cm^{-1} and 2850–2945 cm^{-1} , respectively. The *vasym.* CH₂ and *vsym.* CH₂ modes occur in the range 2942–2960 cm^{-1} and 2868–2895 cm^{-1} , respectively. The *δasym.* CH₃ and *δsym.* CH₃ modes occur in the range 1452–1475 cm^{-1} and 1371–1400 cm^{-1} , respectively. An in-plane ring mode and/or δ CH₂ occur in the range 1450–1453 cm^{-1} .

PHENOXARSINE DERIVATIVES

The compound 10-phenoxarsinyl acetate has the following empirical structure:



IR data for the 10-phenoxarsinyl esters are listed in Table 15.16. In this series 10-phenoxarsinyl acetate, the trichloroacetate, and the trifluoroacetate derivatives, the ν C=O occurs at 1698, 1725, and 1738 cm^{-1} in CCl₄ solution, respectively, and this increase in the ν C=O frequency is attributed to the inductive and field effects of the halogen atoms upon the C=O group (17). In CCl₄ solution, these ν C=O frequencies occur $\sim 50 \text{ cm}^{-1}$ lower in frequency than ν C=O occurs for the corresponding ethyl acetates. This frequency difference can be attributed to the fact that arsenic is less electronegative than oxygen, which would induce some ionic character to the functional group [e.g., R–C(=O)O[−]–As⁺]. This effect would reduce the C=O force constant because the C=O bond would contain less double character due to an increase of π overlap with the free pair of electrons on the O–As oxygen atom (17).

Figure 15.24 show IR spectra of 10-phenoxarsinyl chloroacetate in (A) CCl_4 ($3800\text{--}1333\text{ cm}^{-1}$) and CS_2 ($1333\text{--}450\text{ cm}^{-1}$) solutions and (B) as a split mull (Fluorolube $3800\text{--}1333\text{ cm}^{-1}$ and Nujol, $1333\text{--}450\text{ cm}^{-1}$). In CCl_4 solution, $\nu\text{C}=\text{O}$ bands are noted at 1720 and 1696 cm^{-1} while in the Fluorolube mull $\nu\text{C}=\text{O}$ is noted at 1702 cm^{-1} . This occurs because in solution the chloroacetate derivative exists as rotational conformers while in the solid phase only one rotational conformer exists. The 1720 cm^{-1} rotational conformer in CCl_4 solution and the 1702 cm^{-1} band in the solid phase are assigned to the rotational conformer where the Cl atom is near in space to the carbonyl oxygen atom while the 1696 cm^{-1} CCl_4 solution band is assigned to the rotational conformer where the Cl atom is near in space to the O–As oxygen atom.

The 10-phenoxarsinyl thiol esters of form As-S-C(=O)R exhibit $\nu\text{C}=\text{O}$ in the range $1670\text{--}1681\text{ cm}^{-1}$. Comparison of the As-S-C(=O)CH_3 vs the $\text{AsO-C(=O)(CH}_3)_3$ (1681 cm^{-1} vs 1698 cm^{-1}) shows that there is a frequency decrease of $\sim 17\text{ cm}^{-1}$ with the substitution of sulfur for oxygen; the reason for this is presented in a discussion on ordinary thiol esters [R-C(=O)-S-R'] that will follow.

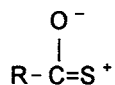
The S-(10-phenoxarsinyl) thiol aryl esters of form $\text{As-S-C(=O)C}_6\text{H}_5$ exhibit $\nu\text{C}=\text{O}$ in the range $1638\text{--}1650\text{ cm}^{-1}$, and the decrease in the $\nu\text{C}=\text{O}$ frequency compared to As-S-C(=O)R analogs is attributed to conjugation of the phenyl ring with the $\text{C}=\text{O}$ group (17).

Compounds such as S-(10-phenoxarsinyl) α -(2,4,5-trichlorophenoxy) thiol acetate exhibit rotational conformer 1 at 1691 cm^{-1} and rotational conformer 2 at 1665 cm^{-1} in CCl_4 solution. In the solid phase, the $\nu\text{C}=\text{O}$ band at 1650 cm^{-1} is assigned to the more stable structure conformer 2. Rotational conformer 1 is where the phenoxy oxygen atom is near in space to the carbonyl oxygen atom and rotational conformer 2 is where the phenoxy oxygen atom is near in space to the As–S sulfur atom.

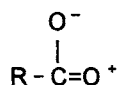
The compound, S-(10-phenoxarsinyl)-thiol-2-furoate exhibits rotational conformer 1 at 1646 cm^{-1} and rotational conformer 2 at 1631 cm^{-1} in CCl_4 solution, and the more stable conformer 1 at 1630 cm^{-1} in the solid state. Rotational conformer 1 is where the furan ring oxygen atom is near in space to the carbonyl oxygen atom while rotational conformer 2 is where the furan ring oxygen atom is near in space to As-S sulfur atom.

THIOL ESTERS

Thiol esters of form R-C(=O)-S-R' exhibit $\nu\text{C}=\text{O}$ near 1690 cm^{-1} while esters of form R-C(=O)-O-R' exhibit $\nu\text{C}=\text{O}$ at $\sim 1735 \pm 5\text{ cm}^{-1}$ (18). The reason substitution of sulfur for oxygen causes $\nu\text{C}=\text{O}$ to vibrate at a lower frequency needs to be addressed. This change in the $\nu\text{C}=\text{O}$ frequency is attributed principally to the change in the $\text{C}=\text{O}$ force constants. The resonance form



for thiol esters is more important than resonance form



for ordinary esters. In terms of electronic theory, there appears to be a greater tendency toward overlap of the carbonyl carbon atom π -electron with a nonbonding electron pair of the sulfur atom than with a nonbonding of the oxygen atom. This weakens the C=O bond, and causes $\nu\text{C}=\text{O}$ to vibrate at a lower frequency than in the case of comparable ordinary esters (18). Otherwise, as will be discussed, the $\nu\text{C}=\text{O}$ frequencies for thiol esters are affected by resonance, inductive, field, and hydrogen bonding.

Table 15.17 lists IR data for alkyl and phenyl thiol esters (18). The frequencies reported in the region $3800\text{--}1333\text{ cm}^{-1}$ are for CCl_4 solution, and in the region of 1333 cm^{-1} and below they are CS_2 solution data. In all cases, the thiol esters of form $\text{R}-\text{C}(=\text{O})-\text{S}-\text{C}_6\text{H}_5$ exhibit higher $\nu\text{C}=\text{O}$ frequencies than those for the corresponding $\text{R}-\text{C}(=\text{O})-\text{S}-\text{C}_4\text{H}_9$ or $\text{R}-\text{C}(=\text{O})-\text{S}-\text{C}_6\text{H}_{13}$ analogs. This occurs because the inductive effect of the phenyl ring is larger than that for the $\text{S}-\text{R}$ alkyl group.

The inductive and field effects of halogen atoms on the α -carbon of thiol ester also increase the $\nu\text{C}=\text{O}$ frequencies for compounds of forms: $\text{CHCH}_3\text{C}(=\text{O})-\text{S}-\text{C}_4\text{H}_9$ (1695 cm^{-1}) $\text{Cl}_3\text{C}(=\text{O})-\text{S}-\text{C}_4\text{H}_9$ (1699 cm^{-1}), and $\text{Cl}_3\text{C}(=\text{O})-\text{S}-\text{C}_4\text{H}_9$ (1710 cm^{-1}), and for $\text{CH}_3\text{C}(=\text{O})-\text{S}-\text{C}_6\text{H}_5$ (1711 cm^{-1}), $\text{CCl}_3\text{C}(=\text{O})-\text{S}-\text{C}_6\text{H}_5$ (1711 cm^{-1}), and $\text{CF}_3\text{C}(=\text{O})-\text{S}-\text{C}_6\text{H}_5$ (1722 cm^{-1}).

In the case of the mono- and dichloro thiol acetates in CCl_4 solution, both the $\text{S}-\text{R}$ and $\text{S}-\text{C}_6\text{H}_5$ analogs exhibit rotational conformers (see Table 15.17a). The higher frequency $\nu\text{C}=\text{O}$ band for the $\text{ClCH}_2-\text{C}(=\text{O})-\text{S}-\text{R}$ or $-\text{S}-\text{C}_6\text{H}_5$ and $\text{Cl}_2\text{CH}-\text{C}(=\text{O})-\text{S}-\text{R}$ or $-\text{S}-\text{C}_6\text{H}_5$ analogs results from the rotational conformer 1 where the Cl atom (s) is (are) near in space to the carbonyl oxygen atom. The lower frequency $\nu\text{C}=\text{O}$ band is assigned to rotational conformer 2. In this case the Cl atom (s) is (are) near in space to $\text{S}-\text{R}$ or $\text{S}-\text{C}_6\text{H}_5$ sulfur atom (18).

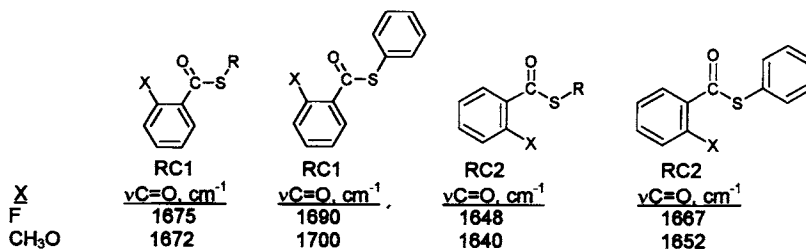
Thiol esters of oxalic ester have two C=O groups $[\text{R}-\text{S}-\text{C}(=\text{O})-]_2$ and $[\text{C}_6\text{H}_5-\text{S}-\text{C}(=\text{O})-]_2$; however, in each case only one $\nu\text{C}=\text{O}$ band is observed (at 1680 and 1698 cm^{-1} for the $\text{S}-\text{C}_4\text{H}_9$ and $\text{S}-\text{C}_6\text{H}_5$ analogs, respectively). Thus, these S, S'-dialkyl or S, S'-diphenyl dithiol oxalates exist in a trans configuration where the molecular structure has a center of symmetry lying between the $\text{O}=\text{C}-\text{C}=\text{O}$ groups. Only the out-of-phase $(\text{C}=\text{O})_2$ stretching mode is IR active; the in-phase $(\text{C}=\text{O})_2$ stretching mode is Raman active.

The S-butyl thiol formate and S-phenyl thiol formate exhibit $\nu\text{C}=\text{O}$ at 1675 and 1693 cm^{-1} , respectively. These compounds are readily identified by the formate $\nu\text{C}-\text{H}$ and $2\delta\text{CH}$ frequencies, which occur in the region $2825\text{--}2835\text{ cm}^{-1}$ and $2660\text{--}2680\text{ cm}^{-1}$, respectively. The δCH mode occurs in the range $1340\text{--}1345\text{ cm}^{-1}$. In all cases these three C-H modes for the $\text{S}-\text{C}_6\text{H}_5$ analog occur at lower frequency than for the $-\text{S}-\text{C}_4\text{H}_9$ analog. Thus, the C-H bond is stronger for $\text{H}-\text{C}(=\text{O})\text{S}-\text{R}$ than for $\text{H}-\text{C}(=\text{O})\text{S}-\text{C}_6\text{H}_5$.

Thiol esters of form $\text{C}_6\text{H}_5-\text{C}(=\text{O})-\text{S}-\text{C}_6\text{H}_5$ exhibit $\nu\text{C}=\text{O}$ at higher frequency than the correspondingly ring-substituted thiol benzoates of form $\text{C}_6\text{H}_5-\text{C}(=\text{O})-\text{S}-\text{R}$ (see Table 15.17b). This is attributed to the inductive effect of the $\text{S}-\text{C}_6\text{H}_5$ being larger than the $\text{S}-\text{R}$ group.

Both the $\text{S}-\text{R}$ and $\text{S}-\text{C}_6\text{H}_5$ analogs of 2-fluoro-thiol benzoate and 2-methoxy thiol benzoate exist as rotational isomers in CCl_4 solution. The higher frequency band in each set is assigned to

rotational conformer 1, the lower frequency band in each set is assigned rotational conformer 2. In these two cases, rotational isomers are presented here:



The phenyl 2-Cl, 2-Br, and 2-I thiol benzoates exhibit $\nu_{C=O}$ at 1696, 1700, and 1698 cm^{-1} in CS_2 solution, respectively. In these cases, all exist as conformer 1, as the $C=O$ group can not be coplanar with the phenyl group due to the bulky S atom of the $S-R$ or $S-C_6H_5$ group.

Phenyl thiol salicylate exhibits $\nu_{C=O} \cdots HO$ at 1640 cm^{-1} , and this relatively low frequency is mainly the result of the intramolecular hydrogen bond between the 2-OH proton and the free pair of electrons on the carbonyl oxygen atom (18).

THIOL ACIDS

Table 15.17c lists IR data for thiol acids, thiol anhydrides, and potassium thiol benzoate (18). Thiol acids exist as $R-C(=O)-SH$ and $C_6H_5-C(=O)-S-H$, and this is in marked contrast to carboxyl acids ($R-CO_2H$ and $C_6H_5CO_2H$), which exist as cyclic intermolecularly hydrogen-bonded dimers in the condensed phase (see Chapter 10).

Thiol acetic acid exhibits $\nu_{C=O}$ and ν_{S-H} at 1712 and 2565 cm^{-1} in CCl_4 solution, respectively, and thiol benzoic acid exhibits $\nu_{C=O}$ and ν_{S-H} at 1690 and 2585 cm^{-1} in CCl_4 solution, respectively. Conjugation lowers the $\nu_{C=O}$ frequency as shown for thiol benzoic acid vs thiol acetic acid. The $S-H$ proton for thiol acetic acid is more acidic than that for thiol benzoic acid, and consequently its ν_{S-H} frequency occurs at lower frequency than it does for thiol benzoic acid. In CCl_4 solution, there is most likely intermolecular hydrogen bonding between the $S-H$ proton and CCl_4 (e.g., $SH \cdots ClCCl_3$).

THIOL ACID ANHYDRIDES

Thiol benzoic anhydride or (dibenzoyl sulfide) exhibits IR bands at 1739, 1709, and 1680 cm^{-1} , and only two $\nu_{C=O}$ modes are expected. An IR band assigned as $=C-S$ stretching occurs at 860 cm^{-1} , and its first overtone would be expected at below 1720 cm^{-1} . Most likely, the third IR band in this region of the spectrum results from Fermi resonance of $2\nu_{C-S}$ with ν in-phase $(C=O)_2$ stretching (1680 cm^{-1}). The higher frequency IR band most likely results from the ν out-of-phase $(C=O)_2$ mode (see Fig. 15.25, which compares the IR spectra of thiol benzoic anhydride (dibenzoyl sulfide) and benzoic anhydride (dibenzoyl oxide)).

Potassium thiol benzoate exhibits *vasym.* COS at 1525 cm^{-1} and its $\nu\text{C-S}$ mode at 948 cm^{-1} (18).

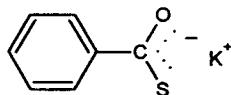


Table 15.18 lists Raman data and probable assignments for propargyl acrylate and propargyl methacrylate. As noted in Table 15.18, $\nu\text{C}\equiv\text{C}$ exhibits the most intense Raman band at 2132 cm^{-1} for both acrylate and methacrylate. The next most intense Raman band is assigned to $\nu\text{C}=\text{C}$ and it is less intense than $\nu\text{C}\equiv\text{C}$ by a factor of 7/9 and 5/9 for the acrylate and methacrylate, respectively. The $\nu\text{C}=\text{O}$ modes occur at 1728 and 1724 cm^{-1} for the acrylate and methacrylate, respectively. The lower $\nu\text{C}=\text{O}$ frequency for the methacrylate is attributed to the inductive contribution of the α -methyl group, which weakens the $\text{C}=\text{O}$ bond. Apparently this causes the depolarization of the electron cloud to be larger in the case of methacrylates compared to the acrylates, since the relative Raman band intensity is 3 for the methacrylate and only 2 for the acrylate.

OTHER ESTER VIBRATIONS

Table 15.19 lists IR vapor-phase data for carboxylic acid esters (1).

Alkyl alkanoates and dialkyl diesters exhibit a strong IR band in the range $1110\text{--}1250\text{ cm}^{-1}$, which results from a complex mode involving $\text{R}-\text{C}(=\text{O})-\text{OR}'$ stretching. In the case of alkyl formate, $\text{H}-\text{C}(=\text{O})-\text{OR}'$, the mode most likely includes $=\text{C}-\text{O}$ stretching, and it occurs in the range $1152\text{--}1180\text{ cm}^{-1}$. In the case of alkyl acetates, the mode occurs in the range $1231\text{--}1250\text{ cm}^{-1}$ for compounds of form $\text{CH}_3-\text{C}(=\text{O})-\text{OR}'$, and in the range $1201\text{--}1215\text{ cm}^{-1}$ when R' is vinyl, isopropenyl, or phenyl. These data suggest that the stretching mode is complex and involves $\text{CH}_3-\text{C}(=\text{O})-\text{OR}'$ skeletal stretching.

Study of α -substitution on the alkyl acetate series shows that the skeletal $\text{C}-\text{C}(=\text{O})-\text{O}-\text{R}'$ stretching mode decreases as the 2-alkyl group increases in length from 2-methyl through 2-butyl. Moreover, the skeletal $\text{C}-\text{C}(=\text{O})-\text{OR}'$ stretching mode decrease steadily in frequency as the substitution of α -methyl groups increases (e.g. $(\text{CH}_3)_2\text{CH}-\text{C}(=\text{O})-\text{OR}'$, $1145\text{--}1159\text{ cm}^{-1}$ and $(\text{CH}_3)_3\text{C}-\text{C}(=\text{O})-\text{OR}'$, $1110\text{--}1156\text{ cm}^{-1}$). These data support the conclusion that the $\text{C}-\text{C}(=\text{O})-\text{OR}'$ mode includes stretching of the $\text{C}-\text{C}(=\text{O})-\text{OR}'$, $(\text{C}-)_2\text{C}(=\text{O})-\text{R}'$, or $(\text{C}-)_3\text{C}(=\text{O})-\text{OR}'$ groups.

Table 15.20 lists IR vapor-phase data for conjugated esters (1). The alkyl aromatic esters skeletal $\text{aryl}-\text{C}(=\text{O})-\text{OR}'$ stretching modes in the range $1229\text{--}1311\text{ cm}^{-1}$ (strong) and in the range $1082\text{--}1145\text{ cm}^{-1}$ (medium). The alkyl crotonates exhibit skeletal $\text{C}=\text{C}-\text{C}(=\text{O})-\text{OR}'$ stretching modes in the range $1176\text{--}1190\text{ cm}^{-1}$ (strong) and $1021\text{--}1048\text{ cm}^{-1}$ (medium).

All esters show strong or medium IR bands in these general regions of the vibrational spectrum. It is always helpful to have a collection of IR and/or Raman standard reference spectra available for comparison and positive identification. The most comprehensive sets of IR and Raman spectra for all types of organic materials are available from Sadtler Research Laboratories, a Division of Bio-Rad Laboratories, Inc.

REFERENCES

1. Nyquist, R. A. (1984). *The Interpretation of Vapor-Phase Infrared Spectra: Group Frequency Data*, Philadelphia: Sadtler Research Laboratories, Division of Bio-Rad.
2. Nyquist, R. A. (1994). *Vib. Spectrosc.*, **7**, 1.
3. Buckingham, A. D. (1960). *Can J. Chem.*, **308**, 300.
4. Timmermans, J. (1959). *Physical-Chemical Constants of Binary Systems*, Vol. 1, pp. 308, 309, New York: Interscience Publishers.
5. Nyquist, R. A. (1991). *Vib. Spectrosc.*, **2**, 221.
6. Gutman, V. (1978). *The Donor-acceptor Approach to Molecular Interactions*, New York: Plenum.
7. Nyquist, R. A. (1986). *Appl. Spectrosc.*, **40**, 336.
8. Nyquist, R. A. (1986). *Appl. Spectrosc.*, **40**, 79.
9. Nyquist, R. A., Fouchea, H. A., Hoffman, G. A., and Hasha, D. L. (1991). *Appl. Spectrosc.*, **45**, 860.
10. Nyquist, R. A. and Settineri, S. E. (1990). *Appl. Spectrosc.*, **44**, 791.
11. Nyquist, R. A. and Settineri, S. E. (1990). *Appl. Spectrosc.*, **44**, 1629.
12. Nyquist, R. A., Putzig, C. L., Clark, T. L., and McDonald, A. T. (1996). *Vib. Spectrosc.*, **12**, 93.
13. Nyquist, R. A. (1972). *Appl. Spectrosc.*, **26**, 81.
14. (1996). *View Master-Raman Basic Monomers and Polymers*, Philadelphia: Sadtler Research Laboratories, A Division of Bio-Rad.
15. Nyquist, R. A. and Streck, R. (1994). *Vib. Spectrosc.*, **8**, 71.
16. Nyquist, R. A. and Streck, R. (1995). *Spectrochim. Acta*, **51A**, 475.
17. Nyquist, R. A., Sloane, H. J., Dunbar, J. E., and Strycker, S. J. (1966). *Appl. Spectrosc.*, **20**, 90.
18. Nyquist, R. A. and Potts, W. J. Jr. (1959). *Spectrochim. Acta*, **15**, 514.

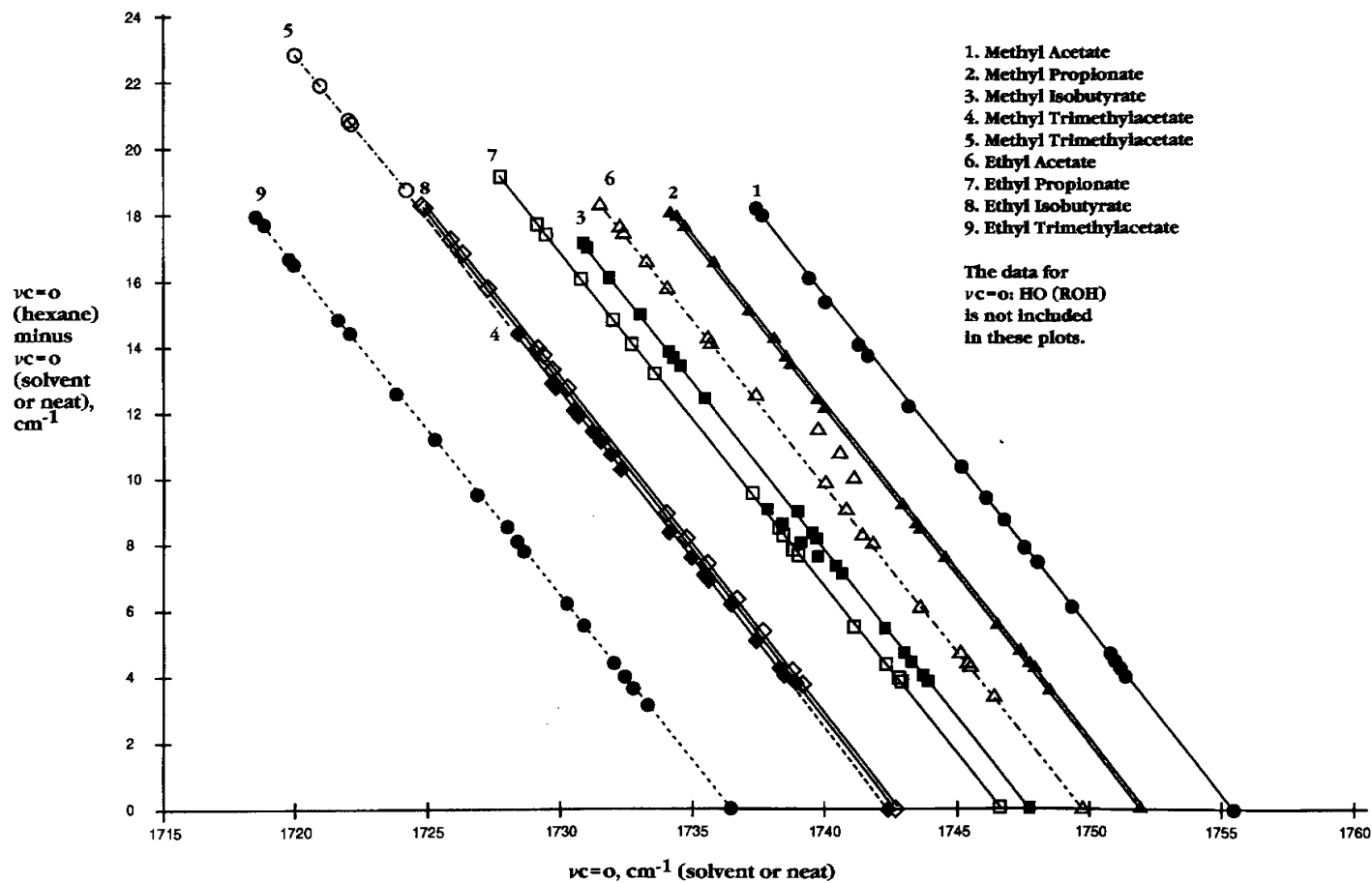
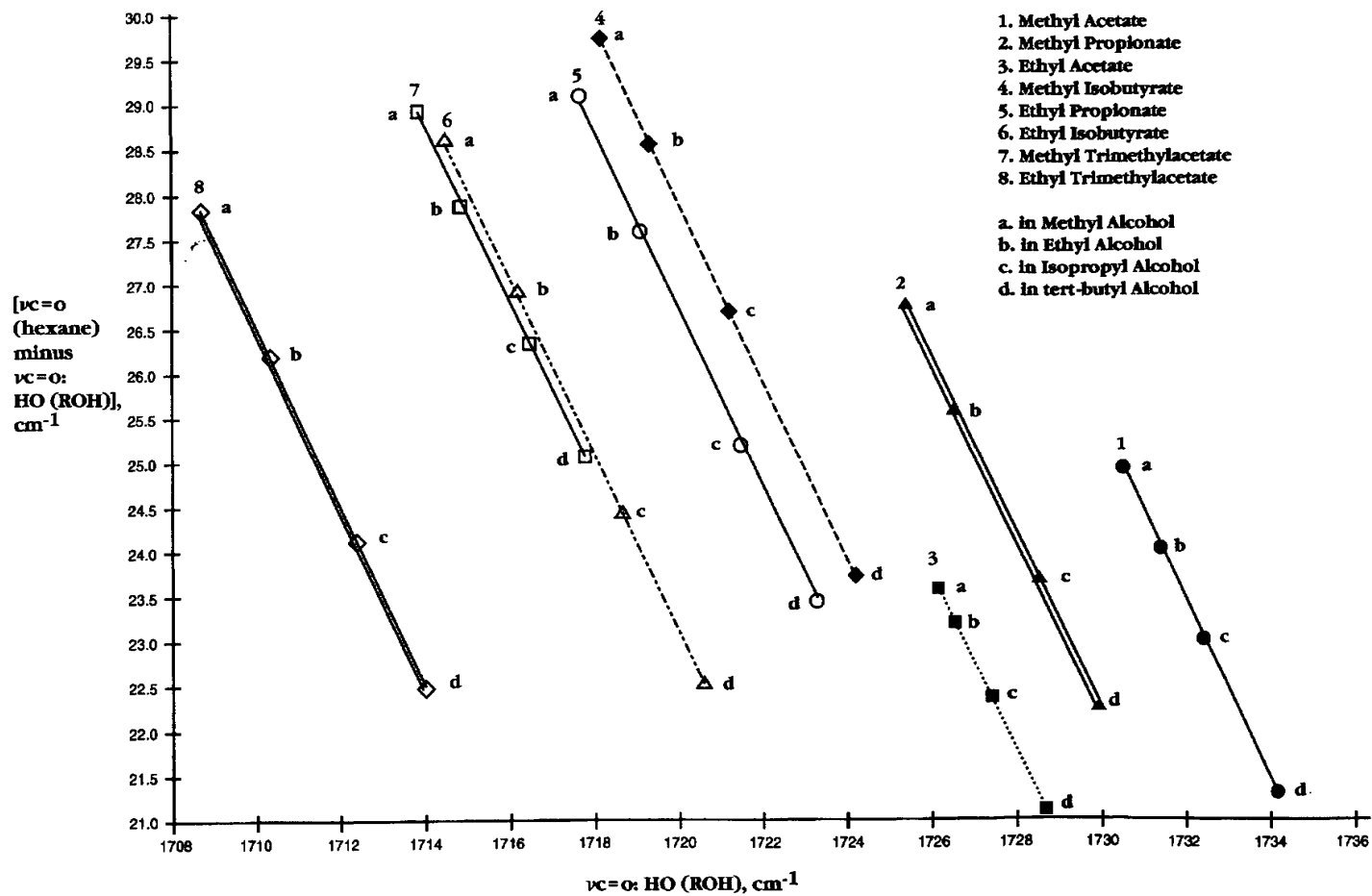


FIGURE 15.1 Plots of ν_{CO} (solvent or neat) vs ν_{CO} (hexane) minus ν_{CO} (solvent or neat) for alkyl alkanoate.

FIGURE 15.2 Plots of $\nu_{CO} \dots HO(ROH)$ vs $\nu_{C=O}$ (hexane) minus $\nu_{CO} \dots HO(ROH)$ for alkyl alkanooates.

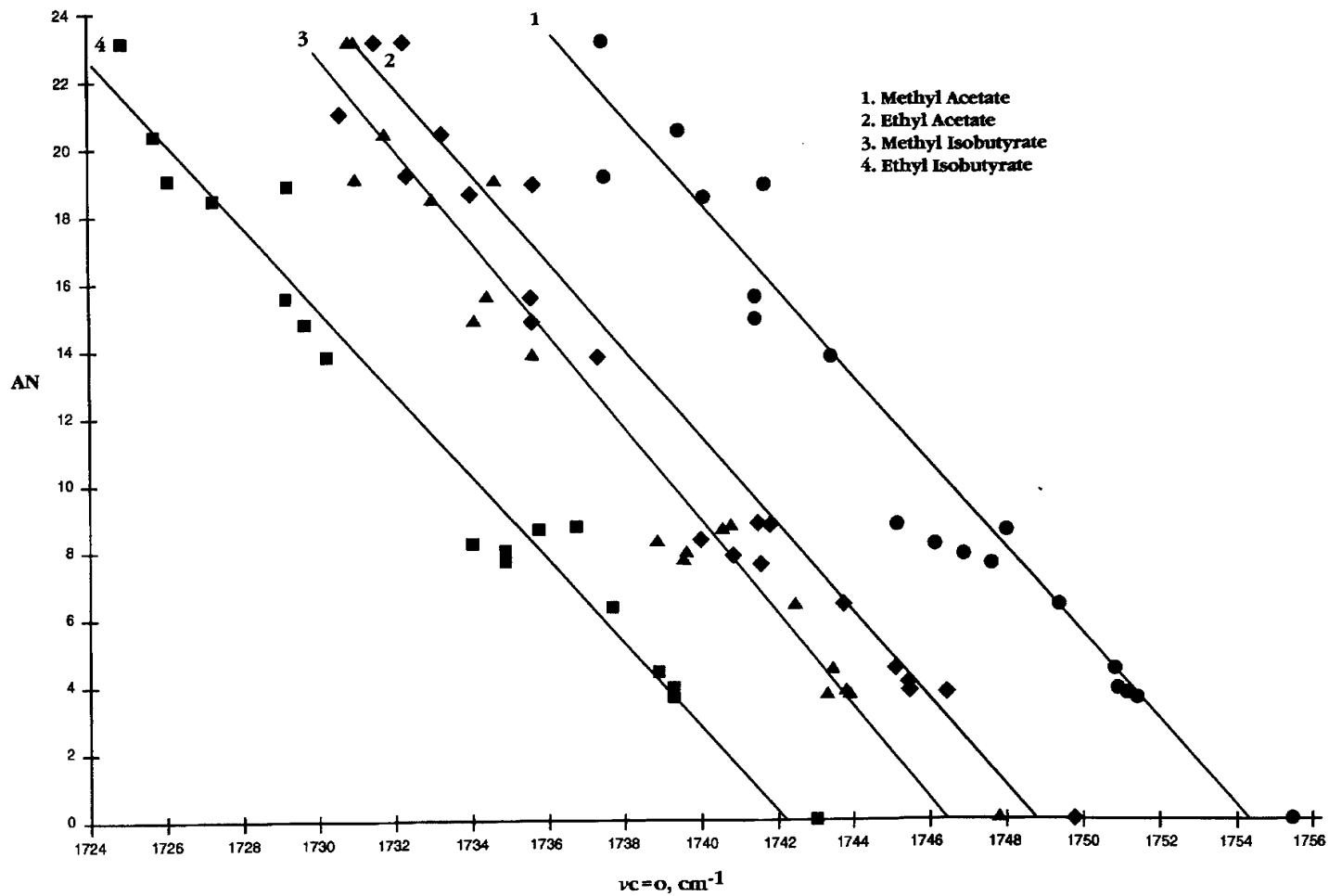
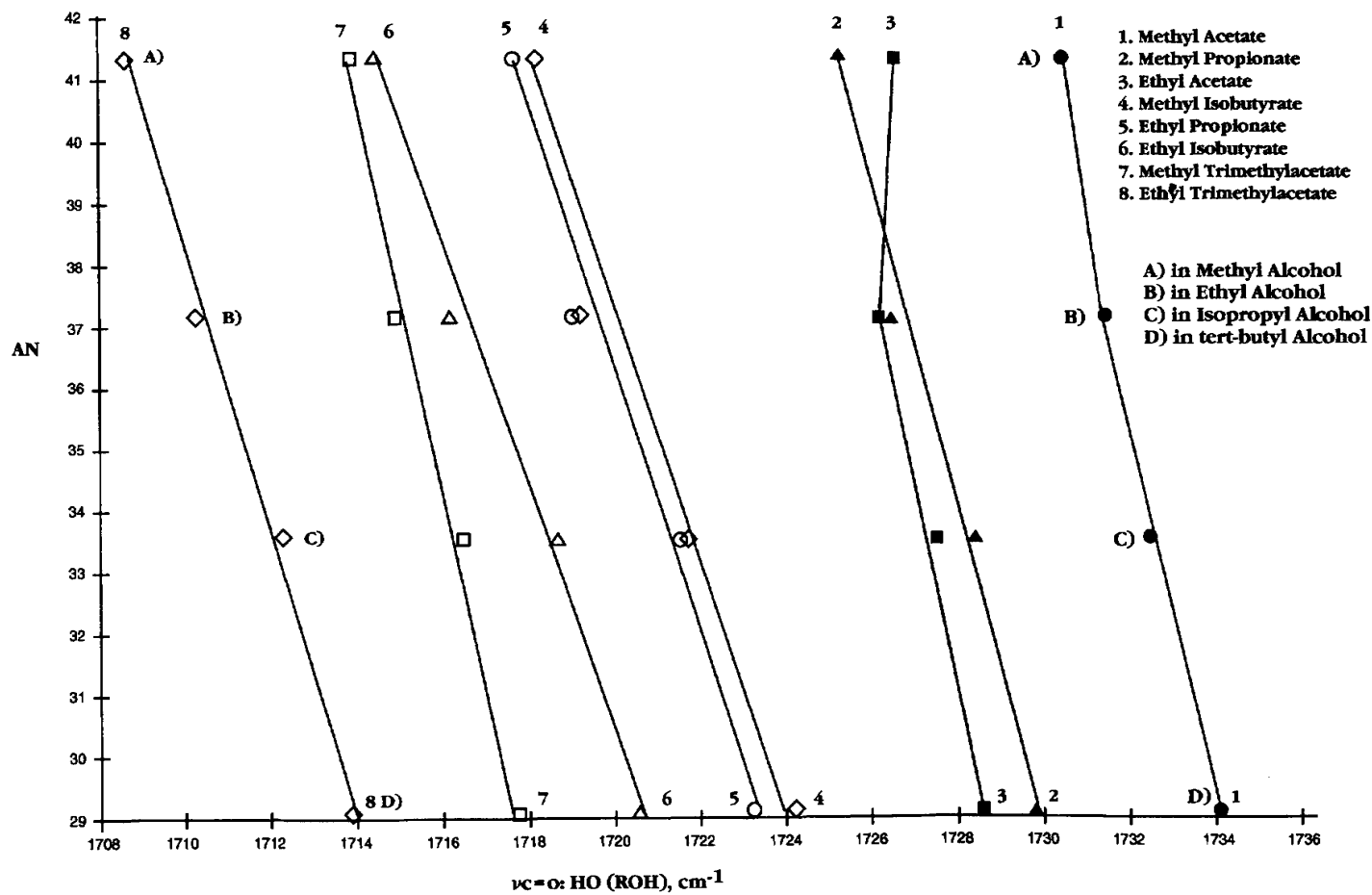


FIGURE 15.3 Plots of ν_{CO} for alkyl alkanoates vs the solvent acceptor number (AN) or neat alkyl alkanoate.

FIGURE 15.4 Plots of $\nu_{\text{CO}\cdots\text{HO(ROH)}}$ vs the solvent acceptor number (AN) in alkyl alcohols.

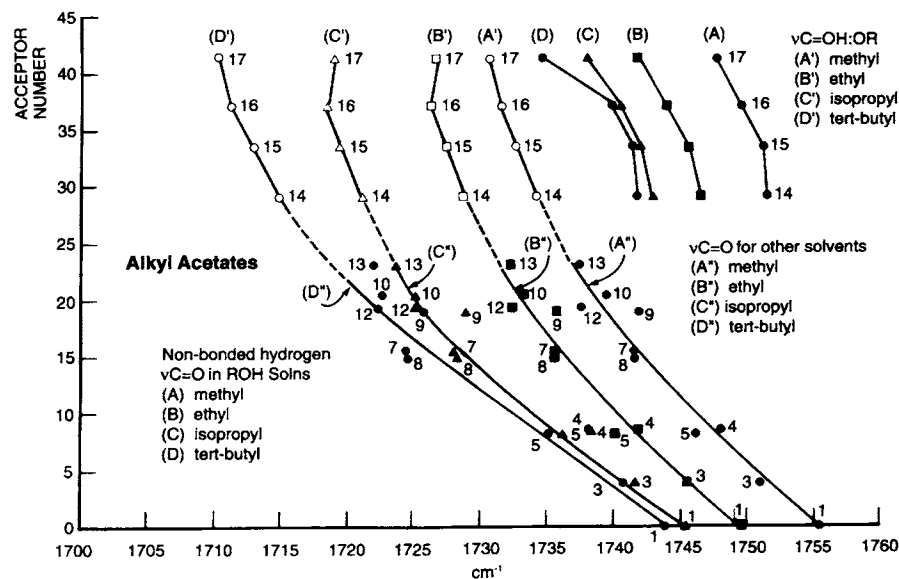


FIGURE 15.5 Plots of the ν_{CO} and $\nu_{\text{CO}} \cdots \text{HO(ROH)}$ frequencies vs. the solvent acceptor number (AN). Extrapolation of the points on curve A to A, curve B to B, curve C to C, and curve D to D yields the postulated AN values of 9.15, 4.15, 3.00, and 2.06 for methyl alcohol through tert-butyl alcohol, respectively.

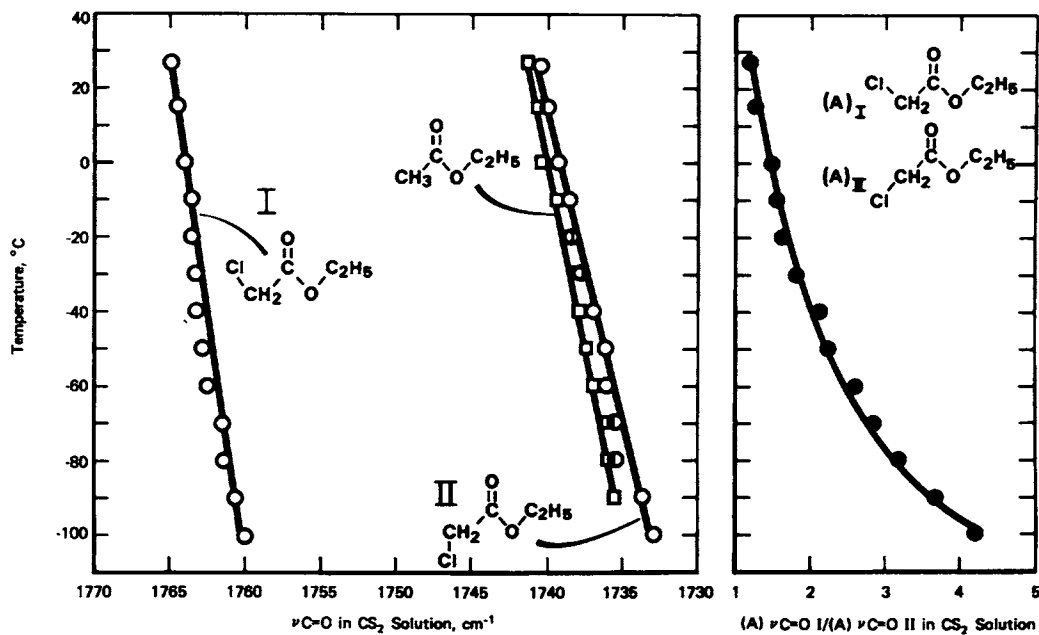


FIGURE 15.6 The left figure shows plots of ν_{CO} rotational conformers 1 and 2 for ethyl 2-chloroacetate and ν_{CO} for ethyl acetate frequencies in CS_2 solution vs. temperature in $^{\circ}\text{C}$. The right figure shows a plot of the absorbance ratio for ν_{CO} rotational conformer 1/rotational conformer 2 vs. temperature in $^{\circ}\text{C}$.

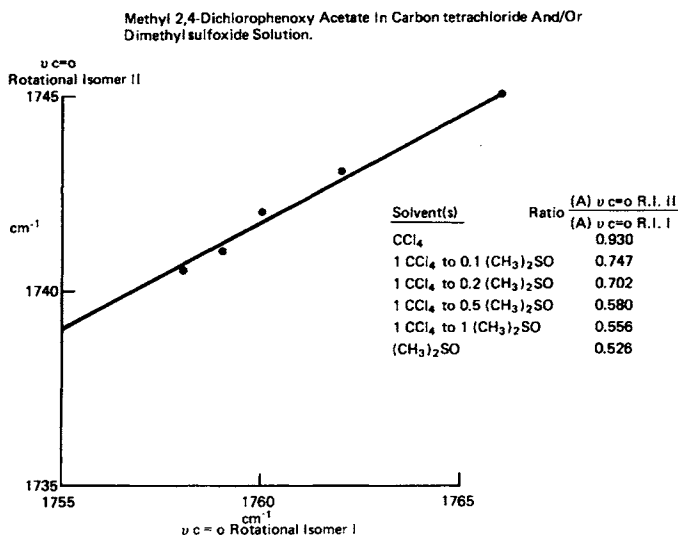


FIGURE 15.7 A plot of the ν CO frequencies for rotational conformer 1 vs ν CO for rotational conformer 2 for methyl 2,4-dichlorophenoxyacetate with change in the CCl₄ to (CH₃)₂SO ratio.

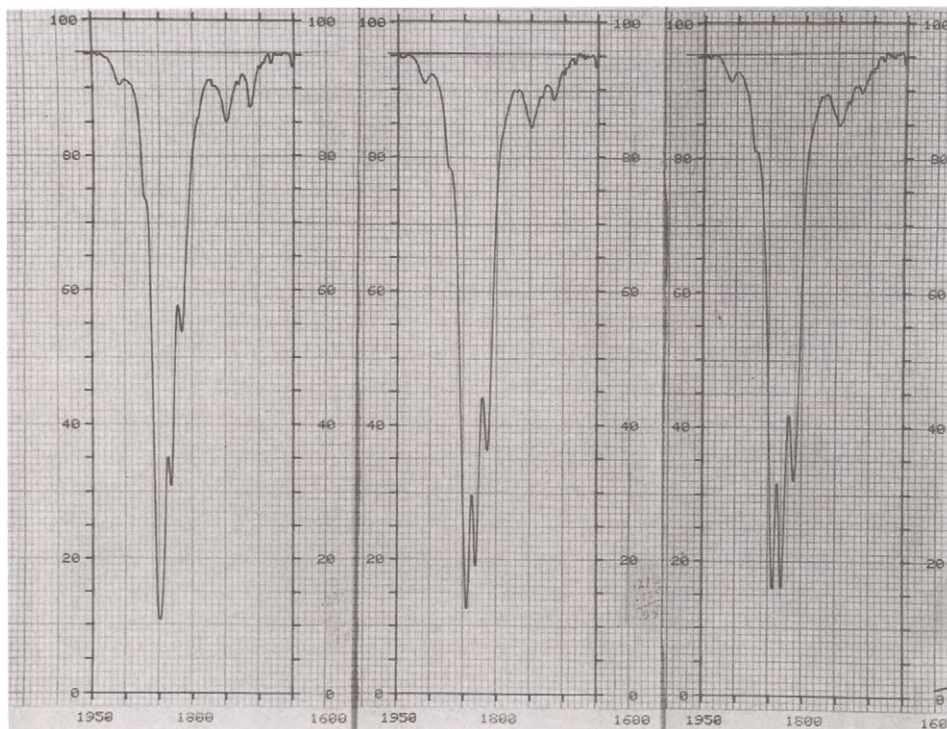


FIGURE 15.8 Infrared spectra of β -propiolactone in CCl₄ solution (left), 52 mol % CHCl₃/CCl₄ solution (middle), and CHCl₃ solution (right).

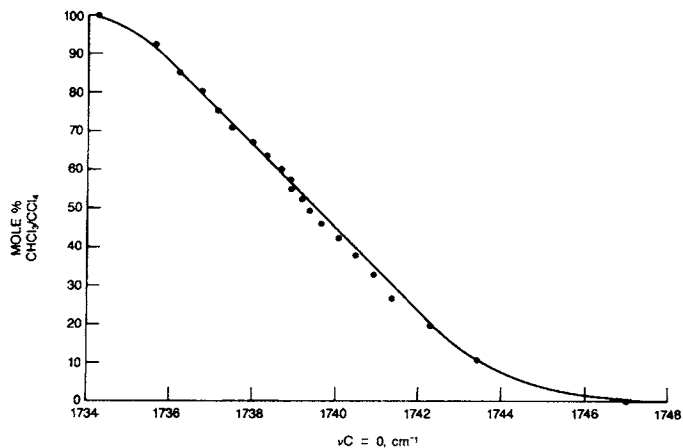


FIGURE 15.9 A plot of unperturbed ν_{CO} frequencies for coumarin in 1% wt./vol. $\text{CHCl}_3/\text{CCL}_4$ solutions vs mole % $\text{CHCl}_3/\text{CCL}_4$.

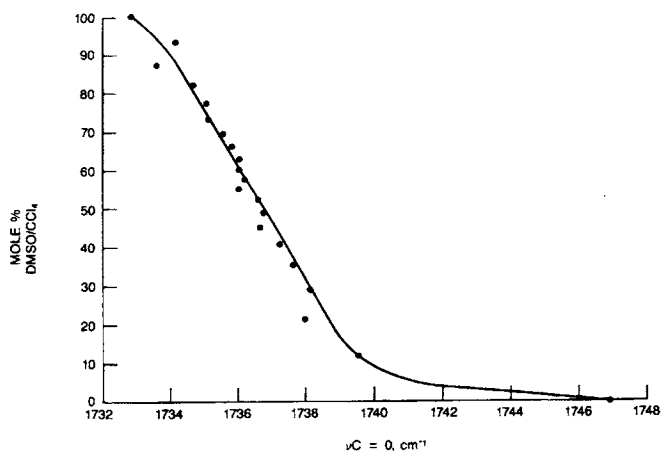


FIGURE 15.10 A plot of unperturbed ν_{CO} frequencies for coumarin in 1% wt./vol. $(\text{CH}_3)_2\text{SO}/\text{CCL}_4$.

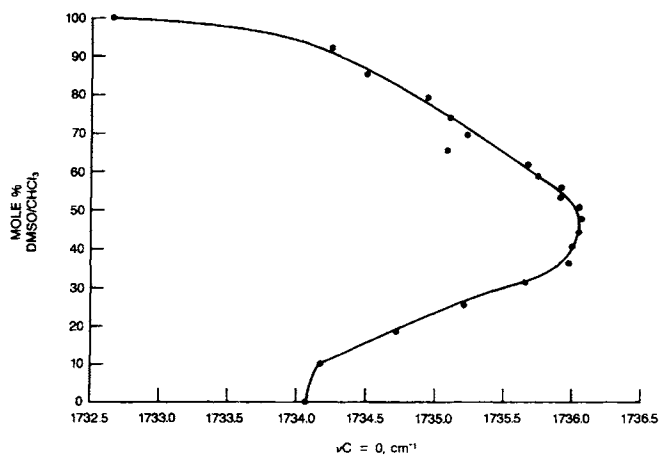


FIGURE 15.11 A plot of unperturbed ν_{CO} frequencies for coumarin 1% wt./vol. in $(\text{CH}_3)_2\text{SO}/\text{CHCl}_3$ solutions vs mole % $(\text{CH}_3)_2\text{SO}/\text{CHCl}_3$.

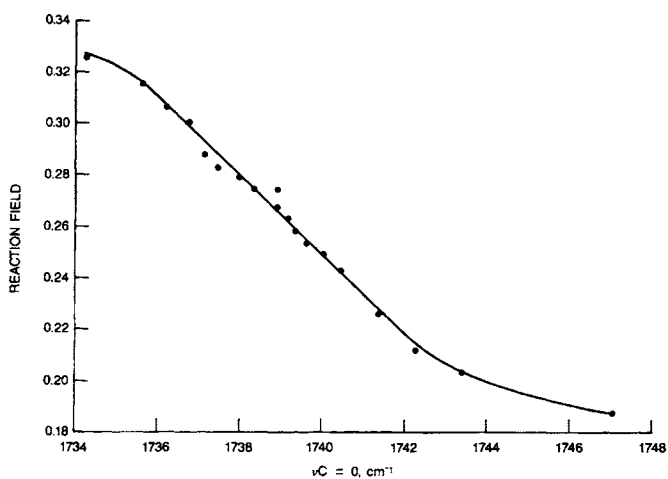


FIGURE 15.12 A plot of the unperturbed ν_{CO} frequencies for coumarin 1% wt./vol. in $\text{CHCl}_3/\text{CCl}_4$ solution vs the reaction field for $\text{CHCl}_3/\text{CCl}_4$ solutions.

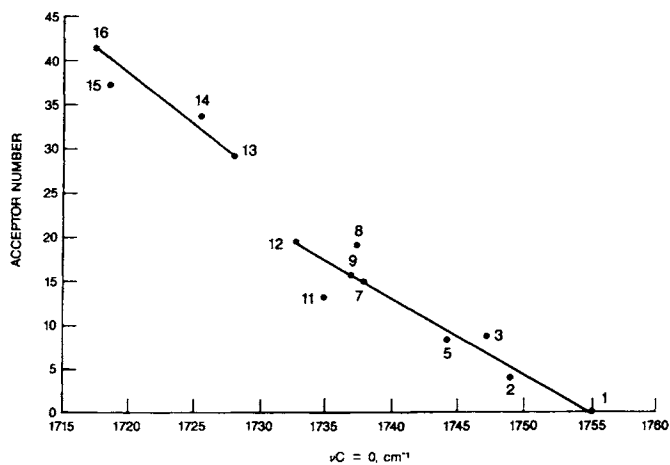


FIGURE 15.13 Plots of unperturbed ν_{CO} frequencies for coumarin 1% wt./vol. in various solvents vs the solvent acceptor number (AN).

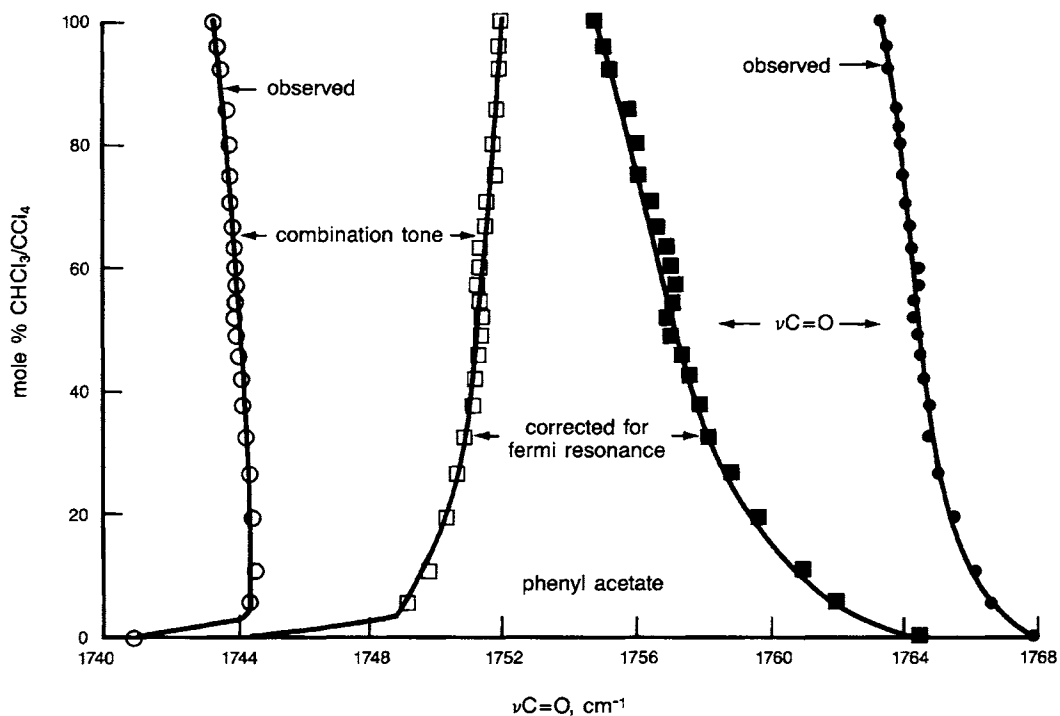


FIGURE 15.14 Plots of ν_{CO} and a combination tone in Fermi resonance and their unperturbed ν_{CO} and CT frequencies for phenyl acetate after correction for Fermi resonance vs mole % $\text{CHCl}_3/\text{CCl}_4$.

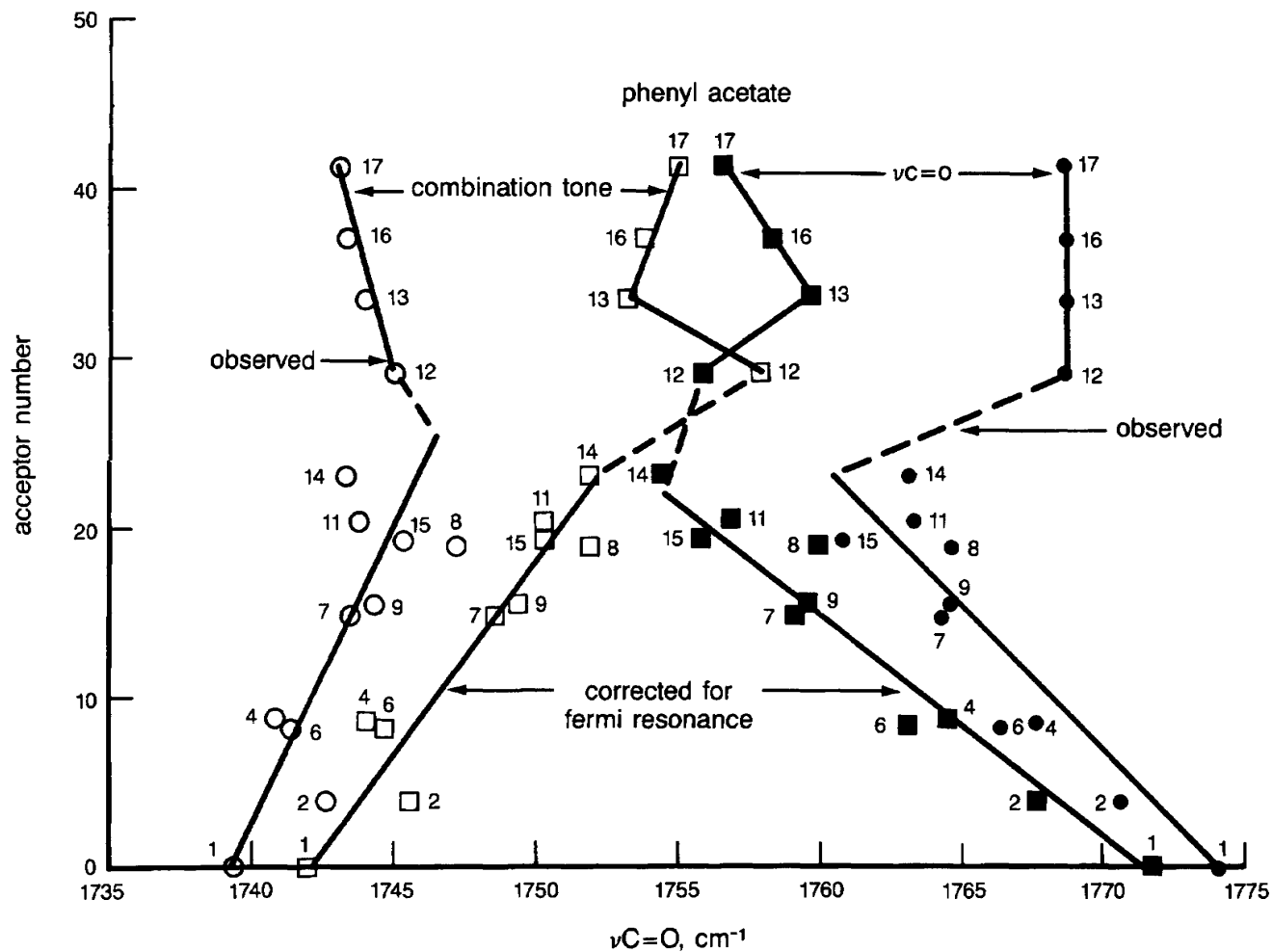


FIGURE 15.15 Plots of $\nu_{C=O}$ and a combination tone in Fermi resonance and their unperturbed $\nu_{C=O}$ and CT frequencies for phenyl acetate after correction for Fermi resonance vs the solvent acceptor number (AN).

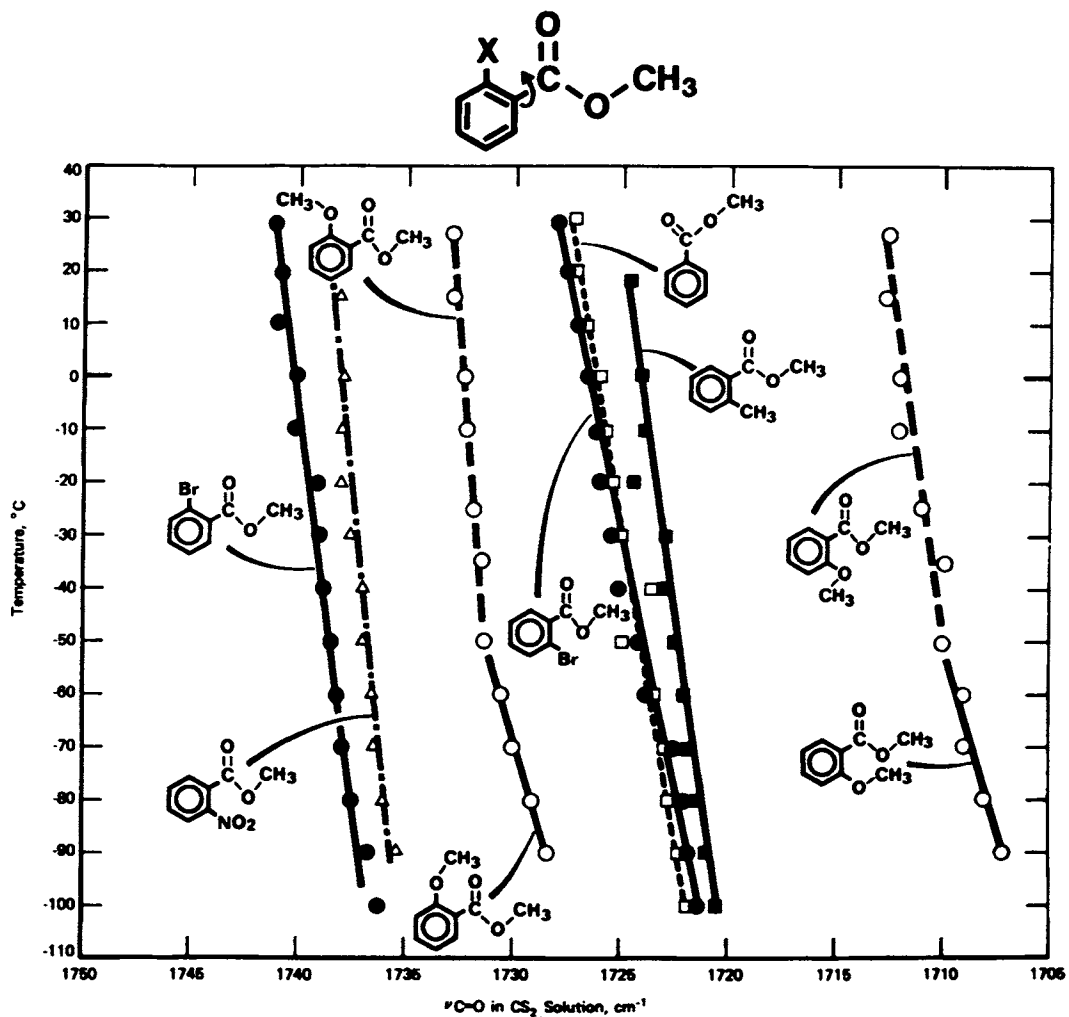


FIGURE 15.16 Plots of ν_{CO} for methyl benzoates in CS_2 solution vs temperature in $^{\circ}\text{C}$.

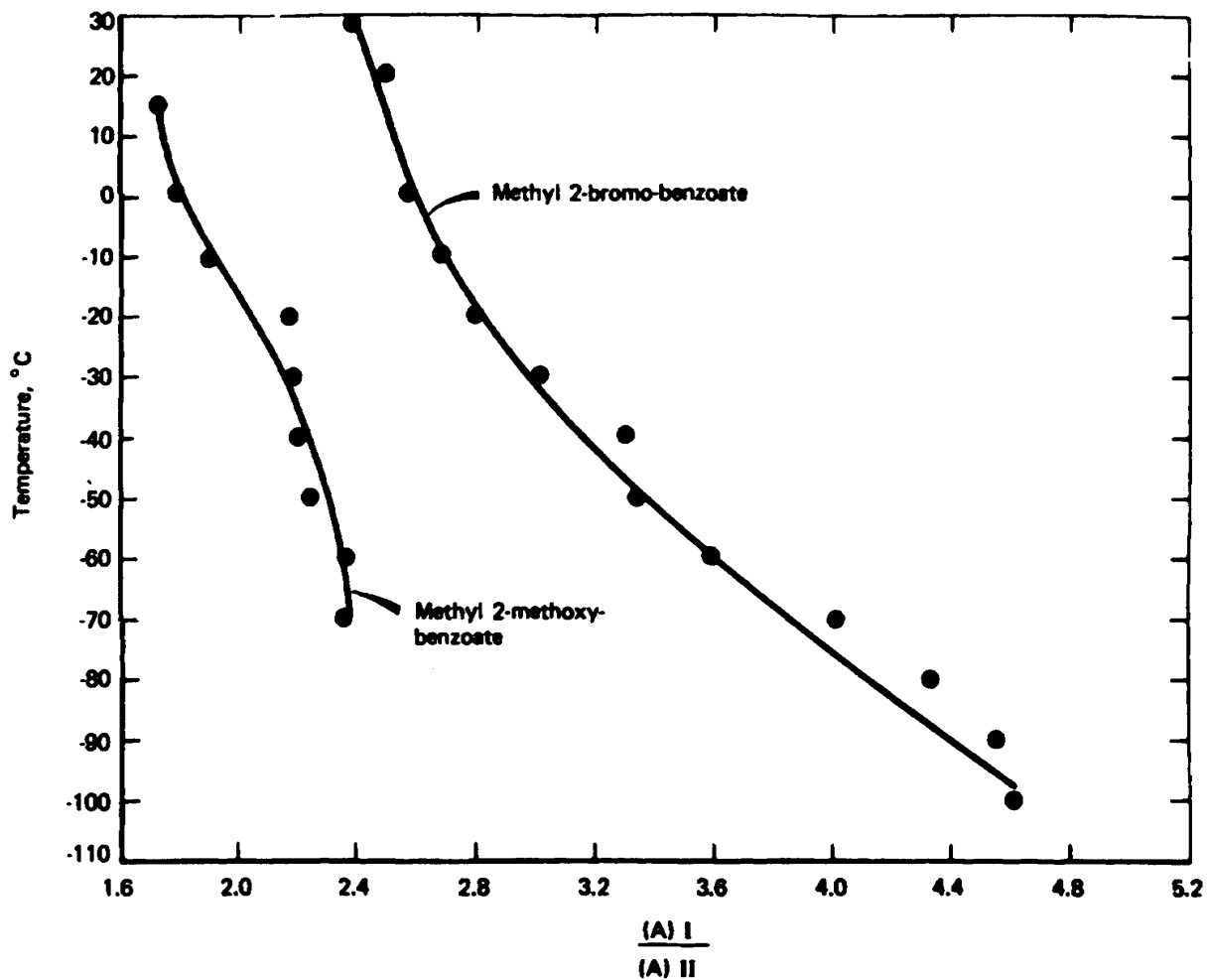


FIGURE 15.17 Plots of the absorbance ratio for $A(\nu\text{CO, rotational conformer 1})/A(\nu\text{CO, rotational conformer 2})$ for methyl 2-methoxybenzoate and methyl 2-bromobenzoate in CS_2 solution vs temperature in $^\circ\text{C}$.

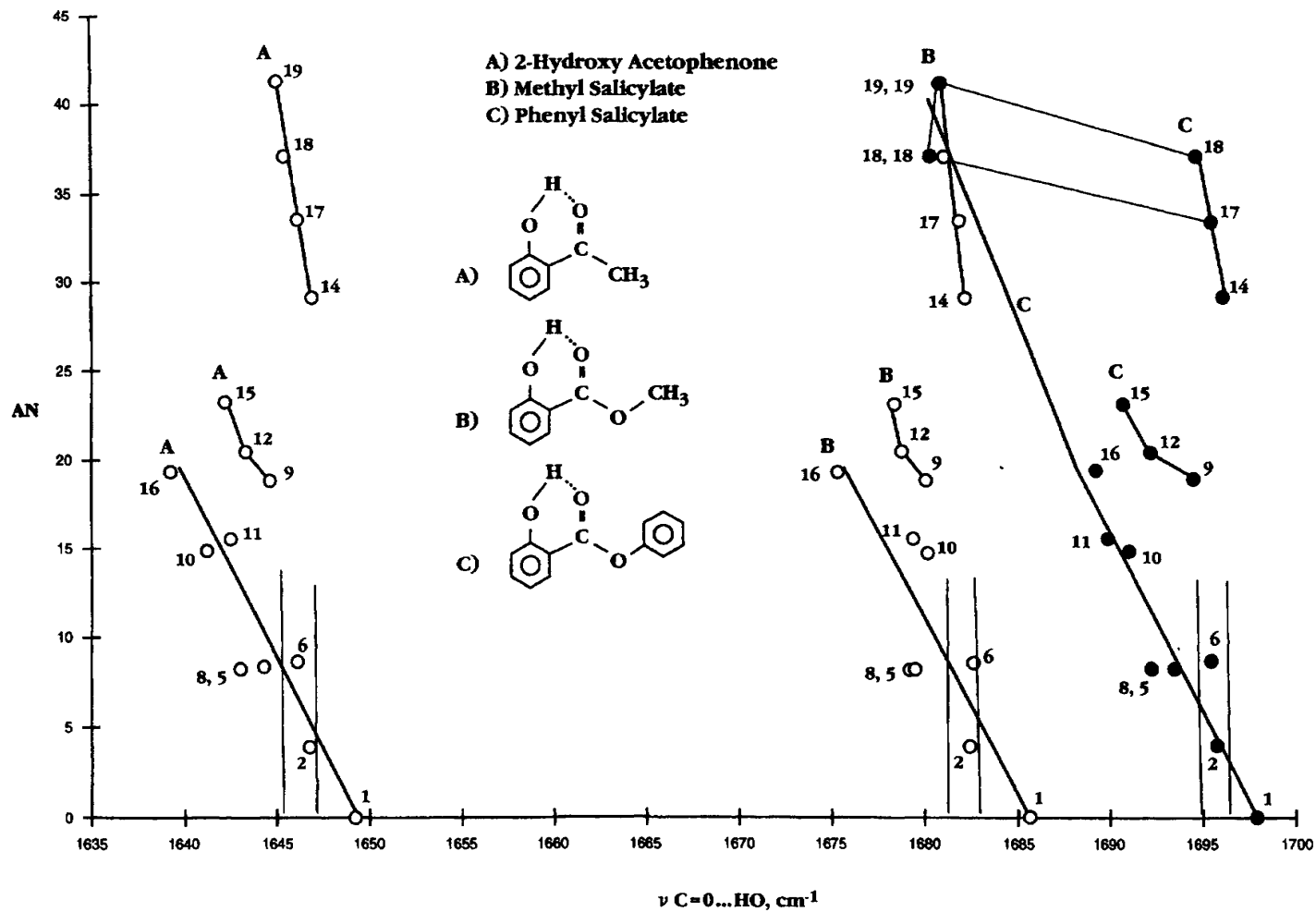


FIGURE 15.18 Plots of $\nu_{\text{CO}\cdots\text{HO}}$ frequencies for 2-hydroxyacetophenone, methyl salicylate, and phenyl salicylate vs the solvent acceptor number (AN) for each of the solvents used in the study.

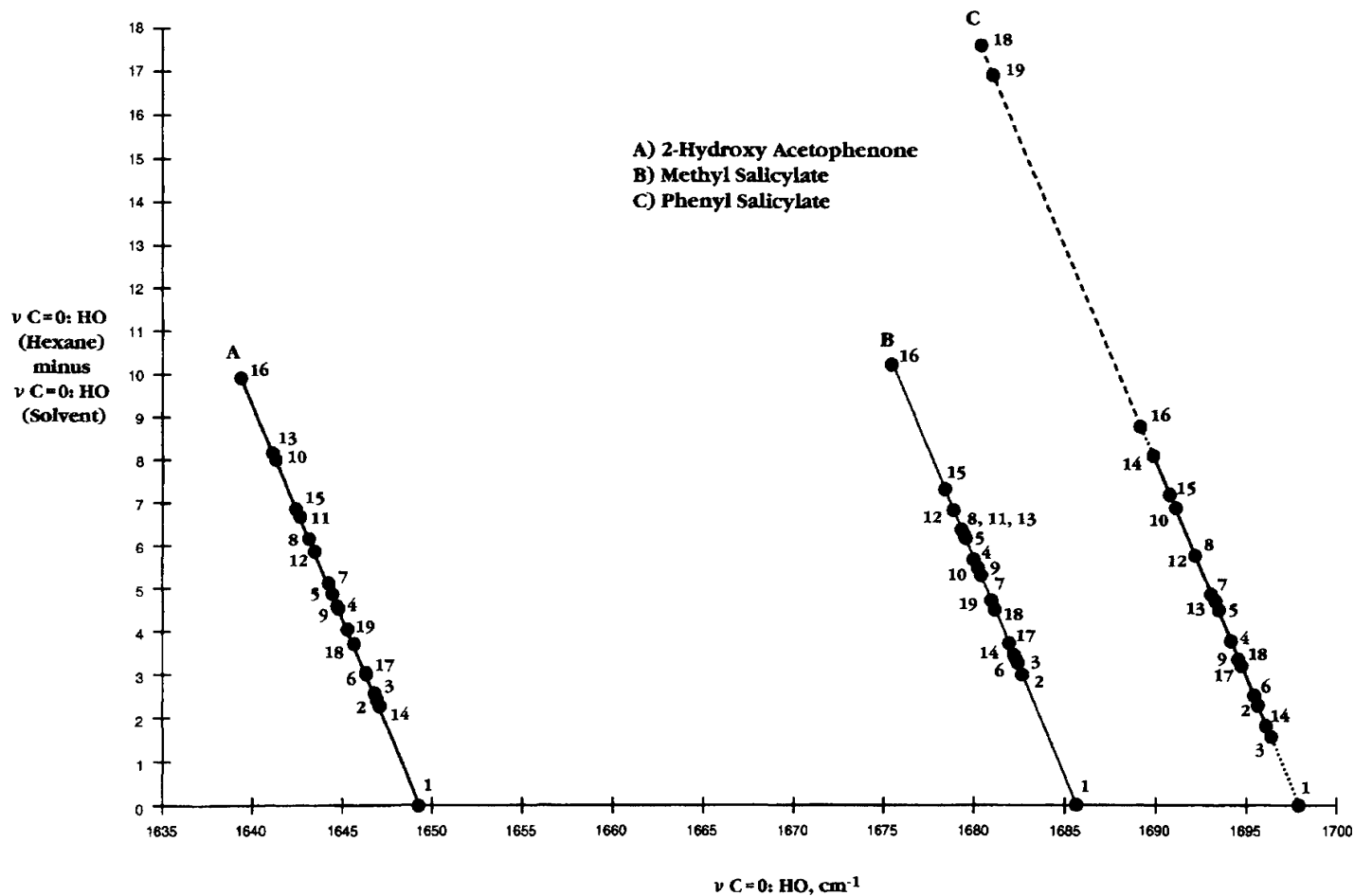


FIGURE 15.19 Plots of $\nu \text{CO} \cdots \text{HO}$ for 2-hydroxyacetophenone, methyl salicylate, phenyl salicylate vs the frequency difference between $\nu \text{CO} \cdots \text{HO}$ (hexane) and $\nu \text{CO} \cdots \text{HO}$ (solvent) for each of the other solvents.

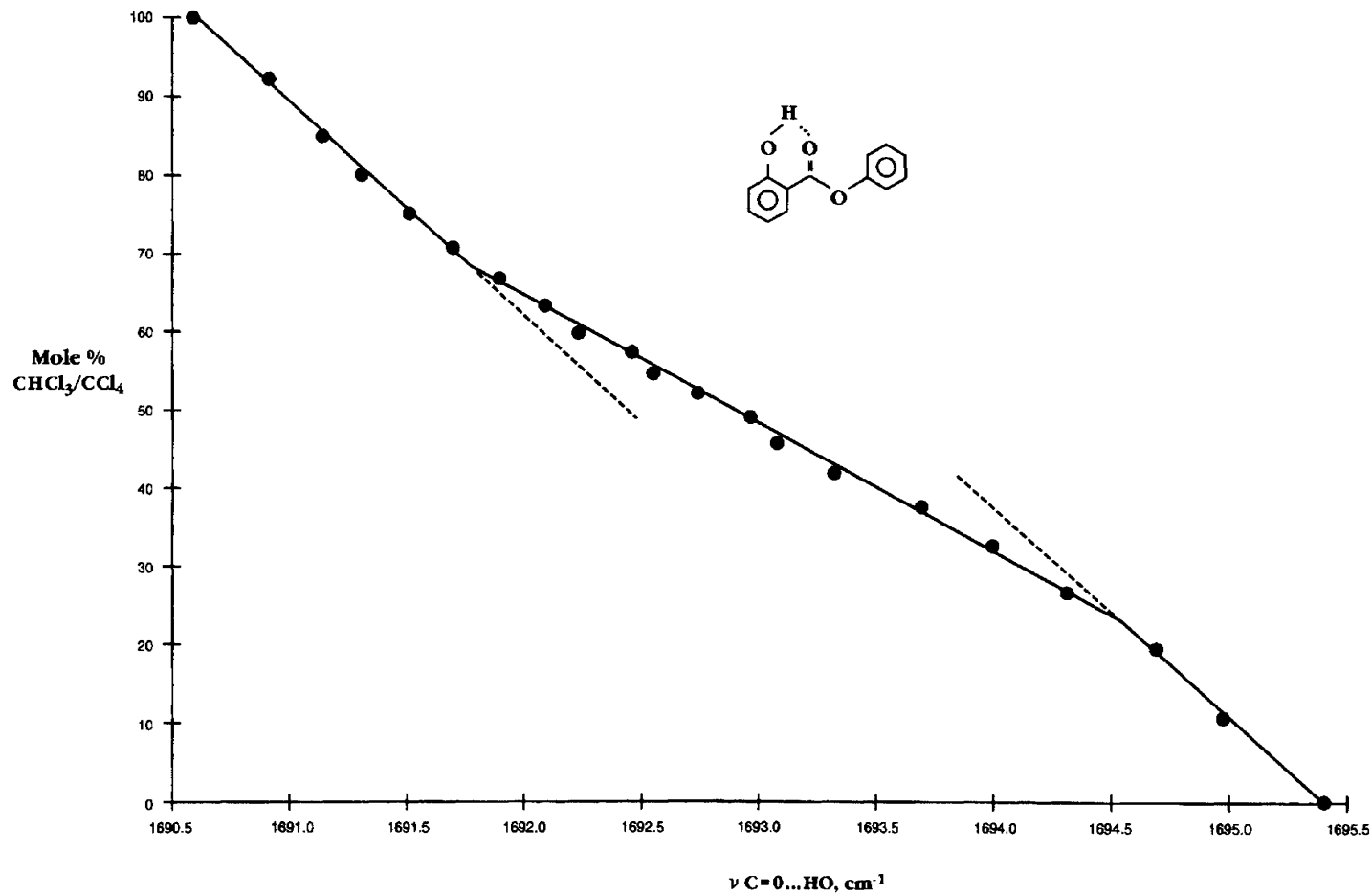


FIGURE 15.20 A plot of $\nu_{\text{CO}\cdots\text{HO}}$ frequencies of phenyl salicylate vs mole % $\text{CHCl}_3/\text{CCl}_4$.

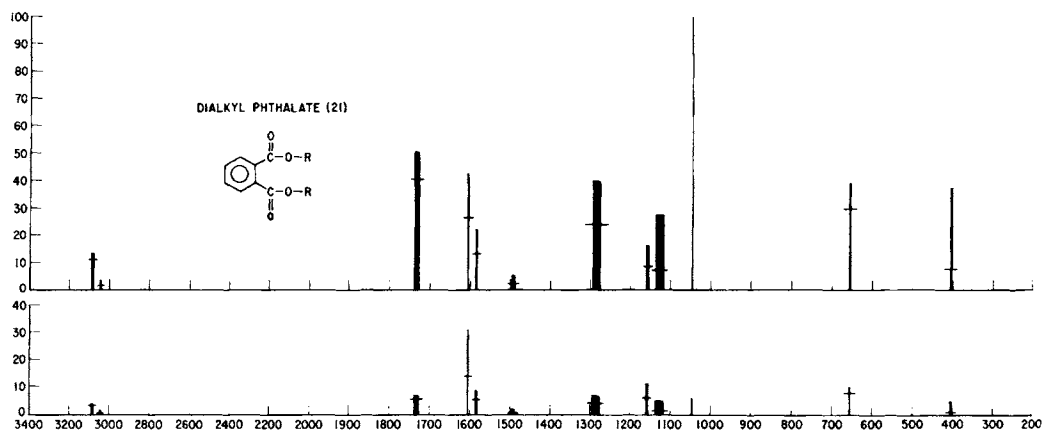
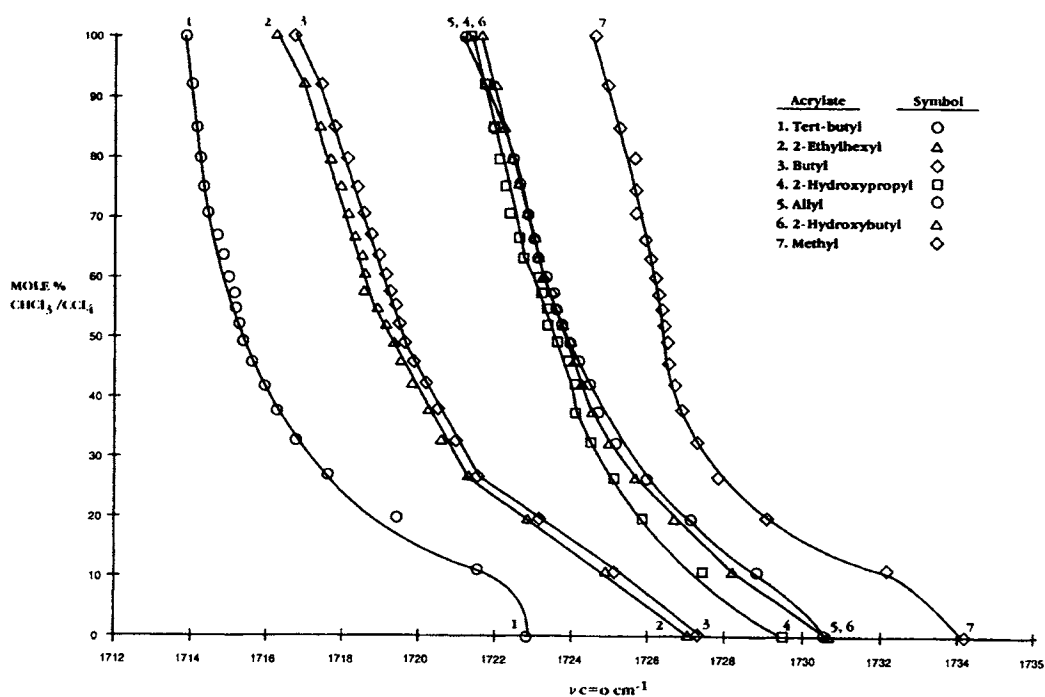


FIGURE 15.21 Bar graphs of the Raman group frequency data for 21 dialkyl phthalates.

FIGURE 15.22 Plots of ν_{CO} for seven alkyl acrylates in 1% wt./vol. $CHCl_3/CCl_4$ solutions vs mole % $CHCl_3/CCl_4$.

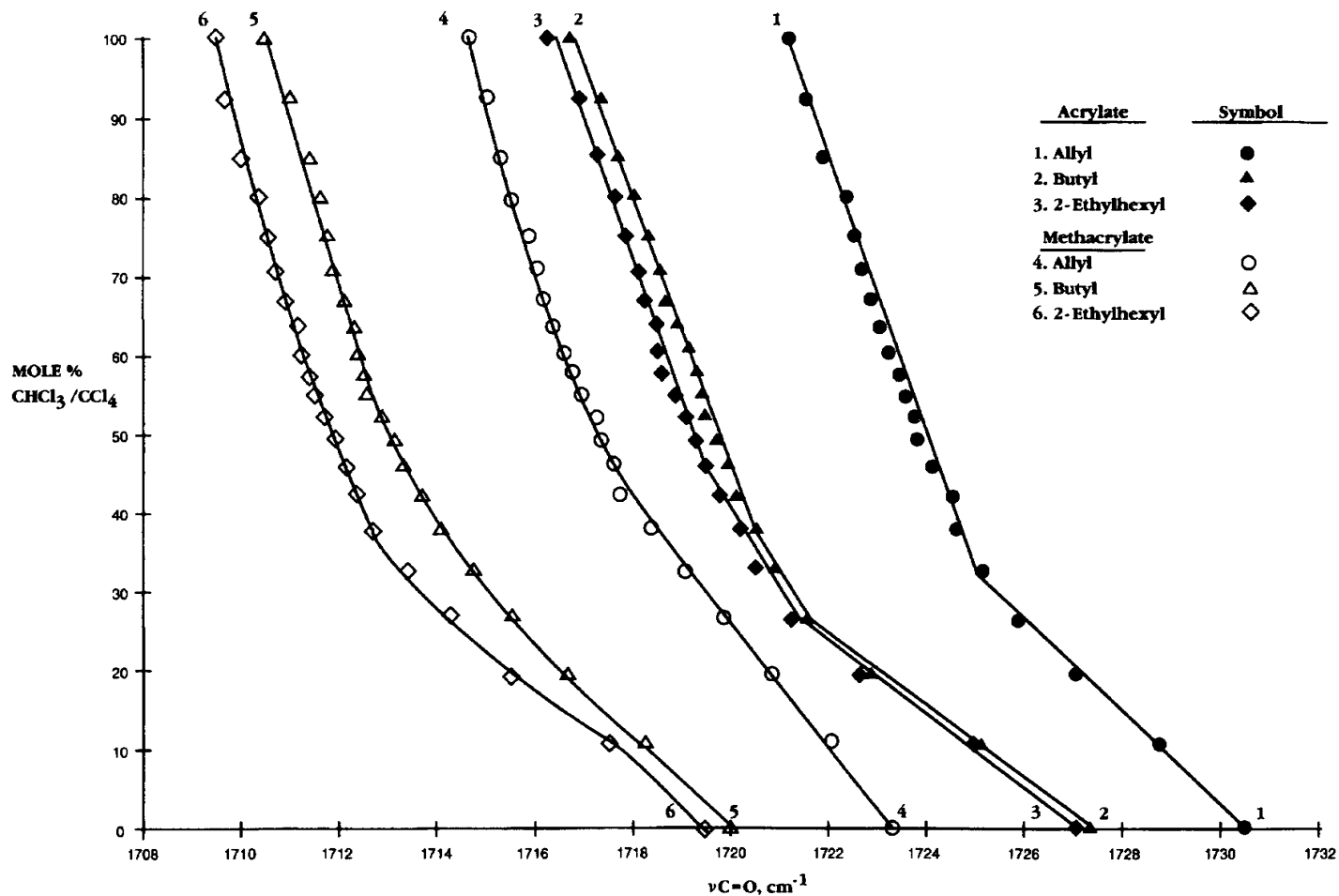
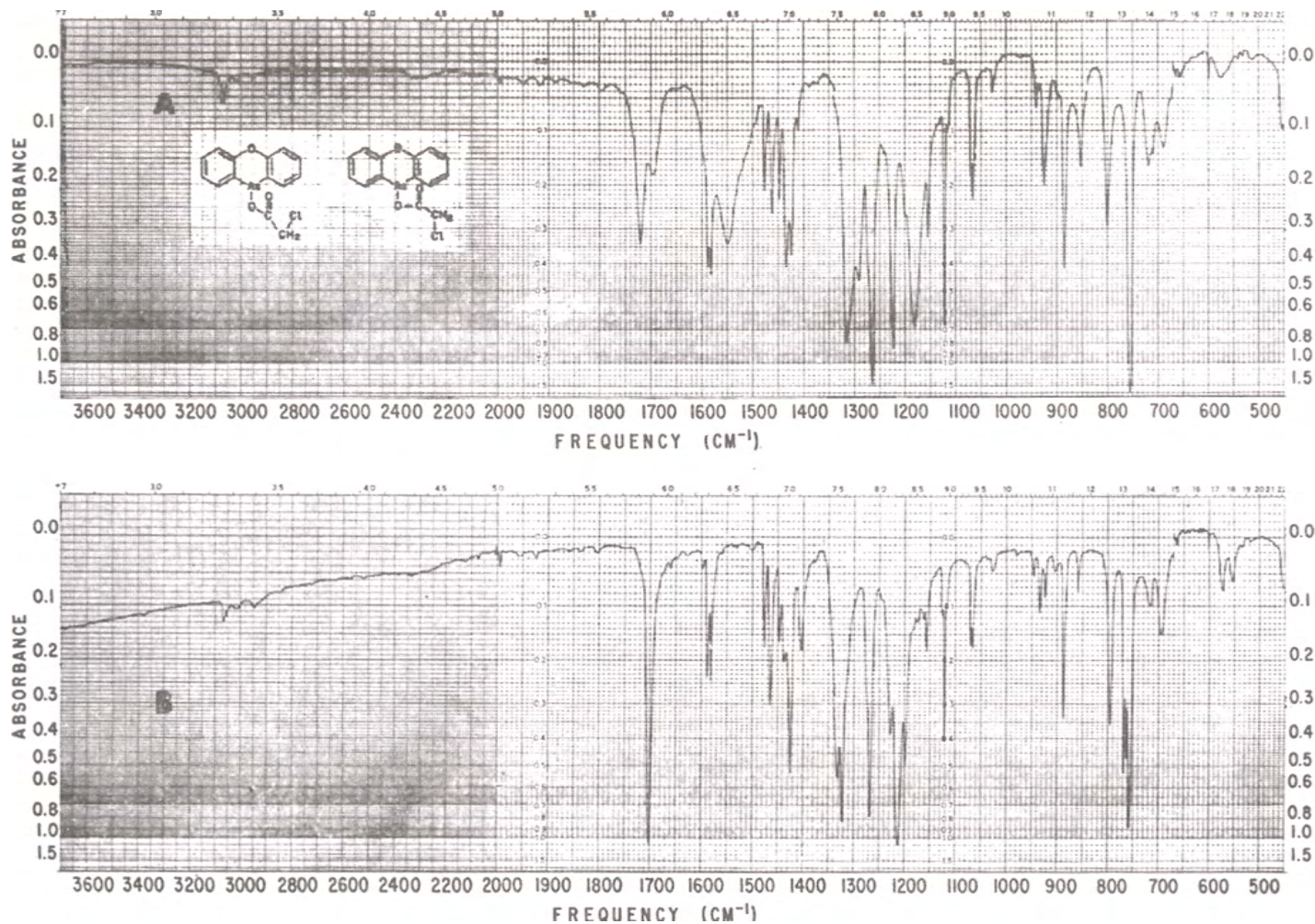


FIGURE 15.23 Plots of $\nu_{\text{C=O}}$ for corresponding alkyl acrylates and alkyl methacrylates vs mole % $\text{CHCl}_3/\text{CCl}_4$ solutions.

FIGURE 15.24 10-phenoxyarsinyl chloroacetate. (a) Saturated in CCl₄ and CS₂ solution, (b) split mull.

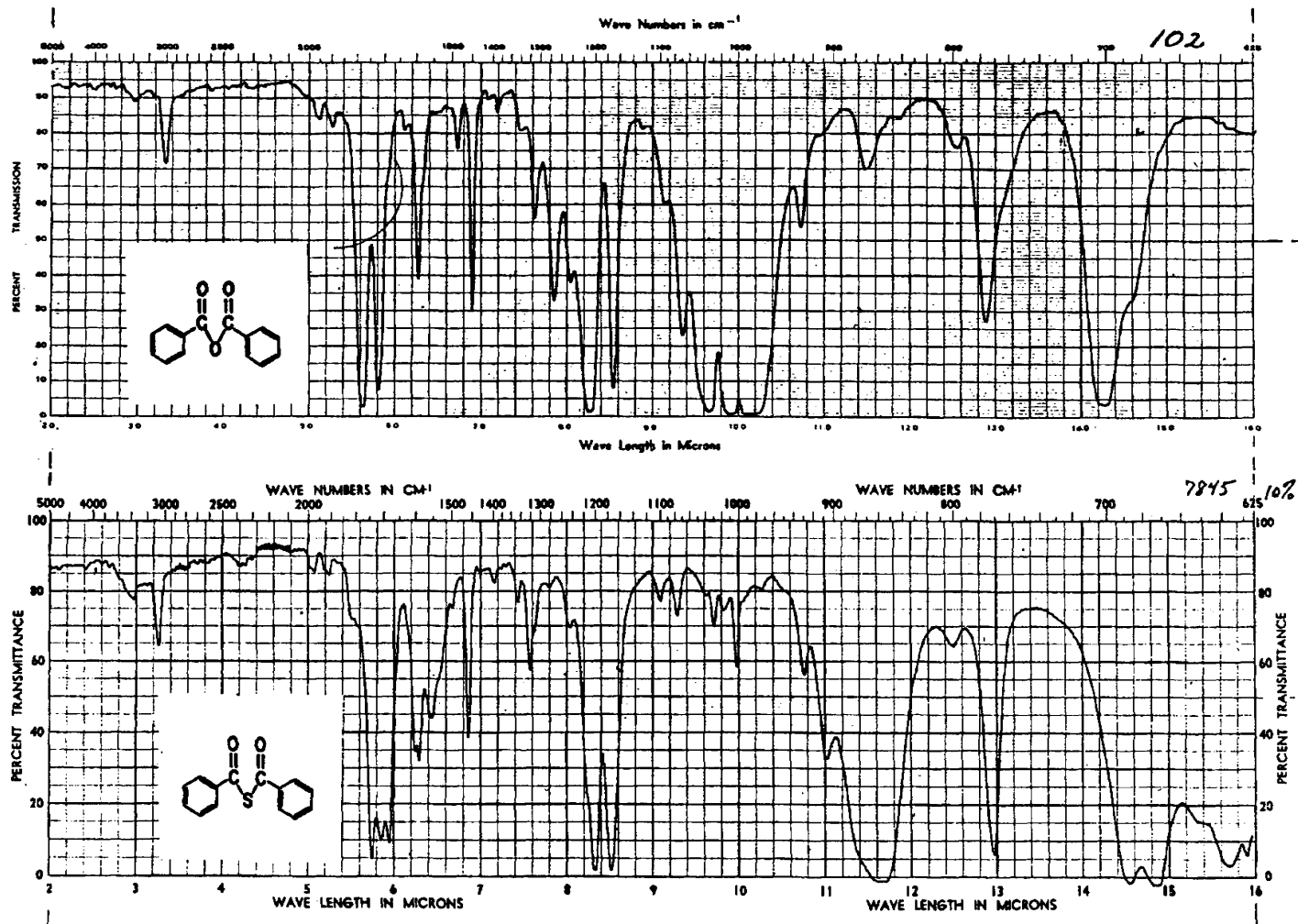


FIGURE 15.25 IR spectra of thiolbenzoic anhydride (dibenzoyl sulfide) and benzoic anhydride (dibenzoyl oxide).

TABLE 15.1 Carbonyl stretching frequencies for some carboxylic acid esters

Compound	C=O str. vapor cm ⁻¹	C=O str. liquid cm ⁻¹	Compound	C=O str. vapor cm ⁻¹	C=O: H-O str liquid cm ⁻¹
Alkyl formate	1741–1751	1715–1730			
Alkyl acetate	1755–1769	1735–1750			
Phenyl acetate	1781–1786				
Vinyl acetate	1784				
Alkyl propionate	1751–1762	1725–1740	Alkyl acrylate	1746–1751	
Phenyl propionate	1781				
Vinyl propionate	1777				
Alkyl isobutyrate	1751–1760		Alkyl methacrylate	1739–1741	
Alkyl butyrate	1750–1760				
Alkyl valerate	1752–1761		Alkyl benzoate	1737–1749	
Alkyl hexanoate	1749–1759		Phenyl benzoate	1760	
Alkyl heptanoate	1752–1759		Methyl 2-nitrobenzoate	1751	
Alkyl octanoate	1751–1759				
Alkyl nonoate	1751–1759		Dialkyl phthalate	1735–1753	
Alkyl decanoate	1751–1760		Dialkyl isophthalate	1740–1746	
Vinyl decanoate	1780		Dialkyl terephthalate	1739–1749	
Alkyl undecanoate	1751–1760				
Alkyl octanoate	1740–1759		Alkyl isonicotinate	1750–1753	
Vinyl octanoate	1771				
Dialkyl malonate	1750–1770		Alkyl salicylate	1740–1755	1687–1698
Dialkyl succinate	1751–1761		Phenyl salicylate	1750–1762	1695–1705
Dialkyl adipate	1750–1760				

TABLE 15.2 The C=O stretching frequencies for alkyl alkanooates in the vapor phase and in various solvents

Solvent* ¹	MA C=O str. cm ⁻¹	MP C=O str. cm ⁻¹	MIB C=O str. cm ⁻¹	MTMA C=O str. cm ⁻¹	MTMA C=O str. cm ⁻¹	EA C=O str. cm ⁻¹	E C=O str. cm ⁻¹	EIB C=O str. cm ⁻¹	ETMA C=O str. cm ⁻¹	AN
[vapor]	1769	1662	1760	1755	1755	1761	1755	1752	1750	
Hexane	1755.4	1752.1	1747.9	1742.8		1749.8	1746.7	1743	1736.4	0
Diethyl ether	1751	1747.8	1743.8	1739		1745.4	1742.8	1739.3	1732.4	3.9
Methyl t-butyl ether	1750.8	1747.3	1743.5	1738.7		1745.1	1742.4	1738.9	1732	[4.4]
Carbon tetrachloride	1748	1744.6	1740.6	1735.8		1741.8	1739.1	1735.7	1728.3	8.6
Benzene	1746.1	1742.9	1738.9	1734.4		1740	1737.2	1734	1726.9	8.2
1,2-Dichlorobenzene	1743.5	1739.7	1735.5	1732.5		1737.3	1733.6	1730.3	1723.8	[13.8]
Nitrobenzene	1741.5	1739.9	1734.1	1734.4		1735.5	171.9	1729.7	1725.3	14.8
Acetonitrile	1741.8	1738.7	1734.6	1731.6	1724.2	1735.7	1732.7	1729.3	1722	18.9
Benzonitrile	1741.4	1738.5	1734.3	1731.9	1722.1	1735.6	1732.7	1729.1	1721.6	1720
Nitromethane	1740.1	1737.1	1732.9	1738.8	1722.3	1734	1730.7	1727.2	1720	[18.5]
Methylene chloride	1739.4	1735.8	1731.8	1730.6	1721	1733.2	1729.4	1725.17	1718.7	20.4
Chloroform	1737.4	1734.1	1730.9	1729.9	1720	1732.2	1727.7	1724.9	1718.36	23.1
Chloroform-d	1737.5	1734.2	1730.8	1729.7	1720	1731.5	1727.7	1724.9	1718.9	23.1
t-Butyl alcohol	1751.4	1747.7	1743.3	1738.6		1746.4	1742.8	1739.3	1733.2	[3.7]
Isopropyl alcohol	1751.2	1748.6	1743.9	1738.6		1745.4	1742.9	1739.3	1732.8	[3.7]
Ethyl alcohol	1749.5	1746.6	1742.5	1738.6		1743.7	1741.2	1737.7	1731	[6.3]
Methyl alcohol	1747.6	1743.7	1739.5	1737.5		1741.5	1738.4	1734.9	1728.6	[7.6]
Dimethyl sulfoxide	1737.5	1734.6	1731	1728.5	1720.9	1732.3	1729.1	1726.1	1719.9	19.1
[neat]	1745.2	1743	1740.8	1736.6		1741.5	1738.9	1736.7	1730.3	[8.7]
Carbon disulfide	1746.9	1743.6	1739.6	1735.1		1740.8	1738.2	1734.9	1727.9	[7.9]

*¹ Abbreviations for the various solvents are spelled out in the text.

TABLE 15.3 The frequency difference between $\nu\text{C}=\text{O}$ and $\nu\text{C}=\text{O}:\text{HOR}$ for alkyl alkanooates in alkyl alcohols [0.5 wt./vol. solute in solvent]

Alcohol	MA cm^{-1}	MP cm^{-1}	EA cm^{-1}	MIB cm^{-1}	EP cm^{-1}	EIB cm^{-1}	MTMA cm^{-1}	ETMA cm^{-1}	[M + E]/2 cm^{-1}
tert-Butyl	17.32	17.82	17.55	19.16	19.55	18.77	20.81	19.26	18.78
Isopropyl	18.75	20.12	17.99	22.25	21.39	20.61	20.11	20.39	20.45
Ethyl	17.98	20.16	17.54	23.14	22.07	21.56	22.57	20.68	20.71
Methyl	17.05	18.33	14.97	21.36	20.71	20.42	21.81	20.01	19.33

TABLE 15.4 The frequency difference between $\nu\text{C}=\text{O}$ and $\nu\text{C}=\text{O}:\text{HO}$ for alkyl acetates in alkyl alcohols

Alcohol	Methyl acetate delta cm^{-1}	Ethyl acetate delta cm^{-1}	Isopropyl acetate delta cm^{-1}	tert-Butyl acetate delta cm^{-1}
Methyl	17.05	14.97	18.97	18.04
Ethyl	18.07	17.54	21.91	22.77
Isopropyl	17.75	18.02	22.43	23.41
tert-Butyl	17.32	17.75	21.67	23.13

TABLE 15.5 The C=O stretching frequencies for alkyl 2,2-dichloroacetates and alkyl acetates in the vapor and neat phases

Alkyl	[A] Alkyl 2,2-dichloroacetate [vapor phase] C=O str., Conformer 1 cm^{-1}	[B] Alkyl 2,2-dichloroacetate [vapor phase] C=O str., Conformer 2 cm^{-1}	[C] Alkyl acetate [vapor phase] C=O str. cm^{-1}	[A]-[C] cm^{-1}	[A]-[C] cm^{-1}	[B]-[C] cm^{-1}	[vapor]-[neat] cm^{-1}
	Methyl	1790	1765	1769	25	21	-4
Ethyl	1785	1762	1761	23	24	1	
Ethyl[neat]	[1771]	[1750]		[21]			[14]:[12]
Hexyl	1783	1761	1760	22	23	1	
Hexyl[neat]	[1767]	[1750]		[17]			[16]:[11]
Nonyl	1782	1761	1761	21	21	0	
Dodecyl	1782	1761	1761	21	21	0	
sec-Butyl	1779	1758	1755	21	24	3	
Methyl			1751				
t-Butyl			1740				
[delta C=O str.]			[11]				

TABLE 15.5A IR data for ethyl acetate and ethyl 2-chloroacetate in CS₂ solution between 27 and -100°C

°C	Ethyl acetate	°C	Ethyl 2-chloroacetate	Ethyl 2-chloroacetate	A[conformer 1] A[conformer 2]	[conformer 1]- [conformer 1]-
	[CS ₂] cm ⁻¹		conformer 1 [CS ₂] cm ⁻¹	conformer 2 [CS ₂] cm ⁻¹		cm ⁻¹
27	1741.3	26	1765	1740.5	1.19	24.5
15	1740.7	15	1764.5	1740	1.25	24.5
0	1740.5	0	1764.1	1739.4	1.47	24.7
-10	1739.5	-10	1763.6	1738.5	1.55	25.1
-20	1738.6	-20	1763.6	1738.5	1.6	25.1
-30	1738	-30	1763.5	1738	1.81	25.5
-40	1738	-40	1763.4	1737	2.14	26.4
-50	1737.6	-50	1762.8	1736.2	2.32	26.6
-60	1737	-60	1762.5	1736.1	2.62	26.4
-70	1736	-70	1761.6	1735.5	2.85	26.1
-80	1736	-80	1761.3	1735.4	3.18	26.2
-90	1735.5	-90	1760.6	1733.6	3.69	27
-100		-100	1759.8	1732.8	4.2	27
delta C	delta C=O str.	delta C	delta C=O str.	delta C=O str.	delta	delta cm ⁻¹
[-117]	[-5.8]	[-126]	[-5.2]	[-7.7]	[A(conformer 1)]- [A(conformer 2)]- [3.01]	[2.22]

TABLE 15.6 IR data for β-propiolactone in various solvents

β-Propiolactone 1% wt./vol. solutions in the solvents listed below	C=O str., A' cm ⁻¹	v6 + v13, A' cm ⁻¹	2v10, A' cm ⁻¹	C=O str., A' corrected for FR. cm ⁻¹	v6 + v13A' corrected for FR. cm ⁻¹	2v10, A' corrected for FR. cm ⁻¹
Hexane	1857.18	1832.01	1817.52	1850.21	1830.69	1826.81
Diethyl ether	1852.24	1838.04	1814.14	1843.8	1834.65	1825.97
Carbon tetrachloride	1850.5	1833.08	1816.28	1841.78	1831.62	1831.62
Nitrobenzene	1830.93	1843.31	1808.44	1828.74	1830.62	1823.33
Acetonitrile	1832.18	1845.07	1810.23	1830.55	1832.56	1824.37
Benzonitrile	1830.77	1843.31	1829.78	1829.72	1831.92	1825.23
Methylene chloride	1831.46	1844.86	1812.36	1830.87	1832.43	1825.38
chloroform	1845.02	1831.7	1813.04	1834.7	1829.67	1825.39
Nitromethane	1831.8	1845.07	1809.8	1830.12	1832.48	1824.07
t-Butyl alcohol	1832.02	1845.66	1813.4	1830.79	1833.28	1821.01
Isopropyl alcohol	1833.07	1845.72	1810.82	1830.84	1832.72	1826.05
Ethyl alcohol	1833.81	1845.72	1810.37	1831.14	1832.78	1825.99
Methyl alcohol	1834.23	1843.23	1809.89	1830.72	1832.01	1825.35

TABLE 15.7 IR group frequency data for coumarin and derivatives in the vapor phase and in solution

Compound vapor phase	2(C=O) cm ⁻¹ (A)	C=O str. cm ⁻¹ (A)	CCOC str. cm ⁻¹ (A)	CCOC str. cm ⁻¹ (A)	o.p. Ring cm ⁻¹ (A)	o.p. Ring cm ⁻¹ (A)
Coumarin	3530(0.015)	1776(1.240)	1265(0.078)	1178(0.160)	751(0.131)	825(0.140)
3,4-dihydro	3590(0.021)	1802(1.250)	1235(0.710)	1140(1.040)	755(0.295)	
3-chloro	3545(0.020)	1775(1.210)	1242(0.160)	1120(0.199)	750(0.354)	
6-methyl	3525(0.010)	1755(1.240)	1260(0.118)	1163(0.210)	897(0.141)	819(0.172)

Coumarin 1 wt. % (0.1 mm KBr) solvent	C=O str. corrected for FR. cm ⁻¹	C=O: HO corrected for FR.	AN	C=O str. not corrected for FR. cm ⁻¹
Hexane	1755.16		0	1758.56
Diethyl ether	1748.93		3.9	1755.16
Carbon tetrachloride	1747.16		8.6	1741.25
Carbon disulfide	1744.47			1739.49
Benzene	1744.18		8.2	1738.64
Toluene	1743.96			1739.3
Nitrobenzene	1737.82		14.8	1733.47
Acetonitrile	1737.31		18.9	1733.58
Benzonitrile	1736.84		15.5	1733.5
Nitromethane	1735.28			1732.06
Chloroform	1734.89		23	1729.94
Dimethylsulfoxide	1732.82		19.3	1729.22
Tert-butyl alcohol		1727.9	29.1	
Isopropyl alcohol		1725.45	33.5	
Ethyl alcohol		1718.53	37.1	1739.74
Methyl alcohol		1717.38	41.3	1738.18

TABLE 15.8 IR data for phenyl acetate in CHCl₃/CCl₄

Phenyl acetate	C=O str. in FR. cm ⁻¹	CT in FR. cm ⁻¹	A[1]	A[2]	A[1]/A[2]	C=O str. corrected for FR. cm ⁻¹	CT corrected for FR. cm ⁻¹
Mole % CHCl ₃ /CCl ₄							
0	1767.71	1740.99	0.433	0.059	0.133	1764.6	1744.1
52	1764.22	1743.94	0.612	0.35	0.572	1756.8	1751.3
100	1763.19	1743.32	0.287	0.217	0.756	1754.6	1751.9
delta C=O	-4.52	2.33				-9.9	7.8

TABLE 15.9 IR data for phenyl acetate in various solvents

Phenyl acetate 1 % wt./vol. solutions [.207 mm KBr cell]	C=O str. in FR. cm ⁻¹	CT* ¹ in FR. cm ⁻¹	C=O str. corrected for FR. cm ⁻¹	CT corrected for FR. cm ⁻¹	AN* ²
Solvent					
Hexane	1774.21	1736.5	1771.8	1741.9	0
Diethyl ether	1770.62	1742.62	1767.6	1745.6	3.9
Methyl t-butyl ether	1770.22	1743.3	1766.7	1746.8	
Carbon tetrachloride	1767.71	1740.99	1764.6	1744.1	8.6
Carbon disulfide	1766.46	1737.6	1763.9	1740.2	
Benzene	1766.39	1741.24	1763.1	1744.6	8.2
Nitrobenzene	1764.31	1743.48	1759.2	1748.6	14.8
Acetonitrile	1764.65	1747.24	1759.9	1751.9	18.9
Benzonitrile	1764.6	1744.34	1759.5	1749.4	15.5
Nitromethane	1763.88	1754.76	1758.1	1751.6	
Methylene chloride	1763.37	1743.79	1756.8	1750.3	20.4
t-Butyl alcohol	1768.72	1745.05	1755.9	1757.9	29.1
Isopropyl alcohol	1768.79	1744.07	1759.6	1753.3	33.5
Chloroform	1763.19	1743.32	1754.6	1751.9	23.1
Dimethyl sulfoxide	1760.83	1745.34	1755.8	1750.3	19.3
Ethyl alcohol	1768.82	1743.4	1758.3	1753.9	37.1
Methyl alcohol	1768.51	1743.17	1756.6	1755.1	41.3

*¹CT = combination tone.*²AN = acceptor number.

TABLE 15.10 IR data for alkyl 2-benzoates in CS₂ solution between 29 and -100°C

°C	Methyl 2-bromo- benzoate C=O str. conformer 1	Methyl 2-bromo- benzoate C=O str. conformer 2	[conformer 1]- [conformer 2]	°C	Methyl 2-methoxy- benzoate C=O str. conformer 1	Methyl 2-methoxy- benzoate C=O str. conformer 2	[conformer 1]- [conformer 2]
	[CS ₂] cm ⁻¹	[CS ₂] cm ⁻¹	cm ⁻¹		[CS ₂] cm ⁻¹	[CS ₂] cm ⁻¹	cm ⁻¹
29	1741.2	1728	13.2	15	1732.8	1712.8	20
10	1741	1728	13				
0	1740	1727	13	0	1732.3	1712.2	20.1
-10	1740.2	1726.5	13.7	-10	1732.3	1712.1	20.2
-20	1739.2	1726	13.2	-24.5	1731.7	1711	20.7
-30	1739	1725.5	13.5	-35	1731.5	1709.8	21.7
-40	1738.8	1725	13.8	-40			
-50	1738.5	1724.2	14.3	-50	1731.5	1710.1	21.4
-60	1738.2	1723.8	14.4	-60	1730.5	1709	21.5
-70	1738	1722.5	15.5	-70	1730	1709	21
-80	1737.5	1722	15.5	-80	1729.1	1708	21.1
-90	1736.7	1722	14.7	-90	1728.5	1707.2	21.3
-100	1736.2	1721.5	14.7				
delta C	delta C=O str.	delta C=O str.		delta C	delta C=O str.	delta C=O str.	
[-129]	[-5.0]	[-6.5]	[1.5]	[115]	[-4.3]	[-5.6]	[1.3]

°C	Ethyl 2-Nitro- benzoate C=O str.	°C	Methyl benzoate C=O str.	°C	Methyl 2-Methyl benzoate C=O str.
	cm ⁻¹		cm ⁻¹		cm ⁻¹
15	1738.2	30	1727	18	1724.7
0	1738	0	1726	0	1724.3
-10	1738	-10	1725.8	-10	1724
-20	1738	-20	1725.4	-20	1723.5
-30	1737.6	-30	1725	-30	1723
-40	1737	-40	1724.5	-40	1723.3
-50	1737	-50	1724	-50	1722.6
-60	1737.5	-60	1723.5	-60	1722
-70	1736.5	-70	1723	-70	1722
-80	1736	-80	1722.8	-80	1721.5
-90	1735.5	-90	1722.3	-90	1721.1
		-100	1721.7	-100	1720.6
delta C	delta C=O str.	delta C	delta C=O str.	delta C	delta C=O str.
[-115]	[-2.7]	[-130]	[-5.3]	[-118]	[-4.1]

TABLE 15.11 The C=O stretching frequencies for methyl salicylate, phenyl salicylate, and 2-hydroxyacetophenone in various solvents

2-Hydroxy- acetophenone C=O: H-O cm ⁻¹	Methyl salicylate C=O: H-O cm ⁻¹	Phenyl salicylate C=O: H-O cm ⁻¹	Phenyl salicylate C=O: (O-H) ₂ cm ⁻¹	Solvent	AN
1649.2	1685.6	1697.9		Hexane	0
1646.8	1682.3	1695.7		Diethyl ether	3.9
1646.7	1682.2	1696.3		Methyl t-butyl ether	
1644.7	1679.9	1694		Toluene	
1644.4	1679.4	1693.4		Benzene	8.2
1646.2	1682.5	1695.4		Carbon tetrachloride	8.6
1644.1	1680.4	1693		Carbon disulfide	
1643	1679.2	1692.1		1,2-Dichlorobenzene	8.2
1644.6	1680.1	1694.5		Acetonitrile	18.9
1641.2	1680.1	1691		Nitrobenzene	14.8
1642.5	1679.4	1689.8		Benzonitrile	15.5
1643.3	1678.7	1692.1		Methylene chloride	20.4
1641	1679.3	1693.2		Nitromethane	
1647	1682.1	1696.1		t-Butyl alcohol	29.1
1642.3	1678.3	1690.7		Chloroform	23.1
1639.3	1675.3	1689.1		Dimethyl sulfoxide	19.3
1646.2	1681.8	1695.5		Isopropyl alcohol	33.5
1645.5	1681.1	1694.7	1680.3	Ethyl alcohol	37.1
1645.1	1680.2		1680.9	Methyl alcohol	41.3

TABLE 15.12 Raman group frequency correlations for dialkyl phthalates in the neat phase

Dimethyl phthalate cm ⁻¹	RI ^{*1}	DR ^{*2}	Di-(isooctyl) phthalate cm ⁻¹	RI	DR
3082	11.1	0.31	3079	11.6	0.31
3042	2.1	0.64	3039	1.5	0.75
1731	45.3	0.14	1731	45.7	0.14
[1753 vapor, IR]					
1604	26.7	0.77	1603	31.9	1.76
1584	14	0.43	1583	15.9	0.45
1494	3.8	0.31	1492	2.2	0.33
1287	26.2	0.16	1278	30.8	0.19
1170	9	0.83	1167	14.2	0.73
1129	17	0.1	1135	9.4	0.15
1044	100	0.05	1043	100	0.06
652	30.2	1.3	652	32.6	0.27
405	37	0.11	405	13.1	0.14

*¹RI = relative intensity.*²DR = depolarization ratio.

TABLE 15.13 Raman data for C=O and C=C stretching for acrylates

Group	[R]C=O str. cm ⁻¹	RI	C=C str. cm ⁻¹	RI	C=O str.-C=C str. cm ⁻¹	RI C=O/ RI C=C
Methyl	1726	4	1636	9	90	0.44
Propyl	1723	5	1639	9	84	0.56
Butyl	1723	4	1639	9	84	0.44
Heptyl	1725	4	1639	9	86	0.44
Nonyl	1726	3	1639	8	87	0.38
Undecyl	1726	3	1640	9	86	0.33
2-Ethylhexyl	1725	4	1638	7	87	0.57
Isopropyl	1721	3	1640	9	81	0.33
Cyclohexyl	1720	3	1639	6	81	0.51
isoButyl	1725	3	1638	9	87	0.33
isoAmyl	1725	5	1639	9	86	0.56
Benzyl	1723	1	1636	2	87	0.51
2-Phenylethyl	1722	1	1637	4	85	0.25
2-(2-Ethoxyethoxy) ethyl	1724	4	1639	9	85	0.44
2-Hydroxyethyl	1722	3	1639	9	83	0.33
2-Hydroxypropyl	1722	3	1639	9	83	0.33
2-Hydroxybutyl	1721	3	1638	9	83	0.33
2-Methoxyethyl	1723	4	1639	9	84	0.44
3-Methoxybutyl	1724	5	1639	9	85	0.56
Triethyleneglycol,di-	1721	4	1638	9	83	0.44
1,4-Tetramethylene,di	1720	4	1636	9	82	0.44
Ethylene,di	1723	4	1639	9	85	0.44
1,2-Propanediol,di	1724	5	1638	9	86	0.56
1,3-Propanediol,di	1721	4	1637	7	84	0.57
1,6-Hexamethylene,di	1721	4	1638	9	83	0.44
1,10-Decanediol,di	1722	5	1638	9	84	0.56
2,-Butene-1,4-diol,di	1722	4	1637	9	85	0.44
Cinnamyl	1722	1	1637	3	85	0.33
2-Bromoethyl	1726	2	1637	5	89	0.41
2,3-Dibromopropyl	1717	1	1636	3	81	0.33
Tribromoneopentyl	1730	1	1637	3	93	0.33
2,2,2,Trifluoroethyl	1748	4	1638	9	110	0.44
Hexafluorobutyl	1746	4	1639	9	107	0.44
Pentafluorooctyl	1752	4	1639	9	113	0.44
1,H,1H,11H-Eicos-fluorodecanyl	1747	1	1639	2	108	0.51
Hexafluorisopropyl	1757	3	1640	4	117	0.75
Phenyl	1739	1	1635	3	104	0.33
p-Chlorophenyl	1742	3	1637	9	105	0.33
p-Nitrophenyl	1748	~ 0.51	1632	2	116	~ 0.25
2,4,6,Tribromophenyl	1737	2	1623	~ 0.50	114	~ 0.13
Pentabromophenyl	1738	2	1625	~ 0.25	113	~ 4.0
Pentachlorophenyl	1752	1	1638	3	114	0.33
Pentafluorophenyl	1774	2	1636	5	138	0.41
p-Phenylene,di-	1726	5	1637	6	89	0.83
Bisphenol A,di-	1726	6	1626	5	100	1.21
1-Naphthyl	1731	1	1637	1	94	1
2-Naphthyl	1735	1	1634	2	101	0.51

(continued)

TABLE 15.13 (continued)

Group	[R]C=O str. cm ⁻¹	RI	C=C str. cm ⁻¹	RI	C=O str.-C=C str. cm ⁻¹	RI C=O/ RI C=C
Vinyl	1740	4	1630	9	110	0.44
Propargyl	1728	2	1637	7	91	0.29
N,N-dimethylaminoethyl	1724	4	1638	9	86	0.44
2-(N-morpholino)ethyl	1723	4	1637	4	86	0.57
3-Dimethylamino-neopentyl	1725	4	1636	7	89	0.57
3-Sulfopropyl potassium salt	1719	1	1638	4	81	0.25
Range	1717-1774		1623-1640		81-138	

TABLE 15.13A IR C=O stretching frequency data and other group frequency for alkyl acrylates [CHCl₃ and CCl₄ solutions]

Mole % CHCl ₃ /CCl ₄	Methyl acrylate C=O str.	2-Hydroxy- butyl acrylate C=O str.	Allyl acrylate C=O str.	2-Hydroxy- propyl acrylate C=O str.	Butyl acrylate C=O str.	2-Ethyl- hexyl acrylate C=O str.	tert-Butyl acrylate
[vapor]	1751				1741		
0	1734.1	1730.6	1730.5	1729.4	1727.3	1727.1	1722.9
100	1724.5	1721.6	1727.1	1721.3	1716.7	1716.3	1713.8
[delta cm ⁻¹]	16.9;26.5;9.6	9	3.4	8.1	13.8;24.3;10.6	10.8	9.1
	s-trans C=C str.	s-trans C=C str.	s-trans C=C str.	s-trans C=C str.	s-trans C=C str.	s-trans C=C str.	s-trans C=C str.
0	1635.3	1636.5	1635.4	1637	1637.2	1635.7	1635.6
100	1635.1	1636.1	1635.4	1636.6	1635.8	1636.3	1635.8
[delta cm ⁻¹]	-0.2	-0.4	0	-0.4	-1.4	0.6	0.2
	s-cis	s-cis	s-cis	s-cis	s-cis	s-cis	s-cis
0	1620.4	1619.3			1619.7		1619.2
100	1619.9				1619.2		1618.5
[delta cm ⁻¹]	-0.5				-0.5		-0.7
	CH ₂ =bend	CH ₂ =bend	CH ₂ =bend	CH ₂ =bend	CH ₂ =bend	CH ₂ =bend	CH ₂ =bend
0		1406.4	1404.6	1406.6	1407.2	1406.5	1401.6
100		1409.4	1407	1409.5	1410.3	1409.9	1404
[delta cm ⁻¹]		3	2.4	2.9	3.1	3.4	2.4
	HC=CH twist	HC=CH twist	HC=CH twist	HC=CH twist	HC=CH twist	HC=CH twist	HC=CH
0	984.9	982.6	984.7	983.3	983.5	983.6	984.45
100	985	983.4	984.4	983.9	984.3	984.5	985.6
[delta cm ⁻¹]	0.1	0.8	-0.3	0.6	0.8	0.9	1.1
	C=CH ₂ wag	C=CH ₂ wag	C=CH ₂ wag	C=CH ₂ wag	C=CH ₂ wag	C=CH ₂ wag	C=CH ₂ wag
0	968.1	982.6			968.4		966.3
100	970.3	983.4			969		966.5
[delta cm ⁻¹]	2.2	0.8			0.6		0.2

TABLE 15.14 Raman data for methacrylates in the neat phase and summary of IR data in CHCl₃ and CCl₄ solutions

	C=O str.	RI	C=C str.	RI	C=O str. minus C=C str.	RI C=O str./ RI C=C str.	C=O str.Acr.– C=O str. Methacr.	C=C str.Methacr.– C=C str.Acr.
Methyl [IR vapor]	1741							
Propyl	1719	5	1641	7	78	0.71	4	2
Pentyl [IR vapor]	1739							
Pentyl	1719	4	1641	6	78	0.67		
Hexyl	1720	3	1640	5	80	0.6		
Heptyl	1720	3	1640	4	80	0.75	5	1
Octyl	1720	3	1641	4	79	0.75		
Nonyl	1720	3	1641	79	0.75	6	2	
Decyl [IR vapor]	1739							
Decyl	1720	3	1641	4	79	0.75		
Undecyl	1720	3	1641	9	79	0.33	6	1
Dodecyl	1721	2	1641	3	80	0.67	6	2
Hexadecyl	1721	2	1641	2	80	1	7	3
Octadecyl	1721	1	1640	2	81	0.5		
2-Ethylhexyl	1720	3	1641	4	79	0.75	5	3
Oleyl	1720	2	1641	3	79	0.67	8	2
Isopropyl	1716	4	1641	6	75	0.67	5	1
sec-Butyl	1715	4	1640	5	75	0.8		
isoBornyl	1716	2	1640	3	76	0.67	6	2
isoButyl	1719	5	1641	7	78	0.71	6	3
isoAmyl	1719	4	1640	6	79	0.67	6	1
isoDecyl	1720	3	1641	4	79	0.75		
2-Phenylethyl	1717	2	1641	2	77	1	5	3
2-Phenoxyethyl	1720	1	1639	2	81	0.5		
2-Ethylethyl	1719	4	1640	79	0.67			
Ethoxytriethylene glycol	1719	4	1640	5	79	0.8		
2-Hydroxyethyl	1718	5	1640	9	78	0.56	4	1
2-Hydroxybutyl	1716	4	1639	9	77	0.44	5	1
2-Methoxypropyl	1717	5	1640	7	77	0.71		
2-Methoxybutyl	1718	4	1640	6	78	0.67	6	1
Glyceryl tri-	1721	7	1639	9	82	0.78		
Ethylene, di-	1720	6	1640	9	80	0.67	3	1
1,9-Nonanediol,di	1717	4	1640	6	77	0.67		
1,10-Decanediol,di	1717	4	1640	6	77	0.67	5	2

(continued)

TABLE 15.14 (continued)

	C=O str.	RI	C=C str.	RI	C=O str. minus C=C str.	RI C=O str./ RI C=C str.	C=O str.Acr.– C=O str. Methacr.	C=C str.Methacr.– C=C str.Acr.
2-Bromoethyl	1720	1	1639	2	81	0.5	6	2
tribromoepentyl	1723	1	1639	2	84	0.5	7	2
Trichloroethyl	1742	2	1637	1	105		2	
2,2,2-Trifluoroethyl	1738	6	1640	9	98	0.67	10	2
1,H,1H,3H-Tetra-fluoropropyl	1735	6	1640	9	95	0.67		
Hexafluorobutyl	1736	6	1641	9	95	0.67	10	2
Dodecafluoro-1-heptyl	1739	4	1641	7	98	0.57		
Pentadecylfluoro-octyl	1743	5	1641	7	102	0.71	9	2
1H,1H,2H-Hepta-decylfluorodecyl	1727	3	1642	4	85	0.75		
Phenyl	1735	3	1639	4	96	0.75	4	4
p-Nonylphenyl	1738	4	1639	5	99	0.8		
p-Nitrophenyl	1742	2	1636	1	106	2	6	4
Pentabromophenyl	1737	1	1635	1	102	1	1	10
Pentachlorophenyl	1745	4	1637	1	108	1.33	7	-1
Pentafluorophenyl	1762	2	1639	2	123	1	12	3
Bisphenol A, di-	1718	5	1639	7	79	0.79	8	13
4-Hydroxy-benzophenone	1737	2	1629	7	108	0.29		
2-Naphthyl	1729	2	1639	2	90	1	6	5
Methylallyl	1720	5	1640	8	80	0.63		
Allyl	1720	5	1641	8	79	0.63		
Propargyl	1724	3	1640	5	84	0.6		
N,N-Dimethylamino-ethyl	1719	6	1640	8	79	0.75	5	2
2-(1-Aziridinyl) ethyl	1718	6	1640	8	78	0.75		
2-Aminoethyl hydrochloride	1719	4	1639	8	78	0.5		
Trimethylammonium ethyl methosulfate	1717	1	1640	3	77	0.33		
3-Sulfopropyl	1713	2	1639	3	74	0.67	6	1
Range	1713–62		1635–42		77–123			
Infrared Range in CCl ₄ soln.	1719–26		1637.3–38					
Infrared Range in CHCl ₃ soln.	1709.5–18		1635.7–37.3					

TABLE 15.15 IR vapor-phase data and assignments for alkyl cinnamates [C=C stretching, CH=CH twisting, and C=O stretching]

Cinnamate	C=O str.	C=C str.	[(A)C=C]/ [(A)C=O]	HC=CH twist	[(A)HC=CH twist]/ [(A)C=C str.]	[(A)HC=CH twist]/ [(A)C=O str.]
Methyl	1740(1.141)	1640(0.431)	0.38	975(0.181)	0.42	0.16
Ethyl	1735(1.050)	1640(0.370)	0.35	975(0.169)	0.46	0.16
Butyl	1731(1.141)	1641(0.379)	0.33	978(0.205)	0.54	0.18
Isobutyl	1735(0.806)	1641(0.310)	0.38	975(0.130)	0.42	0.16
Isopentyl	1737(0.830)	1642(0.282)	0.34	980(0.171)	0.61	0.21
Isopropyl	1731(1.250)	1641(0.500)	0.41	982(0.310)	0.62	0.25
Tert-butyl	1727(1.030)	1640(0.370)	0.36	972(0.247)	0.67	0.24
Cyclohexyl	1731(0.654)	1642(0.214)	0.33	980(0.129)	0.6	0.2
Benzyl	1739(0.959)	1640(0.371)	0.39	980(0.246)	0.66	0.26

TABLE 15.15A IR vapor-phase data and assignments for alkyl cinnamates [in-plane and out-of-plane phenyl ring vibrations]

Cinnamate	[1] cm ⁻¹ (A)	[2] cm ⁻¹ (A)	[3] cm ⁻¹ (A)	[4] CCO str. cm ⁻¹ (A)	[5] COC str. cm ⁻¹ (A)	[6] i.p.o.p.5H Ring def. cm ⁻¹ (A)	[7] o.p.Ring def. cm ⁻¹ (A)
Methyl	1314(0.750)	1269(0.850)	1199(0.700)	1166(1.240)	1045(0.180)	765(0.199)	695(0.159)
Ethyl	1309(0.599)	1259(0.690)	1199(0.490)	1165(1.240)	1042(0.325)	761(0.158)	690(0.120)
Butyl	1309(0.490)	1265(0.605)	1199(0.465)	1170(1.240)		764(0.136)	688(0.110)
Isobutyl	1310(0.440)	1250(0.500)	1199(0.460)	1161(1.240)		763(0.115)	690(0.080)
Isopentyl	110(0.470)	1252(0.450)	1200(0.370)	1165(1.210)		764(0.110)	688(0.072)
Isopropyl	1309(0.690)	1268(0.770)	1199(1.250)	1171(1.250)		763(0.162)	688(0.130)
Tert-butyl	1314(0.589)	1276(0.559)	1199(0.580)	1155(1.250)		761(0.166)	685(0.094)
Cyclohexyl	1307(0.280)	1268(0.365)	1199(0.292)	1170(1.240)	1042(0.180)	764(0.081)	690(0.061)
Benzyl	1304(0.511)	1245(0.750)	1198(0.480)	1154(1.234)	1011(0.331)	750(0.192)	696(0.345)
	[(A)[1]]/[(A)[4]]	[(A)[2]]/[(A)[4]]	[(A)[3]]/[(A)[4]]		[(A)[6]]/[(A)[7]]	[(A)C=C str.]/[(A)[4]]	
Methyl	0.61	0.68	0.56		1.25	0.35	
Ethyl	0.48	0.56	0.41		1.32	0.31	
Butyl	0.41	0.48	0.38		1.24	0.31	
Isobutyl	0.35	0.4	0.37		1.44	0.25	
Isopentyl	0.39	0.37	0.31		1.53	0.23	
Isopropyl	0.55	0.62	0.48		1.25	0.41	
Tert-butyl	0.47	0.45	0.46		1.75	0.31	
Cyclohexyl	0.23	0.29	0.24		1.32	0.17	
Benzyl	0.41	0.61	0.39		0.56	0.131	

TABLE 15.15B IR data for alkyl cinnamates

Cinnamate	2(C=O) cm ⁻¹ (A)	Ring C-H cm ⁻¹ (A)	Ring C-H cm ⁻¹	a.CH ₃ str. cm ⁻¹ (A)	a.CH ₂ str. cm ⁻¹ (A)	s.CH ₃ str. cm ⁻¹ (A)	s.CH ₂ str. cm ⁻¹ (A)	a.CH ₃ def. cm ⁻¹ (A)	CH ₂ bend+ Ring cm ⁻¹ (A)	s.CH ₃ def. cm ⁻¹ (A)
Methyl	3470(0.010)	3075(0.200)	3040(0.150)	2961(0.281)		2850(0.051)		1442(0.290)		
Ethyl	3459(0.010)	3070(0.160)	3035(0.100)	2985(0.211)	2942(0.119)	2910(0.070)	2885(0.050)	1470(0.090)	1450(0.110)	1400(0.070)
Butyl	3458(0.005)	3075(0.149)	3040(0.090)	2984(0.392)	2943(0.199)		2895(0.112)	1452(0.132)		1385(0.122)
Isobutyl	3458(0.005)	3075(0.080)	3040(0.081)	2975(0.350)	2960(0.200)		2885(0.129)	1469(0.080)	1451(0.100)	1379(0.150)
Isopentyl	3458(0.005)	3075(0.120)	3040(0.070)	2969(0.440)	2950(0.190)	2920(0.170)	2882(0.120)	1470(0.101)	1451(0.110)	1390(0.090)
Isopropyl	3446(0.011)	3075(0.175)	3040(0.115)	2985(0.487)		2945(0.142)	2888(0.060)	1470(0.090)	1451(0.140)	1380(0.169)
Cyclohexyl	3446(0.005)	3075(0.0830)	3040(0.052)		2942(0.652)		2868(0.159)		1453(0.095)	
Tert-butyl	3435(0.008)	3065(0.150)	3030(0.090)	2984(0.420)		2939(0.161)		1475(0.090)	1451(0.120)	1395(0.170)
Benzyl	3469(0.005)	3070(0.289)	3039(0.080)		2960(0.099)	2899(0.029)			1371(0.300)	
									1450(0.143)	

TABLE 15.16 The C=O stretching frequencies for phenoxarsine derivatives in the solid state and in CCl₄ solution

Phenoxarsine X=O-(C=O)-R	C=O str. [CCl ₄ soln.] cm ⁻¹	C=O str. [Nujol mull] cm ⁻¹
R		
methyl	1698	
chloromethyl	1720	1702
	1696	
trichloromethyl	1725	1717
trifluoromethyl	1738	1737
X=S-(C=O)-R		
R		
methyl	1681	
ethyl	1680	1671
propyl	1671	1661
isopropyl	1675	1669
isobutyl	1675	
octyl	1677	
cyclohexyl	1669	1660
2-cyclohexylethyl	1671	1661
benzyl	1670[CS2]	1671
phoxymethyl	1694;1665	
2,4,5-trichloro-phoxymethyl	1691;1665	1650
alpha-(2,4,5-tri-chlorophenoxy)ethyl	1682;1665	
carbethoxy	1759;1675	1762;1670
	1742	
2-furyl	1646;1631	1630
phenyl	1645	
4-t-butylphenyl	1650	
4-methoxyphenyl	1638[CS2]	1628
4-n-butoxyphenyl	1641	
4-n-pentoxyphenyl	1643	1635
3,4,5-triethoxyphenyl		1625
diethylamino	1624	
piperidino	1631	

TABLE 15.17 IR data for alkyl thiol esters and phenyl thiol esters

Alkyl thiol ester R-C(=O)-S-R' R' is C ₄ H ₉ or C ₆ H ₁₃	C=O str. cm ⁻¹	C=O str. cm ⁻¹	Phenyl thiol ester R-C(=O)-S-C ₆ H ₅	C-C≡str. R' analog cm ⁻¹	C-C≡str. C ₆ H ₅ analog cm ⁻¹	S-C≡str. R' analog cm ⁻¹	S-C≡str. C ₆ H ₅ analog cm ⁻¹
R			R				
Formate*	1675	1693	Formate			755	730
Acetate	1695	1711	Acetate	1137	1111	955	947
chloro-	1671(s)	1691(s)	chloro-	1089	1065	1000	986
	1699(m)	1725(m)					
dichloro-	1682(s)	1700(s)	dichloro-	1085	1070	990	976
	1703(m)	1736(m)					
trichloro-	1699	1711	trichloro-	?	?	1032	1018
trifluoro-	1710	1722	trifluoro-	?	955	?	930
Propionate	1691	1710	Propionate	1090	1088	937	925
Butyrate	1693	1710	Butyrate	1111	1111	989	975
Dialkyl dithiol esters							
Oxalate	1680	1698	Oxalate			790	770
Succinate	1690	1705	Succinate	~ 1050	~ 1050	985	970
Adipate		1710			~ 1010		~ 940
	C-H str. cm ⁻¹	C-H str. cm ⁻¹		C-H bend cm ⁻¹	C-H bend cm ⁻¹	2(C-H bend) cm ⁻¹	2(C-H bend) cm ⁻¹
Formate*	2835	2825		1345	1340	2680	2660

TABLE 15.17A IR data for alkyl thioesters and phenyl thiol esters

Alkyl thiol ester R-C(=O)-S-R' R' is C ₄ H ₉ or C ₆ H ₁₃	C=O str. cm ⁻¹	C=O str. cm ⁻¹	Phenyl thiol ester R-C(=O)-S-C ₆ H ₅
R			R
Acetate	1695	1711	Acetate
chloro-	1671(s)	1691(s)	chloro-
	1699(m)	1725(m)	
dichloro-	1682(s)	1700(s)	dichloro-
	1703(m)	1736(m)	
trichloro-	1699	1711	trichloro-
trifluoro-	1710	1722	trifluoro-
Propionate	1691	1710	Propionate
Butyrate	1693	1710	Butyrate

TABLE 15.17B IR data for Thiobenzoates

Thiol benzoate ring substitution	Alkyl thiol benzoate C=O str. cm ⁻¹	Phenyl thiol benzoate C=O str. cm ⁻¹	Alkyl analog C-C str. cm ⁻¹	Phenyl analog C-C str. cm ⁻¹	Alkyl analog S-C str. cm ⁻¹	Phenyl analog S-C str. cm ⁻¹
Thiol benzoate	1665	1685	1203	1205	915	898
2-F	1648 1675 1701(w)	1667 1690 1701(w)	1205	1196	920	906
2-Cl		1696		1198		898
2-Br		1700		1198		898
2-I	1679	1698	1205	1200	910	897
2-CH ₃ O	1640 1672	1652 1700	1193	1190	904	888
2-HO		1640		1192		918
3-I	1670	1689	1195	1191	938	913
3-NO ₂		1689		1203		939
4-Br	1669	1681	1204	1199	913	898
4-NO ₂		1683		1197		907
Dithiol phthalate diphenyl		1675 1690		1193 1211		913

TABLE 15.17C IR data for thiol acids, thiol anhydrides, and potassium thiol benzoate

Compound	C=O str.	C-C str.	S-C str.	S-H str.	S-H bend
Thiol acetic acid	1712	1122	988	2565	828
Thiol benzoic acid	1690	1210	950	2585	835
2-chloro-	1700	1207	945	2580	837
	[O=C]2-S str.				
Thiol benzoic anhydride	1739 1709 1680	1202 1178	860		
Potassium thiol benzoate	asym. COS str. 1525	1203	948		

TABLE 15.18 Raman data and assignments for propargyl acrylate and propargyl methacrylate

Propargyl acrylate	Assignment	Propargyl methacrylate
3111(1)	a.CH ₂ =str.	3110(1)
3042(2)	s.CH ₂ =str.	
2994(1)	a.CH ₂ str.	2998(2)
2953(1)	s.CH ₂ str.	
	s.CH ₃ str.	2933(2)
2132(9)	CC str.	2132(9)
1728(2)	C=O str.	1724(3)
1637(7)	C=C str.	1640(5)
1439(1)	CH ₂ bend	1439(1)
1410(2)	CH ₂ =bend	1405(3)
1368(0)	CH ₂ wag	1372(1)
	CH=rock	1319(0)
1293(2)	CH=rock	
1073(0)	CH ₂ =rock	
	s.COC str.	1016(1)
992(2)	CH ₂ rock	
958(2)	s.COC=str.	962(2)
	CH ₃ rock?	946(2)
935(1)	C-C str.	
	C-C str.	922(0)
	C-C str.	852(1)
842(2)	C-C str.	
	CH ₂ =twist	820(3)
		605(1)
		592(1)
		564(0)
408(1)		377(1)
	C-O-O ₃ bend,a'	350(2)
309(5)	C-CC bend,a''	306(5)
238(6)	C-CC bend,a'	227(5)

TABLE 15.19 IR vapor-phase data for R-C(=)-OR' skeletal stretching

R-C(=O)-O-R'	R' is Alkyl cm ⁻¹	R' is Allyl cm ⁻¹	R' is Benzyl cm ⁻¹	R' is Vinyl cm ⁻¹	R' is Isopropenyl cm ⁻¹	R' is Phenyl cm ⁻¹
Formate	1158-1180		1152-1159			
Acetate	1231-1250	1231		1215	1202	1201-1203
Propionate	1182-1194	1180		1162		1200
Butyrate	1176-1185		1170	1155		
Valerate	1171-1178	1165				
Hexanoate	1168-1171					
Heptanoate	1165-1170					
Octanoate	1165-1169	1160				
Nonanoate	1162-1169	1160				
Decanoate	1160-1169			1151		
Tetradecanoate	1170-1177					
Octadecanoate	1165-1178			1150		
Acetate	1231-1250					
2-Methylacetate	1182-1194					
2-Ethylacetate	1176-1181					
2-Propylacetate	1173-1178					
2-Butylacetate	1168-1171					
2-Alkylacetates	1165-1172					
2,2-Dimethylacetate	1145-1159					
2,2,2-Trimethylacetate	1110-1156					
2,-Cyanoacetate	1160-1172					
2-Chloroacetate	1159-1171					
2,2-Dichloroacetate	1160					1101
2,2,2-Trichloroacetate	1235-1241					1181
Diesters						
Oxalate	1152-1164					
Malonate	1139-1153					
Succinate	1159-1166					
Glutarate	1170-1175					
Adipate	1151-1179					
Sebacate	1161-1171					

TABLE 15.20 IR vapor-phase data for conjugated esters [aryl-C(=)-OR or C=C-C(=)-OR skeletal stretching

Compound	Alkyl or Dialkyl cm ⁻¹	Phenyl cm ⁻¹	Alkyl or Dialkyl cm ⁻¹	Phenyl cm ⁻¹
Benzoate	1235-1294	1260	1089-1145	1200
Phthalate	1260-1281		1111-1128	
Isophthalate	1229-1240		1092-1095	
Terephthalate	1263-1270		1100-1107	
Nicotinate	1272-1280		1105-1111	
Isonicotinate	1272-1281		1115-1120	
Picolinate	1305-1311		1130-1131	
Salicylate	1300-1305	1300	1082-1111	1061
Crotonate	1176-1190		1021-1048	

Organic Carbonates, Thiol Carbonates, Chloroformates, Thiol Chloroformates, Acetyl Chloride, Benzoyl Chloride, Carbamates, and an Overview of Solute-Solvent Effects upon Carbonyl Stretching Frequencies

Carbonates $(-O-)_2C=O$	392
Monothio Carbonates $-O-C(=O)-S-$	393
Chloroformates $R-O-C(=O)Cl$ and $\phi-O-C(=O)Cl$	393
Dithiol Carbonates $(-S-C(=O)-S-)$	393
Ring Strain	393
Thiol Chloroformates $Cl-C(=O)-S$	394
Intramolecular Hydrogen Bonding	396
An Overview of the Solute-Solvent Effects Upon Carbonyl Stretching Frequencies	397
Solvent Acceptor Numbers (AN)	398
Concentration Effects	399
Dipolarity-Polarizability Effect	399
References	400

Figures

Figure 16-1a	402	Figure 16-4	407 (394)
Figure 16-1b	403	Figure 16-5	408 (394)
Figure 16-1c	404	Figure 16-6	409 (395)
Figure 16-2	405	Figure 16-7	410 (399)
Figure 16-3	406 (394)		

Tables

Table 16-1	409 (390)	Table 16-3	411
Table 16-2	410 (392)	Table 16-4	412 (392)

Table 16-4a	413 (392)	Table 16-5	415 (393)
Table 16-4b	413 (392)	Table 16-6	415 (392, 293)
Table 16-4c	414 (393)	Table 16-7	416 (393, 397)
Table 16-4d	414 (393)	Table 16-8	417

*Numbers in parentheses indicate in-text page reference.

In developing spectra-structure correlations it is helpful to know the molecular vibrations of some relatively simple model compounds. In this case, these include dihalocarbonyl compounds such as $F_2C=O$, $FCIC=O$, and $Cl_2C=O$. The normal modes as obtained by Overend and Scherer (1) for these three carbonyl halides are depicted in Figs. 16.1a-c. The normal skeletal stretching modes for $F_2C=O$ and $Cl_2C=O$ are best described as symmetric and asymmetric X_2C stretching, while for $FCIC=O$ they are best described as C-X and C-Y stretching. These model compounds are useful in predicting where the similar molecular vibrations for compounds of forms $(R-O)_2C=O$, $(R-S)_2C=O$, $(R-S)(R-O)C=O$, $(R-S)C(=O)Cl$, $(R-O)C(=O)Cl$, $(R-O)C(=O)NH_2$, etc. are expected to occur in the IR region of the electromagnetic spectrum.

In addition, Overend and Evans (2) have shown that the force constant of the out-of-plane skeletal deformation is similar to the sum of Taft σ_R and σ_1 parameters, therefore, it is expected that this out-of-plane skeletal deformation is sensitive to the mass as well as the resonance and inductive parameters of the X and Y substituents for compounds containing the $XYC=O$ skeletal structure.

Table 16.1 summarizes the IR group frequency data for organic carbonates, thiol carbonates, chloroformates, thiol chloroformates, carbamates and related compounds (3). In all of the compounds listed in Table 16.1 it is noted that when compounds whose carbonyl substituents are phenyl-O- or phenyl-S- are compared to analogous compounds whose substituents are alkyl-O- or alkyl-S-, consistent frequency differences are noted: (1) the carbonyl stretching frequency is always higher for the aromatic containing compounds than for the aliphatic containing compounds; (2) the frequency of the asymmetric $X_2C=$ or $Y_2C=$ stretch, or the X-C= stretch in unsymmetrical $XYC=O$ compounds, is always lower for the aromatic compounds than for the analogous aliphatic compounds; and (3) the carbonyl stretching frequency for the alkyl-O- or phenyl-O- always occurs at higher frequency than the analogous alkyl-S- or phenyl-S- $X_2C=O$ or $XYC=O$ compounds.

A possible explanation for these frequency shifts is that they are caused by resonance competition between the π -electron of the phenyl ring and the π -electron of the carbonyl atom for overlap with the nonbonding electron pair of oxygen or sulfur: increase of electron overlap between the phenyl π electron and a nonbonding pair on oxygen or sulfur takes place at the expense of overlap between the carbonyl carbon π -electron and oxygen or sulfur non-bonding pairs; this results in a reduced force constant and stretching frequency for $X_2C=$, $Y_2C=$ and $XYC=$ bonds, but increased force constant and stretching frequency of the $C=O$ bond (3).

CARBONATES $(-O-)_2C=O$

The carbonyl stretching frequency for compounds of type $(R-O-)(R'-O)C=O$ is $\sim 1739\text{ cm}^{-1}$, for compounds of type $(\phi-O-)(R-O)C=O$, the range is $1754\text{--}1787\text{ cm}^{-1}$, and it is 1775--

1819 cm^{-1} for compounds of type $(\phi-\text{O}-)_2\text{C}=\text{O}$. These carbonates exhibit asymmetric $\text{C}(-\text{O}-)_2$ stretching in the range 1205–1280 cm^{-1} , and the out-of-plane skeletal deformation occurs in the range 785–800 cm^{-1} (3).

MONOTHIOL CARBONATES $-\text{O}-\text{C}(=\text{O})-\text{S}-$

Compounds of types $(\text{R}-\text{O}-)\text{C}(=\text{O})-\text{S}-\text{R}$ and $(\phi-\text{O}-)\text{C}(=\text{O})(-\text{S}-\text{R})$ exhibit their carbonyl stretching frequencies in the range 1702–1710 cm^{-1} and 1730–1739 cm^{-1} , respectively, while for compounds of type $(\text{R}-\text{O}-)\text{C}(=\text{O})(-\text{S}-\phi)$ in the range 1719–1731 cm^{-1} . The band in the range 1056–1162 cm^{-1} is assigned to the $\text{C}-\text{O}$ stretching vibration. The out-of-plane skeletal deformation occurs in the range 650–670 cm^{-1} .

CHLOROFORMATES $\text{R}-\text{O}-\text{C}(=\text{O})\text{Cl}$ AND $\phi-\text{O}-\text{C}(=\text{O})\text{Cl}$

The alkyl chloroformates exhibit the carbonyl stretching frequency in the range 1775–1780 cm^{-1} , and it occurs at 1784 cm^{-1} in the case of phenyl chloroformate. The $\text{C}-\text{O}$ stretching vibration is assigned in the range 1139–1169 cm^{-1} and at 1113 cm^{-1} for alkyl chloroformates and phenyl chloroformate, respectively.

DITHIOL CARBONATES $(-\text{S}-\text{C}(=\text{O})-\text{S}-)$

The carbonyl stretching frequencies for the dithiol carbonates occur in the range 1640–1655, 1649, and 1714–1718 cm^{-1} for compounds of $(\text{R}-\text{S})_2\text{C}=\text{O}$, $(\text{R}-\text{S}-)(\phi-\text{S}-)\text{C}=\text{O}$, and $(\phi-\text{S}-)_2\text{C}=\text{O}$, respectively. The strong band in the range 827–880 cm^{-1} is assigned to the asymmetric $\text{S}_2\text{C}=\text{stretching}$ vibration (see Fig. 16.2), which shows the IR spectrum of diallyl dithiol carbonate (upper) and dipropyl dithiol carbonate (lower), respectively. The weak band in the range 554–595 cm^{-1} is assigned to the out-of-plane carbonyl skeletal deformation. A weak band in the region 700–750 cm^{-1} is assigned to $\text{C}-\text{S}$ stretching.

The asymmetric $\text{S}_2\text{C}=\text{mode}$ exhibits a strong first overtone that is sometimes higher or lower in frequency than the carbonyl stretching absorption band and it is in Fermi resonance with $\nu\text{C}=\text{O}$. The $\nu\text{C}=\text{O}$ frequencies are corrected in Table 16.1.

RING STRAIN

Ethylene carbonate, ethylene monothiol carbonate, and ethylene dithiol carbonate exhibit $\nu\text{C}=\text{O}$ at 1818.3, 1757, and ~ 1687 cm^{-1} , respectively. These $\nu\text{C}=\text{O}$ frequencies occur at higher frequency than their analogous open chain analogs by approximately 70, 50, and 40 cm^{-1} , respectively, after correction for Fermi resonance. This is the order of increasing ring size due to the fact that sulfur is larger than oxygen. As the ring size becomes smaller, there is a decrease in the $\text{X}-\text{C}-\text{X}$ bond angle, which makes it more difficult for the carbonyl carbon atom to vibrate in and out of the 5-membered ring. Thus, as the ring strain is increased, the carbonyl stretching mode increases in frequency.

THIOL CHLOROFORMATES $\text{Cl}-\text{C}(=\text{O})-\text{S}$

Alkyl thiol chloroformates and aryl thiol chloroformates exhibit $\nu\text{C}=\text{O}$ in the range $1766\text{--}1772\text{ cm}^{-1}$ and $1769\text{--}1775\text{ cm}^{-1}$, respectively, which is not as much difference as shown between alkyl chloroformates and phenyl chloroformate ($1775\text{--}1780\text{ cm}^{-1}$ and 1784 cm^{-1}). However, the $\nu\text{C}=\text{O}$ mode for alkyl thiol chloroformate is $\sim 1760\text{ cm}^{-1}$ CCl_4 solution after correction for Fermi resonance vs $1769\text{--}1775\text{ cm}^{-1}$ for aryl thiol chloroformate (see Fig. 16.3 for a comparison of the IR spectrum of methyl thiol chloroformate vs phenyl chlorothiol chloroformate). The strong IR band at $\sim 845\text{ cm}^{-1}$ for the methyl ester and the strong IR band at $\sim 815\text{ cm}^{-1}$ for the phenyl ester are assigned to asymmetric $\text{S}-\text{C}-\text{Cl}$ stretching. A more comprehensive vibrational assignment for methyl thiol chloroformate will be presented later in Table 16.6.

Ethylene carbonate has C_{2v} symmetry, its vibrational spectrum has been assigned, and its carbonyl stretching mode has been reported to be in Fermi resonance with the first overtone of the skeletal breathing mode. The skeletal breathing mode occurs at 897 cm^{-1} in the liquid phase, at 894 cm^{-1} in CHCl_3 solution, at 880 cm^{-1} in the vapor phase, and at 900 cm^{-1} in water solution, while the perturbed $\text{C}=\text{O}$ stretching mode is located in the region $1810\text{--}1870\text{ cm}^{-1}$, depending upon the physical state of the sample (4).

Table 16.2 lists the carbonyl stretching frequency for ethylene carbonate in various solvents. The IR band in the ranges $1770\text{--}1780\text{ cm}^{-1}$ and $1790\text{--}1815\text{ cm}^{-1}$ is in Fermi resonance. In each solvent system, the $\nu\text{C}=\text{O}$ mode has been corrected for Fermi resonance, and it occurs as low as 1791.7 cm^{-1} in solution in methanol and as high as 1812.5 cm^{-1} in solution in carbon tetrachloride (5).

Figure 16.4 shows plots of the $\nu\text{C}=\text{O}$ frequencies of ethylene carbonate corrected for Fermi resonance vs the solvent acceptor number (AN). Two separate plots are apparent. The upper plot includes methylene chloride, chloroform, tert-butyl alcohol, isopropyl alcohol, ethyl alcohol, and methyl alcohol while the lower plot includes diethyl ether, carbon tetrachloride, benzene, nitrobenzene, acetonitrile, benzonitrile, and dimethyl sulfoxide. Thus, it is apparent that the protic solvents correlate in a different manner than the so-called aprotic solvents. Thus, it again shows that the AN values do not take into account the factors determining the strength of the intermolecular hydrogen bond formed between the carbonyl oxygen atom of ethylene carbonate and the OH or C-H proton of the solvent system (5).

Figure 16.5 shows a plot of the carbonyl stretching frequencies of ethylene carbonate corrected for Fermi resonance vs the reaction field of the $\text{CHCl}_3/\text{CCl}_4$ solutions. The linear plot demonstrates a good correlation between $\nu\text{C}=\text{O}$ and its surrounding reaction field.

Table 16.3 compares the vibrational assignments for methyl chloroformate, 3-propynyl chloroformate, and chlorofluoro carbonyl (6). This comparison shows the value of utilizing the vibrational modes of a model compound such as $\text{FCl C}=\text{O}$ in assigning the six OCI $\text{C}=\text{O}$ skeletal vibrations for the alkyl chloroformates (6). It was shown that 3-propynyl chloroformate exists as rotational conformers.

Tables 16.4, 4a, and 4b list IR and Raman data and assignments for acetyl chloride, acetyl- d_3 chloride, and acetyl- d_1 chloride (7). These data serve as model compounds in the development of spectra structure correlations for compounds of forms $\text{CH}_3-\text{C}(=\text{O})(-\text{S}-\text{R})$ and $\text{CH}_3-\text{C}(=\text{O})(-\text{S}-\text{aryl})$. In the case of the d_1 analog, the presence of trans and gauche conformers is apparent (7). The $\nu\text{C}=\text{O}$ mode occurs at 1807 , 1812 , and 1802 cm^{-1} for the

CH₃, CD₃, and CDH₂ analogs, respectively. Data such as these show that the C=O stretching mode is not a "pure" molecular vibration.

Table 16.4c lists IR spectra-structure correlations for carboxylic acid halides in the vapor phase. Comparison of the $\nu\text{C}=\text{O}$ frequency for acetyl fluoride (1869 cm⁻¹) to $\nu\text{C}=\text{O}$ for benzoyl fluoride (1832 cm⁻¹) shows that the benzoyl analog exhibits $\nu\text{C}=\text{O}$ 37 cm⁻¹ lower in frequency than the acetyl analog. This lower $\nu\text{C}=\text{O}$ frequency is the result of conjugation of the phenyl group with the CO group, which weakens the C=O bond.

The $\nu\text{C}=\text{Cl}$ mode for compounds of form R-C(=O)Cl occurs in the range 570–601 cm⁻¹, and in the range 821–889 cm⁻¹ for compounds of form $\phi\text{-C(=O)Cl}$. The $\nu\text{C-F}$ mode for acetyl fluoride is assigned at 827 cm⁻¹ and for benzoyl fluoride it is assigned at 1022 cm⁻¹.

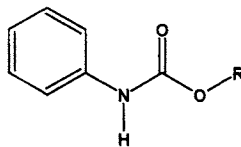
Table 16.4d lists IR spectra-structure correlations for benzoyl halides in the neat phase. Most of these compounds exhibit IR bands in the region 1750–1812 cm⁻¹ and in the region 1693–1815 cm⁻¹. The presence of two IR bands is the result of $\nu\text{C}=\text{O}$ being in Fermi resonance with an overtone or a combination tone of a lower lying fundamental (s). The $\nu\text{C}=\text{O}$ and the overtone have been corrected for Fermi resonance (see Table 16.4d).

An IR band in the region 1172–1245 cm⁻¹ is assigned to a complex mode involving aryl-C stretching. The $\nu\text{C-X}$ mode is assigned in the region 840–1000 cm⁻¹ in the neat phase.

Table 16.5 lists IR data for benzoyl chloride in CS₂ solution at temperatures between 31 and -70 °C. Figure 16.6 shows plots of $\nu\text{C}=\text{O}$, $2\nu\text{C-C(=)Cl}$, and $\nu\phi\text{-C(=)Cl}$ frequencies for benzoyl chloride in CS₂ vs temperature in °C. The carbonyl stretching frequency is in Fermi resonance with the first overtone of the C₆H₅-C-Cl stretching mode in the case of benzoyl chloride. Neither $\nu\text{C}=\text{O}$ nor $2\nu\phi\text{-C-Cl}$ has been corrected for Fermi resonance in this case (8). Perturbed $\nu\text{C}=\text{O}$ decreases in frequency from 1774.6 cm⁻¹ at 31 °C to 1771.2 cm⁻¹ at -70 °C while perturbed $2\nu\text{C-C-Cl}$ decreases in frequency from 1732.5 cm⁻¹ at 31 °C to 1731.3 cm⁻¹ at -70 °C. Moreover, $\nu\text{C-C-Cl}$ increases in frequency from 871.5 cm⁻¹ at 31 °C to 874.1 cm⁻¹ at -70 °C. In addition, the absorbance ratio $A[\nu\text{C}=\text{O}]/A[2\nu\text{C-C-Cl}]$ decreases from 4.44 at 31 °C to 3.03 at -70 °C. Thus, the absorbance of $2\nu\text{C-C-Cl}$ becomes larger as the $\nu\text{C-C-Cl}$ frequency increases with a decrease in temperature. These experimental data prove conclusively that the extent of Fermi interaction between these two vibrational modes increases with decreases in temperature. Of course, the combination or overtone must belong to the same symmetry species as the fundamental vibration. In this case $\nu\text{C}=\text{O}$ and $2\nu\text{C-C-Cl}$ belong to the A' symmetry species.

Table 16.6 compares the vibrational data for S-methyl thiol chloroformate with those for Cl₂C=O and s-methyl phosphoro-dichloridithioate. These comparisons show the value of model compounds in making the vibrational assignments for the S-C(=O)Cl group based on the molecular vibrations for Cl₂C=O. Moreover, the value of comparing vibrational assignments for a compound containing the CH₃-S- group is also demonstrated (9).

Table 16.7 lists IR spectra-structure correlations for carbamic acid: aryl-, alkyl esters (10). These carbamates have the following empirical structure:



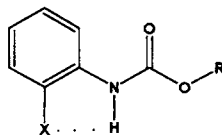
In CCl_4 solution these compounds exhibit the $\text{C}=\text{O}$ stretching mode in the range $1730\text{--}1755\text{ cm}^{-1}$ and the intermolecularly hydrogen-bonded $\nu\text{C}=\text{OH}-\text{N}$ frequency in the range $1705\text{--}1734\text{ cm}^{-1}$. In the solid state, $\nu\text{C}=\text{O}$ occurs at lower frequency at $\sim 1690\text{ cm}^{-1}$. The $\text{N}-\text{H}$ stretching mode occurs in the range $3409\text{--}3461\text{ cm}^{-1}$ and $\nu\text{N}-\text{H}\cdots\text{O}=\text{C}$ occurs in the range $3295\text{--}3460\text{ cm}^{-1}$. These IR bands are no longer present in dilute CCl_4 solution because in dilute solution these carbamates are not intermolecularly hydrogen bonded.

The in-plane bending and out-of-plane $\text{N}-\text{H}$ bending modes occur in the ranges $1504\text{--}1546\text{ cm}^{-1}$ and $503\text{--}570\text{ cm}^{-1}$, respectively. In the solid phase the out-of-phase $\text{N}-\text{H}$ bending mode occurs at even higher frequency, $624\text{--}680\text{ cm}^{-1}$. A complex mode involving aryl- N stretching is assigned in the range $1237\text{--}1282\text{ cm}^{-1}$.

In solution, an IR band occurs in the range $1195\text{--}1225\text{ cm}^{-1}$ and shifts to the range $1219\text{--}1257\text{ cm}^{-1}$ in the solid phase. This complex mode most likely is a mixture of $\text{N}-\text{C}-\text{O}$ stretching and $\text{N}-\text{H}$ in-plane bending (10).

INTRAMOLECULAR HYDROGEN BONDING

These carbamates have the following empirical structure:



where X is a halogen atom or a phenyl group.

The $\nu\text{N}-\text{HX}$ mode for 2-substituted carbamates occurs at 3345 , 3419 , 3409 , and 3425 cm^{-1} in 10 % wt./vol. in CCl_4 solution where X is F, Cl, Br, and phenyl, respectively. Comparable 3- and 4-substituted carbamates show IR evidence for intermolecular hydrogen bonding, but only the 2-F analog shows IR evidence for a small amount of intermolecular hydrogen bonding. In this case, F forms the weakest hydrogen bond in the series, which is most likely due to the relatively small size of the F atom. The strength of the intramolecular hydrogen $\text{N}-\text{H}\cdots\text{X}$ bond increases in the order F, Cl, and Br, and this is in the order of increasing size of the halogen atom. The larger size of Cl and Br also sterically interferes with intermolecular hydrogen bonding, and most likely contributes to the stabilization of the intramolecular hydrogen bond (10).

In the case of the 2-phenyl analog, the $\nu\text{N}-\text{H}\cdots\phi$ mode occurs at 3425 cm^{-1} . The 2-phenyl group in this case has to be perpendicular to the carbamate phenyl group in order for the $\text{N}-\text{H}$ group to intramolecularly hydrogen bond to its π system.

The 1-naphthyl alkyl carbamates differ from the 2-naphthyl alkyl carbamates in that they exhibit $\nu\text{N}-\text{H}$ in the ranges $3441\text{--}3461\text{ cm}^{-1}$ and $3425\text{--}3442\text{ cm}^{-1}$ while the 2-naphthyl analog only exhibits a band near 3445 cm^{-1} . The two $\nu\text{N}-\text{H}$ bands in the case of the 1-naphthyl analogs are attributed to the existence of rotational conformers [rotation about the naphthyl- N bond (10)].

The $\nu\text{N}-\text{H}$ frequencies within each series vary by as much as 20 cm^{-1} depending on the nature of the $\text{O}-\text{R}$ group in compounds of form $\phi-\text{N}-\text{H}-\text{C}(=\text{O})-\text{O}-\text{R}$. Compounds of form $\phi-\text{NH}-\text{C}(=\text{O})-\text{O}-\text{CH}_2-\text{CH}_2-\text{N}(-\text{CH}_3)_2$ exhibit the lowest $\text{N}-\text{H}$ frequencies in each series

studied, and occur in the region 3411–3440 cm^{-1} . These data suggest that there is a weak intramolecular hydrogen bond formed between the N–H proton and the β -nitrogen atom of the O–R group (10).

AN OVERVIEW OF THE SOLUTE-SOLVENT EFFECTS UPON CARBONYL STRETCHING FREQUENCIES

In $\text{CHCl}_3/\text{CCl}_4$ solutions the carbonyl stretching mode for a variety of compounds decreases in frequency as the mole % solvent is increased from 0 to 100. Mole % solvent is directly equivalent to the Reaction field surrounding the solute molecules. The Reaction field (R) involves both the dielectric constant and the refractive index of the solvent system.

$$|R| = (\epsilon - 1)/(2\epsilon + n^2)$$

where ϵ is the dielectric constant and n is the refractive index of the solvent.

$$\epsilon = \frac{Q_1 Q_2}{fr^2} \quad (\text{Reference 11})$$

Q_1 and Q_2 are the two charges of the solvent.

f is the force between the two charges.

r is the distance between the two charges.

Thus, the carbonyl stretching mode decreases in frequency as the Reaction field (R) increases; this is due mainly to the increasing electrically charged solvent molecules surrounding the solute molecules. In an aprotic solvent system such as $\text{CCl}_4/\text{C}_6\text{H}_{14}$ the carbonyl stretching frequency for a compound such as 1,1,3,3-tetramethylurea decreases in a linear manner as the mole % CCl_4 increases from 0 to 100. However, in the $\text{CHCl}_3/\text{CCl}_4$ solvent system the carbonyl stretching frequency for 1,1,3,3-tetramethylurea decreases in frequency in linear segments A, B, and C. It is suggested that segment A represents $\text{TMU}(\text{CHCl}_3)_1$, segment B represents $\text{TMU}(\text{CHCl}_3)_2$, and segment C represents $\text{TMU}(\text{CHCl}_3)_3$ complexes within the $\text{CHCl}_3/\text{CCl}_4$ solvent system (10). In contrast, acetone in $\text{CHCl}_3/\text{CCl}_4$ solvent system exhibits only one point of deviation from linearity as the mole % is increased from 0 to 100. In this case, the decrease due to intermolecular $\text{C}=\text{OHCCl}_3$ occurs within 17 mol % $\text{CHCl}_3/\text{CCl}_4$ (12).

The degree of carbonyl stretching frequency decrease in going from solution in CCl_4 to solution depends upon the basicity of the carbonyl group. For example, the carbonyl stretching frequency for acetone occurs at 1717.5 cm^{-1} in CCl_4 and at 1710.5 cm^{-1} in CHCl_3 , a decrease of 7 cm^{-1} (12). In the cases of 1,1,3,3-tetramethylurea, 1,1,3,3-tetraethylurea, and 1,1,3,3-tetra-butylurea the carbonyl stretching frequency in going from CCl_4 to CHCl_3 solution decreases by 25.6, 26.1, and 27.0, respectively (13). The carbonyl group becomes more basic as the four alkyl groups become larger as reflected by larger frequency decrease in going from CCl_4 to CHCl_3 solution.

The carbonyl stretching frequency for acetone occurs at 1735 cm^{-1} in the vapor phase and at 1713 cm^{-1} in the liquid phase while for 1,1,3,3-tetramethylurea it occurs at 1685 cm^{-1} in the vapor phase and at 1649.6 cm^{-1} in the liquid phase (10, 12). Thus, acetone shows a decrease of 22 cm^{-1} and 1,1,3,3-tetramethylurea shows a decrease of 35.4 cm^{-1} in going from the vapor to

the neat phase. These data indicate that the dipolar interaction between carbonyl groups $[(+C=O^-)_n]$ is larger in the case of 1,1,3,3-tetramethylurea than in the case of acetone (12). This is what is expected, as the carbonyl group of 1,1,3,3-tetramethylurea is more basic than the carbonyl group for acetone.

It has been shown that the carbonyl stretching frequency for ketones and esters is affected by steric factors of the $R-(C=O)-R'$ groups and for the R_1 group of $R_1-(C=O)-OR$. The steric factor of these alkyl groups increases as the dipolar distance increases between the dipolar sites in the solute and the dipolar sites of the solvent.

In summary, factors affecting solute-solvent interactions include the following:

- a. basicity of the $C=O$ group (dipolarity);
- b. acidity of the solvent group;
- c. the dielectric constant of the solvent (dipolarity);
- d. the refractive index of the solvent;
- e. steric factors of the solvent;
- f. steric factors of the solute;
- g. other basic sites in the solute; and
- h. concentration of the solute in the solvent.

Thus, the dipolar interaction between sites in the solute and solvent which causes shifts in the carbonyl stretching mode is complex and the magnitude of the carbonyl stretching shift can not be determined by a simple equation.

SOLVENT ACCEPTOR NUMBERS (AN)

Gutman developed solvent acceptor numbers utilizing NMR spectroscopy (14). The AN is defined as a dimensionless number related to the relative chemical shift of ^{31}P in $(C_2H_5)_3PO$ in that particular solvent with hexane as the reference solvent on one hand, and $C_2H_5)_3PO \cdot SbCl_5$ in 1,2-dichloroethane on the other—to which the acceptor numbers 0 and 100 have been assigned, respectively:

$$AN = \frac{\delta_{\text{corr}} - 100}{\delta_{\text{corr}}(C_2H_5)_3PO \cdot SbCl_5} = \text{Corr} - 2.348$$

Studies included in this book show that these AN values for the alcohols also included intermolecular hydrogen bonding between $C=O \cdot HOR$. In cases where both $C=O$ and $C=O \cdot \cdot HOR$ were determined, the carbonyl frequencies for the ketones or esters not intermolecularly hydrogen bonded, but surrounded by intermolecularly hydrogen-bonded alkyl alcohols, exhibit their carbonyl stretching mode at frequencies comparable to those recorded in dialkyl ethers. Thus, a large portion of the AN value for each alkyl alcohol is due to intermolecular hydrogen bonding, and a smaller portion of the AN value results from the $R-O$ portion of the alcohol complex.

Steric factors of the solute and solvent also appear to affect a linear correlation of carbonyl stretching frequencies vs AN. However, the AN values do help in spectra-structure identification of unknown chemical compounds.

CONCENTRATION EFFECTS

In an aprotic solvent such as CCl_4 dialkyl ketones would tend to cluster due to dipolar interaction between molecules $[(+\text{C}-\text{O}^-)_n]$, where n becomes larger as the wt. % solute/volume solvent increases. The carbonyl stretching frequency for diisopropyl ketone decreases 0.24 cm^{-1} in going from 0.75 to 7.5 % wt./vol. In CCl_4 solution and for di-tert-butyl ketone it decreases 0.05 cm^{-1} in going from 0.8 to 6.56 % wt./vol. In CCl_4 ; and although this carbonyl frequency decrease is attributed to clustering of ketone molecules, steric factors of the tert-butyl group prevent close interaction of the carbonyl groups compared to that for diisopropyl ketone (15).

In the case of CHCl_3 , the carbonyl stretching frequency for diisopropyl ketone increases 0.53 cm^{-1} in going from 0.22 % wt./vol. to 8.6 % wt./vol. in CHCl_3 solution, and for di-tert-butyl ketone 0.1 cm^{-1} in going from 0.40 % wt./vol. to 5.78 % : wt./vol. in CHCl_3 . This suggests that clustering of the diisopropyl ketone molecules at higher % wt./vol. solutions decreases the effect of intermolecular hydrogen bonding by a small amount. The effect appears to be small in the case of the tert-butyl analog due to steric effects of the tert-butyl groups compared to the isopropyl groups (14).

DIPOLARITY-POLARIZABILITY EFFECT

Recently, it has been reported that there is a coupled dipolarity-polarizability influence of the solvent upon the carbonyl stretching mode for 1,1,3,3-tetramethylurea (16). This observation is based in part on an SCRF-MO model, which assumes that the solute is located in a spherical cavity within an unstructured dielectric continuum. It is stated that the solvent dipolarity appears to exert the larger effect, along with making solvent polarizability detectable. However, it does not predict the effect of hydrogen bonding upon the carbonyl stretching frequency for 1,1,3,3-tetramethylurea (15).

It is interesting to compare the IR data used to develop the SCRF-MO model developed by Kolling (16) and the data reported by Nyquist (10, 13) and Wohar (17) as shown in Table 16.8. The AN values are those developed by Gutman (14) with the exception of the AN values in brackets, which are estimated from IR spectra-structure correlations.

Comparison of columns A, B, and C shows that there are some serious discrepancies between the three sets of data generated in three different laboratories.

It should be pointed out that with the exception of chloroform, methyl alcohol, ethyl alcohol, isopropyl alcohol, and tert-butyl alcohol, the carbonyl stretching frequencies correlate in a linear manner in the case of 1,1,3,3-tetramethylurea (10). The four alkyl alcohols also show two linear relationships vs AN. The linear relationship for the $\nu\text{C}=\text{O} \cdots \text{HOR}$ frequencies includes intermolecular hydrogen bonding in the Gutman AN value. The linear relationship for the $\nu\text{C}=\text{O}$ frequency (molecules surrounded by intermolecular hydrogen-bonded alcohols, but where $\text{C}=\text{O}$ is not hydrogen bonded) vs AN occurs at a significantly lower frequency. Projecting the points on the linear segment of $\nu\text{C}=\text{O}$ vs AN onto points on the plot for the aprotic solvents indicates that the AN values for intermolecularly hydrogen-bonded tert-butyl alcohol, isopropyl alcohol, and ethyl alcohol are approximately 5, 7, and 10, respectively (see Fig. 16.7). Thus, approximately 26–27 of the Gutman AN values for the four alkyl alcohols appear to be the result of

intermolecular hydrogen bonding (e.g., $\text{C}=\text{O} \cdots \text{HOR}$). The AN values of 5, 7, and 10 for tert-butyl alcohol, isopropyl alcohol, and ethyl alcohol for intermolecularly hydrogen-bonded alcohols, respectively, are comparable to the AN values for diethyl ether [3.9], methyl tert-butyl ether [5.0], and tetrahydrofuran [8.9] (10).

In the writer's opinion there are two reasons why the Gutman AN values are not a precise predictor of $\nu\text{C}=\text{O}$ frequencies in solvent systems. The first reason is intermolecular hydrogen bonding. The second is the steric factor of the solute and of the solvent, which alters the distance between the carbonyl group and the interactive site of the solvent molecules. Otherwise the AN values are useful in predicting the general direction of $\nu\text{C}=\text{O}$ frequency shift in a particular or similar type solvent.

The Nyquist values do correlate well with the AN values. However, there are serious discrepancies in the three sets of IR data for $\nu\text{C}=\text{O}$ for 1,1,3,3-tetramethylurea in hexane, diethyl ether, tetrahydrofuran, and hexamethyl phosphoramidate (see Table 16.8). In these four cases the data are significantly lower than the Nyquist (12) or Wohar data (17).

In the writer's opinion, the Kolling model is not correct in assuming that the solute is located in a spherical cavity within an unstructured dielectric continuum because steric factors of both the solute and solvent alter the spatial distance between the dipolar interactive sites between the solute and solvent. Furthermore, the accuracy of the experimental data is in question. The presence of a more polar solvent not flushed from the IR cell, or from the presence of water in the solute-solvent system would lower the $\nu\text{C}=\text{O}$ frequencies. Further experimental data are suggested to help clarify the theoretical aspects of solute-solvent interaction.

Finally, carbonyl stretching vibrations are often perturbed by Fermi interaction. Solvents either increase or decrease the amount of Fermi resonance between $\nu\text{C}=\text{O}$ and a combination or overtone of the same symmetry species as $\nu\text{C}=\text{O}$. Therefore, in order to obtain the exact frequency for $\nu\text{C}=\text{O}$ in this case in any solvent or solvent system, it is necessary to correct for Fermi resonance ($\nu\text{C}=\text{O}$ for 1,1,3,3-tetramethylurea is not in Fermi resonance).

REFERENCES

1. Overend, J. and Scherer, J. R. (1960). *J. Chem. Phys.*, **32**, 1296.
2. Overend, J. and Evans, J. C. (1959). *Trans. Faraday Soc.*, **551**, 1817.
3. Nyquist, R. A. and Potts, W. J. Jr. (1961). *Spectrochim. Acta*, **17**, 679.
4. Angell, C. L. (1956). *Trans. Faraday Soc.*, **52**, 1178.
5. Nyquist, R. A. and Settineri, S. E. (1991). *Appl. Spectrosc.*, **45**, 1075.
6. Nyquist, R. A. (1972). *Spectrochim. Acta*, **28A**, 285.
7. Overend, J., Nyquist, R. A., Evans, J. C., and Potts, W. J. Jr. (1961). *Spectrochim. Acta*, **17**, 1205.
8. Nyquist, R. A. (1986). *Appl. Spectrosc.*, **40**, 79.
9. Nyquist, R. A. (1967-68). *J. Mol. Structure*, **1**, 1.
10. Nyquist, R. A. (1973). *Spectrochim. Acta*, **29A**, 1635.
11. Lange, N. A. (ed.) (1961). *Handbook of Chemistry* p. 1728, 10th ed., New York: McGraw-Hill.
12. Nyquist, R. A., Putzig, C. L., and Hasha, D. L. (1989). *Appl. Spectrosc.*, **43**, 1049.
13. Nyquist, R. A. and Luoma, D. A. (1991). *Appl. Spectrosc.*, **45**, 1491.

14. Gutman, V. (1978). *The Donor-Acceptor Approach to Molecular Interactions*, p. 29, New York: Plenum Press.
15. Nyquist, R. A. and Putzig, C. L. (1989). *Appl. Spectrosc.*, 43, 983.
16. Kolling, O. W. (1999). *Appl. Spectrosc.*, 53, 29.
17. Wohar, M., Seehra, J., and Jagodzinski, P. (1988). *Spectrochim. Acta*, 44A, 999.

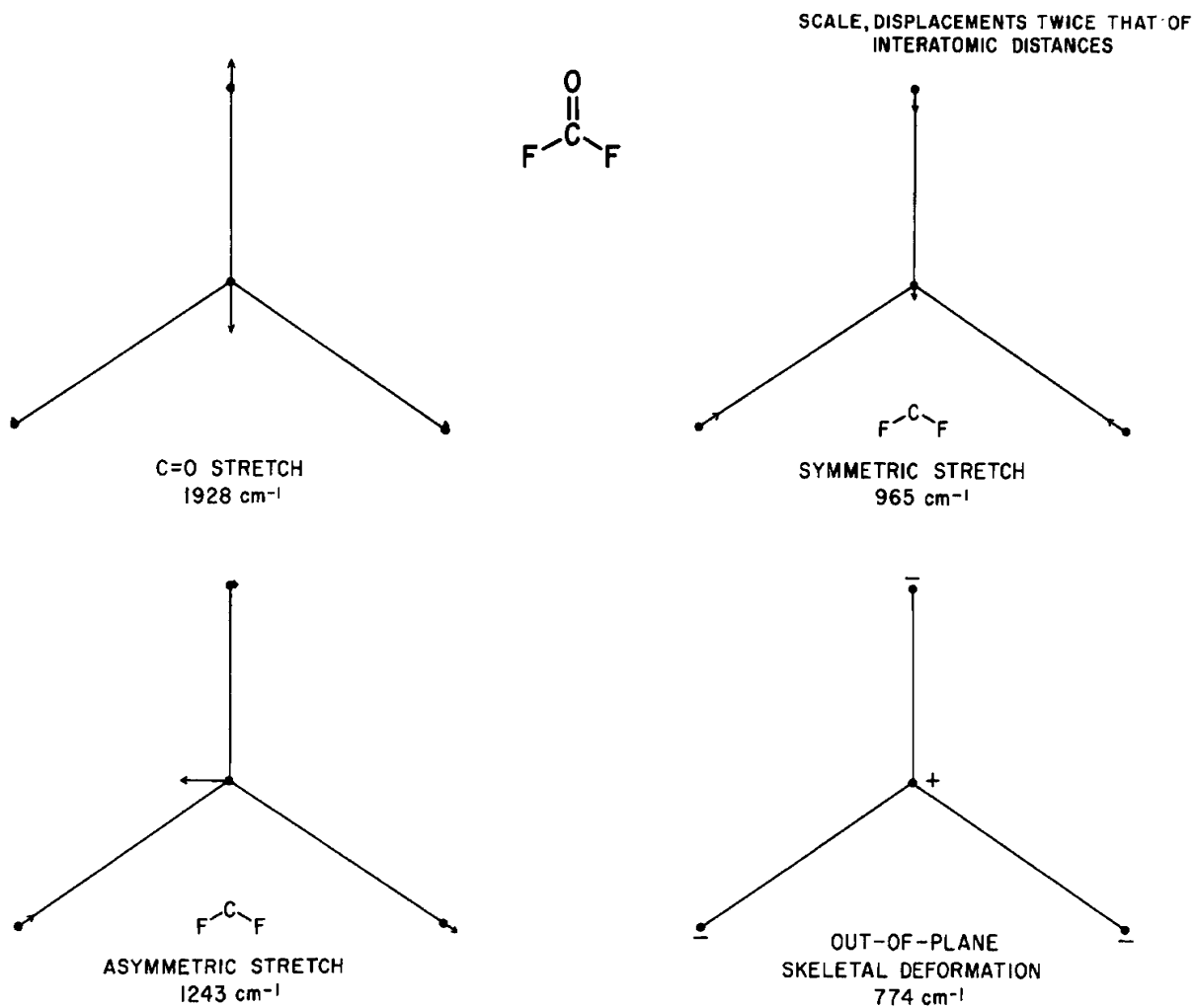


FIGURE 16.1a Normal modes for COF_2 .

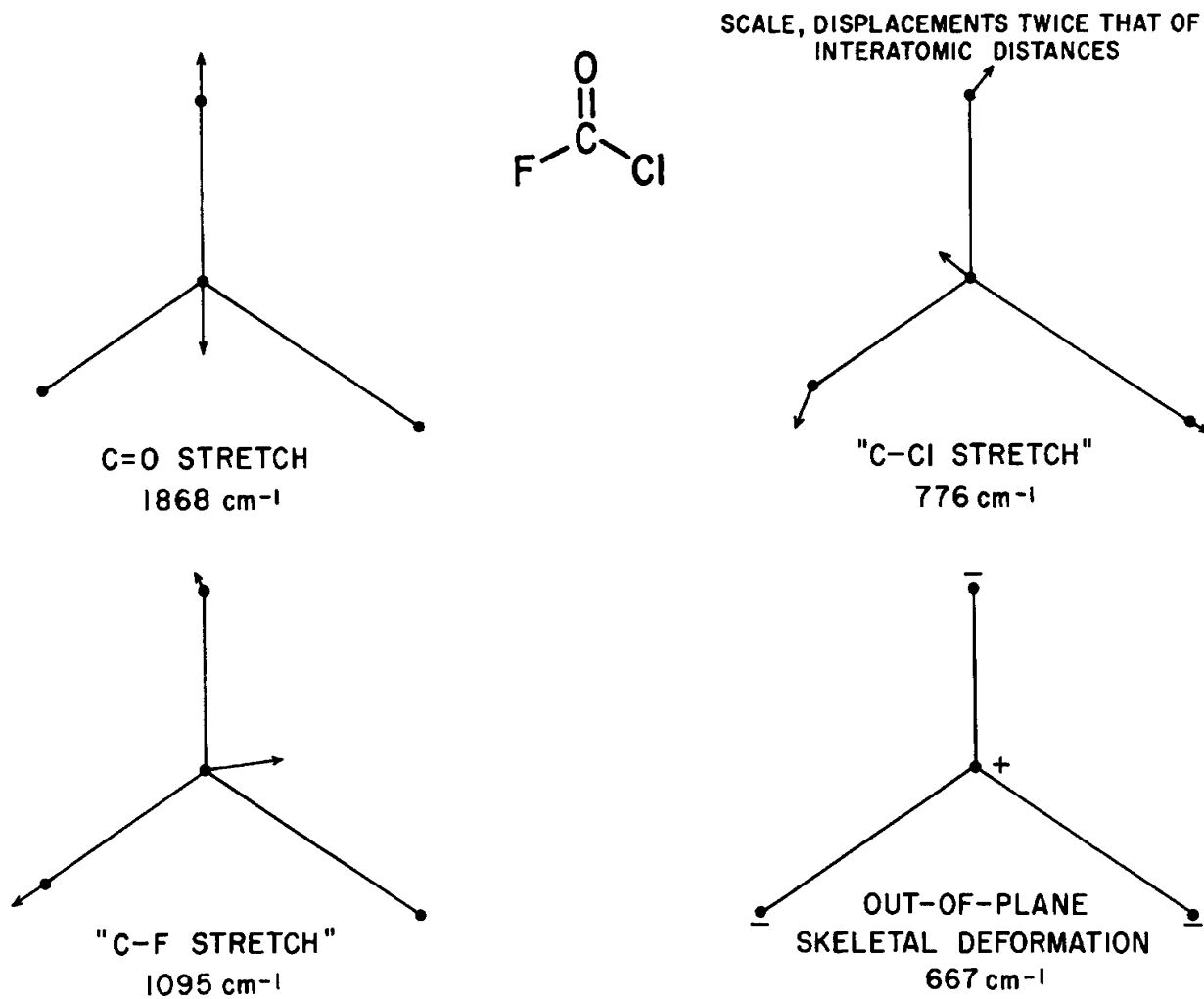


FIGURE 16.1b Normal modes for COClF

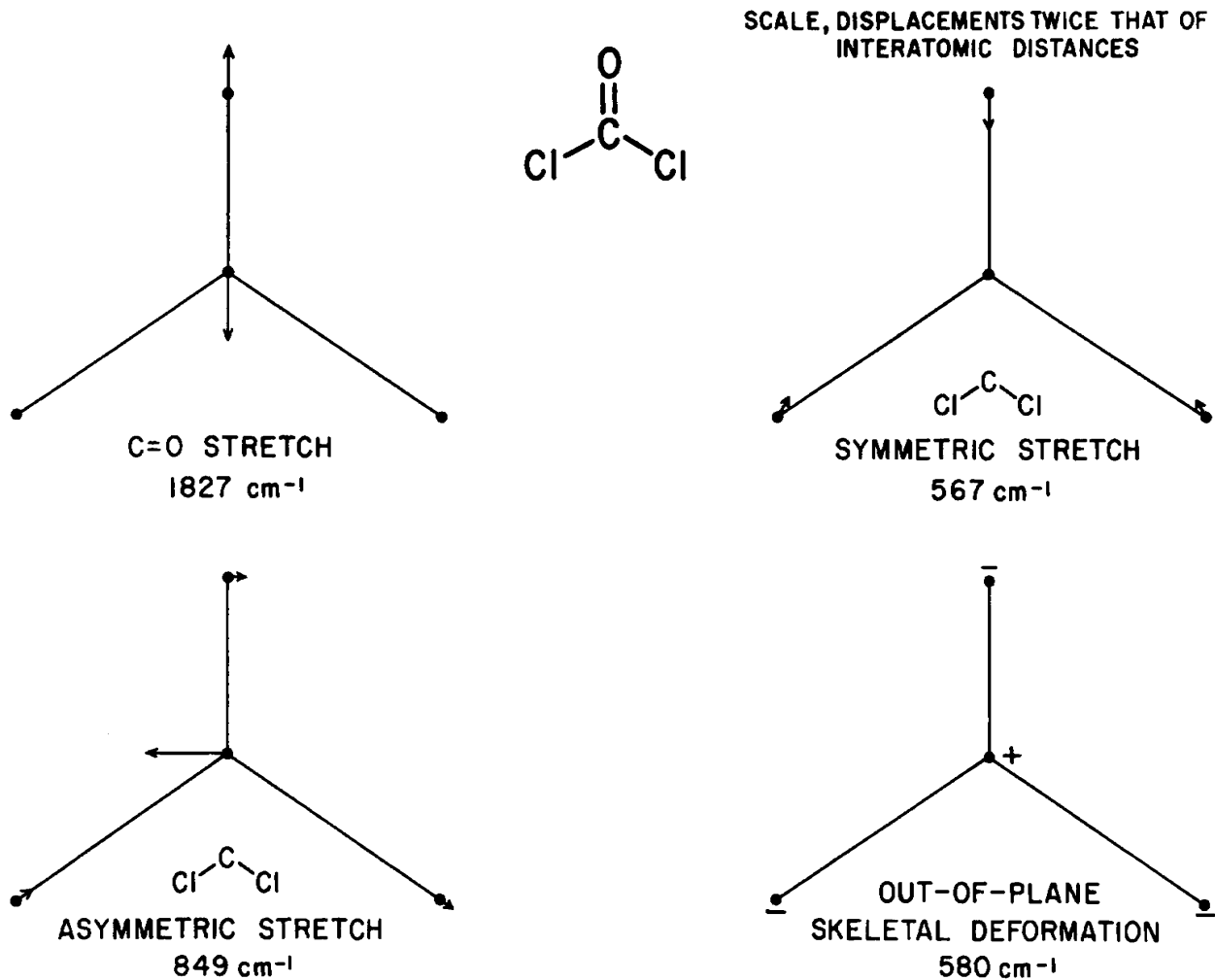


FIGURE 16.1c Normal modes for COCl_2 .

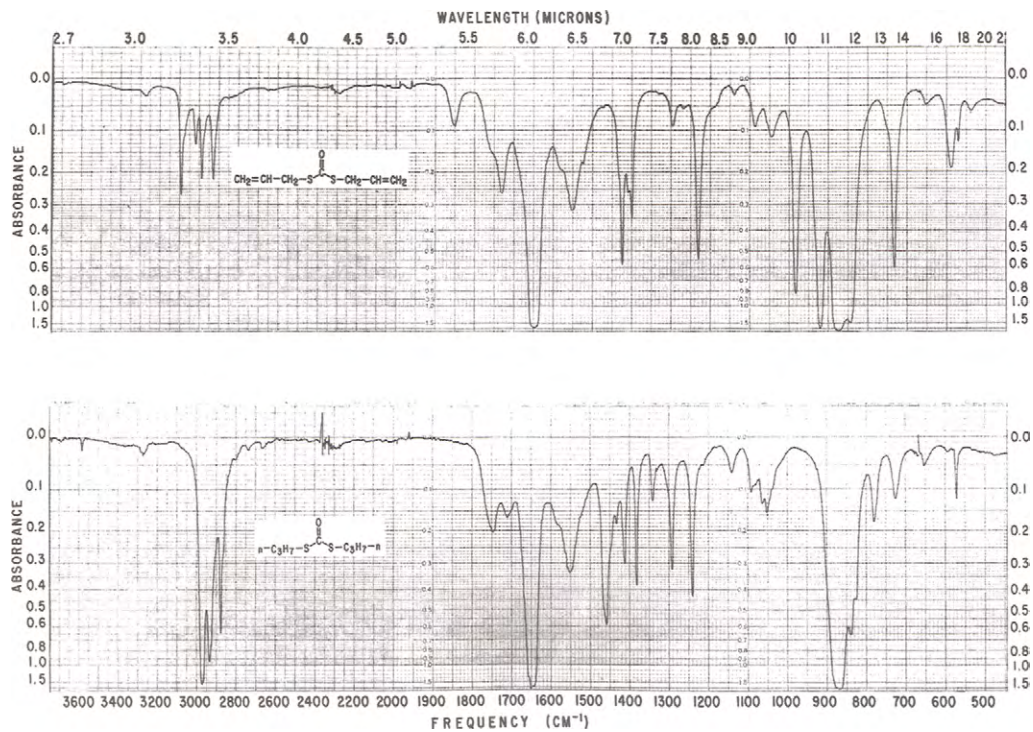


FIGURE 16.2 (Upper)—Infrared spectrum of diallyl dithiol carbonate. (Lower)—Infrared spectrum of dipropyl dithiol carbonate.

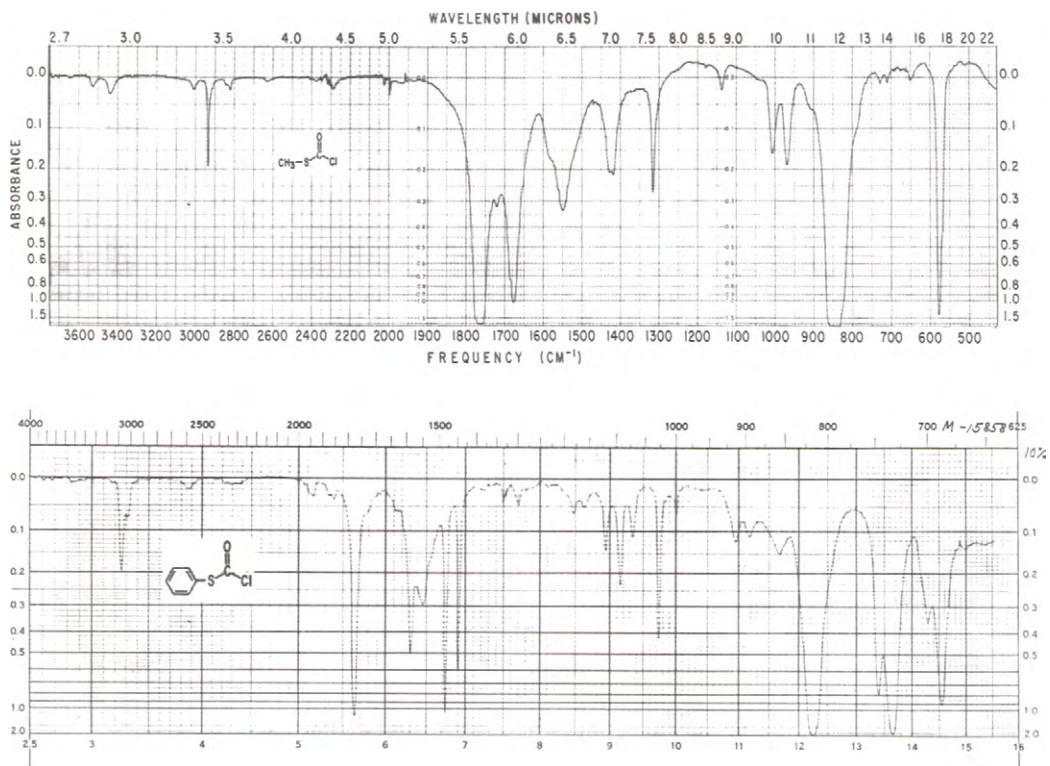
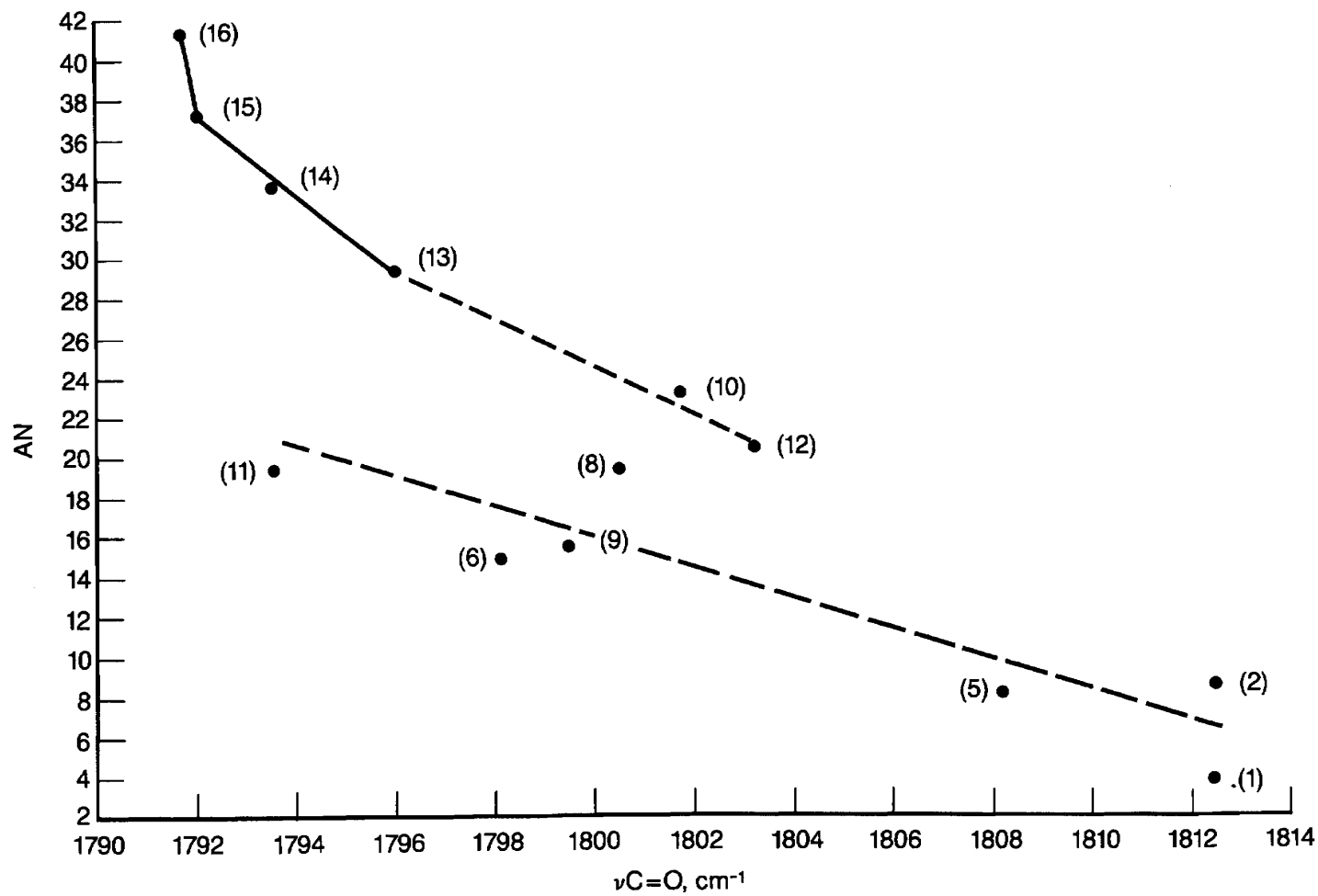


FIGURE 16.3 (Upper)—Infrared spectrum of methyl thiol chloroformate. (Lower)—Infrared spectrum of phenyl thiol chloroformate.

FIGURE 16.4 Plots of $\nu\text{C}=\text{O}$ frequencies of ethylene carbonate corrected for Fermi resonance vs the solvent acceptor number (AN).

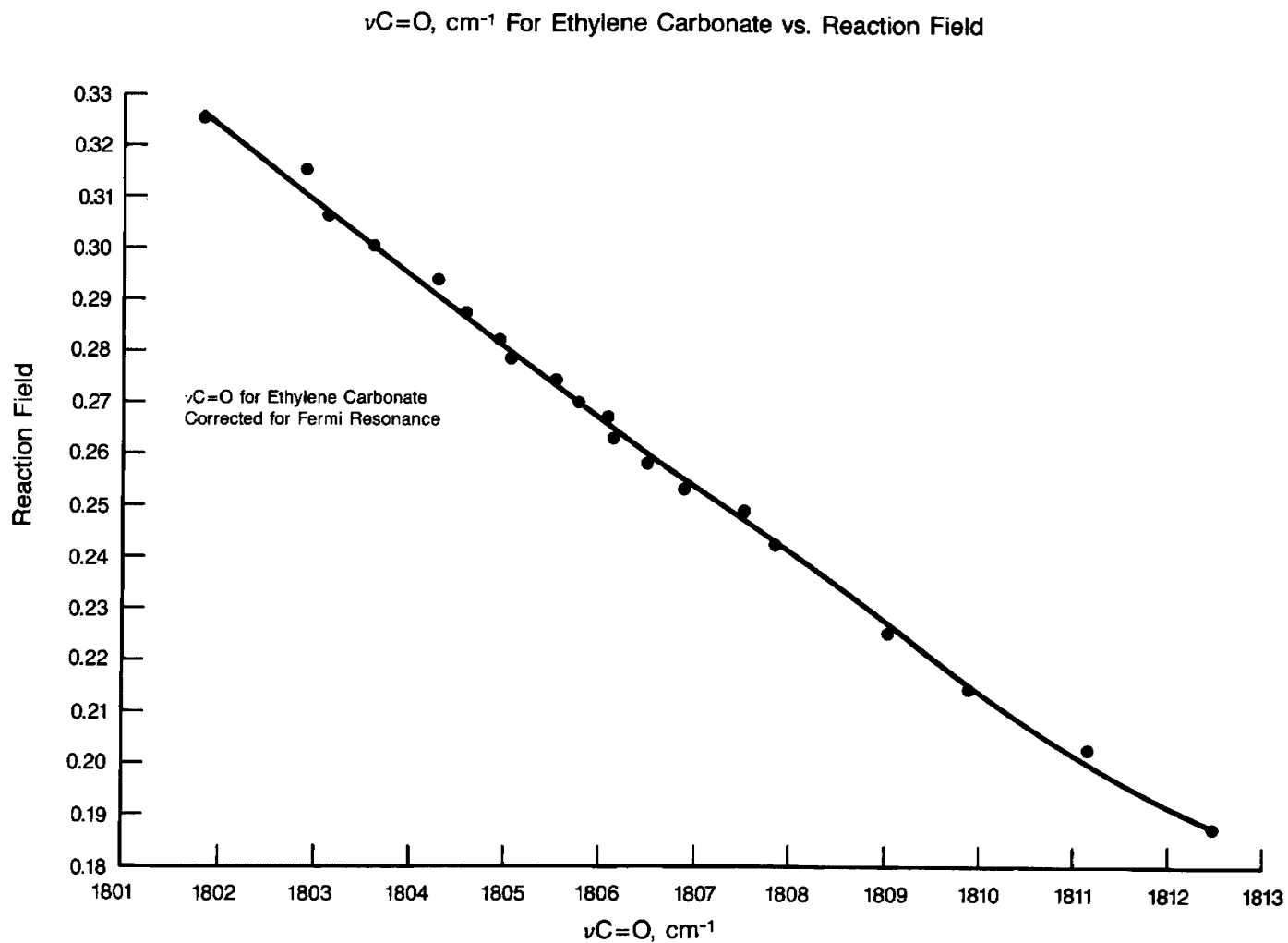


FIGURE 16.5 A plot of the $\nu\text{C}=\text{O}$ frequencies for ethylene carbonate corrected for Fermi resonance vs the reaction field of the $\text{CHCl}_3/\text{CCl}_4$ solutions.

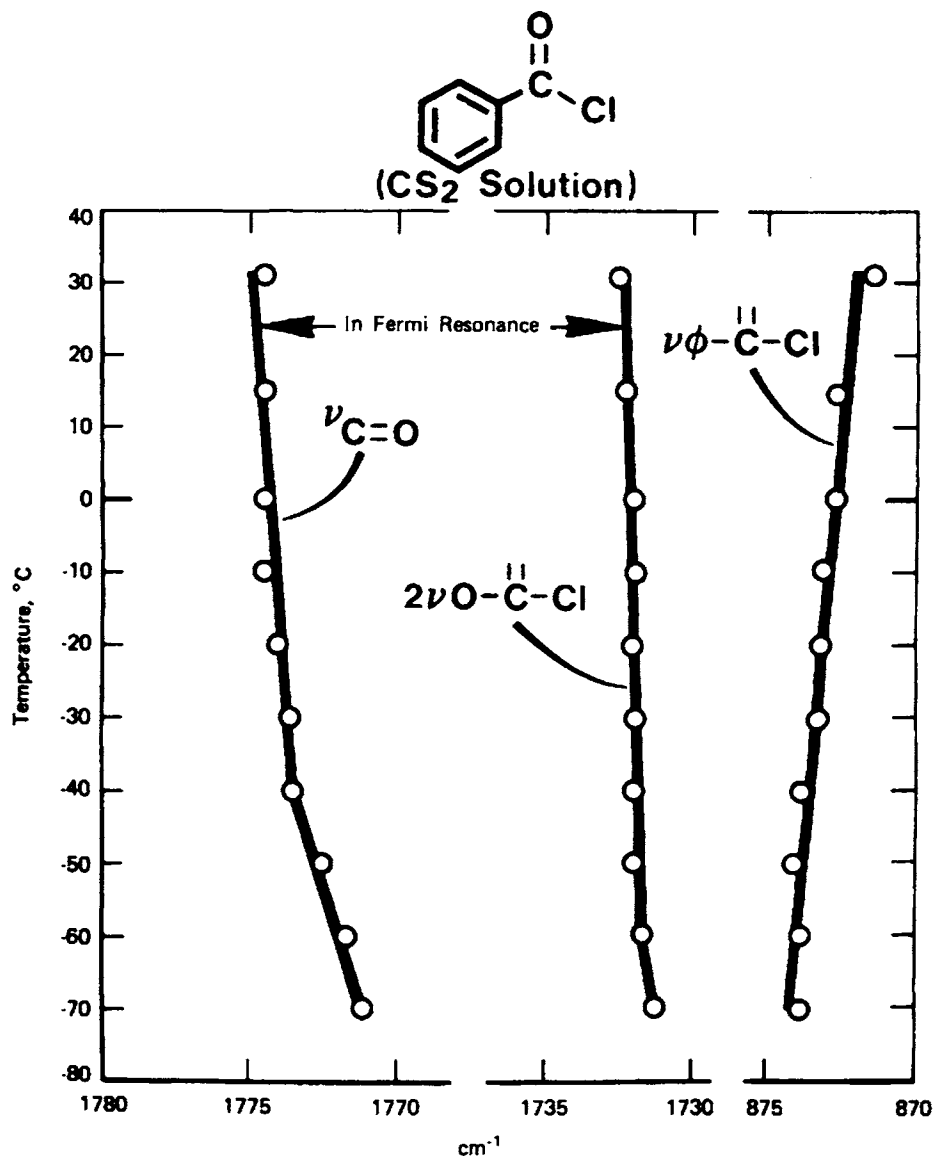


FIGURE 16.6 Plots of $\nu_{\text{C}=\text{O}}$, $2\nu_{\text{C}-\text{C}(=\text{O})-\text{Cl}}$, and $\nu_{\phi-\text{C}(=\text{O})-\text{Cl}}$ frequencies for benzoyl chloride in CS₂ solution vs temperature in °C.

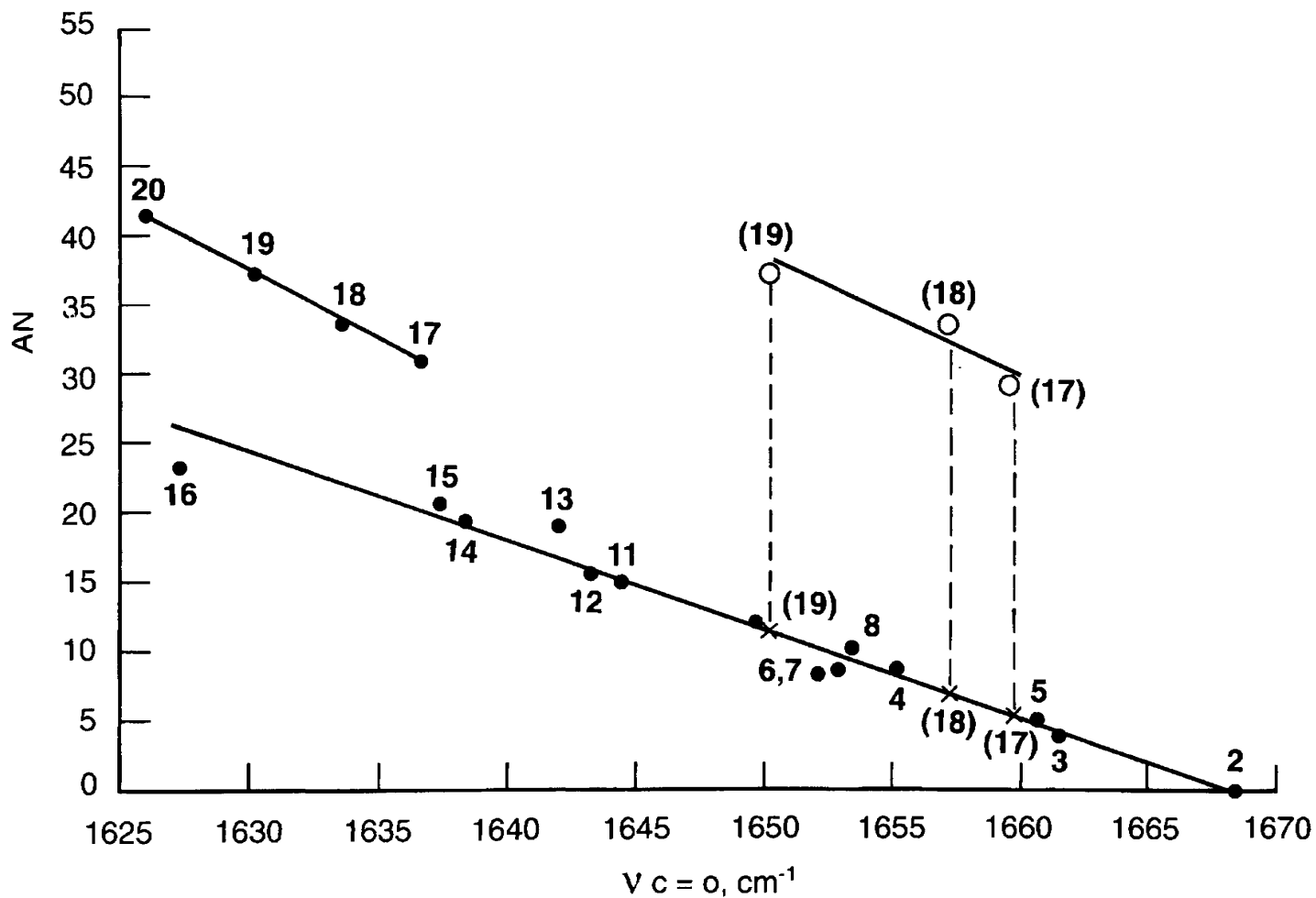


FIGURE 16.7 Plots of $\nu_{C=O}$ for tetramethylurea in various solvents vs the solvent acceptor number (AN).

TABLE 16.1 IR group frequency correlations for organ carbonates, thiol carbonates, chloroformates, and thiol chloroformates

Compound type	C=O str. cm ⁻¹	a.X-C-X str. cm ⁻¹	s.X-C-X str. cm ⁻¹	C-X str. cm ⁻¹	C-Y str. cm ⁻¹	a.Y-C-Y str. cm ⁻¹	s.Y-C-Y str. cm ⁻¹	ABC=O o.p.def. A and B =X or Y cm ⁻¹	C=O str. Corrected for Fermi Res. cm ⁻¹
(R-O-)2C=O	1739-41	1240-80	~ 900					785-80	
(R-O-)C=O(-O-C ₆ H ₅)	1754-87	1211-48	~ 900					~ 800	
C ₆ H ₅ -O-)2C=O	1775-1819	1205-21							
(CH ₂ -O-)2C=O	1818.3	~ 1140	~ 900						1812.5*
(R-S-)2C=O	1640-66					870-80	~ 572	~ 593	~ 1655*
(R-S-)C=O(-S]-C ₆ H ₅)	1649					839	~ 567	~ 554	~ 1664*
(C ₆ H ₅ -S-)2C=O	1714-18					827-33	~ 560	~ 572	~ 1690*
(CH ₂ -S-)2C=O	~ 1678					880			~ 1694*
(R-O-)C=O(-S-R)	1702-10			1142-62		~ 800		~ 670	
(R-O-)C=O(-S-C ₆ H ₅)	1719-31			1125-451		~ 800		~ 670	
(C ₆ H ₅ -O-)C=O(-S-R-)	1730-9			1056-1102				650-655	
(-O-CH ₂ CH ₂ -S-)C=O	1757			1070 or 1040					[C=N str. [1649-56]
(R-S-)C=O(O-N=C(R') ₂)	1720-25			1117-19		~ 800			
(R-O-)C=O(Cl)	1775-80			1139-69				685-87	
(C ₆ H ₅ -O-)C=O(Cl)	1784			1113		~ 800			
(R-S-)C=O(Cl)	1766-72					840-50	579	~ 560	~ 1760[CCl ₄]* ~ 1763[vapor]* for CH ₃ -S-C=O(Cl)
(C ₆ H ₅ -S-)C=O(Cl)	1769-75					814-16	595	~ 560	
(R-O-)C=O(NHR')	1732-38	1210-1250						760-80	N-H str.(not N-H: O=C in dilute soln.) a.NH ₂ str.,3530 s.NH ₂ str.,3414 (not H-bonded in dilute soln.)
(R-S-)C=O(NH ₂)	1699								N-H str.,3431 (in dilute soln.) N-H str.,3289-3320
(R-S-)C=O(NHR')	1690-95			1170-1230					
(R-S-)C=O(NHC ₆ H ₅)	1652-59			1152-60					
(R-S-)C=O(N(R') ₂)	1650-60			1220-65					i.p.N-H def.,1517-56
(C ₆ H ₅ -S-)C=O(N(R') ₂)	1666			1248					
(R-S-)C=O(N(C ₆ H ₅) ₂)	1670			~ 1275					
(R) ₂ NC=O(Cl)	1739			1091?		671		660?	C=O str.,1763[vapor] for C ₂ H ₅ analog
(C ₆ H ₅) ₂ NC=O(Cl)	1743 1751sh			1138?				661?	

*Corrected for Fermi resonance.

TABLE 16.2 The C=O stretching frequency for ethylene carbonate in various solvents [1% wt./vol.]

Ethylene carbonate 1 % wt./vol. in different solvents		C=O corrected for FR.			
Solvent	cm ⁻¹	cm ⁻¹	cm ⁻¹	cm ⁻¹	AN
Diethyl ether	1771.2	1818.69	1812.43	1777.46	3.9
Carbon tetrachloride	1771.93	1818.31	1812.45	1777.79	8.6
Carbon disulfide	1769.98	1816.82	1811.73	1775.07	
Toluene	1772.14	1715.24	1810.58	1776.8	
Benzene	1772.67	1714.72	1808.14	1779.25	8.2
Nitrobenzene	1775.06	1807.9	1798.12	1784.84	14.8
Nitromethane	1778.26	1806.91	1799.03	1786.14	
Acetonitrile	1777.9	1807.86	1800.51	1785.25	19.3
Benzonitrile	1775.69	1807.93	1799.46	1784.16	15.5
chloroform	1778.97	1810.27	1801.74	1787.44	23.1
Dimethyl sulfoxide	1774.37	1801.73	1793.54	1782.56	19.3
Methylene chloride	1777.57	1810.16	1803.21	1784.52	20.4
t-Butyl alcohol	1779.23	1806.43	1796	1789.66	[29.3]
Isopropyl alcohol	1778.88	1804.95	1793.53	1790.3	33.5
Ethyl alcohol	1779.14	1804.17	1793.01	1791.3	37.1
Methyl alcohol	1778.77	1804.68	1791.68	1791.77	41.3

TABLE 16.3 Vibrational assignments for methyl and 3-propynyl chloroformate, and FCl(C=O)

Methyl chloroformate cm ⁻¹	3-Propynyl chloroformate cm ⁻¹	F-C(=O)Cl cm ⁻¹	Assignment
1797	1782	1868	C=O str.
1150	1141(conformer 1) 1121(conformer 2)		a.C-O-C(=) str.
		1095	C-F str. s.C-O-C(=) str.
954	1014(conformer 1) 974(conformer 2)		
822	834(conformer 1) 807(conformer 2)	776	C-Cl str.
690	687	667	out-of-plane C=O def.
484	479	501	O=C=O or F-C=O bend
413	362	415	O-C-Cl or F-C-Cl bend
277	255		C-O-R bend
167	~170		C-O-R torsion
3044			a.CH ₃ str.
3018			a.CH ₃ str.
2961			s, CH ₃ str.* ¹
2844			2(s.CH ₃ bend)* ¹
1453			a.CH ₃ bend
1434			s.CH ₃ bend
1202			CH ₃ rock
	3314		C-H str.
	3012		a.CH ₂ str.
	2959		s.s.CH ₂ str.
	2149		CC str.
	1459(conformer 1)		CH ₃ bend
	1439(conformer 2)		
	1366		CH ₂ wag
	1366		CH ₂ twist
	992		CH ₂ rock
	916(conformer 1_		C-C str.
	937(conformer 2		C-C str.
	687		in-plane C-H bend
	634		out-of-plane C-H bend
	531(conformer 1)		out-of-plane C-C-O bend
	574(conformer 2)		out-of-plane C-C-O bend
	306		out-of-plane C-CC
	222		in-plane C-CC bend

*¹on Fermi resonance.

TABLE 16.4 IR and Raman data and assignments for acetyl chloride, acetyl-d₃ chloride, and acetyl-d₁ chloride

CH ₃ C(=O)Cl cm ⁻¹	CD ₃ C(=O)Cl cm ⁻¹	Assign- ment	Descrip- tion	CH ₂ DCC(=O)Cl cm ⁻¹ [trans]	Assign- ment	CH ₂ DCC(=O)Cl cm ⁻¹ [gauche]	Descrip- tion
3010		v1,v11		2955	v1		s.CH ₂ str.
	2248	v1		2245	v2	3020	a.CH ₂ str.
					v2	2955	C-D str.
					v3	2245	s.CH ₂ str.
2930		v2		1802	v3		C-D str.
	2104	v2		1397	v4	1802	C=O str.
					v5		C=O str.
1807	1812	v3	C=O str.	1254	v5		CH ₂ bend
					v6	1281	
1421		v4,v12		1011	v6		
	1132	v4		908	v7	1254	
					v8	1088	C-D wag
1361		v5		554	v8		C=O bend
	1040	v5		437	v9		C(=O)Cl bend
					v10	852	CD wag+C-C str.
1098		v6		340	v10		CCCl bend
	962	v6		3005	v11	588	C=O bend
					v11		a.CH ₂ str.
					v12	487	gamma C=O
953		v7		1281	v12		
	818	v7		973	v13	437	C(=O)Cl bend
					v14		
594	563	v8		503	v14	340	CCCl bend
436	438	v9		?	v15	?	gamma C=O
348	317	v10					
3010		v11,v1					
	2257	v11					
1421		v12,v4					
1021		v13					
	887	v13					
514	522	v14					
238	?	v15					

TABLE 16.4a IR and Raman data and assignments for acetyl chloride and acetyl-d₃ chloride

Mode	CH ₃ C(=O)Cl Calculated cm ⁻¹	CH ₃ C(=O)Cl Observed cm ⁻¹	Approximate description	Mode	CD ₃ C(=O)Cl Calculated cm ⁻¹	CD ₃ C(=O)Cl Observed cm ⁻¹	Approximate description
A'				A'			
v1	3002	3029	a > CH ₃ str.	v1	2232	2280	a.CH ₃ str.
v2	2939	2934	s.CH ₃ str.	v2	2114	2104	s.CD ₃ str.
v3	1780	1822	C=O str.	v3	1777	1820	C=O str.
v4	1441	1432	a.CH ₃ bend	v4	1147	1132	s.CD ₃ bend+a.CCCL str.
v5	1378	1370	s.CH ₃ bend	v5	1031	1040	a.CD ₃ bend
v6	1104	1109	CH ₃ rock + C-C str.	v6	986	962	a.CCCL +s.CD ₃ bend
v7	962	958	C-C str.+CH ₃ rock	v7	802	818	CD ₃ rock
v8	661	608	C-Cl str.	v8	601	563	CCl str.
v9	469	436	O=C-Cl bend	v9	462	437	O=CCl bend
v10	391	348	CCCl bend	v10	355	317	CCCl bend
A''				A''			
v11	3000	3029	a.CH ₃ str.	v11	2227	2280	a.CD ₃ str.
v12	1444	1432	a.CH ₃	v12	1031	1040	a.CD ₃
v13	1040	1029	CH ₃ rock	v13	854	877	CD ₃ rock
v14	568	514	gamma C=O	v14	516	498	gamma C=O
v15	136	238	CH ₃ torsion	v15	100	?	CS ₃ torsion

TABLE 16.4b IR and Raman data and assignments for acetyl-d₁ chloride

Mode	CH ₂ DC(=O)Cl	CH ₂ DC(=O)Cl	Approximate description	Mode	CH ₂ DC(=O)Cl	CH ₂ DC(=O)Cl	Approximate description
	Calculated trans [D-eclipsed] cm ⁻¹	Observed trans [D-eclipsed] cm ⁻¹			Calculated gauche [H-eclipsed] cm ⁻¹	Observed gauche [H-eclipsed] cm ⁻¹	
A'				A'			
v1	2962	2972	a.CH ₂ str.	v1	3002	3020	a.CH ₂ str.
v2	2192	2255	C-D str.	v2	2962	2972	s.CH ₂ str.
v3	1778	1820	C=O str.	v3	2189	2255	C-D str.
v4	1418	1408	bend	v4	1780	1820	C=O-H ₂ str.
v5	1266	1265	CH ₂ wag	v5	1417	1422	CH ₂ bend
v6	1033	1020	C-C str.	v6	1300	1290	CH ₂ wag
v7	899	909	C-D wag.	v7	1260	1265	CH ₂ rock
v8	607	565	C-Cl str.	v8	1085	1088	C-C str.+CH ₂ rock
v9	467	437	O=CCl	v9	968	987	C-D bend+C-C str.
v10	381	340	CCCl bend	v10	847	851	C-D bend+C-C str.
A''				A''			
v11	3000	3020	a.CH ₂	v11	657	588	C-Cl str.
v12	1306	1290	CH ₂ twist	v12	539	489	gamma C=O
v13	974	987	C-D o.p.bend	v13	467	437	O=CCl bend
v14	568	507	gamma C=O	v14	378	340	CCCl bend
v15	120	?	CH ₂ D torsion	v15	121	?	CH ₂ D torsion

TABLE 16.4c IR spectra-structure correlations for carboxylic acid halides in the vapor phase

Carboxylic acid halides	$\nu\text{C=O}$ cm^{-1}	See Text cm^{-1}	$\nu\text{C-X}$ cm^{-1}	gamma C=O cm^{-1}
acetyl fluoride	1869	1032	827	599
acetyl chloride	1818	1108	601	514
acetyl bromide	1818	1095	552	
trichloroacetyl chloride	1814	1023	591	622
hexanoyl chloride	1810	960	577	
octanoyl chloride	1809	965	570	
benzoyl fluoride	1832	1251	1022	
3-fluoro, benzoyl chloride	1790	1255	821	
4-trifluoromethyl, benzoyl chloride	1782.7* ¹	1181	882	
2-fluoro, benzoyl chloride	1794.9* ¹	1198	889	
2-bromo, benzoyl chloride	1801.8* ¹	1200	874	
2,6-dichloro, benzoyl chloride	1802* ¹			

*¹Corrected for Fermi resonance.

TABLE 16.4d IR spectra-structure correlations for benzoyl halides in neat phase

Benzoyl halide	perturbed C=O str. $\text{cm}^{-1}[\text{A}]$	perturbed overtone $\text{cm}^{-1}[\text{A}]$	C=O str. corrected for F.R. cm^{-1}	overtone corrected for F.R. cm^{-1}	complex aryl-C str. cm^{-1}	complex aryl-C-X str. cm^{-1}
fluoride	1812[0.94]	1778[0.75]	1796.9	1793.1	1000	
chloride	1785[0.88]	1735[0.66]	1762.9	1757.1	1205	875
bromide	1775[0.67]	1693[0.10]	1764.4	1703.6	1190	847
3-bromo, bromide	1775[0.84]	1754[0.84]	1764.5	1764.5	1179	875
2-methyl, chloride	1765[0.87]	1710[0.38]	1757.2	1717.8	1203	870
2-trifluoromethyl, chloride	1803[1.12]	1750[0.38]	1789.6	1763.4	1200	871
2-fluoro, chloride	1788[1.07]	1756[0.94]	1774	1771	1195	884
2-chloro, chloride	1780[0.94]	1735[0.45]	1765.4	1749.6	1190	865
2-bromo, chloride	1797[1.13]	1747[0.21]	1789.2	1754.8	1200	864
2-nitro, chloride* ¹	1800[0.70]	1758[0.37]	1785.5	1772.5	1195	870
3-fluoro, chloride	1771[1.03]	1741[1.03]	1756	1756	1245	785
3-chloro, chloride	1765[1.03]	1815[0.15]	1780	1798.8	1200	918
3-bromo, chloride	1750[1.15]	1795[0.59]	1765.3	1779.7	1172	884
3-nitro, chloride* ²	1752[1.14]	1783[0.74]	1758.3	1776.7	1191	840?
4-methyl, chloride	1775[1.04]	1740[0.85]	1769.3	1745.7	1203	875
4-tert-butyl, chloride	1782[1.13]	1730[0.94]	1758.4	1753.6	1210	874
4-trifluoromethyl, chloride	1775[0.58]	1740[0.55]	1758	1757	1200	879
4-chloro, chloride	1780[1.15]	1732[0.95]	1768	1743.8	1190	860

*¹vasym.NO₂, 1530 cm^{-1} ; vsym.NO₂, 1342 cm^{-1} .*²vasym.NO₂, 1529 cm^{-1} ; vsym.NO₂, 1340 cm^{-1} .

TABLE 16.5 IR data for benzoyl chloride in CS₂ solution in the temperature between 31 and -70°C

Benzoyl chloride [CS ₂] °C	C=O str. in Fr cm ⁻¹	2[C ₆ H ₅ -C-Cl str.] in FR cm ⁻¹	C ₆ H ₅ -C-C] str. cm ⁻¹	A[C=O str.] /A[2(C ₆ H ₅ -C-Cl str.)]
31	1774.6	1732.5	871.5	4.44
15	1774.5	1732.2	873	4.31
0	1774.5	1732	873	4.17
-10	1774.4	1732	873.5	3.82
-20	1774	1732.1	873.7	3.62
-30	1773.6	1732	873.7	3.53
-40	1773.5	1732	873.9	3.5
-50	1772.4	1732	874.3	3.25
-60	1771.5	1731.7	873.8	3.25
-70	1771.2	1731.3	874.1	3.03
delta C [-101]	delta C=O str. [-3.4]	delta 2[C ₆ H ₅ -C-Cl] [-1.2]	delta C ₆ H ₅ -C-Cl [-2.6]	delta A[C=O str.] /A[2(C ₆ H ₅ -C-Cl)] [-1.41]

TABLE 16.6 Vibrational assignments for S-methyl thiol chloroformate

CH ₃ -S-C(=O)Cl S-C(=O)Cl fundamentals	Infrared 25 % solutions in 0.1 KBr cell cm ⁻¹	C(=O)Cl ₂ fundamentals	Infrared cm ⁻¹	CH ₃ -S-C(=O)Cl Raman liquid cm ⁻¹ (R.I.)	Dep. ratio
C=O str.	1767.2(0.862)*	C=O str.	1827	1757(14.9)	0.34
asym.S-C-Cl str.	846.4(0.831)*	asym.Cl-C-Cl str.	847	840(5.2)	0.74
sym.S-C-Cl str.	580.7(0.137)*	sym.Cl-C-Cl str.	567	5881(100.0)	0.09
gamma C=O	571sh	gamma C=O	580		
C=O rock	430.2(0.371)	C=O rock	440	422(43.2)	0.45
S-C-Cl bend	304	Cl-C-Cl bend	285	305(89.8)	0.29
C-S-C fundamentals					
C-S str.	712.8(0.059)			710(50.0)	0.22
C-S-C bend	205			199(5.6)	0.32
C-S-C torsion	126				
CH ₃ -S fundamentals		CH ₃ -S-P(=O)Cl ₂ CH ₃ fundamentals			
asym.CH ₃ str.	3020.5(0.065)	asym.CH ₃ str.	3011	3013(2.8)	0.64
sym.CH ₃ str.	2938.3(0.435)	sym.CH ₃ str.	2938	2932(36.0)	0.05
asym.CH ₃ bend	1422.3(0.608)	asym.CH ₃ bend	1431	1420	
sym.CH ₃ bend	1316.5(0.605)	sym.CH ₃ bend	1321	1311(2.0)	0.44
CH ₃ rock	972.7(0.464)	CH ₃ rock	972	967(2.5)	0.35
CH ₃ torsion	?	CH ₃ torsion	?		

* 2 % solutions in 0.1 mm KBr cell] [CCl₄ solution 3800-1333 cm⁻¹] [CS₂ solution 1333-400 cm⁻¹].

TABLE 16.7 IR spectra-structure correlations for carbamic acid: aryl-, alkyl esters

Aryl-NH-C(=O)-O-R	R	C=O str. cm ⁻¹	C=O: H-N str. intermolecular* ¹ cm ⁻¹	N-HO=C str. intermolecular* ¹ cm ⁻¹	N-H str. cm ⁻¹	2-X: H-N str. intramolecular cm ⁻¹	N-H i.p.-bend cm ⁻¹	N-H o.p.-bend cm ⁻¹	Aryl-N str. cm ⁻¹	N-C-O and N-H bend cm ⁻¹
Phenyl										
2-, 3-, or 4-										
F, Cl, Br, or C ₆ H ₅	H-CCCH ₂	1730-1758	1705-1734	3295-3460 1690* ²	3409-3461		1504-1546	503-570	1237-1282 624-680* ²	1195-1225 1219-1257* ²
	(CH ₃) ₂ N(CH ₂) ₂					3411-3440				
2-F	H-CC-CH ₂					3435				
2-Cl	H-CC-CH ₂					3419				
2-Br	H-CC-CH ₂					3409				
2-C ₆ H ₅	H-CC-CH ₂					3425				
1-Naphthyl	H-CC-CH ₂				3325-3340	3441-3461				
2-Naphthyl	H-CC-CH ₂				3360	3445				

*¹Disappears upon dilution.*²Solid phase.

TABLE 16.8 The carbonyl stretching frequency for 1,1,3,3-tetramethylurea in aprotic solvents [Nyquist data vs Kolling and Wohar data] vs solvent parameters

Solvent	AN* ³	[A]	[B]	[C]	[A]-[B]	[A]-[C]	[B]-[C]	e* ¹	n* ²
		C=O str. Nyquist data cm ⁻¹	C=O str. Kolling data cm ⁻¹	C=O str. Wohar data cm ⁻¹					
Hexane	0	1668.4	1658	1656	10.4	12.4	2	1.88	1.3719
Diethyl ether	3.9	1661.5	1651	1658	10.5	3.5	-7	4.33	1.3494
Methyl tert-butyl ether	[5.0]	1660.7							
Tetrahydrofuran	[8.8]	1655.1	1646		9.1			7.58	1.405
Carbon disulfide	[10.1]	1653.2	1652		1.4			2.64	1.6241
Carbon tetrachloride	8.6	1652.9		1653		-0.1		2.24	1.457
Benzene	8.2	1652.1	1654	1654	-1.9	-1.9	0	2.28	1.5017
Hexamethylphosphoramide	10.6		1643	1649			-6	30	1.457
Acetone	12.5		1646	1648			-2	20.7	1.356
Nitrobenzene	14.8	1644.4	1642.		2.4			34.82	1.55
Benzonitrile	15.5	1643.2		1642			1.2	25.2	1.5257
Acetonitrile	19.3	1638.4	1639	1638	-0.6	0.4	1	46.68	1.4771

*¹e = dielectric constant.*²n = refractive index.*³AN = solvent acceptor number.

List of Tables

CHAPTER 3

3.1	IR data for a. and s. CH ₃ stretching for <i>n</i> -alkanes in 0.5 mol % solutions in CCl ₄ , in CDCl ₃ , and 54.6 mol % CHCl ₃ /CCl ₄	41
3.2	IR absorbance data for <i>n</i> -alkanes: a. and s.CH ₂ and CH ₃ stretching and CH ₂ bending	42
3.2a	Absorbance ratios for CH ₃ and CH ₂ groups for <i>n</i> -alkanes	43
3.3	IR data for a. and s.CH ₂ stretching for <i>n</i> -alkanes in 0.5% solutions in Cl ₄ , 54.6 mol % CDCl ₃ /CCl ₄ , and CDCl ₃	44
3.4	The frequency separation between the a. and s.CH ₃ and the a. and s.CH ₂ stretching vibrations for <i>n</i> -alkanes in CCl ₄ , CDCl ₃ /CCl ₄ , and CDCl ₃ solutions	45
3.5	The CH ₃ and CH ₂ bending frequencies and frequency separations for <i>n</i> -alkanes	45
3.6	IR vapor-phase data for the alkyl group of 1,2-epoxyalkanes	46
3.7	IR and Raman data for (CH ₃) ₂ PO ₂ Na in water and in the solid phase	47
3.8	IR data and assignments for CH ₃ HgSCH ₃ , CH ₃ SC(C=O)C, and (CH ₃) ₂ Hg	47
3.9	IR vapor-phase data for cycloalkanes	48
3.10	Raman data for compounds containing cycloalkyl groups	49
3.11	Raman data for the CH stretching and bending modes of the alkyl group, and C—C—C=O skeletal bending for monomers and polymers	50
3.12	IR vapor-phase data for cyclopropane derivatives	52
3.13	IR data for octadecane, octadecane-D38, tetracosane, and tetracosane-D50	53

CHAPTER 4

4.1	IR vapor-phase data and assignments for 1-alkenes	72
4.2	The IR vapor-phase frequencies and assignments for the X—CH=CH ₂ group	73
4.2a	IR absorbance ratio and assignments for X—CH=CH ₂ compounds	74
4.2b	Raman data and assignments for X—CH=CH ₂ compounds	75
4.2c	IR vapor-phase data for vinyl alkyl ethers	76
4.3	CH ₂ = frequencies vs (sigma ρ-sigma') for group G	77

4.3a	IR carbon disulfide solution data for the CH=CH twist frequency for compounds of form G-CH ₂ CO ₃ H vs σ' of G and pK _a of G-CH ₂ CO ₂ H	77
4.4	IR data and assignments for the cis and gauche conformers of allyl halides	78
4.5	IR data and assignments for cyclopentene, cyclohexene, 1,4-cyclohexadiene, and 1,3-cyclohexadiene [C=C and (C=O) ₂ stretching]	78
4.5a	IR vapor-phase data and assignments for cis-cycloalkene derivatives	78
4.6	IR C=O stretching frequency data for alkyl acrylates [CHCl ₃ and CCl ₄ solutions]	79
4.6a	IR data and assignments for alkyl methacrylates in CHCl ₃ and CCl ₄ solutions [C=O and C=C stretching]	80
4.7	IR vapor-phase data for trans-alkenes	81
4.8	IR data for the CH=CH twist frequency for trans disubstituted ethylenes	82
4.9	IR data for the =CH ₂ wag and its overtone for 1,1-disubstituted ethylenes	82
4.10	A comparison of the fundamentals for 1,1-dihaloethylenes	83
4.11	IR vapor-phase data and assignments for alkyl cinnamates [C=C stretching, CH=CH twisting, and C=O stretching]	84
4.11a	IR vapor-phase data and assignments for cinnamyl esters	85
4.12	Raman data and assignments for vinyl esters of carboxylic acids	85
4.13	Raman data and assignments for styrene monomers	86
4.14	IR group frequency data for styrene and substituted styrenes	87
4.15	IR group frequency data for α -halostyrenes, α -methylstyrenes, and related compounds	88
4.16	IR vapor-phase data for butadienes and propadienes	90
4.17	IR vapor-phase data for carbon hydrogen stretching vibrations and other vibrations for 1-alkenes	90
4.18	IR data and assignments for the alkyl group of vinyl alkyl ethers	91

CHAPTER 5

5.1	IR data and assignments for terminal acetylenic compounds	106
5.2	IR and Raman data and assignments for 3-halopropynes	107
5.3	IR vapor-phase data and assignments for 1-alkynes	108
5.4	IR data and assignments for 1-chloropropyne and 1-bromopropyne	109
5.4a	Coriolis coupling constants for 1-halopropyne-1, propyne, and propyne-1-d	109
5.5	IR data for phenylacetylene in CHCl ₃ /CCl ₄ solutions	109
5.6	IR data and assignments for 1,4-diphenylbutadiyne in CHCl ₃ /CCl ₄ solutions	110
5.6a	IR data for phenylacetylene in various solvents	110
5.7	Vibrational assignments for propargyl alcohol, propargyl alcohol-od, propargyl alcohol-1d, od, and propargyl fluoride	111
5.8	Vibrational data for 1,3-dichloropropyne and 1,3-dibromopropyne	112
5.9	Vibrational data and assignments for phenylacetylene and phenylacetylene-1d	113

CHAPTER 6

- 6.1 IR and Raman data and assignments for 1-halopropadienes and 1-bromopropadiene-1d 123

CHAPTER 7

- 7.1 IR vapor-phase data and assignments for alcohols 135
7.2 IR vapor-phase data for substituted phenols 137
7.3 A comparison of OH:X stretching frequencies in the vapor and CCl₄ solution phases 138
7.4 The OH stretching frequency for 4-hydroxybenzaldehyde in 0 to 100 mol % CHCl₃/CCl₄ solutions 139
7.5 The OH stretching frequencies for phenol and intramolecular hydrogen-bonded phenols and the OH torsion frequency for phenol and the out-of-plane OH:X deformation frequencies for intramolecularly hydrogen-bonded phenols 140

CHAPTER 8

- 8.1 IR vapor-phase data and assignments for primary alkyl amines 147
8.2 Raman data and assignments for primary amines 148

CHAPTER 9

- 9.1 IR data for the a. and s. NH₂ stretching frequencies of 3-X and 4-X-anilines in the vapor phase, and in *n*-C₆H₁₄, CCl₄, and CHCl₃ solutions 158
9.2 The calculated NH₂ bond angles for 3-X and 4-X anilines in *n*-C₆H₁₄, CHCl₃, and CCl₄ solutions 159
9.3 IR data for the frequency separation between a.NH₂ and s.NH₂ stretching in the vapor, and in *n*-C₆H₁₄, CCl₄, and CHCl₃ solutions for 3-X and 4-X-anilines 160
9.3a IR data for the frequency separation between a. and s.NH₂ bending for 3-X and 4-X-anilines in the vapor-phase and in solutions with *n*-C₆H₁₄, CCl₄, and CHCl₃ 161
9.4 IR data for the NH₂ stretching frequencies of aniline and 4-chloroaniline in CS₂ solution in the temperature between 27 and -60 °C 162
9.5 IR and Raman data and assignments for azines 163
9.6 IR and Raman data for glyoximes in the solid state [(N=C-) ₂ stretching vibrations] 164

CHAPTER 10

10.1	IR vapor-phase data, CCl ₄ and CHCl ₃ solution-phase data, and assignments for aliphatic carboxylic acids	194
10.2	Raman data and assignments for out-of-phase and in-phase (C=O) ₂ stretching modes and C=C stretching modes for carboxylic acids	195
10.3	IR group frequency data for acetic acid and its derivatives in the vapor and solution phases	196
10.4	IR data and assignments for 4-X-benzoic acids in the vapor and solution phases	197
10.4a	Factors affecting the CO ₂ H and (CO ₂) ₂ groups for 4-X-benzoic acids in CHCl ₃ and/or CCl ₄ solutions	198
10.5	IR vapor-phase data and assignments for anthranilic acids	199
10.6	Infrared data for methacrylic acid and acrylic acid in CHCl ₃ and/or CCl ₄ solutions	200
10.7	Raman data and assignments for carboxylic acid salts	201
10.8	The asymmetric and symmetric CO ₂ stretching frequencies for carboxylic acid salts	202
10.9	IR data for carboxylic acid salts	203

CHAPTER 11

11.1	IR vapor-phase data and Raman data in the neat phase for anhydrides	210
11.2	Raman data and assignments for carboxylic anhydrides	210
11.3	IR data for maleic anhydride in <i>n</i> -C ₆ H ₁₄ /CHCl ₃ , CHCl ₃ /CCl ₄ , and <i>n</i> -C ₆ H ₁₄ /CCl ₄ solutions	211
11.4	The in-phase and out-of-phase (C=O) ₂ stretching vibrations for carboxylic anhydrides in the vapor phase and in various solution phases	212

CHAPTER 12

12.1	A comparison of primary, secondary, and tertiary amides in various physical phases	241
12.1a	The NH stretching frequencies and absorbance data for N-methyl acetamide in concentration ranging from 1.37×10^{-3} to 1.37 mols/liter in CCl ₄ solution	242
12.1b	The NH stretching, C=O stretching, amide II, and amide III frequencies for N-methyl acetamide in CHBr ₃ solutions	242
12.1c	The overtone for amide II of N-methyl acetamide and N-methyl chloroacetamide in varying concentrations in CCl ₄ solutions	243
12.2	IR data and assignments for N-alkyl acetamides, and N-alkyl α -substituted acetamides in dilute solutes	244

12.2a	The NH stretching frequencies for N-alkyl acetamides, N-alkyl X-halo, X,X-dihalo-, X,X,X-trihaloacetamides, and N-alkyl methoxyacetamide in CCl ₄ solutions	246
12.3	IR data for N-alkyl α -substituted acetamides in 10% wt./vol. CCl ₄ and 0.002 M CCl ₄ solutions	248
12.4	A comparison of primary and secondary amides in the solid phase	249
12.4a	A comparison of IR data for tertiary amides in the neat or solid phase	249
12.5	A comparison of Raman data and assignments for acrylamide, methacrylamide, and their polymers	250
12.5a	Raman data and assignments for N-alkyl or N-aryl acrylamides and methacrylamides	251
12.6	IR C=O stretching frequencies for p-x acetanilides and p-x, α -haloacetanilides in CCl ₄ and CHCl ₃ solutions	252
12.7	The NH stretching frequencies for p-x-acetanilides and p-x, α -haloacetanilides in CCl ₄ and CHCl ₃ solutions	252
12.8	The NH and C=O stretching frequencies for N-alkyl p-methoxybenzamide, N-alkyl p-chlorobenzamide, and N-alkylmethyl carbamate in CCl ₄ solutions	254
12.9	IR and Raman data for N,N'-dialkyl oxamide and N,N'-diaryl oxamide	255
12.10	IR data and assignments for dimethylacetamide and tetraalkylurea in the vapor, neat and solution phases	256
12.11	IR vapor-phase data and assignments for urea, thiourea, and guanidine derivatives	257
12.12	IR data and assignments for tetramethylurea and 1,3-dimethyl-2-imidazolidinone in various solvents	258
12.13	IR data and assignments for 1,3-dimethyl-2-imidazolidinone 1% wt./vol. in various solutions	259
12.14	The in-phase and out-of-phase (C=O) ₂ stretching frequencies for caffeine, isocaffeine, 1,3,5-trimethyluracil, 1,3,6-trimethyluracil, and 1,3-dimethyl-2,4-(1H,3H) 2, quinazolinedione in CCl ₄ and CHCl ₃ solutions	260
12.15	IR data for uracils in the solid phase	261
12.16	IR vapor-phase data and assignments for imides	262
12.17	IR data for the in-phase and out-of-phase stretching frequencies of 4-bromobutyl phthalimide in CHCl ₃ /CCl ₄ solutions	264
12.18	IR data and assignments for hydantoins in the vapor and solid phase	265
12.19	IR data and assignments for tri-allyl-1,3,5-triazine-2,4,6-(1H,3H,5H) trione in CHCl ₃ /CCl ₄ solutions	266
12.20	IR data and assignments for tri-allyl-1,3,5-triazine-2,4,6-(1H,3H,5H) trione in various solvents	266

CHAPTER 13

13.1	A comparison of IR data of nonconjugated aldehydes in different phases	282
13.1a	Raman data and assignments for aldehydes	282

13.2	IR data and assignments for 4-X-benzaldehydes in the vapor and CHCl ₃ and CCl ₄ solution	282
13.3	The C=O stretching frequency for 4-X-benzaldehydes in various solvents	283
13.4	The CH bending vibration for 4-X-benzaldehydes in CCl ₄ and CHCl ₃ solutions and in the vapor phase	284
13.5	The overtone of =CH bending in Fermi resonance with =CH stretching for 4-X-benzaldehydes corrected for Fermi resonance	285
13.16	IR data and assignments for the observed and corrected-for Fermi resonance CH stretching frequencies for 4-X-benzaldehydes in CCl ₄ and CHCl ₃ solutions	286

CHAPTER 14

14.1	IR vapor phase and Raman data for acetone and acetone-d ₆	311
14.2	Application of the KBM equation using IR data for acetone C=O stretching frequencies in various solvents	312
14.2a	The calculated values for $A-1/2A + 1$ and $X-Y/X$ where A and Y equal 0 to 85 and X equals 85 [the KBM equation]	313
14.3	The C=O stretching frequencies for aliphatic ketones in the vapor phase and various solvents	314
14.3a	A comparison of the carbonyl stretching frequency difference (Δ C=O str. in cm ⁻¹) for dialkyl ketones in hexane and each of the other solvents	315
14.3b	A comparison of the carbonyl stretching frequency difference (Δ C=O str. in cm ⁻¹) for dialkyl ketones in methyl alcohol and the other protic solvents	315
14.3c	A comparison of the differences in the carbonyl stretching frequencies (Δ C=O str. in cm ⁻¹) of dialkyl ketones in hexane solution and in alcohol solution [non-H-bonded C=O]	316
14.4	The C=O stretching frequencies for <i>n</i> -butyrophenone and tert-butyrophenone in 0 to 100 mol % CHCl ₃ /CCl ₄ solutions	316
14.5	IR data for acetone, α -chloroacetone, acetophenone, and benzophenone in CS ₂ solution between \sim 29 and -100° C	317
14.6	A comparison of carbonyl stretching frequencies for 2% wt./vol. ketone in dimethyl sulfoxide and/or carbon tetrachloride solution	318
14.7	IR vapor-phase data for conjugated ketones	319
14.7a	Other fundamental vibrations for conjugated ketones	320
14.8	Infrared data for 2-hydroxy-5-X-acetophenone in CCl ₄ and CS ₂ solutions	321
14.9	IR vapor-phase data and assignments for cyclobutanone and cyclopentanone	322
14.10	The C=O stretching frequencies for cyclopentanone and cyclohexanone in the vapor, neat, and solution phases	323
14.11	IR data for 14H-dibenzo[a,j] xanthen-14-one in CHCl ₃ /CCl ₄ and various solvents	324
14.12	IR and Raman data for 1,4-benzoquinones in CCl ₄ and CHCl ₃ solutions	325
14.13	IR data for tetrafluoro-1,4-benzoquinone in CCl ₄ , CHCl ₃ , and C ₆ H ₁₄ solutions	326
14.14	IR data for tetrachloro-1,4-benzoquinone in CHCl ₃ / <i>n</i> -C ₆ H ₁₄ , CCl ₄ / <i>n</i> -C ₆ H ₁₄ , and CHCl ₃ /CCl ₄ solutions	327

14.15	IR data for tetrabromo-1,4-benzoquinone in $\text{CCl}_4/\text{C}_6\text{H}_{14}$, $\text{CHCl}_3/\text{C}_6\text{H}_{14}$, and $\text{CHCl}_3/\text{CCl}_4$ solutions	328
14.16	IR data for chloro-1,4-benzoquinone in $\text{CHCl}_3/n\text{-C}_6\text{H}_{14}$, $\text{CCl}_4/n\text{-C}_6\text{H}_{14}$, and $\text{CHCl}_3/\text{CCl}_4$ solutions	328
14.17	IR data for 2,5-dichlorobenzoquinone on $\text{CHCl}_3/n\text{-C}_6\text{H}_{14}$, $\text{CCl}_4/n\text{-C}_6\text{H}_{14}$, and $\text{CHCl}_3/\text{CCl}_4$ solutions	329
14.18	IR data for 3,3',5,5'-tetraalkyl-1,4-diphenoquinone in CHCl_3 solution and in the solid phase	329
14.19	The dependence of the $\text{C}=\text{O}$ stretching frequency upon solute concentrations of dialkyl ketones in $\text{CCl}_4/\text{CHCl}_3$ solutions	330

CHAPTER 15

15.1	Carbonyl stretching frequencies for some carboxylic acid esters	371
15.2	The $\text{C}=\text{O}$ stretching frequencies for alkyl alkanooates in the vapor phase and in various solvents	372
15.3	The frequency difference between $\nu\text{C}=\text{O}$ and $\nu\text{C}=\text{O}:\text{HOR}$ for alkyl alkanooates in alkyl alcohols [0.5 wt./vol. solute in solvent]	373
15.4	The frequency difference between $\nu\text{C}=\text{O}$ and $\nu\text{C}=\text{O}:\text{HO}$ for alkyl acetates in alkyl alcohols	373
15.5	The $\text{C}=\text{O}$ stretching frequencies for alkyl 2,2-dichloroacetates and alkyl acetates in the vapor and neat phases	373
15.5a	IR data for ethyl acetate and ethyl 2-chloroacetate in CS_2 solution between 27 and -100°C	374
15.6	IR data for β -propiolactone in various solvents	374
15.7	IR group frequency data for coumarin and derivatives in the vapor phase and in solution	375
15.8	IR data for phenyl acetate in $\text{CHCl}_3/\text{CCl}_4$	375
15.9	IR data for phenyl acetate in various solvents	376
15.10	IR data for alkyl 2-benzoates in CS_2 solution between 29 and -100°C	377
15.11	The $\text{C}=\text{O}$ stretching frequencies for methyl salicylate, phenyl salicylate, and 2-hydroxyacetophenone in various solvents	378
15.12	Raman group frequency correlations for dialkyl phthalates in the neat phase	378
15.13	Raman data for $\text{C}=\text{O}$ and $\text{C}=\text{C}$ stretching for acrylates	379
15.13a	IR $\text{C}=\text{O}$ stretching frequency data and other group frequency for alkyl acrylates [CHCl_3 and CCl_4 solutions]	380
15.14	Raman data for methacrylates in the neat phase and summary of IR data in CHCl_3 and CCl_4 solutions	381
15.15	IR vapor-phase data and assignments for alkyl cinnamates [$\text{C}=\text{C}$ stretching, $\text{CH}=\text{CH}$ twisting, and $\text{C}=\text{O}$ stretching]	383
15.15a	IR vapor-phase data and assignments for alkyl cinnamates [in-plane and out-of-plane phenyl ring vibrations]	383
15.15b	IR data for alkyl cinnamates	384

15.16	The C=O stretching frequencies for phenoxarsine derivatives in the solid state and in CCl ₄ solution	385
15.17	IR data for alkyl thiol esters and phenyl thiol esters	386
15.17a	IR data for alkyl thiol esters and phenyl thiol esters	386
15.17b	IR data for thiolbenzoates	387
15.17c	IR data for thiol acids, thiol anhydrides, and potassium thiol benzoate	387
15.18	Raman data and assignments for propargyl acrylate and propargyl methacrylate	388
15.19	IR vapor-phase data for R-C(=)-OR' skeletal stretching	389
15.20	IR vapor-phase data for conjugated esters [aryl-C(=)-OR or C=C-C(=)-OR skeletal stretching	390

CHAPTER 16

16.1	IR group frequency correlations for organic carbonates, thiol carbonates, chloroformates, and thiol chloroformates	411
16.2	The C=O stretching frequency for ethylene carbonate in various solvents [1% wt./vol.]	412
16.3	Vibrational assignments for methyl and 3-propynyl chloroformate, and FCl(C=O)	413
16.4	IR and Raman data and assignments for acetyl chloride, acetyl-d ₃ chloride, and acetyl-d ₁ chloride	414
16.4a	IR and Raman data and assignments for acetyl chloride and acetyl-d ₃ chloride	415
16.4b	IR and Raman data and assignments for acetyl-d ₁ chloride	415
16.4c	IR spectra-structure correlations for carboxylic acid halides in the vapor phase	416
16.4d	IR spectra-structure correlations for benzoyl halides in the neat phase	416
16.5	IR data for benzoyl chloride in CS ₂ solution in the temperature between 31 and -70° C	417
16.6	Vibrational assignments for S-methyl thiol chloroformate	417
16.7	IR spectra-structure correlations for carbamic acid: aryl-, alkyl esters	418
16.8	The carbonyl stretching frequency for 1,1,3,3-tetramethylurea in aprotic solvents [Nyquist data vs Kolling and Wohar data] vs solvent parameters	419

List of Figures

CHAPTER 1

1.1	Infrared vapor-phase spectrum for hydrogen bromide (5-cm glass cell with KBr windows: 600 mm Hg HBr).	9
1.2	Infrared vapor-phase spectrum for hydrogen chloride (5-cm glass cell with KBr windows: 200 mm Hg HCl, total pressure 600 mm Hg with N ₂).	10
1.3	Infrared vapor-phase spectrum for carbon monoxide (5-cm glass cell with KBr windows: 400 mm Hg CO, total pressure 600 mm Hg with N ₂).	11
1.4	Infrared vapor-phase spectrum for nitrogen oxide, NO.	12
1.5	Infrared vapor-phase spectrum for carbon dioxide (5-cm glass cell with KBr windows: 50 and 200 mm Hg CO ₂ , total pressure 600 mm with N ₂).	13
1.6	Infrared vapor-phase spectrum for carbon disulfide (5-cm glass cell with KBr windows: 2 and 100 mm Hg CS ₂ , total pressure 600 mm Hg with N ₂).	14
1.7	Infrared vapor-phase spectrum for acetylene (5-cm glass cell with KBr windows: 50 mm Hg C ₂ H ₂ , total pressure 600 mm Hg with N ₂).	15
1.8	Infrared vapor-phase spectrum for methane (5-cm glass cell with KBr windows: 150 mm Hg CH ₄ , total pressure 600 mm Hg with N ₂).	16
1.9	Infrared vapor-phase spectrum for carbon tetrafluoride (5-cm glass cell with KBr windows: 100 mm Hg CF ₄ , total pressure 600 mm Hg with N ₂).	17
1.10	Infrared vapor-phase spectrum for methyl chloride (5-cm glass cell with windows: 200 mm Hg CH ₃ Cl, total pressure 600 mm Hg with N ₂).	18
1.11	Infrared vapor-phase spectrum for methyl bromide (5-cm glass cell with KBr windows: 100 mm Hg CH ₃ Br, total pressure 600 mm Hg with N ₂).	19
1.12	Infrared vapor-phase spectrum for methyl iodide (5-cm glass cell with KBr windows: 200-mm Hg CH ₃ I, total pressure 600 mm Hg with N ₂).	20
1.13	Infrared vapor-phase spectrum for 1-bromopropyne, C ₃ H ₃ Br.	21
1.14	Infrared vapor-phase spectrum for 1-iodopropyne, C ₃ H ₃ I.	22
1.15	Infrared vapor-phase spectrum for benzene (5-cm glass cell with KBr windows: 40 mm Hg with C ₆ H ₆ ; total pressure 600 mm Hg with N ₂).	23
1.16	Infrared vapor-phase spectrum for ethylene oxide (5-cm glass cell with KBr windows: 50-mm Hg C ₂ H ₂ O, total pressure 600 mm Hg with N ₂).	24

CHAPTER 3

3.1	Plots of $\nu_{\text{asym. CH}_3}$ vs the molecular weight of each <i>n</i> -alkane.	36
3.2	Plots of $\nu_{\text{sym. CH}_3}$ vs the molecular weight of each <i>n</i> -alkane.	37
3.3	A plot of the absorbance ratio $A(\nu_{\text{asym. CH}_3})/A(\nu_{\text{asym. CH}_2})$ vs the absorbance ratio $A(\nu_{\text{sym. CH}_3})/A(\nu_{\text{sym. CH}_2})$ in CCl_4 solution for C_5H_{12} to $\text{C}_{18}\text{H}_{38}$.	38
3.4	A plot of the absorbance ratio $A(\nu_{\text{asym. CH}_3})/A(\nu_{\text{asym. CH}_2})$ vs the absorbance ratio $A(\nu_{\text{sym. CH}_3})/A(\nu_{\text{sym. CH}_2})$ in CCl_4 solution for C_5H_{12} to $\text{C}_{18}\text{H}_{38}$.	39
3.5	Plots of $\nu_{\text{asym. CH}_2}$ vs $\nu_{\text{sym. CH}_2}$ in CCl_4 , 54.6 mol % $\text{CDCl}_3/\text{CCl}_4$, and CDCl_3 solutions.	39
3.6	Plots of $\nu_{\text{asym. CH}_3}$ vs $\nu_{\text{sym. CH}_3}$ in CCl_4 , 54.6 mol % $\text{CDCl}_3/\text{CCl}_4$, and CDCl_3 solutions.	40
3.7	Plots of the frequency separation ($\nu_{\text{asym. CH}_3}-\nu_{\text{sym. CH}_3}$) vs the frequency separation ($\nu_{\text{asym. CH}_2}-\nu_{\text{sym. CH}_2}$) for each <i>n</i> -alkane in CCl_4 , 54.6 mol % $\text{CDCl}_3/\text{CCl}_4$, and CDCl_3 solutions.	40

CHAPTER 4

4.1	Shows plots of the $\nu_{\text{C=C}}$ or $\nu_{(\text{C=C})_2}$ modes for 1,3-cyclohexadienes, 1,4-cyclohexadienes, cyclopentene, and cyclohexene vs mole % CDCl_3 /or CHCl_3 /solvent system.	68
4.2	Infrared and Raman spectra for 1-bromo-1-chloroethylene.	69
4.3	Plots of the $\text{C}=\text{CH}_2$ wag frequencies for styrenes and ring substituted styrenes vs the pK_a values for correspondingly substituted phenols.	70
4.4	A plot of the frequency separation between $\text{CH}=\text{CH}_2$ twist and $\text{C}=\text{CH}_2$ wag for styrene and ring-substituted styrenes.	70
4.5	A plot of the $\text{C}=\text{CH}_2$ wag frequencies for styrene and ring-substituted styrenes vs the $\text{C}=\text{CH}_2$ wag frequency for α -methyl- α -methyl styrenes.	71

CHAPTER 5

5.1	A plot of absorbance ratios for the 1-alkynes vs the number of carbon atoms in the 1-alkynes.	100
5.2	A plot of $\nu_{\equiv\text{C}-\text{H}}$ for phenylacetylene vs mole % $\text{CHCl}_3/\text{CCl}_4$.	101
5.3	A plot of $\nu_{\text{C}\equiv\text{C}}$ for phenyl acetylene vs mole % $\text{CHCl}_3/\text{CCl}_4$.	101
5.4	A plot of the in-plane $\equiv\text{C}-\text{H}$ mode vs mole % $\text{CHCl}_3/\text{CCl}_4$.	102
5.5	A plot of out-of-plane $\equiv\text{C}-\text{H}$ mode vs the in-plane $\equiv\text{C}-\text{H}$ bending mode.	102
5.6/5.7	Vapor- and solution-phase infrared spectra of 1,3-dichloro-propyne.	103
5.8	The expected normal modes of 1-halopropynes, 3-halopropynes, and 1,3-dihalopropynes.	105

CHAPTER 6

6.1	Infrared solution and vapor-phase spectra of 3-bromopropyne-1d impure with 3-bromopropyne.	118
6.2	Raman spectra of 3-bromopropyne-1d impure with 3-bromopropyne.	118
6.3	IR solution and vapor-phase spectra of 1-bromopropadiene-1d impure with 1-bromopropadiene.	119
6.3a	Raman spectrum of 1-bromopropadiene-1d impure with 1-bromopropadiene.	119
6.4	IR vapor-phase spectra of 1-chloropropadiene.	120
6.5	IR vapor-phase spectra of 1-bromopropadiene.	121
6.6	IR vapor-phase spectra of 1-iodopropadiene.	122
6.7	Plots of the fifteen fundamentals, certain first overtones, and one combination band vs. Pauling electronegativity. The solid lines represent observed data, and the dashed extension is the extrapolation used to predict the partial spectrum of fluoropropadiene (see text).	122

CHAPTER 7

7.1	A plot of ν_{OH} for 4-hydroxybenzaldehyde vs mole % $\text{CHCl}_3/\text{CCl}_4$.	132
7.2	A plot of the $\gamma_{\text{OH}} \cdots \text{X}$ frequencies vs the $\nu_{\text{OH}} \cdots \text{X}$ frequencies for 2-X-substituted phenols.	133
7.3	A plot of Tafts $(\sigma_p - \sigma') + (\sigma_m - \sigma')$ vs $\gamma_{\text{OH}} \cdots \text{O}=\text{C}$ frequencies.	134
7.4	Plots of intramolecular hydrogen-bonded $\text{OH}:\text{Cl}$ stretching frequencies for chlorinated phenols in CS_2 solution vs temperature in $^{\circ}\text{C}$.	134

CHAPTER 9

9.1	A plot of $\nu_{\text{asym. NH}_2}$ for 3-X and 4-X anilines in CCl_4 solutions vs Hammett σ_m and σ_p values for the 3-X and 4-X atoms or groups. The open circles are for 3-X anilines and the closed circles are for 4-X anilines.	155
9.2	A plot of $\nu_{\text{sym. NH}_2}$ for 3-X and 4-X anilines in CCl_4 solutions vs Hammett σ_m and σ_p values for the 3-X and 4-X atoms or group. The open circles are for 3-X anilines and the closed circles are for 4-X anilines.	155
9.3	A plot of $\nu_{\text{asym. NH}_2}$ vs $\nu_{\text{sym. NH}_2}$ for 3-X and 4-X anilines in solution with C_6H_{14} , CCl_4 , and CHCl_3 .	156
9.4	A plot of σ_m and σ_p vs the calculated NH_2 bond angles for the <i>m</i> - and <i>p</i> -substituted anilines.	156
9.5	A plot of both ν_{NH_2} frequencies for aniline and 4-chloroaniline in CS_2 solution vs $^{\circ}\text{C}$.	157

CHAPTER 10

10.1	Plots of the number of protons on the acid α -carbon atom of the carboxylic acid vs $\nu_{\text{C}=\text{O}}$ for alkyl carboxylic acids in 2% wt./vol. in CCl_4 and in 2% wt./vol. CHCl_3 solutions.	175
------	--	-----

10.2	Plots of the mole % $\text{CHCl}_3/\text{CCl}_4$ vs $\nu\text{C=O}$ for alkyl carboxylic acids in 2% wt./vol. CHCl_3 and/or CCl_4 solutions.	176
10.3	Plots of the mole % $\text{CHCl}_3/\text{CCl}_4$ vs $\nu_{\text{op}}(\text{C=O})_2$ for alkyl carboxylic acids in 2% wt./vol. CHCl_3 and/or CCl_4 solutions.	177
10.4	Plots of the mole % $\text{CHCl}_3/\text{CCl}_4$ vs absorbance [$\nu(\text{C=O})$]/absorbance [$\nu_{\text{op}}(\text{C=O})_2$] for the alkyl carboxylic acids in 2% wt./vol. CHCl_3 and/or CCl_4 solutions.	178
10.5	A schematic of the number of possible rotational isomers for the tri-, di-, and haloacetic acids not in the form of intermolecular hydrogen-bonded dimers. X is a halogen atom, 2X is two halogen atoms, 3X is three halogen atoms.	179
10.6	Plots of $\nu\text{C=O}$ for each carboxylic acid in CCl_4 solution vs the pK_a value for each carboxylic acid.	180
10.7	Plots of $\nu\text{C=O}$ for each carboxylic acid in CHCl_3 solution vs the pK_a value for each carboxylic acid.	181
10.8	Plots of $\nu_{\text{op}}(\text{C=O})_2$ for each carboxylic acid in CCl_4 solution vs the pK_a value for each carboxylic acid.	182
10.9	Plots of $\nu_{\text{op}}(\text{C=O})_2$ for each carboxylic acid in CHCl_3 solution vs the pK_a value for each carboxylic acid.	183
10.10	Plots of $\nu\text{C=O}$ for each carboxylic acid in CCl_4 solution vs the σ^* value for each carboxylic acid.	184
10.11	Plots of $\nu(\text{C=O})$ for each carboxylic acid in CHCl_3 solution vs the σ^* value for each carboxylic acid.	185
10.12	Plots of $\nu_{\text{op}}(\text{C=O})_2$ for each carboxylic acid in CHCl_3 solutions vs the σ^* value for each carboxylic acid.	186
10.13	Plots of $\nu(\text{C=O})_2$ for trihalo, dihalo, and haloacetic acids vs mole % $\text{CHCl}_3/\text{CCl}_4$.	187
10.14	Plots of $\nu_{\text{op}}(\text{C=O})_2$ for trihalo, dihalo, and haloacetic acids vs mole % $\text{CHCl}_3/\text{CCl}_4$.	188
10.15	Plots of the νOH mode for 4-X-benzoic acids in CCl_4 solution and in CHCl_3 solution vs σ_p values for the 4-X atom or group.	189
10.16	Plots of the $\nu(\text{C=O})$ mode for 4-X-benzoic acids in CCl_4 solution and in CHCl_3 solution vs σ_p values for the 4-X atom or group.	190
10.17	Plots of the $\nu_{\text{op}}(\text{C=O})_2$ frequencies for 4-X-benzoic acids in CCl_4 solution and CHCl_3 solution vs σ_p values for the 4-X atom or group.	191
10.18	Plots of the $\nu_{\text{op}}(\text{C=O})_2$ frequencies for 4-X-benzoic acids vs mole % $\text{CHCl}_3/\text{CCl}_4$.	192
10.19	(a) Parts of the infrared spectrum of mulls containing sodium hydrogen diacetate; above 1330 cm^{-1} Fluorolube was used and below 1330 cm^{-1} , Nujol. (b) A Nujol mull spectrum of $\text{NaH}(\text{CD}_4\text{COO})_2$.	193

CHAPTER 11

11.1	IR spectra of phthalic anhydride in the region $2000\text{--}1600\text{ cm}^{-1}$. The spectrum on the left is for a saturated solution in CCl_4 , the center spectrum is for a saturated solution in a 23.1% vol. $\text{CHCl}_3/\text{CCl}_4$, and the spectrum on the right is for a saturated solution in CHCl_3 .	209
------	--	-----

CHAPTER 12

- 12.1 Plots of the $\nu\text{N-H}\cdots\text{O}=\text{C}$ frequencies for N-methylacetamide and N-methyl chloroacetamide vs the absorption maximum at each of the $\nu\cdots\text{O}=\text{C}$ frequencies. 232
- 12.2 IR spectra of N-methyl acetamide, N-ethyl acetamide, N-isopropyl acetamide, N-tert-butyl acetamide, and acetanilide in CCl_4 solution in the region $3800\text{--}3300\text{ cm}^{-1}$. 233
- 12.3 Plots of the $\nu\text{C}=\text{O}$ frequencies for α -bromo-*p*-x-acetanilide, *p*-x-acetanilide, and α,α,α -trichloro-*p*-x-acetanilide in 0.002 M solutions or less in CCl_4 and CHCl_3 vs Hammett σ_p values. 234
- 12.4 Plots of $\nu\text{C}=\text{O}$ for 1% wt./vol. solutions of acetone, dimethylacetamide, and tetramethylurea vs mole % $\text{CHCl}_3/\text{CCl}_4$. 235
- 12.5 Plots of $\nu\text{C}=\text{O}$ of 1,3-dimethyl-2-imidazolidazolidinone (DMI) and 1,1,3-tetramethylurea (TMU) in the neat phase or in 1 of the 19 solvents vs $\nu\text{C}=\text{O}$ (hexane) minus $\nu\text{C}=\text{O}$ (solvent). 236
- 12.6 Plots of $\nu\text{C}=\text{O}$ for 1,1,3,3-tetramethylurea (TMU) and 1,3-dimethyl-2-imidazolidinone (DMI) vs the solvent acceptor number (AN). 237
- 12.7 Plots of $\nu\text{C}=\text{O}$ for 1,1,3,3-tetramethylurea (TMU) and 1,3-dimethyl-2-imidazolidinone (DMI) vs mole % $\text{CHCl}_3/\text{CCl}_4$. 238
- 12.8 A plot of $\nu_{\text{op}}(\text{C}=\text{O})_3$ for triallyl-1,3,5-triazine-2,4,6-(1H,3H,5H) trione (T_3 one) vs mole % $\text{CHCl}_3/\text{CCl}_4$. 239
- 12.9 A plot of $\nu_{\text{op}}(\text{C}_3\text{N}_3)$ for triallyl-1,3,5-triazine-2,4,6-(1H,3H,5H) trione (T_3 one) vs mole % $\text{CHCl}_3/\text{CCl}_4$. 239
- 12.10 A plot of $\text{C}=\text{CH}_2$ wag for triallyl-1,3,5-triazine-2,4,6-(1H,3H,5H) trione (T_3 one) vs mole % $\text{CHCl}_3/\text{CCl}_4$. 239
- 12.11 A plot of $\nu_{\text{op}}(\text{C}=\text{O})_3$ and $\nu_{\text{op}}(\text{C}=\text{O})_3\cdots\text{HOR}$ for triallyl-1,3,5-triazine-2,4,6-(1H,3H,5H) trione vs the solvent acceptor number (AN). 240

CHAPTER 13

- 13.1 Plots of $\nu\text{C}=\text{O}$ corrected for Fermi resonance for each of the 4-X-benzaldehyde vs σ_p for the 4-X atom or group. The points on each line correspond to $\nu\text{C}=\text{O}$ frequencies for 0–100% $\text{CHCl}_3/\text{CCl}_4$ solutions. 271
- 13.2 Plots of $\nu\text{C}=\text{O}$ corrected for Fermi resonance in CCl_4 solution vs the frequency difference between ($\nu\text{C}=\text{O}$ corrected for FR in CCl_4 solution minus $\nu\text{C}=\text{O}$ corrected for FR for each of the mole % $\text{CHCl}_3/\text{CCl}_4$ solutions) for each of the 4-X-benzaldehydes. 272
- 13.3 Plots of $\nu\text{C}=\text{O}$ and an overtone in Fermi resonance and their corrected frequencies vs mole % $\text{CHCl}_3/\text{CCl}_4$ for 4-(trifluoromethyl) benzaldehyde. 273
- 13.4 Plots of the $\nu\text{C}=\text{O}$ frequency for each of the 4-X-benzaldehydes in a solvent vs the $\nu\text{C}=\text{O}$ frequency difference between the $\nu\text{C}=\text{O}$ frequency in hexane solution and the $\nu\text{C}=\text{O}$ frequency in each of the other solvents used in the study. 274

13.5	A plot of $\nu_{\text{C=O}}$ vs Hammett σ_p for each of the 4-X-benzaldehydes in dimethyl sulfoxide solution.	275
13.6	A plot of $\nu_{\text{C=O}}$ for 4-(dimethylamino) benzaldehyde vs the solvent acceptor number (AN) for each of the solvents.	276
13.7	Plots of half of the Fermi doublet for each of the 4-X-benzaldehydes in the range 2726–2746 cm^{-1} vs mole % $\text{CHCl}_3/\text{CCl}_4$.	277
13.8	Plots of half of the Fermi doublet for each of the 4-X-benzaldehydes in the range 2805–2845 cm^{-1} vs mole % $\text{CHCl}_3/\text{CCl}_4$.	278
13.9	Plots of unperturbed ν_{CH} for each of the 4-X-benzaldehydes vs mole % $\text{CHCl}_3/\text{CCl}_4$.	279
13.10	Plots of ν_{CH} and $2\delta_{\text{CH}}$ in Fermi resonance and ν_{CH} and δ_{CH} corrected for FR for benzaldehyde vs mole % $\text{CHCl}_3/\text{CCl}_4$.	280
13.11	Plots of $\nu_{\text{C=H}}$ and $2\delta_{\text{CH}}$ in Fermi resonance and ν_{CH} and δ_{CH} corrected for FR for 4-phenylbenzaldehyde vs mole % $\text{CHCl}_3/\text{CCl}_4$.	281

CHAPTER 14

14.1	Plots of the number for A or Y vs the corresponding calculated value multiplied by a factor of 10 (see Table 14.2a).	301
14.2	A plot of $\nu_{\text{C=O}}$ for tert-butyrophenone (phenyl tert-butyl ketone) vs mole % $\text{CHCl}_3/\text{CCl}_4$.	302
14.3	Plots of the $\nu_{\text{C=O}}$ frequencies for acetone, α -chloroacetone, acetophenone, and benzophenone in CS_2 solution between ~ 29 and -100°C .	303
14.4	Plots of $\nu_{\text{C=O}}$ for 2% wt./vol. solutions of (A) benzophenone, (B) 4-methoxyacetophenone, (C) acetophenone, (D) 4-nitroacetophenone, (E) 2,4,6-trimethylacetophenone, and (F) acetone in mole % $(\text{CH}_3)\text{SO}/\text{CCl}_4$ solutions.	303
14.5	A plot of $\nu_{\text{C=O}}$ for 1% wt./vol. cyclohexanone vs mole % $\text{CHCl}_3/n\text{-C}_6\text{H}_{14}$ solutions.	304
14.6	A plot of $\nu_{\text{C=O}}$ for 1% wt./vol. cyclohexanone vs mole % $\text{CCl}_4/n\text{-C}_6\text{H}_{14}$.	305
14.7	A plot of $\nu_{\text{C=O}}$ for 0.345 mol % acetone vs mole % $\text{CHCl}_3/\text{CCl}_4$ solutions.	306
14.8	A plot of the reaction field vs $\nu_{\text{C=O}}$ for 0.345 mole % acetone in $\text{CHCl}_3/\text{CCl}_4$ solutions.	307
14.9	IR spectra for 14 H-dibenzo [a,j] X anthen-14-one. (A) Saturated solution in hexane; (B) saturated solution in carbon tetrachloride; (C) 0.5% wt./vol. solution in chloroform.	308
14.10	Plots of $\nu_{\text{C=O}}$ and OT or CT in Fermi resonance and their corrected unperturbed frequencies for 14H-dibenzo [a,j] xanthen-14-one vs mole % $\text{CHCl}_3/\text{CCl}_4$. The solid squares and open squares represent uncorrected frequency data, the solid circle represents $\nu_{\text{C=O}}$ corrected for Fermi resonance and the open circles represent OT or CT corrected for Fermi resonance.	308
14.11	Plots of $\nu_{\text{C=O}}$ and OT or CT uncorrected and corrected for Fermi resonance for 14H-dibenzo [a,j]-xanthen-14-one vs the solvent acceptor number (A) for (1)	

- hexane; (2) carbon tetrachloride; (3) carbon disulfide; (4) benzene; (5) tetrahydrofuran; (6) methylene chloride; (7) nitrobenzene; and (8) chloroform. 309
- 14.12 Plots of $\nu_{\text{op}}(\text{C}=\text{O})_2$ and a B_{1u} CT in Fermi resonance and their unperturbed frequencies after correction for Fermi resonance for 1,4-benzoquinone vs mole % $\text{CHCl}_3/\text{CCl}_4$. 309
- 14.13 Plots of $\nu_{\text{op}}(\text{C}=\text{O})_2$ and $\nu_{\text{op}}(\text{C}=\text{C})_2$ for tetrafluoro-1,4-benzoquinone vs mole % $\text{CHCl}_3/\text{CCl}_4$. 310

CHAPTER 15

- 15.1 Plots of $\nu_{\text{C}=\text{O}}$ (solvent or neat) vs $\nu_{\text{C}=\text{O}}$ (hexane) minus $\nu_{\text{C}=\text{O}}$ (solvent or neat) for alkyl alkanoates. 352
- 15.2 Plots of $\nu_{\text{C}=\text{O}} \cdots \text{HO}(\text{ROH})$ vs $\nu_{\text{C}=\text{O}}$ (hexane) minus $\nu_{\text{C}=\text{O}} \cdots \text{HO}(\text{ROH})$ for alkyl alkanoates. 353
- 15.3 Plots of $\nu_{\text{C}=\text{O}}$ for alkyl alkanoates vs the solvent acceptor number (AN) or neat alkyl alkanoate. 354
- 15.4 Plots of $\nu_{\text{C}=\text{O}} \cdots \text{HO}(\text{ROH})$ vs the solvent acceptor number (AN) in alkyl alcohols. 355
- 15.5 Plots of the $\nu_{\text{C}=\text{O}}$ and $\nu_{\text{C}=\text{O}} \cdots \text{HO}(\text{ROH})$ frequencies vs the solvent acceptor number (AN). Extrapolation of the points on curve A to A, curve B to B, curve C to C, and curve D to D yields the postulated AN values of 9.15, 4.15, 3.00, and 2.06 for methyl alcohol through tert-butyl alcohol, respectively. 356
- 15.6 The left figure shows plots of $\nu_{\text{C}=\text{O}}$ rotational conformers 1 and 2 for ethyl 2-chloroacetate and $\nu_{\text{C}=\text{O}}$ for ethyl acetate frequencies in CS_2 solution vs temperature in $^\circ\text{C}$. The right figure shows a plot of the absorbance ratio for $\nu_{\text{C}=\text{O}}$ rotational conformer 1/rotational conformer 2 vs temperature in $^\circ\text{C}$. 356
- 15.7 A plot of the $\nu_{\text{C}=\text{O}}$ frequencies for rotational conformer 1 vs $\nu_{\text{C}=\text{O}}$ for rotational conformer 2 for methyl 2,4-dichlorophenoxyacetate with change in the CCl_4 to $(\text{CH}_3)_2\text{SO}$ ratio. 357
- 15.8 Infrared spectra of β -propranolone in CCl_4 solution (left), 52 mol % $\text{CHCl}_3/\text{CCl}_4$ solution (middle), and CHCl_3 solution (right). 357
- 15.9 A plot of unperturbed $\nu_{\text{C}=\text{O}}$ frequencies for coumarin in 1% wt./vol. $\text{CHCl}_3/\text{CCl}_4$ solutions vs mole % $\text{CHCl}_3/\text{CCl}_4$. 358
- 15.10 A plot of unperturbed $\nu_{\text{C}=\text{O}}$ frequencies for coumarin in 1% wt./vol. $(\text{CH}_3)_2\text{SO}/\text{CCl}_4$. 358
- 15.11 A plot of unperturbed $\nu_{\text{C}=\text{O}}$ frequencies for coumarin 1% wt./vol. in $(\text{CH}_3)_2\text{SO}/\text{CHCl}_3$ vs mole % $(\text{CH}_3)_2\text{SO}/\text{CHCl}_3$. 359
- 15.12 A plot of the unperturbed $\nu_{\text{C}=\text{O}}$ frequencies for coumarin 1% wt./vol. in $\text{CHCl}_3/\text{CCl}_4$ solution vs the reaction field for $\text{CHCl}_3/\text{CCl}_4$ solutions. 359
- 15.13 Plots of unperturbed $\nu_{\text{C}=\text{O}}$ frequencies for coumarin 1% wt./vol. in various solvents vs the solvent acceptor number (AN). 360
- 15.14 Plots of $\nu_{\text{C}=\text{O}}$ and a combination tone in Fermi resonance and their unperturbed $\nu_{\text{C}=\text{O}}$ and CT frequencies for phenyl acetate after correction for Fermi resonance vs mole % $\text{CHCl}_3/\text{CCl}_4$. 360

15.15	Plots of $\nu_{\text{C=O}}$ and a combination tone in Fermi resonance and their unperturbed $\nu_{\text{C=O}}$ and CT frequencies for phenyl acetate after correction for Fermi resonance vs the solvent acceptor number (AN).	361
15.16	Plots of $\nu_{\text{C=O}}$ for methyl benzoates in CS_2 solution vs temperature in $^{\circ}\text{C}$.	362
15.17	Plots of the absorbance ratio for $A(\nu_{\text{C=O}}, \text{rotational conformer 1})/A(\nu_{\text{C=O}}, \text{rotational conformer 2})$ for methyl 2-methoxybenzoate and methyl 2-bromobenzoate in CS_2 solution vs temperature in $^{\circ}\text{C}$.	363
15.18	Plots of $\nu_{\text{C=O}} \cdots \text{HO}$ frequencies for 2-hydroxyacetophenone, methyl salicylate, and phenyl salicylate vs the solvent acceptor number (AN) for each of the solvents used in the study.	364
15.19	Plots of $\nu_{\text{C=O}} \cdots \text{HO}$ for 2-hydroxyacetophenone, methyl salicylate, phenyl salicylate vs the frequency difference between $\nu_{\text{C=O}} \cdots \text{HO}$ (hexane) and $\text{C=O} \cdots \text{HO}$ (solvent) for each of the other solvents.	365
15.20	A plot of $\nu_{\text{C=O}} \cdots \text{HO}$ frequencies of phenyl salicylate vs mole % $\text{CHCl}_3/\text{CCl}_4$.	366
15.21	Bar graphs of the Raman group frequency data for 21 dialkyl phthalates.	367
15.22	Plots of $\nu_{\text{C=O}}$ for seven alkyl acrylates in 1% wt./vol. $\text{CHCl}_3/\text{CCl}_4$ solutions vs mole % $\text{CHCl}_3/\text{CCl}_4$.	367
15.23	Plots of $\nu_{\text{C=O}}$ for corresponding alkyl acrylates and alkyl methacrylates vs mole % $\text{CHCl}_3/\text{CCl}_4$ solutions.	368
15.24	10-phenoxarsinyl chloroacetate. (a) Saturated in CCl_4 and CS_2 solution, (b) split mull.	369
15.25	IR spectra of thiolbenzoic anhydride (dibenzoyl sulfide) and benzoic anhydride (dibenzoyl oxide).	370

CHAPTER 16

16.1a	Normal modes for COF_2 .	402
16.1b	Normal modes for COClF .	403
16.1c	Normal modes for COCl_2 .	404
16.2	(Upper)—Infrared spectrum of diallyl dithiol carbonate. (Lower)—Infrared spectrum of dipropyl dithiol carbonate.	405
16.3	(Upper)—Infrared spectrum of methyl thiol chloroformate. (Lower)—Infrared spectrum of phenyl thiol chloroformate.	406
16.4	Plots of $\nu_{\text{C=O}}$ frequencies of ethylene carbonate corrected for Fermi resonance vs the solvent acceptor number (AN).	407
16.5	A plot of the $\nu_{\text{C=O}}$ frequencies for ethylene carbonate corrected for Fermi resonance vs the reaction field of the $\text{CHCl}_3/\text{CCl}_4$ solutions.	408
16.6	Plots of $\nu_{\text{C=O}}$, $2\nu_{\text{C}-\text{C}(=\text{O})\text{Cl}}$, and $\nu_{\phi-\text{C}(=\text{O})\text{Cl}}$ frequencies for benzoyl chloride in CS_2 solution vs temperature in $^{\circ}\text{C}$.	409
16.7	Plots of $\nu_{\text{C=O}}$ for tetramethylurea in various solvents vs the solvent acceptor number (AN).	

Name index

A

Alain, M., 153n14
Albert, N., 174n19
Angell, C. L., 400n4

B

Badger, R. M., 174n19
Baker, A. W., 131n8
Baraceló, J. R., 173n9
Bardet, L., 153n14
Basillia, M. R., 270nn10, 11
Bauer, E., 299n5
Bellamy, L. J., 131n2, 154n19, 208n2, 270n1, 300n7
Bellanato, J., 173n9
Bennett, G. M., 131n7
Bondybey, V. E., 153n8
Bowell, R. J., 30n6
Bowles, A. J., 300n14
Boyd, D.R.J., 99n9
Brooks, C.J.W., 173n12
Brooks, G. L., 131n7
Brown, T. L., 230n3
Buckingham, A. D., 173n4, 351n3
Budde, P. B., 153n7

C

Califano, S., 153n3
Cherskaya, N. O., 153n15
Chiorboli, P., 208n5
Chrisman, R. W., 231n12
Christensen, J. J., 173n8
Chrzan, V., 300n12
Clark, T. D., 173nn2, 7, 14, 231n16, 351n12
Cleveland, F. F., 99n8
Coggeshall, N. D., 270n8
Cole, K. C., 153n12
Coleyshaw, E. E., 30n6
Colthup, N. B., xvnn3, 10, 8n4, 67n9, 10, 131n12, 146n3, 154n18, 230n4, 270n3, 300n13
Connelly, B. J., 208n2
Cottee, F. H., 300n15
Cousins, L. R., 270nn10, 11
Crawford, B., Jr., 8n8

Cronyn, M., 231n10
Cross, P. C., xvn2, 8n2

D

Daly, L. H., xvn3, 8n4, 67n9
Dauben, W. S., 208n1
Davidson, D. W., 99n8
Decius, J. C., xvn2, 8n2
de Haseth, J. A., xvn8
Deno, N. C., 131n10
Dunbar, J. E., 351n17
Dutz, H., 131n11

E

Edwards, R. T., 299n4
Eglinton, G., 173n12
Epstein, W. W., 208n1
Evans, J. C., 30n4, 67nn17, 18, 99nn2, 6, 17, 116n1, 117n3, 131n6, 174n20, 400nn2, 7

F

Fateley, W. G., xvn10, 67n10, 131n12, 146n3, 154n18, 230n4, 270n3, 300n13
Fiedler, S. L., 35n1, 99n14, 231n18
Forbes, J. W., 300n23
Forbes, W. F., 300n15
Fouchea, H. A., 8n10, 351n9
Fuson, N., 300n6

G

George, W. O., 300n14
Glasstone, S., 131n7
Golden, J.D.S., 173n10
Gordon, J. M., 300n23
Grasselli, J. G., xvn10, 67n10, 131n12, 146n3, 154n18, 230n4, 270n3, 300n13
Griffith, W. P., 30n6
Griffiths, P. R., xvn8
Grisenthwaite, H.A.J., 99n10
Guttman, V., 231n17, 351n6, 401n14

H

Hallam, H. E., 299n3, 300n7
 Hammaker, R. M., 270n12
 Hansen, L. D., 173n8
 Hasha, D. L., 8n10, 173n5, 300n19, 351n9, 400n12
 Herzberg, G., xvnl, 8n1
 Hoffman, G. A., 8n10, 351n9
 Houck, J., 300n12

I

Isatt, R. M., 173n8

J

Jagodzinski, P., 401n17
 Jameson, D. A., 231n11
 Johnson, A. L., 99n16
 Josien, M. L., 300n6
 Joyner, P., 67n15

K

Kagel, R. O., xvnl2
 Kahovec, L., 154n17
 Kallos, G. J., 99nn4, 5, 116n2, 117n4
 Killingsworth, R. B., 153n10
 King, S. T., 153n13
 Kirkwood, J. G., 299n4
 Kirrman, A., 153n9
 Kitaev, Yu P., 153n11
 Klemperer, W., 231n10
 Kohlrausch, K. W., 154n17
 Kolling, O. W., 401n16
 Kriegsman, H., 131n11
 Krueger, P. J., 153n5

L

Lange, N. A., 400n11
 Langseth, A., 8n9
 Leugers, M. A., xvnl1, 30n5, 174n17
 Linnett, I. W., 153n4
 Lin-Vien, D., xvnl0, 67n10, 131n12, 146n3, 154n18,
 230n4, 270n3, 300n13
 Lo, Y.-S., 67nn17, 18, 99n16, 116n1
 Lord, R. C., 8nn7, 9, 99n11
 Loy, B. R., 231n12
 Luoma, D. A., 131n4, 153n1, 231nn13-15, 270n5,
 300nn20, 21, 400n13
 Lutz, E.T.G., 131n3

M

Maddams, W. F., 300n14
 Magot, M., 299n5
 Maki, A., 231n10
 Mann, J. R., 35n4
 McDonald, A. T., 351n12
 McLachlan, R. D., 67n7, 230n5
 Merrifield, R. E., 99n11
 Mills, H. H., 174n18
 Mills, I. M., 8n8
 Mirone, P., 208n5
 Mitsch, R. A., 153n13
 Moccia, R., 153n3, 231n9
 Moran, J. F., 173n12

N

Nakamoto, K., xvnn13, 14
 Nibbler, J. W., 153n8
 Nivorozhkin, L. E., 153n11
 Nolin, B., 8n7
 Nyquist, I. M., 8n8
 Nyquist, R. A., xvnn5-6, 11, 12, 8nn5, 6, 10, 30nn3-5,
 35nn1-6, 67nn1-5, 7, 8, 11-13, 17, 18, 99nn1-7,
 13-17, 116nn1, 2, 117nn3, 6, 131nn1, 4, 5, 13,
 146n.1, 153nn1, 2, 6, 7, 173nn1, 2, 5, 7, 14-16,
 174n17, 208nn3, 4, 6, 7, 230nn1, 5, 6, 231nn7, 12-
 16, 18-20, 270nn2, 5-7, 299n2, 300nn8-12, 17-22,
 351nn1, 2, 5, 7-18, 400nn3, 5-10, 12, 13, 401n15

O

Ogden, P. H., 153n13
 Ogilvie, J. F., 153n12
 Overend, J., 67n16, 153n13, 400nn1, 2, 7
 Owen, N. L., 67n6

P

Pauling, L., 117n7
 Pawloski, C. E., 117n5
 Person, W. B., 8n8
 Peters, T. L., 153n7
 Phillpots, A. R., 208n2
 Pimentel, G., 231n10
 Pinchas, S., 270n9
 Plegontov, S. A., 153n11
 Potts, W. J., Jr., xvnl4, 8n3, 30n1, 67n5, 99n1, 117n6,
 351n18, 400nn3, 7
 Pozefsky, A., 270n8
 Puehl, C. W., 153n1, 231n20

Putzig, C. L., xvnn11, 30n5, 99n13, 173n5, 174n17,
231nn12, 16, 20, 300nn10, 19, 21, 351n12, 400n12,
401n15

R

Raevskii, O. A., 153n11
Raktin, O. A., 153n15
Reder, T. L., 99nn4, 5, 116n2
Regan, J. E., 230n3
Richards, R. E., 230n2
Rock, S. L., 270n12
Russell, R. A., 231n8

S

Saier, E. L., 270nn10, 11
St. Fleet, M., 173n11
Scherer, J. R., 67n16, 400n1
Scheutz, D. R., 230n3
Schrader, B., 208n8, 270n4, 299n1
Seehra, J., 401n17
Settineri, S. E., 131n4, 173n15, 270n5, 351nn10, 11,
400n5
Sheppard, N., 67n6
Shilton, R., 300n15
Shlyapochnikov, V. A., 153n15
Shulgin, A. T., 131n8
Simon, A., 131n11
Skell, P. S., 131n10
Sloane, H. J., 351n17
Slockler, G., 67n15
Socrates, G., xvnn9
Splakman, J. C., 174n18
Stec, F. F., 99n5, 116n2
Sternberg, J., 230n3
Stewart, R. L., 117n5, 173n2
Straugham, B. P., 300n15

Streck, R., 67n11, 173n2, 351nn15, 16
Strycker, S. J., 351n17
Sundaram, S., 99n8

T

Taft, R. W., Jr., 131nn9, 10, 173n3
Thompson, H. W., 99nn9, 10, 230n2, 231nn8, 9, 11
Thompson, J. W., 67n13
Timmermans, J., 351n4
Timmons, C. J., 300n15
Titova, S. Z., 153n11

V

van der Maas, J. H., 131n3

W

Ward, G. R., 99n4
Welti, D., 30n2, 173n13
West, W., 153n10, 299n4
Westover, L. B., 117n4
Wiebenga, E. H., 99n12
Wilberley, S. E., xvnn3, 8n4, 67n9
Wilkening, D., 300n20
Williams, A. L., 208n2
Williams, R. L., 270n1, 300n7
Wilson, E. B., Jr., xvnn2, 8n2
Wilti, D., 30n2
Winter, R., 67n14
Wohar, M., 401n17
Woodward, R. W., 231n12

Y

Yurga, L., 300n10

Subject index

A

- Absorbance ratios, band, 57–58
- Acceptor number (AN) values, 269, 276, 354, 355, 356
solvent, 398, 399–400
- Acetamides, 215, 216–217, 242–248
dimethyl, 224–225, 256
- Acetanilides, 222–223, 252, 253
- Acetates, 369, 373, 374
- Acetone, 288, 306, 307, 311
- Acetophenone, hydroxy-, 341–342, 378
- Acetyl chloride, 414, 415
- Acetylene, 3–4, 15
phenylacetylene, 96–97, 99, 101, 109, 113
terminal, 93–94, 106
- Acid halides. *See* Carboxylic acid halides
- Acrolein, 268
- Acrylates, 62–63, 79–80, 343–345, 379–380, 388
- Acrylic acid, 172, 200
- Acrylonitrile, 56, 57, 73, 74
- Adipate, 371
- Alcohol(s)
C–O stretching, 127
OH stretching, 125–127, 135
primary, 125, 127
propargyl, 98, 111
secondary, 125, 126
tertiary, 125
- Aldehydes
benzaldehydes, 268–270, 282, 283
conjugated, 267
Fermi resonance, 268, 270, 273, 280, 281
inductive effect, 268
IR data, 267, 282
nonconjugated, 267, 282
plots of half Fermi doublet versus mole %
CHCl₃/CCl₄, 277, 278
plots of unperturbed ν_{CH} versus CHCl₃/CCl₄, 279,
280
plots of $\nu_{\text{C=O}}$ (4-phenylbenzaldehyde) versus mole %
CHCl₃/CCl₄, 281
plots of $\nu_{\text{C=O}}$ versus acceptor number, 276
plots of $\nu_{\text{C=O}}$ versus $\nu_{\text{C=O}}$ (hexane) and $\nu_{\text{C=O}}$
(solvents), 274
plots of $\nu_{\text{C=O}}$ versus mole % CHCl₃/CCl₄, 268, 273
plots of $\nu_{\text{C=O}}$ versus σ_{p} , 268, 271, 275
Raman data, 268, 282
- Aliphatic amines. *See* Amines, aliphatic
- Alkanes, 31–34, 36, 37, 41–45
- Alkanoates, 333–335, 352, 353, 354
- Alkenes, 55, 58, 67, 90
stretching vibrations, 60
trans, 63–64, 81
- Alkyl acetamide, 216–217
- Alkyl acrylates and methacrylates, 62–63, 79–80
- Alkyl alkanoates, 333–335, 352, 353, 354
- Alkylamines. *See* Amines, aliphatic
- Alkyl benzoates, 341, 377
- Alkyl carbon-hydrogen vibrations, 31–32
cycloalkanes, 35, 48
cycloalkyl groups, 35, 49–53
epoxyalkanes, 34, 46
methylthiomethyl mercury, dimethylmercury, and
methylthiochloroformate, 35, 47
sodium dimethylphosphonate (CH₃)₂P(O)₂Na,
34–35, 47
summary, 32–34
- Alkyl chloroacetamide, 216–217
- Alkylcinnamates, 64, 84
- Alkyl ethers, vinyl, 67, 91
- Alkyl groups, 67, 90
- Alkynes, 93, 94–95, 108
absorbance ratios versus number of α -carbon atoms,
95, 100
- Allyl halides, 61, 78
- Amides
acetamides, 215, 216–217, 242–248
carboxamides, 213, 214, 215, 241
inductive effects, 219
intramolecular hydrogen bonding, 215, 219
N–H intensity, 219–222, 232
primary, 214, 220, 241, 249
secondary, 214, 220, 241, 249
tertiary, 214, 220–221, 241, 249
trans and/or cis secondary, 217–219
- Amines, aliphatic
chemical reactions of primary and secondary,
145–146
primary, NH₂ bending for alkylamines, 145
primary, Raman data for, 145, 148
primary, NH₂ stretching, 143–144, 150–151

- Amines, aliphatic (*continued*)
 primary, symbol for, 143
 primary, wag frequencies, 144
 secondary, 143, 146
 symbols for, 143
 tertiary, 143
- AN. *See* Acceptor number
- Anhydrides
 conjugated, 205, 206
 Fermi resonance, 206, 207
 in- and out-of-phases, 207–208, 212
 inductive effect, 206
 IR vapor-phase data and Raman data, 210
 maleic, 207–208, 211
 phthalic, 206–207, 209
 ring strain, 206
 structures of, 205
 thiol acid, 349–350, 387
- Anilines (arylamines), 149–150
 bond angles, 156
 plot of ν_{asym} , 155, 156
 plot of ν_{sym} , 155
 stretching frequencies versus temperature, 150–151
- Anthranilic acids, 171–172, 199
- Asymmetric molecules, 6
- Azines, 151–152, 163
- B**
- Benzaldehydes, 268–270, 282, 283
- Benzamides, 215
 N-alkyl, 223, 254
- Benzene, 5, 23
- Benzoates, 341, 377
- Benzoic acids, 170–172, 189, 191, 192, 197–198
- Benzoquinones, 297–299, 309, 310
- Benzoyl chloride, 409, 417
- Benzoyl halides, 416
- Bromobutylphthalimide, 229, 264
- Bromocyclohexane, 49
- Bromocyclopropane, 52
- Bromopropadiene, 115–123
- Bromopropyne, 5, 21
- Butadienes, 66, 89
- Butyrate, 371
- Butyrophenone, 290, 316
- C**
- Caffeine, 226–227, 260
- Carbamates, 395, 396, 418
- Carbanates, N-alkyl methyl, 223
- Carbonates, 392–393
 dithiol, 393, 405
- Fermi resonance, 408
 monothiol, 393
 thiol, 411
- Carbon-carbon double bonds (C=C), 55
 absorbance ratios and frequency separations, 57–58
 alkene stretching vibrations, 60
 alkyl acrylates and methacrylates, 62–63, 79–80
 alkyl cinnamates, 64, 84
 alkyl groups of alkenes and vinyl alkyl ethers, 67, 90, 91
 allyl halides, 61, 78
 butadienes, 66, 89
 cinnamyl esters, 64, 85
 cycloalkenes and cycloalkadienes, 61–62, 78
 disubstituted ethylenes, 65, 82
 in-plane vibrations, 56
 out-of-plane vibrations, 56–57
 propadienes, 66, 89
 Raman data, 58, 75
 rotational conformers (rotamers) and Fermi resonance, 58–60
 styrenes, 65–66, 86, 87, 88
 trans-alkenes, 63–64, 81
 twist frequencies versus σ' , 60
 vinyl alkyl ethers, 67, 91
 wag frequencies versus sigma, 60, 77
- Carbon dioxide, 3, 13
- Carbon disulfide, 3, 14
- Carbon-hydrogen vibrations, 127
- Carbon monoxide, 3, 11
- Carbon tetrafluoride, 4, 17
- Carbonyl bond angle effects, 412
- Carbonyl Fermi resonance, 407
- Carbonyl halides, 392, 402–404
- Carbonyl stretching frequencies, solute-solvent effects on, 397–398
- Carbonyl temperature effects, 409, 417
- Carboxamides, 213
 intramolecular hydrogen bonding, 215
 primary, 214, 241
 secondary, 214, 241
 tertiary, 214, 241
- Carboxylic acid halides, 416
- Carboxylic acids
 acrylic and methacrylic acids, 172, 200
 asymmetric and symmetric stretching, 172, 202
 benzoic acids, 170–172, 189, 191, 192, 197–198
 half salts of, 172–173
 inductive effects, 168, 169
 IR data for salts, 172, 203
 IR group frequency data, 167–168, 196
 IR vapor-phase data, 166, 194
 IR vapor-phase data for anthranilic acids, 171–172, 199

- mole % $\text{CHCl}_3/\text{CCl}_4$ versus absorbance $\nu\text{C}=\text{O}$ and $\nu_{\text{op}}\text{C}=\text{O}_2$, 178
 - mole % $\text{CHCl}_3/\text{CCl}_4$ versus $\nu\text{C}=\text{O}$, 176
 - mole % $\text{CHCl}_3/\text{CCl}_4$ versus $\nu_{\text{op}}\text{C}=\text{O}_2$, 177
 - plots of $\nu\text{C}=\text{O}$ and $\nu_{\text{op}}\text{C}=\text{O}_2$, 168–169, 180–191
 - plots of $\nu\text{C}=\text{O}$ versus α^* , 184, 185
 - plots of $\nu\text{C}=\text{O}$ versus α_{p} , 190
 - plots of $\nu\text{C}=\text{O}$ versus pK_{a} , 180, 181
 - plots of $\nu_{\text{op}}\text{C}=\text{O}_2$ versus $\text{CHCl}_3/\text{CCl}_4$, 187, 188
 - plots of $\nu_{\text{op}}\text{C}=\text{O}_2$ versus α^* , 186
 - plots of $\nu_{\text{op}}\text{C}=\text{O}_2$ versus α_{p} , 191
 - plots of $\nu_{\text{op}}\text{C}=\text{O}_2$ versus pK_{a} , 182, 183
 - plots of mole, 166–167, 176–178
 - plots of OH versus α_{p} , 189
 - plots of $\nu_{\text{c}}=\text{O}$ versus mole % $\text{CHCl}_3/\text{CCl}_4$, 192
 - proton numbers on α -carbon atom, 175
 - Raman data, 167, 195
 - Raman data for salts, 172, 201
 - reaction field, 167
 - rotational conformers, 168, 179
 - salts, 172
 - structures of, 165–166, 168
 - vinyl esters of, 65, 85
 - Carboxylic acid salts, 172, 331
 - acrylates, 62–63, 79–80, 343–345, 379–380, 388
 - alkyl benzoates, 341, 377
 - cinnamates, 345–346, 383, 384
 - conjugation effects, 332
 - diesters, 333
 - ester vibrations, 350
 - Fermi resonance, 360, 361
 - field effects, 348
 - half salts of, 172–173
 - inductive effects, 332, 348
 - intermolecular hydrogen bonding, 334
 - intramolecular hydrogen bonding, 333, 341
 - lactones, 337–340
 - methacrylates, 62–63, 79–80, 343–345, 388
 - phenoxarsine derivatives, 346–347, 385
 - phthalates, 342, 378
 - plot of νCO for alkyl acrylates and methacrylates versus mole % $\text{CHCl}_3/\text{CCl}_4$, 368
 - plot of νCO for alkyl acrylates versus mole % $\text{CHCl}_3/\text{CCl}_4$, 367
 - plot of νCO HO versus acceptor number, 364
 - plot of νCO HO(ROH) versus acceptor number, 355
 - plot of νCO HO versus mole % $\text{CHCl}_3/\text{CCl}_4$, 366
 - plot of νCO rotational conformer I versus II, 357
 - plot of νCO versus acceptor number, 354, 355, 356
 - rotational conformers, 335–337, 356, 357, 363
 - salicylates, 341–342, 378
 - temperature effects, 356, 362, 363
 - thiol acid anhydrides, 349–350, 387
 - thiol acids, 349, 387
 - thiol esters, 347–349, 386
 - vapor versus solution phases, 333–335
 - Center of symmetry, glyoximes and, 153
 - Chalcone, 294
 - Chloride
 - acetyl, 414, 415
 - benzoyl, 409, 417
 - Chloroformates, 393, 411, 413
 - thiol, 394–396, 406, 411, 417
 - Chloropropadiene, 116, 120
 - Christiansen effect, 25–26
 - Cinnamates, 345–346, 383, 384
 - Cinnamyl esters, 64, 85
 - Concentration effects, 299, 399
 - Condensed IR spectra, vapor-phase versus, 7
 - Conjugation effects, 332
 - Coriolis coupling constants, 95, 96
 - C–O stretching, alcohol, 127
 - Coumarin, 339–340
 - Cycloalkadienes, 61–62, 78
 - Cycloalkanes, 35, 48
 - Cycloalkanols, 127
 - Cycloalkanones, 295–297
 - Cycloalkenes, 61–62, 78
 - Cycloalkyl groups, 35, 49–53
 - Cyclohexanone, 304, 305
 - Cyclohexene, 61–62, 68, 78
 - Cyclopentene, 61, 62, 68, 78
- D**
- Depolarization, 30
 - Dialkyl ketones, 289, 290, 315, 316
 - Dielectric constant, 288, 296, 334, 397
 - Diesters, 333
 - Dihalopropynes, 98–99, 112
 - Dimethylacetamide, 224–225, 256
 - Dimethylmercury, 35, 47
 - Dimethyl-2,4-quinazolinone, 226–227, 260
 - Dimethyl-2-imidazolidinone (DMI), 225–226, 258, 259
 - Diphenylbutadiyne, 97–98, 110
 - Dipolar interaction, 221, 269, 288, 398
 - Dipolarity-polarizability effect, 399–400
 - Dipole moment change, 33
 - Disubstituted ethylenes, 65, 82
 - Dithiol carbonates, 393, 405
 - Divinylsulfone, 56, 57, 73, 74
- E**
- Epoxyalkanes, 34, 46
 - Esters
 - cinnamyl, 64, 85
 - thiol, 347–349, 386

Esters (*continued*)

- vinyl, 65, 85
- Ethers, vinyl, 58–60, 67, 91
- Ethylene carbonates, 393, 407, 408, 412
- Ethylene oxide (C₂H₂O), 6, 24
- Ethylenes, disubstituted, 65, 82
- Ethyl isobutyrate, 333
- Ethyl acetate, 333
- Ethyl propionate, 333
- Ethyl trimethylacetate, 333
- Evans Transmission Hole, 173, 193

F

- Fermi resonance (FR.), 58–60, 206, 207, 217, 360, 361
- aldehydes, 268, 270, 273, 280, 281
- carbonate, 407, 408
- correcting for, 7–8
- ketones, 290–291
- Field effects, 348
- Fluoride, propargyl, 98, 111
- Fluorolube, 26
- Foramides, 220
- Formates, 371
- Frequency separations, 57–58
- Fumarate, 50

G

- Gas chromatography, 29, 30
- Glyoximes, 152–153, 164
- Group frequencies, 30
- phthalates and Raman, 367
- Group Theory, 2
- Guanidine derivatives, 225, 257

H

- Half salts of carboxylic acids, 172–173
- Halogenated acetic acids, rotational conformers, 168, 169
- Halopropadienes, 115–123
- Halopropynes, 94, 95–96, 107
- Hammett values, 170, 222, 268, 269
- Hydantoins, 229, 265
- Hydrogen bonding, 206–207
- intermolecular, 97, 125, 126, 127, 169, 170, 171, 216, 220, 288, 289, 290, 334
- intramolecular, 126–127, 128, 131, 152, 169, 215, 216, 219, 268, 294–295, 333, 341, 396–397
- Hydrogen bromide, 3, 9
- Hydrogen chloride, 3, 10
- Hydroxyacetophenone, 341–342, 378

I

- Imides, 227–229, 262–263
- Infrared (IR) spectra
- acetamides, 217–218, 233, 244–245
- acetylene, 3–4, 15
- alkanoates, 372
- benzene, 5, 23
- bromochloroethylene, 69
- bromopropadiene, 115, 116, 118, 119, 121, 123
- bromopropyne, 5, 21, 115, 118, 119
- carbon dioxide, 3, 13
- carbon disulfide, 3, 14
- carbon monoxide, 3, 11
- carbon tetrafluoride, 4, 17
- carboxylic acid esters, 371
- chloropropadiene, 116, 120
- dichloropropyne, 98, 103, 104
- dithiol carbonate, 405
- ethylene oxide, 6, 24
- halopropadienes, 115–123
- hydrogen bromide, 3, 9
- hydrogen chloride, 3, 10
- iodopropadiene, 116, 122
- iodopropyne, 5, 22
- maleic anhydride, 207, 211
- methane, 4, 16
- methyl bromide, 4–5, 19
- methyl chloride, 4–5, 18
- methyl iodide, 4–5, 20
- nitrogen oxide, 3, 12
- phthalic anhydride, 206–207, 209
- propiolactone, 357
- thiol benzoic anhydrides and benzoic anhydrides, 370
- thiol chloroformate, 406
- vapor-phase versus condensed, 7
- Infrared (IR) spectra, obtaining
- liquid films, 27–28
- mull technique, 26
- potassium bromide disk technique, 26
- solids (excluding single crystals), 25–27
- solutions technique, 27
- vapors and gases, 28–30
- In-plane vibrations, 56
- Iodopropadiene, 116, 122
- Iodopropyne, 5, 22
- Isocaffeine, 226–227, 260

K

- KBM (Kirkwood, Bauer, Magot) equation, 288, 301, 312, 313
- KBr (potassium bromide) disk technique, 26
- Ketones, 287
- acetone, 288, 306, 307, 311

- aliphatic, 288–289
 - chalcones, 294
 - chemical and physical effects, 291
 - concentration effects, 299
 - conjugated carbonyl containing compounds, 291–294, 319–320
 - cycloalkanones, 295–297
 - dialkyl, 289, 290, 315, 316
 - dimethyl, 289
 - hydroxyacetophenone, 341–342, 378
 - inductive, resonance, and temperature effects, 290–291
 - intramolecular hydrogen bonding, 294–295
 - plot of reaction field, 307
 - plot of $\nu_{\text{C=O}}$ and σ_{p} , 291
 - reaction field, 296
 - ring deformation, 295
 - solute-solvent interaction affected by steric factors, 289–290
 - solvent-induced frequency shifts, 288–289
 - substituted benzoquinones, 297–299, 309, 310
- L**
- Lactams, 217
 - Lactones, 337–340, 357
 - Linear molecules, 2–4
 - Liquid films, 27–28
- M**
- Maleic anhydrides, 207–208, 211
 - Malonates, 371
 - Methacrylates, 62–63, 79–80, 343–345, 388
 - Methacrylic acid, 172, 200
 - Methane, 4, 16
 - Methyl acetamide, 216–217, 242, 243
 - Methyl acetate, 333
 - Methyl bromide, 4–5, 19
 - Methyl carbanates, N-alkyl, 223
 - Methyl chloride, 4–5, 18
 - Methyl chloroacetamide, 217, 243
 - Methyl iodide, 4–5, 20
 - Methyl isobutyrate, 333
 - Methyl methacrylamide, 216
 - Methyl propionate, 333
 - α -Methylstyrenes, 65–66, 86, 87
 - Methylthiochloroformate, 35, 47
 - Methylthiomethyl mercury, 35, 47
 - Methyl trimethylacetate, 333
 - Molecular structure, examples of
 - asymmetric, 6
 - linear, 2–4
 - mull technique, 26
 - spherical, 4
 - symmetric, 4–5
 - Molecular weight
 - absorbance ratios versus number of carbon atoms, 95, 100
 - vasym, 31, 36
 - vsym, 31, 37
 - Monothiol carbonates, 393
 - Mull technique, 26
- N**
- N–H intensity, 219–222
 - Nitrogen oxide, 3, 12
 - Nujol, 26
 - Nyquist Rule, xiv
- O**
- OH groups
 - bending, 128
 - intermolecular hydrogen bonding, 128
 - intramolecular hydrogen bonding, 128–131
 - mole % $\text{CHCl}_3/\text{CCl}_4$, 128
 - stretching for alcohols, 125–127, 135
 - stretching for phenols, 127
 - unassociated, 127
 - Out-of-plane vibrations, 56–57
 - Oxamides, 223–224, 255
 - Oxide, ethylene, 6, 24
 - Oximes, 152–153
- P**
- Parallel band, 3
 - Perpendicular band, 3
 - Perturbation theory, 173
 - Phenols, 125
 - intramolecular hydrogen bonding, 130–131
 - OH bending, 128
 - OH stretching, 127
 - temperature effects, 131
 - Phenoxarsine derivatives, 346–347, 385
 - Phenyl acetate, 340, 360, 361
 - Phenyl acetylene, 96–97, 99, 101, 109, 113
 - Phenyl ring, 223
 - Phthalates, 342, 367, 378
 - Phthalic anhydrides, 206–207, 209
 - Phthalimide, bromobutyl, 229, 264
 - Polarization, de-, 30
 - Potassium bromide disk technique, 26
 - Pressure effect, 6
 - Propadienes, 66, 89, 115–123
 - Propargyl alcohol and fluoride, 98, 111

Propynes

- dihalo, 98–99, 112
- halo, 94, 95–96, 107

Pyrone, 338

Pyrrolidone, 219–220

Q

Quinazolidinedione, 226–227, 260

Quinones, benzo-, 297–299, 309, 310

R

Raman data

- for anhydrides, 206, 210
- for bromochloroethylene, 69
- for bromopropadiene, 115, 116, 118, 119, 121, 123
- for bromopropyne, 5, 21, 115, 118, 119
- for primary amines, 145, 148
- for styrenes, 65–66, 86
- for vinyl esters of carboxylic acids, 65, 85
- for X-CH=CH₂ compounds, 58, 75

Rayleigh scattering, 25

Reaction field, 296, 334, 339, 397

Refractive index, 340, 397

Ring strain, 225, 337, 338, 393

Rotational conformers (rotamers), 7, 58–60

- carbonyl groups, 168, 179, 335–337, 356, 357, 363

S

Salicylates, 341–342, 378

Sigma, wag frequencies versus, 60, 77

Sodium dimethylphosphonate, 34–35, 47

Sodium hydrogen diacetate, 172–173

Solids (excluding single crystals), samples, 25–27

Solute-solvent effects

- affected by steric factors, 289–290
- carbonyl stretching frequencies and, 397–398

Solutions technique, 27

Solvent acceptor number, 398, 399–400

Solvent Field effect, 128

Solvent-induced frequency shifts, 288–289

Spherical molecules, 4

Steric factors, 289–290

Styrenes, 65–66, 86, 87, 88

Sulfides, dibenzoyl, 370

Sulfones

- divinyl, 56, 57, 73, 74
- vinyl phenyl, 58

Sulfoxide, dimethyl, 207

Symmetric molecules, 4–5

T

Temperature effects, 6–7, 131, 409, 417

- carboxylic acid esters, 356, 362, 363

- ketones, 290–291

- NH₂ stretching frequencies versus temperature, 150–151

Tert-butylphenone, 290, 302, 316

Tetraalkylurea, 224–225, 256

Tetrabutylurea (TBU), 224–225, 258

Tetraethylurea (TEU), 224–225, 258

Tetramethylurea (TMU), 224–226, 258, 410, 419

Thiol acid anhydrides, 349–350, 387

Thiol acids, 349, 387

Thiol carbonates, 411

Thiol chloroformates, 394–396, 406, 411, 417

Thiol esters, 347–349, 386

Thiourea, 225, 257

Trans-alkenes, 63–64, 81

s-triazinetriene, 229–230, 266

Trichloroacetaldehyde, 268

Trimethyluracil, 226–227, 260

Twist frequencies versus σ' and pK_a, 60

Twist vinyl group, 57–58

U

Uracils, 261

- trimethyl, 226–227, 260

Urea

- cyclic, 225

- tetraalkylurea, 224–225, 256

- tetrabutylurea (TBU), 224–225, 258

- tetraethylurea (TEU), 224–225, 258

- tetramethylurea (TMU), 224–226, 258

- thiourea, 225, 257

V

Vapor-phase

- trans CH=CH, 294

- versus condensed IR spectra, 7

Vibrational spectroscopy

- examples of molecular structure, 2–6

- Fermi resonance, 7–8

- pressure effect, 6

- temperature effect, 6–7

- theory of, 1–2

- vapor-phase versus condensed IR spectra, 7

Vinyl groups

- absorbance ratios and frequency separations, 57–58

- alkyl ether, 59–60

- allyl halides, 61, 78

- conjugated, 58

cycloalkadienes, 61–62, 78
cycloalkenes, 61–62, 78
esters, 65, 85
ethers, 58–59, 67, 91
phenyl sulfone, 58
rotational conformers (rotamers) and Fermi
 resonance, 58–60
twist, 57–58
twist frequencies versus σ' and pK_a , 60

wag, 57–58
wag frequencies versus sigma, 60, 77

W

Wag frequencies
 for aliphatic amines, 144
 versus sigma, 60, 77
Wag vinyl group, 57–58

Epoxides and Ethers

Epoxides	1
Glycidyl Ethers and Glycidylacrylate	4
Cyclic Ethers	5
Open Chain Aliphatic and Aliphatic Aromatic Ethers	5
Vinyl Ethers	6
References	6

Figures

Figure 1-1	8 (1)
Figure 1-2	9 (2)
Figure 1-3	10 (2)
Figure 1-4	10 (3)
Figure 1-5	11 (3)
Figure 1-6	12 (3, 4)
Figure 1-7	13 (4)
Figure 1-8	13 (4)
Figure 1-9	14 (5)

Tables

Table 1-1	15 (1)
Table 1-2	16 (2, 3)
Table 1-2a	17 (2, 3, 4)
Table 1-2b	18 (4)
Table 1-3	19 (4)
Table 1-4	20 (4)
Table 1-5	21 (5)
Table 1-6	22 (5)
Table 1-7	23 (5)
Table 1-8	24 (6)
Table 1-9	25 (6)

*Numbers in parentheses indicate in-text page reference.

EPOXIDES

Ethylene oxide is a cyclic three-membered ring with the molecular formula C_2H_4O , and it has C_{2v} symmetry. The vapor-phase infrared (IR) spectrum of ethylene oxide is shown in Figure 1.1, and Potts has assigned its vibrational spectrum (1). However, assignment of the antisymmetric B_1 ring deformation was not apparent using 1 cm^{-1} resolution. A vapor-phase IR spectrum of ethylene oxide has been recorded using 0.25 cm^{-1} resolution and the antisymmetric ring deformation was observed at 897 cm^{-1} (2). The fundamental vibrations of ethylene oxide are given in Table 1.1.

The three characteristic ring modes in ethylene oxide are ring breathing, symmetric ring deformation, and antisymmetric ring deformation. These three modes are illustrated here:

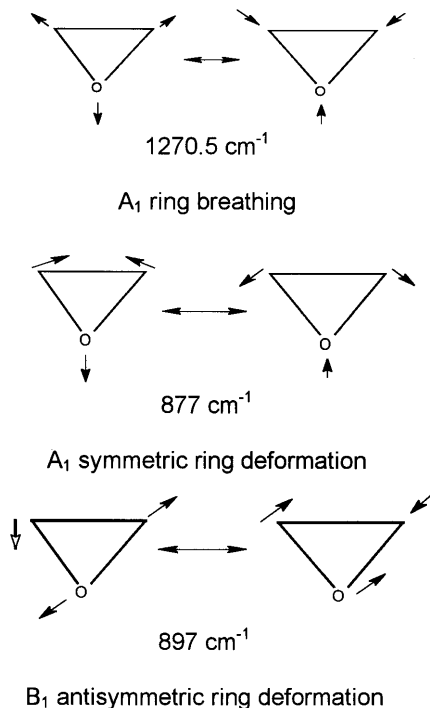


Figure 1.2 shows a vapor-phase IR spectrum of 1,2-propylene oxide. This molecule does not even have a plane of symmetry, and its molecular symmetry is C_1 . The vapor-phase IR bands near 1269, 839, and 959 cm^{-1} are assigned as ring breathing, symmetric ring deformation, and antisymmetric ring deformation, respectively. For the 1,2-epoxyalkanes (3-alkyl-1,2-ethylene oxide) studied (3), these three fundamentals occur in the ranges 1248–1271, 830–877, and 883–941 cm^{-1} , respectively.

The ring breathing mode decreases in frequency as the 3-carbon atom becomes increasingly branched. Thus, the ring breathing mode occurs at 1265, 1259, 1256, and 1248 cm^{-1} for the 3-methyl, 3-ethyl, 3-isopropyl and 4-tert-butyl analogs respectively, of 3-alkyl-1,2-ethylene oxide in CCl_4 solution. It is suggested that the ring breathing mode frequency decrease is due to the electron release of the 3-alkyl group to the C_2 atom, which increases with increased branching in the C_3 atom and which then weakens the bonds, respectively (see Tables 1.2 and 1.2a).

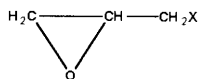


An extensive study of styrene oxide in $\text{CDCl}_3/\text{CCl}_4$ shows that the epoxy ring breathing mode increases in frequency in a systematic manner from 1252.4 cm^{-1} in CCl_4 solution to 1252.9 cm^{-1} in 52 mol % $\text{CDCl}_3/\text{CCl}_4$ solution to 1253.5 cm^{-1} in CDCl_3 solution. Figure 1.3 shows a plot of mole % $\text{CDCl}_3/\text{CCl}_4$ vs the epoxy ring breathing mode frequency for styrene

oxide, which illustrates the smooth increase in frequency as the mol % $\text{CDCl}_3/\text{CCl}_4$ is increased (4). Figure 1.4 shows a plot of the symmetric ring deformation frequency for styrene oxide vs mole % $\text{CHCl}_3/\text{CCl}_4$. This plot shows that symmetric ring deformation decreases in frequency as the mole % $\text{CHCl}_3/\text{CCl}_4$ is increased (4). Figure 1.5 is a plot of antisymmetric ring deformation frequency for styrene oxide vs $\text{CDCl}_3/\text{CCl}_4$, and it shows that this mode increases in frequency as the mole % $\text{CDCl}_3/\text{CCl}_4$ is increased (4). The reaction field becomes larger as the mole % $\text{CDCl}_3/\text{CCl}_4$ is increased, and, consequently, there is a larger dipolar interaction between styrene oxide as the mole % $\text{CDCl}_3/\text{CCl}_4$ is increased. The linear frequency shift is attributed to dipolar effects between styrene oxide and the solvent system. Breaks in the plots are attributed to hydrogen bonding to the oxygen atom of the epoxy group and to the π system of the phenyl group of styrene oxide (4).

The compound 2,4-dichlorostyrene oxide exhibits bands at 1249, 989, and 880 cm^{-1} , which are assigned to epoxy ring breathing, asymmetric deformation, and symmetric deformation, respectively. These assignments are comparable to those exhibited by styrene oxide (see Table 1.2a).

The epihalohydrins, or 3-halo-1,2-epoxypropanes, have the empirical structure:



Electron-diffraction studies of epichlorohydrin (5) and epibromohydrin (6) in the vapor phase have shown that both exist in a molecular configuration where the $\text{C}(3)\text{-X}$ bond eclipses the $\text{C}(2)\text{-H}$ bond and where the halogen atom is almost trans relative to the midpoint of the $\text{C}(1)\text{-O}$ bond about the $\text{C}(2)\text{-C}(3)$ bond.

Table 1.2 lists the characteristic epoxy ring modes for the F, Cl, Br, and I analogs for the epihalohydrins. The RT rotational conformer corresponds to the rotational conformer, which is nearly trans to the midpoint of the C-O bond (7, 8). In solution or neat phases, the IR bands, which decrease in intensity with a decrease in temperature, correspond to the trans rotational conformer (RT). The bands, which increase in intensity with decrease in temperature, are assigned to the rotational conformer (R1). Ring breathing, antisymmetric deformation, and symmetric deformation fall within the same ranges exhibited by the 1,2-epoxyalkanes (see Table 1.2). Complete vibrational assignments for the epihalohydrins have been made using IR and Raman data (see Table 1.2a) (7).

Trans-2,3-epoxybutane (or trans-1,2-dimethyl ethylene oxide) exhibits epoxy ring breathing at 1252 cm^{-1} in CS_2 solution while the corresponding mode for the cis isomer occurs at 1273 cm^{-1} . Both the cis and the trans isomer exhibit epoxy antisymmetric deformation at 885 cm^{-1} in CS_2 solution. In the case of epoxy symmetric deformation, the trans isomer occurs at 810 cm^{-1} and it occurs at 778 cm^{-1} for the cis isomer. Thus, the cis and the trans isomers of 2,3-epoxybutane exhibit symmetric epoxy deformation at lower frequency than those exhibited by the 1,2-epoxyalkanes ($883\text{--}985\text{ cm}^{-1}$) (see Table 1.2). The IR vapor-phase spectrum for trans-2,3-epoxybutane is shown in Figure 1.6. The ring breathing, antisymmetric deformation, and symmetric deformation are assigned near 1258 , 885 , and 817 cm^{-1} in the vapor phase.

Tetrachloroethylene oxide has C_{2v} symmetry and the A_1 ring breathing mode is assigned at 1332 cm^{-1} , the A_1 symmetric ring deformation at 890 cm^{-1} , and the B_1 antisymmetric ring deformation at 978 cm^{-1} . All three of these epoxy in-plane ring modes occur at higher frequency

than do the corresponding modes for ethylene oxide (1270, 877, and 897 cm^{-1} , respectively). The rise in frequency for each mode most likely results from the positive inductive effect of the four Cl atoms, which has the effect of strengthening the bonds of the group.



Vibrational assignments for the CH_2X groups for 3-halo-1,2-epoxypropanes are compared to those for 3-halopropynes, 3-halopropenes, and PCH_2X -containing compounds and they are presented in Table 1.3. In several cases, there is spectral evidence for rotational conformers.

Table 1.2b also lists the symmetric CH_3 bending, in-phase $(\text{CH}_3)_2$ or $(\text{CH}_3)_3$ bending, and out-of-phase $(\text{CH}_3)_2$ or $(\text{CH}_3)_3$ bending modes for some 1,2-epoxy alkanes. These fundamentals are useful in distinguishing between the 1,2-epoxyalkanes.

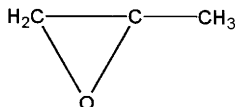
Table 1.4 lists both the frequency and absorbance data for oxirane ring breathing, oxirane symmetric in-plane ring deformation, and oxirane asymmetric in-plane ring deformation for 1,2-epoxyalkanes (3). The oxirane CH_2 modes are also listed (3). The oxirane asym. CH_2 stretching mode occurs in the range 3038–3065 cm^{-1} , the oxirane sym. CH_2 stretching mode in the range 2990–3001 cm^{-1} , the oxirane CH_2 bending mode in the range 1479–1501 cm^{-1} , and the oxirane CH_2 wagging mode in the range 1125–1130 cm^{-1} .

Figure 1.6 is a plot of the absorbance data (A) for the oxirane ring breathing mode divided by (A) for the oxirane antisymmetric CH_2 stretching mode vs the number of carbon atoms for the 1,2-epoxy alkanes (the exception is the data point for the ethylene oxide).

Figure 1.7 is a plot of (A) for the ring breathing mode divided by (A) for the oxirane antisymmetric CH_2 stretching mode vs the number of carbon atoms in 1,2-epoxyalkanes. Figure 1.8 is a plot of (A) for oxirane antisymmetric CH_2 stretching divided by (A) for antisymmetric CH_2 stretching of the alkyl group vs the number of carbon atoms in the 1,2-epoxyalkanes (3). The plots for both figures show a relatively smooth correlation and that the absorbance ratios decrease as the length of the alkyl group increases.

GLYCIDYL ETHERS AND GLYCIDYLACRYLATE

The glycidyl group is also named 2,3-epoxypropyl, and the sym. epoxy ring deformation, asym. epoxy ring deformation, and the epoxy ring breathing vibration for four compounds occur in the ranges 840–853 cm^{-1} , 912–920 cm^{-1} , and near 1241–1251 cm^{-1} , respectively, for bis-(2,3-epoxypropyl) ether, 2,3-epoxy propyl phenyl ether, di-glycidyl ether of bis-phenol-A, and 2,3-epoxypropyl acrylate (see Table 1.2a). Strong absorption from a band involving phenyl-oxygen stretching near 1240 cm^{-1} appears to mask the epoxy ring breathing vibrations. Further, the strong absorption from C–C–O stretching in the case of the acrylate also masks the epoxy ring breathing vibration. Monomers of this type are important in the manufacture of epoxy-based paints.



CYCLIC ETHERS

Figure 1.9 is a vapor-phase IR spectrum of tetrahydrofuran. The IR bands near 1071 and 817 cm^{-1} are assigned to antisymmetric and symmetric C–O–C stretching, respectively. In the IR the antisymmetric C–O–C mode is more intense than the symmetric C–O–C mode while the opposite is observed in the Raman spectrum.

Table 1.5 lists correlations for the ring stretching vibrations for cyclic ethers. Study of this table shows that there is a trend for the antisymmetric C–O–C stretching vibration to increase in frequency while the symmetric C–O–C stretching vibration decreases in frequency as the number of atoms in the ring increase from 3 to 6.

OPEN CHAIN ALIPHATIC AND ALIPHATIC AROMATIC ETHERS

Dimethyl ether has the basic structure $(\text{CH}_3)_2\text{O}$, and it is the first member of the open chain aliphatic ethers. The antisymmetric $(\text{C}-)_2\text{O}$ and symmetric $(\text{C}-)_2\text{O}$ vibrations are assigned at 1102 and 929 cm^{-1} , respectively (14). In the vapor phase, asymmetric $(\text{C}-)_2\text{O}$ occurs in the range 1111–1140 cm^{-1} in the series $(\text{C}_2\text{H}_5)_2\text{O}$ through $(\text{C}_{10}\text{H}_{21})_2\text{O}$, and it tends to decrease in frequency as n increases in the $(\text{C}_n\text{H}_{2n+1})_2\text{O}$ series (15). Table 1.6 lists IR data for several ethers. The situation becomes more complex when the ether alpha carbon atoms become branched. There is considerable mixing of $(\text{C}-)_n\text{C}$ stretching and C–O stretching, and the correlations are not as straightforward as those for $(n\text{-C}_n\text{H}_{2n+1})_2\text{O}$. In the case of branched ethers such as methyl tert-butyl, ether bands at 1187 and 1070 cm^{-1} involve stretching of the $(\text{CH}_3)_3\text{C}-\text{O}$ and CH_3-O groups.

Both methyl phenyl ether, commonly named anisole (1248 and 1041 cm^{-1}), and ethyl phenyl ether, commonly named phenetole (1245 and 1049 cm^{-1}), exhibit two bands in the IR assigned to the phenyl–O–R group. These may be assigned as antisymmetric and symmetric phenyl–O–R stretching, respectively. However, the 1245–1248 cm^{-1} band involves a complex mode involving phenyl-oxygen stretching. The 1041–1049 cm^{-1} band could be viewed as C–O stretching.

Poly (ethyleneglycol), poly (propyleneglycol), and poly (epichlorohydrin) exhibit a strong IR band near 1100, 1105, and 1105 cm^{-1} , respectively. These bands are assigned to antisymmetric $(\text{C}-)_2\text{O}$ stretching in these polymer chains.

In a study of the correspondingly ring-substituted anisoles and phenetoles in the vapor phase, several correlations were developed (16). The phenyl-oxygen-stretching mode for anisole occurs in the range 1243–1280 cm^{-1} and for phenetole in the range 1240–1260 cm^{-1} . Moreover, ring-substituted anisoles occur at higher frequency than those for correspondingly ring-substituted phenetoles. The C–O stretching frequency for the anisoles occurs in the range 1041–1059 cm^{-1} and for phenetoles in the range 1040–1051 cm^{-1} . The C–O stretching frequencies for the phenetoles are not consistently higher in frequency than those for the corresponding ring-substituted anisoles (16).

Table 1.7 lists IR data for 3-X- and 4-X-anisoles in the neat and CS_2 solution phases. The CH_3-O stretching vibration in the neat phase for 3-X- and 4-X-anisoles occurs in the range 1021–1052 cm^{-1} . In the vapor phase, it occurs at higher frequency [e.g., 4- NO_2 , 1022 (neat) vs

1041 (vapor)]. Strong IR bands in the region 1198–1270 cm^{-1} are assigned to the complex phenyl-oxygen stretching vibration.

Table 1.8 lists Raman data for vinyl phenyl ether and alkyl vinyl ethers (17). Tentative assignments are presented for these data.

In the case of phenyl vinyl ether, the Raman bands at 1026, 1002 and 615 cm^{-1} whose relative intensities are 4, 9, and 1 are characteristic of mono-substituted benzenes. These bands are very insensitive to substituent groups (18). Infrared spectra and assignments for vinyl ethers are given in Reference 19.

VINYL ETHERS

Infrared bands in the regions 933–972 cm^{-1} and 800–826 cm^{-1} are assigned to vinyl twist and vinyl CH_2 wag, respectively. These vinyl groups exist in *cis* and *gauche* forms where $\text{C}=\text{C}$ stretching vibrations occur in the region 1600–1665 cm^{-1} . The higher frequency band is assigned to the *gauche* isomer while the lower frequency band is assigned to the *cis* isomer. Another band present is due to the first overtone of vinyl CH_2 wag being in Fermi resonance with $\text{C}=\text{C}$ stretching. An IR strong band in the region 1165–1210 cm^{-1} results from $\text{C}=\text{C}-\text{O}$ stretching.

In the case of divinyl ether, *gauche* and *cis* $\text{C}=\text{C}$ stretching are assigned at 1650 and 1626 cm^{-1} , respectively (19).

Aryl vinyl ethers exhibit *gauche* and *cis* $\text{C}=\text{C}$ stretching in the regions 1639–1645 cm^{-1} and 1623–1631 cm^{-1} , respectively (19). In addition to the medium strong IR band in the region 1137–1156 cm^{-1} assigned as $\text{C}=\text{C}-\text{O}$ stretching, the vinyl aryl ethers exhibit a strong IR band at higher frequency (1190–1250 cm^{-1}) assigned to a complex mode involving stretching of the phenyl-oxygen bond. This vibration appears to increase in frequency as the phenyl ring becomes increasingly substituted (19).

Table 1.8 for vinyl ethers shows that the Raman band intensity for the *cis* $\text{C}=\text{C}$ stretching conformer is usually more intense than for the *gauche* $\text{C}=\text{C}$ stretching conformer while in the case of IR the *cis* $\text{C}=\text{C}$ stretching band intensity is also usually more intense than it is for band intensity for the *gauche* $\text{C}=\text{C}$ stretching vibration. Temperature studies of 2-ethylhexyl vinyl ether has shown that the *cis* conformer is the more stable form (20).

Table 1.9 lists vapor-phase IR data for the alkyl group of vinyl alkyl ethers (21). These data are helpful in spectra-structure identification of compounds of this type. The Sadtler collection of vapor-phase IR spectra are essential for spectroscopists utilizing the GC/FT-IR techniques (21).

REFERENCES

1. Potts, W. J. (1965). *Spectrochim. Acta*, **21**: 511.
2. Nyquist, R. A. and Putzig, C. L. (1986). *Appl. Spectrosc.*, **40**: 112.
3. Nyquist, R. A. (1986). *Appl. Spectrosc.*, **40**: 275.
4. Nyquist, R. A. and Fiedler, S. (1994). *Vib. Spectrosc.*, **7**: 149.
5. Igarashi, M. (1955). *Bull. Chem. Soc. Japan*, **28**: 58.

6. Igarashi, M. (1961). *Bull. Chem. Soc. Japan*, **34**: 165.
7. Nyquist, R. A., Putzig, C. L., and Skelly, N. E. (1986). *Appl. Spectrosc.*, **40**: 821.
8. Evans, J. C. and Nyquist, R. A. (1963). *Spectrochim. Acta*, **19**: 1153.
9. Nyquist, R. A., Reder, T. L., Ward, G. R., and Kallos, G. J. (1971). *Spectrochim. Acta*, **27A**: 541.
10. Nyquist, R. A., Reder, T. L., Stec, F. F., and Kallos, G. J. (1971). *Spectrochim. Acta*, **27A**: 897.
11. McLachlan, R. D. and Nyquist, R. A. (1968). *Spectrochim. Acta*, **24A**: 103.
12. Nyquist, R. A. (1968). *Appl. Spectrosc.*, **22**: 452.
13. Nyquist, R. A. (1984). *The Interpretation of Vapor-Phase Infrared Spectra, Group Frequency Data*. Philadelphia: Sadtler Research Laboratories, A Division of Bio-Rad Laboratories, p. 428.
14. Herzberg, G. (1945). *Molecular Spectra and Molecular Structure II. Infrared and Raman Spectra of Polyatomic Molecules*. Princeton, NJ: D. Van Nostrand Company, Inc.
15. Nyquist, R. A. (1984). *The Interpretation of Vapor-Phase Infrared Spectra, Group Frequency Data*. Philadelphia: Sadtler Research Laboratories, A Division of Bio-Rad Laboratories, p. 434.
16. Nyquist, R. A. (1984). *The Interpretation of Vapor-Phase Infrared Spectra, Group Frequency Data*. Sadtler Research Laboratories, A Division of Bio-Rad Laboratories, p. 440.
17. Sadtler Standard Raman Spectral Data.
18. Nyquist, R. A. and Kagel, R. O. (1977). *Organic Materials. Infrared and Raman Spectroscopy, Part B, Practical Spectroscopy Series*, vol. 1, E. G. Brame and J. G. Grasselli, eds., Marcel Dekker, Inc., New York, p. 476.
19. Nyquist, R. A. (1989). *The Infrared Spectra Building Blocks of Polymers*. Philadelphia: Sadtler Research Laboratories, Division of Bio-Rad Laboratories Inc., p. 33 and IR spectra 1–158 through 1–171.
20. Owen, N. L. and Sheppard, N. (1964). *Trans. Faraday Soc.*, **60**: 634.
21. (1977). *Sadtler Standard Infrared Vapor Phase Spectra*. Philadelphia: Sadtler Research Laboratories, Division of Bio-Rad Laboratories Inc.

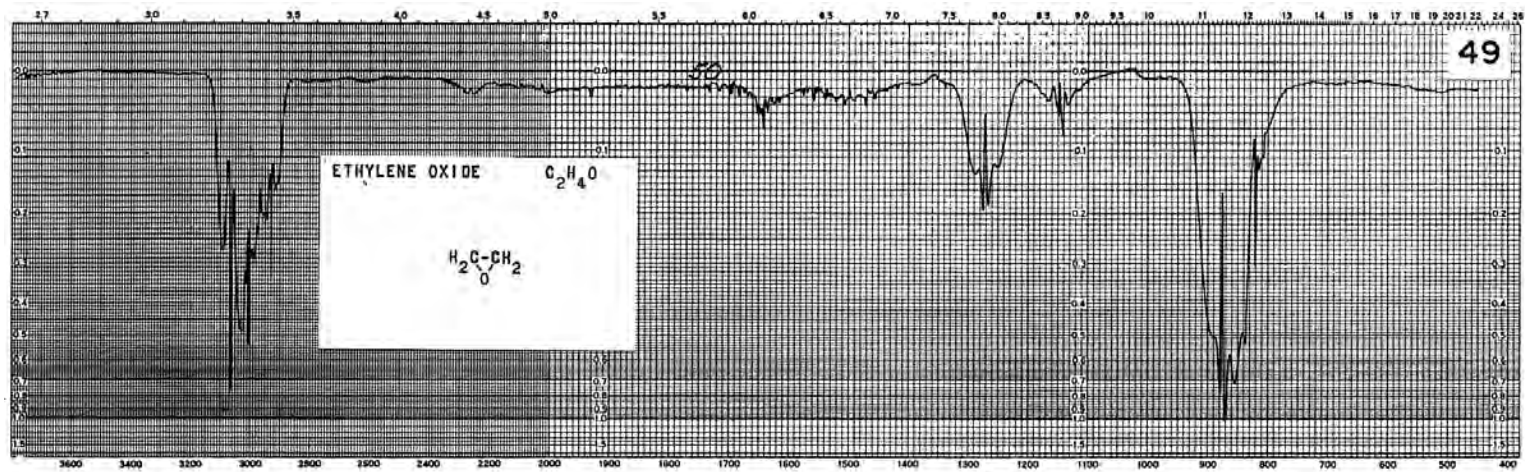


FIGURE 1.1 Vapor-phase IR spectrum of ethylene oxide.

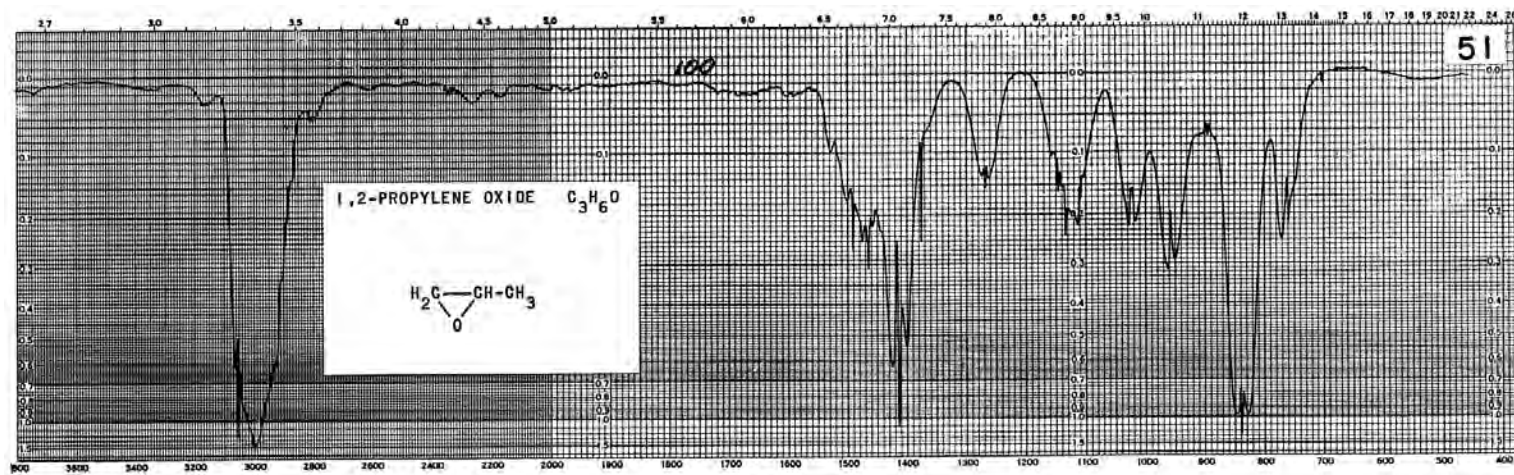


FIGURE 1.2 Vapor-phase IR spectrum of propylene oxide.

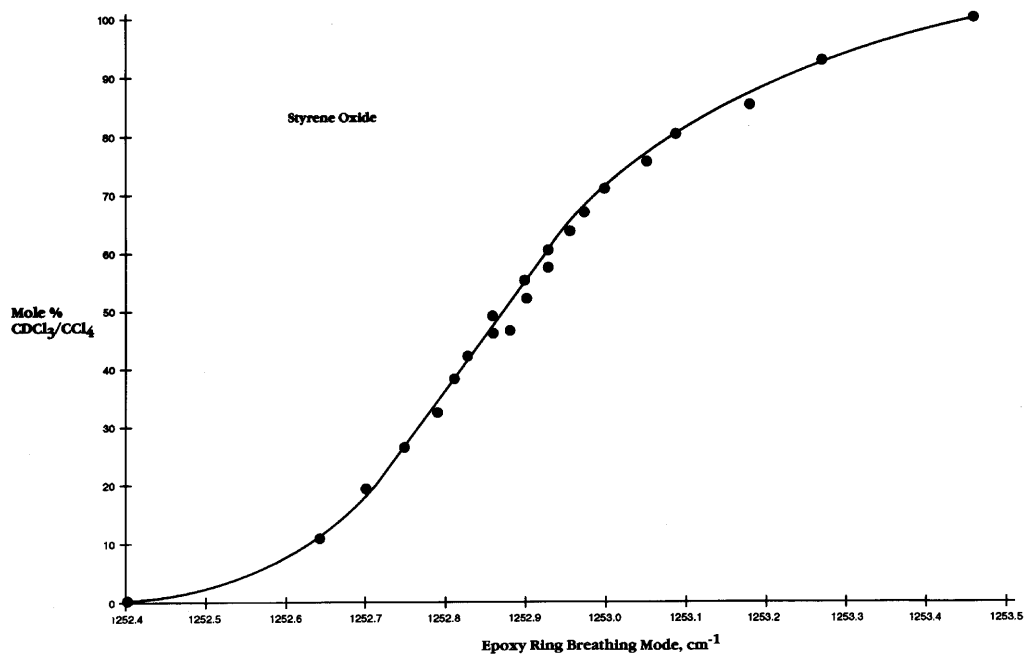


FIGURE 1.3 A plot of the epoxy ring breathing mode frequency for styrene oxide vs the mole % $\text{CDCl}_3/\text{CCl}_4$ (4).

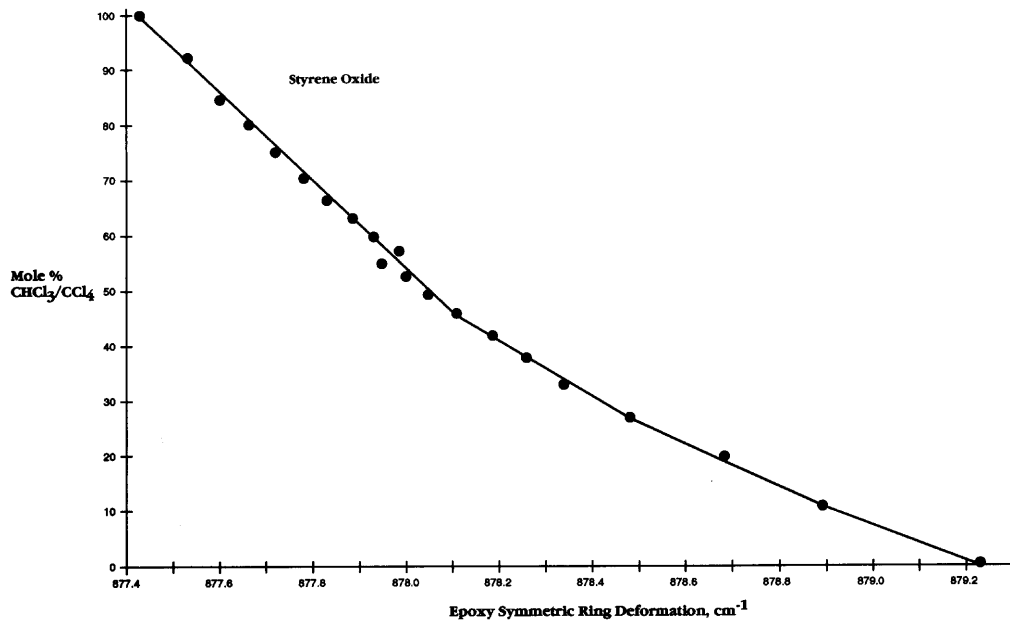


FIGURE 1.4 A plot of the symmetric ring deformation frequency for styrene oxide vs mole % $\text{CDCl}_3/\text{CCl}_4$ (4).

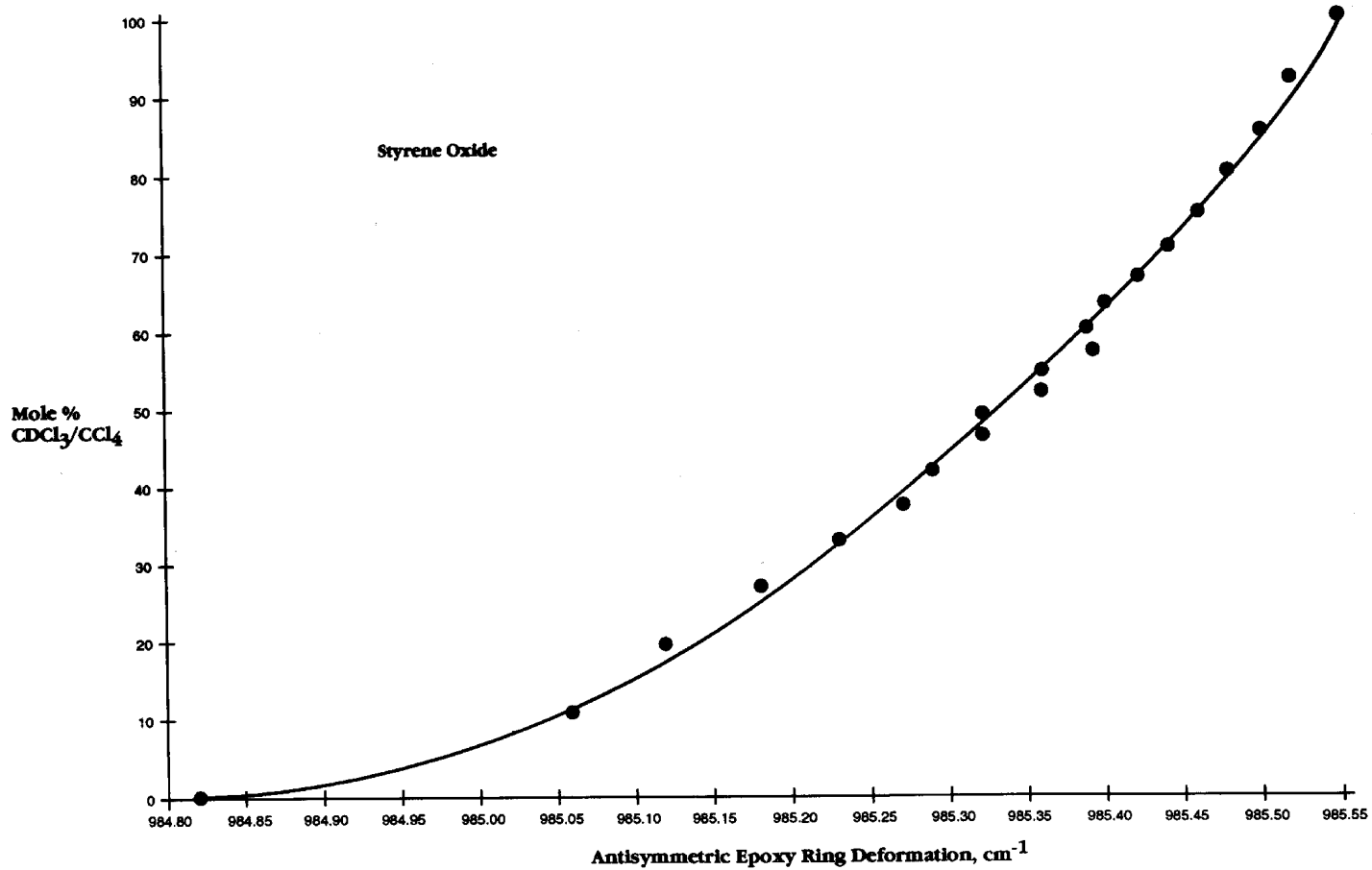


FIGURE 1.5 A plot of the antisymmetric ring deformation frequency for styrene oxide vs mole % $\text{CDCl}_3/\text{CCl}_4$ (4).

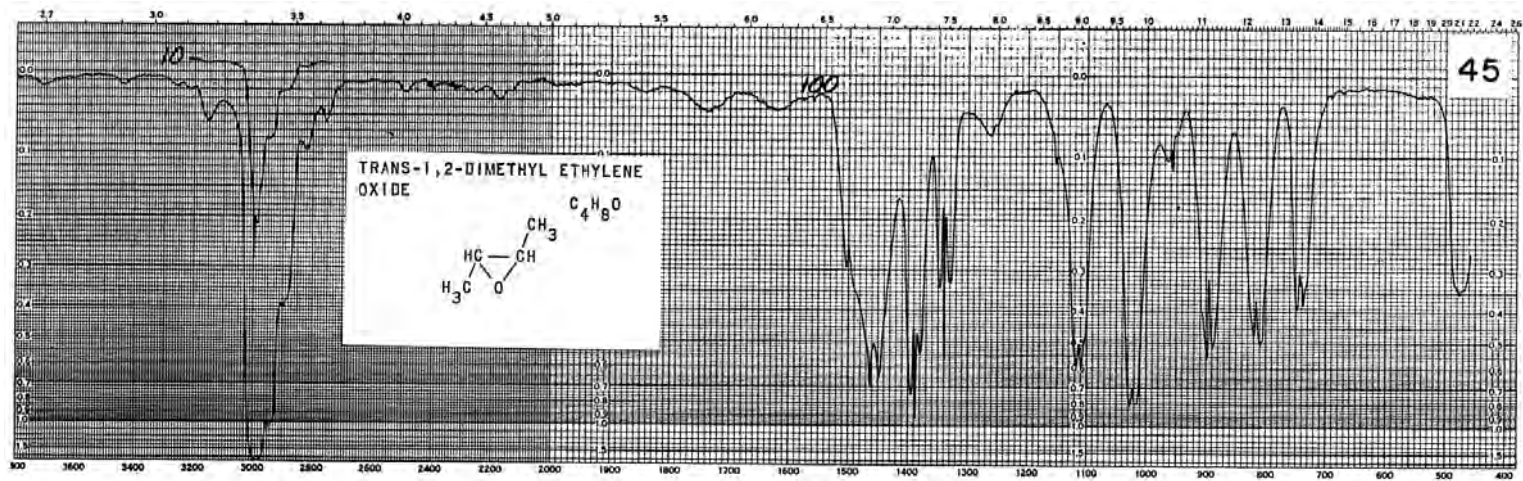


FIGURE 1.6 Vapor-phase IR spectrum of trans-2,3-epoxybutane (or trans-1,2-dimethyl ethylene oxide).

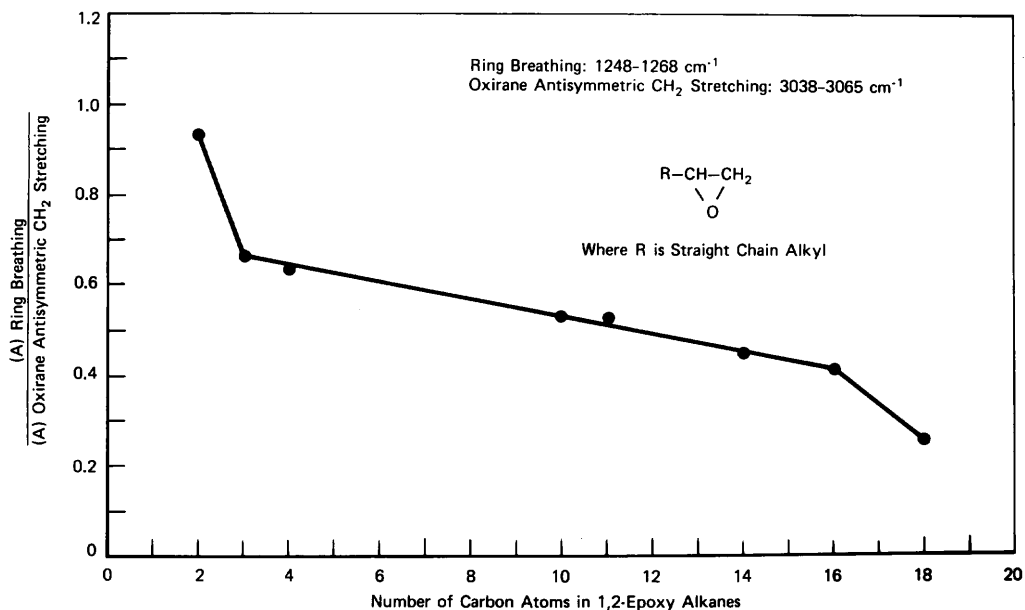


FIGURE 1.7 A plot of the absorbance (A) for the oxirane ring breathing mode divided by (A) for the oxirane antisymmetric CH_2 stretching mode vs the number of carbon atoms for the 1,2-epoxyalkanes (ethylene oxide is the exception).

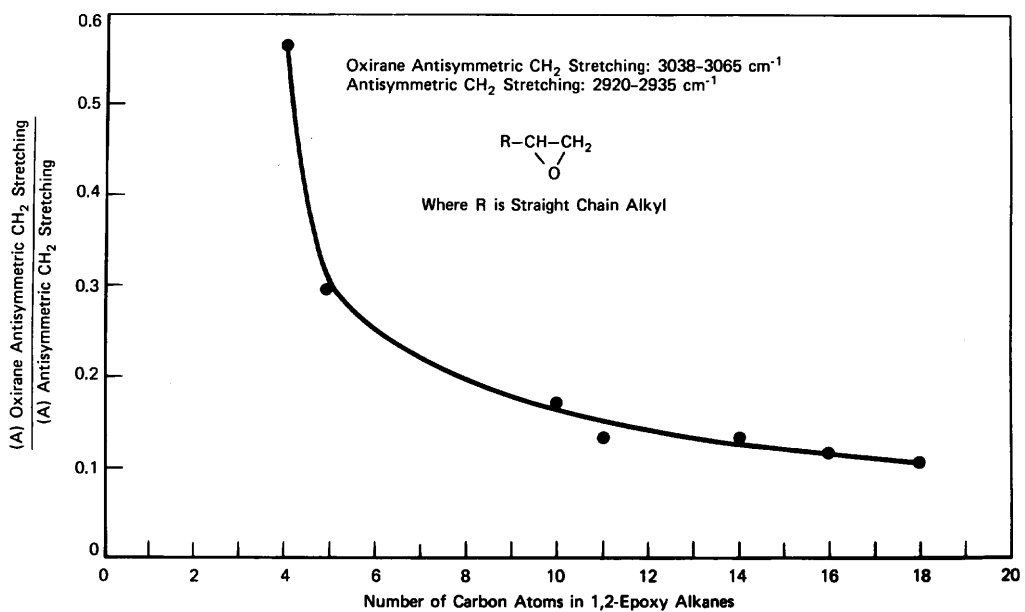


FIGURE 1.8 A plot of (A) for oxirane antisymmetric CH_2 stretching divided by (A) for antisymmetric CH_2 stretching for the alkyl group vs the number of carbon atoms in the 1,2-epoxyalkanes.

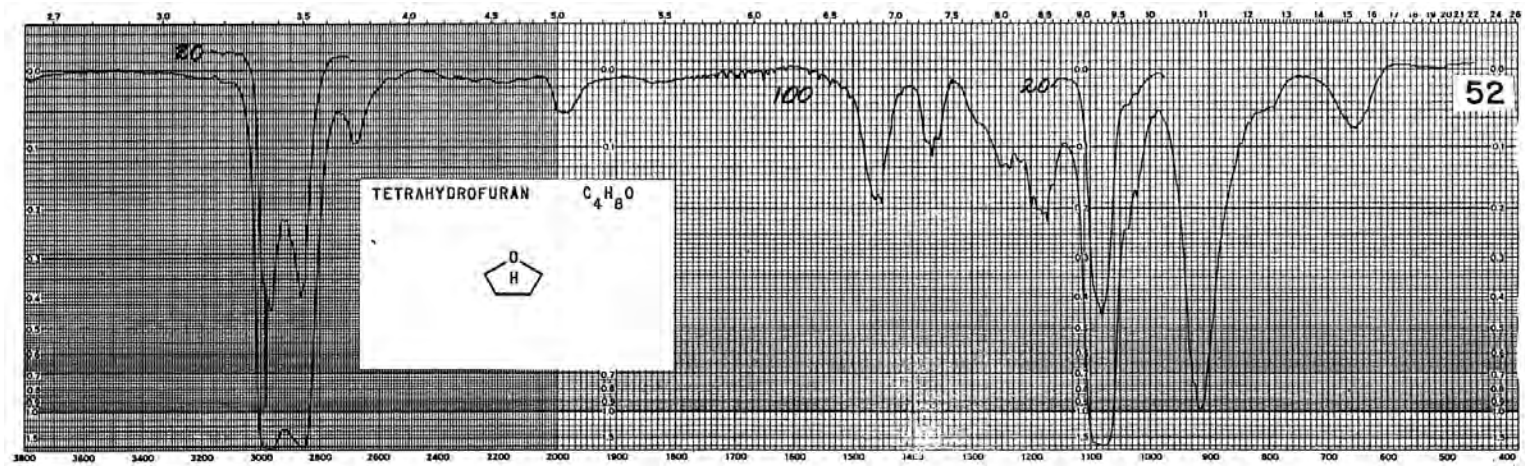


FIGURE 1.9 Vapor-phase IR spectrum of tetrahydrofuran.

TABLE 1.1 Vibrational assignments for ethylene oxide

Species and mode	Ethylene oxide cm ⁻¹
A ₁	(1,2)
s.CH ₂ str.	~ 3006
CH ₂ deformation	1497.5
Ring breathing	1270.5
CH ₂ wagging	~ 1130
s.Ring deformation	897
B ₂	
a.CH ₂ str.	3065
CH ₂ twisting	1412
CH ₂ rocking	821.5
B ₁	
s.CH ₂ str.	3006
CH ₃ deformation	1471.5
CH ₂ wagging	1151
a.Ring deformation	897
A ₂	
a.CH ₂ str.	~ 3065
CH ₂ twisting	~ 1300
CH ₂ rocking	~ 860

TABLE 1.2 Characteristic epoxy ring modes

References	(1,2) Ethylene oxide	(3) 1,2-Epoxy alkanes	(4) Styrene oxide	(5) 1,2-Epoxy- propane 3-fluoro-	(5) 1,2-Epoxy- propane 3-chloro-	(5) 1,2-Epoxy- propane 3-bromo	(5) 1,2-Epoxy- propane 3-iodo-	Rotational isomer	Range
Epoxy ring modes									
Ring breathing	1270.5	1248–1271	1252.4	1257.4 [—]	1254.8 1266.8	1256.1 1262	1260 1253	R1 RT	1248–1271
Antisymmetric deformation	897 [5]	883–941	984.8	906.4	905.8	888.2	911	R1	883–985
Symmetric deformation	877	830–877	879.2	860 838.2	854 845	845.8 833.2	841 862	R1 RT	830–877
RT = trans isomer R1 = gauche isomer?									
Asym. CH ₂ str.	(~3065)	3038–3051		3067.7	3063.4	3059.4	3051		3038–3068
Sym. CH ₂ str.	(~3006)	2989–3001		3011	3003.9	3000	2991		2989–3011
CH ₂ bending	1497.5	1479–1501		1530	1520	1512	1500		1497–1530
CH ₂ wagging	(~1130)	1125–1130							1125–1130
	trans-2,3- epoxy- butane [vapor]; [CS ₂]	3,4-epoxy- 1-butene [vapor]	1,2-epoxy- propane [vapor]	1,2-epoxy- 3-isopropoxy- propane [neat]	cis-2,3-epoxy butane [CS ₂]	tetrachloro- ethylene oxide [CS ₂]	2-methyl-2,3- epoxy- butane [neat]	ethyl 2,3- epoxy- butyrate [CS]	
Ring breathing	[1258]; [1252]	1251	1269	1250	1273	1332	1250	1246?	1246–1332
Antisymmetric deformation	[885]; [885]	915?	959	928	885	978	952	929	885–978
Symmetric deformation	[817]; [810]	825	839	832	778	890	860	864	818–890

? tentative assignment.

TABLE 1.2a Vibrational assignments for 1-halo-1,2-epoxypropanes (or epihalohydrins)

3-Halo,1,2-epoxy-propane or (epihalohydrin)	F	Cl	Br	I	Assignment (7) epoxy group
	3067.7	3063.4	3059.7	3151	a.CH ₂ str.
	3011	3003.9	3000	2991	s.CH ₂ str.
	1484.3	1480.6	1477.4	1475	CH ₂ bend* ¹
	1530	1520	1512	1500	2(CH ₂ rock)* ¹
	1409.8	1398.2	1395	1392	CH ₂ wag
	1164.4	1142	1135.9	1131	CH ₂ twist [R1]
	1137.5	1136.6			CH ₂ twist [RT]* ²
	749.1	781.7	779.9	750	CH ₂ rock [RT]
	766.4	760.7	756.5	770	CH ₂ rock [R1]
	2959.8	2962.8	2967.3	2967	CH str. (see text)
	1252	1208.7	1195.7	1186	CH bend [R1]
		1192.6	1181.7		CH bend [RT]
	1082.4	1081	1081.4	1075	CH wag [R1]
	1113.6				CH wag [RT]
	1257.4	1254.8	1256.1	1260	Ring breath [R1]
		1266.8	1262	1253	Ring breath [RT]
	[906.4]	905.8	888.2	[911]	a.deformation [R1]
	860	854	845.8	841	s.deformation [R1]
	838	845	833.2	862	s.deformation [RT]
					C-CH ₂ -X group
	3007.1	2999	2991	2991	a.CH ₂ str.
	2959.8	2962.8	2967.3	2967	s.CH ₂ str.
	1456.2	1432.5	1428.8	1420	CH ₂ bend
	1363.3	1276.8	1221.2	1212	CH ₂ wag [R1]
	1346.1	1266.8			CH ₂ wag [R1]
	1148	1091.8	1061.4	1018	CH ₂ twist [R1]
			1036.3		CH ₂ twist [RT]
	949.5	961.6	948.6	937	C-C str. [RT]
	[906.4]	926.9	915.7	[911]	C-C str. [R1]
		877	861.2	826	CH ₂ rock [RT]
	~ 983	836		816	CH ₂ rock [R1]
	1018.5	695.8	654.9	604	C-X str. [RT]
	992	727.5	643.5		C-X str. [R1]
	601.1	517.9	461.7	417	Skeletal bend [RT]
	496.5	442.3	426.1	395	Skeletal bend [R1]
	365	373	361	359	Skeletal bend [RT]
	397	363	340	318	Skeletal bend [R1]
	260	222	180	177	Skeletal bend
	~ 150	115	113	105	Torsion

*¹ Solid phase.*² [RT] is the trans rotational conformer.

TABLE 1.2b A comparison of IR data for epoxy ring modes and CH₃, (CH₃)₂ and (CH₃)₃ bending modes

Epoxy Ring modes	Bis-(2,3-epoxy- propyl) ether [CS ₂] cm ⁻¹	2,3-Epoxy- propyl phenyl ether [CS ₂] cm ⁻¹	Di-glycidyl ether of bis-phenol-A [fluorolube] cm ⁻¹	2,3-epoxy- propyl acrylate [CS ₂] cm ⁻¹	Ethyl 2,3-epoxy- butyrate [CS ₂] cm ⁻¹	Styrene oxide [CS ₂] cm ⁻¹	2,4-Dichloro- styrene oxide [neat] cm ⁻¹	2,3-Epoxy-2- methyl-4- decyne [neat] cm ⁻¹	Range cm ⁻¹
Ring breathing	1251	1245 or masked	1241 or masked by C ₆ H ₄ -O str.	masked	1246?	1252	1249	1249	1246?–1252
Antisymmetric deformation	912	918	920	913	929	984	989	972	912–989
Symmetric deformation	846	843	840	853	864	879	880	881	840–881
	1,2-epoxy- propane [CS ₂]	1,2-epoxy-4- methyl-pentane [CS ₂]	1,2-epoxy- butane [CS ₂]	1,2-epoxy-3- methyl-butane [CS ₂]	1,2-epoxy-3,3- dimethyl-butane [CS ₂]	Ethylene oxide [CS ₂]	α-Methyl styreneoxide [CS ₂]		
Ring breathing	1265	1260	1259	1256	1248	1268	1267		1248–1268
Antisymmetric deformation	893	919	908	932	916	897 [vapor]	997		893–997
Symmetric deformation	829	843	830	878	848	877	861		829–878
Symmetric CH ₃ bending	1370 [CCl ₄]		1379 [CCl ₄]		1381 [CCl ₄]				1370–1381
In-phase (CH ₃) ₂ or (CH ₃) ₃ bending		1388 [CCl ₄]		1382 [CCl ₄]	1366 [CCl ₄]				1366–1382
Out-of-phase (CH ₃) ₂ or (CH ₃) ₃ bending		1371 [CCl ₄]		1366 [CCl ₄]					1366–1371

? tentative assignment.

TABLE 1.3 Vibrational assignments for the CH₂X groups for 3-halo-1,2-epoxypropanes, 3-halopropynes, 3-halopropenes, and PCH₂X-containing compounds

[References] Assignment	(7) 1,2-Epoxy- propane 3-fluoro-	(8) 3-Fluoro- propyne	(8) 1,2-Epoxy- propane 3-chloro-	(8) 3-Chloro- propyne	(9) 3-Chloro- propyne-1-d	(7) 1,2-Epoxy- propane 3-bromo-	(8) 3-Bromo- propyne	(10) 3-Bromo- propyne-1-d	(7) 1,2-Epoxy- propane 3-iodo-	(8) 3-Iodo- propyne	Range
Asym. CH ₂ str.	3007.1	2955	2999	2968	2969	2991	2976	2978	2991	2958	2958–3007
Sym. CH ₂ str.	2959.8	2972	2962.8	3002	2992	2967.3	3006	3008	2967	3008	2959–3008
CH ₂ bending	1456.2	1465	1432.5	1441	1442	1428.8	1431	1436	1420	1423	1423–1465
CH ₂ wagging [RT] ^{*1}	1363.3	1381	1276.8	1271	1265	1221.2	1218	1215	1212	1160	1160–1381
CH ₂ wagging [R1] ^{*2}	1346.1		1266.8			—			1172		1172–1267
CH ₂ twisting [R1]	1148	1242	1091.8	1179	1176	1061.4	1152	1151	1018	1116	1061–1092
CH ₂ twisting [RT]	—		—			1036.3			—		1036–—
C-C str. [RT]	949.5	940	961.6	960	943	948.6	961	945	937	959	937–962
C-C str. [R1]	906.4		926.9			915.7			911		906–927
CH ₂ rocking [RT]	—	1018	877	908	908	861.2	866	866	826	810	810–1018
CH ₂ rocking [R1]	983		836			—			816		816–983
C-X str. [RT]	1018.5	1039	695.8	725	723	654.9	621	634	604	570	570–1019
C-X str. [R1]	992		727.5			643.5			—		643–992

References Assignments	(11) 3-Fluoro- propene	(11) 3-Chloro- propene	(11) 3-Bromo- propene	(11) 3-Iodo- propene	(12) ClCH ₂ -PCl ₂ Cs ^{*3} ; Cl ^{*4}	(12) ClCH ₂ -P=OCl ₂ Cs; Cl	(12) ClCH ₂ -P=SCl ₂ Cs; Cl	(12) BrCH ₂ -P=OCl ₂ Cs; Cl	Range	
Asym. CH ₂ str.	2989.6	2990.2	2986.2	2984.4	3000; —	2999; 2989	3000; 2993	3011; 3000	2984–2990	2989–3011
Sym. CH ₂ str. [g] ^{*5}	2939	2958.3	2967.7	2967.8	2937; —	2933; —	2927; —	2946; —	2939–2968	2927–2946
Sym. CH ₂ str. [c] ^{*6}	2956.9	—	—	—					2957–—	
CH ₂ bending [g]	1459.2	1445.5	1442.4	1438.8	1391; —	1389; —	1381; —	1373; 1384	1438–1446	1373–1391
CH ₂ bending [c]	1467.7	—	—	—					1468–—	
CH ₂ wagging [g]	1383	1289.5	1245.2	1201	1188; —	1212; 1207	1207; —	1161; 1169	1201–1333	1161–1212
CH ₂ wagging [c]	1239.8	1201	1195	1186.9					1186–1240	
CH ₂ twisting [g]	1239.8	1178.2	1154	1088	1098; —	1121; 1116	1118; —	1072; 1080	1088–1240	1072–1121
CH ₂ twisting [c]	989.3	985.2	983.9	980.9					980–989	
C-C str. [g]	935	931.1	925.7	919.9					920–935	
C-C str. [c] or P-C str.	901	—	—	—	812; —	818; 811	801; 833	788; 778	901–—	778–833
CH ₂ rocking [g]	1027	895.5	866.2	825.1	775; —	769; —	769; —	757; 772	778–833	757–775
C-X str. [g]	1005.8	739.4	690.6	669.1	682; —	709; —	736; —	636; 623	669–1006	623–709
C-X str. [c]	989.3	—	—	—				989; —		

^{*1} [RT] = trans.^{*2} [R1] = gauche.^{*3} Cs = plane of sym.^{*4} Cl = gauche.^{*5} [g] = gauche.^{*6} [c] = cis.

TABLE 1.4 Vapor-phase IR data for the oxirane ring vibrations of 1,2-epoxyalkenes*

1,2-Epoxy- alkane R	Oxirane ring breathing cm ⁻¹		Oxirane sym. in-plane def. cm ⁻¹		Oxirane asym. in- plane def. cm ⁻¹	
		A		A		A
H	1268	0.362	877	1.677	892	
CH ₃	1265	0.401	829	1.755	893	0.156
C ₂ H ₅	1259	0.279	830	1.25	908	1.23
C ₃ H ₇	1259	0.229	843, 831	0.533, 0.644	883	0.48
iso-C ₄ H ₉	1260	0.26	845, 843	0.622, 0.713	919	0.578
iso-C ₃ H ₇	1256	0.285	878	1.357	932	0.779
<i>t</i> -C ₄ H ₉	1248	0.348	848	1.165	916	1.094
C ₈ H ₁₇	1259	0.079	831	0.21	913	0.13
C ₉ H ₁₉	1259	0.06	834	0.153	915	0.099
C ₁₂ H ₂₅	1259	0.05	831	0.154	912	0.11
C ₁₄ H ₂₉	1259	0.041	830	0.13	911	0.081
C ₁₆ H ₃₃	1255	0.023	830	0.065	909	0.047
Range	1255–1268		830–877		883–932	

R	Oxirane a.CH ₂ str. cm ⁻¹		Oxirane s.CH ₂ str. cm ⁻¹		Oxirane CH ₂ bending cm ⁻¹		Oxirane CH ₂ wagging cm ⁻¹	
		A		A		A		A
H	3065	0.391	3000	0.429	1491	0.025	1130	
CH ₂	3049	0.615	2995	1.305	1501	0.258	1129	
C ₂ H ₅	3044	0.435	masked		1481	0.415	1129	
C ₃ H ₇	3045	0.41	2989	0.736	1481	0.305	1128	
iso-C ₄ H ₉	3049	0.367	2999	0.407	1482	0.232	1126	
iso-C ₃ H ₇	3049	0.359	2996	0.57	1484	0.387	1128	
<i>t</i> -C ₄ H ₉	3051	0.265	3001	0.398	1482	0.886	1129	
C ₈ H ₁₇	3040	0.15	2990	sh	1480	0.1	1129	
C ₉ H ₁₉	3041	0.115	2990	sh	1480	0.084	1129	
C ₁₂ H ₂₅	3040	0.111	2990	sh	1480	0.076	1129	
C ₁₄ H ₂₉	3040	0.099	2990	sh	1479	0.06	1125	
C ₁₆ H ₃₃	3038	0.091	2990	sh	1479	0.06	1125	
Range	3038–3065		2990–3001		1479–1501		1125–1130	

* Reference (12).

TABLE 1.5 Correlations for the ring stretching vibrations for cyclic ethers

Compound or type compound	Ring size atoms in ring	asym. C—O—C stretching [vapor]; (13) cm ⁻¹	asym. C—O—C stretching [neat or CS ₂] cm ⁻¹	sym. C—O—C stretching [vapor]; (13) cm ⁻¹	sym. C—O—C stretching [neat or CS ₂] cm ⁻¹
Ethylene oxides and derivatives	3	883–912	883–912	1246–1332	1246–1322
Tetramethylene oxide	4	[—]	986 [CS ₂] IR; stg 980 [neat] R; wk	[—]	1029 [CS ₂] IR; wk 1027 [neat] R; stg
Tetrahydrofuran	5	1170	1060 [neat]	919	903 [neat]
Tetrahydrofuran 3-methyl	5	1194	[—]	919	[—]
Tetrahydropyran	6	1095	[—]	820	[—]
Range for four compounds	6	1094–1132	[—]	820–860	[—]

TABLE 1.6 Infrared data for ethers

Ether	asym. C—O—C str.	asym. C—O—C str.	CH ₂ rocking	in-phase (CH ₃) ₂ bending	out-of-phase (CH ₃) ₂ bending
	neat cm ⁻¹	vapor cm ⁻¹	neat cm ⁻¹	cm ⁻¹	cm ⁻¹
Methyl	[—]	1102			
Ethyl	1121	~ 1140			
Propyl	1115	1133			
Butyl	1116	1130	735		
Hexyl	1111	1126	724		
Octyl	1118	1111	725		
Isopropyl	1125	1121		1379	1363
Bis-(2,3-epoxy- propyl)	1100 [CS ₂]				
Benzyl	1095	1095			
Bis-(alpha-methyl- benzyl)	1085	[—]			
Phenyl	1235	[—]			
4-Methoxyphenyl	1212; [1030]				
Methyl butyl	1126	1129	734		
Ethyl butyl	1127	1129	742		
Ethyl isobutyl	1120	[—]			
Ethyl octadecyl	1121	[—]	720		
Propyl isopropyl	1125	[—]	751	1378	1361
Methyl tert-butyl	1200; 1085	1209; 1091		1382	1360
Ethyl tert-butyl	1187; 1070	[—]		1388	1356
Isopropyl tert- butyl	1195; 1105			1378; 1368	1355
Methyl benzyl	1100	[—]			
Methyl phenyl	1248; 1041	[—]			
Ethyl phenyl	1245; 1049	[—]			
Propyl phenyl	1229; 1064	[—]			
Poly(ethyleneglycol)	~ 1100			CH ₂ bending ~ 1454	CH ₂ wagging ~ 1345
Poly(propyleneglycol)	~ 1105			sym. CH ₃ bending 1371	asym. CH ₃ stretching 2960
Poly(epichlorohydrin)	~ 1105			C—Cl stretching 743; 704	CH ₂ wagging ~ 1335

TABLE 1.7 Infrared data for the a and s Aryl-O-R stretching vibrations for 3-X- and 4-X-anisoles in CS₂ solution, vapor, and in the neat phase

Anisole	a.C ₆ H ₄ -O-CH ₃ str. or C ₆ H ₄ -O str. [neat] cm ⁻¹	s.C ₆ H ₄ -O-CH ₃ str. or CH ₃ -O str. [neat] cm ⁻¹	s.C ₆ H ₄ -O-CH ₃ str. or CH ₃ -O str. [vapor]; (11b) cm ⁻¹	a.C ₆ H ₄ -O-CH ₃ str. or C ₆ H ₄ -O str. [CS ₂ soln.] cm ⁻¹
4-X				
NO ₂	1262	1022	1041	1264
CH ₃ SO ₂	1260	1021	1032	
CH ₃ CO	1249	1021		1261
CO ₂ C ₂ H ₅	1252	1028		1258
CN	1240	1024		1259
H	1248	1042		1246
CH=CH ₂	1248	1040	1043	
C ₆ H ₅	1249	1032		
CH ₂ OH	1245	1030		1248
iso-C ₃ H ₇	1249	1037		
2-ClC ₂ H ₄	1240	1031		
Br	1240	1029	1041	1246
2-BrC ₂ H ₄	1245	1031	1044	
Cl	1242	1032		1247
CH ₃	1242	1028		1244
C ₂ H ₅	1248	1037		1248
n-C ₃ H ₇	1244	1038	1041	
t-C ₄ H ₉	1248	1037	1050	1248
CH ₃ O	1246	1029		1243
C ₆ H ₅ CH ₂ O	1230	1033		
NH ₂	1238	1034		1241
C ₆ H ₅ O	1230	1039		
3-X				
CH ₃ O	1211	1052		
OH	1200	1043	1046	
NH ₂	1198	1029		
Cl	1237	1029		
CH ₃	1259	1042	1054	
CH ₃ CO	1270	1040		
3-BrC ₃ H ₆	1250	1034		

TABLE 1.8 Raman data and assignments for vinyl ethers

Vinyl phenyl ether cm ⁻¹ (A)	Assignment	Vinyl isobutyl ether cm ⁻¹ (A)	Vinyl isoocetyl ether cm ⁻¹ (A)	Vinyl decyl ether cm ⁻¹ (A)	Vinyl docdecyl ether cm ⁻¹ (A)	Vinyl octadecyl ether cm ⁻¹ (A)	Vinyl-2-(2-ethoxy ethyl)ethyl ether cm ⁻¹ (A)	Divinyl ether of butanediol cm ⁻¹ (A)	Divinyl ether of diethyleneglycol cm ⁻¹ (A)	Assignment [possible]
3068 (4)	Ring CH str.	3122 (1)	3121 (0)	3121 (0)	3121 (0)		3120 (1)	3120 (1)	3120 (2)	a.CH ₂ = str.
3035 (3)	CH= str.	3046 (3)	3046 (3)	3046 (2)	3046 (1)	3046 (1)	3045 (2)	3044 (4)	3045 (4)	CH= str.
		3023 (2)	3022 (1)	3022 (1)	3022 (1)			3022 (2)		s.CH ₂ str.
		2962 (5)	2961 (5)				2975 (4)			a.CH ₃ str.
		2943 (4)	2933 (7)				2934 (9)	2924 (4)	2930 (3)	a.CH ₂ str.
		2911 (6)	2913 (7)							a.CH ₂ str.
1644 (3)	C=C str.			2902 (8)	2895 (8)	2890 (7)				
1593 (2)	Ring 4	2876 (9)	2874 (9)	2874 (9)	2874 (8)		2874 (8)	2876 (4)	2880 (3)	s.CH ₃ str.
1311 (2)				2854 (9)	2853 (9)	2852 (9)				s.CH ₂ str.
1232 (1)		2724 (1)		2730 (0)	2728 (0)	2725 (0)				s.CH ₂ str.
1171 (1)	Ring 6	1638 (2)	1638 (1)	1637 (1)	1638 (0)	1638 (0)	1639 (1)	1639 (3)	1639 (3)	C=C gauche
1157 (1)		1612 (3)	1611 (1)	1611 (2)	1610 (1)	1609 (0)	1620 (2)	1616 (4)	1620 (4)	C=C cis
		1464 (2)						1474 (1)		CH ₂ bend
			1450 (3)				1459 (4)		1456 (1)	CH ₂ bend
1026 (4)	Ring 8			1439 (4)	1439 (3)	1439 (3)		1436 (1)		CH ₂ bend
		1415 (0)						1414 (0)	1415 (0)	CH ₂ bend
		1342 (2)								CH ₂ wag
1002 (9)	Ring 9	1322 (7)	1320 (4)	1321 (5)	1320 (4)	1320 (2)	1323 (4)	1322 (9)	1323 (9)	CH= rock

TABLE 1.9 Vapor-phase IR data and assignments for the alkyl group of vinyl alkyl ethers*

Vinyl alkyl ether	a.CH ₃ str.	s.CH ₃ str.	a.CH ₃ bend	CH ₃ rock	CH ₃ rock							
Methyl		2870 (0.100)				1145 (0.260)	1024 (0.186)					
		2958 (0.310)	2860 (0.095)	1460 (0.152)		1136 (0.190)	1011 (0.175)					
		2930 (0.240)	2850 (0.110)			1127 (0.210)	997 (0.171)					
	a.CH ₃ str.	a.CH ₂ str.	s.CH ₃ str.	s.CH ₂ str.	a.CH ₃ bend	s.CH ₃ bend	CH ₂ wag and or C—C str.	CH ₂ twist	CH ₃ rock and or C—C str.	CH ₂ rock	C—Cl str.	C—Cl str.
Ethyl						1391 (0.225)						
	2997 (0.434)	2940 (0.270)	2900 (0.260)		1476 (0.087)	1388 (0.200)	1128 (0.481)	1079 (0.226)	1059 (0.271)			
Butyl	2984 (0.370)					1377 (0.210)						
	2971 (0.790)	2950 (0.690)	2894 (0.410)		1476 (0.135)	1379 (0.190)	1135 (0.249)	1083 (0.270)	1030 (0.177)			
Isobutyl	2965 (0.840)	2925 (0.392)	2897 (0.376)		1475 (0.200)	1388 (0.195)	1145 (0.232)	1080 (0.280)	1019 (0.310)			
2-Ethylhexyl	2970 (1.245)	2938 (1.245)	2882 (0.640)		1470 (0.250)	1380 (0.180)		1079 (0.266)	1015 (0.164)	735 (0.035)		
a.C—O—C str.												
2-Methoxyethyl	2995 (0.322)	2930 (0.902)	2890 (0.555)	2830 (0.327)	1462 (0.185)	1360 (0.185)	1135 (1.150)	1095 (0.560)	1039 (0.250)			
2-Chloroethyl		2980 (0.105)			2895 (0.065)	1466 (0.060)	1377 (0.100)		1086 (0.240)	1013 (0.145) 1010 (0.138) 1001 (0.142)	764 (0.170)	687 (0.082)? and CH=CH ₂ wag?
	Bis[2-(vinylloxy)ethyl]ether		2938 (0.291)		2880 (0.256)	1460 (0.090)	1359 (0.140)	1140 (0.970)	1092 (0.350)	1010 (0.165) 980 (0.200)		

* Reference (13).

Nitriles, Isonitriles, and Dialkyl Cyanamides

Nitriles	27
Isonitriles	30
Dialkyl Cyanamides	31
Organothiocyanates	31
References	31

Figures		Tables	
Figure 2-1	32 (28)	Table 2-1	39 (27)
Figure 2-2	32 (29)	Table 2-2	40 (29)
Figure 2-3	33 (29)	Table 2-3	40 (29)
Figure 2-4	34 (29)	Table 2-4	41 (29)
Figure 2-5	35 (29)	Table 2-5	42 (30)
Figure 2-6	36 (30)	Table 2-6	42 (30)
Figure 2-7	37 (30)	Table 2-7	43 (31)
Figure 2-8	38 (30)		

* Numbers in parentheses indicate in-text page reference.

NITRILES

Table 2.1 lists IR and/or Raman data for nitriles in different physical phases. In the vapor phase, compounds of form R-CN or NC-(CH₂)₄-CN exhibit the CN stretching vibration in the region 2250–2280 cm⁻¹, while in the neat phase the CN stretching vibration for the corresponding compound occurs at a frequency 5 to 22 cm⁻¹ lower than in the vapor phase.

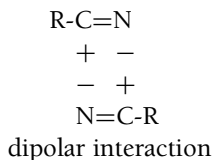
Conjugated organonitriles such as benzonitrile, 2-X-, 3-X- or 4-X-substituted benzonitriles, and acrylonitrile exhibit CN stretching in the region 2222–2240 in the vapor phase, and at a frequency 8–19 cm⁻¹ lower in the neat phase. Conjugation with the CN group causes the CN stretching mode to vibrate at a lower frequency compared to those for alkylnitriles.

Compounds such as 3-halo-propynitrile (or 1-cyano-2-haloacetylene) have the following empirical structure: X-C≡C-C≡N. It is apparent that the CN group is joined to the C≡C group in a linear manner. Thus, the CN and CC groups are conjugated, and one might expect that CN stretching frequencies would occur at lower frequencies than those for alkanonitriles, benzonitriles, and methacrylonitrile. However, it is noted that the CN stretching vibration occurs in the region 2263–2298 cm⁻¹ (CCl₄ solution) and 2270–2293 cm⁻¹ (vapor phase). These CN stretching frequencies are higher than expected. In CCl₄ solution, the C≡C stretching vibration

occurs at 2195, 2122, and 2128 cm^{-1} for the Cl, Br and I analogs of 3-halopropynitrile, respectively (6). It is likely that there is coupling between the $\text{C}\equiv\text{C}-\text{C}\equiv\text{N}$ stretching modes, which causes the CN stretching mode to occur at higher frequency and the $\text{C}\equiv\text{C}$ stretching vibration to occur at lower frequency than expected.

Figure 2.1 is a plot of the Raman data (CN stretching) for acetonitrile, propionitrile, isobutyronitrile, pivalonitrile vs the number of protons on the α -carbon atom and this plot shows that the CN stretching vibration decreases in frequency as the number of α -hydrogen atoms decreases from 3 to 0 (7). Tafts σ^* values for CH_3 , CH_3CH_2 , $(\text{CH}_3)_2\text{CH}$, and $(\text{CH}_3)_3\text{C}$ are 0, -0.100 , -0.190 , and -0.300 , respectively (7). Thus, the CN stretching vibration decreases in frequency as the inductive electron release to the nitrile group is increased. This effect would tend to lengthen the CN bond, causing it to vibrate at a lower frequency.

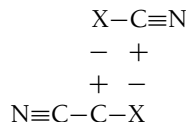
In all cases, in Table 2.1 the CN stretching frequency occurs at a higher frequency in the vapor phase than in the neat or solution phase by 5–47 cm^{-1} . It is of interest to note that the frequency difference between the CN stretching mode in the vapor- and neat phases decreases by 31, 20, 17, and 14 cm^{-1} for acetonitrile, propionitrile, isobutyronitrile, and pivalonitrile, respectively, and this is in decreasing frequency order for both vapor- and neat phases. It is of interest to consider why the frequency difference for CN stretching decreases between the two physical phases progressing in the series from acetonitrile through pivalonitrile. It is suggested that this difference is caused by steric factors of the alkyl groups, which alter the amount of dipolar interaction between nitrile groups in the neat phase, while in the vapor phase the dipolar interaction between the nitrile groups is negligible. The steric constant E_s for CH_3 , C_2H_5 , $(\text{CH}_3)_2\text{CH}$, and $(\text{CH}_3)_3\text{C}$ is 0.00, -0.07 , -0.47 , and -1.54 , respectively (9). Thus, as E_s becomes larger the CN groups in the neat phase are spaced farther apart, which weakens the dipolar interaction between nitrile groups. The inductive effect of the alkyl group most likely contributes to some extent to the amount of dipolar interaction, but this is probably a smaller effect because the inductive effect is independent of physical phase.



The cyanogen halides exhibit the CN stretching vibration at 2290, 2201, 2187, and 2158 cm^{-1} in the neat phase for the F, Cl, Br and I analogs, respectively (4). In the vapor phase the CN stretching for the Cl and Br analogs occurs at frequencies higher by 47 and 13 cm^{-1} , respectively (4, 5).

In this cyanogen halide series the CN stretching vibration decreases as the $\text{C}\equiv\text{N}$ bond length increases. For example, in the solid state the CN bond length in the solid state is 1.26, 1.58, 1.77, and 2.03 Å for FCN, ClCN, BrCN, and ICN, respectively (10). In the vapor phase the CN bond is less restricted, and the $\text{C}\equiv\text{N}$ bond length is 1.67 and 1.79 Å for ClCN and BrCN, respectively (10). The relative steric factor of F, Cl, Br, CH_3 , and I (based on F as zero) is (0.00), -0.31 , -0.49 , -0.49 , and -0.69 , respectively. The inductive value σ^* for F, Cl, Br, and I is 1.10, 1.05, 1.00, and 0.85, respectively (11). Thus, the steric factor of the halogen atom increases as the $\text{C}\equiv\text{N}$ bond length increases, while the inductive effect of the halogen atom decreases progressing in the series FCN through ICN. Combination of the preceding factors is most likely the cause for

the CN stretching frequency for compounds of form R-CN to occur at intermediate frequencies between FCN and ClCN (see Table 2.1). The dipolar interaction between these linear XCN molecules could also be different than for R-CN molecules, which are not linear. For example,



The larger inductive effect of Cl vs Br, and the large steric effect of Br vs Cl could account for the fact that the frequency difference between the vapor and neat phases for the CN stretching frequency is 47 cm^{-1} for ClCN and 13 cm^{-1} for BrCN.

Table 2.2 lists IR data for acetonitrile 1% wt./vol. in various solvents (12). The solvents are numbered 1–15 in Table 2.2. The CN stretching vibration and the combination tone C–C stretching plus symmetric CH_3 bending are in Fermi resonance (FR). The CN stretching vibration has been corrected for FR in each of the solvents. Figure 2.2 shows a plot for unperturbed $\nu\text{C}\equiv\text{N}$ for acetonitrile vs AN, where AN is the solvent acceptor number (12). This plot shows that the νCN frequency does not correlate well with AN, especially the AN value for dimethyl sulfoxide (DMSO).

Figure 2.3 shows plots of $\nu\equiv\text{CN}$ (uncorrected and corrected for FR) vs ($\nu\equiv\text{CN}$ in methyl alcohol) minus ($\nu\equiv\text{CN}$ in solvent). Both plots are linear, and any set of data plotted in this manner yields a linear mathematical relationship (12). The plots clearly show that FR causes νCN to occur at lower frequency due to resonance with the $\nu\text{C}-\text{C} + \delta$ sym. CH_3 combination tone (CT). It should be noted that the numbering sequence is different in both plots. The extent of FR interaction between νCN and CT ($\nu\text{C}-\text{C} + \delta$ sym. CH_3) is altered in each solvent system because $\nu\text{C}-\text{C}$ and δ sym. CH_3 , as well as νCN are affected differently.

Table 2.3 compares IR νCN stretching frequencies for benzonitrile 10 wt./vol.% and 1 wt./vol.% vs those for 1% wt./vol. acetonitrile νCN frequencies corrected for FR in different solvents (12). This table shows that νCN for benzonitrile occurs at lower frequency than νCN for acetonitrile (corrected for FR), from 27 to 34 cm^{-1} in these solvents. The shift to lower frequency in the case of benzonitrile is due to resonance of the CN group with the π system of the phenyl group.

Table 2.3 also shows that νCN for benzonitrile occurs at lower frequency in solution at 10 wt./vol.% than at 1 wt./vol.%. These data are plotted in Figure 2.4. These plots indicate that at higher wt./vol.% solute there is some dipolar interaction between solute molecules, which lowers the νCN frequency.

Figure 2.5 is a plot of unperturbed $\nu\text{C}\equiv\text{N}$, (1% wt./vol. acetonitrile), cm^{-1} vs $\nu\text{C}\equiv\text{N}$ for benzonitrile (1% wt./vol. benzonitrile), cm^{-1} where each compound has been recorded individually in the same solvent. Point 1 for hexane does not fit the essentially linear relationship.

Table 2.4 lists IR data for the νCN frequency for 4-cyanobenzaldehyde in 0 to 100 mol% $\text{CHCl}_3/\text{CCl}_4$ solutions (1 wt./vol.% solutions). Figure 2.6 shows a plot of $\nu\equiv\text{CN}$ for 4-cyanobenzaldehyde vs mol% $\text{CHCl}_3/\text{CCl}_4$ (13). The νCN mode increases in frequency as the mole % $\text{CHCl}_3/\text{CCl}_4$ increases to $\sim 45\%$. It then decreases in frequency to $\sim 75\%$, after which νCN frequency is relatively constant. The νCN frequency for 4-cyanobenzaldehyde is higher in frequency in CHCl_3 solution than in CCl_4 solution, and this same observation has been noted for

benzonitrile (12, 13). The behavior of $\nu\text{C}=\text{O}$ for 4-cyanobenzonitrile has already been discussed; furthermore, its frequency increases as the reaction field is increased (14). Figure 2.6 then shows that $\nu\text{C}\equiv\text{N}$ as well as $\nu\text{C}=\text{O}$ are affected, although not in the same manner.

The nitrile group is not always readily detected in the IR. In the case of compounds such as 2,4,4,4-tetrachloro-butyronitrile, the νCN mode is extremely weak, but in the Raman it is readily detected (15). In the vapor phase, benzonitrile and substituted benzonitriles exhibit νCN in the region $2220\text{--}2250\text{ cm}^{-1}$, and the IR band intensity varies from very-weak to weak-medium compared to the most intense IR band in these spectra (2a). In general, the νCN band intensity is significantly higher for atoms or groups with negative Hammett's σ values (OH, OCH_3 , NH_2 etc.) than for those with positive values (NO_2 , CN, CF_3 etc.). In the vapor phase, the CN group is intramolecularly hydrogen bonded in cases such as 2-hydroxybenzonitrile (νCN , 2225 cm^{-1}) and 2-aminobenzonitrile (νCN , $\sim 2222\text{ cm}^{-1}$) (2a). The highest vapor-phase frequency is noted at 2250 cm^{-1} for 2,6-difluorobenzonitrile, and this overlaps the region for compounds of form $\text{R}-\text{CN}$ (νCN , $2250\text{--}2260\text{ cm}^{-1}$) in the vapor phase (2a). The high frequency exhibited by 2,6-difluorobenzonitrile is attributed to a field effect between F and the CN group.

Table 2.5 lists Raman data for the $\text{C}\equiv\text{N}$ and $\text{C}=\text{C}$ groups of organonitriles. In most cases, the $\nu\text{C}\equiv\text{N}$ mode is the strongest band in the Raman spectrum. However, in the case of 1,1-azo bis-(cyclohexane carbonitrile) the symmetric CH_2 stretching vibration is the most intense Raman band. In the case of crotonitrile and 2-methyl crotonitrile the Raman band for $\nu\text{C}\equiv\text{N}$ is approximately twice as strong as the Raman band for $\nu\text{C}=\text{C}$.

ISONITRILES

Methyl isonitrile, ethyl isonitrile, isopropyl isonitrile, and tert-butyl isonitrile exhibit $\nu\text{N}\equiv\text{C}$ at 2183 , 2160 , 2140 , and 2134 cm^{-1} , respectively (16). Figure 2.7 is a plot of the number of protons on the alkyl $\alpha\text{-C}-\text{N}\equiv$ atom vs $\nu\text{N}\equiv\text{C}$ for alkyl isonitriles. This plot shows that $\nu\text{N}\equiv\text{C}$ decreases in frequency with increased branching on the alkyl $\alpha\text{-C}-\text{N}\equiv$ atom (17). Figure 2.8 shows a plot of Taft's σ^* vs $\nu\text{N}\equiv\text{C}$ for alkyl isonitriles (17). Therefore, $\nu\text{N}\equiv\text{C}$ decreases in frequency as the electron release to the isonitrile group is increased. This effect should increase the $\text{N}\equiv\text{C}$ bond length. Table 2.6 compares the IR data for organonitriles and organoisonitriles.

In the series of alkanonitriles and alkanoisnitriles presented in Table 2.6, νCN occurs in the range $2236\text{--}2249\text{ cm}^{-1}$ and νNC occurs in the range 2134 through 2183 cm^{-1} . The frequency separation between νCN and νNC increases as the electron release of the alkyl group to the CN or NC group is increased (66 to 102 cm^{-1}). In the series 3-x and 4-x substituted benzonitriles and isobenzonitriles presented in Table 2.6, νCN occurs in the range $2226\text{--}2240\text{ cm}^{-1}$ and νNC occurs in the range $2116\text{--}2125\text{ cm}^{-1}$. The frequency separation between νCN and νNC ($101\text{--}122\text{ cm}^{-1}$) tends to increase somewhat as σ_p or σ_m increase in value. The frequency separation between νCN for 4-chlorobenzonitrile (2233 cm^{-1}) and 2-chlorobenzonitrile (2237 cm^{-1}) is 4 cm^{-1} while for 4-chloroisobenzonitrile (2116 cm^{-1}) and 2-chloroisobenzonitrile (2166 cm^{-1}) is 50 cm^{-1} . The frequency separation between νCN and νNC for 2-chlorobenzonitrile and 2-chloroisobenzonitrile is 71 cm^{-1} . The relatively high νNC frequency exhibited by 2-chloroisobenzonitrile suggests that a field effect of the Cl atom upon the N atom of the NC group causes νNC to shift to higher frequency.

DIALKYL CYANAMIDES

Dialkyl cyanamides have the following empirical structure $(R-)_2N-C\equiv N$. In the vapor phase dimethyl cyanamide and diallyl cyanamide exhibit $\nu_{C\equiv N}$ near $\sim 2228\text{ cm}^{-1}$ and 2221 cm^{-1} , respectively (2B). In the neat phase dialkyl cyanamide and dibenzyl cyanamide exhibit $\nu_{C\equiv N}$ at 2200 and 2190 cm^{-1} , respectively.

ORGANOTHIOCYANATES

Table 2.7 compares IR data for the vapor and neat phases of organothiocyanates. In the neat phase alkyl thiocyanates (R-S-CN) exhibit ν_{CN} in the range $2145\text{--}2160\text{ cm}^{-1}$ and in the vapor phase in the range $2161\text{--}2175\text{ cm}^{-1}$. In the neat phase arylthiocyanates ν_{CN} occurs in the range $2166\text{--}2174\text{ cm}^{-1}$, and occur at higher frequency than alkylthiocyanates in the neat phase. The alkyl group releases electrons to the SCN group and the aryl group withdraws electrons from the SCN group. Therefore, ν_{CN} for arylthiocyanates occur at higher frequency than ν_{CN} for alkylthiocyanates.

REFERENCES

1. Nyquist, R. A. (1984). *The Interpretation of Vapor-Phase Infrared Spectra: Group Frequency Data*. vol. 1. Philadelphia: Sadtler Research Laboratories, Division of Bio-Rad Laboratories, Inc., p. 443.
2. Nyquist, R. A. (1984). *Ibid.*, p. 450.
- 2a. Nyquist, R. A. (1984). *Ibid.*, p. 443.
- 2b. Nyquist, R. A. (1984). *Ibid.*, p. 446.
3. *Standard Raman Spectra*. Philadelphia: Sadtler Research Laboratories, Division of Bio-Rad Laboratories, Inc.
4. Colthup, N. B., Daley, L. H., and Wiberley, S. E. (1990). *Introduction to Infrared and Raman Spectroscopy*. 3rd ed., Boston: Academic Press, Inc., p. 183.
5. Nyquist, R. A., Putzig, C. L., and Leugers, M. A. (1997). *Handbook of Infrared and Raman Spectra of Inorganic Compounds and Organic Salts*. Vol. 3, Boston: Academic Press, p. 198.
6. Klæboe, P. and Kloster-Jensen, E. (1967). *Spectrochim. Acta*, 23A: 1981.
7. Nyquist, R. A. (1987). *Appl. Spectrosc.*, 41: 904.
8. Newman, M. S. Editor (1956). *Steric Effects in Organic Chemistry*. New York: John Wiley & Sons, Inc., p. 591; R. W. Taft (1956). *Separation of Polar, Steric, and Resonance Effects in Reactivity*.
9. Newman, M. S. (1956). *Ibid.*, p. 601.
10. Wyckoff, R. (1963). *Crystal Structure*. Vol. 1, New York: John Wiley & Sons, Inc., p. 173.
11. Newman, M. S. (1956). *Steric Effects in Organic Chemistry*. New York: John Wiley & Sons, Inc., p. 595; R. W. Taft (1956). *Separation of Polar, Steric, and Resonance Effects in Reactivity*.
12. Nyquist, R. A. (1990). *Appl. Spectrosc.*, 44: 1405.
13. Nyquist, R. A., Settineri, S. E., and Luoma, D. A. (1992). *Appl. Spectrosc.*, 46: 293.
14. Nyquist, R. A., Settineri, S. E., and Luoma, D. A. (1991). *Appl. Spectrosc.*, 45: 1641.
15. Brame, Jr., E. G. and Grasselli, J. G. (1977). *Infrared and Raman Spectroscopy, Part B, Practical Spectroscopy Series*. Vol. 1, New York: Marcel Dekker, Inc., p. 471; R. A. Nyquist and R. O. Kagel (19XX). *Organic Materials*.
16. Bellamy, L. J. (1968). *Advances In Infrared Group Frequencies*. London: Methuen.
17. Nyquist, R. A. (1988). *Appl. Spectrosc.*, 42: 624.

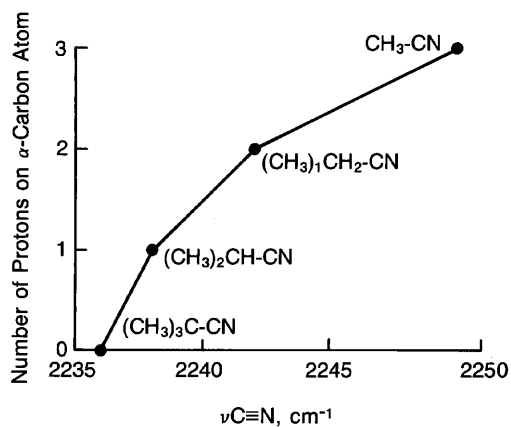


FIGURE 2.1 A plot of $\nu_{C\equiv N}$ for alkanonitriles vs the number of protons on the α -carbon atom.

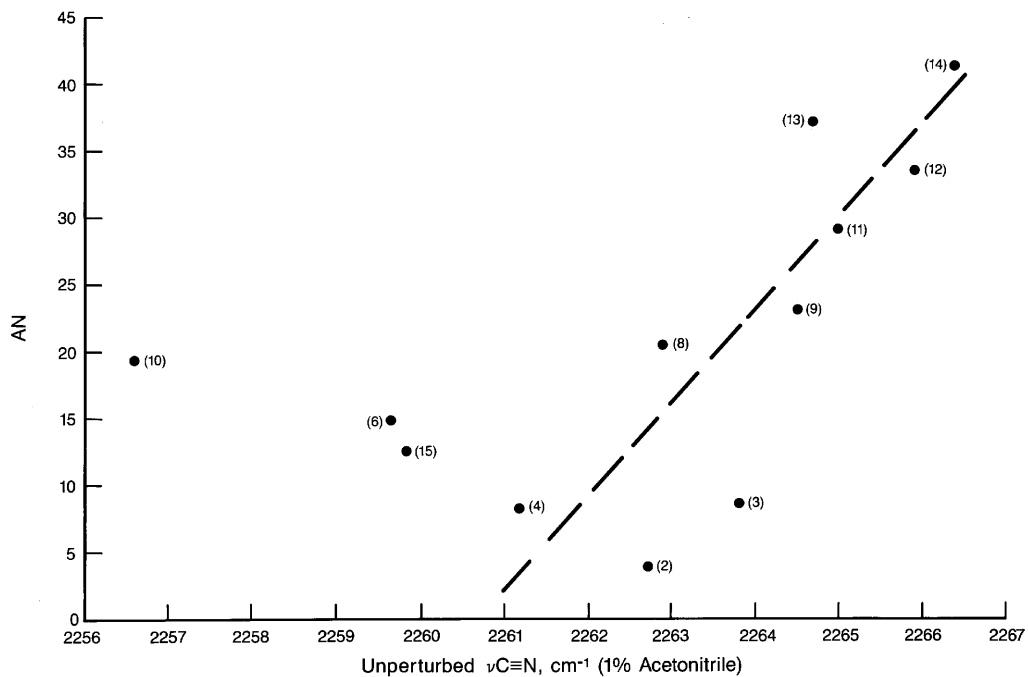


FIGURE 2.2 A plot of unperturbed $\nu_{C\equiv N}$, cm $^{-1}$ (1% wt./vol.) vs AN (the solvent acceptor number).

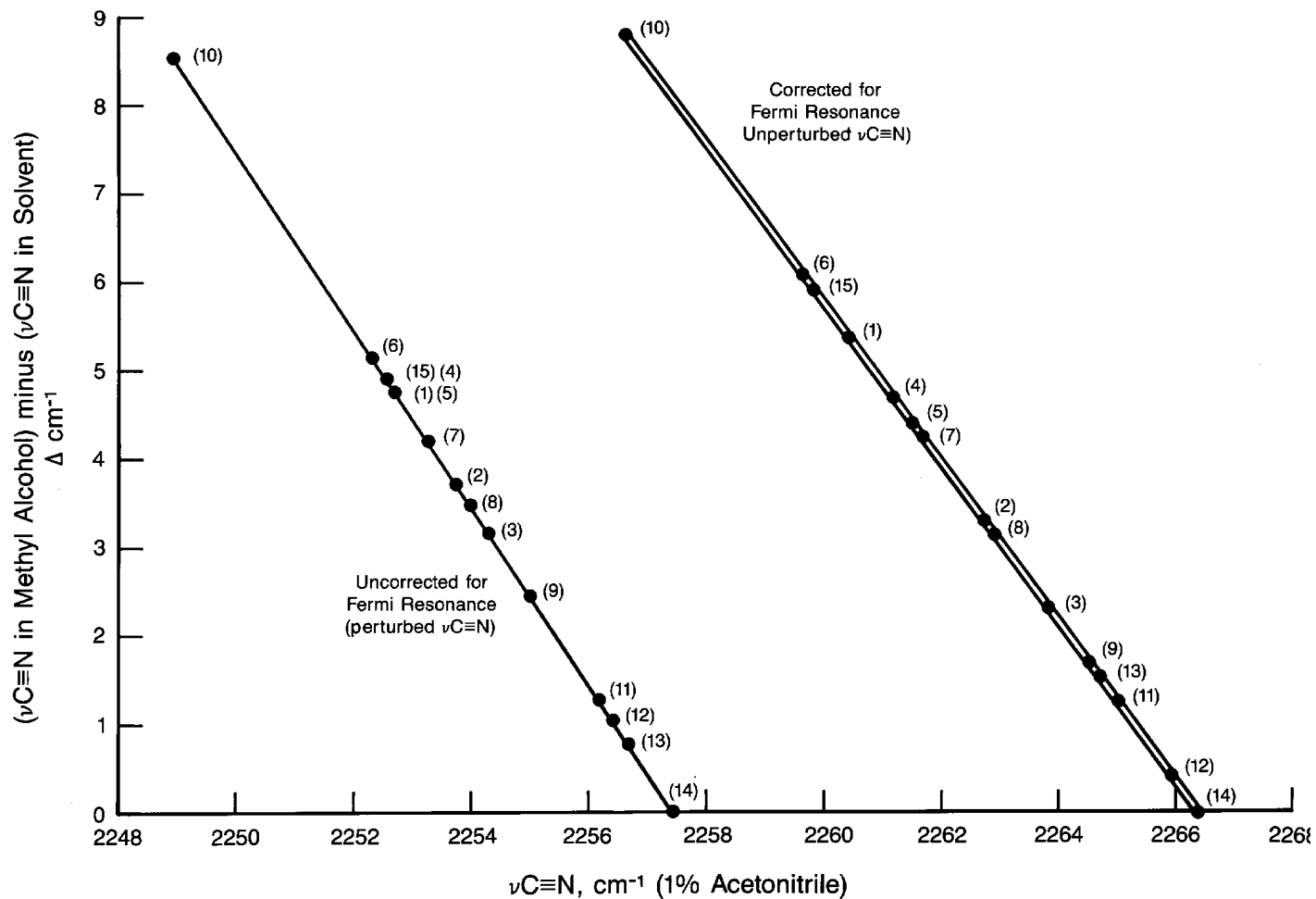


FIGURE 2.3 Plots of $\nu_{\text{C}\equiv\text{N}}$, cm^{-1} for acetonitrile (1 wt./vol.%) vs $(\nu_{\text{C}\equiv\text{N}} \text{ in methyl alcohol}) \text{ minus } (\nu_{\text{C}\equiv\text{N}} \text{ in another solvent})$. The two plots represent perturbed and unperturbed $\nu_{\text{C}\equiv\text{N}}$.

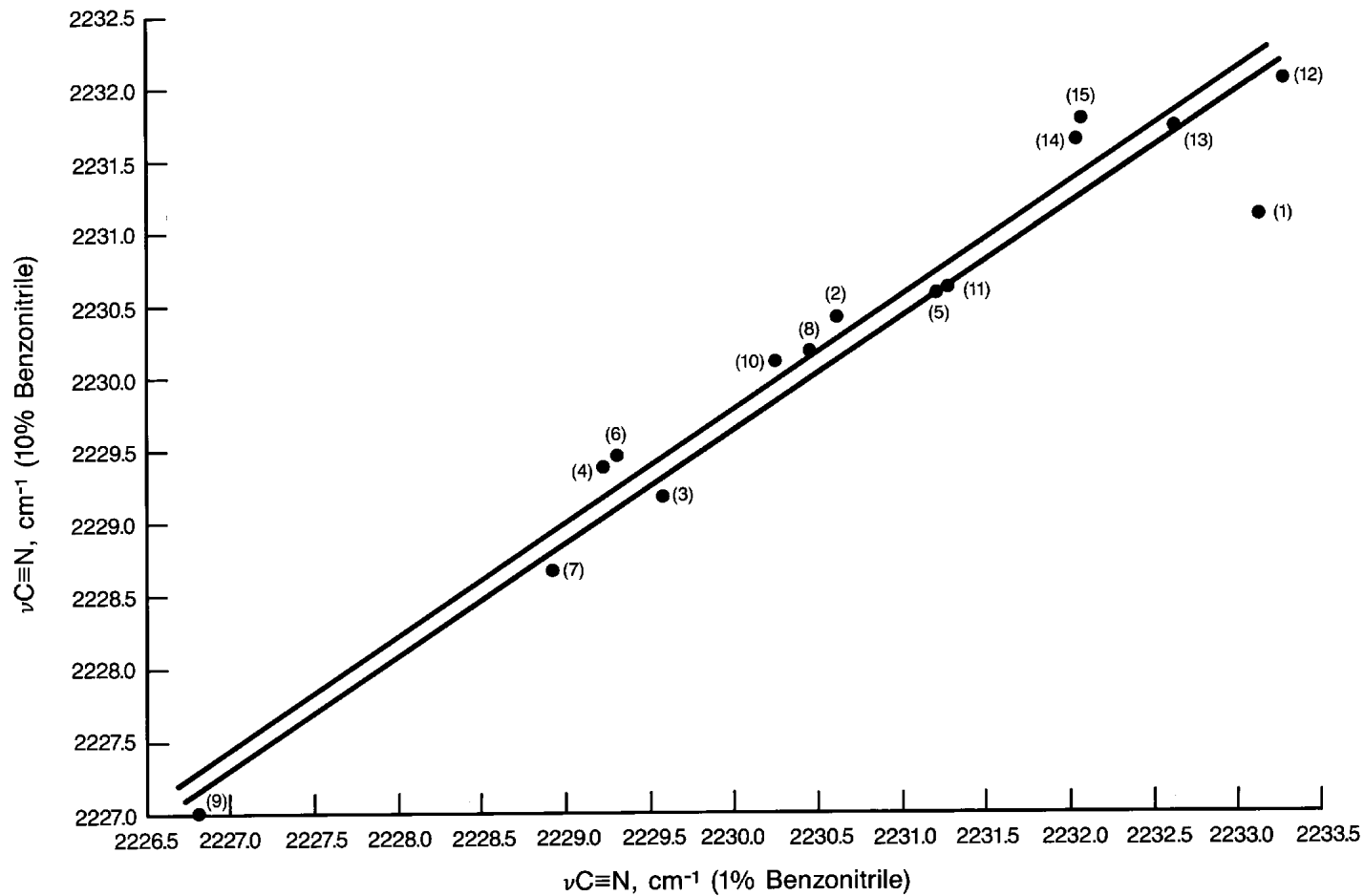


FIGURE 2.4 A plot of $\nu_{\text{C}\equiv\text{N}}$ for 1 wt./vol. % vs $\nu_{\text{C}\equiv\text{N}}$ for 1% wt./vol. in 15 different solvents.

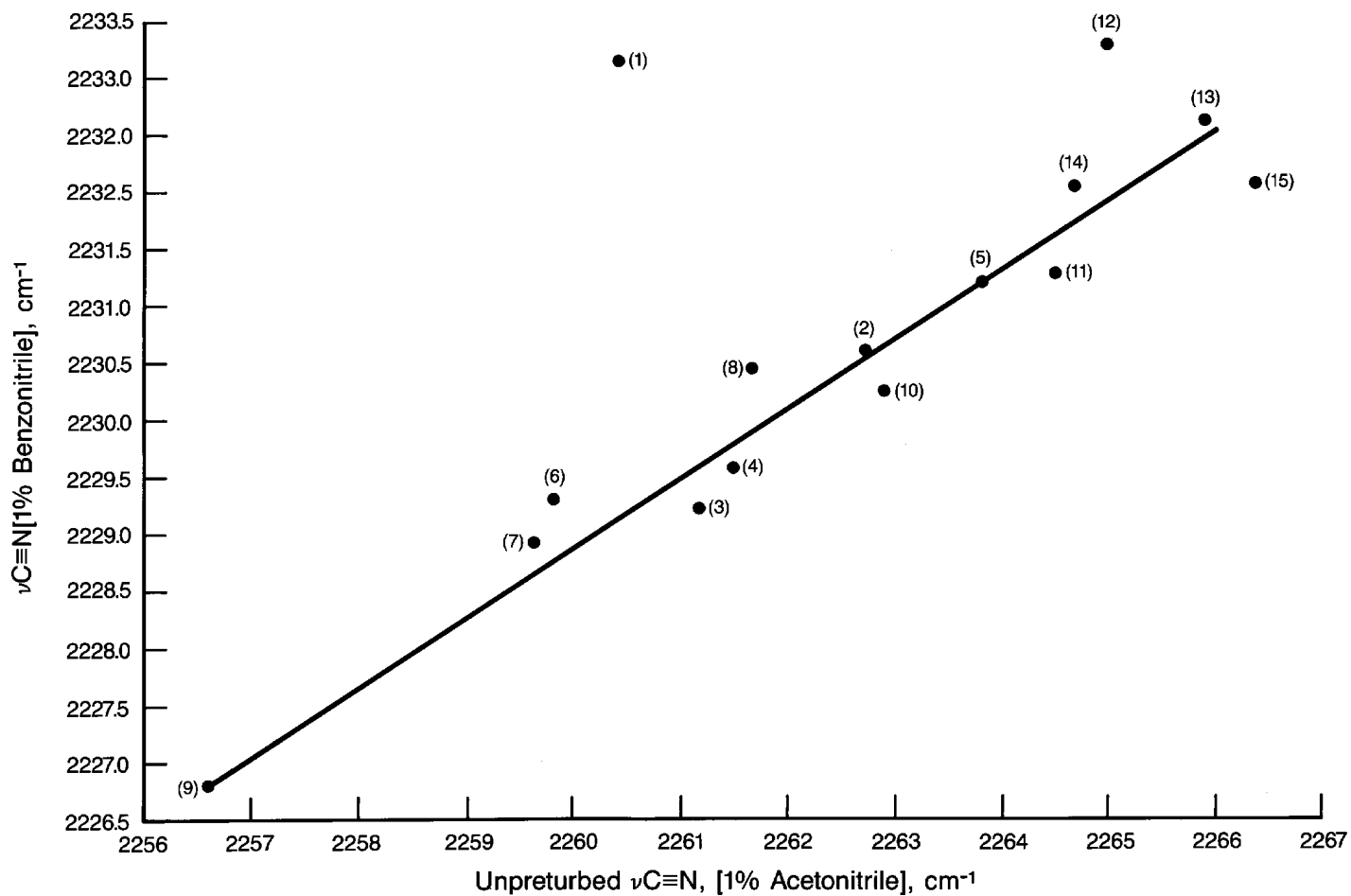


FIGURE 2.5 A plot of unperturbed $\nu_{\text{C}\equiv\text{N}}$ for acetonitrile vs $\nu_{\text{C}\equiv\text{N}}$ for benzonitrile. Both compounds were recorded at 1% wt./vol. separately in each of the 15 solvents.

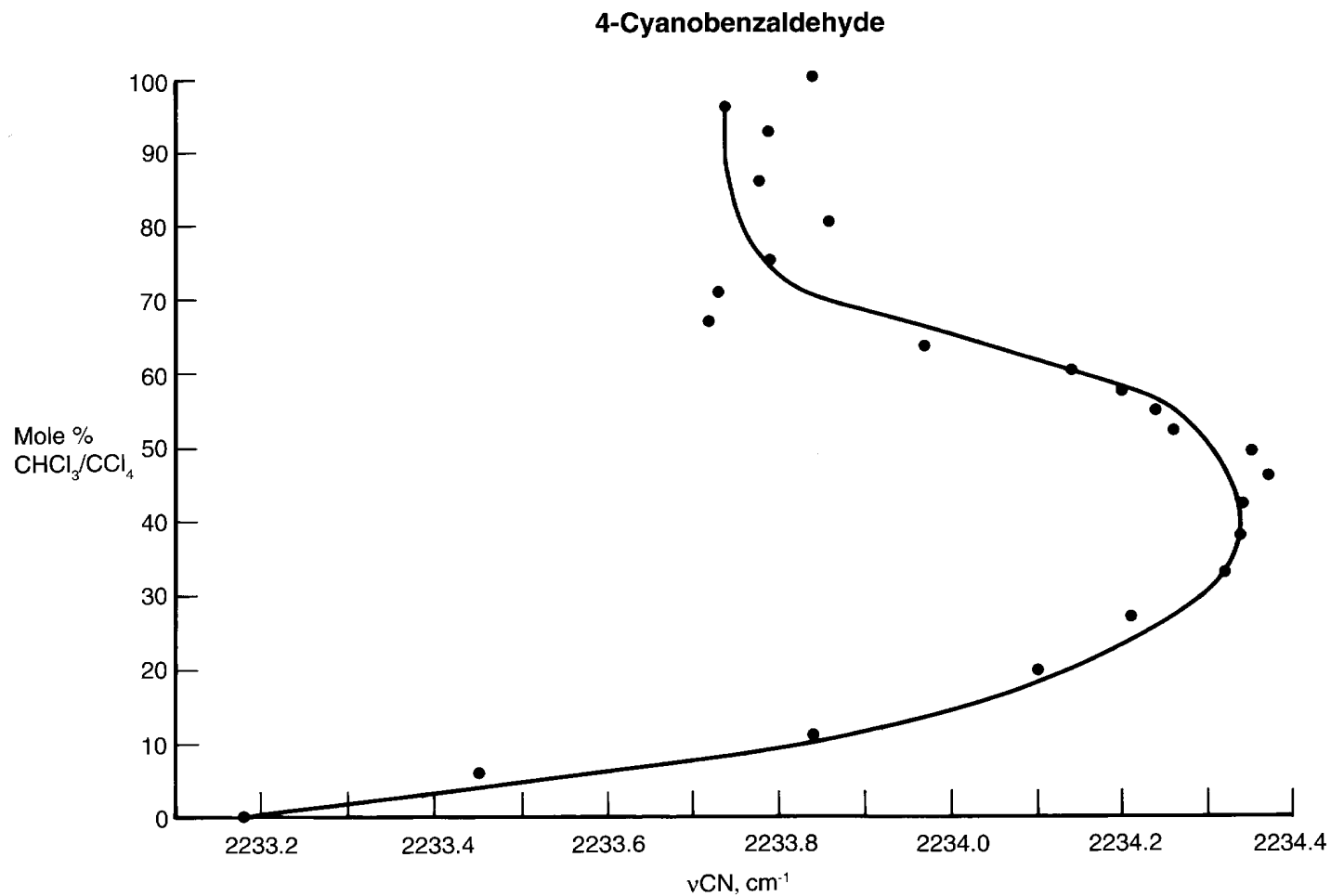
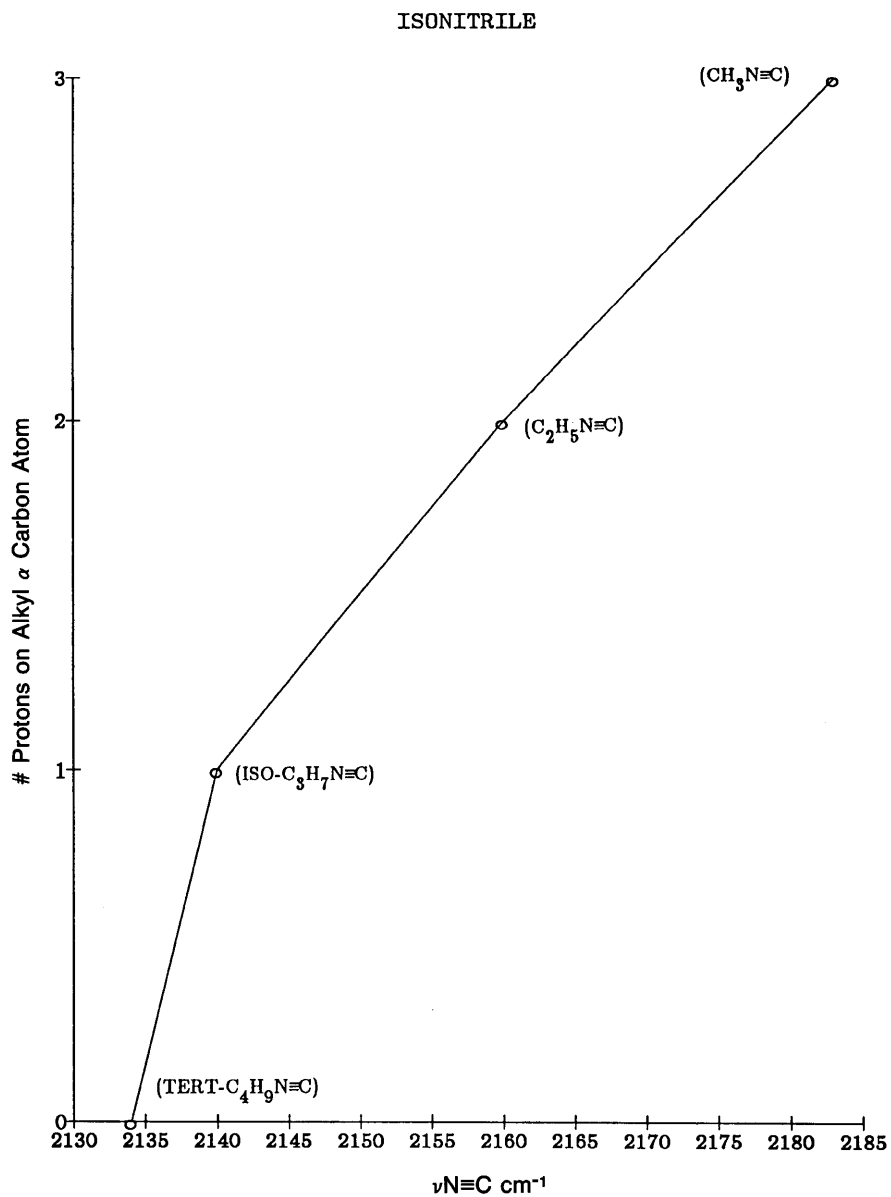


FIGURE 2.6 A plot of $\nu\text{C}\equiv\text{N}$ for 4-cyanobenzaldehyde in cm^{-1} vs mole % $\text{CHCl}_3/\text{CCl}_4$.

FIGURE 2.7 A plot of the number of protons on the alkyl α -C-N atom vs ν_{NC} for alkyl isonitriles.

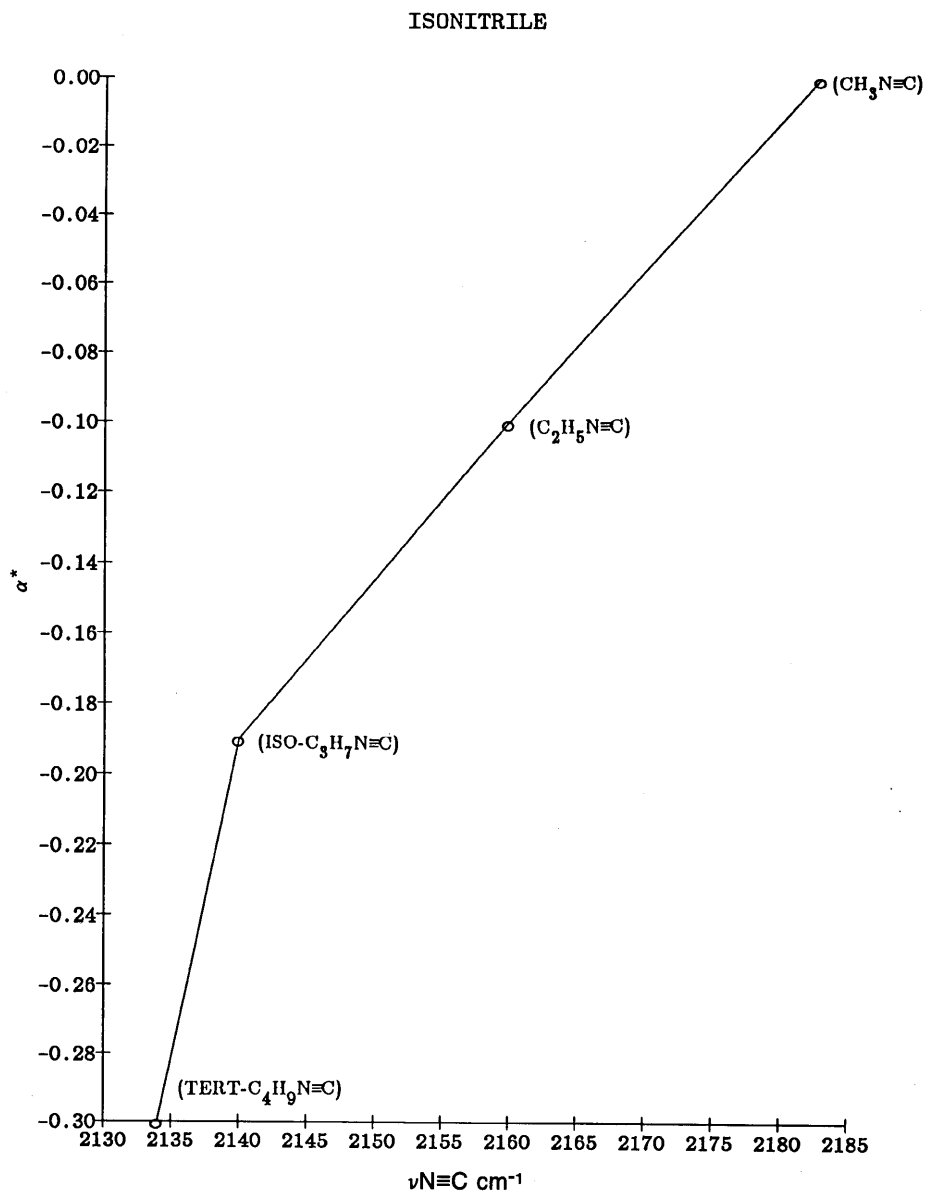
FIGURE 2.8 A plot of Taft's σ^* vs ν_{NC} for alkyl isonitriles.

TABLE 2.1 Infrared data for nitriles and cyanogen halides in the vapor and/or neat phases

	CN str. cm ⁻¹ [vapor]	A	Compound	CN str. cm ⁻¹ [vapor]	A	Compound	CN str. cm ⁻¹ [vapor]	A
IR (1)								
	2320	0.078					2244	0.02
acetonitrile	2280	0.11	benzonitrile	2240	0.118	acrylonitrile	2239	
	2252	0.07	benzonitrile				2221	0.012
butyronitrile	2260	0.03	4-hydroxy	2238	0.156	methacrylonitrile	2230	0.025
isobutyronitrile	2255	0.032	4-bromo	2238	0.12	2-chloroacryl- nitrile	2241	0.039
valeronitrile	2260	0.029	4-nitro	2240	0.011			
isovaleronitrile	2255	0.035	3-hydroxy	2230	0.059			
tetradecanenitrile	2250	0.019	3-chloro	2239	0.115			
adiponitrile	2258	0.051	3-cyano	2241	0.085			
undecanedinitrile	2250	0.049	2-amino 2-hydroxy	2222 2225	0.21 0.21			
	[neat] cm ⁻¹	[vapor]- [neat] cm ⁻¹		[neat] cm ⁻¹	[vapor]- [neat] cm ⁻¹		[neat] cm ⁻¹	[vapor]- [neat] cm ⁻¹
butyronitrile	2250	10	benzonitrile	2221	19	acrylonitrile	2224	15
isobutyronitrile	2240	5				methacrylonitrile	2222	8
valeronitrile	2238	22						
isovaleronitrile	2242	13						
	neat cm ⁻¹	IR [vapor] cm ⁻¹	IR (CCl ₄)					
Raman (2, 3)								
acetonitrile	2249	2280	2264*		31			
propionitrile	2242	2262			20			
isobutyronitrile	2238				17			
pivalonitrile	2236	2250			14			
chloroacetonitrile	2258							
trichloroacetonitrile	2250	2255			5			
acrylonitrile	2222	2239						17
methacrylonitrile	2230	2230						0
benzonitrile	2230	2260						10
2-chloroacrylonitrile	2234	2241						
	CCl ₄							
1-cyano-2-halo-acetylene								
-2-chloro-[IR; (6)]	2292	2301; 2293			5			
-2-bromo-[IR; (6)]	2278	2295; 2289			14			
-2-iodo-[IR; (6)]	2263	2270			7			
cyanogenhalides [IR] neat (4) vapor (5)								
FCN (4)	2290							
ClCN (4)	2201	2248			47			
BrCN (4)	2187	2200			13			
ICN (4)	2158							

* Corrected for Fermi resonance.

TABLE 2.2 Infrared data for acetonitrile in various solvents

Acetonitrile [1 wt./vol. %] Solvent	AN	In FR cm ⁻¹	In FR cm ⁻¹	C—C str. cm ⁻¹	s.CH ₃ bend cm ⁻¹	CN str. cor. for FR cm ⁻¹	[C—C str.] + [s.CH ₃ bend] cor. for FR cm ⁻¹
1. Hexane	0	2292.1	2252.7			2260.4	2284.4
2. Diethyl ether	3.9	2292.1	2253.7			2262.7	2283.1
3. Carbon tetrachloride	8.6	2292.5	2254.3	918.6	1374.7	2263.8	2283
4. Benzene	8.2	2290.8	2252.5	917.9	1373.8	2261.2	2282.2
5. Toluene		2291.2	2252.5			2261.5	2282.3
6. Nitrobenzene	14.8	2291.4	2252.3			2259.6	2284.1
7. Nitromethane		2291.2	2253.2			2261.7	2282.8
8. Methylene chloride	20.4	2292.1	2254	918.1	1373.2	2262.9	2283.2
9. Chloroform	23.1	2292.4	2255	919.8	1373	2264.5	2282.9
10. Dimethyl sulfoxide	19.3	2293.4	2248.9			2256.6	2285.7
11. tert-Butyl alcohol	29.1	2294.9	2256.2			2265	2286.1
12. Isopropyl alcohol	33.5	2294.9	2256.4			2265.9	2285.4
13. Ethyl alcohol	37.1	2295.2	2256.7			2264.7	2287.1
14. Methyl alcohol	41.3	2295.5	2257.4			2266.4	2286.5
15. Acetone	12.5	2293.3	2252.7			2259.8	2286.1

TABLE 2.3 A comparison of the IR ν_{CN} stretching frequencies for acetonitrile [corrected for Fermi resonance] with those for benzonitrile

Solvent	Benzonitrile 10 wt./vol. % cm ⁻¹	Benzonitrile 1 wt./vol. % cm ⁻¹	Acetonitrile 1 wt./vol. % cor. for FR cm ⁻¹	[Acetonitrile]- [Benzonitrile] 1 wt./vol. % cm ⁻¹
Hexane	2231.12	2233.14	2260.42	27.28
Diethyl ether	2230.41	2230.61	2262.72	32.11
Benzene	2229.38	2229.22	2261.17	31.95
Toluene	2229.18	2229.57	2261.49	31.92
Carbon tetrachloride	2230.58	2231.21	2263.8	32.59
Acetone	2229.46	2229.32	2259.81	30.5
Nitrobenzene	2228.67	2228.92	2259.63	30.71
Nitromethane	2230.18	2230.45	2261.66	31.21
Dimethyl sulfoxide	2227.01	2226.81	2256.6	29.79
Methylene chloride	2230.11	2230.25	2262.89	32.64
Chloroform	2230.62	2231.28	2264.49	33.21
tert-Butyl alcohol	2232.06	2233.28	2264.98	31.7
Isopropyl alcohol	2231.73	2232.62	2265.9	33.28
Ethyl alcohol	2231.64	2232.04	2264.67	32.63
Methyl alcohol	2231.78	2232.07	2266.37	34.3

TABLE 2.4 The CN stretching frequency for 4-cyanobenzaldehyde in 0 to 100 mol% CHCl₃/CCl₄ solutions [1 wt./vol. % solutions]

4-Cyanobenzaldehyde 1% (wt./vol.)	CN str. cm ⁻¹	A
Mole % CHCl ₃ /CCl ₄		
0	2233.2	0.065
5.68	2233.5	0.071
10.74	2233.8	0.076
19.4	2234.1	0.083
26.53	2234.2	0.085
32.5	2234.3	0.089
37.57	2234.3	0.092
41.93	2234.3	0.094
45.73	2234.4	0.094
49.06	2234.4	0.097
52	2234.3	0.097
54.62	2234.2	0.098
57.22	2234.2	0.1
60.07	2234.1	0.101
63.28	2234	0.109
66.74	2233.7	0.111
70.65	2233.7	0.112
75.06	2233.8	0.112
80.05	2233.9	0.114
85.75	2233.8	0.118
92.33	2233.8	0.125
96.01	2233.7	0.126
100	2233.8	0.123
Δ CN str.	1.2	
	-0.6	
Δ A		0.061

TABLE 2.5 Raman data for the C≡N group and C=C group of organonitriles*

Compound	CN str. cm ⁻¹	C=C str. cm ⁻¹
Isobutyl 2-cyanoacrylate	2239 (9)	
2,2-Azobis(4-methoxy-2,4-dimethylvaleronitrile)	2239 (8)	
1,1-Azobis(cyclohexane carbonitrile)	2236 (2)	
2,2-Azobis(2-methylbutyronitrile)	2241 (9)	
4,4'-Azobis(4-cyanovaleric acid)	2246 (9)	
Cyanoethylated cellulose	2251 (9)	
Crotononitrile	2223 (9)	1639 (4) 1629 (5)
2-Methyl crotononitrile	2218 (9)	1646 (4)

* Reference (3).

TABLE 2.6 A comparison of infrared data for organonitriles vs organoisonitriles

Compound	CN str. cm ⁻¹	NC str. cm ⁻¹	Compound	σ_p or σ_m	σ_p^- σ'	σ^*	CN str.- NC str. cm ⁻¹
Benzonitrile			Benzoisonitrile				
4-CH ₃ O	2226	2125	4-CH ₃ O	[-0.27]	[-0.50]	[0.52]	101
4-CH ₃	2229	2125	4-CH ₃	[-0.17]	[-0.13]	[-0.10]	104
3-CH ₃	2229	2125	3-CH ₃	[-0.07]	[-0.02]	[-0.10]	104
4-H	2229	2123	4-H	[0.00]	[0.00]	[0.00]	106
4-Cl	2233	2116	4-Cl	[0.23]	[-0.24]	[1.05]	117
4-NO ₂	2238	2116	4-NO ₂	[0.78]	[0.15]	[1.40]	122
3-NO ₂	2240	2120	3-NO ₂	[0.71]	[0.08]	[1.40]	120
2-CH ₃	2226	2122	2-CH ₃				104
2-Cl	2237	2166	2-Cl				71
Alkanonitrile			Alkanoisonitrile				
Acetonitrile	2249	2183	Acetoisonitrile			[0.000]	66
Propionitrile	2242	2160	Propionoisonitrile			[-0.100]	82
Isobutyronitrile	2238	2140	Isobutyroisonitrile			[-0.190]	98
Pivalonitrile	2236	2134	Pivaloisonitrile			[-0.300]	102

TABLE 2.7 A comparison of the infrared data for organothiocyanates in the vapor and neat phases

Thiocyanate	Vapor cm ⁻¹	Neat cm ⁻¹	Vapor-heat cm ⁻¹	Neat cm ⁻¹
Methyl	2175	2160	15	
Ethyl	2165	2160	5	
Pentyl	2165	[—]	[—]	
Isopentyl	2164	[—]	[—]	
Octyl	2161	2145	16	
Decyl	2164	2150	14	
Chloromethyl	2170	2150	20	Raman*
Benzyl	2164	2150	14	2150 (40)
Range	2161–2175	2145–2160		
2,6-Dichlorobenzyl Thiocyanate	[—]	2115	[—]	
Phenyl	[—]	2170	[—]	
4-Nitrophenyl	[—]	2174	[—]	
4-Aminophenyl	[—]	2166	[—]	
Range	[—]	2166–2174	[—]	
	Phenyl ring cm ⁻¹	Phenyl ring cm ⁻¹	Phenyl ring cm ⁻¹	
	1029 (10)	1003 (80)	631 (5)	

* Relative intensity.

Azines, Isocyanates, Isothiocyanates, and Carbodiimides

Azines	45
Isocyanates	46
Isothiocyanates	49
Carbodiimides	50
References	50

Figures

Figure 3-1	51 (47)
Figure 3-2	51 (47)
Figure 3-3	52 (47)
Figure 3-4	52 (47)
Figure 3-5	53 (47)
Figure 3-6	53 (47)
Figure 3-7	54 (47)
Figure 3-8	54 (49)
Figure 3-9	55 (49)
Figure 3-10	55 (49)
Figure 3-11	56 (49)

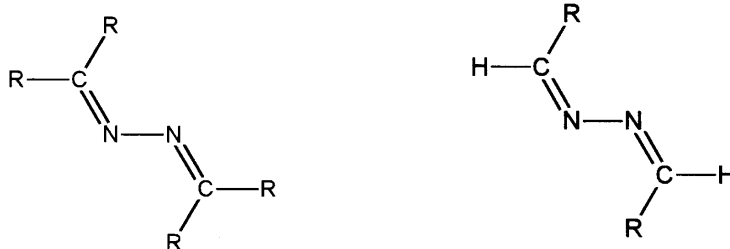
Tables

Table 3-1	57 (46)
Table 3-2	58 (46)
Table 3-3	59 (46)
Table 3-4	60 (48)
Table 3-5	60 (49)
Table 3-6	61 (49)
Table 3-6a	62 (49)
Table 3-7	63 (50)

* Numbers in parentheses indicate in-text page reference.

AZINES

Infrared and Raman studies of aldehyde and ketone azines have been summarized by Dollish *et al.* (1). Azines have the following empirical structures:



(Where R can be hydrogen, alkyl, and/or aryl in the case of aldehyde azines, and in the case of ketone azines R can be alkyl and/or aryl.)

These molecules exist in an *s*-transoid configuration and have a center of symmetry (2–7). In these cases, the antisymmetric $(\text{C}=\text{N}-)_2$ stretching vibration is only IR active while the symmetric $(\text{C}=\text{N}-)_2$ stretching vibration is only Raman active. The compound, $(\text{F}_2\text{C}=\text{N}-)_2$, is reported to have a trans planar structure (6). Infrared and Raman studies of benzaldehyde azines are also reported to have a center of symmetry (7).

Table 3.1 lists IR and Raman data for the benzaldehyde azines (7) and also summarizes the ν asym. $(\text{C}=\text{N}-)_2$ and ν sym. $(\text{C}=\text{N}-)_2$ vibrations for other azines (2–7). The IR bands assigned to ν asym. $(\text{C}=\text{N}-)_2$ were not apparent in the Raman spectrum and Raman bands assigned to ν sym. $(\text{C}=\text{N}-)_2$ were not apparent in the IR spectrum. The ν sym. $(\text{C}=\text{N}-)_2$ mode yields the most intense Raman band in each azine spectrum. For example, ν sym. NO_2 in nitrobenzenes has high Raman band intensity. In the Raman spectrum of 2-nitrobenzaldehyde azine, ν sym. $(\text{C}=\text{N}-)_2$ at 1560 cm^{-1} has twice the intensity of the ν sym. NO_2 vibration at 1348 cm^{-1} (7). With the exception of 2,6-dichlorobenzaldehyde azine, ν sym. $(\text{C}=\text{N}-)_2$ occurs in the region $1539\text{--}1563\text{ cm}^{-1}$ while the 2,6-dichloro analog exhibits ν sym. $(\text{C}=\text{N}-)_2$ at 1587 cm^{-1} . This higher frequency is intermediate between arylaldehyde azines and alkylaldehyde azines (7). This intermediate ν sym. $(\text{C}=\text{N}-)_2$ frequency is due to the fact that the 2,6- Cl_2 atoms prevent the two 2,6-dichlorophenyl groups from being coplanar with the $(\text{C}=\text{N}-)_2$ group. Thus, the resonance effect of the phenyl group, which lowers ν sym. $(\text{C}=\text{N}-)_2$ frequency, is absent in the case of the 2,6-dichloro analog. Further, only the inductive effect operates in this case, causing ν sym. $(\text{C}=\text{N}-)_2$ to occur at the intermediate 1587 cm^{-1} frequency.

In the IR benzaldehyde azines exhibit ν asym. $(\text{C}=\text{N}-)_2$ at lower frequency than those for alkylaldehyde azines ($1606\text{--}1632$ vs $1636\text{--}1663\text{ cm}^{-1}$, respectively) due to resonance of the phenyl groups with the $(\text{C}=\text{N}-)_2$ group (7).

It is interesting to note that in the case of $(\text{F}_2\text{C}=\text{N}-)_2$ the ν sym. $(\text{C}=\text{N}-)_2$ frequency (1758 cm^{-1}) occurs at a higher frequency than that for ν asym. $(\text{C}=\text{N}-)_2$ at 1747 cm^{-1} (6). In all other cases ν asym. $(\text{C}=\text{N}-)_2$ occurs at a higher frequency than that for ν sym. $(\text{C}=\text{N}-)_2$.

ISOCYANATES

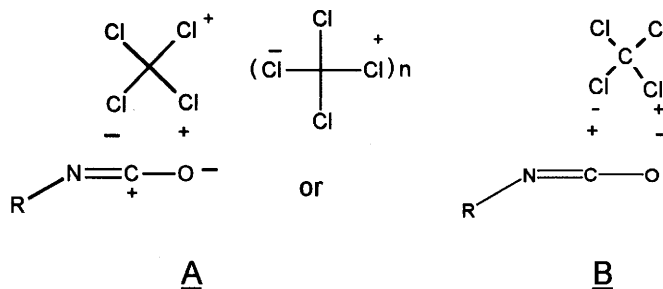
Table 3.2 lists IR data for alkyl and aryl isocyanates in various physical phases. In the liquid phase, methyl, ethyl and isopropyl isocyanate exhibit ν asym. $\text{N}=\text{C}=\text{O}$ at 2288 , 2280 , and 2270 cm^{-1} , respectively, and ν sym. $\text{N}=\text{C}=\text{O}$ at 1437 , 1432 , and 1421 cm^{-1} , respectively (8). Phenyl isocyanate and Cl_3Si isocyanate in the liquid phase exhibit ν asym. $\text{N}=\text{C}=\text{O}$ at 2285 and 2311 cm^{-1} , respectively (9, 10).

In CCl_4 solution, *n*-butyl, *n*-pentyl, isobutyl and sec-butyl isocyanate exhibit ν asym. $\text{N}=\text{C}=\text{O}$ at 2273 , 2274 , 2263 , and 2261 , respectively (11). Aryl isocyanates in CCl_4 solution exhibit ν asym. $\text{N}=\text{C}=\text{O}$ in the region $2242\text{--}2278\text{ cm}^{-1}$ (11) (see Table 3.2). In the case of phenyl isocyanate, two IR bands are observed in the region expected for ν asym. $\text{N}=\text{C}=\text{O}$ and these two bands are reported to arise from ν asym. $\text{N}=\text{C}=\text{O}$ in Fermi resonance (FR) with a combination tone of the same symmetry species (12). The ν sym. $\text{N}=\text{C}=\text{O}$ mode for phenyl isocyanate has been assigned at 1448 cm^{-1} (10).

Table 3.3 lists IR data for alkyl isocyanates in 0 to 100 mol % $\text{CHCl}_3/\text{CCl}_4$ in 0.5 wt./vol.% solutions (13, 14). In the case of methyl isocyanate, IR bands are noted at 2285.6 cm^{-1} (A is

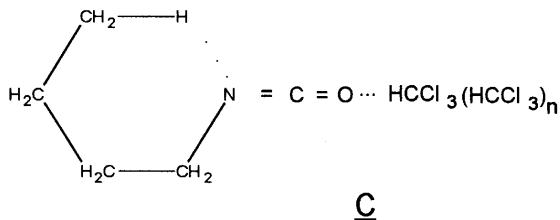
1.176), 2256.3 cm^{-1} (A is 0.716), and 2318.3 cm^{-1} (A is 0.314) in CCl_4 solution, and 2286.0 cm^{-1} (A is 0.478), 2253.3 cm^{-1} (A is 0.478), and 2315.9 cm^{-1} (A is 0.519) in CHCl_3 solution. The data listed in Table 3.3 have been corrected for FR by the method developed in Reference (14), and these frequencies corrected for FR have been plotted vs mole % $\text{CHCl}_3/\text{CCl}_4$ as shown in Figure 3.1. These plots show that unperturbed ν asym. $\text{N}=\text{C}=\text{O}$ and an unperturbed combination tone $\nu(\text{C}_\alpha-\text{N}) + \delta$ sym. CH_3 both increase in frequency while the combination $\nu(\text{C}_\alpha-\text{N}) + \nu$ sym. $\text{N}=\text{C}=\text{O}$ decreases in frequency as the mole % CHCl_3 is increased (14). Figure 3.2 shows a plot of these same bands in FR (14). In the case of the uncorrected IR data where all three bands are in FR, the band with the most intensity has the most contribution from ν asym. $\text{N}=\text{C}=\text{O}$. This band decreases only 0.5 cm^{-1} in going from solution in CCl_4 to solution in CHCl_3 while after correction for FR ν asym. $\text{N}=\text{C}=\text{O}$ decreases 3 cm^{-1} , as might be expected due to intermolecular hydrogen bonding between the CHCl_3 proton and the $\text{N}=\text{C}=\text{O}$ group and the increase in the field effect of the solvent system. Ethyl isocyanate and propyl isocyanate also show that ν asym. $\text{N}=\text{C}=\text{O}$ is in FR with a combination tone (CT), while isopropyl isocyanate and tert-butyl isocyanate exhibit only unperturbed ν asym. $\text{N}=\text{C}=\text{O}$ (14).

Figure 3.3 shows plots of ν asym. $\text{N}=\text{C}=\text{O}$ frequencies for *n*-butyl, isopropyl and tert-butyl isocyanate, and of the frequencies for the most intense IR band for ν asym. $\text{N}=\text{C}=\text{O}$ (uncorrected for FR) for methyl, ethyl and *n*-propyl isocyanate vs the mole % $\text{CHCl}_3/\text{CCl}_4$ (13). Figure 3.4 shows plots of unperturbed ν asym. $\text{N}=\text{C}=\text{O}$ frequencies for the alkyl isocyanates vs mole % $\text{CHCl}_3/\text{CCl}_4$ solutions (in this case the ν asym. $\text{N}=\text{C}=\text{O}$ mode for the methyl, ethyl and *n*-propyl isocyanates have been corrected for FR). In this case, the six plots decrease in frequency in the order methyl, *n*-butyl, ethyl, *n*-propyl, isopropyl and tert-butyl isocyanate. The *n*-butyl analog occurs at a higher frequency than would be predicted by the reasons given here. Figure 3.5 show plots of ν asym. $\text{N}=\text{C}=\text{O}$ for alkyl isocyanates in CCl_4 solution and in CHCl_3 solution vs σ^* (the inductive value of the alkyl group). Figure 3.6 show plots of ν asym. $\text{N}=\text{C}=\text{O}$ for alkyl isocyanates in CCl_4 solution and in CHCl_3 solution vs E_s (the steric parameter of the alkyl group). Figure 3.7 show plots of ν asym. $\text{N}=\text{C}=\text{O}$ frequencies for alkyl isocyanates vs σ^* times E_s . Figures 3.5–3.7 show that ν asym. $\text{N}=\text{C}=\text{O}$ for these six alkyl isocyanates occur at higher frequency in CHCl_3 solution than in CCl_4 solution (13). In addition, the data points for *n*-butyl isocyanate do not correlate with the other five alkyl isocyanates. In CCl_4 solution, the five alkyl isocyanates apparently exist as a complex such as A or B. A complex such as A or B:

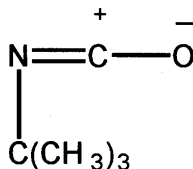


would weaken the $\text{N}=\text{C}=\text{O}$ bond, and it would vibrate at lower frequency (13).

In the case of *N*-butyl isocyanate, ν asym. N=C=O decreases in frequency in the order CHCl_3 (2278.7 cm^{-1}), CCl_4 (2274.5 cm^{-1}), and C_6H_{14} (2270.5 cm^{-1}), and this is the reverse solvent effect order exhibited upon carbonyl stretching frequencies ($\nu \text{ C=O}$). Therefore, a complex between CHCl_3 or CCl_4 must cause the ν asym. N=C=O to vibrate at a higher frequency than occurs in solution with hexane. It is suggested that the complex between CHCl_3 and *n*-butyl isocyanate is either a steric or intramolecular hydrogen-bonded complex such as **C**, which stabilizes the N=C=O group and thus prevents a hydrogen-bonding complex from being formed between the Cl_3CH proton and the isocyanate nitrogen atom.



In the case of tert-butyl isocyanate, the tert-butyl group would have more of an electron release toward the isocyanate group, and it would have the most contribution from the resonance form **D**. The steric factor



of the tert-butyl group is also higher than that of the other alkyl groups. Thus, structures **E** and **A** would help contribute the lower ν asym. N=C=O frequencies exhibited by the tert-butyl analog than when in hexane solution

Table 3.4 lists IR data for ν asym. N=C=O for the alkyl isocyanates in both CCl_4 and CHCl_3 solutions. Examination of Table 3.4 clearly shows that ν asym. N=C=O in CHCl_3 solution always occurs at higher frequency than when in CCl_4 solution (13).

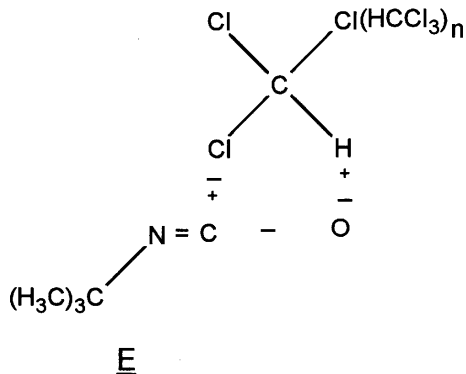


Table 3.5 lists IR and Raman data for alkyl isocyanates. The last column lists the Raman data for these compounds (15). These data show that the frequency of ν sym. N=C=O decreases, progressing in the order of methyl isocyanate through tert-butyl isocyanate; this is the order of electron release of the alkyl group to the isocyanate group.

ISOTHIOCYANATES

Table 3.6 lists IR data for 1% wt./vol. alkyl isothiocyanates in 0 to 100 mol % CHCl₃/CCl₄ or CDCl₃/CCl₄ solution. The unperturbed ν asym. N=C=S frequencies for the alkyl isothiocyanates occur at higher frequency in CHCl₃ or CDCl₃ solution than in CCl₄ (16). Figure 3.8 and Figure 3.9 show plots of ν asym. N=C=S in FR resonance and ν asym. N=C=S corrected for FR, respectively. The propyl analog was not corrected for FR and is not included in Figure 3.9. Both plots show that ν asym. N=C=S generally increases in frequency as the mole % CHCl₃/CCl₄ or CDCl₃/CCl₄ is increased (16). Examination of Figure 3.9 shows that ν asym. N=C=S frequency for the methyl, ethyl and tert-butyl analogs decrease in frequency as the σ^* values decrease (increasing electron release to the C=N=S group). The exception is the *n*-butyl analog. It is suggested that the explanation used here to explain the behavior of ν asym. N=C=O for *n*-butyl isocyanate can also be used to explain the behavior of ν asym. N=C=S for *n*-butyl isothiocyanate (16).

Figure 3.10 shows a plot of ν asym. N=C=S and 2ν C-N in FR and the same two modes corrected for FR for methyl isothiocyanate vs mole % CHCl₃/CCl₄ (16). Figure 3.11 shows a plot of ν C-N for methyl isothiocyanate vs mole % CHCl₃/CCl₄. Figure 3.11 shows that ν C-N decreases in frequency as the mole % CHCl₃/CCl₄ is increased. Figure 3.10 shows that 2ν C-N decreases in frequency while the ν asym. N=C=S increases in frequency as the mole % CHCl₃/CCl₄ is increased. In CCl₄ solution, the amount of FR between ν asym. N=C=S and 2ν C-N is the least; it is the most in CHCl₃ solution because the IR band intensity ratio of perturbed ν N=C=O/perturbed 2ν C-N is $0.808/0.200 = 4.04$ in CCl₄ solution and $0.690/0.371 = 1.86$ in CHCl₃ solution. In addition, that perturbed ν asym. N=C=S increases 18.0 cm^{-1} while perturbed 2ν C-N decreases 10.7 cm^{-1} in going from solution in CCl₄ to solution in CHCl₃. Another way to look at these data is that the frequency separation between perturbed ν asym. N=C=S and perturbed 2ν C-N is 116.5 cm^{-1} in CCl₄ solution and 87.8 cm^{-1} in CHCl₃ solution, while the frequency separation between ν asym. N=C=S and 2ν C-N corrected for FR is 70.2 cm^{-1} in CCl₄ solution and 26.4 cm^{-1} in CHCl₃. In other words, the closer in frequency that unperturbed ν asym. N=C=S and 2ν C-N occur, the larger the amount of Fermi interaction between the fundamental and the first overtone. The first overtone gains intensity from the fundamental during the FR interaction.

The correction for FR is readily performed by application of the equation presented here (17, 18):

$$W^o = \frac{W_a + W_b}{2} \pm \frac{W_a - W_b}{2} \cdot \frac{I_a - I_b}{I_a + I_b}$$

where W_a and W_b are the observed band frequencies, I_a and I_b are their intensities, and the two values of W^o calculated by this equation will be approximately the unperturbed frequencies.

Table 3.6a lists vibrational data for alkyl and aryl isothiocyanates in different physical phases. In the case of heptyl isothiocyanate, ν asym. N=C=S gives a depolarized Raman band at

2090 cm^{-1} and ν sym. $\text{N}=\text{C}=\text{S}$ gives a polarized Raman band at 1070 cm^{-1} . Raman data for the three aryl isothiocyanates are assigned as ν asym. $\text{N}=\text{C}=\text{S}$ in the range 2070–2150 cm^{-1} and ν sym. $\text{N}=\text{C}=\text{S}$ in the range 1245–1250 cm^{-1} .

CARBODIIMIDES

Table 3.7 lists vapor- and neat-phase infrared data for dialkyl and diaryl carbodiimides (19). In the vapor phase the compounds of form $\text{R}-\text{N}=\text{C}=\text{N}-\text{R}$ exhibit ν asym. $\text{N}=\text{C}=\text{N}$ in the region 2118–2128 cm^{-1} and compounds of form $\phi-\text{N}=\text{C}=\text{N}-\phi$ exhibit a doublet. One band of the doublet occurs in the regions 2100–2120 cm^{-1} and the other band of the doublet occurs in the region 2150–2170 cm^{-1} . In the neat phase, the compounds of form $\text{R}-\text{N}=\text{C}=\text{N}-\text{R}$ exhibit a doublet. One band of the doublet occurs in the region 2040–2098 cm^{-1} and the other band of the doublet occurs in the region 2120–2158 cm^{-1} (19). The higher frequency band in the doublet always has more intensity than the lower frequency band. These two bands result from ν asym. $\text{N}=\text{C}=\text{N}$ in FR with a combination tone or an overtone (18). The unperturbed ν asym. $\text{N}=\text{C}=\text{N}$ frequencies for the diaryl carbodiimides occur at higher frequency (2124–2145 cm^{-1}) than do those for the dialkyl carbodiimides (2105–2125 cm^{-1}). The higher frequency for the diaryl analog is attributed to the positive inductive effect of the two aryl groups vs the negative inductive effect of the two alkyl groups. In addition, the ν asym. $\text{N}=\text{C}=\text{N}$ mode occurs at higher frequency in the vapor phase than in the neat phase.

REFERENCES

1. Dollish, F. R., Fateley, W. G., and Bentley, F. K. (1974). *Characteristic Raman Frequencies of Organic Compounds*. New York: Wiley.
2. Kirrman, A. (1943). *Comp Rend.*, **217**: 148.
3. West, W. and Killingsworth, R. B. (1938). *J. Chem. Phys.*, **6**: 1.
4. Kitaev, Yu. P., Nivorozhkin, L. E., Plegontov, S. A., Raevskii, O. A., and Titova, S. Z. (1968). *Dokl. Acad. Sci. USSR*, **178**: 1328.
5. Ogilvie, J. F. and Cole, K. C. (1971). *Spectrochim. Acta*, **27A**: 877.
6. King, S. T., Overend, J., Mitsch, R. A., and Ogden, P. H. (1970). *Spectrochim. Acta*, **26A**: 2253.
7. Nyquist, R. A. and Peters, T. L. (1978). *Spectrochim. Acta*, **34A**: 503.
8. Hirschmann, R. P., Kniseley, R. N., and Fassel, V. A. (1965). *Spectrochim. Acta*, **21**: 2125.
9. Koster, D. F. (1968). *Spectrochim Acta*, **24A**: 395.
10. Stephenson, C. V., Coburn, Jr. W. C., and Wilcox, W. S. (1961). *Spectrochim Acta*, **17**: 933.
11. Hoyer, H. (1956). *Chem. Ber.*, **89**: 2677.
12. Ham, N. S. and Willis, J. B. (1960). *Spectrochim. Acta*, **16**: 279.
13. Nyquist, R. A., Luoma, D. A., and Putzig, C. L. (1992). *Appl. Spectrosc.*, **46**: 972.
14. Nyquist, R. A., Putzig, C. L., and Hasha, D. L. (1989). *Appl. Spectrosc.*, **43**: 1049.
15. Herzberg, G. and Reid, C. (1950). *Discuss. Faraday Soc.*, **9**: 92.
16. Nyquist, R. A. and Puehl, C. W. (1993). *Appl. Spectrosc.*, **47**: 677.
17. Nyquist, R. A., Fouchea, H. A., Hoffman, G. A., and Hasha, D. L. (1991). *Appl. Spectrosc.*, **45**: 860.
18. Nyquist, R. A. (1984). *The Interpretation of Vapor-phase Infrared Spectra: Group Frequency Data*. Vol. 1, Philadelphia: Sadtler Research Laboratories, Division of Bio-Rad Laboratories, Inc., p. 43.
19. Nyquist, R. A. (1984). *Ibid.*, p. 461.

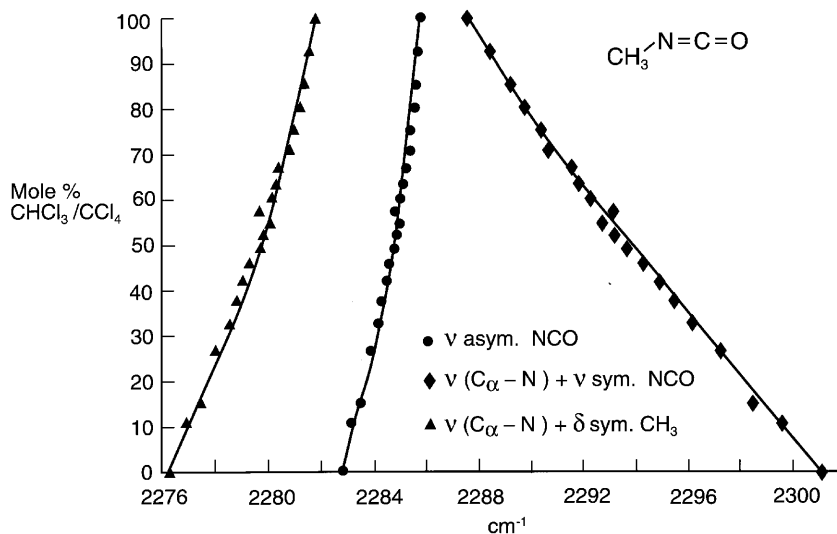


FIGURE 3.1 Plots of ν asym. N=C=O and the combination tone ν ($\text{C}_\alpha\text{-N}$) + ν sym. N=C=O and ν ($\text{C}_\alpha\text{-N}$) + sym. CH_3 for methyl isocyanate all corrected for Fermi resonance.

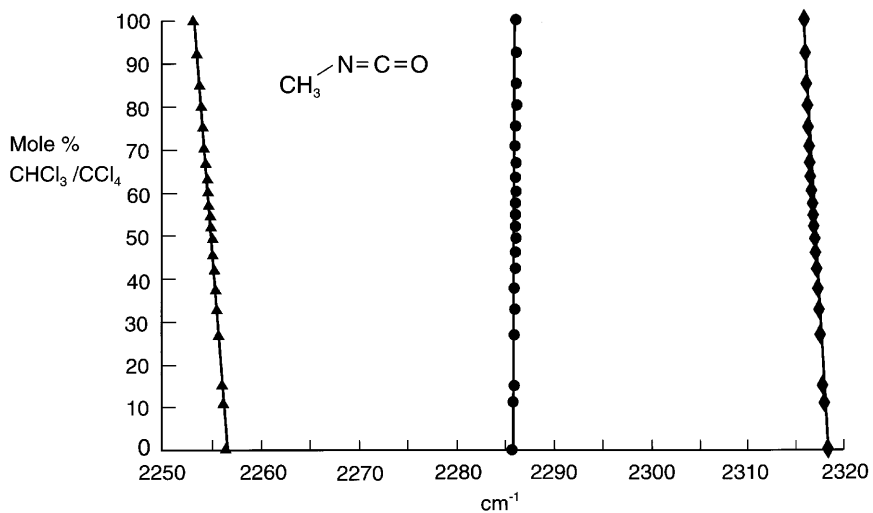


FIGURE 3.2 Plots of the three observed IR bands for methyl isocyanate occurring in the region 2250–2320 vs mole % $\text{CHCl}_3/\text{CCl}_4$.

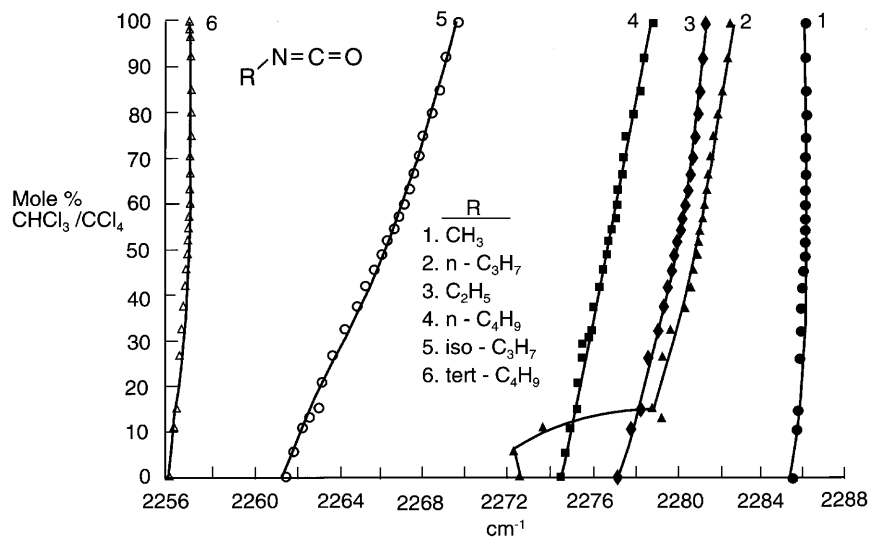


FIGURE 3.3 Plots of the ν asym. NCO frequencies for *n*-butyl, isopropyl and tert-butyl isocyanate and of the frequencies of the most intense IR band for ν asym. N=C=O in FR (uncorrected for FR) for methyl, ethyl and *n*-propyl isocyanate vs mole % $\text{CHCl}_3/\text{CCl}_4$.

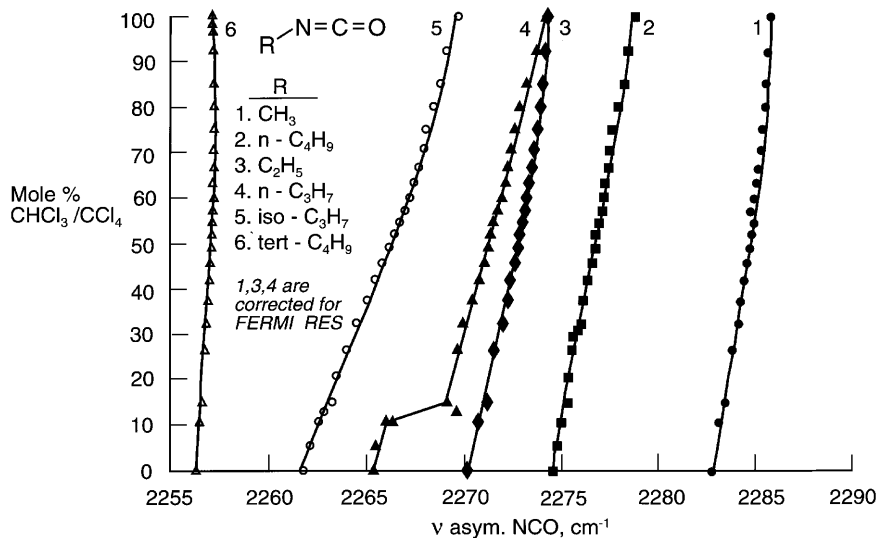


FIGURE 3.4 Plots of unperturbed ν asym. N=C=O for the alkyl isocyanates vs mole % $\text{CHCl}_3/\text{CCl}_4$.

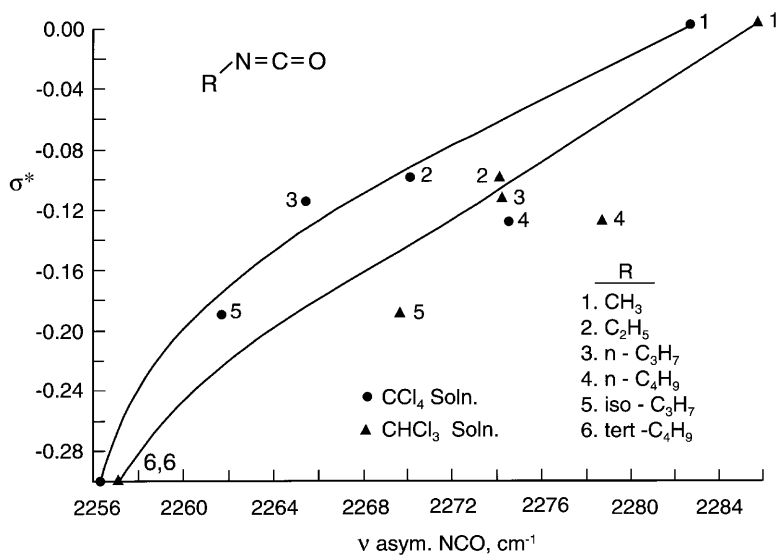


FIGURE 3.5 Plots of ν asym N=C=O frequencies for alkyl isocyanates in CCl_4 solution and in CHCl_3 solution vs σ^* . (The inductive release value of the alkyl group.)

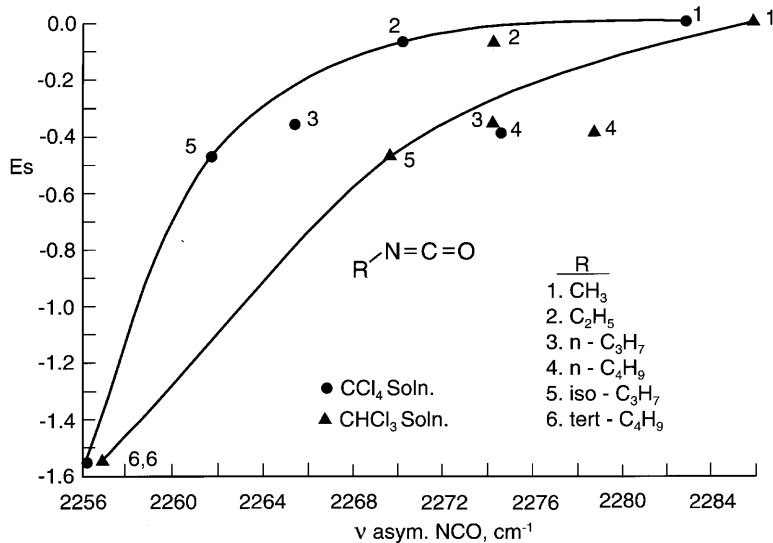


FIGURE 3.6 Plots of ν asym. N=C=O frequencies for alkyl isocyanates in CCl_4 solution and in CHCl_3 solution vs E_s . (The steric parameter of the alkyl group.)

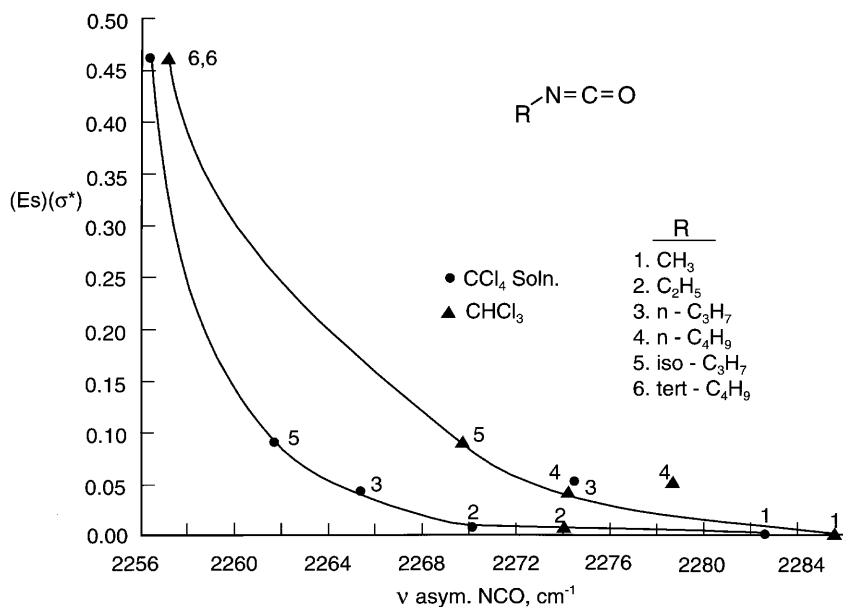


FIGURE 3.7 Plots of ν asym. $N=C=O$ frequencies for alkyl isocyanates in CCl_4 solution and in $CHCl_3$ solution vs (E_s) (σ^*).

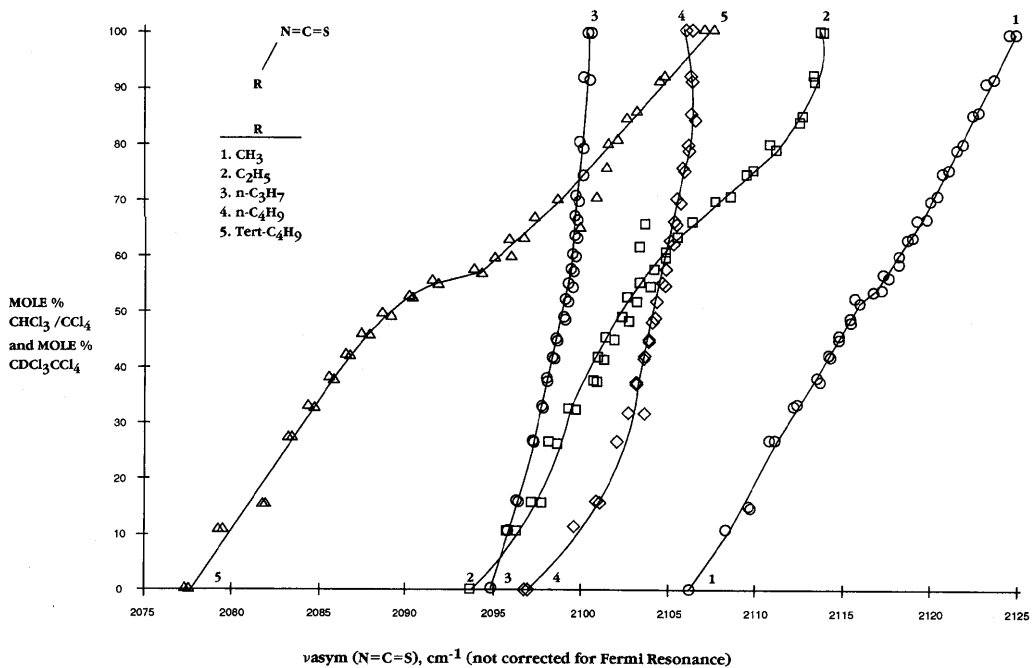


FIGURE 3.8 A plot of perturbed ν asym. $N=C=S$ (not corrected for FR) for five alkyl isothiocyanates vs mole % $CHCl_3/CCl_4$.

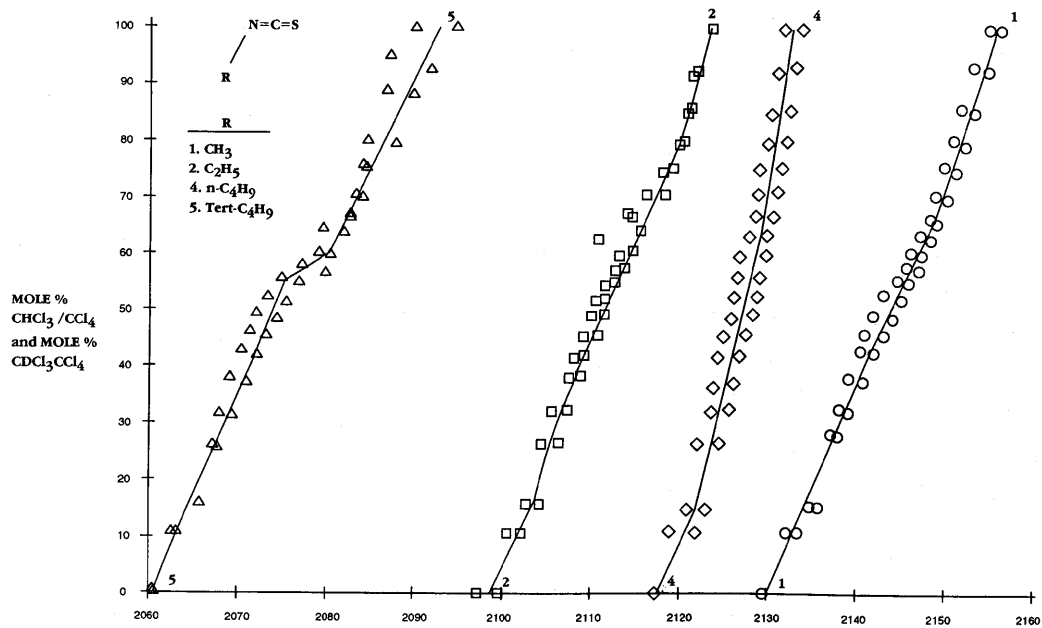


FIGURE 3.9 A plot of unperturbed ν asym. $N=C=S$ (corrected for FR) for four alkyl isothiocyanates vs mole % $CHCl_3/CCl_4$ and $CDCl_3/CCl_4$.

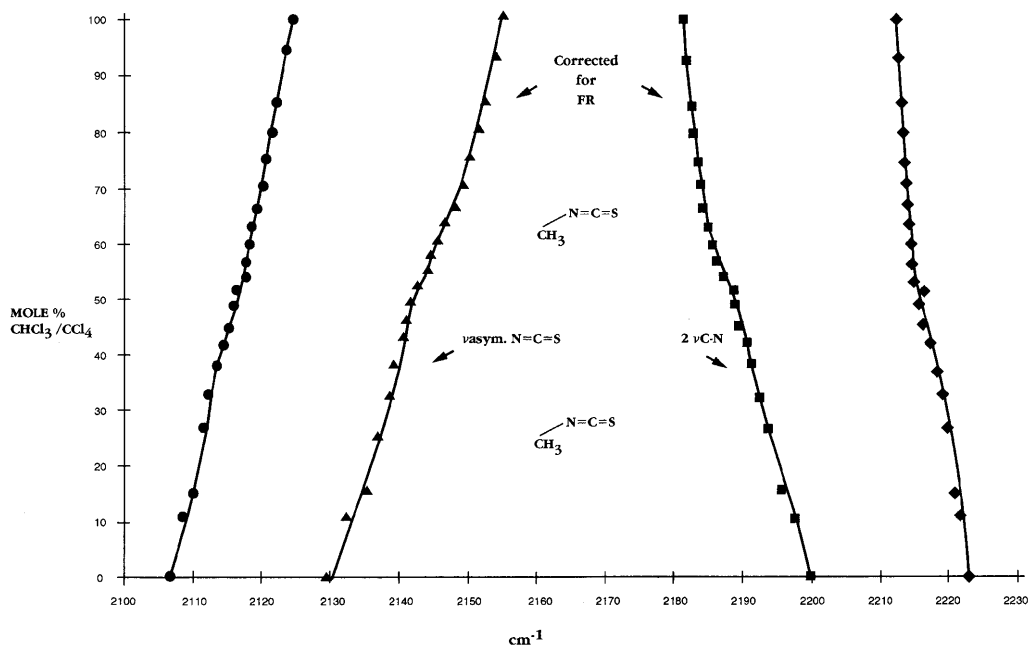


FIGURE 3.10 A plot of perturbed 2ν C-N and perturbed ν asym. $N=C=S$ and unperturbed 2ν C-N and unperturbed ν asym, $N=C=S$ vs mole % $CHCl_3/CCl_4$.

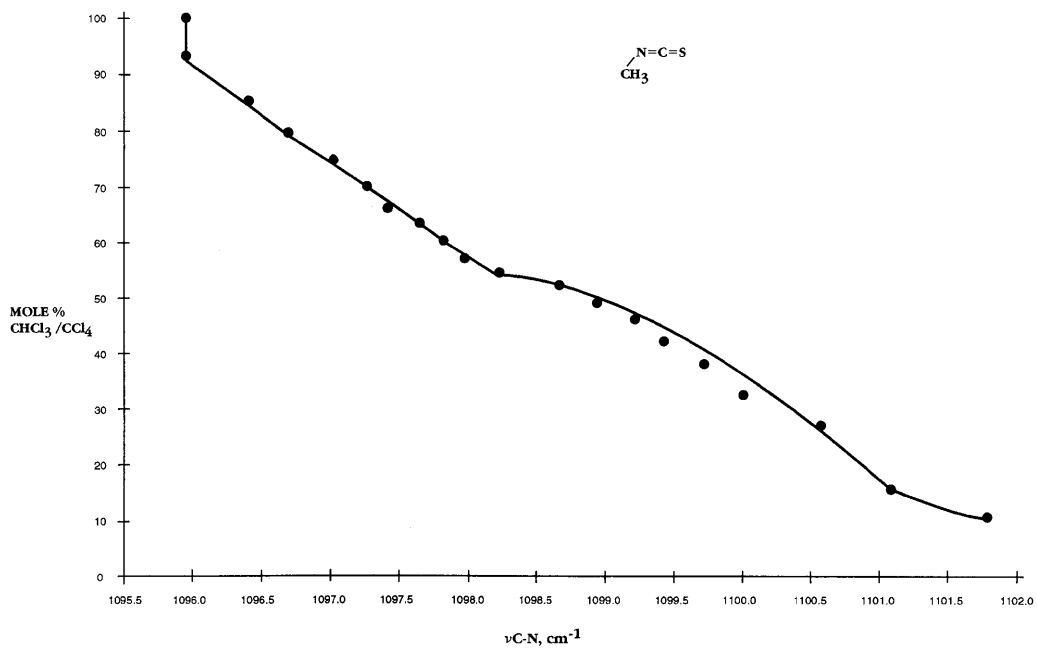


FIGURE 3.11 A plot of $\nu\text{C-N}$ for methyl isothiocyanate vs mole % $\text{CHCl}_3/\text{CCl}_4$.

TABLE 3.1 Infrared and Raman data and assignments for the (C=N-)2 antisymmetric and symmetric stretching vibrations for azines

Azines	asym. (C=N-)2 str. IR active cm ⁻¹	sym. (C=N)2 str. Raman active cm ⁻¹	asym. (C=N)2 str.- sym. (C=N)2 str. cm ⁻¹
4-X-benzaldehyde			
X			
dimethylamino	1608	1539	69
methoxy	1605	1553	52
methyl	1623	1553	70
hydrogen	1628	1556	72
fluoro	1633	1561	72
chloro	1627	1547	80
acetoxo	1631	1562	69
trifluoromethyl	1631	1561	70
cyano	1624	1541	83
2-X-benzaldehyde			
X			
methoxy	1619	1552	67
chloro	1618	not recorded	[-]
hydroxy	1630	1555	75
nitro	1627	1560	67
3-X-benzaldehyde			
X			
nitro	1629	1551	78
benzaldehyde			
2,4-dimethoxy	1617	1546	71
3,4-dimethoxy	1626	1557	69
2-hydroxy-4-methoxy	1630	1554	76
2,4-dihydroxy	1632	1563	69
3-methoxy-4-hydroxy	1629	1558	71
2,6-dichloro	1629	1587	42
Summary			
Azine Type			
benzaldehyde	1606-1632	1539-1563	52-83
2,6-Cl ₂ -benzaldehyde	1629	1587	42
alkylaldehyde and alkylketone	1636-1663	1608-1625	28-38
CF ₂ =	1747	1758	[-11]
Range	1606-1747	1539-1758	

TABLE 3.2 The symmetric and/or antisymmetric stretching frequencies for alkyl and aryl isocyanates in various physical phases

Alkyl and phenyl isocyanate R-N=C=O and C ₆ H ₅ -N=C=O	a.N=C=O cm ⁻¹	s.N=C=O cm ⁻¹	Physical phase	Reference
Methyl	2288	1437	L ^{*1}	8
Ethyl	2280	1432	L	8
Isopropyl	2270	1421	L	8
<i>t</i> -Butyl	2270		L	9
Phenyl	2285	1448	L	10
Cl ₂ Si	2311	1467	L	8
H	2274	1318	V ^{*2}	13
<i>n</i> -Butyl	2273		CCl ₄ ^{*3}	11
<i>n</i> -Pentyl	2274		CCl ₄	11
Isobutyl	2263		CCl ₄	11
sec-Butyl	2261		CCl ₄	11
	2262			11
Cyclohexyl	2255		CCl ₄	11
Benzyl	2266		CCl ₄	11
	2265			
Acetyl	2246		CCl ₄	11
Phenyl	2260		CCl ₄	11
	2278			
4-X-phenyl				
X				
Ethoxy	2274		CCl ₄	11
Chloro	2266		CCl ₄	11
Methyl	2263		CCl ₄	11
Nitro	2261		CCl ₄	11
Cyano	2258		CCl ₄	11
3-X-phenyl				
Methoxyl	2267		CCl ₄	11
Methyl	2266		CCl ₄	11
Chloro	2265		CCl ₄	11
2-X-phenyl				
Methyl	2273		CCl ₄	11

*¹ L is liquid.*² V is vapor.*³ CCl₄ is in CCl₄ solution.

TABLE 3.3 Infrared data for alkyl isocyanates in 0 to 100 mol % CHCl₃/CCl₄ in 0.5 wt./vol % solutions

Methyl isocyanate CH ₃ -N=C=O [0.5% solutions] Mole % CHCl ₃ /CCl ₄	cm ⁻¹	cm ⁻¹	cm ⁻¹	Corrected for FR a.N=C=O str. cm ⁻¹	Corrected for FR C-N str. + s.CH ₃ bend cm ⁻¹	Corrected for FR C-N str. + s.N=C=O str. cm ⁻¹
0	2285.56	2256.26	2318.28	2282.8	2276.3	2301.1
10.74	2285.7	2256.08	2317.87	2283.1	2276.9	2299.6
15.07	2285.8	2255.93	2317.7	2283.5	2277.5	2298.5
26.53	2285.87	2255.74	2317.51	2283.8	2278	2297.2
32.5	2285.93	2255.59	217.31	2284.1	2278.6	2296.1
37.5	2285.92	2255.4	2317.21	2284.3	2278.8	2295.5
41.93	2285.99	2255.3	2317.09	2284.4	2279.1	2294.9
45.73	2285.99	2255.1	2316.99	2284.5	2279.3	2294.3
49.06	2286.04	2255.08	2316.96	2284.7	2279.7	2293.7
52	2286.05	2254.93	2316.84	2284.8	2279.8	2293.2
54.62	2286.06	2254.86	2316.76	2284.9	2280.1	2292.7
57.22	2286.08	2254.78	2316.7	2284.8	2279.7	2293.1
60.07	2286.08	2254.67	2316.62	2285	2280.1	2292.3
63.28	2286.09	2254.56	2316.54	2285.1	2280.3	2291.8
66.73	2286.1	2254.51	2316.49	2285.2	2280.4	2291.5
70.65	2286.1	2254.2	2316.36	2285.3	2280.8	2290.7
75.06	2286.1	2254.23	2316.28	2285.4	2280.9	2290.4
80.06	2286.12	2254.1	2316.21	2285.5	2281.2	2289.7
85.05	2286.12	2253.93	2316.21	2285.6	2281.4	2289.2
92.33	2286.07	2253.6	2316	2285.6	2281.6	2288.4
100	2286.03	2253.27	2315.87	2285.8	2281.8	2287.6
Δ [CCl ₄]-[CHCl ₃]	0.47	-2.99	-2.41	3.02	5.56	-13.51
C ₂ H ₅ N=C=O						
0	2277.25	2220.81		2270.1	2227.9	
100	2281.25	2217.65		2274.1	222.8	
Δ [CCl ₄]-[CHCl ₃]	4	-3.13		4	-3.2	
C ₃ H ₇ -N=C=O						
Δ [CCl ₄]-[CHCl ₃]						
0	2272.63	2259.31		2265.4	2266.6	
100	2282.47	2264.8		2274.3	2273	
Δ [CCl ₄]-[CHCl ₃]	9.84	5.49		8.9	6.5	
C ₄ H ₉ -N=C=O						
0	2274.57					
100	2278.8					
Δ [CCl ₄]-[CHCl ₃]	4.23					

TABLE 3.4 Infrared data for the antisymmetrical N=C=O stretching frequency and two combination tones for alkyl isocyanates in CHCl₃ and CCl₄ solutions

Alkyl isocyanate	cm ⁻¹	cm ⁻¹	cm ⁻¹	Corrected for FR a.N=C=O cm ⁻¹	Corrected for FR C-N str. + s.CH ₃ bend or CT cm ⁻¹	Corrected for FR C-N str. + s.N=C=O str. cm ⁻¹	Solvent
Methyl	2285.6	2256.3	2318.3	2282.8	2276.3	2301.1	CCl ₄ soln.
	2286	2253.3	2315.9	2285.8	2281.8	2287.6	CHCl ₃ soln.
Ethyl	2277.3	2220.8		2270.1	2227.9		CCl ₄ soln.
	2281.3	2217.7		2274.1	2224.8		CHCl ₃ soln.
Propyl	2272.6	2259.3		2265.4	2266.6		CCl ₄ soln.
	2282.5	2264.8		2274.3	2273		CHCl ₃ soln.
<i>n</i> -Butyl	v asym. N=C=O						
	2274.6						CCl ₄ soln.
Isopropyl	2278.8						CHCl ₃ soln.
	2261.7						CCl ₄ soln.
tert-Butyl	2269.7						CHCl ₃ soln.
	2256.3						CCl ₄ soln.
	2257.1						CHCl ₃ soln.

[CT is a combination tone].

TABLE 3.5 Infrared and Raman data for alkyl isocyanates

Raman data for Alkyl isocyanate	IR (13) a.N=C=O str. C ₆ H ₁₄ soln. cm ⁻¹	IR (13) a.N=C=O str. CCl ₄ soln. cm ⁻¹	IR (13) a.N=C=O str. CHCl ₃ soln. cm ⁻¹	Raman (15) s.N=C=O str. liquid cm ⁻¹	E _N *
Methyl	2283.8	2282.8	2285.8	1437	0.000-0.00
Ethyl	2270.8	2270.1	2274.1	1431.7	-0.100-0.07
<i>n</i> -Propyl	2266.9	2265.4	2274.3	1431	-0.115-0.36
<i>n</i> -Butyl	2270.5	2274.5	2278.7	1431	-0.130-0.39
Isopropyl	2262.9	2261.7	2269.7	1422.9	-0.0190-0.47
tert-Butyl	2258.8	2256.3	2257.1	1396.9	-0.300-1.54

* Raman NC=O.

TABLE 3.6 Infrared data for 1 wt./vol. % alkyl isothiocyanates in 0 to 100 mol % $\text{CHCl}_3/\text{CCl}_4$ solutions [the ν asym. $\text{N}=\text{C}=\text{S}$ and the first overtone of $\text{C}-\text{N}$ stretching frequencies in Fermi resonance]

$\text{CH}_3-\text{N}=\text{C}=\text{S}$ [1 wt. % solutions] Mole % $\text{CHCl}_3/\text{CCl}_4$	cm^{-1}	cm^{-1}	Corrected for Fermi res. $\text{N}=\text{C}=\text{S}$ str. cm^{-1}	Corrected for Fermi res. $2(\text{C}-\text{N}$ str.) cm^{-1}
0	2106.35	2222.81	2129.5	2199.7
10.74	2108.14	2221.46	2131.9	2197.7
15.07	2109.64	2220.65	2134.4	2195.9
26.53	2111.07	2219.47	2136.4	2194.2
32.5	2112.17	2218.74	2137.9	2193
37.57	2113.01	2217.54	2138.9	2191.7
41.93	2113.95	2216.91	2140.2	2190.7
45.73	2114.6	2215.93	2141.1	2189.4
49.06	2115.27	2215.42	2141.9	2188.8
52	2115.8	2215.8	2142.9	2188.7
54.62	2117.04	2214.33	2144.6	2186.8
57.22	2117.31	2214.1	2145	2186.4
60.07	2117.96	2213.76	2145.8	2186
63.28	2118.48	2213.57	2146.5	2185.6
66.73	2119.41	2213.34	2148.1	2184.7
70.65	2119.95	2213.16	2148.6	2184.5
75.06	2120.67	2213.01	2141.6	2184.1
80.06	2121.49	2212.73	2150.9	2183.3
85.05	2122.37	2212.55	2152.1	2182.8
92.33	2123.33	2212.35	2153.5	2182.2
100	2124.38	2212.14	2155.1	2181.5
Mole % $\text{CDCl}_3/\text{CCl}_4$				
0	2222.81	2106.3	2129.4	2199.8
10.65	2221.58	2108.1	2129.4	2196.7
14.94	2220.78	2109.75	2135.3	2195.2
26.31	2219.62	2110.87	2137.1	2193.4
32.23	2219.04	2112.03	2138.8	2192.3
37.26	2218.06	2113.27	2140.6	2190.7
41.58	2217.4	2114	2141.7	2189.7
45.35	2216.82	2114.66	2142.8	2188.7
48.65	2216.34	2115.31	2143.6	2188
51.57	2215.73	2115.96	2144.4	2187.3
54.17	2215.31	2116.68	2145.4	2186.6
56.74	2214.96	2117.48	2146.5	2185.9
59.57	2214.64	2117.87	2146.9	2185.6
62.75	2214.51	2118.34	2147.8	2185
66.18	2214.23	2118.82	2148.6	2184.4
70.06	2214	2119.69	2149.8	2183.9
74.44	2213.78	2120.41	2150.8	2183.4
79.39	2213.52	2121.15	2152	2182.7
84.34	2213.35	2122.07	2153.3	2182.1
91.56	2213.12	2122.95	2154.7	2183.3
100	2213.01	2124.66	2157	2180.7

(continues)

TABLE 3.6 (continued)

CH ₃ -N=C=S [1 wt. % solutions] Mole % CHCl ₃ /CCl ₄	cm ⁻¹	cm ⁻¹	Corrected for Fermi res. N=C=S str. cm ⁻¹	Corrected for Fermi res. 2(C-N str.) cm ⁻¹
Mole % CHCl ₃ /CCl ₄				
C ₂ H ₅ -N=C=S				
0	2093.85		2099.6	
100	2113.9		2124	
C ₃ H ₇ -N=C=S				
0	2094.8		(not corrected	
100	2100.09		for FR)	
C ₄ H ₉ -N=C=S				
0	2096.65		2117.6	
100	2106.1		2133.9	
tert C ₄ H ₉ -N=C=S				
0	2077.1		2060.4	
100	2106.7		2090.2	

TABLE 3.6a Vibrational data for organoisothonocyanates

Compound	Phase	a.N=C=S str. cm ⁻¹	2(C-N str.) cm ⁻¹	s.N=C=S str. or 2(s.N=C=S str.) cm ⁻¹	N=C=S bend cm ⁻¹
CH ₃ -N=C=S	vapor [IR]	2085 (1.240)	2228 (0.233)	~1090 (0.020)	685 (0.020)
(CH ₃) ₃ C-N=C=S	liquid [Raman]	2082 (dep.)		1005 (pol.)	625 (pol.)
C ₇ H ₁₅ -N=C=S	liquid [Raman]	2090 (dep.)	2170	1070 (pol.)	655 (pol.)
C ₇ H ₁₅ -N=C=S	vapor [IR]	2061 (1.250)		1110 (0.020)	
	Δ [v-l]	[29]		[40]	
C ₆ H ₅ -N=C=S	liquid [Raman]	2150 (dep.)		1245 (pol.)	
4-Br-C ₆ H ₄ -N=C=S	solid [Raman]	2070	2170sh	1250	
2,4,6-(CH ₃) ₃ -C ₆ H ₂ -N=C=S	solid [Raman]	2150	2120sh	1245	

TABLE 3.7 Vapor- and neat-phase infrared data for dialkyl and diaryl carbodiimides

Carbodiimide	a.N=C=N str. vapor cm ⁻¹	A	Not corrected for FR a.N=C=N str. OT or CT		Corrected for FR a.N=C=N str. CT or OT cm ⁻¹
			neat cm ⁻¹	A	
dicyclohexyl	2128	1.245	2110 2045	1.179 0.51	2090.4 (neat) 2064.6 (neat)
tert-butyl triphenylmethyl	2118	1.225	2110 2040	1.895 0.122	2105.8 (neat) 2044.2 (neat)
	Not corrected for FR a.N=C=N OT or CT				
bis-(2-methylphenyl)	2150 2120	1.246 0.498	2139 2105	1.18 0.88	2124.5 (neat) 2119.5 (neat) 2141.4 (vapor) 2122.6 (vapor)
bis-(2,6-diethylphenyl)	2170 2100	1.231 0.212	2158 2098	1.168 0.323	2145 (neat) 2111 (neat) 2147.4 (vapor) 2122.6 (vapor)

Thiols, Sulfides and Disulfides, Alkanethiols, and Alkanedithiols (S–H stretching)

Alkanethiols (S–H stretching)	65
Benzenethiols (S–H stretching)	66
Alkanethiols and Alkanedithiols (C–S stretching)	66
Alkanethiol, Alkane Sulfides, and Alkane Disulfides	66
Carbon Hydrogen Modes	67
Dialkyl Sulfides (rotational conformers)	67
Dialkyl Disulfides, Aryl Alkyl Disulfides, and Diaryldisulfide	67
4-Chlorobenzenthio	67
Phosphorodithioates (S–H stretching)	68
Alkyl Groups Joined to Sulfur, Oxygen, or Halogen	68
Methyl (Methylthio) Mercury	69
References	69

Figures

Figure 4-1	71 (68)
Figure 4-2	73 (69)
Figure 4-3	73 (69)

Tables

Table 4-1	74 (65, 66)
Table 4-1a	75 (66)
Table 4-2	76 (66, 67)
Table 4-3	78 (67)
Table 4-4	79 (67)
Table 4-5	80 (68)
Table 4-6	81 (68)

*Numbers in parentheses indicate in-text page reference.

ALKANETHIOLS (S–H STRETCHING)

Table 4.1 lists IR and Raman S–H stretching frequency data for alkanethiols and benzenethiols in different physical phases.

In the vapor phase ν S–H for alkanethiols and alkanedithiols exhibit a weak IR which occurs in the region $2584\text{--}2598\text{ cm}^{-1}$. In CCl_4 solution ν S–H occurs at lower frequency in the region $2565\text{--}2583\text{ cm}^{-1}$ (1), and in the liquid phase $2554\text{--}2585\text{ cm}^{-1}$ (2, 3). There is a decrease in the ν S–H frequency in going from vapor to CCl_4 solution, with this most likely resulting from intermolecular hydrogen bonding between S–H and CCl_4 to form $\text{S–H}\cdots\text{ClCCl}_3$.

In going from CCl_4 solution to the liquid phase, the ν S–H frequency decreases $13\text{--}21\text{ cm}^{-1}$ for alkanethiols, with the exception of tert-butylthiol, which increases in frequency by 6 cm^{-1} . This decrease in frequency is attributed to intermolecular hydrogen bonding between S–H groups $(\text{S–H})_n$. In the case of tert-butylthiol the steric factor of the tert-butyl group apparently prevents such a strong intermolecular hydrogen bond from forming between S–H groups.

The Raman band assigned to ν S–H ($2571\text{--}2583\text{ cm}^{-1}$, liquid) has weak-medium to strong intensity and it is polarized (2).

BENZENETHIOLS (S–H STRETCHING)

Benzenethiols exhibit ν S–H in the region $2560\text{--}2608\text{ cm}^{-1}$ in the vapor phase, with most absorbing in the region $2582\text{--}2608\text{ cm}^{-1}$ (1). The compounds 2-aminobenzethiol and toluene-3,4-dithiol exhibit ν S–H \cdots NH₂ at 2560 cm^{-1} and ν S–H \cdots SH at 2570 cm^{-1} . These relatively low frequencies are the result of intramolecular hydrogen bonding between S–H \cdots NH₂ and S–H \cdots SH groups, respectively (1).

ALKANETHIOLS AND ALKANEDITHIOLS (C–S STRETCHING)

The C–S stretching (ν C–S) vibration decreases in frequency as the branching on the sulfur α -carbon atom is increased, and the ν C–S mode is often observed as a doublet in both the IR and Raman due to the existence of rotational conformers (5). For example, Table 4.1 shows that ν C–S for methanethiol occurs at 703 cm^{-1} , butanethiol at 651 cm^{-1} , isopropylthiol at 629 and 616 cm^{-1} , and tert-butyl thiol at 587 cm^{-1} . This decrease in frequency is attributed to the increased electron release to the C–S bond progressing in the order $\text{CH}_3\text{--S}$ to $(\text{CH}_3)_3\text{CSH}$, which weakens the C–S bond.

The major rotational conformer has strong Raman band intensity and the lesser rotational conformer has weak- to medium Raman band intensity depending upon the concentrations of the two rotational conformers. In both cases the ν S–H band is polarized (2). Table 4.1a lists Raman liquid-phase data for some compounds containing SH groups (6).

ALKANETHIOL, ALKANE SULFIDES, AND ALKANE DISULFIDES

Table 4.2 lists IR vapor phase data for alkanethiols, alkane sulfides, and alkane disulfides. The compounds are compared (methanethiol vs dimethyl sulfide vs dimethyl disulfide, etc.) in Table 4.2. In the series for the methyl analog, ν C–S decreases in frequency progressing in the order CH_3SH , $(\text{CH}_3)_2\text{S}$, and $(\text{CH}_3\text{S})_2$. In the case of the dialkyl sulfides vs dialkyl disulfides, weak IR bands are noted in the regions $760\text{--}786\text{ cm}^{-1}$ and $732\text{--}751\text{ cm}^{-1}$. The higher frequency IR band has more intensity than the lower frequency band, and these IR bands are assigned to ν asym.(C)₂S and ν sym.(C)₂S, respectively. In the IR ν asym.(C)₂S and ν sym.(C)₂S are weak, and

these bands are not readily apparent in the higher molecular weight dialkyl sulfides and dialkyl disulfides.

CARBON HYDROGEN MODES

Table 4.2 also lists vibrational assignments for the alkyl groups for the alkanethiols, alkane sulfides, and alkane disulfides as a convenience to the reader.

DIALKYL SULFIDES (ROTATIONAL CONFORMERS)

Table 4.3 lists IR and Raman data for organic sulfides and disulfides (2). Examination of these data show that ν asym.(C)₂ and ν sym.(C)₂ occur at approximately the same frequency in either CS₂ solution or the liquid phase. In the case of methyl ethyl sulfide an IR band at 729 cm⁻¹ and the depolarized medium Raman band at 732 cm⁻¹ are assigned to ν asym.(C)₂S. The IR band at 652 cm⁻¹ and the polarized Raman band at 661 cm⁻¹ are assigned to ν sym.(C)₂S for the low-temperature conformer. The 672 cm⁻¹ IR band and the 684 cm⁻¹ polarized medium Raman band are assigned to ν sym.(C)₂S for the other rotational conformer. In the case of diethyl sulfide, there is both IR and Raman evidence to support the presence of three rotation conformers. One has C₁ symmetry, one has C₂ symmetry, and one has C_{2v} symmetry.

DIALKYL DISULFIDES, ARYL ALKYL DISULFIDES, AND DIARYLDISULFIDE

Table 4.3 lists IR and Raman data for dialkyl disulfides, aryl alkyl disulfide, and diaryl disulfide (2). A weak IR band in the region 502–528 cm⁻¹ and a polarized weak-medium to strong Raman band in the region 501–529 cm⁻¹ are assigned to ν S–S (2). In some cases ν S–S is observed as a doublet in both the IR and Raman spectra due to the existence of rotational conformers.

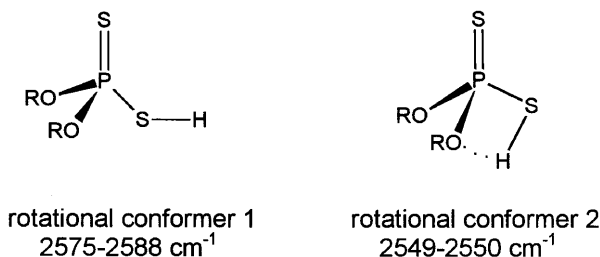
4-CHLOROBENZENTHIOL

Table 4.4 compares the vibrational assignments of 4-chlorobenzenethiol (7) and 1,4-dichlorobenzene (8). Sulfur and chlorine masses are 32 and ~35, respectively, the 30 ring modes occur at very similar frequencies, and they have comparable IR and Raman band intensities. The ν S–H mode is observed at 2579 cm⁻¹ in the solid-phase IR spectrum and at 2569 cm⁻¹ in the liquid Raman spectrum (7). Thus, it is helpful in spectra-structure identification of chlorinated benzenethiol isomers to have IR and Raman spectra of comparable chlorinated benzene isomers for reference. Vibrational data and assignments are available for the chlorinated benzenes (8, 9, 10), and normal coordinates data for these chlorinated benzenes have also been determined (11). In-plane vibrations have also been assigned for a large number of differently substituted

benzenes whose IR spectra have been recorded in the vapor phase (12), and for the out-of-plane deformations and their combination and overtones (13).

PHOSPHORODITHIOATES (S–H STRETCHING)

Table 4.5 lists the ν S–H frequencies for O,O-(dialkyl) phosphorodithioate and O,O-bis-(2,4,5-trichlorophenyl) phosphorodithioate (14). The ν S–H rotational conformer 1 is assigned to a band in the region 2575–2588 cm^{-1} and ν S–H rotational conformer 2 is assigned in the region 2549–2550 cm^{-1} (14). Figure 4.1 shows IR spectra for O,O-bis-(2,4,5-trichlorophenyl) phosphorodithioate in CS_2 solution in the region 2700–2400 cm^{-1} for temperatures ranging from 29 °C to –100 °C. The higher frequency band is more intense than the lower frequency band at 29 °C but the lower frequency band steadily increases in intensity as the temperature is decreased and at –100 °C it is more intense than the higher frequency band (14). These data support the postulation that ν S–H occurs as a doublet due to rotational conformers (15). Rotational conformers 1 and 2 are assigned to the following empirical structures:



The ν S–H \cdots OR mode for conformer 2 is lower in frequency than ν S–H for conformer 1 due to intramolecular hydrogen bonding between the S–H proton and the OR oxygen atom S–H \cdots OR (14).

In summary, the ν S–H or ν S–H \cdots X vibrations are compared here:

	ν S–H cm^{-1}	ν S–H \cdots X cm^{-1}
Phosphorodithioates	2575–2588	2549–2550
Benzenethiols	2582–2608	2560–2570
Alkane thiols	2565–2583	
Range:	2565–2608	2549–2570

ALKYL GROUPS JOINED TO SULFUR, OXYGEN, OR HALOGEN

Table 4.6 compares IR vapor-phase data for compounds where the same alkyl group is joined to S, O, or halogen (1). These data show that it is an aid in spectra structure identification of

unknown chemicals to be able to compare the unknown spectrum with spectra of other chemical compounds containing the same alkyl group.

METHYL (METHYLTHIO) MERCURY

Methyl (methylthio) mercury has the empirical structure $\text{CH}_3\text{-Hg-S-CH}_3$ (16). Figure 4.2 (top) is a liquid-phase IR spectrum of methyl (methylthio) mercury between KBr plates, and Figure 4.2 (bottom) is a liquid-phase IR spectrum of methyl (methylthio) mercury between polyethylene plates. The band at $\sim 72\text{ cm}^{-1}$ is a lattice mode for polyethylene. Figure 4.3 (top) is a Raman liquid-phase spectrum of methyl (methylthio) mercury in a small glass capillary tube. The sample was positioned perpendicularly to both the laser beam and the optical axis of the spectrometer. The bottom Raman spectrum is the same as the top one except that the plane of polarization of the incident beam was rotated through 90° (16).

The 692 cm^{-1} IR band and the 700 cm^{-1} Raman band are assigned to $\nu\text{ C-S}$. The 533 cm^{-1} IR band and 537 cm^{-1} Raman band are assigned to $\nu\text{ C-Hg}$ (16). The $\nu\text{ S-Hg}$ vibration is assigned to the 333 cm^{-1} IR band and the 329 cm^{-1} Raman band. Characteristic CH_3 vibrations for the $\text{CH}_3\text{-S}$ and $\text{CH}_3\text{-Hg}$ group are:

$\text{CH}_3\text{-S}$ cm^{-1}	Assignment	$\text{CH}_3\text{-Hg}$ cm^{-1}
2984	ν asym. CH_3	2984
2919	ν sym. CH_3	2919
1432	δ asym. CH_3	1408
1309	δ sym. CH_3	1177
956	ρ CH_3	765

REFERENCES

1. Nyquist, R. A. (1984). *The Interpretation of Vapor-Phase Infrared Spectra: Group Frequency Data*. Philadelphia: Bio-Rad Laboratories Sadtler Div., p. 468.
2. Nyquist, R. A. and Kagel, R. O. (1977). *Infrared and Raman Spectroscopy*. Part B, Chap. 6, E. G. Brame, Jr. and J. G. Grasselli, eds., New York: Marcel Dekker, Inc., p. 497.
3. Simons, W. W. (ed.) (1978). *The Sadtler Handbook of Infrared Spectra*. Philadelphia: Bio-Rad Laboratories, Sadtler Div., p. 360.
4. Nyquist, R. A. and Evans, J. C. (1961). *Spectrochim. Acta*, **17**: 795.
5. Sheppard, N. (1950). *Trans. Faraday Soc.*, **46**: 429.
6. (19XX). *Sadtler Raman Spectra*. Philadelphia: Bio-Rad Laboratories Sadtler Div.
7. Nyquist, R. A. and Evans, J. C. (1961). *Spectrochim. Acta*, **17**: 795.
8. Stojilykovic, A. and Whiffen, D. H. (1958). *Spectrochim. Acta*, **12**: 47.
9. Scherer, J. R. and Evans, J. C. (1963). *Spectrochim. Acta*, **19**: 1793.
10. Scherer, J. R., Evans, J. C., Muelder, W. W., and Overend, J. (1962). *Spectrochim. Acta*, **18**: 57.
11. Scherer, J. R. (1963). *Planar Vibrations of Chlorinated Benzenes*. Midland, MI: The Dow Chemical Company.

12. Nyquist, R. A. (1984). *The Interpretation of Vapor-Phase Infrared Spectra: Group Frequency Data*. Philadelphia: Bio-Rad Laboratories Sadtler Div., p. 708.
13. Nyquist, R. A. (1984). *The Interpretation of Vapor-Phase Infrared Spectra: Group Frequency Data*. Philadelphia: Bio-Rad Laboratories Sadtler Div., p. 635.
14. Nyquist, R. A. (1969). *Spectrochim Acta*, **25A**: 47.
15. Popov, E. M., Kabachnik, M. I., and Mayants, L. S. (1961). *Russian Chem. Rev.*, **30**: 362.
16. Nyquist, R. A. and Mann, J. R. (1972). *Spectrochim. Acta*, **28A**: 511.

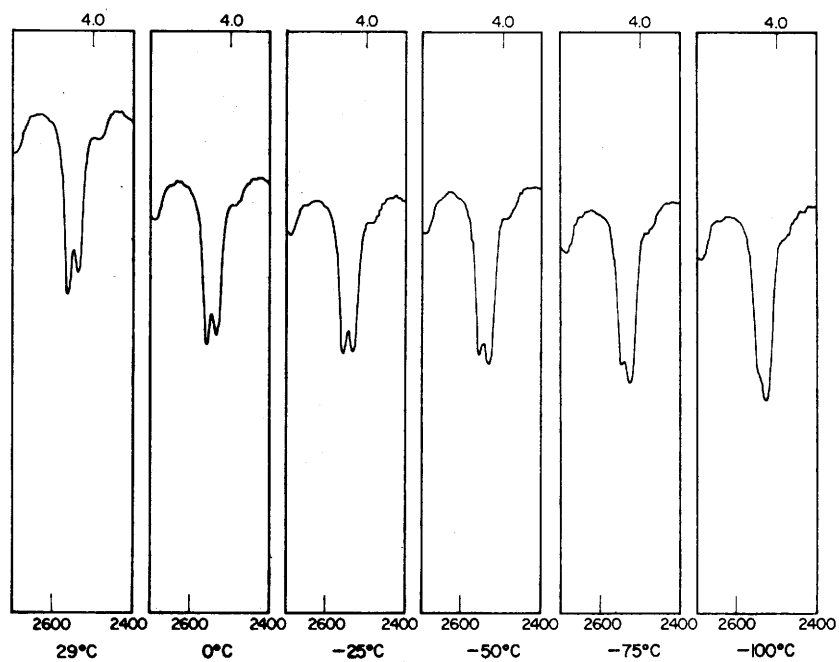


FIGURE 4.1 Infrared spectra of O,O-bis-(2,4,5-trichlorophenyl) phosphorodithioate in 5 wt/vol in CS₂ solution (2700–2400 cm⁻¹) at temperatures ranging from 29 to -100°C.

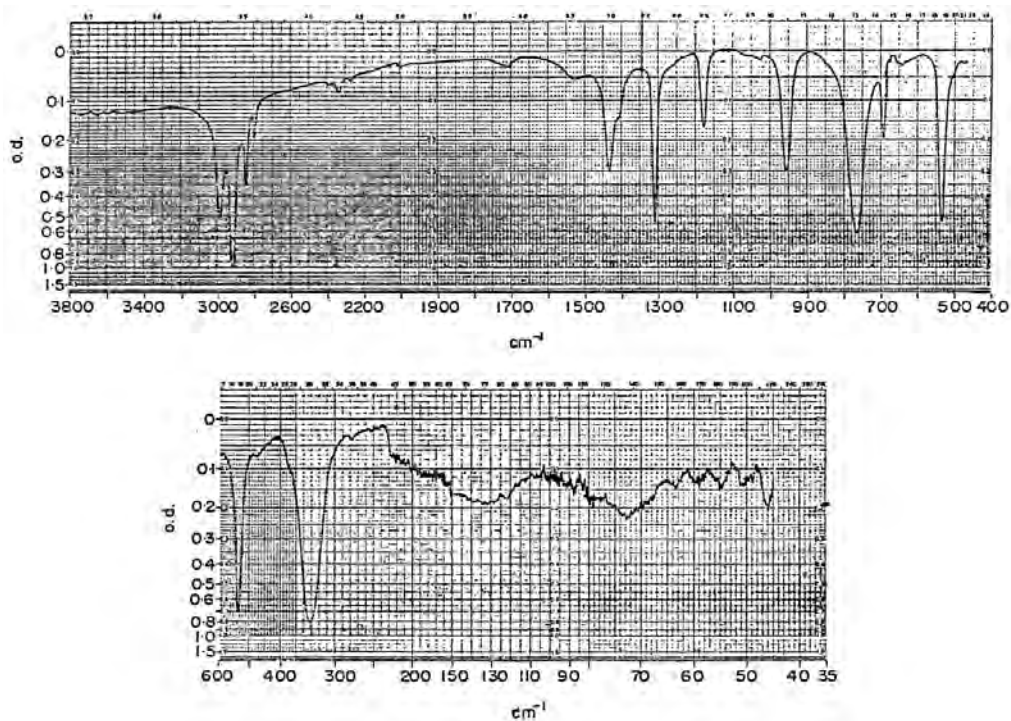


FIGURE 4.2 top: Liquid-phase IR spectrum of methyl (methylthio) mercury between KBr plates in the region 3800–450 cm^{-1} . bottom: Liquid-phase IR spectrum of methyl (methylthio) mercury between polyethylene plates in the region 600–45 cm^{-1} . The IR band near 72 cm^{-1} is due to absorbance from poly(ethylene).

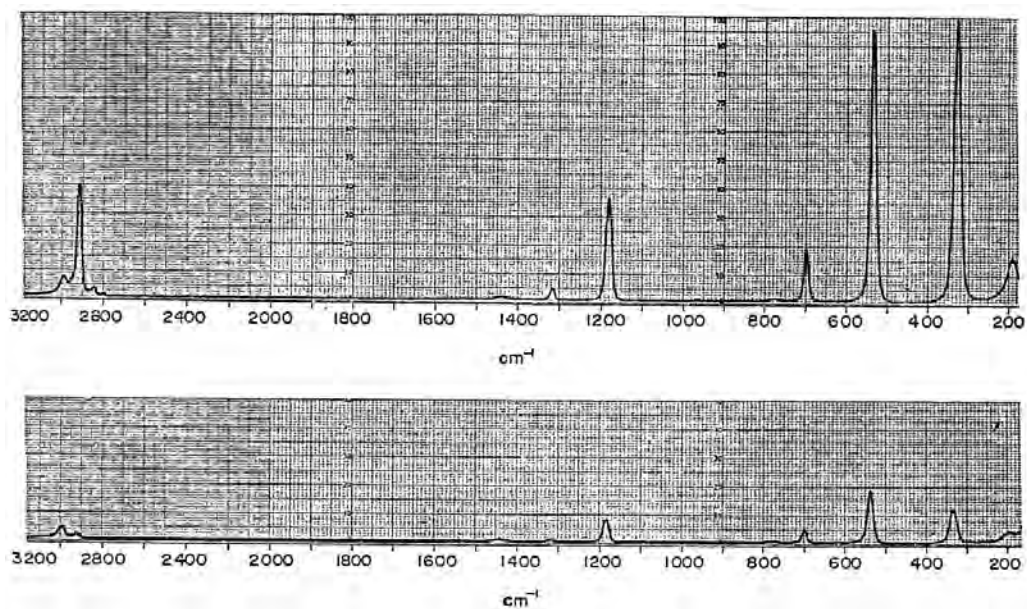


FIGURE 4.3 top: Raman liquid-phase spectrum of methyl(methylthio)mercury in a glass capillary tube. The sample was positioned perpendicularly to both the laser beam and the optical axis of the spectrometer. bottom: Same as top except that the plane of polarization of the incident beam was rotated 90° .

TABLE 4.1A Raman data for organic thiols

Compound	SH str. cm^{-1} (RI)	C=O str. cm^{-1} (RI)
Ethylene bis-(thioglycolate)	2574 (9)	1734 (3)
Ethylene bis-(thiopropionate)	2572 (7)	1734 (3)
Thiophenol	2569 (1)	
Toluenethiol isomers	2570 (4)	
Thioxlenol isomers	2570 (6)	

TABLE 4.2 Vapor-phase infrared data for alkanethiols, alkane sulfides, and alkane disulfides

Compound	a.CH ₃ str. cm ⁻¹ (A)	s.CH ₂ str. cm ⁻¹ (A)	s.CH ₃ str. cm ⁻¹ (A)	s.CH ₂ str. cm ⁻¹ (A)	OT in FR or CT cm ⁻¹ (A)	S–H str. cm ⁻¹ (A)	a.CH ₃ bend and or CH ₂ bend cm ⁻¹ (A)	s.CH ₃ bend cm ⁻¹ (A)	cm ⁻¹ (A)	CH ₂ wag cm ⁻¹ (A)	cm ⁻¹ (A)	CH ₃ rock cm ⁻¹ (A)	C–C str. or a.CCC str. cm ⁻¹ (A)	s.CCC str. cm ⁻¹ (A)	CH ₂ twist cm ⁻¹ (A)	CH ₂ rock cm ⁻¹ (A)	C–S str. cm ⁻¹ (A)	a.(C) ₂ S str. cm ⁻¹ (A)	s.(C) ₂ S str. cm ⁻¹ (A)
Methanethiol*	3028		2882		2822	2820	1470	1348				1089					728		
	(0.240)		(1.240)		(0.140)	(0.022)	(0.140)	(0.150)				(0.135)					(0.030)		
	3018		2864		2864	2601	1452	1331				1071					710		
	(0.250)		(1.040)		(0.100)	(0.015)	(0.090)	(0.060)				(0.095)					(0.037)		
			2858		2828	2592	1445	1319				1060							
		(0.740)		(0.130)	(0.020)	(0.151)	(0.132)				(0.155)								
Methyl sulfide	3000																		
	(0.370)																		
	2968		2935		2860		1439	1311				1011					695		
(0.890)		(1.250)		(0.290)		(0.432)	(0.112)				(0.121)					(0.015)			
		2910		2838															
		(1.150)		(0.220)															
Methyl disulfide	3000		2962		2920		1430										688		
	(0.305)		(1.240)		(0.130)		(0.305)										(0.030)		
Ethanethiol	2991	2960	2900	2880		2598	1455	1390	1280			1100	982			866	659		
	(1.240)	(1.035)	(0.270)	(0.244)		(0.041)	(0.190)	(0.052)	(0.301)			(0.056)	(0.102)			(0.030)	(0.050)		
Ethyl sulfide	2975	2940		2890			1458	1389	1260			1075	975					776	651
	(1.250)	(1.050)		(0.380)			(0.170)	(0.090)	(0.380)			(0.020)	(0.095)					(0.039)	(0.005)
Ethyl disulfide	2987	2940		2884	2838		1454	1383	1251			1045	970					760	645
	(1.250)	(0.930)		(0.315)	(0.060)		(0.190)	(0.110)	(0.470)			(0.055)	(0.081)					(0.081)	(0.010)
Propyl sulfide	2970	2942		2890			1460	1390	1340	1295	1237	1092		896	845			784	742
	(1.235)	(1.035)		(0.585)			(0.185)	(0.104)	(0.030)	(0.149)	(0.202)	(0.040)		(0.095)	(0.019)			(0.050)	(0.039)
Propyl disulfide	2970	2942		2882		2882	1460	1388	1339	1290	1230	1088	1054	894	825			785	732
	(1.240)	(0.610)		(0.340)		(0.040)	(0.140)	(0.078)	(0.045)	(0.139)	(0.170)	(0.020)	(0.019)	(0.020)	(0.015)			(0.040)	(0.019)
1-Butanethiol	2965	2942	2895	2880		2600	1460	1396		1288	1235	1104		960				779	740
	(1.250)	(1.050)	(0.410)	(0.418)		(0.021)	(0.139)	(0.050)		(0.121)	(0.060)	(0.040)		(0.025)				(0.020)	(0.030)
Butyl sulfide	2975	2950		2885			1465	1389	1347	1270	1227	1098	1050	918		880		786	751
	(1.150)	(1.150)		(0.750)			(0.241)	(0.058)	(0.041)	(0.100)	(0.080)	(0.010)	(0.005)	(0.019)		(0.011)		(0.020)	(0.030)
Butyl disulfide	2970	2940		2880			1466	1385	1347	1272	1218	1097	1065	914		876		782	749
	(1.250)	(1.050)		(0.550)			(0.200)	(0.100)	(0.070)	(0.140)	(0.140)	(0.031)	(0.015)	(0.042)		(0.042)		(0.029)	(0.062)

1-Pentanethiol	2972	2940	2880	2600	1462	1385	1348	1277	1226		1102							730
	(1.140)	(1.240)	(0.370)	(0.020)	(0.101)	(0.032)	(0.030)	(0.072)	(0.032)		(0.020)							(0.024)
Pentyl disulfide	2965	2938	2872		1465	1385	1348	1271	1259	1210	1105	1075						730
	(1.122)	(1.230)	(0.385)		(0.240)	(0.060)	(0.090)	(0.080)	(0.080)	(0.050)	(0.010)	(0.010)						(0.035)
Hexanethiol	2962	2938	2868	2596	1460	1384	1350	1295	1254	1214								740
	(0.950)	(1.240)	(1.000)	(0.020)	(0.150)	(0.058)	(0.052)	(0.090)	(0.058)	(0.053)								(0.043)
Hexyl disulfide	2972	2940	2870		1460	1289	1340	1290	1260	1208								730
	(1.010)	(1.220)	(0.491)		(0.151)	(0.061)	(0.070)	(0.081)	(0.075)	(0.030)								(0.035)
Heptyl sulfide	2970	2938	2865		1465	1385	1351	1300	1248		1105		900					728
	(0.580)	(1.220)	(0.420)		(0.120)	(0.031)	(0.049)	(0.040)	(0.048)		(0.005)		(0.005)					(0.015)
Heptyl disulfide	2970	2935	2865		1460	1380	1350	1300	1240									720
	(0.560)	(1.250)	(0.410)		(0.131)	(0.040)	(0.040)	(0.042)	(0.050)									(0.030)
1-Octanethiol	2970	2935	2864	2680	2595	1463	1385	1355	1289	1249	1175	1110						727
	(0.690)	(1.235)	(0.552)	(0.030)	(0.021)	(0.140)	(0.040)	(0.040)	(0.061)	(0.040)	(0.011)	(0.011)						(0.037)
Octyl sulfide	2970	2935	2862		1465	1382	1352	1280	1230									720
	(0.364)	(1.204)	(0.244)		(0.080)	(0.029)	(0.029)	(0.028)	(0.025)									(0.030)
Octyl disulfide	2972	2935	2862		1461	1385	1350	1294	1238		1109							719
	(0.660)	(1.250)	(0.550)		(0.140)	(0.059)	(0.050)	(0.069)	(0.049)		(0.010)							(0.020)
Nonyl sulfide	2970	2936	2862		1461	1380	1350	1301	1255	1191								716
	(0.290)	(1.240)	(0.368)		(0.090)	(0.020)	(0.020)	(0.040)	(0.250)	(0.040)								(0.024)
1-Decanethiol	2970	2935	2860	2595	1464	1380	1352	1308			1110		900					722
	(0.500)	(1.250)	(0.500)	(0.100)	(0.100)	(0.025)	(0.030)	(0.038)			(0.011)		(0.010)					(0.018)
Decyl sulfide	2970	2935	2864		1460	1381												722
	(0.400)	(1.250)	(0.366)		(0.091)	(0.030)												(0.018)
Decyl disulfide	2970	2935	2862		1460		1350	1299										720
	(0.271)	(1.245)	(0.290)		(0.060)		(0.027)	(0.020)										(0.010)
Dodecyl sulfide	2970	2935	2862		1460	1380	1351	1300										720
	(0.320)	(1.220)	(0.400)		(0.080)	(0.005)	(0.026)	(0.020)										(0.010)
1-Tetradecanethiol	2970	2938	2862	2595	1464		1355	1305										715
	(0.120)	(1.250)	(0.330)	(0.005)	(0.053)		(0.022)	(0.020)										(0.025)
1-Octadecanethiol	2970	2935	2861	2595	1460			1300										735
	(0.250)	(1.250)	(0.550)	(0.010)	(0.100)			(0.040)										(0.025)
Cyclohexanethiol			2860	2596	1453		1345		1266	1210	1129	1000	884	818				735
			(0.040)	(0.020)	(0.120)		(0.039)		(0.020)	(0.064)	(0.010)	(0.058)	(0.031)	(0.029)				(0.20)

* [SH bend, 958 (0.058)?].

TABLE 4.3 Infrared and Raman data for organic sulfides and disulfides

R-S-R' R; R'	IR [CS ₂] a.CSC str. cm ⁻¹	IR [neat] a.CSC str. cm ⁻¹	IR [CS ₂] s.CSC str. cm ⁻¹	IR [neat] s.CSC str. cm ⁻¹	R [neat] a.CSC str. cm ⁻¹	RI	Dep. ratio	R [neat] s.CSC str. cm ⁻¹	RI	Dep. ratio
CH ₃ ; CH ₃	743	746	691	693	745	15.3	0.81	696	100	0.11
CH ₃ ; C ₂ H ₅		729		652; 672	732	43.8	0.75	661; 684	100; 40.8	0.19; 0.25*
C ₂ H ₅ ; C ₂ H ₅	761	762	651	652	766	5.9	0.29	651	0.25; C ₁	
	782	781	637	638	782	5.7	0.29	641	0.23; C ₂	
	694	694	694	694	696	55.8	0.66	696	0.66; C _{2v}	
C ₂ H ₅ ; <i>n</i> -C ₄ H ₉	743	743	651	661	750	28.4	0.72	660	100	0.16
								643	38.6	0.19
								694	41.5	0.54
<i>n</i> -C ₄ H ₉ ; <i>n</i> -C ₄ H ₉	745	746	650	660	750	78.6	0.47	659	100	0.25
								670	81.3	0.29
								688	48.6	0.5
R-S-S-R' R; R'	IR S-S str. cm ⁻¹	R S-S str. cm ⁻¹	RI	Dep. ratio						
CH ₃ ; CH ₃	511	511	100	0.06						
C ₂ H ₅ ; C ₂ H ₅	511; 526	511; 528	98.0; 49.2	0.06; 0.12						
iso-C ₄ H ₉ ; iso-C ₄ H ₉	512; 528	516; 528	58.8; 37.5	0.06; 0.14						
tert-C ₄ H ₉ ; tert-C ₄ H ₉	502	515	7.2	0.09						
CH ₃ ; C ₆ H ₅	507; 525	512; 529	24.8; 23.0	0.22; 0.21						
C ₆ H ₅ ; C ₆ H ₅	not observed	[solid] 546	26.8							

* Low-temperature conformer.

TABLE 4.4 Vibrational assignments for 4-chlorobenzenethiol and 1,4-dichlorobenzene

4-Chlorobenzenethiol cm ⁻¹	1,4-Dichlorobenzene cm ⁻¹	Interpretation
a1	a1	
3060	3072	C-H stretch
3050	3050	C-H stretch
1575	1573	C-C stretch
1481	1475	Ring stretch
1178	1169	C-H deformation
1098	1106	Ring stretch
1067	1087	Ring stretch
1017	1013	C-H deformation
745	747	Ring deformation
545	546	C-X stretch
329	405	C-X stretch
a2	a2	
951	951	C-H deformation
817	811	C-H deformation
403	405	Skeleton deformation
b1	b1	
935	934	C-H deformation
812	816	C-H deformation
692	689	Skeleton deformation
485	484	Skeleton deformation
293	299	C-X deformation
122	125	C-X deformation
b2	b2	
3078	3095	C-H stretch
3050	3072	C-H stretch
1575	1573	C-C stretch
1397	1393	C-C stretch
1298	1291	C-H deformation
1260	1260	C-C stretch
1104	1104	C-H deformation
629	628	Ring deformation
342	351	C-X deformation
221	226	C-X deformation
2589		S-H stretch
915		S-H deformation
?		S-H free rotation

TABLE 4.5 The P=S, P–S, and S–H stretching frequencies for O,O-dialkyl phosphorodithioate and O,O-bis-(aryl)phosphorodithioate

$(\text{CH}_3\text{-O-})_2\text{P(=S)SH}$ cm^{-1}	$(\text{C}_2\text{H}_5\text{-O-})_2\text{P(=S)SH}$ cm^{-1}	$(2,4,5\text{-Cl}_3\text{-C}_6\text{H}_4\text{-O-})_2$ P(=S)SH cm^{-1}	Assignment
2588	2582	2575	S–H str., rotational conformer 1
2550	2550	2549	S–H str., rotational conformer 2
670sh	670sh		P=S str., rotational conformer 1
659	659		P=S str., rotational conformer 2
524	535		P–S str. rotational conformer 1
490	499		P–S str., rotational conformer 2

TABLE 4.6 A comparison of the alkyl groups joined to sulfur, oxygen, or halogen

Compound	a.CH ₃ str.	a.CH ₂ str.	s.CH ₃ str.	s.CH ₂ str.	a.CH ₃ bend	CH ₂ bend	o.p.[CH ₃] ₂ bend	i.p.[CH ₃] ₂ bend												
Isobutyl disulfide	2970 (1.250)	2962 (0.581)	2905 (0.390)	2880 (0.430)	1469 (0.189)		1385 (0.180)	1375 (0.160)	1323 (0.080)	1240 (0.150)	1215 (0.080)	1170 (0.101)	1109 (0.021)	1075 (0.030)	946 (0.030)	926 (0.030)	856 (0.030)	800 (0.030)	C-X str. C-X str.	
Isobutyl chloride	2980 (1.040)	2962 (1.240)		2880 (0.310)	1471 (0.200)	1444 (0.170)	1389 (0.160)	1381 (0.170)	1329 (0.090)	1267 (0.080)	1220 (0.020)	1168 (0.030)	1100 (0.020)		951 (0.070)	938 (0.090)	880 (0.025)	808 (0.080)	744 (0.310)	698 (0.090)
Isopentyl sulfide	2962 (1.250)	2925 (0.500)		2882 (0.330)	1470 (0.120)	1444 (0.069)	1390 (0.97)	1373 (0.086)	1350 (0.050)	1280 (0.075)	1226 (0.060)	1170 (0.060)	1110 (0.010)			920 (0.010)	885 (0.007)	745 (0.015)		
Isopentyl disulfide					1471 (0.172)															
Isopentyl chloride	2965 (1.250)	2930 (0.058)		2885 (0.460)	1469 (0.165)	1462 (0.172)	1382 (0.141)	1367 (0.100)	1351 (0.094)	1296 (0.161)	1250 (0.060)	1170 (0.059)			930 (0.025)	872 (0.060)		741 (0.180)	670 (0.135)	
Isopentyl bromide	2965 (1.250)	2940 (0.550)		2885 (0.421)	1470 (0.180)		1385 (0.149)	1370 (0.110)	1351 (0.080)	1267 (0.251)	1220 (0.180)	1170 (0.080)		1025 (0.029)	950 (0.015)	922 (0.029)	860 (0.055)	750 (0.020)	652 (0.121)	570 (0.081)
	a.CH ₃ str.	s.CH ₃ str.	2 (a.CH ₃ bend) in FR. (s.CH ₃)	a.CH ₃ bend	i.p.[CH ₃] ₂ bend		o.p.[CH ₃] ₂ bend													s.C[C] ₂ str. C-X str.
Isopropanethiol ⁺¹	2979 (1.240)	2930 (0.490)	2898 (0.290)	1470 (0.180)	1459 (0.240)	1390 (0.190)	1370 (0.120)		1262 (0.240)	1251 (0.240)	1165 (0.101)	1090 (0.090)	940 (0.020)	861 (0.040)	625 (0.040)					
Isopropyl disulfide	2970 (1.250)	2935 (0.700)	2880 (0.450)	1454 (0.220)			1375 (0.220)	1311 (0.050)	1238 (0.470)	1155 (0.230)	1047 (0.190)	928 (0.021)	876 (0.019)	620 (0.010)						
	2995 (1.240)			1470 (0.180)					1276 (0.330)	1166 (0.160)	1075 (0.190)		897 (0.122)	639 (0.270)						

(continues)

TABLE 4.6 (continued)

Compound	a.CH ₃ str.	a.CH ₂ str.	s.CH ₃ str.	s.CH ₂ str.	a.CH ₃ bend	CH ₂ bend	o.p.[CH ₃] ₂ bend	i.p.[CH ₃] ₂ bend						
Isopropyl chloride	2980 (1.250)	2941 (0.361)	2885 (0.160)	1450 (0.240)	1390 (0.270)		1372 (0.170)	1315 (0.035)	1265 (0.430)	1161 (0.190)	1061 (0.240)	945 (0.020)	885 (0.140)	630 (0.358)
		2925 (0.0140)	2870 (0.120)	1440 (0.120)	1384 (0.250)				1253 (0.350)	1150 (0.172)	1053 (0.160)		87590.120	620 (0.340)
Isopropyl bromide	2998 (1.240)								1235 (0.882)		1051 (0.172)		889 (0.142)	
	2982 (1.240)	2932 (0.630)	2885 (0.291)	1470 (0.270)	1385 (0.380)		1372 (0.260)	1330 (0.037)	1229 (0.932)	1160 (0.520)	1042 (0.210)	945 (0.025)	880 (0.160)	540 (0.345)
									1220 (0.912)		1035 (0.182)		875 (0.150)	
Isopropyl iodide	2998 (1.040)			1465 (0.220)					1210 (0.690)					
	2980 (1.240)	2922 (0.600)	2890 (0.420)	1459 (0.260)	1382 (0.330)		1372 (0.220)	1330 (0.090)	1203 (0.840)	1150 (1.030)	1021 (0.159)	950 (0.060)	874 (0.090)	495 (0.150)
Isopropyl alcohol ⁺²				1471 (0.140)							1090 (0.320)	968 (0.380)		
	2980 (1.250)	2890 (0.460)		1460 (0.151)	1380 (0.510)			1250 (0.275)		1147 (0.540)	1080 (0.300)	951 (0.400)	817 (0.070)	
											1075 (0.320)	941 (0.380)		
Isopropyl ether														
	a.CH ₃ str.	s.CH ₃ str.	O.T.	a.CH ₃ bend	i.p.[CH ₃] ₃ bend		o.p.[CH ₃] ₃ bend	CH ₃ rock	a.C[C] ₃ str.		s.C[C] ₃ str.		C-X str.	
tert-Butyl sulfide		2930 (0.650)												
	2975 (1.250)	2910 (1.250)	2721 (0.029)	1470 (0.230)	1399 (0.100)		1370 (0.360)	1208 (0.100)	1156 (0.560)	1024 (0.010)	926 (0.010)	810 (0.010)	604 (0.021)	
tert-Butyl disulfide		2891 (0.660)												
	2970 (1.250)	2902 (0.550)	2720 (0.021)	1461 (0.241)	1392 (0.090)		1368 (0.410)	1214 (0.080)	1160 (0.620)	1017 (0.011)	931 (0.011)	800 (0.005)	564 (0.030)	
tert-Butyl chloride				1470 (0.170)			1378 (0.631)	1238 (0.180)				819 (0.039)	581 (0.180)	
	2995 (1.224)	2938 (0.500)	2720 (0.020)	1462 (0.220)	1388 (0.329)		1365 (0.290)	1228 (0.212)	1154 (0.550)	1018 (0.015)	930 (0.041)	810 (0.045)	570 (0.340)	500 (0.070)
tert-Butyl bromide				1450 (0.150)										
	2980 (1.139)													
								1238 (0.1300)				810 (0.070)		
	2990 (0.930)	2924 (0.459)	2738 (0.020)	1459 (0.190)	1391 (0.240)		1378 (0.440)	1228 (0.120)	1151 (1.240)		918 (0.020)	802 (0.090)	790 (0.070)	520 (0.172)

[or S-S str.]

Sulfoxides, Sulfones, Sulfates, Monothiosulfates, Sulfonyl Halides, Sulfites, Sulfonamides, Sulfonates, and N-Sulfinyl Anilines

S=O Stretching Frequencies	86
SO ₂ Stretching Frequencies	87
Diakyl Sulfones and Dimethyl Sulfoxide	87
Diaryl Sulfones	88
Sulfate and Thiosulfate Phenoxarsine Derivatives	88
Dialkyl Sulfites	89
Primary Sulfonamides	89
Secondary and Tertiary Sulfonamides	89
Organic Sulfonates	90
Organosulfonyl Chlorides	91
Organosulfonyl Fluorides	91
Summary of S=O and SO ₂ Stretching Frequencies in Different Physical Phases	92
ν asym. SO ₂ and ν sym. SO ₂ Correlations	92
SO ₂ Stretching Vibrations in CHCl ₃ /CCl ₄ Solutions	92
Calculated ν SO ₂ Frequencies	93
Sulfinyl Anilines	93
References	93

Figures

Figure 5-1	96 (86)	Figure 5-5	100 (92)
Figure 5-2	97 (92)	Figure 5-6	101 (92)
Figure 5-3	98 (92)	Figure 5-7	102 (93)
Figure 5-4	99 (92)	Figure 5-8	103 (93)

Tables

Table 5-1A	104 (86)	Table 5-3	109 (88)
Table 5-1B	105 (87)	Table 5-4	110 (89)
Table 5-1C	107 (87)	Table 5-5	111 (89)
Table 5-1D	108 (88)	Table 5-6	111 (89)
Table 5-2	109 (88)	Table 5-6A	112 (89)

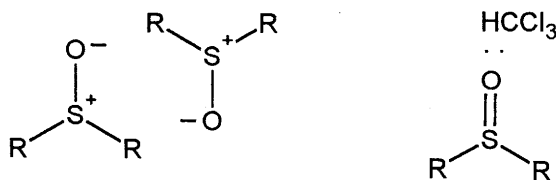
Tables

Table 5-7	112 (90)	Table 5-10	116 (92)
Table 5-8	113 (91)	Table 5-11	117 (92)
Table 5-9	114 (91)	Table 5-12	117 (92)
Table 5-9A	115 (91)		

*Numbers in parentheses indicate in text page reference.

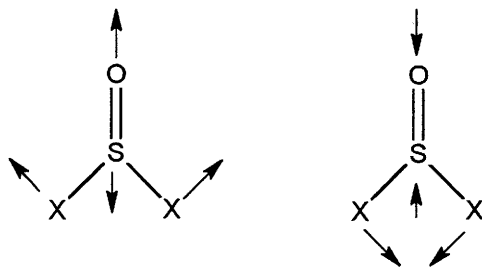
S=O STRETCHING FREQUENCIES

Table 5.1a lists infrared and Raman data for compounds containing an S=O group. In the vapor phase ν S=O occurs in the range 1092–1331 cm^{-1} , and in the neat phase ν S=O usually occurs at lower frequency in the range 1035–1308 cm^{-1} . The decrease in the ν S=O frequency in going from the vapor to the neat phase is attributed to dipolar interaction between the S=O groups of these molecules in the neat phase. In solution, this type of intermolecular interaction is called a reaction field (RF). The equation for determining RF has been presented previously. This equation includes both the dielectric constants of all molecules present and their refractive indices. Because the contribution of the refractive indices is minor compared to the contribution of the dielectric constants in chemical mixtures, the refractive indices are usually ignored in the RF calculations. The ν S=O vibration is highly dependent upon the dielectric surroundings of the S=O groups and the steric factors, which determine the spatial distance between S=O groups or the spatial distance between S=O groups and solvent molecules. Examples are presented here:



Perhaps a better descriptive name for RF is a name such as intermolecular force field association (IFFA).

Figure 5.1 shows plots of the sum of the σ^* constants for the atoms or groups joined to the S=O or SO₂ groups vs the ν S=O frequencies and the mean average of the ν sym. SO₂ and ν sym. SO₂ frequencies (1). The plot for the ν S=O frequencies for (CH₃)₂S=O, (CH₃O)₂S=O, and F₂S=O vs σ^{*} is linear, and the plot for ν S=O for (CH₃O)₂S=O, (CH₃O)(Cl)S=O, and Cl₂S=O vs $\Sigma\sigma'$ is essentially linear. It is also noted that there is a good correlation between the mean average of ν asym. SO₂ and ν sym. SO₂ for the (CH₃)₂SO₂, (CH₃O)₂SO₂, and F₂S=O vs $\Sigma\sigma'$. Both ν S=O for Cl₂S=O and the mean average for the ν SO₂ modes occur at lower frequency than do the linear or pseudolinear plots for the three other S=O analogs. This suggests that mass is also a factor in affecting the ν S=O frequencies. Chlorine is heavier than C, O, and F by a factor of 2 to 3. During a cycle of ν C=O, the X-S-X bond angle opens and closes as depicted here,



This increased mass of Cl would cause ν S=O to vibrate at lower frequency, as the Cl atoms impede the motion of the S atom during a cycle of S=O stretching.

SO₂ STRETCHING FREQUENCIES

Table 5.1b compares the ν asym. SO₂ and ν sym. SO₂ frequencies for a variety of chemical compounds in the vapor and neat phases. In the vapor phase the ν asym. SO₂ vibration occurs in the range 1335–1535 cm⁻¹ and in the neat phase in the range 1295–1503 cm⁻¹. In the vapor phase the ν sym. SO₂ vibration occurs in the range 1141–1300 cm⁻¹ and in the neat phase in the range 1125–1270 cm⁻¹ (1–42).

Study of the last two columns in Table 5.1b shows that in all but two cases the ν asym. SO₂ shifts more to lower frequency than ν sym. SO₂ does in going from the vapor phase to the neat phase. One exception is Cl₂SO₂ where the shift is less for ν asym. SO₂ (24 cm⁻¹) than for ν sym. SO₂ (28 cm⁻¹). The effect of the mass of Cl upon the ν SO₂ mean average was already discussed here, and this may be the reason for the deviation from this group frequency spectra-structure correlation. It should be noted that the shift to lower frequency for ν asym. SO₂ is 18 cm⁻¹ and for ν sym. SO₂ is 19 cm⁻¹ for Cl₂SO₂ in going from the vapor phase to a CCl₄ solution.

DIALKYL SULFONES AND DIMETHYL SULFOXIDE

Table 5.1c lists vapor-phase IR data for methyl sulfoxide and dialkyl sulfones. The ν asym. (C)₂S and ν sym. (C)₂S vibrations are assigned at 755 cm⁻¹ and 669 cm⁻¹ for methyl sulfoxide, respectively. Corresponding vibrations for dimethyl sulfone are assigned at 742 cm⁻¹ and 680 cm⁻¹, respectively. Thus, the ν asym. (C)₂S vibration decreases 13 cm⁻¹ while the ν sym. (C)₂S vibration increases 11 cm⁻¹ when S=O is substituted SO₂[(CH₃)₂S=O to (CH₃)₂SO₂]. The ν asym. (C)₂S (742–812 cm⁻¹) and ν sym. (C)₂S (680–702 cm⁻¹) vibrations increase in frequency, progressing in the series (CH₃)₂SO₂ through (*n*-C₆H₁₃)SO₂. However, ν sym. SO₂ decreases in frequency (1160–1140 cm⁻¹), progressing in the series (CH₃)₂SO₂ through (*n*-C₆H₁₃)SO₂. The ν asym. SO₂ mode also decreases in frequency (1351–1335 cm⁻¹), progressing in the series (CH₃)₂SO₂ through (*n*-C₆H₁₅)SO₂, but not in a decreasing order. It is possible that the ν sym. (C)₂S (680–702 cm⁻¹) and ν sym. SO₂ vibrations (1160–1140 cm⁻¹) are coupled, because both modes belong to the A₁ symmetry species [assuming (CH₃)₂SO₂ has C_{2v} symmetry] together with the fact that as ν sym. (C)₂ increases in frequency, ν sym. CO₂ decreases in frequency. The ν asym. (C)₂S and ν asym. SO₂ vibration can not couple, because ν

asym. $(C)_2S$ and ν asym. SO_2 belong to the B_1 and B_2 symmetry species, respectively. The only mode that could couple with ν asym. SO_2 would be a $\rho (C)_2 B_2$ vibration.

Table 5.1d lists vapor- and solid-phase IR data for dimethyl sulfoxide and dialkyl sulfones. When dimethyl sulfoxide goes from the vapor to the liquid phase the ν asym. $(C)_2S$ and $\nu S=O$ vibrations decrease by 60 cm^{-1} and 50 cm^{-1} while the ν sym. $(C)_2S$ vibration decreases by 5 cm^{-1} . In going from the vapor to the solid phase the ν asym. $(C)_2S$ and ν sym. $(C)_2S$ vibrations decrease in frequency by 8 and 5 cm^{-1} , respectively. In addition, in going from the vapor to solid phase the ν asym. SO_2 and ν sym. SO_2 vibrations decrease in frequency by 65 cm^{-1} and 36 cm^{-1} , respectively. These data are consistent with the spectra-structure correlation that the antisymmetric vibrations of the same group shift more in frequency than the symmetric vibration in going from the vapor phase to the solid or liquid phase.

DIARYL SULFONES

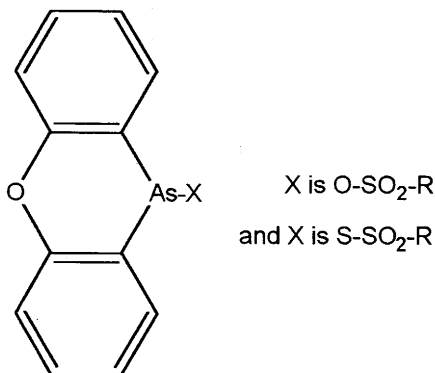
Table 5.2 lists IR vapor- and solid-phase data for diaryl sulfones. In the vapor phase ν asym. SO_2 and ν sym. SO_2 occur in the range $1348\text{--}1354\text{ cm}^{-1}$ and $1161\text{--}1170\text{ cm}^{-1}$, respectively. In the solid phase, ν asym. SO_2 and ν sym. SO_2 occur in the ranges $1318\text{--}1325\text{ cm}^{-1}$, and $1145\text{--}1170\text{ cm}^{-1}$, respectively. In all cases, ν asym. SO_2 shifts more to lower frequency than ν sym. SO_2 in going from the vapor to the solid phase.

SULFATE AND THIOSULFATE PHENOXARSINE DERIVATIVES

Phenoxarsine has the empirical structure presented here:

Table 5.3 lists IR data for these phenoxarsine derivatives in CS_2 solution.

Both of these types of phenoxarsine derivatives exhibit ν asym. SO_2 in the region 1320--



1328 cm^{-1} (35). On the other hand, the ν sym. SO_2 mode for the O-SO₂-R analog occurs in the range $1161\text{--}1171\text{ cm}^{-1}$ while the S-SO₂-R analog exhibits ν sym. SO_2 in the range $1125\text{--}1141\text{ cm}^{-1}$.

Table 5.4 lists IR data for the SO_2 stretching vibrations for compounds in CHCl_3 and CCl_4 solutions (37). Table 5.4 lists data for sulfate, a benzenesulfonate, benzenesulfonyl chloride, and two sulfones. In all cases the ν asym. SO_2 vibration shifts more in frequency than the ν sym. SO_2 vibration in going from solution in CCl_4 to solution in CHCl_3 . In CHCl_3 solution part of the decrease in both ν SO_2 frequencies is the result of intermolecular hydrogen bonding of the form $\text{SO}_2 \cdots \text{HCCl}_3$ and/or $\text{SO}_2(\cdots \text{HCCl}_3)_2$ (see discussion on SO_2 containing compounds in mole % $\text{CHCl}_3/\text{CCl}_4$ solutions). This set of data is consistent with previous discussions about the shifts in ν SO_2 frequencies with change in physical phase.

DIALKYL SULFITES

Table 5.5 lists IR data for dialkyl sulfites (see Reference 5). The ν S=O frequency decreases in frequency by 6 to 13 cm^{-1} in going from the vapor phase to the liquid phase. The IR bands in the ranges $955\text{--}1010 \text{ cm}^{-1}$ and $685\text{--}748 \text{ cm}^{-1}$ are attributed to C–O–S stretching vibrations. These IR bands also shift with change of phase.

PRIMARY SULFONAMIDES

Tables 5.6 and 5.6a list IR data for primary sulfonamides in the vapor and solid phases. In the vapor phase, ν asym. SO_2 occurs in the range $1370\text{--}1382 \text{ cm}^{-1}$, and in the solid phase in the range $1308\text{--}1355 \text{ cm}^{-1}$. In the vapor phase ν sym. SO_2 occurs in the range $1170\text{--}1178 \text{ cm}^{-1}$ and in the solid phase it occurs in the range $1140\text{--}1158 \text{ cm}^{-1}$. In all cases the ν asym. SO_2 vibration shifts more to lower frequency than does the ν sym. SO_2 vibration in going from the vapor phase to the solid phase. Part of the reason both modes shift to lower frequency in the solid phase is that the NH_2 group is intermolecularly hydrogen-bonded to the SO_2 group of another molecule ($\text{NH}_2 \cdots \text{O}_2\text{S}$).

In the vapor phase, the ν asym. NH_2 mode for these primary sulfonamides occurs in the range $3456\text{--}3479 \text{ cm}^{-1}$ and in the solid phase it occurs in the range $3323\text{--}3397 \text{ cm}^{-1}$. The ν sym. NH_2 mode occurs in the range $3365\text{--}3378 \text{ cm}^{-1}$ in the vapor phase and in the range $3228\text{--}3275 \text{ cm}^{-1}$ in the solid phase. The compounds methanesulfonamide, benzenesulfonamide, and 4-toluenesulfonamide all show that ν asym. NH_2 decreases more in frequency than ν sym. NH_2 in going from the vapor phase to the solid phase. The decrease in frequency varies between $137\text{--}155 \text{ cm}^{-1}$ for ν asym. NH_2 and between $120\text{--}137 \text{ cm}^{-1}$ for ν sym. NH_2 in going from the vapor phase to the solid phase. The situation is reversed in the case of 2-toluenesulfonamide. The decrease in the ν sym. NH_2 (90 cm^{-1}) vibration is more than the ν asym. NH_2 (68 cm^{-1}) in going from the vapor phase to the solid phase. Moreover, these frequency decreases are much less than those for the other three sulfonamides. These data indicate that the strength of the intermolecular hydrogen bond ($\text{NH}_2 \cdots \text{O}_2\text{S}$) is less in the case of 2-toluenesulfonamide due to the steric factor of the 2-methyl group, which increases the spatial distance between the $\text{NH}_2 \cdots \text{O}_2\text{S}$ groups in the solid phase as compared to this case for the other sulfonamides. The data for 2,4,6-trimethylbenzenesulfonamide presented in Table 5.6a shows the same correlation as for 2-toluenesulfonamide.

The ν S–N mode is assigned in the range $846\text{--}918 \text{ cm}^{-1}$ and NH_2 bending is assigned in the range $1545\text{--}1569 \text{ cm}^{-1}$. The ν S–N frequency occurs at lower frequency in the vapor phase than

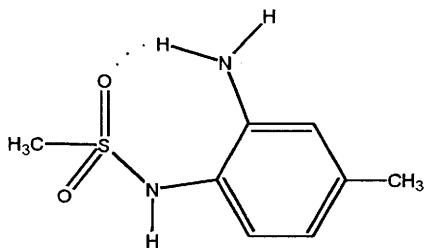
in the solid phase. In the case of NH_2 bending there is no consistent spectra-structure correlation with change in physical phase.

SECONDARY AND TERTIARY SULFONAMIDES

The $\nu\text{N-H}$ frequency for *N*-butyl 4-toluenesulfonamide and 4-toluenesulfonanilide in the vapor phase are assigned at 3419 cm^{-1} and 3402 cm^{-1} , respectively, as listed in Table 5.6a.

Table 5.7 lists IR data for secondary and tertiary sulfonamides. In the vapor phase, compounds of form $\text{R-SO}_2\text{-NHR}'$ (where R and R' can be both alkyl, both aryl, or one aryl and one alkyl group) exhibit $\nu\text{ asym. SO}_2$ in the range $1344\text{--}1360\text{ cm}^{-1}$. The compound whose empirical structure is presented here:

appears to be intramolecularly hydrogen-bonded in the vapor phase, because its $\nu\text{ asym. SO}_2$ frequency occurs at 1325 cm^{-1} . Its $\nu\text{ sym. SO}_2$ vibration is assigned at 1150 cm^{-1} in the vapor phase, and $\nu\text{ sym. SO}_2$ for the other compound occurs at higher frequency in the region $1160\text{--}1175\text{ cm}^{-1}$. In the case of the one secondary sulfonamide studied in both the vapor and solid



states, $\nu\text{ asym. SO}_2$ decreases 66 cm^{-1} while $\nu\text{ sym. SO}_2$ decreases 10 cm^{-1} .

Tertiary sulfonamides of form $\text{R-SO}_2\text{N}(\text{CH}_3)_2$, where R is either CH_3 or aryl, exhibit $\nu\text{ asym. SO}_2$ in the range $1362\text{--}1365\text{ cm}^{-1}$ in the vapor phase and in the range $1324\text{--}1334\text{ cm}^{-1}$ in the solid phase. The $\nu\text{ asym. SO}_2$ vibration occurs in the range $1165\text{--}1169\text{ cm}^{-1}$ in the vapor phase and in the range $1142\text{--}1164\text{ cm}^{-1}$ in the solid phase. Again $\nu\text{ asym. SO}_2$ vibration shifts more the $\nu\text{ sym. SO}_2$ vibration in going from the vapor phase to the liquid phase.

The secondary sulfonamides exhibit $\nu\text{ S-N}$ in the range $825\text{--}920\text{ cm}^{-1}$, and the tertiary sulfonamides in the range $770\text{--}815\text{ cm}^{-1}$ from the limited spectra included in the study.

The νNH frequencies for the secondary sulfonamides in the vapor phase (excluding the intramolecularly hydrogen-bonded compound just discussed) occur in the range $3400\text{--}3422\text{ cm}^{-1}$. In the series, $4\text{-CH}_3\text{C}_6\text{H}_4\text{SO}_2\text{NHR}$ (where R is CH_3 , *n*- CH_4H_9 and *tert*- C_4H_9) $\nu\text{N-H}$ decreases in the order 3422 cm^{-1} , 3418 cm^{-1} , and 3400 cm^{-1} . This is the order of increased branching on the nitrogen α -carbon atom which is also on the order of increasing electron release of the alkyl group to the nitrogen atom. The increasing electron release steadily weakens N-H bond, causing $\nu\text{N-H}$ to vibrate at increasingly lower frequency.

ORGANIC SULFONATES

Table 5.8 lists IR data for organic sulfonates. Sulfonates of form $\text{CH}_3\text{SO}_2\text{OR}$ and $\text{C}_6\text{H}_5\text{SO}_2\text{OR}$ in the vapor-phase exhibit ν asym. SO_2 in the ranges $1368\text{--}1380\text{ cm}^{-1}$ and $1389\text{--}1391\text{ cm}^{-1}$, respectively. Moreover, these same two classes of sulfonates in the vapor phase exhibit ν sym. SO_2 in the ranges $1185\text{--}1190\text{ cm}^{-1}$ and $1188\text{--}1195\text{ cm}^{-1}$, respectively.

The two examples in which vapor-phase and liquid phase data are compared show that the shift in frequency in going from the vapor phase to the liquid phase for these sulfonates is larger for the ν asym. SO_2 vibration than for the ν sym. SO_2 vibration.

Vibrations involving stretching of the C–O–S bonds are assigned in the ranges $934\text{--}1019\text{ cm}^{-1}$ and $751\text{--}810\text{ cm}^{-1}$.

The frequency separation between ν asym. SO_2 and ν sym. SO_2 in the vapor phase increases in the order: $\text{CH}_3\text{SO}_2\text{OR}$, $188\text{--}192\text{ cm}^{-1}$; $\text{C}_6\text{H}_5\text{SO}_2\text{OR}$, $195\text{--}197\text{ cm}^{-1}$; and $4\text{-CH}_3\text{C}_6\text{H}_4\text{SO}_2\text{OR}$, $200\text{--}202\text{ cm}^{-1}$.

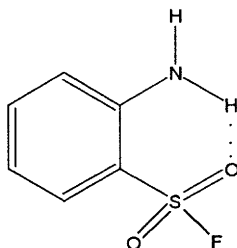
ORGANOSULFONYL CHLORIDES

Table 5.9 lists IR data for organosulfonyl chlorides. Compounds of forms RSO_2Cl and ArSO_2Cl in the vapor phase exhibit ν asym. SO_2 in the range $1390\text{--}1408\text{ cm}^{-1}$ and ν sym. SO_2 in the range $1179\text{--}1192$. In the liquid or solid phase, these same sulfonyl chlorides exhibit ν asym. SO_2 and ν sym. SO_2 in the regions $1362\text{--}1382\text{ cm}^{-1}$ and $1170\text{--}1174\text{ cm}^{-1}$. With change in physical phase from vapor to neat phases, the ν asym. SO_2 vibration shifts more in frequency than the ν sym. SO_2 vibration.

An IR band in the region $529\text{--}599\text{ cm}^{-1}$ is assigned to ν SCl, and the frequency separation between ν asym. SO_2 and ν sym. SO_2 varies between $208\text{--}236\text{ cm}^{-1}$ in the vapor phase and $191\text{--}212\text{ cm}^{-1}$ in the neat phase.

ORGANOSULFONYL FLUORIDES

Table 5.9a lists IR data for organosulfonyl fluorides of form ArSO_2F . In the vapor phase, ν asym. SO_2 and ν sym. SO_2 occur in the ranges $1428\text{--}1441\text{ cm}^{-1}$ and $1211\text{--}1235\text{ cm}^{-1}$, respectively. An exception here is the sulfonyl fluoride substituted in the 2-position with an NH_2 group, because ν asym. SO_2 and ν sym. SO_2 occur at 1411 and 1204 cm^{-1} , respectively. These normal modes occur at lower frequency due to intramolecular hydrogen bonding as presented here:



A

In the liquid phase, ν asym. SO_2 and ν sym. SO_2 occur in the ranges 1399–1420 cm^{-1} and 1186–1214 cm^{-1} , respectively. Compound A in the liquid phase exhibits ν asym. SO_2 and ν sym. SO_2 at 1384 cm^{-1} and 1186 cm^{-1} , respectively. In all cases the ν asym. SO_2 vibration shifts more in frequency than the ν sym. SO_2 vibration in going from the vapor phase to the liquid phase.

The band in the region 750–811 cm^{-1} is assigned to ν S–F in either the liquid or vapor phase. However, ν S–F occurs at higher frequency in the vapor phase compared to the liquid phase. The frequency separation between ν asym. SO_2 and ν sym. SO_2 varies between 207 and 219 cm^{-1} in the vapor phase and between 190 and 206 cm^{-1} in the liquid phase.

SUMMARY OF S=O AND SO_2 STRETCHING FREQUENCIES IN DIFFERENT PHYSICAL PHASES

Tables 5.10 and 5.11 list IR data for S=O and SO_2 containing compounds in different physical phases. In all cases the ν S=O or ν SO_2 vibrations occur at lower frequency in the neat phase than in the vapor phase.

ν asym. SO_2 AND ν sym. SO_2 CORRELATIONS

Figure 5.2 is a plot of ν asym. SO_2 vs ν sym. SO_2 vapor-phase frequencies for 13 compounds. This plot shows that there is an essentially linear relationship between these two ν SO_2 vibrations (24).

Figures 5.3 and 5.4 are plots of ν asym. SO_2 and ν sym. SO_2 , respectively, vs the summation of the inductive σ' values of the atoms or groups joined to the SO_2 group. These plots show that in general both ν SO_2 vibrations decrease in frequency as the electron release of the two groups joined to the SO_2 group decreases in value (24).

SO_2 STRETCHING VIBRATIONS IN $\text{CHCl}_3/\text{CCl}_4$ SOLUTIONS

Figure 5.5 shows plots of the ν asym. and ν sym. SO_2 frequencies for 1 wt./vol. % in mole % $\text{CHCl}_3/\text{CCl}_4$ solutions (36). Both ν SO_2 vibrations decrease in frequency as the mole % $\text{CHCl}_3/\text{CCl}_4$ is increased. The ν asym. SO_2 vibration occurs in the range 1317.7–1325.7 cm^{-1} and the ν sym. SO_2 vibration occurs in the range 1153.2–1157.4 cm^{-1} . Over the 0 to 100 mol % $\text{CHCl}_3/\text{CCl}_4$ the ν asym. SO_2 frequency shifts to lower frequency by ~ 8 cm^{-1} while the ν sym. SO_2 frequency shifts to lower frequency by ~ 4 cm^{-1} . With the first introduction of CHCl_3 to CCl_4 the ν SO_2 vibrations show a marked decrease in frequency, and after ~ 35 mol % $\text{CHCl}_3/\text{CCl}_4$ both plots are essentially linear. This results from the formation of intermolecular hydrogen bonding between $\text{SO}_2 \cdots \text{HCCl}_3$, which lowers the ν SO_2 frequencies. The continued decrease in both ν SO_2 frequencies is the result of the increased RF surrounding methyl phenyl sulfone molecules. Figure 5.6 shows a plot of ν asym. SO_2 vs ν sym. SO_2 for these same solutions. This plot is not linear over the 0–100 mol % $\text{CHCl}_3/\text{CCl}_4$. The break in linearity reflects the formation of different complexes with the methyl phenyl sulfone molecules. This could be where CHCl_3 also intermolecularly hydrogen bonds with the π system of the phenyl group as the mole % $\text{CHCl}_3/\text{CCl}_4$ is increased.

Figure 5.7 shows plots of ν asym. SO_2 and ν sym. SO_2 frequencies for 1 wt./vol. % in mole % $\text{CDCl}_3/\text{CCl}_4$ solutions (36). Both ν SO_2 frequencies decrease as the mole % $\text{CDCl}_3/\text{CCl}_4$ is increased. With the first addition of CDCl_3 , intermolecular deuterio bonds are formed between SO_2 groups of dimethyl sulfate and CDCl_3 (viz. $\text{SO}_2 \cdots \text{DCCl}_3$). After formation of the intermolecular $\text{SO}_2 \cdots \text{DCCl}_3$ complexes, the ν SO_2 vibrations decrease essentially in a linear manner due to the increased RF surrounding dimethyl sulfate molecules.

Figure 5.8 shows a plot of ν asym. SO_2 vs ν sym. SO_2 for 1% solutions of dimethyl sulfate in 0 to 100 mol% $\text{CDCl}_3/\text{CCl}_4$. This plot shows that both ν asym. SO_2 and ν sym. SO_2 decrease essentially in a linear manner as the mole % $\text{CDCl}_3/\text{CCl}_4$ is increased.

CALCULATED ν SO_2 FREQUENCIES

Using dimethyl sulfone ν SO_2 vapor-phase frequencies as the standard, two equations were developed for calculating ν asym. SO_2 and ν sym. SO_2 frequencies within $\pm 7 \text{ cm}^{-1}$ (43). These equations are:

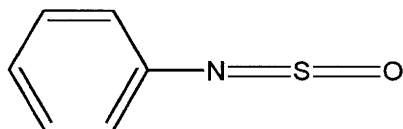
$$\begin{aligned}\nu \text{ asym. } \text{SO}_2 &= 1351 \text{ cm}^{-1} + \Sigma(\text{X} + \text{Y shift constants in cm}^{-1}) \\ \nu \text{ sym. } \text{SO}_2 &= 1160 + \Sigma(\text{X} + \text{Y shift constants in cm}^{-1})\end{aligned}$$

For those interested in applying these equations to predict ν SO_2 frequencies, the series of shift constants are available in Reference 43.

SULFINYL ANILINES

These sulfinyl anilines have the empirical structure presented here:

These molecules have ν asym. $\text{N}=\text{S}=\text{O}$ and ν sym. $\text{N}=\text{S}=\text{O}$ vibrations, where the ν asym. $\text{N}=\text{C}=\text{O}$ has strong IR band intensity and the ν sym. $\text{N}=\text{C}=\text{O}$ IR band has medium intensity. The ν asym. $\text{N}=\text{S}=\text{O}$ and ν sym. $\text{N}=\text{S}=\text{O}$ vibrations occur in the ranges $1254\text{--}1290 \text{ cm}^{-1}$ and



B

$1157\text{--}1173 \text{ cm}^{-1}$, respectively (see Table 5.12 for details). In the cases where both modes of a sulfinyl aniline derivative were recorded in two physical phases, ν asym. $\text{N}=\text{S}=\text{O}$ shifts more in frequency (24 cm^{-1}) than ν sym. $\text{N}=\text{S}=\text{O}$ (14 cm^{-1}) in going from the vapor phase to CS_2 solution.

REFERENCES

1. Nyquist, R. A. (1984). *The Interpretation of Vapor-Phase Infrared Spectra: Group Frequency Data*. Philadelphia: Bio-Rad Lab. Inc., Sadtler Div., p. 509.
2. Dollish, F. R., Fateley, W. G., and Bentley, F. F. (1974). *Characteristic Raman Frequencies of Organic Compounds*. New York: John Wiley & Sons, pp. 46–53.
3. Bellamy, L. J. (1975). *The Infrared Spectra of Complex Molecules*. New York: John Wiley & Sons, pp. 394–410.
4. Lin-Vien, D., Colthup, N. B., Fateley, W. G., and Grasselli, J. G. (1991). *The Handbook of Infrared and Raman Characteristic Frequencies of Organic Molecules*. Boston: Academic Press, Inc., p. 241.
5. Nyquist, R. A. (1984). *The Interpretation of Vapor-Phase Infrared Spectra: Group Frequency Data*. Philadelphia: Bio-Rad Lab. Inc. Sadtler Div., p. 495.
6. Nyquist, R. A. (1984). pp. 479, 517.
7. Klæboe, P. (1968). *Acta Chem. Scand.*, **22**: 2817.
8. Paetzold, R. and Ronsch, E. (1970). *Spectrochim. Acta*, **26A**: 569.
9. Nyquist, R. A., Putzig, C. H., and Leugers, M. A. (1997). *Handbook of Infrared and Raman Spectra of Inorganic Compounds and Organic Salts*. Vol. 3, Boston: Academic Press, p. 285.
10. Nyquist, R. A. *et al.* (1997). *Ibid.*, p. 235.
11. Nyquist, R. A. (1984). *The Interpretation of Vapor-Phase Infrared Spectra: Group Frequency Data*. Philadelphia: Bio-Rad Lab. Inc., Sadtler Div., p. 480.
12. Bender, P. and Wood, Jr. J. M. (1955). *J. Chem. Phys.*, **22**: 1316.
13. Martz, D. E. and Lagemann, R. T. (1956). *J. Chem. Phys.*, **25**: 1277.
14. Stammreich, H., Forneris, R., and Tavares, Y. (1956). *J. Chem. Phys.*, **25**: 1277.
15. Geisler, G. and Hanschmann, G. (1972). *J. Mol. Struct.*, **11**: 283.
16. Detoni, S. and Hadzi, D. (1957). *Spectrochim. Acta*, **11**: 601.
17. Ubo, T., Machida, K., and Hanai, K. (1971). *Spectrochim. Acta*, **27A**: 107.
18. Fawcett, A. H., Fee, S., Stuckey, M., and Walkden, P. (1987). *Spectrochim. Acta*, **43A**: 797.
19. Nyquist, R. A., Putzig, C. H., and Leugers, M. A. (1997). *Handbook of Infrared and Raman Spectra of Inorganic Compounds and Organic Salts*, Vol. 13, Boston: Academic Press, p. 225.
20. Nyquist, R. A. (1984). *The Interpretation of Vapor-Phase Infrared Spectra: Group Frequency Dates*, Philadelphia: Bio-Rad Lab. Inc., Sadtler Div., p. 495.
21. Nyquist, R. A. (1984). *Ibid.*, p. 496.
22. Nyquist, R. A. (1984). p. 489.
23. Nyquist, R. A. (1984). p. 490.
24. Nyquist, R. A. (1984). p. 497.
25. Nyquist, R. A. (1984). p. 474.
26. Nyquist, R. A. (1984). p. 485.
27. Nyquist, R. A. (1984). p. 484.
28. Bouquet, M., Chassaing, G., Corset, J., Favort, J., and Limougi, J. (1981). *Spectrochim. Acta*, **37A**: 727.
29. Joshi, U. C., Joshi, M., and Singh, R. N. (1981). *Ind. J. Pure & Appl. Phys.*, **19**: 1226.
30. Hanai, K., Okuda, T., Uno, T., and Machida, K. (1975). *Spectrochim. Acta*, **31A**: 1217.
31. Uno, T., Machida, K., and Hanai, K. (1966). *Spectrochim. Acta*, **22**: 2065.
32. Tanka, Y., Tanka, Y., and Saito, Y. (1983). *Spectrochim. Acta*, **39A**: 159.
33. Tanka, Y., Yanka, Y., Saito, Y., and Machida, K. (1978). *Bull. Chem. Soc. Jpn.*, **51**: 1324.
34. Hanai, K. and Okuda, T. (1975). *Spectrochim. Acta*, **31A**: 1227.
35. Kanesaki, I. and Kawai, K. (1970). *Bull. Chem. Soc. Jpn.*, **43**: 3298.
36. Nyquist, R. A., Sloane, H. J., Dunbar, J. E., and Strycker, S. J. (1966). *Appl. Spectrosc.*, **20**: 90.

37. Nyquist, R. A. (1990). *Appl. Spectrosc.*, **44**: 594.
38. (1977) *Sadtler Standard Infrared Vapor Phase Spectra*. Philadelphia: Bio-Rad Inc., Sadtler Div.
39. Nyquist, R. A., Putzig, C. H., and Leugers, M. A. (1997). *Handbook of Infrared and Raman Spectra of Inorganic Compounds and Organic Salts*. Vol. 3, Boston: Academic Press, p. 231.
40. Nyquist, R. A. *et al.* (1997). *Ibid.*, p. 232.
41. CS₂ Solution Data. The Dow Chemical Company, Analytical Laboratories.
42. Sportouch, S., Clark, R. J. H., and Gaufres, R. (1974). *J. Raman Spectrosc.*, **2**: 153.
43. Nyquist, R. A. (1984). *The Interpretation of Vapor-Phase Infrared Spectra: Group Frequency Data*. Philadelphia: Bio-Rad Lab. Inc., Sadtler Div., p. 506.

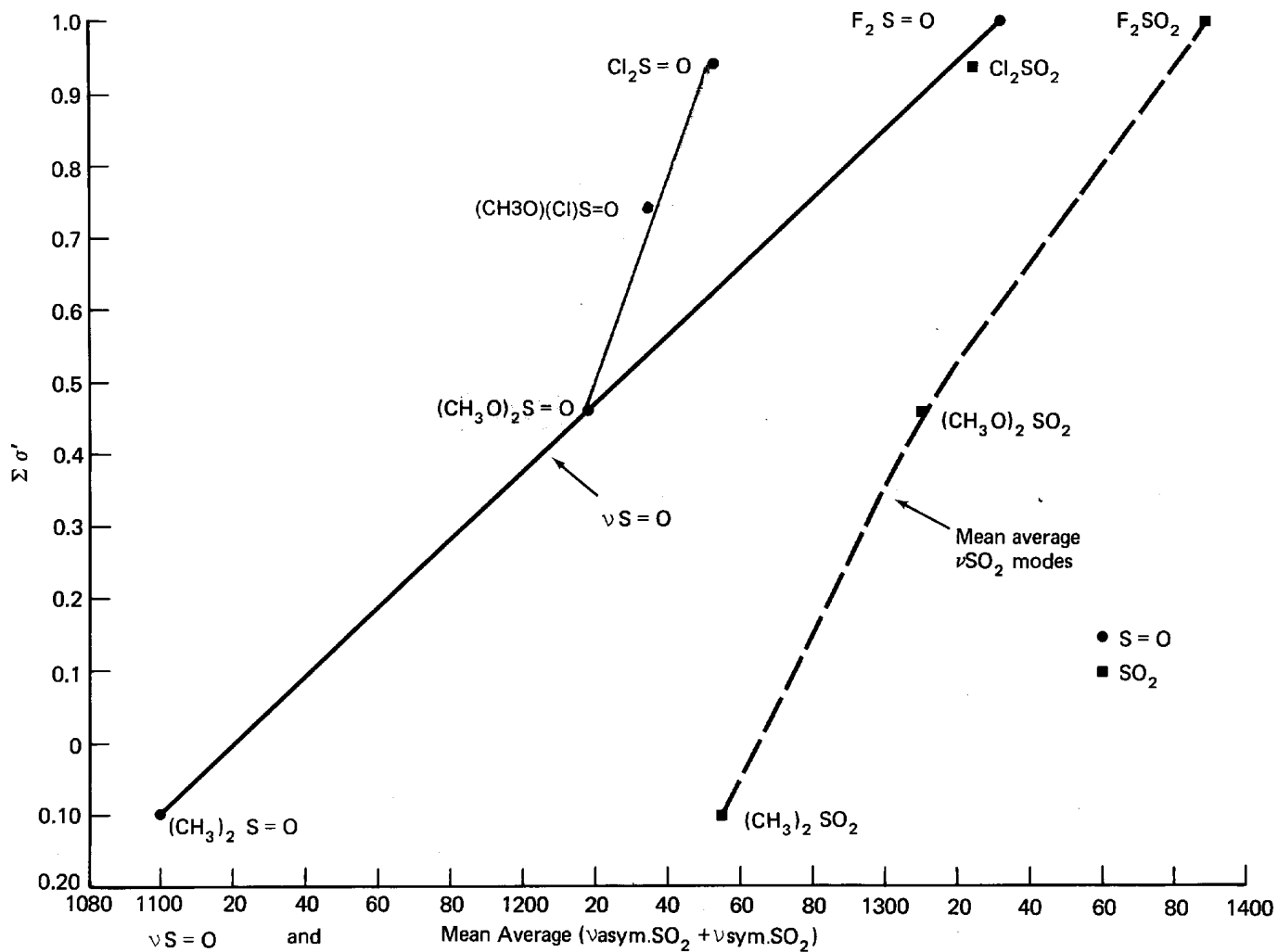


FIGURE 5.1 Plots of $\nu S=O$ and the mean average of $(\nu_{\text{asym.}} SO_2 + \nu_{\text{sym.}} SO_2)$ vapor-phase frequencies for compounds containing the S=O or SO₂ group vs $\Sigma \sigma'$.

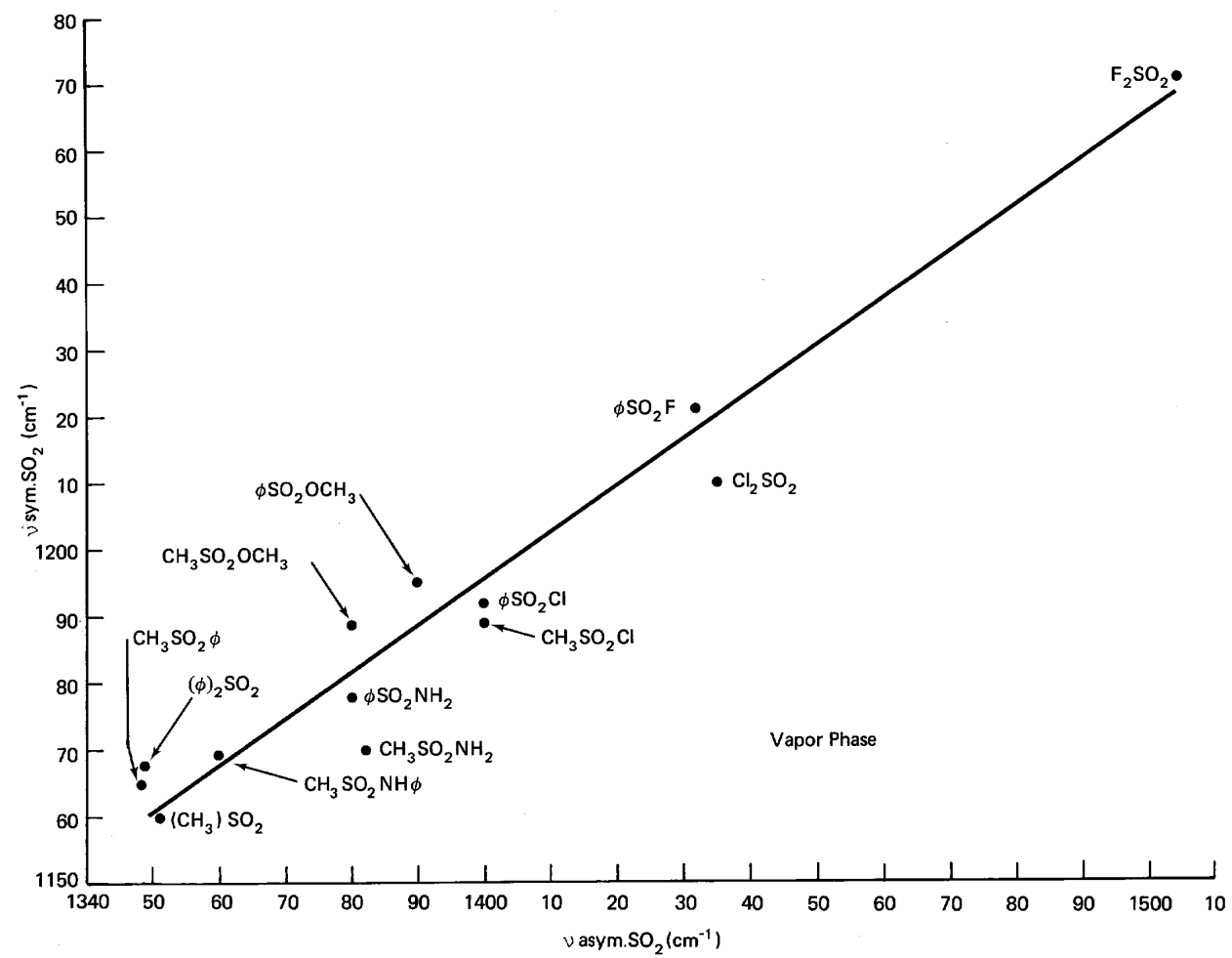


FIGURE 5.2 A plot of $\nu_{\text{asym}} \text{SO}_2$ vs $\nu_{\text{sym}} \text{SO}_2$ vapor-phase frequencies for a variety of compounds containing the SO_2 group.

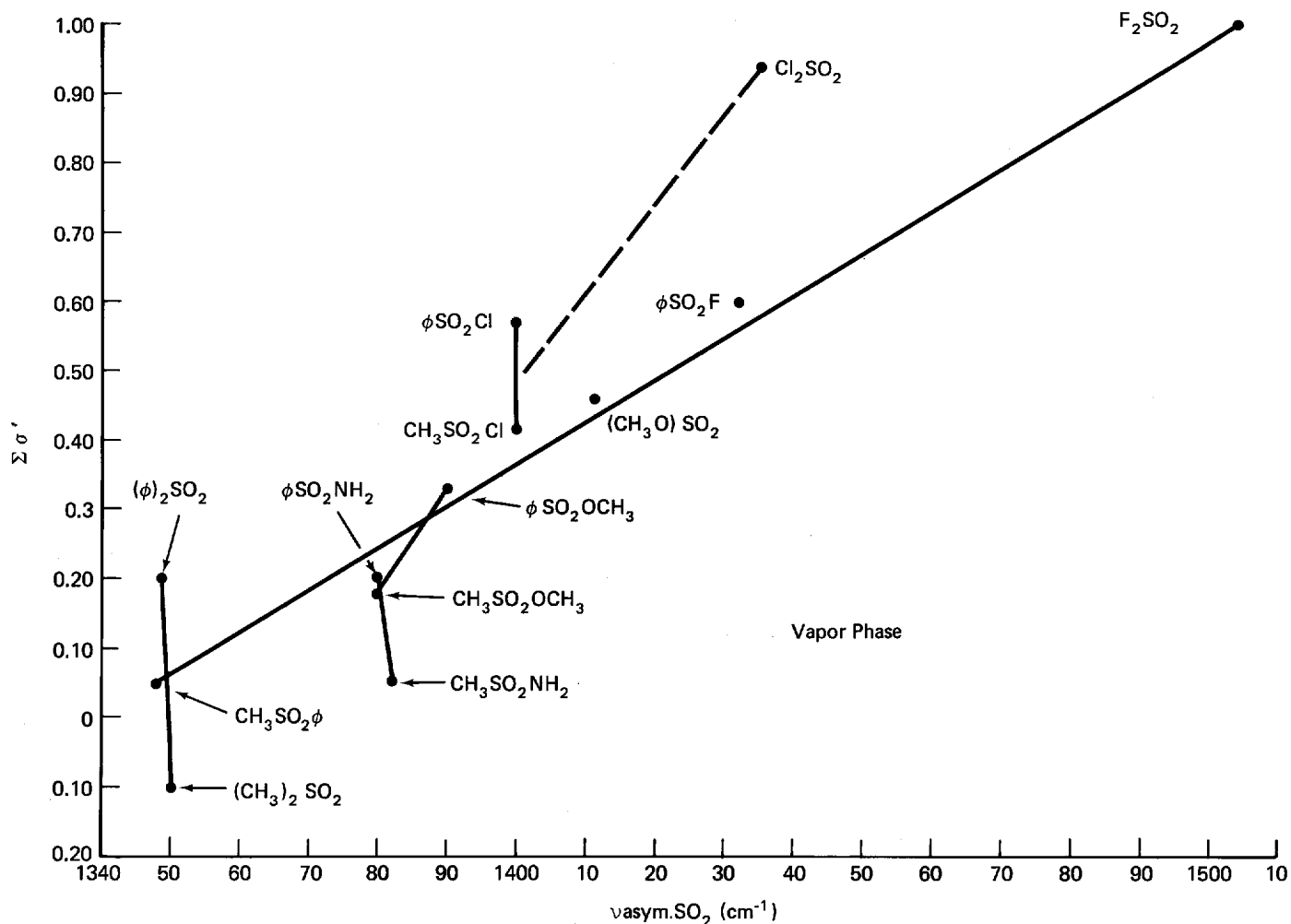


FIGURE 5.3 Plots of $\nu_{\text{asym. SO}_2}$ vapor-phase frequencies for a variety of compounds containing a SO_2 group vs $\Sigma\sigma'$.

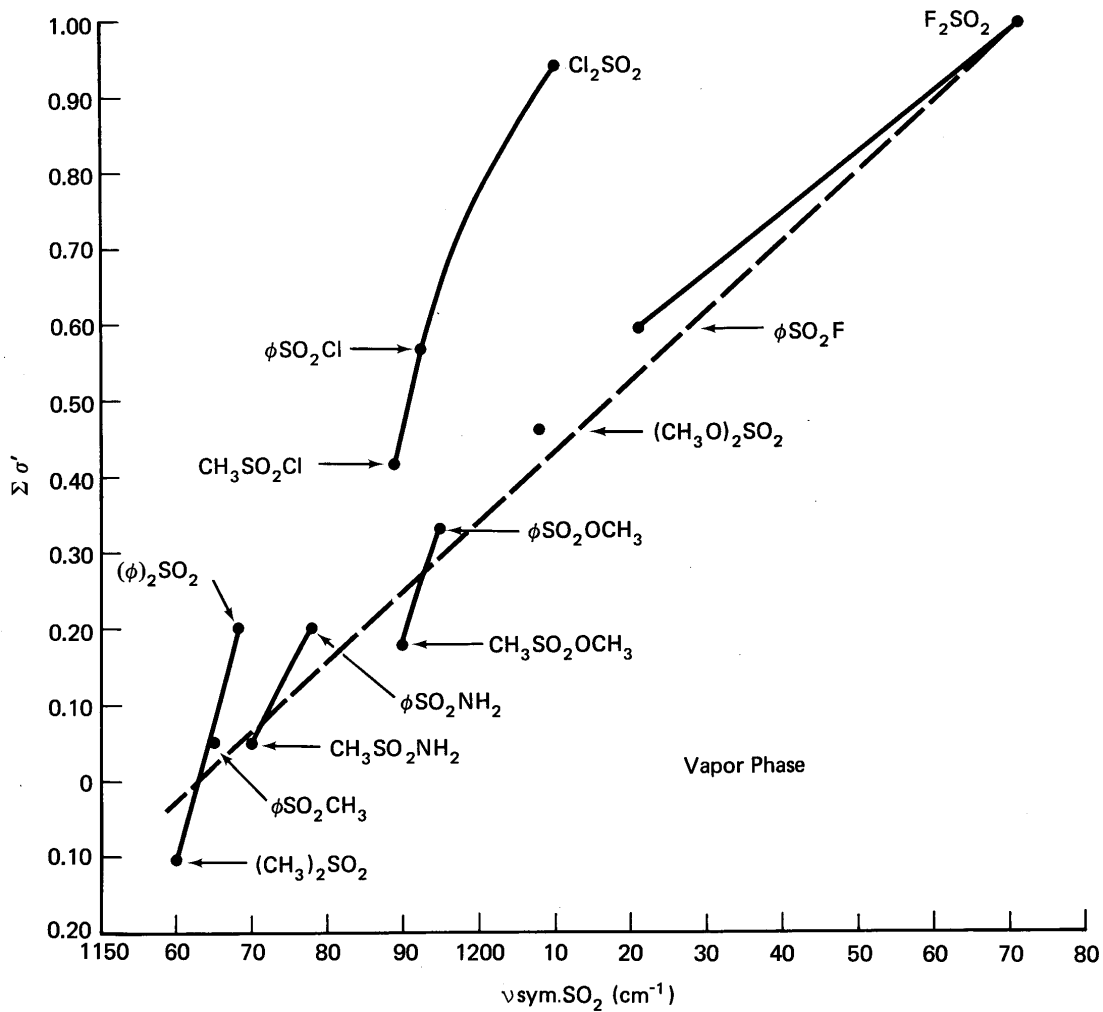


FIGURE 5.4 Plots of $\nu_{\text{sym. SO}_2}$ vapor-phase frequencies for a variety of compounds containing the SO₂ group vs $\Sigma\sigma'$.

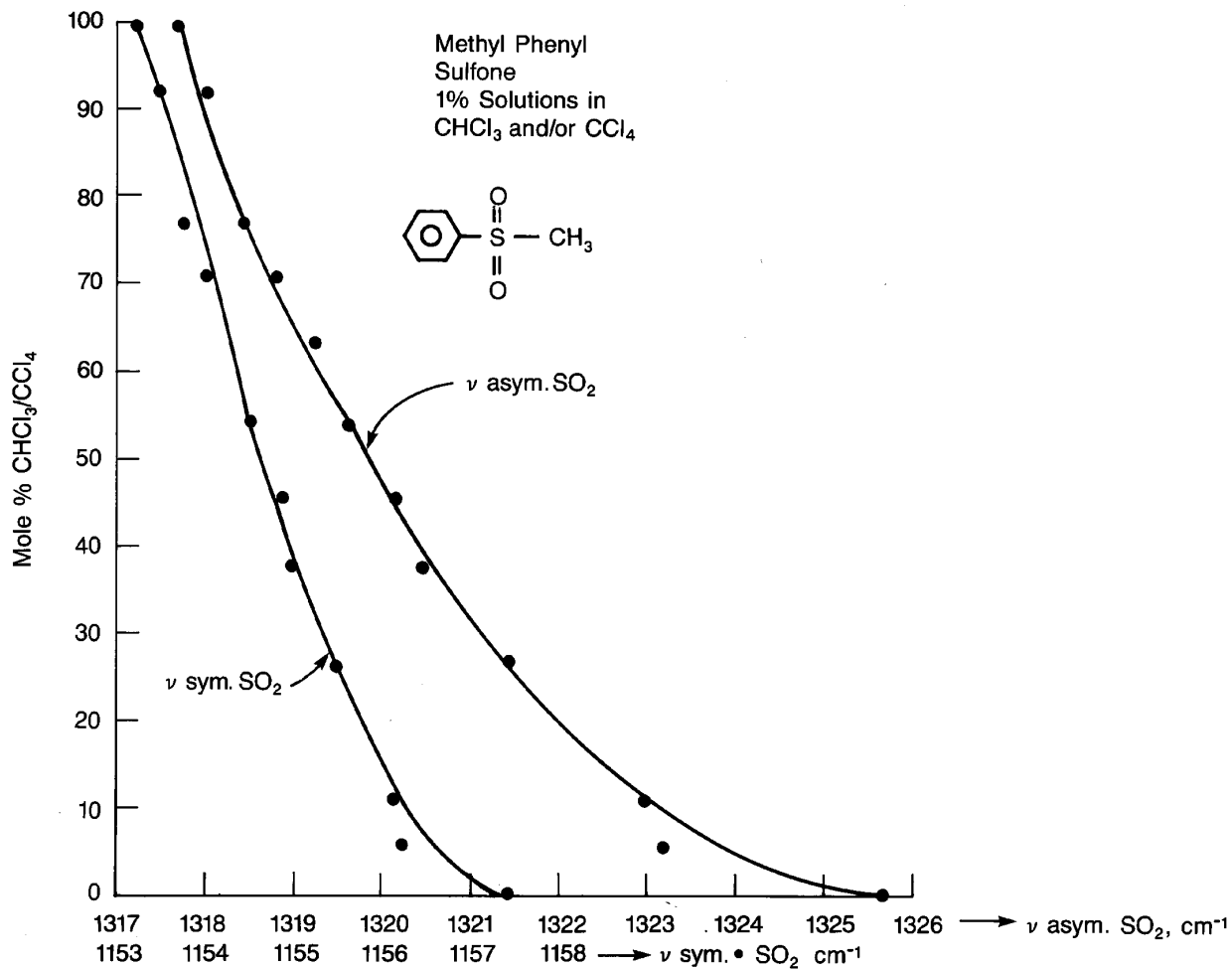
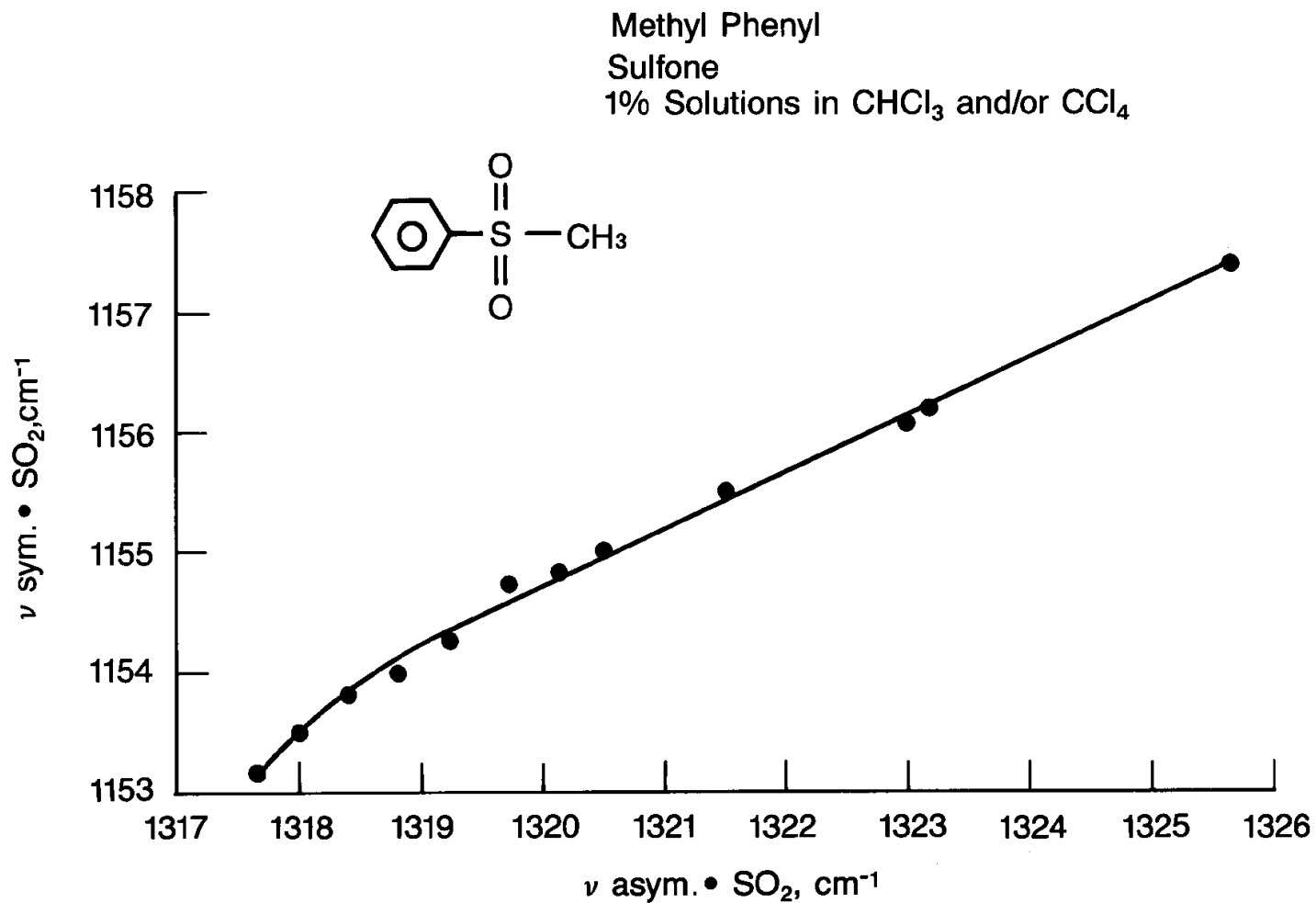


FIGURE 5.5 Plots of ν asym. and ν sym. SO_2 for methyl phenyl sulfone in 10 wt./vol. solvent vs mole % $\text{CHCl}_3/\text{CCl}_4$.

FIGURE 5.6 A plot of $\nu_{\text{asym.}} \text{SO}_2$ vs $\nu_{\text{sym.}} \text{SO}_2$ for methyl phenyl sulfone in 1% wt./vol. solvent vs mole % $\text{CHCl}_3/\text{CCl}_4$.

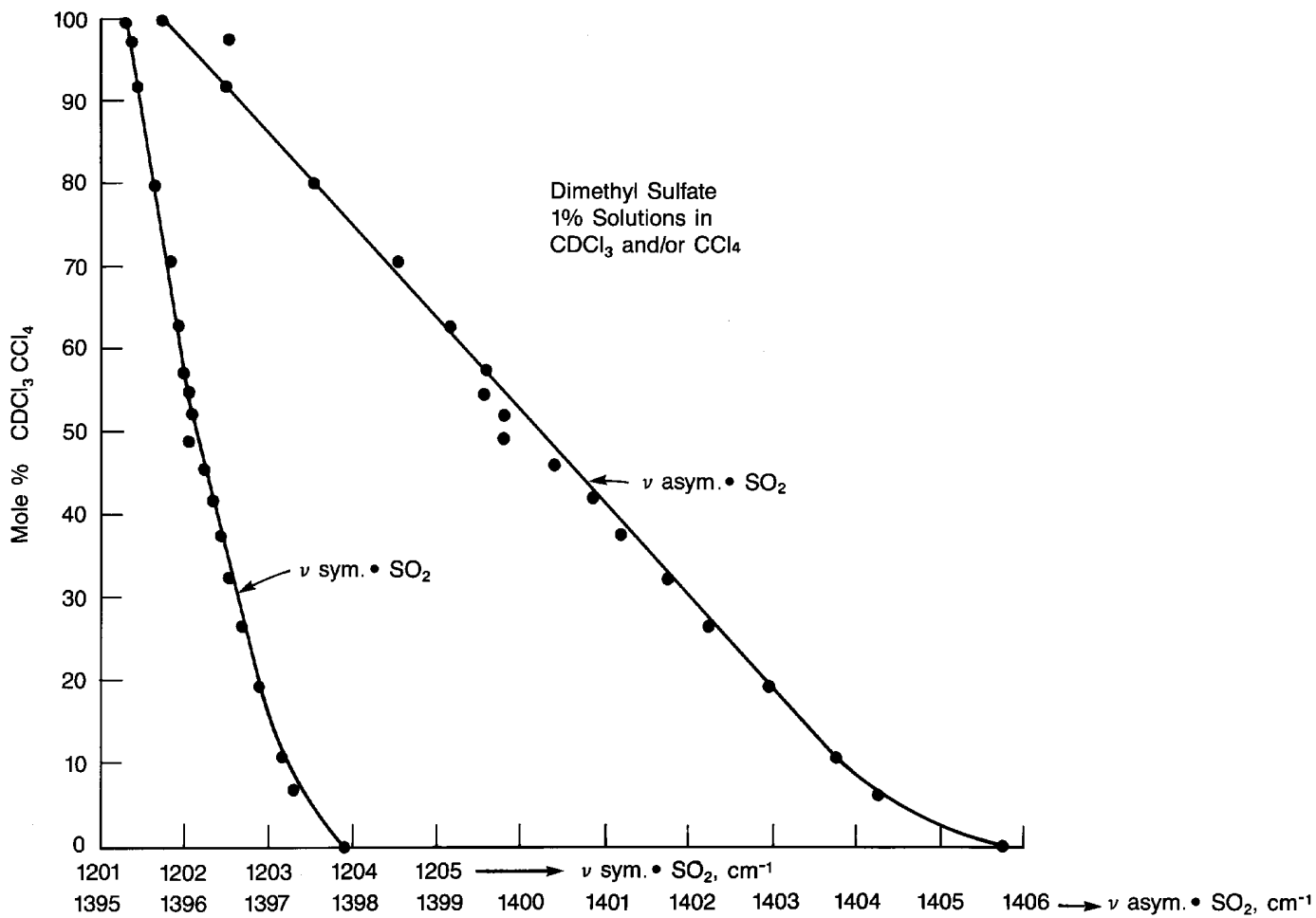


FIGURE 5.7 Plots of ν asym. SO_2 and sym. SO_2 for dimethyl sulfate in 1% wt./vol. solvent vs mole % $\text{CDCl}_3/\text{CCl}_4$.

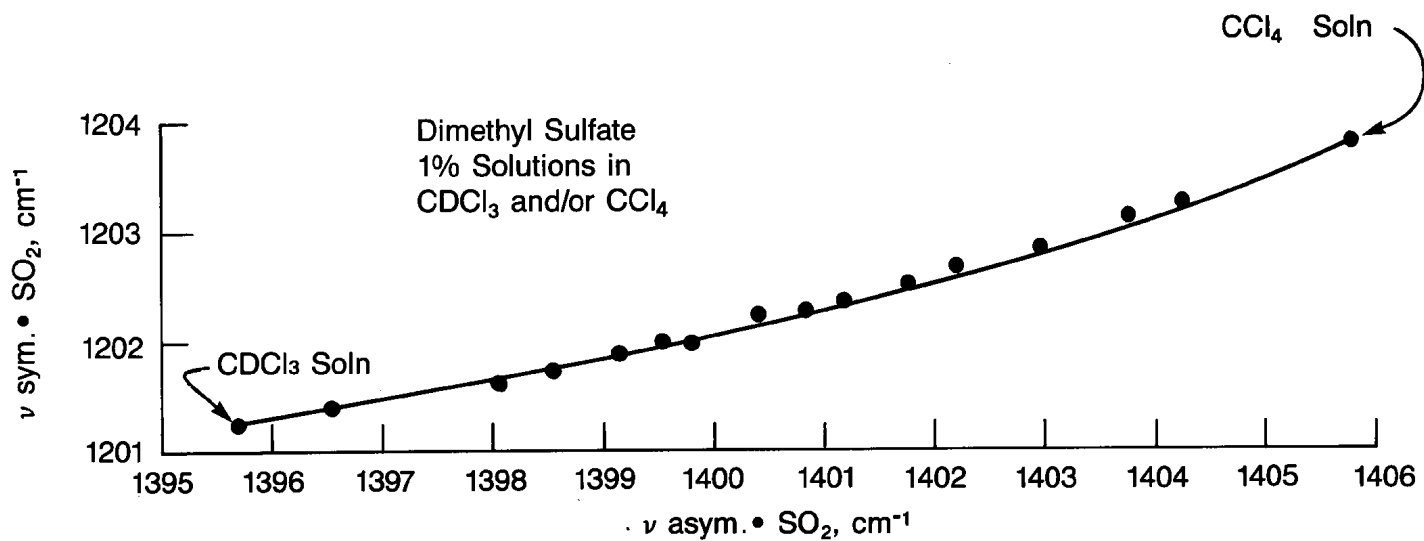
FIGURE 5.8 A plot of ν asym. SO_2 vs ν sym. SO_2 for dimethyl sulfate 1% wt./vol. solvent vs mole % $\text{CDCl}_3/\text{CCl}_4$.

TABLE 5.1a A comparison of the S=O stretching frequencies for S=O containing compounds

Compound or compound type	$\nu_{\text{S=O}}$ vapor cm^{-1}	References	$\nu_{\text{S=O}}$ Ref. 3 cm^{-1}	IR	R	References
(R-) ₂ S=O	[—]		1035–1070	vs	w-m	2, 3, 4
(CH ₃ -) ₂ S=O	1100	5				
(CD ₃ -) ₂ S=O	1092	5				
(R-)S(=O)(-Ar)	[—]		1040–1050	vs	w-m	4
(Ar-) ₂ S=O	[—]		1035–1042	vs	w-m	2, 3, 4
(CH ₃ -O-) ₂ S=O	1218	6	1207	vs	vs, p	7
(R-O-) ₂ S=O	1209–1218	6	1198–1209	s		2, 3, 4
(CH ₂ -O) ₂ S=O	1240	6				
	1230					
[(CH ₃) ₂ N] ₂ S=O	[—]		1108	vs	m	8
(CH ₃) ₂ NS(=O)Cl	[—]		1185	vs	m	8
(R-O-)S(=O)Cl	[—]		1214–1221			2, 4
(CH ₃ -O-)S(=O)Cl	1232	9				
F ₂ S=O	1331	10	1308			12
Cl ₂ S=O	1251	10	1253			13
Br ₂ S=O	[—]		1121			14

TABLE 5.1b A comparison of asym. SO₂ and sym. SO₂ stretching frequencies in different physical phases, and asym. N=S=O and sym. N=S=O frequencies in CS₂ solution

Compound or compound Type	ν asym. SO ₂ vapor cm ⁻¹	ν sym. SO ₂ vapor cm ⁻¹	Ref.	ν asym. SO ₂			ν sym. SO ₂			Ref.	[ν asym. SO ₂ vapor]- [ν asym. neat or CCl ₄] cm ⁻¹	[ν sym. SO ₂ vapor]- [ν sym. neat or CCl ₄] cm ⁻¹
				Ref. 3 cm ⁻¹	IR	R	Ref. 3 cm ⁻¹	IR SO ₂	R SO ₂			
SO ₂	1360	1150	19									
(R-)SO ₂	1335-1371	1141-1160	20	1295-1330	vs	w-m	1125-1152	vs	vs, p 2, 3, 15-18		[40]-[41]	[9]-[8]
(Ar-)SO ₂ (-R)	1346-1349	1159-1172	21	1325-1334	s	w	1150-1160	s	w 3, 28		[21]-[15]	[9]-[12]
(Ar) ₂ SO ₂	1351-1357	1158-1169	21	1328		vs	1162		vs, p 29		[23]-[29]	[-4]-[-7]
(R-)SO ₂ (-OH)	[—]	[—]		1342-1352	vs		1150-1165			16		
(R-)SO ₂ (-OR)	[—]	[—]		1352-1358		m	1165-1172		vs, p 2, 4			
(CH ₃ -)SO ₂ (-OR)	1368-1380	1185-1190	22									
(Ar-)SO ₂ (-OR)	1390-1400	1188-1195	22	1338-1363		w	1185-1192		vs 2, 4		[52]-[37]	[3]-[3]
(Ar-)SO ₂ (-OAr)	1402-1409	1178-1190	23									
Cl-SO ₂ (-OR)				1401-1406		m-s	1184-1191	vs	2, 4			
(R-)SO ₂ (-SR)				1305-1344	m-s	1126-1128		s	2, 4			
(RO-)SO ₂	1408-1420	1200-1219	24	1372-1388		s	1188-1196		vs 2, 4		[36]-[32]	[12]-[26]
(Ar-As-O-)SO ₂ (-OR or -OAr)				1325	s		1161-1171	s	34		[69]	[25]
(CH ₃ -)SO ₂ (-NH ₂)	1382	1170	25	1315	vs	m	1145	vs	vs 28			
(C ₂ H ₅ -)SO ₂ (NH ₂)	1375	1161	25									
(C ₂ H ₅ -)SO ₂ (NH ₂)	1380	1178	25				1157		s 2, 4		[?]	[21]
(Ar-)SO ₂ (NH ₂)	1370-1380	1172-1178	25									
(CH ₃ -)SO ₂ (-NHC ₆ H ₅)	1360	1160	25									
(CH ₃ -)SO ₂ (-2NH ₂ -4-C ₆ H ₅)	1325	1150	25									
(Ar-)SO ₂ (-NHR)	1344-1366	1160-1175	26									
(CH ₃ -)SO ₂ (-N(CH ₃) ₂)	1362	1165	26									
(Ar-)SO ₂ (-N(CH ₃) ₂)	1365	1169	26									
(NH ₂) ₂ SO ₂				1358	vs		1156	vs	31			
((CH ₃) ₂ N-)SO ₂ (-NH ₂)				1335	vs	m	1140	s	s 32			
((CH ₃) ₂ N-)SO ₂ (-Cl)	1411	1190	36	1385	vs	m, dp	1177	vs	s, p 33		[26]	[13]
(CH ₃ -)SO ₂ (-F)				1401		m	1186		vs 2, 4			
(Ar-)SO ₂ (-F)	1428-1442	1211-1229	26	1402-1412		w-m	1167-1197		vs 2, 4		[18]-[32]	[11]-[27]

(continues)

TABLE 5.1b (continued)

Compound or compound Type	ν asym. SO ₂ vapor cm ⁻¹	ν sym. SO ₂ vapor cm ⁻¹	Ref.	ν asym. SO ₂ Ref. 3 cm ⁻¹	IR	R	ν sym. SO ₂ Ref. 3 cm ⁻¹	IR SO ₂	R SO ₂	Ref.	[ν asym. SO ₂ vapor]- [ν asym. neat or CCl ₄] cm ⁻¹	[ν sym. SO ₂ vapor]- [ν sym. neat or CCl ₄] cm ⁻¹
(R-)SO ₂ (-Cl)	1400-1402	1177-1189	27	1366	vs	w	1171	vs	s, p	2, 4	[34]-[36]	[6]-[5]
(Ar-)SO ₂ (-Cl)	1390-1410	1172-1192	27	1361-1384		w-m	1169-1184		vs	2, 4	[29]-[25]	[3]-[8]
(Cl-)SO ₂ (-N=C=O)				1442	vs	m	1182	vs	m	35		
(F-)SO ₂				1497; [1503]		w	1263; [1270]		vs	2, 4	[42]	
(Cl-)SO ₂	1438	1210	39	1414		s	1182		s	2, 3	[24]*	[28]*
(Cl-)SO ₂	[1420, CCl ₄ soln.]	[1191, CCl ₄ soln.]	40								[18]*	[19]*
				ν asym. N=S=O cm ⁻¹			ν sym. N=S=O cm ⁻¹					
(Ar-)N=S=O [in CS ₂ soln.]				1254-1290	s		1158-1175	m		41		

* An exception (see text).

TABLE 5.1c Vapor-phase infrared data for dimethyl sulfoxide and dialkyl sulfones

Sulfone	a.CH ₃ str. cm ⁻¹ (A)	a.CH ₂ str. cm ⁻¹ (A)	s.CH ₃ str. cm ⁻¹ (A)	s.CH ₂ cm ⁻¹ (A)	a.CH ₃ bend cm ⁻¹ (A)	CH ₂ bend cm ⁻¹ (A)	s.CH ₃ bend cm ⁻¹ (A)	CH ₃ rock cm ⁻¹ (A)	a.(C) ₂ S str. cm ⁻¹ (A)	s.(C) ₂ S str. cm ⁻¹ (A)	a.SO ₂ str. cm ⁻¹ (A)	s.SO ₂ str. cm ⁻¹ (A)	Ratio (A) s.SO ₂ str./ s.CH ₂ str.	Ratio (A) s.SO ₂ str./ a.CH ₃ str.	Ratio (A) s.SO ₂ str./ s.(C) ₂ str.	Ratio (A) s.SO ₂ str./ a.(C) ₂ str.	Ratio (A) s.(C) ₂ str./ a.(C) ₂ str.
Methyl	3022 (0.026)		2942 (0.039)		1425 (0.044)		1311 (wk)	932 (0.460)	742 (0.270)	680 (0.093)	1351 (1.250)	1160 (1.040)		40.01	11.18	3.85	0.34
Propyl	2979 (0.930)	2943 (1.230)		2890 (0.480)	1465 (0.185)	1415 (0.125)			779 (0.195)	699 (0.205)	1335 (1.250)	1145 (1.250)	2.61	1.34	6.09	6.41	1.05
Butyl	2975 (1.240)	2942 (0.770)		2885 (0.430)	1464 (0.180)	1414 (0.120)			810 (0.130)	700 (0.130)	1338 (1.240)	1142 (1.040)	2.42	0.84	8.01	8.01	1.01
Hexyl	2970 (0.835)	2935 (1.240)		2875 (0.395)	1461 (0.150)	1412 (0.070)			812 (0.080)	702 (0.080)	1338 (0.680)	1140 (0.580)	1.47	0.69	7.25	7.25	1.01
														Ratio (A) SO str./ s.CH ₃ str.	Ratio (A) SO str./ a.CH ₃ str.		
Sulfoxide																	0.45
Methyl	3000 (0.152)		2921 (0.115)		1441 (0.170)	1420 (0.135)	1310 (0.086)	930 (0.135)	755 (0.020)	669 (0.169)	[1100 (1.220)]		10.61	8.03			

TABLE 5.1d Vapor- and solid-phase infrared data for dimethyl sulfoxide and dialkyl sulfones

Sulfone	Phase	a.(C) ₂ str. cm ⁻¹ (A)	s.(C) ₂ S str. cm ⁻¹ (A)	a.SO ₂ str. cm ⁻¹ (A)	s.SO ₂ str. cm ⁻¹ (A)	[a.SO ₂ str.] - [s.SO ₂ str.] cm ⁻¹	Ratio (A) A[s.SO ₂ str.]/ A[s.(C) ₂ S str.]	Ratio (A) A[s.SO ₂ str.]/ A[a.(C) ₂ str.]	Ratio (A) A[s.(C) ₂ str.]/ A[a.(C) ₂ str.]
Methyl	vapor	742 (0.270)	680 (0.093)	1351 (1.250)	1160 (1.040)	191	11.18	3.85	0.34
Methyl	solid	750 (0.765)	685 (0.245)	1286 (1.145)	1124 (1.031)	162	4.21	1.35	0.33
	Δ [v-s]	[8]	[5]	[-65]	[-36]	[-29]			
Propyl	vapor	779 (0.195)	699 (0.205)	1335 (1.250)	1145 (1.250)	190	6.09	6.41	1.05
Propyl	solid	781 (0.300)	699 (0.170)	1309 (stg)	1127 (stg)	182			0.57
				1280 (stg)		153			
	Δ [v-s]	[2]	[0]	[-26]; [-55]	[-18]	[-8]; [-37]			
Butyl	vapor	810 (0.130)	700 (0.130)	1338 (1.240)	1142 (1.040)	196	8.01	8.01	1.01
Butyl	solid	810 (0.350)	699 (0.150)	1311 (stg)	1117 (stg)	194			0.43
				1290 (stg)		173			
	Δ [v-s]	[0]	[-1]	[-28]; [-48]	[-25]	[-2]; [-23]			
Hexyl	vapor	812 (0.080)	702 (0.080)	1338 (0.680)	1140 (0.580)		7.25	7.25	1.01
Sulfoxide				[SO str.]					
Methyl	vapor	755 (0.020)	669 (0.169)	[1100 (1.220)]					0.45
Methyl	liquid	695 (0.240)	664 (0.094)	1050 (1.050)					0.39
	Δ [v-l]	[-60]	[-5]	[-50]					

TABLE 5.2 Vapor- and solid-phase infrared data for diaryl sulfones

Compound Diaryl sulfone	Phase	a.SO ₂ str. cm ⁻¹ (A)	s.SO ₂ str. cm ⁻¹ (A)	SO ₂ bend cm ⁻¹ (A)	SO ₂ wag cm ⁻¹ (A)	[a.SO ₂ str.] - [s.SO ₂ str.] cm ⁻¹	A[s.SO ₂ str.] / A[a.SO ₂ str.]
(4-CH ₃ -C ₆ H ₄ -)SO ₂	vapor	1348 (0.850)	1165 (1.240)	678 (1.024)	558 (0.950)	183	1.46
(4-CH ₃ -C ₆ H ₄ -)SO ₂	solid	1318 (0.840)	1152 (1.150)	677 (0.930)	554 (0.830)	166	1.37
		1301 (0.611)			546 (0.835)	149	1.88
	Δ [v-s]	[-30]; [-47]	[-13]	[-1]	[-4]; [-12]	[-17]; [-34]	
(4-F-C ₆ H ₄ -) ₂ SO ₂	vapor	1351 (0.470)	1161 (1.240)	680 (0.321)	550 (1.250)	190	2.64
(4-F-C ₆ H ₄ -) ₂ SO ₂	solid	1325 (0.860)	1155 (1.168)	671 (0.392)	550 (1.032)	170	1.36
	Δ [v-s]	[-26]	[-6]	[-9]	[0]	[-20]	
(4-Cl-C ₆ H ₄ -) ₂ SO ₂	vapor	1352 (0.534)	1169 (0.773)	631 (1.010)	581 (0.180)	183	1.45
(4-Cl-C ₆ H ₄ -) ₂ SO ₂	solid	1319 (0.840)	1145 (1.240)	628 (0.855)	574 (0.575)	174	1.48
	Δ [v-s]	[-33]	[-24]	[-3]	[-7]	[-9]	
(4-NO ₂ -C ₆ H ₄ -)SO ₂ - C ₆ H ₅ *	vapor	1354 (0.790)	1170 (0.750)	607 (1.240)	564 (0.255)	184	0.95
	solid	1318 (0.650)	1164 (1.150)	608 (0.950)	564 (0.766)	154	1.77
		1301 (0.839)				137	
	Δ [v-s]	[-36]; [-53]	[-6]	[1]	[0]	[-30]; [-47]	
			a.NO ₂ str.	s.NO ₂ str.	A[s.NO ₂ str.] / A[a.NO ₂ str.]	[a.NO ₂ str.] - [s.NO ₂ str.]	
(4-NO ₂ -C ₆ H ₄)SO ₂ -C ₆ H ₅	vapor	1548 (0.500)	1354 (0.970)		1.94	194	
(4-NO ₂ -C ₆ H ₄)SO ₂ -C ₆ H ₅	solid	1529 (1.150)	1351 (0.950)		0.83	178	
	Δ [v-s]	[-19]	[-3]			[-16]	

TABLE 5.3 Infrared data for phenoxarsine derivatives containing the S(SO₂)R and O(SO₂)R groups in CS₂ solution

Phenoxarsine [CS ₂]	a.SO ₂ str.	s.SO ₂ str.	C-S str.	SO ₂ bend	SO ₂ rock
X=S-SO ₂ -R					
R					
Methyl	1328	1137	740		
Ethyl	1322	1125	751	601	548
<i>n</i> -butyl	1320	1126	753	601	537
Phenyl	1322	1141	715	591	538
X=O-SO ₂ -R					
R					
Methyl	1325	1161			
Phenyl	1325	1171			

TABLE 5.4 Infrared data for the SO₂ stretching vibrations for compounds in CHCl₃ and CCl₄ solutions

Compound	a.SO ₂ str. CCl ₄ soln. cm ⁻¹	a.SO ₂ str. CHCl ₃ soln. cm ⁻¹	[CCl ₄ soln.]– [CHCl ₃ soln.] cm ⁻¹	s.SO ₂ str. CCl ₄ soln. cm ⁻¹	s.SO ₂ str. CHCl ₃ soln. cm ⁻¹	[CCl ₄ soln.]– [CHCl ₃ soln.] cm ⁻¹	[a.SO ₂ str.]– [s.SO ₂ str.] CCl ₄ soln. cm ⁻¹	[a.SO ₂ str.]– [s.SO ₂ str.] CHCl ₃ soln. cm ⁻¹	[CCl ₄ soln.]– [CHCl ₃ soln.] cm ⁻¹
Dimethyl sulfate	1405.7	1395.7	–10	1203.8	1201.8	–2	201.9	193.9	–8
4'-Chlorophenyl 4-chloro- benzenesulfonate	1392.4	1382.9	–9.5	1178.9	1176.8	–2.1	213.5	206.1	–7.4
Benzenesulfonyl chloride	1387.4	1380.3	–7.1	1177.8	1177.1	–0.7	209.6	203.2	–6.4
Diphenyl sulfone	1326.8	1319.1	–7.7	1161.4	1157.6	–3.8	165.4	161.5	–3.9
Methyl phenyl sulfone	1325.7	1317.7	–8	1157.4	1153.2	–4.2	168.3	164.5	–3.8

TABLE 5.5 Infrared data for dialkyl sulfites

Compound		S=O str.		a.C-O-S str.		s.C-O-S str.	
R-O-SO-O-R	Phase	cm ⁻¹	A	cm ⁻¹	A	cm ⁻¹	A
CH ₃	vapor	1218	0.588	979	1.25	685	1.142
CH ₃	liquid	1205	0.85	990	0.721	730	0.48
				955	0.81	685	0.58
C ₂ H ₅	Δ [v-l]	[-13]		[11]; [-24]		[45]; [0]	
C ₂ H ₅	vapor	1210	0.499	1010	0.84	695	0.735
C ₂ H ₅	liquid	1204		1019		748	
				1001		717	
	Δ [v-l]	[-6]		[9]; [-9]		[55]; [22]	

TABLE 5.6 Infrared data for primary sulfonamides in the vapor and solid phases

Compound	a.NH ₂ str.	s.NH ₂ str.		NH ₂ bending		A(NH ₂ bending)/A(NH ₂ bending)/				
R-SO ₂ NH ₂	Phase	cm ⁻¹	A	cm ⁻¹	A	cm ⁻¹	A	A(a.NH ₂ str.)	A(s.NH ₂ str.)	
Methane	vapor	3472	0.19	3378	0.173	1553	0.237	1.25	1.37	
Methane	solid	3335	0.98	3258	0.62	1569	0.09	0.09	0.15	
	Δ [v-s]	[-137]		[-120]		[16]				
Benzene	vapor	3479	0.094	3378	0.135	1552	0.136	1.45	1.01	
Benzene	solid	3339	0.659	3241	0.721	1547	0.225	0.34	0.31	
	Δ [v-s]	[-140]		[-137]		[-5]				
4-Toluene	vapor	3478	0.048	3370	0.074	1552	0.08	1.67	1.08	
4-Toluene	solid	3323	1.02	3238	0.94	1545	0.154	0.15	0.16	
	Δ [v-s]	[-155]		[-132]		[-7]				
2-Toluene	vapor	3465	0.073	3365	0.103	1550	0.14	1.92	1.36	
2-Toluene	solid	3397	0.56	3275	0.635	1558	0.175	0.31	0.28	
	Δ [v-s]	[-68]		[-90]		[8]				
		[a.NH ₂ str.]-(s.NH ₂ str.)	a.SO ₂ str.	s.SO ₂ str.		SN str.		A[s.SO ₂ str.]/A[a.SO ₂ str.]		[a.SO ₂ str.]-(s.SO ₂ str.)
		cm ⁻¹	cm ⁻¹	A	cm ⁻¹	A	cm ⁻¹	A	cm ⁻¹	
Methane	vapor	94	1382	1.262	1170	1.035	856	0.402	0.82	212
Methane	solid	77	1308	1.101	1140	0.82	871	0.135	0.75	168
			1355	0.841	1158	0.65			0.31	197
	Δ [v-s]		[-74]		[-30]		[15]			
	Δ [v-s]		[-27]		[-12]					
Benzene	vapor	101	1380	0.848	1178	1.265	851	0.359	1.49	202
Benzene	solid	98	1325	0.97	1152	0.88	900	0.21	0.91	198
	Δ [v-s]		[-55]		[-26]		[45]			
4-Toluene	vapor	108	1380	0.523	1172	1.248	851	0.231	2.39	208
4-Toluene	solid	85	1325	0.96	1150	0.875	909	0.29	0.91	175
	Δ [v-s]		[-55]		[-22]		[58]			
2-Toluene	vapor	100	1370	1.1	1172	1.245	846	0.312	1.13	198
2-Toluene	solid	122	1311	1.03	1148	1.1	918	0.155	1.03	163
	Δ [v-s]		[-59]		[-24]		[72]			

TABLE 5.6a Infrared data for some NH and NH₂ vibrations for compounds containing SO₂NH₂ or SO₂NH groups in different physical phases

Amides	a.NH ₂ str. cm ⁻¹	s.NH ₂ str. cm ⁻¹	NH ₂ bend cm ⁻¹	Temperature	Physical phase
Methanesulfonamide	3470	3375	1552	280°C	vapor
	3335	~ 3255	~ 1568		KBr
	135	120	[-16]		vapor-KBr
Benzenesulfonamide	3480	3370	1551	280°C	vapor
	~ 3335	~ 3242	~ 1548		KBr
	145	128	[-17]		vapor-KBr
Benzenesulfonamide 2,4,6-trimethyl	3460	3360	1552		vapor
	3370	3258	1551		KBr
	90	102	1		vapor-KBr
NH str.					
<i>p</i> -Toluenesulfonamide	3419			280°C	vapor
N-butyl	~ 3370				KBr
	49				vapor-KBr
<i>p</i> -Toluenesulfonanilide	3402				vapor
					KBr
					vapor-KBr

In KBr it is NH₂:O₂S; str. or NH:O₂S str.

TABLE 5.7 Infrared data for secondary and tertiary sulfonamides

Compound R-SO ₂ -NH-R' R;R'	Phase	NH str. cm ⁻¹	A	a.SO ₂ str. cm ⁻¹	A	s.SO ₂ str. cm ⁻¹	A	SN str. cm ⁻¹	A	A[s.SO ₂ str.]/ A[a.SO ₂ str.]	[a.SO ₂ str.] /[s.SO ₂ str.] cm ⁻¹
CH ₃ ; C ₆ H ₅	vapor	3420	0.07	1360	0.17	1169	1.241	890	0.18	7.3	191
CH ₃ ; 2-NH ₂ -4-CH ₃ -C ₆ H ₃	vapor	3298	0.189	1325	0.67	1150	1.202	881	0.135	1.79	175
C ₆ H ₅ ; <i>n</i> -C ₄ H ₉	vapor	3420	0.062	1355	0.363	1170	1.21	840	0.09	3.33	185
4-CH ₃ -C ₆ H ₄ ; CH ₃	vapor	3422	0.09	1355	0.49	1175	1.248	825	0.35	2.55	180
4-CH ₃ -C ₆ H ₄ ; <i>n</i> -C ₄ H ₉	vapor	3418	0.083	1356	0.42	1169	1.246	839	0.138	2.97	187
4-CH ₃ -C ₆ H ₄ ; tert-C ₄ H ₉	vapor	3400	0.09	1344	0.58	1160	1.22	852	0.2	2.1	184
4-CH ₃ -C ₆ H ₄ ; C ₆ H ₅	vapor	3402	0.07	1403	0.54	1170	1.22	888	0.18	2.56	233
4-CH ₃ -C ₆ H ₄ ; C ₆ H ₅	solid	3255	0.33	1337	0.32	1160	1.07	920	0.25	3.34	177
	Δ [v-s]	[-1.47]		[-66]		[-10]		[32]			
R-SO ₂ -N(-CH ₃) ₂											
R											
CH ₃	vapor			1362	1.25	1165	1.049	770	0.7	0.84	197
CH ₃	liquid			1324	stg.	1142	stg.	770	mstg.		182
	Δ [v-l]			[-38]		[-23]		[0]			
4-CH ₃ -C ₆ H ₄	vapor			1365	0.7	1169	1.25	770	0.87	1.79	196
4-CH ₃ -C ₆ H ₄	solid			1334	stg.	1164	mstg.	815	m		
	Δ [v-s]			[-31]		[-5]		[45]			

TABLE 5.8 Infrared data for organic sulfonates

Compound	Phase	a.SO ₂ str. cm ⁻¹	A	s.SO ₂ str. cm ⁻¹	A	A[s.SO ₂ str.]/ A[a.SO ₂ str.]	[a.SO ₂ str.]- [s.SO ₂ str.] cm ⁻¹	a.COS str. cm ⁻¹	A	s.COS str. cm ⁻¹	A
CH ₃ -SO ₂ -O-R											
R											
CH ₃	vapor	1380	1.25	1190	1.15	0.92	190	1011	1.2	795	0.95
C ₂ H ₅	vapor	1378	1.25	1190	1.15	0.92	188	1020	0.76	790	0.47
<i>n</i> -C ₄ H ₉	vapor	1377	1.16	1185	1.25	1.08	192	950	1.25	800	0.47
<i>n</i> -C ₄ H ₉	liquid	1350	stg.	1173	mstg.		177	934	mstg.	807	m
	Δ [v-l]	[-27]		[-12]			[-15]	[-16]		[7]	
<i>n</i> C ₁₈ H ₃₇	vapor	1368	0.089	1190	0.17	1.91	178	960	0.087	810	0.04
C ₆ H ₅ -SO ₂ -O-R											
R											
CH ₃	vapor	1390	0.53	1195	1.25	2.36	195	1015	0.69	775	0.7
C ₂ H ₅	vapor	1391	0.619	1194	1.24	2	197	1019	0.65	770	0.41
<i>n</i> -C ₄ H ₉	vapor	1390	0.49	1194	1.24	2.53	196	950	0.57	789	0.28
4-CH ₃ -C ₆ H ₄ -SO ₂ - O-R											
R											
CH ₃	vapor	1389	0.531	1189	1.251	2.36	200	1010	0.68	752	0.781
C ₂ H ₅	vapor	1390	0.5	1189	1.24	2.48	201	1012	0.51	751	0.385
<i>n</i> -C ₄ H ₉	vapor	1390	0.275	1188	1.24	4.51	202	949	0.261	772	0.15
<i>n</i> -C ₄ H ₉	liquid	1355	1.14	1173	1.15	1.01	182	940	0.95	785	0.5
	Δ [v-l]	[-35]		[-15]				[-9]		[13]	

TABLE 5.9 Infrared data for organosulfonyl chlorides

Compound R-SO ₂ -Cl	Phase	a.SO ₂ str.	s.SO ₂ str.	S-Cl str.	CS str.	[a.SO ₂ str.]-	A[s.SO ₂ str.]/
		cm ⁻¹ (A)	cm ⁻¹ (A)	cm ⁻¹ (A)	cm ⁻¹ (A)	[s.SO ₂ str.] cm ⁻¹	A[a.SO ₂ str.]
CH ₃	vapor	1400 (1.240)	1189 (0.690)	540 (1.040)	746 (0.200)	211	0.56
CH ₃	liquid	1362 (1.059)	1170 (1.041)	530 (0.656)	742 (0.370)	192	0.98
	Δ [v-l]	[-38]	[-19]	[-10]	[-4]	[-19]	
C ₂ H ₅	vapor	1402 (1.250)	1177 (0.870)	541 (0.480)	704 (0.400)	225	0.7
Aryl-SO ₂ -Cl							
C ₆ H ₅	vapor	1400 (0.581)	1192 (0.679)	549 (0.459)		208	1.17
C ₆ H ₅	liquid	1372 (0.724)	1181 (0.770)	548 (0.810)		191	1.06
	Δ [v-l]	[-28]	[-11]	[1]		[-17]	
4-F-C ₆ H ₄	vapor	1401 (0.579)	1191 (0.910)	525 (0.485)		210	1.57
4-F-C ₆ H ₄	liquid	1372 (0.910)	1174 (0.815)	529 (0.775)		198	0.9
	Δ [v-l]	[-29]	[-17]	[14]		[-12]	
4-CH ₃ -C ₆ H ₄	vapor	1399 (0.836)	1189 (1.234)	533 (0.401)		210	1.48
4-CH ₃ -C ₆ H ₄	solid	1379 (0.940)	1189 (0.620)	530 (0.915)		190	0.66
		1364 (0.920)	1172 (0.670)			192	0.73
	Δ [v-s]	[-20]; [-35]	[0]; [-17]	[-33]		[-20]; [-18]	
2,5-(CH ₃) ₂ -C ₆ H ₃	vapor	1390 (0.650)	1179 (1.060)	562 (0.921)		211	1.63
2,5-(CH ₃) ₂ -C ₆ H ₃	liquid	1369 (0.965)	1171 (0.980)	569 (0.958)		198	0.81
	Δ [v-l]	[-21]	[-8]	[7]		[-13]	
4-Cl,3-NO ₂ -C ₆ H ₃ *	vapor	1408 (1.149)	1190 (1.250)	559 (0.411)		218	1.09
4-Cl,3-NO ₂ -C ₆ H ₃ *	solid	1382 (1.310)	1170 (1.040)	551 (0.810)		212	0.79
	Δ [v-s]	[-26]	[-20]	[-8]		[-6]	
2,3,4-(Cl) ₃ -C ₆ H ₂	vapor	1408 (1.250)	1172 (0.730)	599 (0.481)		236	0.58
2,4,5-(Cl) ₃ -C ₆ H ₂	vapor	1408 (0.850)	1189 (0.939)	560 (1.240)		219	1.1
2,4,5-(Cl) ₃ -C ₆ H ₂	liquid	1371 (1.010)	1170 (0.992)	561 (0.859)		201	0.98
	Δ [v-l]	[-37]	[-19]	[1]		[-18]	
		a.NO ₂ str.	s.NO ₂ str.			[a.NO ₂ str.]-	A[s.NO ₂ str.]
						[s.NO ₂ str.]	A[a.NO ₂ str.]
4-Cl,3-NO ₂ -C ₆ H ₃ *	vapor	1560 (0.620)	1350 (0.465)			210	0.75
4-Cl,3-NO ₂ -C ₆ H ₃ *	solid	1542 (1.310)	1360 (0.910)			182	0.69
	Δ [v-s]	[-18]	[10]			[-28]	

* reference 38.

* Sadtler Standard Infrared Spectra, Philadelphia, PA.

TABLE 5.9a Infrared data for organosulfonyl fluorides

Compound Aryl-SO ₂ F	Phase	asym.SO ₂ cm ⁻¹ (A)	sym.SO ₂ cm ⁻¹ (A)	SF str. cm ⁻¹ (A)	[asym.SO ₂]- [sym.SO ₂] cm ⁻¹	A[sym.SO ₂]/ A[asym.SO ₂]
C ₆ H ₅	vapor	1429 (0.718)	1221 (1.240)	782 (1.232)	208	1.73
C ₆ H ₅	liquid	1404 (1.100)	1204 (1.250)	780 (0.735)	200	1.14
	[v-l]	[25]	[17]	[2]	[8]	
4-CH ₃ -C ₆ H ₄	vapor	1430 (1.085)	1220 (1.240)	775 (1.095)	210	1.14
4-CH ₃ -C ₆ H ₄	solid	1399 (1.011)	1209 (0.920)	750 (0.905)	190	0.91
			1200 (9.30)			0.92
	[v-s]	[31]	[11]	[25]	[20]; [11]	
4-NH ₂ -C ₆ H ₄	vapor	1428 (0.608)	1218 (1.265)	777 (1.027)	210	2.08
3-NH ₂ -C ₆ H ₄	vapor	1430 (0.812)	1211 (1.245)	780 (0.976)	219	1.53
3-NH ₂ ,4-ClC ₆ H ₃	vapor	1431 (1.050)	1219 (1.150)	785 (1.250)	212	1.1
3-NH ₂ ,4-ClC ₆ H ₃	liquid	1399 (0.790)	1208 (0.639)	771 (1.020)	191	0.81
	[v-l]	[32]	[11]	[14]	[21]	
2-NH ₂ -C ₆ H ₄	vapor	1411 (0.598)	1204 (0.950)	785 (1.229)	207	1.59
2-NH ₂ -C ₆ H ₄	liquid	1384 (0.919)	1186 (0.919)	775 (0.690)	198	1
	[v-l]	[27]	[18]	[10]	[9]	
2-NO ₂ -C ₆ H ₄ * ¹	vapor	1438 (0.821)	1228 (1.240)	811 (0.808)	210	1.51
2-NO ₂ -C ₆ H ₄	liquid	1411 (1.124)	1210 (1.113)	800	201	0.99
	[v-l]	[18]	[11]	[11]	[9]	
3-NO ₂ -C ₆ H ₄ * ²	vapor	1440 (0.931)	1235 (1.131)	800 (0.932)	205	1.21
3-NO ₂ -C ₆ H ₄	liquid	1411 (0.770)	1208 (0.870)	790 (0.621)	203	1.13
	[v-l]	[29]	[27]	[10]	[2]	
3-NO ₂ -4-Cl-C ₆ H ₃ * ³	vapor	1441 (0.640)	1222 (1.240)	801 (0.850)	219	1.94
3-NO ₂ -4-Cl-C ₆ H ₃	liquid	1420 (0.680)	1214 (0.715)	796 (0.610)	206	1.05
	[v-l]	[21]	[8]	[5]	[13]	
		asym.NO ₂ str.	sym.NO ₂ str.	[a.NO ₂ str.]– [s.NO ₂ str.]	A[s.NO ₂ str.]/ A[a.NO ₂ str.]	
2-NO ₂ -C ₆ H ₄ * ¹	vapor	1568 (0.939)	1358 (0.349)	210	0.37	
2-NO ₂ -C ₆ H ₄	liquid	1543 (1.270)	1354 (0.974)	189		
	[v-l]	[25]	[4]	[21]		
3-NO ₂ -C ₆ H ₄ * ²	vapor	1551 (0.745)	1352 (0.750)	199	1.01	
3-NO ₂ -C ₆ H ₄	liquid	1530 (0.869)	1347 (0.830)	183	0.96	
	[v-l]	[21]	[5]	[16]		
3-NO ₂ -4-Cl-C ₆ H ₃ * ³	vapor	1562 (0.360)	1351 (0.264)	211	0.73	
3-NO ₂ -4-Cl-C ₆ H ₃	liquid	1545 (0.669)	1350 (0.619)	195	0.93	
	[v-l]	[17]	[1]	[16]		

*¹ reference 38*² reference 38*³ reference 38

TABLE 5.10 Infrared data for organosulfur compounds containing SO₄, SO₃, SO₂N, and SO₂X groups in different physical phases

Compound	a.SO ₂ str. cm ⁻¹ Vapor	s.SO ₂ str. cm ⁻¹ Vapor	Temperature	a.SO ₂ str. cm ⁻¹ Neat	a.SO ₂ str. cm ⁻¹ Neat	s.SO ₂ str. cm ⁻¹ Vapor-Neat	IR or cm ⁻¹ Vapor-Neat	Raman
Dimethyl sulfate	1401	1208	200 °C	1391	1200	10	17	IR
Methanesulfonate								
methyl	1380	1189	200 °C	1340	1169	40	20	IR
ethyl	1378	1188	240 °C	1344	1168	34	20	IR
Propanesultone	1395	1190	280 °C	1344	1165	51	25	IR
<i>p</i> -toluenethiolsulfonic acid, S-methyl ester	1360	1155	175 °C	~ 1319	~ 1134	41	21	IR
Methanesulfonamide	1382	1170	280 °C	1308 KBr	1140	42	30	IR
Benzenesulfonamide	1380	1175	280 °C	1328 KBr	1151	52	24	IR
Benzenesulfonamide 2,4,6-trimethyl	1368	1170	280 °C	1337 KBr	1152	31	18	IR
<i>p</i> -Toluenesulfonamide N-butyl	1410	1170	280 °C	1315	1150	95	20	IR
<i>p</i> -Toluenesulfonanilide	1404	1170	275 °C	1336	1160	68	10	IR
Methanesulfonyl chloride	1393	1189		1375	1172	18	17	IR; R
Benzenesulfonyl chloride	1400	1192		1381	1177	18	15	IR; R
<i>p</i> -Toluenesulfonyl chloride	1399	1188	240 °C	1378	1188 or 1175	21	0 or 13	IR
<i>p</i> -Bromobenzenesulfonyl chloride	1401	1180	200 °C	1370	1162	31	18	IR
		1200			1183		17	IR
<i>m</i> -fluorosulfonylbenzene	1410	1192	200 °C	1390	1184	20	8	IR
sulfonyl chloride	1442	1228		1430	1221	12	7	IR
Benzenesulfonyl fluoride	1429	1221		1411	1215	18	6	IR; R
<i>p</i> -Toluenesulfonyl fluoride	1430	1220	280 °C	1400	1200	30	20	IR

TABLE 5.11 Infrared data for sulfones and sulfoxides in different physical phases

Compound	a.SO ₂ str.	s.SO ₂ str.	Temperature	a.SO ₂ str.	s.SO ₂ str.	a.SO ₂ str.	s.SO ₂ str.
	cm ⁻¹	cm ⁻¹		cm ⁻¹	cm ⁻¹	cm ⁻¹	cm ⁻¹
	Vapor	Vapor		Neat	Neat	Vapor-Neat	Vapor-Neat
Sulfone							
Di-butyl	1336	1142	280 °C	1321CS ₂	1132CS ₂	15* ¹	10* ¹
Methyl <i>p</i> -tolyl	1350	1164	220 °C	1300	1147	50	17
Di-phenyl	1348	1165	280 °C	1324CS ₂	1160CS ₂	24* ¹	5* ¹
Di-phenyl	1348	1165	280 °C	1311	1159	37	6
Phenyl <i>p</i> -tolyl	1347	1167	240 °C	1309	1155	38	12
Di-(<i>P</i> -tolyl)	1348	1165	280 °C	1327CS ₂	1158CS ₂	21* ¹	7* ¹
Sulfoxide							
	SO str.		SO str.	SO str.	SO str.	SO str.	
	cm ⁻¹	Temperature	cm ⁻¹	cm ⁻¹	cm ⁻¹	cm ⁻¹	
	Vapor		Neat	Vapor-Neat	CCL ₄ soln.	Vapor-CCL ₄ soln.	
Dimethyl	1100	200 °C	1050	50	1070	30	
Dimethyl-d ₃	1095	200 °C	1060; 1031	35; 64	1068	27	
Phenyl methyl	1102	160 °C	1050	52	1057	45	
<i>p</i> -Bromophenyl methyl	1101	280 °C	1050	51	—	—	
Di-phenyl	1100	280 °C	1046	~ 54	1052	48	
Di-(<i>p</i> -tolyl)	1098	280 °C	1040	~ 58			
Di-(<i>o</i> -tolyl)	1088	280 °C	1028 KBr	~ 60* ²	—	—	
Di-(<i>p</i> -chlorophenyl)	1090	280 °C	1042 Nujol	~ 48* ³	—	—	

*¹ CS₂ soln.*² KBr.*³ Nujol.TABLE 5.12 Infrared data for N-sulfinyl-4-X-anilines and N,N'-disulfinyl-*p*-phenylenediamine

N-Sulfinyl 4-X-aniline X	asym. N=S=O	sym. N=S=O	[asym. N=S=O]- [sym. N=S=O]	asym. N=S=O	sym. N=S=O
	CS ₂ soln. cm ⁻¹	CS ₂ soln. cm ⁻¹	CS ₂ soln. cm ⁻¹	vapor-CS ₂ soln. cm ⁻¹	vapor-CS ₂ soln. cm ⁻¹
CH ₃ -O	1254	1158	96		
Cl	1272	1162 or 1173	110 or 99		
CH ₃	1283	1157	126		
H	1274; [1298 vapor]	1162; [1176 vapor]	114; [112 vapor]	24	14
NO ₂	1290	1175	115		
	Nujol mull cm ⁻¹	Nujol mull cm ⁻¹	Nujol mull cm ⁻¹		
N,N'-disulfinyl <i>p</i> -phenylenediamine	1271	1166	105		

Halogenated Hydrocarbons

Halogenated Methanes	120
1-Haloalkanes	121
2-Haloalkanes	122
Tertiary Butyl Halides	122
Ethylene Propylene, 1,2-Epoxypropane, and Propadiene Halogenated Analogs	125
Halopropadienes	127
Halogenated Methanes with T_d and C_{3v} Symmetry	127
References	128

Figures

Figure 6-1	129 (120)	Figure 6-21	151 (125)
Figure 6-2	130 (120)	Figure 6-22	152 (125)
Figure 6-3	131 (121)	Figure 6-23	153 (125)
Figure 6-4	132 (122)	Figure 6-24	154 (125, 127)
Figure 6-5	133 (123)	Figure 6-25	154
Figure 6-6	134	Figure 6-26	155
Figure 6-7	135	Figure 6-27	155
Figure 6-8	136	Figure 6-28	156
Figure 6-9	137	Figure 6-29	156
Figure 6-10	138	Figure 6-30	157
Figure 6-11	139	Figure 6-31	157
Figure 6-12	140	Figure 6-32	157
Figure 6-13	141	Figure 6-33	158
Figure 6-14	142 (125)	Figure 6-34	158
Figure 6-15	143 (125)	Figure 6-35	159
Figure 6-16	144, 145 (125)	Figure 6-36	160
Figure 6-17	146, 147 (125)	Figure 6-37	161
Figure 6-18	148 (125)	Figure 6-38	162
Figure 6-19	149 (125)	Figure 6-39	163
Figure 6-20	150 (125)		

Tables

Table 6-1	164 (120, 127)	Table 6-5	168 (123, 127)
Table 6-2	164 (121, 127)	Table 6-6	169 (123, 127)
Table 6-2a	165 (121, 127)	Table 6-7	170 (123, 127)
Table 6-3	166 (121, 127)	Table 6-8	171 (125)
Table 6-4	167 (122, 127)		

*Numbers in parentheses indicate in-text page reference.

HALOGENATED METHANES

The IR and Raman data for halogenated hydrocarbons have been summarized (1, 2), and some examples will be discussed in this chapter.

Table 6.1 lists vapor-phase IR data for the methyl halides (also study Figs. 6.1–6.3). The ν C–X stretching frequencies for the F, Cl, Br, and I analogs occur at 1044, 732, 608, and 530 cm^{-1} , respectively. These ν C–X vibrations decrease in frequency as the mass of the halogen atom increases, as the C–X bond length increases, as the value of the inductive parameter σ' for X decreases, and as the value of the C–X force constants decreases in value in the order F through I. In general, other carbon-halogen stretching frequencies behave similarly. However, in many cases the situation becomes more complex due to the presence of rotational conformers, and also due to the presence of ν asym. CX_n and ν sym. CX_n vibrations.

The methylene halides CH_2X_2 exhibit ν asym. CX_2 and ν sym. CX_2 vibrations. The ν asym. CX_2 (F–I) decrease in frequency in the order 1180, 742, 640, and 570 cm^{-1} , respectively (also study Figs. 6.4 and 6.5). The ν sym. CX_2 (F–I) decrease in frequency in the order 1110, 704, 577, and 480 cm^{-1} , respectively. It is noted that in all cases the ν asym. CX_2 mode always occurs at a higher frequency than does the ν sym. CX_2 mode for each CX_2 analog. Moreover, the Raman band intensity for ν sym. CX_2 is higher than the Raman band intensity for ν asym. CX_2 and in both cases of ν CX_2 the Raman band intensities increase in the order F, Cl, Br, and I (3).

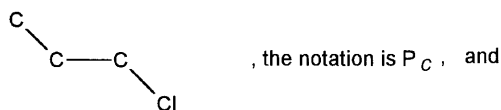
Comparison of the ν asym. CX_2 and ν sym. CX_2 frequency shifts in going from the vapor phase to the liquid phase shows that the ν sym. CX_2 vibration shifts more in frequency (9 to -30 cm^{-1}) compared to ν asym. CX_2 (-1 to -5 cm^{-1}). In other cases discussed in previous chapters, the opposite spectra-structure correlation has been observed. The asymmetric vibration also shifted more in frequency than did the symmetric vibration with change in physical phase. In the case of the CH_2X_2 compounds, the ν asym. CX_2 vibrations occur at lower frequency in the liquid phase than in the vapor phase. However, the ν sym. CX_2 vibration for CH_2Cl_2 occurs at a higher frequency in the liquid phase than in the vapor phase, while for CH_2Br_2 and CH_2I_2 the ν sym. CX_2 vibrations occur at increasingly lower frequencies in the liquid phase than in the vapor phase, progressing in the order of Br_2 to I_2 . In other words, it is apparently easier for ν sym. X_2 for the Br_2 and I_2 analogs to vibrate in the liquid phase than in the vapor phase. Mass and the decreasing C–X force constants progressing in the series F_2 through I_2 apparently account for this frequency behavior during expansion and contraction of surrounding molecules during the ν sym. CX_2 modes. In the case of ν asym. CX_2 , there is an equal tradeoff in energy as the one C–X bond expands toward neighboring molecules and the other C–X bond contracts from neighboring molecules. Hence, there is not as much of a shift in frequency with a change in physical phase for ν asym. CX_2 as there is for ν sym. CX_2 . With a lesser force constant for C–Br and C–I, it is relatively easier for the C–Br or C–I bonds to vibrate without exerting as much pressure against neighboring molecules in the liquid state.

Table 6.2 lists IR and Raman data for trihalomethane and tetrahalomethane (also study Figs. 6.6 through 6.12). The ν asym. F_3 vibration for CHF_3 and the ν asym. CF_4 vibration for CF_4 occur at 1376 cm^{-1} and 1283 cm^{-1} , respectively. The ν sym. F_3 vibration for CHF_3 and the ν sym. F_4 vibration for CF_4 occur at 1165 cm^{-1} and 908 cm^{-1} , respectively. The ν asym. CX_4 mode for the CF_4 , CCl_4 , and CBr_4 occurs at 1283, 797, and 671 cm^{-1} , respectively. In the liquid phase, the ν sym. CX_4 mode for CF_4 through Cl_4 occurs at 908, 790, 662, and 560 cm^{-1} , respectively.

Table 6.2a lists a comparison of CX, CX₂, CX₃, and CX₄ stretching frequencies. The C–F_n, C–Cl_n, C–Br_n, and C–I_n stretching frequencies in this methane series occur in the regions 908–1376 cm⁻¹, 667–797 cm⁻¹, 541–662 cm⁻¹, and 480–572 cm⁻¹, respectively. Moreover, the ν CX₂ vibrations occur at higher and lower frequencies than is the case for the ν C–X vibrations. The ν asym. CX₃ vibrations occur at higher frequencies than those of the ν asym. CX₂ vibrations. The other ν CX_n modes do not correlate as well as the ones just discussed.

1-HALOALKANES

Haloalkanes exist as rotational conformers, and Shipman *et al.* have specified the notation for describing these rotational conformers (4). The notation P, S, and T denote primary, secondary and tertiary carbon atoms to which the halogen atom is joined. Atom X is joined to the β -carbon atom in a trans position to the α -halogen atom in a zig-zag plane together with subscript C or H for the trans X atom denotes the specific rotational conformer. Applying this nomenclature for the planar skeleton trans rotational conformer for *n*-propyl chloride,



for the gauche skeleton rotational conformer,



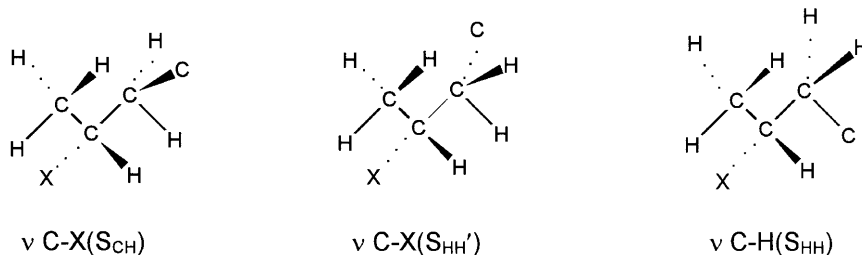
Table 6.3 lists vapor- and liquid-phase IR data for the carbon-halogen stretching frequencies for 1-haloalkanes. The ν CCl (P_c rotational conformers) for the 1-chloroalkanes (C₃–C₁₈) occur in the region 738–750 cm⁻¹ in the vapor phase and in the region 732–758 cm⁻¹ in the liquid phase. The ν CCl P_H gauche (skeletal rotational conformer) occurs in the region 660–664 cm⁻¹ in the vapor phase and in the region 650–659 cm⁻¹ in the liquid phase. Study of the absorbance data for A(ν CCl P_c)/A(ν CCl P_H) for these 1-chloroalkanes shows that the ratio is less in the liquid phase than in the vapor phase. (Another band in this region in the case of the 1-chloroalkanes results from (CH₂)_n rocking.) These data show that the concentration of P_c and P_H rotational conformers change with change in phase. Assuming that the extinction coefficient for the absorbance values are equal for both the P_c and P_H conformers, the concentrations for 1-chloropropane are 55.6% P_c and 44.4% P_H in the vapor phase and 49.1% P_c and 50.9% P_H in liquid phase.

In the case of 1-bromoalkanes, C₄ through C₁₉, ν CBr(P_c) occurs in the region 645–653 cm⁻¹, and ν CBr(P_H) occurs in the region 562–572 cm⁻¹ in the vapor phase. In all cases, these ν CBr modes occur at lower frequency in the liquid phase.

In the case of 1-iodoalkanes, C_3 – C_{16} , the ν Cl(P_c) rotational conformer (P_c) occurs in the region 591 – 598 cm^{-1} and the ν Cl(P_H) rotational conformer occurs in the region 500 – 505 cm^{-1} in the vapor phase. Both ν Cl(P_c) and ν Cl(P_H) occur at lower frequency in the liquid phase and the concentration of the rotational conformer P_c decreases in going from the vapor to the liquid phase. 1-Fluorodecene exhibits ν CF(P_c) at 1050 cm^{-1} and ν CF(P_H) at 1032 cm^{-1} in the vapor phase and ν CF(P_c) at 1042 and ν CF(P_H) at 1005 cm^{-1} in the liquid phase.

2-HALOALKANES

The 2-haloalkanes exist as three rotational conformers, and these are S_{CH} , $S_{HH'}$, and S_{HH} . Vapor- and liquid-phase IR data are listed in Table 6.4 for 2-halobutane and tert-butyl halide. These data for the 2-halobutenes are also shown here under the rotational conformer for which the ν CX vibration is assigned.



	Vapor cm^{-1}	Liquid cm^{-1}	Vapor cm^{-1}	Liquid cm^{-1}	Vapor cm^{-1}	Liquid cm^{-1}
Cl (5)	680	670	625	628	592	609
Br (2)	612	605	529	525	478	480
I (2)	580	570	484	479	—	454

The H' notation is used to specify a rotation of the carbon skeleton away from the zigzag carbon plane at the 3-position where the trans hydrogen is located. In the S_{HH} conformer, the first four carbon atoms are in a planar zigzag configuration while only the first three carbon atoms are in a planar zigzag configuration in the case of conformer $S_{HH'}$.

TERTIARY BUTYL HALIDES

In the liquid phase the tert-butyl halides exhibit ν C–X(T_{HHH}) at Cl (570 cm^{-1}), Br (520 cm^{-1}), and I (492 cm^{-1}). In the case of 2-halo-2-methylbutanes, ν CX(T_{HHH}) occurs at Cl (566 cm^{-1}), Br (510 cm^{-1}), and ν CX(T_{CHH}) occurs at Cl (621 cm^{-1}), Br (577 cm^{-1}) (2).

Table 6.5 lists vapor- and liquid-phase IR data for 1-halocycloalkanes. 1-Halocycloalkanes containing four or more ring carbon atoms can exist in an equatorial or axial configuration as presented here for 1-halocyclohexanes. In general, the ν CX(S_{cc}) vibrations



occur at higher frequencies than ν CH($S_{H'H'}$) vibrations. In the case of 1-halocyclohexane in the vapor phase ν CX(S_{cc}) occurs at 740 cm^{-1} (Cl), 692 cm^{-1} (Br), and 664 cm^{-1} (I), and for ν CX($S_{H'H'}$) it occurs at 690 cm^{-1} (Cl), 661 cm^{-1} (Br), and 635 cm^{-1} (I). The frequency separation between ν CX(S_{cc}) and ν CX($S_{H'H'}$) decrease, progressing in the series Cl through I in both the vapor and liquid phases, where

vapor is Cl (50 cm^{-1}), Br (31 cm^{-1}), and I (29 cm^{-1}), and
liquid Cl (48 cm^{-1}), Br (27 cm^{-1}), and I (18 cm^{-1}).

In addition, study of the absorbance ratios for (A) ν CX($S_{H'H'}$) shows that their concentration changes in going from the vapor to the liquid state. The concentration of conformer S_{cc} is higher than the concentration of conformer $S_{H'H'}$ in the vapor phase than in the liquid phase. If we assume for purposes of comparison that the extinction coefficients for (A) for each conformer are identical in both the liquid and vapor states, the following calculations can be performed for 1-halocyclohexane:

	Vapor % ν CX(S_{cc})	Vapor % ν CS($S_{H'H'}$)	Liquid % ν CX(S_{cc})	Liquid % ν CX($S_{H'H'}$)
Cl	72.3	27.7	70.3	29.7
Br	78.1	21.9	65.3	34.7
I	84.2	15.8	72.9	27.1

In the vapor phase, there is only IR evidence for the presence of ν CX(S_{cc}) for 1-halocyclopentane and their ν CX(S_{cc}) frequencies occur at 620 cm^{-1} (Cl), 520 cm^{-1} (Br), 476 cm^{-1} (I). In the liquid phase ν CCl($S_{H'H'}$) is assigned to a very weak Raman band at 588 cm^{-1} (8). No spectral evidence is reported for the presence of ν CBr($S_{H'H'}$) or ν CH($S_{H'H'}$) conformers.

Table 6.6 lists vapor- and liquid-phase IR data for primary dihaloethane through dihalohexane. These P,P-dihaloalkanes also exist as rotational conformers. It is interesting to compare the highest ν CX vapor-phase frequency in each series:

	ν CCl cm ⁻¹	ν CBr cm ⁻¹	ν Cl cm ⁻¹	
1,2-dihaloethane	730	594	485*	(also study Fig. 6.13)
1,3-dihalopropane	740	655	602	
1,4-dihalobutane	778	659	599	
1,5-dihalopentane	748	654	584*	
1,6-dihalopentane	740	654	600	
Range:	730-778	594-659	485*-602	

* Liquid.

These ν CX frequencies are affected by the number of (CH₂)_n groups between the two CH₂X groups. The ν CX frequencies increase in the order $n = 0, 1, 2$, and then decrease or stay relatively constant in the order $n = 3, 4$.

It is also interesting to compare the lowest ν CX vapor-phase frequency in each series:

	ν CCl cm ⁻¹	ν C Br cm ⁻¹	ν Cl cm ⁻¹
1,2-dihaloethene	660	545*	—
1,3-dihalopropane	660	559	526
1,4-dihalobutane	660	572	505
1,5-dihalopentane	662	571	492*
1,6-dihalohehexane	660	570	509
Range:	660-662	545-572	492*-526

* Liquid.

The ν CX rotational conformer that occurs between the high and low ν CX rotational conformer is not noted in all of the spectra studied. In this case only the liquid-phase data are compared for the intermediate ν CX rotational conformer.

	ν CCl*	ν C Br*	ν Cl*
	cm ⁻¹	cm ⁻¹	cm ⁻¹
1,2-dihaloethane	662	—	—
1,3-dihalopropane	—	585	—
1,4-dihalobutane	735	—	—
1,5-dihalopentane	720	—	604

* Liquid.

A study of the absorbance ratios in Table 6.6 shows that the concentrations of these conformers change with their physical phase. Take for example, 1,3-dibromopropane (assume the extinction coefficient for (A) is equal). Then the % concentrations of the 3-rotational conformers in the vapor and liquid phases are listed here for 1,3-dibromopropane.

Rotational Conformer, cm^{-1}	Vapor Phase %	Liquid Phase %	Rotational Conformer, cm^{-1}
655	30.5	24.8	645
599	26.5	31.4	585
559	43.0	43.8	543

Table 6.7 lists Raman data for the methyl halides and IR and Raman data for tetrabromoalkanes. Vapor-phase IR data for the ν CX frequencies are presented in Table 6.1. Tentative assignments for the ν CBr_2 and ν CBr vibrations are compared here.

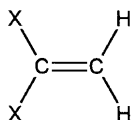
	ν_a CBr_2 cm^{-1}	ν_a CBr cm^{-1}	ν_s CBr_2 cm^{-1}
1,1,2,2- Br_4 ethane	714	664	537
	ν CBr cm^{-1}	ν CBr cm^{-1}	ν CBr cm^{-1}
1,2,3,4- Br_4 butane	702	567	532

ETHYLENE, PROPYNE, 1,2-EPOXYPROPANE, AND PROPADIENE HALOGENATED ANALOGS

Table 6.8 lists carbon halogen stretching frequencies for ethylene, propyne, 1,2-epoxypropane, and propadiene analogs. The first six examples, 3-halopropene through 1,3-dihalopropyne all contain an isolated $\text{CH}_2\text{-X}$ group. (Study Figs. 6.14 through 6.24.) The ranges for ν CF , ν CCl , ν CBr , and ν Cl for the CH_2X group are listed here.

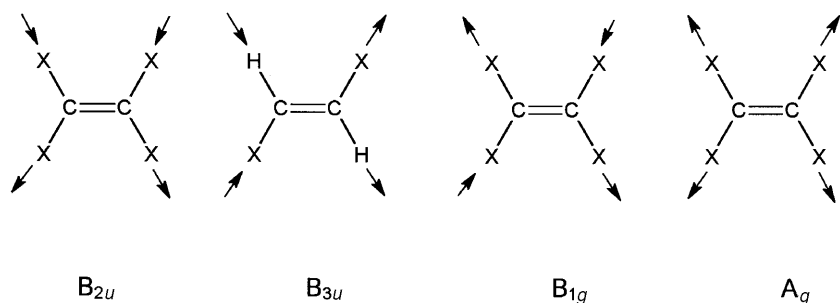
ν CF cm^{-1}	ν CCl cm^{-1}	ν CBr cm^{-1}	ν Cl cm^{-1}
989–1006	695–740	613–691	570–670

The ν CX vibrations for 1-fluoroethylene (vinyl fluoride) and 1-chloroethylene (vinyl chloride) are assigned at 1157cm^{-1} and 719cm^{-1} , respectively. In the case of the 1,1-dihaloethylenes,



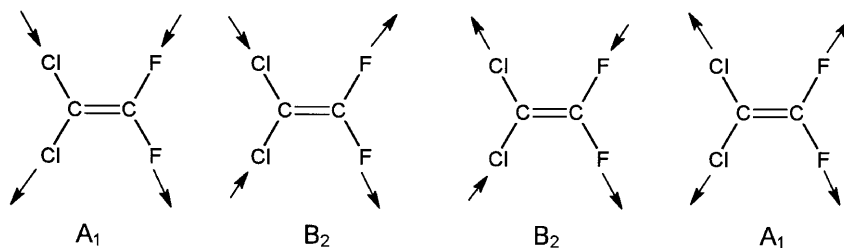
the two vibrations are ν asym. CX_2 and ν sym. CX_2 . These molecules have C_{2v} symmetry, and ν asym. CX_2 vibration belongs to the B_2 symmetry species and the ν sym. CX_2 vibration belongs to the A_1 symmetry species. Both of these vibrations decrease in frequency, progressing in the series CF_2CH_2 through CBr_2CH_2 ; ν asym. CX_2 occurs in the region $1301\text{--}698\text{ cm}^{-1}$, and ν sym. CX_2 occurs in the region $922\text{--}474\text{ cm}^{-1}$. The compounds, 1-bromo-1-chloroethylene, has C_s symmetry, and both modes belong to the A' symmetry species (study Figs. 6.25 and 6.28) (19).

The tetrahaloethylenes have ν_h symmetry, and the four C_2X_4 carbon halogen stretching vibrations are depicted here (see Figs. 6.36 through 6.39).



The B_{2u} and B_{3u} C_2X_4 stretching vibrations are allowed in the IR, and the B_{1g} and A_g C_2X_4 stretching vibrations are allowed in the Raman. In the series C_2F_4 through C_2Br_4 , the B_{2u} ν C_2X_4 mode occurs in the region $909\text{--}1340\text{ cm}^{-1}$ and the B_{3u} ν C_2X_4 mode occurs in the region $632\text{--}875\text{ cm}^{-1}$.

In the case of 1,1-dichloro-2,2-difluoroethylene, the molecular symmetry is C_{2v} , and the two A_1 and two B_2



$C_2Cl_2F_2$ stretching vibrations are IR active. These four modes are assigned in the region $890\text{--}1219\text{ cm}^{-1}$.

The ethylenes of form C_2X_3Y have C_s symmetry. The four C_2X_3Y stretching frequencies belong to the A' symmetry species. Trichloroethylene has three C_2Cl_3 stretching frequencies and one ν CH mode. Three of the C_2X_3Y stretching vibrations occur in the ranges $1329\text{--}1330\text{ cm}^{-1}$, $1202\text{--}1211\text{ cm}^{-1}$, and $1025\text{--}1052\text{ cm}^{-1}$ for both the C_2F_3Cl and C_2F_3Br analogs, and they occur in the ranges $931\text{--}1181\text{ cm}^{-1}$, $852\text{--}987\text{ cm}^{-1}$, and $639\text{--}869\text{ cm}^{-1}$ for both C_2Cl_3F and C_2HCl_3 .

HALOPROPADIENES

The 1-halopropadienes have C_s symmetry and the ν CX vibration decrease in frequency, progressing in the series Cl, 767 cm^{-1} , Br, 681 cm^{-1} , and I, 609 cm^{-1} (study Figs. 6.29–6.35). Evidently these ν CX vibrations are complex, because ν CBr for 1-bromopropadiene-1-d occurs at 636 cm^{-1} while ν CBr for 1-bromopropadiene occurs at 681 cm^{-1} , a shift of 45 cm^{-1} by substitution of D for H on the same C–Br carbon atom. The ν CF vibration for 1-fluoropropadiene is estimated to occur at 1050 cm^{-1} (23).

Halogen atoms joined to a carbon–carbon triple bond occur at relatively low frequency. In the case of 1-halopropyne and 1,3-dihalopropyne the $\nu\equiv\text{C}-\text{X}$ vibrations occur in the range Cl, $574\text{--}617\text{ cm}^{-1}$, Br, $464\text{--}512\text{ cm}^{-1}$, and I, 403 cm^{-1} (study Figs. 6.30 and 6.39) (16, 24).

Figure 6.24 shows the approximate skeletal bending modes of propyne, 3-halopropynes, and 1,3-dihalopropynes. Vibrations involving bending of the carbon–halogen bonds occur at low frequencies (25).

HALOGENATED METHANES WITH T_d AND C_{3v} SYMMETRY

Compounds for form CX_4 have T_d symmetry. The ν asym. CX_4 mode is triply degenerate and decreases in frequency, progressing in the series CF_4 , 1265 cm^{-1} , CCl_4 , 776 cm^{-1} , and CB_4 , 672 cm^{-1} . The ν sym. CX_4 mode decreases in frequency, progressing in the series CF_4 , 904 cm^{-1} , CCl_4 , 458 cm^{-1} , and CBr_4 , 267 cm^{-1} (26).

Compounds of form CX_3Y have C_{3v} symmetry. The ν asym. CX_3 mode is doubly degenerate. These molecules also have a ν sym. CX_3 vibration and a ν CY vibration. These three stretching frequencies also decrease in frequency, progressive in the order F through Br.

Compound: (22)	ν asym. CX_3 cm^{-1}	ν sym. X_3 cm^{-1}	ν CY cm^{-1}
CF_3Cl	1210	1101	780
CF_3Br	1201	1080	759
CCl_3F	840	930	1080

Study of Tables 6.1 through 6.8 shows that different ν CX frequencies overlap in several cases in the Cl through I series. More extensive coverage of the vibrational spectra and frequencies of the halogenated alkanes can be found in References 1–10.

Standard vapor and neat IR spectra and standard Raman spectra of these halogenated materials as well as other organic compounds are readily available from Bio-Rad Sadtler Division, and these spectra are valuable in identifying unknown chemical compositions.

Figures 6.1 through 6.39 are included as a convenience to the reader, since some of the data discussed in this chapter were obtained from these IR and Raman spectra.

REFERENCES

1. Lin-Vien, D., Colthup, N. B., Fateley, W. G., and Grasselli, J. G. (1991). *The Infrared and Raman Characteristic Frequencies of Organic Molecules*. Boston: Academic Press, Inc., p. 29.
2. Nyquist, R. A. (1984). *The Interpretation of Vapor-Phase Infrared Spectra: Group Frequency Data*. Philadelphia: Bio-Rad Laboratories, Sadtler Div.
3. Schrader, B. (1989). *Raman/Infrared Atlas of Organic Compounds*. 2nd Edition, New York, VCH-Verl.-Ges. Weinheim.
4. Shipman, J. J., Folt, V. L., and Krimm, S. (1962). *Spectrochim. Acta*, **18**: 1603.
5. George, W. O., Goodfield, J. E., and Maddams, W. F. (1985). *Spectrochim. Acta*, **41A**: 1243.
6. Rothschild, W. G. (1966). *J. Chem. Phys.*, **45**: 1214.
7. Durig, J. R., Karriker, J. M., and Wertz, D. M. (1969). *J. Mol. Spectrosc.*, **31**: 237.
8. Ekejiuba, I. O. C. and Hallam, H. E. (1969). *Spectrochim. Acta*, **26A**: 59.
9. Rey-Lafon, M., Rouffi, C., Camiade, M., and Forel, M. (1970). *J. Chim. Phys.*, **67**: 2030.
10. Wurrey, C. J., Berry, R. J., Yeh, Y. Y., Little, T. S., and Kalasinsky, V. J. (1983). *J. Raman Spectrosc.*, **14**: 87.
11. McLachlan, R. D. and Nyquist, R. A. (1968). *Spectrochim. Acta*, **24A**: 103.
12. Nyquist, R. A., Putzig, C. L., and Skelly, N. E. (1986). *Appl. Spectrosc.*, **40**: 821.
13. Evans, J. C. and Nyquist, R. A. (1963). *Spectrochim. Acta*, **19**: 1153.
14. Nyquist, R. A., Reder, T. L., Ward, G. F., and Kallos, G. J. (1971). *Spectrochim. Acta*, **27A**: 541.
15. Nyquist, R. A., Stec, F. F., and Kallos, G. J. (1971). *Spectrochim. Acta*, **27A**: 897.
16. Nyquist, R. A., Johnson, A. L., and Lo, Y.-S. (1965). *Spectrochim. Acta*, **21**: 77.
17. Nyquist, R. A. (1984). *The Interpretation of Vapor-Phase Infrared Spectra: Group Frequency Data*. Philadelphia: Bio-Rad Laboratories, Sadtler Div.
18. Nyquist, R. A. and Thompson, J. W. (1977). *Spectrochim. Acta*, **33A**: 63.
19. Joyner, P. and Glockler, G. (1952). *J. Chem. Phys.*, **20**: 302.
20. Winter, F. (1970). *Z. Naturforsch.*, **25a**: 1912.
21. Scherer, J. R. and Overend, J. (1960). *J. Chem. Phys.*, **32**: 1720.
22. Nyquist, R. A. (1989). *The Infrared Spectra Building Blocks of Polymers*. Philadelphia: Bio-Rad, Sadtler Div.
23. Nyquist, R. A., Lo, Y.-S., and Evans, J. C. (1964). *Spectrochim. Acta*, **20**: 619.
24. Nyquist, R. A. (1965). *Spectrochim. Acta*, **21**: 1245.
25. Herzberg, G. (1945). *Molecular Spectra and Molecular Structure II. Infrared and Raman Spectra of Polyatomic Molecules*. New York: Van Nostrand Co., Inc., p. 167.
26. Erley, D. S. and Blake, B. H. (1965). *Infrared Spectra of Gases and Vapors, Vol. II. Grating Spectra*. The Dow Chemical Co.

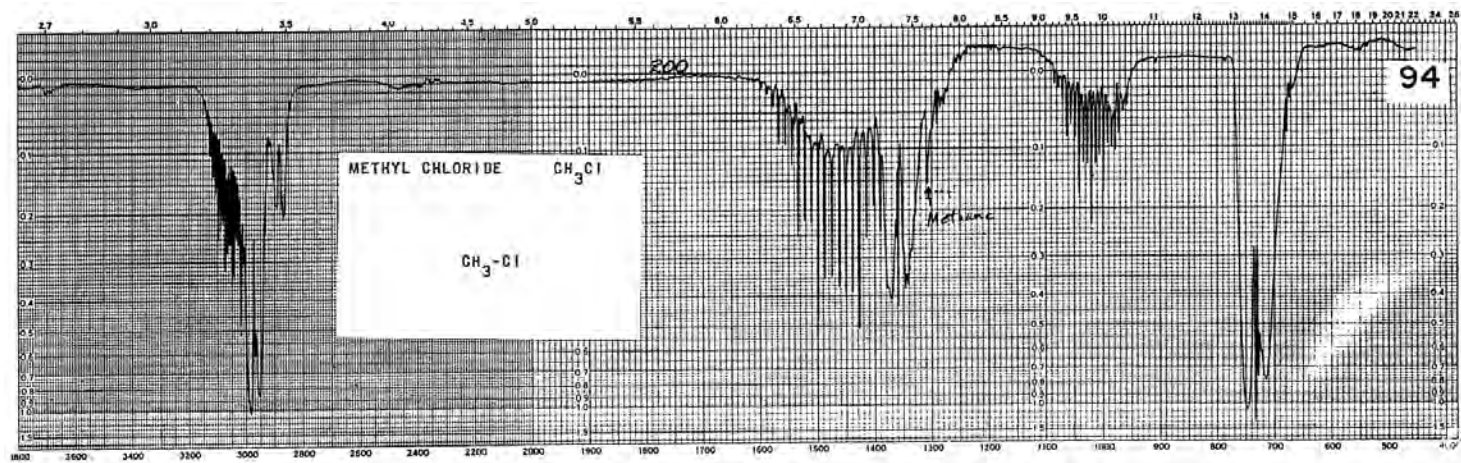


FIGURE 6.1* Methyl chloride (200-mm Hg sample) (26).

*Those vapor-phase infrared spectra figures for Chapter 6 with an asterisk following the figure number have a total vapor pressure of 600-mm Hg with nitrogen (N₂), in a 5-cm KBr cell. The mm Hg sample is indicated in each figure.

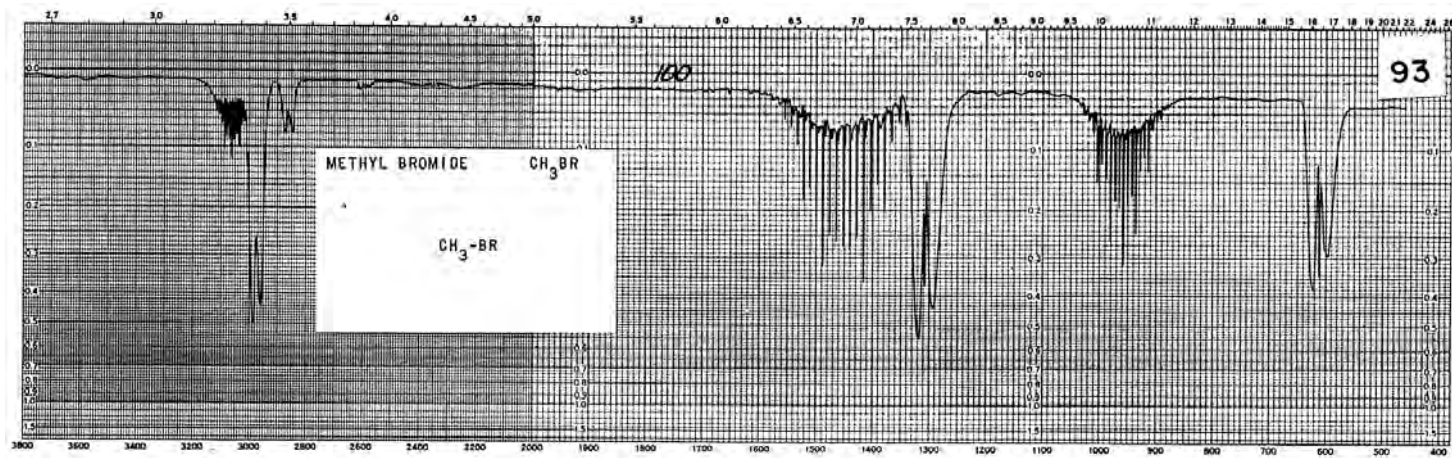


FIGURE 6.2* Methyl bromide (100-mm Hg sample) (26).

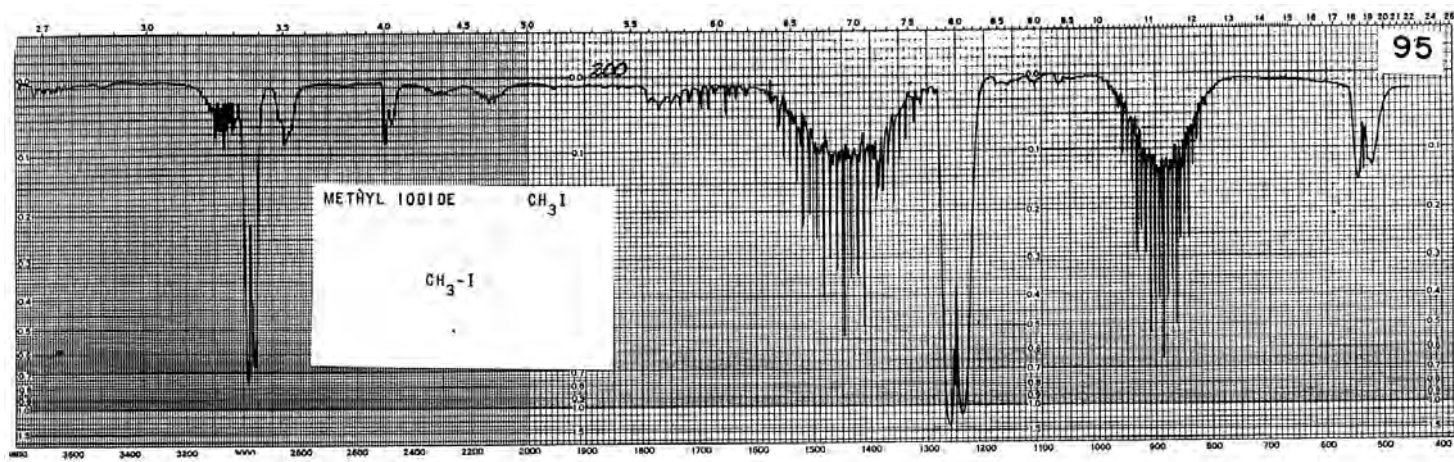


FIGURE 6.3* Methyl iodide (200-mm Hg sample) (27).

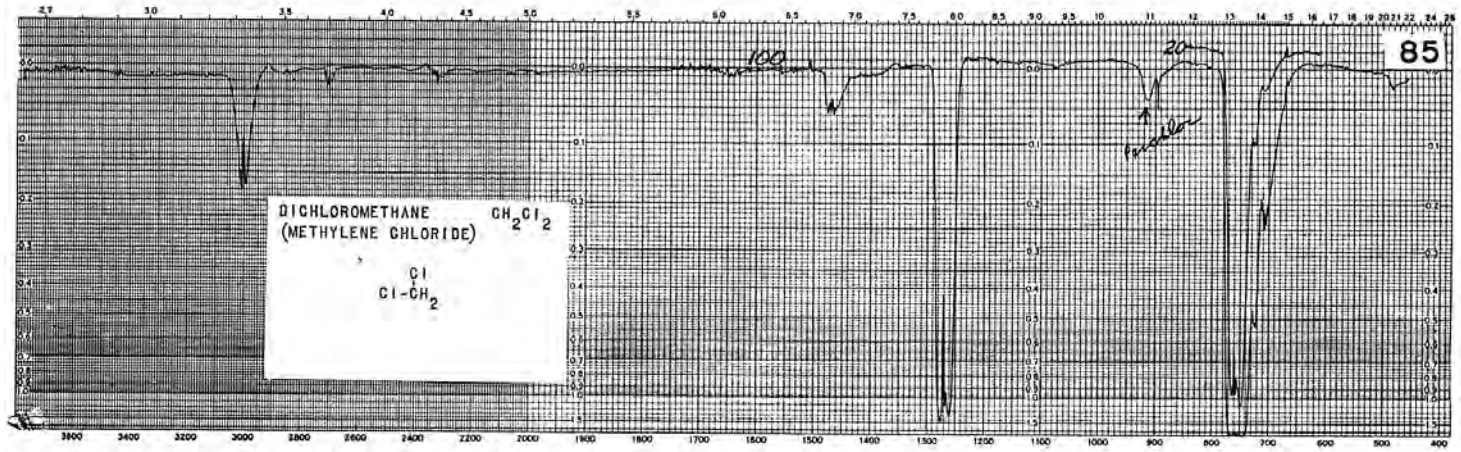


FIGURE 6.4* Methylene chloride (20- and 100-mm Hg sample) (26).

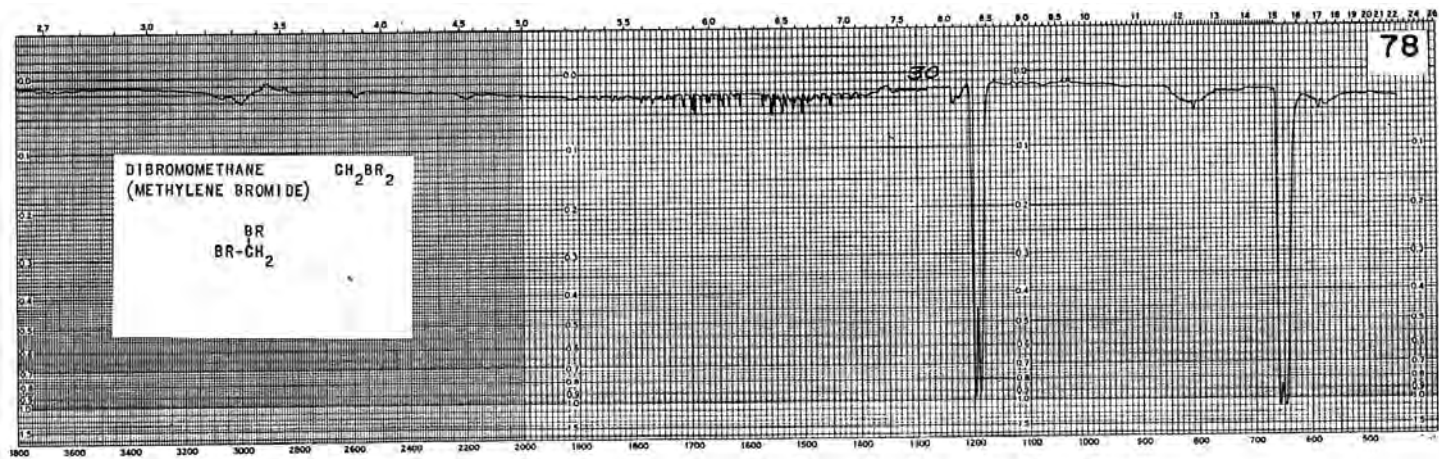


FIGURE 6.5* Methylene bromide (30-mm Hg sample) (26).

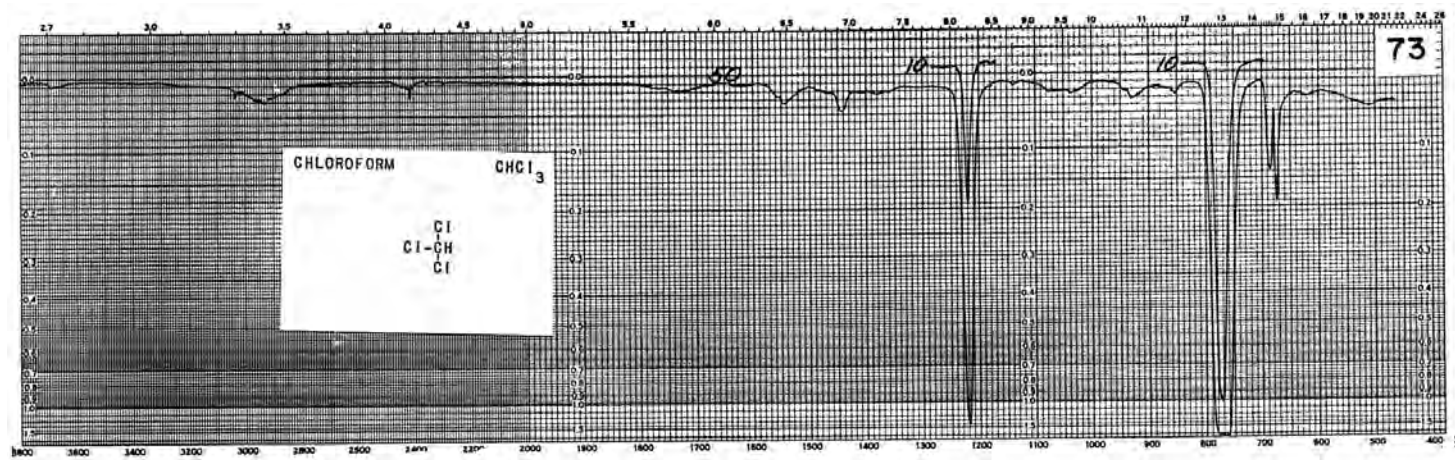


FIGURE 6.6* Trichloromethane (chloroform) (10- and 50-mm Hg sample) (26).

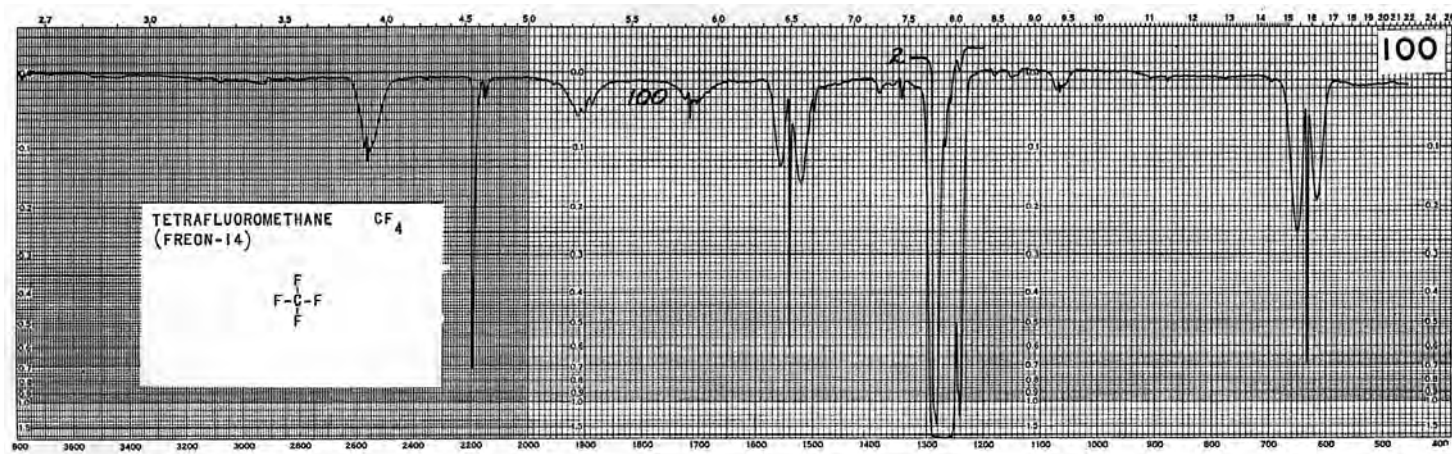


FIGURE 6.7 Tetrafluoromethane (Freon 14) (2 and 100 Hg sample) (26)

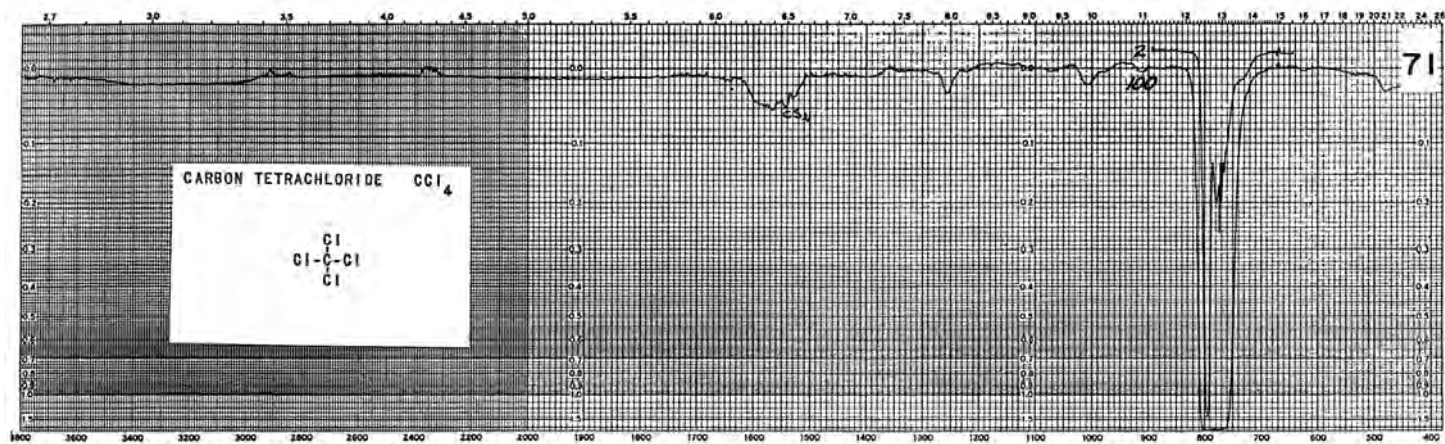


FIGURE 6.8* Tetrachloromethane (carbon tetrachloride) (2- and 100-mm Hg sample) (26).

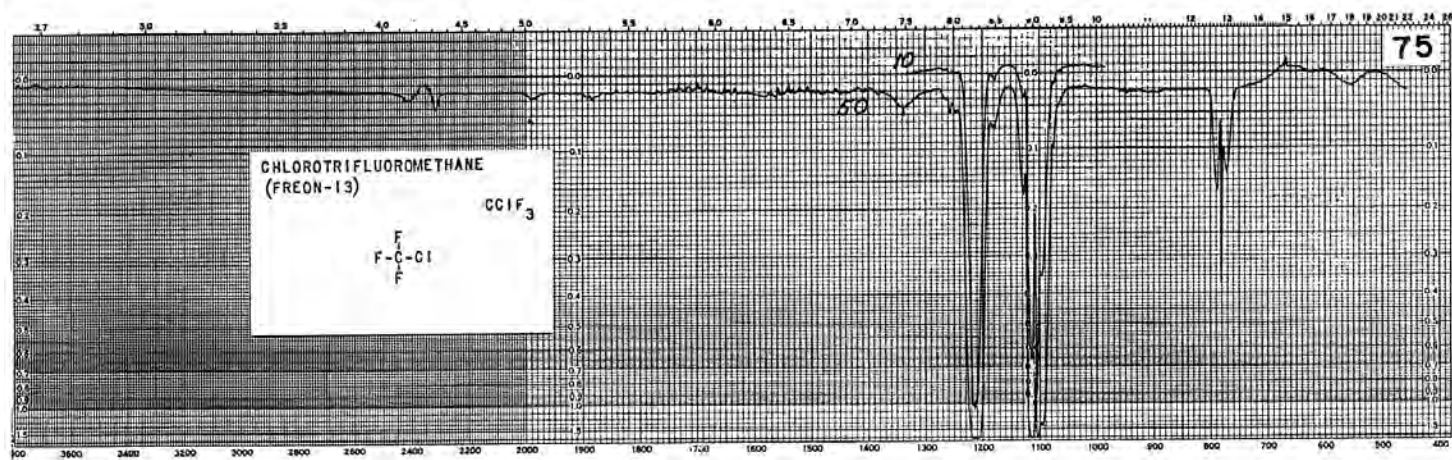


FIGURE 6.9* Chlorotrifluoromethane (10- and 50-mm Hg sample) (26).

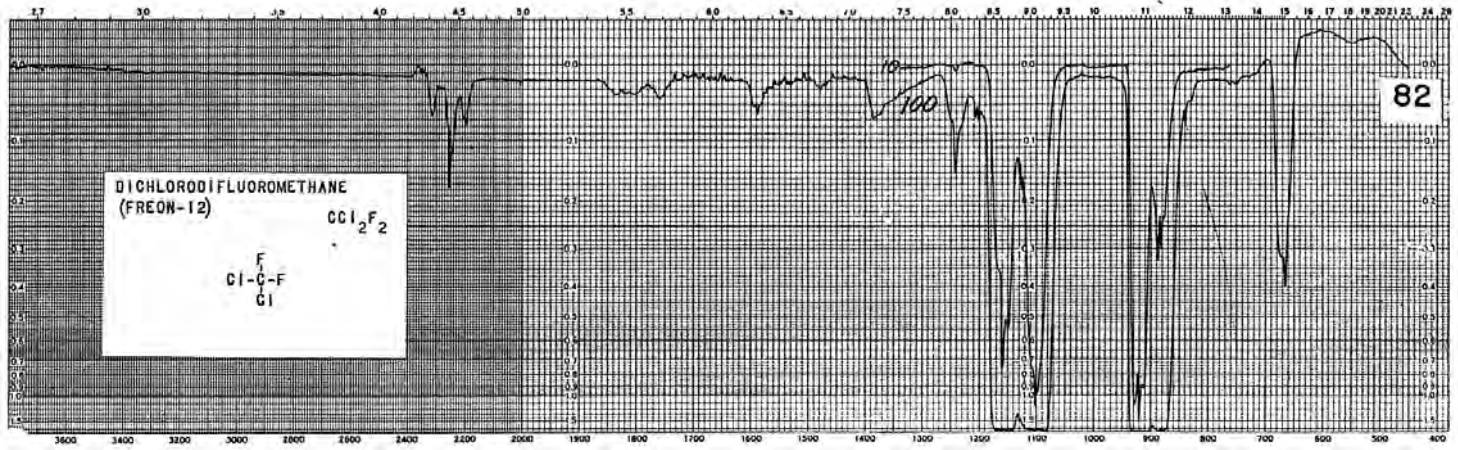


FIGURE 6.10* Dichlorodifluoro methane (10- and 100-mm Hg sample) (26).

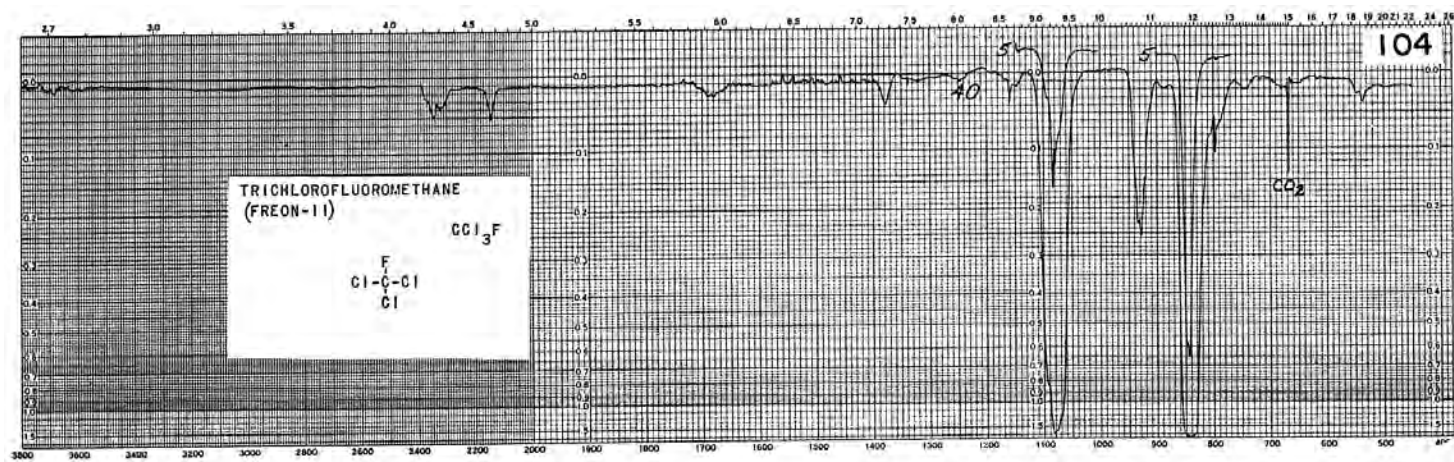


FIGURE 6.11* Trichlorofluoromethane (f and 40-mm Hg sample) (26).

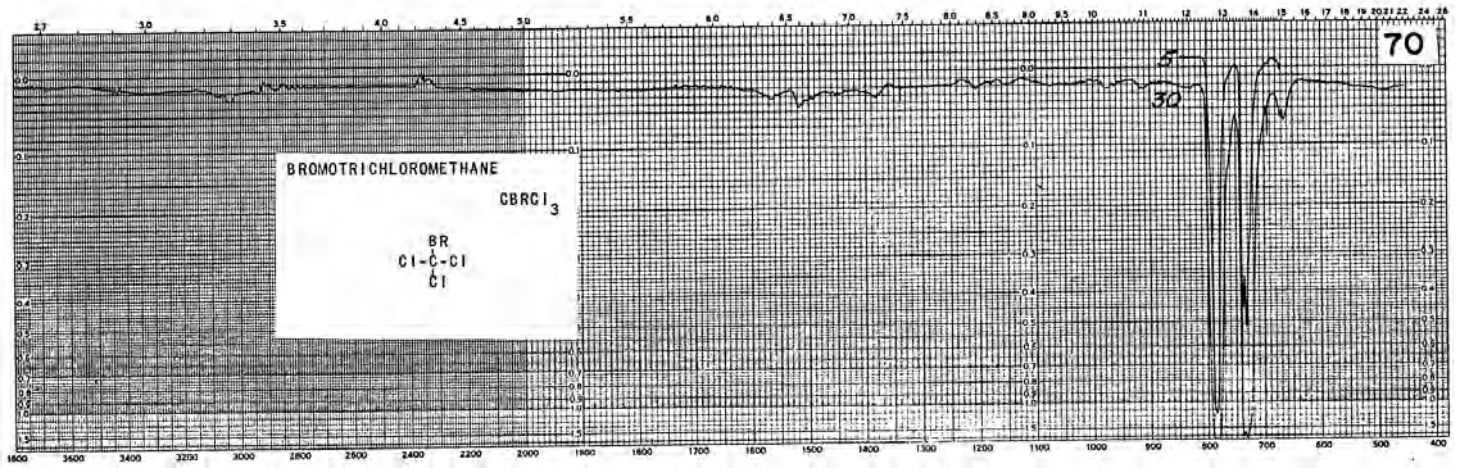


FIGURE 6.12* Bromotrichloromethane (5- and 30-mm Hg sample) (27).

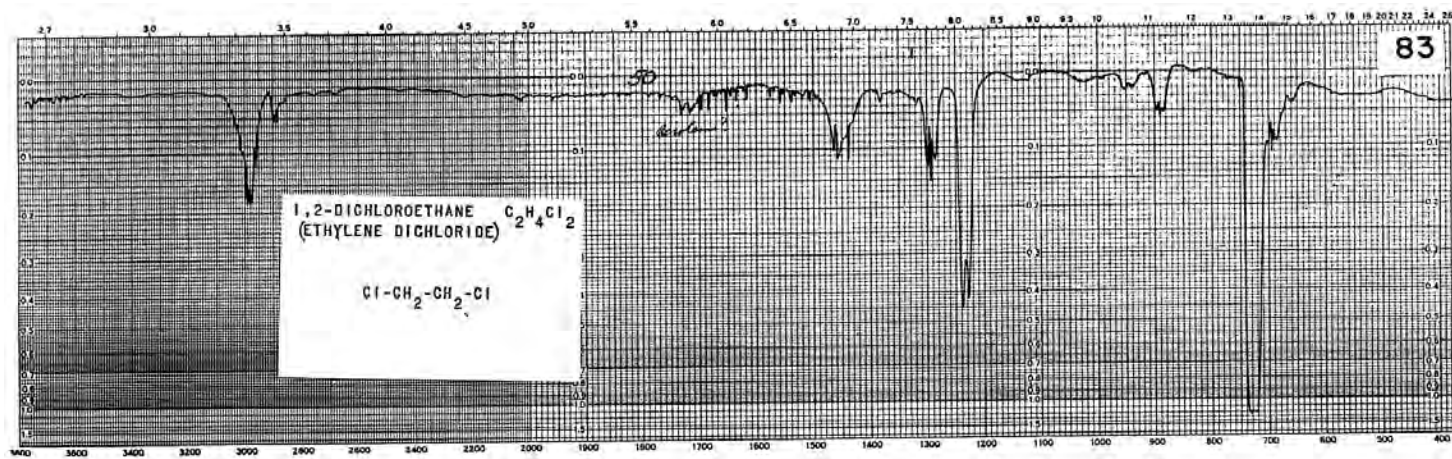


FIGURE 6.13* 1,2-Dichloroethane (ethylene dichloride) (50-mm Hg sample) (27).

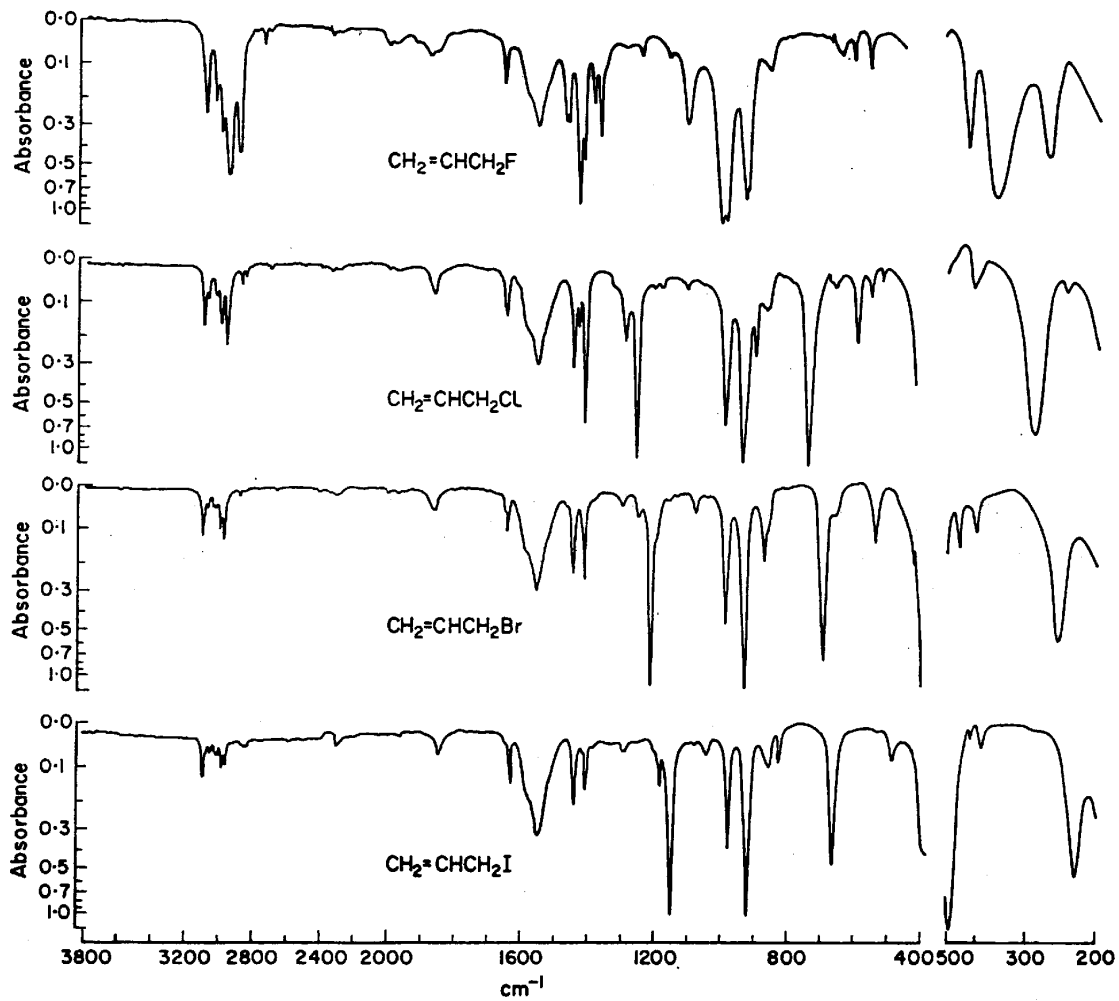


FIGURE 6.14* Infrared spectra of 3-halopropenes (allyl halides) in CCl_4 solution ($3800\text{--}1333\text{ cm}^{-1}$) ($133\text{--}400\text{ cm}^{-1}$) (12).

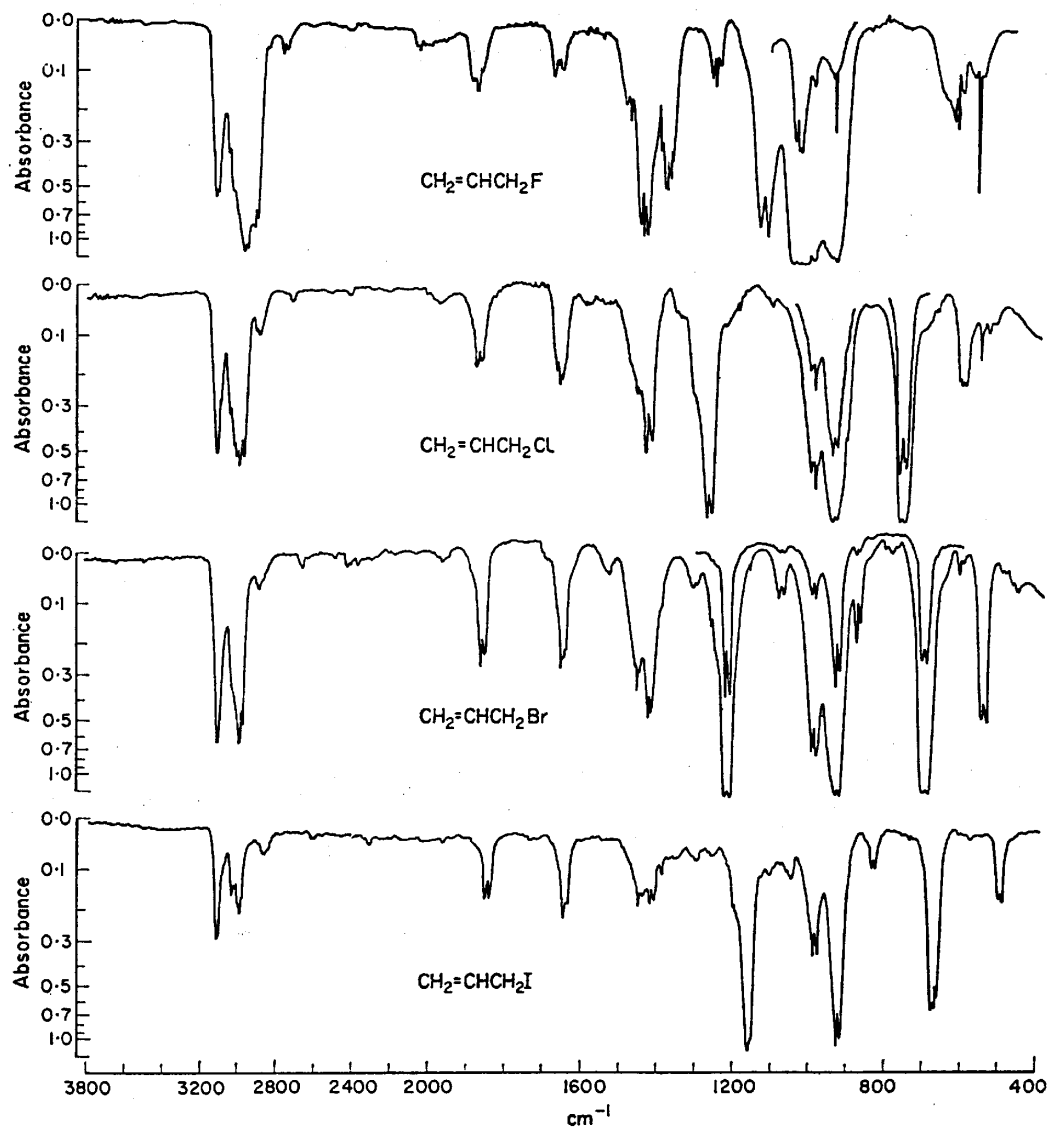


FIGURE 6.15 Vapor-phase infrared spectra of 3-halopropenes (allyl halides) (12).

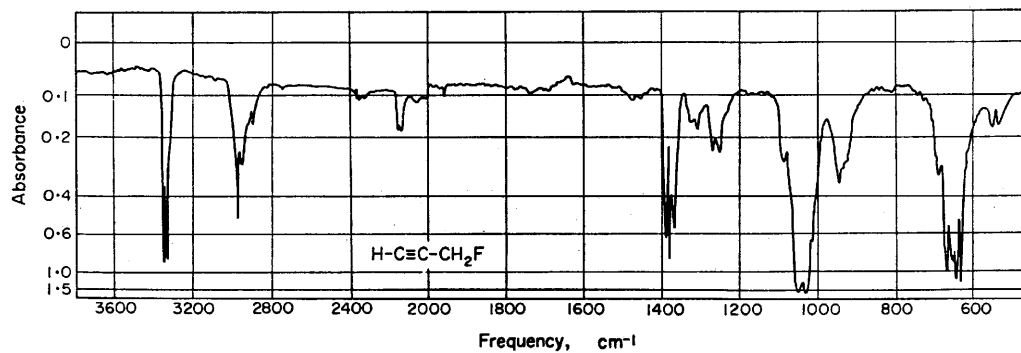


FIGURE 6.16a Vapor-phase IR spectrum of 3-fluoropropyne in a 5-cm KBr cell (50-mm Hg sample).

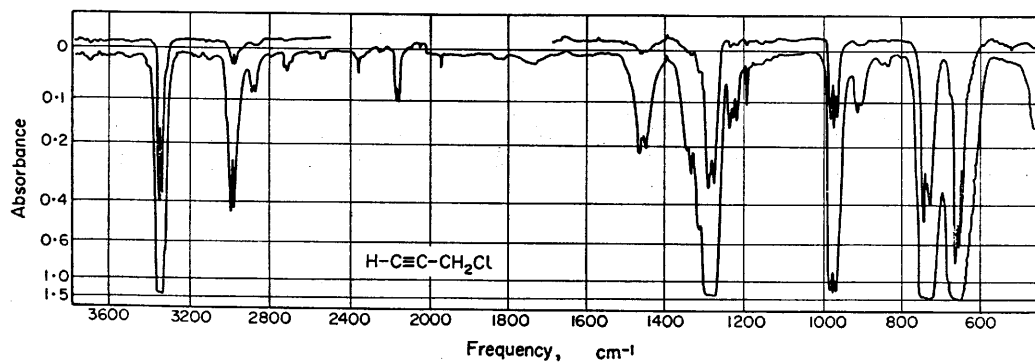


FIGURE 6.16b Vapor-phase IR spectrum of 3-chloropropyne in a 5-cm KBr cell (vapor pressure at -10 and 25°C samples).

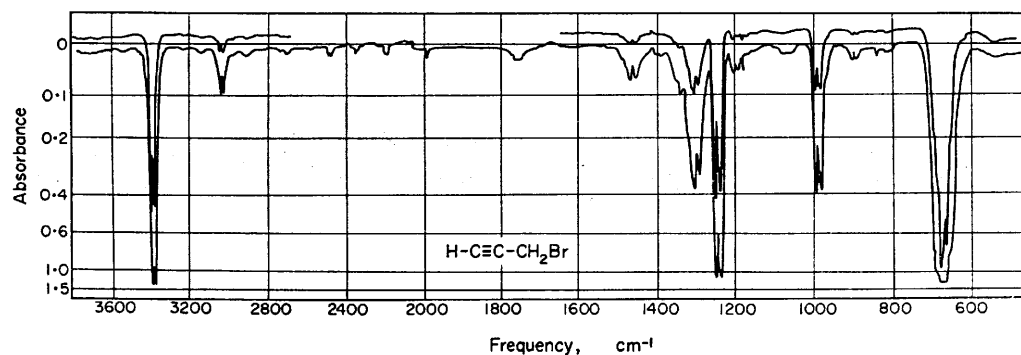


FIGURE 6.16c Vapor-phase IR spectrum of 3-bromopropyne in a 5-cm KBr cell (vapor pressure at 0 and 25°C samples).

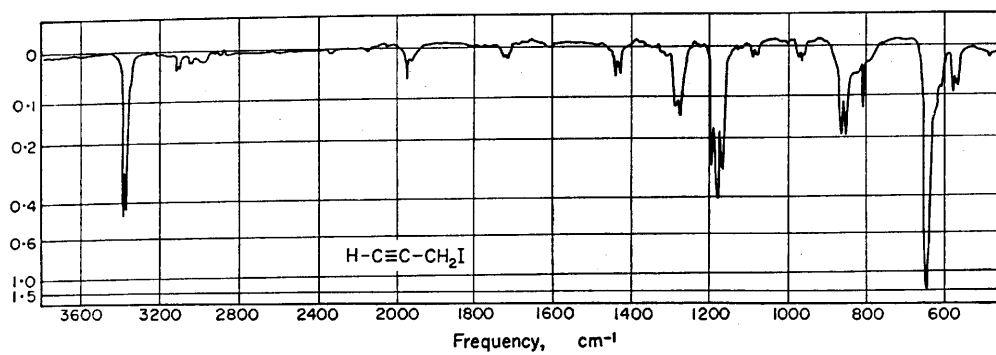


FIGURE 6.16d Vapor-phase IR spectrum of 3-iodopropyne in a 15-cm KBr cell (~ 8 -mm Hg sample).

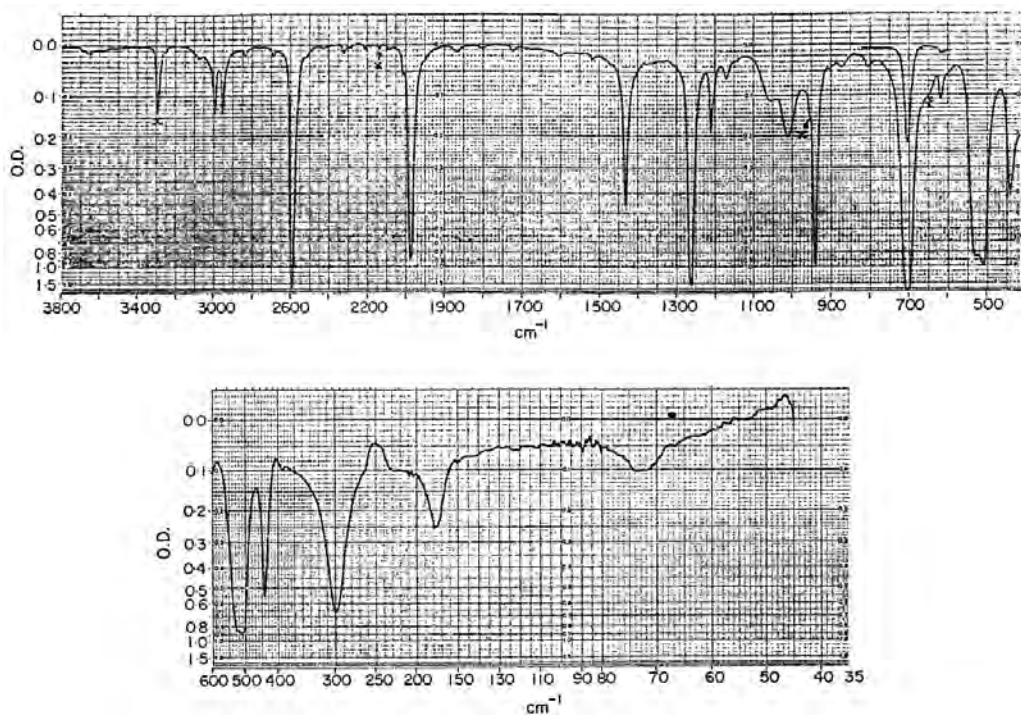


FIGURE 6.17a Top: Liquid-phase IR spectrum of 3-chloropropyne-1-d in a 0.023-mm KBr cell. Bottom: Liquid-phase IR spectrum of 3-chloropropyne-1-d in a 0.1-mm polyethylene cell.

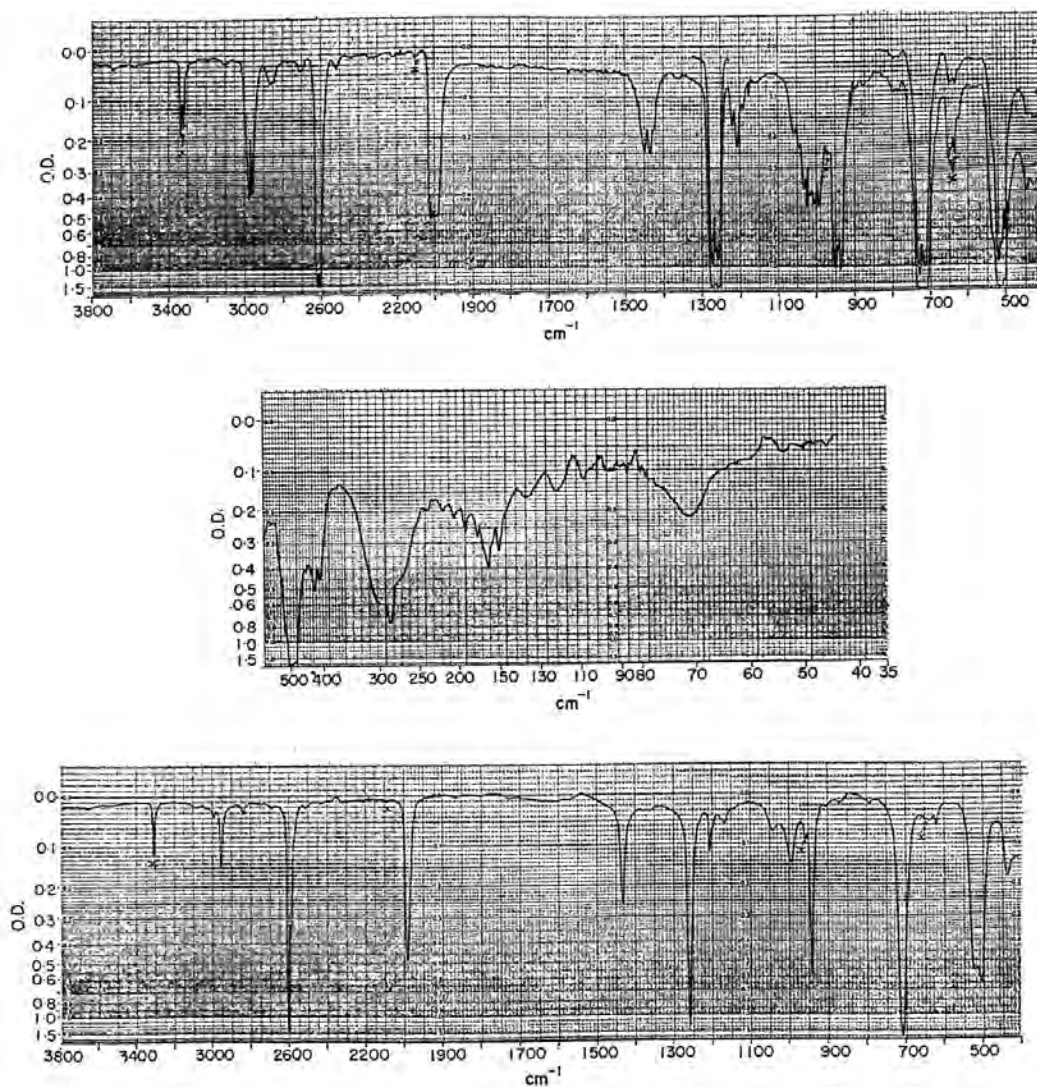


FIGURE 6.17b Top: Vapor-phase IR spectrum of 3-chloropropyne-1-d in a 10-cm KBr cell (33- and 100-mm Hg sample); Middle: 3-chloropropyne-1-d in a 10-cm polyethylene cell. Bottom: Solution-phase IR spectrum of 3-chloropropyne-1-d in 10% wt./vol. CCl₄ (3800–1333 cm⁻¹) and 10% wt./vol. in CS₂ (1333–400 cm⁻¹) using 0.1-mm KBr cells. Bands marked with X are due to 3-chloropropyne.

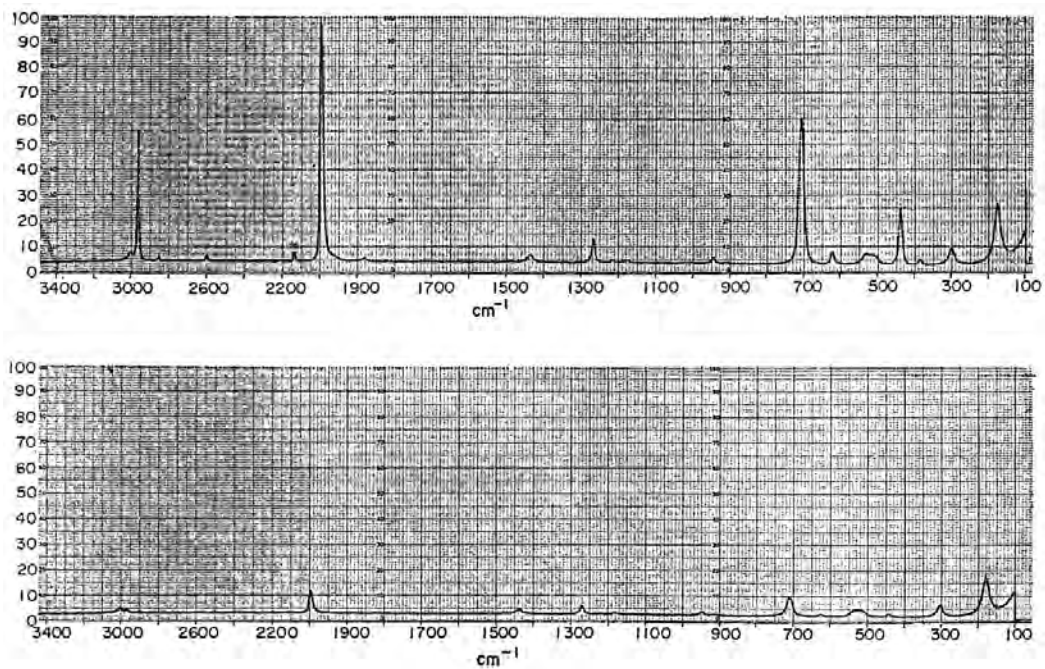


FIGURE 6.18 Top: A Raman liquid-phase spectrum of 3-chloropropyne-1-d. Bottom: A Raman polarized liquid-phase spectrum of 3-chloropropyne-1-d. Some 3-chloropropyne is present (15).

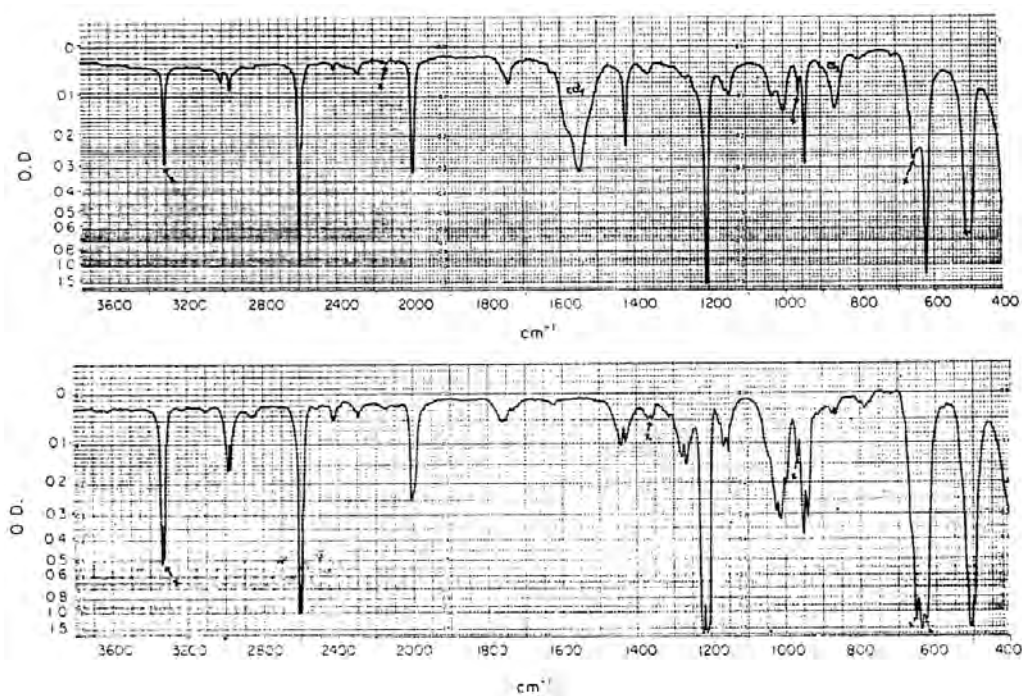


FIGURE 6.19 Top: Solution-phase IR spectrum of 3-bromopropyne-1-d in 10% wt./vol. in CCl₄ (3800–1333 cm⁻¹) and 10% wt./vol. in CS₂ (1333–450 cm⁻¹) using 0.1-mm KBr cells (16). Bottom: A vapor-phase IR spectrum of 3-bromopropyne-1-d in a 10-cm KBr cell (40-mm Hg sample). Infrared bands marked with X are due to the presence of 3-bromopropyne (16).

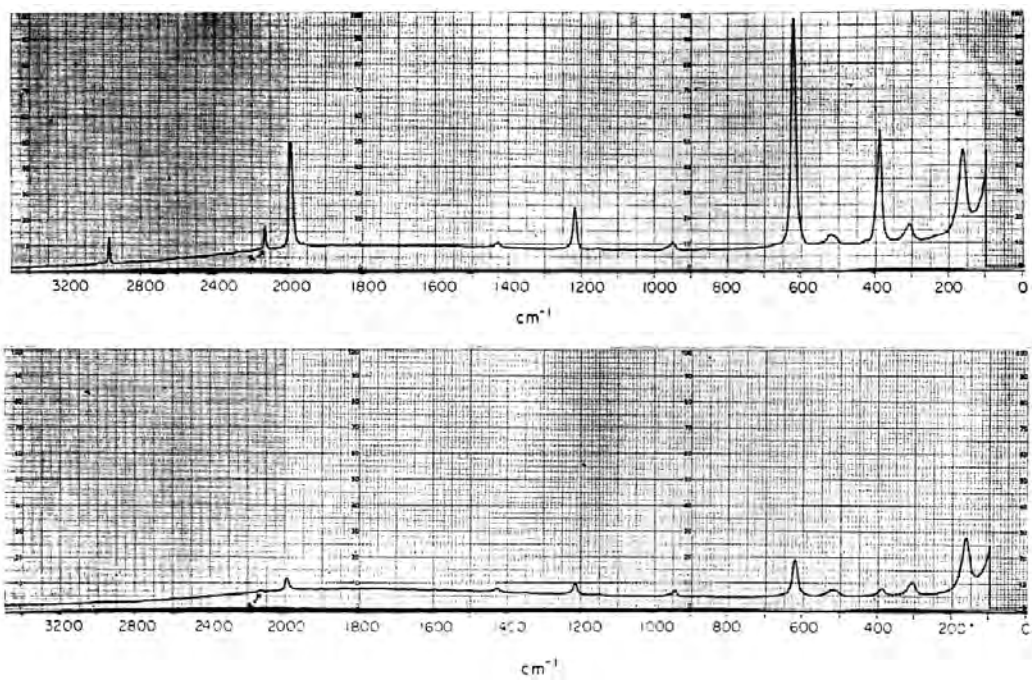


FIGURE 6.20 Top: Raman spectrum of 3-bromopropyne-1-d. Bottom: Polarized Raman spectrum of 3-bromopropyne-1-d. Infrared bands marked with X are due to the presence of 3-bromopropyne (16).

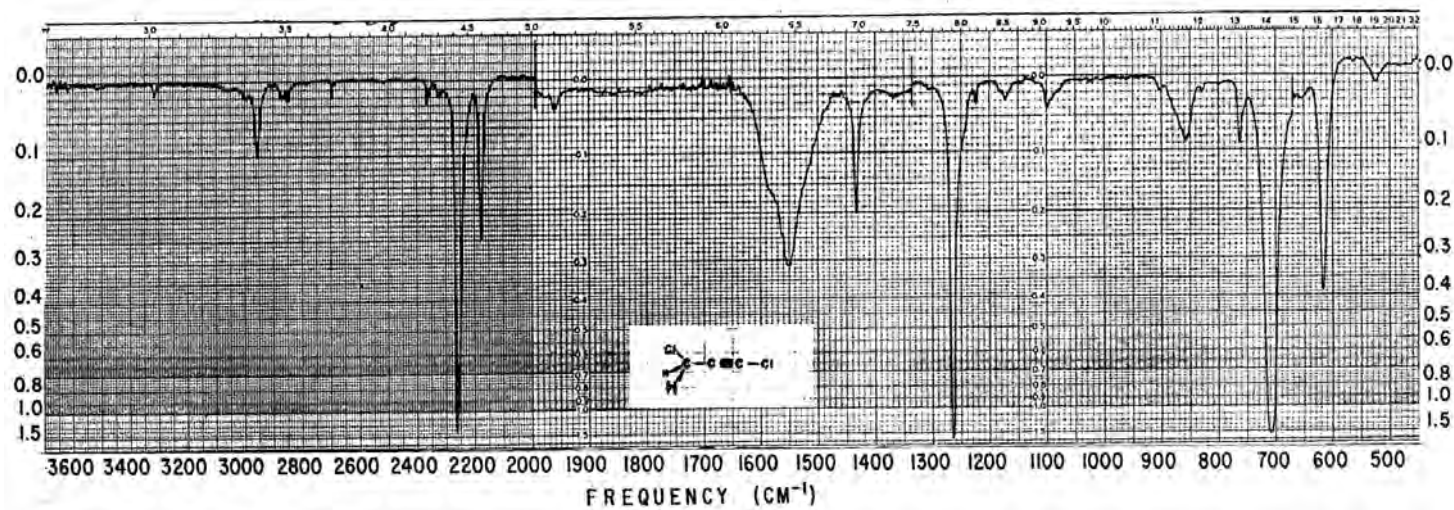


FIGURE 6.21 An IR spectrum of 1,3-dichloropropyne in 10% wt./vol. CCl_4 solution ($3800\text{--}1333\text{ cm}^{-1}$) and in CS_2 solution ($1333\text{--}450\text{ cm}^{-1}$) using 0.1-mm NaCl and KBr cells, respectively. Infrared bands at 1551 and 1580 cm^{-1} are due to CCl_4 and the IR band at 858 cm^{-1} is due to CS_2 (17).

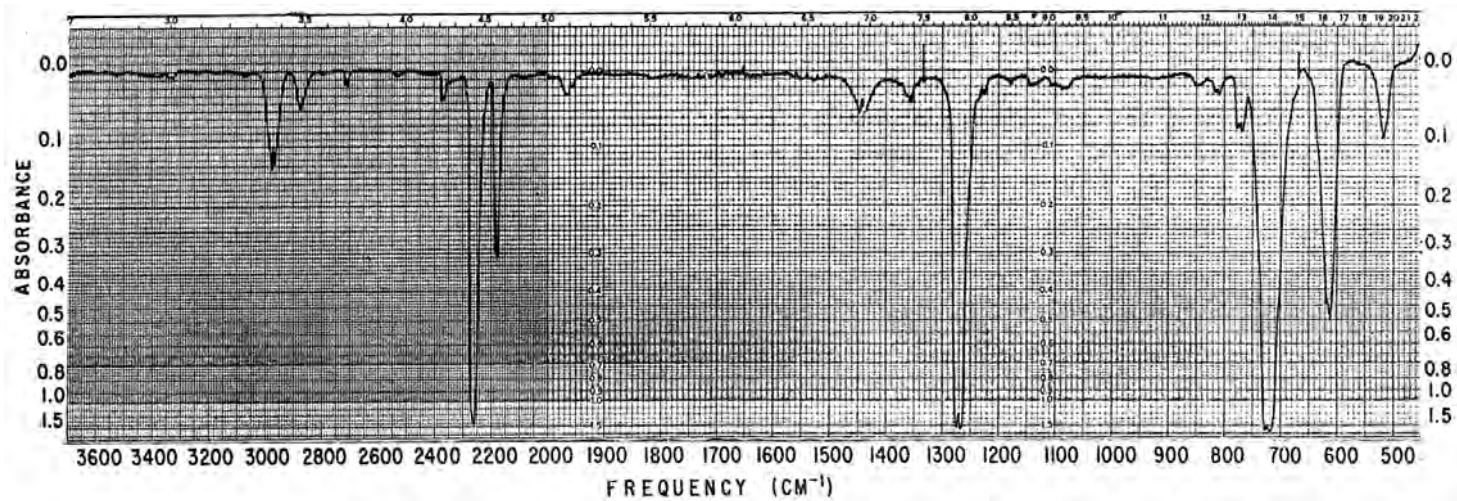


FIGURE 6.22 Vapor-phase IR spectrum of 1,3-dichloropropyne (ambient mm Hg sample at 25°C in a 12.5-cm KBr cell) (17).

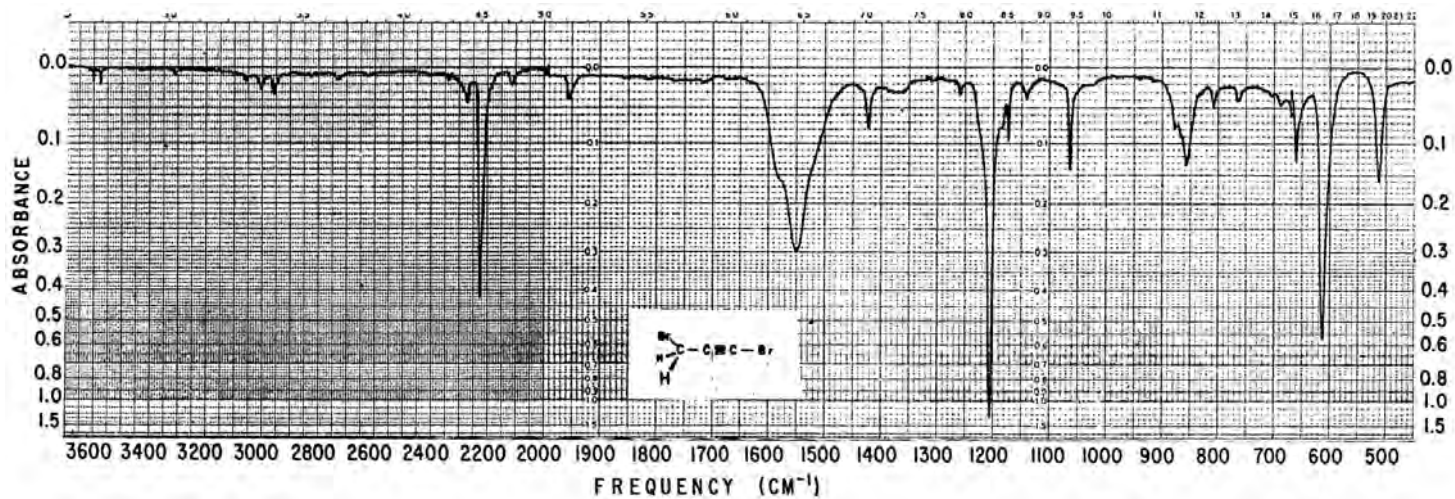


FIGURE 6.23 Solution-phase IR spectrum of 1,3-dibromopropyne in 10% wt./vol. in CCl_4 (3800–1333 cm^{-1}) and in CS_2 solution (1333–450 cm^{-1}) using 0.1-mm NaCl and KBr cells, respectively. Infrared bands at 1551 and 1580 cm^{-1} are due to CCl_4 , and the IR band at 858 cm^{-1} to CS_2 (17).

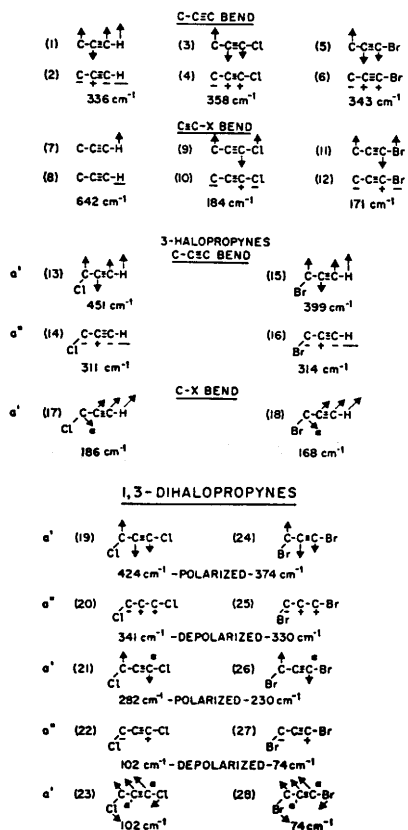
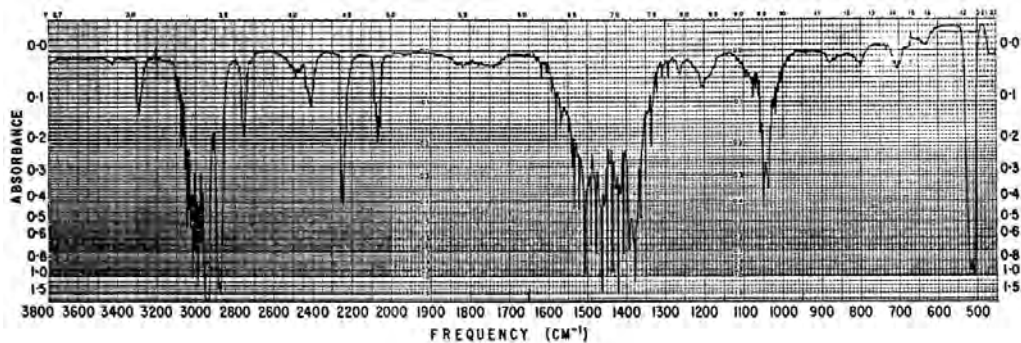


FIGURE 6.24 Approximate normal modes for propyne, 3-halopropynes, and 1,3-dihalopropynes.

FIGURE 6.25 Vapor-phase IR spectrum for 1-bromopropyne in a 12.5-cm KBr cell. The weak IR band at 734 cm^{-1} is due to an impurity. The 1-bromopropyne decomposes rapidly in the atmosphere (25).

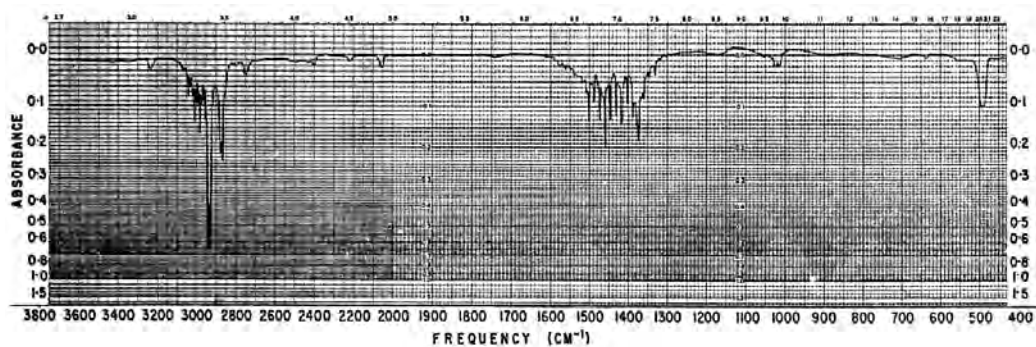


FIGURE 6.26 Infrared vapor spectrum for 1-iodopropyne in a 12.5-cm KBr cell (25).

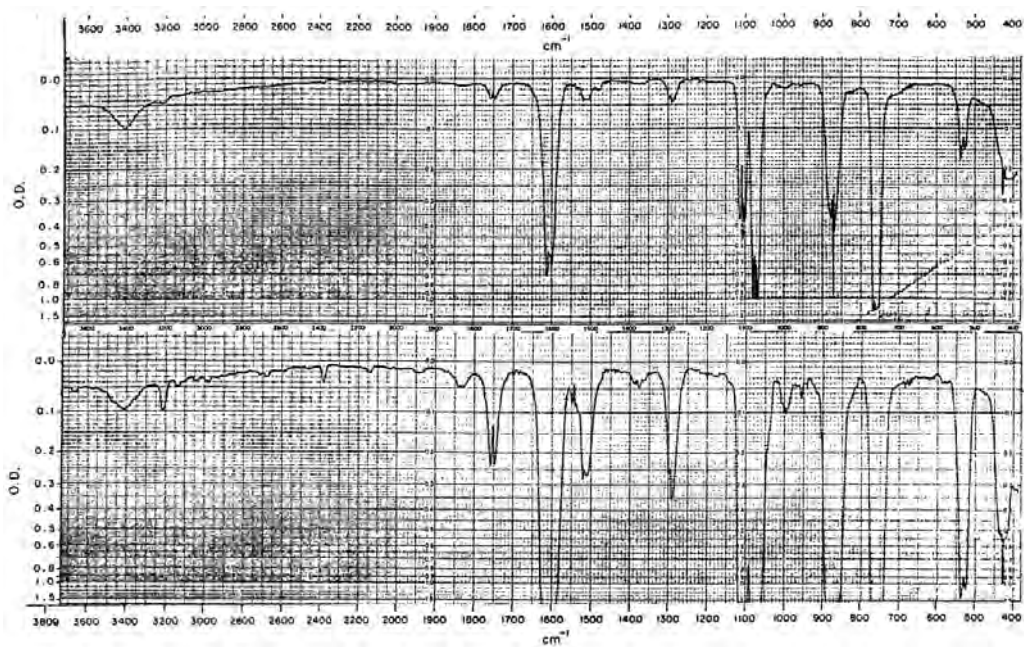


FIGURE 6.27 Top: Vapor-phase IR spectrum of 1-bromo-1-chloroethylene using a 10-cm KBr cell (10-mm Hg sample). Bottom: Same as upper (100-mm Hg sample) (19).

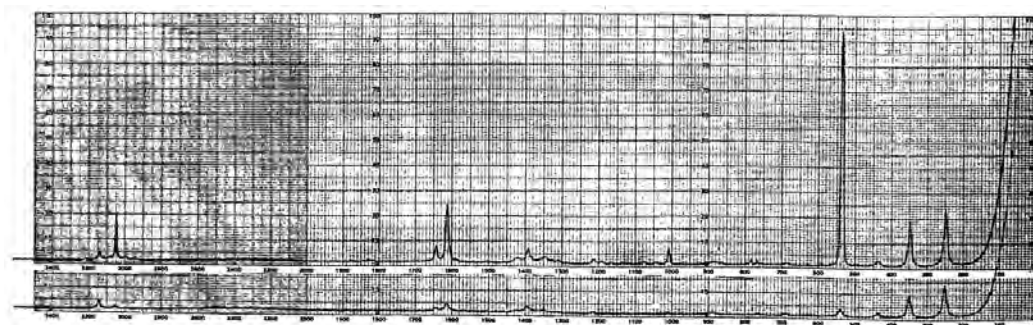


FIGURE 6.28 Raman liquid-phase spectrum of 1-homo-1-chloroethylene. top: Parallel polarization. bottom: Perpendicular polarization.

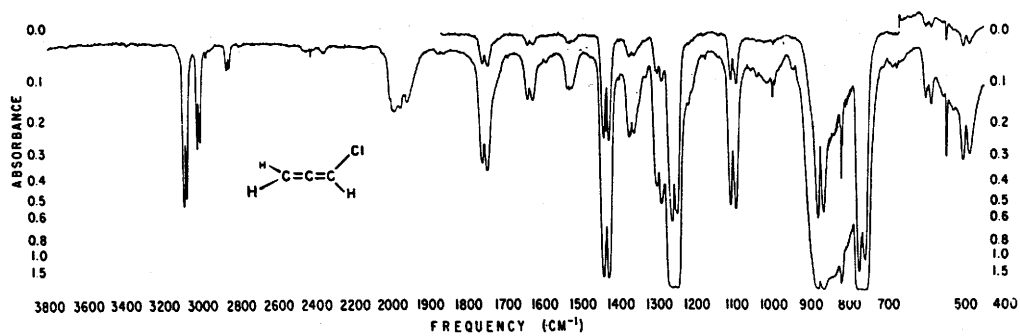


FIGURE 6.29 Vapor-phase IR spectrum of 1-chloropropadiene in a 12.5-cm KBr cell (50- and 100-mm Hg sample) (23).

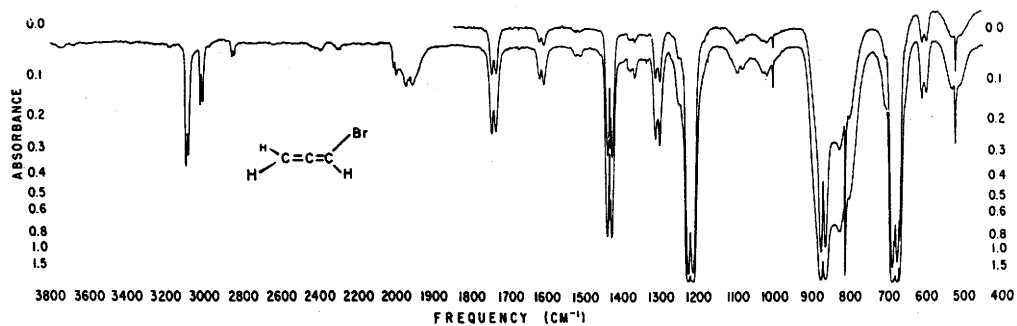


FIGURE 6.30 Vapor-phase IR spectrum of 1-bromopropadiene in a 12.5-cm KBr cell (50- and 100-mm Hg sample).

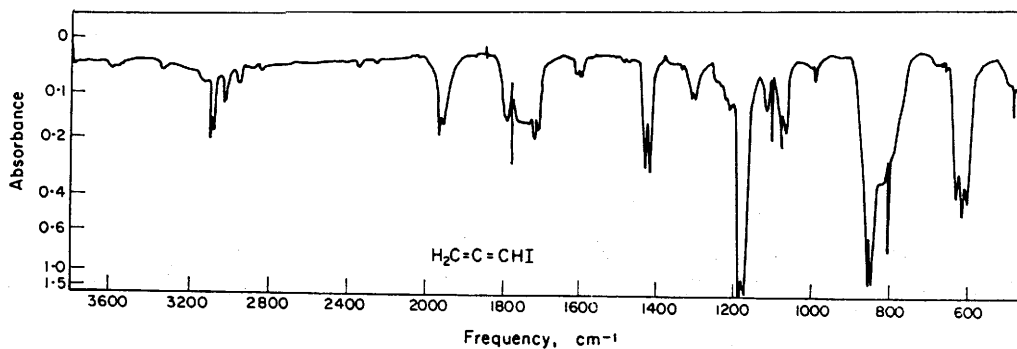


FIGURE 6.31 Vapor-phase IR spectrum of 1-iodopropadiene in a 5-cm KBr cell (vapor pressure at 25 °C). Bands at 1105 and 1775 cm^{-1} are due to the presence of an impurity.

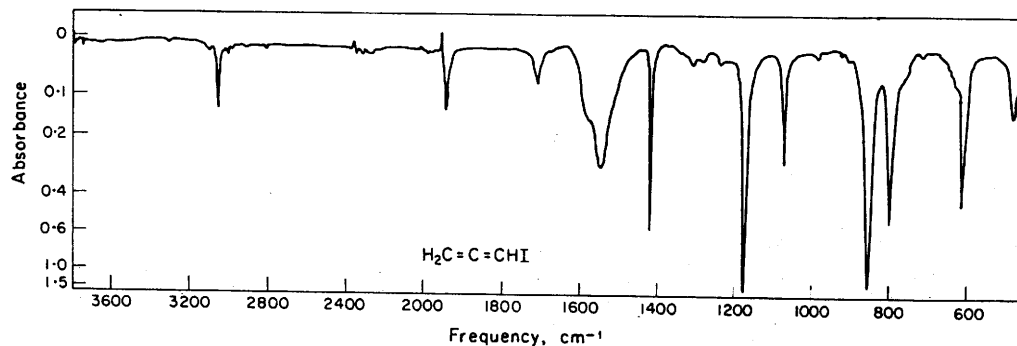


FIGURE 6.32 Infrared spectrum of 1-iodopropadiene in 10% wt./vol. CCl_4 solution (3800–1333 cm^{-1}) and 10% wt./vol. CS_2 solution (1333–450 cm^{-1}) using NaCl and KBr cells, respectively.

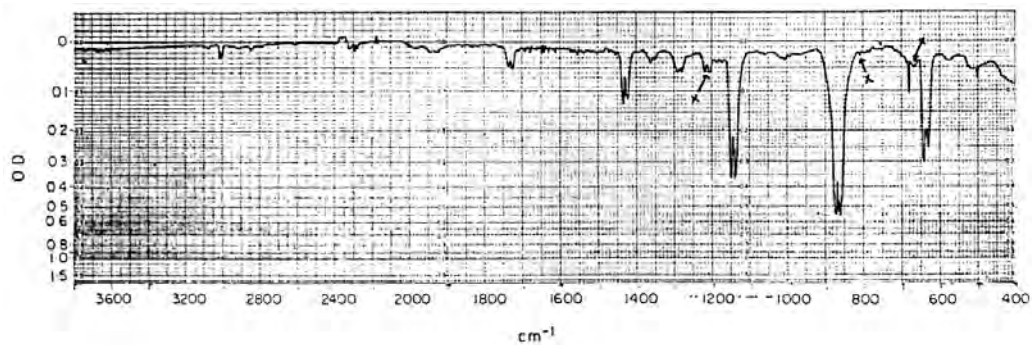


FIGURE 6.33 Vapor-phase IR spectrum of 1-bromopropadiene-1-d in a 12.5-cm KBr cell (50- and 100-mm Hg sample) (16).

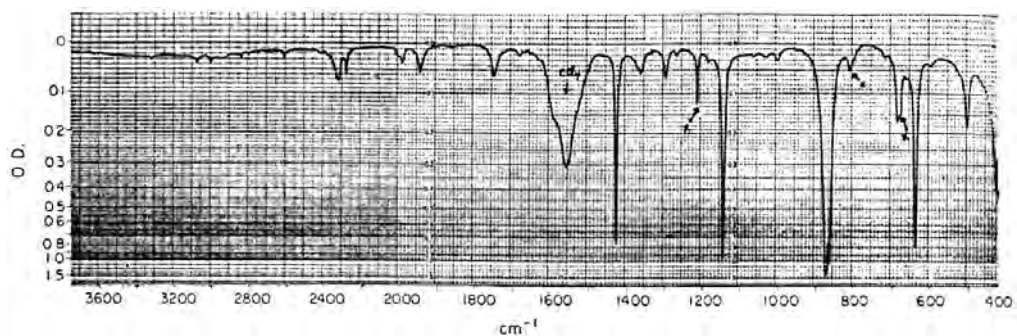


FIGURE 6.34 Solution-phase IR spectrum of 1-bromopropadiene-1-d 10% wt./vol. in CCl₄ (3800–1333 cm⁻¹) and in CS₂ solution using 0.1-mm KBr cells. Infrared bands marked with X are due to the presence of 1-bromopropadiene (16).

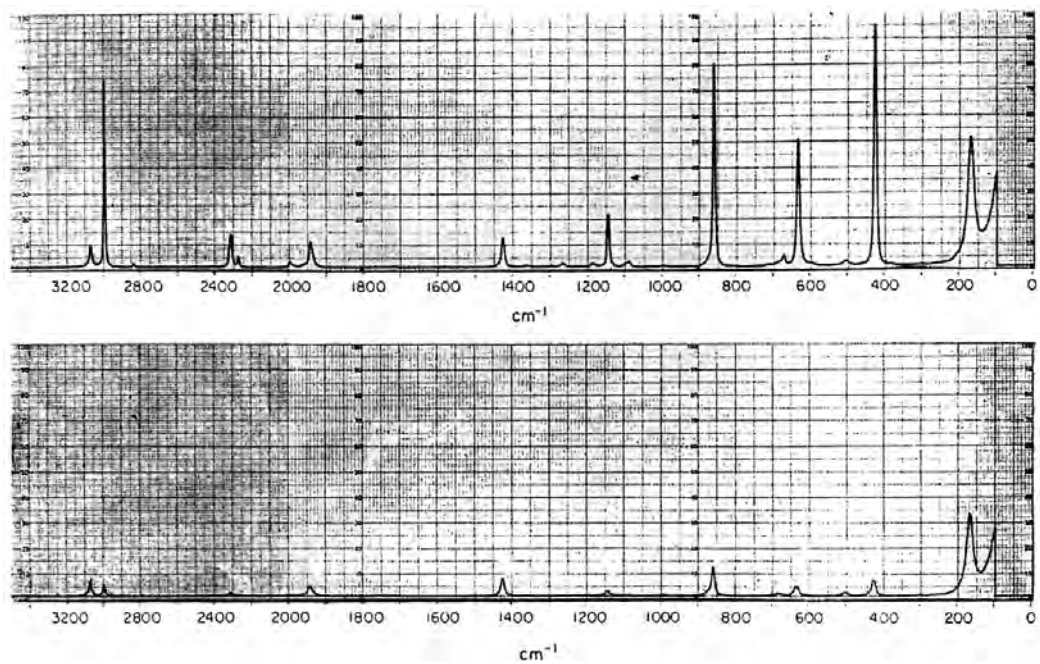


FIGURE 6.35 Top: Raman spectrum of 1-bromopropadiene-1-d using a capillary tube. Bottom: Polarized Raman spectrum of 1-bromopropadiene-1-d (16).

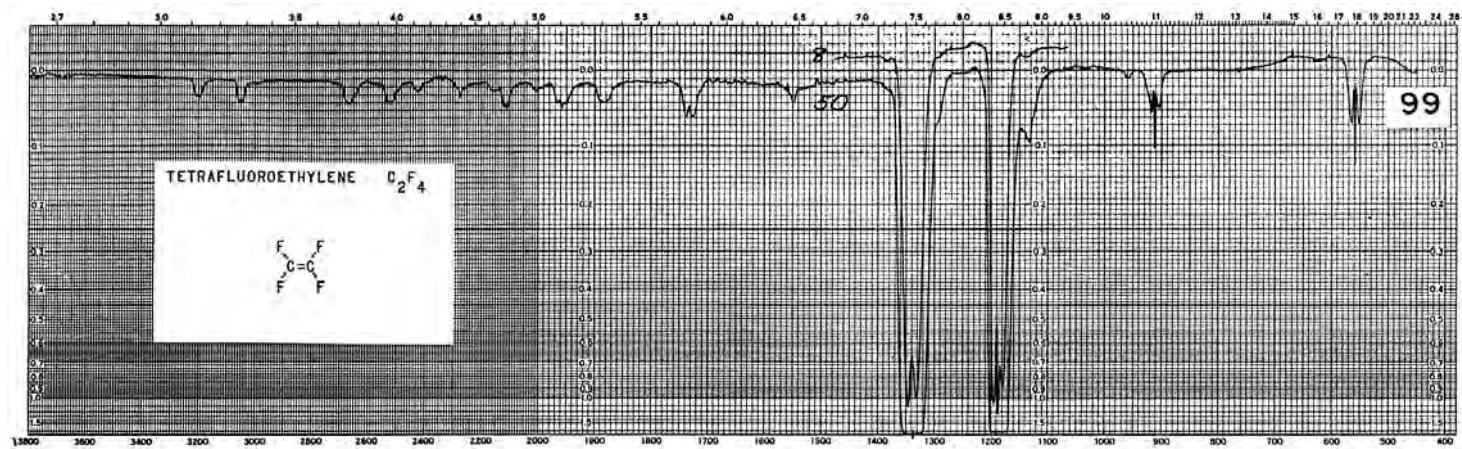


FIGURE 6.36* Vapor-phase IR spectrum of tetrafluoroethylene (8- and 50-mm Hg samples) (26).

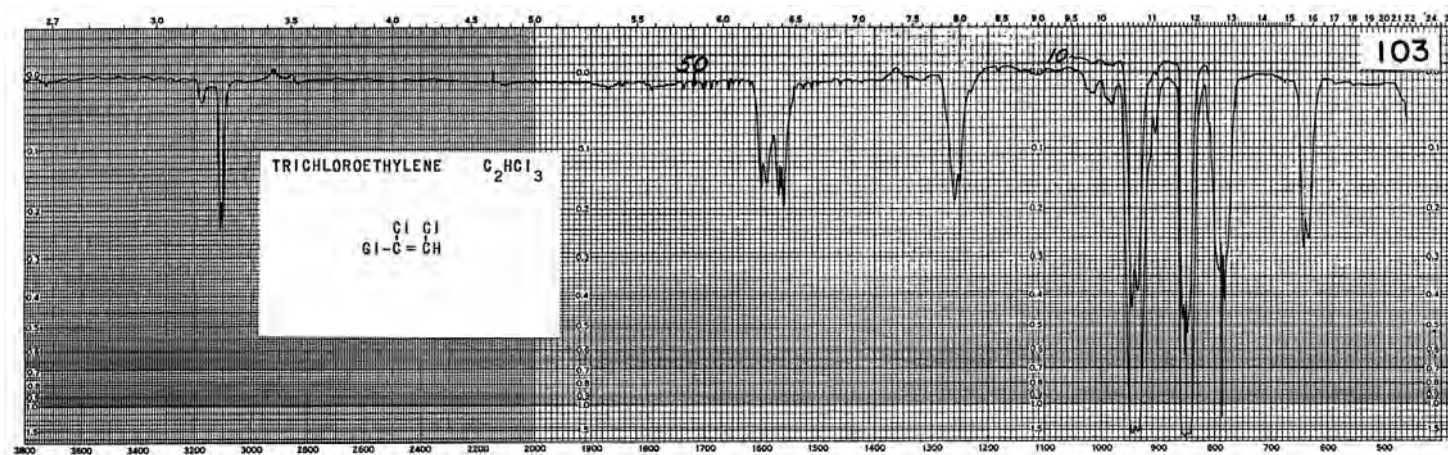


FIGURE 6.37* Vapor-phase IR spectrum of tetrachloroethylene (13-mm Hg sample) (26).

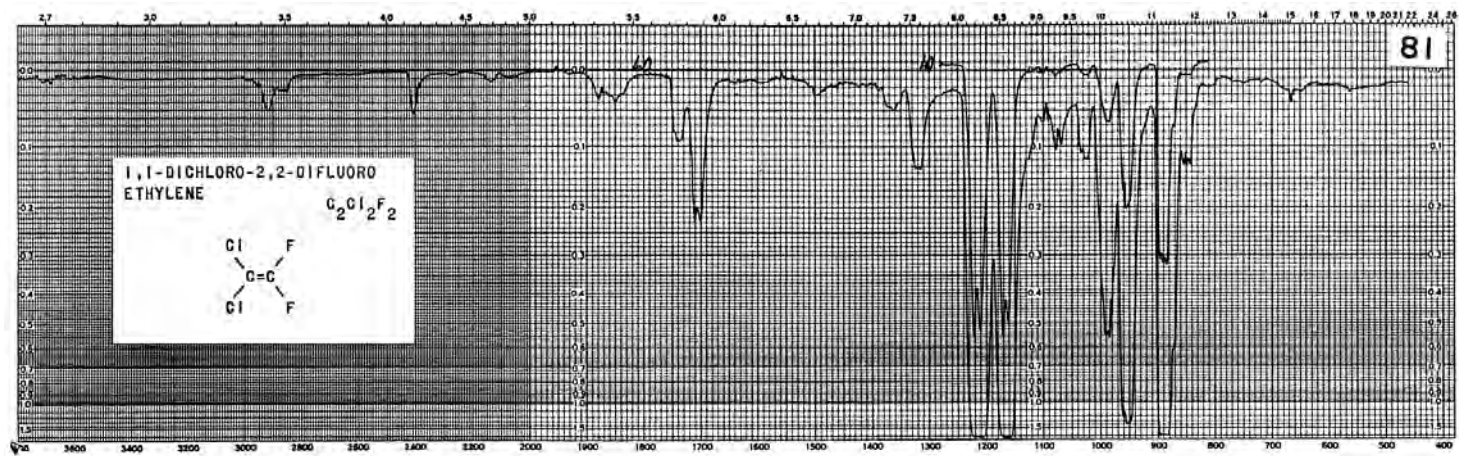


FIGURE 6.38* Vapor-phase IR spectrum of 1,1-dichloro-2,2-difluoroethylene (10- and 60-mm Hg samples) (26).

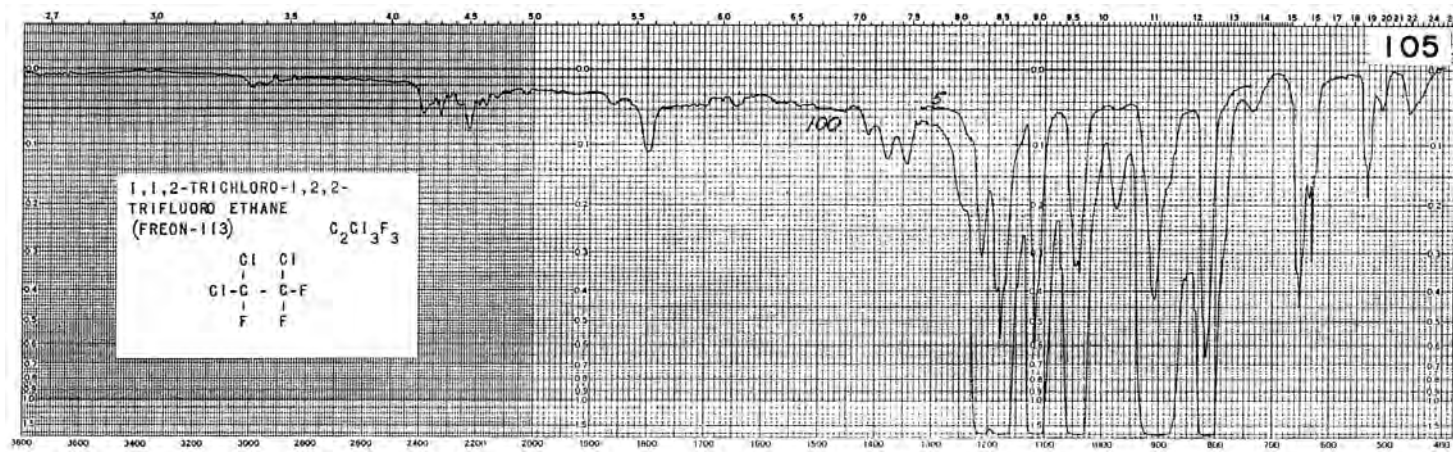


FIGURE 6.39* Vapor-phase IR spectrum of 1,1,2-trichloro-1,2,2-trifluoroethane (5 and 100 mm Hg samples) (26).

TABLE 6.1 Infrared and Raman data for the methylene halides

Compound	a.CH ₂ str. cm ⁻¹ (RI)	s.CH ₂ str. cm ⁻¹ (RI)	a.C-X ₂ str. cm ⁻¹ (RI)	s.C-X ₂ str. cm ⁻¹ (RI)	[a.C-X ₂ str.]- [s.C-X ₂ str.] cm ⁻¹	[a.CH ₂ str.]- [s.CH ₂ str.] cm ⁻¹
Methylene fluoride (3)	3027 (23,p)	2950 (41,p)	1180	1110 (18,p)	70	77
Methylene chloride (3)	3058 (3,p)	2989 (41,p)	742 (4,p)	704 (40,p)	38	69
Methylene bromide (3)	3065 (4,p)	2987 (22,p)	640 (8,p)	577 (88,p)	63	78
Methylene iodide (3)	3048 (1,p)	2967 (14,p)	570 (11,p)	480 (80,p)	90	81
	a.C-X ₂ str. [vapor] cm ⁻¹	a.C-X ₂ str. [liquid] cm ⁻¹	a.C-X ₂ str. [v-p] cm ⁻¹	s.C-X ₂ str. [v- p]	s.C-X ₂ str. [vapor] cm ⁻¹	s.C-X ₂ str. [liquid] cm ⁻¹
Methylene chloride	744	742	-2	9	695	704
Methylene bromide	641	640	-1	-3	580	577
Methylene iodide	575	570	-5	-30	510	480
	C-X str. cm ⁻¹	[C-F str.]- [C-X str.] cm ⁻¹	σ p	[C-I str.]- [C-X str.] cm ⁻¹	Mass X atomic mass	C-X bond length angstroms
Methyl fluoride [IR vap.] (2)	1044	0	0.52	-514	19	0.64
Methyl chloride [IR vap.] (2)	732	312	0.47	-436	35.457	0.99
Methyl bromide [IR vap.] (2)	608	436	0.45	-312	79.916	1.14
Methyl iodide [IR vap.] (2)	530	514	0.39	0	126.92	1.33

TABLE 6.2 Raman and infrared data for trihalomethane and tetrahalomethane

Compound	C-H str. cm ⁻¹ (RI)	a.CX ₃ str. cm ⁻¹ (RI)	s.CX ₃ str. cm ⁻¹ (RI)	CX ₃ bend cm ⁻¹ (RI)
Trifluoromethane	3036 (8,p)	1376 (0.05)	1165 (1,p)	697 (4,p)
Triiodomethane	2975 (9,p)		572 (18,p)	
	a.CX ₄ str. cm ⁻¹ (RI)	s.CX ₄ str. cm ⁻¹ (RI)		
Tetrafluoromethane (3)	1283 (2,p)	908 (46,p)		
Tetrachloromethane (3)	797	790 (8,p)		
Tetrabromomethane (3)	671 (6,p)	662 (7,p)		
Tetraiodomethane (3)		560 (4,p)		
[IR vapor]	cm ⁻¹			
Tetrafluoromethane (2)	1282			
Tetrachloromethane (2)	790			

TABLE 6.2a A comparison of C-X, CX₂, CX₃, and CX₄ stretching frequencies

X	C-X str. cm ⁻¹	a.CX ₂ str. cm ⁻¹	s.CX ₂ str. cm ⁻¹	a.CX ₃ str. cm ⁻¹	s.CX ₃ str. cm ⁻¹	a.CX ₄ str. cm ⁻¹	s.CX ₄ str. cm ⁻¹	Range cm ⁻¹
F	1044	1180	1110	1376	1165	1283	908	908-1376
Cl	732	742	704	[755]	[667]	797	790	667-797
Br	608	640	577	[649]	541	671	662	541-662
I	530	570	480	571	572	[-]	560	480-572

TABLE 6.3 Vapor- and liquid-phase infrared data for 1-haloalkanes

1-Haloalkane F	PC [planar trans rotational conformer] vapor cm ⁻¹ (A)	PH [gauche skeletal rotational conformer] vapor cm ⁻¹ (A)	PC liquid cm ⁻¹ (A)	PH liquid cm ⁻¹ (A)	[PC-PH] vapor cm ⁻¹	[PC-PH] liquid cm ⁻¹	A[PC]/A[PH] vapor	A[PC]/A[PH] liquid	PC cm ⁻¹	PH cm ⁻¹
C ₁₀ H ₂₁	1050 (0.212)	1032 (0.239)	1042 (0.289)	1005 (0.300)	18	37	0.89	0.96	-8	-27
Cl										
C ₃ H ₇	741 (0.150)	661 (0.120)	732 (0.262)	654 (0.320)	80	78	1.25	0.82	-9	-7
C ₄ H ₉	750 (0.210)	661 (0.132)	735 (0.341)	659 (0.460)	79	76	1.59	0.74	-15	-2
C ₅ H ₁₁	740 (0.210)	661 (0.132)	743 (0.250)	665 (0.160)	79	79	1.59	1.56	3	4
C ₇ H ₁₅	740 (0.107)	661 (0.080)	758 (0.028)	652 (0.102)	79	106	1.34	0.27	18	-9
			725 (0.140)			73		1.37		
C ₁₀ H ₂₁	740 (0.080)	662 (0.050)	749 (0.010)	650 (0.080)	78	99	1.6	0.13	9	-12
			721 (0.089)			71		1.11		
C ₁₁ H ₂₃	740 (0.100)	660 (0.071)	751 (0.070)	645 (0.159)	80	106	1.41	0.44		
			711 (0.169)			66		1.06		
C ₁₆ H ₃₃	738 (0.061)	660 (0.040)	758 (0.030)	659 (0.098)	78	99	1.53	0.31		
			725 (0.135)			66		1.38		
C ₁₈ H ₃₇	~ 740 (0.029)	~ 664 (0.020)	750 (0.034)	650 (0.080)	76	100	1.45	0.43		
			~ 720 (0.129)			~ 70		1.61		
Br										
C ₄ H ₉	650 (0.090)	564 (0.074)	638 (0.200)	554 (0.155)	86	84	1.22	1.29	-12	-10
C ₅ H ₁₁	648 (0.118)	568 (0.090)	641 (0.280)	564 (0.241)	80	77	1.31	1.16	-7	-4
C ₆ H ₁₃	652 (0.139)	569 (0.129)	642 (0.305)	565 (0.280)	83	77	1.08	1.09	-10	-4
C ₇ H ₁₅	652 (0.071)	569 (0.090)	645 (0.070)	562 (0.070)	83	83	0.79	1	-7	-7
C ₈ H ₁₇	652 (0.072)	569 (0.060)	640 (0.090)	559 (0.090)	83	81	0.9		-12	-10
C ₁₁ H ₂₃	653 (0.060)	562 (0.050)	642 (0.060)	560 (0.043)	91	82	1.2	1.4	-11	-2
C ₁₂ H ₂₅	650 (0.039)	561 (0.050)	640 (0.082)	560 (0.072)	89	80	0.78	1.14	-10	-1
C ₁₄ H ₂₉	649 (0.050)	568 (0.036)	640 (0.079)	559 (0.066)	81	81	1.39	1.2	-9	-9
C ₁₆ H ₃₃	651 (0.026)	572 (0.019)	646 (0.060)	565 (0.050)	79	81	1.37	1.2	-5	-7
C ₁₉ H ₃₉	~ 645 (0.019)	~ 568 (0.020)	650 (0.059)	574 (0.039)	~ 77	76	0.95	1.51	5	6
I										
C ₃ H ₇	591 (0.080)	500 (0.052)	590 (0.131)	498 (0.110)	91	92	1.53	1.19	-1	-2
C ₄ H ₉	593 (0.090)	505 (0.040)	581 (0.121)	495 (0.061)	88	86	2.3	1.98	-12	-10
C ₉ H ₁₉	598 (0.039)	504 (0.010)	593 (0.071)	493 (0.040)	94	100	3.9	1.78	-5	-11
C ₁₆ H ₃₃	593 (0.030)	500 (0.010)	600 (0.046)	499 (0.031)	93	101	3	1.48	7	-1

TABLE 6.4 Vapor- and liquid-phase infrared data for 2-halobutane and tert-butyl halide

Rotational conformer	S(CH) C-X str.[1] vapor cm ⁻¹ (A)	S(CH) C-X str.[1] liquid cm ⁻¹ (A)	S(HH') C-X str.[2] vapor cm ⁻¹ (A)	S(HH') C-X str.[2] liquid cm ⁻¹ (A)	S(HH) C-X str.[3] vapor cm ⁻¹ (A)	S(HH) C-X str.[3] liquid cm ⁻¹ (A)	A[1]/A[2] vapor	A[1]/A[2] liquid	A[1]/A[3] vapor	A[1]/A[3] liquid
2-Halobutane										
X										
Cl	680 (0.130)	670 (0.392)	625 (0.200)	628 (0.341)	592 (0.045)	609 (0.460)	0.65	1.1	2.9	0.85
Br	612 (0.069)	605 (0.055)	529 (0.070)	525 (0.090)	478 (0.020)	480 (0.030)	0.99	0.61	3.5	2.3
I	580 (0.041)	570 (0.050)	489 (0.041)	479 (0.072)		454 (0.040)	1	0.69		1.02
Rotational conformer tert-Butyl halide										
X	T(HHH)	T(HHH)	C-X str. [v-1] cm ⁻¹							
Cl	580	570	-10							
Br	521	520	-1							
I		492								
2-Halobutane										
X			C-X str.[1] [v-1]	C-X str.[2] [v-1]	C-X str.[3] [v-1]					
Cl			-10	3	17					
Br			-7	-4	2					
I			-10	-10						
	[1]-[2] [C-Cl str.]- [C-X str.] vapor cm ⁻¹	[1]-[2] [C-Cl str.]- [C-X str.] liquid cm ⁻¹	[1]-[3] [C-Cl str.]- [C-X str.] vapor cm ⁻¹	[1]-[3] [C-Cl str.]- [C-X str.] liquid cm ⁻¹						
Cl	55	42	88	61						
Br	83	80	134	125						
I	91	91		116						

TABLE 6.6 Vapor- and liquid-phase infrared data for primary, primary dihaloalkanes

Compound	C-X str.[1] vapor cm ⁻¹ (A)	C-X str.[1] liquid cm ⁻¹ (A)	C-X str.[2] vapor cm ⁻¹ (A)	C-X str.[2] liquid cm ⁻¹ (A)	C-X str.[3] vapor cm ⁻¹ (A)	C-X str.[3] liquid cm ⁻¹ (A)	C-X str.[1] [v-l] cm ⁻¹	C-X str.[2] [v-l] cm ⁻¹	C-X str.[3] [v-l] cm ⁻¹	A[1]/ A[3] vapor	A[1]/ A[3] liquid	A[1]/ A[2] vapor	A[1]/ A[2] liquid
1,2-Dihaloethane X,X													
Cl,Cl	720 (1.230)	710 (0.940)		662 (0.320)	660 (0.070)	655 (0.380)	-10		-5	17.6	2.5		
Br,Br	594 (1.210)	590 (0.440)				545 (0.100)	-4						
I,I		485 (0.785)											
1,3-Dihalopropane X,X													
Cl,Cl	740 (0.240)				660 (0.540)								
Br,Br	655 (0.163)	645 (0.210)	599 (0.142)	585 (0.265)	559 (0.230)	543 (0.370)	-10	-14	-16	0.71	0.57	1.1	0.81
I,I	602 (0.070)	590 (0.105)			526 (0.050)	512 (0.105)	-12		-14	1.4	1		
						483 (0.110)							
1,4-Dihalobutane X,X													
Cl,Cl	778 (0.524)	780 (0.320)	742 (0.434)	735 (0.300)	660 (0.511)	655 (0.415)	2	-7	-5	1.03	0.77	1.21	1.07
Br,Br	659 (0.178)	649 (0.160)			572 (0.311)	560 (0.260)	-10		-12	0.31	0.62		
I,I	599 (0.080)	591 (0.052)			505 (0.078)	502 (0.120)	-8		-3	1.02	0.43		
1,5-Dihalopentane X,X													
Cl,Cl	748 (0.389)	740 (0.285)		720 (0.255)	662 (0.298)	651 (0.379)	-8		-11	1.3	0.75		
Br,Br	654 (0.299)	647 (0.525)			571 (0.309)	570 (0.580)	-7		-1	0.97	0.91		
I,I		584 (0.140)		604 (0.109)		492 (0.140)							
1,6-Dihalohexane X,X													
Cl,Cl	740 (0.350)				660 (0.260)								
Br,Br	654 (0.169)				570 (0.157)								
I,I	600 (0.090)	590 (0.190)			509 (0.047)	498 (0.070)	-10		-11	1.9	2.7	2.7	

TABLE 6.7 Raman data for methyl halides and infrared and Raman data for tetrabromoalkanes

Compound	Phase	a.CH ₃ str. cm ⁻¹ (RI)	s.CH ₃ str. cm ⁻¹ (RI)	2(CH ₃ bend) cm ⁻¹ (RI)	C-X str. cm ⁻¹ (RI)					
Methyl fluoride (3)	vapor		2967 (41,p)	2865 (26,p)	1043 (5,p)					
Methyl chloride (3)	vapor	3052 (4)	2968 (95,p)	2879 (7,p)	729 (36,p)					
Methyl bromide (3)	vapor		2972 (43,p)	2862 (4,p)	609 (42,p)					
Methyl iodide (3)	liquid		3042 (2,p)	2946 (44,p)	523 (96,p)					
	Raman		CH str. cm ⁻¹ (RI)	s.CH ₂ str. cm ⁻¹ (RI)	a.CBr ₂ str. cm ⁻¹ (RI)	a.CBr ₂ str. cm ⁻¹ (RI)	s.CBr ₂ str. cm ⁻¹ (RI)	CBr ₂ bend cm ⁻¹ (RI)	CBr ₂ wag cm ⁻¹ (RI)	CBr ₂ twist cm ⁻¹ (RI)
1,1,2,2-tetrabromoethane	liquid				714 (2)	664 (1)	537 (2)	451 (0)	219 (9)	176 (2)
	Raman				C-Br str.	C-Br str.	C-Br str.	CCBr bend	CCBr torsion	
1,2,3,4-tetrabromobutane	liquid		2967 (1)	2935 (0)	702 (3)	567 (8)	532 (3)	305 (1)	191 (0)	
	IR				cm ⁻¹ (A)	cm ⁻¹ (A)	cm ⁻¹ (A)			
1,1,2,2-tetrabromoethane (2)	vapor				710 (1.240)	642 (0.560) 589 (0.250)	538 (0.135) 619 (1.030)			

TABLE 6.8 Carbon halogen stretching frequencies for ethylene propyne, 1,2-epoxypropane, and propadiene derivatives

Compound	ν C—F cm ⁻¹	ν C—Cl cm ⁻¹	ν C—Br cm ⁻¹	ν C—I cm ⁻¹	Rotational conformer					Ref.	
3-Halopropene	1005.8	739.4	690.6	669.1	gauche					11	
	989.3				cis					11	
3-Halo,1,2-epoxypropane	1018.5	695.8	654.9	604	RT					12	
	992	727.5	643.5		R1					12	
3-Halopropyne	1039	725	621	570						13	
3-Chloropropyne-1d	[—]	723	[—]	[—]						14	
3-Bromopropyne-1d	[—]	[—]	634	[—]						15	
1,3-Dihalopropyne	[—]	709	613	[—]						16	
1-Haloethylene	1157	719	[—]	[—]						17	
	FF va.CF ₂ cm ⁻¹	Cl,Cl va.CCl ₂ cm ⁻¹	Cl,Br va.CClBr cm ⁻¹	Br,Br va.CBr ₂ cm ⁻¹	FF vs.CF ₂ cm ⁻¹	Cl,Cl vs.CCl ₂ cm ⁻¹	Cl,Br vs.CClBr cm ⁻¹	Br,Br vs.CBr ₂ cm ⁻¹			
1,1-Dihaloethylene	1301	788	765	698	922	601	531	474	18–22		
	F ₄	F ₄	Cl ₄	Cl ₄	Br ₄	Br ₄					
Tetrahaloethylene	1340	1189	909	875	768	632	[see text]			17	
Difluorodichloroethylene	1219	1179	956	890			[see text]			21	
Trifluorochloroethylene	1330	1211	1032				[see text]			22	
Trifluorobromoethylene	1329	1202	1025				[see text]			22	
Trichlorofluoroethylene	1181	987	869				[see text]			22	
Trichloroethylene	931	852	639				[see text]			22	
	ν C—F cm ⁻¹	ν C—Cl cm ⁻¹	ν C—Br cm ⁻¹	ν C—I cm ⁻¹							
1-Halopropadiene	est. [1050]	767	681	609							23
1-Bromopropadiene-1d	[—]	[—]	636	[—]							15
1-Halopropyne	[—]	574	464	403							24
1,3-Dihalopropyne	[—]	617	512	[—]							16

Nitroalkanes, Nitrobenzenes, Alkyl Nitrates, Alkyl Nitrites, and Nitrosamines

Nitroalkanes	174
Nitroalkanes: Vapor vs Liquid-Phase Data	176
Tetranitromethane	176
Nitrobenzenes	177
Nitrobenzene in Different Physical Phases	177
4-Nitrobenzaldehyde	178
3-X-Nitrobenzenes	179
2-Nitrobenzenes	180
4-X-Nitrobenzenes in CCl ₄ and CHCl ₃ Solutions	181
Alkyl Nitrates	182
Ethyl Nitrate vs Nitroalkanes and Nitrobenzene	183
Alkyl Nitrites	183
Raman Data for Organonitro Compounds	184
A Summation of $\nu_{\text{asym. NO}_2}$ and $\nu_{\text{sym. NO}_2}$ in Different Physical Phases	184
Nitrosamines	185
References	185

Figures

Figure 7-1	186 (175)	Figure 7-12	196 (182)
Figure 7-2	187 (175)	Figure 7-13	197 (182)
Figure 7-3	188 (175)	Figure 7-14	198 (182)
Figure 7-4	189 (175)	Figure 7-15	199 (182)
Figure 7-5	190 (178)	Figure 7-16	200 (183)
Figure 7-6	190 (178)	Figure 7-17	201 (183)
Figure 7-7	191 (181)	Figure 7-18	202 (184)
Figure 7-8	192 (182)	Figure 7-19	203 (184)
Figure 7-9	193 (182)	Figure 7-20	204 (184)
Figure 7-10	194 (182)	Figure 7-21	205 (184)
Figure 7-11	195 (182)		

Tables

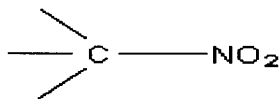
Table 7-1	206 (175)	Table 7-2	208 (175)
Table 7-1a	207 (175)	Table 7-3	209 (176)

Table 7-4	209 (177)	Table 7-19	221 (181)
Table 7-5	210 (177)	Table 7-20	222 (181)
Table 7-6	211 (177)	Table 7-21	223 (181)
Table 7-7	212 (177)	Table 7-22	224 (182)
Table 7-8	213 (177)	Table 7-23	224 (182)
Table 7-9	214 (178)	Table 7-24	225 (183)
Table 7-10	215 (179)	Table 7-25	226 (183)
Table 7-11	216 (179)	Table 7-26	226 (183)
Table 7-12	216 (180)	Table 7-27	227 (184)
Table 7-13	217 (180)	Table 7-28	227 (184)
Table 7-14	218 (180)	Table 7-29	228 (184)
Table 7-15	218 (180)	Table 7-30	229 (184)
Table 7-16	219 (180)	Table 7-31	229 (184)
Table 7-17	220 (180)	Table 7-32	230 (184)
Table 7-18	221 (180)	Table 7-33	230 (185)

*Numbers in parentheses indicate in-text page reference.

NITROALKANES

The variations in frequencies of antisymmetric NO_2 stretching, $\nu_{\text{asym. NO}_2}$, and symmetric NO_2 stretching, $\nu_{\text{sym. NO}_2}$ have been attributed to inductive and/or resonance effects (1, 2). Empirical correlations have been developed for the calculation of $\nu_{\text{asym. NO}_2}$ and $\nu_{\text{sym. NO}_2}$ frequencies in unknown compounds containing this functional group. These correlations relate to the substituent groups joined to the α -carbon atom of nitroalkanes and the wavenumber values of $\nu_{\text{asym. NO}_2}$ and $\nu_{\text{sym. NO}_2}$ for nitromethane (1).



α

$$\text{Vapor phase} \quad \left[\begin{array}{l} \nu_{\text{asym. NO}_2} = 1582 + \Sigma(Y_1 + X_1) \\ \nu_{\text{sym. NO}_2} = 1397 + \Sigma(Y_2 + X_2) \end{array} \right. \quad (1)$$

$$\nu_{\text{asym. NO}_2} \quad \left[\begin{array}{l} Y_1 = -7 \text{ cm}^{-1} \text{ for each CH}_3 \text{ or C}_2\text{H}_5 \text{ group joined to the } \alpha\text{-carbon atom} \\ X_1 = 10 \text{ cm}^{-1} \text{ for each Cl atom joined to the } \alpha\text{-carbon atom} \end{array} \right.$$

$$\nu_{\text{asym. NO}_2} \quad \left[\begin{array}{l} Y_2 = -17 \text{ cm}^{-1} \text{ for each CH}_3 \text{ or C}_2\text{H}_5 \text{ group joined to the } \alpha\text{-carbon atom} \\ X_2 = -29 \text{ cm}^{-1} \text{ for each Cl atom joined to the } \alpha\text{-carbon atom} \end{array} \right.$$

Application of Eqs. (1) and (2) allow one to estimate the observed frequencies to within 16 cm^{-1} in the vapor phase.

Equations 3 and 4 were developed to estimate ν asym. NO_2 and ν sym. NO_2 frequencies in the liquid phase (1). The 1558 cm^{-1} and 1375 cm^{-1} are for nitromethane in

$$\nu \text{ asym. NO}_2 = 1558\text{ cm}^{-1} + \Sigma\Delta R \quad (3)$$

$$\nu \text{ sym. NO}_2 = 1375 + \Sigma\Delta R \quad (4)$$

the liquid phase (1). The ΔR values are for atoms or groups joined to the α - and β - carbon atoms, and their $\Delta\text{ cm}^{-1}$ values are presented here in Table 7.1.

Figures 7.1 and 7.2 show plots of ν asym. NO_2 (observed) vs ν asym. NO_2 (calculated) and ν sym. NO_2 (observed) vs ν sym. NO_2 (calculated), respectively, and the agreement is essentially linear. These correlations do not distinguish between primary, secondary or tertiary nitroalkanes.

Applying Eqs. 3 and 4 to determine the νNO_2 vibrations for CF_3NO_2 is shown here:

$$\nu \text{ asym. NO}_2 = 1558 + 3(17) = 1609\text{ cm}^{-1} \text{ vs } 1607\text{ cm}^{-1} \text{ observed}$$

$$\nu \text{ sym. NO}_2 = 1375 + 3(-23) = 1306\text{ cm}^{-1} \text{ vs } 1311\text{ cm}^{-1} \text{ observed}$$

Figure 7.3 is a vapor-phase IR spectrum for nitromethane. The IR band at 919 cm^{-1} is assigned to C–N stretching, ν C–N, and the IR band at 659 cm^{-1} is assigned to NO_2 bending, δNO_2 . The weak band at 605 cm^{-1} is assigned to NO_2 wagging, WNO_2 , and an IR band at 472 cm^{-1} (liquid phase) is assigned to NO_2 rocking, ρNO_2 (3). Figure 7.4 is a vapor-phase IR spectrum for 2-nitropropane. Presumably the IR band at $\sim 625\text{ cm}^{-1}$ results from δNO_2 , and the WNO_2 mode at 535 cm^{-1} .

Table 7.1a lists the vapor-phase IR data for nitroalkanes. Most primary nitroalkanes exist as a mixture of trans and gauche conformers due to rotation of the C–CNO₂ moiety. The trans ν C–N vibration has been assigned in the range $895\text{--}914\text{ cm}^{-1}$ and the gauche ν C–N vibration has been assigned in the range $868\text{--}894\text{ cm}^{-1}$ (4). Figure 7.4 shows that the absorbance for the 901 cm^{-1} trans ν C–N vibration is much less than the absorbance for the 851 cm^{-1} gauche ν C–N vibration. The gauche ν C–N vibration for 1-nitrobutane, 1-nitropentane, and 1-nitrohexane are assigned in the range $850\text{--}859\text{ cm}^{-1}$.

The δNO_2 vibration for these *n*-alkanes listed in Table 7.1a is assigned in the range $603\text{--}659\text{ cm}^{-1}$.

The frequency separation between ν asym. NO_2 and ν sym. NO_2 for these nitroalkanes in the vapor phase varies between 185 and 205 cm^{-1} , and the absorbance ratio $(A)\nu$ asym. $\text{NO}_2/(A)\nu$ sym. NO_2 varies between 1.94 and 3.47.

Table 7.2 lists the vapor-phase IR data for nitroalkanes. The ν asym. CH_3 vibrations occur in the range $2975\text{--}2995\text{ cm}^{-1}$, the ν asym. CH_2 vibrations occur in the range $2940\text{--}2950\text{ cm}^{-1}$, and the ν sym. CH_2 vibration in the range $2880\text{--}2910\text{ cm}^{-1}$. In the case of 2-nitropropane it appears as though ν sym. CH_3 is in Fermi resonance (FR) with 2δ asym. CH_3 . The δCH_2 and ρCH_2 vibrations occur in the ranges $1446\text{--}1458\text{ cm}^{-1}$ and $1113\text{--}1129\text{ cm}^{-1}$, respectively.

If one calculates the absorbance ratios: $(A)\nu$ sym. $\text{NO}_2/(A)\nu$ sym. CH_2 ; $(A)\nu$ sym. $\text{NO}_2/(A)\nu$ asym. CH_2 ; and $(A)\nu$ sym. $\text{NO}_2/(A)\nu$ asym. CH_3 , the calculated values decrease as the number of carbon atoms in the nitroalkanes increase. Absorbance ratios such as these aid in identifying specific nitroalkanes.

NITROALKANES: VAPOR VS LIQUID-PHASE DATA

Table 7.3 compares vapor- and liquid-phase IR data for the ν NO₂ vibrations for 12 nitroalkanes. In both vapor and liquid phases, ν asym. NO₂ occur in the ranges 1555–621 cm⁻¹ and 1535–1601 cm⁻¹, respectively. Thus, the ν asym. NO₂ vibration for these nitroalkanes decreases in frequency by 17 to 32 cm⁻¹ in going from the vapor to the liquid phase. In the case of ν sym. NO₂, this vibration occurs in the range 1310–1397 cm⁻¹ in the vapor and in the range 1310–1381 cm⁻¹ in the liquid phase. Thus, the ν sym. NO₂ vibration remains constant in the case of trichloronitromethane or decreases in frequency by 1–22 cm⁻¹ in going from the vapor to the liquid phase. Thus, the ν asym. NO₂ vibration decreases much more in frequency than does the ν sym. NO₂ vibration in going from the vapor to the liquid phase.

TETRANITROMETHANE

Tetranitromethane has a maximum symmetry of T_d. In the vapor phase, IR bands are noted at 1651 cm⁻¹ (A = 0.180), 1623 cm⁻¹ (A = 1.240), 1278 cm⁻¹ (A = 0.220), 801 cm⁻¹ (A = 0.330), and very weak bands at ~665 cm⁻¹, and 604 cm⁻¹ (1). In the liquid phase, IR bands are noted at 1642 cm⁻¹ (A = 0.490), 1610 cm⁻¹ (A = 0.840), 1268 cm⁻¹ (A = 0.490), 799 cm⁻¹ (A = 0.611), 662 cm⁻¹ (A = 0.070), and 602 cm⁻¹ (A = 0.113).

Nitroalkanes have been reported to exhibit ν asym. NO₂ in the range 1555–1621 cm⁻¹ (1). The absorbance ratio of the 1623 cm⁻¹/1651 cm⁻¹ bands in the vapor phase is 6.89, and the absorbance ratio of the 1642 cm⁻¹/1610 cm⁻¹ bands in the liquid phase is 1.71. These two IR bands must result from ν asym. (NO₂)₄ vibrations. It is possible that the 1623 cm⁻¹ (VP) and 1610 cm⁻¹ (LP) bands result from out-of-phase ν asym. (NO₂)₄ and the 1651 cm⁻¹ (VP) and 1642 cm⁻¹ (LP) bands result from in-phase ν asym. (NO₂)₄. The ratio of the out-of-phase ν asym. (NO₂)₄ vibrations to the in-phase ν asym. (NO₂)₄ vibrations is higher in the vapor phase at elevated temperature. There are no other spectral features to suggest that these two bands are the result of ν asym. (NO₂)₄ being in FR with a combination tone.

Nitroalkanes in the vapor phase exhibit ν sym. NO₂ in the range 1310–1397 cm⁻¹ (1). It is suggested that the 1278 cm⁻¹ (VP) and the 1268 cm⁻¹ (LP) bands result from out-of-phase ν sym. (NO₂)₄. With T_d symmetry, the in-phase ν sym. (NO₂)₄ vibration would be IR inactive (Raman active). A weak IR band occurs at 2885 cm⁻¹ in the vapor phase and this can be assigned to the combination tone (1623 + 1278 = 2901 cm⁻¹). In the liquid phase the combination tone is (1610 + 1268 = 2878 cm⁻¹ vs 2870 cm⁻¹ observed). This assignment is for the out-of-phase ν asym. (NO₂)₄ + out-of-phase ν sym. (NO₂)₄ combination tone. A weak IR band is observed at 2970 cm⁻¹ in the vapor phase. If we assume that the in-phase ν asym. (NO₂)₄ and in-phase ν sym. (NO₂)₄ also exhibit a combination tone (the 2970 cm⁻¹ IR band), the in-phase ν sym. (NO₂)₄ vibration is calculated to occur at 1319 cm⁻¹. Raman data is required to determine if this assumption is correct.

Weak IR bands are observed at 2550 cm⁻¹ (VP) and 2532 cm⁻¹ (LP), and these can be assigned to the overtone of out-of-phase ν asym. (NO₂)₄.

Infrared bands at 801 cm⁻¹ (VP), 799 cm⁻¹ (A = 0.611) (LP), ~665 cm⁻¹ (VP), 666 cm⁻¹ (A = 0.070) (LP) and 604 (VP), and 602 cm⁻¹ (A = 0.113) (LP) are tentatively assigned to the

$\delta(\text{NO}_2)_4$, $\text{W}(\text{NO}_2)_4$, and $\rho(\text{NO}_2)_4$ vibrations. The decrease in frequency for out-of-phase ν asym. $(\text{NO}_2)_4$ and out-of-phase ν sym. $(\text{NO}_2)_4$ in going from the vapor phase to the liquid phase is 131 cm^{-1} and 10 cm^{-1} , respectively. The data for tetranitromethane was read from Sadtler IR vapor spectra and standard condensed phase IR spectra (1).

It is suggested that the range for ν asym. NO_2 for nitroalkanes extends over the range $1555\text{--}1651\text{ cm}^{-1}$ and that ν sym. NO_2 extends over the range $1278\text{--}1397\text{ cm}^{-1}$.

NITROBENZENES

Study of 131 vapor-phase IR spectra of nitrobenzenes shows that ν asym. NO_2 occurs in the range $1530\text{--}1580\text{ cm}^{-1}$ and ν sym. NO_2 in the range $1325\text{--}1371\text{ cm}^{-1}$. Comparisons of these nitrobenzene data with those data for nitroalkanes show that both ν asym. NO_2 and ν sym. NO_2 vibrations overlap. Comparison of the ν asym. NO_2 frequencies for nitrobenzene (1540 cm^{-1}), nitromethane (1582 cm^{-1}), and trimethylnitromethane (1555 cm^{-1}) show that this mode occurs at lower frequency in the case of nitrobenzene. This decrease in frequency for ν asym. NO_2 is attributed to resonance effects of the phenyl group with the NO_2 group (5). Table 7.4 lists IR data for 4-X-nitrobenzenes in the vapor phase. The ν asym. NO_2 mode occurs at 1530 cm^{-1} for 4-nitroanilines and at 1567 cm^{-1} for 1,4-dinitrobenzene and the σ_p values are -0.66 and $+0.78$, respectively. However, there is no apparent smooth correlation for ν asym. NO_2 vs σ_p . Neither is there a smooth correlation for ν sym. NO_2 vs σ_p .

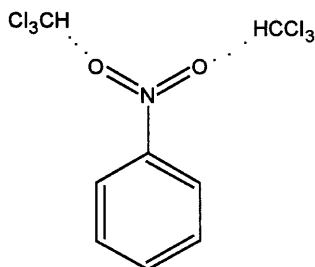
Comparison of the ν sym. NO_2 frequencies for nitrobenzene (1351 cm^{-1}), nitromethane (1397 cm^{-1}), and trimethylnitromethane (1349 cm^{-1}) show that these vibrations occur at similar frequencies. Thus, it would be helpful to have another parameter to help distinguish between nitrobenzenes and nitroalkanes. A distinguishing feature is the absorbance ratio (A) ν asym. NO_2 /(A) ν sym. NO_2 . The band intensity ratio for nitrobenzene is 0.9 compared to 1.9–5.9 for the nitroalkanes. The absorbance ratio for (A) ν asym. NO_2 /(A) ν sym. NO_2 varies between 0.9 and 1.9 for these 4-X-nitrobenzenes.

NITROBENZENE IN DIFFERENT PHYSICAL PHASES

Tables 7.5 through 7.8 list IR frequency data for nitrobenzenes in different physical phases. In all cases ν asym. NO_2 occurs at lower frequency in CHCl_3 solution or in the neat liquid or solid phase than it occurs in the vapor phase. However, ν sym. NO_2 usually occurs at lower frequency in CHCl_3 than in the vapor phase. In certain cases ν sym. NO_2 occurs at higher frequency in the neat phase than in the vapor phase (4-chloronitrobenzene for example, 1360 cm^{-1} vs 1349 cm^{-1} ; see Table 7.5). In all cases, the frequency separation between ν asym. NO_2 and ν sym. NO_2 is larger in the vapor phase than it is in CHCl_3 solution or the neat phases.

Table 7.7 lists IR ν NO_2 data for 4-X-nitrobenzenes and 3-X-nitrobenzenes in CCl_4 and CHCl_3 solution. In all cases the frequency separation between ν asym. NO_2 and ν sym. NO_2 is larger in CCl_4 solution than in CHCl_3 solution. In addition, the ν asym. NO_2 frequency always decreases in going from CCl_4 solution to CHCl_3 solution, while ν sym. NO_2 generally increases in frequency. The exceptions are for 4-nitroaniline, 4-nitroanisole, and 4-nitrodiphenyl oxide. The decrease in frequency for ν asym. NO_2 in going from solution in CCl_4 to solution in CHCl_3

is attributed to intermolecular hydrogen bonding between the CHCl_3 proton and the oxygen atoms of the NO_2 group as shown here:



In the case of $\nu_{\text{sym. NO}_2}$ it is more difficult for the oxygen atoms to vibrate in phase, compared to the $\nu_{\text{asym. NO}_2}$ vibration which causes an increase in frequency due to intermolecular hydrogen bonding. In contrast there is a trade-off in energy during $\nu_{\text{asym. NO}_2}$ because one NO_2 oxygen atom is pulling away from the CHCl_3 proton while the other oxygen atom is expanding toward the CHCl_3 proton. The overall effect is a decrease in the $\nu_{\text{asym. NO}_2}$ frequency.

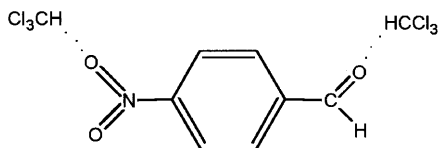
Table 7.8 shows that the frequency separation between $\nu_{\text{asym. NO}_2}$ in the vapor and CHCl_3 solution phase is larger than it is between $\nu_{\text{asym. NO}_2}$ in the vapor and the CCl_4 solution phase, and again this is the result of intermolecular hydrogen bonding in CHCl_3 solution. The reaction field of the solvent also affects ν_{NO_2} frequencies, and part of the decrease in frequency in CHCl_3 solution is attributed to the CHCl_3 reaction field. In the case of CCl_4 , the decrease in frequency is attributed to the reaction field of CCl_4 .

4-NITROBENZALDEHYDE

Table 7.9 lists IR data for $\nu_{\text{asym. NO}_2}$ and $\nu_{\text{sym. NO}_2}$ frequencies of 4-nitrobenzaldehyde 1% wt./vol. in 0 to 100 mol% $\text{CHCl}_3/\text{CCl}_4$ solutions (6). The $\nu_{\text{asym. NO}_2}$ decreases 4.8 cm^{-1} while $\nu_{\text{sym. NO}_2}$ increases 1.5 cm^{-1} in going from solution in CCl_4 to solution in CHCl_3 . Figure 7.5 show plots of $\nu_{\text{asym. NO}_2}$ and $\nu_{\text{C=O}}$ frequencies for 4-nitrobenzaldehyde vs mole% $\text{CHCl}_3/\text{CCl}_4$ (6). Both $\nu_{\text{asym. NO}_2}$ and $\nu_{\text{C=O}}$ decrease in frequency in a linear manner as the mole% $\text{CHCl}_3/\text{CCl}_4$ is increased from 0 to 100 mol%. Moreover, both modes decrease in frequency at approximately the same amount (viz. $\nu_{\text{asym. NO}_2}$, 4.8 cm^{-1} vs $\nu_{\text{C=O}}$, 4.5 cm^{-1}). In contrast the $\nu_{\text{C=O}}$ decrease in frequency for 4-dimethylaminobenzaldehyde is 9.8 cm^{-1} as the mole % is increased from 0 to 100 mol% $\text{CHCl}_3/\text{CCl}_4$. These data indicate that the strength of the intermolecular hydrogen formed between the CCl_3H proton and the $\text{C=O} \cdots \text{HCl}_3$ or $\text{NO}_2 \cdots (\text{HCl}_3)_1$ or $_2$ depends upon the basicity of the oxygen atoms. As these compounds are both 1,4-disubstituted benzenes, this is not a steric factor altering the distance between the site of the oxygen atom and the CCl_3H proton.

Figure 7.6 shows a plot of $\nu_{\text{sym. NO}_2}$ for 4-nitrobenzaldehyde vs mole% $\text{CHCl}_3/\text{CCl}_4$ (6). The plot shows that $\nu_{\text{sym. NO}_2}$ increases in frequency from 0 to 10.74 mol% $\text{CHCl}_3/\text{CCl}_4$, then decreases in frequency from 19.4 to 26.5 mol% $\text{CHCl}_3/\text{CCl}_4$, and then steadily increases in frequency to 100 mol% $\text{CHCl}_3/\text{CCl}_4$. This suggests that at mole% $\text{CHCl}_3/\text{CCl}_4 < 10.74$ the

intermolecular hydrogen bonding in the case of 4-nitrobenzaldehyde is as shown here. At higher concentrations of CHCl_3 , the intermolecular hydrogen bonding is as shown here:



The steady increase in frequency is due to the increased energy required to expand and contract the NO_2 oxygen atoms away from the CHCl_3 protons. This effect is larger than it appears in this plot, because the reaction field increases as the mole % $\text{CHCl}_3/\text{CCl}_4$ is increased, which has the effect of decreasing $\nu_{\text{asym. NO}_2}$ and $\nu_{\text{C=O}}$ frequencies.

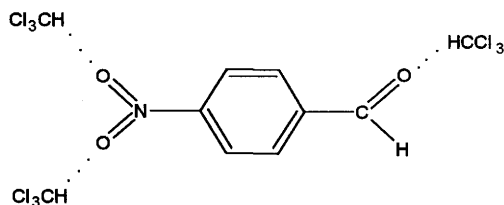


Table 7.10 is a comparison of IR $\nu_{\text{asym. NO}_2}$ and $\nu_{\text{sym. NO}_2}$ frequency data for nitromethane and nitrobenzene in a series of 13 different solvents (7). In both cases, the $\nu_{\text{asym. NO}_2}$ frequency is highest when in solution with hexane (CH_3NO_2 , 1569 cm^{-1} ; $\text{C}_6\text{H}_5\text{NO}_2$, 1535.8 cm^{-1}), and the frequency is lowest in dimethyl sulfoxide (CH_3NO_2 , 1552.8 cm^{-1} ; $\text{C}_6\text{H}_5\text{NO}_2$, 1524.7 cm^{-1}). In this series of solvents, the frequency difference between $\nu_{\text{asym. NO}_2}$ for nitromethane and nitrobenzene varies between 28.1 cm^{-1} and 34.3 cm^{-1} .

In several cases the $\nu_{\text{sym. NO}_2}$ vibration for nitromethane is masked by the solvent, and in two cases for nitrobenzene. The $\nu_{\text{sym. NO}_2}$ mode for nitrobenzene occurs 26.2 to 28 cm^{-1} lower in frequency than $\nu_{\text{sym. NO}_2}$ for nitromethane. Both $\nu_{\text{asym. NO}_2}$ and $\nu_{\text{sym. NO}_2}$ for nitrobenzene occur at lower frequency than the corresponding vibrations for nitromethane, and this is attributed to resonance of the phenyl group with the nitro group.

The frequency difference for $\nu_{\text{asym. NO}_2}$ for nitromethane in hexane and each of the other solvents is more than the frequency difference for $\nu_{\text{asym. NO}_2}$ for nitrobenzene in hexane and each of the other solvents, except for the solvents methylene chloride and chloroform. These exceptions may be attributed to intermolecular hydrogen bonding between the NO_2 oxygen atoms and CHCl_3 or CH_2Cl_2 protons, which is apparently stronger in the case of nitrobenzene.

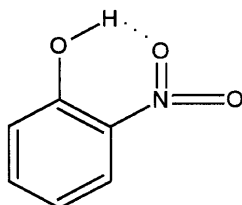
3-X-NITROBENZENES

The vapor-phase IR $\nu_{\text{asym. NO}_2}$ and $\nu_{\text{sym. NO}_2}$ frequencies for 3-X-nitrobenzenes occur in the ranges 1540 – 1553 cm^{-1} and 1349 – 1360 cm^{-1} , respectively (see Table 7.11). In addition the frequency difference between $\nu_{\text{asym. NO}_2}$ and $\nu_{\text{sym. NO}_2}$ ranges between 187 and 204 cm^{-1} , and the absorbance ratio $(A)\nu_{\text{asym. NO}_2}/(A)\nu_{\text{sym. NO}_2}$ varies between 1.07 and 2.16 . The

frequency separation between ν asym. NO_2 and ν sym. NO_2 appears to decrease in the order vapor, CHCl_3 , CHCl_3 , and neat or solid phase (see Tables 7.12 and 7.13).

2-NITROBENZENES

Table 7.14 lists vapor-phase IR data for 2-nitrobenzenes (1). Their ν asym. NO_2 and ν sym. NO_2 frequencies occur in the ranges $1540\text{--}1560\text{ cm}^{-1}$ and $1350\text{--}1360\text{ cm}^{-1}$, respectively. The compound 2-nitrophenol is an exception because ν sym. NO_2 occurs at 1335 cm^{-1} . This relatively low ν sym. NO_2 for 2-nitrophenol is attributed to intramolecular hydrogen bonding between the OH proton and the NO_2 oxygen atom as illustrated here:



Intramolecular hydrogen bonding alters the band intensity ratio $(A)\nu$ asym. $\text{NO}_2/(A)\nu$ sym. NO_2 because this ratio is 0.52 for 2-nitrophenol and varies between 1.09 to 2.59 for the 13 other compounds included in this study. In addition the frequency separation between ν asym. NO_2 and ν sym. NO_2 is 210 cm^{-1} for 2-nitrophenol and varies between 186 and 200 cm^{-1} for the other 13 compounds included in this study.

Tables 7.15 and 7.16 compare the ν asym. NO_2 and ν sym. NO_2 frequency data for 2-X-nitrobenzenes in different physical phases. The frequency separation between ν asym. NO_2 and ν sym. NO_2 is larger in the vapor phase than in either CHCl_3 solution or the neat or solid phases. Moreover, the ν asym. NO_2 vibration decreases more in frequency in going from the vapor phase to the CHCl_3 solution phase or to the neat or solid phase than does the ν sym. NO_2 vibration.

Table 7.17 lists IR data for 1-X-, 3-X- and 4-X-nitrobenzenes in the solid phase, and there does not appear to be a consistent trend in ν asym. NO_2 and ν sym. NO_2 frequencies in the three sets of these substituted nitrobenzenes in the solid phase.

Table 7.18 lists vapor-phase IR data for the ν asym. NO_2 and ν sym. NO_2 frequencies of 2,5- and 2,6-X,Y-nitrobenzenes. The ν asym. NO_2 and ν sym. NO_2 frequencies occur in the ranges $1541\text{--}1560\text{ cm}^{-1}$ and $1349\text{--}1361\text{ cm}^{-1}$, respectively. The exceptions are for those 2,5-X,Y-nitrobenzenes with an OH or an NHCO CH_3 group in the 2-position. These ν sym. NO_2 vibrations occur at 1325 cm^{-1} , 1330 cm^{-1} , and 1340 cm^{-1} , and occur at lower frequency as a result of intramolecular hydrogen bonding. It is also interesting to note that the absorbance ratio $(A)\nu$ asym. $\text{NO}_2/(A)\nu$ sym. NO_2 is 1.07, 0.74, and 0.37 for these same compounds.

In the case of the 2,6-X-Y-nitrobenzenes, the compound 2-nitro-6-methylphenol exhibits ν sym. NO_2 at 1349 cm^{-1} and the absorbance ratio $(A)\nu$ asym. $\text{NO}_2/(A)\nu$ sym. NO_2 is 0.88. These data indicate that the NO_2 group is intramolecularly hydrogen bonded with the phenolic OH group.

In the case of 2,6-dichloronitrobenzene the ν asym. NO_2 frequency occurs at 1568 cm^{-1} and the absorbance ratio $(A)\nu$ asym. $\text{NO}_2/(A)\nu$ sym. NO_2 is 3.60. These data are comparable to those

exhibited by the nitroalkanes. The reason for this is that the NO_2 group and the 2,6-dichlorophenyl group are not coplanar in the case of 2,6-dichloro-1-nitrobenzene. Therefore, the resonance effect upon the NO_2 is no longer possible.

Table 7.19 is a comparison of the frequency difference between ν asym. NO_2 and ν sym. NO_2 in the vapor, neat or solid phases for 2,5-X-Y-nitrobenzenes. These data show that the ν asym. NO_2 decrease more in frequency than ν sym. NO_2 in going from the vapor to the neat or solid phase.

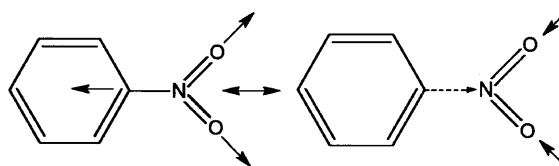
Table 7.20 lists IR data for tri-, tetra- and pentasubstituted nitrobenzenes. The highest ν asym. NO_2 frequencies are exhibited by 1,2-dinitro-3,6-dichlorobenzene, 1580 cm^{-1} , and 1,2-dinitro-3,6-dibromobenzene, 1578 cm^{-1} (1). These two compounds also have the highest absorbance ratio $(A)\nu$ asym. $\text{NO}_2/(A)\nu$ sym. NO_2 , 4.17 and 3.88 for the 3,6- Cl_2 and 3,6- Br_2 analogs, respectively. These data indicate that the NO_2 groups are not coplanar with the 3,6-dihalophenyl group.

In the case of nitrobenzenes where there is at least 2,6-dichloro atoms, the NO_2 group is not coplanar with the 2,6-dichloro phenyl group. Thus, compounds such as 2,4,6-trichloronitrobenzene, 2,3,5,6-tetrachloronitrobenzene, and pentachloronitrobenzene exhibit ν asym. NO_2 at 1562 , 1569 , and 1568 cm^{-1} , respectively. In the same compound order, ν sym. NO_2 is assigned at 1361 , 1333 , and 1332 cm^{-1} , respectively, and the absorbance ratio for $(A)\nu$ asym. $\text{NO}_2/(A)\nu$ sym. NO_2 is 2.67, 1.25, and 1.48, respectively.

4-X-NITROBENZENES IN CCl_4 AND CHCl_3 SOLUTIONS

Table 7.21 lists the ν asym. and ν sym. NO_2 frequencies for 21 4-X-nitrobenzenes in 1% or less wt./vol. in CCl_4 and CHCl_3 solutions (8). Figure 7.7 is a plot of ν asym. NO_2 frequencies in CCl_4 solution vs ν asym. NO_2 frequencies in CHCl_3 solution. This linear plot increases from a low of 1513.9 cm^{-1} vs 1505.3 cm^{-1} for 4-nitroaniline to a high of 1556.1 cm^{-1} vs 1554.4 cm^{-1} for 1,4-dinitrobenzene. At all frequency points, the ν asym. NO_2 vibration occurs at lower frequency in CHCl_3 solution than in CCl_4 solution. As stated previously, the shift to lower frequency in CHCl_3 solution is due to intermolecular hydrogen bonding $[\text{NO}_2(\cdots\text{HCCl}_3)_2]$ and an increased value for the reaction field.

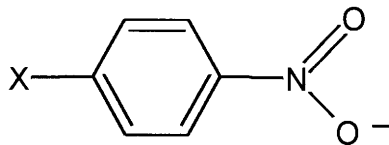
It has been suggested that ν sym. NO_2 couples with an in-plane ring mode as approximated here:



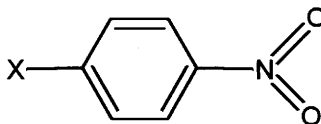
This is because ν sym. NO_2 is not affected in the same manner as ν asym. NO_2 .

In general, the frequency separation between ν asym. NO_2 and ν sym. NO_2 increases progressing in the series 1-21 in both solvents. This is attributed to the nature of the NO_2 bonds. Bellamy has pointed out that the ν asym. NO_2 for 4-X-nitrobenzenes is directly related to

the electron donor or acceptor property of the 4-X substituent (9). For example, substituent groups with negative σ_p values would contribute to a structure such as presented here:



Substituent groups with positive σ_p values would contribute to a structure such as presented here:



Figures 7.8 and 7.9 are plots of $\nu_{\text{asym. NO}_2}$ for 4-X-nitrobenzenes in CCl₄ solution and in CHCl₃ solution vs Hammett σ_p values for the 4-X substituent group, respectively (8). The Hammett σ_p values include both inductive and resonance contributions of the 4-substituent groups (10). Both of these plots show pseudolinear relationships. The most deviant point is 6 for 4-nitrophenol. In this case the OH group is intermolecularly hydrogen bonded to the Cl atom of each solvent (8).

Resonance parameters have been derived for substituted benzenes. When the ring is unperturbed, it is σ_R . When the ring is electron poor, it is σ_{R+} . When the ring is electron rich, it is σ_{R-} . When the ring is in resonance with a carboxylic acid group, it is σ_R (11).

Figures 7.10 and 7.11 are plots of $\nu_{\text{asym. NO}_2}$ frequencies vs σ_{R+} for 4-X-nitrobenzenes in CCl₄ and CHCl₃ solutions, respectively (8). These pseudo-linear relationships show that as σ_{R+} becomes more positive, the $\nu_{\text{asym. NO}_2}$ vibration increases in frequency.

Figures 7.12 and 7.13 are plots of $\nu_{\text{asym. NO}_2}$ vs σ_R for 4-X-nitrobenzenes in CCl₄ and CHCl₃ solutions, respectively (8). These plots show the same trend as for Figs. 7.10 and 7.11.

Figures 7.14 and 7.15 are plots of $\nu_{\text{asym. NO}_2}$ for 4-X-nitrobenzenes vs σ_I , a measure of the inductive power of the 4-X group (10, 11) in CCl₄ and CHCl₃ solutions, respectively (8). These figures show that $\nu_{\text{asym. NO}_2}$ does not correlate well with the inductive parameter of the 4-X group. In conclusion, the $\nu_{\text{asym. NO}_2}$ frequencies for 4-X-nitrobenzenes correlate best with σ_p values, which include both resonance and inductive parameters.

ALKYL NITRATES

Tables 7.22 and 7.23 list IR data and vibrational assignments for alkyl nitrates. Depending upon the physical phase, $\nu_{\text{asym. NO}_2}$ and $\nu_{\text{sym. NO}_2}$ for alkyl nitrates occur in the ranges 1617–1662 cm⁻¹ and 1256–1289 cm⁻¹, respectively. The absorbance for $\nu_{\text{asym. NO}_2}$ is higher than the absorbance for $\nu_{\text{sym. NO}_2}$. The $\nu_{\text{asym. NO}_2}$ vibration decrease more in frequency then the $\nu_{\text{sym. NO}_2}$ vibration in going from the vapor phase to CCl₄ solution or neat phase. Both $\nu_{\text{asym. NO}_2}$ and $\nu_{\text{sym. NO}_2}$ exhibit a first overtone, and $2\nu_{\text{asym. NO}_2}$ decreases more in frequency than $2\nu_{\text{sym. NO}_2}$ in going from the vapor phase to the neat or solution phase.

The ν N–O vibration occurs in the range 854–865 cm^{-1} , and γ NO₂ and δ NO₂ are assigned near 760 cm^{-1} and 700 cm^{-1} , respectively. A vapor-phase IR spectrum for ethyl nitrate is shown in Fig. 7.16.

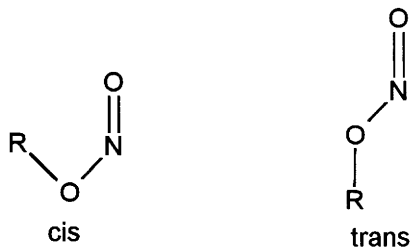
ETHYL NITRATE VS NITROALKANES AND NITROBENZENE

Table 7.24 lists IR data for ethyl nitrate, nitroalkanes, and nitrobenzene in CCl₄ and CHCl₃ solutions (7). In all cases, the ν asym. NO₂ vibration decreases in frequency and the ν sym. NO₂ vibration increases in frequency in going from CCl₄ solution to CHCl₃ solution. The decrease in the ν asym. NO₂ frequency in going from solution in CCl₄ to solution in CHCl₃ is attributed to intermolecular hydrogen bonding [NO₂(\cdots HCCL₃)₂] and an increased reaction field. In the case of ν sym. NO₂, the situation is reversed. The increased reaction is expected to lower the ν sym. NO₂ frequency. This reversal is due to the fact that it requires more energy to expand both NO₂ oxygen atoms against the HCCL₃ protons [NO₂(\cdots HCCL₃)₂] during a cycle of ν sym. NO₂. In the case of ν asym. NO₂, the energy required to expand one NO₂ oxygen atom toward the HCCL₃ proton is canceled by contraction of the other NO₂ oxygen atom away from the HCCL₃ proton.

Another correlation for these compounds is that as the ν asym. NO₂ vibration decreases in frequency from 1637 through 1531 cm^{-1} , the ν sym. NO₂ vibration tends to increase in frequency. The frequency separation between ν asym. NO₂ and ν sym. NO₂ decreases in the order ethyl nitrate through nitrobenzene in both CCl₄ and HCCL₃ solutions (355.8–183.3 cm^{-1} CCl₄ and 348.8–177.6 cm^{-1} in HCCL₃) (7).

ALKYL NITRITES

Alkyl nitrites have the empirical structure R–O–N=O. However, these compounds exist in a cis and trans structure as depicted here:



Therefore, alkyl nitrites exhibit IR bands for cis ν N=O and trans ν N=O. Tables 7.25 and 7.26 list characteristic IR group frequency data for alkyl nitrites. The data in Table 7.26 are from Tarte (12). The ν N=O frequency data reported by Tarte are higher than those reported by Nyquist (1). An IR spectrum for *n*-butyl nitrite is shown in Fig. 7.17. The trans ν N=O vibration (1653–1681 cm^{-1}) occurs at higher frequency than the cis ν N=O vibration (1610–1625 cm^{-1}), and the absorbance ratio (A) trans ν N=O/(A) cis ν N=O varies from 0.95 for methyl nitrite to \sim 50 for tert-butyl nitrite. As the steric factor of the R group becomes larger, the preferred structure is apparently the trans configuration.

The trans ν N–O vibration occurs in the range 751–814 cm^{-1} , and the cis δ O–N=O and trans δ O–N=O vibrations are assigned in the ranges 617–689 cm^{-1} and 564–625 cm^{-1} , respectively (12).

Figure 7.18 shows plots of cis ν N=O and trans ν N=O for alkyl nitrites vs σ^* (the inductive parameter of the alkyl group), and both plots show a pseudo-linear relationship (1).

Figure 7.19 shows a plot of trans ν N–O vs σ^* and this plot also shows a pseudolinear relationship (1).

Figure 7.20 shows a plot of trans ν N=O vs trans ν N–O, and this plot also exhibits a pseudolinear relationship (1).

Figure 7.21 shows plots of the absorbance ratio (A) trans ν N=O/(A) cis ν N=O for 10 alkyl nitrites vs σ^* . These data show that the concentration of the trans conformer increases as the electron release of the alkyl group to the O–N=O group is increased (1).

RAMAN DATA FOR ORGANONITRO COMPOUNDS

Table 7.27 lists Raman data for some organonitro compounds (13). The eight compounds listed show that ν sym. NO_2 is a medium to strong Raman band in the range 1312–1350 cm^{-1} , and a weak to strong Raman band assigned to δ NO_2 in the range 831–882 cm^{-1} . The frequency separation between these two Raman bands varies between 454 and 492 cm^{-1} . The relative Raman band intensity for the absorbance ratio (RI) ν sym. NO_2 /(RI) δ NO_2 varies between 0.56 and 9.

Table 7.28 compares IR and Raman data for nitroalkanes in different physical phases. These data also show that ν asym. NO_2 occurs at lower frequency in the neat phase than in the vapor phase, and it also decreases more in frequency than ν sym. NO_2 , which either decreases or in some cases increases in frequency.

Table 7.29 lists IR and Raman data for nitrobenzenes in different physical phases. Not listed in this Table but worth mentioning is that in the Raman spectrum the ν sym. NO_2 mode is always more intense than in the IR spectrum.

A SUMMATION OF ν asym. NO_2 AND ν sym. NO_2 IN DIFFERENT PHYSICAL PHASES

Tables 7.30–7.32 list IR and/or Raman data in various physical phases. In all cases ν asym. NO_2 changes more in going from the vapor phase to the solution or neat phases than does the ν sym. NO_2 , which sometimes even increases in frequency. Intermolecular hydrogen bonding and the increased reaction field lowers ν NO_2 frequencies. The increased energy required during expansions of the NO_2 oxygen atoms against the CHCl_3 protons offset the increase in the reaction field and hydrogen bonding effects.

NITROSAMINES

Nitrosamines have the empirical structure presented here:

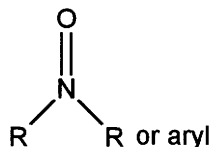
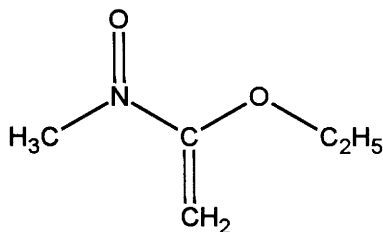


Table 7.33 lists IR data for nitrosamines in different physical phases. These compounds exhibit $\nu\text{N}=\text{O}$ in the region $1482\text{--}1492\text{ cm}^{-1}$ in the vapor phase, and in the region $1438\text{--}1450\text{ cm}^{-1}$ in the liquid phase. Thus, there is a decrease in frequency of between $32\text{--}54\text{ cm}^{-1}$ in going from the vapor to the liquid phase. This frequency decrease is attributed to dipolar interaction between the $\text{N}=\text{O}$ groups in the condensed phase. Another way to look at this $\nu\text{N}=\text{O}$ frequency decrease in going from the vapor to the neat phase is that there is an increase in the reaction field.

The compound illustrated here exhibits $\nu\text{N}=\text{O}$ at 1534 cm^{-1} in the vapor phase and at 1509 cm^{-1} in the neat phase:



REFERENCES

1. Nyquist, R. A. (1984). *The Interpretation of Vapor-Phase Infrared Spectra: Group Frequency Data*. Philadelphia: Sadtler Research Laboratories, pp. 550–608; see also Sadtler Standard vapor- and neat-phase IR collections.
2. Lunn, W. H. (1960). *Spectrochim. Acta*, **16**: 1088.
3. Smith, D. C., Pan, C. Y., and Nielsen, J. R. (1950). *J. Chem. Phys.* **18**: 706.
4. Geiseler, G. and Kesler, G. (1964). *Ber. Bunsenges. Phys. Chem.* **68**: 571.
5. Bellamy, L. J. (1968). *Advances In Infrared Group Frequencies*. London: Methuen & Co. Ltd., p. 231.
6. Nyquist, R. A., Settineri, S. E., and Luoma, D. A. (1991). *Appl. Spectrosc.* **45**: 1641.
7. Nyquist, R. A. (1990). *Appl. Spectrosc.* **44**: 594.
8. Nyquist, R. A. and Settineri, S. E. (1990). *Appl. Spectrosc.* **44**: 1552.
9. Bellamy, L. J. (1968). *Advances in Infrared Group Frequencies*. London: Methuen & Co., p. 228.
10. Taft, R. W. (1956). *Steric Effects in Organic Chemistry*. M. S. Newman, ed., New York: John Wiley.
11. Brownlee, R. T. C. and Topsom, R. D. (1975). *Spectrochim. Acta* **31A**: 1677.
12. Tarte, P. (1952). *J. Chem. Phys.* **20**: 1570.
13. *Sadtler Laboratories Standard Collection of Raman Data for Organic Compounds*. Philadelphia, PA.
14. Bellamy, L. J. (1968). *Advances in Infrared Group Frequencies*. London: Methuen & Co.

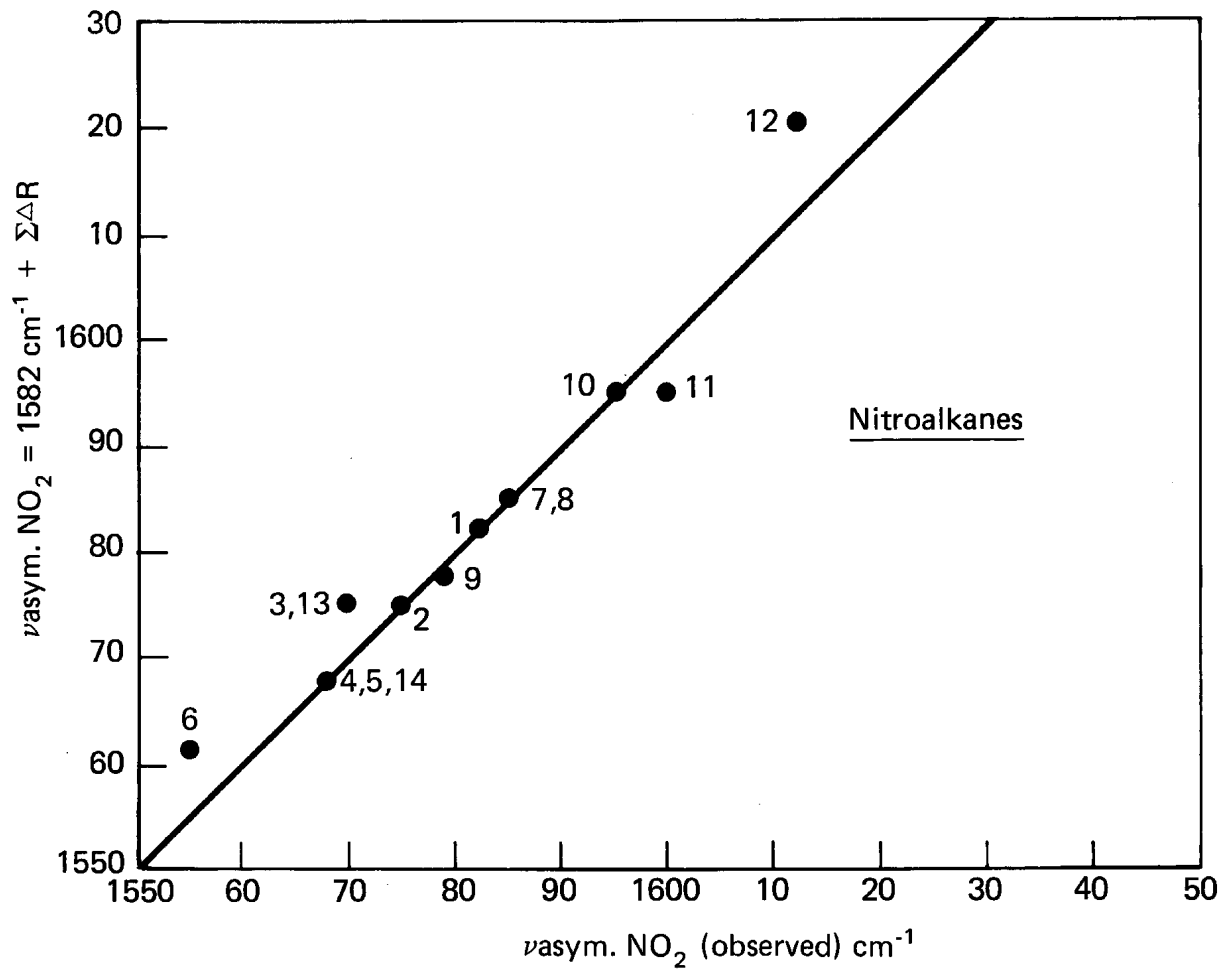


FIGURE 7.1 A plot of the observed $\nu_{\text{asym. NO}_2}$ frequencies vs the calculated $\nu_{\text{asym. NO}_2}$ frequencies for nitroalkanes using the equation $\nu_{\text{asym. NO}_2} = 1582 \text{ cm}^{-1} + \Sigma\Delta R$.

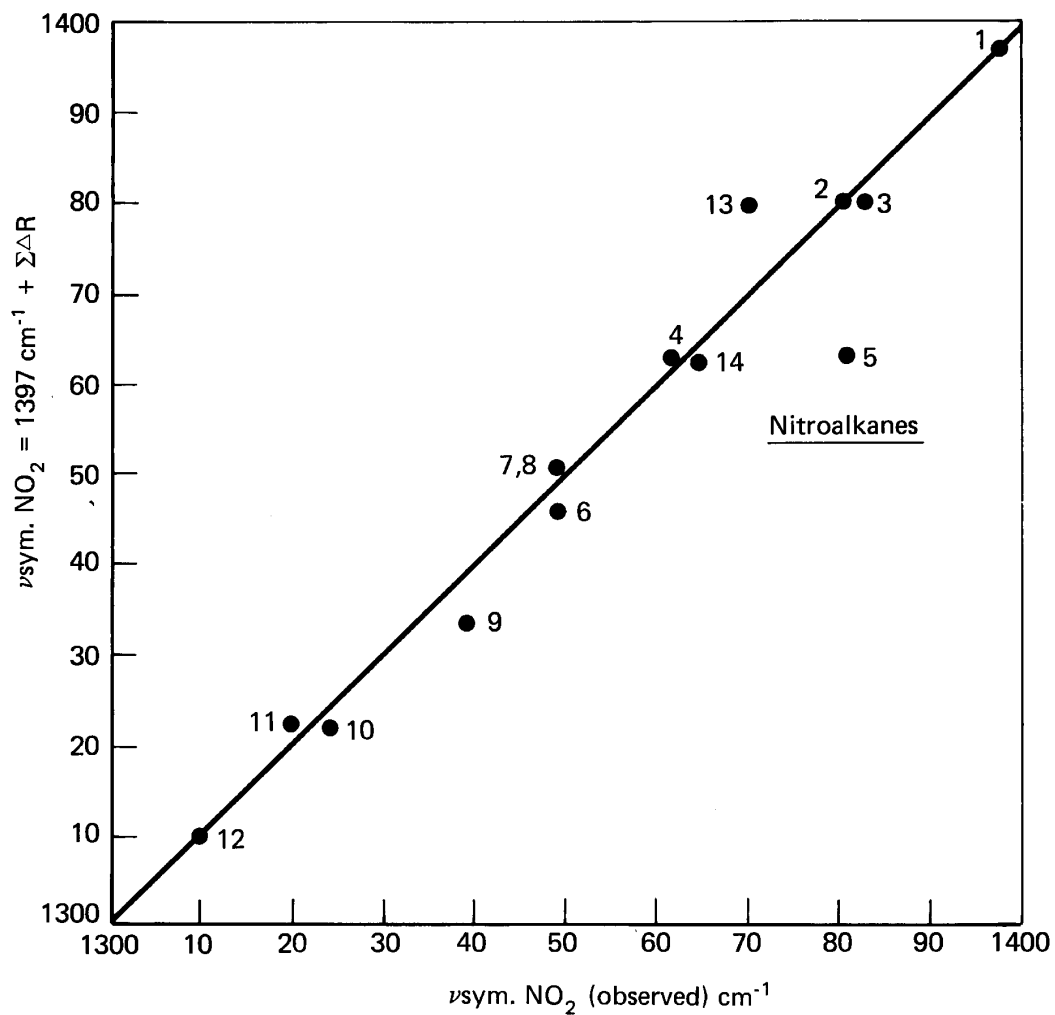


FIGURE 7.2 A plot of the observed $\nu_{\text{sym. NO}_2}$ frequencies vs the calculated $\nu_{\text{sym. NO}_2}$ frequencies using the equation $\nu_{\text{sym. NO}_2} = 1397 \text{ cm}^{-1} + \Sigma\Delta R$.

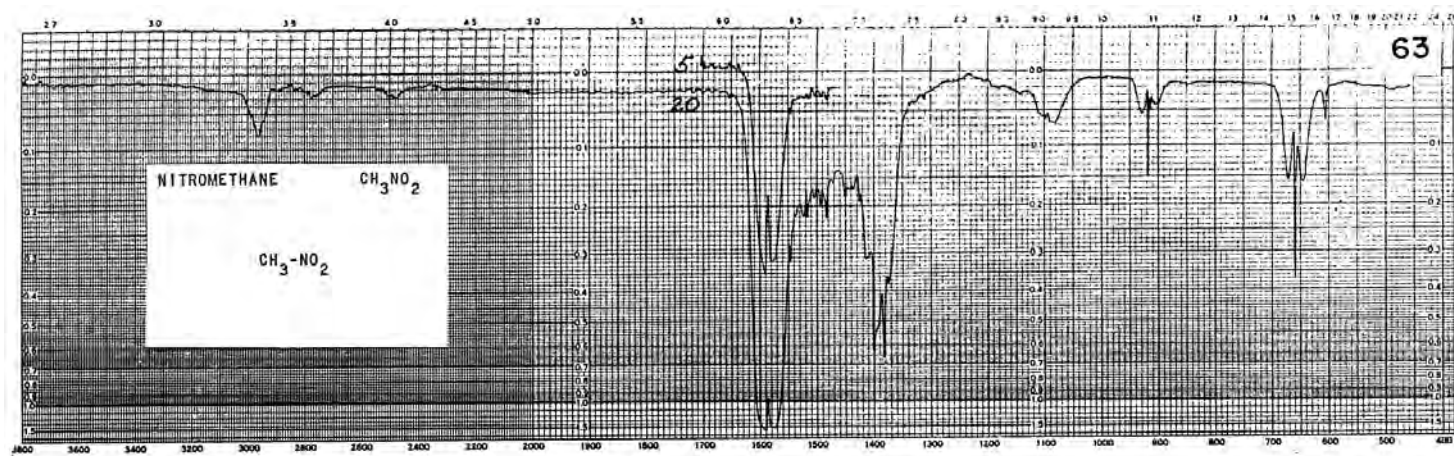


FIGURE 7.3 Vapor-phase IR spectrum for nitromethane in a 5-cm KBr cell (5 and 20 mmHg sample to 600 mmHg with N_2).

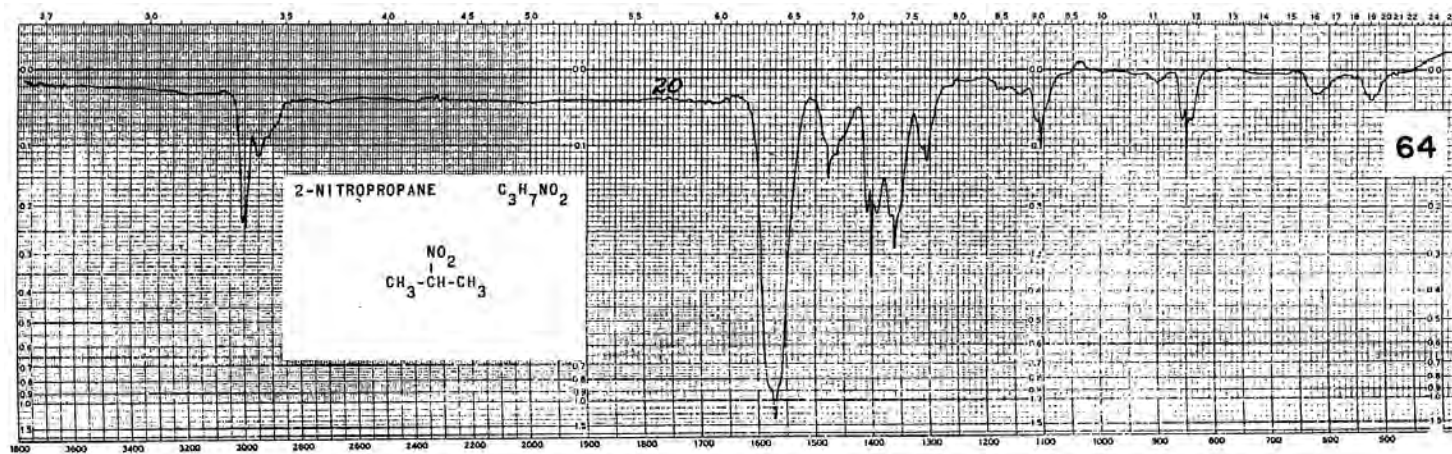
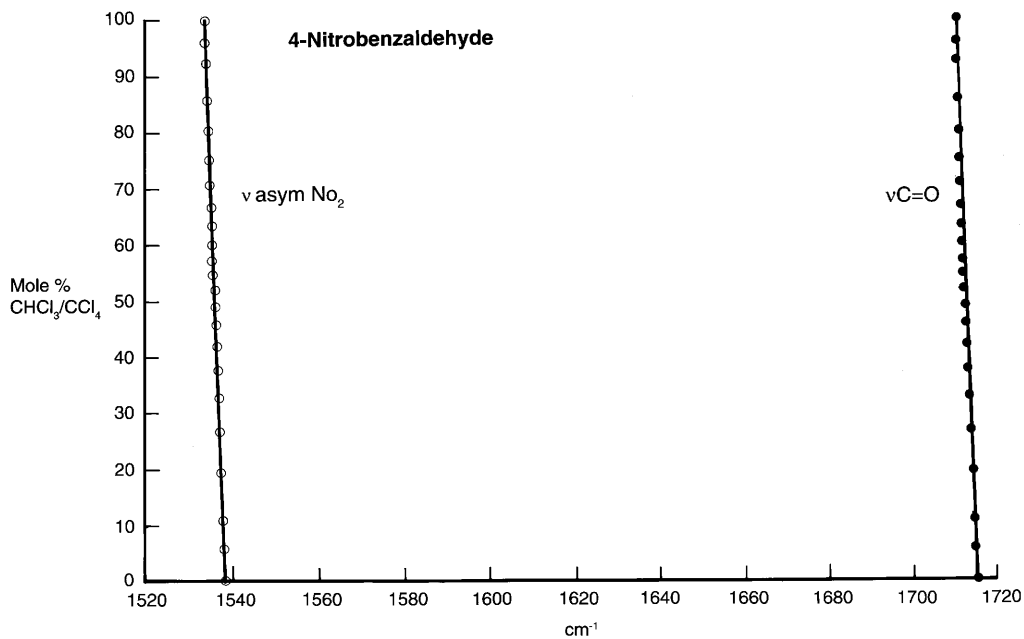
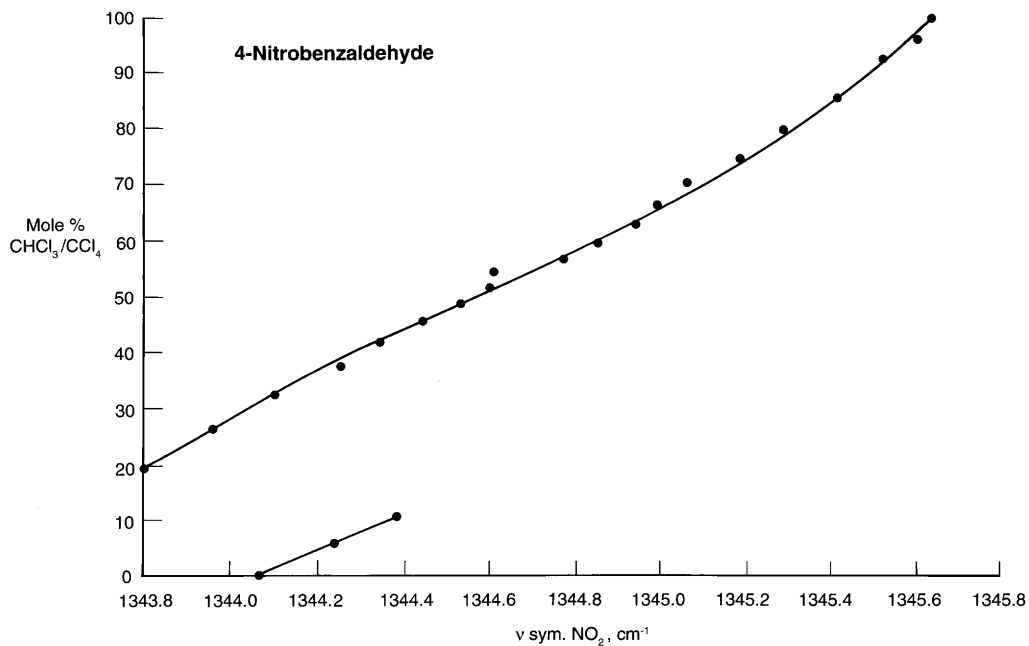


FIGURE 7.4 Vapor-phase IR spectrum for 2-nitropropane in a 5-cm KBr cell (20 mm Hg sample to 600 mm Hg with N₂).

FIGURE 7.5 Plots of ν asym. NO_2 and $\nu \text{C}=\text{O}$ for 4-nitrobenzaldehyde vs mole % $\text{CHCl}_3/\text{CCl}_4$.FIGURE 7.6 Plots of ν sym. NO_2 for 4-nitrobenzaldehyde vs mole % $\text{CHCl}_3/\text{CCl}_4$.

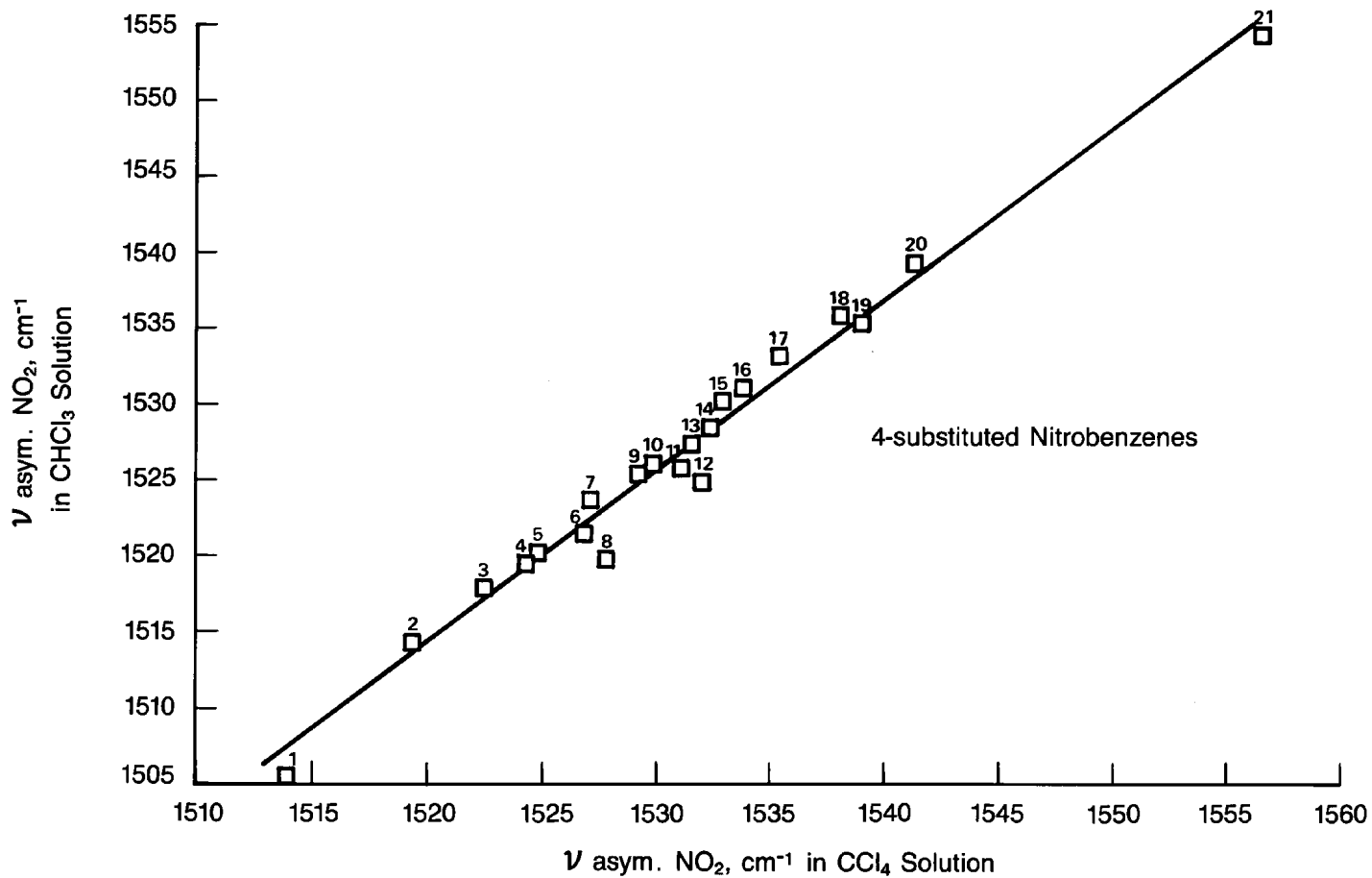


FIGURE 7.7 A plot of ν asym. NO₂ for 4-X-nitrobenzenes in CCl₄ solution vs ν asym. NO₂ in CHCl₃ solution.

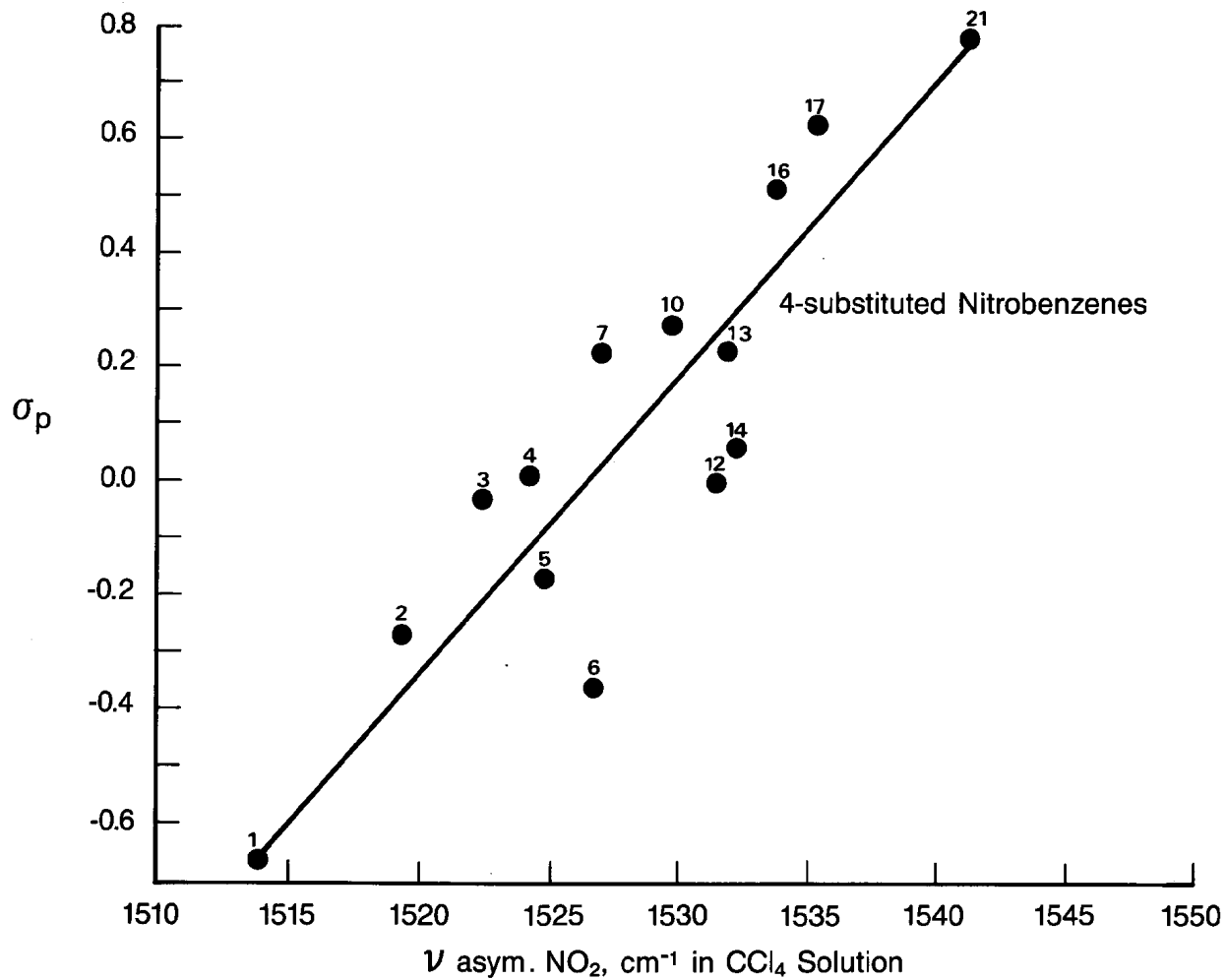
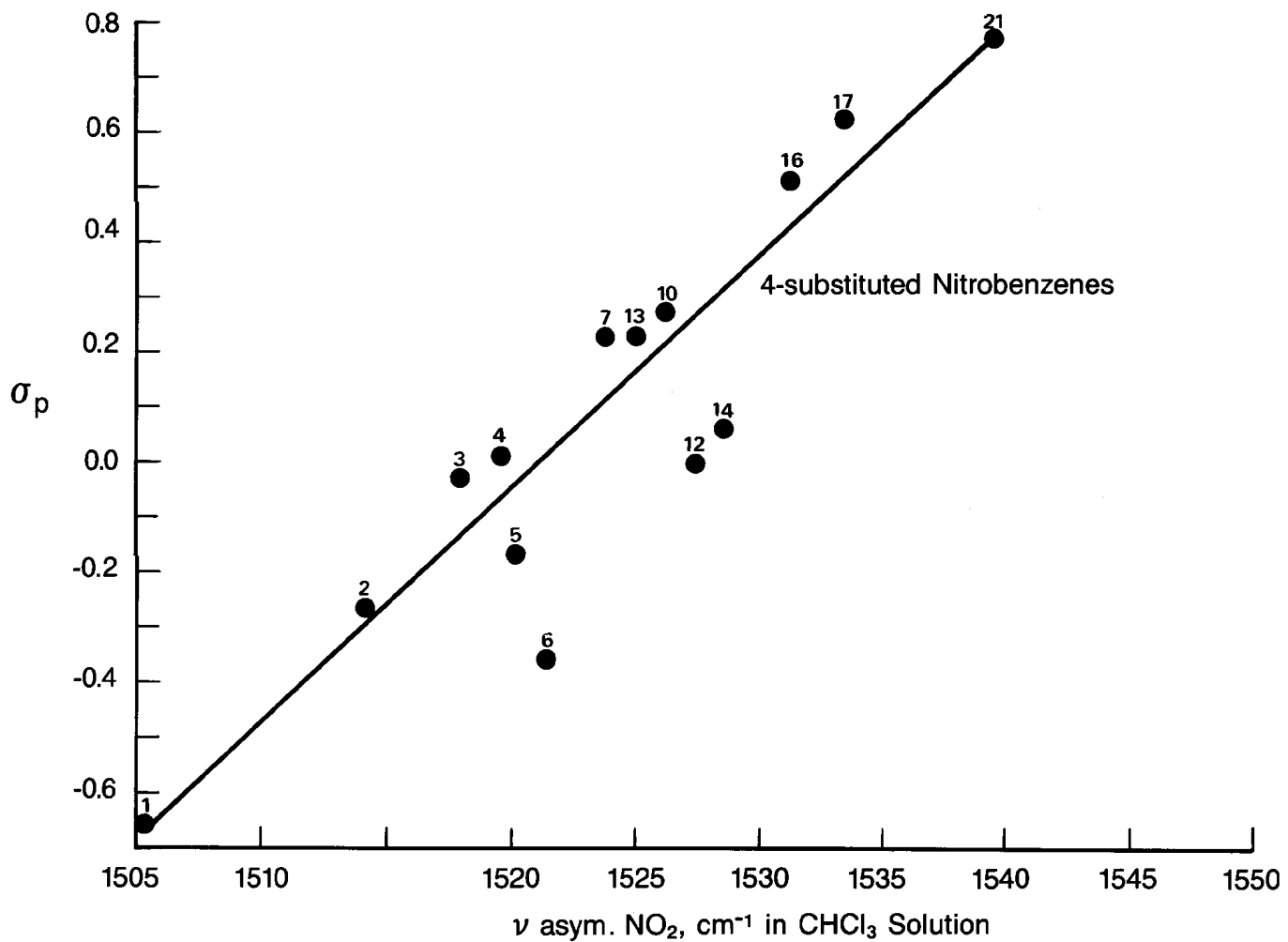
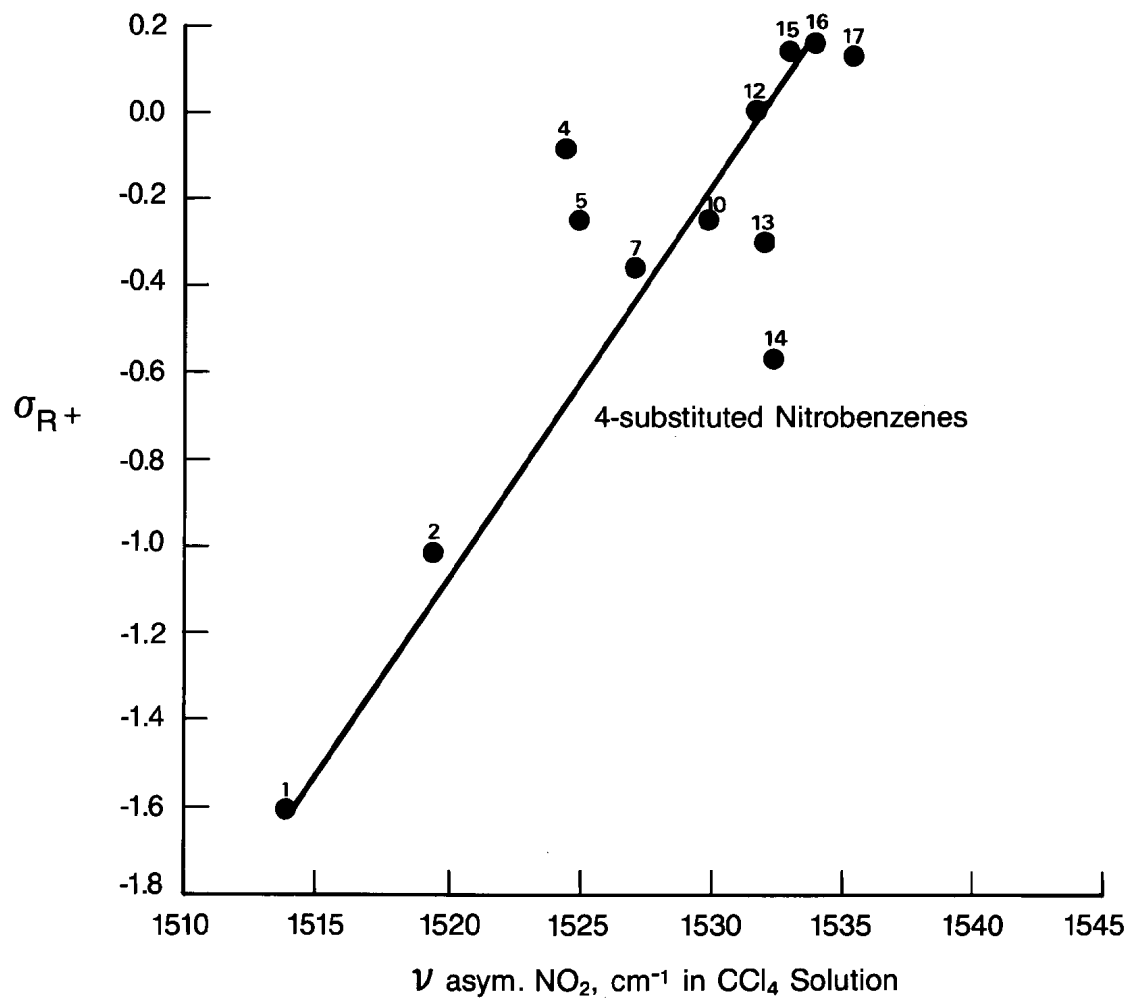
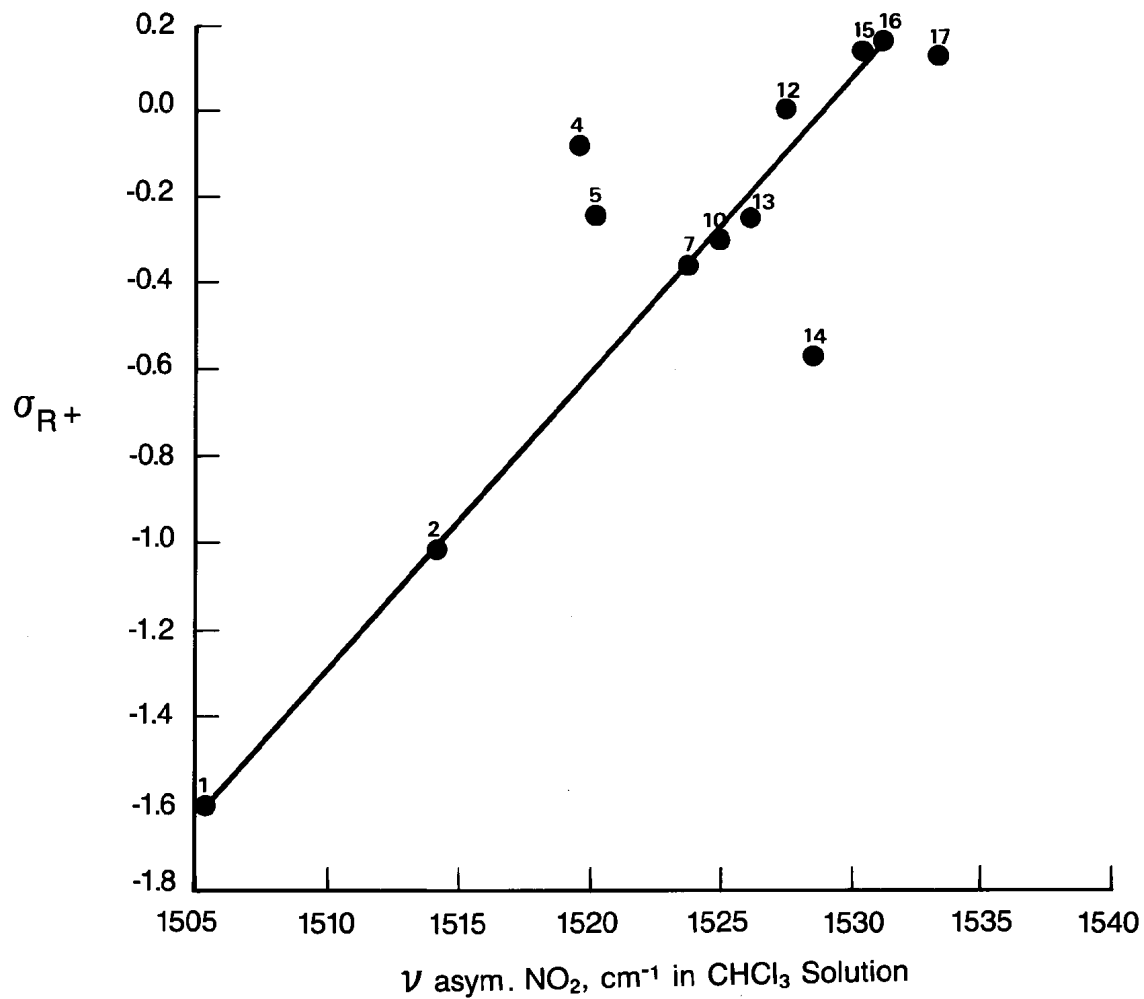
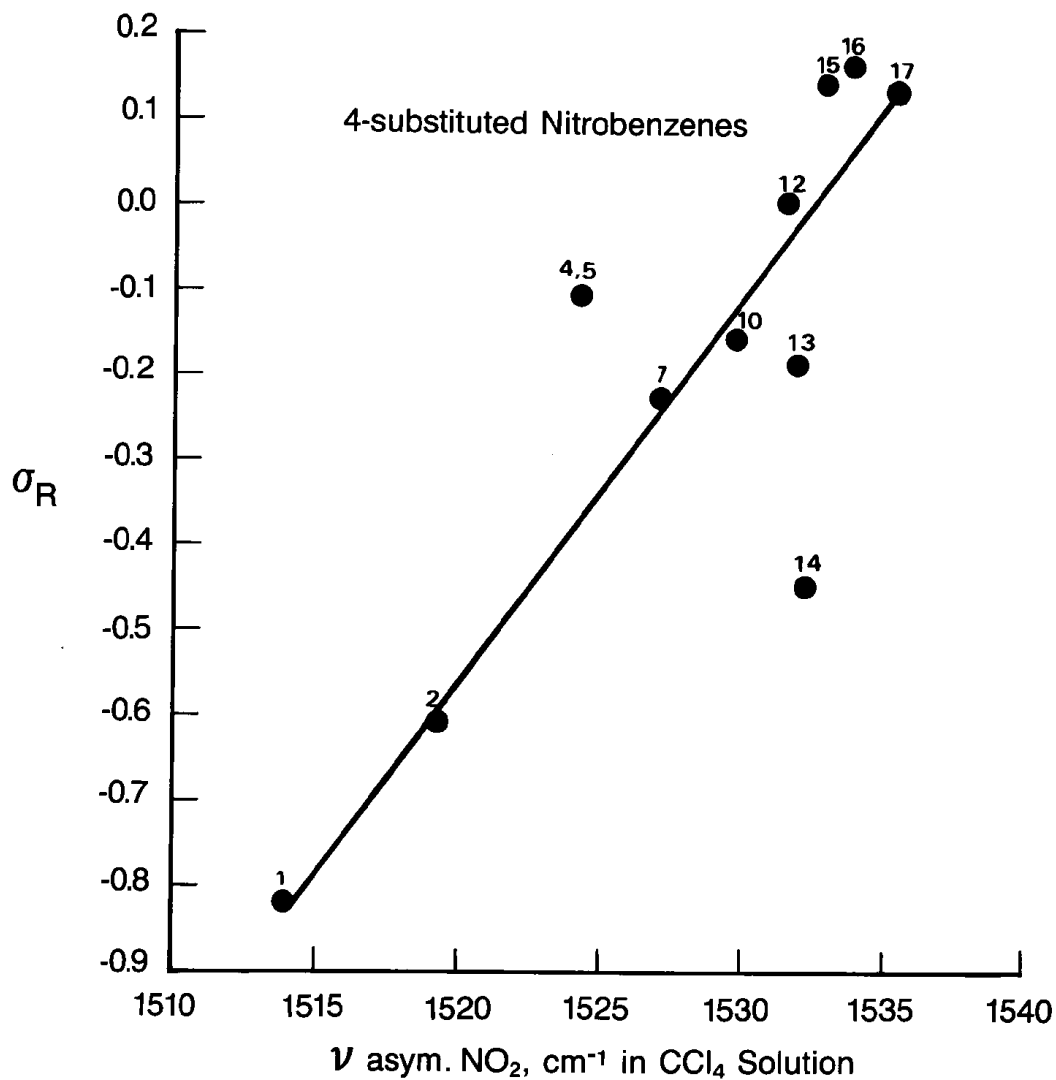


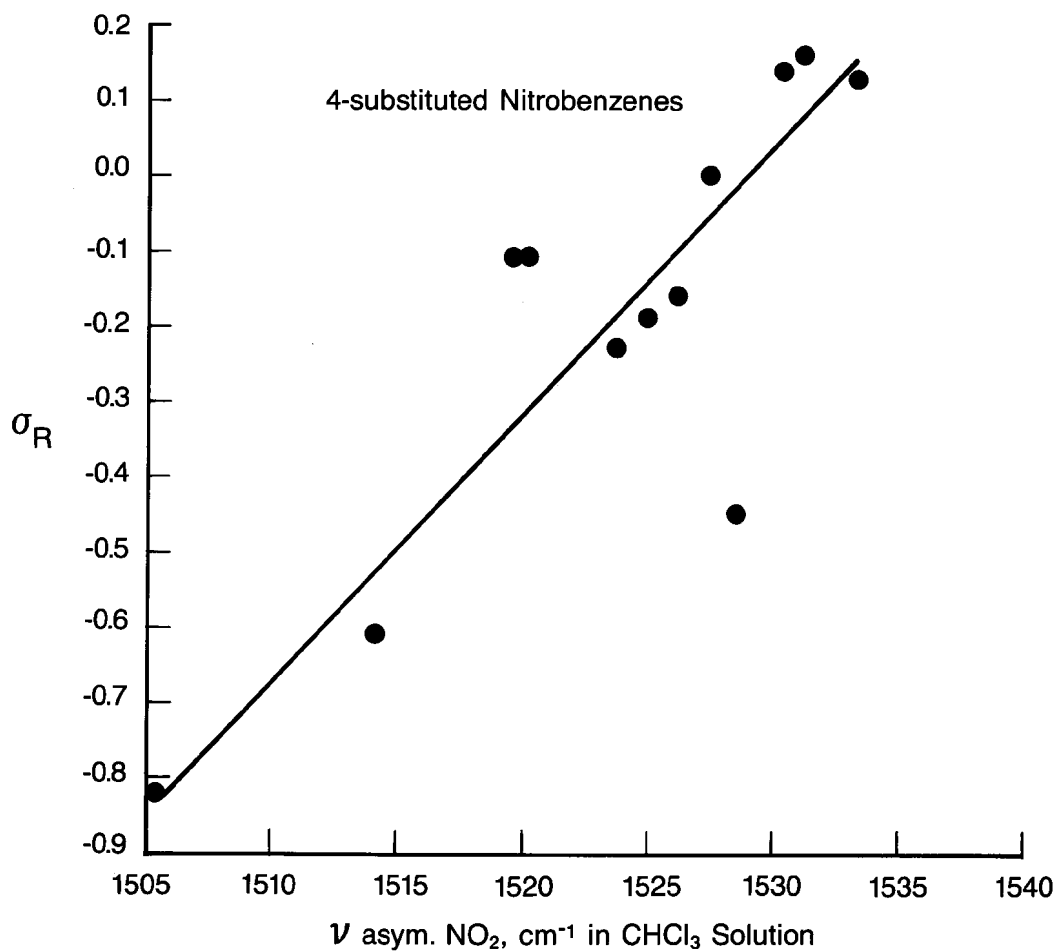
FIGURE 7.8 A plot of ν asym. NO_2 for 4-X-nitrobenzenes in CCl_4 solution vs σ_p .

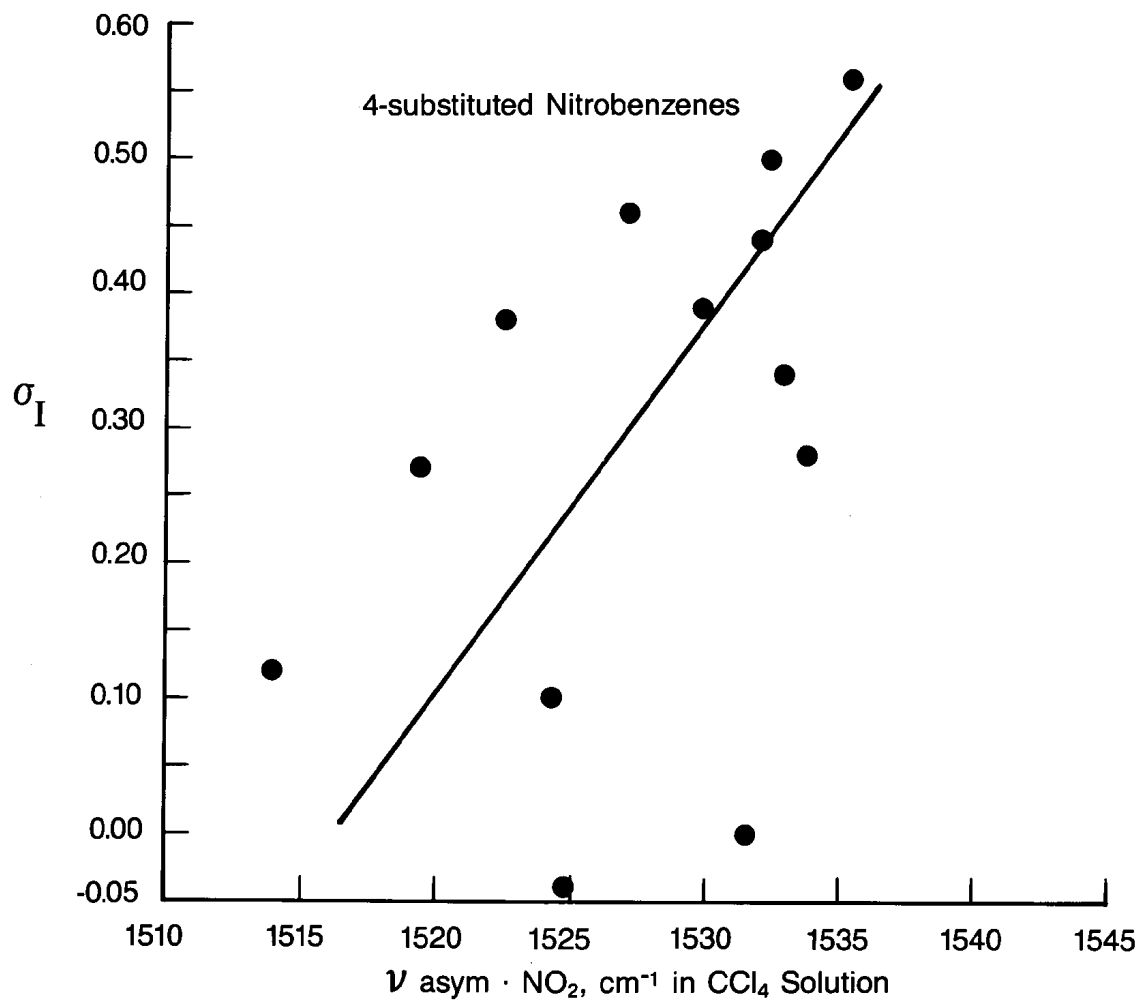
FIGURE 7.9 A plot of ν asym. NO₂ for 4-X-nitrobenzenes in CHCl₃ solution vs σ_p .

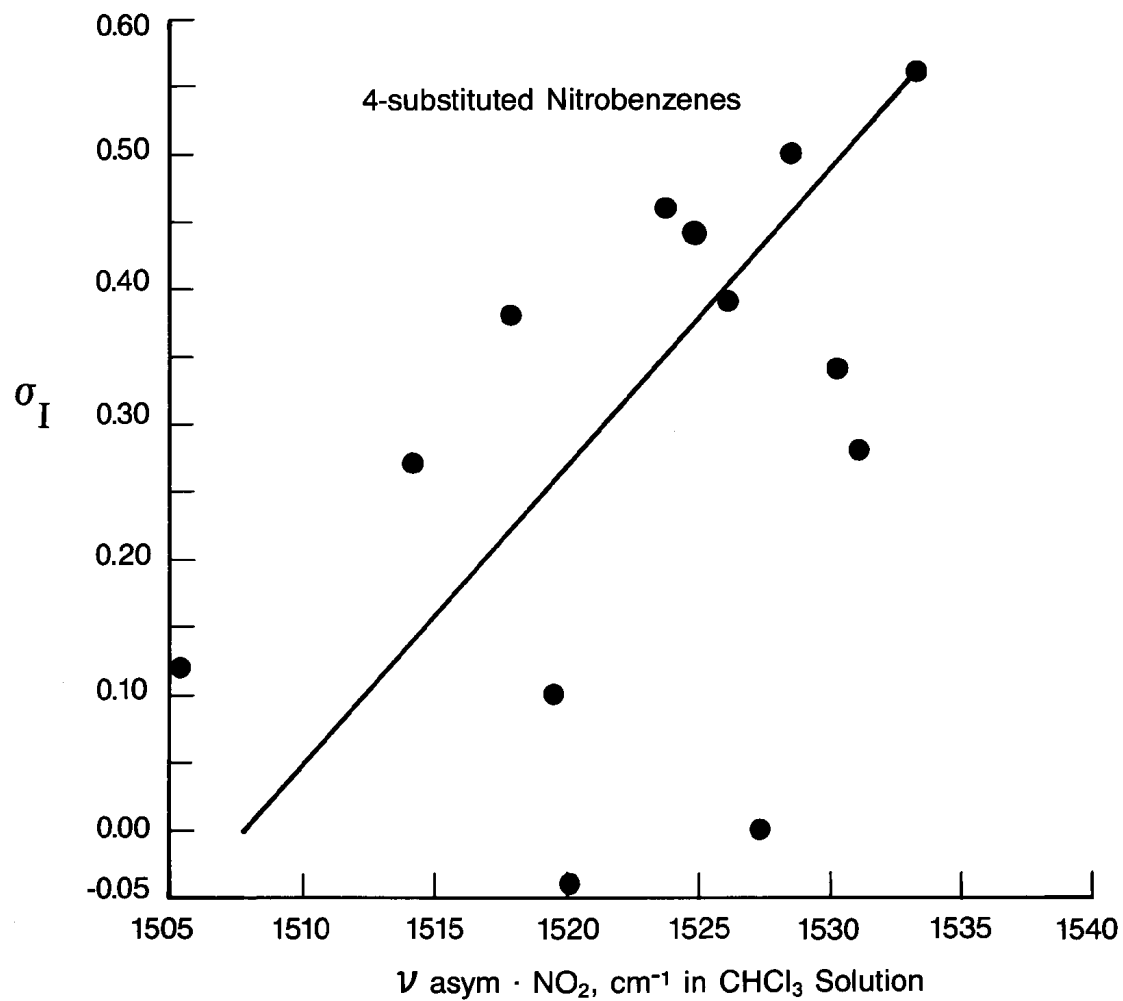
FIGURE 7.10 A plot of ν asym. NO_2 for 4-X-nitrobenzenes in CCl_4 solution vs σ_{R+} .

FIGURE 7.11 A plot of ν asym. NO₂ for 4-X-nitrobenzenes in CHCl₃ solution vs σ_{R+} .

FIGURE 7.12 A plot of ν asym. NO_2 for 4-X-nitrobenzenes in CCl_4 solution vs σ_R .

FIGURE 7.13 A plot of ν asym. NO₂ for 4-X-nitrobenzenes in CHCl₃ solution vs σ_R .

FIGURE 7.14 A plot of $\nu_{\text{asym}} \cdot \text{NO}_2$ for 4-X-nitrobenzenes in CCl_4 solution vs σ_I .

FIGURE 7.15 A plot of $\nu_{\text{asym}} \cdot \text{NO}_2$ for 4-X-nitrobenzenes in CHCl_3 solutions vs σ_I .

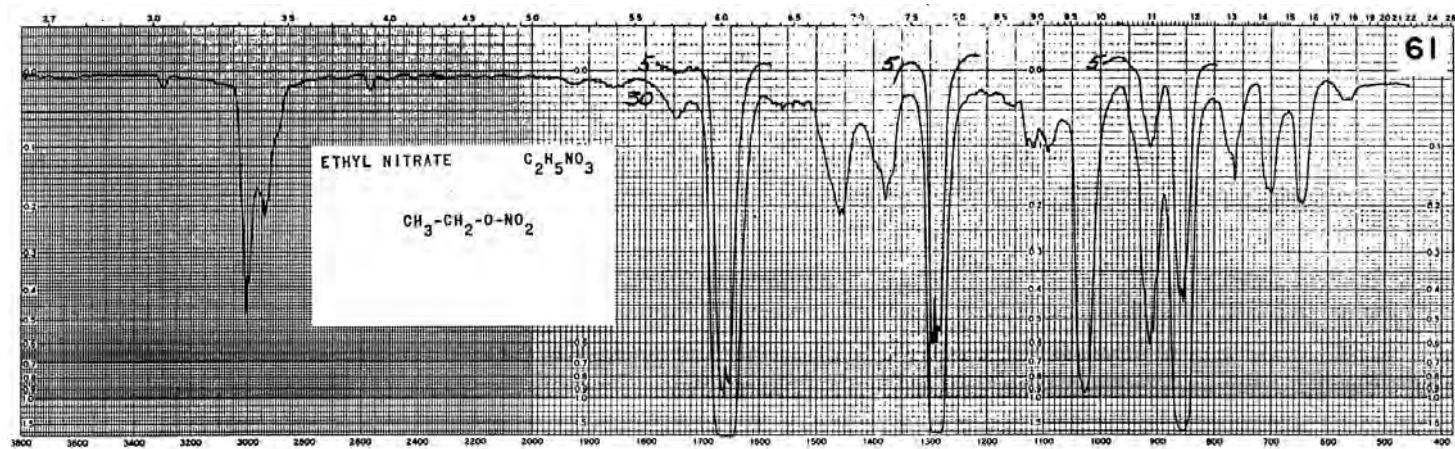


FIGURE 7.16 Vapor-phase IR spectrum for ethyl nitrate in a 5-cm KBr cell (5 and 30 mmHg sample to 600 mm Hg with N₂).

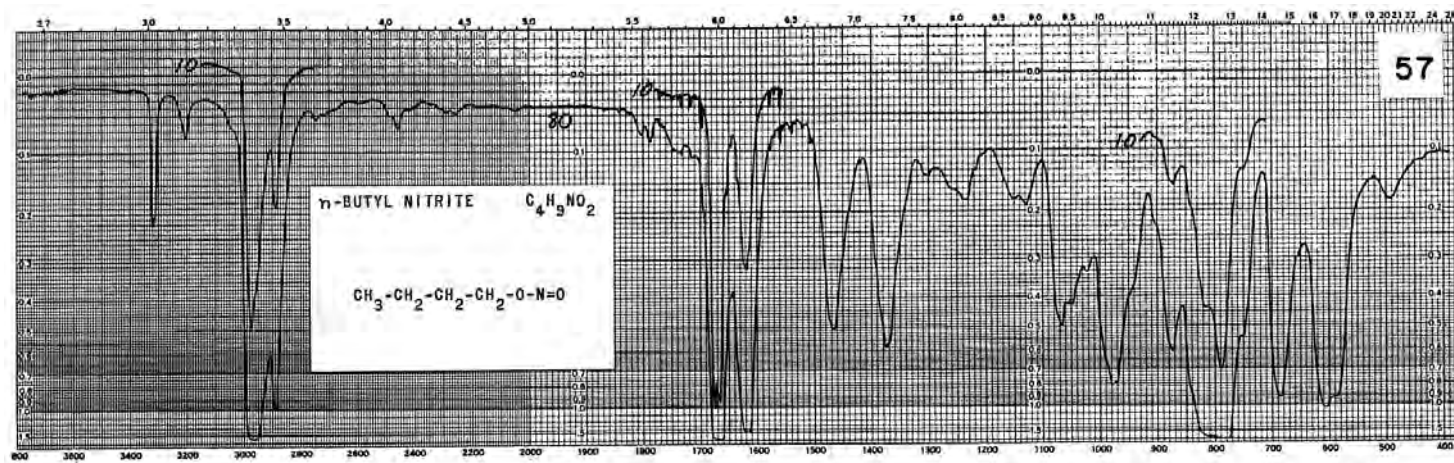
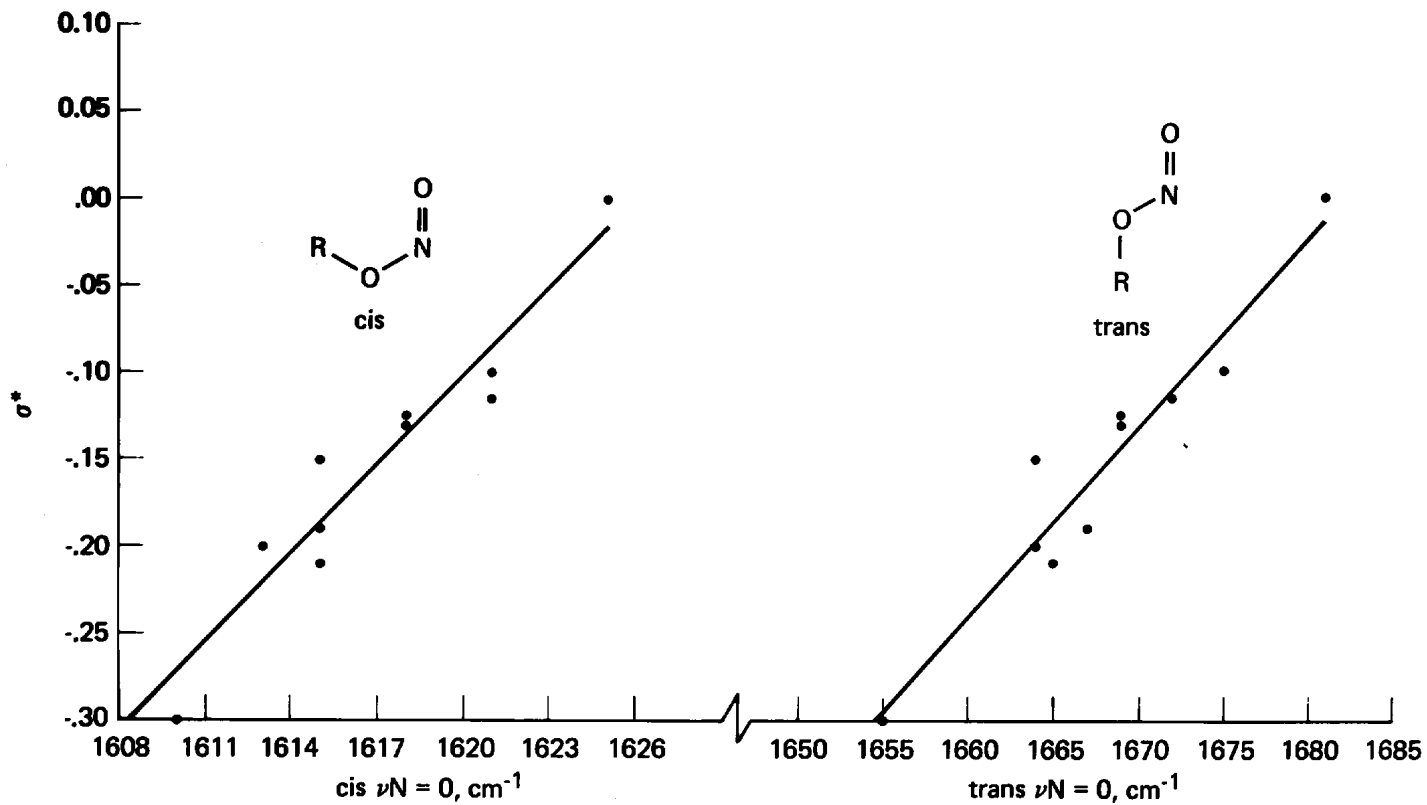
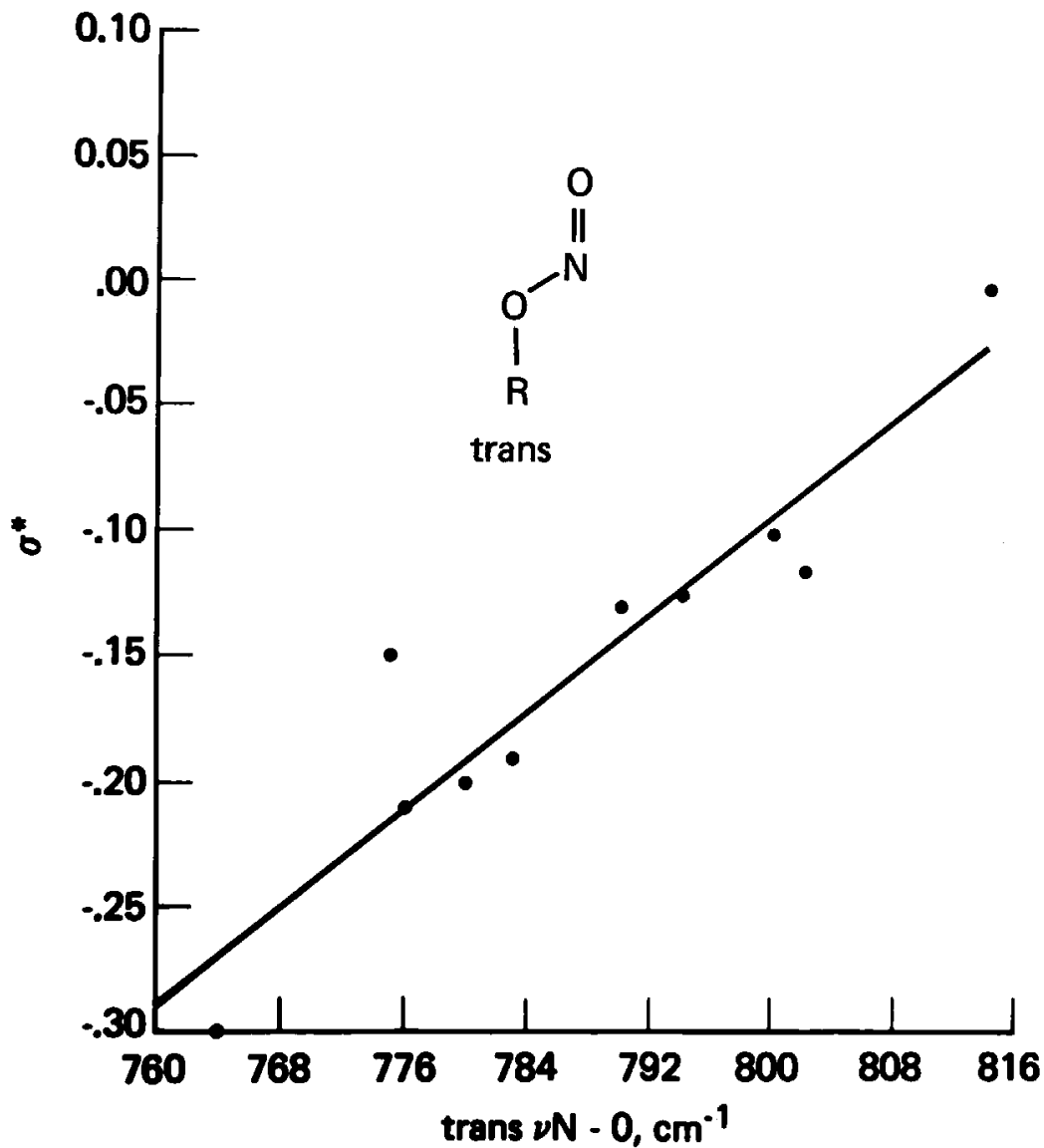


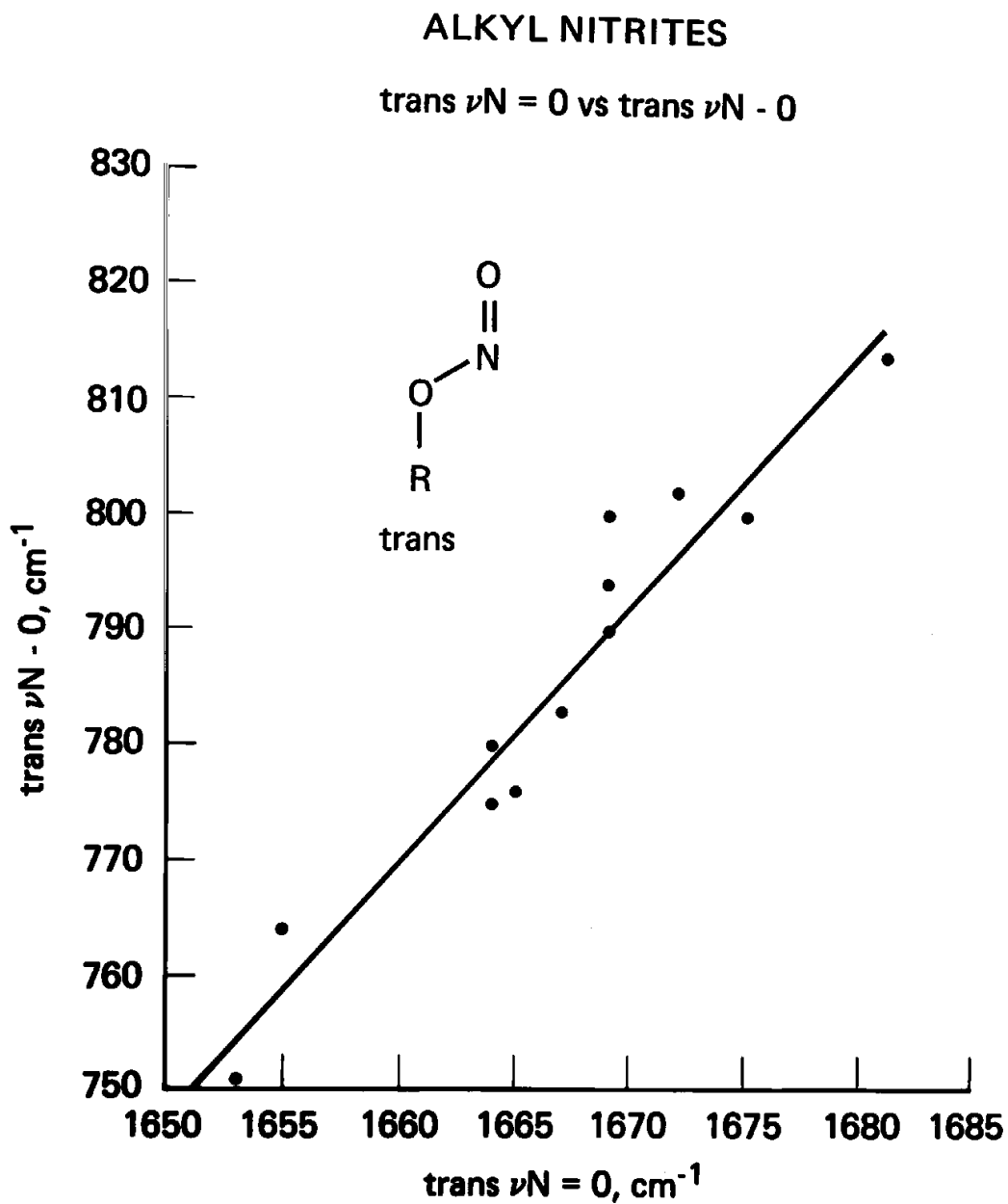
FIGURE 7.17 Vapor-phase IR spectrum for *n*-butyl nitrite in a 5-cm KBr cell (10 and 80 mm Hg sample to 600 mm Hg with N₂).

ALKYL NITRITES

cis and trans $\nu\text{N}=\text{O}$ vs σ^* valuesFIGURE 7.18 Plots of cis $\nu\text{N}=\text{O}$ and trans $\nu\text{N}=\text{O}$ for alkyl nitrites vs σ^* .

ALKYL NITRITES

trans $\nu_{\text{N-O}}$ vs σ^* valuesFIGURE 7.19 A plot of trans $\nu_{\text{N-O}}$ for alkyl nitrites vs σ^* .

FIGURE 7.20 A plot of trans $\nu_{\text{N}=\text{O}}$ vs trans $\nu_{\text{N}-\text{O}}$ for alkyl nitrites.

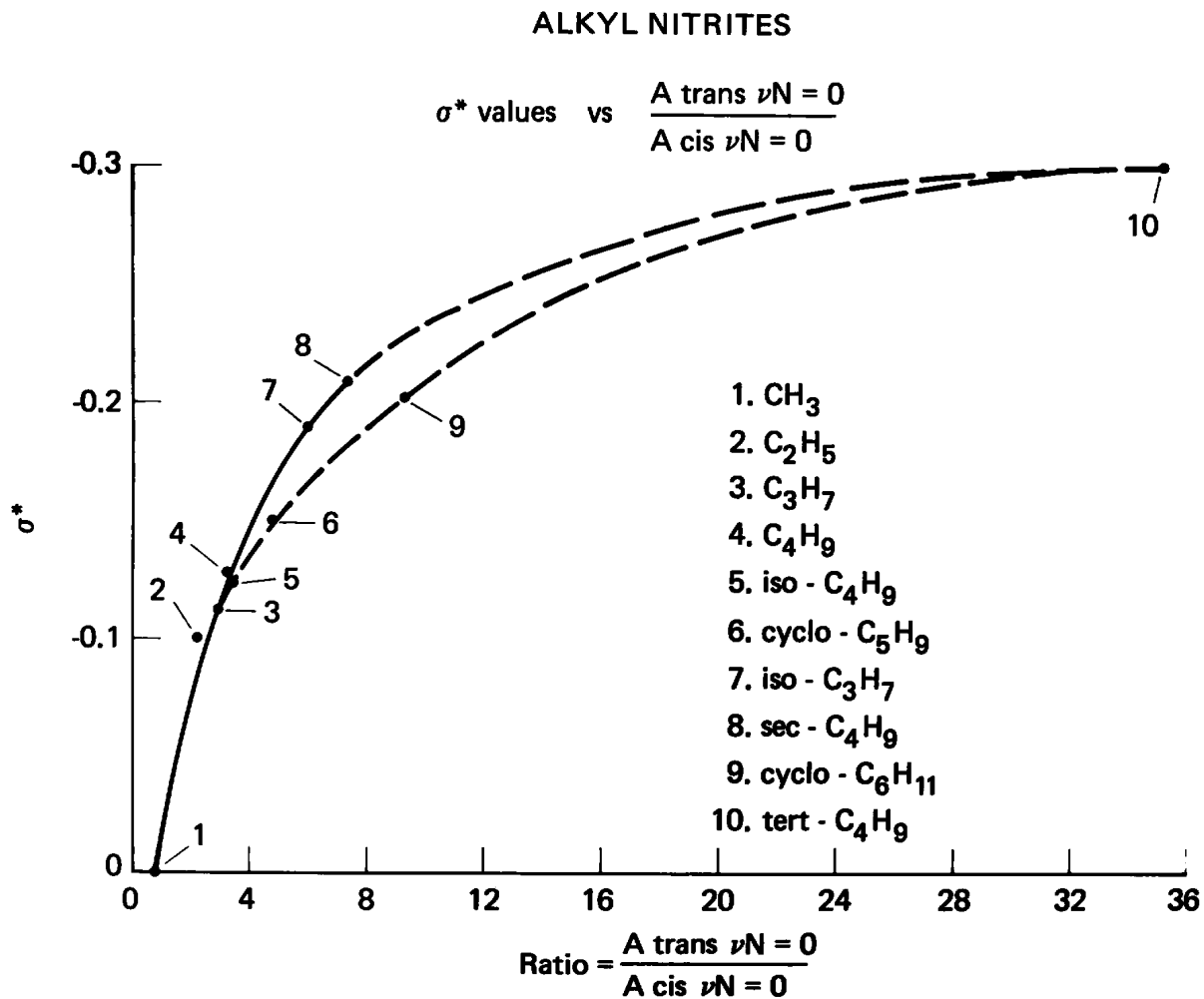
FIGURE 7.21 Plots of the absorbance ratio (A) trans $\nu N=O$ /(A) cis $\nu N=O$ vs σ^* .

TABLE 7.1 The $\nu_{\text{asym. NO}_2}$ and $\nu_{\text{sym. NO}_2}$ frequency shifts of substituted nitro compounds from those for nitromethane in the liquid phase

CH_3NO_2	$\nu_{\text{asym. NO}_2}: 1558 \text{ cm}^{-1}$ $\nu_{\text{asym. NO}_2}$	$\nu_{\text{sym. NO}_2}: 1375 \text{ cm}^{-1}$ $\nu_{\text{sym. NO}_2}$
α -substituent	ΔR	ΔR
H	0	0
CH_3	-5	-8
C_2H_5	-5	-8
C_6H_5	—	-8
C=O (ester)	10	-8
F	17	-23
Cl	17	-23
Br	17	-23
NO_2	29	-29
β -substituent		
H	0	0
OH	-4	-6
Cl	2	-4
Br	2	-4
NO_2	2	-15

TABLE 7.1a Vapor-phase IR data for nitroalkanes

Compound	C-N st. cm ⁻¹ (A)	NO ₂ wag cm ⁻¹ (A)	a.NO ₂ str. cm ⁻¹ (A)	s.NO ₂ str. cm ⁻¹ (A)	[a.NO ₂ str.] - [s.NO ₂ str.] cm ⁻¹	Ratio (A) a.NO ₂ str./ s.NO ₂ str.	Ratio (A) s.NO ₂ str./ s.CH ₂ str.	Ratio (A) s.NO ₂ str./ a.CH ₂ str.	Ratio (A) s.NO ₂ str./ a.CH ₃ str.
Methane	918 (0.060)	659 (0.230)	1582 (1.049)	1397 (0.541)	185	1.94			13.53
Ethane	872 (0.152)	619 (0.080)	1575 (1.152)	1380 (0.442)	195	2.61	6.31	3.13	2.75
1-(\square)Propane	891 (0.040)	603 (0.050)	1570 (1.250)	1382 (0.405)	188	3.09	3.38	1.69	1.23
1-(\square)Butane	859 (0.049)	610 (0.050)	1576 (1.250)	1382 (0.360)	194	3.47	2.01	1.09	0.73
1-(\square)Pentane	850 (0.060)	610 (0.040)	1575 (1.250)	1371 (0.390)	204	3.21	1.32	0.67	0.57
1-(\square)Hexane	850 (0.049)	605 (0.040)	1571 (1.250)	1382 (0.380)	189	3.29	1.06	0.45	0.51
2-(\square)Propane	851 (0.100) ^{*1} 901 (0.030) ^{*2}	618 (0.060)	1565 (1.250)	1360 (0.450)	205	2.78	4.09	2.25	1.09
Cyclohexane	1152 (0.032)		1567 (1.250)	1379 (0.429)	188	2.91	1.03	0.41	

*¹ gauche.*² trans.

TABLE 7.2 Vapor-phase IR data for nitroalkanes

Nitro	a.CH ₃ str.	a.CH ₂ str.	s.CH ₃ str.	s.CH ₂ str.	a.CH ₃ bend	CH ₂ bend	CH ₃ rock	C–N st.	NO ₂ wag	a.NO ₂ str.	s.NO ₂ str.	Ratio (A)	Ratio (A)	Ratio (A)	Ratio (A)
												a.NO ₂ str./ s.NO ₂ str.	s.NO ₂ str./ s.CH ₂ str.	s.NO ₂ str./ a.CH ₂ str.	s.NO ₂ str./ a.CH ₃ str.
Methane	2990 (0.040)		2960 (0.070)					918 (0.060)	655 (0.230)	1582 (1.049)	1397 (0.541)	1.94			13.53
Ethane	3000 (0.161)	2960 (0.141)		2910 (0.070)		1458 (0.170)	1113 (0.100)	872 (0.152)	619 (0.080)	1575 (1.152)	1380 (0.442)	2.61	6.31	3.13	2.75
1-(<i>l</i>)Propane	2982 (0.330)	2950 (0.240)		2900 (0.120)		1450 (0.120)	1125 (0.040)	891 (0.040)	603 (0.050)	1570 (1.250)	1382 (0.405)	3.09	3.38	1.69	1.23
1-(<i>l</i>)Butane	2980 (0.490)	2950 (0.330)		2895 (0.180)	1469 (0.100)	1450 (0.170)	1129 (0.049)	859 (0.049)	610 (0.050)	1576 (1.250)	1382 (0.360)	3.47	2.01	1.09	0.73
1-(<i>l</i>)Pentane	2975 (0.685)	2945 (0.585)		2885 (0.295)	1465 (0.150)	1447 (0.210)	1125 (0.040)	850 (0.060)	610 (0.040)	1575 (1.250)	1371 (0.390)	3.21	1.32	0.67	0.57
1-(<i>l</i>)Hexane	2975 (0.740)	2940 (0.840)		2880 (0.360)	1465 (0.160)	1446 (0.200)	1126 (0.040)	850 (0.040)	605 (0.040)	1571 (1.250)	1382 (0.380)	3.29	1.06	0.45	0.51
2(a.CH ₃ bend)															
2-(<i>l</i>)Propane	2995 (0.411)	2952 (0.200)*	2880 (0.110)*		1460 (0.209)			851 (0.100)	618 (0.060)	1565 (1.250)	1360 (0.450)	2.78	4.09	2.25	1.09
Cyclohexane		2950 (1.070)		2875 (0.418)		1460 (0.232)		1152 (0.032)		1567 (1.250)	1379 (0.429)	2.91	1.03	0.41	

* In Fermi Resonance.

TABLE 7.3 Vapor- and liquid-phase IR data for nitroalkanes

Compound	a.NO ₂ str. vapor cm ⁻¹	a.NO ₂ str. liquid cm ⁻¹	a.NO ₂ str. Δ [v-l] cm ⁻¹	s.NO ₂ str. Δ [v-l] cm ⁻¹	s.NO ₂ str. vapor cm ⁻¹	s.NO ₂ str. liquid cm ⁻¹	Taft σ^*
CH ₃	1582	1558	-24	-22	1397	1375	[0]
C ₂ H ₅	1575	1555	-20	-17	1380	1363	[-0.100]
C ₃ H ₇	1570	1549	-21	-1	1382	1380	[-0.115]
(CH ₃) ₂ CH	1568	1550	-18	-1	1360	1359	[-0.190]
C ₆ H ₁₁	1567	1535	-32	-9	1379	1370	[-0.150]
(CH ₃) ₃ C	1555	1535	-20	-3	1349	1346	[-0.300]
CH ₃ ClCH	1589	1565	-24	-2	1349	1347	[0.95]
C ₂ H ₅ ClCH	1585	1564	-21	10	1348	1358	[0.95]
(CH ₃) ₂ ClC	1579	1554	-25	-3	1339	1336	[0.86]
CH ₃ Cl ₂ C	1600	1581	-19	-2	1324	1322	[1.84]
C ₂ H ₅ Cl ₂ C	1595	1578	-17	-8	1320	1312	[1.82]
Cl ₃ C	1621	~1601	-20	0	1310	1310	[2.65]
Range:	[1555-1621]	[1535-1601]			[1310-1397]	[1310-1381]	
Δ Range:	66	66			87	71	

TABLE 7.4 Vapor-phase IR data for 4-X-nitrobenzenes

Compound	a.NO ₂ str. cm ⁻¹ (A)	s.NO ₂ str. cm ⁻¹ (A)	[a.NO ₂ str.]- [s.NO ₂ str.] cm ⁻¹	A[s.NO ₂ str.]/ A[a.NO ₂ str.]	σ_p
NH ₂	1530 (0.756)	1350 (1.273)	180	1.68	[-0.66]
OH	1539 (0.800)	1350 (1.222)	189	1.53	[-0.36]
OCH ₃	1535 (0.530)	1348 (0.749)	187	1.41	[-0.27]
OC ₆ H ₅	1538 (0.669)	1350 (0.521)	188	0.78	[-0.03]
Cl	1540 (1.230)	1349 (1.225)	191	1	[0.23]
CH ₃	1538 (1.152)	1355 (1.239)	183	1.08	[-0.17]
C ₆ H ₅	1538 (0.669)	1352 (1.240)	186	1.85	[0.01]
H	1540 (1.248)	1351 (1.141)	189	0.91	[0]
CN	1542 (1.145)	1349 (1.242)	193	1.08	[0.86]
NO ₂	1567 (1.275)	1340 (0.974)	227	0.76	[0.78]
CH ₃ CO	1541 (1.250)	1349 (1.250)	192	1	[0.52]
F	1542 (1.030)	1352 (1.240)	190	1.2	[0.06]
Range:	[1530-1567]	[1340-1355]			
Δ Range:	[37]	[15]			

TABLE 7.5 Infrared data for 4-X-nitrobenzenes in different phases

Compound	a.NO ₂ str. vapor cm ⁻¹	a.NO ₂ str. CHCl ₃ cm ⁻¹	a.NO ₂ str. neat or solid cm ⁻¹	[a.NO ₂ str.] - [s.NO ₂ str.] vapor cm ⁻¹	[a.NO ₂ str.] - [s.NO ₂ str.] CHCl ₃ cm ⁻¹	[a.NO ₂ str.] - [s.NO ₂ str.] neat or solid cm ⁻¹	s.NO ₂ str. vapor cm ⁻¹	s.NO ₂ str. CHCl ₃ cm ⁻¹	s.NO ₂ str. neat or solid cm ⁻¹
N(CH ₃) ₂		1487			169			1318	
OCH ₃	1535	1510		187	171		1348	1339	
OH	1539	1517		189	179		1350	1338	
F	1542		1524	190		177	1352		1347
Cl	1540	1522	1522	191	179	162	1349	1343	1360
					180			1342	
Br		1527		172				1355	
				181				1346	
I			1510			160			1350
						175			1335
CH ₃	1538	1520	1510	183	174	159	1355	1346	1351
C ₆ H ₅	1538		1520	186		169	1352		1351
CH ₂ Cl		1527			179		1348		
CN	1542	1536		193	188		1349	1348	
CO ₂ CH ₃		1528			180			1348	
CHO		1535			192			1343	
CH ₃ CO	1541	1530		192	188		1349	1342	
NO ₂	1567	1555		229	217		1340	1338	

TABLE 7.6 A comparison of the frequency differences between asym. NO₂ str. and sym. NO₂ str. in the vapor and CHCl₃ solution and in the vapor and neat or solid phases

Compound	a.NO ₂ str. vapor cm ⁻¹	a.NO ₂ str. CHCl ₃ cm ⁻¹	a.NO ₂ str.				s.NO ₂ str.		s.NO ₂ str. CHCl ₃ cm ⁻¹	s.NO ₂ str. neat or solid cm ⁻¹
			neat or solid cm ⁻¹	[a.NO ₂ str.] [v-CHCl ₃] cm ⁻¹	[s.NO ₂ str.] [v-CHCl ₃] cm ⁻¹	[a.NO ₂ str.] [v-n or -s] cm ⁻¹	[s.NO ₂ str.] [v-n or -s] cm ⁻¹	s.NO ₂ str. vapor cm ⁻¹		
OCH ₃	1535	1510		-25	-9			1348	1339	
OH	1539	1517		-27	-12			1350	1338	
F	1542		1524			-18	-5	1352		1347
Cl	1540	1522	1522	-18	-6	-18	11	1349	1343	1360
						-7			1342	
CH ₃	1538	1520	1510	-18	-28	-9	-4	1355	1346	1351
C ₆ H ₅	1538		1520			-18	-1	1352		1351
CN	1542	1536		-6	-1			1349	1348	
CH ₃ CO	1541	1530		-11	-7			1349	1342	
NO ₂	1567	1555		-12	-2			1340	1338	

TABLE 7.7 Infrared data for the asym. NO₂ and sym. NO₂ stretching frequencies for 3-X and 4-X-nitrobenzene in CCl₄ and CHCl₃ solutions

4-X-Nitrobenzene [1 wt. % solutions or saturated at 1 wt. %] X	a.NO ₂ str. [CCl ₄]	s.NO ₂ str. [CCl ₄]	[a.NO ₂ str.] [s.NO ₂ str.] [CCl ₄]	[a.NO ₂ str.] [s.NO ₂ str.] [CHCl ₃]	a.NO ₂ str. [CHCl ₃]	s.NO ₂ str. [CHCl ₃]	[a.NO ₂ str. (CCl ₄)]- [a.NO ₂ str. (CHCl ₃)]	[s.NO ₂ str. (CCl ₄)]- [s.NO ₂ str. (CHCl ₃)]
NH ₂	1513.94	1338.08	175.86	170.19	1505.34	1335.15	8.6	2.93
CH ₃ O	1519.32	1343.07	176.25	171.36	1514.12	1342.76	5.2	0.31
C ₆ H ₅ O	1522.43	1344.98	177.45	172.97	1517.85	1344.88	4.58	0.1
C ₆ H ₅	1524.26	1346.67	177.59	171.73	1519.47	1347.74	4.79	-1.07
CH ₃	1524.8	1346.18	178.62	173.17	1520.1	1346.93	4.7	-0.75
HO	1526.74	1344.45	182.29	178.95	1521.41	1342.46	5.33	1.99
Cl	1527.01	1344.3	182.71	178.25	1523.64	1345.39	3.37	-1.09
iso-C ₃ H ₇	1527.68	1347.11	180.57	171.72	1519.8	1348.08	7.8	-0.97
CH ₂ Cl	1529.17	1348.01	181.16	175.35	1525.44	1350.09	3.73	-2.08
	1529.78	1348.7	181.08	175.78	1526.08	1350.3	3.7	-1.6
C ₆ H ₅ -C=O	1531.06	1353.19	177.87	170.54	1525.77	1355.23	5.29	-2.04
H	1531.53	1348.24	183.29	177.61	1527.37	1349.76	4.16	-1.52
Br	1531.95	1350.1	179.68	173.42	1524.88	1351.46	7.07	-1.36
F	1532.31	1346.41	185.9	180.22	1528.48	1349.26	3.83	-1.85
CH ₃ CO ₂	1532.87	1348	184.87	180.23	1530.26	1350.03	2.62	-2.03
CH ₃ C=O	1533.76	1345.71	188.05	183.6	1531.06	1347.46	2.7	-1.75
CN	1535.33	1345.37	189.96	185.65	1533.21	1347.56	2.12	-2.19
CH ₃ SO ₂	1537.97	1348.2	189.77	185.3	1535.9	1350.6	2.07	-2.4
CF ₃	1538.91	1354.35	184.56	179.1	1535.44	1356.34	3.47	-1.99
SO ₂ Cl	1541.25	1346.06	195.19	191.4	1539.26	1347.86	1.99	-1.8
NO ₂	1556.41	1338.68	217.73	213.77	1554.37	1340.6	2.04	-1.92
Δ cm ⁻¹	42.47	16.27	41.87	43.58	49.03	20.08		
3-X-Nitrobenzene X								
N(CH ₃) ₂	1535.29	1349.47	185.82	181.83	1531.64	1349.81	3.65	-0.34
CH ₃	1532.78	1350.88	181.9	177.12	1529.16	1352.04	3.62	-1.16
Br	1536.44	1348.28	188.16	183.12	1533.09	1349.97	3.35	-1.69
I	1533.69	1346.97	186.72	181.8	1530.42	1348.62	3.27	-1.65
NO ₂	1544.05	1345.29	198.76	194.19	1541.63	1347.44	2.42	-2.15
Δ cm ⁻¹	11.27	5.59	16.86	17.07	12.47	4.6		

TABLE 7.8 Infrared data for the asym. NO₂ and sym. NO₂ stretching frequencies for 4-X-nitrobenzenes in the vapor, CCl₄ and CHCl₃ solution phases

4-X-Nitrobenzene	σ_p	a.NO ₂ str. [vapor] cm ⁻¹	a.NO ₂ str. [CCl ₄ soln.] cm ⁻¹	a.NO ₂ str. [CHCl ₃ soln.] cm ⁻¹	a.NO ₂ str. [solid] cm ⁻¹	[vapor]- [CCl ₄ soln.] [-cm ⁻¹]	[vapor]- [CHCl ₃ soln.] [-cm ⁻¹]	[vapor]- [solid] [-cm ⁻¹]
NH ₂	-0.66	1530	1513.94	1505.34		16	25	
HO	-0.36	1539	1526.74	1521.41		12	18	
CH ₃ O	-0.27	1535	1519.32	1514.12		15	21	
CH ₃	-0.17	1538	1524.8	1520.1	1510	13	18	28
C ₆ H ₅ O	-0.03	1538	1522.43	1517.85		16	20	
H	0	1540	1531.53	1527.37		9	13	
C ₆ H ₅	0.01	1538	1524.26	1519.47	1520	14	19	18
F	0.06	1542	1532.31	1528.48	1524	10	14	18
Cl	0.23	1540	1527.01	1523.64	1522	13	16	18
CH ₃ C=O	0.52	1541	1532.87	1530.26		8	11	
NO ₂	0.78	1567	1556.41	1554.37		11	13	
CN	0.86	1542	1535.33	1533.21		7	9	
X		s.NO ₂ str. [vapor]	s.NO ₂ str. [CCl ₄ soln.]	s.NO ₂ str. [CHCl ₃ soln.]	s.NO ₂ str. [solid]	[vapor]- [CCl ₄ soln.]	[vapor]- [CHCl ₃ soln.]	[vapor]- [solid]
NH ₂	-0.66	1350	1338.08	1335.15		11.9	14.9	
OH	-0.36	1350	1344.45	1342.46		5.6	7.5	
CH ₃ O	-0.27	1348	1343.07	1342.76		4.9	5.2	
CH ₃	-0.17	1355	1346.18	1346.93	1351	8.8	8.1	4
C ₆ H ₅ O	-0.03	1350	1344.98	1344.88		5	5.1	
H	0	1351	1348.2	1349.76		2.8	1.2	
C ₆ H ₅	0.01	1352	1346.67	1347.74	1350	5.3	4.3	2
F	0.06	1352	1346.41	1349.26	1347	5.6	2.7	5
Cl	0.23	1349	1344.3	1345.39	1342	4.7	1.5	7
CH ₃ C=O	0.52	1349	1345.71	1347.41		3.3	1.6	
NO ₂	0.78	1340	1338.68	1340.6		1.3	-0.6	
CN	0.86	1349	1348.37	1347.56		3.6	1.5	

TABLE 7.9 Infrared data for the asym. NO₂ and sym. NO₂ stretching frequencies of 4-nitrobenzaldehyde 1 wt./vol % in 0 to 100 mol % CHCl₃/CCl₄ solutions

4-Nitrobenzaldehyde 1% (wt./vol.) mole % CHCl ₃ /CCl ₄	a.NO ₂ str. cm ⁻¹	s.NO ₂ str. cm ⁻¹
0	1538.4	1344.1
5.68	1538.1	1344.2
10.74	1537.8	1344.4
19.4	1537.4	1343.8
26.53	1537.1	1344.1
32.5	1537.1	1344.1
37.57	1536.9	1344.3
41.93	1536.6	1344.3
45.73	1536.4	1344.4
49.06	1536.2	1344.5
52	1536.1	1344.6
54.62	1535.4	1344.6
57.22	1535.4	1344.8
60.07	1535.3	1344.9
63.28	1535.1	1344.9
66.74	1535.2	1345.1
70.65	1535.1	1345.1
75.06	1534.9	1345.2
80.05	1534.6	1345.3
85.75	1534.3	1345.4
92.33	1534.1	1345.5
96.01	1533.8	1345.6
100	1533.6	1345.6
Δ C=O	-4.8	1.5

TABLE 7.10 A comparison of infrared data for nitromethane vs nitrobenzene in various solvents

Solvent	Nitromethane a.NO ₂ str. cm ⁻¹	Nitrobenzene a.NO ₂ str. cm ⁻¹	[CH ₃ NO ₂]- [C ₆ H ₅ NO ₂] cm ⁻¹	Nitromethane s.NO ₂ str. cm ⁻¹	Nitrobenzene s.NO ₂ str. cm ⁻¹	[CH ₃ NO ₂]- [C ₆ H ₅ NO ₂] cm ⁻¹	Nitromethane [Hexane]- [Solvent] a.NO ₂ str. cm ⁻¹	Nitrobenzene [Hexane]- [Solvent] a.NO ₂ str. cm ⁻¹	Nitrobenzene [Hexane]- [Solvent] s.NO ₂ str. cm ⁻¹
Hexane	1569	1535.8	33.2	masked	1348.2	[—]	0	0	0
Diethyl ether	1563.6	1532.6	31	masked	1349	[—]	5.4	3.2	0.8
Carbon tetrachloride	1564.5	1531.5	33	1374.4	1348.2	26.2	4.5	4.3	0
Benzene	1560.8	1528.5	32.3	1374.6	1348.3	26.3	8.2	7.3	-0.1
Acetonitrile	1561	1529.4	31.6	1374.2	1350.9	23.3	8	6.4	-2.7
Benzonitrile	1558.7	1526	32.7	1376.2	1348.5	27.7	10.3	9.8	-0.3
Methylene chloride	1562.2	1527.9	34.3	1376.7	1349.7	27	6.8	7.9*	-1.5
<i>t</i> -Butyl alcohol	1562.3	1531.9	30.4	1376.1	1349.5	26.6	6.7	3.9	-1.5
Chloroform	1562.4	1527.4	35	1376.2	1349.8	26.4	6.6	8.4*	-1.6
Isopropyl alcohol	1562.5	1531.6	30.9	1376.4	masked	[—]	6.5	4.2	[—]
Ethyl alcohol	1561.7	1530.7	31	masked	masked	[—]	7.3	5.1	[—]
Methyl alcohol	1561	1529.9	31.1	masked	1350.6	[—]	8	5.9	-2.4
Dimethyl sulfoxide	1552.8	1524.7	28.1	1376.1	1348.1	28	16.2	11.1	-0.1

* (see text).

TABLE 7.11 Vapor-phase infrared data for 3-X-nitrobenzenes

Compound 3-X-Nitrobenzenes X	a.NO ₂ str. cm ⁻¹ (A)	s.NO ₂ str. cm ⁻¹ (A)	[a.NO ₂ str.] - [s.NO ₂ str.] cm ⁻¹	A[s.NO ₂ str.] / A[a.NO ₂ str.]	A[a.NO ₂ str.] / A[s.NO ₂ str.]
OH	1547 (1.230)	1360 (0.870)	187	0.71	1.41
OCH ₃	1550 (1.235)	1353 (0.672)	197	0.54	1.84
OC ₆ H ₅	1550 (1.220)	1353 (0.566)	197	0.46	2.16
Cl	1551 (1.242)	1351 (0.758)	200	0.61	1.64
CH ₃	1545 (1.234)	1358 (1.139)	187	0.92	1.08
C ₆ H ₅	1545 (1.245)	1357 (0.830)	188	0.67	1.5
H	1540 (1.248)	1351 (1.141)	189	0.91	1.09
CH ₂ Br	1550 (1.231)	1355 (0.923)	195	0.75	1.33
NO ₂	1553 (1.271)	1349 (0.904)	204	0.71	1.41
CO ₂ C ₂ H ₅	1550 (0.672)	1351 (0.562)	199	0.84	1.2
CH ₃ CO	1549 (1.229)	1358 (1.148)	191	0.93	1.07
Range:	[1540–1553]	[1349–1360]			
Δ Range:	[13]	[11]			

TABLE 7.12 Infrared data for 3-X-nitrobenzenes in different phases

Compound 3-X-nitro- benzenes X	a.NO ₂ str. vapor cm ⁻¹	a.NO ₂ str. CHCl ₃ cm ⁻¹	a.NO ₂ str.		[a.NO ₂ str.] - [s.NO ₂ str.]		[a.NO ₂ str.] - [s.NO ₂ str.]		s.NO ₂ str. neat or solid cm ⁻¹
			neat or solid cm ⁻¹	[s.NO ₂ str.] vapor cm ⁻¹	[a.NO ₂ str.] - [s.NO ₂ str.] CHCl ₃ cm ⁻¹	[a.NO ₂ str.] - [s.NO ₂ str.] neat or solid cm ⁻¹	s.NO ₂ str. vapor cm ⁻¹	s.NO ₂ str. CHCl ₃ cm ⁻¹	
OCH ₃	1550	1526	[—]	197	178	[—]	1353	1348	[—]
OH	1547	1529	[—]	187	177	[—]	1360	1352	[—]
Cl	1551	1527	1520 1540	200	177	176 196	1351	1350	1344
Br	[—]	1532	[—]	[—]	152	[—]	[—]	1380	[—]
I	[—]	1521	[—]	[—]	[—]	181	[—]	1340	[—]
CH ₃	1545	1531	1521	187	181	174	1358	1350	1347
C ₆ H ₅	1545	1529	1529	188	[—]	178	1357		1351
CH ₂ Cl	[—]	1532	[—]	[—]	179	[—]	[—]	1353	[—]
CN	[—]	1538	[—]	[—]	186	[—]	[—]	1352	[—]
NO ₂	1553	1539	1522	204	193	174	1349	1346	1348

TABLE 7.13 A comparison of the frequency difference between asym. NO₂ str. and sym. NO₂ for 3-X-nitrobenzenes in the vapor and CHCl₃ solution and in the vapor and solid or neat phases

Compound 3-X-nitro- benzene X	a.NO ₂ str. vapor cm ⁻¹	a.NO ₂ str. CHCl ₃ cm ⁻¹	a.NO ₂ str.				s.NO ₂ str.		s.NO ₂ str. CHCl ₃ cm ⁻¹	s.NO ₂ str. neat or solid cm ⁻¹
			neat or solid cm ⁻¹	[a.NO ₂ str.] [v-CHCl ₃] cm ⁻¹	[s.NO ₂ str.] [v-CHCl ₃] cm ⁻¹	[a.NO ₂ str.] [v-n or -s] cm ⁻¹	[s.NO ₂ str.] [v-n or -s] cm ⁻¹	s.NO ₂ str. vapor cm ⁻¹		
OCH ₃	1550	1526		-24	-5			1353	1348	
OH	1547	1529		-18	-8			1360	1352	
Cl	1551	1527	1540 1520	-24	-11	-11 -31	-7	1351	1350	1344
Br		1532							1380	
I			1521							1340
CH ₃	1545	1531	1521	-14	-8	-24	-11	1358	1350	1347
C ₆ H ₅	1545		1529			-16	-6	1357		1351
CH ₂ Cl		1532							1353	
CN		1538							1352	
NO ₂	1553	1539	1522	-14	-3	-31	-1	1349	1346	1348

TABLE 7.14 Vapor-phase infrared data for 2-X-nitrobenzenes

Compound 2-X-Nitrobenzenes X	a.NO ₂ str. cm ⁻¹ (A)	s.NO ₂ str. cm ⁻¹ (A)	[a.NO ₂ str.]- [s.NO ₂ str.] cm ⁻¹	A[s.NO ₂ str.]/ A[a.NO ₂ str.]	A[a.NO ₂ str.]/ A[s.NO ₂ str.]
OH	1545 (0.640)	1335 (1.239)	210	1.94	0.52
OCH ₃	1550 (1.190)	1360 (0.920)	190	0.77	1.29
OC ₂ H ₅	1547 (1.230)	1360 (0.920)	187	0.75	1.34
OC ₄ H ₉	1545 (1.240)	1359 (0.479)	186	0.39	2.59
Cl	1551 (1.220)	1359 (0.700)	192	0.57	1.74
Br	1553 (1.240)	1359 (0.770)	194	0.62	1.61
CH ₃	1542 (1.242)	1350 (0.960)	192	0.77	1.29
I	1550 (1.241)	1353 (0.640)	197	0.52	1.94
C ₆ H ₅	1545 (1.240)	1358 (0.638)	187	0.51	1.94
H	1540 (1.248)	1351 (1.141)	189	0.91	1.09
CF ₃	1560 (1.141)	1360 (0.662)	200	0.58	1.72
CO ₂ CH ₃	1551 (1.240)	1357 (0.818)	194	0.66	1.52
CO ₂ C ₂ H ₅	1551 (1.150)	1352 (0.720)	199	0.63	1.6
F	1549 (1.250)	1354 (1.131)	195	0.9	1.11
Range:	[1540–1560]	[1335–1360]			
Δ Range:	[20]	[25]			

TABLE 7.15 Infrared data for 2-X-nitrobenzenes in different phases

Compound 2-X-nitro- benzene X	a.NO ₂ str. vapor cm ⁻¹	a.NO ₂ CHCl ₃ cm ⁻¹	a.NO ₂ neat or solid cm ⁻¹	[a.NO ₂ str.]- [s.NO ₂ str.]		[a.NO ₂ str.]- [s.NO ₂ str.]		s.NO ₂ str. CHCl ₃ cm ⁻¹	s.NO ₂ str. neat or solid cm ⁻¹
				vapor cm ⁻¹	CHCl ₃ cm ⁻¹	neat or solid cm ⁻¹	vapor cm ⁻¹		
OCH ₃	1550	1530		190	173		1360	1357	
OH	1545	1537		210	202		1335	1335	
F	1549		1520	195		180	1354		1340
Cl	1551	1537	1528	192	180	176	1359	1357	1352
Br	1553	1536	1520	194	179	175	1359	1356	1345
CH ₃	1542	1527	1520	192	173	175	1350	1354	1345
C ₆ H ₅	1545		1520	187		170	1358		1350
CO ₂ CH ₃	1551	1537		194	184		1357	1353	
CHO		1532			185			1347	
NO ₂			1546			176			1370
			1529			175			1354

TABLE 7.16 A comparison of the frequency differences between asym. NO₂ and sym. NO₂ str. for 2-X-nitrobenzenes in the vapor, CHCl₃ solution, and in the vapor, neat or solid phases

Compound 2-X-nitro- benzene X	a.NO ₂ str.	a.NO ₂ str.	a.NO ₂ str.		[a.NO ₂ str.]	[s.NO ₂ str.]	[a.NO ₂ str.]	[s.NO ₂ str.]	s.NO ₂ str.	s.NO ₂ str.	s.NO ₂ str.
	vapor cm ⁻¹	CHCl ₃ cm ⁻¹	neat or solid cm ⁻¹	[v-CHCl ₃]	[v-CHCl ₃]	[v-n or -s]	[v-n or -s]	vapor cm ⁻¹	CHCl ₃ cm ⁻¹	neat or solid cm ⁻¹	
OCH ₃	1550	1530		-20	-3			1360	1357		
OH	1545	1537		-8	0			1335	1335		
F	1549		1520			-29	-14	1354		1340	
Cl	1551	1537	1528	-14	-2	-23	-7	1359	1357	1352	
Br	1553	1536	1520	-17	-3	-33	-14	1359	1356	1345	
CH ₃	1542	1527	1520	-15	4	-22	-5	1350	1354	1345	
C ₆ H ₅	1545		1520			-25	-8	1358		1350	
CO ₂ CH ₃	1551	1537		-14	-4			1357	1353		
CHO		1532							1347		
NO ₂			1546							1370	
			1529							1354	

TABLE 7.17 Infrared data for nitrobenzenes in the solid and CCl₄ solution phases

1-X-2-Nitro- benzene a.NO ₂ str. [solid] cm ⁻¹	1-X-3-Nitro- benzene a.NO ₂ str. [solid] cm ⁻¹	1-X-4-Nitro- benzene a.NO ₂ str. [solid] cm ⁻¹	X	1-X-2-Nitro- benzene s.NO ₂ str. [solid] cm ⁻¹	1-X-3-Nitro- benzene s.NO ₂ str. [solid] cm ⁻¹	1-X-4-Nitrobenzene s.NO ₂ str. [solid] cm ⁻¹	[a.NO ₂ str.]- [s.NO ₂ str.] 1,2- [solid] cm ⁻¹	[a.NO ₂ str.]- [s.NO ₂ str.] 1,3- [solid]; [CCl ₄ -solid] cm ⁻¹	[a.NO ₂ str.]- [s.NO ₂ str.] 1,4- [solid]; [CCl ₄ -solid] cm ⁻¹
1534* ¹	1512* ²	1500* ³	OH	1330	1351	1324	204	170	176
1500	1522		NHC ₂ H ₅	1337	1348		163		
1520	1521	1510	CH ₃	1344	1347	1351	176	174; 181.9	159; 178.6
1524		1509	C ₂ H ₅	1349		1334	175		175
1520	1529	1520	C ₆ H ₅	1350	1351	1350	170		170; 177.6
1520		1524	F	1340		1347	180		177; 185.9
1529	1521	1522	Cl	1351	1345	1342	178	180; 182	
1520			Br	1343			177		
	1520	1510	I	1366; 1355	1339	1328			182; 181* ¹
1548; 1530	1522		NO ₂		1348		182; 165		
1-X-2,4-di- Nitrobenzene a.NO ₂ str. [solid] cm ⁻¹	4-X-2,4-di- Nitrobenzene a.NO ₂ str. [solid] cm ⁻¹	1-X-3,5-di- Nitrobenzene a.NO ₂ str. [solid] cm ⁻¹	X	1-X-2,4-di- Nitrobenzene s.NO ₂ str. [solid] cm ⁻¹	4-X-di-2,4- Nitrobenzene s.NO ₂ str. [solid] cm ⁻¹	1-X,3,5-di- Nitrobenzene s.NO ₂ str. [solid] cm ⁻¹	[a.NO ₂ str.]- [s.NO ₂ str.] cm ⁻¹	2-OH,3-Cl- Nitrobenzene* ⁴ a.NO ₂ str.; s.NO ₂ str. [solid] cm ⁻¹	2-OH,3,5-di- Nitrobenzene* ⁵
1538			F	1345			193		
1540			Br	1341			199		
	1534		N(CH ₃) ₂		1310		224		
		1544	NO ₂			1348	196		
			OH; Cl				180	1515; 1335	
			OH; NO ₂ ; NO ₂	188				1528; 1340	
				240				1550; 1310	

*¹ OH; O₂N str. 3260.*² OH str. 3380.*³ OH str. 3325.*⁴ OH; O₂N str. 3230.*⁵ OH; NO₂ str. ~3230 (broad).

TABLE 7.18 Vapor-phase infrared data for 2,5- and 2,6-X,Y-nitrobenzenes

Compound 2,5- X,Y-nitrobenzenes X,Y	a.NO ₂ str. cm ⁻¹ (A)	s.NO ₂ str. cm ⁻¹ (A)	[a.NO ₂ str.] - [s.NO ₂ str.] cm ⁻¹	A[s.NO ₂ str.] / A[a.NO ₂ str.]	A[a.NO ₂ str.] / A[s.NO ₂ str.]
CH ₃ , NH ₂	1541 (1.250)	1360 (0.508)	181	0.4	2.46
OH, CH ₃	1545 (1.240)	1325 (1.155)	220	0.93	1.07
CH ₃ , CH ₃	1541 (1.241)	1359 (0.610)	182	0.49	2.03
CH ₃ , CH ₂ OH	1542 (1.240)	1355 (0.660)	187	0.53	1.88
CH ₃ , NO ₂	1550 (1.240)	1351 (1.225)	199	0.99	1.01
OH, NO ₂	1552 (0.671)	1345 (1.210)	207	1.8	0.55
		1330 (0.910)	222	1.36	0.74
Cl, CH ₃	1558 (1.230)	1361 (0.661)	197	0.54	1.86
Cl, Cl	1555 (1.250)	1352 (0.849)	203	0.7	1.47
Cl, NO ₂	1553 (1.348)	1349 (1.140)	204	0.85	1.18
Cl, CF ₃	1560 (0.341)	1357 (0.175)	203	0.51	1.9
F, CF ₃	1560 (0.417)	1352 (0.219)	208	0.53	1.9
F, NO ₂	1559 (1.230)	1349 (1.225)	210	1	1
NHCOCH ₃ , NO ₂	1541 (0.460)	1340 (1.230)	201	2.67	0.37
CH ₃ O, CH ₃ CO	1552 (0.668)	1360 (0.542)	192	0.81	1.23
F, CH ₃	1555 (1.240)	1351 (0.590)	204	0.48	2.1
2,6-X,Y-nitrobenzenes					
X,Y					
OH, CH ₃	1547 (0.590)	1349 (0.672)	198	1.14	0.88
CH ₃ , CH ₃	1545 (1.341)	1371 (0.590)	174	0.44	2.27
Cl, Cl	1568 (1.230)	1360 (0.342)	208	0.28	3.6

TABLE 7.19 A comparison of the frequency difference between asym. NO₂ str. and sym. NO₂ str. in the vapor, neat or solid phase

Compound 2,5-X,Y-nitrobenzene X,Y	a.NO ₂ str. vapor cm ⁻¹	a.NO ₂ str. neat or solid cm ⁻¹	[a.NO ₂ str.] [v-n or -s] cm ⁻¹	[s.NO ₂ str.] [v-n or -s] cm ⁻¹	s.NO ₂ str. vapor cm ⁻¹	s.NO ₂ str. neat or solid cm ⁻¹
CH ₃ , CH ₃	1541	1514	-27	-19	1359	1340
F, NO ₂	1559	1537	-22	-3	1349	1346

TABLE 7.20 Vapor-phase infrared data for tri-X,YZ-, W,X,Y,Z-tetra-, and V,W,X,Y,Z-penta-nitrobenzenes

Compound 2,3,4-X,Y,Z-nitrobenzenes X,Y,Z	a.NO ₂ str.	s.NO ₂ str.	[a.NO ₂ str.] - [s.NO ₂ str.]	A[s.NO ₂ str.] / A[a.NO ₂ str.]	A[a.NO ₂ str.] / A[s.NO ₂ str.]
Cl, CH ₃ , Cl	1552 (1.241)	1359 (0.735)	193	0.59	1.69
Cl, Cl, Cl	1560 (1.050)	1351 (1.232)	209	1.17	0.85
2,3,5-X,Y,Z-nitrobenzenes X,Y,Z					
OH, Br, Br	1545 (1.230)	1338 (0.678)	207	0.55	1.81
OH, Cl, Cl	1550 (1.240)	1335 (0.740)	215	0.6	1.68
OH - s- C ₄ H ₉ , NO ₂	1561 (0.680)	1348 (1.240)	213	1.82	0.55
OH, CH ₃ , NO ₂	1564 (0.750)	1347 (1.240)	217	1.65	0.6
Br, NO ₂ , Br	1561 (1.241)	1340 (0.541)	221	0.44	2.29
Cl, NO ₂ , Cl	1567 (1.220)	1350 (0.570)	217	0.47	2.14
2,3,6-X,Y,Z-nitrobenzenes X,Y,Z					
NH ₂ , Cl, Cl	1541 (1.250)	1359 (0.442)	182	0.35	2.83
NO ₂ , Br, Br	1578 (1.242)	1348 (0.320)	230	0.26	3.88
NO ₂ , Cl, Cl	1580 (1.250)	1350 (0.300)	230	0.24	4.17
2,4,5-X,Y,Z-nitrobenzenes X,Y,Z					
Br, NO ₂ , Br	1552 (1.250)	1339 (0.405)	213	0.32	3.09
NH ₂ , Cl, Cl	1561 (0.531)	1340 (0.585)	221	1.1	0.91
Cl, NO ₂ , Cl	1565 (1.230)	1340 (0.530)	225	0.43	2.32
Cl, Cl, Cl	1565 (1.240)	1335 (0.512)	230	0.41	2.42
2,4,6-X,Y,Z-nitrobenzenes X,Y,Z					
CH ₃ , OH, CH ₃	1538 (1.229)	1362 (0.404)	176	0.33	3.04
Cl, Cl, Cl	1562 (1.248)	1361 (0.488)	201	0.38	2.67
3,4,5-X,Y,Z-nitrobenzenes X,Y,Z					
CH ₃ , OH, CH ₃	1543 (0.660)	1357 (1.201)	186	1.82	0.55
CH ₃ , CH ₃ O, CH ₃	1540 (0.780)	1359 (1.210)	181	1.55	0.64
2,3,4,5-W,X,Y,Z-nitrobenzenes W,X,Y,Z					
Cl, Cl, Cl, Cl	1560 (0.922)	1332 (1.240)	228	1.34	0.74
F, F, F, F	1570 (1.330)	1360 (0.625)	210	0.47	2.13

(continues)

TABLE 7.20 (continued)

Compound 2,3,4-X,Y,Z-nitrobenzenes X,Y,Z	a.NO ₂ str.	s.NO ₂ str.	[a.NO ₂ str.] - [s.NO ₂ str.]	A[s.NO ₂ str.] / A[a.NO ₂ str.]	A[a.NO ₂ str.] / A[s.NO ₂ str.]
2,3,5,6-W,X,Y,Z- nitrobenzenes					
Cl, Cl, Cl, Cl	1569 (1.199)	1333 (0.961)	236	0.8	1.25
2,3,4,5,6-V,W,X,Y,Z-penta- nitrobenzenes V,W,X,Y,Z					
Cl, Cl, Cl, Cl, Cl	1568 (1.239)	1332 (0.838)	236	0.68	1.48

TABLE 7.21 Infrared data for 4-X-nitrobenzenes in CCl₄ and CHCl₃ solutions (1% wt./vol. or less)

4-X-Nitrobenzene	v asym.NO ₂ CCl ₄ soln. cm ⁻¹	v sym.NO ₂ CCl ₄ soln. cm ⁻¹	v asym.NO ₂ CHCl ₃ soln. cm ⁻¹	v sym.NO ₂ CHCl ₃ soln. cm ⁻¹
X				
1 NH ₂	1513.9	1338.1	1505.3	1335.2
2 OCH ₃	1519.3	1343.1	1514.1	1342.8
3 OC ₆ H ₅	1522.4	1345	1517.9	1344.9
4 C ₆ H ₅	1524.3	1346.7	1519.5	1347.7
5 CH ₃	1524.8	1346.2	1520.1	1346.9
6 OH	1526.7	1344.5	1521.4	1342.5
7 Cl	1527	1344.3	1523.6	1345.4
8 iso-C ₃ H ₇	1527.7	1347.1	1519.8	1348.1
9 CH ₂ Cl	1529.2	1348	1525.4	1350.1
10 I	1529.8	1348.7	1526.1	1350.3
11 (C=O)C ₆ H ₅	1531.1	1353.2	1525.8	1355.2
12 H	1531.5	1348.2	1527.4	1349.8
13 Br	1532	1350.1	1524.9	1351.5
14 F	1532.3	1346.4	1528.5	1349.3
15 CO ₂ CH ₃	1532.9	1348	1530.3	1350
16 (C=O)CH ₃	1533.8	1345.7	1531.1	1347.5
17 CN	1535.3	1345.4	1533.2	1347.6
18 SO ₃ CH ₃	1538	1348.2	1535.9	1350.6
19 CF ₃	1538.9	1354.4	1535.4	1356.3
20 SO ₂ Cl	1541.3	1346.1	1539.3	1347.9
21 NO ₂	1556.4	1338.7	1554.4	1340.6
Δ cm ⁻¹	42.5	16.3	49	20.1

TABLE 7.22 Infrared data and assignments for alkyl nitrates

Compound R-O-NO ₂ R	a.NO ₂ str. cm ⁻¹	s.NO ₂ str. cm ⁻¹	A[s.NO ₂ str.]/ A[a.NO ₂ str.]	A[a.NO ₂ str.]/ A[s.NO ₂ str.]	NO str. cm ⁻¹	A[NO str.]/ A[a.NO ₂ str.]	γ NO ₂ cm ⁻¹	Δ NO ₂ cm ⁻¹
C ₂ H ₅ [vapor]	1662 (0.932)	1289 (0.625)	0.67	1.49	854 (0.455)	0.49	764	700
iso-C ₃ H ₇ [vapor]	1651 (1.265)	1282 (0.619)	0.49	2.04	860 (0.525)	0.42	760	700
C ₃ H ₇ [liquid]	1622 (stg)	1268 (stg)			861 (stg)		760 (wm)	699 (wm)
C ₅ H ₁₁ [liquid]	1617 (stg)	1256 (stg)			865 (stg)		760 (wm)	700 (wm)

TABLE 7.23 Infrared data for alkyl nitrates in various phases

Compound R-O-NO ₂ R	a.NO ₂ str. vapor cm ⁻¹	a.NO ₂ str. CCl ₄ or neat cm ⁻¹	[a.NO ₂ str.]- [v-CCl ₄ or -neat]	[s.NO ₂ str.]- [v-CS ₂ or -neat]	s.NO ₂ str. vapor cm ⁻¹	s.NO ₂ str. CS ₂ or neat
C ₂ H ₅ [CCl ₄ and CS ₂]	1662	1637	-25	-9	1289	1280
Iso-C ₃ H ₇ [neat]	1651	1620	-31	-8	1282	1274
		[a.NO ₂ str.]- [s.NO ₂ str.] vapor cm ⁻¹	[a.NO ₂ str.]- [s.NO ₂ str.] CCl ₄ ; CS ₂ or neat cm ⁻¹	[2(a.NO ₂ str.)]- [2(s.NO ₂ str.)] vapor cm ⁻¹	[2(a.NO ₂ str.)]- [2(s.NO ₂ str.)] CCl ₄ ; CS ₂ or neat cm ⁻¹	
C ₂ H ₅ [CCl ₄ and CS ₂]		373	357	731	691	
Iso-C ₃ H ₇ [neat]		369	346	730	672	
	2(a.NO ₂ str.) vapor cm ⁻¹	2(a.NO ₂ str.) CCl ₄ or neat cm ⁻¹	[2(a.NO ₂ str.)]- [v-CCl ₄ or neat] cm ⁻¹	[2(s.NO ₂ str.)]- [v-CS ₂ or neat] cm ⁻¹	2(s.NO ₂ str.) vapor cm ⁻¹	2(s.NO ₂ str.) CS ₂ or neat cm ⁻¹
C ₂ H ₅ [CCl ₄ and neat]	3299	3250	-49	-9	2568	2559
[calculated]	[3334]	[3274]	-60	-12	[2578]	[2560]
[Δ obs. -calc.]	[-35]	[-24]			[-10]	[-1]
Iso-C ₃ H ₇ [neat]	3290	~3210	-80	-22	~2560	2538
[calculated]	[3302]	[3240]	-62	-16	[2564]	[2548]
[Δ obs. -calc.]	[-12]	[-30]			[-4]	[-10]

TABLE 7.24 Infrared data for ethyl nitrate, nitroalkanes, and nitrobenzene in CCl₄ and CHCl₃ solutions

Compound	a.NO ₂ str. CCl ₄ soln. cm ⁻¹	a.NO ₂ str. CHCl ₃ soln. cm ⁻¹	[CCl ₄ soln.]- [CHCl ₃ soln.] cm ⁻¹	s.NO ₂ str. CCl ₄ soln. cm ⁻¹	s.NO ₂ str. CHCl ₃ soln. cm ⁻¹	[CCl ₄ soln.]- [CHCl ₃ soln.] cm ⁻¹	[a.NO ₂ str.]- [s.NO ₂ str.] CCl ₄ soln. cm ⁻¹	[a.NO ₂ str.]- [s.NO ₂ str.] CHCl ₃ soln. cm ⁻¹	[CCl ₄ soln.]- [CHCl ₃ soln.] cm ⁻¹
Ethyl nitrate	1637.3	1631.7	-5.6	1281.5	1282.9	1.4	355.8	348.8	-7
Trichloronitromethane	1608.2	1606.5	-1.7	1307.5	1309.6	2.1	300.7	296.8	-3.8
Tribromonitromethane	1595.1	1593.3	-1.8	1305.9	1308.7	2.8	289.2	284.6	-4.6
Nitromethane	1564.5	1562.4	-2.1	1374.4	1376.2	1.8	190.1	182.2	-3.9
Nitrobenzene	1531.5	1527.4	-4.1	1348.2	1349.8	1.6	183.3	177.6	-5.7

TABLE 7.25 Vapor-phase infrared data for alkyl nitrites

Compound R-O-N=O R	[trans N=O str.]		[cis N=O str.]		cis C-O str. cm ⁻¹ (A)	trans C-O str. cm ⁻¹ (A)	
	cis N=O str. cm ⁻¹ (A)	trans N=O str. cm ⁻¹ (A)	cis N=O str. cm ⁻¹	trans N=O str. cm ⁻¹ (A)			
CH ₃	1619 (0.726)	1676 (0.426)	57	835 (0.230)	795 (0.821)	1020 (w)	1055 (w)
C ₃ H ₇	1614 (0.300)	1669 (0.850)	55		794 (0.710)		
iso-C ₄ H ₉	1609 (0.170)	1668 (0.690)	59	849 (0.280)	781 (0.560)	982 (w)	1039 (w)
sec-C ₄ H ₉	1611 (0.211)	1660 (0.721)	49	850 (0.220)	766 (0.870)	?	1120 (w)
tert-C ₄ H ₉	~1610 (0.020)	1653 (1.148)	43		759 (1.240)		
tert-C ₄ H ₉ [liquid]	1554	1619	65		760 (stg)		1190 (m)
Δ [vap. - liq.]	[-56]	[-34]	[22]		[1]		

TABLE 7.26 Vapor-phase infrared data of the characteristic vibrations of alkyl nitrites*

Compound R-O-N=O R	N=O str.		N-O str.	Δ O-N=O		σ†	A[trans N=O str.]/ A[cis N=O str. ~values
	cis cm ⁻¹	trans cm ⁻¹	trans cm ⁻¹	cis cm ⁻¹	trans cm ⁻¹		
CH ₃	~1625	1681	814	617	565	[0.000]	0.95
C ₂ H ₅	1621	1675	~800	691	581	[-0.100]	2.3
C ₃ H ₇	1621	1672	802	687	602	[-0.115]	3
C ₄ H ₉	1618	1669	790	689	610	[-0.130]	3.3
iso-C ₄ H ₉	1618	1669	794	680	625	[-0.125]	3.5
iso-C ₅ H ₁₁	1618	1669	800	687	617		305
iso-C ₃ H ₇	1615	1667	783	688	605	[-0.190]	6
sec-C ₄ H ₉	1615	1665	776	678	600	[-0.210]	7.2
sec-C ₅ H ₁₁	1618	1664	775	678	594		10
cyclo-C ₅ H ₉	1613	1664	780	682	604	[-0.150]	4.7
cyclo-C ₆ H ₁₁	1615	1664	775			[-0.200]	9.3
tert-C ₄ H ₉	1610	1655	764		621?	[-0.300]	~30
tert-C ₅ H ₁₁	~1613	1653	751		613?		~50

* See Tarte (12).

† σ* is a polar value for the alkyl group.

TABLE 7.27 Raman data for organonitro compounds

Compound	s.NO ₂ str. cm ⁻¹ (RI)	NO ₂ bend cm ⁻¹ (RI)	[s.NO ₂ str.]- [NO ₂ bend] cm ⁻¹	RI[s.NO ₂ str.]/ RI[NO ₂ bend]
2-Nitro-2-methyl propyl methacrylate	1350 (5)	858 (8)	492	0.63
4-Nitrostyrene	1343 (9)	859 (2)	484	4.5
Poly(4-nitrostyrene)	1347 (9)	859 (1)	488	9
3-Nitrostyrene	1349 (9)			
4-Nitrophenyl acrylate	1349 (9)	866 (3)	483	3
4-Nitrophenyl methacrylate	1351 (9)	866 (3)	485	3
4,4'-Diamino-3,3- dinitrophenyl ether	1336 (5)	882 (9)	454	0.56
1,3-Diamino-4,6- dinitrobenzene	1312 (9)	831 (4)	481	2.3

TABLE 7.28 Infrared and Raman data for nitroalkanes in different physical phases

Compound	asym.NO ₂ str. [vapor] cm ⁻¹	asym.NO ₂ str. [neat] cm ⁻¹	asym.NO ₂ str. [vapor]- [neat] cm ⁻¹	sym.NO ₂ str. [vapor]- [neat] cm ⁻¹	sym.NO ₂ str. [vapor] cm ⁻¹	sym.NO ₂ str. [neat] cm ⁻¹	IR or Raman
	CH ₃ NO ₂	1582	1558 1562	24 20	22 13	1397	
C ₂ H ₅ NO ₂	1575	1555 1559	20 16	17 5	1380	1363 1375	IR R
(CH ₃) ₂ CHNO ₂	1568	1550 1552	18 16	1 [-2]	1360	1359 1362	IR R
(CH ₃) ₃ CNO ₂	1555	1535	20	3	1349	1346	IR
(CH ₃) ₂ ClCNO ₂	[-]	1564	[-]	[-]	[-]	1346	R
CH ₃ ClHCNO ₂	1589	1565 1572	24 17	2 [-7]	1349	1347 1356	IR R
CH ₃ Cl ₂ CNO ₂	1600	1581 1587	19 13	2 [-6]	1324	1322 1330	IR R
C ₂ H ₅ ClHCNO ₂	1585	1564 1570	21 15	[-10] [-14]	1348	1358 1362	IR R
C ₂ H ₅ Cl ₂ CNO ₂	1595	1578 1585	17 10	8 [-3]	1320	1312 1323	IR R
Cl ₃ NO ₂	1621	~1601	20	0	1310	1310	IR

TABLE 7.29 Infrared and Raman data for nitrobenzenes in different physical phases

Group	4-Nitro- benzene [vapor] asym.NO ₂ str. cm ⁻¹	4-Nitro- benzene [CHCl ₃] asym.NO ₂ str. cm ⁻¹	4-Nitro- benzene [neat] asym.NO ₂ str. cm ⁻¹	3-Nitro- benzene [vapor] asym.NO ₂ str. cm ⁻¹	3-Nitro- benzene [CHCl ₃] asym.NO ₂ str. cm ⁻¹	3-Nitro- benzene [neat] asym.NO ₂ str. cm ⁻¹	2-Nitro- benzene [vapor] asym.NO ₂ str. cm ⁻¹	2-Nitro- benzene [CHCl ₃] asym.NO ₂ str. cm ⁻¹	2-Nitro- benzene [neat] asym.NO ₂ str. cm ⁻¹	IR or Raman IR
CH ₃ O	1535	1510	[—]	1550	1526	[—]	1550	1530	[—]	IR
HO	1539	1517	[—]	1547	1529	[—]	1545	1537	[—]	IR
Cl	1540	1522	1522	1551	1527	1530	1551	1537	1528	IR
F	1542	1525		1530						R [neat] IR
CH ₃	1538	1528 1520	1510	1545	1531	1522	1542 1525	1527 R	1521	R IR
NO ₂	1567	1555	[—]	1553	1539	1522	[—]	[—]	1530 [KBr]	R [neat] IR
	sym.NO ₂ str.	sym.NO ₂ str.	sym.NO ₂ str.	sym.NO ₂ str.	sym.NO ₂ str.	sym.NO ₂ str.	sym.NO ₂ str.	sym.NO ₂ str.	sym.NO ₂ str.	
CH ₃ O	1348	1339	[—]	1353	1348	[—]	1360	1357	[—]	IR
HO	1350	1338	[—]	1360	1352	[—]	1335	1335	[—]	IR
Cl	1350	1343	1342	1351	1350	1345	1359	1357	1352	IR
F	1352	1347								IR
CH ₃	1355	1346 1350	1351	1358	1350	1350	1350 1350	1354	1344	R [neat] IR
NO ₂	1340	1338	[—]	1349	1346	1344	[—]	[—]	[—]	R [neat] IR

TABLE 7.30 A comparison of the frequency separation between asym. NO₂ stretching and sym. NO₂ stretching [vapor-phase data minus CHCl₃ solution data] and [vapor-phase data minus neat-phase data] for nitrobenzenes

Group	4-Nitro- benzene asym.NO ₂ str. [vapor]- [CHCl ₃] cm ⁻¹	4-Nitro- benzene sym.NO ₂ str. [vapor]- [CHCl ₃] cm ⁻¹	3-Nitro- benzene asym.NO ₂ str. [vapor]- [CHCl ₃] cm ⁻¹	3-Nitro- benzene asym.NO ₂ str. [vapor]- [CHCl ₃] cm ⁻¹	2-Nitro- benzene asym.NO ₂ str. [vapor]- [CHCl ₃] cm ⁻¹	2-Nitro benzene asym.NO ₂ str. [vapor]- [CHCl ₃] cm ⁻¹	IR or Raman
	[vapor]- [neat] cm ⁻¹	[vapor]- [neat] cm ⁻¹	[vapor]- [neat] cm ⁻¹	[vapor]- [neat] cm ⁻¹	[vapor]- [neat] cm ⁻¹	[vapor]- [neat] cm ⁻¹	
CH ₃ O	25	9	24	5	20	3	IR
HO	22	12	18	8	8	0	IR
Cl	18	6	24	1	14	2	IR
CH ₃	18	9	14	8	14	[-4]	IR
NO ₂	12	2	14	3	[-]	[-]	IR
Cl	18 15	7 0	21	6	23	7	IR IR; R
F	14	5					IR; R
CH ₃	28 18	4 5	23	12	21	6	IR IR; R
NO ₂	[-]	[-]	14	0	[-]	[-]	IR

TABLE 7.31 Infrared data for organonitro compounds in different physical phases

Nitro- Compounds	a.NO ₂ str. cm ⁻¹ vapor	s.NO ₂ str. cm ⁻¹ vapor	Tempera- ture	a.NO ₂ str. cm ⁻¹ neat	s.NO ₂ str. cm ⁻¹ neat	a.NO ₂ str. cm ⁻¹ vapor-neat	s.NO ₂ str. cm ⁻¹ vapor-neat
	CCl ₄	CCl ₄		Vapor-CCl ₄	Vapor-CCl ₄		
Benzene							
Nitro	1540	1352	20 °C	1520	1345	20	7
1,2-Dinitro	1563	1353	280 °C	1529	1353	34	0
1,3-Dinitro	1555	1349	280 °C	1532	1349	23	0
1,4-Dinitro	1565	1340	240 °C	1562	1339	3	1
Phenol 2-Nitro	1545	1333	280 °C	1530 Melt	1322	15	11
				CCl ₄	CCl ₄	Vapor-CCl ₄	Vapor-CCl ₄
Benzene							
1,2,4,5-Cl ₄ -3-NO ₂	1569	1333		1556 neat	1337	13	[-4]
				1559	1339	10	[-6]
Cl ₅ -NO ₂	1569	1335		1556	1338	13	[-3]
1,2,3,4-Cl ₄ -5-NO ₂	1562	1338		1532	1338	30	0
1-Cl-2-NO ₂	1551	1359		~1535	1352	16	1
1-Cl-3-NO ₂	1551	1351		1542	1351	9	0
1-Cl-4-NO ₂	1540	1349		1527	1344	13	5

TABLE 7.32 Infrared and Raman data for organonitrates, organonitrites, and 1,4-dinitropiperazine in different physical phases

Nitrate	asym.NO ₂ str. [vapor] cm ⁻¹	asym.NO ₂ str. [CCl ₄] cm ⁻¹	asym.NO ₂ [vapor]- [CCl ₄] cm ⁻¹	sym.NO ₂ [vapor]- [CCl ₄] cm ⁻¹	sym.NO ₂ str. [vapor] cm ⁻¹	sym.NO ₂ str. [CCl ₄] cm ⁻¹	IR or Raman
	C ₂ H ₅	1660	1637	23	9	1289	
		[neat] cm ⁻¹	[vapor]- [neat] cm ⁻¹	[vapor]- [neat] cm ⁻¹		[neat] cm ⁻¹	IR
(CH ₃) ₂ CH	1651	1620	31	8	1282	1274	IR
C ₃ H ₇	[—]	1625	[—]	[—]	1277	[—]	IR
		1635 wk			1282 stg		R
C ₅ H ₁₁	[—]	1624	[—]	[—]	1275	[—]	IR
	trans N=O str. [vapor] cm ⁻¹	trans N=O str. [CCl ₄] cm ⁻¹	trans N=O str. [vapor]- [CCl ₄] cm ⁻¹	cis N=O str. [vapor]- [CCl ₄] cm ⁻¹	cis N=O str. [vapor] cm ⁻¹	cis N=O str. [CCl ₄] cm ⁻¹	
CH ₃	1681	1685	[—4]	[—5]	1625	1630	
C ₄ H ₉	1673	[—]	[—]	[—]	1618	[—]	IR
iso-C ₅ H ₁₁	1669	1672	[—3]	[—2]	1618	1620	IR
tert-(CH ₃) ₃ C	1655	1661	[—6]	0	1610	~1610	IR
N—NO ₂		asym.NO ₂ str. [neat] cm ⁻¹			sym.NO ₂ str. [neat] cm ⁻¹		
1,4-Dinitropiperazine		1543			1234		IR

TABLE 7.33 The N=O stretching frequencies for nitrosamines in different physical phases

X,Y	XYNN=O vapor N=O str. cm ⁻¹	Temp. °C	XYNN=O N=O str. cm ⁻¹	State	XYNN=O* CCl ₄ soln. N=O str. cm ⁻¹	Vapor- state Δ N=O str. cm ⁻¹	Vapor- CCl ₄ soln. Δ N=O str. cm ⁻¹
	CH ₃ , CH ₃		1485		200 °C	1438	neat
C ₂ H ₅ , C ₂ H ₅	1482	200 °C	1450	neat	1454	32	28
C ₃ H ₇ , C ₃ H ₇	1482	200 °C	1449	neat	[—]	33	[—]
C ₄ H ₉ , C ₄ H ₉	1482	200 °C	1448	neat	[—]	34	[—]
CH ₃ , C ₆ H ₅	1492	200 °C	1438	neat	[—]	54	[—]
CH ₃ , O=C—OC ₂ H ₅	1534	200 °C	1509	neat	[—]	25	[—]
iso-C ₃ H ₇ , iso-C ₃ H ₇	[—]	[—]	[—]	[—]	1438	[—]	[—]
sec-C ₄ H ₉ , sec-C ₄ H ₉	[—]	[—]	[—]	[—]	1437	[—]	[—]

* See Reference 14.

Phosphorus Compounds

Introduction	233
Phosphorus-Halogen	234
Phosphorus Halogen Stretching F or Organophosphorus Halides	235
O-Methyl Phosphorodichloridothioate	236
O-Ethyl Phosphorodichloridothioate, O-Ethyl-1,1-d ₂ Phosphorodichloridothioate, and O-Ethyl-2,2,2-d ₃ Phosphorodichloridothioate	236
O,O-Dimethyl Phosphorochloridothioate	236
P-Cl Stretching	237
CH ₃ , CD ₃ , C ₂ H ₅ , CH ₃ CD ₂ and CD ₃ CH ₂ Vibrational Assignments for (R-O)P=OCl ₂ and (RO)P(=S)Cl ₂ Analogs	237
P=O Stretching, ν P=O	237
O,O-Dimethyl O-(2-Chloro 4-X-Phenyl) Phosphate	238
Phenoxarsine Derivatives	238
ν P=O vs ν P=S	239
P=S Stretching, ν P=S	239
S-Methyl Phosphorodichloridothioate	239
Skeletal Modes of the (C-O-) ₃ P Group of Trimethyl Phosphite and Trimethyl Phosphate	240
ν P=S, ν P-S, and ν S-H	240
Dialkyl Hydrogenphosphonate and Diphenyl Hydrogenphosphonate	240
The C-O-P Stretching Vibrations	241
C-P Stretching, ν C-P	241
Compounds Containing P-NH-R Groups	242
O-Alkyl O-Aryl N-Methylphosphoramidate vs O-Alkyl O-Aryl N-Methylphosphoramidothioate	243
Primary Phosphoramidothioates, P(=S)NH ₂	244
P(=S)NH ₂ , P(=S)NH, P(=S)ND ₂ , P(=S)NHCH ₃ , and R(=S)NDCH ₃	244
O-Methyl O-(2,4,5-trichlorophenyl) N-alkylphosphoramidates	245
Summary of PNH ₂ and PNH ₂ Vibrations	245
Summary of Vibrational Assignments for N-Alkyl Phosphoramidodichloridothioate and Deuterated Analogs	245
O,O-Dimethyl O-(2,4,5-Trichlorophenyl) Phosphorothioate, and Its P=O and (CD ₃ O) ₂ Analogs	245
A Comparison of IR Data for O,O-Dialkyl Phosphorochlorothioate and O,O,O-Trialkyl Phosphorothioate in Different Physical Phases	246
A Comparison of IR Data for Organophosphates and Organohydrogenphosphonates in Different Physical Phases	246
A Comparison of O-alkyl Phosphorodichloridothioate and S-alkyl Phosphorodichloridothioate in Different Physical Phases	247

Infrared Data for O,O-diethyl <i>N</i> -alkylphosphoramidates in Different Physical Phases	247
Vibrational Assignments for CH ₃ -PO ₃ ²⁻ , CD ₃ -PO ₃ ²⁻ , H-PO ₃ ²⁻ , and PO ₄ ³⁻	247
Vibrational Data for Sodium Dimethylphosphinate, Potassium Dimethylphosphinate, and Sodium Dialkylphosphinate	248
Solvent Effects P=O Stretching, ν P=O	248
PCl ₃ and PCl ₂ Vibrations	250
Absorbance Ratios for ROP(=O)Cl ₂ Molecules	250
Alkyl Group Vibrations	250
The ν C-C Mode for the C ₂ H ₅ OP Group	251
The ν COP Group	251
ν C-D for CDCl ₃ in CCl ₄ Solutions	252
Reference Spectra	252
References	253

Figures

Figure 8.1	255 (236)	Figure 8.32	281 (243)
Figure 8.2	256 (236)	Figure 8.33	282 (243)
Figure 8.3	257 (236)	Figure 8.34	283 (243)
Figure 8.4	258 (236)	Figure 8.35	283 (243)
Figure 8.5	259 (236)	Figure 8.36	284 (243)
Figure 8.6	260 (236)	Figure 8.37	284 (243)
Figure 8.7	261 (236)	Figure 8.38	285 (243)
Figure 8.8	262 (236)	Figure 8.39	285 (244)
Figure 8.9	263 (236)	Figure 8.40	286 (244)
Figure 8.10	264 (236)	Figure 8.41	287 (244)
Figure 8.11	265 (236)	Figure 8.42	288 (244)
Figure 8.12	266 (236)	Figure 8.43	289 (244)
Figure 8.13	267 (237)	Figure 8.44	290 (244)
Figure 8.14	268 (239)	Figure 8.45	291 (246)
Figure 8.15	269 (239)	Figure 8.46	292 (246)
Figure 8.16	270 (239)	Figure 8.47	293 (248)
Figure 8.17	271 (240)	Figure 8.48	294 (247)
Figure 8.18	272 (240)	Figure 8.49	295 (247)
Figure 8.19	272 (240)	Figure 8.50	296 (247)
Figure 8.20	273 (240)	Figure 8.51	297 (248)
Figure 8.21	273 (240)	Figure 8.52	298 (248)
Figure 8.22	274 (241)	Figure 8.53	299 (248)
Figure 8.23	274 (241)	Figure 8.53a	300 (248)
Figure 8.24	275 (241)	Figure 8.53b	300 (249)
Figure 8.25	275 (241)	Figure 8.54	301 (249)
Figure 8.26	276 (241)	Figure 8.55	301 (249)
Figure 8.27	277 (242)	Figure 8.56	302 (249)
Figure 8.28	278 (242)	Figure 8.57	302 (249)
Figure 8.29	279 (242)	Figure 8.58	303 (249)
Figure 8.30	279 (242)	Figure 8.59	303 (249)
Figure 8.31	280 (243, 244)	Figure 8.60	304 (250)

Figure 8.61	304 (250)	Figure 8.74	311 (251)
Figure 8.62	305 (250)	Figure 8.75	311 (251)
Figure 8.63	305 (250)	Figure 8.76	312 (251)
Figure 8.64	306 (250)	Figure 8.77	312 (251)
Figure 8.65	306 (250)	Figure 8.78	313 (251)
Figure 8.66	307 (250)	Figure 8.79	313 (251)
Figure 8.67	307 (250)	Figure 8.80	314 (251)
Figure 8.68	308 (250)	Figure 8.81	314 (252)
Figure 8.69	308 (250)	Figure 8.82	315 (252)
Figure 8.70	309 (251)	Figure 8.83	315 (252)
Figure 8.71	309 (251)	Figure 8.84	316 (252)
Figure 8.72	310 (251)	Figure 8.85	316 (252)
Figure 8.73	310 (251)	Figure 8.86	317 (252)

Tables

Table 8.1	318 (234)	Table 8.18	333 (240)
Table 8.2	319 (234)	Table 8.19	334 (240)
Table 8.3	320 (234)	Table 8.20	336 (241)
Table 8.4	321 (235)	Table 8.21	338 (241)
Table 8.5	322 (237)	Table 8.22	338 (241)
Table 8.5a	323 (237)	Table 8.23	339 (243)
Table 8.6	323 (237)	Table 8.24	340 (244)
Table 8.7	324 (237)	Table 8.25	341 (245)
Table 8.8	325 (237)	Table 8.26	342 (245)
Table 8.8a	326 (237)	Table 8.27	343 (245)
Table 8.9	326 (238)	Table 8.28	344 (245)
Table 8.10	327 (238)	Table 8.29	345 (246)
Table 8.11	327 (239)	Table 8.30	346 (246)
Table 8.12	328 (239)	Table 8.31	347 (246)
Table 8.13	329 (239)	Table 8.32	348 (247)
Table 8.14	331 (239)	Table 8.33	349 (247)
Table 8.15	331 (239)	Table 8.34	349 (247)
Table 8.16	332 (240)	Table 8.35	350 (248)
Table 8.17	332 (240)		

*Numbers in parentheses indicate in-text page reference.

INTRODUCTION

There has been interest in phosphorus compounds for many years, because these compounds have been found to be useful as chlorinating agents, flame retardants, antioxidants, fertilizers, and pesticides. On the other hand certain phosphorus derivatives have been manufactured for poisonous war gases, and this application is not positive for mankind. Therefore, many articles covering IR and Raman spectral data and assignments for these materials have been published and reviewed (1–55).

PHOSPHORUS-HALOGEN

Tables 8.1 through 8.3 list vibrational data and assignments for compounds of forms PX_3 , $P(=S)X_3$, and $P(=O)X_3$. The νPX_3 , νPX_2 and νPX vibrations for these inorganic phosphorus compounds decrease in frequency in the X order: F, Cl, Br, and I. The overall frequency ranges for the νPX_n modes for PX_3 , $P(=S)X_3$ and $P(=O)X_3$ analogs are:

$$PF_{1-3}, 817-981 \text{ cm}^{-1}$$

$$PCl_{1-3}, 431-618 \text{ cm}^{-1}$$

$$PBr_{1-3}, 299-466 \text{ cm}^{-1}$$

$$PI_3, 303-325 \text{ cm}^{-1}$$

The ν asym. PF_3 modes for $P(=O)F_3$, $P(=S)F_3$, and PF_3 decrease in the order 982 cm^{-1} , 981 cm^{-1} , and 840 cm^{-1} , and the ν sym. PF_3 modes for $P(=S)F_3$, PF_3 , and $P(=O)F_3$ decrease in the order 981 cm^{-1} , 890 cm^{-1} , and 875 cm^{-1} . Thus, the compound order for the ν asym. PF_3 frequency decrease $P(=O)F_3$, $P(=S)F_3$, and PF_3 is not the same as the compound order $P(=S)F_3$, PF_3 , and $P(=O)F_3$ for ν sym. PF_3 (Table 8.1). In the case of the $P=O$ analog, the $\nu P=O$ vibration occurs at 1405 cm^{-1} (see the Table 8.8 discussion on page 237), and $\nu P=O$ and ν sym. PF_3 belong to the A_1 species. Therefore, it is possible for $\nu P=O$ and ν sym. PF_3 to couple, causing $\nu P=O$ to occur at higher frequency and ν sym. PF_3 to occur at a lower frequency than ν sym. PF_3 for both the $P(=S)F_3$ and PF_3 analogs. On the other hand, the $\nu P=S$ vibration for $P(=S)F_3$ occurs at 695 cm^{-1} , and $\nu P=S$ and ν sym. PF_3 both belong to the A_1 species. Therefore, it also appears that these two modes are coupled, causing ν sym. PF_3 to occur at a higher frequency and $\nu P=S$ to occur at a lower frequency than otherwise expected. A similar argument has been given for the frequency behavior of νPCl_2 for the compound $P(=S)Cl_2F$ (9).

The ν asym. PCl_3 and ν asym. PBr_3 vibrations and the ν sym. PCl_3 and ν sym. PBr_3 vibrations for the PX_3 , $P(=O)X_3$, and $P(=S)X_3$ are compared here:

ν asym. $PX_3 \text{ cm}^{-1}$	Compound	ν sym. $PX_3, \text{ cm}^{-1}$
484	PCl_3	511
547	$P(=S)Cl_3$	431
581	$P(=O)Cl_3$	486
400	PBr_3	380
438	$P(=S)Br_3$	299
488	$P(=O)Br_3$	340
325	PI_3	303

The ν asym. PX_3 vibration increases in frequency in the order PX_3 , $P(=S)X_3$, and $P(=O)X_3$ for both the PCl_3 and PBr_3 analogs. The ν asym. PX_3 belongs to the e species and the $\nu P=O$ and $\nu P=S$ vibration belong to the a_1 species. Therefore, it is not possible for these two modes to couple. On the other hand, it is possible for ν sym. PX_3 and $\nu P=S$ to couple, because both modes

belong to the a_1 species. Coupling between ν P=S and ν sym. PX_3 causes ν sym. PCl_3 and ν sym. Br_3 to occur at lower frequency in the case of the $\text{P}(=\text{S})\text{X}_3$ analogs than in the case of the $\text{P}(=\text{O})\text{X}_3$ analogs.

Frequencies in parentheses in Tables 8.2 and 8.3 are estimated based upon spectra-structure correlations presented in Nyquist *et al.* (51).

PHOSPHORUS HALOGEN STRETCHING FOR ORGANOPHOSPHORUS HALIDES

Table 8.4 lists the ν asym. PCl_2 and ν sym. PCl_2 frequencies for compounds of form XPCl_2 , $\text{XP}(=\text{O})\text{Cl}_2$, and $\text{XP}(=\text{S})\text{Cl}_2$. It is of interest to compare these vibrations for a series of analogs:

ν asym. PCl_2 , cm^{-1}	Compound	ν sym. PCl_2 , cm^{-1}
506	CH_3OPCl_2	453
579/607	$\text{CH}_3\text{OP}(=\text{O})\text{Cl}_2$	515/548
531/560	$\text{CH}_3\text{OP}(=\text{S})\text{Cl}_2$	456/478
505	CD_3OPCl_2	456
531/552	$\text{CD}_3\text{OP}(=\text{S})\text{Cl}_2$	452/471
576/600	$\text{C}_2\text{H}_5\text{OP}(=\text{O})\text{Cl}_2$	516/550
528/558	$\text{C}_2\text{H}_5\text{OP}(=\text{S})\text{Cl}_2$	472-490
525/550	$\text{CH}_3\text{CD}_2\text{OP}(=\text{S})\text{Cl}_2$	465/484
531/552	$\text{CD}_3\text{CH}_2\text{OP}(=\text{S})\text{Cl}_2$	462-483
560	$\text{CH}_3\text{NHP}(=\text{O})\text{Cl}_2$	517
512	$\text{CH}_3\text{NHP}(=\text{S})\text{Cl}_2$	450/468
560	$(\text{CH}_3)_2\text{NP}(=\text{O})\text{Cl}_2$	517
512	$(\text{CH}_3)_2\text{NP}(=\text{S})\text{Cl}_2$	450

In all cases, the ν asym. PCl_2 and ν sym. PCl_2 vibrations occur at higher frequency for the $\text{P}=\text{O}$ analog than for the $\text{P}=\text{S}$ analog. It is suggested that ν P=S and ν sym. PCl_2 are coupled to some degree. It is interesting to note that both ν asym. PCl_2 and ν sym. PCl_2 are affected by substitution of CD_3O for CH_3O , and $\text{CH}_3\text{CD}_2\text{O}$ and $\text{CH}_3\text{CH}_2\text{O}$ for $\text{C}_2\text{H}_5\text{O}$ in compounds of form $\text{ROP}(=\text{S})\text{Cl}_2$. These data show that these vibrations involve more than just stretching of the PCl_2 bonds. In addition, two frequencies are listed for the ν asym. PCl_2 and ν sym. PCl_2 vibrations for many compounds, and these doublets are due to the existence of rotational conformers (22). The low-temperature rotational conformer is always listed first in each set.

O-METHYL PHOSPHORODICHLORIDOTHIOATE

Figure 8.1 illustrates how a model compound such as dichlorofluorophosphorothioate can be used to help assign the vibrational assignments for the nine $\text{OP}(=\text{S})\text{Cl}_2$ skeletal vibrations for $\text{CH}_3\text{OP}(=\text{S})\text{Cl}_2$. In addition, substitution of CD_3O for CH_3O aids in the vibrational assignments for the CH_3 and CD_3 groups. Variable temperature experiments aided in showing which bands resulted from each rotational conformer (21).

Figures 8.1 and 8.2 show the IR spectrum for $\text{P}(=\text{S})\text{Cl}_2\text{F}$ in the vapor and solution phases and a complete vibrational assignment is presented in Reference 9.

Figure 8.3 shows the IR spectrum for phosphoryl chloride, $\text{P}(=\text{O})\text{Cl}_3$. The vibrational assignment for $\text{P}(=\text{S})\text{Cl}_2\text{F}$ was aided by comparison with the vibrational assignment for $\text{P}(=\text{O})\text{Cl}_3$ (see Fig. 8.4). The a_1 modes for $\text{P}(=\text{O})\text{Cl}_3$ correspond to a' modes for $\text{P}(=\text{S})\text{Cl}_2\text{F}$, and the doubly degenerate e modes for $\text{P}(=\text{O})\text{Cl}_3$ correspond to a' and a'' modes for $\text{P}(=\text{S})\text{Cl}_2\text{F}$ (9).

Figure 8.5 shows IR spectra for $\text{CH}_3\text{OP}(=\text{S})\text{Cl}_2$, $\text{CD}_3\text{OP}(=\text{S})\text{Cl}_2$, and $\text{CH}_3\text{OP}(=\text{O})\text{Cl}_2$ (21). Figure 8.6 shows an IR spectrum for $\text{CH}_3\text{OP}(=\text{S})\text{Cl}_2$, and Figure 8.7 shows an IR spectrum for $\text{CD}_3\text{OP}(=\text{S})\text{Cl}_2$ (25). Vibrational assignments for these compounds have been reported (21, 25).

Because these molecules exist as rotational conformers, several of the vibrational modes for $\text{CH}_3\text{OP}(=\text{S})\text{Cl}_2$ and $\text{CD}_3\text{OP}(=\text{S})\text{Cl}_2$ appear as doublets. Rotational conformer 1 is assigned to the sets of IR bands that increase in intensity (A) with decrease in temperature (T), and rotational conformer 2 is assigned to IR bands that decrease in intensity (A) with a decrease in temperature (T).

Figure 8.8 compares the vibrational assignments for $\text{CH}_3\text{OP}(=\text{S})\text{Cl}_2$, $\text{CD}_3\text{OP}(=\text{S})\text{Cl}_2$, $\text{P}(=\text{S})\text{Cl}_2\text{F}$, $\text{CH}_3\text{OP}(=\text{O})\text{Cl}_2$, and $\text{P}(=\text{O})\text{Cl}_3$ (25).

O-ETHYL PHOSPHORODICHLORIDOTHIOATE, O-ETHYL-1,1-d₂ PHOSPHORODICHLORIDOTHIOATE, AND O-ETHYL-2,2,2-d₃ PHOSPHORODICHLORIDOTHIOATE

Complete vibrational assignments have been reported for $\text{C}_2\text{H}_5\text{OP}(=\text{S})\text{Cl}_2$, $\text{CH}_3\text{CD}_2\text{OP}(=\text{S})\text{Cl}_2$, and $\text{CD}_3\text{CH}_2\text{OP}(=\text{S})\text{Cl}_2$. These compounds exist as rotational conformers and conformers 1 and 2 were determined experimentally in the same manner as those reported for $\text{CH}_3\text{OP}(=\text{S})\text{Cl}_2$ and $\text{CD}_3\text{OP}(=\text{S})\text{Cl}_2$ (22, 25).

Figures 8.9, 8.10, and 8.11 show IR spectra for $\text{C}_2\text{H}_5\text{OP}(=\text{S})\text{Cl}_2$, $\text{CH}_3\text{CD}_2\text{OP}(=\text{S})\text{Cl}_2$, and $\text{CD}_3\text{CH}_2\text{OP}(=\text{S})\text{Cl}_2$, respectively (22). Comparison of Figs. 8.9–8.11 with Figs. 8.5–8.7 should help the reader identify the $\text{ROP}(=\text{S})\text{Cl}_2$ skeletal vibrations.

O,O-DIMETHYL PHOSPHOROCHLORIDOTHIOATE

The compound $\text{P}(=\text{S})\text{ClF}_2$ was used as a model compound for the vibrational assignments for $(\text{CH}_3)_2\text{P}(=\text{S})\text{Cl}$. Vibrational assignments for $\text{P}(=\text{S})\text{ClF}_2$ used are presented by Durig and Clark (11). Figure 8.12 shows IR spectra for O,O-dimethyl phosphorochloridothioate in the solution

and liquid phases. Figure 8.13 shows IR spectra for O,O-dimethyl-d₆ phosphorochloridothioate in the solution and liquid phases. Figure 8.14 shows IR spectra of (CH₃O)₂P(=S)Cl and (CD₃O)₂P(=S)Cl in solution (27). Tables 8.5 and 8.5a list the vibrational assignments for these three compounds. Several of the vibrations for the (CO)₂P(=S)Cl analogs appear as doublets due to the existence of rotational conformers (27).

P–Cl STRETCHING

Table 8.6 lists the ν P–Cl frequencies for P=O and P=S derivatives. All but the [(CH₃)₂N]₂ and [(C₂H₅)₂N]₂ derivatives exhibit ν P–Cl as a doublet due to the existence of rotational conformers. The P=O analogs exhibit ν P–Cl at higher frequency(ies) than corresponding P=S analogies [e.g., (CH₃O)₂P(=O)Cl, 553/598 cm⁻¹ vs (CH₃O)₂P(=S)Cl, 486/525 cm⁻¹] (27). For the compounds studied, ν P–Cl for the P=O series occur in the range 532–557 cm⁻¹ and for the P=S series in the range 470–543 cm⁻¹.

CH₃, CD₃, C₂H₅, CH₃CD₂ AND CD₃CH₂ VIBRATIONAL ASSIGNMENTS FOR (R-O)P=OCl₂ AND (RO)P(=S)Cl₂ ANALOGS

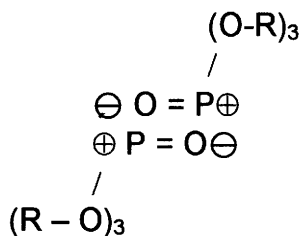
Table 8.7 lists vibrational assignments of the alkyl groups of O-methyl phosphorodichloridothioate, O-methyl-d₃ phosphorodichloridothioate, methyl phosphorodichloridate, O-ethyl phosphorodichloridothioate, O-ethyl-1,1-d₂ phosphorodichloridothioate, and O-ethyl-2,2,2-d₃ phosphorodichloridothioate (21, 22, 25, 27). The ratios ν CH₂/ ν CD₂ and ν CH₃/ ν CD₃ vary from 1.14 to 1.52 vs a theoretical value of 1.414.

P=O STRETCHING, ν P=O

Table 8.8 lists the P=O stretching, ν P=O, frequencies for a variety of compounds. For the compounds studied, ν P=O occurs in the range 1243–1405 cm⁻¹. Many of the phosphate esters exhibit ν P=O as a doublet due to the existence of rotational conformers, and the frequency separation for these doublets varies between 7 and 29 cm⁻¹.

Table 8.8a lists ν P=O frequencies for organophosphorus compounds in different physical phases. In the liquid phase many of the organophosphorus esters exhibit only a single ν P=O frequency; however, in CS₂ solution ν P=O is observed as a doublet due to the existence of rotational conformers. The ν P=O frequency difference between these rotational conformers varies between 7 and 22 cm⁻¹.

In the liquid phase the structural configuration may be stabilized by the intermolecular association shown here:



O,O-DIMETHYL O-(2-CHLORO 4-X-PHENYL) PHOSPHATE

Table 8.9 lists the $\nu\text{P-O}$ frequencies for the rotational conformers for the X-analogs of O,O-dimethyl O-(2-chloro 4-X-phenyl) phosphate (20). The Hammett σ_p values for the 4-X group are also listed.

The frequency separation between the $\nu\text{P=O}$ rotational conformers varies between 15.6 and 18.4 cm^{-1} . The high frequency $\nu\text{P=O}$ conformer occurs in the range 1303.2–1308.5 cm^{-1} , and the low frequency P=O conformer occurs in the range 1285.8–1291.1 cm^{-1} . There is a trend that the $\nu\text{P=O}$ vibration decreases in frequency as σ_p changes from positive to negative.

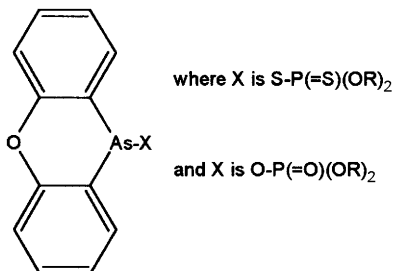
Thomas and Chittenden have developed an equation to predict $\nu\text{P=O}$ frequencies for a variety of organophosphorus compounds. Their equation is presented here (30):

$$\nu\text{P=O}(\text{cm}^{-1}) = 930 + 40 \Sigma \pi$$

Table 8.10 lists π constants for group G for compounds of form G-P(=O)Cl_2 . The calculated and observed frequencies vary between 2 and 28 cm^{-1} of the observed frequencies. In the case of organophosphorus compounds in the vapor phase, the 930 cm^{-1} constant should most likely be raised 10 to 20 cm^{-1} to account for the higher $\nu\text{P=O}$ frequencies observed in the vapor phase. In general, the $\nu\text{P=O}$ frequencies are lower in the neat phase, and this is attributed to the higher field effect in the neat phase as compared to the field effect in solution or the relative absence of the field effect in the vapor phase.

PHENOXARSINE DERIVATIVES

These compounds have the empirical structure presented here:



The $\nu\text{P}=\text{S}$ vibration occurs in the range 645–648 cm^{-1} , and the $\nu\text{P}=\text{O}$ vibration occurs in the range 1228–1235 cm^{-1} (31). See Table 8.11 for more specific data.

$\nu\text{P}=\text{O}$ VS $\nu\text{P}=\text{S}$

A normal coordinate analysis of phosphorus oxyhalides and their derivatives has shown that the $\nu\text{P}=\text{O}$ frequencies exhibit an accidental relationship between mass and electronegativity for the halogen atoms. The good agreement obtained between the calculated and observed $\nu\text{P}=\text{O}$ frequencies for all the phosphorus oxyhalides indicates that kinetic energy does have a significant effect on the $\nu\text{P}=\text{O}$ frequency. The calculated potential energy distribution indicates that the $\text{P}=\text{O}$ fundamental in each molecule results from over 85% $\nu\text{P}=\text{O}$, and mixes only slightly with other molecular vibrations of the same symmetry species (47). These calculations show that the force constant for $\nu\text{P}=\text{O}$ for $\text{CH}_3\text{P}(\text{=O})\text{Cl}_2$ is closer to that for $\text{P}(\text{=O})\text{Cl}_3$ than the force constant for $(\text{CH}_3)_3\text{P}(\text{=O})$.

Table 8.12 lists IR data for $\nu\text{P}=\text{O}$ and $\nu\text{P}=\text{S}$ for $\text{P}(\text{=O})\text{X}_3$ ν and $\text{P}(\text{=S})\text{X}_3$ -type compounds. This table shows that $\nu\text{P}=\text{O}$ decreases in frequency progressing in the series $\text{P}(\text{=O})\text{F}_3$, 1415 cm^{-1} to $\text{P}(\text{=O})\text{Cl Br}_2$, 1275 cm^{-1} . The $\nu\text{P}=\text{S}$ vibration does not show the same trend and, as stated before, $\nu\text{P}=\text{S}$ couples with other fundamental vibrations.

$\text{P}=\text{S}$ STRETCHING, $\nu\text{P}=\text{S}$

The $\nu\text{P}=\text{S}$ vibration couples with other fundamentals as discussed previously. The characteristic $\nu\text{P}=\text{S}$ vibration occurs in the range 565–742 cm^{-1} . These limits are set by $[(\text{CH}_3)_2\text{N}]_3\text{P}=\text{S}$ and $(\text{HCCCH}_2\text{O})\text{P}(\text{=S})\text{Cl}_2$ as listed in Table 8.13. Many of these $\text{P}=\text{S}$ containing compounds exist as rotational conformers as shown in Table 8.13.

The frequency separation between these rotational conformers varies between 11 and 47 cm^{-1} .

S-METHYL PHOSPHORODICHLORIDIOTHIOATE

This compound has the empirical structure $\text{CH}_3\text{SP}(\text{=O})\text{Cl}_2$ (23). This compound also exists as rotational conformers. The $\nu\text{P}=\text{O}$ frequencies are 1275/1266 cm^{-1} and the vibrational assignments are presented in Table 8.14.

Figure 8.15 (top) is an IR spectrum of S-methyl phosphorodichloridothioate in the range 3800–400 cm^{-1} . Figure 8.15 (bottom) is a spectrum of S-methyl phosphorodichloridothioate in the range 600–45 cm^{-1} . Figure 8.16 (top) is a Raman spectrum of S-methyl phosphorodichloridothioate, and Fig. 8.16 (bottom) is a polarized spectrum of S-methyl phosphorodichloridothioate in the range 3000–100 cm^{-1} . The skeletal vibrations for S- $\text{P}(\text{=O})\text{Cl}_2$ are similar to those for $\text{P}(\text{=O})\text{Cl}_3$ (23). Consequentially, the $\nu\text{sym. PCl}_3$, a_1 mode for $\text{P}(\text{=O})\text{Cl}_3$ at 483 cm^{-1} corresponds to the rotational conformers at 450 and 471 cm^{-1} for the $\text{SP}(\text{=O})\text{Cl}_2$ skeletal vibration. The doubly degenerate $\nu\text{asym. PCl}_3$, e mode for $\text{P}(\text{=O})\text{Cl}_3$ corresponds to the 593/579 cm^{-1} a'' rotational conformers (23).

SKELETAL MODES OF THE (C–O)₃P GROUP OF TRIMETHYL PHOSPHITE AND TRIMETHYL PHOSPHATE

Table 8.15 compares the P(–O–C)₃ vibrations for (CH₃O)₃P and (CH₃O)₃P=O. These skeletal vibrations occur at similar frequencies. The vibrational assignments for the CH₃ vibrations for trimethyl phosphite are listed in Table 8.16. Infrared spectra of trimethyl phosphite in different physical phases are presented in Figs. 8.17–8.19.

ν P=S, ν P–S, AND ν S–H

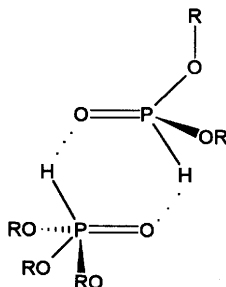
The ν P=S, ν P–S and ν S–H vibrations in compounds of form (RO)₂P(=S)SH and (ArO)₂P(=S)SH exist as a doublet due to the existence of rotational conformers (see Table 8.17). The ν SH rotational conformers were discussed in Chapter 4 in the section on thiols. The lower frequency ν S–H rotational conformer was assigned to the rotational conformer where the S–H group was intramolecularly hydrogen bonded to the free pair of electrons of the POR group (viz. SH···OR). The ν P=S rotational conformers 1 and 2 are assigned 670/659 cm⁻¹ and ν P–S rotational conformers are assigned 524–538 cm⁻¹/490–499 cm⁻¹, respectively (32).

Figure 8.20 compares the IR spectrum for O,O-dimethyl phosphorodithioic acid with the IR spectrum for O,O-dimethyl phosphorochloridothioate. Figure 8.21 compares the IR spectrum for O,O-diethyl phosphorodithioic acid with the IR spectrum for O,O-diethyl phosphorochloridothioate. The IR group frequencies just discussed are readily apparent in these spectra.

DIALKYL HYDROGENPHOSPHONATE AND DIPHENYL HYDROGENPHOSPHONATE

These compounds are often named phosphites, but the phosphorus atom is actually pentavalent in these cases and has the empirical structure (RO)₂P(=O)H.

In the neat phase ν P–H occurs in the range 2410–2442 cm⁻¹, δ P–H in the range 955–1028 cm⁻¹, and ν P=O in the range 1241–1260 cm⁻¹. In the vapor phase ν PH occurs 19–25 cm⁻¹ higher in frequency, δ P–H 8–20 cm⁻¹ higher in frequency, and ν P=O 27–41 cm⁻¹ higher in frequency than they occur in the neat phase. These frequency changes going from the neat to vapor phase suggest that in the neat phase these compounds are intermolecularly hydrogen bonded, such as in the one illustrated here:



In other compounds $\nu\text{P}=\text{O}$ does not shift as much to lower frequency in going from the vapor to the liquid phase as do these hydrogenphosphonates (see Table 8.18).

In CS_2 solution, compounds of form $(\text{RO})_2\text{P}(=\text{O})\text{H}$ exhibit $\nu\text{P}=\text{O}$ in the range 1273–1283 cm^{-1} and $\nu\text{P}=\text{O}$ in the range 1257–1266 cm^{-1} . The higher frequency $\nu\text{P}=\text{O}$ is often seen as a shoulder. It is possible that the higher frequency $\nu\text{P}=\text{O}$ is due to unassociated $(\text{RO})_2\text{P}(=\text{O})\text{H}$ molecules.

Figures 8.22 and 8.23 show the IR spectra of dimethyl hydrogenphosphonate and dimethyl deuterophosphonate in solution. Figures 8.24 and 8.25 show the IR spectra of diethyl hydrogenphosphonate and diethyl deuterophosphonate in solution (32). Figure 8.26 shows Raman spectra of dimethyl hydrogenphosphonate in the liquid phase (32). These spectra aid the reader in recognizing the group frequencies discussed in this chapter.

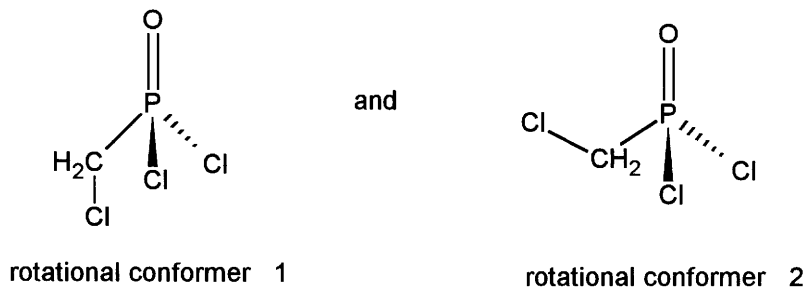
THE C–O–P STRETCHING VIBRATIONS

The C–O–P group frequencies are complex, and are often described as “C–O stretching”, $\nu\text{C}-\text{O}$, and “P–O stretching”, $\nu\text{P}-\text{O}$. Tables 8.19 and 8.20 list IR group frequency assignments for $\nu\text{C}-\text{O}$, $\nu\text{P}-\text{O}$ for C–O–P and $\nu\text{aryl}-\text{O}$ and $\nu\text{P}-\text{O}$ for aryl–O–P. The $\nu\text{C}-\text{O}$ frequencies occur in the range 990–1065 cm^{-1} , and the $\nu\text{P}-\text{O}$ frequencies occur in the range 739–861 cm^{-1} for the P–O–C group. The $\nu\text{aryl}-\text{O}$ frequencies occur in the range 1160–1261 cm^{-1} and $\nu\text{P}-\text{O}$ in the range 920–962 cm^{-1} for the aryl–O–P group.

Table 8.21 lists the aryl–O stretching frequencies for the O-methyl O-(X-phenyl N-methylphosphoramidates, and $\nu\text{aryl}-\text{O}$ occurs in the range 1207–1259 cm^{-1} (39).

C–P STRETCHING, $\nu\text{C}-\text{P}$

Table 8.22 lists the $\nu\text{C}-\text{P}$ frequencies for a variety of compounds containing this group, with $\nu\text{C}-\text{P}$ occurring in the range 699–833 cm^{-1} . In compounds such as $\text{ClCH}_2\text{P}(=\text{O})\text{Cl}_2$ and $\text{ClCH}_2\text{P}(=\text{S})\text{Cl}_2$, $\nu\text{C}-\text{P}$ exhibits a doublet (811/818 cm^{-1} at 25 °C) for $\nu\text{C}-\text{P}$ due to the presence of rotational conformers:



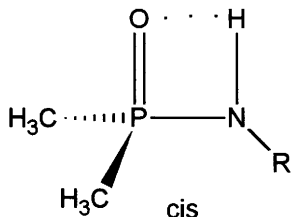
In the case of a compound such as $(\text{CH}_3)_2\text{PO}_2\text{Na}$ the IR bands at 737 cm^{-1} and 700 cm^{-1} are assigned to $\nu\text{asym. PC}_2$ and $\nu\text{sym. PC}_2$, respectively (41).

Figure 8.27 shows the IR spectrum of chloromethyl phosphonic dichloride in CS_2 solution at 0°C and at -75°C . Note that several bands occur as doublets due to the presence of rotational conformers, and that one band in each set of doublets increases in intensity (A) with a decrease in temperature (T). The higher frequency band of the doublet in the range $800\text{--}820\text{ cm}^{-1}$ increases in (A) with a decrease in (T). The lower frequency band in the range $1270\text{--}1300\text{ cm}^{-1}$ increases in (A) with a decrease in (T). Thus, the lower frequency $\nu\text{P=O}$ band near 1280 cm^{-1} and the band near 818 cm^{-1} for $\nu\text{C-P}$ are assigned to rotational conformer 2. The IR bands near 1282 cm^{-1} and 810 cm^{-1} are assigned to $\nu\text{P=O}$ and $\nu\text{C-P}$ for rotational conformer 1. On this same basis, $\nu\text{asym. PCl}_2$ rotational conformers 1 and 2 are assigned near 559 cm^{-1} and 570 cm^{-1} , respectively and the $\nu\text{sym. PCl}_2$ rotational conformers 1 and 2 are assigned near 490 cm^{-1} and 510 cm^{-1} , respectively.

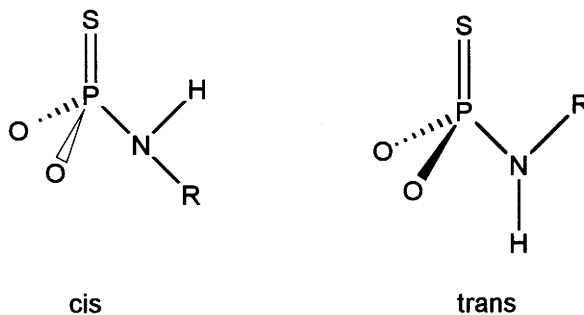
Figures 8.28 and 8.29 are IR spectra for $\text{ClCH}_2\text{P(=O)Cl}_2$ and $\text{ClCH}_2\text{P(=S)Cl}_2$, respectively (17). Vibrational assignments have been reported for $\text{ClCH}_2\text{PCl}_2$, $\text{CH}_3\text{P(=O)Cl}_2$, $\text{ClCH}_2\text{P(=S)Cl}_2$, $\text{CH}_3\text{P(=S)Cl}_2$, and $\text{BrCH}_2\text{P(=O)Br}_2$ (17). The $\nu\text{P=S}$ frequency for $\text{CH}_3\text{P(=S)Cl}_2$ occurs at 696 cm^{-1} , and the $\nu\text{P=S}$ rotational conformers 1 and 2 for $\text{ClCH}_2\text{P(=S)Cl}_2$ occur at 683 and 657 cm^{-1} (17). The $\nu\text{P=O}$ rotational conformers 1 and 2 occur at 1264 and 1275 cm^{-1} for $\text{BrCH}_2\text{P(=O)Br}_2$, and $\nu\text{asym. PBr}_2$ rotational conformers 1 and 2 occur at 463 and 481 cm^{-1} (17) (see Fig. 8.30).

COMPOUNDS CONTAINING P-NH-R GROUPS

The compounds containing the R-NH-P(=O) group exist in a cis configuration in dilute solution as shown here:



This cis configuration is stabilized by the intramolecular bonding between the N-H proton and the free pair of electrons on the P=O group (viz. $\text{N-H}\cdots\text{O=P}$). In the case of compounds containing the R-NH-P(=S) group the N-H group in dilute solution exists in both a cis and trans configuration as shown here:



The cis ν N–H frequencies occur in the range 3388–3461 cm^{-1} and trans ν N–H frequencies occur in the range 3380–3434 cm^{-1} (see Table 8.23). The frequency separation between cis ν N–H and trans ν N–H varies between 18 and 44 cm^{-1} .

Figure 8.31 shows the solution-phase IR spectrum of N-methyl phosphoramidodichloridothioate. The cis ν N–H frequency is assigned at 3408 cm^{-1} and that shoulder 3300 cm^{-1} is assigned to intermolecularly bonded ν N–H. The bands at 1094 and 838 cm^{-1} are assigned to “ ν C–N” and “P–N” for the P–N–C group. Infrared bands at 725 and 690 cm^{-1} are assigned to ν P=S rotational conformers 1 and 2, respectively (24). Figure 8.32 shows an IR spectrum of N-methyl- d_3 phosphoramidodichloridothioate (24). The ν N–H frequency is assigned at 3409 cm^{-1} and intermolecularly hydrogen bonded ν N–H at 3301 cm^{-1} . The “ ν C–N” and “ ν P–N” for the P–N–C group are assigned at 1117 cm^{-1} and 785 cm^{-1} , respectively. The ν P=S rotational conformers 1 and 2 are assigned at 711 cm^{-1} and 683 cm^{-1} , respectively.

Figure 8.33 is an IR spectrum for the N–D analog of N-methyl phosphoramidodichloridothioate (a small amount of the N–H analog is present as an impurity). The ν N–D mode is assigned at 2522 cm^{-1} and the intermolecular, ν N–D mode is assigned at 2442 cm^{-1} . The ν NH/ND ratio 3408 cm^{-1} /2522 cm^{-1} is 1.35, and the intermolecularly bonded ν NH/ ν ND ratio 3300 cm^{-1} /2442 cm^{-1} is 1.35. In this case, “ ν C–N” and “ ν P–N” for the group C–N–P occur at 1107 cm^{-1} and 846 cm^{-1} /825 cm^{-1} , respectively (24). The ν P=S conformers 1 and 2 are 728 cm^{-1} /681 cm^{-1} . Figure 8.34 is an IR spectrum for the N–D analog of N-methyl- d_3 phosphoramidodichloridothioate (a small amount of the N–H analog is also present). The “ ν P–N” mode is assigned at 780 cm^{-1} and “ ν C–N” at 1107 cm^{-1} . The ν P=S rotational conformers 1 and 2 are assigned at 701 cm^{-1} /673 cm^{-1} (24).

O-ALKYL O-ARYL N-METHYLPHOSPHORAMIDATE VS O-ALKYL O-ARYL N-METHYLPHOSPHORAMIDOTHIOATE

In Fig. 8.35 IR spectrum 1 is for a 10% CCl_4 solution spectrum of O-alkyl O-aryl N-methylphosphoramidate in a 0.1-mm NaCl cell and IR spectrum 2 is for a 10% CCl_4 solution of O-alkyl O-aryl N-methyl-phosphoramidothioate. In Fig. 8.31, spectrum 1, the strong IR band at 3235 cm^{-1} is assigned to intermolecularly hydrogen-bonded ν N–H, and the IR band 3442 cm^{-1} from cis ν N–H (42). In Figure 8.35, spectrum 2, the IR bands at 3440 cm^{-1} , 3402 cm^{-1} , and 3320 cm^{-1} are assigned to cis ν N–H, trans ν N–H, and intermolecularly hydrogen-bonded ν N–H, respectively. Study of Fig. 8.35 shows that it is a rather simple task to distinguish between $\text{CH}_3\text{NH–P=O}$ and $\text{CH}_3\text{NH–P=S}$ groups (42).

Figure 8.36 is a plot of the ν N–H frequencies of O-alkyl O-aryl N-alkylphosphoramidates vs an arbitrary assignment of one for each proton joined to the N- α -carbon atom. Figure 8.37 is a comparable plot for the O-alkyl O-aryl N-alkylphosphoramidothioates. However, in this case (with the exception of the N-tert-butyl analog) both cis ν N–H and trans ν N–H frequencies are observed (42). In the case of the N-tert-butyl analog, only the cis configuration is possible, because the N-tert-butyl group is sterically prevented from being in a cis position with the P=S group (42).

Figure 8.38 shows IR spectra in the range 3300–3500 cm^{-1} for O-alkyl O-aryl N-alkylphosphoramidothioates as obtained in ~ 0.01 molar or less CCl_4 solutions using a 14-mm NaCl cell. In spectrum A the N–R group is N– CH_3 , B is N– C_2H_5 , C is N– C_3H_7 , D is N-iso- C_4H_9 , E is

N_4H_9 , F is N -iso- C_3H_7 , G is N -sec- C_4H_9 , and H is N -tert- C_4H_9 . Spectra I and J are O, O-dialkyl N-methylphosphoramidothioate and O,O-dialkyl N-isopropylphosphoramidothioate, respectively. These data show that the νNH vibrations decrease in frequency with increased branching on the N - α -carbon atom. The electron release of the N -alkyl group to the nitrogen atom increases in the order methyl, ethyl, isopropyl, and tert-butyl. Thus, as the electron release to the nitrogen atom increases, the $N-H$ bond weakens, causing it to vibrate at a lower frequency.

Figure 8.39 shows IR spectra of O-alkyl N, N' -dialkylphosphorodiamidothioate in the range 3300–3500 cm^{-1} . Spectrum A is where N, N' is dimethyl, B is N, N' -diethyl, E is N, N' -dipropyl, D is N, N' -dibutyl, F is N, N' -diisopropyl, G is N, N' -di-sec-butyl, and H is the N, N' -dibenzyl analog. The I and J are for O-aryl N, N' -di-isopropylphosphorodiamidothioate and O-aryl N -isopropyl, N' -methyl phosphorodiamidothioate, respectively. These diamido compounds differ from the mono-amido compounds in that the intensity ratio is higher for the lower-frequency $\nu N-H$ band to the higher frequency $\nu N-H$ band. This indicates that there is a higher fraction of trans $\nu N-H$ in the diamides, but the cis $\nu N-H$ isomeric is still predominant. Spectra A through J are 0.01 molar or less solutions in 3-mm NaCl cells. Spectra D and J are for the N, N' -dibutyl analog; however, spectrum J is for a 10% CCl_4 solution using a 0.1-mm NaCl cell. The broad band in J is due to intermolecularly hydrogen-bonded $\nu N-H$ (42).

PRIMARY PHOSPHORAMIDOTHIOATES, $P(=S)NH_2$

Figure 8.40 shows an IR spectrum (coded R on the figure) of O-alkyl O-aryl phosphoramidothioate and an IR spectrum of O,O-dialkyl phosphoramidothioate (coded S) in the range 3300–3500 cm^{-1} . Samples were prepared as 0.01 molar CCl_4 solutions, and the spectra were recorded utilizing a 3-mm NaCl cell. The IR band near 3490 cm^{-1} is assigned as ν asym. NH_2 and the IR band near 3390 cm^{-1} is assigned as ν sym. NH_2 (42).

$P(=S)NH_2$, $P(=S)NH$, $P(=S)ND_2$, $P(=S)NHCH_3$, AND $R(=S)NDCH_3$

Figures 8.41, 8.42, and 8.43 are IR spectra of O,O-dimethyl phosphoramidothioate and its ND_2 analog, O,O-diethyl phosphoramidothioate and its D_2 analog, and O,O-diethyl N-methylphosphoramidothioate, and its $N-D$ analog. The vibrational assignments for the NH_2 , ND_2 , NHD vibrations are presented in Table 8.24. The values for the $\nu NH_2/\nu ND_2$ and $\nu NH/\nu ND$ are also presented in Table 8.24. The ν asym. NH_2 and asym. ND_2 modes occur near 3480 cm^{-1} and 2600–2611 cm^{-1} , respectively, and ν sym. NH_2 and ν sym. ND_2 occur near 3390 cm^{-1} and 2490 cm^{-1} , respectively. Both cis and trans νNH and νND modes are also assigned.

The δNH_2 and δND_2 modes are assigned near 1542 cm^{-1} and 1171 cm^{-1} , respectively (37).

The IR spectrum for O,O-dimethyl N-methylphosphoramidothioate is given in Fig. 8.44. Compare Fig. 8.44 with Fig. 8.43. upper spectrum for O,O-dimethyl N-methylphosphoramidothioate. The IR band at 954 cm^{-1} results from $\nu C-C$ for the $P-O-C_2H_5$ group in Fig. 8.43 (not from a $\nu N-C$ mode).

O-METHYL O-(2,4,5-TRICHLOROPHENYL) N-ALKYLPHOSPHORAMIDATES

Table 8.25 lists the N–H and N–D frequencies for O-methyl O-(2,4,5-trichlorophenyl) N-alkyl phosphoramidates in CCl_4 solution. The frequency separation between $\nu\text{N–H}$ and $\nu\text{N–D}$ is $\sim 200\text{ cm}^{-1}$ while for the $\nu\text{N–H}$ and $\nu\text{N–D}$ intermolecularly bonded species it varies between 144 and 155 cm^{-1} . In the case of the O-methyl O-(2,4,5-trichlorophenyl) N-alkylphosphoramidothioates the frequency separation between the cis $\nu\text{N–H}$ and trans $\nu\text{N–H}$ is in the range of $31\text{--}34\text{ cm}^{-1}$. The cis $\nu\text{N–H}$ frequencies decrease in the order of N– CH_3 , N-ethyl, N-isopropyl, and N-tert-butyl (3442, 3429, 3419, and 3402 cm^{-1} , respectively). The trans $\nu\text{N–H}$ frequencies decrease in the same order, N– CH_3 , N-ethyl, and N-isopropyl (3409, 3398, and 3385 cm^{-1} , respectively). The trans $\nu\text{N–H}$ mode is not observed for the N-tert-butyl analog.

SUMMARY OF PNH AND PNH₂ VIBRATIONS

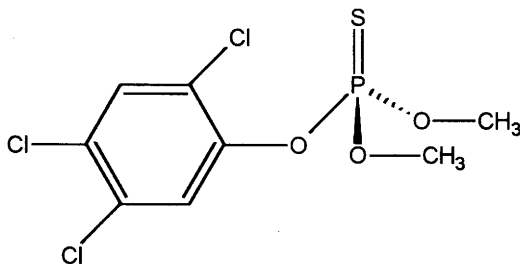
Table 8.26 lists the cis and trans νNH frequencies for compound types containing the P(=O)NHR , P(=S)NHR groups, and P(=S)NH_2 groups (37). The N–H bending mode, $\nu\text{N–H}$, is assigned in the range $1372\text{--}1416\text{ cm}^{-1}$. In all cases cis $\nu\text{N–H}$ occurs at higher frequency than trans νNH by 16 through 36 cm^{-1} .

SUMMARY OF VIBRATIONAL ASSIGNMENTS FOR N-ALKYL PHOSPHORAMIDODICHLORIDOTHIOATE AND DEUTERATED ANALOGS

Table 8.27 lists a summary of the vibrational assignments for N-alkyl phosphoramidodichloridothioates (24). For a more detailed discussion of these vibrational frequency assignments, the reader is referred to Reference 24.

O,O-DIMETHYL O-(2,4,5-TRICHLOROPHENYL) PHOSPHOROTHIOATE, AND ITS P=O AND $(\text{CD}_3\text{O})_2$ ANALOGS

Table 8.28 lists vibrational assignments for O,O-dimethyl O-(2,4,5-trichlorophenyl) phosphorothioate, and its P=O and $(\text{CD}_3\text{O})_2$ analogs (43). O,O-dimethyl O-(2,4,5-trichlorophenyl) phosphorothioate has the empirical structure presented here:



This phosphorus compound has 66 fundamental vibrations. Eighteen fundamentals result from vibrations with the two methyl groups. Thirty fundamentals result from vibration within the 2,4,5-trichlorophenoxy group, and 18 fundamentals result from vibrations within the $(C-O)_2(aryl-O)P=S$ group.

Vibrational assignments for the 2,4,5-trichlorophenoxy group were aided by comparison with the vibrational assignments for 1-fluoro-2,4,5-trichlorobenzene (52). The assignments for these ring modes are compared in Table 8.29.

Figure 8.45 (top) is an IR spectrum for O,O-dimethyl O-(2,4,5-trichlorophenyl) phosphorothioate, and Fig. 8.45 (bottom) is an IR spectrum for O,O-dimethyl O-(2,4,5-trichlorophenyl) phosphate. Figure 8.46 (top) is an IR spectrum for O,O-dimethyl- d_6 O-(2,4,5-trichlorophenyl) phosphorothioate, and Fig. 8.46 (bottom) is an IR spectrum for O,O-dimethyl- d_6 O-(2,4,5-trichlorophenyl)phosphate. It is easy to distinguish between the $P=S$ and $P=O$ analogs in this case. The $\nu P=O$ rotational conformers 1 and 2 are readily apparent by the doublet in the range $1275\text{--}1310\text{ cm}^{-1}$. Note that these IR bands are not present in the $P=S$ analogs. It should be noted that the $\nu P=O$ rotational conformer vibrations occur at lower frequency ($1300/1285\text{ cm}^{-1}$) in the case of the $(CH_3-O)_2$ analog than for the $(CD_3-O)_2$ analog ($1306\text{ cm}^{-1}/1292\text{ cm}^{-1}$). Thus, this frequency difference shows that $\nu P=O$ involves motion other than simple stretching of the $P=O$ bond.

The strongest Raman band in the spectrum of O,O-dimethyl O-(2,4,5-trichlorophenyl) phosphorothioate and its O,O-dimethyl- d_6 analog occur at 616 cm^{-1} and 617 cm^{-1} in the solid phase, respectively. This Raman band is assigned to $\nu P=S$. The out-of-plane ring mode (25 for the 2,4,5-trichlorophenoxy group occurs as a weak IR band in the range $627\text{--}629\text{ cm}^{-1}$ (43). However, another weak IR band is noted at 615 cm^{-1} for O,O-dimethyl O-(2,4,5-trichlorophenyl) phosphorothioate and at 607 cm^{-1} for the O,O-dimethyl- d_6 analog in CS_2 solution. These weak IR bands are assigned to $\nu P=S$.

A COMPARISON OF IR DATA FOR O,O-DIALKYL PHOSPHOROCHLOROTHIOATE AND O,O,O-TRIALKYL PHOSPHOROTHIOATE IN DIFFERENT PHYSICAL PHASES

Table 8.30 lists IR data for O,O-dialkyl phosphorochlorothioate and O,O,O-trialkyl phosphorothioate in different physical phases. It is interesting to note that the combination tone $\nu C-O + \nu P-O$ occurs at higher frequency in the vapor phase than in the neat phase. In the vapor phase at 200°C , O,O-dimethyl phosphorochloridothioate and O,O,O-trimethyl phosphorothioate each exist as one rotational conformer.

A COMPARISON OF IR DATA FOR ORGANOPHOSPHATES AND ORGANOHYDROGENPHOSPHONATES IN DIFFERENT PHYSICAL PHASES

The $\nu P=O$ rotational conformers generally occur at higher frequency in the vapor phase than in CS_2 solution (see Table 8.31).

A COMPARISON OF O-alkyl PHOSPHORODICHLORIDOTHIOATE AND S-alkyl PHOSPHORODICHLORIDOTHIOATE IN DIFFERENT PHYSICAL PHASES

Table 8.32 compares IR data for O-alkyl phosphorodichloridothioates and S-alkyl phosphorodichloridothioates in different physical phases. These data show that some molecular vibrations increase in frequency while other molecular vibrations decrease in frequency with change of physical phase.

INFRARED DATA FOR O,O-diethyl N-ALKYLPHOSPHORAMIDATES IN DIFFERENT PHYSICAL PHASES

Table 8.33 lists IR data for O,O-diethyl N-alkylphosphoramidates in different physical phases. In the vapor phase $\nu\text{P}=\text{O}$ occurs in the region $1274\text{--}1280\text{ cm}^{-1}$ and in the neat phase $\nu\text{P}=\text{O}:\text{H}$ occurs in the region $1210\text{--}1240\text{ cm}^{-1}$. The decrease in the $\nu\text{P}=\text{O}$ frequency in going from the vapor phase is attributed mainly to intermolecular hydrogen bonding between the free pair of electrons on the $\text{P}=\text{O}$ oxygen atom and the N-H proton (viz. $\text{P}=\text{O}\cdots\text{H}-\text{N}$). The $\nu\text{N-H}$ mode occurs in the region $3420\text{--}3460\text{ cm}^{-1}$ in the vapor phase, and occurs in the region $3198\text{--}3240\text{ cm}^{-1}$ in the neat phase. Thus, intermolecular hydrogen bonding causes $\nu\text{N-H}\cdots\text{O}=\text{P}$ to occur $205\text{--}225\text{ cm}^{-1}$ lower in frequency than it occurs in the vapor phase.

VIBRATIONAL ASSIGNMENTS FOR $\text{CH}_3\text{--PO}_3^{2-}$, $\text{CD}_3\text{--PO}_3^{2-}$, H--PO_3^{2-} , AND PO_4^{3-}

Table 8.34 lists vibrational assignments for $\text{CH}_3\text{--PO}_3\text{Na}_2$, $\text{CD}_3\text{--PO}_3\text{Na}_2$, HPO_3^{2-} , and PO_4^{3-} . Fig. 8.47 (top) is an IR spectrum of disodium methanephosphonate in the solid phase and Fig. 8.47 (bottom) is an IR spectrum of disodium methane- d_3 -phosphonate in the solid phase. Fig. 8.48 (top) is an IR spectrum of disodium methanephosphonate in water solution, and Fig. 8.48 (bottom) is an IR spectrum of disodium methane- d_3 -phosphonate in water solution (40). Figure 8.49 (top) is an IR spectrum of disodium methanephosphonate in the solid phase, Fig. 8.49 (middle) is an IR spectrum of disodium methane- d_3 -phosphonate in the solid phase, and Figure 8.49 (bottom) is an IR spectrum of dipotassium methanephosphonate in the solid phase (40). Figure 8.50 is a solid-phase IR spectrum for disodium n-octadecanephosphonate (40).

The model compounds containing the H--PO_3^{2-} and PO_4^{3-} anions (44,45) aid in the vibrational assignments for the CPO_3^{2-} skeletal vibrations. Vibrational assignments for the CH_3 and CD_3 groups are presented in Table 8.34. It is apparent that the e fundamentals for the PO_3^{2-} groups are split in the case of the CPO_3^{2-} skeletal modes. Thus, $\nu_{\text{asym. PO}_3^{2-}}$ for $\text{CH}_3\text{PO}_3\text{Na}_2$ occurs near 1110 and 1080 cm^{-1} and near 1100 and 1070 cm^{-1} in the case of

$\text{CD}_3\text{PO}_3\text{Na}_2$. The ν sym. PO_3 vibration occurs at 993 cm^{-1} for the CH_3 analog and at 972 cm^{-1} for the CD_3 analog.

In H_2O solution ν asym. PO_3^{2-} occurs at 1060 cm^{-1} and ν sym. PO_3^{2-} occurs at 975 cm^{-1} for the CH_3 analog, and at 1060 cm^{-1} and 969 cm^{-1} for the CD_3 analog. Comparison of the IR band near 2330 cm^{-1} for $\text{CH}_3\text{-PO}_3\text{Na}_2$ with the IR band near 185 cm^{-1} for $\text{CH}_3\text{-PO}_3\text{K}_2$ indicates that these bands arise from a lattice vibration (see Figure 8.48 (top and bottom)). In the case of $n\text{-C}_{18}\text{H}_{37}\text{-PO}_3\text{Na}_2$, the IR bands in the region $1050\text{--}1130$ are assigned to ν sym. PO_3^{2-} vibrations, the IR band near 987 cm^{-1} is assigned to (sym. PO_3^{2-} , and the IR band near 771 cm^{-1} is assigned as $\nu\text{ C-P}$.

VIBRATIONAL DATA FOR SODIUM DIMETHYLPHOSPHINATE, POTASSIUM DIMETHYLPHOSPHINATE, AND SODIUM DIALKYLPHOSPHINATE

Table 8.35 lists IR data and assignments for the $(\text{CH}_3)_2\text{PO}_2^-$ anion (41). Figure 8.51 upper is an IR spectrum of sodium dimethylphosphinate, $(\text{CH}_3)_2\text{PO}_2\text{Na}$ in the solid phase and Fig. 8.51 (bottom) is an IR spectrum of the same compound in water solution. Figure 8.52 (top) is an IR spectrum for $(\text{CH}_3)_2\text{PO}_2\text{Na}$ and Fig. 8.52 (bottom) is an IR spectrum for $(\text{CH}_3)_2\text{PO}_2\text{K}$. Both spectra were recorded in the solid phase. Figure 8.53 gives Raman spectra of $(\text{CH}_3)_2\text{PO}_2\text{Na}$ saturated in water solution.

Vibrational assignments for these dialkyl phosphinate salts were aided by vibrational assignments for $\text{H}_2\text{PO}_2\text{K}$ (44), $(\text{CH}_3)_3\text{P}$ (53), and $(\text{CH}_3)_3\text{P=O}$ (54).

The IR bands for $(\text{CH}_3)_2\text{PO}_2\text{Na}$ at 1169 cm^{-1} and 1065 cm^{-1} in the solid phase and at 1128 cm^{-1} and 1040 cm^{-1} in water solution are assigned to ν asym. PO_2 and ν sym. PO_2 , respectively (41). The IR band for $(\text{CH}_3)_2\text{PO}_2\text{Na}$ in the solid phase at 725 cm^{-1} and 695 cm^{-1} , and at 738 cm^{-1} (depolarized Raman band) and 700 cm^{-1} (polarized Raman band) in water solution are assigned as ν asym. PC_2 and ν sym. PC_2 , respectively. The ν asym. PO_2 and ν sym. PO_2 near 1150 cm^{-1} and 1050 cm^{-1} for sodium diheptyl phosphinate and sodium dioctylphosphinate are readily apparent in Fig. 8.53a.

The IR bands near 1300 cm^{-1} , and in the region $840\text{--}920\text{ cm}^{-1}$ are assigned to δ sym. CH_3 modes and ρCH_3 modes, respectively. For more detailed vibrational assignments see Reference 41.

SOLVENT EFFECTS P=O STRETCHING, $\nu\text{ P=O}$

Solvent effects aid the spectroscopist in interpreting the vibrational spectra of organophosphorus compounds. These studies also allow one to gain information upon solute solvent interactions. Intermolecular hydrogen bonding between a solvent and a basic site affects the vibrational spectrum. Field effects of a solvent system also alter the vibrational spectrum. Often both of

these effects operate simultaneously on the vibrational frequencies of chemical molecular vibrations (26, 55).

Figure 8.54 shows separate plots of $\nu\text{P}=\text{O}$ frequencies for $\text{P}(\text{=O})\text{Cl}_3$ vs the mole % $\text{CCl}_4/\text{C}_6\text{H}_{14}$, mole % $\text{C}_6\text{H}_{14}/\text{CHCl}_3$, and mole % $\text{CHCl}_3/\text{CCl}_4$ solvent systems. These are 1% wt./vol. solutions of $\text{P}(\text{=O})\text{Cl}_3$, and at this concentration the field effect of $\text{P}(\text{=O})\text{Cl}_3$ is minimal and constant in these solvent systems. In all three solvent systems $\nu\text{P}=\text{O}$ decreases in frequency as the mole % solvent system increases. The $\text{CCl}_4/\text{C}_6\text{H}_{14}$ solvent system has the least effect upon $\nu\text{P}=\text{O}$, and $\nu\text{P}=\text{O}$ decreases as the mole % $\text{CCl}_4/\text{C}_6\text{H}_{14}$ increases. Thus, the $\nu\text{P}=\text{O}$ frequency decreases as the field effect of the solvent system increases. The same trend is noted for the $\text{C}_6\text{H}_{14}/\text{CHCl}_3$ and $\text{CHCl}_3/\text{CCl}_4$ solvent systems and the $\nu\text{P}=\text{O}$ frequency decreases in the order of the increased field effect of the solvent system. However, there is a distinct difference in the solvent systems containing CCl_3H . The $\nu\text{P}=\text{O}$ frequency is rapid with the first addition of CHCl_3 into the solvent system, and this is attributed to the formation of intermolecular hydrogen bonding between the CCl_3H proton and the free pair of electrons of the $\text{P}=\text{O}$ oxygen atom (viz. $\text{CCl}_3\text{H}\cdots\text{O}=\text{P}$) (26).

Figure 8.55 show a plot of $\nu\text{P}=\text{O}$ for methanephosphonic dichloride $\text{CH}_3\text{P}(\text{=O})\text{Cl}_2$ vs mole % CDCl_3 and plots of $\nu\text{P}=\text{O}$ for 1,1-dimethylethane-phosphonic dichloride vs mole % $\text{CHCl}_3/\text{CCl}_4$ and vs mole % $\text{CDCl}_3/\text{CCl}_4$. The $\nu\text{P}=\text{O}$ vibration for $(\text{CH}_3)_3\text{CP}(\text{=O})\text{Cl}_2$ occurs at lower frequency than $\nu\text{P}=\text{O}$ for $\text{CH}_3\text{P}(\text{=O})\text{Cl}_2$ at all mole % concentrations of $\text{CDCl}_3/\text{CCl}_4$. The $\text{P}=\text{O}$ group is more basic in the case of the $(\text{CH}_3)_3\text{C}$ analog than for the CH_3 analog, because the electron release of the $(\text{CH}_3)_3\text{C}$ group to the $\text{P}=\text{O}$ group is larger than that of the CH_3 group to the $\text{P}=\text{O}$ group. With the first addition of CHCl_3 or CDCl_3 to the solvent system $\nu\text{P}=\text{O}$ decreases in frequency due to intermolecular hydrogen bonding (viz. $\text{CCl}_3\text{D}\cdots\text{O}=\text{P}$) (26). In the case of $(\text{CH}_3)_3\text{CP}(\text{=O})\text{Cl}_2$ there appears to be a second break in the plot after ~ 60 mol% $\text{CDCl}_3/\text{CCl}_4$. Perhaps this is the result of a second intermolecular hydrogen bond between the CDCl_3 or CHCl_3 and the $\text{P}=\text{O}$ group (viz. $(\text{CCl}_3\text{H})_2\cdots(\text{O}=\text{P})$). The second intermolecular hydrogen bond may occur because the $\text{P}=\text{O}$ group is more basic than the $\text{P}=\text{O}$ group for $\text{CH}_3\text{P}(\text{=O})\text{Cl}_2$. This is apparently unique because the steric factor of the $(\text{CH}_3)_3\text{C}$ group is significantly larger than the steric factor for the CH_3 group.

Figure 8.56 shows plots of the $\nu\text{P}=\text{O}$ rotational conformers 1 and 2 for O-methyl phosphorodichloridate and O-ethyl phosphorodichloridate vs mole % $\text{CHCl}_3/\text{CCl}_4$ (26). Both $\nu\text{P}=\text{O}$ rotational conformers 1 and 2 decrease in frequency with the first addition of CHCl_3 , and this is attributed to intermolecular hydrogen bonding (viz. $\text{CCl}_3\text{H}\cdots\text{O}=\text{P}$)₂. The $\nu\text{P}=\text{O}$ frequency separation between rotational conformers 1 and 2 is larger in CCl_4 solution than in CHCl_3 solution, and this reflects the effect of hydrogen bonding. There appears to be a second intermolecular hydrogen bond formed in all but rotational conformer 2 for $\text{C}_2\text{H}_5\text{OP}(\text{=O})\text{Cl}_2$. In all of these plots the general decrease in the $\nu\text{P}=\text{O}$ frequencies is due to the increased field effect of the solvent system.

Figure 8.57 shows plots of $\nu\text{P}=\text{O}$ rotational conformers 1 and 2 for trimethyl phosphate vs mole % $\text{CHCl}_3/\text{CCl}_4$. The IR band in the range 1273.4 cm^{-1} through 1289.9 cm^{-1} is assigned to $\nu\text{P}=\text{O}$ rotational conformer 1, and the IR band in the range 1258 cm^{-1} through 1270.9 cm^{-1} is assigned to $\nu\text{P}=\text{O}$ rotational conformer 2. Complexes such as $\text{CCl}_3\text{H}\cdots\text{O}=\text{P}$ and $(\text{CCl}_3\text{H}\cdots)_2\text{O}=\text{P}$ are apparently formed between solute and solvent.

Figures 8.58 and 8.59 show plots of $\nu\text{P}=\text{O}$ conformers 1 and 2 for triethyl phosphate and tributyl phosphate, respectively. The apparent decrease in the $\nu\text{P}=\text{O}$ frequencies for rotational

conformers 1 and 2 reflects the initial intermolecular hydrogen-bond formation. As the mole % $\text{CHCl}_3/\text{CCl}_4$ is increased $\nu\text{P}=\text{O}$ for the rotational conformer increases in frequency for both $(\text{C}_2\text{H}_5\text{-O})_3\text{P}=\text{O}$ and $(\text{C}_4\text{H}_9\text{O})_3\text{P}=\text{O}$ while rotational conformer 1 for $(\text{C}_4\text{H}_9\text{O})_3\text{P}=\text{O}$ remains relatively constant. These data suggest that as the alkyl group becomes larger it sterically shields the $\text{P}=\text{O}$ group from the solvent field effect. Thus, the $\nu\text{P}=\text{O}$ frequencies are not continually lowered in frequency due to the field effect of the solvent system.

PCl_3 AND PCl_2 VIBRATIONS

Figures 8.60 through 8.62 show plots of ν asym. PCl_3 or ν asym. PCl_2 vs mole % solvent system for $\text{P}(\text{=O})\text{Cl}_3$, $\text{CH}_3\text{P}(\text{=O})\text{Cl}_2$, $(\text{CH}_3)_3\text{CP}(\text{=O})\text{Cl}_2$, and $(\text{RO})\text{P}(\text{=O})\text{Cl}_2$. In all cases, the ν asym. PCl_3 or ν sym. PCl_2 vibration increases in frequency as the mole % $\text{CCl}_4/\text{C}_6\text{H}_{14}$, mole % $\text{CHCl}_3/\text{C}_6\text{H}_{14}$, or $\text{CHCl}_3/\text{CCl}_4$ is increased. In the case of $(\text{CH}_3\text{O})\text{P}(\text{=O})\text{Cl}_2$ or $(\text{C}_2\text{H}_5\text{O})\text{P}(\text{=O})\text{Cl}_2$, the ν asym. PCl_2 mode is a doublet due to the presence of rotational conformers 1 and 2.

Figures 8.63–8.66 show plots of ν sym. PCl_3 or ν sym. PCl_2 for $\text{P}(\text{=O})\text{Cl}_3$, $\text{CH}_3\text{P}(\text{=O})\text{Cl}_2$, $(\text{CH}_3)_3\text{CP}(\text{=O})\text{Cl}_2$, and $(\text{RO})\text{P}(\text{=O})\text{Cl}_2$. With the exception of the solvent system $\text{CCl}_4/\text{C}_6\text{H}_{14}$, the ν sym. PCl_3 or ν sym. PCl_2 vibration increases in frequency as the mole % solvent system is increased. Therefore, both the ν sym. $\text{PCl}_{3\text{or}2}$ and ν asym. $\text{PCl}_{3\text{or}2}$ vibrations in mole % $\text{CHCl}_3/\text{CCl}_4$ solutions increase in frequency as the $\nu\text{P}=\text{O}$ vibrations decrease in frequency. Thus, as the field effect of the solvent increases, it requires more energy to vibrate these PCl_3 or PCl_2 bonds.

Figure 8.66 shows plots of ν asym. PCl_2 vs ν sym. PCl_2 for $\text{CH}_3\text{OP}(\text{=O})\text{Cl}_2$, $\text{C}_2\text{H}_5\text{OP}(\text{=O})\text{Cl}_2$, $(\text{CH}_3)_3\text{CP}(\text{=O})\text{Cl}_2$, and $\text{CH}_3\text{P}(\text{=O})\text{Cl}_2$. These plots show that ν asym. PCl_2 occurs within the range $545\text{--}615\text{ cm}^{-1}$ and that ν sym. PCl_2 occurs within the range $495\text{--}555\text{ cm}^{-1}$.

ABSORBANCE RATIOS FOR $\text{ROP}(\text{=O})\text{Cl}_2$ MOLECULES

Figures 8.67 and 8.68 show plots of the absorbance ratios $A(\text{conformer 1})/A(\text{conformer 2})$ for the $\nu\text{P}=\text{O}$, νCOP , ν asym. PCl_2 and ν sym. PCl_2 vibrations vs mole % $\text{CHCl}_3/\text{CCl}_4$ for $(\text{CH}_3\text{O})\text{P}(\text{=O})\text{Cl}_2$ and $(\text{C}_2\text{H}_5\text{O})\text{P}(\text{=O})\text{Cl}_2$, respectively. In all cases the ratio $A(\text{conformer 1})/A(\text{conformer 2})$ increases as the mole % $\text{CHCl}_3/\text{CCl}_4$ increases. These data indicate that as the field effect of the solvent system increases, the concentration of rotational conformer 1 increases while the concentration of conformer 2 decreases.

ALKYL GROUP VIBRATIONS

Figure 8.69 shows a plot of ν sym. CH_3 for $\text{CH}_3\text{P}(\text{=O})\text{Cl}_2$ vs mole % $\text{CHCl}_3/\text{CCl}_4$. This symmetric CH_3 bending vibration increases in frequency in an essentially linear manner as the mole % $\text{CHCl}_3/\text{CCl}_4$ increases. The effect is small, as the frequency difference is only $\approx 0.5\text{ cm}^{-1}$ (26).

Figure 8.70 is a plot of ρ CH₃ for CH₃P(=O)Cl₂ vs mole % CHCl₃/CCl₄. The CH₃ rocking vibration increases in frequency in a nonlinear manner as the mole % CHCl₃/CCl₄ increases. The effect is small, as the frequency difference is <0.5 cm⁻¹.

Figure 8.71 shows plots of the in-phase δ sym. (CH₃)₃ and out-of-phase δ sym. (CH₃)₃ frequencies for (CH₃)₃CP(=O)Cl₂ vs mole % CHCl₃/CCl₄. The in-phase symmetric (CH₃)₃ deformation decreases in frequency while the out-of-phase symmetric (CH₃)₃ deformation increases in frequency as the mole % CHCl₃/CCl₄ increases. These solvent effects are small because the frequency differences are ≈ 1 cm⁻¹.

Figure 8.72 shows plots of the ρ CH₃ modes for (C₂H₅O)P(=O)Cl₂ vs mole % CHCl₃/CCl₄. The a' CH₃ rocking vibration (~ 1103 cm⁻¹) decreases in frequency while the a'' CH₃ rocking vibration (~ 1165 in) increases in frequency as the mole % CHCl₃/CCl₄ increases. Figure 8.73 shows plots of ρ CH₃ modes for (C₂H₅O)₃P=O vs mole % CHCl₃/CCl₄. The a'' ρ (CH₃) mode decreases in frequency while the a' ρ CH₃ mode decreases in frequency until ~ 16 mol % CHCl₃/CCl₄, and then the frequency remains relatively constant.

THE ν C–C MODE FOR THE C₂H₅OP GROUP

Figures 8.74 and 8.75 show a plot of ν C–C for (C₂H₅O)P(=O)Cl₂ and for (C₂H₅O)₃P=O vs mole % CHCl₃/CCl₄, respectively. This plot shows that the C–C stretching vibration for the C₂H₅OP group increases in frequency as the mole % CHCl₃/CCl₄ is increased (26, 55).

THE ν COP GROUP (26, 55)

Figure 8.76 shows plots of ν C–O for the COP group of CH₃OP(=O)Cl₂ and C₂H₅OP(=O)Cl₂ vs mole % CHCl₃/CCl₄. The ν CO frequency for rotational conformer 1 of the COP group decreases in frequency as the mole % CHCl₃/CCl₄ is increased. In case of rotational conformer 2, ν C–O for CH₃OP(=O)Cl₂ increases in frequency while ν C–O for C₂H₅OP(=O)Cl₂ decreases in frequency (26, 55).

Figure 8.77 shows plots of ν P=O for rotational conformers 1 and 2 for (CH₃O)₃ P=O vs mole % CHCl₃/CCl₄. The erratic behavior of these two plots shows the effect of intermolecular hydrogen bonding upon the ν (C–O)₃ modes of the (CH₃O)₃ groups. These data suggest that the molecular configuration of the rotational conformers is changing. Figure 8.78 shows a plot of ν P–O for the (C–O)₃ P groups for (CH₃O)₃ P=O vs mole % CHCl₃/CCl₄. The ν P(–O)₃ vibrations first decrease in frequency and then increase in frequency as the mole % CHCl₃/CCl₄ is increased. These data indicate that the rotational configuration of the rotational conformers is changing as the mole % CHCl₃/CCl₄ is increased.

Figures 8.79 and 8.80 show plots of ν ϕ -O and ν O–P for the ϕ -O–P groups of (C₆H₅O)₃P=O vs mole % CHCl₃/CCl₄, respectively. These plots show that as ν Φ -O decreases in frequency, ν P–O increases in frequency to a point in the range near 50 mol % CHCl₃/CCl₄. At higher mole % CHCl₃/CCl₄ concentrations, ν ϕ -O increases in frequency while ν P–O decreases in frequency. These plots indicate that the rotational conformers are changing as the mole % CHCl₃/CCl₄ is increased.

Figure 8.81 shows plots of ν P=O rotational conformers 1 and 2 for triphenyl phosphate. Both ν P=O rotational conformers decrease in frequency as the mole % $\text{CHCl}_3/\text{CCl}_4$ is increased. Figure 8.82 shows a plot of the absorbance ratio $A(\nu \text{P=O, conformer 1})/A(\nu \text{P=O, conformer 2})$ for triphenyl phosphate vs mole % $\text{CHCl}_3/\text{CCl}_4$. A break is noted in the plot near 10 mol % $\text{CHCl}_3/\text{CCl}_4$ in Figure 8.8, which corresponds to the break in the plot of ν P=O, conformer 1. This break is attributed to the formation of the intermolecular hydrogen bond for rotational conformer 1. The absorbance ratio decreases as the mole % $\text{CHCl}_3/\text{CCl}_4$ is increased, which shows that the concentration of conformer 2 increases while the concentration of conformer 1 decreases (see Figure 8.82).

Figure 8.83 shows a plot of the in-plane hydrogen deformation for the phenyl groups of triphenyl phosphate vs mole % $\text{CHCl}_3/\text{CCl}_4$. This vibration increases in frequency at a more rapid rate below 10 mol % $\text{CHCl}_3/\text{CCl}_4$ with the formation of the intermolecular hydrogen bonds, and then increases in a linear manner as the mol % $\text{CHCl}_3/\text{CCl}_4$ is increased.

Figure 8.84 shows a plot of the out-of-plane ring deformations for the phenyl groups of triphenyl phosphate vs mole % $\text{CHCl}_3/\text{CCl}_4$. This out-of-plane ring deformation increases in frequency as the field effect of the solvent system increases.

ν C–D FOR CDCl_3 IN CCl_4 SOLUTIONS

Figure 8.85 shows a plot of ν C–D for CDCl_3 vs mole % $\text{CDCl}_3/\text{CCl}_4$. This plot shows that ν C–D increases in frequency as the mole % $\text{CDCl}_3/\text{CCl}_4$ is increased in essentially a linear manner (55). The ν C–D frequency decreases as the concentration of CCl_4 is increased. The Cl atoms of CCl_4 are more basic than the Cl atoms of CDCl_3 . Thus, ν C–D of CDCl_3 decreases as the surrounding field of CCl_4 molecules is increased in the $\text{CCl}_3\text{-D}:\text{CCl}_4$ equilibrium.

Figure 8.86 shows a plot of ν C–D for CDCl_3 containing 1 % wt./vol. triethyl phosphate in $\text{CDCl}_3/\text{CCl}_4$ solutions. In this case ν C–D does not decrease in a linear manner as the mole % $\text{CDCl}_3/\text{CCl}_4$ is increased. The more rapid decrease in the ν C–D frequency at lower mole % $\text{CDCl}_3/\text{CCl}_4$ concentrations is due to intermolecular hydrogen bonding with $(\text{CH}_3\text{O})_3\text{P=O}$ molecules in conjunction with competing intermolecular hydrogen bonding with CCl_4 molecules. Thus, in all cases of $\text{CHCl}_3/\text{CCl}_4$ there is an equilibrium of $(\text{CCl}_3\text{H})_n \cdots (\text{ClCCl}_3)_m$ with intermolecular hydrogen bonding with solute molecules.

For further discussion of solvent effects on phosphorus compounds the reader is referred to References 26 and 55.

REFERENCE SPECTRA

Reference IR and Raman spectra are available for identification of unknown samples containing phosphorus. These spectra are available in references such as 48–51, or from the Sadler Research Laboratories. The book *Analytical Chemistry of Phosphorus Compounds* is an excellent source for other techniques required for the solution of chemical problems involving phosphorus derivatives (50).

REFERENCES

1. Wilson, M. K. and Polo, S. R. (1952) *J. Chem. Phys.* **20**: 16.
2. Delwaulle, M. L. and Francois, F. (1949) *J. Chem. Phys.* **46**: 87.
3. Gutowsky, H. S. and Liehr, A. D. (1952). *J. Chem. Phys.* **20**: 1652.
4. Wilson, M. K. and Polo, S. R. (1953) *J. Chem. Phys.* **21**: 1426.
5. Eucken, A., Hellwege, K. H. and Landolt-Bornstein, I. (1951). *Band, Atomic Und Molekulorphsk. 2 Terl, Molekeln I.* Berlin: Springer-Verlag, p. 247.
6. Stammereich, H., Foreris, R. and Tavares, Y. (1956). *J. Chem. Phys.* **25**: 580.
7. Durig, J. R. and Clark, J. W. (1967) *J. Chem. Phys.* **46**: 3057.
8. Delwaulle, M. L. and Francois, F. (1946) *Comp. Rend.* **22**: 550.
9. Nyquist, R. A., (1967) *Spectrochim. Acta.* **23A**: 845.
10. Gerding, H. and Westrick, R. (1942). *Rec. Trav. Chem.* **61**: 842.
11. Durig, J. R. and Clark, J. W. (1967) *J. Chem. Phys.* **46**: 3057.
12. Delwaulle, M. L. and Francois, F. (1948). *Comp. Rend.* **226**: 894.
13. Delwaulle, M. L. and Francois, F. (1946). *Comp. Rend.* **22**: 550.
14. Eucken, A., Hellewege, K. H. and Landolt-Bornstein, I. (1951). *Band, Atomic Und Moleknlorphsk. 32 Terl. Molcheln I.* Berlin: Springer-Verlage, p. 278.
15. Delwaulle, M. L. and Francois, F. (1945) *Comp. Rend.* **220**: 817.
16. Nyquist, R. A. (1987). *Appl. Spectrosc.* **41**: 272.
17. Nyquist, R. A. (1968). *Appl. Spectrosc.* **22**: 452.
18. Durig, J. R., Black, F. and Levin, J. W. (1965). *Spectrochim. Acta* **21**: 1105.
19. Durig, J. and Di Yorio, J. (1960) *Chem. Phys.* **48**: 4154.
20. The Dow Chemical Company Data in CS₂ solution.
21. Nyquist, R. A. and Muelder, W. W. (1966) *Spectrochem. Acta.* **22**: 1563.
22. Nyquist, R. A., Muelder, W. W. and Wass, M. N. (1970). *Spectrochim. Acta* **26A**: 769.
23. Nyquist, R. A. (1971). *Spectrochim. Acta* **27A**: 697.
24. Nyquist, R. A., Wass, M. N. and Muelder, W. W. (1970). *Spectrochim. Acta* **26A**: 611.
25. Nyquist, R. A. (1967). *Spectrochim. Acta* **23A**: 1499.
26. Nyquist, R. A. and Puehl, C. W. (1999). *Appl. Spectrosc.* **46**: 1552; Mortimer, F. S. (1957). *Spectrochim. Acta.* **9**: 270.
27. Nyquist, R. A. and Muelder, W. W. (1968) *Spectrochim. Acta* **24A**: 187.
28. Dow Chemical Company data in CCl₄ solution.
29. Taft, R. W. (ed.). (1976). *Progress in Physical Organic Chemistry*, Vol. 12, New York: John Wiley & Sons, p. 74.
30. Thomas, L. C. and Chittenden, R. A. (1964). *Spectrochim. Acta* **20**: 489.
31. Nyquist, R. A., Sloane, H. J., Dunbar, J. E. and Stycker, S. J. (1966). *Appl. Spectrosc.* **20**: 90.
32. Nyquist, R. A. (1969). *Spectrochim. Acta* **25A**: 47.
33. Durig, J. R. and Clark, J. W. (1967) *J. Chem. Phys.* **46**: 3057.
34. Delwaulle, M. L. and Francois, F. (1946). *Comp. Rend.* **22**: 550.
35. Nyquist, R. A. and Muelder, W. W. (1968). *J. Mol. Structure* **2**: 465.
36. Nyquist, R. A. (1966) *Spectrochim. Acta* **22**: 1315.
37. Nyquist, R. A., Blair, E. H. and Osborne, D. W. (1967) *Spectrochim. Acta* **23A**: 2505.
38. Herrail, F. (1965). *Comp. Rend.* **261**: 3375.
39. Neely, W. B., Unger, I., Blair, E. H. and Nyquist, R. A. (1964). *Biochemistry* **3**: 1477.
40. Nyquist, R. A. (1968) *J. Mol. Structure* **2**: 123.
41. Nyquist, R. A., (1968) *J. Mol. Structure* **2**: 111.

42. Nyquist, R. A. (1963) *Spectrochim. Acta* **19**: 713.
43. Nyquist, R. A. and Muelder, W. W. (1971). *Appl. Spectrosc.* **25**: 449.
44. Tsubio, M. (1957). *J. Amer. Chem. Soc.* **79**: 1351.
45. Herzberg, G. (1945). *Infrared and Raman Spectra of Polyatomic Molecules*. New York: Van Nostrand.
46. Corbridge, D. E.C. (1969). *Topics in Phosphorus Chemistry*, Vol. 6, M. Grayson and E. J. Griffiths, eds, *The Infrared Spectra of Phosphorus Compounds*. New York: Interscience, p. 235.
47. King, S. T. and Nyquist, R. A. (1970). *Spectrochim. Acta* **26A**: 1481.
48. Nyquist, R. A. and Craver, C. D. (1977). In *The Coblenz Society Desk Book of Infrared Spectra*. (C. D. Craver, ed.), Kirkwood, MO: The Coblenz Society.
49. Lin-Vien, D., Cotthup, N. B., Fateley, W. C. and Grasselli, J. G. (1991). *The Handbook of Infrared and Raman Characteristic Frequencies of Organic Molecules*. San Diego, CA: Academic Press, Inc.
50. Nyquist, R. A. and Potts, Jr., W. J. (1972). Vibrational Spectroscopy of Phosphorus Compounds, Ch. 5, in *Analytical Chemistry of Phosphorus Compounds*. Vol. 37, M. Halmann, ed., New York: Wiley-Interscience.
51. Nyquist, R. A., Putzig, C. L., Leugers, M. A. and Kagel, R. O. (1997). *Handbook of Infrared and Raman Spectra of Inorganic Compounds and Organic Salts*. Vols. 1–4, San Diego: Academic Press.
52. Nyquist, R. A. (1970) *Spectrochim. Acta* **26A**: 849.
53. Bouquet, S. and Bigorne, M. (1967). *Spectrochim. Acta* **23A**: 1231.
54. Daasch, L. W. and Smith, D. C. (1951). *J. Chem. Phys.* **19**: 22.
55. Nyquist, R. A. and Puehl, C. W. (1992). *Appl. Spectrosc.* **46**: 1564.

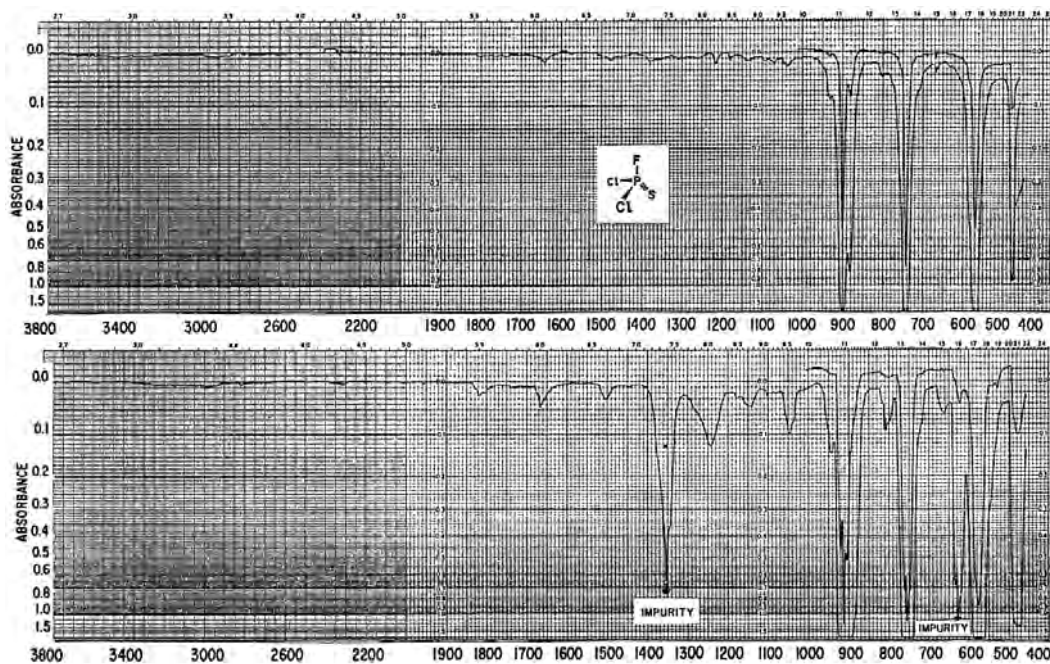


FIGURE 8.1 Top: Infrared spectrum of thiophosphoryl dichloride fluoride 10% wt./vol. in CCl_4 solution ($3800\text{--}1333\text{ cm}^{-1}$) and 10% wt./vol. in CS_2 solution. Bottom: Vapor-phase spectrum of thiophosphoryl dichloride fluoride in the region $3800\text{--}450\text{ cm}^{-1}$ (9).

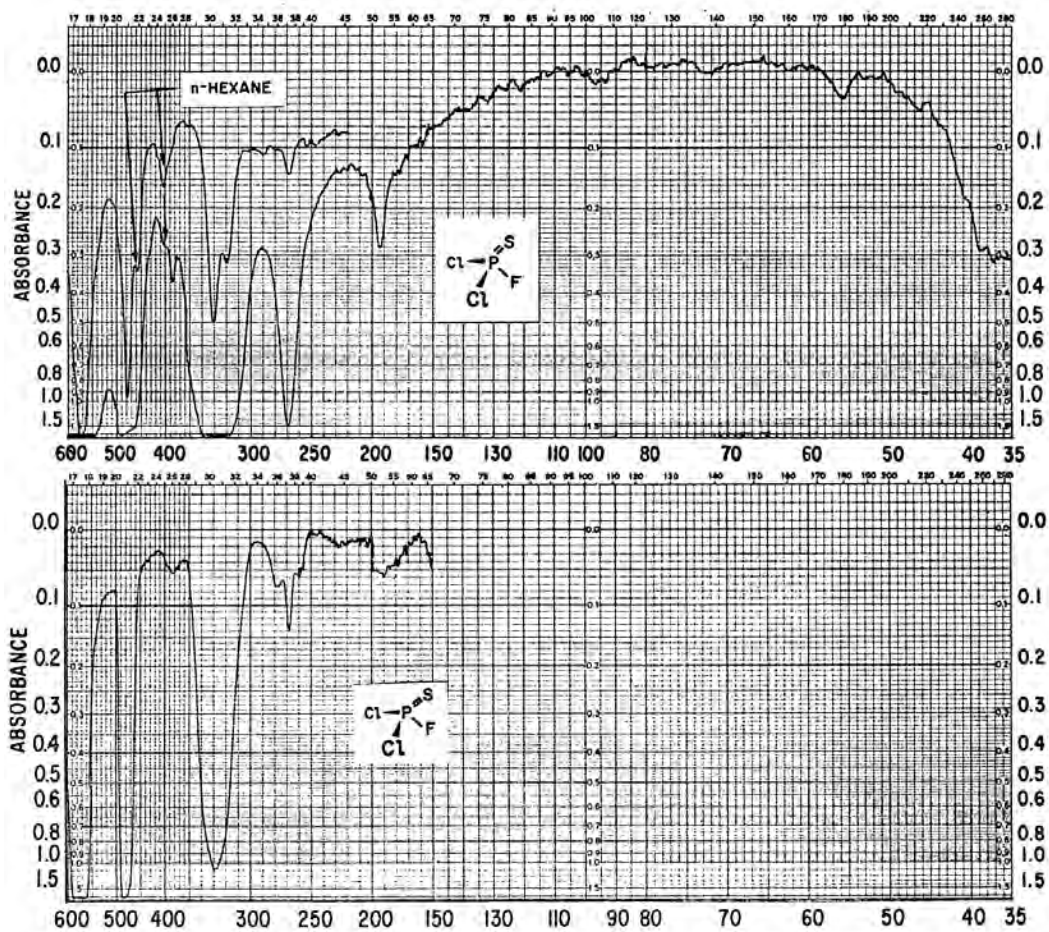


FIGURE 8.2 Top: Infrared spectrum of thiophosphoryl dichloride fluoride in hexane solution using polyethylene windows in the region $600\text{--}40\text{ cm}^{-1}$. Bottom: Vapor-phase IR spectrum of thiophosphoryl dichloride fluoride using polyethylene windows in the region $600\text{--}150\text{ cm}^{-1}$ (9).

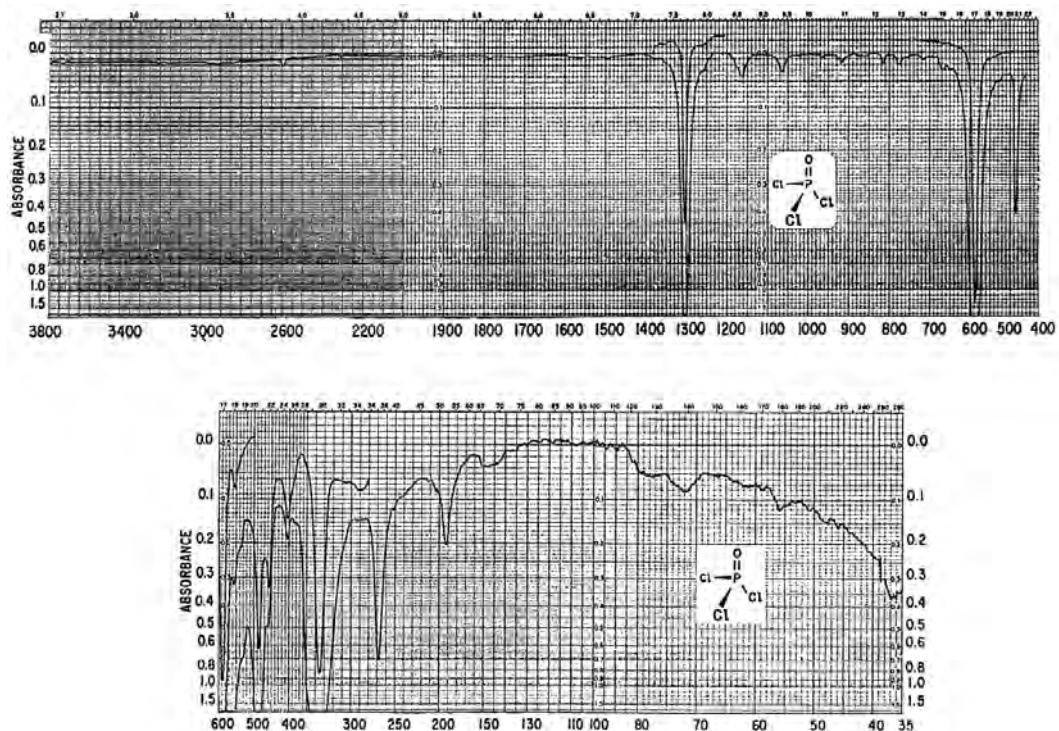


FIGURE 8.3 Top: Infrared spectrum of phosphoryl chloride in CCl_4 solution ($3800\text{--}1333\text{ cm}^{-1}$) and in CS_2 solution ($1333\text{--}45\text{ cm}^{-1}$). Bottom: Infrared spectrum of phosphoryl chloride in hexane solution (9).

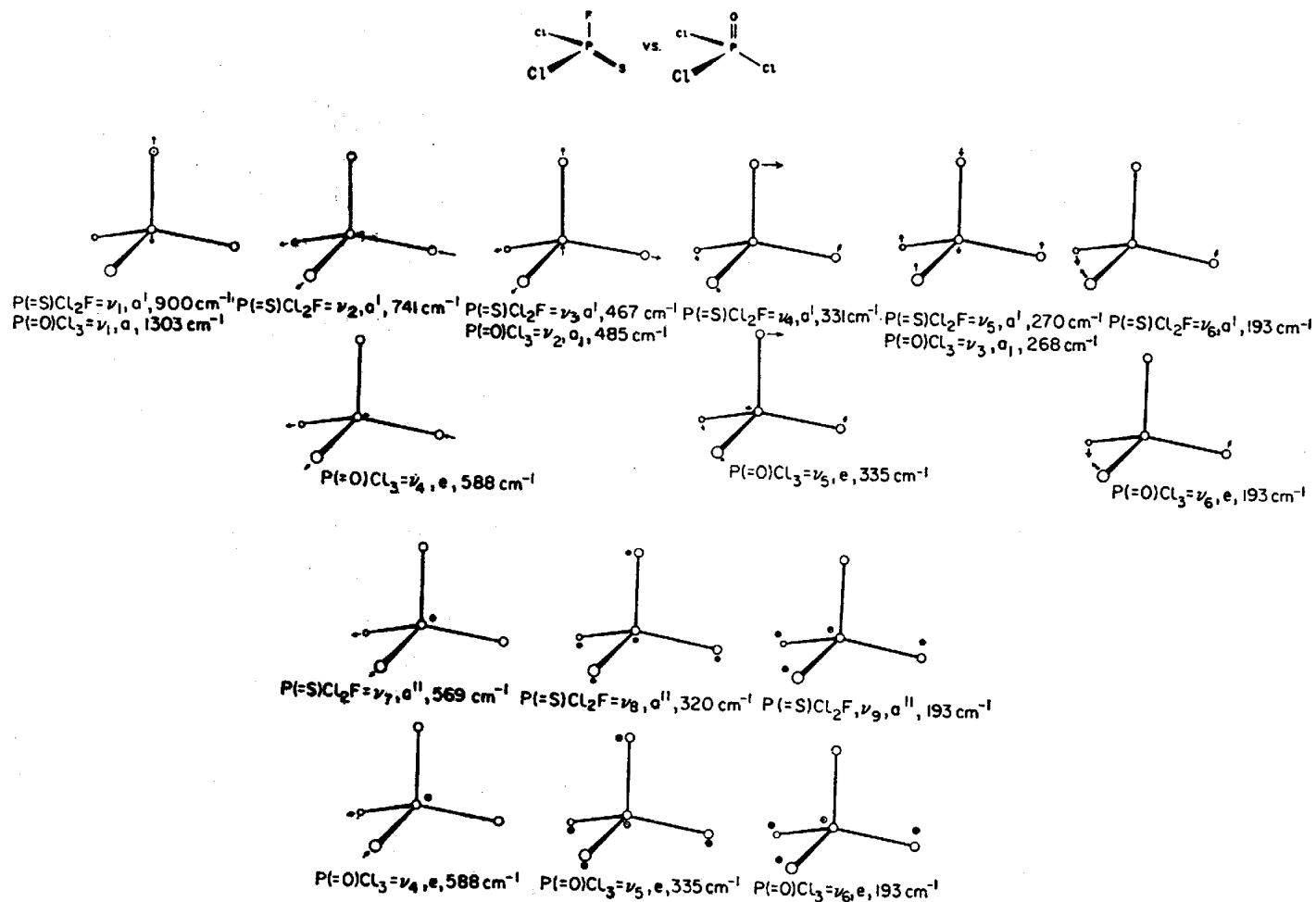


FIGURE 8.4 A comparison of the approximate normal vibrations of thiophosphoryl dichloride fluoride vs those for phosphoryl chloride (9).

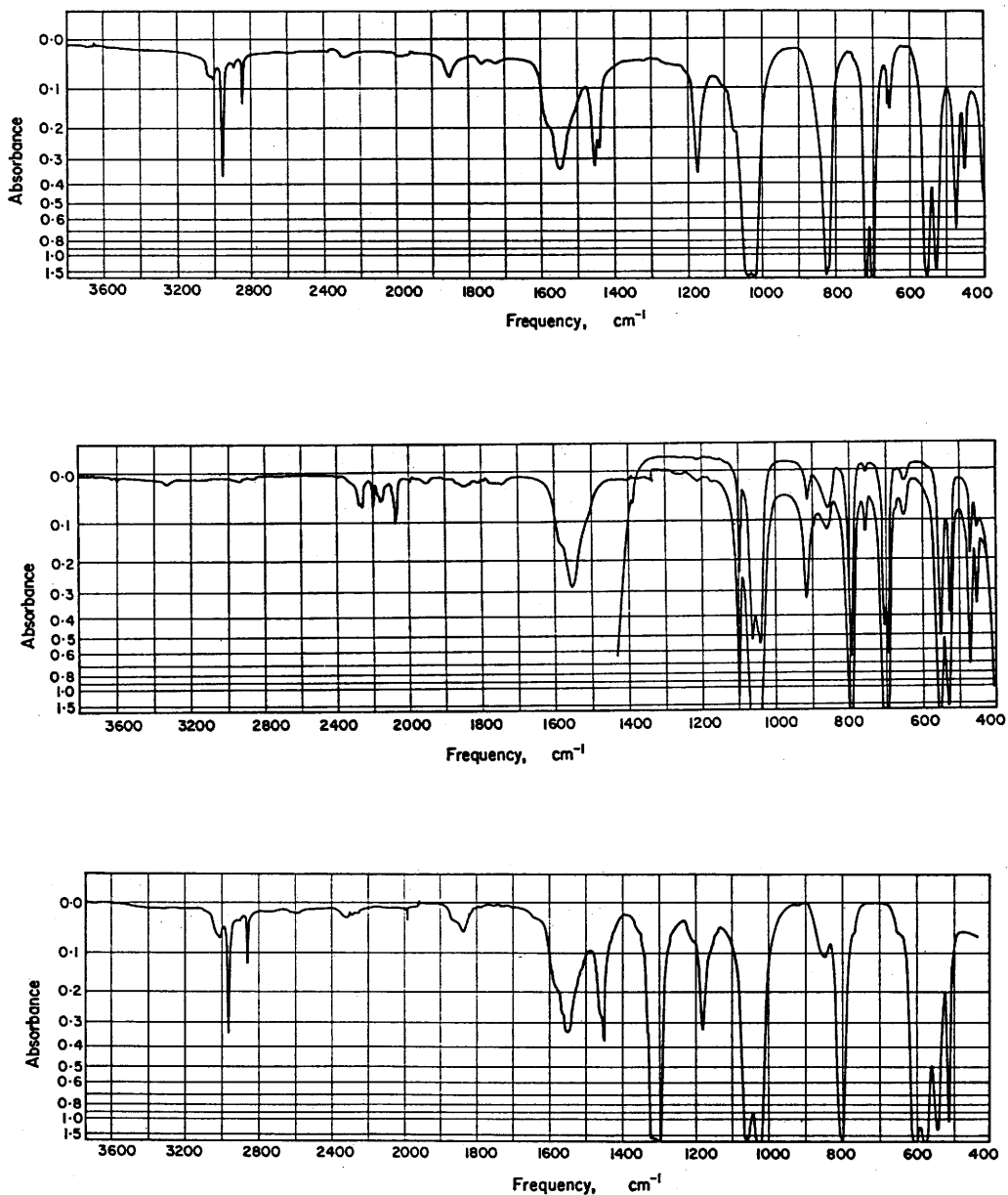


FIGURE 8.5 Top: Infrared spectrum of O-methyl phosphorodichloridothioate in 10 wt./vol. % in CCl₄ solution (3800–1333 cm⁻¹) and in 10 wt./vol. % in CS₂ solution (1333–400 cm⁻¹) using 0.1-mm KBr cells. The weak band at ~752 cm⁻¹ is due to the presence of a trace amount of P(=S)Cl₃. The band at 659 cm⁻¹ is due to the presence of ~4% O,O-dimethyl phosphorochloridothioate. Middle: Infrared spectrum of O-methyl-d₃ phosphorodichloridothioate in 10 wt./vol. % in CCl₄ solution (3800–1333 cm⁻¹) and 10 + 2 wt./vol. % in CS₂ solution (1333–400 cm⁻¹) using 0.1-mm KBr cells. Bottom: Infrared spectrum of O-methyl phosphorodichloridate in 10 wt./vol. % in CCl₄ solution (3800–1333 cm⁻¹) and 10 wt./vol. % in CS₂ solution (1333–450 cm⁻¹) using 0.1-mm KBr cells (21).

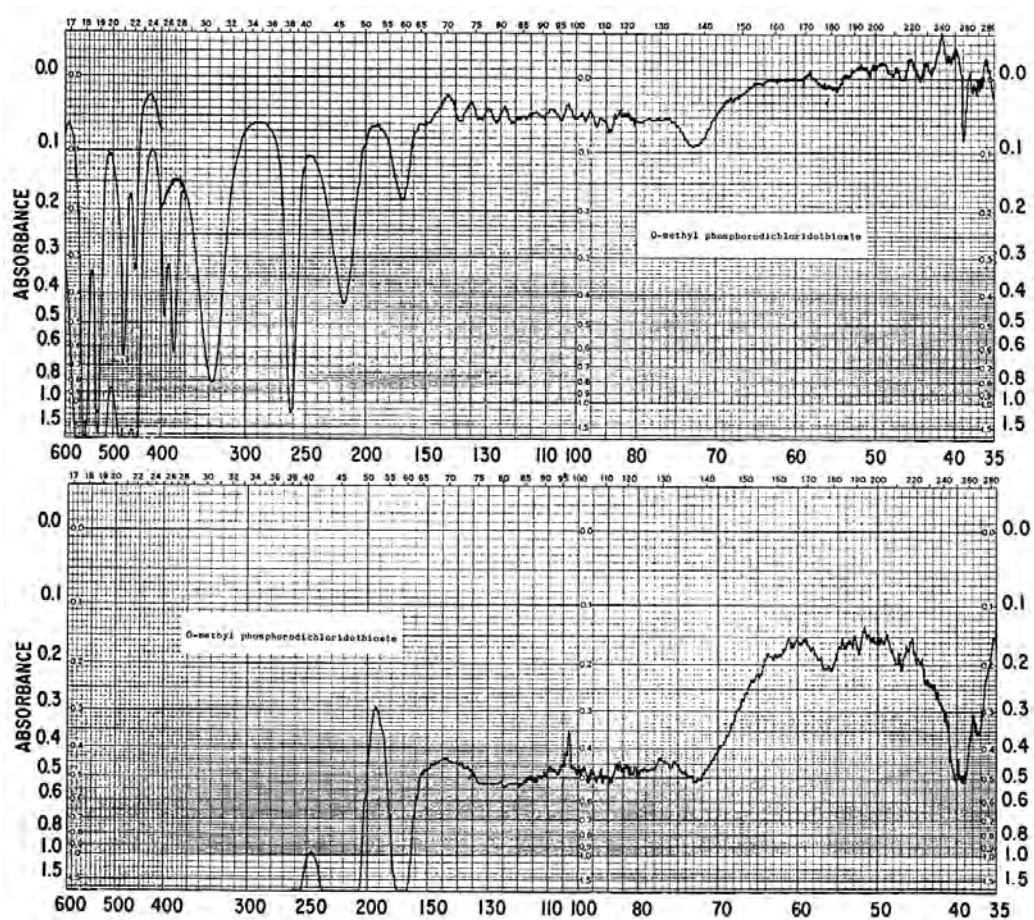


FIGURE 8.6 Top: Infrared spectrum of O-methyl phosphorodichloridothioate in 10 wt./vol. % in hexane solution in a 1-mm polyethylene cell. Bottom: Infrared spectrum of O-methyl phosphorodichloridothioate in 25 wt./vol. % in hexane solution in a 2-mm polyethylene cell (25).

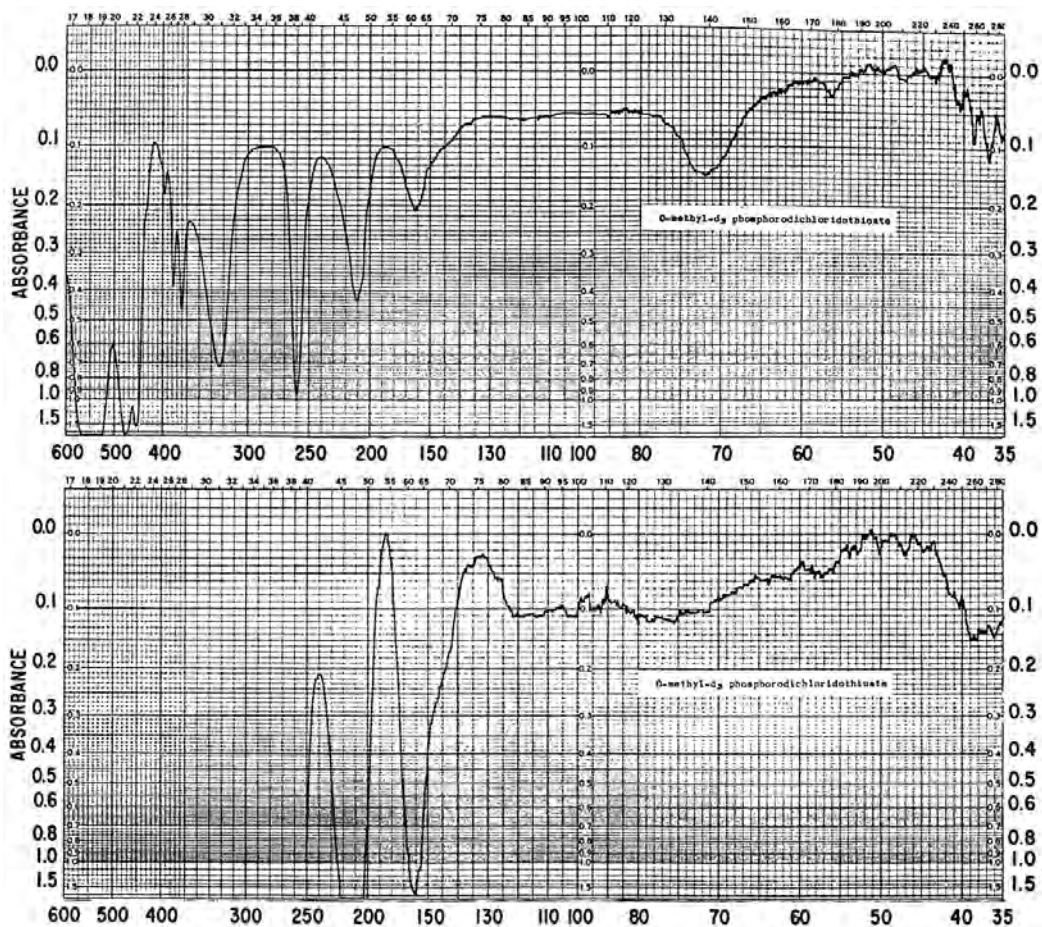


FIGURE 8.7 Top: Infrared spectrum of O-methyl-d₃ phosphorodichloridothioate in 10 wt./vol. % hexane solution in a 1-mm polyethylene cell. Bottom: Infrared spectrum of O-methyl-d₃ phosphorodichloridothioate in 25 wt./vol. % hexane solution in a 2-mm polyethylene cell and compensated with polyethylene (25).

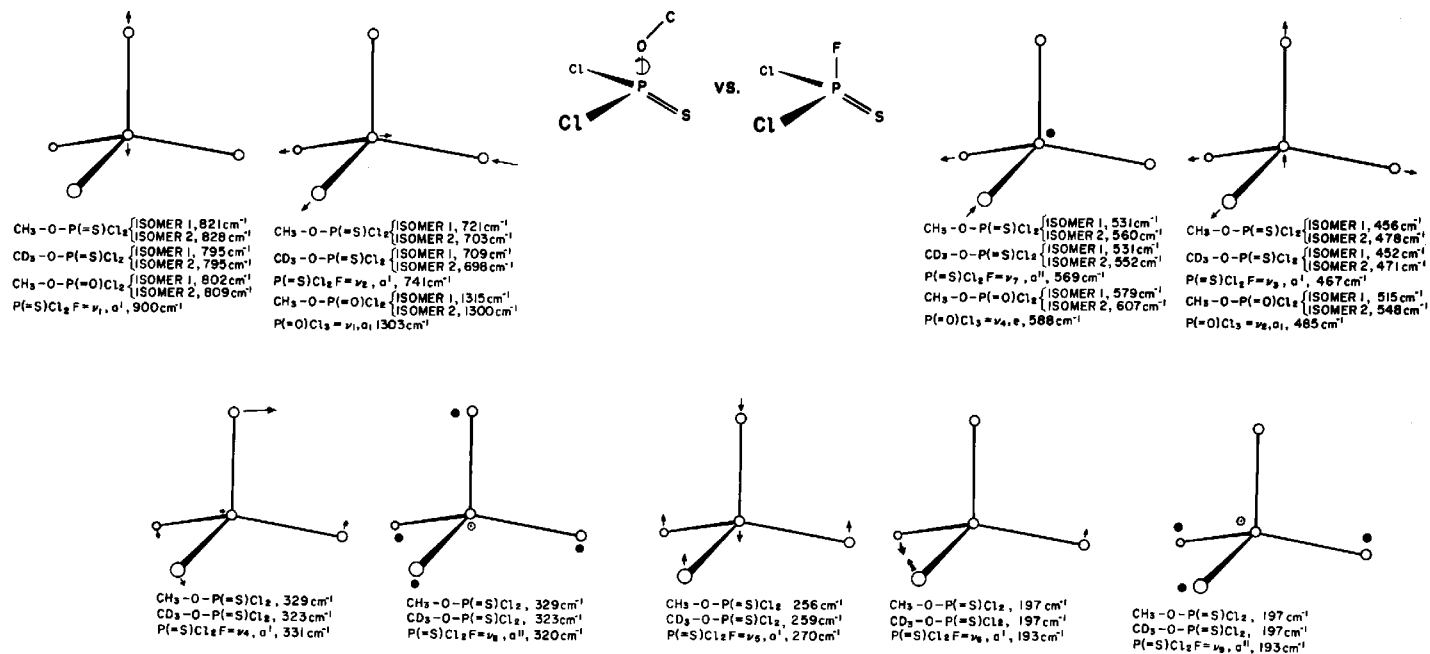


FIGURE 8.8 Assumed normal vibrations of organophosphorus and inorganic phosphorus compounds (25).

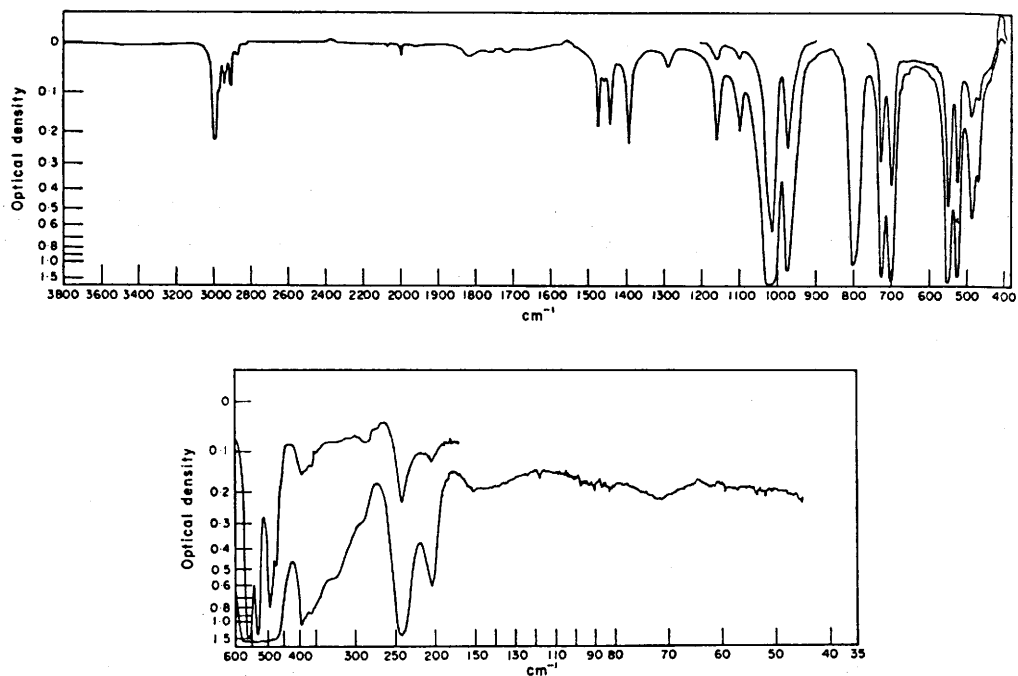


FIGURE 8.9 Top: Infrared spectrum of O-ethyl phosphorodichlorodithioate 10 wt./vol. % in CCl_4 solution ($3800\text{--}1333\text{ cm}^{-1}$) and 10 and 2 wt./vol. % in CS_2 solution ($1333\text{--}400\text{ cm}^{-1}$) in 0.1-mm KBr cells. The solvents were compensated. Bottom: Infrared spectrum of O-ethyl phosphorodichlorodithioate in 25 and 2 wt./vol. % in hexane solution ($600\text{--}45\text{ cm}^{-1}$) in a 1-mm polyethylene cell (22).

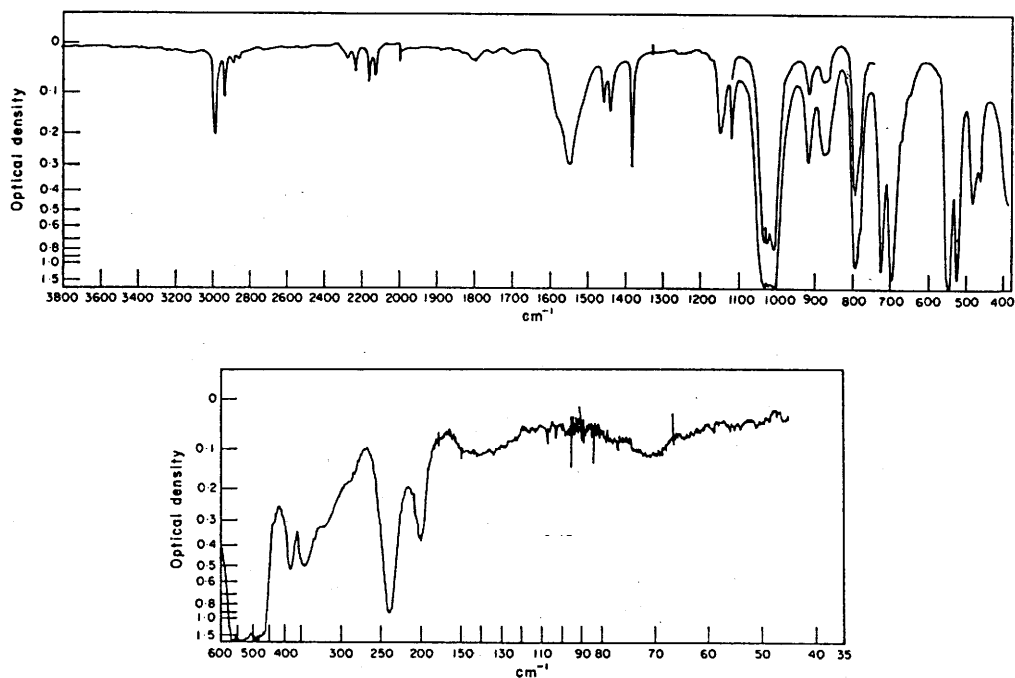


FIGURE 8.10 Top: Infrared spectrum of O-ethyl-1,1-d₂ phosphorodichloridothioate in 10 wt./vol. % in CCl₄ solution (3800–1333 cm^{-1}) and 10 and 2.5 wt./vol. % in CS₂ solution (1333–400 cm^{-1}) in 0.1-mm KBr cells. The solvents are compensated. Bottom: Infrared spectrum of O-ethyl-1,1-d₂ phosphorodichloridothioate in 10 wt./vol. hexane solution (600–45 cm^{-1}) in a 1-mm polyethylene cell (22).

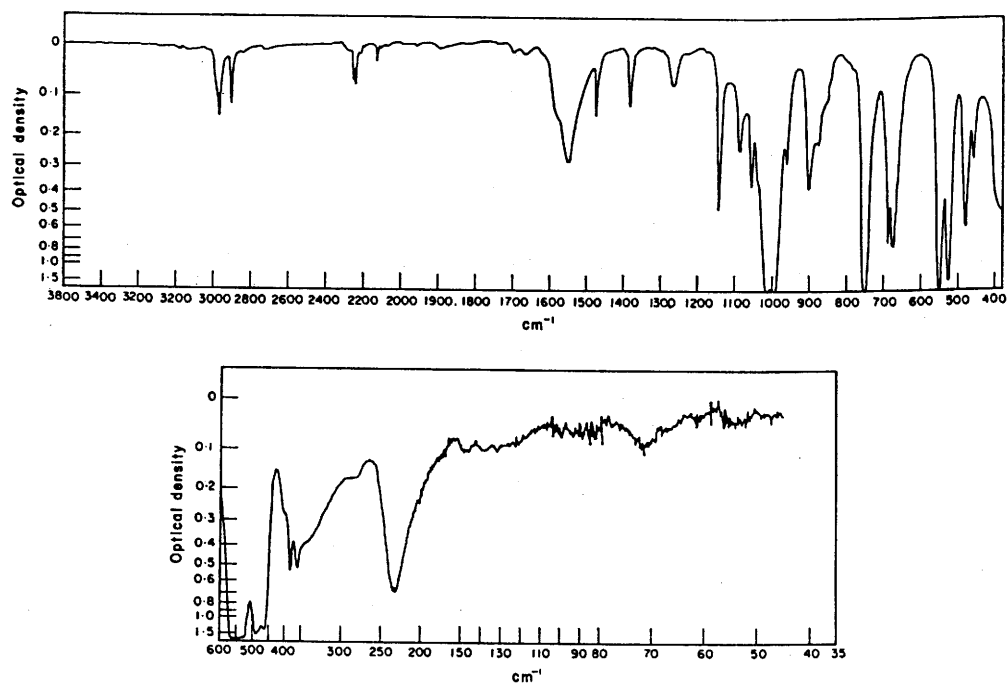


FIGURE 8.11 Top: Infrared spectrum of O-ethyl-2,2,2-d₃ phosphorodichloridothioate in 10 wt./vol. % CCl₄ solution (3800–1333 cm⁻¹) and 10 wt./vol. % CS₂ solution (1333–400 cm⁻¹) in 0.1-mm KBr cells. The solvents are not compensated. Bottom: Infrared spectrum of O-ethyl-2,2,2-d₃ phosphorodichloridothioate in 10 wt./vol. hexane solution in a 1-mm polyethylene cell (22).

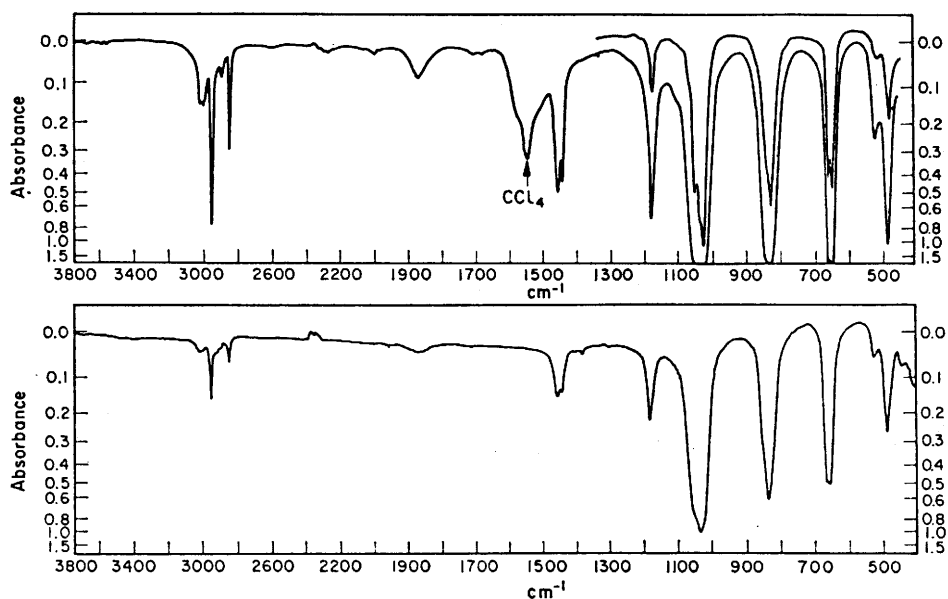


FIGURE 8.12 Top: Infrared spectrum of O,O-dimethyl phosphorochloridothioate in 10 wt./vol. % in CCl_4 solution ($3800\text{--}1333\text{ cm}^{-1}$) and 10 and 2 wt./vol. % in CS_2 solution ($1333\text{--}450\text{ cm}^{-1}$) in 0.1-mm KBr cells. The solvents have not been compensated. Bottom: Liquid-phase IR spectrum of O,O-dimethyl phosphorochloridothioate between KBr plates (27).

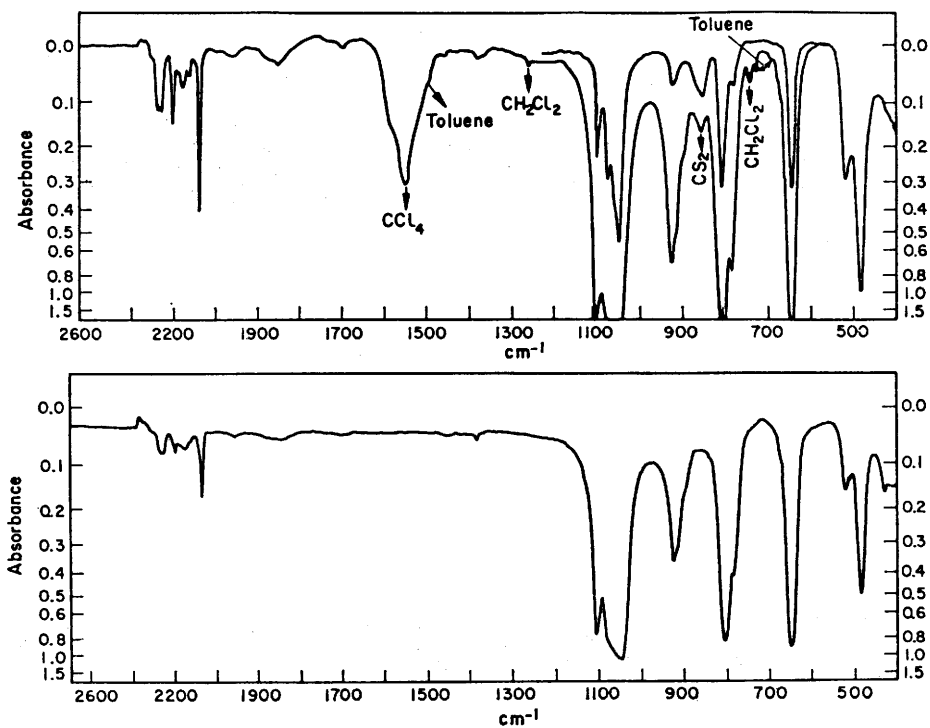


FIGURE 8.13 Top: Infrared spectrum of O,O-dimethyl- d_6 phosphorochloridothioate in 10 wt./vol. % in CCl_4 solution ($3800\text{--}1333\text{ cm}^{-1}$) and 10 and 1 wt./vol. % in CS_2 solution ($1333\text{--}400\text{ cm}^{-1}$) in 0.1-mm KBr cells. Traces of toluene and methylene chloride are present. Bottom: Liquid-phase IR spectrum of O,O-dimethyl- d_6 phosphorochloridothioate between KBr plates (27).

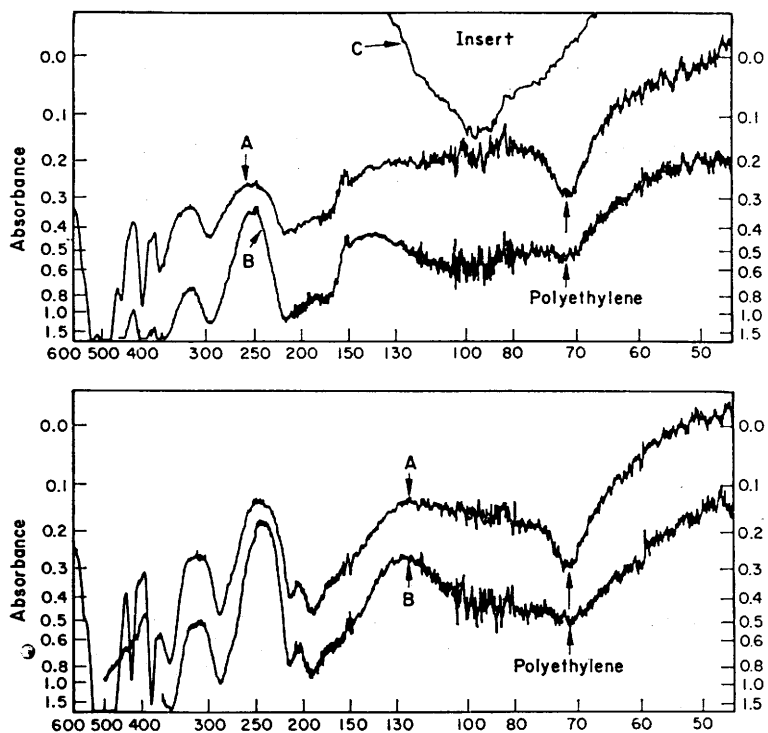


FIGURE 8.14 Top: Infrared spectrum of O,O-dimethyl phosphorochloridothioate in 2-mm polyethylene cells. The polyethylene has been compensated. Bottom: Infrared spectrum of O,O-dimethyl-d₆ phosphorochloridothioate in 10 wt./vol. % n-hexane in 1- and 2-mm polyethylene cells, respectively (27).

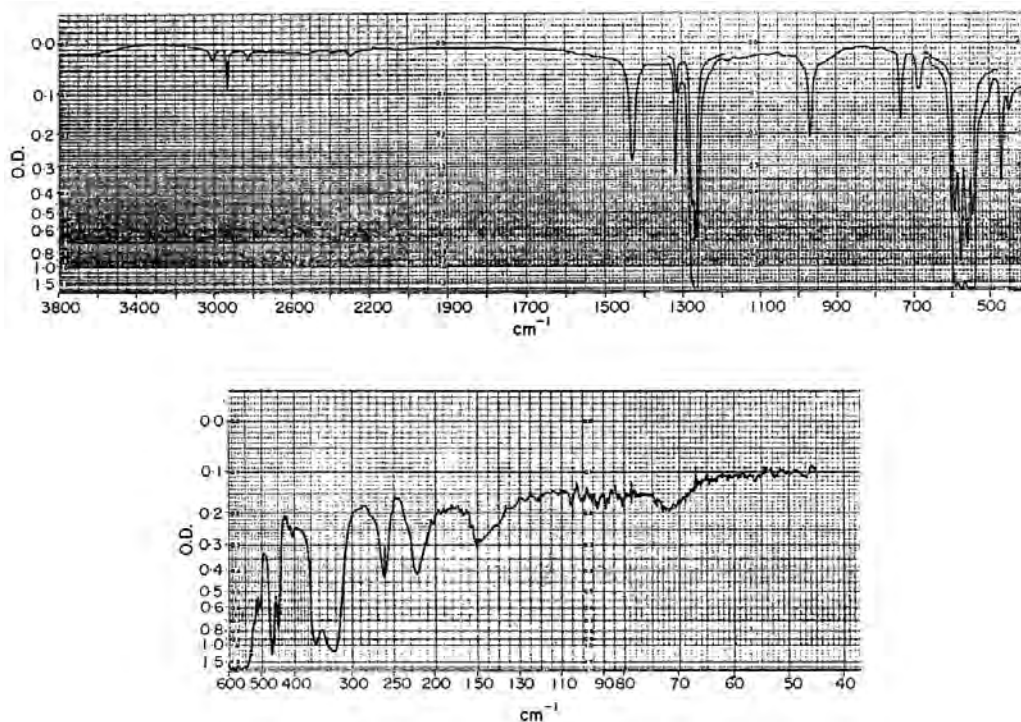


FIGURE 8.15 Top: Infrared spectrum of *S*-methyl phosphorodichloridothioate in 10 wt./vol. % in CCl_4 solution ($3800\text{--}1333\text{ cm}^{-1}$) and in 10 and 2 wt./vol. % in CS_2 solution ($1333\text{--}400\text{ cm}^{-1}$) in 0.1-mm KBr cells. Bottom: Infrared liquid phase spectrum of *S*-methyl phosphorodichloridothioate in 10 wt./vol. % hexane solution ($600\text{--}45\text{ cm}^{-1}$) in a 1-mm polyethylene cell (23).

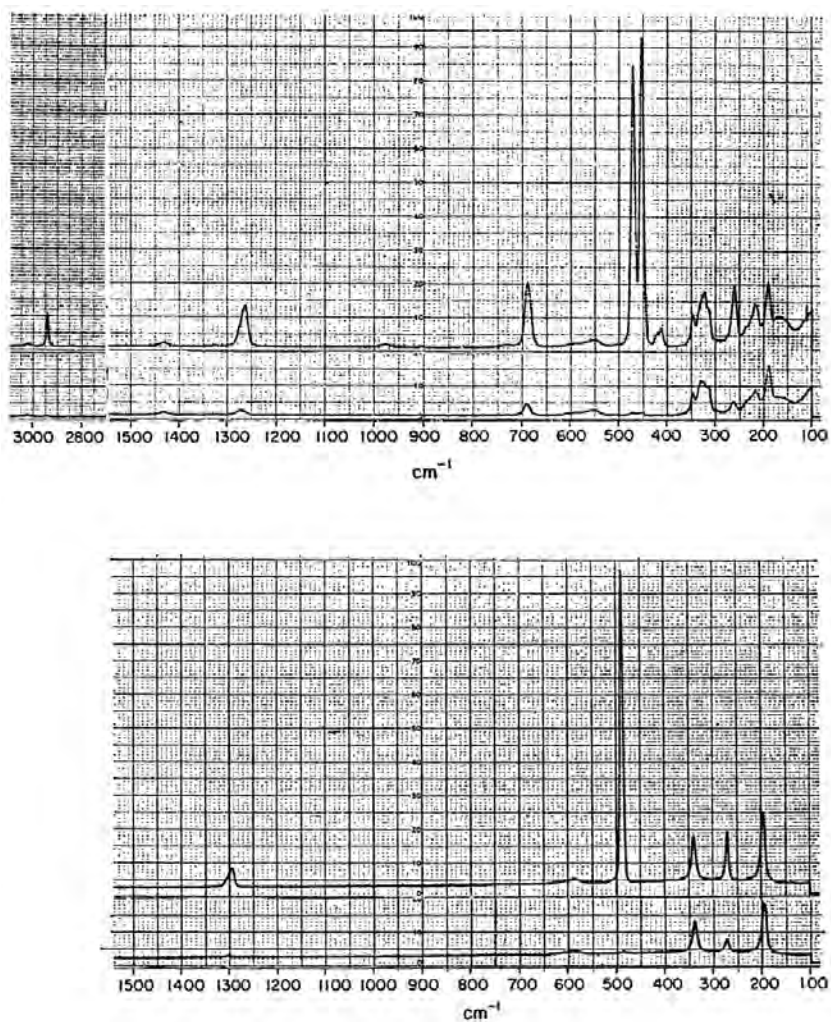


FIGURE 8.16 Top: upper: Raman liquid-phase spectrum of S-methyl phosphorodichloridothioate. Lower: Polarized Raman liquid-phase spectrum of S-methyl phosphorodichloridothioate (23). Bottom upper: Raman liquid-phase spectrum of phosphoryl chloride. Lower: Polarized Raman spectrum of phosphoryl chloride (23).

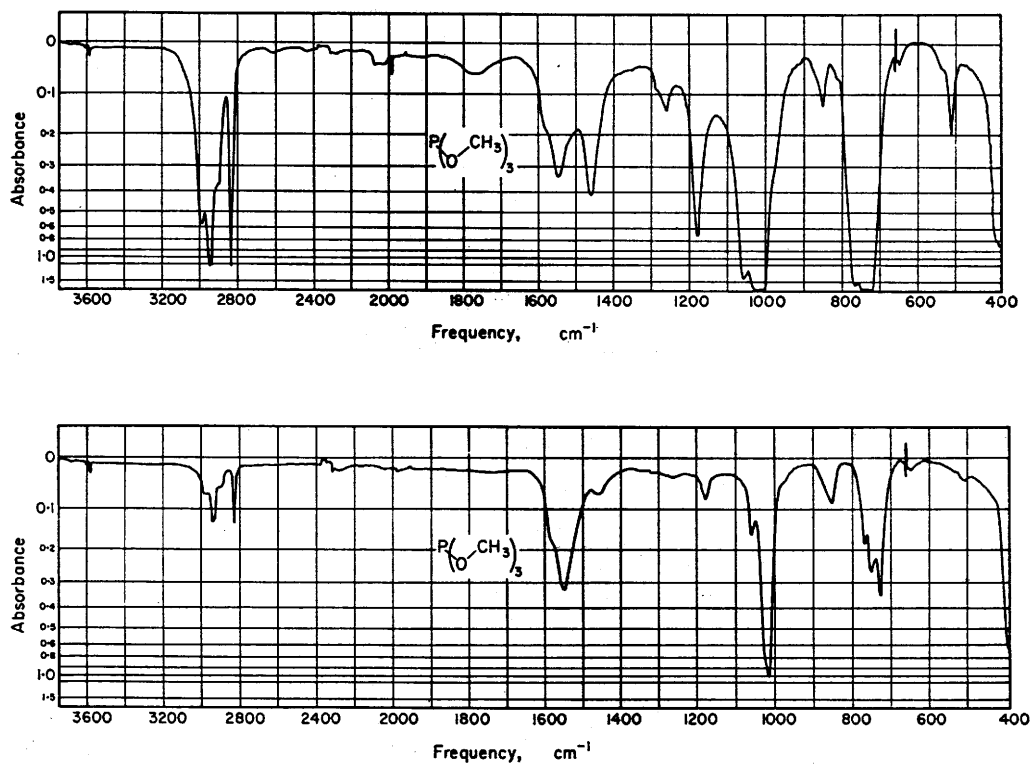


FIGURE 8.17 Top: Infrared spectrum of trimethyl phosphite 10 wt./vol. % in CCl₄ solution (3800–1333 cm⁻¹) and 10 wt./vol. % in CS₂ solution (1333–400 cm⁻¹) in 0.1-mm KBr cells. The solvents have not been compensated. Bottom: Infrared spectrum of trimethyl phosphite in 1 wt./vol. % CCl₄ solution (3800–1333 cm⁻¹) and in 1 wt./vol. % CS₂ solution (1333–400 cm⁻¹) using 0.1-mm KBr cells. The solvents have not been compensated (36).

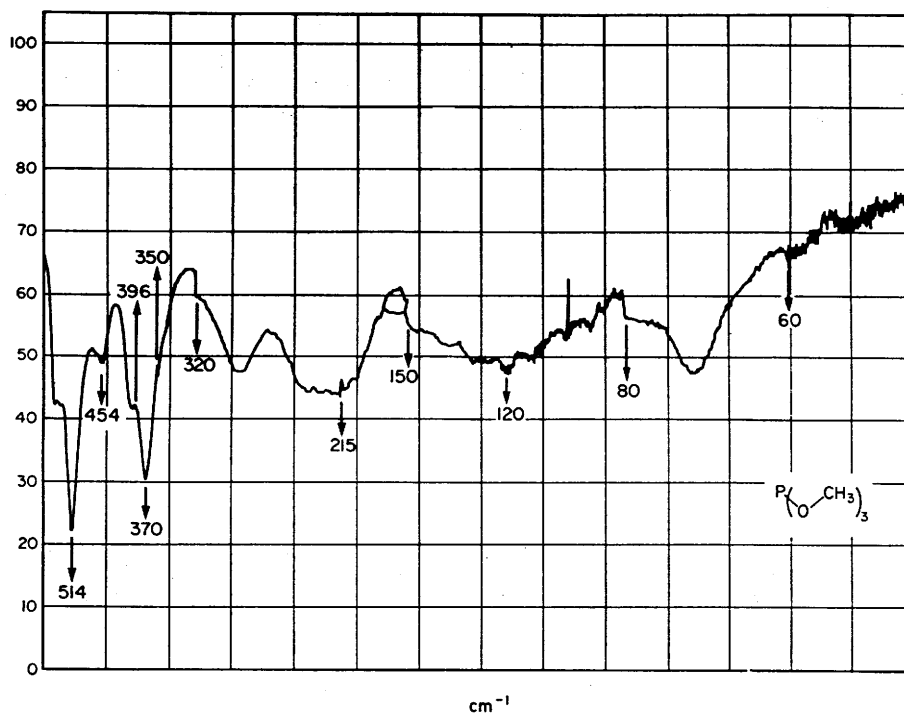


FIGURE 8.18 Infrared spectrum of trimethyl phosphite in 10 wt./vol. % hexane solution in a 0.1-mm polyethylene cell. The IR band at $\sim 70 \text{ cm}^{-1}$ in a lattice mode for polyethylene (36).

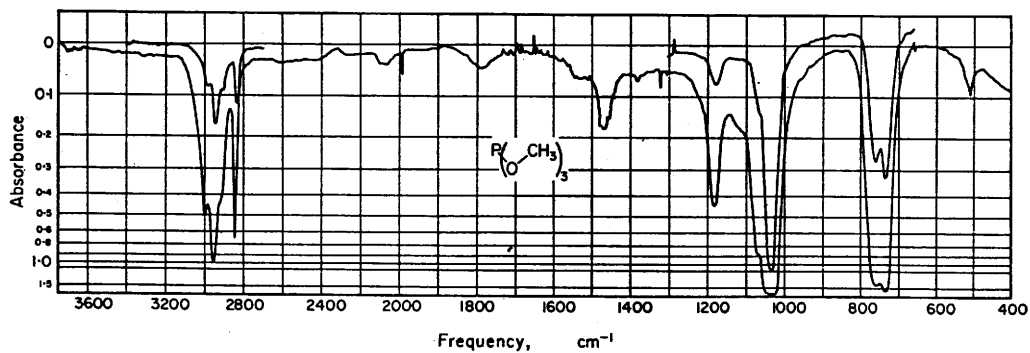


FIGURE 8.19 Vapor-phase IR spectrum of trimethyl phosphite in a 10-cm KBr cell (36).

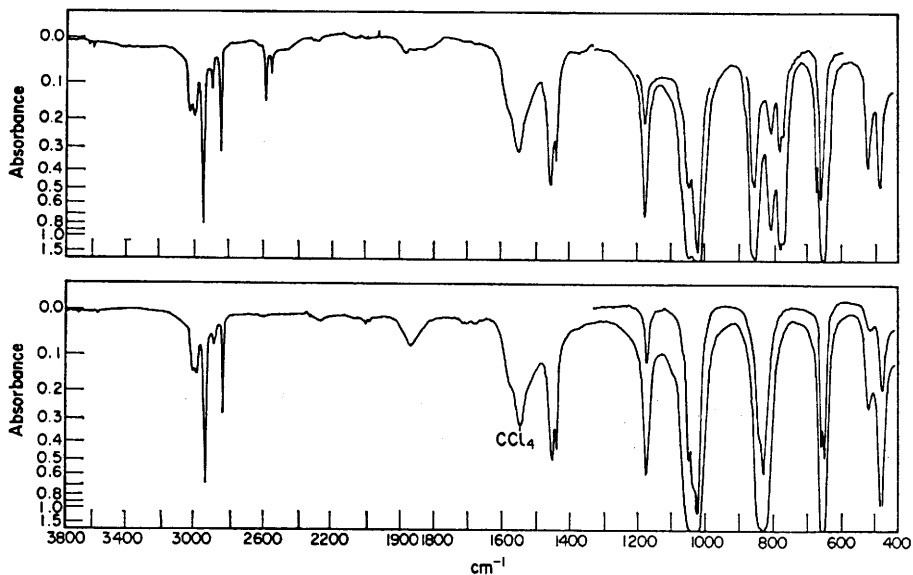


FIGURE 8.20 Top: Infrared spectrum of O,O-dimethyl phosphorodithioic acid in 10 wt./vol. % in CCl₄ solution (3800–1333 cm⁻¹) and 10 and 2 wt./vol. % in CS₂ solution (1333–450 cm⁻¹) in 0.1-mm KBr cells. Bottom: Infrared spectrum of O,O-dimethyl phosphorochloridothioate in CCl₄ solution (3800–1333 cm⁻¹) and 10 and 2 wt./vol. % in CS₂ solutions (1333–450 cm⁻¹) in 0.1-mm KBr cells (32).

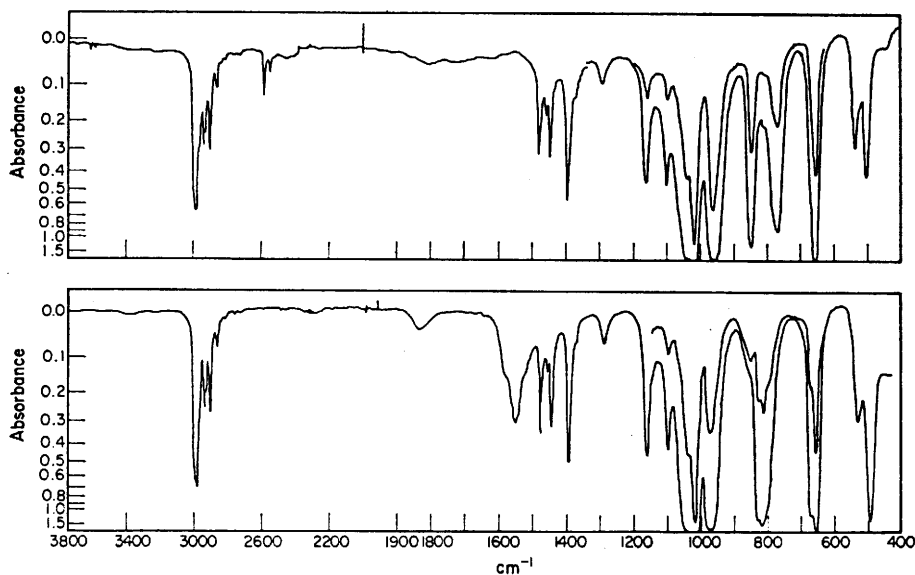


FIGURE 8.21 Top: Infrared spectrum of O,O-diethyl phosphorodithioic acid in 10 wt./vol. % in CCl₄ solution (3800–1333 cm⁻¹) and 10 and 2 wt./vol. % in CS₂ solutions (1333–400 cm⁻¹) in 0.1-mm KBr cells. The solvents have been compensated. Bottom: Infrared spectrum of O,O-diethyl phosphorochloridothioate in 10 wt./vol. % in CCl₄ solution and in 10 and 2 wt./vol. % CS₂ solutions (1333–450 cm⁻¹) in 0.1-mm KBr cells (32).

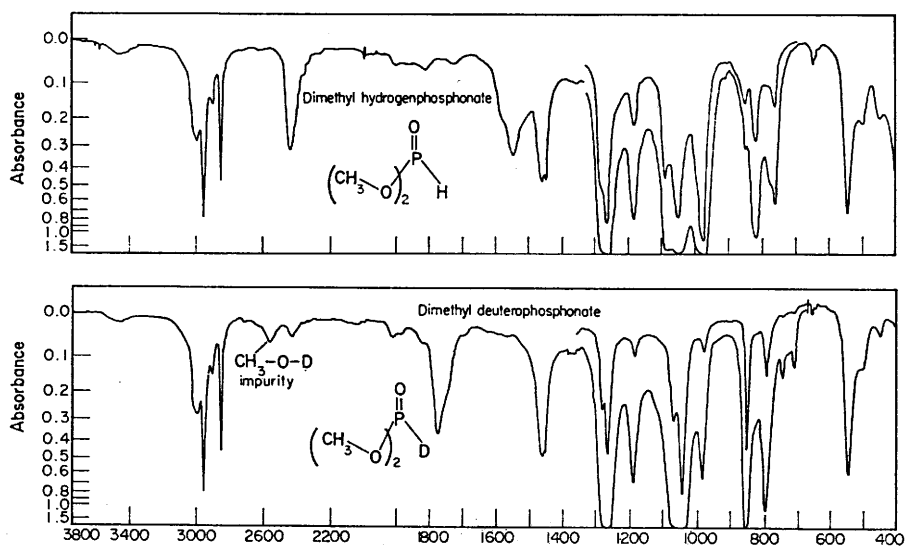


FIGURE 8.22 Top: Infrared spectrum of dimethyl hydrogenphosphonate in 10 wt./vol. % in CCl_4 solution ($3800\text{--}1333\text{ cm}^{-1}$) and in 10 and 2 wt./vol. % CS_2 solutions in 0.1-mm KBr cells. The solvents have not been compensated. Bottom: Infrared spectrum of dimethyl deuterophosphonate in 10% wt./vol. CCl_4 solution ($3800\text{--}1333\text{ cm}^{-1}$) and in 10 and 2 wt./vol. % solutions in CS_2 solution ($1333\text{--}400\text{ cm}^{-1}$). The solvents have been compensated (32).

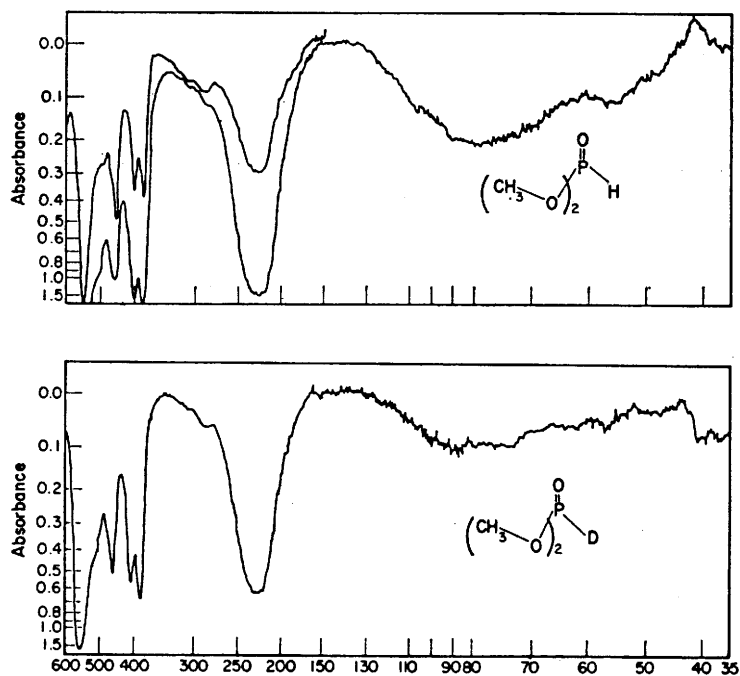


FIGURE 8.23 Top: Infrared spectrum of dimethyl hydrogenphosphonate saturated in hexane solution ($600\text{--}35\text{ cm}^{-1}$) in a 2-mm polyethylene cell. Bottom: Infrared spectrum of dimethyl deuterophosphonate saturated in hexane solution ($600\text{--}35\text{ cm}^{-1}$) in a 2-mm polyethylene cell (32).

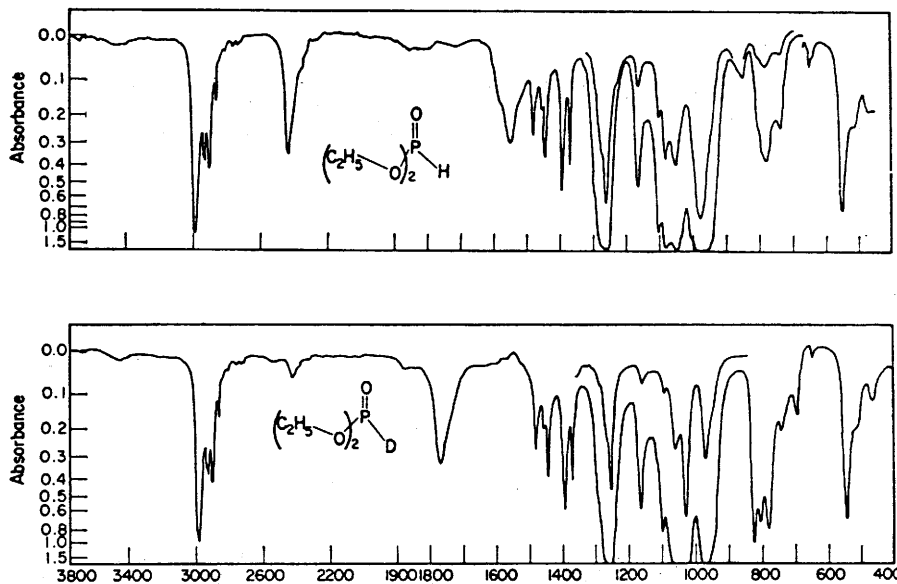


FIGURE 8.24 Top: Infrared spectrum of diethyl hydrogenphosphonate in 10 wt./vol. % in CCl_4 solution ($3800\text{--}1333\text{ cm}^{-1}$) and in 10 and 2 wt./vol. % in CS_2 solutions ($1333\text{--}400\text{ cm}^{-1}$) in 0.1-mm KBr cells. The solvents have not been compensated. Bottom: Infrared spectrum of diethyl deuterophosphonate in 10% wt./vol. % in CCl_4 solution ($3800\text{--}1333\text{ cm}^{-1}$) and 10 and 2 wt./vol. % CS_2 solutions ($1333\text{--}400\text{ cm}^{-1}$) in 0.1-mm KBr cells. The solvents have been compensated (32).

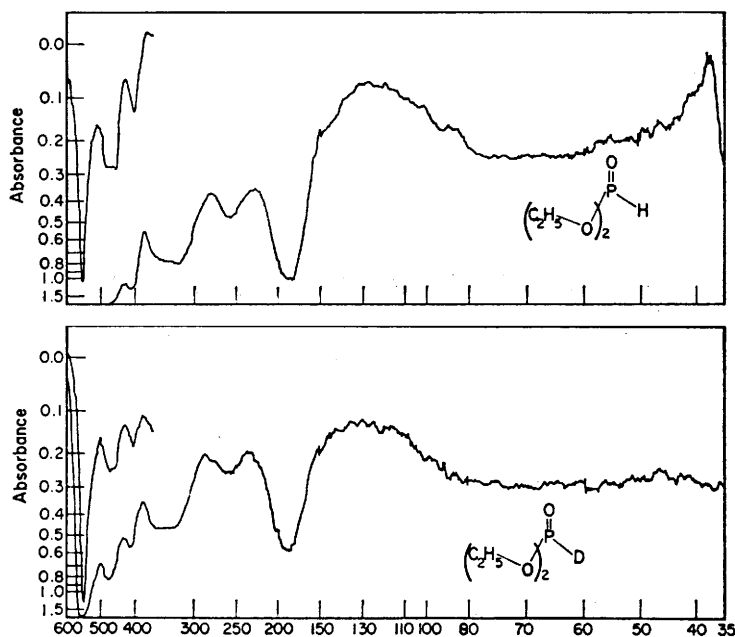


FIGURE 8.25 Top: Infrared spectrum for diethyl hydrogenphosphonate in 0.25 and 5 wt./vol. % hexane solutions ($600\text{--}35\text{ cm}^{-1}$) in a 2-mm polyethylene cell. Bottom: Infrared spectrum for diethyl deuterophosphonate in 10 wt./vol. % hexane solution ($600\text{--}35\text{ cm}^{-1}$) in a 1-mm polyethylene cell.

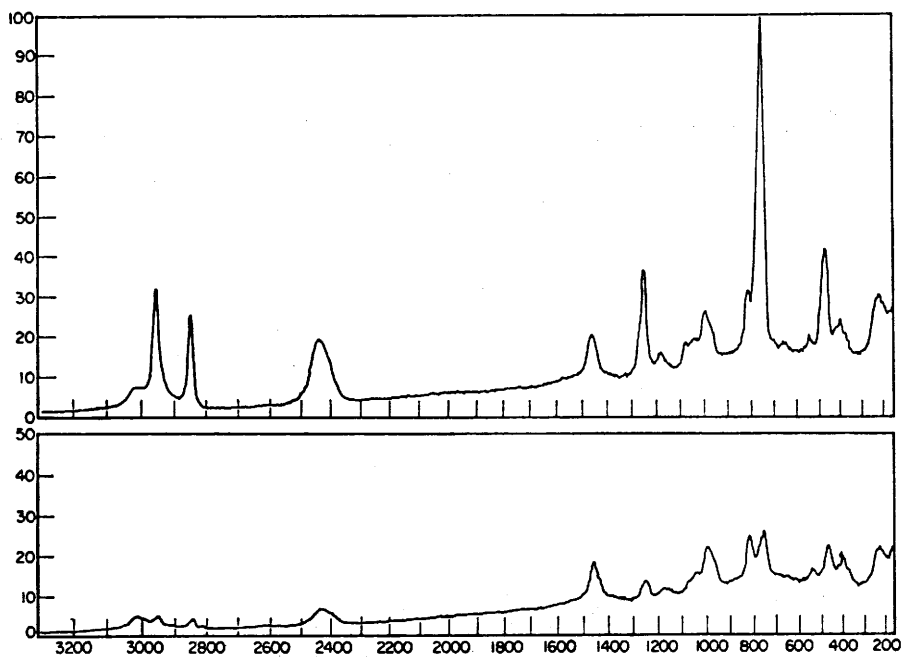


FIGURE 8.26 Top: Raman liquid-phase spectrum of dimethyl hydrogenphosphonate in a 2.5-ml multipass cell, gain 7, spectral slit-width 0.4 cm^{-1} . Bottom: Same as top but with the plane of polarization of the incident beam rotated through 90° (32).

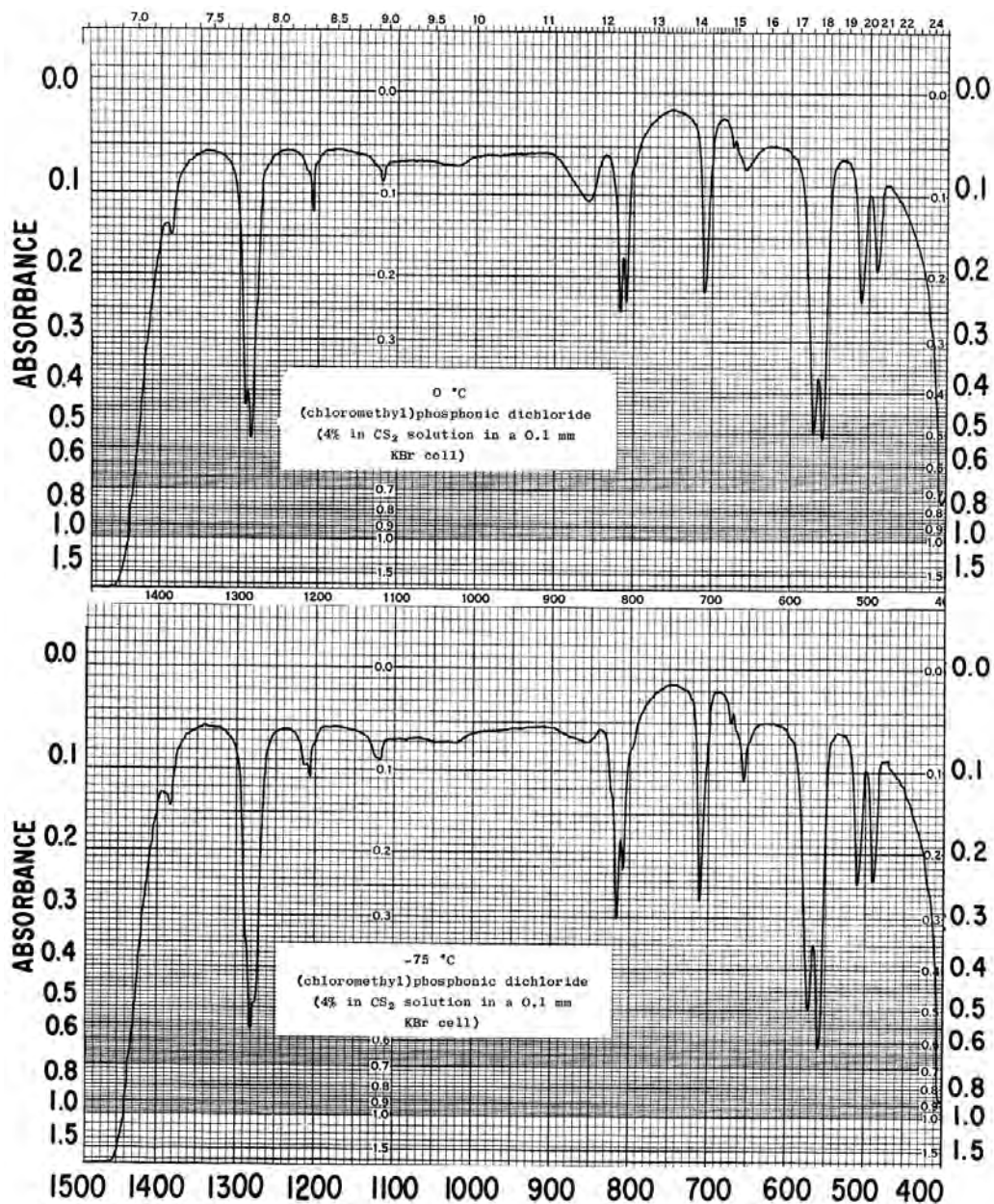


FIGURE 8.27 Top: Infrared spectrum of (chloromethyl) phosphonic dichloride in 4 wt./vol. % CS₂ solution (1500–400 cm⁻¹) at 0 °C in a 0.1-mm KBr cell. Bottom: Same as above except at -75 °C.

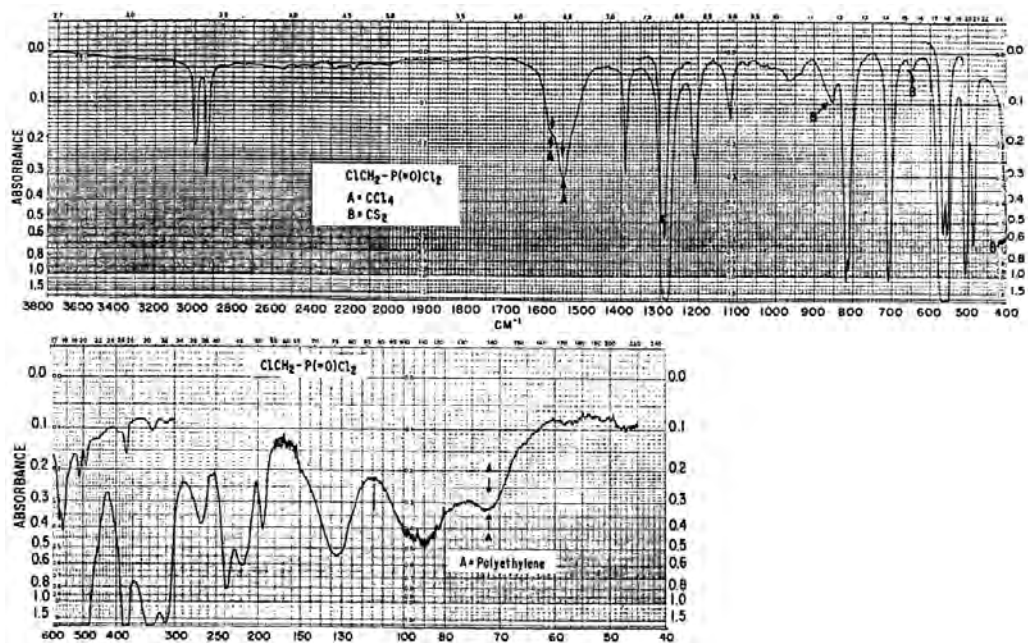


FIGURE 8.28 Top: Infrared spectrum of (chloromethyl) phosphonic dichloride in 10 wt./vol. % in CCl_4 solution ($3800\text{--}1333\text{ cm}^{-1}$) and 10 wt./vol. % in CS_2 solution ($1333\text{--}400\text{ cm}^{-1}$) in 0.1-mm KBr cells. Bottom: Infrared spectrum of (chloromethyl) phosphonic dichloride in 20 wt./vol. % hexane solution ($600\text{--}45\text{ cm}^{-1}$) in a 1-mm polyethylene cell (17).

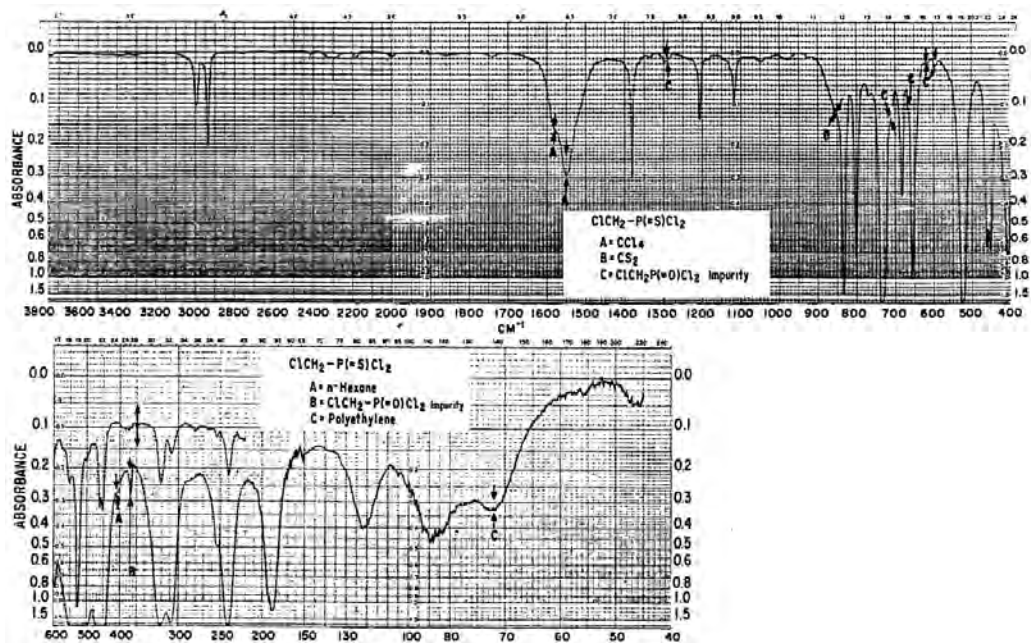


FIGURE 8.29 Top: Infrared spectrum of (chloromethyl) phosphonothioic dichloride in 10 wt./vol. % CCl_4 solution ($3800\text{--}1333\text{ cm}^{-1}$) and in 10 wt./vol. % CS_2 solution ($1333\text{--}400\text{ cm}^{-1}$) in 0.1-mm KBr cells. Bottom: Infrared spectrum of (chloromethyl) phosphonothioic dichloride in 20 wt./vol. % hexane solution ($600\text{--}45\text{ cm}^{-1}$) in a 1-mm polyethylene cell (17).

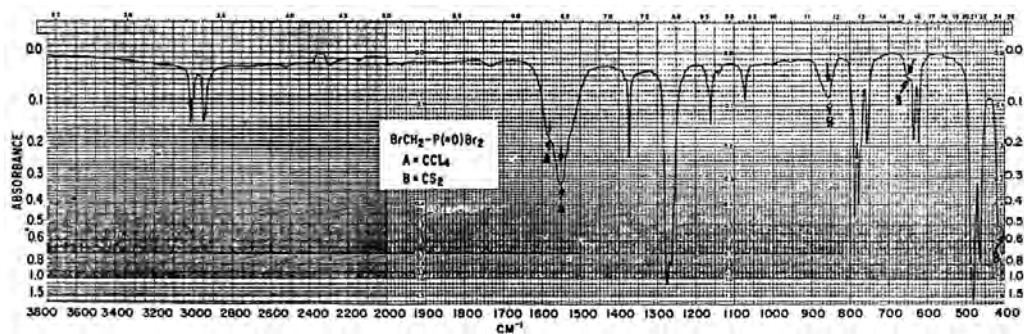


FIGURE 8.30 Infrared spectrum of (bromomethyl) phosphonic dibromide in 10 wt./vol. % CCl_4 solution ($3800\text{--}1333\text{ cm}^{-1}$) and 10 wt./vol. % in CS_2 solution ($1333\text{--}400\text{ cm}^{-1}$) in 0.1-mm KBr cells (17).

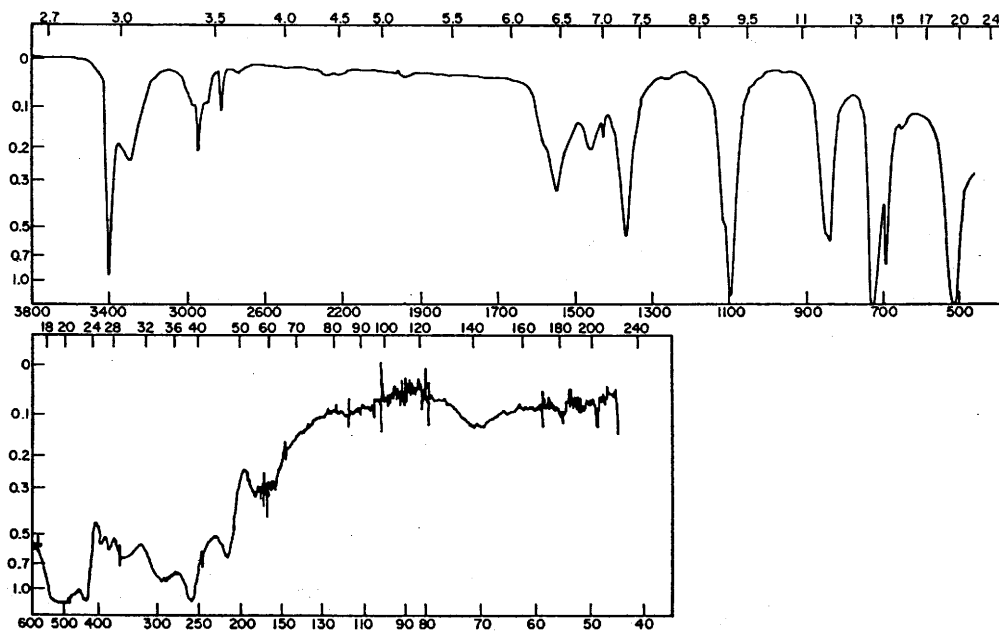


FIGURE 8.31 Top: Infrared spectrum of N-methyl phosphoramidodichloridothioate 10 wt./vol. % in CCl_4 solution ($3800\text{--}1333\text{ cm}^{-1}$) and 10 wt./vol. % in CS_2 solution ($1333\text{--}45\text{ cm}^{-1}$) in 0.1-mm KBr cells. The solvents have not been compensated. Bottom: Infrared spectrum of N-methyl phosphoramidodichloridothioate in 10 wt./vol. hexane solution ($600\text{--}45\text{ cm}^{-1}$) in a 1-mm polyethylene cell (24).

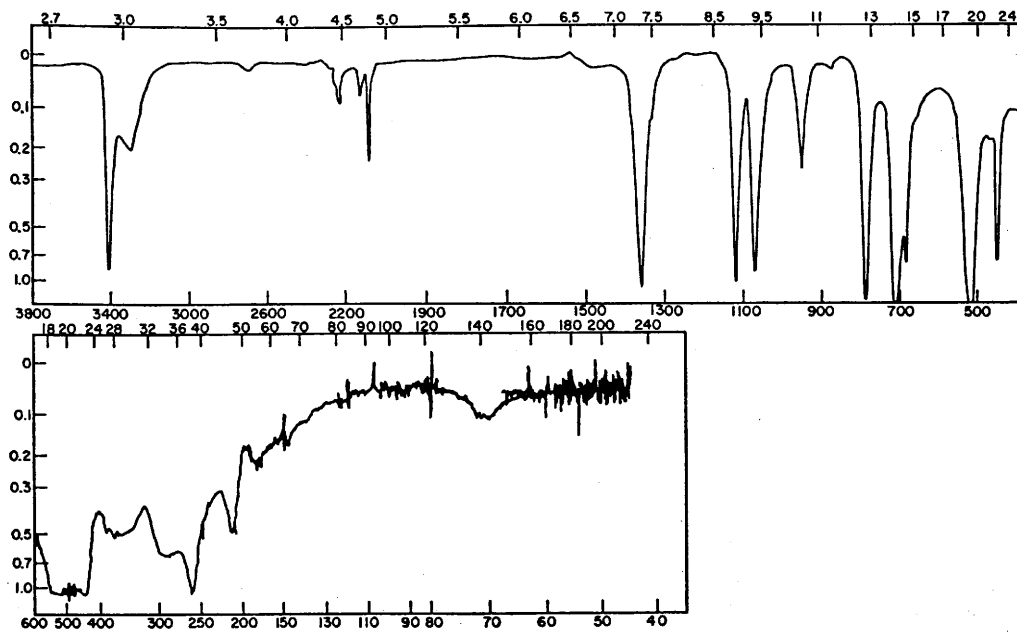


FIGURE 8.32 Top: Infrared spectrum of N-methyl-d₃ phosphoramidodichloridothioate in 10 wt./vol. % in CCl₄ (3800–1333 cm⁻¹) and 10 wt./vol. % in CS₂ solution (1333–45 cm⁻¹) in 0.1-mm KBr cells. Bottom: Infrared spectrum of N-methyl-d₃ phosphoramidodichloridothioate in 10 wt./vol. % in hexane solution (600–45 cm⁻¹) in a 1-mm polyethylene cell (24).

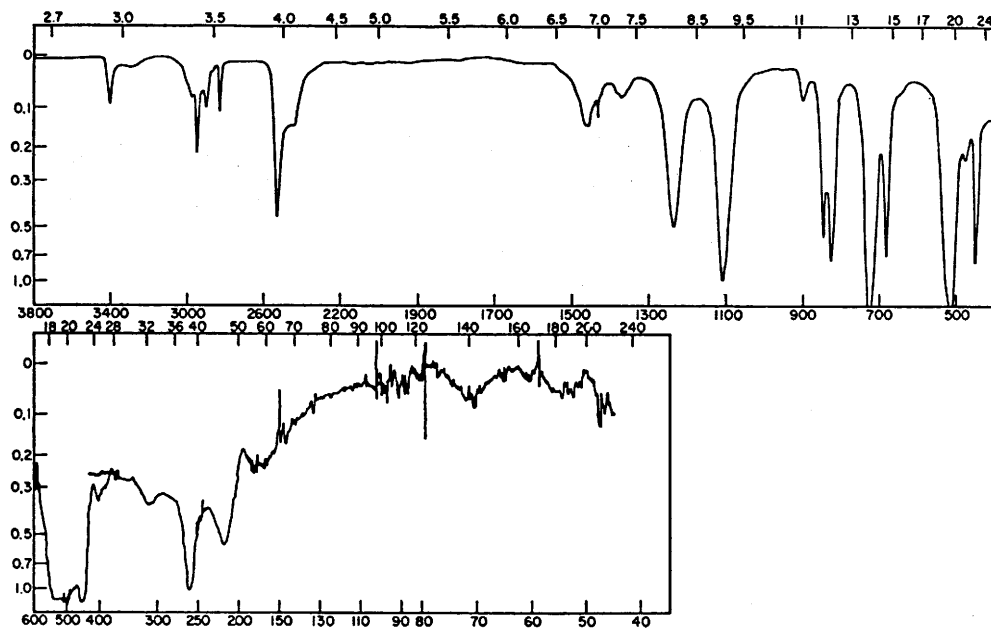


FIGURE 8.33 Top: Infrared spectrum of N-D, N-methyl phosphoramidodichloridothioate in 10 wt./vol. % CCl₄ solution (3800–1333 cm⁻¹) and in 10 wt./vol. % in CS₂ solution (1333–45 cm⁻¹) in 0.1-KBr cells. The solvents have been compensated. Bottom: Infrared spectrum of N-D, N-methyl phosphoramidodichloridothioate in 10 wt./vol. % hexane solution in a 1-mm polyethylene cell. Both samples contain N-methyl phosphoramidodichloridothioate as an impurity (24).

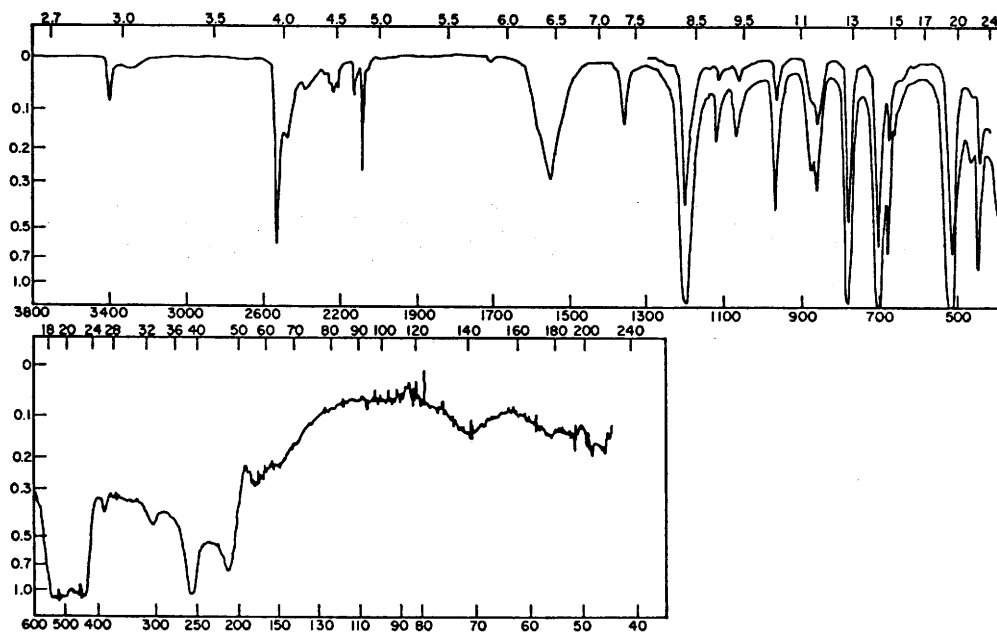


FIGURE 8.34 Top: Infrared spectrum for N-D, N-methyl-d₃ phosphoramidodichloridothioate in 10 wt./vol. % CCl₄ solution (3800–1333 cm⁻¹) and 10 and 2 wt./vol. % in CS₂ solutions (1333–400 cm⁻¹) in 0.1-mm KBr cells. The solvent bands are compensated. Bottom: Infrared spectrum of N-D, N-methyl-d₃ phosphoramidodichloridothioate in 10 wt./vol. % hexane solution in a 1-mm polyethylene cell. This sample contains N-methyl-d₃ phosphoramidodichloridothioate as an impurity (24).

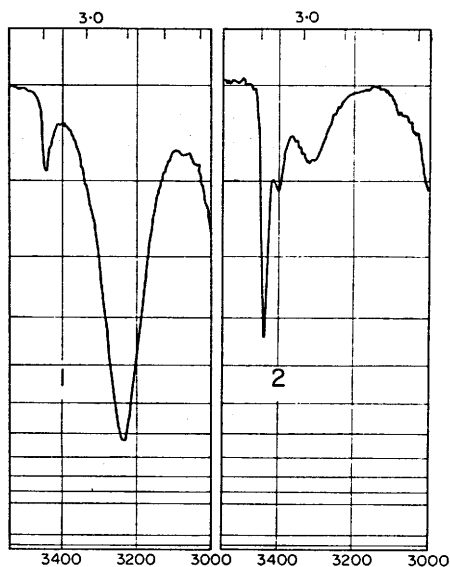


FIGURE 8.35 Infrared spectrum 1 is for O-alkyl O-aryl N-methylphosphoramidate in 10 wt./vol. % CCl₄ solution (3500–3000 cm⁻¹) in a 0.1-mm NaCl cell. Infrared spectrum 2 is for O-alkyl O-aryl N-methylphosphoramidodithioate in 10 wt./vol. % in CCl₄ solution (3500–300 cm⁻¹) in a 0.1-mm NaCl cell (42).

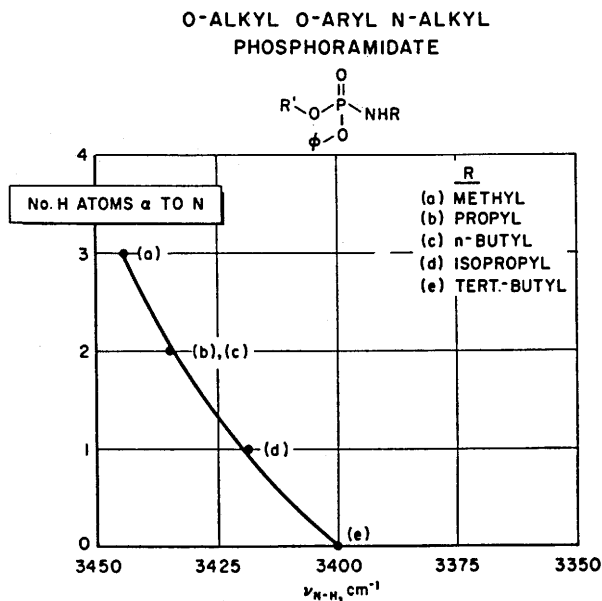


FIGURE 8.36 A plot of N-H stretching frequencies of O-alkyl O-aryl N-alkylphosphoramidates in the region 3450–3350 cm^{-1} vs an arbitrary assignment of one for each proton joined to the N- α -carbon atom (42).

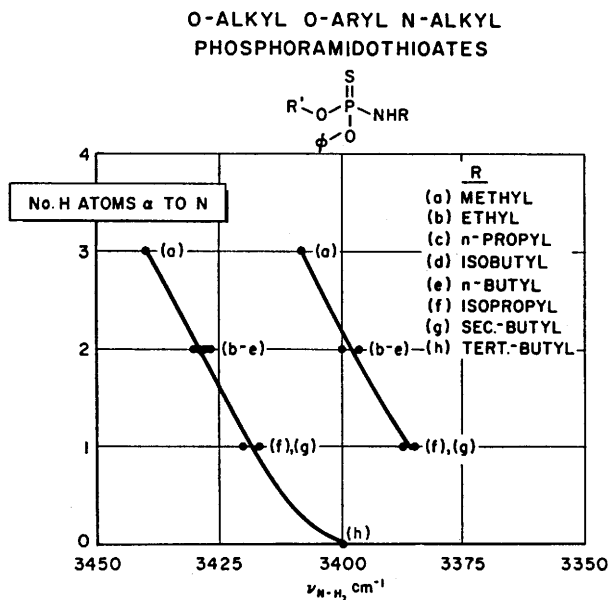


FIGURE 8.37 Plots of cis and trans N-H stretching frequencies of O-alkyl O-aryl N-alkylphosphoramidothioates in the region 3450–3350 cm^{-1} vs an arbitrary assignment of one for every proton joined to the N- α -carbon atom (42).

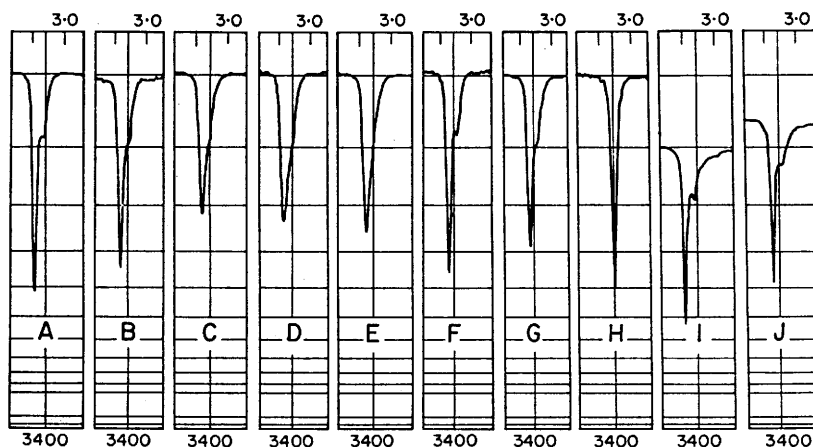


FIGURE 8.38 Infrared spectra of the *cis* and *trans* N–H stretching absorption bands of O-alkyl O-aryl N-alkylphosphoramidothioates in 0.01 molar or less in CCl_4 solutions ($3450\text{--}3350\text{ cm}^{-1}$) in a 14-mm NaCl cell. The N-alkyl group for A is methyl, B is ethyl, C is *n*-propyl, D is isobutyl, E is *n*-butyl, F is isopropyl, G is *sec*-butyl, and H is *tert*-butyl. Spectra I and J are O,O-dialkyl N-methylphosphoramidothioate and O,O-dialkyl N-propylphosphoramidothioate, respectively (42).

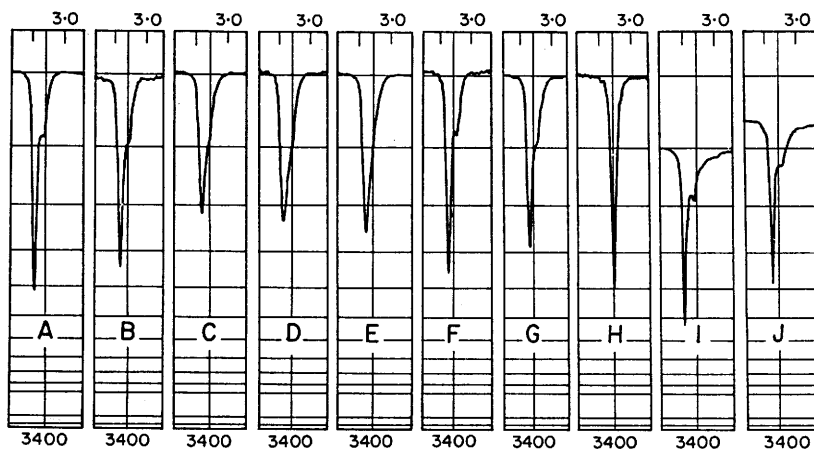


FIGURE 8.39 Infrared spectra of the N–H stretching absorption bands of O-alkyl N,N'-dialkyl phosphorodiamidothioates. The N,N'-dialkyl group for A is dimethyl, B is diethyl, C is dipropyl, D is dibutyl, E is diisopropyl, F is di-*sec*-butyl, G is dibenzyl. The H and I are IR spectra for the N–H stretching bands of O-aryl N,N'-diisopropylphosphorodiamidothioate and O-aryl N-isopropyl, N-methylphosphorodiamidothioate, respectively. Spectra A through J were recorded for 0.01 molar or less in CCl_4 solutions using 3-mm KBr cells. Spectra D and J are for O-aryl N,N'-dibutylphosphorodiamidothioate in 0.01 molar CCl_4 solution in a 3-mm cell and 10 wt./vol. % in CCl_4 solution in a 0.1-mm KBr cell (42).

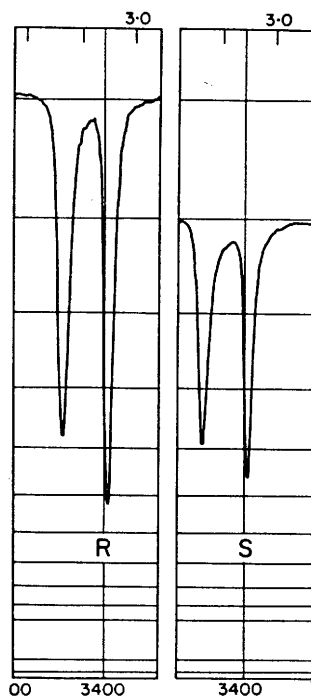


FIGURE 8.40 Infrared spectrum R gives the N–H stretching absorption bands for O-alkyl O-aryl phosphoramidothioate in 0.01 molar CCl_4 solution in a 3-mm NaCl cell. Infrared spectrum S gives O,O-dialkyl phosphoramidothioate in 0.01 molar CCl_4 solution in a 3-mm NaCl cell (42).

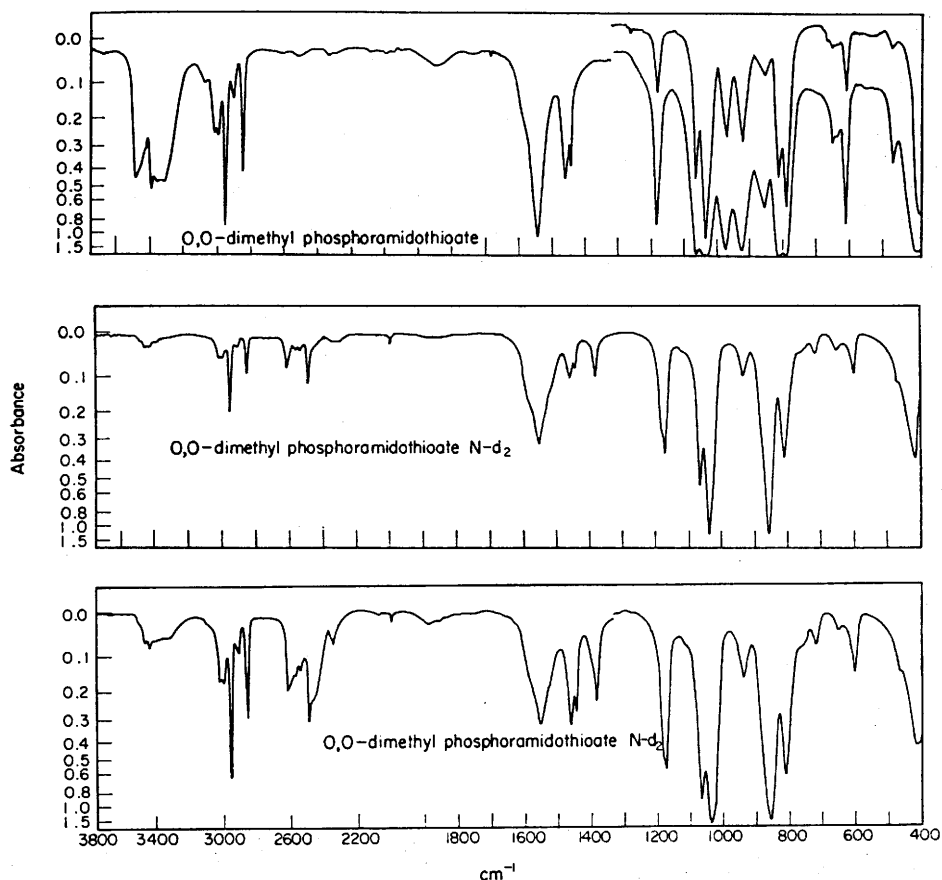


FIGURE 8.41 Top: Infrared spectrum of O,O-diethyl methylphosphoramidothioate in 10 wt./vol. % CCl₄ solution (3800–1333 cm⁻¹) and 10 and 2 wt./vol. % CS₂ solutions (1333–400 cm⁻¹) in 0.1-mm KBr cells. Middle: Infrared spectrum of O,O-diethyl N-methyl, N-D-phosphoramidothioate in 2 wt./vol. % in CCl₄ solution (3800–1333 cm⁻¹) and in 2 wt./vol. % in CS₂ solution (1333–400 cm⁻¹) in 0.1-mm KBr cells. Bottom: Infrared spectrum of O,O-diethyl N-methyl, N-D-phosphoramidothioate 10 wt./vol. % in CCl₄ solution (3800–1333 cm⁻¹) and in 10 wt./vol. % CS₂ solution (1333–400 cm⁻¹) in 0.1-mm KBr cells (37).

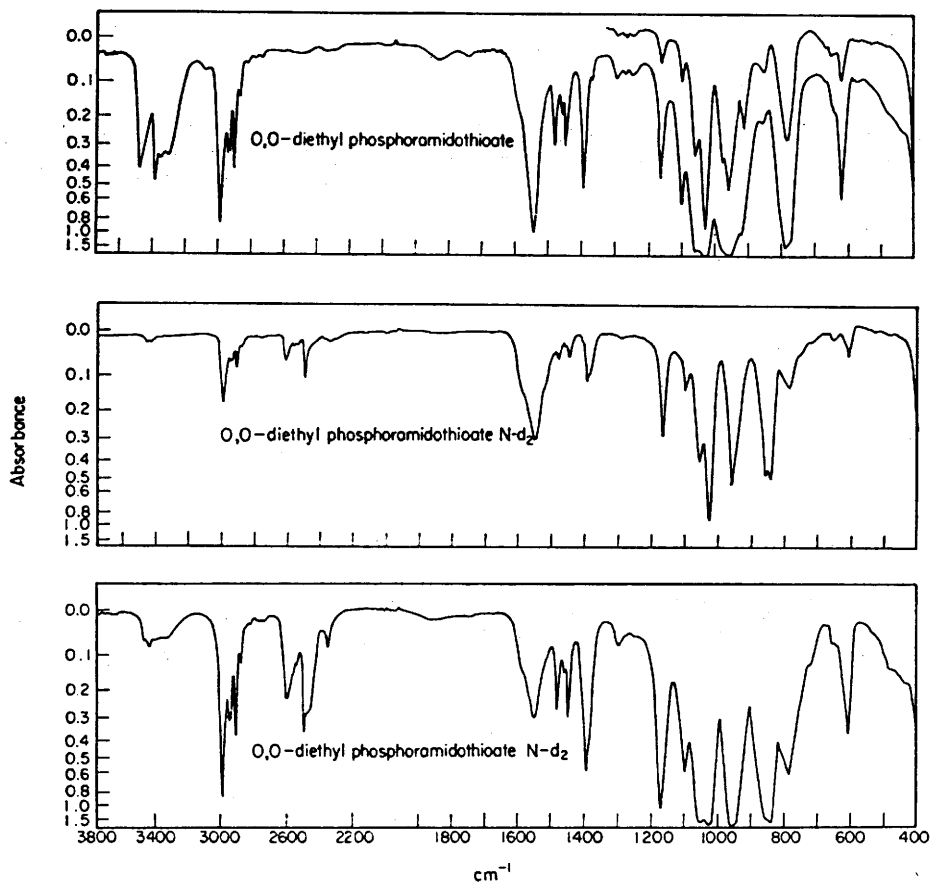


FIGURE 8.42 Top: Infrared spectrum of O,O-diethyl phosphoramidothioate in 10 wt./vol. % in CCl₄ solution (3800–1333 cm⁻¹) and 2 and 10 wt./vol. % in CS₂ solutions (1333–400 cm⁻¹) in 0.1-mm KBr cells. Middle: Infrared spectrum of O,O-diethyl phosphoramidothioate-N-D₂ in 2 wt./vol. % in CCl₄ solution (3800–1333 cm⁻¹) and in 2 wt./vol. % CS₂ solution (1333–400 cm⁻¹) in 0.1-mm KBr cells. Bottom: Infrared spectrum of O,O-diethyl phosphoramidothioate-N-D₂ 10 wt./vol. % in CCl₄ solution (3800–1333 cm⁻¹) and 10 wt./vol. % in CS₂ solution (1333–400 cm⁻¹) in 0.1-mm KBr cells (37).

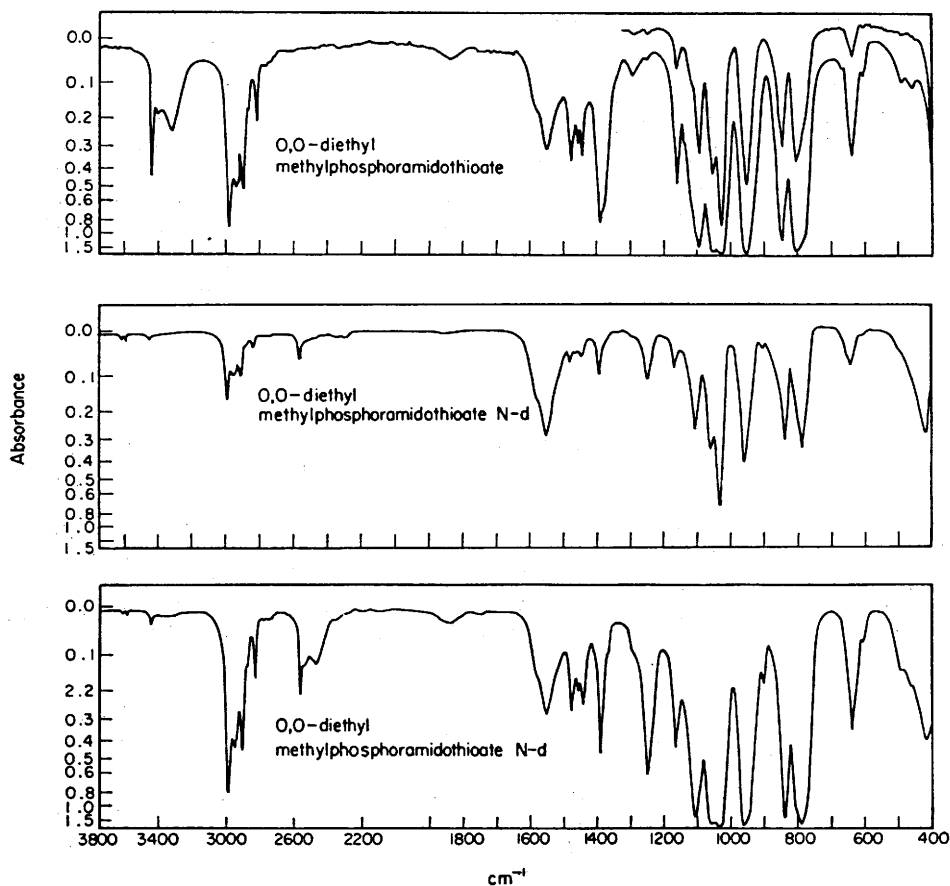


FIGURE 8.43 Top: Infrared spectrum of O,O-diethyl N-methylphosphoramidothioate 10 wt./vol. % in CCl_4 solution ($3800\text{--}1333\text{ cm}^{-1}$) and 10 and 2 wt./vol. % in CS_2 solutions ($1333\text{--}400\text{ cm}^{-1}$) in 0.1-mm KBr cells. Middle: Infrared spectrum of O,O-diethyl N-methyl, N-D phosphoramidothioate in 2 wt./vol. % CCl_4 solution ($3800\text{--}1333\text{ cm}^{-1}$) and 2 wt./vol. % in CS_2 solution ($1333\text{--}400\text{ cm}^{-1}$) in 0.1-mm KBr cells. Bottom: Infrared spectrum of O,O-diethyl N-methyl, N-D-phosphoramidothioate in 10 wt./vol. % CCl_4 solution ($1333\text{--}400\text{ cm}^{-1}$) in 0.1-mm KBr cells. The solvents are not compensated (37).

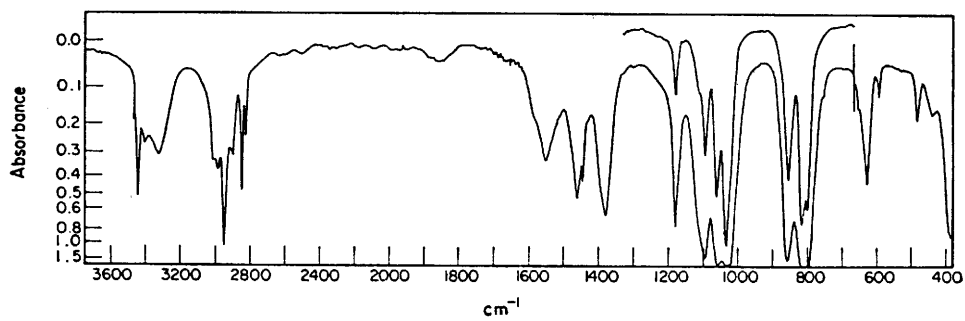


FIGURE 8.44 Infrared spectrum of O,O-dimethyl N-methylphosphoramidithioate in 10 wt./vol. % in CCl₄ solution (3800–1333 cm⁻¹) and 10 and 2 wt./vol. % in CS₂ solutions (1333–400 cm⁻¹) in 0.1-mm KBr cells (37).

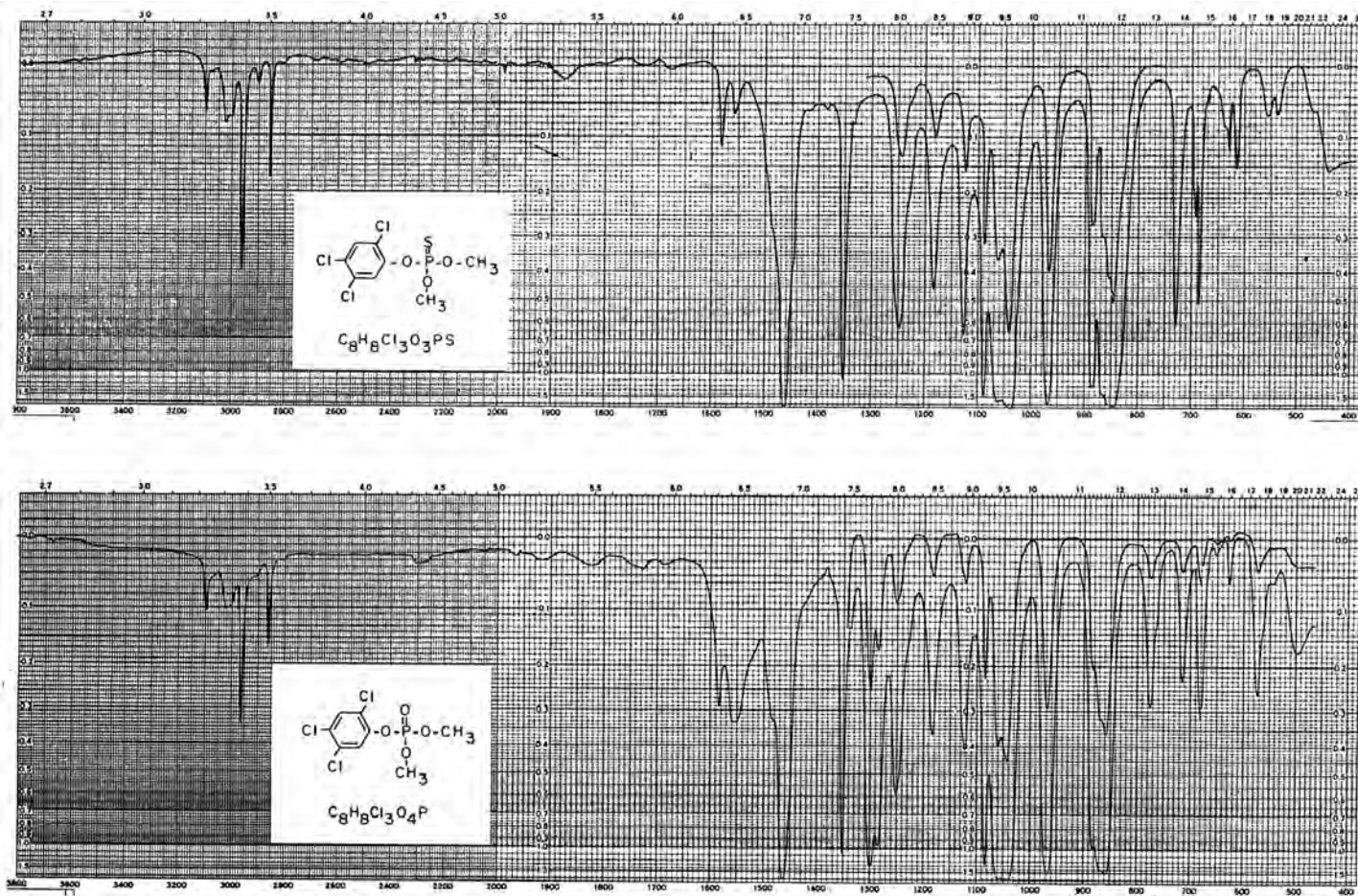


FIGURE 8.45 Top: Infrared spectrum of O,O-dimethyl O-(2,4,5-trichlorophenyl) phosphorothioate 10 wt./vol. % in CCl_4 solution ($3800\text{--}1333\text{ cm}^{-1}$) and 10 and 2 wt./vol. % in CS_2 solutions ($1333\text{--}400\text{ cm}^{-1}$) in 0.1-mm KBr cells. Bottom: Infrared spectrum of O,O-dimethyl O-(2,4,5-trichlorophenyl) phosphate in 10 wt./vol. % in CCl_4 solution ($3800\text{--}1333\text{ cm}^{-1}$) in 0.1-mm KBr cells. The solvents are not compensated (43).

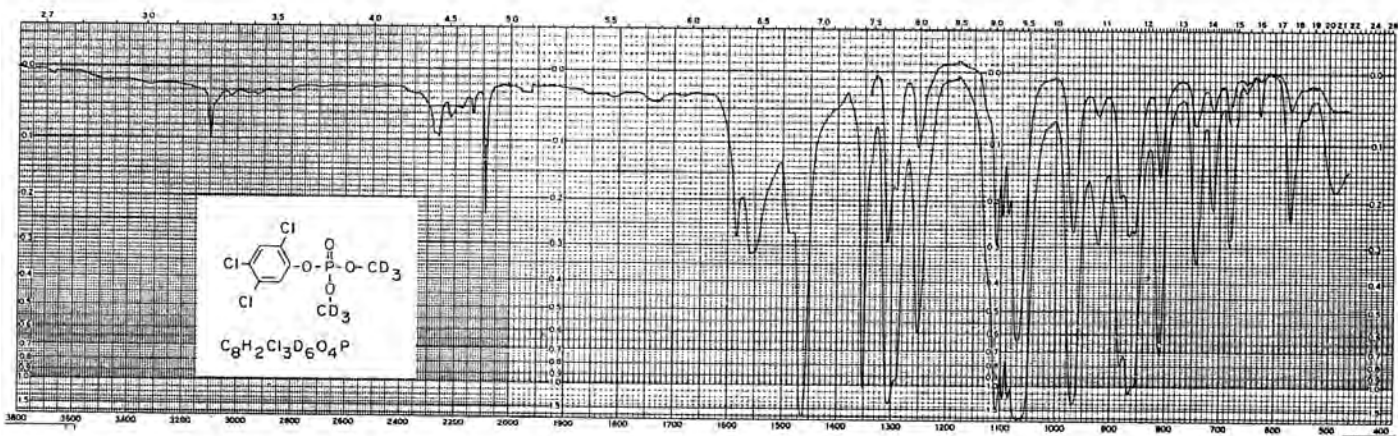
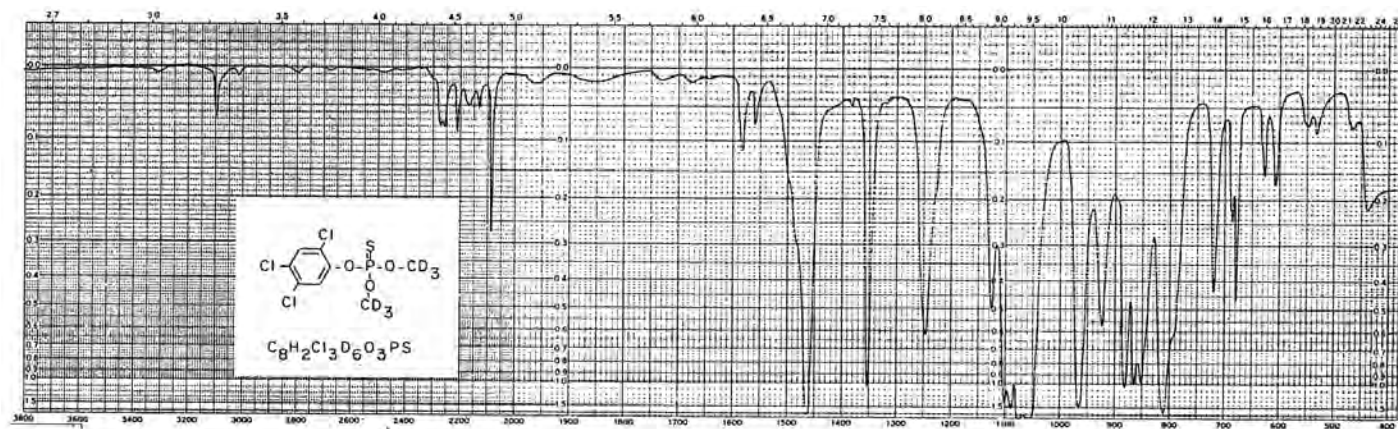


FIGURE 8.46 Top: Infrared spectrum for O,O-dimethyl-d₆ O-(2,4,5-trichlorophenyl) phosphorothioate in 10 wt./vol. % CCl₄ solution (3800–1333 cm⁻¹) and in 10 and 2 wt./vol. % CS₂ solution (1333–400 cm⁻¹) in 0.1-mm KBr cells. Bottom: Infrared spectrum for O,O-dimethyl-d₆ O-(2,4,5-trichlorophenyl) phosphate in 10 wt./vol. % CS₂ solutions (1333–450 cm⁻¹) in 0.1-mm KBr cells. The solvents have not been compensated (37).

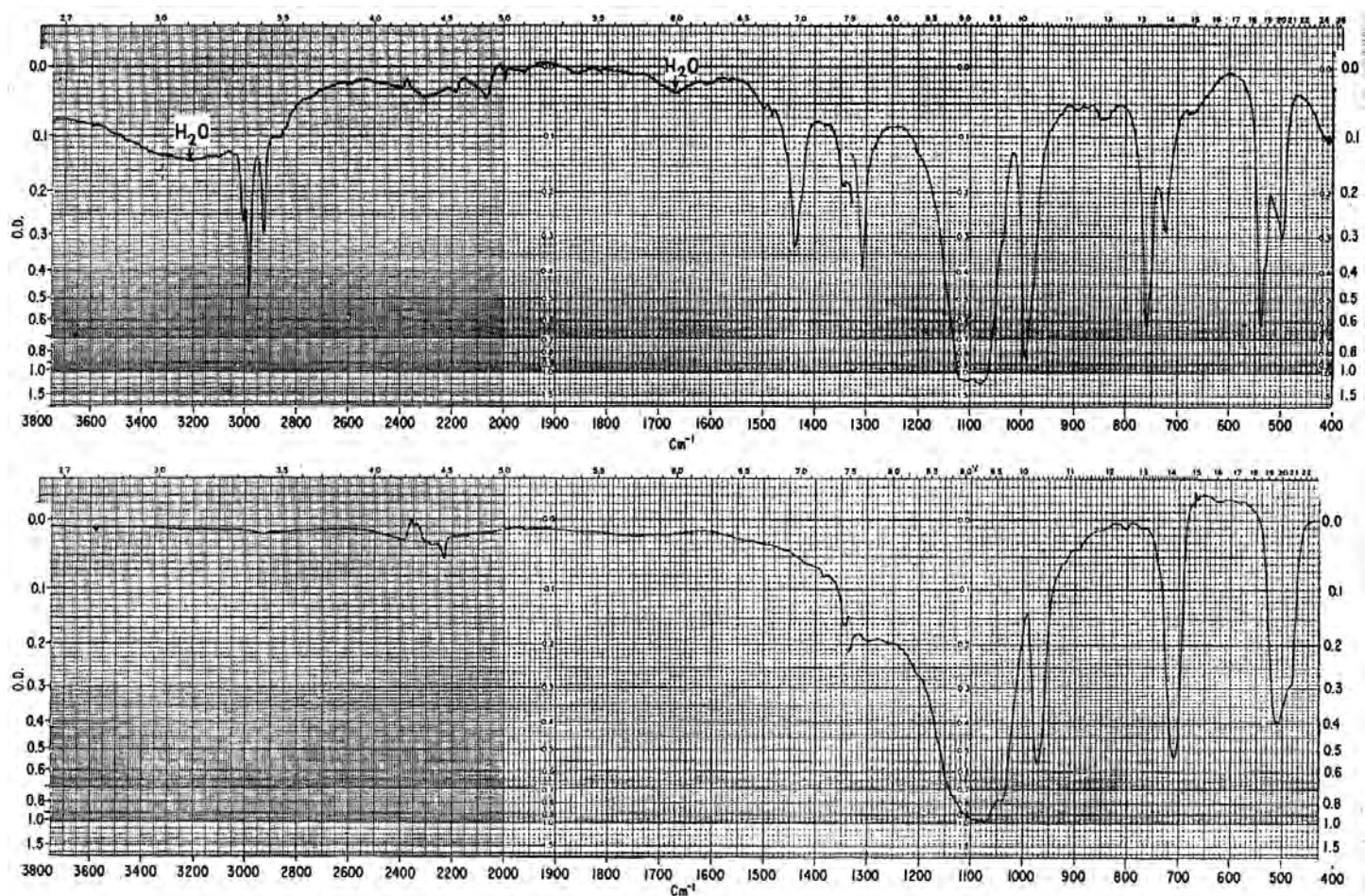


FIGURE 8.47 Top: Infrared spectrum of disodium methanephosphonate. Bottom: Infrared spectrum of disodium methane- d_3 -phosphonate. In fluorolube oil mull ($3800\text{--}1333\text{ cm}^{-1}$) and in Nujol oil mull ($1333\text{--}400\text{ cm}^{-1}$) (40). These mulls were placed between KBr plates.

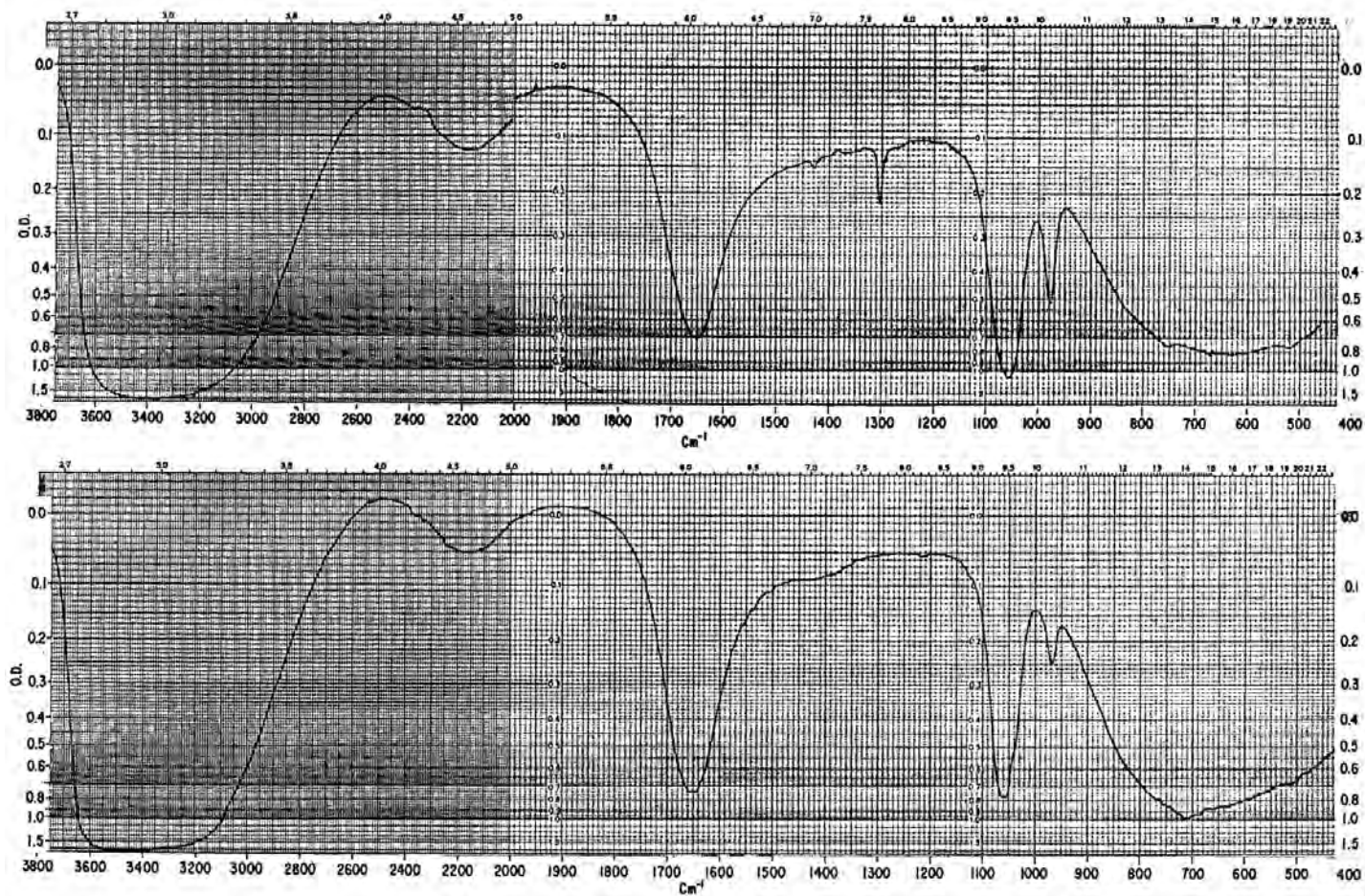


FIGURE 8.48 Top: Infrared spectrum of disodium methanephosphonate in water solution between AgCl plates. Bottom: Infrared spectrum of disodium methane- d_3 -phosphonate in water solution between AgCl plates (40).

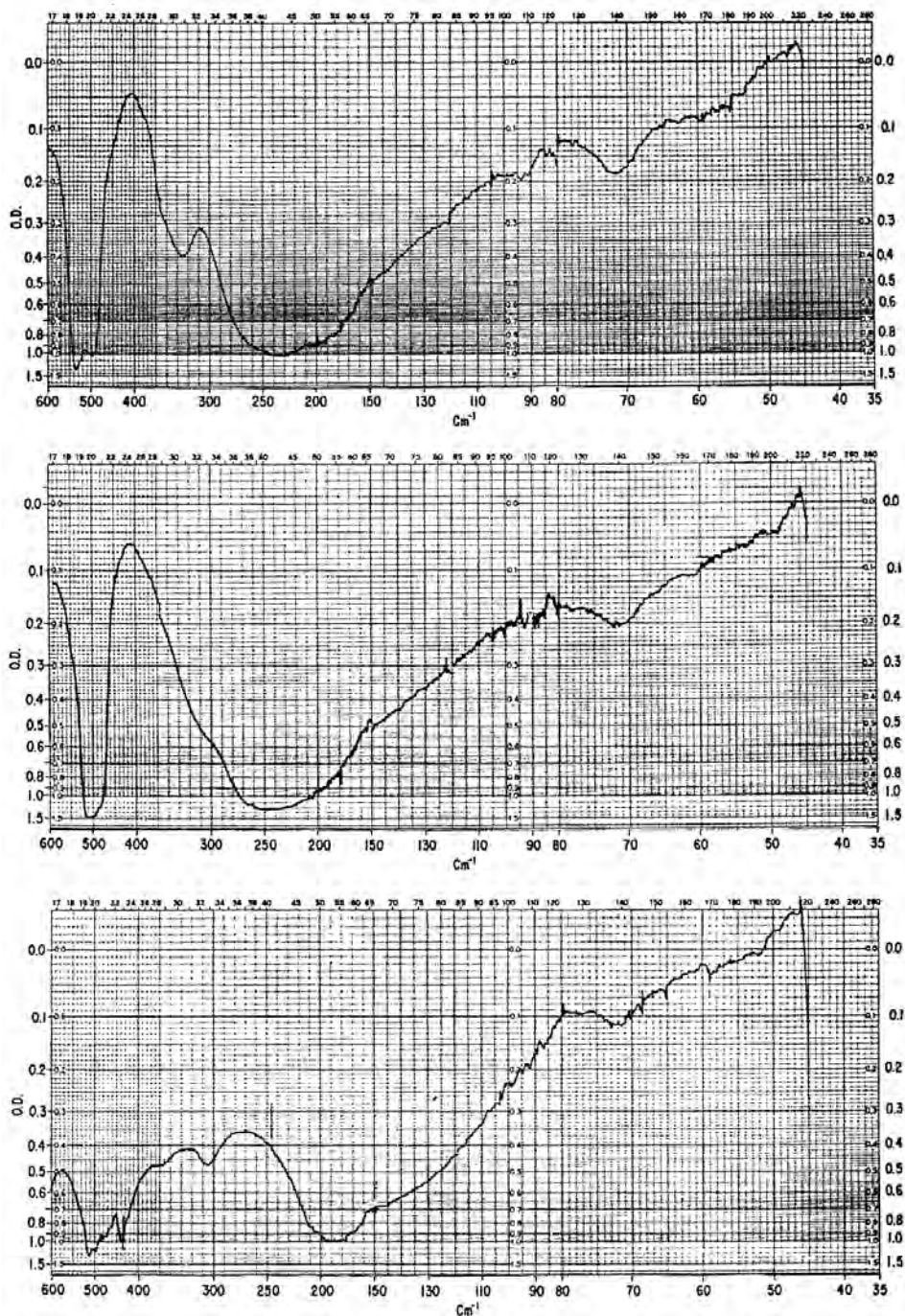


FIGURE 8.49 Top: Infrared spectrum of disodium methanephosphonate. Middle: Infrared spectrum of disodium methane-d₃-phosphonate. Bottom: Infrared spectrum of dipotassium methanephosphonate. These spectra were recorded from samples prepared as Nujol mulls between polyethylene film (600–45 cm⁻¹) (40).

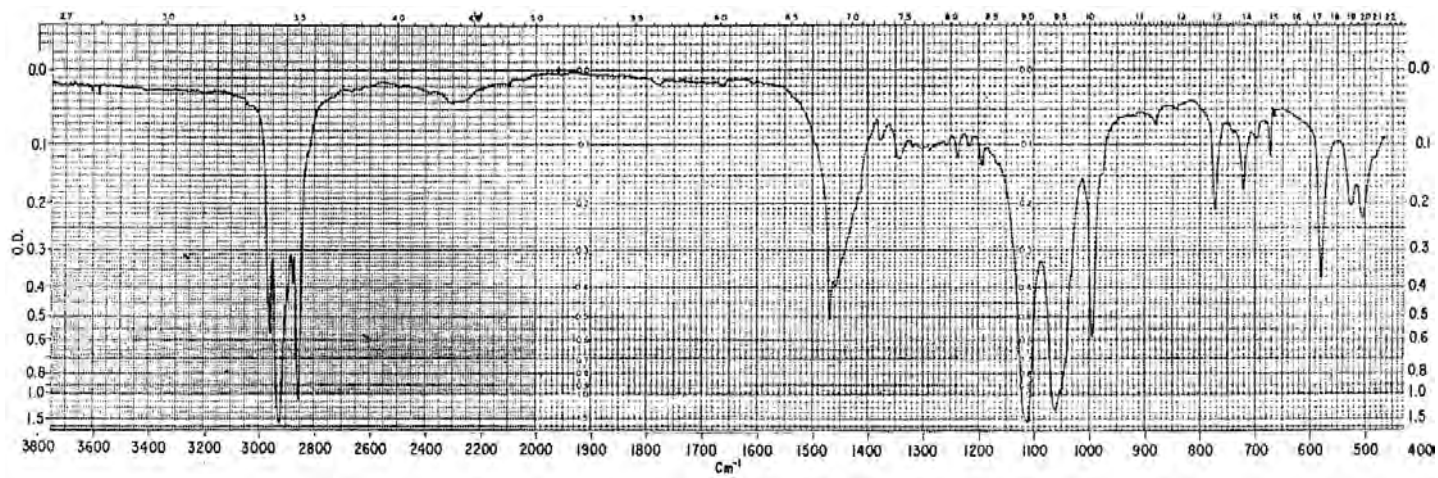


FIGURE 8.50 Infrared spectrum of disodium n-octadecanephosphonate prepared as a fluoroluble mull (3800–1333 cm^{-1}) prepared as a Nujol mull (1333–450 cm^{-1}) (40).

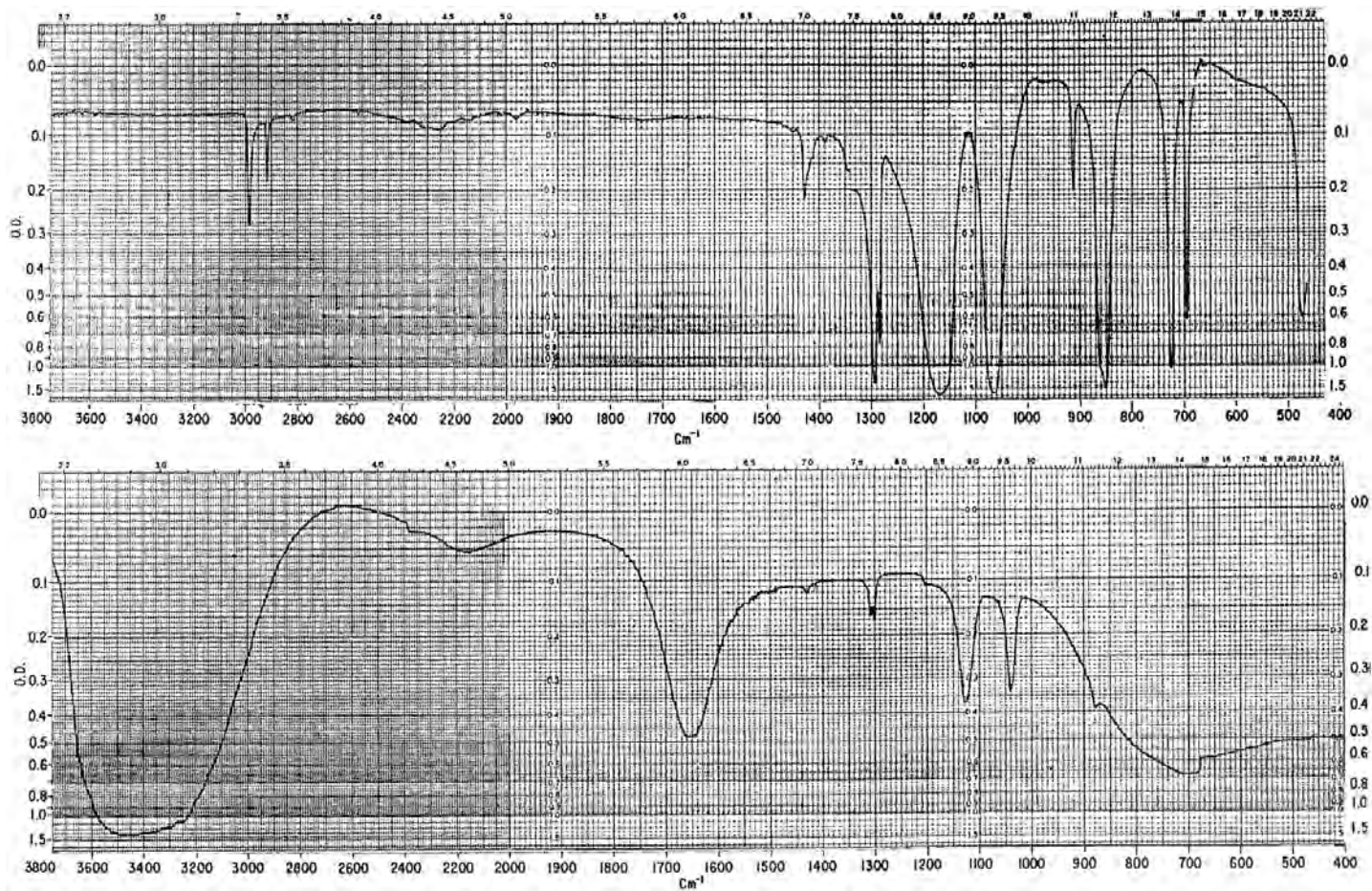


FIGURE 8.51 Top: Infrared spectrum of sodium dimethylphosphate prepared as a fluoroluble mull (3800–1333 cm⁻¹) and prepared as a Nujol mull (1333–400 cm⁻¹) between KBr plates. Bottom: Infrared spectrum of sodium dimethylphosphate saturated in water solution between AgCl plates (41).

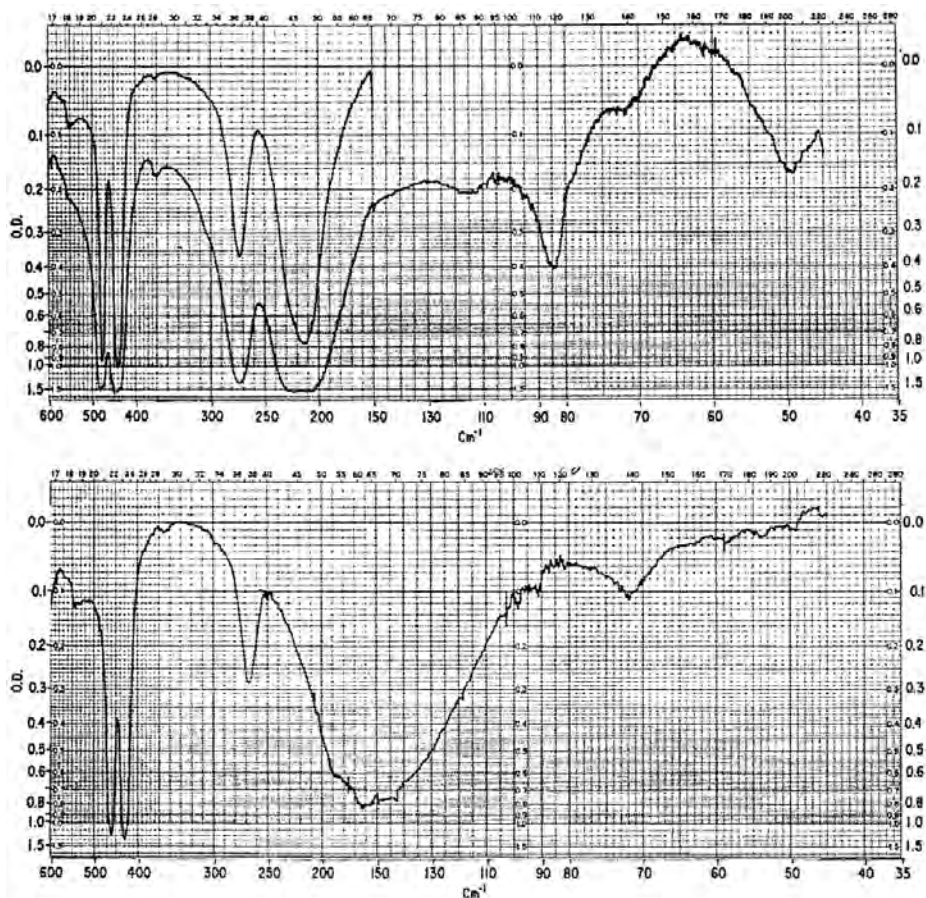


FIGURE 8.52 Top: Infrared spectrum of sodium dimethylphosphinate prepared as Nujol mull between polyethylene film ($600\text{--}45\text{ cm}^{-1}$). Bottom: Infrared spectrum of potassium dimethylphosphinate prepared as a Nujol mull between polyethylene film ($600\text{--}45\text{ cm}^{-1}$) (41).

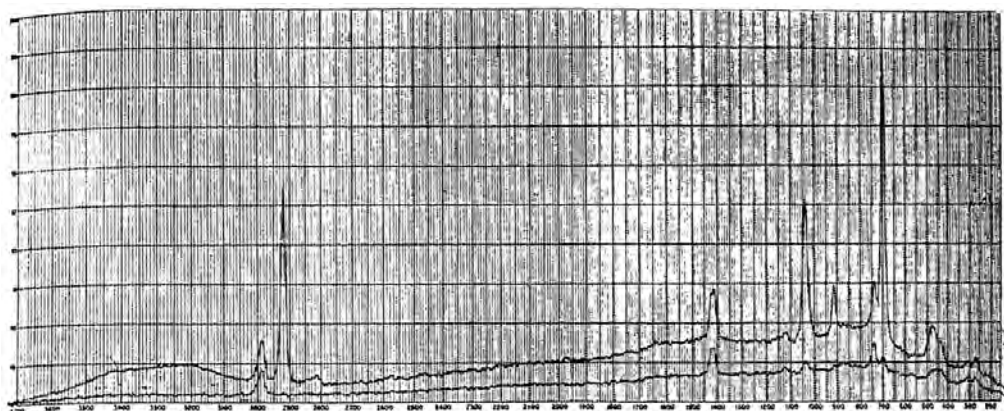


FIGURE 8.53 Top: Raman saturated water solution of sodium dimethylphosphinate using a 0.25-ml multipass cell, gain 13.4, spectral slit 10 cm^{-1} . Bottom: Same as above, except with the plane of polarization of the incident beam rotated 90° (41).

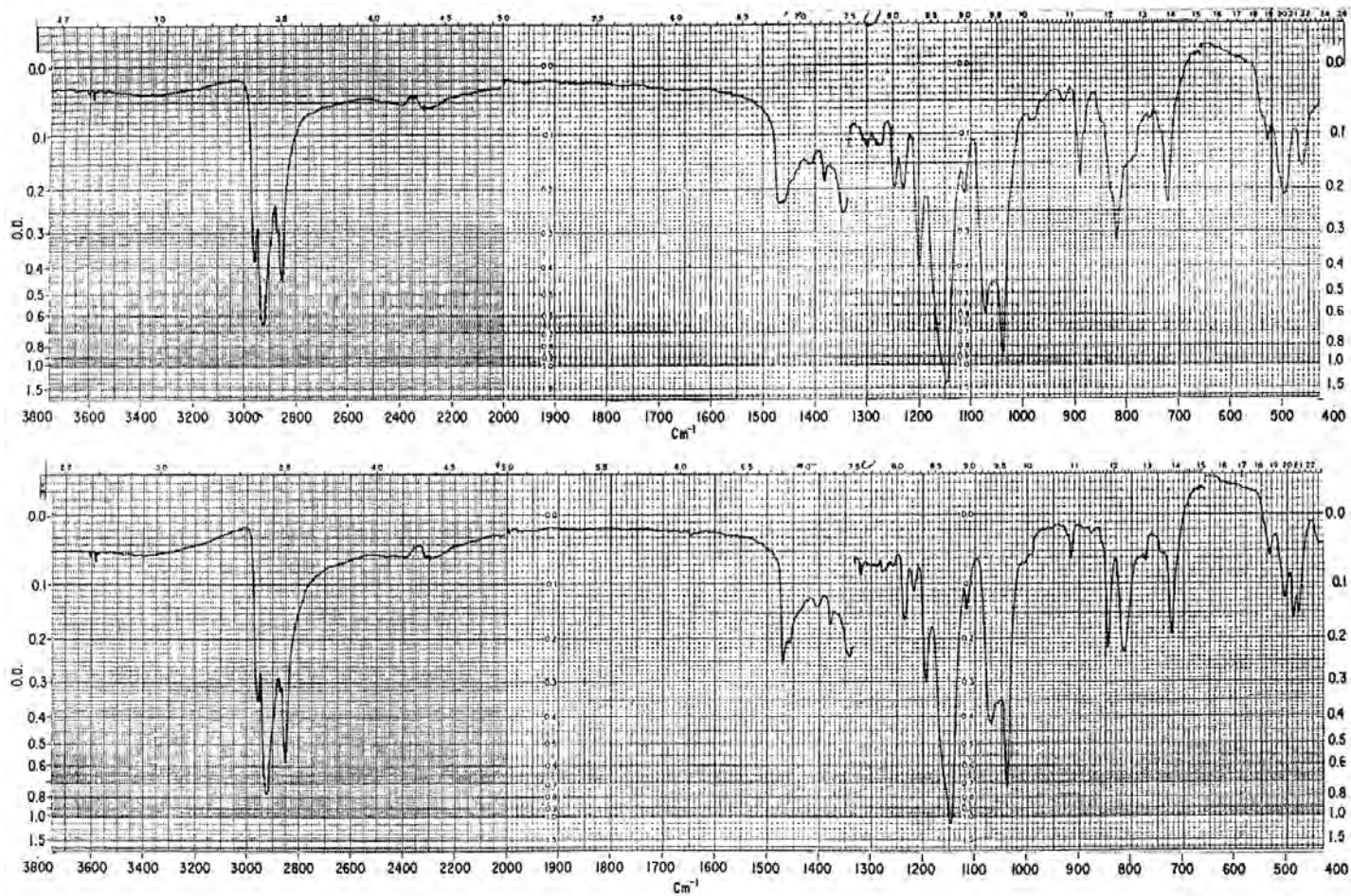


FIGURE 8.53a Top: IR spectrum for sodium diheptylphosphinate. (Bottom): IR spectrum for sodium dioctylphosphinate.

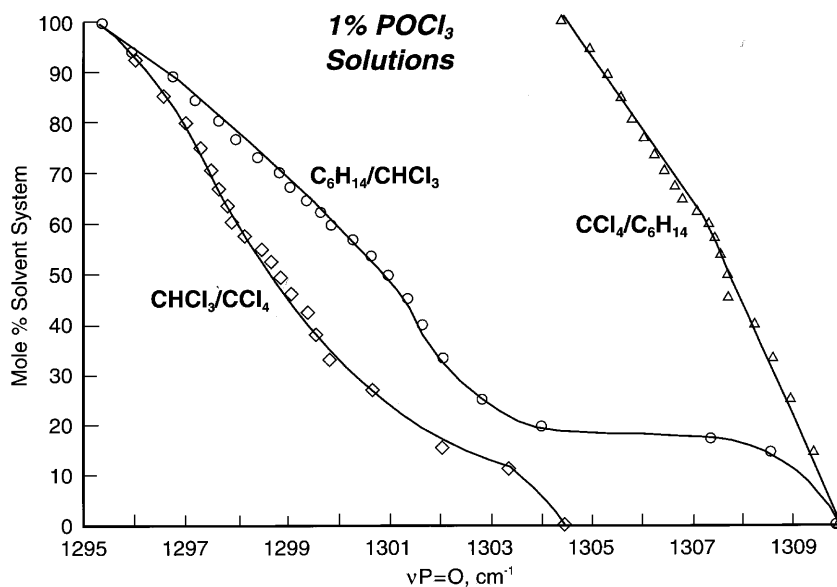


FIGURE 8.54 Plots of ν P=O for P(=O)Cl₃ vs mole % solvent system. The open triangles represent CCl₄/C₆H₁₄ as the solvent system. The open circles represent CHCl₃/C₆H₁₄ as the solvent system; and the open diamonds represent CHCl₃/CCl₄ as the solvent system (26).

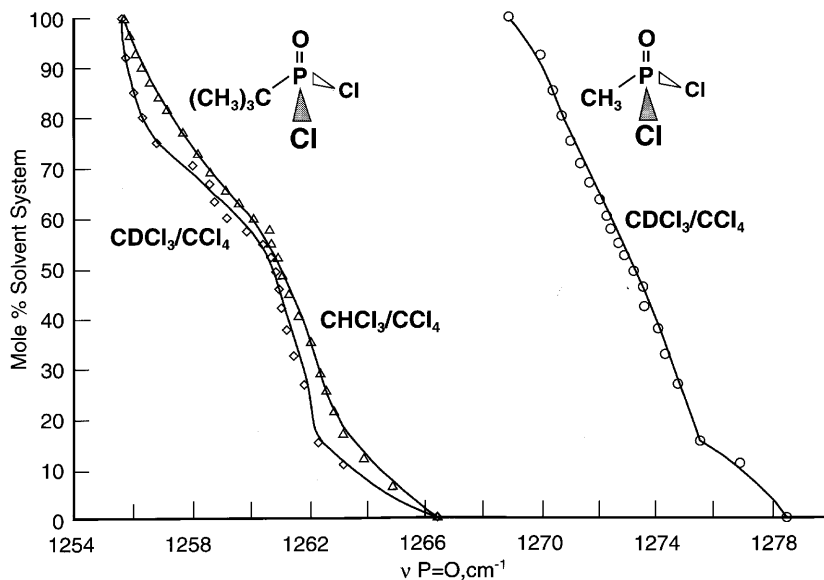


FIGURE 8.55 A plot of ν P=O for CH₃P(=O)Cl₂ vs mole % CDCl₃/CCl₄ as represented by open circles, and plots of ν P=O for (CH₃)₃C P(=O)Cl₂ vs mole % CHCl₃/CCl₄ (open triangles) and mole % (CDCl₃/CCl₄) (open diamonds) (26).

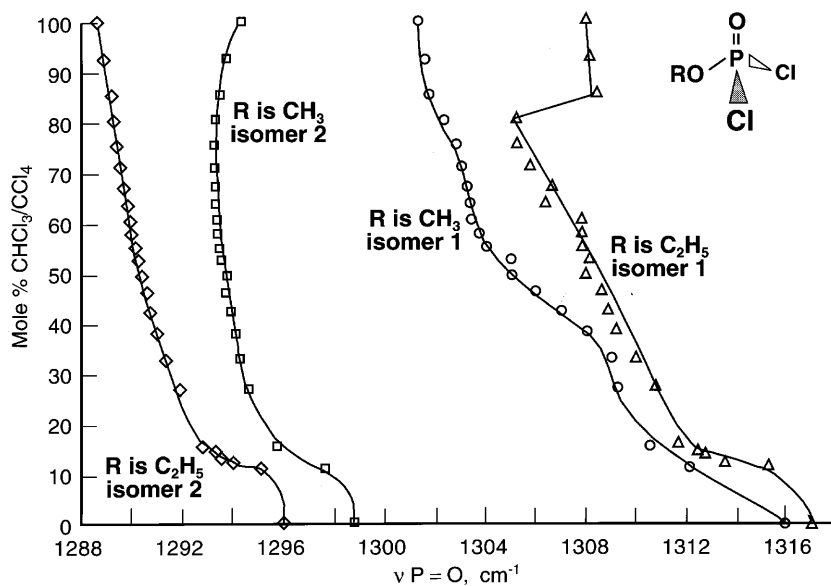


FIGURE 8.56 Plots of $\nu \text{P}=\text{O}$ rotational conformers 1 and 2 for $\text{CH}_3\text{O P}(=\text{O})\text{Cl}_2$ (conformer 1, open circles; conformer 2, open squares), and for $\text{C}_2\text{H}_5\text{OP}(=\text{O})\text{Cl}_2$ (conformer 1, open triangles; conformer 2, open diamonds) vs mole % $\text{CHCl}_3/\text{CCl}_4$ (26).

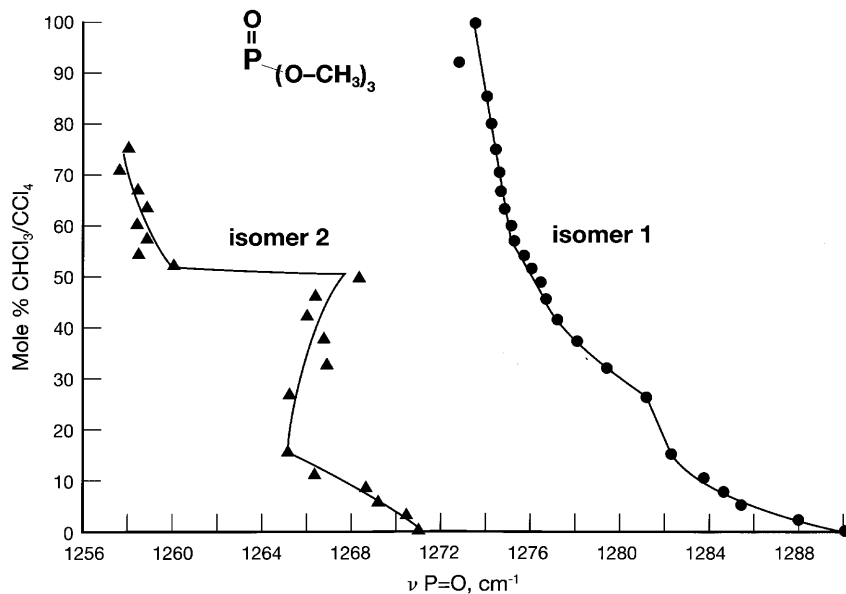


FIGURE 8.57 Plots of $\nu \text{P}=\text{O}$ rotational conformers 1 and 2 for $(\text{CH}_3\text{O})_3\text{P}=\text{O}$ vs mole % $\text{CHCl}_3/\text{CCl}_4$ (conformer 1, solid circles, and conformer 2, solid triangles) (55).

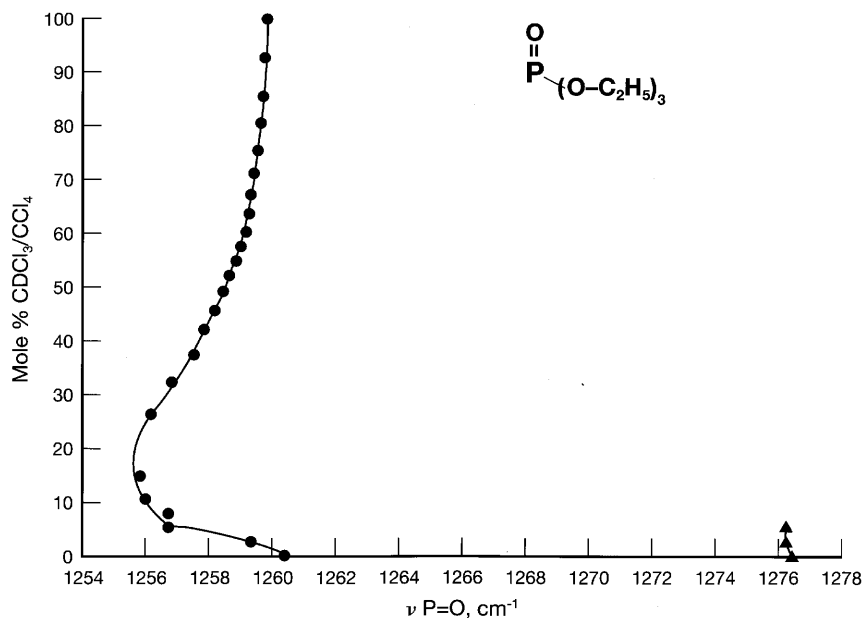


FIGURE 8.58 Plots of ν P=O rotational conformers 1 and 2 for $(\text{C}_2\text{H}_5\text{O})_3\text{P}=\text{O}$ vs mole % $\text{CDCl}_3/\text{CCl}_4$ (conformer 1, solid triangles, conformer 2, closed circles) (55).

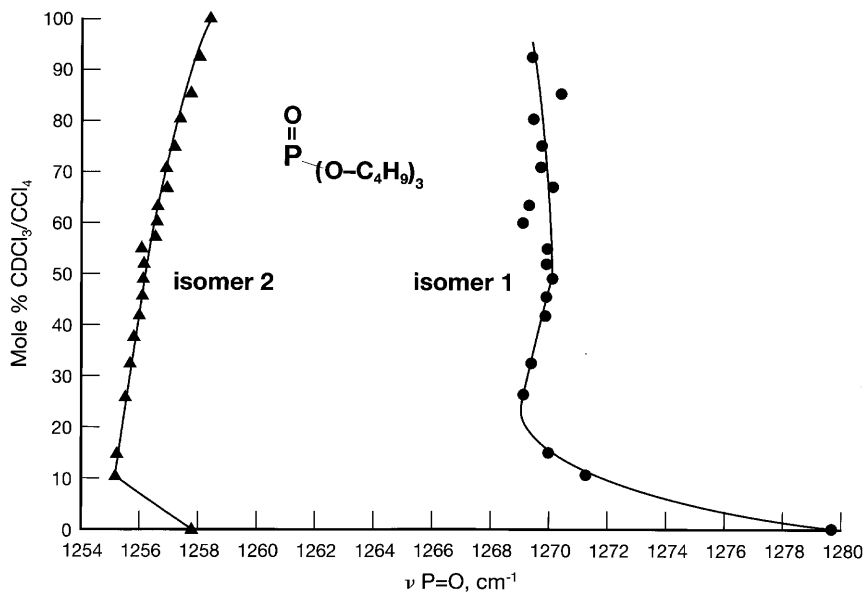


FIGURE 8.59 Plots of ν P=O rotational conformers 1 and 2 for $(\text{C}_4\text{H}_9\text{O})_3\text{P}=\text{O}$ vs mole % $\text{CDCl}_3/\text{CCl}_4$ (conformer 1, solid circles, conformer 2, solid triangles) (55).

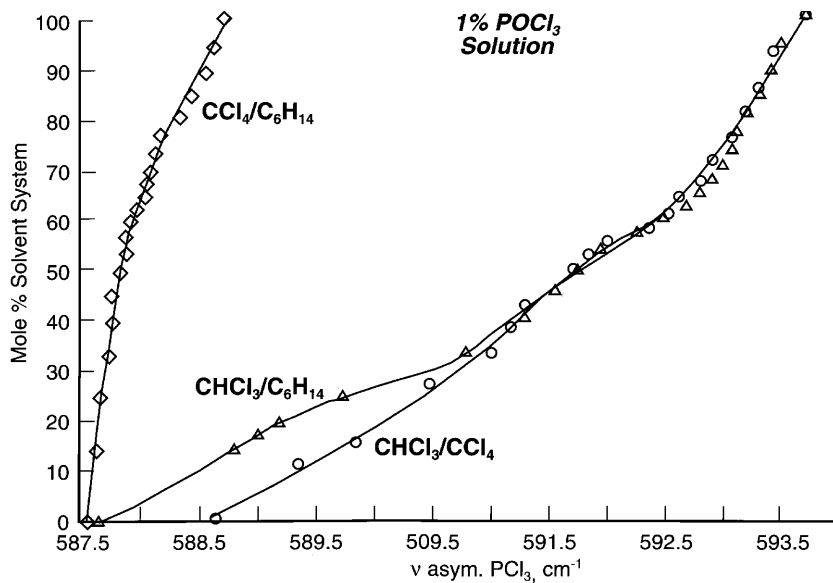


FIGURE 8.60 Plots of ν asym. PCl_3 for $\text{P}(\text{=O})\text{Cl}_3$ vs mole % solvent system. The open circles represent the $\text{CHCl}_3/\text{CCl}_4$ solvent system; the open triangles represent the $\text{CHCl}_3/\text{C}_6\text{H}_{14}$ solvent system; and the open diamonds represent the $\text{CCl}_4/\text{C}_6\text{H}_{14}$ solvent system (26).

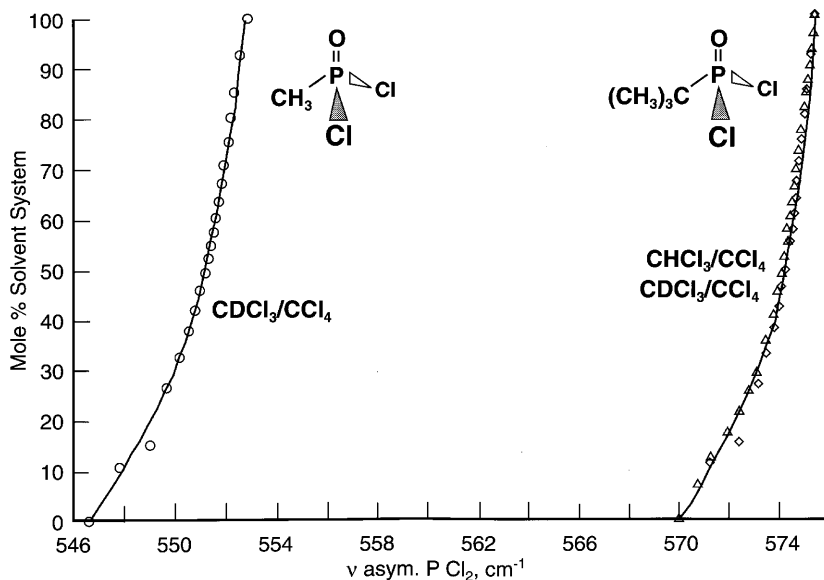


FIGURE 8.61 Plots of ν asym. PCl_2 frequencies for $\text{CH}_3\text{P}(\text{=O})\text{Cl}_2$ (open circles) and for $(\text{CH}_3)_3\text{CP}(\text{=O})\text{Cl}_2$ (open triangle and open diamonds) vs mole % $\text{CDCl}_3/\text{CCl}_4$ and $\text{CHCl}_3/\text{CCl}_4$ (26).

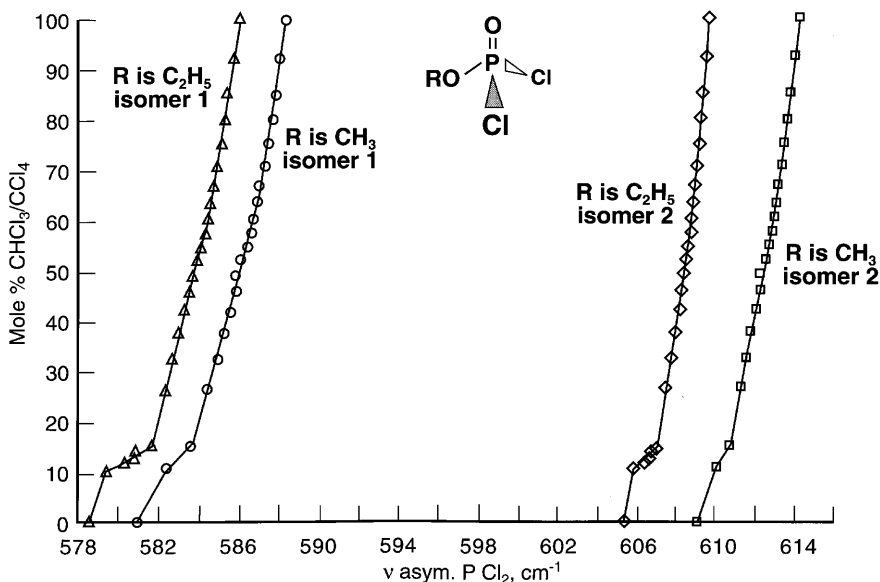


FIGURE 8.62 Plots of ν asym. PCl_2 rotational conformers 1 and 2 frequencies for $\text{CH}_3\text{OP}(=\text{O})\text{Cl}_2$ (conformer 1, open circles; conformer 2, open squares) and for $\text{C}_2\text{H}_5\text{OP}(=\text{O})\text{Cl}_2$ (conformer 1, open triangles, conformer 2, open diamonds) frequencies vs mole % $\text{CHCl}_3/\text{CCl}_4$ (26).

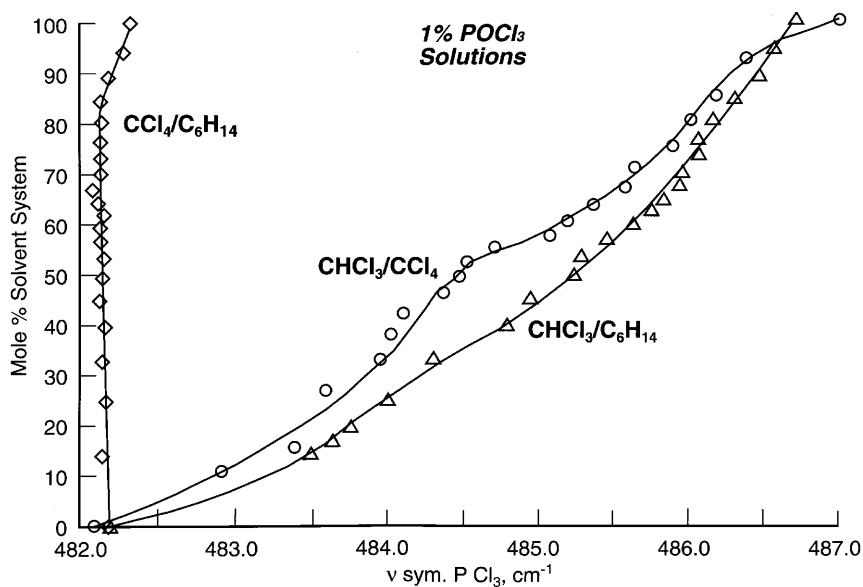


FIGURE 8.63 Plots of ν sym. PCl_3 frequencies for $\text{P}(=\text{O})\text{Cl}_3$ vs mole % solvent system. The open circles represent $\text{CHCl}_3/\text{CCl}_4$ as the solvent system, the open triangles represent the $\text{CHCl}_3/\text{C}_6\text{H}_{14}$ solvent system, and the open diamonds represent the $\text{CCl}_4/\text{C}_6\text{H}_{14}$ solvent system.

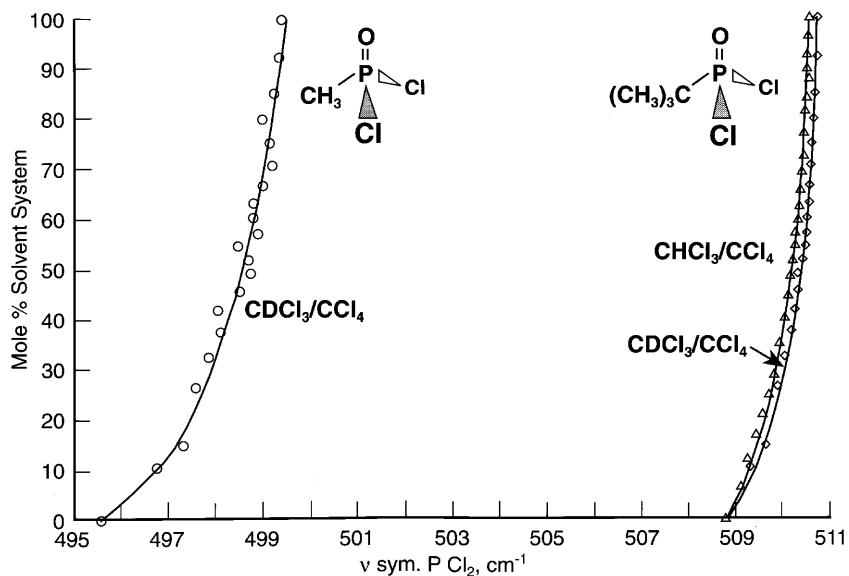


FIGURE 8.64 A plot of $\nu_{\text{sym. PCl}_2}$ frequencies for $\text{CH}_3\text{P}(=\text{O})\text{Cl}_2$ vs mole % $\text{CDCl}_3/\text{CCl}_4$ (open circles) and plots of $\nu_{\text{sym. PCl}_2}$ frequencies for $(\text{CH}_3)_3\text{CP}(=\text{O})\text{Cl}_2$ vs mole % $\text{CHCl}_3/\text{CCl}_4$ (open triangles) and mole % $\text{CDCl}_3/\text{CCl}_4$ (open diamonds) (26).

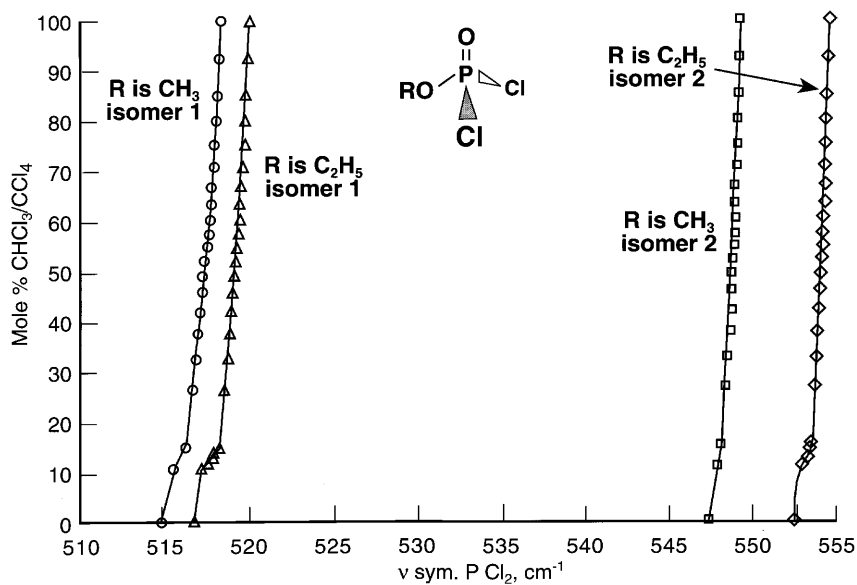


FIGURE 8.65 Plots of $\nu_{\text{sym. PCl}_2}$ rotational conformers 1 and 2 vs mole % $\text{CHCl}_3/\text{CCl}_4$. The open circles and open squares are for $\text{CH}_3\text{OP}(=\text{O})\text{Cl}_2$ conformers 1 and 2, respectively. The open triangles and open diamonds are for $\text{C}_2\text{H}_5\text{OP}(=\text{O})\text{Cl}_2$ conformers 1 and 2, respectively (26).

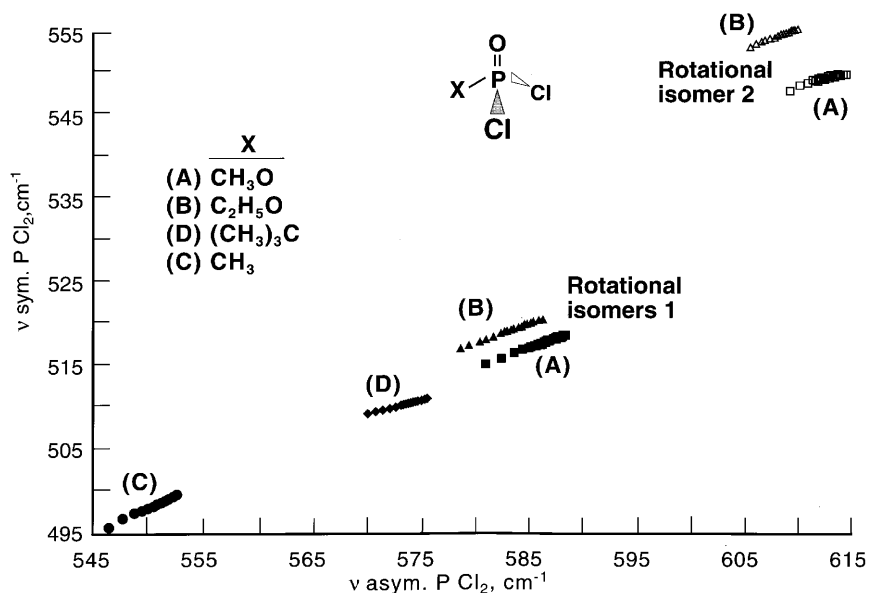


FIGURE 8.66 Plots of $\nu_{\text{asym. PCl}_2}$ frequencies vs $\nu_{\text{sym. PCl}_2}$ frequencies for CH₃OP(=O)Cl₂ (conformer 1, solid squares); CH₃OP(=O)Cl₂ (conformer 2, open squares); C₂H₅OP(=O)Cl₂ (conformer 1, solid triangles); C₂H₅OP(=O)Cl₂ (conformer 2, open triangles); (CH₃)₃CP(=O)Cl₂ (solid diamonds); and CH₃P(=O)Cl₂ (solid circles) (26).

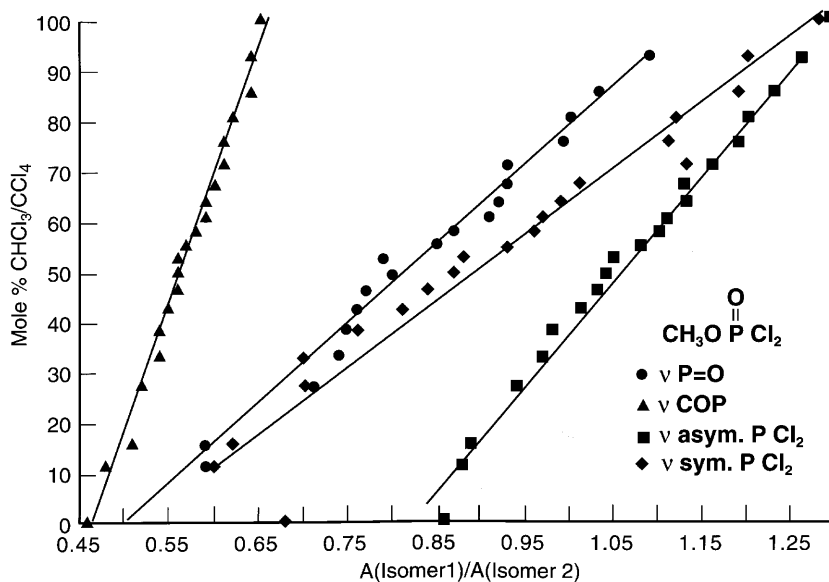


FIGURE 8.67 Plots of the absorbance (A) ratio of rotational conformer 1 and 2 band pairs for $\nu_{\text{P=O}}$ (solid circles), ν_{COP} (solid triangles), $\nu_{\text{asym. PCl}_2}$ (solid squares), and $\nu_{\text{sym. PCl}_2}$ (solid diamonds) for CH₃OP(=O)Cl₂ vs mole % CHCl₃/CCl₄ (26).

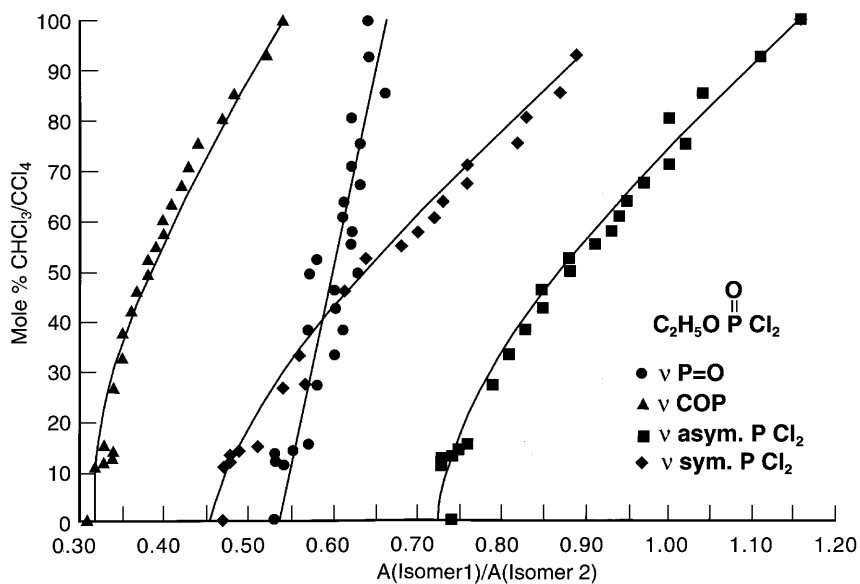


FIGURE 8.68 Plots of the absorbance (A) ratio of conformer 1 and 2 band pairs for ν P=O (solid circles), ν COP (solid triangles), ν asym. P Cl₂ (solid squares), and ν sym. P Cl₂ (solid diamonds) for C₂H₅OP(=O)Cl₂ vs mole % CHCl₃/CCl₄ (26).

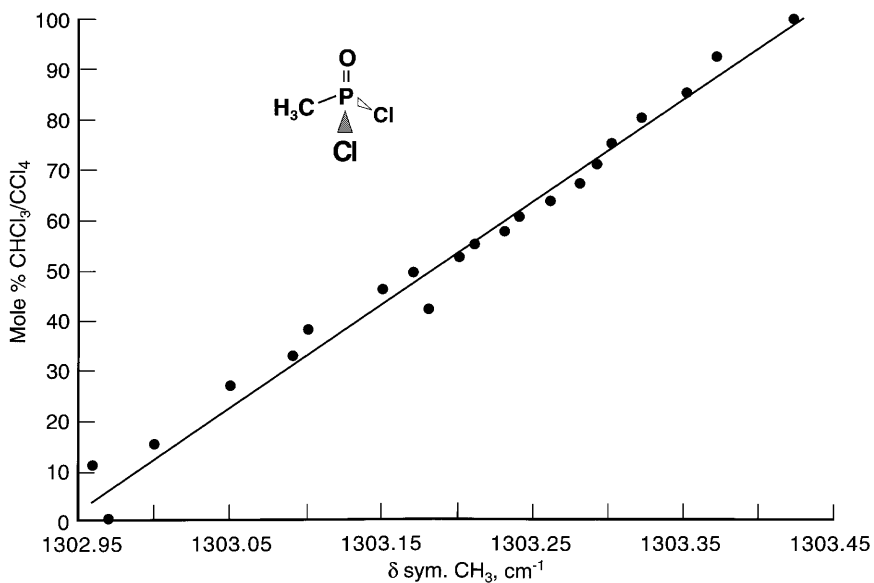


FIGURE 8.69 A plot of Δ sym. CH₃ frequencies for CH₃P(=O)Cl₂ vs mole % CHCl₃/CCl₄ (26).

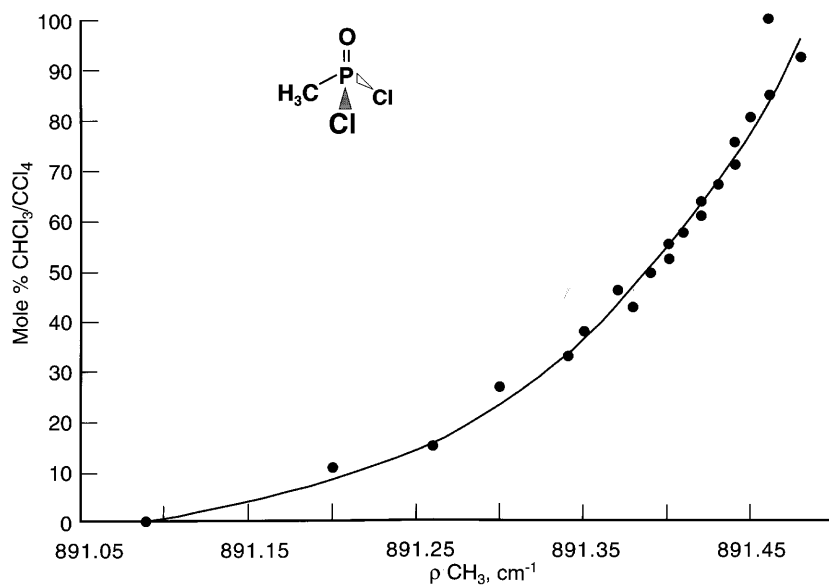


FIGURE 8.70 A plot of ρCH_3 frequencies for $\text{CH}_3\text{P}(=\text{O})\text{Cl}_2$ vs mole % $\text{CHCl}_3/\text{CCl}_4$ (26).

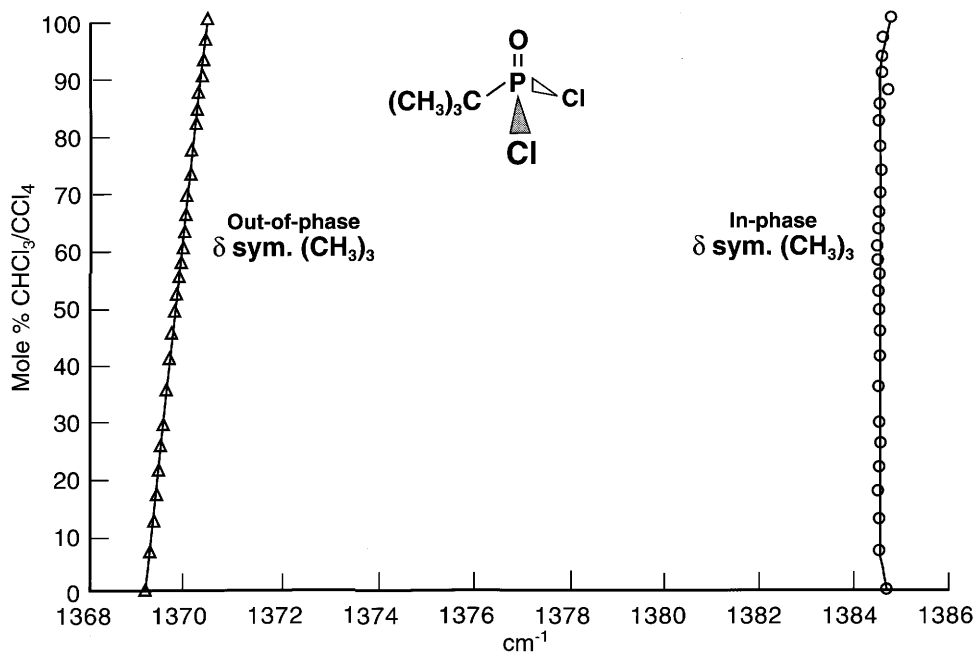


FIGURE 8.71 Plots of the in-phase δ sym. $(\text{CH}_3)_3$ frequencies (open circles) and the out-of-phase δ sym. $(\text{CH}_3)_3$ frequencies (open triangles) vs mole % $\text{CHCl}_3/\text{CCl}_4$ (26).

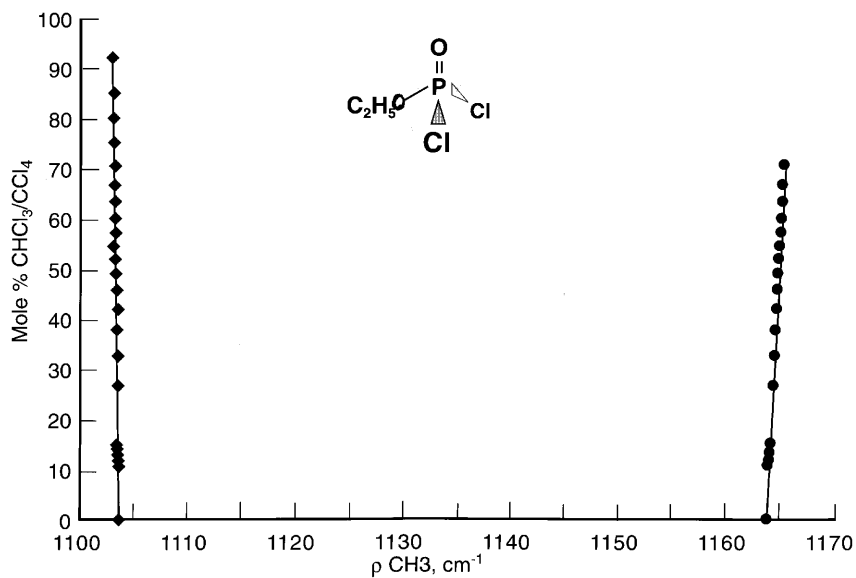


FIGURE 8.72 Plots of the a' and a'' ρCH_3 frequencies for $\text{C}_2\text{H}_5\text{O P}(=\text{O})\text{Cl}_2$ vs mole % $\text{CHCl}_3/\text{CCl}_4$ (26).

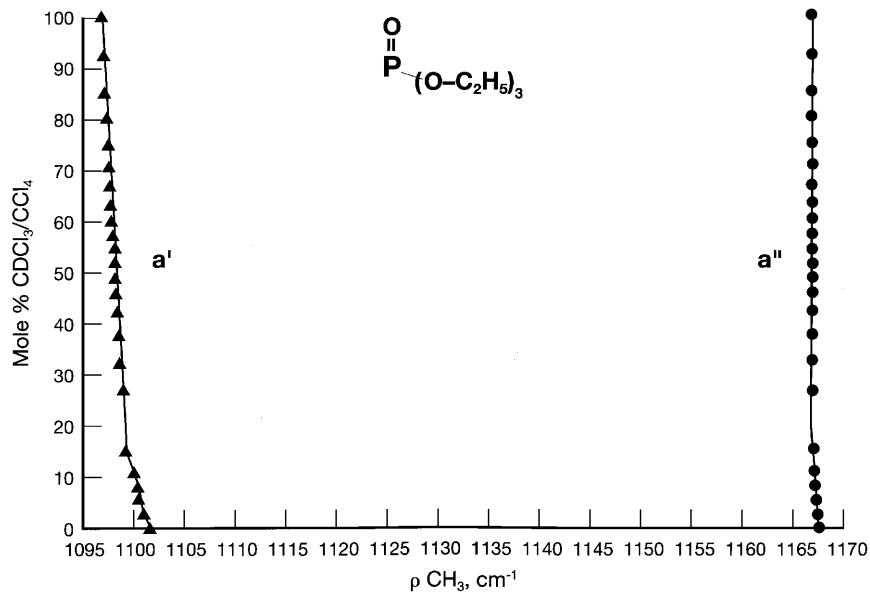


FIGURE 8.73 Plots of the a' and a'' ρCH_3 modes of $(\text{C}_2\text{H}_5\text{O})_3\text{P}=\text{O}$ vs mole % $\text{CDCl}_3/\text{CCl}_4$ (55).

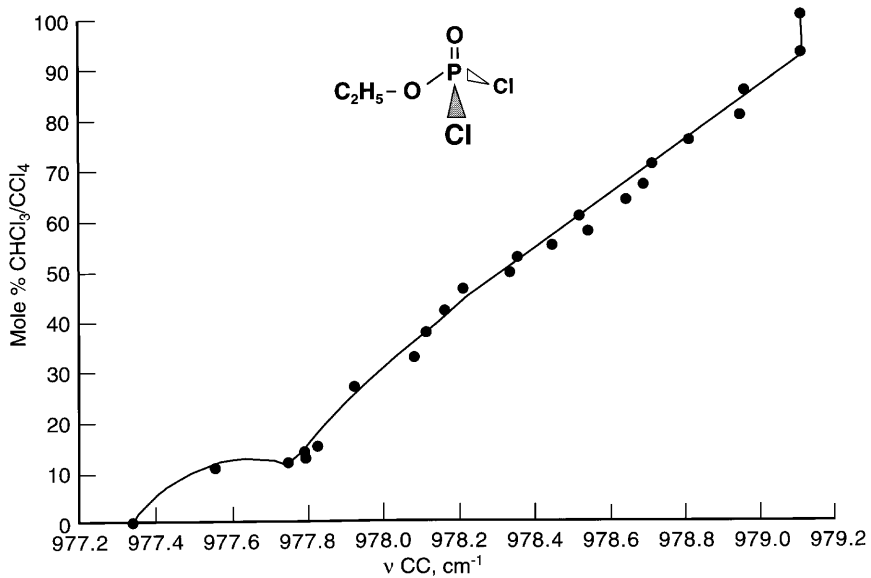


FIGURE 8.74 A plot of ν CC for $C_2H_5OP(=O)Cl_2$ vs mole % $CHCl_3/CCl_4$ (26).

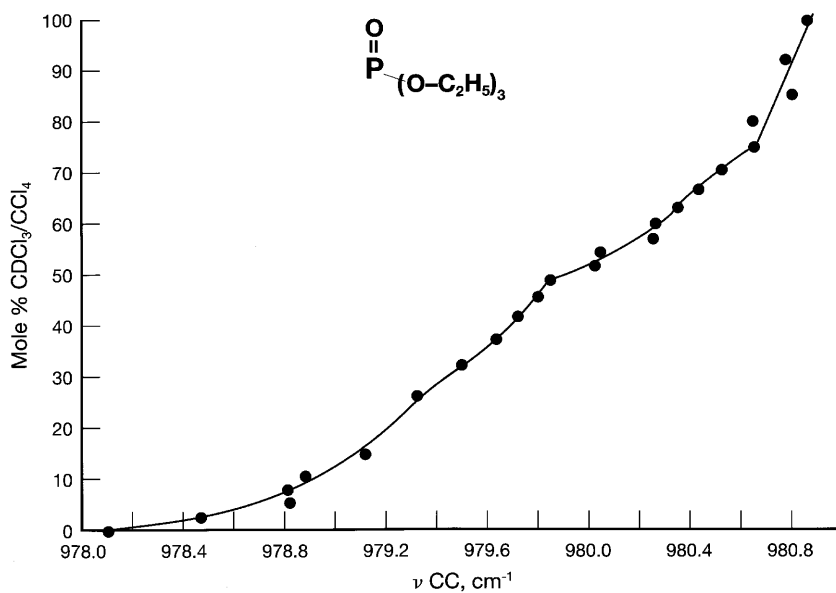


FIGURE 8.75 A plot of ν CC for $(C_2H_5O)_3P=O$ vs mole % $CDCl_3/CCl_4$ (55).

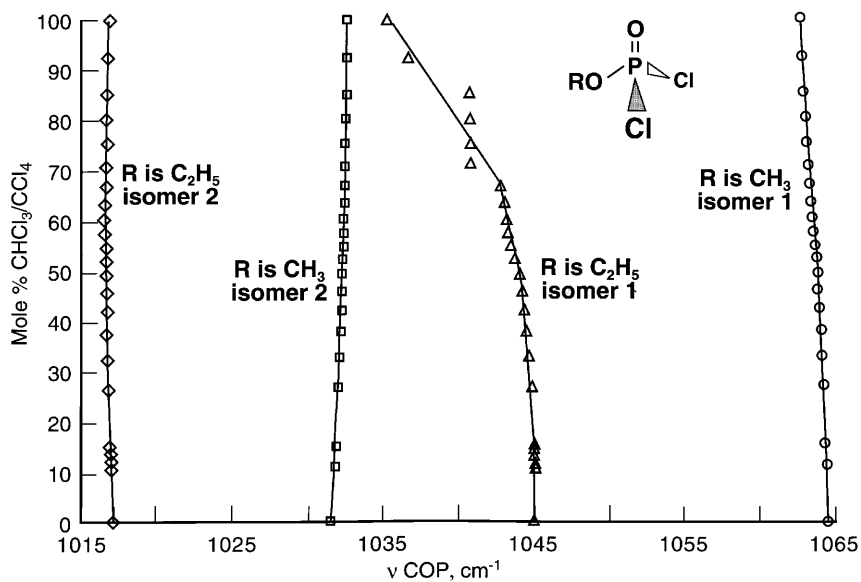


FIGURE 8.76 Plots of ν COP rotational conformers 1 and 2 for $\text{CH}_3\text{O P(=O)Cl}_2$ and $\text{C}_2\text{H}_5\text{OP(=O)Cl}_2$ vs mole % $\text{CDCl}_3/\text{CCl}_4$ (26).

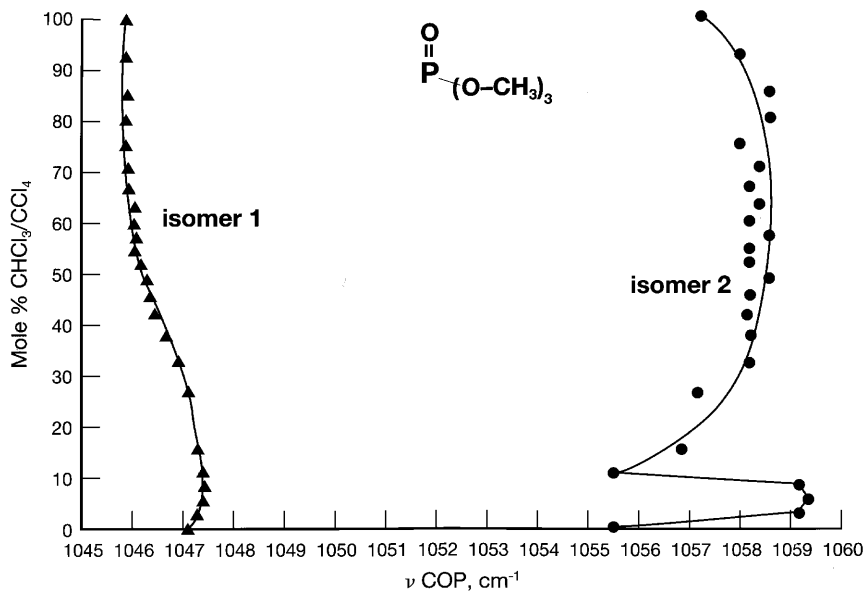


FIGURE 8.77 Plots of ν COP rotational conformers 1 and 2 frequencies for $(\text{CH}_3\text{O})_3\text{P=O}$ vs mole % $\text{CHCl}_3/\text{CCl}_4$. The solid triangles represent conformer 1 and the solid circles represent conformer 2 (55).

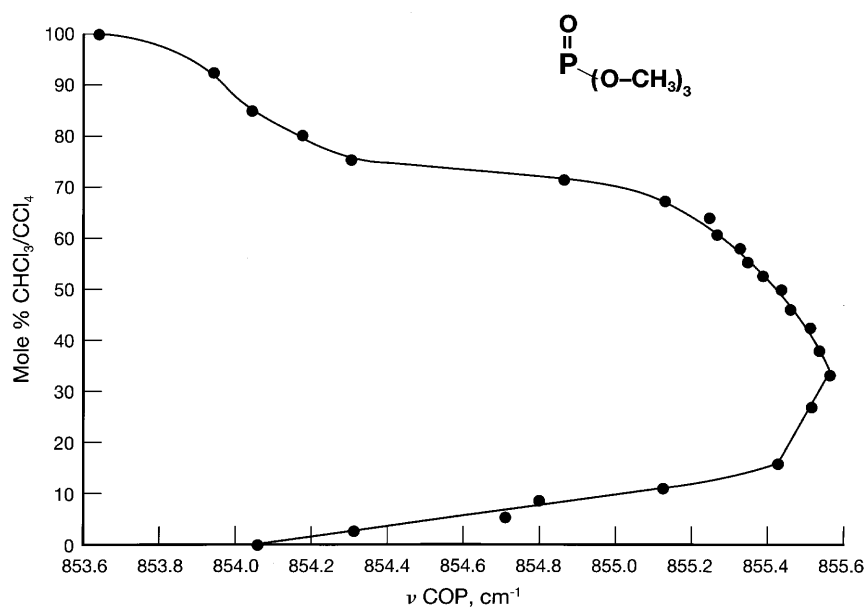


FIGURE 8.78 A plot of $\nu \text{ COP}$ frequencies for $(\text{CH}_3\text{O})_3\text{P}=\text{O}$ vs mole % $\text{CHCl}_3/\text{CCl}_4$ (55).

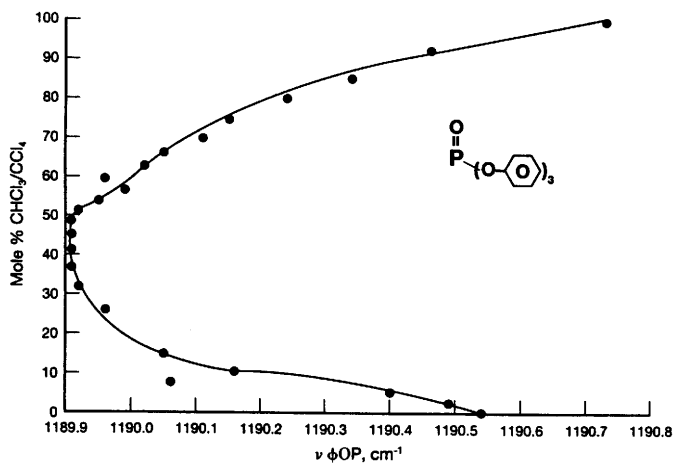


FIGURE 8.79 A plot of $\nu(\phi\text{OP})$, " $\nu \Phi\text{-O}$ ", frequencies for triphenyl phosphate vs mole % $\text{CHCl}_3/\text{CCl}_4$ (55).

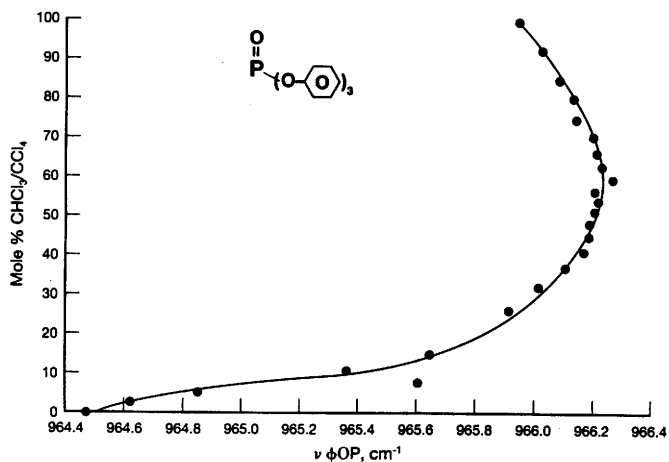


FIGURE 8.80 A plot of $\nu(\Phi\text{OP})$, “ $\nu\text{P-O}$ ”, frequencies for triphenyl phosphate vs mole % $\text{CHCl}_3/\text{CCl}_4$ (55).

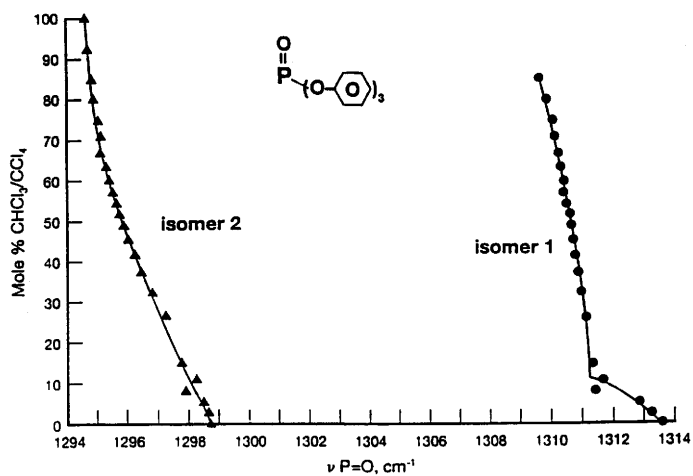


FIGURE 8.81 A plot of the in-plane hydrogen deformation frequencies for the phenyl groups of triphenyl phosphate vs mole % $\text{CHCl}_3/\text{CCl}_4$ (55).

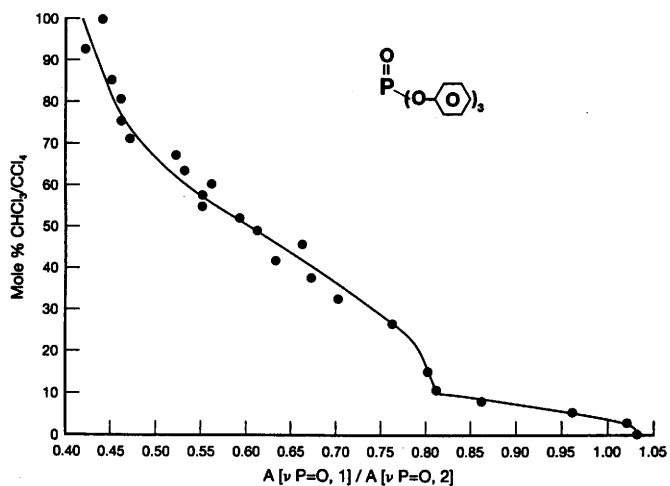


FIGURE 8.82 A plot of the out-of-plane ring deformation frequencies for the phenyl groups of triphenyl phosphate vs mole % CHCl₃/CCl₄ (55).

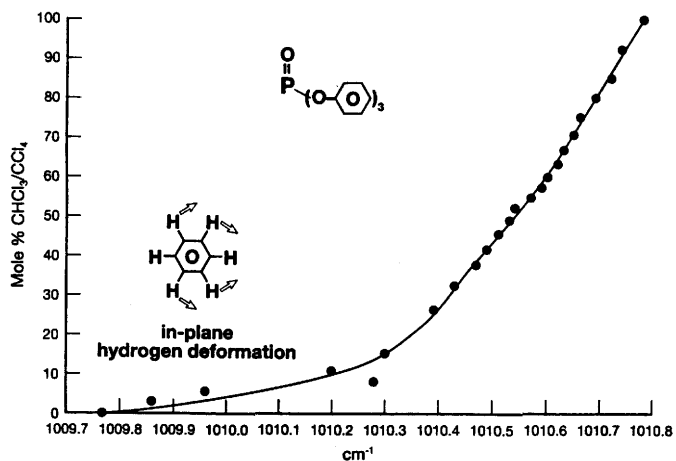


FIGURE 8.83 A plot of ν_{CD} frequencies (for the solvent system CDCl₃/CCl₄) vs mole % CDCl₃/CCl₄ (55).

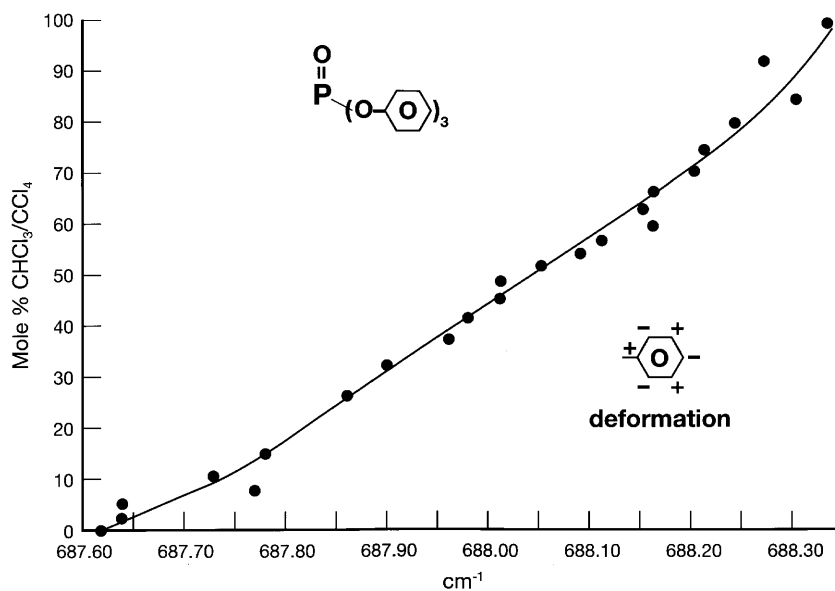


FIGURE 8.84 A plot of the ν CD frequencies for CDCl₃ vs mole % CDCl₃/CCl₄ for the CDCl₃/CCl₄ solvent system containing 1 wt./vol. % triphenylphosphate (55).

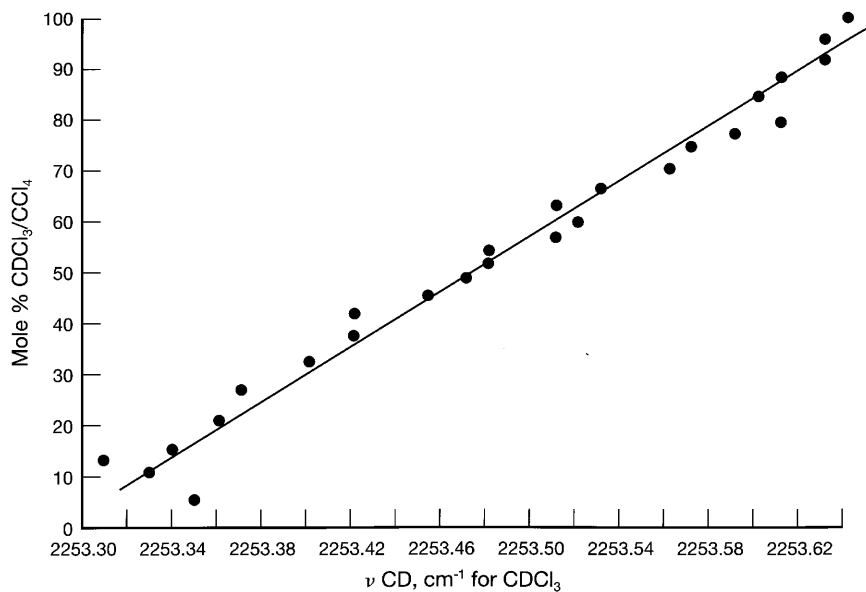


FIGURE 8.85 A plot of ν CD for CDCl₃ vs mole % CDCl₃/CCl₄.

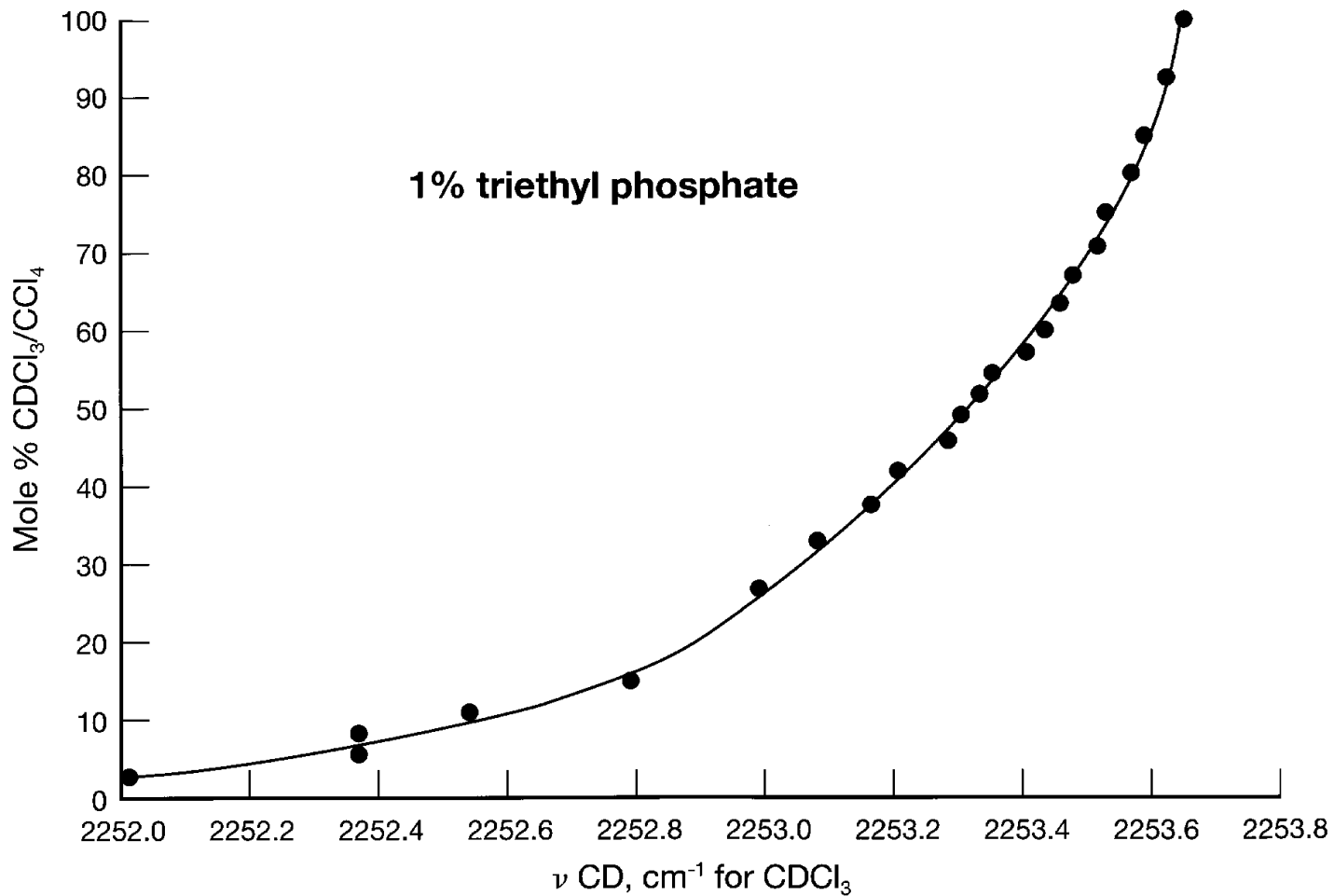
FIGURE 8.86 A plot of $\nu \text{ CD}$ for CDCl_3 vs mole% $\text{CDCl}_3/\text{CCl}_4$ containing 1% triethylphosphate.

TABLE 8.1 Phosphorus halogen stretching frequencies for inorganic compounds*

Compound PX ₃ X	F stretching cm ⁻¹	Cl stretching cm ⁻¹	Br stretching cm ⁻¹	I stretching cm ⁻¹	Assignment	References
F ₃	890(s.);840(a.)				v1,a1;v3,e	1,2,3,4
FCl ₂	827	524(s.);496(a.)			a' ; a' ; a''	5
FClBr	822	500	415		a ; a ; a	5
FBr ₂	817		421(s.);393(a.)		a' ; a' ; a''	5
Cl ₃		511(s.);484(a.)			v1,a1;v3,e	6
Cl ₂ Br		510(s.);480(a.)	~ 400		a' ; a'' ; a'	5
ClBr ₂		~ 480	400(s.);380(a.)		a' ; a' ; a''	5
Br ₃			380(s.);400(a.)		v1,a1;v3,e	5
I ₃				303(s.);325(a.)	v1,a1;v3,e	6
P(=S)X ₃						
X						
F ₃	981(s.);945(a.)				v2,a1;v4,e	7
F ₂ Cl	946(s.);920(a.)	541			a' ; a'' ; a'	7
F ₂ Br	930(s.);899(a.)		~ 468		a' ; a'' ; a'	8
FCl ₂	900	476(s.);567(a.)			a' ; a'' ; a'	9
Cl ₃		431(s.);547(a.)			v2,a1;v4,e	10,11
Br ₃			299(s.);438(a.)		v2,a1;v4,e	12
P(=O)X ₃						
X						
F ₃	875(s.);982(a.)				v2,a1;v4,e	1
F ₂ Cl	895(s.);948(a.)	618			a' ; a'' ; a'	13
F ₂ Br	888(s.);940(a.)		554		a' ; a'' ; a'	13
FCl ₂	894	547(s.);620(a.)			a' ; a' ; a''	14
FClBr	890	590	495		a ; a ; a	13
FBr ₂	880		466(s.);538(a.)		a' ; a' ; a''	13
Cl ₃		486(s.);581(a.)			v2,a1;v4,e	15
Cl ₂ Br		545(s.);580(a.)	432		a' ; a'' ; a'	13
ClBr ₂		552	391(s.);492(a.)		a' ; a' ; a''	13
Br ₃			340(s.);488(a.)		v2,a1;v4,e	8,15

*See Reference 16.

TABLE 8.2 The PX_3 bending frequencies for compounds of form PX_3 , PXY_2 , and $PXYZ$ *¹

Compounds & symmetry	Species & Assignment s. bending	Compound & symmetry	Species & Assignment	Compound & symmetry	Species & Assignment	Compound References
C3v	v2,a1 cm ⁻¹	Cs	v3,a' cm ⁻¹	Ci	v4,a cm ⁻¹	see Table 8.1
PF ₃	486	PClF ₂	[390–400]* ²			
		PBF ₂	[367–375]			
		PF ₂ I	[327–340]			
		PCl ₂ F	327			
		PBr ₂ F	257	PBrClF	302	
				PClFI	[250–275]	
PCl ₃	261			[PBrFI]	[220–252]	
		PBrCl ₂	230			
		PF ₂ I	[190–220]			
		PBr ₂ Cl	197			
		PCl ₂ I	[175–202]			
PBr ₃	165			PBrClI	[167–195]	
		PBr ₂ I	[135–157]			
		PClI ₂	[133–155]			
		PbrI ₂	[120–135]			
PI ₃	113					

*¹See Reference 16.*²All numbers in brackets are estimated frequencies.

TABLE 8.3 Vibrational data and assignments for PX_3 , $P(=O)X_3$, and $P(=S)X_3$ *¹

	P C3v,e	P=O C3v,e	P=S C3v,e	P Cs,a'	P=O Cs,a'	P=S Cs,a'	P Ci,a	P=O Ci,a	P=S Ci,a	Compound References
PX(1-3)	v4,cm ⁻¹	v6,cm ⁻¹	v6,cm ⁻¹	v6,cm ⁻¹	v6,cm ⁻¹	v6,cm ⁻¹	v6,cm ⁻¹	v9,cm ⁻¹	v9,cm ⁻¹	
F3	347	345	276							See Table 8.1
ClF				[245-262]* ²	274	209				
BrF ₂				[166-178]	[170-190]	175				
F ₂ l				[126-145]	[140-150]	[130-140]				
Cl ₂ F				200	207	191				
BrClF							161	173	[140-160]	
Br ₂ F				126	134	[125-135]				
ClFl							[126-136]	[130-140]	[125-135]	
Cl ₃	191	193	172							
BrFl							[109-119]	[125-135]	[110-130]	
BrCl ₂				149	161	[135-155]				
Fl ₂				[97-105]	[100-120]	[100-120]				
Br ₂ Cl				123	130	[115-130]				
Cl ₂ l				[119-129]	[125-135]	[115-130]				
Br ₃	116	118	115							
BrClI							[105-116]	[110-125]	[100-120]	
Br ₂ l					[90-115]	[90-115]				
ClI ₂				[94-101]	[90-115]	[90-115]				
BrI ₂				[87-93]	[90-110]	[90-110]				
I ₃	85	[70-90]	[70-90]							

*¹See Reference 16.*²All numbers in brackets are estimated frequencies.

TABLE 8.4 The asym. and sym. PCl₂ stretching frequencies for XPCl₂, XP(=O)Cl₂, and XP(=S)Cl₂ groups

Compound	a.PCl ₂ str. cm ⁻¹	s.PCl ₂ str. cm ⁻¹	Ref.	[a.PCl ₂ str.]– [s.PCl ₂ str.] cm ⁻¹	Compound	a.PCl ₂ str. cm ⁻¹	s.PCl ₂ str. cm ⁻¹	Ref.	[a.PCl ₂ str.]– [s.PCl ₂ str.] cm ⁻¹
CH ₃	495	495	17,18	0					
ClCH ₂	490	490	17	0					
CH ₃ –O	506	453	19	53					
CH ₃ –O	505	456	19	49					
X – P(=O)Cl ₂	[CCl ₄]/[CHCl ₃]	[CCl ₄]/[CHCl ₃]			X–P(=S)Cl ₂				
X	cm ⁻¹	cm ⁻¹							
CH ₃	552	497	17,18	55	CH ₃	520	464	17,18	56
CH ₃	[546.6* ¹]/[552.8* ²]	[495.6* ¹]/[499.4* ²]	26	51* ¹ , 53.4* ²					
(CH ₃) ₃ C	[570.1* ¹]/[575.5* ²]	[508.8* ¹]/[510.6* ²]	26	61.3* ¹ ; 64.9* ²					
ClCH ₂	556/566	487/508	17	69:61	ClCH ₂	527	452/461	17	65; or 75
C ₆ H ₅	565	542	20	23	C ₆ H ₅	521	501	20	20
CH ₃ –O	579–607	515/548	21	64:59	CH ₃ –O	531/560	456/478	21,25	75:82
					CD ₃ –O	531/552	452/471	21,25	79:81
CH ₂ H ₃ –O	576/600	516/550	22	60:50	C ₂ H ₅ –O	528/558	472/490	22	56:68
					CH ₃ –CD ₂ –O	525/550	465/484	22	69:66
					CD ₃ –CH ₂ –O	531/552	462/483	22	69:69
					iso-C ₃ H ₇ –O	521/548	483/500	20	59:69
					iso-C ₄ H ₉ –O	528/553	473/493	20	55:60
					s.-C ₄ H ₉ –O	525/547	485/500	20	40:47
					iso-C ₅ H ₁₁ –O	528/552	455/465	20	73:87
					H–CC–CH ₂ –O	529/557	440/474	26	89:83
4-Cl–C ₆ H ₄ –O	585/600	?/555	20	[–; 45]	4-Cl–C ₆ H ₄ –O	560	?/471	20	89
					2,4-Cl ₂ –C ₆ H ₃ –O	?/551	?	20	[–]
					2,6-Cl ₂ –C ₆ H ₃ –O	555	472	20	83
2,4,5-Cl ₃ –C ₆ H ₂ –O	587/602	?	20	[–; –]	2, 4, 5-Cl ₃ –C ₆ H ₂ –O	?/565	?/448	20	117?
CH ₃ –S	547/560	449/471	23	98:89					
CH ₃ –NH	560	517	24	43	CH ₃ –NH	512	450/468	24	62; or 44
					CD ₃ –NH	515	446/463	24	69; or 52
					CH ₃ –ND	513	447/470	24	66; or 43
					CD ₃ –ND	510	443/461	24	67; or 49
					C ₂ H ₅ –NH	512	?463	24	[–; 49]
					iso-C ₃ H ₇ –NH	514	?/481	24	[–; 33]
(CH ₃) ₂ –N	560	517	20	43	(CH ₃) ₂ –N	512	450	20	62
(C ₂ H ₅) ₂ –N	560	523	20	37	(C ₂ H ₅) ₂ –N	522	481	20	41

*¹In CCl₄ soln.*²In CHCl₃ soln. Other data are in CS₂ soln.

TABLE 8.5 Vibrational assignments for $F_2P(=S)Cl$, $(CH_3-O-)_2P(=S)Cl$, and $(CD_3-O-)_2P(=S)Cl$

Assignment	[11] $ClF_2P(=S)$ cm^{-1}	[27] $Cl(CH_3-O-)_2P(=S)$ cm^{-1}	[27] $Cl(CD_3-O-)_2P(=S)$ cm^{-1}	[(CH_3O) ₂]- [(CD_3O_2)] cm^{-1}	Assignment
s.PF ₂ str., a'	939	~ 845	783.2	61.8	s.p(-O-) ₂ str.
a.PF ₂ str., a''	913	836.2	807.3	28.9	a.p(-O-) ₂ str.
P=S str., a'	727	666.1	649.1	17	P=S str.* ¹
		654.7	649.1	5.6	P=S str.* ¹
P-Cl str., a'	536	524.7	519.6	5.1	P-Cl str.* ¹
		485.7	482	3.7	P-Cl str.* ¹
PF ₂ wag, a'	394	396	376	2	P(-O-) ₂ wag* ¹
		375	348	27	P(-O-) ₂ wag* ¹
PF ₂ wag, a'	359	352	341	11	P(-O-) ₂ bend
PF ₂ twist, a''	314	291	288	3	p(-O-) ₂ twist* ¹
		276	272	4	P(-O-) ₂ twist* ¹
Cl-P(=S)	251	233	215	18	Cl-P(=S)
out-of-plane bend, a''					out-of-plane bend
Cl-P(=S)	207	217	215	2	Cl-P(=S)
in-of-plane bend, a''					in-of-plane bend
		1055.9	1076.4	[-20.5]	s.(C-O-) ₂ P str.* ¹
		1042	1059	[-17.0]	s.(C-O-) ₂ P str.* ¹
		1031.1	1050	[-18.9]	a(C-O-) ₂ P str.
		449	428	21	(C-O-) ₂ P bend, a'
		426	405	21	(C-O-) ₂ P bend, a''
		171	157	14	(C-O-) ₂ P, a' & a''
				CH ₃ /CD ₃	
		3025.7	2273	1.33	a.CH ₃ str. or a.CD ₃ str., a''
		3002.2	2255.3	1.33	a.CH ₃ str. or a.CD ₃ str., a'
		2952.3	2077.1	1.42	s.CH ₃ str. or CD ₃ str., a'
		[2922.3]* ²	[2109.3]* ¹	1.39	2(CH ₃ bend) or 2(CD ₃ bend). a'
		2848	2203	1.29	
		[2878]* ¹	[2170.9]* ¹	1.33	
		1456.9	1099.4	1.33	a.CH ₃ or a.CD ₃ bend a' & a''
		1443.1	1099.4	1.31	s.CH ₃ or CD ₃ bend, a'
		1179.9	926.1	1.27	CH ₃ or CD ₃ rock, a' (in-plane)
		1160	900	1.29	CH ₃ or CD ₃ rock, a'' (out-of-plane)
		200	189	1.06	CH ₃ or CD ₃ torsion a' & a''

*¹Rotational conformers.

TABLE 8.5a The PCl_2 stretching frequencies for methyl phosphorodichloridate and O-methyl phosphorodichlorothioate*

Mode	[A] $\text{CH}_3\text{-O-P(=O)Cl}_2$ cm^{-1}	[B] $\text{CH}_3\text{-O-P(=S)Cl}_2$ cm^{-1}	[A]-[B] cm^{-1}	[C] $\text{CD}_3\text{-O-P(=S)Cl}_2$ cm^{-1}	[A]-[C] cm^{-1}	[B]-[C] cm^{-1}
a. PCl_2 str.						
conformer 1	579	531	48	531	48	0
conformer 2	607	560	47	552	55	8
delta[$\text{C}_2\text{-C}_1$]	[28]	[29]	[1]	[21]	[7]	[8]
s. PCl_2 str.						
conformer 1	515	456	59	452	63	4
conformer 2	548	478	70	471	77	7
delta[$\text{C}_2\text{-C}_1$]	[33]	[22]	[11]	[19]	[14]	[3]

*See Reference 21.

TABLE 8.6 P-Cl stretching frequencies

Compound	P-Cl str.	Ref.	Frequency separation between rotational conformers	Compound	P-Cl str.	Ref.	Frequency separation between rotational conformers
X-P(=O)Cl				X-P(=S)Cl			
X				X			
$(\text{CH}_3\text{-O})_2$	553/598	27	45	$(\text{CH}_3\text{-O})_2$	486/525	27	39
$(\text{C}_2\text{H}_5\text{-O})_2$	554/589	20	35	$(\text{CD}_3\text{-O})_2$	482/519	27	37
$(\text{n-C}_3\text{H}_7\text{-O})_2$	557/597	20	40	$(\text{C}_2\text{H}_5\text{-O})_2$	502/539	32	37
$[(\text{CH}_3)_2\text{N-}]_2$	540	20		$(\text{n-C}_3\text{H}_7\text{-O})_2$	505/538	20	33
$(\text{CH}_3\text{-O})(\text{CH}_3\text{-NH})$	532/583	20	51	$[(\text{CH}_3)_2\text{N-}]^2$	493	20	
				$[(\text{C}_2\text{H}_5)_2\text{N-}]_2$	515	20	
				$(\text{CH}_3\text{-O})(\text{CH}_3\text{-NH})$	479/530	20	51
				$(\text{CH}_3\text{-O})[(\text{CH}_3)_2\text{N}]$	470/528	20	58
				$(\text{CH}_3\text{-O})(\text{CH}_3\text{-NH})$	491/543	20	52
				$(\text{CH}_3\text{-O})(\text{iso-C}_3\text{H}_7\text{-NH})$	508/538	20	30
				$(\text{C}_2\text{H}_5\text{-O})(\text{CH}_3\text{-NH})$	479/532	20	53
				$(\text{C}_2\text{H}_5\text{-O})(\text{C}_2\text{H}_5\text{-NH})$	483/532	20	49
				$(\text{C}_2\text{H}_5\text{-O})(\text{iso-C}_3\text{H}_7\text{-NH})$	501/536	20	35
				$(\text{iso-C}_3\text{H}_7\text{-O})(\text{CH}_3\text{-NH})$	483/531	20	48
				$(\text{iso-C}_3\text{H}_7\text{-O})(\text{C}_2\text{H}_5\text{-NH})$	485/532	20	47
				$(\text{iso-C}_3\text{H}_7\text{-O})(\text{iso-C}_3\text{H}_7\text{-NH})$	498/532	20	34

TABLE 8.7. Vibrational assignments for the CH₃, CD₃, C₂H₅, CH₃CD₂ and CD₃CH₂ groups of R–O–R(=O)Cl₂ and R–O–P(=S)Cl₂ analogs

[A] Compound CH ₃ –O–P(=S)Cl ₂ cm ⁻¹	[B] Compound CD ₃ –O–P(=S)Cl ₂ cm ⁻¹	[C] Compound	[D] Compound CH ₃ –O–P(=O)Cl ₂ cm ⁻¹	Assignment [22]	[A]/[B]
3030	2279		3030	a.CH ₃ str., a'' or CD ₃ , a''	1.33
3004	2250		3008	a.CH ₃ str., a' or CD ₃ , a'	1.34
2959	2198		2960	s.CH ₃ str., a' [in Fermi res.] or CD ₃ , a'	1.35
2848	2071		2852	2(CH ₃ bend), a' [in Fermi res.] or CD ₃ , a'	1.38
1455	1100		1455	a.CH ₃ bend, a' and a'' or CD ₃ , a'	1.32
1442	1095		1448	s.CH ₃ bendR, a' or CD ₃ , a'	1.32
1175* ¹	913		1178	CH ₃ rock, a' and a'' or CD ₃ , a''	1.29
?	?		?	CH ₃ torsion, a'' or CD ₃ , a''	[?]
C ₂ H ₅ –O–P(=S)Cl ₂ cm ⁻¹	CH ₃ – CD ₂ –O–P(=S)Cl ₂ cm ⁻¹	CD ₃ – CH ₂ –O–P(=S)Cl ₂ cm ⁻¹	C ₂ H ₅ –O–P(=O)Cl ₂ cm ⁻¹		[D]/[C]
3000	2988	2258	3000	a.CH ₃ str., a'' or CD ₃ , a''	1.33
2990	2988	2244	2991	a.CH ₃ str., a' or CD ₃ , a'	1.33
2945	2938	2129	2944	s.CH ₃ str., a' or CD ₃ , a'	1.38
1458	1458	1086	1457	a.CH ₃ bend, a'' or CD ₃ , a''	1.34
1443	1441	1143	1445	a.CH ₃ bend, a' or CD ₃ , a'	1.26
1394	1383	1055	1374	s.CH ₃ bend, a' or CD ₃ , a'	1.3
1159	1148	876	1160	CH ₃ rock, a'' or CD ₃ , a''	1.32
1100	1148	962	1100	CH ₃ rock, a' or CD ₃ , a'	1.14
		masked ? (200–300)			[D]/[B]
325?	320?			CH ₃ torsion, a'' or CD ₃ , a''	[-]
2990	2275	2980	2991	a.CH ₂ str., a'' or CD ₂ , a''	1.31
2972	2168	2970	2970	s.CH ₂ str., a' or CD ₂ , a'	1.37
1475	1119	1472	1479	CH ₂ bend, a' or CD ₂ , a'	1.32
1394	1034	1383	1394	CH ₂ wag, a' or CD ₂ , a'	1.35
1290	917	1268	1394	CH ₂ twist, a'' or CD ₂ , a''	1.52
masked near 800	masked near 550	785	810	CH ₂ rock, a'' or CD ₂ , a''	[?]
951/876					

TABLE 8.8 The P=O stretching frequencies for inorganic and organic phosphorus compounds

Compound P=O(X) ₃ X	References	P=O str. Rotational conformers/ cm ⁻¹	Frequency difference between rotational conformers cm ⁻¹	P=O str. for the other compounds minus P=O str. for P(=O)Cl ₃ at 1303 cm ⁻¹ cm ⁻¹
F ₃	1	1405		102
Cl ₃	15	1303		0
Br ₂	13	1277		[-26]
Br ₂ (BrCH ₂)	17	1275/1264	11	[-28]/[-39]
Cl ₂ (CH ₃)	17,18	1277		[-26]
Cl ₂ (CH ₃)	26	[1278.5* ¹ ;1268.9* ²]		[-24.5* ¹]/[-34.6* ²]
Cl ₂ (tert-C ₄ H ₉)	26	[1266.4* ¹ ;1255.6* ²]		[-36.6* ¹]/[-47.4* ²]
Cl ₂ (ClCH ₂)	17	1295/1288	7	[-8]/[-15]
Cl ₂ (C ₆ H ₅)	20	1280		[-23]
cl ₂ (CH ₃ -O)	21	1322/1300	22	[19]/[-3]
Cl ₂ (C ₂ H ₅ -O)	22	1317/1296	21	[14]/[-7]
Cl ₂ (n-C ₃ H ₇ -O)	20	1313/1294	19	[10]/[-9]
Cl ₂ (n-C ₄ H ₉ -O)	20	1313/1295	18	[10]/[-8]
Cl ₂ (C ₆ H ₅ -O)	20	1316/1305	11	[13]/[2]
Cl ₂ (4-Cl-C ₆ H ₄ -O)	20	1315/1306	9	[12]/[3]
Cl ₂ (CH ₃ -NH)	24	1292/1279* ³	13	[-11]/[-24]
	20	1267* ⁴		[-36]
Cl ₂ [(CH ₃) ₂ N]	20	1270		[-33]
Cl ₂ [(C ₂ H ₅) ₂ N]	20	1280		[-23]
Cl ₂ (CH ₃ -S)	23	1279/1271	8	[-24]/[-32]
Cl(CH ₃ -O) ₂	27	1308/1293	15	[5]/[-10]
Cl(C ₂ H ₅ -O) ₂	20	1298/1285	13	[-5]/[-18]
Cl(n-C ₃ H ₇ -O) ₂	20	1303/1285	18	[0]/[-18]
Cl(O-CH ₂ CH ₂ -O)	20	1315		[12]
Cl(C ₆ H ₅ -O) ₂	20	1313/1301	12	[10]/[-2]
Cl[(CH ₃) ₂ -N]	20	1243		[-60]
Cl[(C ₂ H ₅) ₂ -N]	20	1258		[-45]
Cl(CH ₃)[(CH ₃) ₂ -N]	20	1248		[-55]
Cl(CH ₃ -O)(CH ₃ -NH)	20	1260* ⁴		[-43]
(CH ₃ -O) ₃	20,26(mortimer)	1291/1272	19	[-12]/[-31]
(C ₂ H ₅ -O) ₃	20	1280/1263	17	[-23]/[-40]
(n-C ₃ H ₇ -O) ₃	20	1279/1265	14	[-24]/[-38]
(n-C ₄ H ₉ -O) ₃	20	1280/1265	15	[-23]/[-32]
(iso-C ₃ H ₇ -O) ₃	20	1272/1257	15	[-31]/[-46]
CH ₃ -O) ₂ (C ₆ H ₅ -O)	20	1305/1297(1281)	8;24	[3]/[-6]/[-22]
(C ₂ H ₅ -O) ₂ (C ₆ H ₅ -O)	20	1305/1292(1276)	13;29	[2]/[-11]/[-27]
(CH ₃ -O)(C ₆ H ₅ -O) ₂	20	1307/1298(1286)	9;21	[4]/[-5]/[-17]
(C ₂ H ₅ -O)(C ₆ H ₅ -O) ₂	20	1306/1292(1285)	14;21	[3]/[-11]/[-18]
(C ₆ H ₅ -O) ₃	20	1312/1298	14	[9]/[-5]
(CH ₃ -O) ₂ (CH ₃)	20	1268/1252	16	[-35]/[-51]
(C ₂ H ₅ -O)(CH ₃)	20	1268/1248	20	[-35]/[-55]
(CH ₃ -O) ₂ (C ₆ H ₅)	20	1258		[-45]
(CH ₃ -O)[(CH ₃) ₂ -N]	20	1260		[-43]
[(CH ₃) ₂ -N] ₃	20	1209		[-94]
[(n-C ₃ H ₇ -O)(C ₂ H ₅ -NH)P-O] ₂ (-O-)	20	~ 1248* ⁴		[-55]
[(CH ₃) ₂ -N] ₃ P=O] ₂ (-O-)	20	~ 1255* ⁴		[-48]

*¹[CCl₄ soln.]*²[CHCl₃ soln.]*³[dilute soln.]*⁴[concentrated soln.]

TABLE 8.8a A comparison of P=O stretching frequencies in different physical phases

Compound	P=O str. liquid cm ⁻¹	P=O str. rotational conformers CS ₂ soln. cm ⁻¹	P=O str. vapor cm ⁻¹	Frequency difference between rotational conformers cm ⁻¹	P=O str. (CS ₂) minus P=O str. (liquid) or (solid) cm ⁻¹	P=O str. (vapor) minus P=O str. (liquid) cm ⁻¹	P=O str. (vapor) minus P=O str. (CS ₂ soln.) cm ⁻¹
CH ₃ -O-P(=O)Cl ₂	1296	1322/1300		22	26		
C ₂ H ₅ -O-P(=O)Cl ₂	1303/1289	1317/1296		21	14/7		
C ₆ H ₅ -O-P(=O)Cl ₂	1304	1316/1305	1324	11	14	20	8
(CH ₃ -O-) ₃ P=O	1290 (solid) 1275	1291/1272		19	18 16		
(C ₂ H ₅ -O) ₃ P=O	1270 (solid) 1290/1270	1280/1263	1300/1280	17/20	20/17	[10/10]	20/17
		1261(CDCl ₃)					
(C ₃ H ₇ -O-P) ₃ =O	1269	1279/1265	1300/1282	14/18	10	31	21/17
(C ₄ H ₉ -O-) ₃ P=O	1270	1280/1265	1300/1282	16/18	10	20/17	
(C ₆ H ₅ CH ₂ -O-) ₃ P=O	1255						
(CH ₃ -O-) ₂ (CH ₆ H ₅ -O-)P=O	1285	1305/1297		20			
(CH ₃ -O-)(C ₆ H ₅ -O-) ₂ P=O	1297sh/1291	1307/1298		[10/7]			
(C ₆ H ₅ -O-) ₃ P=O	1314/1298	1312/1298	1311/1300	16/14/11			

TABLE 8.9 Infrared data for the rotational conformer P=O stretching frequencies for O,O-dimethyl O-(2-chloro-4-X-phenyl) phosphate

O,O-Dimethyl O-(2-chloro-4-X-phenyl) phosphate X	$\sigma_p(29)$	P=O str. rotational conformers (20) CS ₂ soln. cm ⁻¹	Frequency separation between rotational conformers cm ⁻¹
NO ₂	0.78	1307.4/1291.1	16.3
CN	0.66	1308.5/1291.0	17
Cl	0.23	1304.5/1288.4	15.6
H	0	1303.6/1287.8	15.8
C(CH ₃) ₃	-0.27	1304.2/1285.8	18.4
CH ₃ -O	-0.27	1303.2/1286.7	16.5

TABLE 8.10 Infrared observed and calculated P=O stretching frequencies compared*¹

G - P(=O)Cl ₂ Substituent Group G	π	P=O str. Calc. by Eq. 1 cm ⁻¹	P=O str. observed cm ⁻¹	δ P=O str. cm ⁻¹	Average δ P=O str. cm ⁻¹
R	2	1262	1277	15	
R ₂ N	2.4	1278	1280	2	
C ₆ H ₅	2.4	1278	1280	2	
C=C	2.4	1278			
H	2.5	1282			
C=O	2.5	1282			
ClCH ₂	2.7	1290	1295/1288	5/-2	1.5
R-O	2.8	1294	1322/1300	28/6	17
Cl ₂ CH	2.9	1298			
CCl ₃	3	1302			
C ₅ H ₆ -O	3	1302	1316/1305	14/3	8.5
Br	3.1	1306	1295	-11	
C=C-O	3.1	1306			
CF ₃	3.3	1314			
R(C=O)-O	3.4	1318			
Cl* ²	3.4	1318	1300	-18	
CN	3.5	1322			
F	3.9	1338	1340	2	

*¹The calculated frequencies were obtained using the equation developed by Thomas and Chittenden (30).

*²[2(π) for ₂Cl is 6.3 not 6.8].

$$\nu_{\text{P=O}}(\text{cm}^{-1}) = 930 + 40\sigma\pi.$$

TABLE 8.11 The P=O and P=S stretching frequencies for phenoxarsine derivatives

Phenoxarsine	[31] P=S str. [CS ₂] cm ⁻¹
X=S-P=S(O-R) ₂	
R	
methyl	648
isopropyl	645
X=OP=O(O-R) ₂	P=O str.
R	
ethyl	1235
isopropyl	1228

TABLE 8.12 The P=O and P=S stretching frequencies for P(=O)X₃ and P(=S)X₃ type compounds

X ₃	P(=O)X ₃ P=O str. cm ⁻¹	P(=S)X ₃ [P=S str.] cm ⁻¹	[P=O str.]– [P=S str.] cm ⁻¹	[P=O.]/ [P=S str.]	References
F ₃	1415	695	720	2.04	1,2,3,4
F ₂ Cl	1358				7
F ₂ Br	1350				7
FCl ₂	1331	755	576	1.76	9
Cl ₃	1326	771	555	1.72	8
FBr ₂	1303				10,11
Cl ₂ Br	1285				5
Br ₃	1277	730	547	1.75	5
ClBr ₂	1275				4
					5

TABLE 8.13 The P=S stretching frequencies for inorganic and organic phosphorus compounds

Compound P=SX ₃ X	P=S str. rotational conformers cm ⁻¹	Ref.	Frequency separation between rotational conformers	Compound P=SX ₃ X	P=S str. rotational conformers/ cm ⁻¹	Ref.	Frequency separation between rotational conformers
F ₃	696	33		CH ₃ -O) ₃	620/600	20	20
F ₂ Cl	727	33		(C ₂ H ₅ -O) ₃	635/614	20	21
F ₂ Br	711	34		(isoC ₃ H ₇ -O) ₃	672/650	20	22
FCl ₂	741	9,33		(CH ₃)(C ₂ H ₅ -O) ₂	~632	20	
Cl ₃	752	33		(C ₆ H ₅)(CH ₃ -O) ₂	624	20	
Br ₃	730	5		(CH ₃ -O) ₂ [(CH ₃) ₂ -N]	588	20	
Cl ₂ (CH ₃)	670	7,18		(C ₂ H ₅ -O) ₂ (N ₃)	640/627	20	13
Cl ₂ (ClCH ₂)	683/657	17	26	(CH ₃ -O) ₂ (CH ₃ -NH)	630/597	20	33
Cl ₂ (C ₆ H ₅)	690	20		(C ₂ H ₅ -O) ₂ (CH ₃ -NH)	640/608	20	32
Cl ₂ (CH ₃ -O)	721/703	21,25	18	(CH ₃ -O) ₂ (isoC ₃ H ₇ -NH)	645/611	20	34
Cl ₂ (CD ₃ -O)	709/698	21,25	11	(C ₂ H ₅ -O) ₂ (isoC ₃ H ₇ -NH)	650/617	20	33
Cl ₂ (C ₂ H ₅ -O)	728/701	22	27	(CH ₃ -O) ₂ (NH ₂)	635/611	20	24
Cl ₂ (CH ₃ -CD ₂ -O)	727/699	22	28	(C ₂ H ₅ -O) ₂ (NH ₂)	641/618	20	23
Cl ₂ (CD ₃ -CH ₂ -O)	695/675	22	30	(isoC ₃ H ₇ -O) ₂ (NH ₂)	643/621	20	22
Cl ₂ (isoC ₄ H ₉ -O)	737/715	20	22	(n-C ₄ H ₉ -O) ₂ (NH ₂)	653/628	20	25
Cl ₂ (H-CC-CH ₂ -O)	742/716	35	26	(isoC ₄ H ₉ -O)(NH ₂)	665/641	20	24
Cl ₂ (4-Cl-C ₆ H ₄ -O)	721	20		[(CH ₃) ₂ -N] ₃	565	20	
Cl ₂ (CH ₃ -NH)	725/690	22	35	[(CH ₃) ₂ -N] ₂ (N ₃)	607	20	
Cl ₂ (CD ₃ -NH)	711/683	22	28	[(CH ₃) ₂ -N] ₂ (NH ₂)	579	20	
Cl ₂ (CH ₃ -ND)	728/681	22	47	(CH ₃)[(CH ₃) ₂ -N] ₂	569	20	
Cl ₂ (CD ₃ -ND)	701/673	22	28	(C ₂ H ₅ -S) ₃	685	20	
Cl ₂ (C ₂ H ₅ -NH)	725/688	22	37	(isoC ₂ H ₇ -S) ₃	685	20	
Cl ₂ (isoC ₃ H ₇ -NH)	727/690	22	37	(C ₂ H ₅ -S)(CH ₃ -NH)	693/663	20	30
Cl ₂ [(CH ₃) ₂ -N]	673	20		(CH ₃) ₂ (P=S)(P=S)(CH ₃) ₂	576	20	
Cl ₂ [(C ₂ H ₅) ₂ -N]	667	20		[(C ₂ H ₅ -O) ₂ (P=S)] ₂ (-O-)	~636	20	
Cl ₂ (C ₂ H ₅ -S)	730			[(CH ₃ -O)(CH ₃ -NH)P=S] ₂ (-O-)	651/635	20	16
Cl(CH ₃ -O) ₂	666/655	27	11	[(CH ₃ -O)(C ₂ H ₅ -NH)P=S] ₂ (-O-)	660/642	20	18
Cl(CD ₃ -O) ₂	~650	27		[(CH ₃ -O)(n-C ₃ H ₇ -NH)P=S] ₂ (-O-)	660/642	20	18
Cl(C ₂ H ₅ -O) ₂	673/660	32	13	[(CH ₃ -O)(isoC ₃ H ₇ -NH)P=S] ₂ (-O-)	666/647	20	19
Cl(n-C ₃ H ₇ -O) ₂	675/661	20	14	[(CH ₃ -O)(isoC ₄ H ₉ -NH)P=S] ₂ (-O-)	660/645	20	15
Cl[(CH ₃) ₂ -N] ₂	613	20		(C ₂ H ₅ -O)(CH ₃ -NH)P=S] ₂ (-O-)	654/641	20	13

(continues)

TABLE 8.13 (continued)

Compound P= SX ₃ X	P=S str. rotational conformers cm ⁻¹	Ref.	Frequency separation between rotational conformers	Compound P= SX ₃ X	P=S str. rotational conformers/ cm ⁻¹	Ref.	Frequency separation between rotational conformers
Cl[(C ₂ H ₅) ₂ -N] ₂	611	20		[(n-C ₃ H ₇ -O)(CH ₃ -NH)P=S] ₂ (-O-)	660/645	20	15
Cl[-N(CH ₃)CH ₂ CH ₂ (CH ₃)N-]	603	20		[(isoC ₃ H ₇ -O)(CH ₃ -NH)P=S] ₂ (-O-)	~652/638	20	14
Cl(CH ₃ -O)[(CH ₃) ₂ -N]	633	20		[(isoC ₃ H ₇ -O)(C ₂ H ₅ -NH)P=S] ₂ (-O-)	652/639	20	13
Cl(CH ₃ -O)(CH ₃ -NH)	660/639	20	21	[(isoC ₃ H ₇ -O)(NH ₂)P=S] ₂ (-O-)	632	20	
Cl(CH ₃ -O)(C ₂ H ₅ -NH)	663/639	20	24	[(CH ₃) ₂ -N] ₂ P=S] ₂ (-O-)	598	20	
Cl(CH ₃ -O)(isoC ₃ H ₇ -NH)	673/643	20	30	[(C ₂ H ₅ -O) ₂ P=S] ₂ (-S-)	~645	20	
Cl(C ₂ H ₅ -O)(CH ₃ -NH)	666/643	20	23	[(C ₂ H ₅ -O) ₂ P=S(-S-)] ₂	662	20	
Cl(C ₂ H ₅ -O)(C ₂ H ₅ -NH)	663/643	20	20				
Cl(C ₂ H ₅ -O)(isoC ₃ H ₇ -NH)	673/647	20	26				
Cl(isoC ₃ H ₇ -O)(CH ₃ -NH)	660/639	20	21				
Cl(isoC ₃ H ₇ -O)(C ₂ H ₅ -NH)	663/642	20	21				
Cl(isoC ₃ H ₇ -O)(isoC ₃ H ₇ -NH)	665/645	20	20				
Cl(C ₂ H ₅ -S) ₂	705	20					
Cl(isoC ₃ H ₇ -S) ₂	705	20					

TABLE 8.14 Vibrational assignments for the skeletal modes of S-methyl phosphorothiodichloride and phosphoryl chloride

$\text{CH}_3\text{-S-P(=O)Cl}_2$ cm^{-1}	Assignment(23)	P(=O)Cl_3 cm^{-1}	Species
1275	P=O str., a', rotational conformer 1	1303	a1
1266	P=O str., a', rotational conformer 2		
450	s.PCl ₂ S str.,a'	483	a1
471	s.PCl ₂ S str., a'		
235	s.PCl ₂ S bend, a', rotational conformer 1	268	a1
262	s.PCl ₂ S bend, a', rotational conformer 2		
593	a.PCl ₂ S str., a', rotational conformer 1	588	e
579	a.PCl ₂ S str., a', rotational conformer 2		
547	a.PCl ₂ S str., a'', rotational conformer 1		
560	a.PCl ₂ S str., a'', rotational conformer 2		
323	P=O rock, a'	335	e
344	P=O rock, a''		
190	PCl ₂ S bend, a' and a''	193	e
698	C-S str., rotational conformer 1		
732	C-S str., rotational conformer 2		
223	P-S-C bend, a'		
168 or 148	P-S-C torsion, a''		

TABLE 8.15 Vibrational assignments of the P(-O-C)₃ group of trimethyl phosphite and trimethyl phosphate

[36] $(\text{CH}_3\text{-O})_3\text{P}$ cm^{-1}	[26-mortimer] $(\text{CH}_3\text{-O})_3\text{P=O}$ cm^{-1}	Assignment	Number of modes
1059* ¹	1045	s.P(-O-C) ₃ str.	1
1016	1080	a.P(-O-C) ₃ str.	2
769* ¹	750	s.P(-O-) ₃ str.	1
750	865	a.P(-O-) ₃ str.	2
732	858	a.P(-O-) ₃ str.	
513* ¹	533* ²	s.P(-O-C) ₃ bending	1
534	510* ²	a.P(-O-C) ₃ bending	2
370* ¹	367(R)* ³	s.P(-O-) ₃ bending	1
280* ¹	239(R)	a.P(-O-) ₃ bending	2
225		a.P(-O-) ₃ bending	
190	184?(R)	s.P-O-C torsion	1
120(?)	(?)	a.P-O-C torsion	2

*¹Raman polarized band.*²Assignments were reversed by Mortimer (26a).*³Abbreviations: R = Raman; s. = symmetric; and a. = antisymmetric.

TABLE 8.16 Vibrational assignments for the CH₃ groups of trimethyl phosphite

(CH ₃ -O) ₃ P cm ⁻¹	Number of normal modes	Assignment (36)
2990	6	a.CH ₃ str.
2949		
2939	3	s.CH ₃ str.
1459	6	a.CH ₃ bend
1436	3	s.CH ₃ bend
1179* ³	3	CH ₃ rock* ¹
1159(R)	3	CH ₃ rock* ²
* ⁴	3	CH ₃ torsion

*¹ Out of P-O-C plane.*² In P-O-C plane.*³R = Raman.*⁴ Well below 300 cm⁻¹.

TABLE 8.17 The P=S, P-S, and S-H stretching frequencies for O,O-dialkyl phosphorodithioate and O,O-diaryl phosphorodithioate

(CH ₃ -O) ₂ P(=S)SH cm ⁻¹	(C ₂ H ₅ -O) ₂ P(=S)SH cm ⁻¹	(2,4,5-Cl ₃ -C ₆ H ₄ -O) ₂ P(=S)SH cm ⁻¹	Assignment(32)
2588	2582	2575	S-H str., rotational conformer 1
2550	2550	2549	S-H str., rotational conformer 2
670sh	670sh		P=S str., rotational conformer 1
659	659		P=S str., rotational conformer 2
524	535		P-S str., rotational conformer 1
490	499		P-S str., rotational conformer 2

TABLE 8.18 The P=O, PH stretching and PH bending vibrations for O,O-dialkyl hydrogenphosphonates*

(R-O-) ₂ P(=O)H R	P-H str. [CCl ₄] cm ⁻¹	P=O str. [CS ₂] cm ⁻¹	P-H bend [CS ₂] cm ⁻¹	P-H str. neat cm ⁻¹	P=O str. neat cm ⁻¹	P-H bend neat cm ⁻¹	P-H str. cm ⁻¹	P-H bend cm ⁻¹	delta P=O str. cm ⁻¹
CH ₃	2438	1283sh 1266	979	2415	1255	968	23	11	28;11
C ₂ H ₅	2439	1275sh 1262	~980	2419	1250	970	24	10	25;12
n-C ₃ H ₇	2441	1273sh 1261	973						
isoC ₄ H ₉	2435	~1275 1257	~975						
2-C ₂ H ₅ -C ₆ H ₁₃	2431	1273 1257	~970	2410	1250	955	21	15	23;7
2-(2-C ₂ H ₅ -C ₆ H ₁₂ -O-) C ₂ H ₄	2445	1273 1261	968						

*See Reference 32.

TABLE 8.19 The "C–O" and "P–O" stretching frequencies for the C–O group

Compound	"C–O stretching" cm ⁻¹	"P–O stretching" cm ⁻¹	References
(C–O) ₃ P	1059(s.) 1016(a.)	769(s.) 750,732(a.)	36
(C ₂ H ₅ –O–) ₃ P	1060(s.) 1035[1025](a.)	765(s.) 736(a.)	20
(C ₆ H ₅ –O–) ₃ P	[1200]1190,1162	878,862	20
CH ₃ –O–P(=O)Cl ₂	1060/1027	809/802	26 (mortimer)
C ₂ H ₅ –O–P(=O)Cl ₂	1041/1013	779	22
n-C ₃ H ₇ –O–P(=O)Cl ₂	1032,1013[995]	794	20
n-C ₄ H ₉ –O–P(=O)Cl ₂	[1034,1032,1013,995]	794	20
CH ₃ –O–P(=S)Cl ₂	1041/1023	828/821	20
C ₂ H ₅ –O–P(=S)Cl ₂	1028/1014	790/804	20
n-C ₃ H ₇ –O–P(=S)Cl ₂	1050,1036,1020[1000]	838	20
H–CC–CH ₂ –OP(=S)Cl ₂	1015/984	857/822	20
(CH ₃ –O=)(CH ₃ –NH–)P(=S)Cl	~1043	~820	20
(C ₂ H ₅ –O–)(CH ₃ –NH–)P(=S)Cl	~1030	~808	20
(isoC ₃ H ₇ –O–)(CH ₃ –NH–)P(=S)Cl	~990	~780	20
(CH ₃ –O–)(C ₂ H ₅ –NH–)P(=S)Cl	~1041	~812	20
(C ₂ H ₅ –O–)(C ₂ H ₅ –NH–)P(=S)Cl	~1025	~799	20
(isoC ₃ H ₇ –O–)(C ₂ H ₅ –NH–)P(=S)Cl	~990	~781	20
(CH ₃ –O–)(isoC ₃ H ₇ –NH–)P(=S)Cl	~1040	~835(?)	20
(C ₂ H ₅ –O–)(isoC ₃ H ₇ –NH–)P(=S)Cl	~1030	~787(?)	20
(isoC ₃ H ₇ –O–)(isoC ₃ H ₇ –NH–)P(=S)Cl	~990	~778	20
CH ₃ –O[(CH ₃) ₂ N–]P(=S)Cl	~1042	~828	20
[(isoC ₃ H ₇ –O–)(NH ₂ –)P(=S)] ₂ (–O–)	1050	816	20
[(C ₂ H ₅ –O–)(CH ₃ NH–)P(=S)] ₂ (–O–)	~1045	811	20
[(n-C ₃ H ₇ –O–)(CH ₃ –NH–)P(=S)] ₂ (–O–)	1060[1007]	~855	20
[(isoC ₃ H ₇ –O–)(CH ₃ –NH–)P(=S)] ₂ (–O–)	~1005	~795	20
[(CH ₃ –O–)(C ₂ H ₅ –NH–)P(=S)] ₂ (–O–)	1050	815	20
[(isoC ₃ H ₇ –O–)(C ₂ H ₅ –NH–)P(=S)] ₂ (–O–)	~1000	~780	20
[(CH ₃ –O–)(n-C ₃ H ₇ –NH–)P(=S)] ₂ (–O–)	1050	819	20
[(CH ₃ –O–)(isoC ₃ H ₇ –NH–)P(=S)] ₂ (–O–)	1040	805	20
[(CH ₃ –O–)(isoC ₄ H ₉ –NH–)P(=S)] ₂ (–O–)	~1045	810	20
(CH ₃ –O–) ₂ P(=O)Cl	1068,1044[1036]	[845]779,769	27
(C ₂ H ₅ –O–) ₂ P(=O)Cl	1057,1030[1022]	800,763	27
(n-C ₃ H ₇ –O–) ₂ P(=O)Cl	1060,1050[1025]	853,827	20
(–O–CH ₂ –CH ₂ –O–)P(=O)Cl	1031	861,826	20
(CH ₃ –O–) ₂ P(=O)H	1051(s.) 1080(a.)	820(a.) 765(s.)	32
(CH ₃ –O–) ₂ P(=O)D	1068(s.) 1040(a.)	850(a.) 791(s.)	32
(C ₂ H ₅ –O–) ₂ P(=O)H	1081(s.) 1052(a.)	782(a.) 741(s.)	32
(C ₂ H ₅ –O–) ₂ P(=O)D	1061(s.) 1030(a.)	8216(a.) 781(s.)	32
(C ₂ H ₅ –O–) ₂ (CH ₃ –)P(=O)	1061[1032]	770,713	20
(CH ₃ –O–) ₂ (C ₆ H ₅ –)P(=O)	1059[1029]	828,788	20
(CH ₃ –O–) ₂ (CH ₃ –NH–)P(=O)	1063[1033]	[830]742	37
(C ₂ H ₅ –O–) ₂ (CH ₃ –NH–)P(=O)	1059[1032]	793,740	37

(continues)

TABLE 8.19. (continued)

$(\text{CH}_3-\text{O}-)_2[(\text{CH}_3)_2\text{N}-]\text{P}(=\text{O})$	1065[1030]	[825]808	20
$(\text{CH}_3-\text{O}-)_2\text{P}(=\text{S})\text{Cl}$	1056/1042(s.)	845(s.)	18
	1040(s.)	831(s.)	20
$(\text{C}_2\text{H}_5-\text{O}-)_2\text{P}(=\text{S})\text{Cl}$	1017(a.)	819(a.)	20
$(\text{C}_2\text{H}_5-\text{O}-)_2(\text{CH}_3-)\text{P}(=\text{S})$	1054[1048]	762.755	20
$(\text{CH}_3-\text{O}-)_2(\text{C}_6\text{H}_5-)\text{P}(=\text{S})$	1058[1030]	817,794	20
$(\text{CH}_3-\text{O}-)_2(\text{NH}_2-)\text{P}(=\text{S})$	1065[1034]	790(?)	20
$(\text{C}_2\text{H}_5-\text{O}-)_2(\text{NH}_2-)\text{P}(=\text{S})$	1058[1028]	781	20
$(\text{isoC}_3\text{H}_7-\text{O}-)_2(\text{NH}_2-)\text{P}(=\text{S})$	1011[982]	803[771]	20
$(\text{n-C}_4\text{H}_9-\text{O}-)_2(\text{NH}_2-)\text{P}(=\text{S})$	1065,1048[1022][979]	839,823[798]	20
$(\text{isoC}_4\text{H}_9-\text{O}-)_2(\text{NH}_2-)\text{P}(=\text{S})$	1050[1110]	[859]839,820	20
$(\text{CH}_3-\text{O}-)_2(\text{CH}_3-\text{NH}-)\text{P}(=\text{S})$	1061[1033]	[816]799	20
$(\text{C}_2\text{H}_5-\text{O}-)_2(\text{CH}_3-\text{NH}-)\text{P}(=\text{S})$	1055[1029]	809,775	20
$(\text{CH}_3-\text{O}-)_2(\text{isoC}_3\text{H}_7-\text{NH}-)\text{P}(=\text{S})$	1060[1033]	805,784	20
$(\text{C}_2\text{H}_5-\text{O}-)_2(\text{iso}(\text{C}_3\text{H}_7-\text{NH}-)\text{P}(=\text{S}))$	1058[1035]	780	20
$(\text{CH}_3-\text{O}-)_2[(\text{CH}_3)_2\text{N}-]\text{P}(=\text{S})$	1060[1030]	821,803	20
$(\text{C}_2\text{H}_5-\text{O}-)_2(\text{N}_3-)\text{P}(=\text{S})$	1044[1019]	820,800	20
$(\text{CH}_3-\text{O}-)_2(\text{HS}-)\text{P}(=\text{S})$	1050/1037(s.)	801(s.)	32
$(\text{C}_2\text{H}_5-\text{O}-)_2(\text{HS}-)\text{P}(=\text{S})$	1040(s.)	849	32
	1017(a.)	810(?)	
$[(\text{C}_2\text{H}_5-\text{O}-)_2\text{P}(=\text{S})]_2(-\text{O}-)$	1059[1030]	755/739(s.)	20

TABLE 8.20. The “C–O” and “P–O” stretching frequencies for compounds containing C–O–P=O, C–O–P=S, and C–O–P=Se groups

Compound	Ref.	“C–O stretching”	“P–O stretching”	“Aryl-O stretching”	“P–O stretching”
		R–O–P cm ⁻¹	R–O–P cm ⁻¹	Aryl–O–P cm ⁻¹	Aryl–O–P cm ⁻¹
(CH ₃ –O–) ₃ P=O	26 (Mortimer)	1085(s.) 1-55/1040(a.)	755/739(s.) 835/844(a.)		
(C ₂ H ₅ –O–) ₃ P=O	20	1073(s.) 1033(a.)	744(s.) 892/798(a.)		
(n-C ₃ H ₇ –O–) ₃ P=O	20	1053,1039[1008]	888,863,756		
(isoC ₃ H ₇ –O–) ₃ P=O	20	1028[1002]	[791]752		
(n-C ₄ H ₉ –O–) ₃ P=O	20	1058[1030]1003,987	862,850,770		
(CH ₃ –O–) ₃ P=S	20	1071(s.) 1043(a.)	812(s.) 832(a.)		
(C ₂ H ₅ –O–) ₃ P=S	20	1063(s.) 1031(a.)	792(s.) 825(a.)		
(isoC ₄ H ₉ –O–) ₃ P=S	20	1058[1018]	[865]822		
(CH ₃ –O–) ₃ P=Se	38	1028(s.) 1028(a.)	780(s.) 826(a.)		
Cl ₂ (C ₆ H ₅ –O–)P=O	20			[1183]1160	957[942]
Cl ₂ (4–Cl–C ₆ H ₄ –O–)P=O	20			[1185]1160	953,931
Cl ₂ (C ₆ H ₅ –O–)P=S	20			[1180]1157	964[932]
Cl ₂ (4–Cl–C ₆ H ₄ –O–)P=S	20			[1187]1158	[937,920]

Table 8.20 (continued)

$\text{Cl}(\text{C}_6\text{H}_5\text{-O-})_2\text{P=O}$	20			1205[1180]1159	[962]940
$\text{Cl}(\text{C}_6\text{H}_5\text{-O-})_2\text{P=S}$	20			{1201,1182,1161}	~940
$(\text{C}_6\text{H}_5\text{-O-})_3\text{P=O}$	20			[1190]1160	~960
$(\text{CH}_3\text{-O-})_2(\text{C}_6\text{H}_5\text{-O-})\text{P=O}$	20	1069[1047]	[854]796(?)	[1213]1165	[951]937
$(\text{C}_2\text{H}_5\text{-O-})_2(\text{C}_6\text{H}_5\text{-O-})\text{P=O}$	20	1063[1036]	820,802[780]	[1215]1165	[960]940
$(\text{CH}_3\text{-O-})(\text{C}_6\text{H}_5\text{-O-})_2\text{P=O}$	20	1050	823,812	1220[1192]1161	951
$(\text{C}_2\text{H}_5\text{-O-})(\text{C}_6\text{H}_5\text{-O-})_2\text{P=O}$	20	1041	792,770	1230[1192]1162	950
$(\text{CH}_3\text{-O-})_2(\text{C}_6\text{H}_5\text{-O-})\text{P=S}$	20	1066[1041]	[834]818	1207[1165]	938
$(\text{C}_2\text{H}_5\text{-O-})_2(\text{C}_6\text{H}_5\text{-O-})\text{P=S}$	20	1062[1035]	[828]822	1212[1165]	948
$(\text{C}_2\text{H}_5\text{-O-})(\text{C}_6\text{H}_5\text{-O-})_2\text{P=S}$	20	1048	[837]816	1211[1187]1161	938
$(\text{CH}_3\text{-O-})_2(2\text{-Cl}_6\text{H}_4\text{-O-})\text{P=O}$	20	1073[1056]	859	[1234]	950,938
$(\text{CH}_3\text{-O-})_2(2\text{-Cl-4-NO}_2\text{-C}_6\text{H}_3\text{-O-})\text{P=O}$	20	1071[1050]	861	[1261]	941
$(\text{CH}_3\text{-O-})_2(2\text{-Cl}_4\text{-CN-C}_6\text{H}_3\text{-O-})\text{P=O}$	20	1075[1056]	862	[1256]	941
$(\text{CH}_3\text{-O-})_2(2,4\text{-Cl}_2\text{-C}_6\text{H}_3\text{-O-})\text{P=O}$	20	1073[1075]	859	{1260,1238}	949,937
$(\text{CH}_3\text{-O-})_2(2\text{-Cl}_4\text{-t-C}_4\text{H}_9\text{-C}_6\text{H}_3\text{-O-})\text{P=O}$	20	1075p1053]	858	{1263,1243}	954,944
$(\text{CH}_3\text{-O-})_2(2\text{-Cl}_4\text{-CH}_3\text{-O-C}_6\text{H}_3\text{-O-})\text{P=O}$	20	1071[1048]	857	{1263,1214}	951,941
$(\text{CH}_3\text{-O-})_2(2\text{-Cl-C}_6\text{H}_4\text{-O-})\text{P=S}$	20	1067,1052[1038]	838	1232	938,928
$(\text{CH}_3\text{-O-})_2(2\text{-Cl}_4\text{-NO}_2\text{-C}_6\text{H}_3\text{-O-})\text{P=S}$	20	1061[1040]	844	1260	928
$(\text{CH}_3\text{-O-})_2(2\text{-Cl}_4\text{-CN-C}_6\text{H}_3\text{-O-})\text{P=S}$	20	1065,1049[1035]	840	1248	922
$(\text{CH}_3\text{-O-})_2(2,4\text{-Cl}_2\text{-C}_6\text{H}_3\text{-O-})\text{P=S}$	20	1065,1052[1038]	845	{1259,1238}	952,940
$(\text{CH}_3\text{-O-})_2(2\text{-Cl}_4\text{-t-C}_4\text{H}_9\text{-C}_6\text{H}_3\text{-O-})\text{P=S}$	20	1066,1051[1040]	841	{1261,1239}	948,937

TABLE 8.21 The aryl-O stretching frequencies for O-methyl O-(X-phenyl) N-methylphosphoramidate

Compound	Aryl-O stretching
O-methyl O-(x-Phenyl)	
N-methylphosphoramidate	[39]
X	cm ⁻¹
4-nitro	1237
2,4,5-trichloro	1259
2,4-dichloro	1245
2-chloro	1235
4-chloro	1228
hydrogen	1213
4-methoxy	1207
3-tert-butyl	1209
4-tert-butyl	1225
2-chloro-4-tert-butyl	1243

TABLE 8.22. The C-P stretching for organophosphorus compounds

Compound	Ref.	C-P str.	Assignment	Frequency separation between rotational conformers
Cl ₂ (CH ₃ -)P	17	699		
Cl ₂ (CH ₃ -)P(=O)	17	757		
Cl ₂ (CH ₃ -)P(=S)	17	810		
Cl ₂ (ClCH ₂ -)P	17	812	[not split by rotational conformers]	0
Cl ₂ (ClCH ₂ -)P(=O)	17	811,818	[rotational conformers]	7
Cl ₂ (ClCH ₂ -)P(=S)	17	801,833	[rotational conformers]	32
Cl ₂ (BrCH ₂ -)P(=O)	17	778,788	[rotational conformers]	10
CH ₃ -PO ₃ Na ₂	40	753		
(CH ₃ -) ₂ PO ₂ Na.	41	737	a.PC2 str.	
	41	700	s.PC2 str.	
(CH ₃ -O-) ₂ (CH ₃ -)P(=O)	20	711		
(CH ₃ -O-) ₂ (CH ₃ -)P(=S)	20	793		
Range		699-833		

TABLE 8.23 The trans and/or cis N-H stretching frequencies for compounds containing the P-NH-R group

Compound	Ref.	NH str. cis CCl ₄ soln. cm ⁻¹	NH str. trans CCl ₄ soln. cm ⁻¹	Frequency separation [cis]-[trans] cm ⁻¹
Cl ₂ (CH ₃ -NH-)P(=O)	24	3408		
Cl ₂ (CH ₃ -NH-)P(=S)	24,42	3408		
Cl ₂ (CD ₃ -NH-)P(=S)	24,42	3409		
Cl ₂ (C ₂ H ₅ -NH-)P(=S)	24,42	3397		
Cl ₂ (isoC ₃ H ₇ -NH-)P(=S)	24,42	3388		
Cl(CH ₃ -O-)(CH ₃ -NH-)P(=S)	28	3425		
Cl(CH ₃ -O-)(C ₂ H ₅ NH-)P(=S)	28	3411		
Cl(CH ₃ -O-)(isoC ₃ H ₇ -NH-)P(=S)	28	3403	3385sh	18
Cl(C ₂ H ₅ -O-)(CH ₃ -NH-)P(=S)	28	3430	~3400sh	30
Cl(C ₂ H ₅ -O-)(C ₂ H ₅ -NH-)P(=S)	28	3402		
Cl(C ₂ H ₅ -O-)(isoC ₃ H ₇ -NH-)P(=S)	28	3408	3390sh	18
Cl(isoC ₃ H ₇ -O-)(CH ₃ -NH-)P(=S)	28	3422		
Cl(isoC ₃ H ₇ -O-)(C ₂ H ₅ -NH-)P(=S)	28	3409		
Cl(isoC ₃ H ₇ -O-)(isoC ₃ H ₇ -NH-)P(=S)	28	3405	3390sh	15
(CH ₃ -O-) ₂ (CH ₃ -NH-)P(=O)	28	3444		
(CH ₃ -O-) ₂ (CH ₃ -NH-)P(=S)	28	3447	3403	44
(C ₂ H ₅ -O-) ₂ (CH ₃ -NH-)P(=O)	28	3439		
(C ₂ H ₅ -O-) ₂ (CH ₃ -NH-)P(=S)	28	3442	3404	38
(CH ₃ -O-) ₂ (isoC ₃ H ₇ -NH-)P(=S)	28	3429	3387	42
(C ₂ H ₅ -O-) ₂ (isoC ₃ H ₇ -NH-)P(=S)	28	3419	3380	39
(CH ₃ -O-)(2,4,5-Cl ₃ -C ₆ H ₂ -O-)(CH ₃ -NH-)P(=O)	28	3429*		
(CH ₃ -O-)(2,4,5-Cl ₃ -C ₆ H ₂ -O-)(CH ₃ -NH-)P(=S)	28	3442	3409	31
(cH ₃ -O-)(2,4,5-Cl ₃ -C ₆ H ₂ -O-)(C ₂ H ₅ -NH-)P(=O)	28	3425		
(CH ₃ -O-)(2,4,5-Cl ₃ -C ₆ H ₂ -O-)(C ₂ H ₅ -NH-)P(=S)	28	3429	3398	31
(CH ₃ -O-)(2,4,5-Cl ₃ -C ₆ H ₂ -O-)(iso-C ₄ H ₉ -NH-)P(=O)	28	3428		
(CH ₃ -O-)(2,4,5-Cl ₃ -C ₆ H ₂ -O-)(iso-C ₄ H ₉ -NH-)P(=S)	28	3431	3400	31
(CH ₃ -O-)(2,4,5-Cl ₃ -C ₆ H ₂ -O-)(isoC ₃ H ₇ -NH-)P(=O)	28	3413		
(CH ₃ -O-)(2,4,5-Cl ₃ -C ₆ H ₂ -O-)(isoC ₃ H ₇ -NH-)PP(=S)	28	3419	3385	34
(CH ₃ -O-)(2,4,5-Cl ₃ -C ₆ H ₂ -O-)(t-C ₄ H ₉ -NH-)P(=O)	28	3401		
(CH ₃ -O-)(2,4,5-Cl ₃ -C ₆ H ₂ -O-)(t-C ₄ H ₉ -NH-)P(=S)	37	3402		
(CH ₃ -O-) ₂ (HDN-)P(=S)	37	3461	3434	27
(C ₂ H ₅ -O-) ₂ (HDN-)P(=S)	37	3452	3427	25

*In CH₂Cl₂ solution.

TABLE 8.24 The NH₂, NHD, NH₂, NH and ND frequencies for O,O-dimethyl phosphoramidothioate, O,O-diethyl phosphoramidothioate, and N-methyl O,O-dimethylphosphoramidothioate

O,O-dimethyl phosphoramidothioate NH ₂ :ND ₂ cm ⁻¹	[NH ₂],[ND ₂]	O,O-diethyl phosphoramidothioate NH ₂ :ND ₂ cm ⁻¹	[NH ₂]/[NH ₂]	O,O-diethyl N-methyl- phosphoramidothioate NH:ND cm ⁻¹	[NH]/[ND]	Assignment(37)
3480:2611	1.33	3481:2600	1.34			a.NH ₂ or a.ND ₂ str.
3390:2490	1.36	3389:2491	1.36			s.NH ₂ or s.ND ₂ str.
3450:(2515)* ¹	1.37	~3450				NH ₂ or ND ₂ str. bonded
3350:(2410)* ¹	1.39	~3352:~2460	1.36			
3310:~2450	1.35	~3305				
NHD:NHD		NHD:NHD				
3461:2561	1.35	3452:2553	1.35	3442:2562	1.34	cis NH or ND str.
3434:2535	1.34	3427:2530	1.35	3404:2539	1.34	trans NH or ND str.
				3320:2470	1.34	NH or ND str. bonded
~3070		2342		~3070:2345	1.31	2(NH or ND bend)
1542:1171	1.32	1542:1170 (1179)* ¹	1.32			NH ₂ or ND ₂ bend
				1380:1250	1.1	NH or ND bend
NHD		NHD				
~1382		~1385				NHD bend
971:760	30:43:12	977:785	1.24			NH ₂ or ND ₂ wag* ²
922:718	1.28	913:721	1.27			NH ₂ or ND ₂ twist* ²
:938		:masked* ²				NHD twist

*¹Liquid.*²See text.

TABLE 8.25 The N–H and N–D stretching and bending frequencies for O-alkyl O-(2,4,5-trichlorophenyl) N-alkylphosphoramidate and O-methyl O-(2,4,5-trichlorophenyl) N-alkylphosphoramidothioate

	NH str. [CCl ₄] * ²	ND str. [CCl ₄] * ³	δ [CCl ₄] cm ⁻¹	NH str. [CH ₂ Cl ₂] * ²	ND str. [CH ₂ Cl ₂] * ³	δ [CH ₂ Cl ₂] cm ⁻¹	O-methyl O-(2,4,5-trichlorophenyl) N-alkylphosphoramidothioate	NH str. cis [CCl ₄] cm ⁻¹	NH str. trans [CCl ₄] cm ⁻¹	[NH str. cis]- [NH str. trans] cm ⁻¹
N-alkyl methyl	insol.	insol.		3429 [2550]* ¹	3256 [2432]	173 118	N-alkyl	3442	3409	33
(NH/ND) ethyl	3425 [~2545]	3224 [~2394]	201	3415	3245	170		3429	3398	31
(NH/ND) isobutyl	3428 [2545]	3228 [2412]	151 200	3417	3249	168		3431	3400	31
(NH/ND) isopropyl	3413 [2538]	3213 [2384]	200 154	3405	3230	175		3419	3385	34
(NH/ND) t-butyl	3401 [2528]	3201 [2384]	200 144	3395	3214	181		3402		
[NH/ND]	1.34 δ [CCl ₄]* ²	(~1.34) δ [CCl ₄]* ³	δ NH [CH ₂ Cl ₂]* ²	δ ND [CH ₂ Cl ₂]* ³						
methyl			1397	1426				1397		
ethyl	1415	~1442 [1214]	1415	1442				1403		
(NH/ND) isobutyl	~1418	(~1.19) ~1440	1421					1406		
isopropyl	~1417	~1442 1440 [~1211]	1417					1404		
(NH/ND) t-butyl	1396	(~1.19) 1440 : 1408 [1222?]	1393	1425 1410				1382		
(NH/ND)		(~1.18 or ~1.15)								

*¹N–D frequencies.*²Monomer.*³Bonded.

TABLE 8.26. The cis and trans NH stretching frequencies for compounds containing O=P–NH–R or S=P–NH=R groups*¹

Compound	N-Alkyl	N–H str. cis cm ⁻¹	N–H str. trans cm ⁻¹	[NH str. cis]- [N–H str. Trans.] cm ⁻¹	N–H bending cm ⁻¹
O-alkyl kO-aryl N-alkylphosphoramidate	CH ₃ C ₂ H ₅ n-C ₃ H ₇ n-C ₄ H ₉ isoC ₃ H ₇ t-C ₄ H ₉	3444 3428 3430 3430 3418 3400			1393 1413 1415 1416 1415 1396
O-aryl N,N'-dialkyl phosphorodiamidate	CH ₃ , CH ₃	3436			1390
O-alkyl O-aryl N-alkylphosphoramido- thioate	CH ₃ C ₂ H ₅ n-C ₃ H ₇ iso-C ₄ H ₉ n-C ₄ H ₉ iso-C ₃ H ₇ s-C ₄ H ₉ t-C ₄ H ₉	3440 3430 3428 3431 3427 3419 3417 3400	3408 3399 3401 3410 3402 3385 3387	32 31 27 21 25 34 30	1381 1400 1403 1404 1402 1408 1406 1383
O,O-dialkyl N-alkyl phosphoramidothioate	CH ₃ isoC ₃ H ₇	3443 3421	3408 3385	35 36	1377 1402
N-alkylphosphoramidodichloridothioate	CH ₃ C ₂ H ₅ isoC ₃ H ₇	3414 3397 3388			1372 1393 1403
O-alkyl N,N'-dialkylphos- phorodiamidothioate	CH ₃ C ₂ H ₅ n-C ₃ H ₇ n-C ₄ H ₉ isoC ₃ H ₇ s-C ₄ H ₉ C ₆ H ₅ CH ₂	3448 3433 3430 3429 3419 3414 3421	3414 3404 3405 3401 3397 3398 3395	34 29 25 28 22 16 26	1378 1400 1400 1401 1402 1402 1399
O-aryl N,N'-dialkylphos- phorodiamidothioate	isoC ₃ H ₇ CH ₃ , isoC ₃ H ₇	3415 3438;3415	3396 3415;3395	19	1403 1387;1403
N-alkylphosphoramidodi-chloridate	CH ₃	3408 3195(H-bonded)			1390 1418(H-bonded)
		a.NH ₂ str.	s.NH ₂ str.		NH ₂ bending
O-alkyl O-aryl phosphor- amidothioate	H	* ²			1579* ³
O,O-dialkylphosphoramido- thioate	H	3490	3390		1539* ³
O-alkyl O-arylphosphor- amidothioate	H	3490	3390		1538* ³

*¹See Reference 37.

*²Not studied in dilute solution.

*³Solid phase.

TABLE 8.27. Vibrational assignments for N-alkyl phosphoramidodichloridithioate and the CD₃NH, CD₃ND and CH₃ND analogs

CH ₃ -NH-P(=S)Cl ₂ cm ⁻¹	CD ₃ -NH-P(=S)Cl ₂ cm ⁻¹	C ₂ H ₅ -NH-P(=S)Cl ₂ cm ⁻¹	isoC ₃ H ₇ -NH-P(=S)Cl ₂ cm ⁻¹	CH ₃ -ND-P(=S)Cl ₂ cm ⁻¹	CD ₃ -ND-P(=S)Cl ₂ cm ⁻¹	Assignment(24)
1094	1117	1112	1129	1107	1197 or 965	C-N str. or a.P-N-C str., a'
838	785	780	812	825	780	P-N str. or s.P-N-C str., a'
725	711	725	727	728	701	P=S str., rotational conformer 1, a'
690	683	681	690	681	673	P=S str., rotational conformer 2, a'
512	515	512	514	513	510	a.PCl ₂ str., a''
468	463			470	461	s.PCl ₂ str., rotational conformer 2, a'
450	446			447	443	s.PCl ₂ str. rotational conformer 1, a'
395	384			404	386	C-N-P bend, rotational conformer 2, a'
370	360			382	362	C-N-P bend, rotational conformer 1, a'
masked	masked			310	305	P-N rock, a' and a''
261	251			260	258	s.PSCl ₂ bend, a'
216	213			218	213	a.PSCl ₂ def., a' and a''
180	183			180	180	P-N-C torsion, a''
3408	3409			2532	2532	NH or ND str., monomer, a'
3300	3301			2242	2477	NH or ND str., bonded
2745	2892			near 2442	2384	2(NH or ND bend), A'
1370	1359			1234	1197	NH or ND bend, a'
340	350			near 260	near 258	γ NH or ND, bonded
295	292			near 218	near 213	γ NH or ND, monomer, a''

TABLE 2.28 Vibrational assignments for O,O-dimethyl O-(2,4,5-trichlorophenyl) phosphorothioate and its P=O and (CD₃-O-)₂ analogs

(CH ₃ -O-) ₂ P=S (2,4,5-Cl ₃ -C ₆ H ₂ -O-) cm ⁻¹	(CD ₃ -O-) ₂ P=S (2,4,5-Cl ₃ -C ₆ H ₂ -O-) cm ⁻¹	(CH ₃ -O-) ₂ P=O (2,4,5-Cl ₃ -C ₆ H ₂ -O-) cm ⁻¹	(CD ₃ -O-) ₂ P=O (2,4,5-Cl ₃ -C ₆ H ₂ -O-) cm ⁻¹	Assignment(43)
1062	1076	1061	1107	s.(C-O-) ₂ P str.
1041	1061	1043	1070	a.(C-O-)P str.
847	793	776	742	s.P(-O-) ₂ str.
830	811	859	810	a.P(-O-) ₂ str.
1248	1247	1251	1252	(C ₆ H ₂ -O-)P str.
968	965	968	968	(P-O-)C ₆ H ₂ str.
616	617	1284	1292	P=S str. or P=O* ¹
		1300	1306	P=O* ¹
3022	2272	3021	2275	a.CH ₃ or a.CD ₃ str., a''
3001	2258	3001	2260	a.CH ₃ or a.CD ₃ str., a'
2960	2088	2961	2089	s.CH ₃ or s.CD ₃ str., a'* ²
2857	2211	2861	2219	2(CH ₃ or CD ₃ bend)* ²
masked	1101	masked	1097	a.CH ₃ or CD ₃ bend, a' and a''
1447	1101	masked	1097	s.CH ₃ or s.CD ₃ bend, a'
1183	923	1184	922	CH ₃ or CD ₃ rock, a' (P-O-C plane)
1183	masked	1184	masked	CH ₃ or CD ₃ rock, a''(P-O-C plane)
				CH ₃ or CD ₃ torsion, a' and a''

*¹Rotational conformers.*²In Fermi Resonance.

TABLE 8.29 Vibrational assignments for 1-fluoro-2,4,5-trichlorobenzene and the ring modes for O,O-dimethyl O-(2,4,5-trichlorophenyl) phosphorothioate and its P=O and (CD₃-O-)₂ analogs

[43] (CH ₃ -O-) ₂ P=S (2,4,5-Cl ₃ -C ₆ H ₂ -O-) cm ⁻¹	[43] (CD ₃ -O-) ₂ P=S (2,4,5-Cl ₃ -C ₆ H ₂ -O-) cm ⁻¹	[43] (CH ₃ -O-) ₂ P=O (2,4,5-Cl ₃ -C ₆ H ₂ -O-) cm ⁻¹	[43] (CD ₃ -O-) ₂ P=O (2,4,5-Cl ₃ -C ₆ H ₂ -O-) cm ⁻¹	[9] 1-F,2,4,5Cl ₃ - C ₆ H ₂ - cm ⁻¹	Assignment
a' species					
3099	3098	3085	3098	3098	v1
3075	3070	3075	3075	3061	v2
1582	1583	1583	1587	1589	v3
1557	1560	1559	1562	1571	v4
1463	1463	1463	1465	1461	v5
1352	1353	1352	1352	1357	v6
1260	1258	1257	1258	1263	v7
1248	1247	1251	1251	1251	v8
1230	1228	1239 or 1220	1228	1239	v9
1127	1125	1122	1122	1128	v10
1088	1076	1087	1084	1086	v11
?	?	911	911	934	v12
729	720	712	715	725	v13
686	679	688	681	677	v14
556	548	570	572	572	v15
537	532	544	545	528	v16
383	375	364	365	390	v17
330	322	335	335	373	v18
257	250	247	246	275	v19
210	200	203	202	211	v20
170	180?	172	170	196	v21
a'' species					
887	882	882	882	882	v22
872	852	866	869	863	v23
689	686	680 or 688	687	669	v24
629	627	627	629	622	v25
440	439	452	460	447	v26
360	355	347	354	373	v27
231	225	225	230	249	v28
157	153	152	152	154	v29
95?	~90?	~80?	88?	93?	v30

TABLE 8.30 Infrared data for O,O-dialkyl phosphorochloridothioate and O,O,O-trialkyl phosphorothioate in different physical phases

O,O-Dialkyl phosphorochloridothioate	C—O str. +P—O str. cm ⁻¹	C—O str. cm ⁻¹	P—O str. cm ⁻¹	P=S str. cm ⁻¹	P—Cl str. cm ⁻¹	C—C str. cm ⁻¹	Physical state
Dimethyl	1888	1045	845	665	490		vp, 200 °C
Dimethyl	1878.7bd	[1055.9,1042sh]	[836.2,845sh]	[666.1,654.9]	[485.7,524.7]		solution
Dimethyl	1868.9bd	[1050.1035.4]	[835.4,850sh]	[665,656.4]	[486.8,526.9]		liquid
Diethyl	1845	1030	821	662	499	966	vp, 200 °C
Diethyl	~1820	1010	809	668,652	~490,529	969	neat
	25	20	12	6,10	9,30		
Dipropyl	~1870	[1005,1055]	853	664	504		vp, 200 °C
Dipropyl	~1855	[1005,1055]	858	664	509		neat
	15	[0,0]	-5	0	-5		
O,O,O-trialkyl phosphorothioate							
trimethyl	1885	1054	834	605			vp, 200 °C
trimethyl	~1863	~1025	820	616,595			neat
	22	29	14	[-11,10]			
triethyl	~1850	~1040	828	614		960	vp, 200 °C
triethyl		~1018	~815	631,604		960	neat
		22	13	[-17,10]			

TABLE 8.31 Infrared data for organophosphates and organohydrogenphosphonates in different physical phases

Compound	P=O str. cm ⁻¹	P=O str. cm ⁻¹	PH bend cm ⁻¹	POC str. cm ⁻¹	POC str. cm ⁻¹	PO ₃ sym. str. cm ⁻¹	Physical state
Phosphate							
Triethyl	1300	*1280		1045	810	748	Vapor, 216 °C
Triethyl	1277	1262		1033	821;797	744	CS ₂ soln.
	23	18		12	[-11];[13]	4	vapor-CS ₂ soln.
Propyl	1299	*1282		[1050],*[1009]	820	750	Vapor, 280 °C
Propyl	1270	1270		[1055],*[1004]	860	751	neat
	19	12		[-5],[5]	-40	-1	vapor-neat
Butyl	1300	*1280		[1060],*[1030]	815	736	Vapor, 289 °C
Butyl	1280	1280		[1055],[1021]	802	731	neat
	20	0		[5],[9]	13	5	vapor-neat
Phenyl	*1311	1300		1191	955	770	Vapor, 280 °C
Phenyl	1300	*1288		1171	950	765	neat
	11	12		20	5	5	vapor-neat
Diphenyl methyl	1316	1316		1198	[821],[952]	765	Vapor, 280 °C
Diphenyl methyl	1305	*1290		1182	[815],[950]	762	neat
	11	26		16	[6],[2]	3	vapor-neat
Phosphonate							
		PH str. CCl ₄ soln. cm ⁻¹	PH bend cm ⁻¹				
Dimethyl hydrogen	1290	~2439	985	1065	815	770	Vapor, 200 °C
Dimethyl hydrogen	[1282],*[1264] [8],[26]	2435	988	1055	821	766	CS ₂ soln.
		4	-3	10	-6	4	vapor-CS ₂ soln. vapor-CCl ₄ soln.
Diethyl hydrogen	1281	~2435	~983	1061	780	749	Vapor.200 °C
Diethyl hydrogen	[1280],*[1262] [1],[19]	~2438	~978	[1084],*[1054]	784	741	CS ₂ soln.
		~ -3	5	[-23],[7]	-4	8	vapor-CS ₂ soln.

*Strongest band in the doublet.

TABLE 8.32 Infrared data for O-alkyl phosphorodichloridothioates and S-alkyl phosphorodichloridothioates in different physical phases

O-alkyl Phosphorodichloridothioate	C–O str.	C–O str.	P–O str.	P–O str.	a.PCl ₂ str.	a.PCl ₂ str.	s.PCl ₂ str.	s.PCl ₂ str.	P=O str.	P=O str.	Physical phase
	isomer 1 cm ⁻¹	isomer 2 cm ⁻¹	isomer 1 cm ⁻¹	isomer 2 cm ⁻¹	isomer 1 cm ⁻¹	isomer 2 cm ⁻¹	isomer 1 cm ⁻¹	isomer 2 cm ⁻¹	isomer 1 cm ⁻¹	isomer 2 cm ⁻¹	
O-ethyl	1026	1014	804	790	528	552	472	490	728	701	CS ₂ soln.
	~1027	977	789bd	798bd	533	555	473	490	728	701	liquid
O-ethyl-1,1-d ₂	-1	37	15	-8	-5	-3	-1	0	0	0	CS ₂ -liquid
	1025	1008	783	796	525	550	465	484	727	699	CS ₂ soln.
O-ethyl-2,2,3d ₃	1025	1010	782	797	529	551	466	474	726	700	liquid
	0	-2	1	-1	-4	-1	-1	-10	1	-1	CS ₂ -liquid
O-(2-Propynyl) [32]	1013	995	750	750	526	551	460	481	688	691	CS ₂ -soln.
	1010	998	750	750	531	552	462	?	675	677	liquid
O-(2-Propynyl) [32]	3	-3	0	0	-5	-1	-2	?	13	14	CS ₂ -liquid
	1015	984	857	822	529	557	440	474	742	716	CS ₂ -soln.
O-(2-Propynyl) [32]	1014	982	853	821	533	556	440	473	739	714	liquid
	1	2	4	1	-4	1	0	1	3	2	CS ₂ -liquid
S-methyl Phosphorodichloridothioate	C–S str. isomer 1 cm ⁻¹	C–S str. isomer 2 cm ⁻¹	a.PSCL ₂ str. isomer 1	a.PSCL ₂ str. isomer 2	a.PSCL ₂ str. isomer 1 cm ⁻¹	a.PSCL ₂ str. isomer 2 cm ⁻¹	s.PSCL ₂ str. isomer 1 cm ⁻¹	s.PSCL ₂ str. isomer 2 cm ⁻¹	P=O str. isomer 1 cm ⁻¹	P=O str. isomer 2 cm ⁻¹	CS ₂ soln. liquid CS ₂ -liquid
	689	732	547a''	560a''	593a'	579a'	450	471	1275	1266	
S-methyl Phosphorodichloridothioate	685	729	547a''	555a''	598a'	582a'	451	470	1261		
	4	3	0	5	-5	-3	-1	1	14		

TABLE 8.33 Infrared data for O,O-diethyl N-alkylphosphoramidates in different physical phases

Alkylphosphoramidic acid, diethyl ester N-alkyl	P=O str. cm ⁻¹ vapor phase	P=O:H str. cm ⁻¹ neat phase	POC str. cm ⁻¹ vapor phase	POC str. cm ⁻¹ vapor phase	PO ₂ N str. cm ⁻¹ vapor phase	NH str. cm ⁻¹ vapor phase	NH:O=P str. cm ⁻¹ neat phase	Physical phase
Methyl	1275	1225	1041	842	749	3460	3240	240 °C
Ethyl	1275	1230	1044	795	750	3440	~3235	240 °C
Hexyl	1275	1230	1044	798	750	3450	~3230	240 °C
Phenethyl	1280	1229	1045	803	749	3440	~3230	280 °C
Isopropyl	1274	1230	1037	794	755	3430	3220	240 °C
Cyclohexyl	1275	1240	1040	795	755	3422	3198	280 °C
Tert-butyl	1275	1237	1045	796	760	3420	3208	240 °C
Phenyl	1275	1210	1039	796	749	3435	3210	280 °C

	P=O str.- P=O:H str. cm ⁻¹	NH str.- NH:O=P str. cm ⁻¹	cm ⁻¹ neat phase	cm ⁻¹ neat phase	cm ⁻¹ neat phase
Methyl	50	220	1024	860	791
Ethyl	45	205	1030	790	740
Hexyl	45	220	1030	792	755
Phenethyl	51	210	1020	791	745
Isopropyl	34	210	1030	790	745
Cyclohexyl	35	224	1053	793	752
Tert-butyl	38	212	1024	789	760
Phenyl	65	225	1010	791	745

TABLE 8.34 Vibrational assignments for [CH₃-PO₃]²⁻, [CD₃-PO₃]²⁻, [H-PO₃]²⁻, and [PO₄]₃-

[40] [CH ₃ -PO ₃] ²⁻ cm ⁻¹	[40] [CD ₃ -PO ₃] ²⁻ cm ⁻¹	C _{3v} symmetry	[44] [H-PO ₃] ²⁻ cm ⁻¹	C _{3v} symmetry	[45] [PO ₄] ₃ - cm ⁻¹	Td symmetry
1057	1060	a.PO ₃ str.,e	1085	a.PO ₃ str.,e	1082	a.PO ₄ str., f ₂
753	720	C-P str.,a ₁				
977	972	s.PO ₃ str.,a ₁	979	s.PO ₃ str.,a ₁	980	s.PO ₄ str., a ₁
510	510	e	465	a.PO ₃ bend,e	515	a.PO ₄ bend, f ₂
485	495	s.PO ₃ bend,a ₁	567	s.PO ₃ bend,a ₁		
335	~320	e			363	PO ₄ def., e

	CH ₃ (cm ⁻¹)/CD ₃ (cm ⁻¹)	Assignment
2983	~2225	1.34 a.CH ₃ str. or a.CD ₃ str.
2921	2142	1.36 s.CH ₃ str. or s.CD ₃ str.
1425	?	? a.CH ₃ bend or a.CD ₃ bend
842	~622	1.35 s.CH ₃ rock or s.CD ₃ rock
?	?	? CH ₃ torsion or CD ₃ torsion

TABLE 8.35 Infrared data and assignments for the $(\text{CH}_3)_2\text{PO}_2^-$ anion

$(\text{CH}_3)_2\text{P}(\text{O})_2\text{Na}$ cm^{-1}	Assignment for C_{2v} symmetry	$\text{H}_2\text{P}(\text{O})_2\text{K}$ cm^{-1}	Assignment for C_{2v} symmetry
1120	a. PO_2 str., b1	1180	a. PO_2 str., b2
1040	s. PO_2 str., a1	1042	s. PO_2 str., a1
479	PO_2 bend,a1	469	PO_2 bend,a1
		$[\text{PO}_4]^{3-}$	for Td symmetry
1120	a. PO_2 str., b1		
738	a. $\text{P}(\text{C})_2$ str., b2	1082	a. PO_4 str., f2
700	s. $\text{P}(\text{C})_2$ str., a1		
1040	s. PO_2 str., a1	980	s. PO_4 str., a1
479	s. $(\text{C})_2\text{P}(\text{O})_2$ bend,a1		
440	a. $(\text{C})_2\text{P}(\text{O})_2$ bend, b1 and b2	515	a. PO_4 bend,f2
352			
315	$(\text{C})_2\text{P}(\text{O})_2$ twist,a2	363	PO_4 defor., e
272	$(\text{C})_2\text{P}(\text{O})_2$ defor., a1		
		$(\text{CH}_3)_3\text{P}$	for C_{3v} symmetry
738	a. $\text{P}(\text{C})_2$ str., b2	708	a. $\text{P}(\text{C})_3$ str., e
700	s. $\text{P}(\text{C})_2$ str., a1	653	s. $\text{P}(\text{C})_3$ str., a1
		305	a. $\text{P}(\text{C})_3$ bend,a1
		263	s. $\text{P}(\text{C})_3$ bend,a1
		$(\text{CH}_3)_3\text{PO}$	for C_{3v} symmetry
735	a. $\text{P}(\text{C})_3$ str., b2	756	a. $\text{P}(\text{C})_3$ str., e
700	s. $\text{P}(\text{C})_3$ str., a1	671	s. $\text{P}(\text{C})_3$ str., a1
		311	$\text{P}(\text{C})_3$ bend, e
		256	$\text{P}(\text{C})_3$ bend, a1

Benzene and Its Derivatives

Introduction	353
Polychlorobiphenyls	353
An A_1 Fundamental for Toluene and Related Analogs	355
Styrene-4-Methylstyrene Copolymers	355
Styrene-Acrylic Acid Copolymer	358
Styrene Acrylamide Copolymer	359
Styrene/2-Isopropenyl-2-Oxazoline Copolymer (SIPO Copolymer)	359
Ethynylbenzene and Ethynylbenzene-d	359
Bromodichlorobenzenes	360
Raman Data for 1,2-Disubstituted Benzenes	360
Vibrational Data for 1,3-Dichlorobenzene and Raman Data for 1,3-Disubstituted Benzenes	361
Raman Data and Assignments for Some In-Plane Ring Modes 1,4-Distributed Benzenes	361
Raman Data for Decabromobiphenyl and Bis (Pentabromophenyl) Ether	361
Infrared Data and Assignments for Benzene, Benzene-d ₆ , Benzyl Alcohol, and Benzyl -2, 3, 4, 5, 6 - d ₅ Alcohol	361
Out-of-Plane Deformations and Their Combination and Overtones for Substituted Benzenes	362
Polystyrene and Styrene Copolymers	362
Ethynylbenzene	363
1,2-Disubstituted Benzenes	363
1,3-Disubstituted Benzenes	364
1,4-Disubstituted Benzenes	364
1,3,5-Trisubstituted Benzenes	364
1,2,3-Trisubstituted Benzenes	364
1,2,4-Trisubstituted Benzenes	365
1,2,3,4-Tetrasubstituted Benzenes	365
1,2,3,5-Tetrasubstituted Benzenes	365
1,2,4,5-Tetrasubstituted Benzenes	365
1,2,3,4,5-Pentasubstituted Benzenes	366
Summary of the Out-of-Plane Hydrogen Deformations for Substituted Benzenes and the Out-of-Plane Ring Deformation for Mono-substituted Benzenes, and Their Combination and Overtones	366
Correlation Chart	366
2,3,4,5,6-Pentachlorobiphenyl	366
References	367

Figures

Figure 9-1	368 (354)	Figure 9-25	383 (357)
Figure 9-2	368 (354)	Figure 9-26	384 (358)
Figure 9-3	369 (554)	Figure 9-27	385 (358, 362)
Figure 9-4	369 (354)	Figure 9-28	386 (358)
Figure 9-5	370 (354)	Figure 9-29	387 (359, 362)
Figure 9-6	370 (354)	Figure 9-30	388 (359, 362)
Figure 9-7	371 (354)	Figure 9-31	388 (359)
Figure 9-8	371 (354)	Figure 9-32	389 (359, 363)
Figure 9-9	372 (354)	Figure 9-33	390 (359)
Figure 9-10	372 (354)	Figure 9-34	391 (359)
Figure 9-11	373 (354)	Figure 9-35	392 (359)
Figure 9-12	373 (354)	Figure 9-36	393 (362)
Figure 9-13	374 (354)	Figure 9-37	394 (363)
Figure 9-14	374 (354)	Figure 9-38	395 (363)
Figure 9-15	375 (354)	Figure 9-39	396 (364)
Figure 9-16	375 (354)	Figure 9-40	397 (364)
Figure 9-17	376 (355)	Figure 9-41	398 (364)
Figure 9-18	377 (355)	Figure 9-42	399 (364)
Figure 9-19	378 (355, 362)	Figure 9-43	399 (365)
Figure 9-20	378 (355, 362)	Figure 9-44	400 (365)
Figure 9-21	379 (355, 362)	Figure 9-45	400 (365)
Figure 9-22	380 (355, 362)	Figure 9-46	401 (365)
Figure 9-23	381 (355, 362)	Figure 9-47	401 (366)
Figure 9-24	382 (356, 362)	Figure 9-48	402 (366)

Tables

Table 9-1	403 (357)	Table 9-13	417 (354)
Table 9-2	404 (354)	Table 9-14	418 (355)
Table 9-3	405 (354)	Table 9-15	418 (360)
Table 9-4	406 (354)	Table 9-16	419 (360)
Table 9-5	407 (354)	Table 9-17	419 (361)
Table 9-6	408 (354)	Table 9-18	420 (361)
Table 9-7	409 (354)	Table 9-19	420 (361)
Table 9-8	411 (354)	Table 9-20	421 (361)
Table 9-9	413 (354)	Table 9-21	422 (362)
Table 9-10	414 (354)	Table 9-22	422 (362)
Table 9-11	415 (354)	Table 9-23	423 (362)
Table 9-12	416 (354)	Table 9-24	423 (366)

*Numbers in parentheses indicate in-text page reference.

INTRODUCTION

Benzene has 30 fundamental vibrations, and benzene substituted with atoms such as halogen also has 30 fundamental vibrations. Twenty-one fundamentals are in-plane vibrations, and nine fundamentals are out-of-plane vibrations. Moreover, there are 30 fundamental benzene ring vibrations for all of its derivatives. Thus, for a compound such as toluene, which has 39 fundamental vibrations, 30 fundamentals result from C_6H_5C vibrations, and 9 fundamentals result from CH_3 vibrations.

Benzene and derivatives of benzene, which have a center of symmetry, have IR vibrations that are IR active (allowed in the IR) and vibrations that are Raman active (allowed in the Raman). Therefore, it is most helpful in the spectra-structure identification of benzene and its derivatives to obtain both IR and Raman data. Of course, a standard IR or Raman spectrum, if available for comparison, is sufficient to identify a chemical compound when the spectrum of the sample and standard reference are identical.

In the case of IR, it is helpful to obtain a spectrum in the vapor phase. This is because the IR band shapes help in determining which vibrations are in-plane vibrations and which vibrations are out-of-plane vibrations. In the case of Raman, it is helpful to obtain polarized and depolarized data to help distinguish between in-plane and out-of-plane vibrations. In certain cases, a fundamental is both IR and Raman inactive. Moreover, compounds with no molecular symmetry, but with only its identity, have molecular vibrations that are both IR and Raman active. Another helpful feature in interpreting IR and Raman data is that normal vibrations with strong IR band intensity have weak Raman band intensity and vice-versa.

Several publications are available to assist one in the spectra-structure identification of benzene and its derivatives (1–6). Reference 6 discusses in detail both in-plane and out-of-plane normal vibrations for substituted benzenes together with schematics of their approximated normal vibrations. This reference is recommended for those who are unfamiliar with this topic.

Some of the topics covered in this section are the result of chemical problems submitted to us for spectra-structure identification by The Dow Chemical Company.

POLYCHLOROBIPHENYLS

Polychlorobiphenyls have been utilized in the electrical power industry. These chemicals are alleged to be carcinogenic materials, and their possible presence in the environment requires methods for their detection and identification.

There are 66 possible pentachlorobiphenyl isomers, and 16 of these isomers are included here. These spectra were recorded utilizing the DRIFT technique (diffuse reflectance infrared Fourier transform), because it is especially useful in obtaining IR spectra of liquid chromatograph (LC) fractions where the amount of sample available is limited (7). All 16 spectra were recorded by using 1–5 μ g of sample deposited from hexane solution via a syringe on approximately 100 mg of KBr powder placed in the sample cup. The solvent was evaporated using an IR heat lamp.

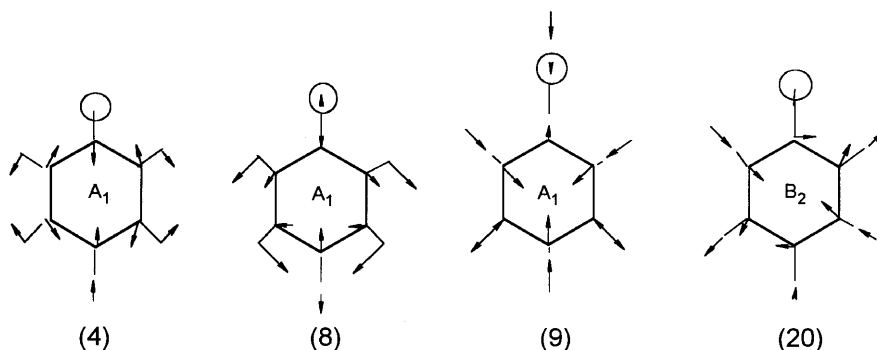
Biphenyl and each polychlorobiphenyl isomer have 60 fundamental vibrations; therefore, it is twice as difficult to determine ring substitution for the polychlorobiphenyl isomers as it is, for

example, benzene and any of the chlorinated benzenes. Moreover, there is no indication which ring modes belong to one substituted phenyl group from the other substituted phenyl group in the case of polychlorobiphenyl isomers. In order to be able to predict which bands belong to each substituted phenyl group, it is necessary to know the potential energy distribution for each of the normal modes for both 1,2,4-trichlorobenzene and 1,2,4,5-tetrachlorobenzene to determine whether the structure of a pentachlorobiphenyl isomer is 2,2',4,4',5-pentachlorobiphenyl or 2,3',4,4',5-pentachlorobiphenyl, for example. This is because normal vibrations, including a significant potential energy contribution from carbon-chlorine stretching, are expected to be affected significantly by substitution of a 2,4-dichlorophenyl group or a 3,4-dichlorophenyl group from 1,2,4-trichlorophenyl for a chlorine atom of 1,2,4,5-tetrachlorobenzene. Scherer (3) has performed normal coordinate calculations for chlorobenzenes and deuterated chlorobenzenes, and the resulting potential energy distribution data were used to enable the development of IR group frequency verification of these 16 polychlorobiphenyl isomers. The IR spectra and assignments are reported in the literature (7).

The diffuse reflectance FT-IR spectra are presented in Figs. 9.1 through 9.16, and vibrational assignments for the 16 polychlorobiphenyl isomers are presented in Tables 9.1 through 9.12 (7); these assignments are compared to those for correspondingly substituted chlorobenzenes.

Out-of-plane ring hydrogen deformations are also useful in characterizing substituted benzenes, and these spectra-structure correlations for polychlorobiphenyls are discussed later in this chapter.

Table 9.13 lists Raman data for a variety of compounds containing the phenyl group (8). It has been reported that two planar polarized Raman bands and one planar depolarized Raman band yield characteristic frequencies and intensities regardless of the nature of the substituent group (9). These three planar ring vibrations together with a fourth planar ring mode are shown here:



Ring mode 9 is essentially a ring breathing vibration, and its Raman band occurs in the region 994–1010 cm^{-1} . This Raman band is usually the most intense band in the spectrum, and it is polarized. Notable exceptions are exhibited by cinnamic acid, glycidyl cinnamate, and 1,6-diphenyl-1,3,5-hexatriene.

Ring mode 8 occurs in the region 1010–1032 cm^{-1} , and this polarized Raman band is relatively weak. Ring mode 20 occurs in the region 603–625 cm^{-1} , and the Raman band is depolarized and has weak intensity. Ring mode 4 occurs in the region 1585–1610 cm^{-1} , and the Raman band has variable intensity.

The relative Raman band intensity ratio for Ring 4/Ring 9 varies between 0.11 and 1.14, for Ring 8/Ring 9 it varies between 0.06 and 0.33, and for Ring 20/Ring 9 it varies between 0.06 and 0.25. All of these Raman data help in the spectra-structure identification of the phenyl group in organic materials.

AN A_1 FUNDAMENTAL FOR TOLUENE AND RELATED ANALOGS

Lau and Snyder performed a normal coordinate analysis for toluene and related compounds (10). They determined that the potential energy distribution of the 790 cm^{-1} planar A_1 fundamental for toluene is 32% ring CCC bend, 31% C–C ring stretch, 30% C–C stretch for methyl-to-ring bond. The 790 cm^{-1} Raman band for toluene is strong, and it is also polarized. Strong Raman bands that are also polarized are observed near 760, 740, and 705 cm^{-1} for ethylbenzene, isopropylbenzene, and tert-butylbenzene, respectively (8).

Figure 9.17 shows a plot of the planar A_1 fundamental for toluene, ethylbenzene, isopropylbenzene, and tert-butylbenzene in the region $700\text{--}790\text{ cm}^{-1}$ vs the number of protons on the ring α -carbon atom (11), and Fig. 9.18 shows a plot of the planar A_1 fundamental for toluene, ethylbenzene, isopropylbenzene, and tert-butylbenzene in the region $700\text{--}790\text{ cm}^{-1}$ vs Tafts σ^* values of 0, -0.01 , -0.19 , and -0.30 for methyl, ethyl, isopropyl, and tert-butyl groups, respectively (11, 12). Both plots are essentially linear.

Table 9.14 lists IR and Raman data for this A_1 fundamental. These Raman band correlations for this A_1 fundamental were used to assign the comparable Raman band at 773.4 cm^{-1} for α -syndiotactic polystyrene and at 785 cm^{-1} for isotactic polystyrene (13). Copies of the syndiotactic polystyrene uniaxially stretched film (perpendicular) and (parallel) polarized IR spectra are presented in Figs. 9.19 and 9.20, respectively (13).

Variable temperature studies of isotactic polystyrene have shown that most of the IR bands shift to lower frequency by 1 to 5 cm^{-1} as the temperature is raised from $30\text{ }^\circ\text{C}$ to $180\text{ }^\circ\text{C}$ (14). A variable-temperature study of syndiotactic polystyrene film cast from a solution of 1,2-dichlorobenzene shows that it changes crystalline form at temperatures of $190\text{ }^\circ\text{C}$ and above (14). Figure 9.21 shows the IR spectra of syndiotactic polystyrene of the cast film from boiling 1,2-dichlorobenzene, and Fig. 9.22 is an ambient temperature IR spectrum of the same syndiotactic polystyrene film used to record Fig. 9.21 except that the film was heated to $290\text{ }^\circ\text{C}$ and then allowed to cool to ambient temperature (15).

Spectral differences between Figs. 9.21 and 9.22 will be discussed under the section for the out-of-plane vibrations for the phenyl group.

STYRENE-4-METHYLSTYRENE COPOLYMERS

Figure 9.23 is an IR spectrum of a syndiotactic styrene (98%) –4-methylstyrene (2%) copolymer. This film was cast on a cesium iodide plate from boiling 1,2-dichlorobenzene (16). A comparison of Fig. 9.23 with Fig. 9.21 shows that the syndiotactic copolymer has the same crystal structure as the syndiotactic polystyrene. The IR band at 1511 cm^{-1} is due to an in-

plane ring mode and the 816 cm^{-1} band is due to the out-of-plane hydrogen deformation for the 4-methylphenyl group in the copolymer (16). Figure 9.24 is an IR spectrum of syndiotactic styrene (93%) –4-methylstyrene (7%) copolymer. This film was cast on a cesium iodide plate from boiling 1,2-dichlorobenzene. A comparison of Fig. 9.24 with Fig. 9.22 shows that the syndiotactic copolymer has the same crystal structure as syndiotactic polystyrene. The IR band near 1511 cm^{-1} is due to an in-plane ring deformation, and the band near 816 cm^{-1} is due to an out-of-plane hydrogen deformation for the 4-methylphenyl group in the copolymer (16).

It is possible to utilize IR spectroscopy in the quantitative analyses of copolymer films where the film thickness is unknown. This method requires measurement of an absorbance band for each of the components in the copolymer. This analysis can be performed using one of the following methods.

A sample containing known concentrations of the monomer units is required in all cases. A film of the copolymer is then cast on a suitable IR plate such as preheated potassium bromide (KBr) placed under an IR heat lamp in a nitrogen (N_2) atmosphere.

The absorbance (A) is proportional to the concentration of each component in the copolymer. Thus,

$$\begin{aligned} C_a &= kA_a; C_b = kA_b \\ \frac{C_a}{C_b} &= K \frac{A_a}{A_b} \quad K = \frac{C_a}{C_b} \cdot \frac{A_b}{A_a} \end{aligned} \quad (1)$$

As an example, component (a) of the copolymer is 70% and component (b) of the copolymer is 30%. The absorbance of a band at 1730 cm^{-1} is 0.753 for component (a) and the absorbance of a band at 1001 cm^{-1} for component (b) is 0.542. These numbers are used to determine the value of K .

$$K = \frac{70}{30} \cdot \frac{0.542}{0.753} = 1.680$$

The copolymer containing components (a) and (b) of unknown concentrations is submitted for analysis. The absorbance (A) for component (a) is measured at 1730 cm^{-1} and for component (b) is measured at 1001 cm^{-1} . The A for (a) is found to be 0.664 and for (b) A is 0.557.

Equation 1 is then utilized using the value for K of 1.680

$$\frac{C_a}{C_b} = 1.680 \frac{(0.664)}{(0.557)} = 2.003; C_a = 2.003 C_b$$

Then $C_a + C_b = 100\%$.

$$\begin{aligned} 2.003 C_b + C_b &= 100\% \\ C_b &= 100\% = 33.3\% \\ &3.003 \end{aligned}$$

Then $C_a = 66.7\%$.

Quantitation of a copolymer consisting of three different components can also be analyzed by application of IR spectroscopy. A copolymer of known composition is required. The measured values of the IR spectrum for the known concentration of the copolymer are:

C_a is 42%; A_a (at 2230 cm^{-1}) is 0.452

C_b is 26%; A_b (at 1730 cm^{-1}) is 0.847

C_c is 32%; A_c (at 700 cm^{-1}) is 0.269

$$K_1 = \frac{C_a}{C_b} \cdot \frac{A_b}{A_a} \quad K_1 = \frac{42}{26} \cdot \frac{0.847}{0.542} = 2.524$$

$$K_2 = \frac{C_c}{C_b} \cdot \frac{A_b}{A_c} \quad K_2 = \frac{32}{26} \cdot \frac{0.847}{0.269} = 3.875$$

The spectrum of the unknown copolymer containing components (a), (b), and (c) is obtained, and the following absorbance bands are measured:

The IR band at 2230 cm^{-1} has an absorbance of 0.757

The IR band at 1730 cm^{-1} has an absorbance of 0.798

The IR band at 700 cm^{-1} has an absorbance of 0.345.

Then

$$\frac{C_{(a)}}{C_{(b)}} = K_1 \frac{A_{(a)}}{A_{(b)}}; \frac{C_{(a)}}{C_{(b)}} = 2.524 \times \frac{0.757}{0.798} = 2.394; C_{(a)} = 2.394 C_{(b)}$$

$$\frac{C_{(c)}}{C_{(b)}} = K_2 \frac{A_{(c)}}{A_{(b)}}; \frac{C_{(c)}}{C_{(b)}} = 3.875 \times \frac{0.345}{0.798} = 1.675 \quad C_{(c)} = 1.675 C_{(b)}$$

Then

$$C_{(a)} + C_{(b)} + C_{(c)} = 100$$

$$2.394 C_{(b)} + C_{(b)} + 1.675 C_{(b)} = 100\%$$

$$C_{(b)} = 100/5.069 = 19.73\%$$

$$C_{(a)} = 2.394 C_{(b)} = 2.394 (19.73\%) = 47.23\%$$

$$C_{(c)} = 1.675 C_{(b)} = 1.675 (19.73\%) = 33.05\%$$

$$C_{(a)} = 47.23 + C_{(b)} = 19.73\%; C_{(b)} = 33.05\% = 100.01\%$$

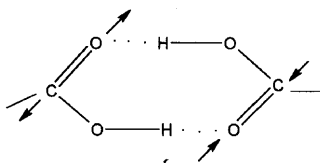
Another way to set up a quantitative method for the analysis of a copolymer is to record IR spectra of known quantitative composition over a range of concentrations that are to be manufactured. The IR spectra of a series of styrene-p-methylstyrene copolymers were prepared and the % p-methylstyrene in the copolymer is: 1,2,3,5 and 7%. Absorbance (A) for styrene was measured near 900 cm^{-1} , and the absorbance (A) also was measured for p-methylstyrene at 1511 cm^{-1} and near 816 cm^{-1} . Figure 9.25 shows a plot of the absorbance ratio $A(1511\text{ cm}^{-1})/A(901-904\text{ cm}^{-1})$ vs % p-methylstyrene in the styrene-p-methylstyrene copoly-

mer; Fig. 9.26 shows the plot of the absorbance ratio $A(815\text{--}817\text{ cm}^{-1})/A(900\text{--}904\text{ cm}^{-1})$ vs % p-methylstyrene in the styrene-p-methylstyrene copolymer. Both plots are linear in this concentration range, and either method is suitable for a routine analytical method for this copolymer.

A matrix method for the quantitative IR multicomponent analysis for films with indeterminate path-length has been reported (17).

STYRENE-ACRYLIC ACID COPOLYMER

Figure 9.27 (top) is an IR spectrum of styrene (92%)—acrylic acid (8%) copolymer recorded at 35 °C, and Fig. 9.27 (bottom) is an IR spectrum of the same copolymer at 300 °C (18). There are significant differences between these two IR spectra of the same copolymer. The ratio of the IR band intensities at 1742 to 1700 cm^{-1} is low in the upper spectrum and is high in the lower spectrum. The 1700 cm^{-1} IR band results from acrylic acid intermolecular hydrogen bonded dimers, and it is actually an out-of-phase $\nu(\text{CO}_2\text{H})_2$ vibration as depicted here:



out-of-phase $\nu(\text{CO}_2\text{H})_2$

The broad IR band in the region 3500–2000 cm^{-1} with subsidiary maxima results for $(\text{OH})_2$ stretching of the $(\text{CO}_2\text{H})_2$ groups in Fermi resonance with combinations and overtones. Note how there is less absorption in this region at high temperature than there is at 35 °C. The three bands in the region 3000–3100 cm^{-1} result from phenyl hydrogen stretching vibrations, and the two bands in the region 2950–2800 cm^{-1} result from CH_2 stretching vibrations. The IR bands near 3520 and 1125 cm^{-1} in the lower spectrum result from $\nu\text{ OH}$ and $\nu\text{ C-O}$ for the CO_2H group not existing in the $(\text{CO}_2\text{H})_2$ dimer form. The IR band near 3470 cm^{-1} is assigned to $\nu\text{ O-H}$ intermolecularly hydrogen bonded to the π system of the phenyl groups in the copolymer (18).

It is interesting to study Fig. 9.28, which shows five plots of absorbance ratios vs °C from 30 to ~310 °C. The plots are all parallel below ~150 °C, and then they increase or decrease essentially in a linear manner. These changes do not take place until the copolymer becomes molten, and the $(\text{CO}_2\text{H})_2$ groups are free to form two CO_2H groups. The 1600 cm^{-1} IR band results from a phenyl ring bend-stretching vibration, and the 752 cm^{-1} IR band results from the five hydrogen atoms vibrating in-phase out-of-the plane of the phenyl groups. The 1742 cm^{-1} and 1700 cm^{-1} IR bands have been assigned previously; R_1 is the ratio of $A(\text{CO}_2\text{H})/A(\text{CO}_2\text{H})_2$, and it increases as the sample temperature is increased; R_2 is the ratio of $A(\text{CO}_2\text{H})/A(\phi)$, and it increases as the sample temperature is increased; R_3 is the ratio of $A(\text{CO}_2\text{H})_2/A(\phi)$, and it decreases as the sample temperature is increased; R_4 is the ratio $A(\text{CO}_2\text{H})/A(\phi)$, and it increases as the sample temperature is increased; and R_5 is the ratio $A(\text{CO}_2\text{H})_2/A(\phi)$, and it decreases as

the sample temperature is increased. All of these absorbance ratios show that after $\sim 150^\circ\text{C}$ the $(\text{CO}_2\text{H})_2$ groups split into two CO_2H groups. Upon cooling to ambient temperature the CO_2H groups reform $(\text{CO}_2\text{H})_2$ groups (18).

STYRENE ACRYLAMIDE COPOLYMER

Figure 9.29 (top) is an IR spectrum of styrene acrylamide recorded at 27°C , and Fig. 9.29 (bottom) is an IR spectrum of the same copolymer recorded at 275°C . The $\nu\text{C}=\text{O}$ vibration for acrylamide in the copolymer occurs at 1682 cm^{-1} at 27°C and at 1690 cm^{-1} at 275°C . Moreover, this change in the $\nu\text{C}=\text{O}$ frequency occurs between 125 to 167°C . In addition, $\nu\text{ asym. NH}_2$ occurs at 3480 cm^{-1} and $\nu\text{ sym. NH}_2$ occurs at 3380 cm^{-1} at temperature below 125°C , and $\nu\text{ asym. NH}_2$ occurs at 3499 cm^{-1} and $\nu\text{ sym. NH}_2$ occurs near 3380 cm^{-1} in the temperature range 27 to 275°C . In addition, bands in the region $3200\text{--}3370\text{ cm}^{-1}$ in the 27°C spectrum are not present in the 275°C spectrum. These data show that the NH_2 groups are not hydrogen bonded to $\text{C}=\text{O}$ groups in temperature above 167°C . Upon cooling the intermolecular hydrogen, bonds reform (18).

STYRENE/2-ISOPROPENYL-2-OXAZOLINE COPOLYMER (SIPO COPOLYMER)

Figure 9.30 is an IR spectrum of a styrene (93.8%)/2-isopropenyl-2-oxazoline (6.2%) copolymer film cast from methylene chloride onto a KBr plate (19). The IR band at 1656 cm^{-1} is assigned to $\nu\text{C}=\text{N}$ of the oxazoline ring. The IR band at 1600 cm^{-1} results from an in-plane bend-stretching vibration of the phenyl ring. Figure 9.31 is a plot of the wt % IPO in the SIPO copolymer vs the absorbance ratio $A(1656\text{ cm}^{-1})/A(1600\text{ cm}^{-1})$ for 10 SIPO copolymers. This plot is linear over the % SIPO copolymers studied, and the calculated and % IPO values agree within 0.15% (19).

ETHYNYLBENZENE AND ETHYNYLBENZENE-D

Figure 9.32 (top) is a vapor-phase IR spectrum of ethynylbenzene (phenylacetylene) in a 4-m cell with the vapor pressure of the liquid sample at 25°C . Figure 9.32 (bottom) is a vapor-phase IR spectrum of ethynylbenzene-d run under the same conditions as the top spectrum (20).

Figure 9.33 (top) is a solution-phase IR spectrum of ethynylbenzene, and Fig. 9.33 (bottom) is a solution-phase IR spectrum of ethynylbenzene-d (20).

Figure 9.34 (top) is an IR spectrum of ethynylbenzene in the liquid phase, and Fig. 9.34 (bottom) is an IR spectrum of ethynylbenzene-d in the liquid phase (20).

Figure 9.35 (top) is a Raman spectrum of ethynylbenzene, and Fig. 9.35 (bottom) is a Raman spectrum of ethynylbenzene-d (20).

The $\nu\equiv\text{C}-\text{H}$ mode occurs at 3340 ; 3320 sh cm^{-1} in the vapor, at 3315 ; 3305 sh cm^{-1} in CCl_4 solution, and at 3291 ; 3310 sh cm^{-1} in the liquid phase. The $\nu\equiv\text{C}-\text{D}$ mode occurs at 2608 cm^{-1}

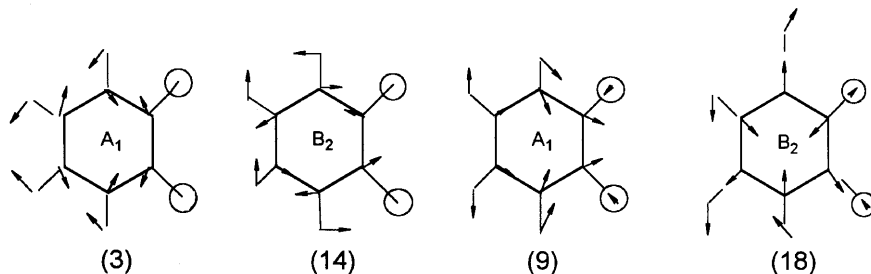
in the vapor, at 2596 cm^{-1} ; 2560 sh cm^{-1} in CCl_4 solution, and at 2550 cm^{-1} in the liquid phase (20). Both $\nu\equiv\text{C}-\text{H}$ and $\nu\equiv\text{C}-\text{D}$ shift to lower frequency in the order: vapor, CCl_4 solution, and liquid phase. The $\nu\text{ C}\equiv\text{C}$ mode for the $\text{C}\equiv\text{C}-\text{H}$ group occurs at 2122 cm^{-1} in the vapor, at 2119 cm^{-1} in CCl_4 solution, and at 2118 cm^{-1} in the liquid phase while the $\nu\text{ C}\equiv\text{C}$ mode for the $\text{C}\equiv\text{C}-\text{D}$ group occurs at 1989 cm^{-1} in CCl_4 solution and at 1983 cm^{-1} in the liquid phase. The in-plane $\equiv\text{C}-\text{H}$ deformation occurs at 648 cm^{-1} in the vapor, at 648 cm^{-1} in CS_2 solution, and at 653 cm^{-1} in the vapor phase. By contrast, the out-of-plane deformation occurs at 612 cm^{-1} in the vapor, at 610 cm^{-1} in CS_2 solution, and at 619 cm^{-1} in the liquid phase. The in-plane $\equiv\text{C}-\text{D}$ deformation occurs at 481 cm^{-1} in the vapor, 482 cm^{-1} in CS_2 solution, and at 486 cm^{-1} in the liquid phase. The out-of-plane $\equiv\text{C}-\text{D}$ deformation appears to be coincident with the in-plane $\equiv\text{C}-\text{D}$ deformation in the case due to coupling with a $\text{C}-\text{C}\equiv\text{C}$ bending mode (20). As discussed in Volume 1, Chapter 5, $\nu\equiv\text{C}-\text{D}$ and $\nu\text{ C}\equiv\text{C}$ are coupled.

BROMODICHLOROBENZENES

There are six isomers of bromodichlorobenzene, and these are: 1-bromo,3,5-dichlorobenzene; 1-bromo, 2,6-dichlorobenzene; 1-bromo,2,3-dichlorobenzene; 1-bromo,2,4-dichlorobenzene; 1-bromo,2,5-dichlorobenzene; and 1-bromo,3,4-dichlorobenzene. There is no problem in distinguishing between the 1,3,5-; 1,2,3-; and 1,2,4-positions by application of IR spectroscopy; however, the problem arises in the unambiguous identity of 1-Br,2,6- $\text{Cl}_2\phi$ from 1-Br,2,3- $\text{Cl}_2\phi$ 3- $\text{Cl}_2\phi$, and between 1-Br, 2,4- $\text{Cl}_2\phi$, 1-Br,2,5- $\text{Cl}_2\phi$, and 1-Br,3,4- $\text{Cl}_2\phi$. Both IR and Raman spectroscopy were used to correctly identify each of the six bromodichlorobenzenes (21). These assignments were made possible by knowing the potential energy distributions for the corresponding trichlorobenzene isomers for planar vibrations involving carbon-halogen stretching (3). Table 9.15 lists the vibrational assignments for the six bromodichlorobenzene isomers as well as the molecular symmetry of each isomer (21).

RAMAN DATA FOR 1,2-DISUBSTITUTED BENZENES

Raman spectra for 1,2-disubstituted benzenes exhibit characteristic group frequencies (see Table 9.16). A strong Raman band occurs in the region $1020\text{--}1044\text{ cm}^{-1}$, and a weaker Raman band occurs in the region $642\text{--}668\text{ cm}^{-1}$. Raman bands also occur in the region $1595\text{--}1610\text{ cm}^{-1}$ and in the region $1577\text{--}1586\text{ cm}^{-1}$, and the higher frequency band is more intense than the lower frequency band (8). The approximate normal vibrations for ring modes 3, 14, 18, and 9 are presented here.



VIBRATIONAL DATA FOR 1,3-DICHLOROBENZENE AND RAMAN DATA FOR 1,3-DISUBSTITUTED BENZENES

Vibrational assignments for the in-plane modes of 1,3-dichlorobenzene have been reported (3). Table 9.17 lists Raman data for 1,3-disubstituted benzenes (8). A strong Raman band occurs in the region 995–1005 cm^{-1} , and a weak to medium Raman band occurs in the region 1574–1618 cm^{-1} .

RAMAN DATA AND ASSIGNMENTS FOR SOME IN-PLANE RING MODES FOR 1,4-DISUBSTITUTED BENZENES

Table 9.18 lists Raman data and assignments for some in-plane ring modes for 1,4-disubstituted benzenes (8). Weak to strong Raman bands occur in the regions 1591–1615 cm^{-1} ; 1268–1308 cm^{-1} ; 819–881 cm^{-1} ; 801–866 cm^{-1} , and 625–644 cm^{-1} .

RAMAN DATA FOR DECABROMOBIPHENYL AND BIS (PENTABROMOPHENYL) ETHER

Raman data for decabromobiphenyl and bis-(pentabromophenyl) ether are listed in Table 9.19 (8). Ring mode assignments are also listed for the pentabromophenyl group.

INFRARED DATA AND ASSIGNMENTS FOR BENZENE, BENZENE-d₆, BENZYL ALCOHOL, AND BENZYL -2,3,4,5,6-d₅

The task of assigning the infrared and Raman data of a molecule is aided by obtaining deuterium analogs. In Table 9.20, vapor-phase infrared data for benzene and benzyl alcohol are compared to the vapor-phase infrared data for benzene-d₆ and benzyl-2,3,4,5,6-d₅ alcohol, respectively. Benzene has a center of symmetry, and overtones are not allowed in the infrared spectrum. Molecular vibrations involving primarily motion of the H atoms joined to the benzene carbon atoms are expected to decrease in frequency by a factor of the square root of 2 or approximately 1.41. Thus, for benzene and benzene-d₆ the assignments where corresponding vibrations decrease in frequency by a factor of over 1.3 involve primarily motion of 6H or 6D atoms. For example, benzene exhibits a type-C band whose strong Q-branch occurs at 670 cm^{-1} (with P- and R- branches and 688 cm^{-1} , respectively). Benzene-d₆ exhibits the corresponding type-C band at 505 cm^{-1} , 491 cm^{-1} , and 470 cm^{-1} . The frequency ratio of 670/491 is 1.365. These bands are due to a vibration where either the 6 H atoms or the 6 D atoms bend in-phase out of the plane of the benzene ring.

Benzyl alcohol and benzyl-2,3,4,5,6-d₅ alcohol exhibit a vapor-phase infrared band at 738 cm^{-1} and 534 respectively. The frequency ratio 738/534 is 1.382. This molecular vibration is where the 5 H atoms or 5 C atoms based in-phase out of the plane of the phenyl group.

OUT-OF-PLANE DEFORMATIONS AND THEIR COMBINATION AND OVERTONES FOR SUBSTITUTED BENZENES

Young *et al.* have shown the substitution pattern for mono-through hexa-substituted benzenes, in the region $5\text{--}6\mu$ $2000\text{--}1666.7\text{ cm}^{-1}$, and their correlation presentation is shown in Fig. 9.36 (2). The substitution patterns are less complex with increased benzene substitution or with fewer protons joined directly to the benzene ring. In fact, hexa-substituted benzenes do not contain protons directly joined to the benzene ring. However, extensive studies of benzene derivatives have shown that most of the IR bands in this region of the spectrum result from combination and overtones of the out-of-plane hydrogen deformations (see Reference 6).

Table 9.21 lists a number of mono-substituted benzenes in the order of increasing σ_p values (6,22). These vibrational modes are listed I through V for the five out-of-plane hydrogen deformations for a mono-substituted benzene in the order of decreasing frequency. The number VI normal vibration is the out-of-plane ring deformation.

A study of Table 9.21 shows that modes I through III generally increase in frequency as the σ_p value is increased. These out-of-plane hydrogen deformations are also dependent upon the physical phase. This phase dependence is the result of the reaction field between the mono-substituted benzene molecules. This reaction field could also affect these spectra-structure conditions. However, a linear correlation is not obtained for data recorded in the vapor phase vs σ_p values (6).

POLYSTYRENE AND STYRENE COPOLYMERS

Tables 9.22 and 9.23 summarize the out-of-plane hydrogen deformation and the out-of-plane ring deformation for substituted benzenes and their combination and overtones, respectively (6).

Figures 9.19–9.24, 9.27, 9.29 and 9.30 are IR spectra for either polystyrene or a copolymer containing styrene units. Compare Figs. 9.19–9.30 with the mono-pattern shown in Fig. 9.36. The pattern for the styrene units is the same as that shown in Fig. 9.36.

In the IR spectra of α - and β -syndiotactic polystyrene the IR bands in the region $2000\text{--}1666.7\text{ cm}^{-1}$ are assigned as presented here (13):

α -Syndiotactic Polystyrene		
Parallel Polarization cm^{-1}	Perpendicular Polarization cm^{-1}	Assignment (13)
1955	—	$2(977.5) = 1955$; 2 I
—	1960	$2(980) = 1960$; 2 I
1941.7	—	$977.5 + 964.4 = 1941.9$; I + II
—	1943.6	$980 + 964 = 1944$; I + II
1869.1	—	$964.4 + 903 = 1867.4$; II + III
—	1871.3	$964 + 904.8 = 1869$; II + III
1800.9	—	$964.4 + 841 = 1805.4$; II + IV

—	1802.8	$964 + 840.7 = 1805$; II + IV
1744.2	—	$903 + 841 = 1744$; III + IV
—	1746.3	$904.8 + 840.7 = 1745.5$; III + IV
1704	—	$2(852.75) = 1705.5$; 2 IV
1673.3	—	$977.5 + 695.3 = 1672.8$; I + VI
—	1675.2	$980 + 695.9 = 1676$

ETHYNYLBENZENE

In the case of ethynylbenzene (Fig. 9.33 in CCl_4 solution) the combination and overtone assignments are as presented here:

Ethynylbenzene	Assignment
1964	$2\nu_{29}(A_1)$; $2(983) = 1966$; 2 I
1947	$\nu_{29} + \nu_{26}(B_1) = 983 + 967 = 1950$; I + II
1895	$\nu_{29} + \nu_{30}(A_1) = 983 + 917 = 1900$; I + III
1871	$\nu_{26} + \nu_{30}(B_1) = 967 + 917 = 1884$; II + III
1820	$\nu_{29} + \nu_{27}(B_1) = 983 + 842 = 1825$; I + IV
1802	$\nu_{26} + \nu_{27}(A_1) = 967 + 842 + 1809$; II + IV
1751	$\nu_{30} + \nu_{27}(B_1) = 917 + 842 = 1759$; II + IV

These assignments are in good agreement with the summary for out-of-plane hydrogen deformation and their combination and overtones for monosubstituted benzenes (see Fig. 9.37).

In the case of mono-substituted benzenes, modes I, II, and V belong to the B_1 symmetry species for molecules with C_{2v} symmetry, and modes I, II and V belong to the A'' symmetry species for molecules with C_s symmetry. Moreover, modes II and IV belong to the A_2 symmetry species for molecules with C_{2v} symmetry, and modes II and IV for molecules that belong to the A'' species for molecules with C_s symmetry. Thus, the author finds it most convenient to term these vibrations I through V in the order of their decreasing frequency.

It is only possible for vibrations belonging to the same symmetry species to couple. Thus, there is more probability of coupling between the A'' vibrations in the case of mono-substituted benzenes with C_s symmetry than there is between the B_1 fundamentals and between the A_2 fundamentals for mono-substituted benzenes with C_{2v} symmetry. This may be one of the reasons that modes I through V do not correlate on a one-to-one basis with σ_p . Another factor is that not all spectra were recorded in the same physical phase.

1,2-DISUBSTITUTED BENZENES

Figure 9.38 is a summary of the out-of-hydrogen deformations and their combination and overtones for 1,2-disubstituted benzenes (6). For 1,2-disubstituted benzenes with C_{2v} symmetry modes I and II belong to the A_2 species and modes III and IV belong to the B_1 species. For 1,2-disubstituted benzenes with C_s symmetry, modes I through IV belong to the A'' species. Modes I through IV occur in the regions $956\text{--}989\text{ cm}^{-1}$; $915\text{--}970\text{ cm}^{-1}$, $833\text{--}886\text{ cm}^{-1}$, and 725--

791 cm^{-1} , respectively. The two overtone and five combination tones of modes I through IV are presented on Fig. 9.38.

1,3-DIBSUBSTITUTED BENZENES

Figure 9.39 is a summary of the out-of-plane hydrogen deformations and their combination and overtones for 1,3-disubstituted benzenes (6). For 1,3-disubstituted benzenes with C_{2v} symmetry, modes I, III and IV belong to the B_1 symmetry species and mode II belongs to the A_2 symmetry species. For 1,3-disubstituted benzenes with C_s symmetry, modes I through IV belong to the A'' species. Modes I through IV occur in the regions 947–999 cm^{-1} , 863–941 cm^{-1} , 831–910 cm^{-1} , and 761–815 cm^{-1} , respectively. The three overtones and four combination tones of modes I through IV are presented in Fig. 9.39.

1,4-DISUBSTITUTED BENZENES

Figure 9.40 is a summary of the out-of-plane hydrogen deformations and their combination and overtones for 1,4-disubstituted benzenes (6). For 1,4-disubstituted benzenes with V_h symmetry, modes I through IV belong to the A_u , B_{2g} , B_{1g} , and B_{3u} species, respectively. For molecules with C_{2v} symmetry, modes I and III belong to the A_2 species and modes II and IV belong to the B_1 species. For molecules with C_s symmetry, modes I through IV belong to the A'' species. For molecules with a center of symmetry such as 1,4-disubstituted benzenes with V_h symmetry, overtones of fundamentals are not allowed in the IR. A study of Fig. 9.40 shows that overtones are not present in the region 2000–1600 cm^{-1} for any of the 1,4-disubstituted benzenes. Modes I through IV occur in the regions 1852–1957 cm^{-1} , 916–971 cm^{-1} , 790–852 cm^{-1} , and 794–870 cm^{-1} , respectively. Four combinations tones of modes I through IV are listed in Fig. 9.40.

1,3,5-TRISUBSTITUTED BENZENES

Figure 9.41 is a summary of the out-of-plane deformations and their combination and overtones for 1,3,5-trisubstituted benzenes (6). For 1,3,5-trisubstituted benzenes with D_{3h} symmetry modes, the Ia and Ib modes are degenerate. For molecules with C_{2v} symmetry, the degeneracy is split into two B_1 modes and the A_2'' mode for molecules with D_{3h} symmetry becomes an A_2 fundamental. In the case of 1,3,5-trisubstituted benzenes with C_s symmetry, all three modes belong to the A'' species. The Ia and Ib modes occur in the region 819–920 cm^{-1} and mode II occurs in the region 786–910 cm^{-1} . The 2I overtone occurs in the regions 1635–1840 cm^{-1} , and the mode I + II combination occurs in the region 1605–1840 cm^{-1} .

1,2,3-TRISUBSTITUTED BENZENES

Figure 9.42 is a summary of the out-of-plane hydrogen deformations and their combination and overtones for 1,2,3-trisubstituted benzenes (6). For molecules with C_{2v} symmetry, modes I and

III belong to the B_1 species and mode II belongs to the A_2 species. For molecules with C_s symmetry, modes I through III belong to the A'' species. Modes I through III occur in the ranges $930\text{--}989\text{ cm}^{-1}$, $848\text{--}930\text{ cm}^{-1}$, and $731\text{--}810\text{ cm}^{-1}$, respectively; 2I and 2II occur in the regions $1860\text{--}1975$ and $1700\text{--}1860\text{ cm}^{-1}$, respectively. The combination I + II occurs in the region $1848\text{--}1930\text{ cm}^{-1}$.

1,2,4-TRISUBSTITUTED BENZENES

Figure 9.43 is a summary of the out-of-plane hydrogen deformations and their combination and overtones for 1,2,4-trisubstituted benzenes (6). As long as these molecules have a plane of symmetry their molecular symmetry is C_s . Modes I through III belong to the A'' species and occur in the regions $926\text{--}982\text{ cm}^{-1}$, $841\text{--}923\text{ cm}^{-1}$, and $790\text{--}852\text{ cm}^{-1}$, respectively. Their three overtones and two combinations are shown in Fig. 9.43.

1,2,3,4-TETRASUBSTITUTED BENZENES

Figure 9.44 is a summary of the out-of-plane hydrogen deformations and their combination and overtones for 1,2,3,4-tetrasubstituted benzenes (6). For molecules with C_{2v} symmetry, mode I and mode II belong to the A_2 and B_1 species, and for molecules with C_s symmetry, modes I and II belong to the A'' species. Modes I and II occur in the regions $919\text{--}949\text{ cm}^{-1}$ and $770\text{--}821\text{ cm}^{-1}$, respectively. Their two overtones and one combination are shown in Fig. 9.44.

1,2,3,5-TETRASUBSTITUTED BENZENES

Figure 9.45 is a summary of the out-of-plane hydrogen deformations and their combination and overtones for 1,2,3,5-tetrasubstituted benzenes (6). For molecules with C_{2v} symmetry, modes I and II belong to the A_2 and B_1 species, and occur in the regions $821\text{--}942\text{ cm}^{-1}$ and $839\text{--}920\text{ cm}^{-1}$, respectively. The overtones I and II occur in the regions $1635\text{--}1860\text{ cm}^{-1}$ and $1638\text{--}1841\text{ cm}^{-1}$, respectively. The combination I + II occurs in the region $1659\text{--}1862\text{ cm}^{-1}$.

1,2,4,5-TETRASUBSTITUTED BENZENES

Figure 9.46 is a summary of the out-of-plane hydrogen deformations and their combination and overtones for 1,2,4,5-tetrasubstituted benzenes (6). For molecules with v_h symmetry, modes I and II belong to the B_{3u} and B_{2g} species, respectively. For molecules with C_{2v} symmetry, modes I and II belong to the B_1 and A_2 species, respectively, and for molecules with C_s symmetry both modes belong to the A'' species. Modes I and II occur in the regions $861\text{--}911\text{ cm}^{-1}$ and $828\text{--}980\text{ cm}^{-1}$, respectively. These two overtones, if allowed, occur in the regions $1725\text{--}1830\text{ cm}^{-1}$ and $1651\text{--}1770\text{ cm}^{-1}$, respectively, and the combination occurs in the region $1695\text{--}1799\text{ cm}^{-1}$.

1,2,3,4,5-PENTASUBSTITUTED BENZENES

Figure 9.47 is a summary of the out-of-plane hydrogen deformation and its first overtone for pentasubstituted benzenes (6). For molecules with C_{2v} symmetry, mode I belongs to the B_1 species, and for molecules with C_s symmetry mode I belongs to the A'' species. Its first overtone occurs in the region $1655\text{--}1848\text{ cm}^{-1}$.

SUMMARY OF THE OUT-OF-PLANE HYDROGEN DEFORMATIONS FOR SUBSTITUTED BENZENES AND THE OUT-OF-PLANE RING DEFORMATION FOR MONO-SUBSTITUTED BENZENES, AND THEIR COMBINATION AND OVERTONES

Table 9.22 is a summary of the frequency ranges for 11 types of substituted benzenes (6). The number of ranges for each class of substituted benzenes decreases as the number of protons joined to the ring decreases.

Table 9.23 is a summary of the frequency ranges for the combination and overtones of the out-of-plane hydrogen deforms for the 11 types of substitute benzenes (6). The number of ranges within each class of substituted benzenes decreases as the number of protons joined to the ring decreases.

CORRELATION CHART

Figure 9.48 is a correlation chart for the out-of-plane hydrogen deformations and their combination and overtones for substituted benzenes. The thickness of each bar graph for modes I through V and their combination and overtones indicates the relative band intensities exhibited within each class of substituted benzenes for most of the compounds within each class. The band intensities for the combination and overtones are generally 10 to 100 times less intense than the most intense IR band for the fundamental out-of-plane hydrogen deformations exhibited by each class of substituted benzenes.

It should be remembered that other overtones such as those for vinyl wag and vinylidene CH_2 wag also occur in the region $2000\text{--}1666\text{ cm}^{-1}$ (see Volume 1, Chapter 4). Of course, the vast majority of compounds containing a carbonyl group exhibit $\nu\text{ C=O}$ in the region $2000\text{--}1666\text{ cm}^{-1}$, and these $\nu\text{ C=O}$ modes have strong IR band intensity that mask many of the combination and overtone bands (see Volume 1, Chapters 10–16).

2,3,4,5,6-PENTACHLOROBIPHENYL

Table 9.24 compares vibrational data for hexachlorobenzene vs 2,3,4,5,6-pentachlorobiphenyl. Eight fundamentals of the pentachlorophenyl group are assigned (7).

REFERENCES

1. Varsanyi, G. (1969). *Vibrational Spectra of Benzene Derivatives*. New York/London: Academic Press.
2. Young, C. W., Du Vall, R. B., and Wright, N. (1951). *Anal. Chem.* **23**: 709.
3. Scherer, J. R. (1964). *Planar Vibrations of Chlorinated Benzenes*. Midland, MI: The Dow Chemical Company.
4. Scherer, J. R., and Evans, J. C. (1963). *Spectrochim Acta* **19**: 1763.
5. Scherer, J. R., Evans, J. C., Muelder, W. W., and Overend, J. (1962). *Spectrochim. Acta* **18**: 57.
6. Nyquist, R. A. (1984). *The Interpretation of Vapor-Phase Infrared Spectra: Group Frequency Data*. Philadelphia: Sadtler.
7. Nyquist, R. A., Putzig, C. L., and Peterson, D. P. *Appl. Spectrosc.* **37**: 140.
8. *Sadtler Standard Raman Spectral Collection*. Philadelphia: Sadtler Research Laboratories.
9. Nyquist, R.A., and Kagel, R. O. (1977). Organic Materials. Chapter 6, in *Infrared and Raman Spectroscopy*, Part B, E. G. Frame, Jr. and J. G. Grassellie, eds., New York: Marcel Dekker, Inc., p. 476.
10. Lau, C. L., and Snyder, R. G. (1971) *Spectrochim. Acta* **27A**: 2073.
11. Nyquist, R. A. (1988). *Appl. Spectrosc.* **13**: 14.
12. Taft, Jr., R. W. (1956) *Steric Effects in Organic Chemistry*. M. S. Newman, ed., New York: Wiley & Sons, p. 592.
13. Nyquist, R. A., Putzig, C. L., Leugers, M. A., McLachlan, R. D., and Thill, B. (1992). *Appl. Spectrosc.* **46**: 981.
14. Nyquist, R. A. (1984). *Appl. Spectrosc.* **38**: 264.
15. Nyquist, R. A. (1989). *Appl. Spectrosc.* **43**: 440.
16. Nyquist, R. A., and Malanga, M. (1989) *Appl. Spectrosc.* **43**: 442.
17. Loy, B. R., Chrisman, R. W., Nyquist, R. A., and Putzig, C. L. (1979). *Appl. Spectrosc.* **33**: 638.
18. Nyquist, R. A., Platt, A. E., and Priddy, D. B. (1982). *Appl. Spectrosc.* **36**: 417.
19. Nyquist, R. A., and Schuetz, J. E. (1985). *Appl. Spectrosc.* **39**: 595.
20. Evans, J. C., and Nyquist, R. A. (1960). *Spectrochim. Acta* **16**: 918.
21. Nyquist, R. A., Loy, B. R., and Chrisman, R. W. (1981). *Spectrochim. Acta* **37A**: 319.
22. Taft, R. W. (1976) *Progress in Physical Organic Chemistry*. vol. 12, New York: Interscience Publication, J. Wiley, p. 74.

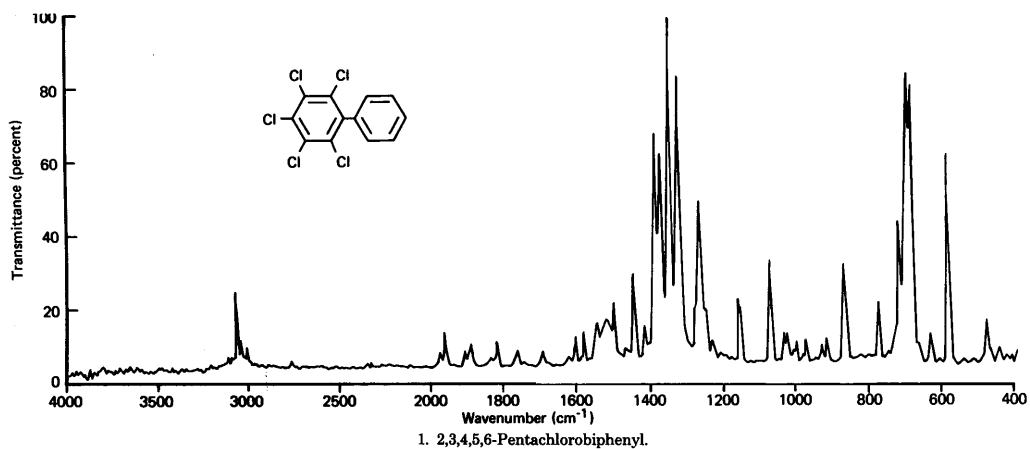


FIGURE 9.1 Infrared spectrum for 2,3,4,5,6-pentachlorobiphenyl.

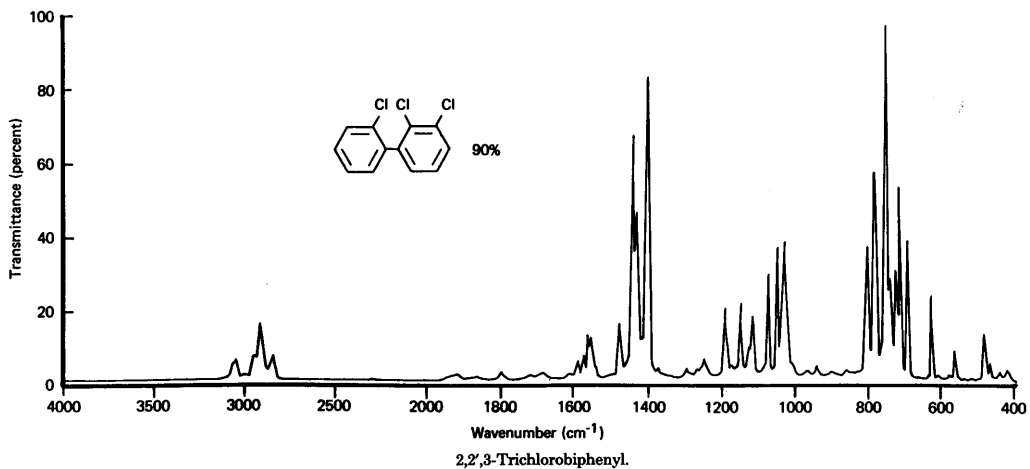


FIGURE 9.2 Infrared spectrum for 2,2',3-trichlorobiphenyl.

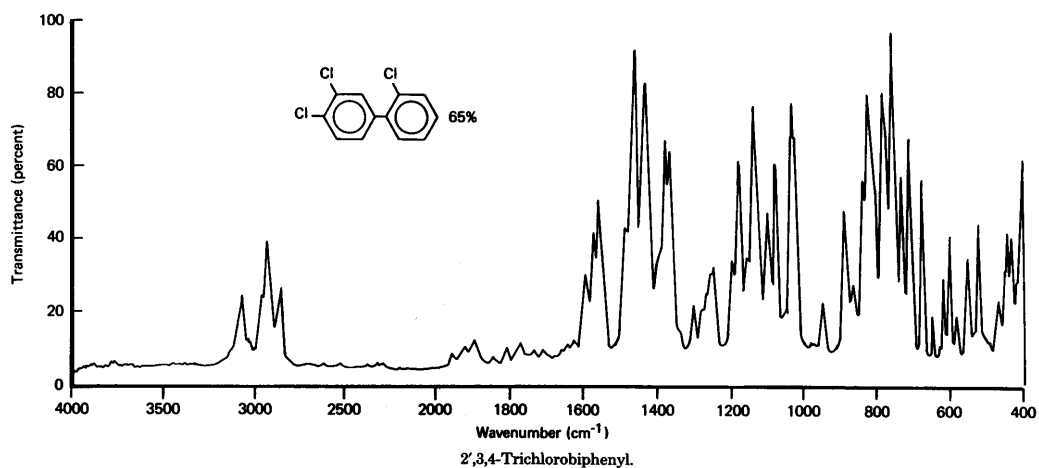


FIGURE 9.3 Infrared spectrum for 2',3,4-trichlorobiphenyl.

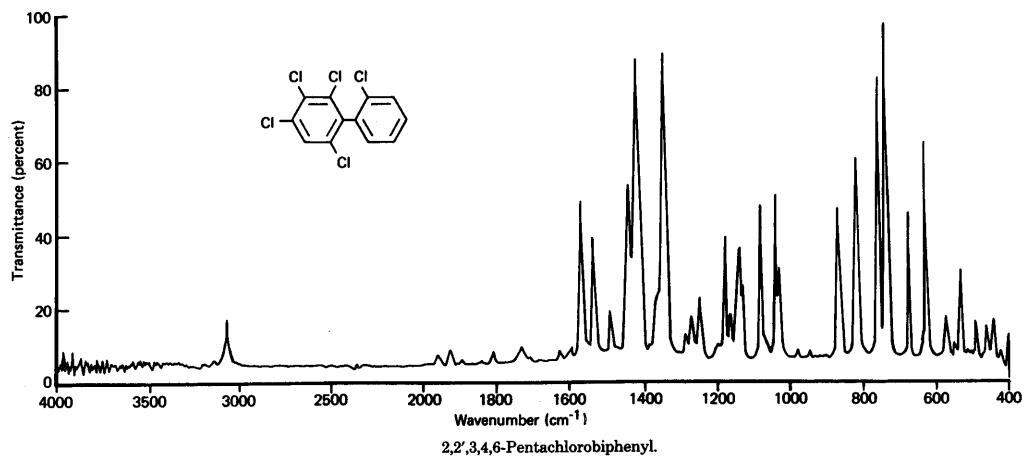


FIGURE 9.4 Infrared spectrum for 2,2',3,4,6-pentachlorobiphenyl.

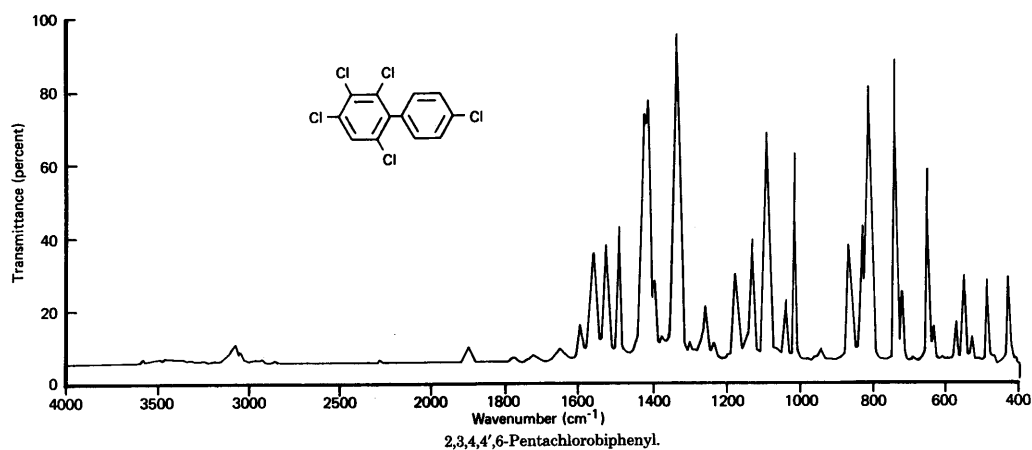


FIGURE 9.5 Infrared spectrum for 2,3,4,4',6-pentachlorobiphenyl.

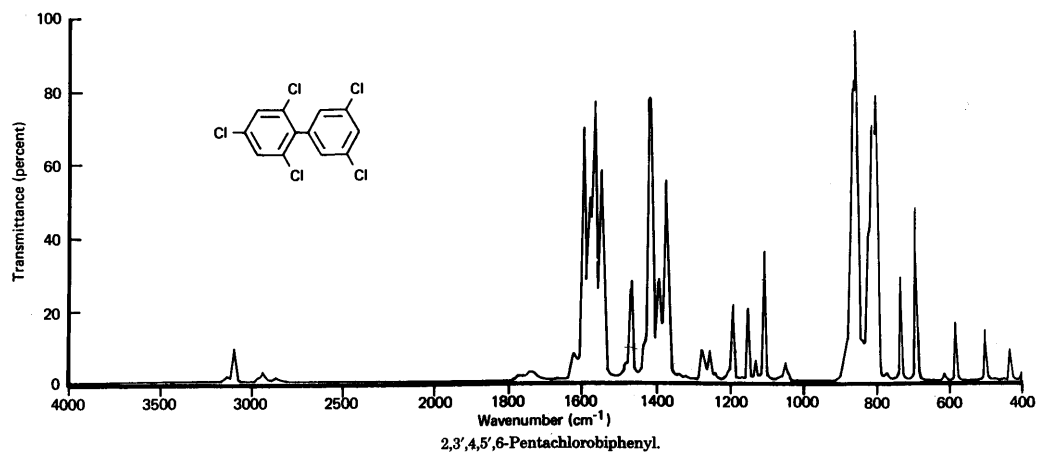


FIGURE 9.6 Infrared spectrum for 2,3',4,5',6-pentachlorobiphenyl.

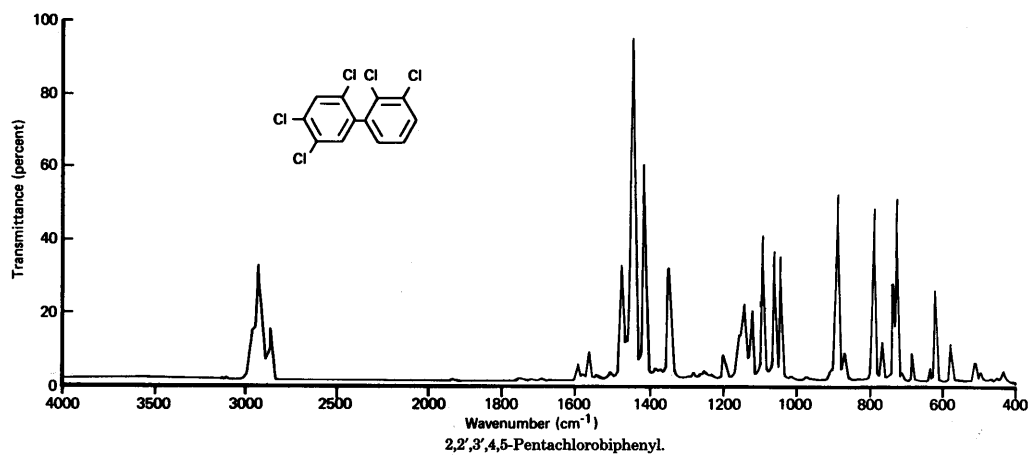


FIGURE 9.7 Infrared spectrum for 2,2',3',4,5-pentachlorobiphenyl.

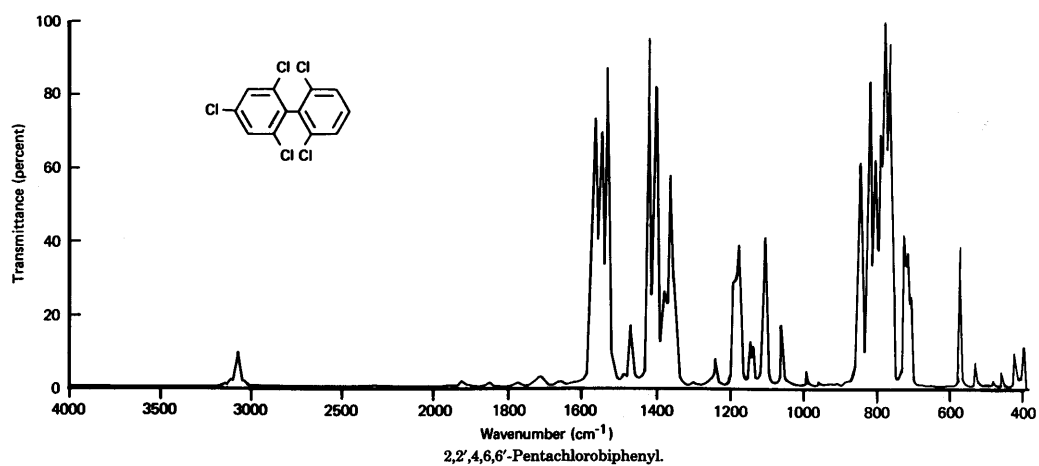


FIGURE 9.8 Infrared spectrum for 2,2',4,6,6'-pentachlorobiphenyl.

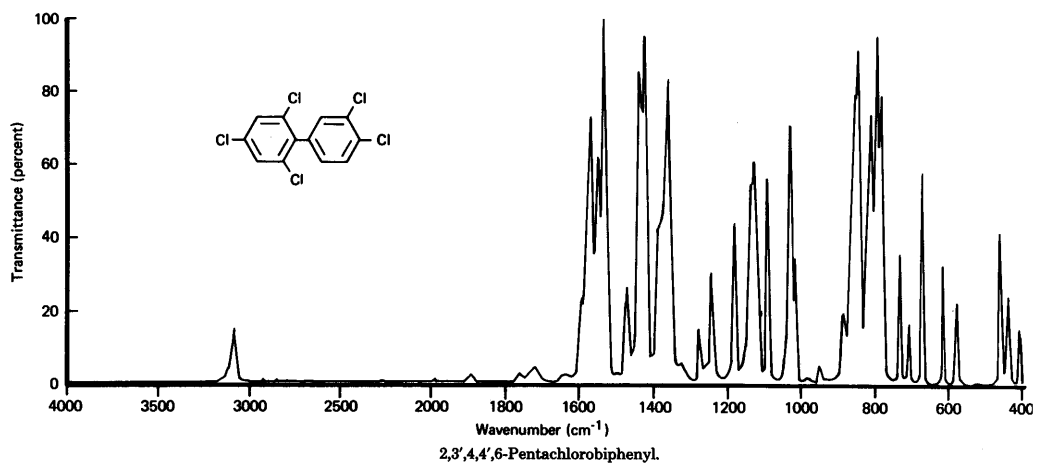


FIGURE 9.9 Infrared spectrum for 2,3',4,4',6-pentachlorobiphenyl.

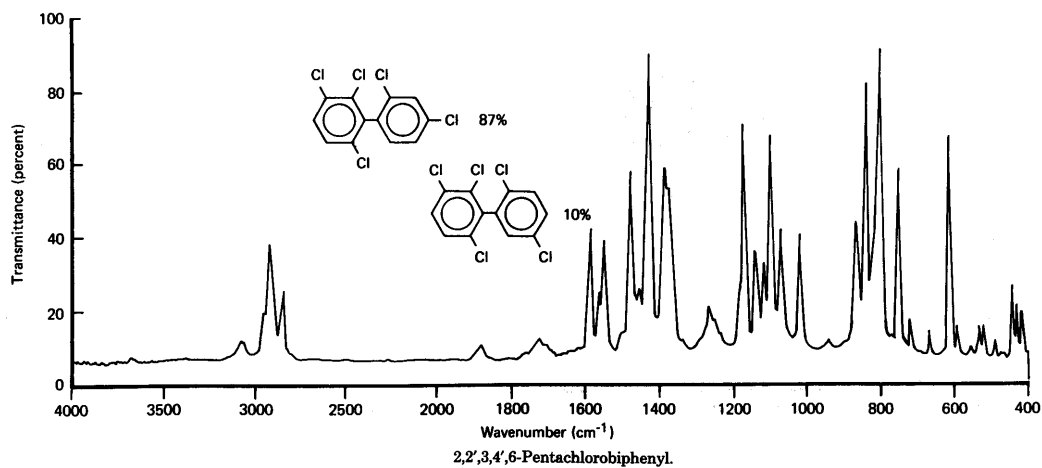


FIGURE 9.10 Infrared spectrum for 2,2',3,4',6-pentachlorobiphenyl.

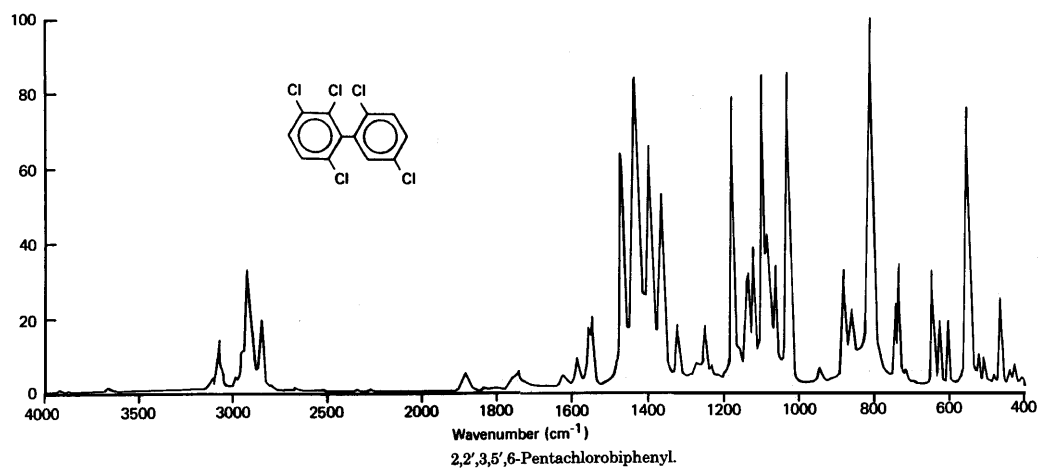


FIGURE 9.11 Infrared spectrum for 2,2',3,5',6-pentachlorobiphenyl.

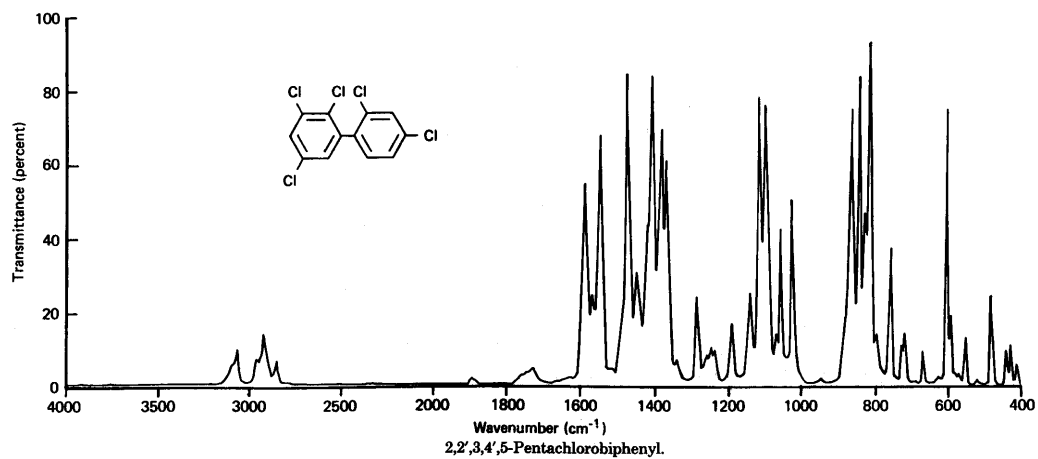


FIGURE 9.12 Infrared spectrum for 2,2',3,4',5-pentachlorobiphenyl.

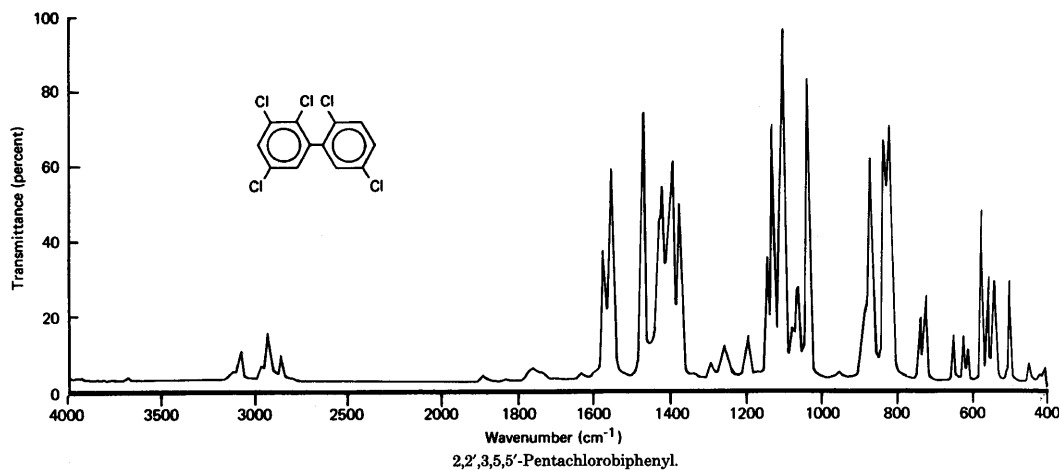


FIGURE 9.13 Infrared spectrum for 2,2',3,5,5'-pentachlorobiphenyl.

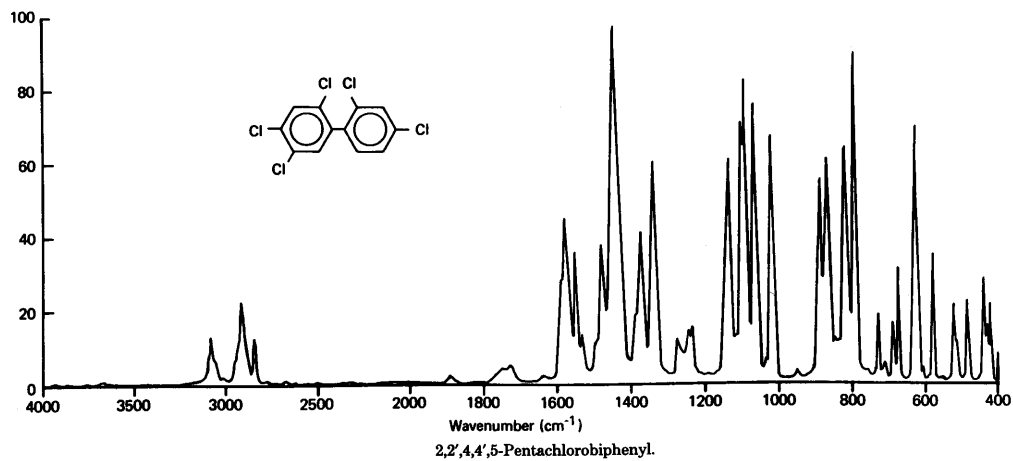


FIGURE 9.14 Infrared spectrum for 2,2',4,4',5-pentachlorobiphenyl.

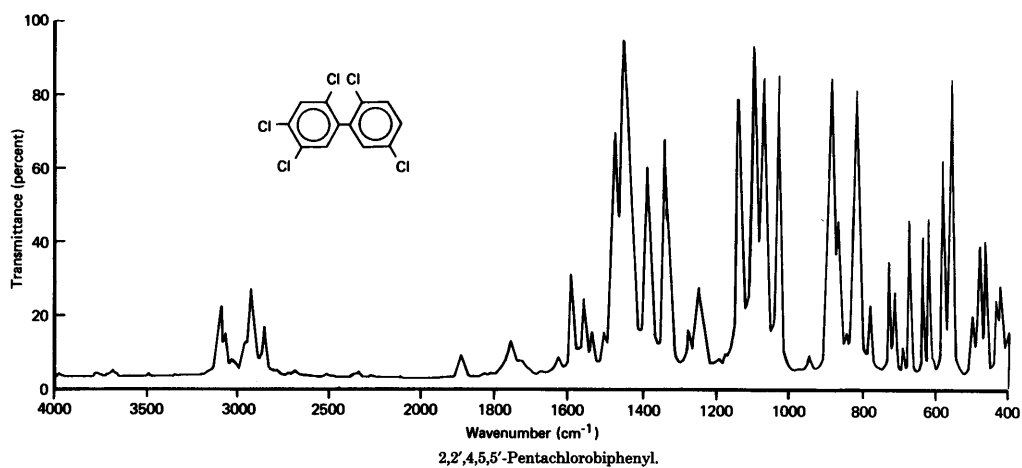


FIGURE 9.15 Infrared spectrum for 2,2',4,5,5'-pentachlorobiphenyl.

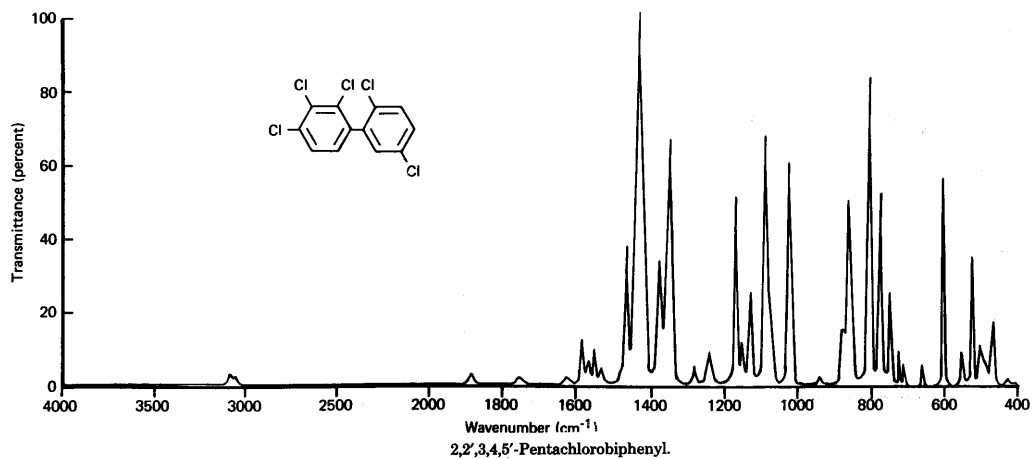


FIGURE 9.16 Infrared spectrum for 2,2',3,4,5'-pentachlorobiphenyl.

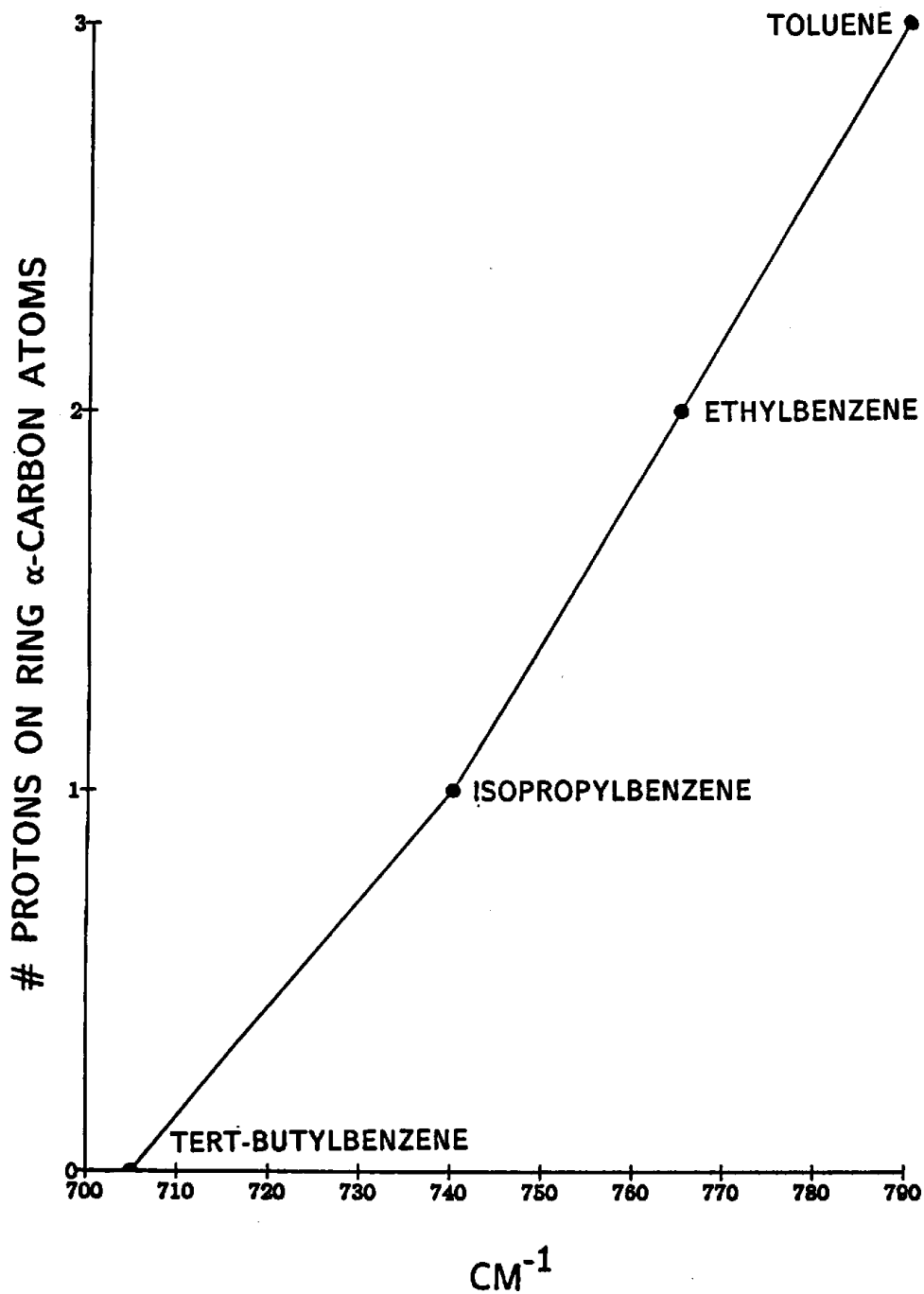
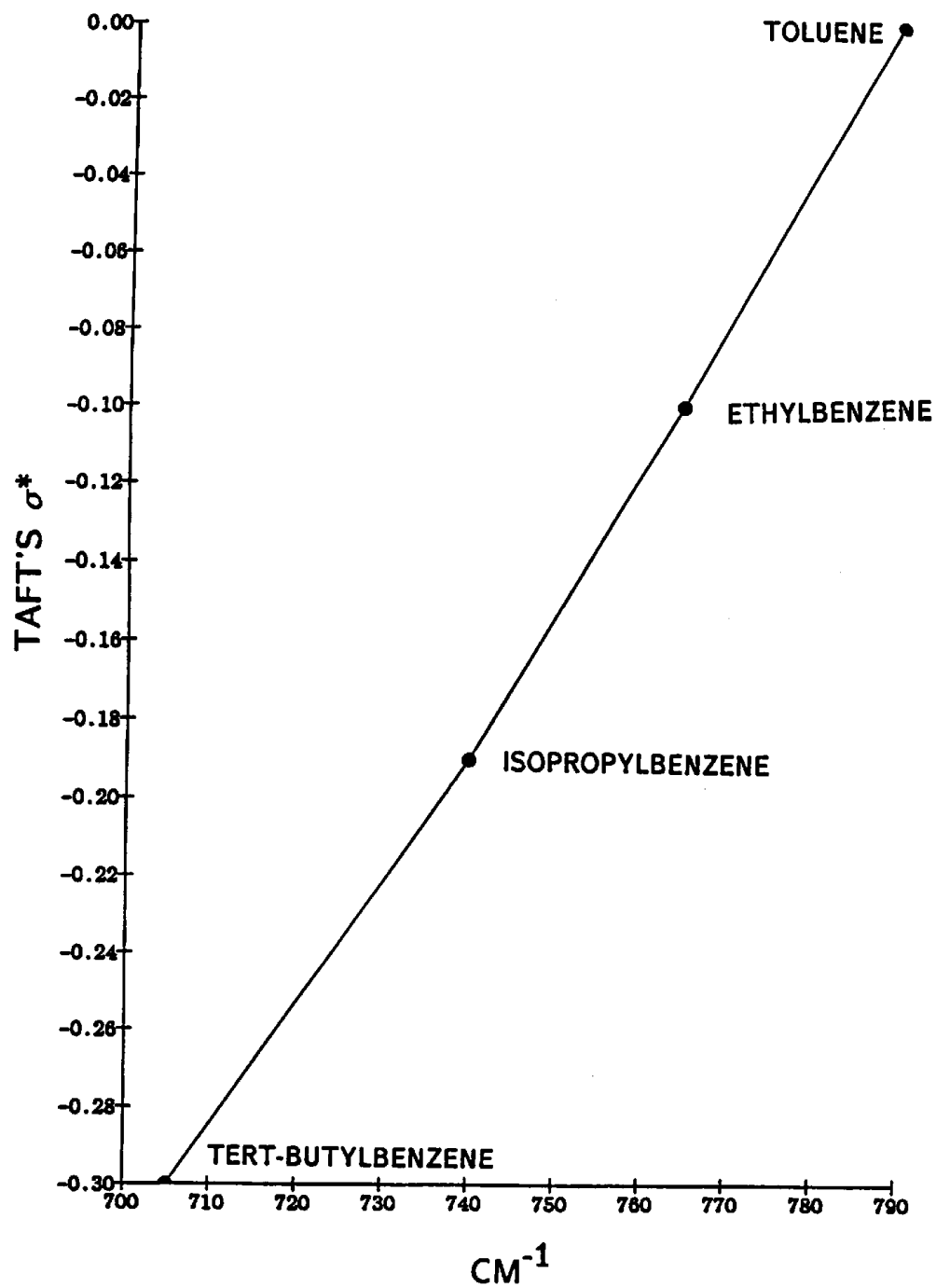


FIGURE 9.17 A plot of an A_1 fundamental for mono-substituted benzenes vs the number of protons on the ring α -carbon atom.

FIGURE 9.18 A plot of an A_1 fundamental for mono-substituted benzenes vs Tafts σ^* .

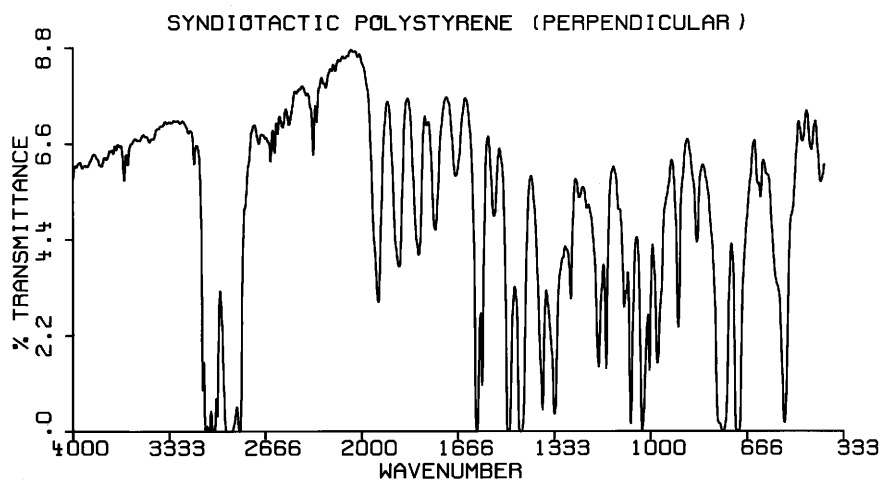


FIGURE 9.19 An IR spectrum for a uniaxially stretched syndiotactic polystyrene film (perpendicular polarization).

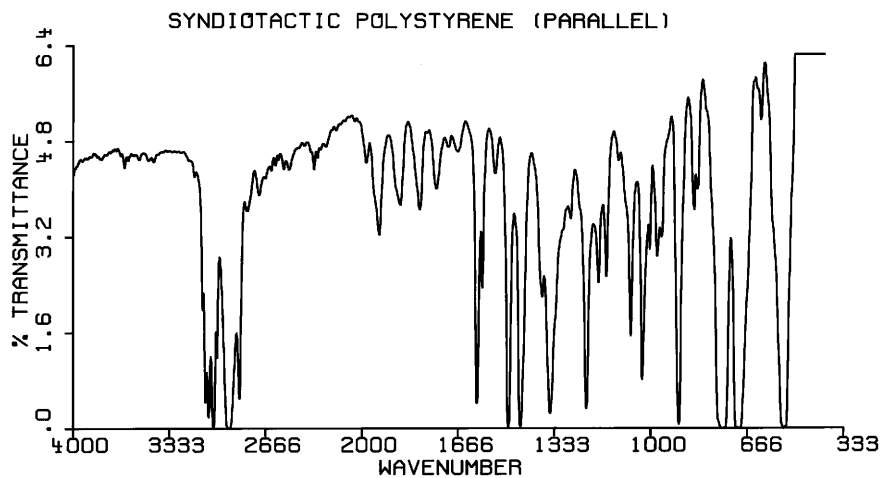


FIGURE 9.20 An IR spectrum for a uniaxially stretched syndiotactic polystyrene film (parallel polarization).

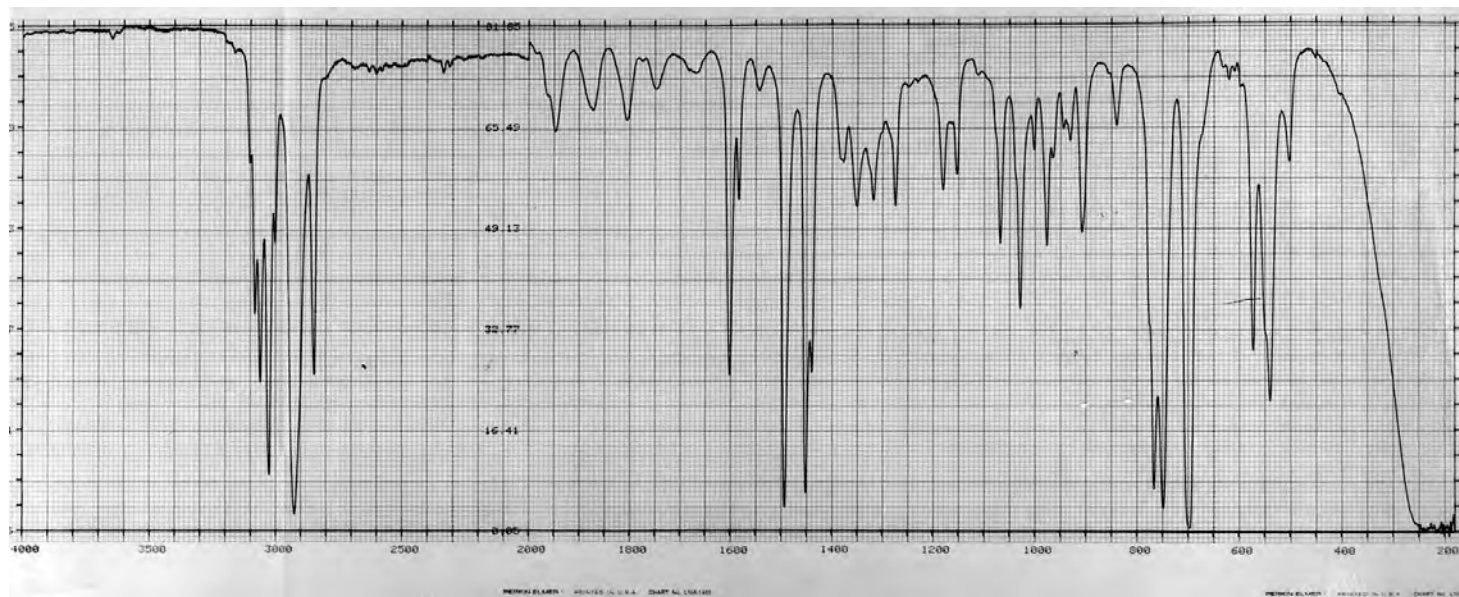


FIGURE 9.21 An IR spectrum of syndiotactic polystyrene film cast from boiling 1,2-dichlorobenzene onto a KBr plate.

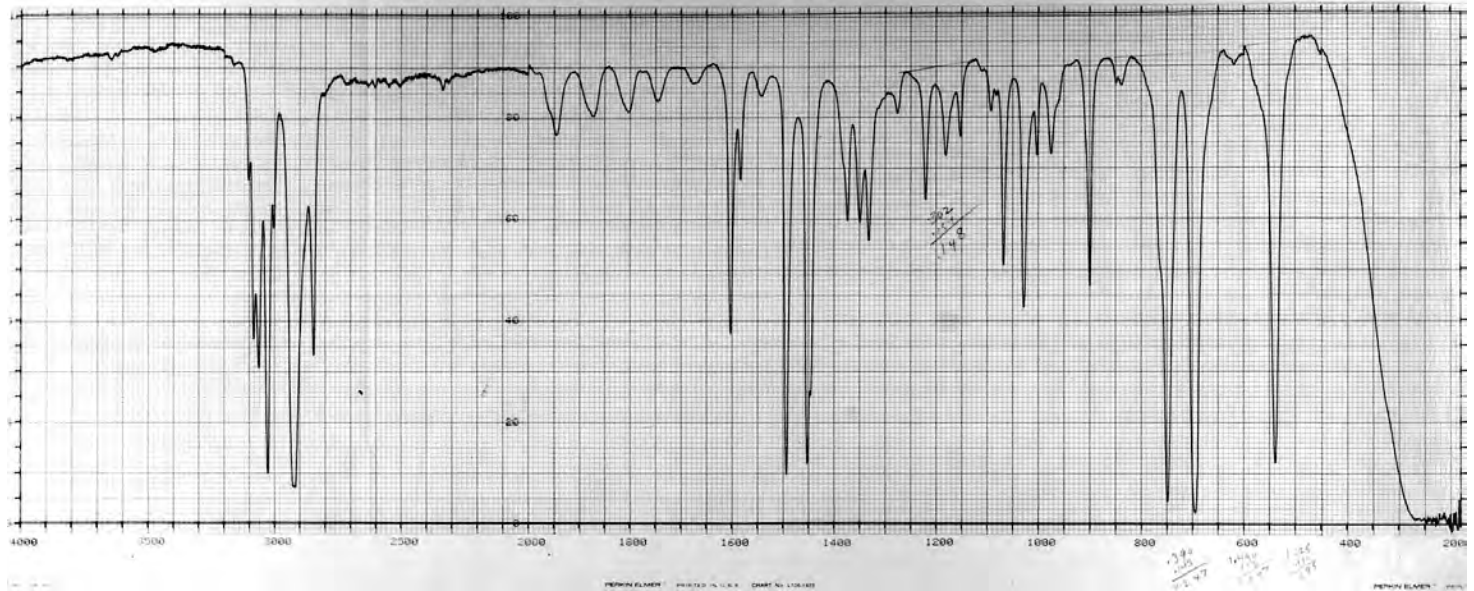


FIGURE 9.22 An IR spectrum of the same film used to record the IR spectrum shown in Fig. 9.21 except that the film was heated to 290°C then allowed to cool to ambient temperature before recording the IR spectrum of syndiotactic polystyrene.

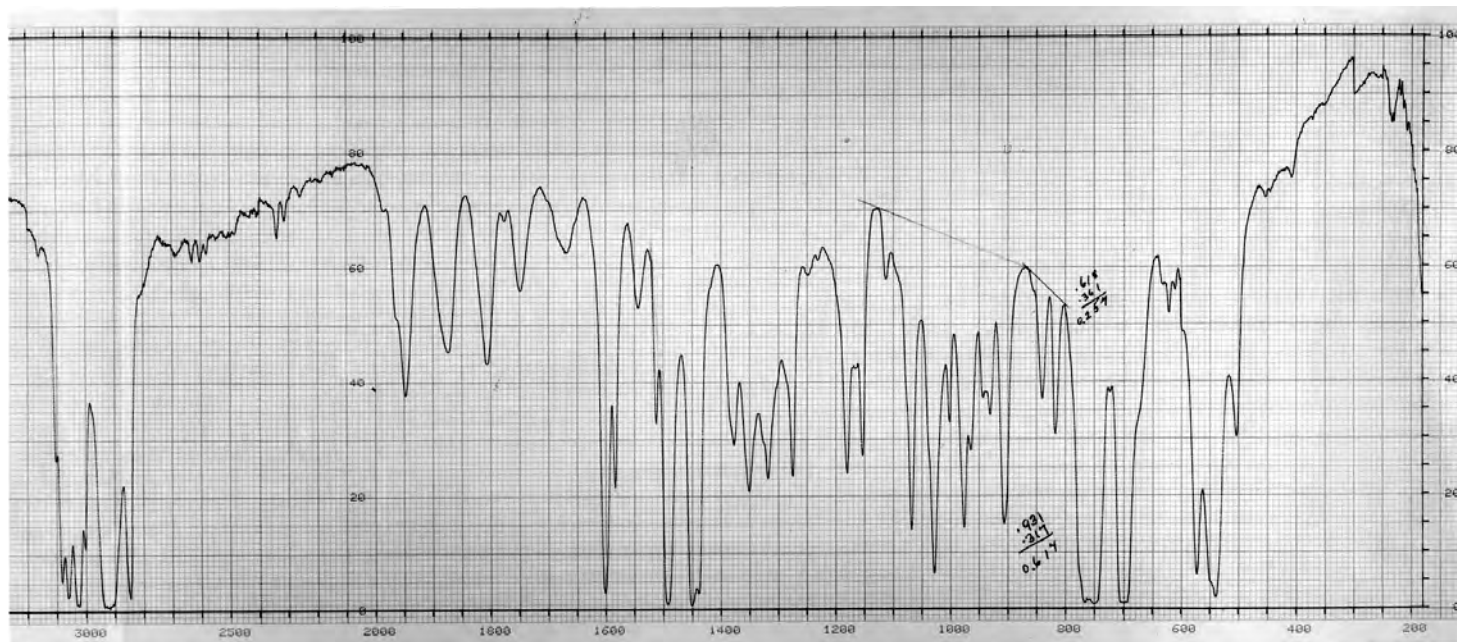


FIGURE 9.23 An IR spectrum syndiotactic styrene (98%)-4-methylstyrene (2%) copolymer cast from boiling 1,2-dichlorobenzene onto a C_sI plate.

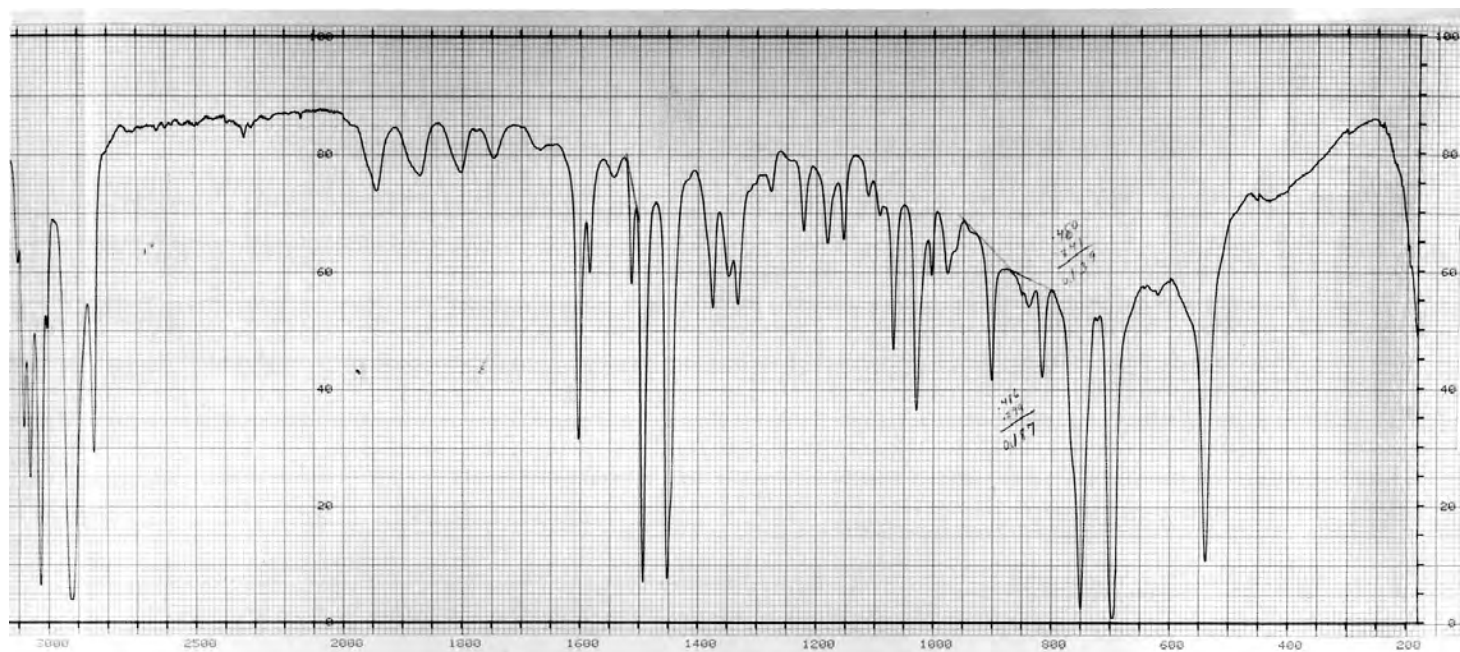


FIGURE 9.24 An IR spectrum of a styrene (93%)-4-methylstyrene (7%) copolymer cast from boiling 1,2-dichlorobenzene onto a C_{60} plate.

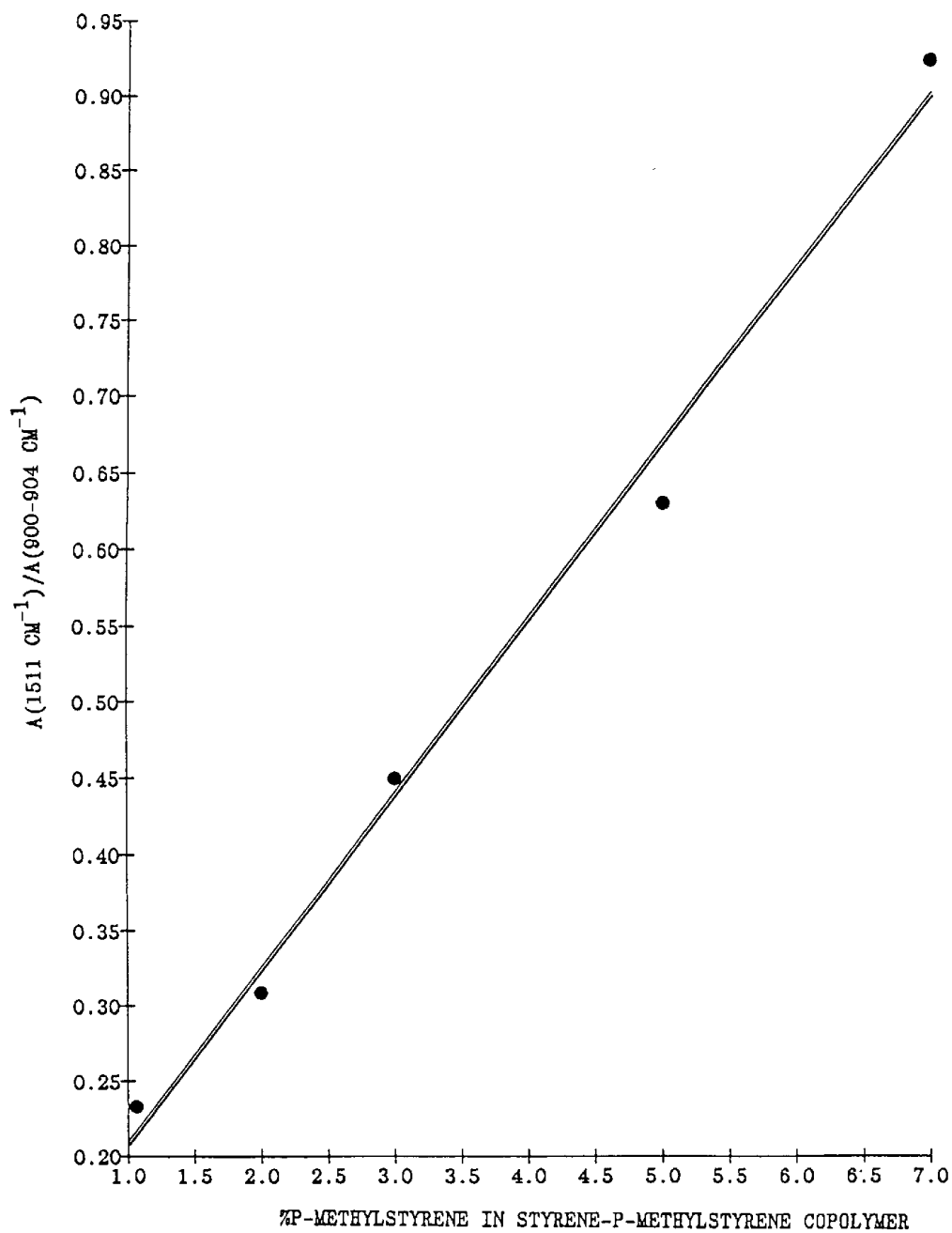


FIGURE 9.25 A plot of the IR band intensity ratio $A(1511 \text{ cm}^{-1})/A(900-904 \text{ cm}^{-1})$ vs the weight % 4-methylstyrene in styrene-4-methylstyrene copolymers.

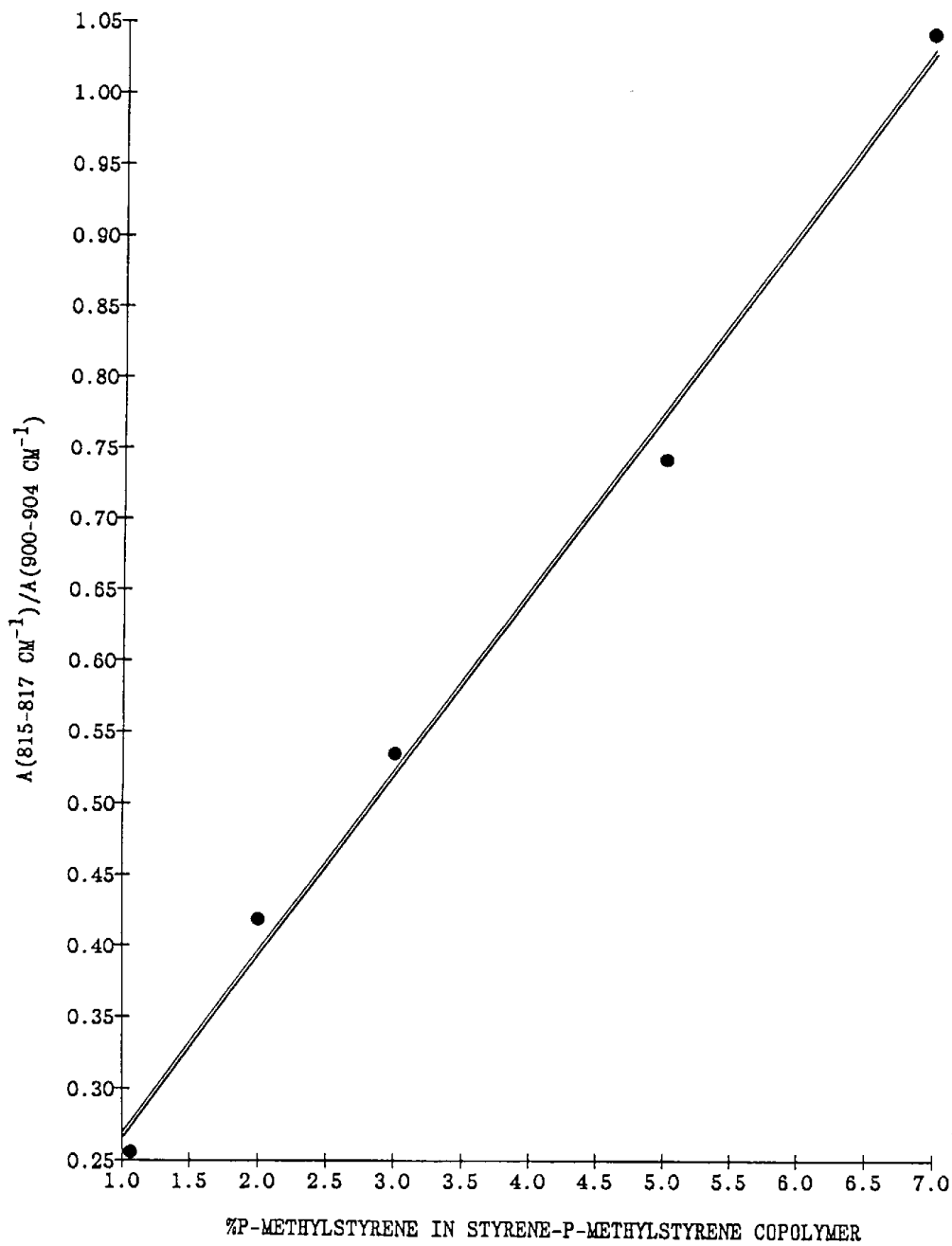


FIGURE 9.26 A plot of the IR band intensity ratio $A(815-817 \text{ cm}^{-1})/A(900-904 \text{ cm}^{-1})$ vs the weight % 4-methylstyrene in styrene-4-methylstyrene copolymers.

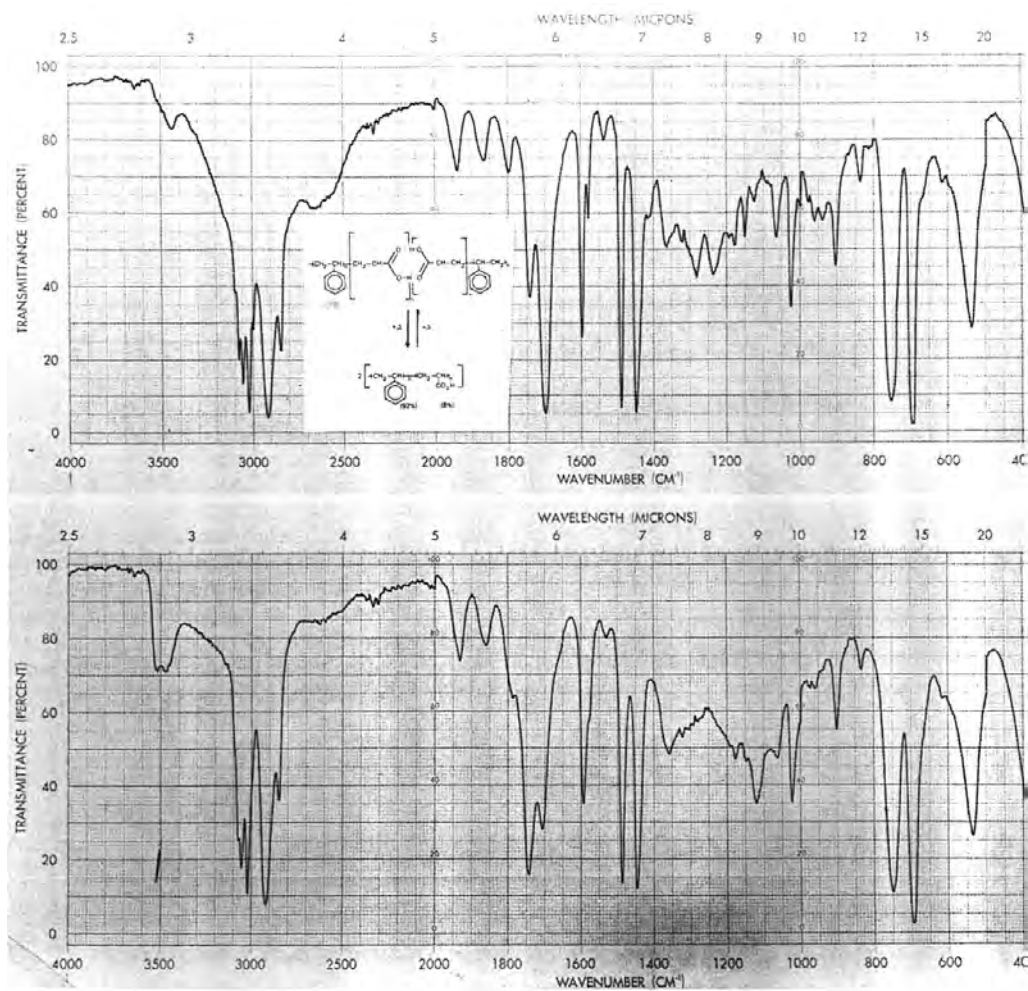


FIGURE 9.27 Top: Infrared spectrum of styrene (92%) -acrylic acid (8%) copolymer recorded at 35 °C. Bottom: Infrared spectrum of styrene (92%) -acrylic acid (8%) copolymer recorded at 300 °C.

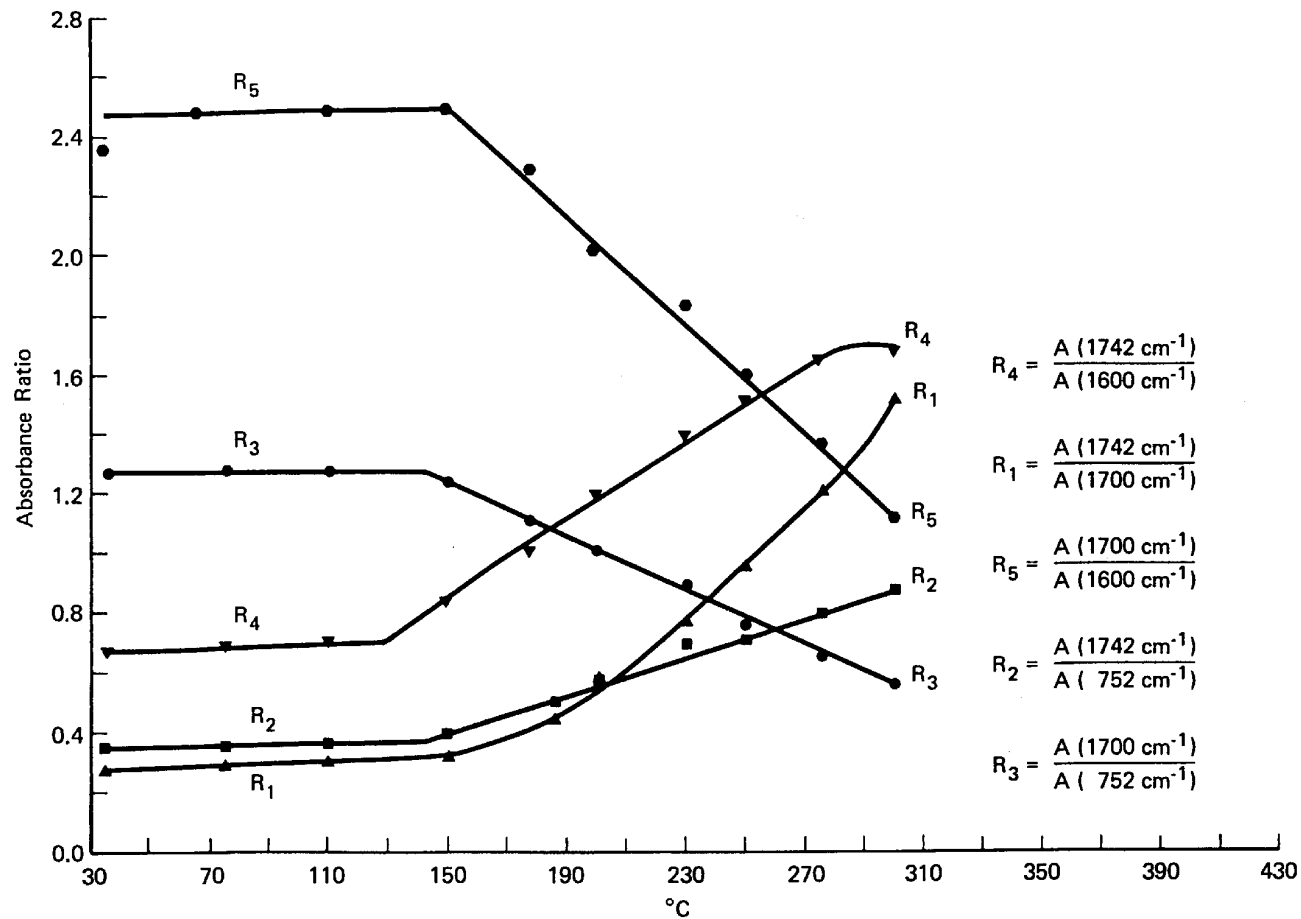


FIGURE 9.28 Styrene (92%)–acrylic acid (8%) copolymer absorbance ratios at the indicated frequencies vs copolymer film temperatures in °C; R₁, R₂, and R₄ indicate an increase in CO₂H concentrations at temperatures >150 °C; R₃ and R₅ indicate a decrease in (CO₂H)₂ concentrations at >150 °C. Base line tangents were drawn from 1630–1780 cm⁻¹, 1560–1630 cm⁻¹ and 720–800 cm⁻¹ in order to measure the absorbance values at 1746 cm⁻¹ and 1700 cm⁻¹, 1600 cm⁻¹ and 752 cm⁻¹, respectively.

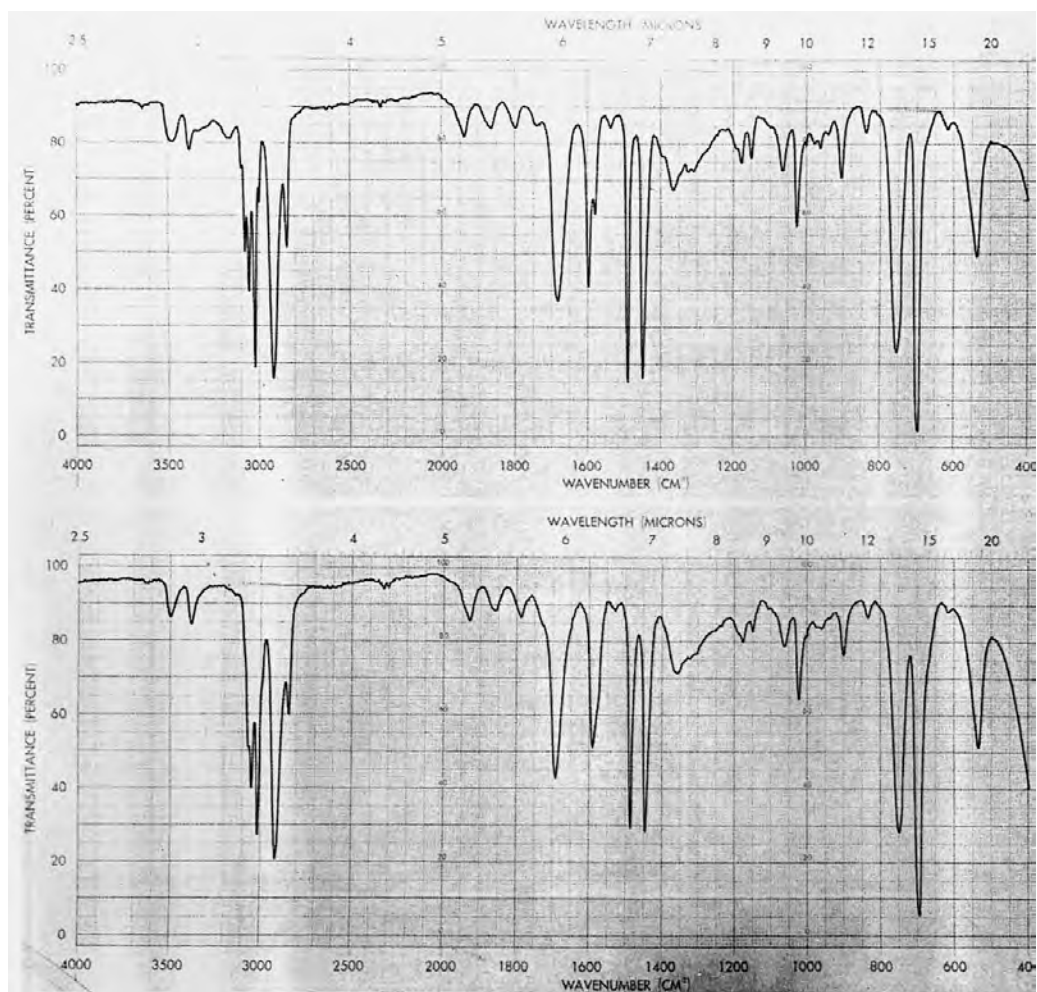


FIGURE 9.29 Top: Infrared spectrum of styrene-acrylamide copolymer recorded at 27°C. Bottom: Infrared spectrum of styrene-acrylamide copolymer recorded at 275°C.

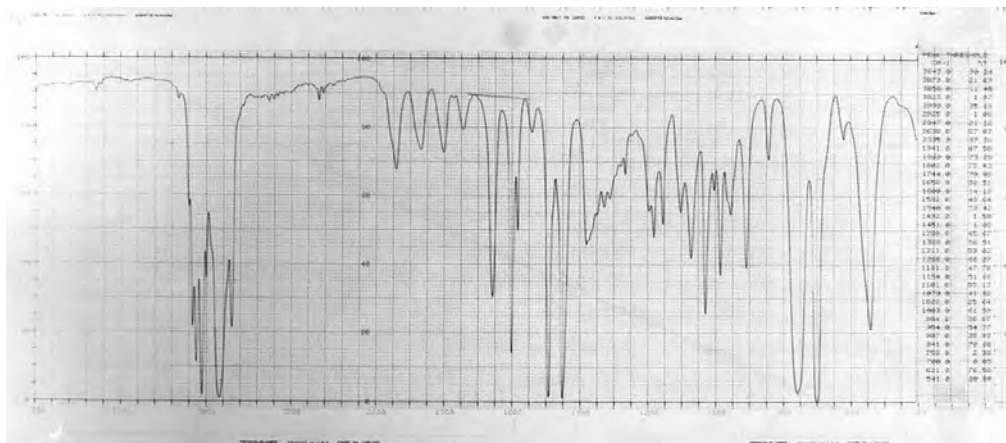


FIGURE 9.30 An IR spectrum for a styrene-2-isopropenyl-2-oxazoline copolymer (SIPO) cast from methylene chloride onto a KBr plate.

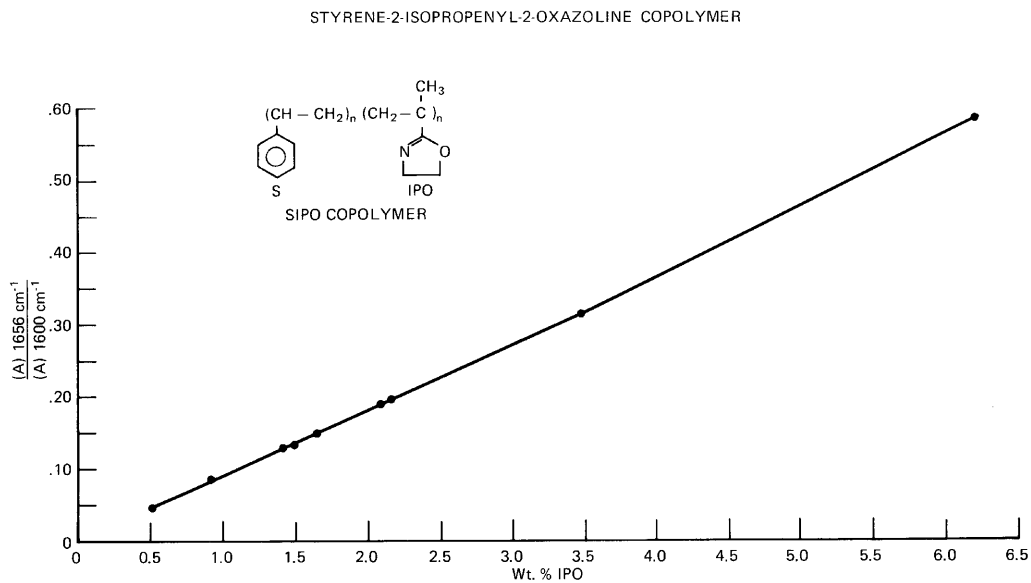


FIGURE 9.31 A plot of the weight % IPO in the SIPO copolymer vs the absorbance ratio $(A)(1656\text{ cm}^{-1}) / (A)(1600\text{ cm}^{-1})$.

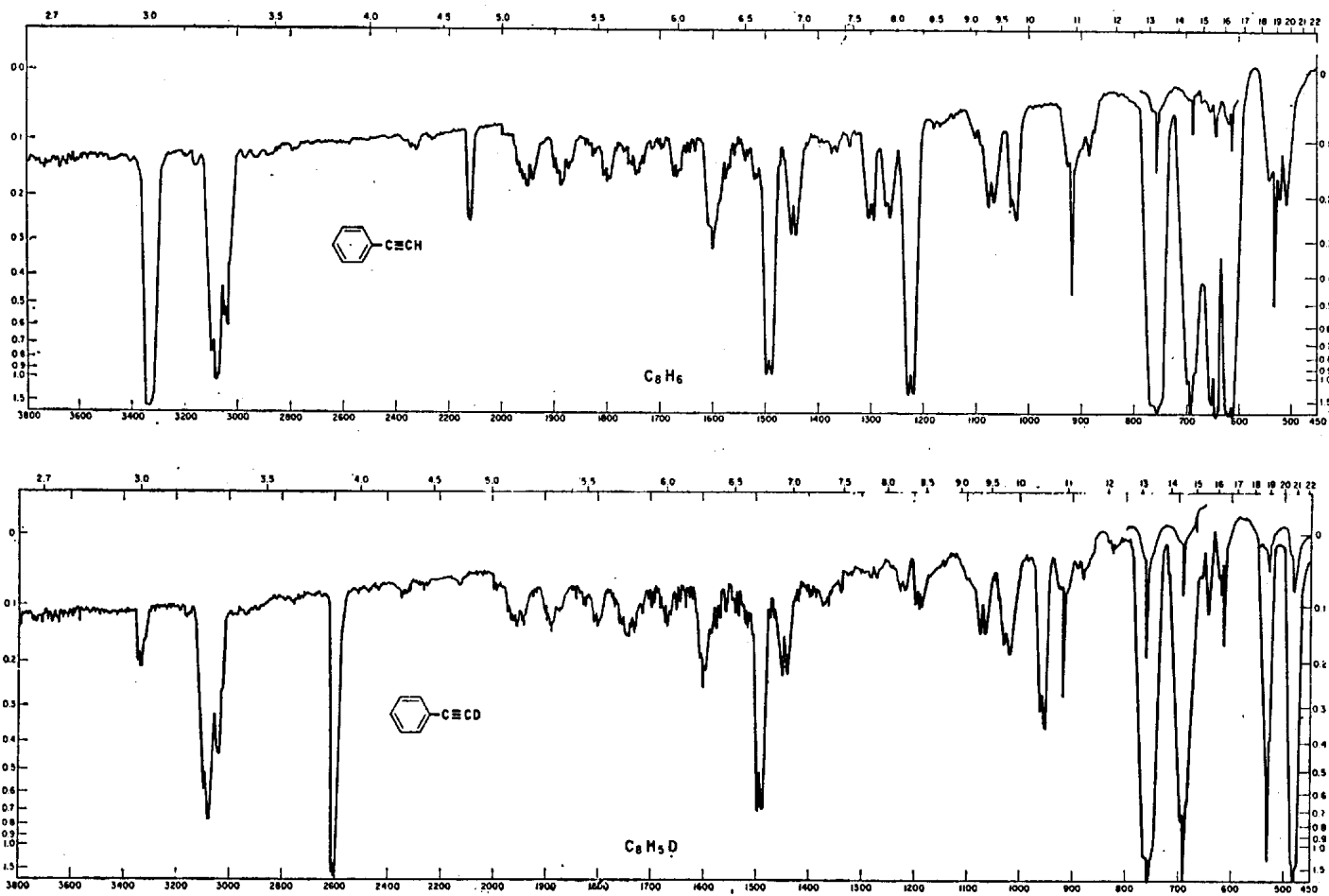


FIGURE 9.32 Top: Vapor-phase IR spectrum of ethynylbenzene in a 4-m cell (vapor pressure is in an equilibrium with the liquid at 25 °C). Bottom: Vapor-phase IR spectrum of ethynylbenzene-d in a 4-m cell (vapor pressure is in an equilibrium with the liquid at 25 °C).

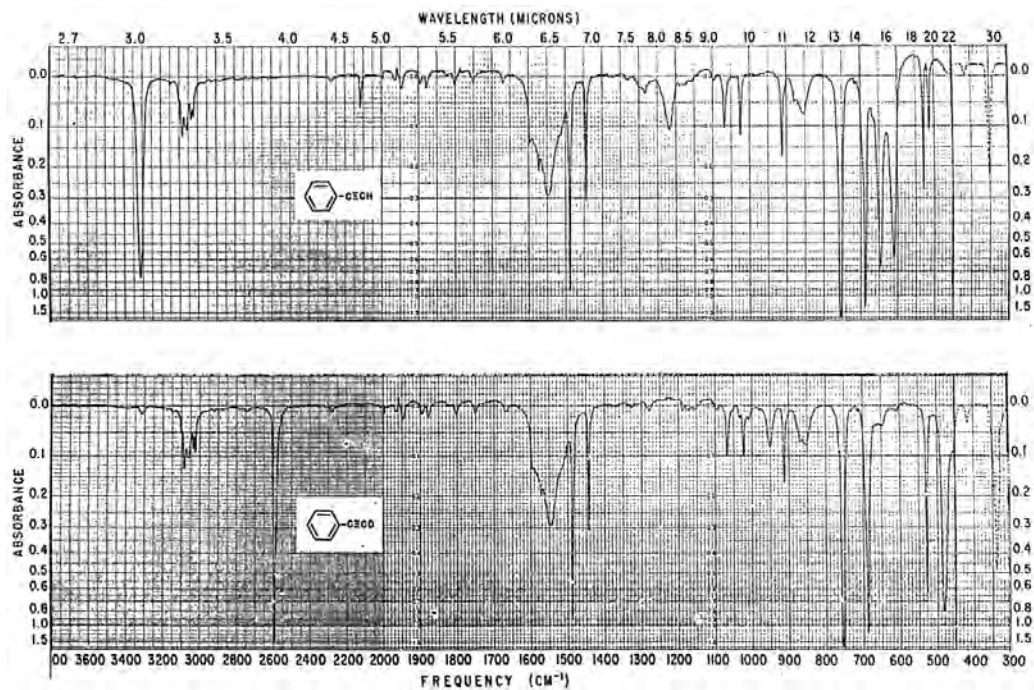


FIGURE 9.33 Top: An IR solution spectrum for ethynylbenzene ($3800\text{--}1333\text{ cm}^{-1}$ in CCl_4 (0.5 M) solution in a 0.1 mm NaCl cell), ($1333\text{--}450\text{ cm}^{-1}$ in CS_2 (0.5 M) solution in a 0.1 mm KBr cell), and in hexane (0.5 M) solution using a 2 mm cis I cell. The IR band at 1546 and 853 cm^{-1} is due to the solvents. Bottom: An IR solution spectrum for ethynylbenzene-d recorded under the same conditions used to record the top spectrum.

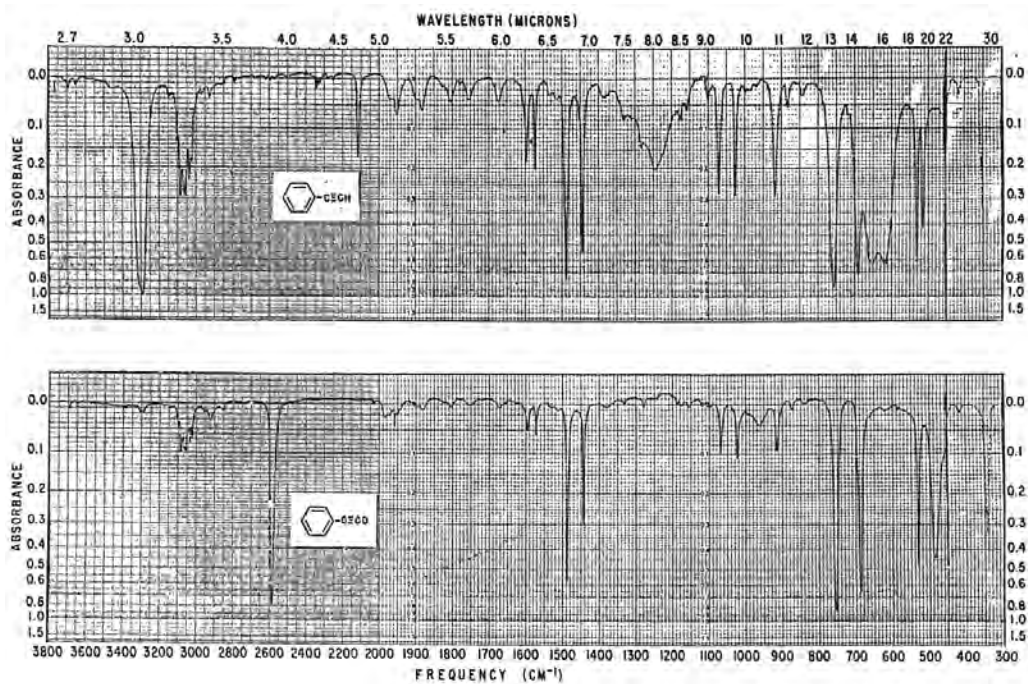


FIGURE 9.34 Top: Liquid-phase IR spectrum ethynylbenzene between KBr plates in the region 3800–450 cm⁻¹, and between C₆I plates in the region 450–300 cm⁻¹. Bottom: Liquid-phase IR spectrum of ethynylbenzene-d recorded under the same conditions as the top spectrum.

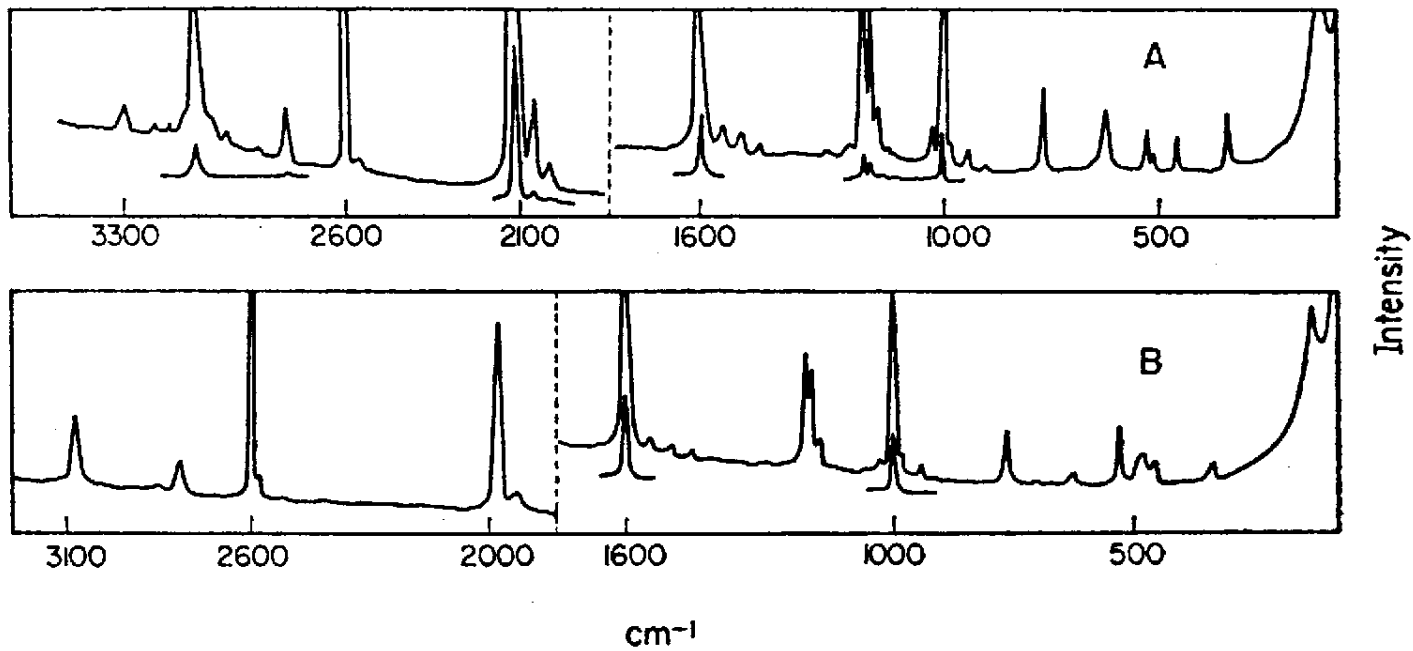


FIGURE 9.35 Top: Raman spectra for ethynylbenzene in the liquid phase. Bottom: Raman spectra for ethynylbenzene-d in the liquid phase.

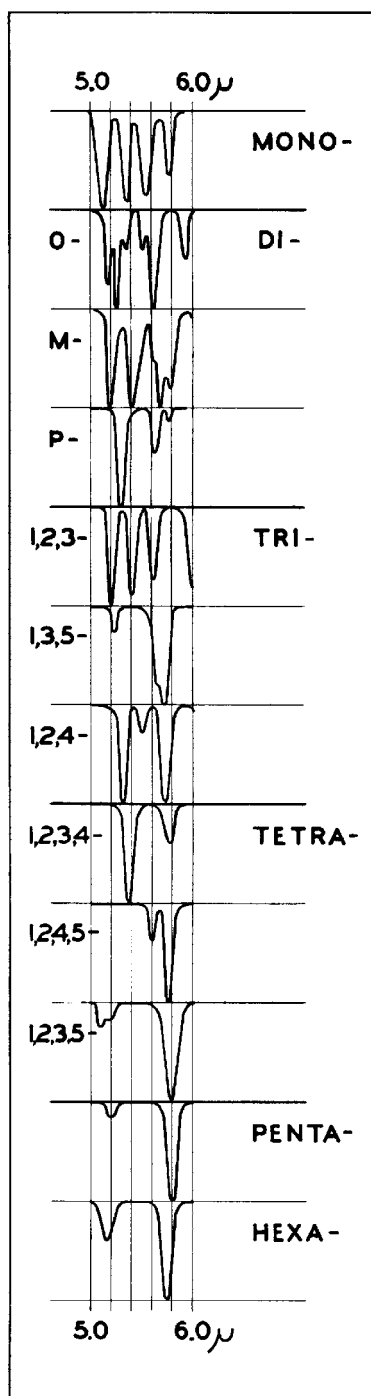


FIGURE 9.36 A correlation chart for substituted benzenes in the region 5–6 μ (after Young, DuVall, and Wright).

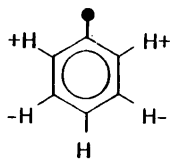
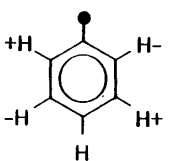
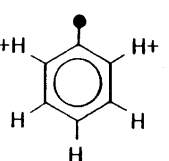
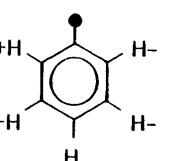
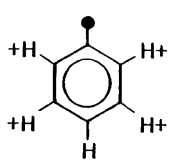
					
	I	II	III	IV	V
<u>Symmetry</u>					
C_{2v}	B_1	A_2	B_1	A_2	B_1
C_s planar	A''	A''	A''	A''	A''
C_s perpendicular plane	A'	A''	A'	A''	A'
C_1 range	965.5-996 cm^{-1}	945-981 cm^{-1}	862-940 cm^{-1}	789-852 cm^{-1}	(725-810)
<u>Symmetry</u>					
C_{2v}	$2 \times I = 2 \times B_1 = A_1$	$I + II = B_1 \times A_2 = B_2$	$I + III = B_1 \times B_1 = A_1$		
C_s planar	$2 \times I = 2A'' = A'$	$I + II = A'' \times A'' = A'$	$I + III = A'' \times A'' = A'$		
C_s perpendicular plane	$2 \times I = 2 \times A' = A''$	$I + II = A' \times A'' = A''$	$I + III = A' \times A' = A''$		
range	1931-1992 cm^{-1}	1915-1976 cm^{-1}	1815-1936 cm^{-1}		
<u>Symmetry</u>					
C_{2v}	$II + III = A_2 \times B_1 = B_2$	$II + IV = A_2 \times A_2 = A_1$	$III + IV = B_1 \times A_2 = B_2$		
C_s planar	$II + III = A'' \times A'' = A'$	$II + IV = A'' \times A'' = A'$	$III + IV = A'' \times A'' = A'$		
C_s perpendicular plane	$II + III = A'' \times A' = A''$	$II + IV = A'' \times A'' = A'$	$III + IV = A' \times A'' = A''$		
range	1815-1914 cm^{-1}	1737-1829 cm^{-1}	1680-1787 cm^{-1}		
<u>Symmetry</u>					
C_{2v}	$III + V = B_1 \times B_1 = A_1$				
C_s planar	$III + V = A'' \times A'' = A'$				
C_s perpendicular plane	$III + V = A' \times A' = A''$				
range	1611-1748 cm^{-1}				

FIGURE 9.37 Summary of out-of-plane hydrogen deformations and their combination and overtones for mono-substituted benzenes.

	I	II	III	IV
<u>Symmetry</u>				
C_{2v}	A_2	B_1	A_2	B_1
C_s	A''	A''	A''	A''
range	956–989 cm^{-1}	915–970 cm^{-1}	833–886 cm^{-1}	725–791 cm^{-1}
<u>Symmetry</u>				
C_{2v}	$2 \times I = 2 \times A_2 = A_1$	$I + II = A_2 \times B_1 = B_2$	$2 \times II = 2 \times B_1 = A_1$	$I + III = A_2 \times A_2 = A_1$
C_s	$2 \times I = 2A'' = A'$	$I + II = A'' \times A'' = A'$	$2 \times II = 2 \times A'' = A'$	$I + III = A'' \times A'' = A'$
range	1912–1979 cm^{-1}	1869–1952 cm^{-1}	1828–1932 cm^{-1}	1789–1875 cm^{-1}
<u>Symmetry</u>				
C_{2v}	$II + III = B_1 \times A_2 = B_2$	$2 \times III = 2 \times A_2 = A_1$	$II + IV = B_1 \times B_1 = A_1$	
C_s	$II + III = A'' \times A'' = A'$	$2 \times III = 2 \times A'' = A'$	$II + IV = A'' \times A'' = A'$	
range	1748–1849 cm^{-1}	1666–1772 cm^{-1}	1658–1758 cm^{-1}	

FIGURE 9.38 Summary of out-of-plane hydrogen deformations and their combination and overtones for 1,2-disubstituted benzenes.

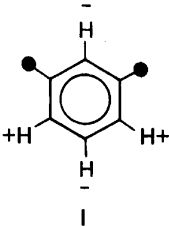
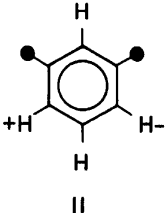
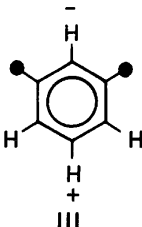
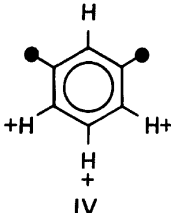
				
	I	II	III	IV
<u>Symmetry</u>				
C_{2v}	B_1	A_2	B_1	B_1
C_s	A''	A''	A''	A''
range	947–999 cm^{-1}	863–941 cm^{-1}	831–910 cm^{-1}	761–815 cm^{-1}
<u>Symmetry</u>				
C_{2v}	$2 \times I = 2 \times B_1 = A_1$	$I + II = B_1 \times A_2 = B_2$	$2 \times II = 2 \times A_2 = A_1$	$II + III = A_2 \times B_1 = B_2$
C_s	$2 \times I = 2 \times A'' = A'$	$I + II = A'' \times A'' = A'$	$2 \times II = 2 \times A'' = A'$	$II + III = A'' \times A'' = A'$
range	1910–1991 cm^{-1}	1820–1940 cm^{-1}	1724–1885 cm^{-1}	1709–1839 cm^{-1}
<u>Symmetry</u>				
C_{2v}	$I + IV = B_1 \times B_1 = A_1$	$2 \times III = 2 \times B_1 = A_1$	$II + IV = A_2 \times B_1 = B_2$	
C_s	$I + IV = A'' \times A'' = A'$	$2 \times III = 2 \times A'' = A'$	$II + IV = A'' \times A'' = A'$	
range	1710–1810 cm^{-1}	1680–1820 cm^{-1}	1637–1760 cm^{-1}	

FIGURE 9.39 Summary of out-of-plane hydrogen deformations and their combination and overtones for 1,3-disubstituted benzenes.

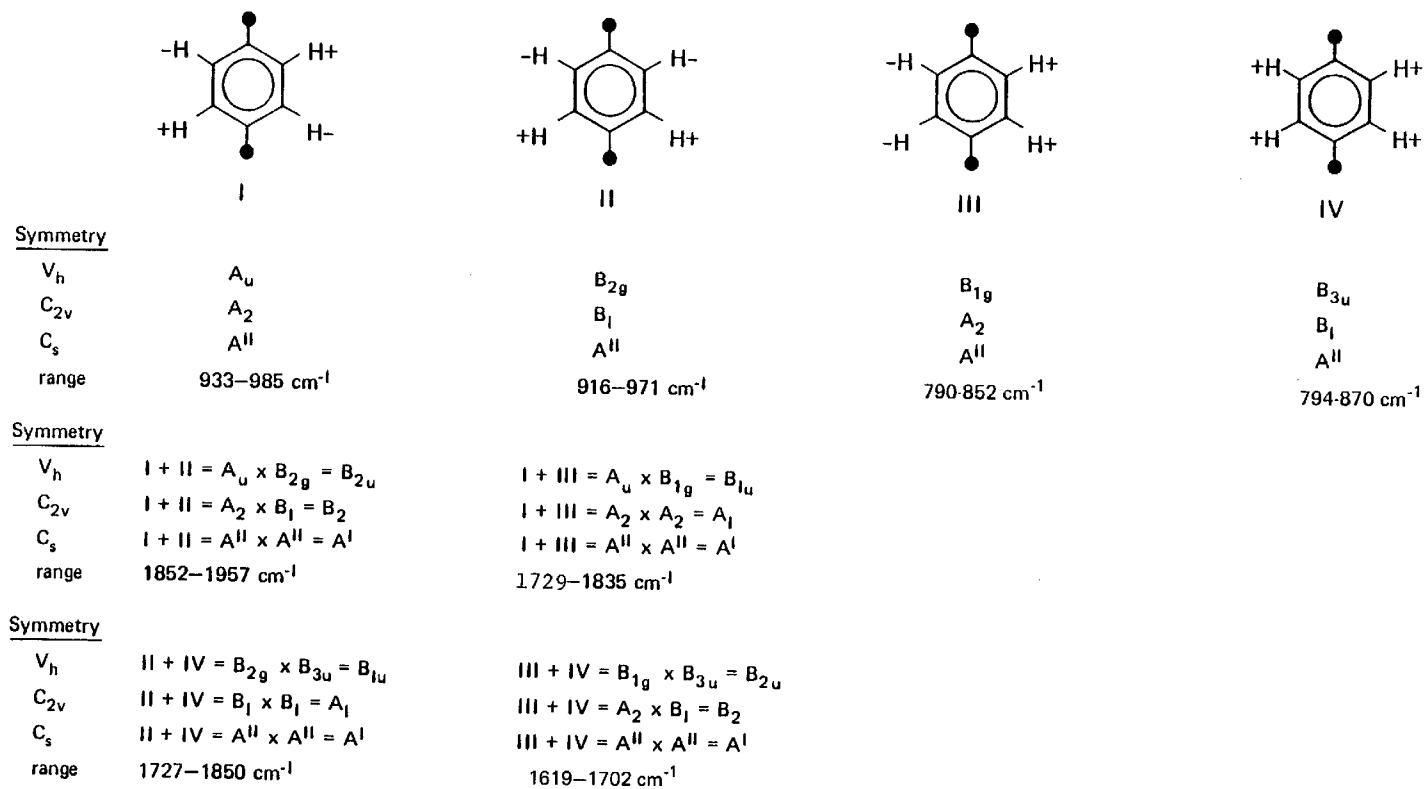


FIGURE 9.40 Summary of out-of-plane hydrogen deformations and their combination and overtones for 1,4-disubstituted benzenes.

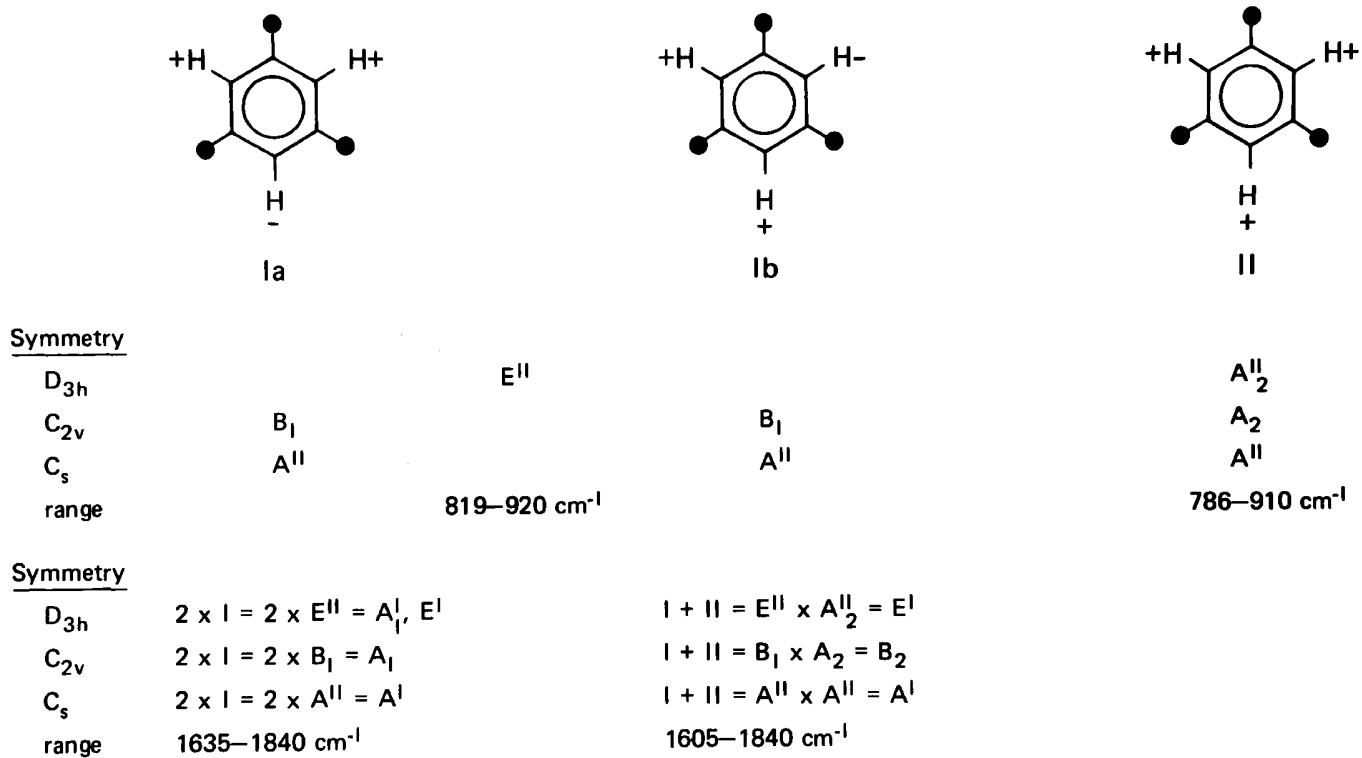


FIGURE 9.41 Summary of out-of-plane hydrogen deformations and their combination and overtones for 1,3,5-trisubstituted benzenes.

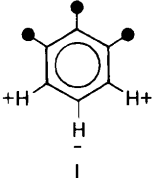
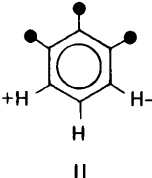
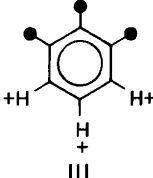
			
<u>Symmetry</u>			
C_{2v}	B_1	A_2	B_1
C_s	A''	A''	A''
range	930–989 cm^{-1}	848–930 cm^{-1}	731–810 cm^{-1}
<u>Symmetry</u>			
C_{2v}	$2 \times I = 2 \times B_1 = A_1$	$I + II = B_1 \times A_2 = B_2$	$2 \times III = 2 \times B_1 = A_1$
C_s	$2 \times I = 2A'' = A'$	$I + II = A'' \times A'' = A'$	$2 \times III = 2 \times A'' = A'$
range	1860–1975 cm^{-1}	1795–1899 cm^{-1}	1700–1860 cm^{-1}

FIGURE 9.42 Summary of out-of-plane hydrogen deformations and their combination and overtones for 1,2,3-trisubstituted benzenes.

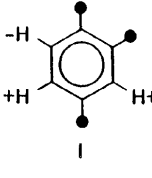
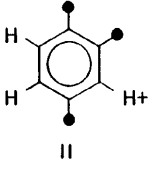
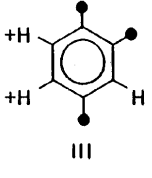
			
<u>Symmetry</u>			
C_s	A''	A''	A''
range	926–982 cm^{-1}	841–923 cm^{-1}	790–852 cm^{-1}
<u>Symmetry</u>			
C_s	$2 \times I = 2 \times A'' = A'$	$I + II = A'' \times A'' = A'$	$I + III = A'' \times A'' = A'$
range	1844–1961 cm^{-1}	1776–1890 cm^{-1}	1712–1829 cm^{-1}
C_s	$2 \times II = 2 \times A'' = A'$	$2 \times III = 2 \times A'' = A'$	
range	1683–1845 cm^{-1}	1580–1704 cm^{-1}	

FIGURE 9.43 Summary of out-of-plane hydrogen deformations and their combination and overtones for 1,2,4-trisubstituted benzenes.

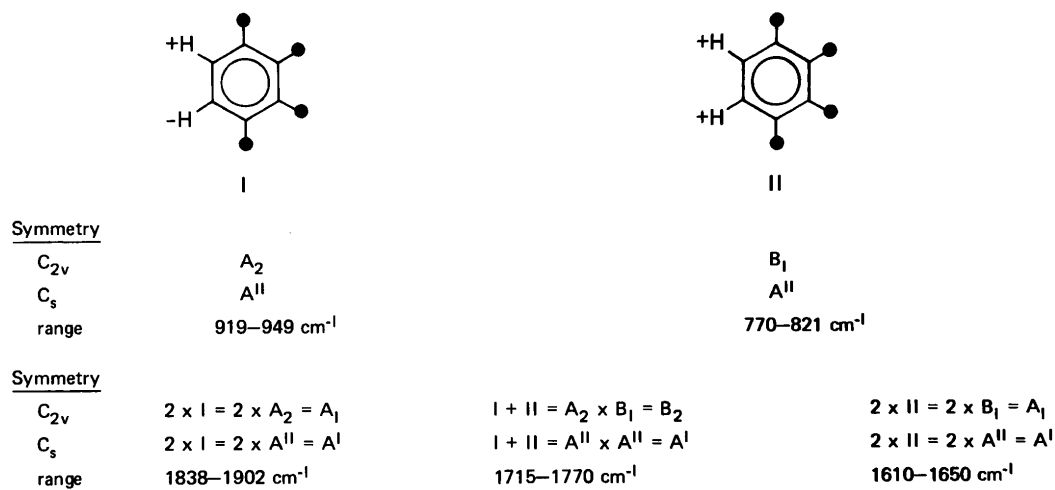


FIGURE 9.44 Summary of out-of-plane hydrogen deformations and their combination and overtones for 1,2,3,4-tetrasubstituted benzenes.

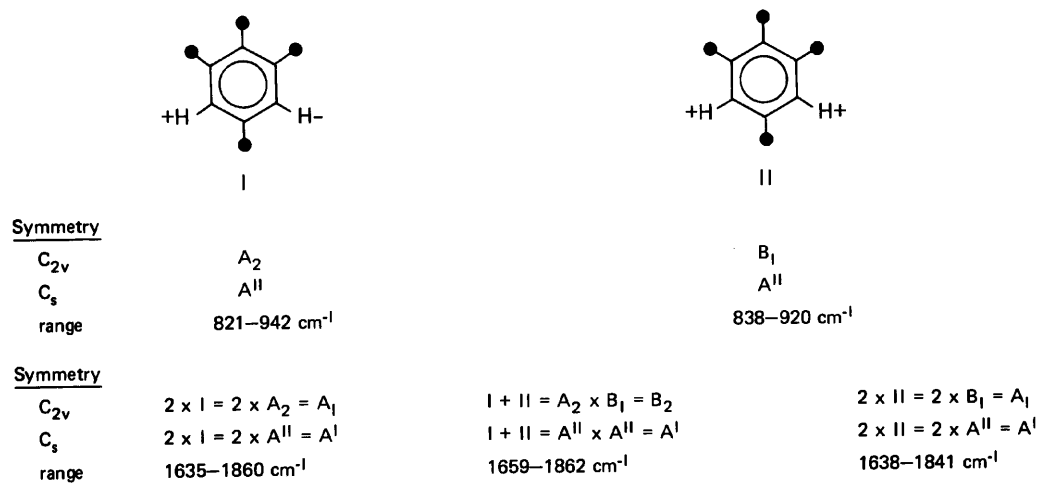


FIGURE 9.45 Summary for out-of-plane hydrogen deformations and their combination and overtones for 1,2,3,5-tetrasubstituted benzenes.

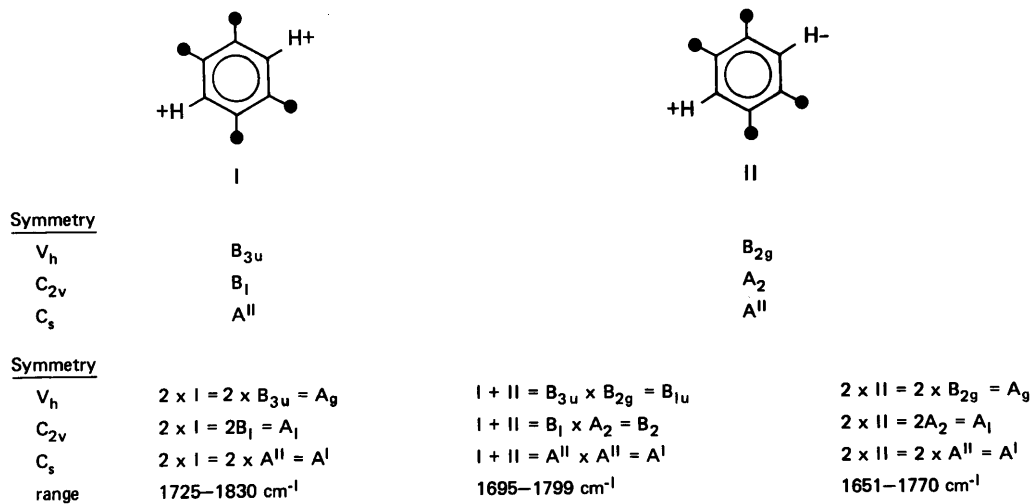


FIGURE 9.46 Summary of out-of-plane hydrogen deformations and their combination and overtones for 1,2,4,5-tetrasubstituted benzenes.

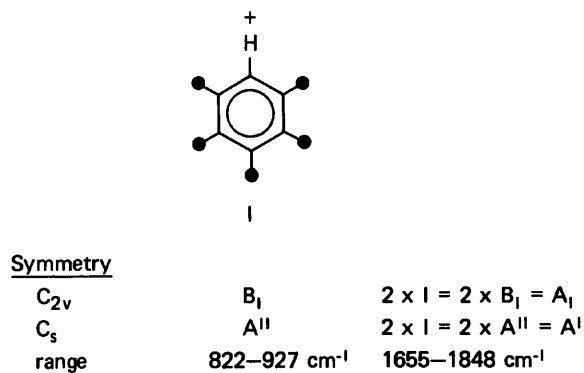


FIGURE 9.47 Summary of out-of-plane hydrogen deformation and its first overtone for 1,2,3,4,5-pentasubstituted benzenes.

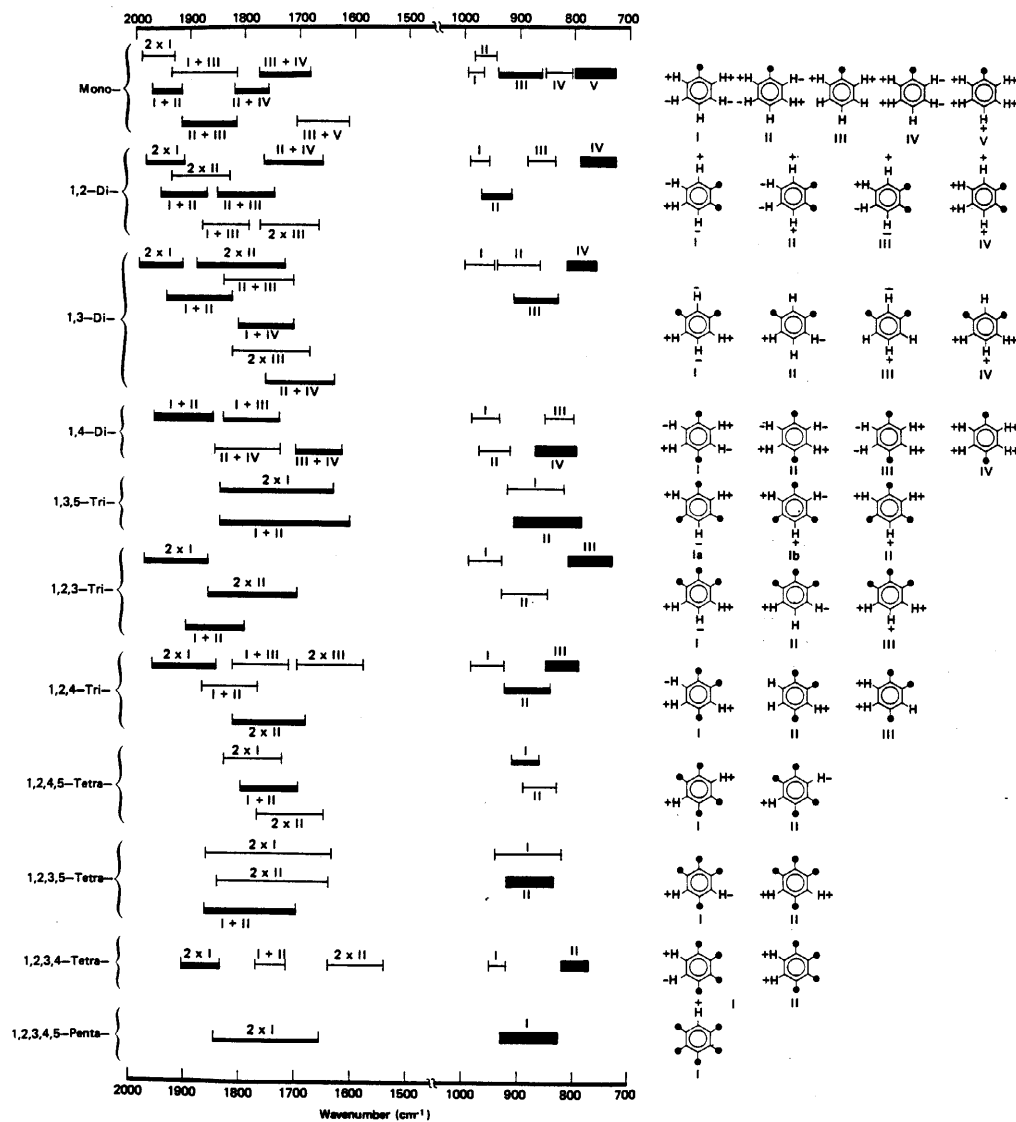


FIGURE 9.48 Infrared correlation chart for out-of-plane hydrogen deformations and their combination and overtones for substituted benzenes.

TABLE 9.1 Vibrational data for chlorobenzene vs chlorinated biphenyls

Chlorobenzene vs phenyl In plane modes	Chlorobenzene cm ⁻¹	2,3,4,5,6-Pentachlorobiphenyl cm ⁻¹
A1	3087	3068
	3072	3030
	3067	3000
	1584	1602
	1480	1497
	1174	1155
	1084	1151?
	1023	1023
	1002	1000
	703	719
	418	449
B2	3087	3058
	3059	3030
	1584	1580
	1447	1442
	1325	?
	1272	1262
	1157	1157
	1068	1070
	613	610
297	?	
A2	957	974
	825	[845]
		414?
B1	976	982
	897	918
	734	773
	679	686
	?	472
	?	?

? tentative assignment or not assigned.

TABLE 9.2 Vibrational data for 1,2-dichlorobenzene vs chlorinated biphenyls

1,2-Dichlorobenzene cm ⁻¹	2,2',3-Trichlorobiphenyl cm ⁻¹	2,3'4'-Trichlorobiphenyl cm ⁻¹	2,2',3,4,6-Pentachlorophenyl cm ⁻¹
A1 species			
3070	3068	3060	3062
3070	3068	3060	3062
1575	1592	1589	1592
1458	1479	1481	1481
1276	1278	1274	1279
1162	1178	1175	1175 or 1182
1130	1135	1151?	1125 or 1132
1041	1029	1021	1032 or 1025
660	715	710	?
480	627	648	628
203	?	?	?
B2 species			
3072	3068	3060	3062
3072	3068	3060	3062
1575	1578	1570	1562
1438	1421	1429	1417
1252	1250	1242	1040
1130	1129	1131	1132
1038	1029	1029	1025
740	735	730?	748sh
429	422	430	423
334	?	?	?
Out-of-plane modes			
A2 species			
975	977	978	974
850	[861]	[863]	[862.5]
695	725	730?	728sh
564	580	581	570
154	?	?	?
B1 species			
940	941	944	941
749	751	751	754
435	434	431	438

? not assigned.

TABLE 9.3 Vibrational data for 1,3-dichlorobenzene vs 2,3,3',5,6-pentachlorobiphenyl

1,3-Dichlorobenzene In-plane modes	Assignment cm ⁻¹	2,3,3',5,6-Cl ₅ biphenyl cm ⁻¹
A ₁	3093.8	
	3085.8	
	3064.6	
	1574.6	1575.8
	1392.6	1390.4
	1126.2	
	1075.2	1083.9
	995.6	
	662.6	658
	401.4	
	201.4	
B ₂	3083.6	
	1586.2	
	1474.5	1475.4
	1326.7	
	1238.9	1247.4
	1169	1165.1
	1069.2	1063.6
	786.3	792.1
	422	
370.6		

TABLE 9.4 Vibrational data for 1,4-dichlorobenzene vs chlorinated biphenyls

Species	1,4-Dichlorobenzene cm ⁻¹	2,3,4,4',6-Pentachlorobiphenyl cm ⁻¹
In-plane modes		
Ag[R]	3087	3078
	1574	1599
	1169	1176
	1096	1131
	747	?
	328	?
B3g	3065	3042
	1574	[1560]
	1290	1300
	626	638
	350	?
B1u	0	3078
	390	
	1477	1492
	1090	1091
	1015	1013
	550	550
B2u	3090	3078
	1394	1397
	1221	1234
	1107	1102sh
	226	?
Out-of-plane modes		
B1g(R)	815	[817]
B2g(R)	934	941
	687	721
	298	?
Au	951	959
	407	410?
B3u	819	815
	485	488
	125	?

? not assigned.

TABLE 9.5 Vibrational data for 1,3,5-trichlorobenzene vs chlorinated biphenyls

Species	1,3,5-Trichlorobenzene cm ⁻¹	2,3',4,5',6-Pentachlorobiphenyl cm ⁻¹
In-plane modes		
A1'	3084	3080
	1149	1131
	997	997
	379	?
A2'	1379	1386
	1249	1233
	471	449
E'	3089	3080
	1570	1590 & 1575
	1420	1459
	1098	1099
	816	805
	429	[430]
	191	?
Out-of-plane modes		
A2''	853	849
	662	689
	148.5	?
E''	868.5	[870]
	530	[525]
	215	?

? not assigned.

TABLE 9.6 Vibrational data for 1,2,3-trichlorobenzene vs 2,2',3-trichlorobiphenyl, 2,2',3',4,5-pentachlorobiphenyl, and 2,2',4,6,6'-pentachlorobiphenyl

Species	1,2,3-Trichloro- benzene cm ⁻¹	2,2',3-Trichloro- biphenyl cm ⁻¹	2,2',3',4,5-Pentachloro- biphenyl cm ⁻¹	2,2',4,6,6'-Pentachloro- biphenyl cm ⁻¹
A1				
	3090			
	1566	1591	1590	1559 or masked
	1416	1401	1411	1411
	1161	1150	1139	1146
	1087	1072	1088	1113
	1049	1050	1040	1069
	737	740	731	733
	513	562	575	580
	352[R]	?	?	?
	212[R]	?	?	?
B2				
	3060			
	1566	1557	1560	1559
	1436	1431	1440	1430
	1260	1250	1249	1248
	1196	1190	1195	1195sh or 1184
	1156[R]	1174?	1150?	1151?
	791	803	762	787
	486	483	484	491
	398	?	?	?
Out-of-plane modes				
A2				
	896	900	masked	892
	524	527?	510?	490?
	212[R]	?	?	?
B1				
	963	967	969	968
	773	782	784	772
	697	692	680 or 721	680 or 721
	500	?	?	?
	242[R]	?	?	?
	90[R]	?	?	?

? not assigned.

TABLE 9.7 Vibrational data for 1,2,4-trichlorobenzene vs chlorinated biphenyls

Species	1,2,4-Trichlorobenzene cm ⁻¹	2',3,4-Trichlorobiphenyl cm ⁻¹	2,3',4,4',6-Pentachlorobiphenyl cm ⁻¹	2,2,3',4',6-Pentachlorobiphenyl cm ⁻¹	2,2',3,5',6-Pentachlorobiphenyl cm ⁻¹
In-plane modes					
A'					
	3094	3060	3079	?	?
	3072	3060	3079	?	?
	1571	1570	1573	1589	?
	1562	1557	1552	1565	?
	1461	1466	1472	1479	?
	1377	1372	1347sh	1382	?
	1267	1272	1278	1280	?
	1245	1249	1244	1250	?
	1156	1151	1152sh		?
	1132	1131	1130	1119	1119
	1096	1094	1093	1100	1091
	1036	1035	1031	1021	1026
	817	885	884	?	?
	697	710	708	?	?
	576	615	615	612	?
	456	469	459	471	463
	396	?	405	?	?
	328	?	?	?	?
	211	?	?	?	?
	1578	1590	1586	1572	1571
	1551	1556	1568	1550	?
	1469	1472	1472	1469	1471
	1270	1272	1285	1285	1288
	1244	1245	1246	1249	1248

(continues)

TABLE 9.7 (continued)

Species	1,2,4-Trichlorobenzene cm ⁻¹	2',3,4-Trichlorobiphenyl cm ⁻¹	2,3',4,4',6-Pentachlorobiphenyl cm ⁻¹	2,2,3',4',6-Pentachlorobiphenyl cm ⁻¹	2,2',3,5',6-Pentachlorobiphenyl cm ⁻¹
	1163	1162sh	?	?	?
	1098	?	?	?	1135sh
	1089	1093	1100	1094	1096
	1020	1028	1024	1029	1031
	621	552?	602	?	612
	481	461	480	?	474
Out-of-plane modes					
A'					
	942	944	951	943	943
	869	863	855	863	859
	811	820	812	809	
	688	672	672	668	695
	551	550	[572]	534	551
	305	?	?	?	?
	183	?	?	?	?
	117	?	?	?	?
	947	946	947	946	[947]
	862	863	860	863	866
	818	812	811	813	812
	670	674	?	644?	668
	575	577	549	551	557
	?	?	439	442	435

? not assigned.

TABLE 9.8 Vibrational data for 1,2,4,5-tetrachlorobenzene vs chlorinated biphenyls

Species	1,2,3,4,5-Tetrachlorobenzene cm ⁻¹	2,2',4,4',5-Pentachlorobiphenyl cm ⁻¹	2,2',4,5,5'-Pentachlorobiphenyl cm ⁻¹	2,2',3',4,5-Pentachlorobiphenyl cm ⁻¹
In-plane modes				
Ag	3070			
	1549	1550	1557	1560
	1165	1167	masked	1150?
	684	723	723	731
	352			
	190			
B3g	1566	1533	1536	1540
	1240	1245	1244	1248
	868			
	511	481	495	494
	312			
B1u	3094			
	1327	1337	1334	1342
	1063	1063	1067	1057
	510	510 or 518	510 or 524	510
	218			
B2u	1473 in FR	1479 in FR	1472 in FR	1472 in FR
	[860 + 600]	[862 + 603]	[605 + 863]	[865 + ?]
	1448 in FR	1443 in FR	1446 in FR	1440 in FR

(continues)

TABLE 9.8 (continued)

Species	1,2,3,4,5-Tetrachlorobenzene cm ⁻¹	2,2',4,4',5-Pentachlorobiphenyl cm ⁻¹	2,2',4,5,5'-Pentachlorobiphenyl cm ⁻¹	2,2',3',4,5-Pentachlorobiphenyl cm ⁻¹
	1226	1233	~1235sh	1229
	1118	1133	1138	1139
	645	670	668	679
	209			
Out-of-plane modes				
B1g	348			
B2g	860	862 or masked	863	865
	681	684	679	680
	225			
Au	600	603?	605?	618 or masked
	80			
B3u	878	882	880	882
	442	429	430	432
	140			

? tentative assignment.

TABLE 9.9 Vibrational data for 1,2,3,5-tetrachlorobenzene vs chlorinated biphenyls

Species	1,2,3,5-Tetra- chloro- benzene cm ⁻¹	2,3',4,4',6-Penta- chloro- biphenyl cm ⁻¹	2,3',4,5',6-Penta- chloro- biphenyl cm ⁻¹	2,2',4,6,6'-Penta- chloro- biphenyl cm ⁻¹	2,2',3,4',5-Penta- chloro- biphenyl cm ⁻¹	2,2',3,5,5'-Penta- chloro- biphenyl cm ⁻¹
In-plane modes						
A1	3078	3079	3080		3065	3065
	1566	1573	1560	1573	1568	1571
	1412	1425	1411	1411	1407	1417
	1170	1182	1183	1184	1188	1190
	1120	1138 or 1130	1142	1115	1119	1121
	1049	1032	1040	1069	1056	1056
	836	812 masked	815sh	830	841	827
	598 stg	580sh	610?wk	580	601 stg	601 stg
	326					
	206					
B2	3078		3080		3065	3065
	1550	1539	1542	1542	1549	1550
	1378	1362	1368	1371	1369	1371
	1254	1260	1269	1248	1246	1250
	1191	1182	1182	1183	1188	1190
	810[FR]	797	797	800	819	829
	521	[572]	579	580	550	551
	431	[435]	[430]	431	439	442
	215					
	192					
Out-of-plane modes						
A2	871	884	[870]	[870]	[869]	[867]
	520	521?	[525?]	525?	520	520
	215					
B1	859	855	855	855	861	863
	692	732	729	733	716	719
	560	572	579	580	569	570
	316					
	147					
	80					

TABLE 9.10 Infrared data for 1,2,3,4-tetrachlorobenzene vs chlorinated biphenyls

Species	1,2,3,4-Tetra- chlorobenzene cm ⁻¹	2,2',3,4',6-Penta- chlorophenyl cm ⁻¹	2,2',3,5,6-Penta- chlorobiphenyl cm ⁻¹	2,2',3',4,5'-Penta- chlorobiphenyl cm ⁻¹
In-plane modes				
A1	3074			
	1560	1565	1557	
	1364	1372?	1362?	1358
	1248	1250	1249	1248
	1178	1173	1175	1176
	1132	1140	1132	1135
	836	865	870	882
	515	590	602	612
B2	3074			
	1560	1551	1550	1559
	1428	1431	1433	1438
	1168			
	1077	1100	1091	1096
	775	808sh	806(masked)?	781
	609	[612]	602	[612]
	482	490	463	473
	356			
	202			
Out-of-plane modes				
A2	940			[947]
	756[R]			
	307[R]			
B1	808	800	806	813
	557	557	[549]	532
	240[R]			
	116[R]			

TABLE 9.11 Vibrational data for pentachlorobenzene vs 2,2',3,4,6-pentachlorobiphenyl and 2,3,4,4',6-pentachlorobiphenyl

Species	Pentachlorobenzene cm ⁻¹	2,2',3,4,6-Pentachlorobiphenyl cm ⁻¹	2,3,4,4',6-Pentachlorobiphenyl cm ⁻¹
In-plane modes			
A1	3069	3064	3078
	1528	1529	1529
	1338	1338	1337
	1198[R]	1191	masked
	1087	1076	masked
	823	811	820
	563	570	573
B2	1559	1562	[1560]
	1398	1417	1421
	1235[R]	1230	1235
	1169	1171	1177
	[863]calc.	[862.5]calc.	[862.5]calc.
	683	671	650
	556	548	549
Out-of-plane modes			
A2	597		
B1	863	862	863
	701	735sh?	741?
	526	529	529
		1725 = 2[862.5]	

? tentative assignment.

TABLE 9.12 Vibrational data for 1,2,3,4,5,6-hexachlorobenzene vs 1,2,3,4,5-pentachlorobiphenyl

Species	Hexachlorobenzene cm ⁻¹	2,3,4,5,6-Pentachlorobiphenyl cm ⁻¹
A _{1g}	1210[R] 372[R]	1206
B _{1u}	1108 369	
A _{2g}	630 est.	632
B _{2u}	1224 Comb. 230 est.	1230
E _{2g}	1512 870[R] 323[R] 219[R]	1516 & 1497 868
E _{1u}	1350 699 218	1344 & 1320 685
A _{2u}	209	
B _{2g}	704 Comb. 97 Comb.	750?
E _{1g}	340[R]	
E _{2u}	594 80 Comb.	586

TABLE 9.13 Raman data for mono-substituted benzenes

Compound	Ring 4	Ring 8	Ring 9	Ring 20	R.I.[Ring 4]/	R.I.[Ring 8]/	R.I.[Ring 20]/
					R.I.[Ring 9]	R.I.[Ring 9]	R.I.[Ring 9]
Allylbenzene	1604(1)	1031(2)	1004(9)	621(0)	0.11	0.22	0.06
N-Benzyl acrylamide		1031(1)	1004(9)	622(1)		0.11	0.11
Benzyl acrylate	1609(1)	1031(2)	1004(9)	622(1)	0.11	0.22	0.11
N-Benzyl methacrylamide	1604(2)	1030(2)	1003(9)	621(1)	0.22	0.22	0.11
Cinnamyl acrylate		1031(2)	1002(9)	620(1)		0.22	0.11
Cinnamic acid	1600(8)	1027(2)	1001(7)	620(0)	1.14	0.29	0.07
Benzil	1595(4)	1020(2)	1000(9)	616(1)	0.44	0.22	0.11
Benzoin ethyl ether	1599(7)	1033(3)	1005(9)	617(2)	0.77	0.33	0.22
Diphenyl divinyl silane	1590(2)	1030(2)	999(9)	620(0)	0.22	0.22	0.06
1,6-Diphenyl-1,3,5-hexatriene	1592(9)		1000(1)		0.11		
Glycidyl cinnamate	1601(6)	1030(1)	1001(5)		1.2	0.2	
2-Hydroxy-4-acryoxyethoxy benzophenone	1602(5)	1027(3)	1001(9)	618(1)	0.56	0.33	0.11
Hydroxy-4-dodecyloxy benzophenone	1601(9)	1030(2)	1001(8)	618(2)	1.13	0.25	0.25
2-Hydroxy-4-methoxy-5-sulfonic acid	1598(7)	1029(3)	1003(9)	617(1)	0.77	0.33	0.11
4-Methacryloxy-2-hydroxy benzophenone	1600(7)	1030(3)	1002(9)	621(1)	0.77	0.33	0.11
α -Methylstyrene	1602(4)	1029(2)	1001(9)		0.44	0.22	
Phenyl acrylate	1594(2)	1025(3)	1007(9)	615(1)	0.22	0.33	0.11
2-Phenylethyl acrylate	1606(2)	1032(3)	1004(9)	622(1)	0.22	0.33	0.11
2-Phenylethyl methacrylate	1606(2)	1032(3)	1004(9)	622(1)	0.22	0.33	0.11
Phenyl glycidyl ether	1601(1)	1026(2)	997(9)	615(1)	0.11	0.22	0.11
N-Phenyl methacrylamide	1598(4)	1031(1)	1002(9)	616(1)	0.44	0.11	0.11
Phenyl methacrylate	1594(2)	1026(3)	1002(9)	615(2)	0.22	0.33	0.22
Phenyl vinyl sulfone	1585(4)	1025(1)	1002(9)	616(1)	0.44	0.11	0.11
Vinyl benzoate	1603(3)	1028(1)	1004(9)	618(1)	0.33	0.11	0.11
Diphenyl terephthalate	1610(3)	1026(1)	1001(9)	614(0)	0.33	0.11	0.06
Diphenyl isophthalate	1607(1)	1022(0)	1004(9)	615(1)	0.11	0.06	0.11

TABLE 9.14 Infrared and Raman data for an A_1 fundamental for mono-X-benzenes

Compound	Raman(liquid) A_1 Fundamental cm^{-1} strong	IR(liquid) A_1 Fundamental cm^{-1} weak	# Protons on α carbon	Taft σ^*	Es
Toluene	790	781	3	0	0
Ethylbenzene	760	770	2	-0.1	-0.07
Isopropylbenzene	740	741	1	-0.19	-0.47
s-Butylbenzene		731	1	-0.21	
t-Butylbenzene	705	masked	0	-0.3	-1.54
α -Syndiotactic polystyrene	773.4[solid]				
Isotactic polystyrene	785[solid]				

TABLE 9.15 Vibrational assignments for the bromodichlorobenzene

	1-Br,3,5-Cl ₂ benzene C_{2v} symmetry	1-Br,2,6-Cl ₂ benzene C_{2v} symmetry	1-Br,2,3-Cl ₂ benzene C_{2v} symmetry	1-Br,2,4-Cl ₂ benzene C_{2v} symmetry	1-Br,2,5-Cl ₂ benzene C_{2v} symmetry	1-Br,3,4-Cl ₂ benzene C_{2v} symmetry
In-plane vibrations	3090	3060	3059	3087	3088	3089
	3090	3060	3059	3075	3070	3065
	3090	3060	3059	3075	3070	3065
	1570	1578	1580	1562	1569	1561
	1559	1561	1558	1553	1555	1554
	1417	1431	1431	1450	1454	1452
	1417	1403	1411	1368	1369	1369
	1365	1261	1252	1258	1259	1260
	1230	1189	1190	1240	1241	1244
	1142	1150	1155	1141	1115	1137
	1097	1144	1144	1135	1124	1119
	1097	1080	1078	1088	1097	1075
	999	1032	1040	1019	1927	1031
	801	791	749	811	792	791
	766	710	728	678	661	684
	470	460	500	518	570	547
	435	470	461	449	429	449
419	401	382	402	349	381	
311	305	287	270	329	266	
187	199	209	202	200	207	
160	171	170	171	161	170	
Out-of-plane vibrations	867.5	965	963	942	943	941
	867.5	884	891.5	865	870	869
	850	774	770	805	811	809
	660	691	693	667	681	675
	527.5	522	512	544	540	541
	527.5	480	492	430	431	432
	218	249	250	300	313	304
	218	213	215	189	171	182
	140	91	91	108	118	110

TABLE 9.16 Raman data and assignments for some in-plane ring modes of 1,2-disubstituted benzenes

Compound	3 cm ⁻¹ (R.I.)	14 cm ⁻¹ (R.I.)	18 cm ⁻¹ (R.I.)	9 cm ⁻¹ (R.I.)
Bis(1-acryloxy-2-hydroxypropyl) phthalate	1600(6)	1581(2)	1042(9)	653(3)
Mono(2-methacryloxy-ethyl) phthalate	1602(6)	1582(4)	1042(9)	646(1)
Isooctadecyl 2-sulfobenzoate NA salt	1595(4)	1577(1)	1044(7)	642(2)
Poly(vinyl hydrogen phthalate)	1601(8)	1582(3)	1042(9)	645(3)
Diallyl phthalate	1602(6)		1041(9)	
Poly (diallyl phthalate)	1601(8)	1580(3)	1041(9)	657(2)
2-Ethylhexyl salicylate	1615(3)	1586(2)	1034(9)	668(4)
N-vinylphthalimide	1610(2)		1020(2)	666(0)
Poly(hexamethylene terephthalamide)	1614(9)	1566(1)		634(1)

TABLE 9.17 Raman data and assignments for some in-plane ring modes for 1,3-disubstituted benzenes

Compound	4 cm ⁻¹ (R.I.)	13 cm ⁻¹ (R.I.)	8 cm ⁻¹ (R.I.)	9 cm ⁻¹ (R.I.)
1,3-Dichlorobenzene	1574	1586	995	662
N,N'-(m-phenylene) Bis-maleimide	1608(2)	1588(3)	1005(5)	683(9)
Bis-maleimide Diallyl phthalate	1609(4)		1004(9)	658(2)
Poly(diallyl isophthalate)	1608(4)	1590(2)	1004(9)	657(2)
1,3-Diisopropenyl benzene	1599(4)	1577(2)	1000(9)	692(4)
3-Fluorostyrene	1603(4)		1002(9)	
3-Chlorostyrene	1596(3)		999(9)	
3-Nitrostyrene	1618(1)		1001(7)	

TABLE 9.18 Raman data and assignments for some in-plane ring modes for 1,4-disubstituted benzenes

Compound	2 cm ⁻¹ (R.I.)	9 cm ⁻¹ (R.I.)	5? cm ⁻¹ (R.I.)	cm ⁻¹ (R.I.)	10 cm ⁻¹ (R.I.)
Diethyl terephthalate	1615(9)	1276(3)	853(3)	836(2)	634(2)
Bis(2-hydroxyethyl) terephthalate	1615(9)	1284(4)	850(3)		634(2)
4-Ethylstyrene	1612(5)	1308(1)	819(1)	805(2)	641(1)
4-Fluorostyrene	1603(4)	1295(1)	842(4)		637(1)
4-Nitrophenyl acrylate	1591(4)		866(3)	848(1)	625(1)
4-Nitrophenyl methacrylate	1591(4)		866(3)	866(3)	632(1)
4-Nitrostyrene	1599(5)		859(2)	859(2)	
4-Nonylphenyl methacrylate	1606(4)	1296(1)	881(2)	812(4)	639(2)
4-Phenoxystyrene	1609(4)	1296(0)		801(2)	
1,4-Phenylene diacrylate	1597(3)	1285(3)	859(5)	803(0)	636(3)
α,α -Dihydroxy	1615(2)				639(2)
Poly(4-methylstyrene)	1614(9)		830(9)	809(9)	644(8)
Poly(4-vinylphenol)	1612(6)		843(9)	826(7)	644(5)
Poly(4-tert-butylstyrene)	1612(9)		845(1)		643(4)
Poly(ethylene terephthalate)	1615(9)	1288(2)	857(2)		633(3)
Poly(1,4-butylene terephthalate)	1614(9)	1277(9)	857(3)		633(3)
1,4-Bis(hydroxymethyl) benzene	1616(2)		839(9)		639(4)
1,4-Dimethoxybenzene	1615(1)	1268(3)		821(9)	638(3)
4-Vinylbenzoic acid	1609(8)	1288(2)		826(3)	638(1)
4-Na vinylbenzenesulfonate	1600(8)	1300(1)		808(1)	637(1)
Bisphenol A/epichlorohydrin liquid epoxy	1610(8)	1298(3)		823(9)	639(8)
4-Vinylphenyl acetonitrile	1607(4)	1302(1)		825(1)	

TABLE 9.19 Raman data and tentative assignments for decabromobiphenyl and bis-(pentabromophenyl) ether

Decabromobiphenyl cm ⁻¹ (R.I.)	Assignment Ring modes	Bis(pentabromophenyl) ether cm ⁻¹ (R.I.)	Assignment Ring modes
1559(1)	3	1524(1)	3
1521(1)	9	1514(1)	9
1256(2)	1		
392(3)	16,20?	431(0)	16,20?
359(9)	2	322(1)	8
345(4)	16,20?	237(7)	5,11
327(4)	8	226(9)	6,12,&14?
250(4)	5,11	208(3)	17,21
217(4)	6,12,&14?		

TABLE 9.20 Vibrational assignments for benzene, benzene d₆, benzyl alcohol and benzyl-2,3,4,5,6-d₅ alcohol

Compound	v12(e1u) in FR. cm ⁻¹ (A)	v12 + v16(E1u) in FR. cm ⁻¹ (A)	v2 + v4(A2u) cm ⁻¹ (A)	v18 + v19(A2u) cm ⁻¹ (A)	v4 + v11(E1u) cm ⁻¹ (A)	v12(e1u) cm ⁻¹ (A)	v14(e1u) cm ⁻¹ (A)	v4(a2u) cm ⁻¹ (A)	
Benzene	3099 (0.510)	3050 (0.600)	1964 (0.065) 1960 (0.067) 1948 (0.070)	1829 (0.080) 1810 (0.080) 1801 (0.100) 1628 (0.025)	1520 (0.040)	1498 (0.190) 1485 (0.240) 1472 (0.185) 1345 (0.019) 1330 (0.040)	1385 (0.029) 1038 (0.180) 1022 (0.100) 825(0.070)	686 (0.950) 670 (1.250) 651 (0.860) 505 (0.360) 491 (1.250)	
Benzene-d ₆	2380 (0.039)	2282 (0.600)	1675 (0.020)	1619 (0.023) 1610 (0.026)	1154 (0.015) 1146 (0.020)	1154 (0.040) 1315 (0.025)	811 (0.120) 800 (0.080)	470 (1.250) 439 (0.439)	
Benzene/Benzene-d ₆	1.302	1.337	1.169	1.118	1.317	1.117	1.279	1.365	
Benzyl alcohol	vC-H 3082 (0.351)	vC-H 3048 (0.380)	4,14 1605 (0.020)	5 1499 (0.089)	7 [1080 CP]	8 [1035 CP]	905 (0.055)	738 (0.600)	697 (0.630)
Benzyl-2,3,4,5,6-d ₅ alcohol	vC-D 2395 (0.010)	vC-D 2282 (0.320)	4,14 1228 (0.120)	5 1145 (0.200)	7 782 (0.0156)	8 735 (0.030)	634 (0.030)	534 (0.529)	
Benzyl alcohol/Benzyl-2,3,4,5,6-d ₅ alcohol	1,287	1,336	1,309	1,309	1,381	1,408	1,427	1,382	
Benzyl alcohol	OH str. 3658 (0.161)	a.CH ₂ str. 2935 (0.240)	s.CH ₂ str. 2895 (0.318)	CH ₂ bend 1462 (0.139) 1460 (0.110) 1451 (0.141)	COH bend 1385 (0.375)	CH ₂ wag 1204 (0.195)	CH ₂ twist masked	C-O str. 1020 (1.220)	CH ₂ rock 800 (0.030)
Benzyl-2,3,4,5,6-d ₅ alcohol	3645 (0.165)	2921 (0.219)	2842 (0.300)	1467 (0.025)	1378 (0.310)	1184 (0.129)	masked	1018 (1.250)	824 (0.080) 820 (0.058) 812 (0.062)
Benzyl alcohol	2(I) 1958 (0.039)	1 + II 1945 (0.020)	1 + III 1882 (0.020)	II + III 1808 (0.025)	III + IV 1750 (0.010)				
Benzyl-2,3,4,5,6-d ₅ alcohol	1740 (0.020)	1605 (0.0250)	1565 (0.011)	1555 (0.011)	1505 (0.011)				
Benzyl alcohol/Benzyl-2,3,4,5,6-d ₅ alcohol	1.125	1.212	1.203	1.162	1.162				

TABLE 9.21 Infrared data for the out-of-plane deformations for mono-x-benzenes

Group	I cm ⁻¹	II cm ⁻¹	III cm ⁻¹	IV cm ⁻¹	V cm ⁻¹	VI cm ⁻¹	σ_p
N(CH ₃) ₂	966	945	862	823	749	689	[—]
NHCH ₃	966	947	867	812	749	691	[—]
NH ₂	968	957	874	823	747	689	-0.66
OH	971	952	882	825	750	688	-0.37
OCH ₃	970	953	881	814	753	691	-0.27
C(CH ₃) ₃	979	964	905	841	763	698	-0.2
CH ₃	973	963	895	789	730	697	-0.17
C ₂ H ₅	978	963	903	841	748	699	-0.15
C ₃ H ₇ -iso	979	961	905	840	762	701	-0.15
F	972	952	890	827	750	682	0.06
I	986	959	901	825	730	685	0.18
Cl	976	957	897	825	734	679	0.23
Br	980	960	902	830	738	685	0.23
CHO	989	970	919	809	753	689	0.42
CO ₂ H	995	973	940	852	810	707	0.45
S(=O)CH ₃	988	969	913	843	744	690	0.49
CF ₃	984	965	920	830;847	769	693	0.54
CN	987	967	920	843	756	685	0.66
SO ₂ CH ₃	994	972	928	849	741	690	0.72
NO ₂	990	969	932	840	793	705	0.78

TABLE 9.22 Summary of the out-of-plane hydrogen deformations for substituted benzenes, and the out-of-plane ring deformation for mono-substituted benzenes

Benzenes	I cm ⁻¹	II cm ⁻¹	III cm ⁻¹	IV cm ⁻¹	V cm ⁻¹	VI cm ⁻¹
Mono-substituted	965.5–996	945–981	862–940	789–852	725–810	679–720
1,2-Disubstituted	956–989	915–970	833–886	715–791	683–729	
1,3-Disubstituted	947–999	863–949	831–910	761–815	639–698	
1,4-Disubstituted	933–985	916–971	790–852	794–870	641–735	
1,3,5-Trisubstituted	819–927	786–910	642–739			
1,2,3-Trisubstituted	930–989	848–930	731–810	684–744		
1,2,4-Trisubstituted	926–982	841–923	790–852	652–750		
1,2,4,5-Tetrasubstituted	861–911	828–890				
1,2,3,5-Tetrasubstituted	821–942	838–920				
1,2,3,4-Tetrasubstituted	919–949	770–821				
Pentasubstituted	822–927					

TABLE 9.23 Combination and overtones of the out-of-plane hydrogen deformations for substituted benzenes

Benzenes	2xI cm ⁻¹	I + II cm ⁻¹	I + III cm ⁻¹	II + III cm ⁻¹	II + IV cm ⁻¹	III + IV cm ⁻¹	III + V cm ⁻¹
Mono-substituted	1931–1992	1915–1976	1815–1936	1815–1914	1737–1829	1680–1787 2xII cm ⁻¹	1611–1748 2xIII cm ⁻¹
1,2-Disubstituted	1912–1997	1869–1952	1789–1875 I + IV cm ⁻¹	1748–1849	1655–1758	1828–1932	1666–1772
1,3-Disubstituted	1910–1991	1820–1940	1709–1820	1709–1852	1637–1760	1724–1890	1680–1820
1,4-Disubstituted		1852–1957	1729–1835		1727–1850	1619–1702	
1,3,5-Trisubstituted	1635–1849	1605–1840					
1,2,3-Trisubstituted	1860–1975	1792–1914				1700–1860	
1,2,4-Trisubstituted	1844–1961	1776–1890	1712–1829			1683–1845	1580–1704
1,2,4,5-Tetrasubstituted	1725–1830	1695–1799				1651–1770	
1,2,3,5-Tetrasubstituted	1635–1876	1659–1862				1675–1841	
1,2,3,4-Tetrasubstituted	1838–1902	1715–1770				1610–1650	
Pentasubstituted	1655–1848						

TABLE 9.24 Hexachlorobenzene vs Penta-chlorobiphenyl

Species	Hexachloro- benzene cm ⁻¹	2,3,4,5,6-Cl ₅ biphenyl cm ⁻¹
A1g	1210(R) 372(R)	1205 [—]
B1u	1108 369	[—] [—]
A2g	630(est)	632
B2u	1224Comb. 230(est)	1230 [—]
E2g	1512 870(R) 323(R) 219(R)	1516&1497 868 [—] [—]
E1u	1350 699 218	685 [—] [—]
A2u	209	[—]
B2g	704Comb. 340(R)	750? [—]
E2u	594 80Comb.	586 [—]

The Nyquist Vibrational Group Frequency Rule

Aliphatic Hydrocarbons — The Nyquist Vibrational Group Frequency Rule	426
Anilines — The Nyquist Vibrational Group Frequency Rule	427
Anhydrides, Imides and 1,4-Benzoquinones — The Nyquist Vibrational Group Frequency Rule	428
Substituted Hydantoins — The Nyquist Vibrational Group Frequency Rule	428
1,4-Diphenylbutadiyne and 1-Halopropadiene — The Nyquist Vibrational Group Frequency Rule	429
3-Nitrobenzenes and 4-Nitrobenzenes — The Nyquist Vibrational Group Frequency Rule	430
Organic Sulfates, Sulfonate, Sulfonyl Chloride and Sulfones — The Nyquist Vibrational Group Frequency Rule	430
References	431

Tables

Table 10-1	423 (426)
Table 10-2	433 (427)
Table 10-3	434 (428)
Table 10-4	435 (428)
Table 10-5	435 (429)
Table 10-6	436 (430)
Table 10-7	437 (430)

*Numbers in parentheses indicate in-text page reference.

The *Nyquist Vibrational Group Frequency Rule* is distinctly different from the *Nyquist Frequency*. The sampling rate, called the *Nyquist Frequency*, is defined here. A signal is made up of various frequency components. If the signal is sampled at regular intervals, then there will be no information lost if the rate at which it is sampled is twice the frequency of the highest frequency component of the signal. The author of this text has been asked many times if he developed the *Nyquist Frequency*. The answer is NO! This answer always causes a look of disappointment. When this question arises, I respond with this reply, “No, but I developed the *Nyquist Vibrational Group Frequency Rule*.”

The *Nyquist Vibrational Group Frequency Rule* is defined here. With change in the physical phase or environment of a chemical compound, the group frequency shift for the antisymmetric stretching vibration is larger than it is for the symmetric vibration (or out-of-phase vs in-phase stretching vibrations) for a chemical group within the molecular structure of a chemical

compound. This relative change between the group frequency shifts is caused by the difference in energy required in order for the particular chemical group to vibrate in the antisymmetric and symmetric (or out-of-phase and in-phase) modes in two physical phases. The Nyquist Vibrational Group Frequency Rule was developed from studies of alkanes, anhydrides, anilines, imides, nitro-containing compounds, and SO₂-containing compounds in different solutions (CCl₄ and CHCl₃), in the vapor phase vs solution or neat phase. This energy differential is believed to result from the difference in the dipolar interaction of the chemical group within the solute and the surrounding change in its reaction field. This change can also result from intermolecular hydrogen bonding between solvent molecules and the chemical group within the solute, or from intermolecular hydrogen bonding between molecules in the vapor phase compared to the molecules in the vapor phase that are not intermolecularly hydrogen-bonded (1).

ALIPHATIC HYDROCARBONS — THE NYQUIST VIBRATIONAL GROUP FREQUENCY RULE

Table 10.1 lists IR data for the ν asym. CH₃, ν sym. CH₃, ν asym. CH₂ and ν sym. CH₂ vibrations for *n*-alkanes in CCl₄ and CDCl₃ solutions, and the frequency difference between each of these vibrations in CCl₄ and CDCl₃ solutions (2). In all cases, the ν asym. CH₃ and ν asym. CH₂ vibrations occur at higher frequency in CDCl₃ solution than in CCl₄ solution. In all cases, the ν sym. CH₃ and ν sym. CH₂ vibrations occur at lower frequency in CDCl₃ solution than in CCl₄ solution.

The Cl atoms in CCl₄ are more basic in the case of CCl₄ than they are in CDCl₃ or CHCl₃. If there is intermolecular hydrogen bonding between aliphatic hydrocarbon protons and the Cl atoms in CCl₄ and CDCl₃, one would expect the strongest intermolecular association to be formed between the protons of the aliphatic hydrocarbon and the Cl atoms of CCl₄.

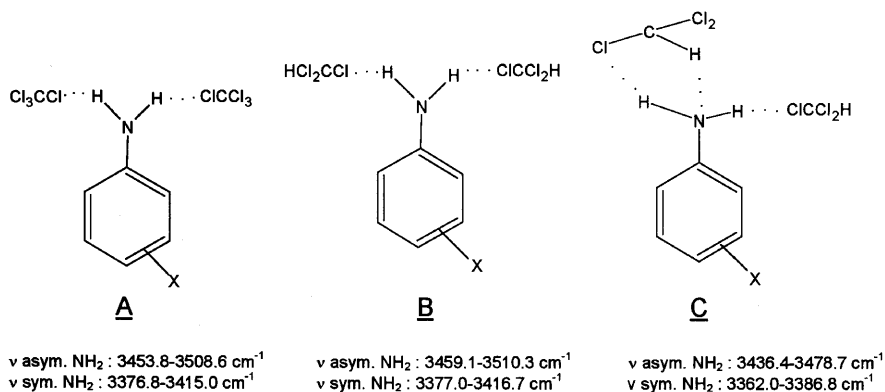
This appears to be the case, because both ν asym. CH₃ and ν asym. CH₂ occur at lower frequency by 0.08 to 0.22 cm⁻¹ in CCl₄ solution than in CDCl₃ solution. If so, another factor must be considered in the case of ν sym. CH₃ and ν sym. CH₂, because these vibrations occur at higher frequency in CDCl₃ solution than in CCl₄ solution. During the ν asym. CH₃ and ν asym. CH₂ vibration there is a trade-off in energy arising from simultaneous expansion and contraction of the CH₃···Cl-C and CH₂···Cl-C bonds while it requires more energy to expand and contract these same CH₃···Cl-C and CH₂···Cl-C bonds in phase. These factors more than offset the expected decrease in ν sym. CH₃ and ν sym. CH₂ frequencies due to the strength of the intermolecular hydrogen bond formed between the solute and solvent. Thus, the ν CH₃ and ν CH₂ vibrations conform to the Nyquist Vibrational Group Frequency Rule.

Progressing in the series pentane through octadecane, the ν asym. CH₃ vibration decreases in frequency by a factor of 2 to 3 times that exhibited by ν sym. CH₃. In the case of the CH₂ vibrations, ν asym. CH₂ decreases in frequency by a factor of ~1/6 of that exhibited by ν sym. CH₂. Progressing in the series pentane through octadecane, the frequency separation between ν asym. CH₃ and ν asym. CH₂ decreases progressively from 31.82 cm⁻¹ to 30.65 cm⁻¹ in CCl₄ solution and from 31.52 cm⁻¹ to 30.56 cm⁻¹ in CDCl₃ solution. Progressing in the series pentane through octadecane, the frequency separation between ν sym. CH₃ and ν sym. CH₂

increases progressively from 11.30 cm^{-1} to 17.76 cm^{-1} in CDCl_3 solution. These data indicate that as n increases in the series $\text{CH}_3(\text{CH}_2)_n\text{CH}_3$ there is less coupling between ν asym. CH_3 and ν asym. CH_2 and there is more coupling between ν sym. CH_3 and ν sym. CH_2 .

ANILINES — THE NYQUIST VIBRATIONAL GROUP FREQUENCY RULE

Table 10.2 list IR data for the ν asym. NH_2 and ν sym. NH_2 frequencies for 4-X and 3-X anilines in both CCl_4 and CHCl_3 solutions and the frequency separation between ν asym. NH_2 in CCl_4 and CHCl_3 solutions and the frequency separation between ν sym. NH_2 in CCl_4 and CHCl_3 solutions (3). The ν asym. NH_2 and ν sym. NH_2 frequencies for these anilines in CCl_4 solution are suggested to result from complexes such as A:



Two sets of ν asym. NH_2 and ν sym. NH_2 are noted for these anilines in CHCl_3 solution. The higher frequency set is suggested to result from a complex such as B, and the lower frequency set is suggested to result from a complex such as C (3).

The intermolecular hydrogen-bonded complexes formed for A are stronger than those complexes for B, because ν asym. NH_2 in CCl_4 solution occurs at lower frequency by 1.16 to 9.19 cm^{-1} than those for the corresponding aniline in CHCl_3 solution.

However, in the case of complex C, ν asym. NH_2 occurs at lower frequency than in complex A by 17.4 to 29.7 cm^{-1} . The CCl_3H proton intermolecularly hydrogen bonded to the free pair of electrons on the nitrogen atom in complex B weakens the NH_2 bonds, causing their ν asym. NH_2 vibration to occur at even lower frequency than in the case of complex B. The ν sym. NH_2 vibrations shift to lower frequency by a factor of 2 to 8.5 times more than the ν asym. NH_2 vibrations for the correspond 3-X and 4-X-aniline. This frequency difference between the ν asym. NH_2 and ν sym. NH_2 vibrational in complexes B and C is attributed to the Nyquist Vibrational Group Frequency Rule. During the ν sym. NH_2 vibration in complexes B and C, the NH_2 vibrations expand and contract in phase from the chlorine atoms of the CCl_3H molecules. The amount of energy required during the compression of the $\text{NH}_2(\cdots\text{ClCCl}_2\text{H})_2$ intermolecular hydrogen bonds is larger in the case of ν sym. NH_2 than the amount of energy required for ν asym. NH_2 where the compression of one $\text{NH}\cdots\text{ClCCl}_2\text{H}$ intermolecular hydrogen bond is

offset by the expansion of the other intermolecular $\text{NH}\cdots\text{ClCCl}_2\text{H}$ hydrogen bond in complexes such as B and C.

ANHYDRIDES, IMIDES AND 1,4-BENZOQUINONES — THE NYQUIST VIBRATIONAL GROUP FREQUENCY RULE

Table 10.3 lists IR data for anhydrides, imides, and 1,4-benzoquinones (4–8). The out-of-phase and in-phase $(\text{C}=\text{O})_2$ stretching frequencies for these compounds in CCl_4 and CHCl_3 solution are listed as well as the frequency difference between $\nu_{\text{op}}(\text{C}=\text{O})_2$ in CCl_4 solution and $\nu_{\text{op}}(\text{C}=\text{O})_2$ in CHCl_3 solution, and the frequency difference between $\nu_{\text{ip}}(\text{C}=\text{O})_2$ in CCl_4 solution and $\nu_{\text{ip}}(\text{C}=\text{O})_2$ in CHCl_3 solution.

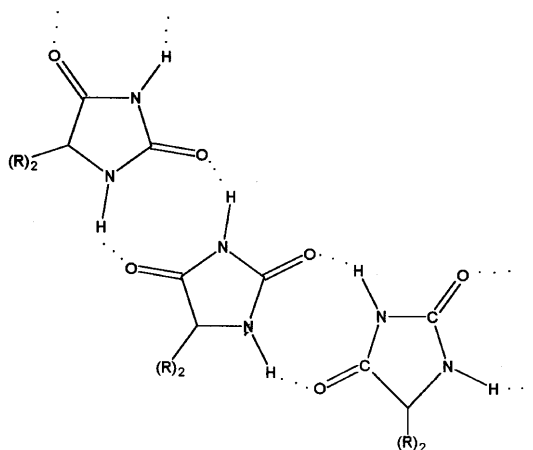
In all cases of anhydrides and imides $\nu_{\text{op}}(\text{C}=\text{O})_2$ and $\nu_{\text{ip}}(\text{C}=\text{O})_2$ occur at lower frequency in CHCl_3 solution than in CCl_4 solution. These lower $\nu(\text{C}=\text{O})_2$ frequencies in CCl_3H solution are attributed to complexes such as $(\text{C}=\text{O}\cdots\text{HCCl}_3)_2$. In the 1,4-benzoquinone series the $\nu_{\text{op}}(\text{C}=\text{O})_2$ mode occurs at lower frequency in CCl_3H solution than in CCl_4 solution while $\nu_{\text{ip}}(\text{C}=\text{O})_2$ (with one exception) increases in frequency in CHCl_3 solution compared to the corresponding compounds in CCl_4 solution.

The carbonyl-containing compounds differ from those for the aliphatic hydrocarbons and aniline in that the former compounds involve stretching of the $(\text{C}=\text{O})_2$ bond while the latter compounds involve stretching of CH_3 , CH_2 and NH_2 bonds. Intermolecular hydrogen bonding of two CCl_3H protons with two oxygen atoms $(\text{C}=\text{O}\cdots\text{HCCl}_3)_2$ lowers $\nu_{\text{op}}(\text{C}=\text{O})_2$ from 1.7 to 5.2 cm^{-1} for the anhydrides, by 5.7 to 10.6 cm^{-1} for the imide type compounds, and by 0.9 to 2.9 cm^{-1} for the 1,4-benzoquinones. Intermolecular hydrogen bonding in the case of $\nu_{\text{ip}}(\text{C}=\text{O})_2$ does not lower this vibrational mode as much in frequency as the $\nu_{\text{op}}(\text{C}=\text{O})_2$ vibration, because it requires more energy to compress two $\text{C}=\text{O}\cdots\text{HCCl}_3$ intermolecular hydrogen bonds in the case of $\nu_{\text{ip}}(\text{C}=\text{O})_2$ than it requires to expand one $\text{C}=\text{O}\cdots\text{HCCl}_3$ bond while the other $\text{C}=\text{O}\cdots\text{HCCl}_3$ contracts during the $\nu_{\text{op}}(\text{C}=\text{O})_2$ vibration. Thus, the $\nu(\text{C}=\text{O})_2$ frequency behavior for these compounds conforms to the Nyquist Vibrational Group Frequency Rule.

SUBSTITUTED HYDANTOINS — THE NYQUIST VIBRATIONAL GROUP FREQUENCY RULE

Table 10.4 lists IR data for the $\nu_{\text{op}}(\text{C}=\text{O})_2$ and $\nu_{\text{ip}}(\text{C}=\text{O})_2$ vibrations for substituted hydantoins in the vapor- and solid phases (7). The in-phase mode occurs in the region 1809–1825 cm^{-1} in the vapor phase and in the region 1761–1783 cm^{-1} in the solid phase. These $\nu_{\text{ip}}(\text{C}=\text{O})_2$ vibrations occur at lower frequency by 29–48 cm^{-1} in the solid phase than they occur in the vapor phase. The out-of-phase $(\text{C}=\text{O})_2$ mode occurs in the region 1774–1785 cm^{-1} in the vapor phase, and in the region 1707–1718 cm^{-1} in the solid phase. These $\nu_{\text{op}}(\text{C}=\text{O})_2$ vibrations occur at lower frequency by 56–68 cm^{-1} in the solid phase than in the vapor phase.

The hydantoin listed in Table 10.4 exists as intermolecular hydrogen bonded dimers in the solid phase as depicted here:

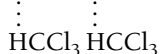


However, in the vapor phase these 5,5-dialkyl hydantoin are not intermolecularly hydrogen bonded. The $\nu_{\text{ip}}(\text{C}=\text{O})_2$ modes shift to lower frequency in the solid phase because of the intermolecular hydrogen-bond formation between the $\text{N}-\text{H}\cdots\text{O}=\text{C}$ groups, but the $\nu_{\text{ip}}(\text{C}=\text{O})_2$ mode does not shift as much to lower frequency due to the fact that it requires more energy to compress two intermolecular $\text{N}-\text{H}\cdots\text{O}=\text{C}$ bonds than is required to compress one intermolecular $\text{N}-\text{H}\cdots\text{O}=\text{C}$ bond and expand one $\text{N}-\text{H}\cdots\text{O}=\text{C}$ intermolecular bond in the case of $\nu_{\text{op}}(\text{C}=\text{O})_2$. Thus, these group frequencies fulfill the requirement of the Nyquist Vibrational Group Frequency Rule.

1,4-DIPHENYLBUTADIYNE AND 1-HALOPROPADIENE — THE NYQUIST VIBRATIONAL GROUP FREQUENCY RULE

Table 10.5 lists the $\nu_{\text{op}}(\text{CC})_2$, $\nu_{\text{ip}}(\text{CC})_2$, $\nu_{\text{op}}\text{C}=\text{C}=\text{C}$, and $\nu_{\text{ip}}\text{C}=\text{C}=\text{C}$ vibrations for 1,4-diphenylbutadiyne and the 1-halopropadiene in CCl_4 solution and in CHCl_3 solution, and their frequency differences between each of these vibrations in CCl_4 and CHCl_3 solutions (9 11).

In the case of 1,4-diphenylbutadiyne, both $\nu_{\text{op}}(\text{CC})_2$ and $\nu_{\text{ip}}(\text{CC})_2$ occur at lower frequency in CCl_3H solution than in CCl_4 solution. These frequency decreases are attributed to intermolecular hydrogen bonding between the π systems of the $(\text{C}\equiv\text{C})_2$ groups and CCl_3 H protons (eg. $-\text{C}\equiv\text{C}-\text{C}\equiv\text{C}-$). Most likely the CCl_3 protons also intermolecularly hydrogen



bond to the π system of the two phenyl groups. The $\text{C}\equiv\text{C}-\text{C}\equiv\text{C}$ group is a linear rod and the CCl_3H molecules would be surrounding and intermolecularly hydrogen bonding with the two $\text{C}\equiv\text{C}$ groups. The $\nu_{\text{ip}}(\text{CC})_2$ vibration takes relatively more energy to vibrate due to the compression and expansion of the intermolecularly hydrogen-bonded CCl_3H molecules than the energy required during $\nu_{\text{op}}(\text{CC})_2$ where one intermolecularly hydrogen-bonded $\text{C}\equiv\text{C}$ is



compressed while the other $\text{C}\equiv\text{C}$ group is expanded. In the $\nu_{\text{op}}(\text{CC})_2$ case there is less

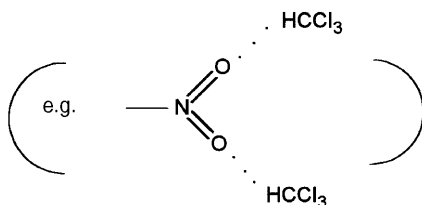


interaction between the CCl_3H molecules than in the case of $\nu_{\text{ip}}(\text{CC})$ interactions with CCl_3H molecules. Thus, $\nu_{\text{op}}(\text{CC})_2$ decreases twice as much as $\nu_{\text{ip}}(\text{CC})_2$ in going from solution in CCl_4 to solution in CHCl_3 .

The ν asym. $\text{C}=\text{C}=\text{C}$ vibration decreases in frequency in going from the vapor phase to the liquid phase while under the same physical conditions ν sym. $\text{C}=\text{C}=\text{C}$ does not decrease as much in frequency as the ν asym. $\text{C}=\text{C}=\text{C}$ vibration or else actually increases in frequency (9–11). These data fulfill the Nyquist Vibrational Group Frequency Rule.

3-NITROBENZENES AND 4-NITROBENZENES — THE NYQUIST VIBRATIONAL GROUP FREQUENCY RULE

Table 10.6 lists IR data for ν asym. NO_2 and ν sym. NO_2 in both CCl_4 and CCl_3H solutions and their frequency difference in CCl_4 and CCl_3H solutions (5,12). The ν asym. NO_2 mode decreases in frequency by 1.7 to 8.6 cm^{-1} in going from CCl_4 to CCl_3H solution while the ν sym. NO_2 mode for the same compound decreases less in frequency or in many cases actually increases in frequency. In CCl_3H solution the NO_2 group is intermolecularly hydrogen-bonded to the oxygen atoms of the NO_2 group.

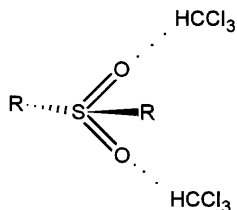


It takes more energy to compress and expand the intermolecular hydrogen-bonded NO_2 groups during the ν sym. NO_2 vibration than it does to expand one $\text{N}=\text{O}\cdots\text{HCCl}_3$ intermolecular hydrogen bond and compress one $\text{N}=\text{O}\cdots\text{HCl}_3$ during $\nu_{\text{op}} \text{NO}_2$. Thus, the νNO_2 most conform to the Nyquist Vibrational Group Frequency Rule.

ORGANIC SULFATES, SULFONATE, SULFONYL CHLORIDE AND SULFONES — THE NYQUIST VIBRATIONAL GROUP FREQUENCY RULE

Table 10.7 lists ν asym. SO_2 and ν sym. SO_2 frequencies in both CCl_4 and CCl_3H solutions and their frequency differences in each solvent. In all cases the νSO_2 vibrations decrease in frequency in going from solution in CCl_4 to solution in CCl_3H , and this decrease in frequency is larger for

ν asym. SO_2 than for ν sym. SO_2 by a factor of ~ 2 to 10. In CCl_3H solution, the SO_2 oxygen atoms are intermolecularly hydrogen bonded as presented here:



The energy to expand and contract the $(\text{S}=\text{O}\cdots\text{HCCl}_3)_2$ intermolecular hydrogen bonds during ν sym. SO_2 is greater than that needed to compress one $\text{S}=\text{O}\cdots\text{HCCl}_3$ intermolecular hydrogen bond and expand one $\text{S}=\text{O}\cdots\text{HCCl}_3$ intermolecular hydrogen bond during ν asym. SO_2 .

REFERENCES

1. Nyquist, R. A. (1994). *Structural Information From Infrared Studies on Solute-Solvent Interactions*. Ph. D. Thesis, Utrecht University, The Netherlands, ISBN 90-393-0743-1, p. 260.
2. Nyquist, R. A. and Fiedler, S. L. (1993). *Appl. Spectrosc.* 47: 1670.
3. Nyquist, R. A., Luoma, D. A., and Puehl, C. W. (1992). *Appl. Spectrosc.* 46: 1273.
4. Nyquist, R. A. (1990). *Appl. Spectrosc.* 44: 438.
5. Nyquist, R. A. (1990). *Appl. Spectrosc.* 44: 594.
6. Nyquist, R. A. (1990). *Appl. Spectrosc.* 44: 783.
7. Nyquist, R. A. and Fielder, S. L. (1995). *Vib Spectrosc.* 8: 365.
8. Nyquist, R. A., Luoma, D. A., and Putzig, C. L. (1992). *Vib. Spectrosc.* 3: 181.
9. Nyquist, R. A. and Putzig, C. L. (1992). *Vib. Spectrosc.* 3: 35.
10. Nyquist, R. A., Lo, Y-S., and Evans, J. C. (1964). *Spectrochim. Acta* 20: 619.
11. Nyquist, R. A., Reder, T. L., Stec, F. F., and Kallos, G. J., (1971). *Spectrochem. Acta* 27A: 897.
12. Nyquist, R. A. and Settineri, S. E. (1990). *Appl. Spectrosc.* 44: 1552.

TABLE 10.1 Aliphatic hydrocarbons — the Nyquist Rule

Compound	a.CH ₃ str. CCl ₄ soln. cm ⁻¹	a.CH ₃ str. CDCl ₃ soln. cm ⁻¹	s.CH ₃ str. CCl ₄ soln. cm ⁻¹	s.CH ₃ str. CDCl ₃ soln. cm ⁻¹	a.CH ₃ str. [CCl ₄]-[CDCl ₃] cm ⁻¹	s.CH ₃ str. [CCl ₄]-[CDCl ₃] cm ⁻¹
Pentane	2959.55	2959.66	2873.12	2872.67	-0.11	0.45
Hexane	2958.69	2958.8	2872.92	2872.34	-0.11	0.58
Hexane	2959.23	2959.31	2873.05	2872.54	-0.08	0.51
Heptane	2958.86	2958.98	2872.81	2872.23	-0.12	0.58
Octane	2958.62	2958.73	2872.82	2872.2	-0.11	0.62
Nonane	2958.46	2958.58	2872.79	2872.17	-0.12	0.62
Decane	2958.35	2958.49	2872.78	2872.14	-0.14	0.64
Undecane	2958.14	2859.33	2872.7	2872.05	-0.19	0.65
Dodecane	2958.03	2958.23	2872.66	2871.96	-0.2	0.7
Tridecane	2957.94	2958.1	2872.65	2871.91	-0.16	0.74
Tetradecane	2957.79	2957.99	2872.6	2871.81	-0.2	0.79
Octadecane	2957.26	2957.48	2872.35	2871.5	-0.22	0.85
Δ cm ⁻¹	2.29	2.18	0.77	1.17		
Compound	a.CH ₂ str. CCl ₄ soln. cm ⁻¹	a.CH ₂ str. CDCl ₃ soln. cm ⁻¹	s.CH ₂ str. CCl ₄ soln. cm ⁻¹	s.CH ₂ str. CDCl ₃ soln. cm ⁻¹	a.CH ₂ str. [CCl ₄]-[CDCl ₃] cm ⁻¹	s.CH ₂ str. [CCl ₄]-[CDCl ₃] cm ⁻¹
Pentane	2927.73	2928.14	2861.82	2861.21	-0.41	0.61
Hexane	2928	2928.25	2859.4	2859.14	-0.25	0.26
Hexane	2927.89	2928.12	2859.12	2858.74	-0.23	0.38
Heptane	2927.29	2927.58	2857.81	2857.37	-0.29	0.44
Octane	2926.95	2927.26	2856.55	2856.22	-0.31	0.33
Nonane	2926.79	2927.07	2855.68	2855.58	-0.28	0.1
Decane	2926.83	2927.13	2855.31	2855.25	-0.3	0.06
Undecane	2926.76	2927.03	2855.09	2855.05	-0.27	0.04
Dodecane	2926.72	2927.01	2854.92	2854.88	-0.29	0.04
Tridecane	2926.7	2926.98	2854.83	2854.79	-0.28	0.04
Tetradecane	2926.66	2926.96	2854.77	2854.71	-0.3	0.06
Octadecane	2926.61	2926.92	2854.59	2854.55	-0.31	0.06
Δ cm ⁻¹	1.12	1.22	7.23	6.66		
Compound	a.CH ₃ str.-a.CH ₂ str. CCl ₄ soln. cm ⁻¹	a.CH ₃ str.-a.CH ₂ str. CDCl ₃ soln. cm ⁻¹	s.CH ₃ str.-s.CH ₂ str. CCl ₄ soln. cm ⁻¹	s.CH ₃ str.-s.CH ₂ str. CDCl ₃ soln. cm ⁻¹		
Pentane	31.82	31.52	11.3	11.46		
Hexane	30.69	30.55	13.52	13.2		
Hexane	31.34	31.19	13.93	13.8		
Heptane	31.57	31.4	15	14.86		
Octane	31.67	31.15	16.27	15.98		
Nonane	31.67	31.51	17.11	16.59		
Decane	31.52	31.36	17.47	16.89		
Undecane	31.38	32.3	17.61	17		
Dodecane	31.31	31.22	17.82	17.08		
Tridecane	31.24	31.12	17.82	17.12		
Tetradecane	31.13	31.03	17.83	17.1		
Octadecane	30.65	30.56	17.76	16.95		
Δ cm ⁻¹	0.69	0.96	6.46	5.49		

TABLE 10.2 Anilines — the Nuquist Rule

4-X-Aniline	a.NH ₂ str. CCl ₄ soln. cm ⁻¹	a.NH ₂ str. CHCl ₃ soln. cm ⁻¹	a.NH ₂ str. CHCl ₃ soln. cm ⁻¹	s.NH ₂ str. CCl ₄ soln. cm ⁻¹	s.NH ₂ str. CHCl ₃ soln. cm ⁻¹	s.NH ₂ str. CHCl ₃ soln. cm ⁻¹	a.NH ₂ str. [CCl ₄]-[CHCl ₃] cm ⁻¹	s.NH ₂ str. [CCl ₄]-[CHCl ₃] cm ⁻¹	a.NH ₂ str. [CCl ₄]-[CHCl ₃] cm ⁻¹	s.NH ₂ str. [CCl ₄]-[CHCl ₃] cm ⁻¹
4-X										
OH	[-]	3468.9	3440.31	[-]	3386.8	3367.89	[-]	[-]	[-]	[-]
OCH ₃	3459.71	3468.9	3441.09	3381.41	3388.75	3366.62	-9.19	-7.34	18.62	14.79
N(CH ₃) ₂	3454.12	3459.13	3435.4	3377.35	3377.02	3362.02	-5.01	0.33	18.72	15.33
NH ₂	3453.81	[-]	3436.41	3376.79	3388.75	3362.43	[-]	-11.96	17.4	14.63
OC ₆ H ₅	3468.78	3474.77	3445.62	3387.3	3389.28	3373.49	-5.99	-1.98	23.16	13.81
F	3472.02	3476.72	3449.2	3390.56	3390.71	3374.57	-4.7	-0.15	22.82	15.99
Cl	3484.52	3486.89	3457.74	3398.35	3400.11	3380.93	-2.37	-1.76	26.78	17.42
Br	3486.23	3488.96	3459.32	3399.48	3401.15	3380.93	-2.73	-1.67	26.91	18.55
H	3480.29	3481.75	3453.95	3394.77	3396.43	3378.03	-1.46	-1.66	26.34	16.74
H	3480.53	3481.57	3453.78	3394.88	3396.75	3377.76	-1.04	-1.87	26.75	17.12
C ₂ H ₅	3471.32	3478.68	3446.47	3389.44	3390.77	3377.91	-7.63	-1.33	24.85	11.53
C(CH ₃) ₃	3472.72	3480.63	3447.29	3390.13	3391.79	3373.96	-7.91	-1.66	25.43	16.17
C ₆ H ₅	3483.8	3486.75	3454.79	3396.84	3399.33	3378.79	-2.95	-2.49	29.01	18.05
C(=O)OC ₂ H ₅	3500.08	3504.25	3478.68	3408.59	3411.06	[-]	-4.17	-2.47	21.4	[-]
CN	3504.31	3507.43		3412.05	3413.73	[-]	-3.12	-1.68	[-]	[-]
CF ₃	3498.73	3501.31	3476.72	3408.35	3409.82	3386.8	-2.59	-1.47	22.01	21.55
C(=O)CH ₃	3501.51	3505.77	[-]	3409.6	3412.09	[-]	-4.26	-2.49	[-]	[-]
NO ₂	3508.61	3510.27	[-]	3414.96	3416.69	[-]	-1.66	-1.73	[-]	[-]
3-X										
OCH ₃	3483.54	3485.08	3457.05	3397.02	3399.07	3380.93	-1.54	-2.05	26.49	16.09
F	3491.35	3492.65	3464.99	3402.99	3404.16	3380.93	-1.3	-1.17	26.36	22.06
Cl	3490.49	3492.02	3464.99	3401.94	3403.23	3380.93	-1.53	-1.29	25.5	21.01
Br	3490.31	3491.94	3463.79	3401.31	3403.05	3378.98	-1.63	-1.74	26.52	22.33
CH ₃	3479.05	3482.59	3453.48	3393.8	3395.42	3377.62	-3.54	-1.62	25.57	16.18
C(=O)OC ₂ H ₅	3486.72	3488.89	3459.56	3399.26	3401.39	3380.93	-2.17	-2.13	27.16	18.33
CN	3494.7	3496.96	3474.77	3405.49	3406.75	3382.89	-2.26	-1.26	19.93	22.6
CF ₃	3492.74	3493.9	3463.04	3403.81	3404.53	3378.98	-1.16	-0.73	29.7	24.83

TABLE 10.3 Andryrides imides, and 1,4-benzoquinones—the Nyquist Rule

Anhydride	op.(C=O) ₂ str. CCl ₄ soln. cm ⁻¹	op(C=O) ₂ str. CHCl ₃ soln. cm ⁻¹	ip(C=O) ₂ str. CCl ₄ soln. cm ⁻¹	ip(C=O) ₂ str. CHCl ₃ soln. cm ⁻¹	op(C=O) ₂ str. [CCl ₄]-[CHCl ₃] cm ⁻¹	ip(C=O) ₂ str. [CCl ₄]-[CHCl ₃] cm ⁻¹
Hexahydrophthalic	1792.7	1787.5	1861.4	1859.1	5.2	2.3
Phthalic	1784.6	1779.4	1856	1853	5.2	3
Tetrachlorophthalic	1790.7	1786.8	1845.9	1845.5	3.9	0.4
Tetrabromophthalic	1795.6	1790.3	1867.2	1863.4	5.3	3.8
Maleic	1787.1	1785.4	1851.74	1851.68	1.7	0.06
Dichloromaleic	1799	1796.4	1876.7	1876.2	2.6	0.5
Phthalimide						
N-(4-bromobutyl)	1718.7	1713	1773.8	1772.2	5.7	1.6
Caffeine	1667.5	1658.4	1710.6	1707.9	9.1	2.7
Isocaffeine* ¹	1673.2	1664	1716.7	1711.3	9.2	5.4
1,3,5-Trimethyluracil	1663.4* ²	1652.4* ²	1706.6	1700	11	6.6
1,3,6-Trimethyluracil	1668.8* ²	1658.2* ²	1710.8	1702	10.6	8.8
1,3-Dimethyl-2,4-(1H,3H)-quinazolinone	1667* ²	1657.4* ²	1711.6	1703.7	9.6	7.9
1,4-Benzoquinone						
Tetrafluoro-	1702.71	1701.42	1696.8	1697.7	1.29	-0.9
Tetrachloro-	1694.68	1693.37			1.31	
Trichloro-	[1694]* ³		[1657]* ³			
Tetrabromo-	1687.48	1685.37			2.11	
2,5-Dichloro-	1682.18	1681.25	1672.5	1673.6	0.9	-1.1
Chloro-	1681.89	1680.95	1659.3	1659.3	0.94	0
Unsubstituted	1663.51* ²	1662	1661.4	1661.8	1.51	-0.4
Methyl-	1662.47	1659.57	1665.7	1665.9	2.9	-0.2
2,6-Dimethyl-	1657					

*¹ 10.74 mol % CHCl₃/CCl₄.*² corrected for Fermi resonance.*³ In CS₂ solution.

TABLE 10.4 Substituted hydantoin— the Nyquist Rule

Hydantion	op(C=O) ₂ str. vapor cm ⁻¹	op(C=O) ₂ str. solid cm ⁻¹	ip(C=O) ₂ str. vapor cm ⁻¹	ip(C=O) ₂ str. solid cm ⁻¹	op(C=O) ₂ str. [vapor]-[solid] cm ⁻¹	ip(C=O) ₂ str. [vapor]-[solid] cm ⁻¹
1,3,5-						
H,H,CH ₃ ,C ₃ H ₇	1774	1707	1809	1761	67	48
H,H,CH ₃ ,isoC ₃ H ₇	1774	1712	1808	1770	62	38
H,H,H,H	1785	1717	1825	1783	68	42
H,H,CH ₃ ,isoC ₄ H ₉	1774	1718	1809	1780	56	29

TABLE 10.5 1,4-Diphenylbutadiyne and 1-halopropadiene— the Nyquist Rule

Compound	op(CC) ₂ str. CCl ₄ cm ⁻¹	op(CC) ₂ str. CHCl ₃ cm ⁻¹	ip(CC) ₂ str. CCl ₄ cm ⁻¹	ip(CC) ₂ str. CHCl ₃ cm ⁻¹	op(CC) ₂ str. [CCl ₄]-[CHCl ₃] cm ⁻¹	ip(CC) ₂ str. [CCl ₄]-[CHCl ₃] cm ⁻¹
1,4-Diphenylbutadiyne	2152.23	2150.22	2220.51	2219.45	2.01	1.06
Propadiene	a.C=C=C str. CCl ₄ cm ⁻¹	a.C=C=C str. liquid cm ⁻¹	s.C=C=C str. CS ₂ cm ⁻¹	s.C=C=C str. liquid cm ⁻¹	a.C=C=C str. [CCl ₄]-[liquid] cm ⁻¹	s.C=C=C str. [CS ₂]-[liquid] cm ⁻¹
1-Chloro-	1958	1951	1101	1095	7	6
1-Bromo-	1957	1954	1082	1086	3	-4
1-Bromo,1-d-	1940	1943	857	861	-3	-4
1-Iodo-	1947	1947	1076	1076	0	0
Propadiene	a.C=C=C str. vapor cm ⁻¹	a.C=C=C str. CCl ₄ cm ⁻¹	s.C=C=C str. vapor cm ⁻¹	s.C=C=C str. CCl ₄ cm ⁻¹	a.C=C=C str. [vapor]-[CCl ₄] cm ⁻¹	s.C=C=C str. [vapor]-[CCl ₄] cm ⁻¹
1-Chloro-	1971	1958	1108	1101	13	7
	1956		1094		-2	-7
1-Bromo-	1969	1957	1081	1082	12	-1
	1954		1076		-3	-6
1-Bromo,1-d-	1943	1940	861	857	3	-4
	1929				-11	
1-Iodo-	1958	1947	1081	1076	11	5
	1947		1071		0	-5
Propadiene	a.C=C=C str. vapor cm ⁻¹	a.C=C=C str. liquid cm ⁻¹	s.C=C=C str. vapor cm ⁻¹	s.C=C=C str. liquid cm ⁻¹	a.C=C=C str. [vapor]-[liquid] cm ⁻¹	s.C=C=C str. [vapor]-[liquid] cm ⁻¹
1-Chloro-	1971	1951	1108	1095	20	13
	1956		1094		-1	-1
1-Bromo-	1969	1954	1081	1086	15	-5
	1954		1076		0	-1
1-Bromo,1-d-	1943	1940	861	861	3	0
	1929				-11	
1-Iodo-	1958	1947	1081	1076	11	5
	1947		1071		0	-5

TABLE 10.6 3=Nitrobenzenes and 4-nitrobenzenes — the Nyquist Rule

	a.NO ₂ str. CCl ₄ soln.CHCl ₃ soln. cm ⁻¹	a.NO ₂ str. HCCl ₄ soln. cm ⁻¹	s.NO ₂ str. CHCl ₃ soln. cm ⁻¹	s.NO ₂ str. [CCl ₄]-[CHCl ₃] cm ⁻¹	a.NO ₂ str. [CCl ₄]-[CHCl ₃] cm ⁻¹	s.NO ₂ str. [CCl ₄]-[CHCl ₃] cm ⁻¹
4-X						
NH ₂	1513.94	1505.34	1338.08	1335.15	8.6	2.93
CH ₃ O	1519.32	1514.12	1343.07	1342.76	5.2	0.31
C ₆ H ₅ O	1522.43	1517.85	1344.98	1344.88	4.58	0.1
C ₆ H ₅	1524.26	1519.47	1346.67	1347.74	4.79	-1.07
CH ₃	1524.8	1520.1	1346.18	1346.93	4.7	-0.75
HO	1526.74	1521.41	1344.45	1342.46	5.33	1.99
Cl	1527.01	1523.64	1344.3	1345.39	3.37	-1.09
isoC ₃ H ₇	1527.68	1519.8	1347.11	1348.08	7.8	-0.97
CH ₂ Cl	1529.17	1525.44	1348.01	1350.09	3.73	-2.08
I	1529.78	1526.08	1348.7	1350.3	3.7	-1.6
C ₆ H ₅ -C=O	1531.06	1525.77	1353.19	1355.23	5.29	-2.04
H	1531.53	1527.37	1348.24	1349.76	4.16	-1.52
Br	1531.95	1524.88	1350.1	1351.46	7.07	-1.36
F	1532.31	1528.48	1346.41	1349.26	3.83	-1.85
CH ₃ CO ₂	1532.87	1530.26	1348	1350.03	2.62	-2.03
CH ₃ C=O	1533.76	1531.06	1345.71	1347.46	2.7	-1.75
CN	1535.33	1533.21	1345.37	1347.56	2.12	-2.19
CH ₃ SO ₂	1537.97	1535.9	1348.2	1350.6	2.07	-2.4
CF ₃	1538.91	1535.44	1354.35	1356.34	3.47	-1.99
SO ₂ Cl	1541.25	1539.26	1346.06	147.86	1.99	-1.8
NO ₂	1556.41	1554.37	1338.68	1340.6	2.04	-1.92
Δ cm ⁻¹	42.47	49.03	16.27	20.08		
3-X-Nitrobenzene						
3-X						
N(CH ₃) ₂	1535.29	1531.64	1349.47	1349.81	3.65	-0.34
CH ₃	1532.78	1529.16	1350.88	1352.04	3.62	-1.16
Br	1536.44	1533.09	1348.28	1349.97	3.35	-1.69
I	1533.69	1530.42	1346.97	1348.62	3.27	-1.65
NO ₂	1544.05	1541.63	1345.29	1347.44	2.42	-2.15
Δ cm ⁻¹	11.27	12.47	5.59	4.6		
Nitromethane	1564.5	1562.4	1374.4	1376.2	2.1	-1.8
Trichloronitromethane	1608.2	1606.5	1307.5	1309.6	1.7	-2.1
Tribromonitromethane	1595.1	1593.3	1305.9	1308.7	1.8	-2.8
Ethyl nitrate	1637.3	1631.7	1281.5	1282.9	5.6	-1.4

TABLE 10.7 Organic sulfate, sulfonate, sulfonyl chloride, and sulfones — the Nyquist Rule

Compound	a.SO ₂ str. CCl ₄ soln. cm ⁻¹	a.SO ₂ str. CHCl ₃ soln. cm ⁻¹	s.SO ₂ str. CCl ₄ soln. cm ⁻¹	s.SO ₂ str. CHCl ₃ soln. cm ⁻¹	a.SO ₂ str. [CCl ₄]-[CHCl ₃] cm ⁻¹	s.SO ₂ str. [CCl ₄]-[CHCl ₃] cm ⁻¹
Dimethyl sulfate	1405.7	1395.7	1203.8	1201.8	-10	-2
4'-Chlorophenyl 4-chlorophenyl benzenesulfonate	1392.4	1382.9	1178.9	1176.8	-9.5	-2.1
Benzenesulfonyl chloride	1387.4	1380.3	1177.8	1177.1	-7.1	-0.7
Diphenyl sulfone	1326.8	1319.1	1161.4	1157.6	-7.7	-3.8
Methyl phenyl sulfone	1325.7	1317.7	1157.4	1153.2	-8	-4.2

Infrared, Raman, and Nuclear Magnetic Resonance Spectra-Structure Correlations for Organic Compounds

Introduction	441
4-x-Anilines	441
3-x and 4-x Benzoic Acids	442
4-x-Acetanilides	442
4-x-Benzaldehydes	443
4-x-Acetophenones	443
4-x and 4,4'-x,x-Benzophenones	444
Alkyl 3-x and 4-x-Benzoates	444
$\nu\text{C}=\text{O}$ vs $\delta^{13}\text{C}=\text{O}$	444
Acetone In $\text{CHCl}_3/\text{CCl}_4$ Solutions	445
N,N'-Dimethylacetamide in $\text{CHCl}_3/\text{CCl}_4$ Solutions	445
Maleic Anhydride (MA) in $\text{CHCl}_3/\text{CCl}_4$ Solutions	446
3-x and 4-x-Benzonitriles	446
Organonitriles	446
Alkyl Isonitriles	447
Nitroalkanes	447
Alkyl Isocyanates	448
Alkylamines	448
A Summary of the Correlations for the Nitrogen Compounds	449
Organophosphorus Compounds	450
A Summary of Correlations for the Phosphorus Compounds	452
Anisoles	453
Mono-Substituted Benzenes	454
4-x and 4,4'-x,x'-Biphenyls in CHCl_3 Solutions	454
Tetramethylurea (TMU)	454
Dialkylketones	455
Acetates	456
Acrylates and Methacrylates	456
References	457

Figures

Figure 11-1	459 (441)	Figure 11-3	461 (441)
Figure 11-2	460 (441)	Figure 11-4	462 (441)

Figure 11-5	463 (442)	Figure 11-52	509 (448)
Figure 11-6	464 (442)	Figure 11-53	510 (448)
Figure 11-7	465 (443)	Figure 11-54	511 (448)
Figure 11-8	466 (442)	Figure 11-55	512 (449)
Figure 11-9	467 (442)	Figure 11-56	513 (449)
Figure 11-10	468 (442)	Figure 11-57	514 (449)
Figure 11-11	469 (472)	Figure 11-58	515 (450)
Figure 11-12	470 (442)	Figure 11-59	516 (450)
Figure 11-13	471 (442)	Figure 11-60	517 (450)
Figure 11-14	472 (442)	Figure 11-61	518 (450)
Figure 11-15	473 (442)	Figure 11-62	519 (450)
Figure 11-16	474 (442)	Figure 11-63	520 (450)
Figure 11-17	475 (442)	Figure 11-64	521 (450)
Figure 11-18	476 (443)	Figure 11-65	522 (450)
Figure 11-19	477 (443)	Figure 11-66	523 (450)
Figure 11-20	478 (443)	Figure 11-67	524 (450)
Figure 11-21	479 (448)	Figure 11-68	525 (450)
Figure 11-22	480 (443)	Figure 11-69	526 (451)
Figure 11-23	481 (443)	Figure 11-70	527 (451)
Figure 11-24	482 (443)	Figure 11-71	528 (451)
Figure 11-25	483 (444)	Figure 11-72	529 (451)
Figure 11-26	484 (444)	Figure 11-73	530 (451)
Figure 11-27	485 (444)	Figure 11-74	531 (451)
Figure 11-28	486 (444)	Figure 11-75	532 (451)
Figure 11-29	487 (444)	Figure 11-76	533 (452)
Figure 11-30	488 (444)	Figure 11-77	534 (452)
Figure 11-31	489 (444)	Figure 11-78	535 (452)
Figure 11-32	490 (444)	Figure 11-79	536 (452)
Figure 11-33	491 (445)	Figure 11-80	537 (452)
Figure 11-34	492 (445)	Figure 11-81	538 (452)
Figure 11-35	493 (445)	Figure 11-82	539 (452)
Figure 11-35a	493 (445)	Figure 11-83	540 (452)
Figure 11-35b	494 (446)	Figure 11-84	541 (452)
Figure 11-35c	494 (446)	Figure 11-85	542 (453)
Figure 11-36	495 (446)	Figure 11-86	543 (453)
Figure 11-37	496 (446)	Figure 11-87	544 (453)
Figure 11-38	497 (446)	Figure 11-88	544 (453)
Figure 11-39	498 (446)	Figure 11-89	545 (453)
Figure 11-40	498 (447)	Figure 11-90	545 (454)
Figure 11-41	499 (447)	Figure 11-91	546 (454)
Figure 11-42	500 (447)	Figure 11-92	547 (454)
Figure 11-43	501 (447)	Figure 11-93	548 (457)
Figure 11-44	502 (447)	Figure 11-94	549 (454)
Figure 11-45	503 (447)	Figure 11-95	550 (454)
Figure 11-46	504 (448)	Figure 11-96	551 (454)
Figure 11-47	505 (448)	Figure 11-97	552 (454)
Figure 11-48	506 (448)	Figure 11-98	552 (454)
Figure 11-49	507 (448)	Figure 11-99	553 (454)
Figure 11-50	508 (448)	Figure 11-100	554 (454)
Figure 11-51	509 (448)	Figure 11-101	555 (455)

Figure 11-102	556 (455)	Figure 11-104	558 (456)
Figure 11-103	557 (455)	Figure 11-105	559 (456)

Tables

Table 11-1	560 (441)	Table 11-14	571 (448)
Table 11-2	561 (442)	Table 11-15	571 (450)
Table 11-3	562 (443)	Table 11-16	572 (450)
Table 11-4	563 (443)	Table 11-17	574 (453)
Table 11-5	564 (444)	Table 11-17a	575 (453)
Table 11-6	565 (444)	Table 11-18	576 (454)
Table 11-7	566 (444)	Table 11-19	577 (454)
Table 11-8	567 (444)	Table 11-20	577 (454)
Table 11-9	567 (445)	Table 11-21	578 (455)
Table 11-10	568 (445)	Table 11-22	578 (455)
Table 11-11	569 (446)	Table 11-23	579 (456)
Table 11-12	570 (446)	Table 11-24	579 (456)
Table 11-13	570 (446)		

*Numbers in parentheses indicate in-text page reference.

INTRODUCTION

Spectra-structure correlations exist for IR, Raman and nuclear magnetic resonance (NMR) data. Spectra-structure correlations have been developed for the carbonyl stretching frequencies and the carbon-13 NMR chemical shift data for over 600 compounds (1), and this work has aided us in the solution of many complex chemical problems. Development of other spectra-structure cross correlations between IR, Raman and NMR data would be most helpful in the solution of many complex problems arising in both academia and industry.

4-x-ANILINES

Table 11.1 lists NMR ^{13}C chemical shift data for anilines in CCl_3H solution (2,3). Figure 11.1 is a plot of the $\delta\text{C-1}$ chemical shift for 4-x-anilines in CHCl_3 solution vs Hammett σ_p values for the 4-x atom or group, and Fig. 11.2 is a plot of the NMR $\delta^{13}\text{C-1}$ chemical shift data for 4-x-anilines in CHCl_3 solution vs Taft σ_{Re} values for the 4-x atom or group. Both plots show a pseudolinear relationship (2).

Figure 11.3 is a plot of ν asym. NH_2 frequencies for 4-x-anilines in the vapor phase (4) vs the $\delta^{13}\text{C-1}$ chemical shift data for 4-x-anilines in CHCl_3 solution (2,3).

Compound 24 (4-aminoacetophenone) does not correlate well with the other aniline derivatives, and this most likely results from the intermolecular hydrogen bond formed between the C=O group and the CCl_3H proton ($\text{C=O}\cdots\text{HCCl}_3$). Otherwise, this IR-NMR spectra-structure correlation shows a pseudolinear relationship.

Figure 11.4 is a plot of ν asym. NH_2 frequencies for 3-x- and 4-x-anilines in hexane solution vs the $\delta^{13}\text{C-1}$ chemical shift data of 3-x- and 4-x-aniline in CHCl_3 solution (2,3). This IR-NMR spectra-structure correlation shows a pseudolinear relationship.

Figure 11.5 is a plot of ν asym. NH_2 frequencies for 3-x- and 4-x-anilines in CCl_4 solution vs the $\delta^{13}\text{C}-1$ chemical shift data for 3-x- and 4-x-anilines in CHCl_3 solution. Compounds 17 (4-amino-acetophenone) and 18 (4-nitroaniline) do not fit as well to this pseudolinear correlation between IR and NMR data, and this may be due to the fact that both the oxygen atoms of the $\text{C}=\text{O}$ and NO_2 groups are intermolecularly hydrogen bonded in CCl_3H solution [$\text{C}=\text{O}\cdots\text{HCCl}_3$ and $\text{NO}_2(\cdots\text{HCCl}_3)_2$] (2,3).

Figure 11.6 is a plot of the ν asym. NH_2 frequencies for 3-x- and 4-x-anilines in CHCl_3 solution vs $\delta^{13}\text{C}-1$ chemical shift data for 3-x- and 4-x-anilines in CHCl_3 solution. Both plots show a pseudolinear relationship between IR and NMR data (2,3).

Figure 11.7 is a plot of the ν sym. NH_2 frequencies for 4-x-anilines in the vapor phase vs $\delta^{13}\text{C}-1$ chemical shift data for 3-x- and 4-x-anilines in CHCl_3 solution. This plot shows a pseudolinear relationship between IR and NMR data.

Figure 11.8 is a plot of ν sym. NH_2 frequencies for 3-x- and 4-x-anilines in hexane solution vs the $\delta^{13}\text{C}-1$ chemical shift data for 3-x- and 4-x-anilines in CHCl_3 solution. This plot shows a pseudolinear relationship between IR and NMR data (2,3).

Figure 11.9 is a plot of the ν sym. NH_2 frequencies for 3-x- and 4-x-anilines in CCl_4 solution vs the $\delta^{13}\text{C}-1$ chemical shift data for 3-x- and 4-x-anilines in CHCl_3 solution. This plot shows a pseudolinear relationship between IR and NMR data (2,3).

Figure 11.10 is a plot of the ν sym. NH_2 frequencies for 3-x- and 4-x-anilines in CHCl_3 solution vs the $\delta^{13}\text{C}-1$ chemical shift data for 3-x- and 4-x-anilines in CHCl_3 solution. Both plots show a pseudolinear relationship between IR and NMR data (2,3).

Figure 11.11 is a plot of the frequency difference between ν asym. NH_2 and ν sym. NH_2 for 3-x- and 4-x-anilines in hexane solution vs $\delta^{13}\text{C}-1$ chemical shift data for 3-x- and 4-x-anilines in CHCl_3 solution. This plot shows a pseudolinear relationship between IR and NMR data (2,3).

Figure 11.12 is a plot of the frequency difference between ν asym. NH_2 and ν sym. NH_2 for 3-x- and 4-x-anilines in CCl_4 solution vs the $\delta^{13}\text{C}-1$ chemical shift data for 3-x- and 4-x-anilines in CHCl_3 solution. This plot shows a pseudolinear relationship between IR and NMR data (2,3).

Figure 11.13 is a plot of the frequency difference between ν asym. NH_2 and ν sym. NH_2 for 3-x- and 4-x-anilines in CHCl_3 solution vs the $\delta^{13}\text{C}-1$ chemical shift data of 3-x- and 4-x-anilines in CHCl_3 solution (2,3).

Figure 11.14 is a plot of the absorbance ratio $A(\nu \text{ asym. } \text{NH}_2)/A(\nu \text{ sym. } \text{NH}_2)$ for 3-x- and 4-x-anilines in CCl_4 solution vs $\delta^{13}\text{C}-1$ chemical shift data for 3-x- and 4-x-anilines in CHCl_3 solution (2,3). This plot shows that a pseudolinear relation exists between IR and NMR data.

Figure 11.15 is a plot of $\delta^{13}\text{C}-1$ chemical shift data for 4-x-anilines in CHCl_3 solution vs Taft's (σ_{R} values for the 4-x atom or group. This plot shows that there is a pseudolinear relationship between $\delta^{13}\text{C}-1$ and the resonance parameter of the 4-x group.

3-X AND 4-X BENZOIC ACIDS

Table 11.2 lists IR and NMR data for 3-x- and 4-x-benzoic acids (1,3,4). Figure 11.16 is a plot of $\delta^{13}\text{C}-1$ for 3-x- and 4-x-benzoic acids vs Hammett σ values for the x group. The Hammett σ values are from Kalinowski *et al.* (5). This plot shows that $\delta^{13}\text{C}-1$ generally increases as the σ_m and σ_p values increase (4).

Figure 11.17 show plots of $\nu \text{ C}=\text{O}$ vs Hammett σ values for 3-x- and 4-x-benzoic acids. The solid circles are for IR data in the vapor phase. The open circles are for IR dilute CCl_4 solution

data for unassociated benzoic acids (4). Both sets of data are for unassociated benzoic acids (3-x- and 4-x- $C_6H_4CO_2H$). Both plots increase in frequency as the value of σ_p and σ_m values increases.

Figure 11.18 show plots of $\nu C=O$ vs $\delta^{13}C-1$ for 3-x- and 4-x-benzoic acids. The NMR data are for $CDCl_3$ solutions. The open circles are for IR CCl_4 solution data, and the closed circles include vapor-phase IR data (4). This cross correlation shows that in general $\nu C=O$ increases in frequency as $\delta^{13}C-1$ increases in frequency.

4-X-ACETANILIDES

Table 11.3 lists NMR data in $CHCl_3$ solution and IR data in CCl_4 and $CHCl_3$ solution for 4-x-acetanilides (3,6). Figure 11.19 is a plot of $\delta^{13}C-1$ vs Hammett σ_p for 4-x-acetanilides. This plot shows a pseudolinear relationship between Hammett σ_p values and $\delta^{13}C-1$ for 4-x-acetanilides.

Figure 11.20 is a plot of $\nu C=O$ vs Hammett σ_p for 4-x-acetanilides (4). The solid circles represent IR CCl_4 solution data and the solid squares represent IR $CHCl_3$ solution data. The IR solution data are for dilute solutions of the 4-x-acetanilides where the acetanilide molecules are not intermolecularly hydrogen bonded via $C=O \cdots H-N$. In this case $\nu C=O$ occurs at lower frequency in $CHCl_3$ solution as the result of $C=O \cdots HCCl_3$ intermolecular hydrogen bonding plus the difference in the refraction field between $CHCl_3$ and CCl_4 .

4-X-BENZALDEHYDES

Table 11.4 lists IR and NMR data for 4-x-benzaldehydes in $CHCl_3$ and/or CCl_4 solution (3,4,7). Figure 11.21 is a plot of $\delta^{13}C-1$ vs Taft σ_{R^o} for 4-x-benzaldehydes, and there is a pseudolinear correlation between these two parameters. This correlation shows that as σ_{R^o} increases in value the $\delta^{13}C-1$ value increases in frequency. The chemical significance of increasingly more negative values is that there is an increasing amount of π electron contribution to the C-1 atom. Thus, with an increasing contribution of π electrons to the C-1 atom from the atom or group joined to the C-4 atom there is more π overlap with the π system of the $C=O$ group. Consequently, the $\nu C=O$ mode should decrease in frequency as the σ_{R^o} value decreases. Figure 11.22 is a plot of $\nu C=O$ for 4-x-benzaldehydes vs Taft σ_{R^o} . The solid circles represent $\nu C=O$ frequencies in CCl_4 solution and the solid triangles represent $\nu C=O$ frequencies in $CHCl_3$ solution. In general, the pseudolinear relationships noted for the two sets of solution data support the preceding hypothesis. The $\nu C=O$ frequencies are lower in $CHCl_3$ solution than they are in CCl_4 solution, and this is due in part to intermolecular hydrogen bonding (e.g., $C=O \cdots HCCl_3$) together with an increased field effect in going from solution in CCl_4 to solution in $CHCl_3$.

Figure 11.23 is a plot of $\nu C=O$ for 4-x-benzaldehydes vs Hammett σ_p . The solid circles represent $\nu C=O$ frequencies in CCl_4 solution and the solid triangles represent $\nu C=O$ frequencies in $CHCl_3$ solution. The σ_p values include both resonance and inductive effects. These plots also exhibit pseudolinear relationships, which indicates that there must be some contribution from the σ electrons to the shift of $\nu C=O$ with change in the 4-x atom or group.

Figure 11.24 gives plots of $\nu C=O$ vs $\delta^{13}C-1$ for 4-x-benzaldehydes in CCl_4 solution and in $CHCl_3$ solution (4). The filled-in circles represent $\nu C=O$ frequencies in CCl_4 solution and the filled-in triangles represent $\nu C=O$ frequencies in $CHCl_3$ solution. The $\delta^{13}C-1$ data are for $CDCl_3$ solutions. Both plots show a pseudolinear relationship.

4-X-ACETOPHENONES

Table 11.5 lists IR and NMR data for 4-x-acetophenones. Figure 11.25 is a plot of $\delta^{13}\text{C-1}$ chemical shifts data in CDCl_3 solution vs Taft σ_{R} for 4-x-acetophenones (4). This plot shows a pseudolinear relationship. Figure 11.26 is a plot of $\nu \text{C=O}$ frequencies for 4-x-acetophenones in CHCl_3 solution vs Taft σ_{R} , and this plot shows a pseudolinear relationship. Figure 11.27 is a plot of $\nu \text{C=O}$ frequencies for 4-x-acetophenones in CHCl_3 solution vs $\delta^{13}\text{C-1}$ chemical shifts for 4-x-acetophenones in CDCl_3 solution. This plot shows that, in general, $\nu \text{C=O}$ increases in frequency as $\delta^{13}\text{C-1}$ increases in frequency.

4-X AND 4,4'-X,X-BENZOPHENONES

Table 11.6 lists vapor-phase IR and NMR CHCl_3 solution-phase data for 4-x- and 4,4'-x,x-benzophenones (4,8). Figure 11.28 is a plot of $\delta^{13}\text{C-1}$ vs Taft σ_{R} for the 4-x and 4,x,x atoms or groups for 4-x- and 4,4'-x,x-benzophenones in CHCl_3 solution (4). The first group in parentheses is plotted vs its σ_{R} value. This relationship between $\delta^{13}\text{C-1}$ and σ_{R} appears to be pseudolinear (4). Figure 11.29 is a plot of the $\nu \text{C=O}$ frequencies vs $\delta^{13}\text{C-1}$ chemical shift frequencies for 4-x-benzophenone and vs $\delta^{13}\text{C-1}$ for 4,4'-x,x-benzophenones. Figure 11.30 is a plot of $\nu \text{C=O}$ frequencies vs Hammett σ_{p} for 4-x-benzophenones and the sum of σ_{p} , σ_{p} for 4,4'-x,x-benzophenones. With the exception of the 4-methoxy analog, the 4-x and 4,4'-x,x-benzophenones yield separate relationships where $\nu \text{C=O}$ increases in frequency as the sum of the σ_{p} values increases.

ALKYL 3-X AND 4-X-BENZOATES

Table 11.7 lists IR and NMR data for methyl and/or ethyl 3-x or 4-x-benzoates (4,8). Figure 11.31 shows plots of $\delta^{13}\text{C-1}$ vs Hammett σ values for methyl and ethyl 3-x- and/or 4-x-benzoates (4). These plots show that, in general, $\delta^{13}\text{C-1}$ increases in frequency as the Hammett σ value increases, and that the $\delta^{13}\text{C-1}$ chemical shift for the ethyl analogs generally occurs at higher frequency than for the methyl analogs.

$\nu \text{C=O}$ VS $\delta^{13}\text{C=O}$

Table 11.8 is a summary of some of the IR and NMR data for C=O containing compounds (4).

Figure 11.32 shows plots of the range of $\nu \text{C=O}$ frequencies for the compounds studied in different physical phases vs the range of $\delta^{13}\text{C=O}$ for the compounds studied in CDCl_3 solutions. The IR data for plots 1,4,6, and 7 have been recorded in CCl_4 solution, and plots 1,4,6, and 7 are for 4-x-acetophenones, 4-x-benzaldehydes, 4-x-acetonilides, and 3-x and 4-x-benzoic acids, respectively. Infrared plots for 3 and 5 have been recorded in CHCl_3 solution, and these plots are for 4-x-benzaldehydes and 4-x-acetonilides, respectively. The IR data for 2,8,9, and 10 have been recorded in the vapor phase. Plots 2, 8, 9, and 10 are for 4-x and 4,4'-x,x-

benzophenones, ethyl 3-x and 4-x-benzoates, methyl 3-x and 4-x-benzoates, and 3-x and 4-x-benzoic acids, respectively. These data show that ν C=O is affected by change of phase.

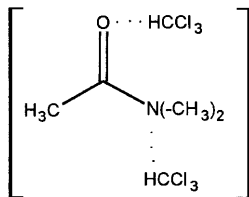
ACETONE IN $\text{CHCl}_3/\text{CCl}_4$ SOLUTIONS

Table 11.9 lists IR data for ν C=O and δ $^{13}\text{C}=\text{O}$ for acetone in mol % $\text{CHCl}_3/\text{CCl}_4$ solutions. Figure 11.33 is a plot of δ $^{13}\text{C}=\text{O}$ in ppm for acetone vs mol % $\text{CHCl}_3/\text{CCl}_4$, and δ $^{13}\text{C}=\text{O}$ increases in frequency as the mol % $\text{CHCl}_3/\text{CCl}_4$ is increased.

Figure 11.34 shows a plot of ν C=O vs δ $^{13}\text{C}=\text{O}$ for acetone, and this plot is essentially a linear relationship. In Volume I the deviation from linearity at low mol % $\text{CHCl}_3/\text{CCl}_4$ was attributed to intermolecular hydrogen bonding between solute and solvent (viz. $(\text{CH}_3)_2\text{C}=\text{O} \cdots \text{HCCl}_3$). The steady decrease in the ν C=O frequency and the steady decrease in δ $^{13}\text{C}=\text{O}$ with increase in the mol % $\text{CHCl}_3/\text{CCl}_4$ is attributed to the field effect of the solvent system (9).

N,N'-DIMETHYLACETAMIDE IN $\text{CHCl}_3/\text{CCl}_4$ SOLUTIONS

Table 11.10 lists IR and NMR data for N,N'-dimethylacetamide in $\text{CHCl}_3/\text{CCl}_4$ solutions (10). Figure 11.35 is a plot of ν C=O for N,N'-dimethylacetamide vs mol % $\text{CHCl}_3/\text{CCl}_4$ (10). The plot shows that ν C=O decreases in frequency by 26.27 cm^{-1} in going from 1650.50 cm^{-1} in CCl_4 solution to 1634.23 cm^{-1} in CHCl_3 solution. At 5.68 mol % $\text{CHCl}_3/\text{CCl}_4$ ν C=O has decreased 9.20 cm^{-1} or 35% of the entire ν C=O decrease in going from solution in CCl_4 to solution in CHCl_3 . The principal cause for this 35% ν C=O frequency decrease is attributed to intermolecular hydrogen bonding (viz. $\text{C}=\text{O} \cdots \text{HCCl}_3$). Between 5.68 and 41.93 mol % $\text{CHCl}_3/\text{CCl}_4$ there is a linear relationship in the ν C=O frequency decrease, and this is attributed to the increase of the field effect of the solvent system. The second break suggests that a second intermolecular hydrogen bond is formed,



and the continued ν C=O frequency decrease is attributed to a further continued increase of the solvent field effect.

Figure 11.35a is a plot of δ $^{13}\text{C}=\text{O}$ for dimethylacetamide vs mol % $\text{CHCl}_3/\text{CCl}_4$. The δ $^{13}\text{C}=\text{O}$ frequency increases as the mol % $\text{CHCl}_3/\text{CCl}_4$ is increased.

The data in Table 11.10 show that as the mol % $\text{CHCl}_3/\text{CCl}_4$ is increased from 0 to 100 the δ $^{13}\text{C}=\text{O}$ increases in frequency from 168.4 to 170.8 ppm while ν C=O decreases in frequency from 1660.5 to 1634.2 cm^{-1} .

MALEIC ANHYDRIDE (MA) IN CHCl₃/CCl₄ SOLUTIONS

Table 11.11 lists IR and NMR data for maleic anhydride (MA) in CHCl₃/CCl₄ solutions (11,12). The out-of-phase ν (C=O)₂ mode is in FR with a combination tone (560 cm⁻¹, A and B₁ fundamental at 1235 cm⁻¹, and an A₁ fundamental yielding at 1795 cm⁻¹, B₁ combination tone). The out-of-phase ν (C=O)₂ mode for maleic anhydride listed in Table 11.11 has been corrected for FR. The δ ¹³C=O chemical shift increases from 163.2 ppm in CCl₄ solution to 164.1 ppm in CHCl₃ solution while ν out-of-phase (C=O)₂ corrected for FR decreases in frequency from 1787.1 cm⁻¹ in CCl₄ solution to 1785.4 cm⁻¹ in CHCl₃. The ν in-phase (C=O)₂ mode decreases 0.06 cm⁻¹ in going from solution in CCl₄ to solution in CHCl₃.

Figure 11.35b is a plot of δ ¹³C=O for maleic anhydride vs mol % CHCl₃/CCl₄. This plot shows two linear segments with a break point near 37 mol % CHCl₃/CCl₄. The δ ¹³C=O chemical shift increases in frequency as the mol % CHCl₃/CCl₄ is increased. These data suggest that at <37 mol % CHCl₃/CCl₄, the CHCl₃/CCl₄ complex with (MA) is most likely forming C=O... (HCCL₃)_x(CCl₄)_x type complexes and > ~37 mol % HCCL₃/CCl₄ solution CHCl₃/CCl₄ is forming (C=O)₂... (HCCL₃)_x(CCl₄) type complexes. Complexes with the C=C π system are also likely (see in what follows).

Figure 11.35c is a plot of δ ¹³C=O vs δ ¹³C=C for maleic anhydrides. This plot shows a linear relationship between these two parameters, and both chemical shifts increase in frequency as the mol % CHCl₃/CCl₄ increases from 0 to 100.

3-X AND 4-X-BENZONITRILES

Table 11.12 lists IR and NMR data for 3-x- and 4-x-benzonitriles (4). Figure 11.36 is a plot of δ ¹³C-1 vs Taft σ_{R^o} values for 3-x- and 4-x-benzonitriles, and Fig. 11.37 is a plot of δ ¹³C-1 vs Hammett σ values for x for 3-x and 4-x-benzonitriles. Both plots show that δ ¹³C-1 increases in frequency as σ_p , σ_m and σ_{R^o} increase in value. However, the plot of δ ¹³C-1 vs σ_{R^o} has a better pseudolinear relationship than the plot of δ ¹³C-1 vs σ_p and σ_m .

Figure 11.38 is a plot of δ ¹³CN vs Hammett σ values for 3-x and 4-x-benzonitriles. The δ ¹³CN values are in the range 116.3 ppm and 120.6 ppm. The literature assignments for δ ¹³CN and δ ¹³C-1 for 4-cyanoacetophenone are 118.0 ppm and 116.3 ppm, respectively (3). However, Fig. 11.38 suggests that the δ ¹³CN chemical shift should be 116.3 ppm rather than 118.0 ppm (3). The δ ¹³CN decreases in frequency as the σ_p and σ_m values increase. It has been shown that ν CN frequencies and intensities correlate with Hammett σ_p and σ_m values (13–16). Electron-donating groups such as OCH₃ and NH₂ increase the IR intensity and decrease the ν CN frequency, while electron-withdrawing groups such as NO₂ and CH₃-C=O have the opposite effect (increase the ν CN frequency and decrease its IR band intensity). The ν CN mode for benzonitriles occurs in the range 2220–2241 cm⁻¹.

ORGANONITRILES

Table 11.13 lists IR, Raman and NMR data for some organonitriles (17). Figure 11.39 is a plot of ν CN vs δ ¹³CN for some organonitriles. In the series CH₃CN through (CH₃)₃CCN, ν CN

decreases in frequency while the $\delta^{13}\text{CN}$ frequency increases in essentially a linear manner with increased branching on the α -carbon atom. Substitution of an α -Cl atom raises the ν CN frequency and lowers the $\delta^{13}\text{CN}$ frequency. In addition, conjugation lowers both ν CN frequencies.

Figure 11.40 is a plot of $\delta^{13}\text{CN}$ vs the number of protons on the α -carbon atom (17). This plot shows that $\delta^{13}\text{CN}$ increases in frequency with increased branching on the α -carbon atom. The σ electron donation to the CN group also increases with increased branching on the α -carbon atom. Therefore, $\delta^{13}\text{CN}$ increases in frequency with increased electron donation to the nitrile group, and ν CN decreases in frequency with increased electron donation to the nitrile group.

ALKYL ISONITRILES

The ν NC frequencies for methyl isonitrile (2183 cm^{-1}), ethyl isonitrile (2160 cm^{-1}), isopropyl isonitrile (2140 cm^{-1}), and tert-butyl isonitrile (2134 cm^{-1}) decrease in frequency in the order of increased branching on the alkyl α -carbon atom (18). The $\delta^{15}\text{N}$ chemical shift for methyl isonitrile (-219.6 ppm), ethyl isonitrile (-205.1 ppm), isopropyl isonitrile (-193.4 ppm), and tert-butyl isonitrile (-184.9 ppm) increases in frequency with increased branching in the alkyl α -carbon atom. The $\delta^{15}\text{N}$ frequencies reported for these isonitriles are based upon nitromethane as the $\delta^{15}\text{N}$ reference point (19).

Figure 11.41 is a plot of $\delta^{15}\text{N}$ vs Taft σ^* for alkyl isonitriles (18). With increased electron contribution to the isonitrile group, the $\delta^{15}\text{N}$ chemical shift increases in frequency. Figure 11.42 is a plot of ν NC vs $\delta^{15}\text{N}$ for alkyl isonitriles. This plot shows that as the ν NC vibration decreases in frequency the $\delta^{15}\text{N}$ increases in frequency. With increased electron contribution to the isonitrile group the ν NC vibration decreases in frequency while the $\delta^{15}\text{N}$ chemical shift increases in frequency.

NITROALKANES

In the vapor phase both ν asym. NO_2 and ν sym. NO_2 decrease in frequency with increased branching on the alkyl α -carbon atom. For example, the ν asym. NO_2 and ν sym. NO_2 frequencies for the alkyl group are CH_3 (1582 cm^{-1} , 1397 cm^{-1}), C_2H_5 (1575 cm^{-1} , 1380 cm^{-1}), iso- C_3H_7 (1568 cm^{-1} , 1360 cm^{-1}), and tert-butyl (1555 cm^{-1} , 1349 cm^{-1}) (8). On the other hand, the $\delta^{13}\text{C}$ (20) and $\delta^{15}\text{N}$ (21) chemical shifts for the alkyl α -carbon atom and the NO_2 nitrogen atom both increase in frequency with increased branching on the alkyl α -carbon atom. For example $\delta^{13}\text{C}$ and $\delta^{15}\text{N}$ are, respectively, CH_3 (63.0 ppm, -0.77 ppm), C_2H_5 (70.9 ppm, 9.37 ppm), iso- C_3H_7 (79.2 ppm, 19.40 ppm), and tert-butyl (84.3 ppm, 25.95 ppm). [The $\delta^{13}\text{C}$ values in CDCl_3 solution referred to TMS (20), and the $\delta^{15}\text{N}$ values in neat nitromethane; samples in 0.3 M in acetone (21)].

Figure 11.43 shows plots of ν asym. NO_2 and ν sym. NO_2 vs the number of protons on the α -carbon atom of the nitroalkanes. Figure 11.44 shows plots of ν asym. NO_2 and ν sym. NO_2 vs $\delta^{13}\text{C}$ for the nitroalkanes, and Fig. 11.45 shows plots of ν asym. NO_2 and ν sym. NO_2 vs $\delta^{15}\text{N}$ for the nitroalkanes (18).

These plots show that with increased electron donation of the alkyl group to the NO₂ group, both ν NO₂ vibrations decrease in frequency while the δ ¹³C and δ ¹⁵N chemical shifts increase in frequency.

Figures 11.46, 11.47, and 11.48 are plots of δ ¹³C vs Taft σ^* , δ ¹⁵N vs Taft σ^* , and δ ¹³C vs δ ¹⁵N for the nitroalkanes (18), respectively. Both δ ¹³C and δ ¹⁵N vs σ^* show a linear relationship for the methyl through isopropyl analogs. However, the plot of δ ¹³C vs δ ¹⁵N shows a linear relationship for methyl through the tert-butyl analogs.

ALKYL ISOCYANATES

The ν asym. N=C=O vibrations for alkyl isocyanates decrease in frequency with an increase in branching on the alkyl α -carbon atom. The ν asym. N=C=O frequencies for the alkyl isocyanates are CH₃ (2288 cm⁻¹), C₂H₅ (2280 cm⁻¹), (CH₃)₂CH (2270 cm⁻¹), and (CH₃)₃C (2252 cm⁻¹) (22). The δ ¹⁵N (neat liquid, referred to neat nitromethane) values are CH₃ (-365.4 ppm), C₂H₅ (-348.6 ppm), (CH₃)₂CH (-335.5 ppm), and (CH₃)₃C (-326.0 ppm) (19).

Figure 11.49 is a plot of ν asym. N=C=O for alkyl isocyanates vs the δ ¹⁵N for the N=C=O group. The ν asym. N=C=O vibrations decrease in frequency as the δ ¹⁵N chemical shifts increase in frequency (18).

Figure 11.50 shows a plot of δ ¹⁵N vs Taft's σ^* for both alkyl isocyanates and alkyl isothiocyanates. The δ ¹⁵N chemical shifts decrease in frequency as the Taft σ^* values increase in value. [Taft σ^* values are CH₃(O), C₂H₅(-0.10), (CH₃)₂CH(-0.19), and (CH₃)₃C -0.30] (23). The CH₃ and C₂H₅ analogs of alkyl isothiocyanate exhibit δ ¹⁵N for alkyl isothiocyanates at higher frequency by 75.6 ppm and 71.6 ppm for the CH₃ and C₂H₅ analogs than for the corresponding methyl and ethyl analogs of alkyl isocyanates (18).

Figure 11.51 shows plots of δ ¹³C for the N=C=O group of alkyl isocyanates or diisocyanates vs the number of protons on the alkyl α -carbon atom (24). These plots show that, in general, the chemical shift δ ¹³C for the isocyanate group increases as the number of protons on the alkyl α -carbon atom decreases. Therefore, the δ ¹³C for the isocyanate group increases in frequency as the electron donation of the alkyl group to the isocyanate group is increased.

Figure 11.52 shows plots of ν asym. N=C=O vs δ ¹³C for the N=C=O group for alkyl isocyanates or diisocyanates. These data show that as the ν asym. N=C=O vibration decreases in frequency the δ ¹³C chemical shift increases in frequency. Thus, as the electron contribution of the alkyl group to the isocyanate group is increased, ν asym. N=C=O decreases in frequency while δ ¹³C increases in frequency (24).

ALKYLAMINES

Table 11.14 compares δ ¹⁵N data for primary, secondary and tertiary amines (25). Figure 11.53 is a plot of δ ¹⁵N vs ν C-N for four primary alkylamines. This plot shows that both ν C-N and δ ¹⁵N increase in frequency with increased branching on the alkyl α -carbon atom (8,18,25).

Figure 11.54 is a plot of δ ¹⁵N vs ω NH for dialkylamines (8,18,25). This plot shows that as δ ¹⁵N decreases in frequency the ω NH vibration for dialkylamines increases in frequency.

The ω NH vibration decreases in frequency as more electrons are donated to the NH group by the two alkyl groups while the $\delta^{15}\text{N}$ chemical shift increases in frequency.

Figures 11.55 and 11.56 are plots of $\nu\text{C-N}$ and $\delta^{15}\text{N}$ for primary alkylamines vs Taft's σ^* values, respectively (18). Both plots increase in frequency as the σ^* values decrease. Thus, the $\nu\text{C-N}$ and $\delta^{15}\text{N}$ increase in frequency as the electron contribution of the alkyl group to the nitrogen atom increases.

Figure 11.57 shows plots of $\delta^{15}\text{N}$ vs the number of protons on the alkyl group(s) α -carbon atom(s) for alkylamines (18). These plots show a series of relationships. With methyl and ethyl groups, the correlations are more nearly linear. Deviation from linearity is apparent for the isopropyl and tert-butyl groups. These deviations suggest that steric factors are also important in determining the $\delta^{15}\text{N}$ values, because a steric factor would alter the C-N-C bond angles (18).

A SUMMARY OF THE CORRELATIONS FOR THE NITROGEN COMPOUNDS

1. The cis and trans $\nu\text{N=O}$ frequencies for alkyl nitrites decrease with increased branching on the alkyl α -carbon atom. A plot of $\nu\text{N=O}$ cis vs $\nu\text{N=O}$ trans is linear for the alkyl nitrites with the exception of tert-butyl nitrite. This exception may be due to a steric factor of the $\text{C}(\text{CH}_3)_3$ group, which causes a change in the R-O-N=O bond angle.
2. Both $\nu\text{sym. NO}_2$ and $\nu\text{asym. NO}_2$ decrease in frequency with increased branching on the $\alpha\text{-C-NO}_2$ carbon atom. A plot of $\nu\text{sym. NO}_2$ vs $\nu\text{asym. NO}_2$ is linear for nitroalkanes, with the exception of 1,1-dimethylnitroethane. This exception is attributed to a steric factor of the $\text{C}(\text{CH}_3)_3$ group.
3. Both $\nu\text{sym. NO}_2$ and $\nu\text{asym. NO}_2$ correlate with the number of protons on the $\alpha\text{-C-NO}_2$ carbon atom, with $\delta^{13}\text{C}$ of $\alpha\text{-C-NO}_2$, with $\delta^{15}\text{N}$ of C-NO₂, and with Taft σ^* values. Thus, $\nu\text{sym. NO}_2$ and $\nu\text{asym. NO}_2$ decrease in frequency with increased branching on the $\alpha\text{-C-NO}_2$ carbon atom, and this frequency decrease is in the order of electron release to the alkyl group to the NO₂ group.
4. A nearly linear correlation exists between $\delta^{13}\text{C}$ for the $\alpha\text{-C-NO}_2$ carbon atom and both the $\nu\text{sym. NO}_2$ and $\nu\text{asym. NO}_2$ vibrations for nitroalkanes.
5. A nearly linear correlation exists between $\delta^{15}\text{N}$ and $\nu\text{sym. NO}_2$ and $\nu\text{asym. NO}_2$ for nitroalkanes.
6. A linear correlation exists between the chemical shifts $\delta^{15}\text{N}$ and $\delta^{13}\text{C}$ for the $\alpha\text{-C-NO}_2$ carbon atom for nitroalkanes.
7. The $\delta^{15}\text{N}$ chemical shift increases in frequency while the $\nu\text{asym. N=C=O}$ decreases in frequency with increased branching on the alkyl group $\alpha\text{-C-N}$ carbon atom for alkyl isocyanates.
8. The $\nu\text{asym. N=C=O}$ mode decreases in frequency and $\delta^{15}\text{N}$ increases in frequency with increasing electron release of the alkyl group in alkyl isocyanates. The chemical shift $\delta^{15}\text{N}$ for alkyl isothiocyanates occurs at higher frequency than does $\delta^{15}\text{N}$ for the corresponding alkyl isocyanate analogs.
9. The νNC mode decreases in frequency and the $\delta^{15}\text{N}$ chemical shift increases in frequency with increased branching on the $\alpha\text{-C-NC}$ carbon atom for alkyl isonitriles R-NC. With the exception of the tert-butyl analog a linear correlation exists between δ

- ^{15}N and νNC for alkyl isonitriles. Comparable linear correlations exist between the electron release of the alkyl group and νNC , and between electron release of the alkyl group and $\delta^{15}\text{N}$ for alkyl isonitriles.
10. The chemical shift $\delta^{15}\text{N}$ increases in frequency with increased branching on the $\alpha\text{-C-N}$ atom(s), progressing in and within the series, alkylamines, dialkylamines, and trialkyl amines.
 11. A linear correlation exists between $\delta^{15}\text{N}$ for alkylamines and the corresponding alkyl analogs of dialkylamines.
 12. A correlation exists between $\nu \text{C-N}$ and $\delta^{15}\text{N}$ for alkylamines. Both $\delta^{15}\text{N}$ and $\nu \text{C-N}$ increase in frequency with increased electron release of the alkyl group to the N atom.
 13. A correlation between ωNH and $\delta^{15}\text{N}$ exists for dialkylamines. In this case ωNH decreases in frequency as $\delta^{15}\text{N}$ increases in frequency.

ORGANOPHOSPHORUS COMPOUNDS

Table 11.15 lists NMR data for organophosphorus and organonitrogen compounds. Figure 11.58 is a plot of $\delta^{31}\text{P}$ for trialkylphosphines vs the sum of the protons on the $\alpha\text{-C-P}$ carbon atoms. Figure 11.59 is a plot of $\delta^{31}\text{P}$ for trialkylphosphines vs the sum of Taft σ^* values for the three alkyl groups. Both plots exhibit a linear relationship, and the $\delta^{31}\text{P}$ chemical shift increases in frequency with increased branching on the $\alpha\text{-carbon}$ atom and with increased electron contribution to the phosphorus atom (26).

Figure 11.60 shows plots of $\delta^{31}\text{P}$ vs $\delta^{15}\text{N}$ for R-PH_2 vs R-NH_2 , $(\text{R-})_2\text{PH}$ vs $(\text{R-})\text{NH}$, and $(\text{R-})_3\text{P}$ vs $(\text{R-})_3\text{N}$. These plots show that both $\delta^{31}\text{P}$ and $\delta^{15}\text{N}$ increase in frequency with increased alkyl substitution on the P or N atoms and with increased electron contribution from the number of alkyl groups to the P and N atoms (26).

Figure 11.61 shows plots of the number of protons on the $\alpha\text{-C-P}$ atom(s) vs $\delta^{31}\text{P}$ for PH_3 , RPH_2 , and $(\text{R-})_2\text{PH}$ (26). The plots show that $\delta^{31}\text{P}$ increases in frequency in the order PH_3 , R-PH_2 , and $(\text{R-})_2\text{PH}$ and in the order of increased branching on the $\alpha\text{-C-P}$ atom(s).

Table 11.16 lists IR and NMR data for organophosphorus compounds (26). Figure 11.62 is a plot of the sum of Taft σ^* values for the alkyl groups of trialkylphosphine oxides vs $\delta^{31}\text{P}$. This plot shows that $\delta^{31}\text{P}$ increases in frequency with increased electron contribution to the P atom. Figure 11.63 is a plot of the sum of the number of protons on the $\alpha\text{-C-P}$ carbon atom(s) vs $\delta^{31}\text{P}$ for trialkylphosphine oxides. The $\delta^{31}\text{P}$ chemical shift increases in frequency with increased branching on the $\alpha\text{-C-P}$ carbon atom (26).

Figure 11.64 shows plots of $\nu \text{P=O}$ rotational conformers vs the sum of the protons on the $\alpha\text{-C-O-P}$ carbon atoms for trialkyl phosphates (26). Both plots show that $\nu \text{P=O}$ decreases in frequency as the branching is increased on the $\alpha\text{-C-O-P}$ carbon atom. Figure 11.65 shows plots of $\nu \text{P=O}$ rotational conformers vs $\delta^{31}\text{P}$ for trialkyl phosphates. Both $\nu \text{P=O}$ and $\delta^{31}\text{P}$ decrease in frequency with increased branching on the $\alpha\text{-C-O-P}$ carbon atom. Trialkyl phosphates exist as rotational conformers and exhibit $\nu \text{P=O}$ rotational conformers I and II at different frequencies; therefore, the P=O frequencies are affected by the molecular geometric configuration of the molecule because the electronic contribution of the O-alkyl groups to the P=O group is independent of the rotational molecular configuration of the trialkyl phosphate molecules.

Figures 11.66, 11.67, and 11.68 show plots of $\delta^{31}\text{P}$ vs the sum of the number of protons on the $\alpha\text{-C-O-P}$ carbon atoms for trialkyl phosphates, O,O,O-trialkyl phosphorothioates, and

O,O,O-trialkyl phosphoroselenates (26). In all cases $\delta^{31}\text{P}$ decreases in frequency with increased branching on the $\alpha\text{-C-O-P}$ carbon atom. In Fig. 11.66 the plot is essentially linear, but the plots in Figs. 11.67 and 11.68 show that the tert-butyl analogs deviate considerably from linearity. The electronegativity of oxygen, sulfur, and selenium decreases in the order 3.5; 2.5; and 2.4, respectively (32). The tetrahedral covalent radii of oxygen, sulfur, and selenium increases in the order 0.66; 1.04, and 1.14 Å, respectively (32). The $\delta^{31}\text{P}$ frequency difference between the isopropyl and tert-butyl analogs of the P=O, P=S and P=Se analogs are 7.3 ppm, 21.3 ppm, and 36.6 ppm, respectively. The difference in the electronegativity of S and Se is only 0.1, and the difference in the tetrahedral covalent radii between S and Se is 0.1 Å. These differences do affect the $\delta^{31}\text{P}$ chemical shifts of the tert-butyl analogs for O,O,O-tri-tert-butyl phosphorothioate and O,O,O-tri-tert-butyl phosphoroselenate. It is suggested that this difference in the $\delta^{31}\text{P}$ chemical shifts is caused by a steric effect of the tert-butyl groups. The steric effect most likely changes the PO_3 bond angles in both the P=S and P=Se tri-tert-butyl analogs.

Figure 11.69 shows plots of $\delta^{31}\text{P}$ vs the sum of the number of protons on the $\alpha\text{-C-P}$ carbon atoms and the $\alpha\text{-C-O-P}$ carbon atoms for $\text{RP}(=\text{O})(\text{OC}_2\text{H}_5)_2$ and $(\text{R})_2\text{P}=\text{O}(\text{OR})$. These plots show that $\delta^{31}\text{P}$ decreases in frequency with increased branching on the $\alpha\text{-C-O-P}$ carbon atoms, and increases in frequency with increased branching in the $\alpha\text{-C-P}$ carbon atom and by substitution of $(\text{CH}_3)_2\text{P}$ for $(\text{CH}_3)_1\text{P}$.

Figure 11.70 shows plots of $\delta^{31}\text{P}$ for $\text{RP}(=\text{O})(\text{OC}_2\text{H}_5)_2$ vs $\delta^{13}\text{C}=\text{O}$ for $\text{RC}(\text{O})(\text{OCH}_3)$ and $\delta^{31}\text{P}$ for $\text{CH}_3\text{P}(=\text{O})(\text{OR})_2$ vs $\delta^{13}\text{C}=\text{O}$ for $\text{CH}_3\text{C}(\text{O})(\text{OR})$. Both $\delta^{13}\text{C}=\text{O}$ and $\delta^{31}\text{P}$ decrease in frequency with decreased branching on the $\alpha\text{-C-P}$ carbon atom or $\alpha\text{-C-C}=\text{O}$ carbon atom and with increased branching on the $\alpha\text{-C-O-P}$ carbon atom or the $\text{O}=\text{C}-\text{O}-\text{C}$ α -carbon atom.

Figure 11.71 shows plots of $\delta^{31}\text{P}$ vs the sum of the protons on the $\alpha\text{-C-O-P}$ carbon atoms. These plots show that $\delta^{31}\text{P}$ for $(\text{RO})_2\text{P}(=\text{S})\text{H}$ analogs occurs at higher frequency (≈ 60 ppm) than it does for the corresponding analogs. Moreover, $\delta^{31}\text{P}$ decrease in frequency with increased branching in the $\alpha\text{-C-O-P}$ carbon atom (26).

The sulfur atom is less electronegative than the oxygen atom (2.5 vs 3.5), and, consequently, the P=O analogs occur at lower frequency than the P=S analogs.

Figure 11.72 is a plot of $\delta^{31}\text{P}$ for $(\text{RO})_2\text{P}(=\text{O})\text{H}$ analogs vs $\delta^{31}\text{P}$ for the corresponding $(\text{RO})_2\text{P}(=\text{S})\text{H}$ alkyl analogs. The two plots are for different $\delta^{31}\text{P}$ literature values (27,28). This plot shows that the $\delta^{31}\text{P}$ chemical shift values decrease in frequency with increased branching on the $\alpha\text{-C-O-P}$ carbon atom (26).

Figure 11.73 shows plots of the number of protons on the $\alpha\text{-C-P}$ carbon atoms vs $\delta^{31}\text{P}$ for $\text{RP}(=\text{O})\text{Cl}_2$ and $\text{RP}(=\text{S})\text{Cl}_2$ (26). The $\delta^{31}\text{P}$ chemical shift increases in frequency with increased branching on the $\alpha\text{-C-P}$ carbon atom. The $\delta^{31}\text{P}$ chemical shifts for the $\text{RP}(=\text{S})\text{Cl}_2$ analogs are larger than they are for the corresponding $\text{RP}(=\text{O})\text{Cl}_2$ analogs (26). Changes in the bond angles caused by steric factors of the alkyl group could be the cause of the increased $\Delta\delta^{31}\text{P}$ values with increased branching on the $\alpha\text{-C-P}$ carbon atom (P=O vs P=S analogs: CH_3 , 34.9 ppm; C_2H_5 , 42.4 ppm; and iso C_3H_7 , 46.6 ppm).

Figure 11.74 is a plot of $\delta^{31}\text{P}$ for $\text{RP}(=\text{S})\text{Cl}_2$ vs $\delta^{31}\text{P}$ for $\text{RP}(=\text{O})\text{Cl}_2$, and the plot shows an essentially linear relationship (26). Both $\delta^{31}\text{P}$ chemical shifts increase in frequency with increased branching on the $\alpha\text{-C-P}$ carbon atom.

Figure 11.75 is a plot of $\delta^{31}\text{P}$ for $\text{RP}(=\text{O})\text{F}_2$ vs the number of protons on the $\alpha\text{-C-P}$ carbon atom. The $\delta^{31}\text{P}$ chemical shift increases in frequency with increased branching on the $\alpha\text{-C-P}$ carbon atom.

Figure 11.76 is a plot of α $\delta^{31}\text{P}$ for $\text{RP}(=\text{S})\text{Br}(\text{OC}_3\text{H}_7\text{-iso})$ vs the number of protons on the $\alpha\text{-C-P}$ carbon atom and the number of protons on the $\alpha\text{-C-O-P}$ carbon atom. The $\delta^{31}\text{P}$ increases in frequency with increased branching on the α -carbon atoms.

Figure 11.77 shows plots of $\delta^{31}\text{P}$ vs the number of chlorine atoms joined to phosphorus for $\text{PCl}_{3-x}(\text{OR})_x$ (26). These plots show that $\delta^{31}\text{P}$ decreases in frequency with a decrease in the number of atoms joining to the phosphorus atom, and that the ethyl analogs occur at lower frequency than the corresponding methyl analogs (26).

Figure 11.78 shows plots of $\delta^{31}\text{P}$ for $\text{PX}_{3-n}\text{R}_n$ vs the number of protons on the $\alpha\text{-C-P}$ carbon atom(s) (26). These plots show that $\delta^{31}\text{P}$ decreases in frequency with decreased branching on the $\alpha\text{-C-P}$ carbon atom(s), and that $\delta^{31}\text{P}$ for the Br analog occurs at lower frequency than the corresponding $\delta^{31}\text{P}$ chemical shift for the corresponding Cl analog.

Figure 11.79 is a plot of $\delta^{31}\text{P}$ vs the number of protons on the $\alpha\text{-C-O-P}$ carbon atoms for $(\text{RO})_2\text{P}(=\text{O})\text{Cl}_2$ (26). This plot shows that $\delta^{31}\text{P}$ decreases in frequency with increased branching on the $\delta\text{-C-O-P}$ carbon atom.

Figure 11.80 shows plots of the number of Cl atoms joined to the P atom vs $\nu\text{P=O}$ frequencies for $\text{P}(=\text{O})\text{Cl}_3$ through $\text{P}(=\text{O})\text{Cl}_{3-x}(\text{OR})_x$ where R is CH_3 or C_2H_5 (26). In all cases $\nu\text{P=O}$ for rotational conformer I occurs at higher frequency than $\nu\text{P=O}$ for rotational conformer II. The $\nu\text{P=O}$ frequencies decrease in frequency as the number of Cl atoms joined to P are decreased. The $\nu\text{P=O}$ frequencies for the CH_3O analogs occur at higher frequency than those exhibited by the $\text{C}_2\text{H}_5\text{O}$ analogs.

Figure 11.81 is a plot of the number of Cl atoms joined to P vs $\nu\text{P=O}$ for $\text{P}(=\text{O})\text{Cl}_{3-x}[\text{N}(\text{CH}_3)_2]_x$. The $\nu\text{P=O}$ frequency decreases with the decrease in the number of Cl atoms joined to the P atom.

Figure 11.82 is a plot of $\delta^{31}\text{P}$ for $\text{P}(=\text{S})(\text{OR})_3$ vs $\delta^{31}\text{P}$ for the corresponding alkyl analogs of $\text{P}(=\text{O})(\text{OR})_3$ (26). The $\delta^{31}\text{P}$ chemical shifts decrease in frequency with increased branching on the $\alpha\text{-C-O-P}$ carbon atoms. The deviation from linearity for the tert-butyl analogs suggests that this results from a steric factor causing a change in the PO_3 bond angles.

Figure 11.83 is a plot of $\delta^{31}\text{P}$ for $\text{P}(=\text{Se})(\text{OR})_3$ vs $\delta^{31}\text{P}$ for the corresponding alkyl analogs of $\text{P}(=\text{O})(\text{OR})_3$ (26). The $\delta^{31}\text{P}$ chemical shifts decrease in frequency with increased branching on the $\alpha\text{-C-O-P}$ carbon atoms. Deviation from linearity for the tert-butyl analogs supports the analysis that this is the result of a steric factor causing a change in the PO_3 bond angles.

Figure 11.84 shows plots of $\delta^{31}\text{P}$ for $\text{RP}(=\text{O})\text{Cl}_2$ vs $\delta^{31}\text{P}$ for $\text{RP}(=\text{O})\text{Cl}_2$ vs $\delta^{31}\text{P}$ for corresponding alkyl analogs of $\text{RP}(=\text{O})\text{F}_2$. The double plot presents the $\delta^{31}\text{P}$ range given in the references for the $\text{RP}(=\text{O})\text{Cl}_2$ analogs. The $\delta^{31}\text{P}$ chemical shift decreases in frequency with decreased branching on the $\alpha\text{-C-O-P}$ carbon atom (26).

A SUMMARY OF CORRELATIONS FOR THE PHOSPHORUS COMPOUNDS

1. Increased branching on the $\alpha\text{-C-P}$ carbon atom causes $\delta^{31}\text{P}$ to occur at increasingly higher frequency in a systematic manner. The $\delta^{31}\text{P}$ chemical shift increases in frequency with increased electron release of the alkyl groups.

2. Correlations exist between $\delta^{31}\text{P}$ and $\delta^{15}\text{N}$ for corresponding alkyl analogs of RPH_2 vs RNH_2 , $(\text{R})_2\text{PH}$ vs $(\text{R})_2\text{NH}$, and $(\text{R})_3\text{P}$ vs $(\text{R})_3\text{N}$.
3. The $\nu \text{P}=\text{O}$ frequency and $\delta^{31}\text{P}$ frequency decrease with increased branching on the $\alpha\text{-C-O-P}$ carbon atoms for $\text{P}(\text{=O})(\text{OR})$ analogs, and a correlation exists between $\nu \text{P}=\text{O}$ and $\delta^{31}\text{P}$.
4. The chemical shift $\delta^{31}\text{P}$ decreases in frequency with increased branching on the $\alpha\text{-C-O-P}$ carbon atoms for $\text{P}(\text{=S})(\text{OR})_3$ and $\text{P}(\text{=Se})(\text{OR})_3$.
5. The chemical shift $\delta^{31}\text{P}$ increases in the order $\text{P}=\text{O}$, $\text{P}=\text{S}$, and $\text{P}=\text{Se}$ for trialkyl esters, with the exception of the tert-butyl analog. It is suggested that the tert-butyl analogs sterically cause the $(\text{RO})_3\text{P}=\text{S}$ and $(\text{RO})_3\text{P}=\text{Se}$ bond angles to change so that $\delta^{31}\text{P}$ does not change in a linear manner, as in the case of the lesser branched alkyl groups.
6. Correlations exist between $\delta^{31}\text{P}$ for comparable $(\text{RO})_3\text{P}=\text{O}$, $(\text{RO})_3\text{P}=\text{S}$ and $(\text{RO})_3\text{P}=\text{Se}$ alkyl analogs.
7. The chemical shift value for $\delta^{31}\text{P}$ is higher for R-P than for R-O-P .
8. The $\nu \text{P}=\text{O}$ frequency decreases with increased substitution of RO for Cl in the series $\text{P}(\text{=O})\text{Cl}_{3-x}(\text{OR})_x$. The decrease in $\nu \text{P}=\text{O}$ frequency is in the order of decreasing electronegativity of the sum of the Cl atoms and RO groups.
9. For RPX_2 analogs, $\delta^{31}\text{P}$ decreases in frequency in the order Cl , Br , and I , which is in the order of decreasing electronegativity. However, $\delta^{31}\text{P}$ for $\text{RP}(\text{=O})\text{Cl}_2$ occurs at higher frequency than $\delta^{31}\text{P}$ for corresponding $\text{RP}(\text{=O})\text{F}_2$ analogs.
10. Correlations exist between $\delta^{31}\text{P}$ for $\text{RP}(\text{=O})(\text{OC}_2\text{H}_5)_2$ vs $\delta^{13}\text{C}=\text{O}$ for $\text{RC}(\text{=O})(\text{OCH}_3)$ and $\text{CH}_3\text{P}(\text{=O})(\text{OR})_2$ vs $\delta^{13}\text{C}=\text{O}$ for $\text{CH}_3\text{C}(\text{=O})(\text{OR})$.

ANISOLES

Goldman *et al.* have reported that ν asym. $\phi\text{-O-C}$ for *p*-substituted anisoles increases in frequency with the electron withdrawing power of the *p*-substituent (30). Brown and Okamoto have reported a linear relationship between ν asym. $\phi\text{-O-C}$ and σ^+ values (33).

Tables 11.17 and 11.17a list NMR and IR data for substituted anisoles, respectively (29). Figure 11.85 is a plot of ν asym. $\phi\text{-O-C}$ vs $\delta^{13}\text{C-1}$ for 4-*x*-anisoles. This plot shows that, in general, both ν asym. $\phi\text{-O-C}$ and $\delta^{13}\text{C-1}$ increase in frequency, progressing in the series 4-methoxy anisole through 4-nitroanisole (29).

Figure 11.86 is a plot of σ_{R° values vs $\delta^{13}\text{C-1}$ for 3-*x*- and 4-*x*-anisoles (29). With the exception of point 22 (4-phenoxyanisole), there is a pseudolinear relationship between $\delta^{13}\text{C-1}$ and Taft σ_{R° . The plot in Fig. 11.86 using $\delta^{13}\text{C-1}$ of 150.4 ppm indicates that $\delta^{13}\text{C-1}$ is misassigned. Assignment of $\delta^{13}\text{C-1}$ at 156.0 ppm is indicated, and thus, we then assign the $\delta^{13}\text{C-4}$ at 150.4 ppm for 4-phenoxyanisole.

Figure 11.87 is a plot of $\delta^{13}\text{C-1}$ vs Hammett σ values for 3-*x* and 4-*x*-anisoles. The point 22 is for 4-phenoxyanisole, and it appears that the correct assignment for $\delta^{13}\text{C-1}$ for this compound is 156.0 ppm rather than 150.4 ppm. The 150.4 ppm apparently results from $\delta^{13}\text{C-4}$ (29).

Figure 11.88 is a plot of Taft σ_{R° values vs $\delta^{13}\text{C-1}$ for 4-*x*-anisoles (29), and this plot exhibits a pseudolinear relationship between these two parameters. Figure 11.89 is a plot of Taft σ_{R° values vs ν asym. $\phi\text{-O-C}$ for 4-*x*-anisoles (26), and this plot shows that in general ν asym. $\phi\text{-O-C}$ increases in frequency as the Taft σ_{R° increases in value.

Figure 11.90 is a plot of $\delta^{13}\text{C-1}$ vs Hammett σ_p values for 4-x-anisoles, and this plot exhibits a pseudolinear relationship between these two parameters. The $\delta^{13}\text{C-1}$ chemical shift increases in frequency as Hammett σ_p values increase.

Figure 11.91 is a plot of $\delta^{13}\text{C-1}$ vs $\delta^{13}\text{C-5}$ for 2-x-anisoles (29), and this plot shows a pseudolinear relationship between these two values. This plot includes 2-nitroanisole, the literature assignment for $\delta^{13}\text{C-5}$ was given as 134.4 ppm, and $\delta^{13}\text{C-3}$ was given as 125.3 ppm. The plot in Fig. 11.91 indicates that the $\delta^{13}\text{C-3}$ and $\delta^{13}\text{C-5}$ assignments should be reversed, and we have done so in the plot shown here.

MONO-SUBSTITUTED BENZENES

Table 11.18 lists IR and NMR data for mono-x-benzenes (4,34,35). Figure 11.92 is a plot of $\delta^{13}\text{C-4}$ for mono-substituted benzenes vs Taft σ_{R^o} values, and these parameters correlate in a pseudolinear manner. The significance of Taft σ_{R^o} is that there is a significant contribution of π electrons to the C-4 atom from the atom or group joined to the C-1 atom (4).

Figure 11.93 is a plot of the out-of-plane hydrogen deformation mode I vs Taft σ_{R^o} values, and these parameters correlate in a pseudolinear manner (4).

Figure 11.94 is a plot of the out-of-plane hydrogen deformation mode III vs Taft σ_{R^o} values, and these parameters correlate in a pseudolinear manner (4).

Figures 11.95 and 11.96 plot the out-of-plane hydrogen deformation modes I and III vs $\delta^{13}\text{C-4}$, respectively, and these parameters show that modes I and III increase in frequency as $\delta^{13}\text{C-4}$ increases in frequency (4).

4-X AND 4,4'-X,X'-BIPHENYLS IN CHCl_3 SOLUTIONS

Table 11.19 lists NMR data for 4-x and 4,4'-x,x-biphenyls in CHCl_3 solution (3). Figure 11.97 is a plot of $\delta^{13}\text{C-1}$ vs Taft σ_{R^o} for 4-x, and 4,4'-x,x-biphenyls and, in general, $\delta^{13}\text{C-1}$ increases in frequency as the Taft σ_{R^o} values increase (4).

TETRAMETHYLUREA (TMU)

Table 11.20 lists NMR data for 1 wt./vol. % tetramethylurea (TMU) in mol % $\text{CHCl}_3/\text{CCl}_4$ solutions. Figure 11.98 is a plot of $\delta^{13}\text{C=O}$ for TMU vs mol % $\text{CHCl}_3/\text{CCl}_4$ (36). Figure 11.98 is a plot of $\delta^{13}\text{C=O}$ for TMU vs mol % $\text{CHCl}_3/\text{CCl}_4$. This plot shows that $\delta^{13}\text{C=O}$ increases in frequency (shifts down field) in a nonlinear manner as the mol % is increased from 0 to 100. These data indicate that there is changing solute-solvent interaction between TMU and $\text{CHCl}_3/\text{CCl}_4$ as the mol % $\text{CHCl}_3/\text{CCl}_4$ is increased from 0 to 100.

Figure 11.99 is a plot of $\nu \text{C=O}$ (37) vs $\delta^{13}\text{C=O}$ for TMU in 0–100 mol % $\text{CHCl}_3/\text{CCl}_4$ solutions. This plot shows that $\nu \text{C=O}$ decreases in frequency while $\delta^{13}\text{C=O}$ increases in frequency as the mol % $\text{CHCl}_3/\text{CCl}_4$ goes from 0–100 mol % $\text{CHCl}_3/\text{CCl}_4$ (36).

Figure 11.100 is a plot of $\delta^{13}\text{C=O}$ for TMU vs $\delta^{13}\text{CH}_3$ in 0–100 mol % $\text{CHCl}_3/\text{CCl}_4$ solutions. This plot shows that $\delta^{13}\text{C=O}$ increases in frequency (shifts down-field) while

$\delta^{13}\text{CH}_3$ decreases in frequency (shifts up-field) as the mol % $\text{CHCl}_3/\text{CCl}_4$ is increased from 0 to 100 (34). Because the $\delta^{13}\text{C}=\text{O}$ chemical shift increases in frequency in going from CCl_4 solution to CHCl_3 solution, the CCl_4 deshields the carbonyl carbon atom more than CHCl_3 does. Simultaneously, CHCl_3 shields the CH_3 carbon atoms of atoms of TMU more than CCl_4 does, because $\delta^{13}\text{CH}_3$ decreases in frequency as the mol % $\text{CHCl}_3/\text{CCl}_4$ is increased.

Table 11.21 lists NMR data for 1 wt./vol. % TMU in various solvents (36). Figure 11.101 is a plot of $\delta^{13}\text{C}=\text{O}$ for TMU vs the solvent acceptor number (AN) for each of the 21 solvents. The solvents are presented in order, 1 through 21, in Table 11.21. This plot shows that in general there is a pseudolinear relationship between $\delta^{13}\text{C}=\text{O}$ and AN, but the scatter of data points shows that this is not a precise indicator of the $\delta^{13}\text{C}=\text{O}$ chemical shifts. If the AN values were a precise indicator of $\delta^{13}\text{C}=\text{O}$ frequencies, the $\delta^{13}\text{C}=\text{O}$ chemical shift for TMU in hexane would be expected to occur at lower frequency by approximately 0.8 ppm by extrapolation from the pseudolinear relationship exhibited by most of the solvents, AN values, and the corresponding $\delta^{13}\text{C}=\text{O}$ frequencies.

These results indicate that the AN values do not take into account the steric effect of the solute and solvent, which alters the distance between the sites of solute-solvent interaction. Thus, there is not a comparable solute-solvent interaction between different but similar carbonyl compounds in the same solvent due to steric differences of the solute and solvent.

Figure 11.102 is a plot of $\delta^{13}\text{C}=\text{O}$ for TMU in each of the solvents vs the difference between $\delta^{13}\text{C}=\text{O}$ for TMU in acetic acid solution and each of the other solvents (see Table 11.21). There is no chemical significance in this linear plot, because this type of mathematical treatment of any data set always produces a linear relationship. It does help show that the AN values are not a precise indicator of $\delta^{13}\text{C}=\text{O}$ chemical shifts. As examples: (A) The AN values for solvent 7 (tert-butyl alcohol) and solvent 14 (acetone) are 29.1 and 12.5, respectively; (B) The AN values for solvent 6 (isopropyl alcohol) and solvent 11 (acetonitrile) are 33.5 and 18.9, respectively; and (C) The AN values for solvent 13 (nitrobenzene), solvent 17 (benzene), and solvent 18 (methyl tert-butyl ether) are 14.8, 8.2, and 5.0, respectively. The $\delta^{13}\text{C}=\text{O}$ frequencies for (A), (B), and (C) are 166.0, 166.1, and 165.1 ppm, respectively, yet the AN values for the solvents vary considerably. These data clearly show that the AN values are not a precise indicator of solute-solvent interactions (36).

DIALKYLKETONES

Table 11.22 lists NMR data for dialkylketones in various solvents at 1 wt./vol. % concentrations (36). Figure 11.103 is a plot of $\delta^{13}\text{C}=\text{O}$ for dialkylketones at 1 wt./vol. % in different solvents vs the AN value for each of the solvents. Plots 1–6 show a pseudolinear relationship for each of the dialkylketones and $\delta^{13}\text{C}=\text{O}$ increases in frequency with increased branching on the α -carbon atoms. In addition, plots 1–6 and 1'–6' yield separate relationships. Plots 1'–6' are $\delta^{13}\text{C}=\text{O}$ frequencies for these dialkylketones in each of the four alcohols included in this study, and these plots are distinctly different from plots 1–6. An IR study of these same dialkylketones in solution with each of these four alcohols has shown that these ketones exist in alcoholic solution in two forms. These are: an intermolecularly hydrogen-bonded form $[(\text{R})_2\text{C}=\text{O} \cdots \text{HOR}]$, and a form in which $(\text{R})_2\text{C}=\text{O}$ is not intermolecularly hydrogen bonded, but surrounded by intermolecularly

hydrogen-bonded alcohol molecules (38). This is why dialkylketones in alkyl alcohols differ from those in nonalcoholic solution.

Plots 1–6 also show that $\delta^{13}\text{C}=\text{O}$ for these dialkylketones increases in frequency as the electron contribution of the alkyl groups increases, progressing in the series dimethyl ketone through di-tert-butyl ketone.

Figure 11.104 shows plots of $\delta^{13}\text{C}=\text{O}$ (solvent) vs the $\delta^{13}\text{C}=\text{O}$ chemical shift difference between each dialkylketone in methanol and the same ketone in each of the other solvents (36). It is noted that the $\delta^{13}\text{C}=\text{O}$ chemical shifts for these dialkylketones increase in the order dimethyl ketone through ethyl isopropyl ketone, di-tert-butyl ketone, and di-isopropyl ketone. The inductive donation of electrons to the carbonyl group increases in the order dimethyl ketone through di-tert-butyl ketone. The di-tert-butyl ketone is out of order in this sequence because the steric effects of the tert-butyl group prevent a closer solute-solvent interaction with the carbonyl group as in the case of di-isopropyl ketone. Further support for this supposition is gained by study of these ketones in the four alcohols. One would expect the strongest intermolecular hydrogen bond ($\text{C}=\text{O}\cdots\text{HO}$) to be formed between methanol and di-tert-butyl ketone. However, as methanol is the reference point in each plot, it does not provide support for the steric factor supposition. Comparison of the points on the plots for alcohols 2, 3, and 6 show that change for $\delta^{13}\text{C}=\text{O}$ (methanol) minus $\delta^{13}\text{C}=\text{O}$ (ethyl alcohol) is the least for di-tert-butyl ketone in going from solution in methanol to solution in ethanol, and the change is more in going from solution in isopropyl alcohol and tert-butyl alcohol. With the exception of diethyl ketone in benzonitrile, in going from solution in methanol to solution in any one of the other solvents, the $\delta^{13}\text{C}=\text{O}$ frequency changes least in the case of di-tert-butyl ketone. These $\delta^{13}\text{C}=\text{O}$ frequency shifts are what is expected when steric factors of the solute and solvent affect the distance between the sites of the solute-solvent interaction. The larger the steric factor, the less solute-solvent interaction regardless of the electrophilicity of the solvent and/or the acidity of the OH protons (36).

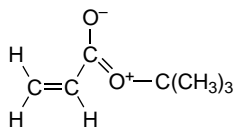
ACETATES

Table 11.23 lists NMR data for alkyl acetates and phenyl acetate 1 wt./vol. % in various solvents (36). Figure 11.105 is a plot of $\delta^{13}\text{C}=\text{O}$ for alkyl acetates and phenyl acetate vs the difference of $\delta^{13}\text{C}=\text{O}$ in methanol and $\delta^{13}\text{C}=\text{O}$ in each of the other solvents (36). The numbers in each plot correspond to a particular solvent, and it can be seen that with the exception of methyl alcohol, the difference values for $\delta^{13}\text{C}=\text{O}$ are not the same for each of the alkyl acetates and phenyl acetate. If the AN value for a solvent is constant, some other factor must be causing the change in the difference values for $\delta^{13}\text{C}=\text{O}$ for each of the other acetates. This other factor is a steric factor, which causes the distance in space between sites of solute and solvent interaction to vary in the acetates studied.

ACRYLATES AND METHACRYLATES

Table 11.24 lists IR and NMR data for alkyl acrylates and alkyl methacrylates in CCl_4 and CHCl_3 solution (39). The $\nu \text{C}=\text{O}$ for alkyl acrylates in mol % $\text{CHCl}_3/\text{CCl}_4$ solutions continuously

decreases, from 1722.9–1734.1 cm^{-1} in CCl_4 to 1713.8–1724.5 cm^{-1} in CHCl_3 solution while $\delta^{13}\text{C}=\text{O}$ continually increases in frequency from 164.2–165.2 ppm in CCl_4 solution to 165.7–166.7 ppm in CHCl_3 solution (39). The $\nu \text{C}=\text{O}$ frequency for alkyl methacrylates is lower than the frequencies for the corresponding alkyl acrylates. This decrease in $\nu \text{C}=\text{O}$ frequency is the result of the electron contribution of the CH_3 group to the $\text{C}=\text{O}$ group, which weakens the $\text{C}=\text{O}$ bond via $\text{C}-\text{O}$ and thus causes the $\nu \text{C}=\text{O}$ mode to vibrate at a lower frequency. The $\nu \text{C}=\text{O}$ for alkyl methacrylates in mol % $\text{CHCl}_3/\text{CCl}_4$ solutions continuously decrease in frequency from 1719.5–1726.0 cm^{-1} in CCl_4 solution to 1709.5–1718.0 cm^{-1} in CHCl_3 solution, while $\delta^{13}\text{C}=\text{O}$ continuously increase in frequency from 165.6–166.7 ppm in CCl_4 solution to 167.1–167.8 ppm in CHCl_3 solution. Moreover, the $\delta^{13}\text{C}=\text{O}$ frequencies for the alkyl methacrylates are higher than those for the corresponding alkyl acrylate analog. Methyl acrylate exhibits the highest $\nu \text{C}=\text{O}$ frequency and highest $\delta^{13}\text{C}=\text{O}$ chemical shift, while tert-butyl acrylate exhibits the lowest $\delta^{13}\text{C}=\text{O}$ chemical shift for the seven alkyl acrylates included in the study. This difference is caused by the larger inductive-mesomeric contribution of the tert-butyl group to the carbonyl group relative to the contribution of the methyl group to the carbonyl group:



Both $\nu \text{C}=\text{O}$ and $\delta^{13}\text{C}=\text{O}$ for alkyl methacrylates shift in a manner comparable to that shown for comparable alkyl acrylates. The behavior of $\nu \text{C}=\text{O}$ and $\delta^{13}\text{C}=\text{O}$ is a function of the electron density on the carbonyl carbon atom. As the electron density on the carbonyl carbon atom increases, both $\nu \text{C}=\text{O}$ and $\delta^{13}\text{C}=\text{O}$ decrease in frequency.

The $\text{C}=\text{O}$ group in CHCl_3 solution is intermolecularly hydrogen bonded ($\text{C}=\text{O} \cdots \text{HCCl}_3$) and surrounded by other CHCl_3 molecules and the $\text{C}=\text{O}$ groups are less shielded by Cl atoms when in CCl_4 solutions. Consequently, the $\delta^{13}\text{C}=\text{O}$ chemical shift occurs at higher frequency in CHCl_3 than in CCl_4 solution. Intermolecular hydrogen bonding ($\text{C}=\text{O} \cdots \text{HCCl}_3$) causes the $\text{C}=\text{O}$ mode to vibrate at lower frequency in CHCl_3 solution than in CCl_4 solution. Other factors that affect both $\nu \text{C}=\text{O}$ and $\delta^{13}\text{C}=\text{O}$ are attributed to the reaction field of the solvent system and steric factors of the solute. As the reaction field is increased in going from 0 to 100 mol % $\text{CHCl}_3/\text{CCl}_4$, the $\nu \text{C}=\text{O}$ frequency is steadily decreased and $\delta^{13}\text{C}=\text{O}$ is steadily increased (39).

REFERENCES

1. Nyquist, R. A. (1986). *IR and NMR Spectral Data-Structure Correlations for the Carbonyl Group*. Philadelphia: Sadtler.
2. Nyquist, R. A. (1993). *Appl. Spectrosc.* 47: 411.
3. *The Sadtler Standard Collection of NMR Carbon-13 NMR Spectra*. Philadelphia: Sadtler Research Laboratories.
4. Nyquist, R. A. and Hasha, D. L. (1991). *Appl. Spectrosc.* 45: 849.
5. Kalinowski, H. O., Berger, S., and Braun, S. (1988). *Carbon-13 NMR Spectroscopy*. New York: John Wiley & Sons, p. 313.
6. Nyquist, R. A. (1963). *Spectrochim. Acta* 19: 1595.
7. Nyquist, R. A., Settineri, S. E., and Luoma, D. A. (1991). *Appl. Spectrosc.* 45: 1641.

8. Nyquist, R. A. (1984). *The Interpretation of Vapor-Phase Infrared Spectra: Group Frequency Data*. Vol. 1, Philadelphia: Sadtler Res. Labs.
9. Nyquist, R. A., Putzig, C. L., and Hasha, D. L. (1989). *Appl. Spectrosc.* **43**: 1049.
10. Nyquist, R. A. and Luoma, D. A. (1991). *Appl. Spectrosc.* **45**: 1501.
11. Nyquist, R. A. (1990). *Appl. Spectrosc.* **44**: 438.
12. Nyquist, R. A., Streck, R., and Jeschek, G. (1996). *J. Mol. Struct.* **377**: 113.
13. Bellamy, L. J. (1975). *The Infrared Spectra of Complex Molecules*. New York: John Wiley & Sons; p. 295.
14. Rao, C. N. R. and Venkataraghavan, R. (1961). *Can. J. Chem.* **39**: 1757.
15. Deady, L., Katritzky, A. R., Shanks, R. A., and Topsom, R. D. (1973). *Spectrochim. Acta* **29A**: 115.
16. Saito, T., Yamakawa, M., and Takasuka, M. (1981). *J. Mol. Spectrosc.* **90**: 359.
17. Nyquist, R. A. (1987). *Appl. Spectrosc.* **41**: 904.
18. Nyquist, R. A. (1988). *Appl. Spectrosc.* **42**: 624.
19. Witanowski, M., Steaniak, L., and Webb, G. A. (1981). *Annual Reports on NMR Spectroscopy*. Vol. 11B, Nitrogen NMR Spectroscopy. New York: Academic Press, p. 301.
20. *Sadtler Research Laboratories Standard Carbon-13 NMR Spectra*.
21. Witanowski, M., Steaniak, L., and Webb, G. A. (1981). *Annual Reports on NMR Spectroscopy*. Vol. 11b, Nitrogen NMR Spectroscopy. New York: Academic Press, p. 385.
22. Hirschmann, R. P., Kniseley, R. N., and Fassel, V. A. (1965). *Spectrochim. Acta* **21**: 2125.
23. Taft, Jr., R. W. (1956). in *Steric Effects in Organic Chemistry*. M. S. Newman, ed., New York: J. Wiley & Sons, Inc., p. 590.
24. Nyquist, R. A. and Jewett, G. L. (1992). *Appl. Spectrosc.* **46**: 841.
25. Witanowski, M., Steaniak, L., and Webb, G. A. (1981). *Annual Reports on NMR Spectroscopy*, Volume 11B, Nitrogen NMR Spectroscopy. New York: Academic Press, p. 305.
26. Nyquist, R. A. (1988). *Appl. Spectrosc.* **42**: 854.
27. Mavel, G. (1973). *Annual Reports on NMR Spectroscopy, NMR Studies of Phosphorus Compounds (1965–1969)*, Vol. 5B, E. F. Mooney, ed., London/New York: Academic Press, pp. 103–288.
28. Mark, V., Dungan, C. H., Crutchfield, M. M., and Van Wazer, J. R. (1967). Compilation of ^{31}P NMR Data. in *Topics in Phosphorus Chemistry*, Vol. 5, Chap. 4, M. Grayson and E. J. Griffiths, eds., New York: Wiley Interscience, pp. 227–447.
29. Nyquist, R. A. (1991). *Appl. Spectrosc.* **45**: 1649.
30. Goldman, G. K., Lehman, H., and Rao, C. N. R. (1960). *Can. J. Chem.* **38**: 171.
31. Nyquist, R. A. and Potts, W. J. (1972). Vibrational Spectroscopy of Phosphorus Compounds. in *Chemical Analysis Series, Analytical Chemistry of Phosphorus Compounds*. M. Holman, ed., New York: John Wiley Interscience, pp. 189–293.
32. L. Pauling (1948). *The Nature of the Chemical Bond*. Ithaca, NY: Cornell University Press, pp. 60, 179.
33. Brown, H. C. and Okamoto, Y. J. (1958). *J. Am. Chem. Soc.* **80**: 4979.
34. Nyquist, R. A. (1984). *The Interpretation of Vapor-Phase Infrared Spectra: Group Frequency Data*. Vol. 1, Philadelphia: Sadtler Res. Labs., p. A-17.
35. Breitmaier, E. and Voelter, W. (1987). *Carbon-13 NMR Spectroscopy*. Federal Republic of Germany: VCH, Weinheim, p. 256.
36. Nyquist, R. A., Steck, R., and Jeschek, G. (1996). *J. Mol. Struct.* **377**: 113.
37. Nyquist, R. A. and Luoma, D. A. (1991). *Appl. Spectrosc.* **45**: 1491.
38. Nyquist, R. A. (1994). *Vib. Spectrosc.* **7**: 1.
39. Nyquist, R. A. and Streck, R. (1995). *Spectrochim. Acta* **51A**: 475.

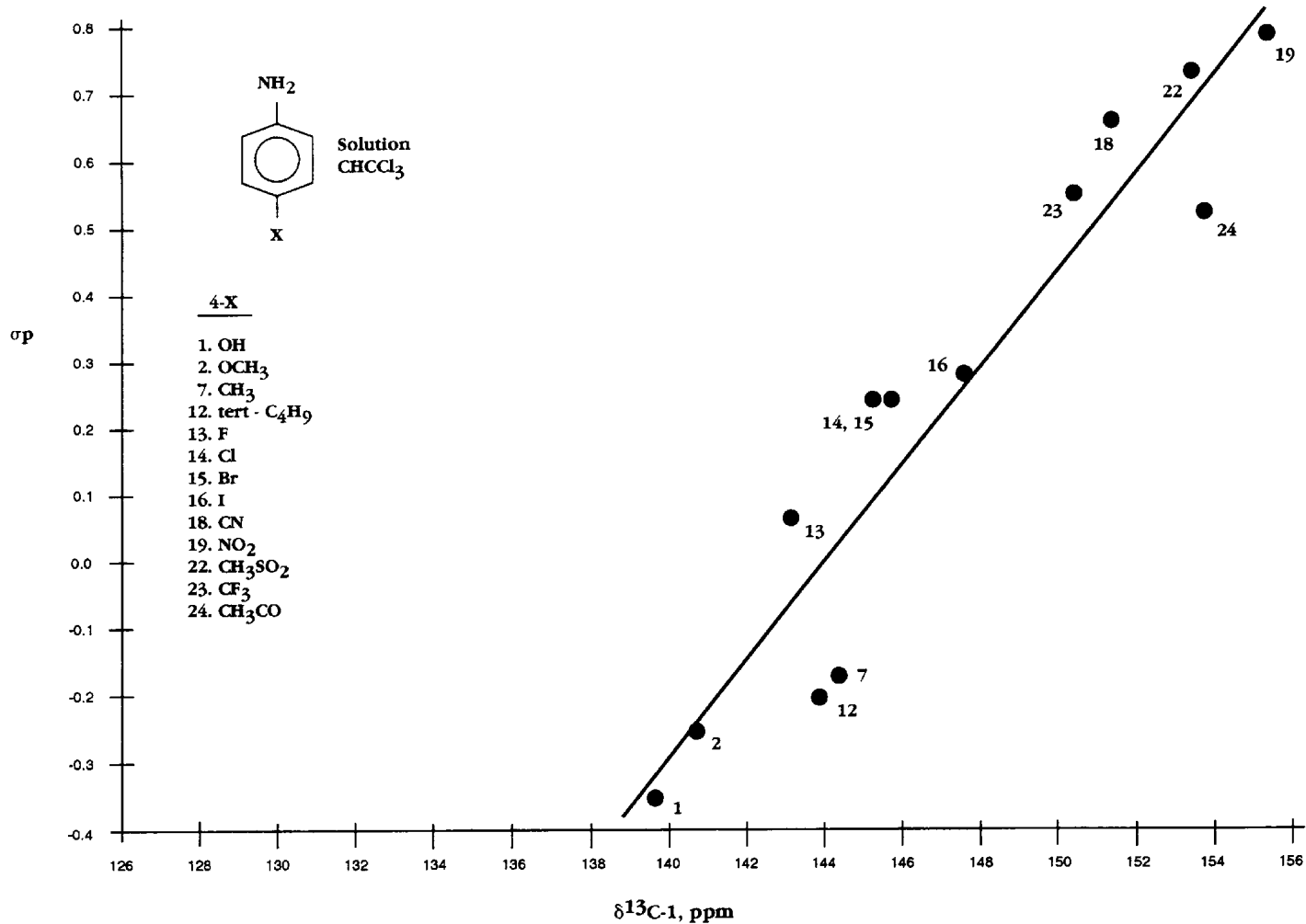


FIGURE 11.1 A plot of the NMR $\delta^{13}\text{C-1}$ chemical shift data for 4-x-anilines in CHCl_3 solution vs Hammett σ_p values for the 4-x atom or group.

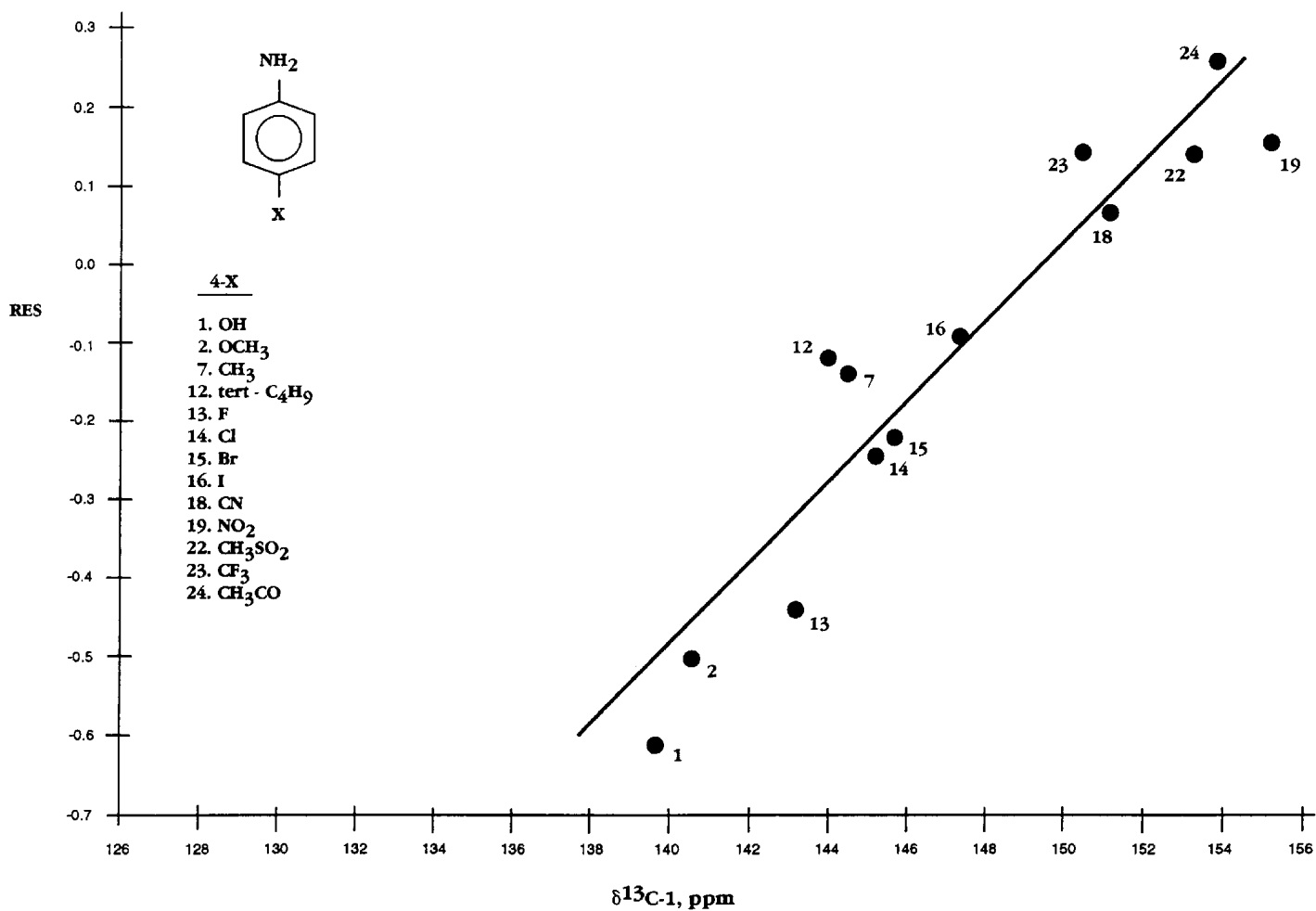


FIGURE 11.2 A plot of the NMR $\delta^{13}\text{C-1}$ chemical shift data for 4-x-anilines in CHCl_3 solution vs Taft σ_R values for the 4-x atom or group.

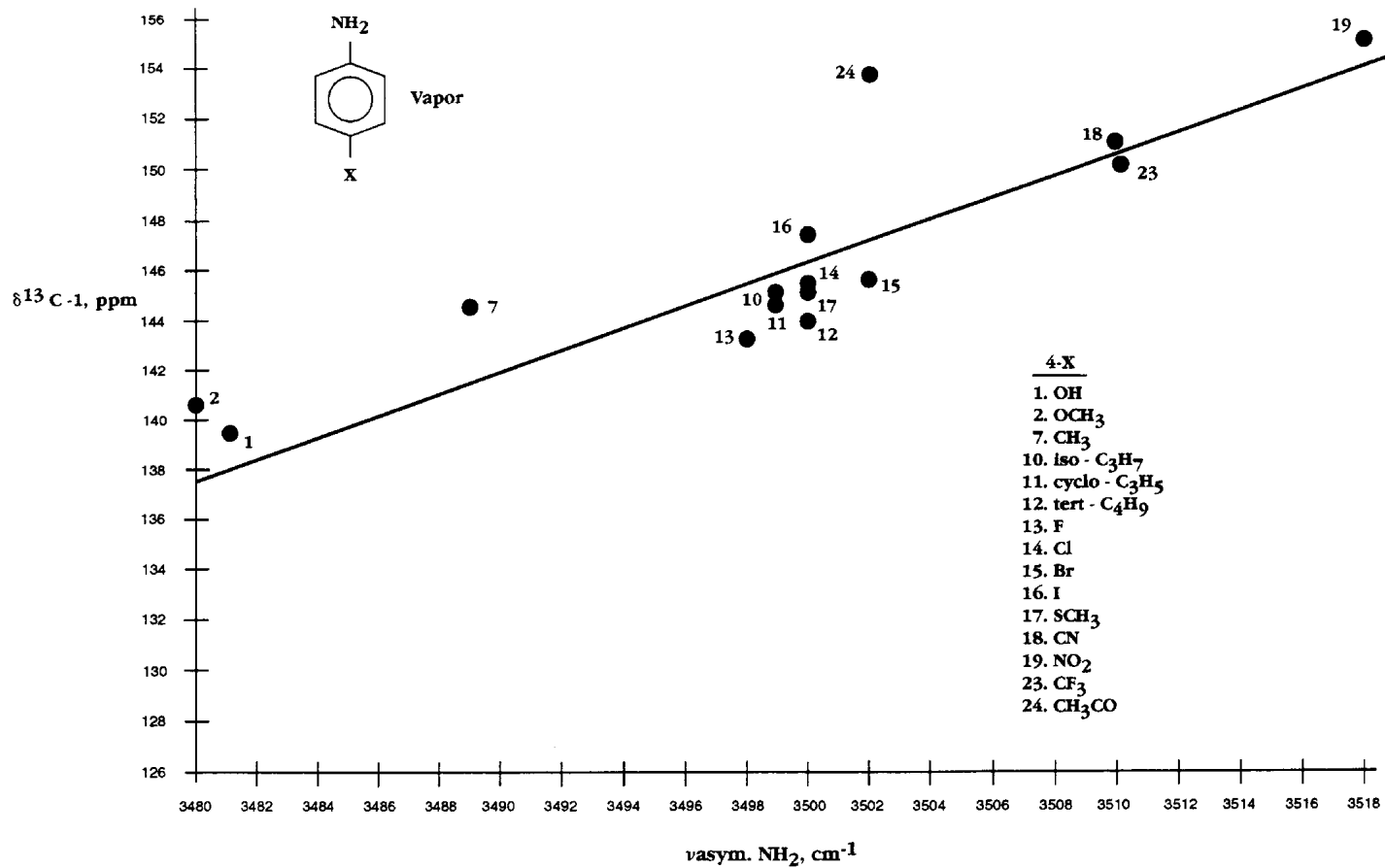


FIGURE 11.3 A plot of $\nu_{\text{asym. NH}_2}$ frequencies for 4-x-anilines in the vapor phase vs $\delta^{13}\text{C-1}$ chemical shift data for 4-x-anilines in CHCl_3 solution.

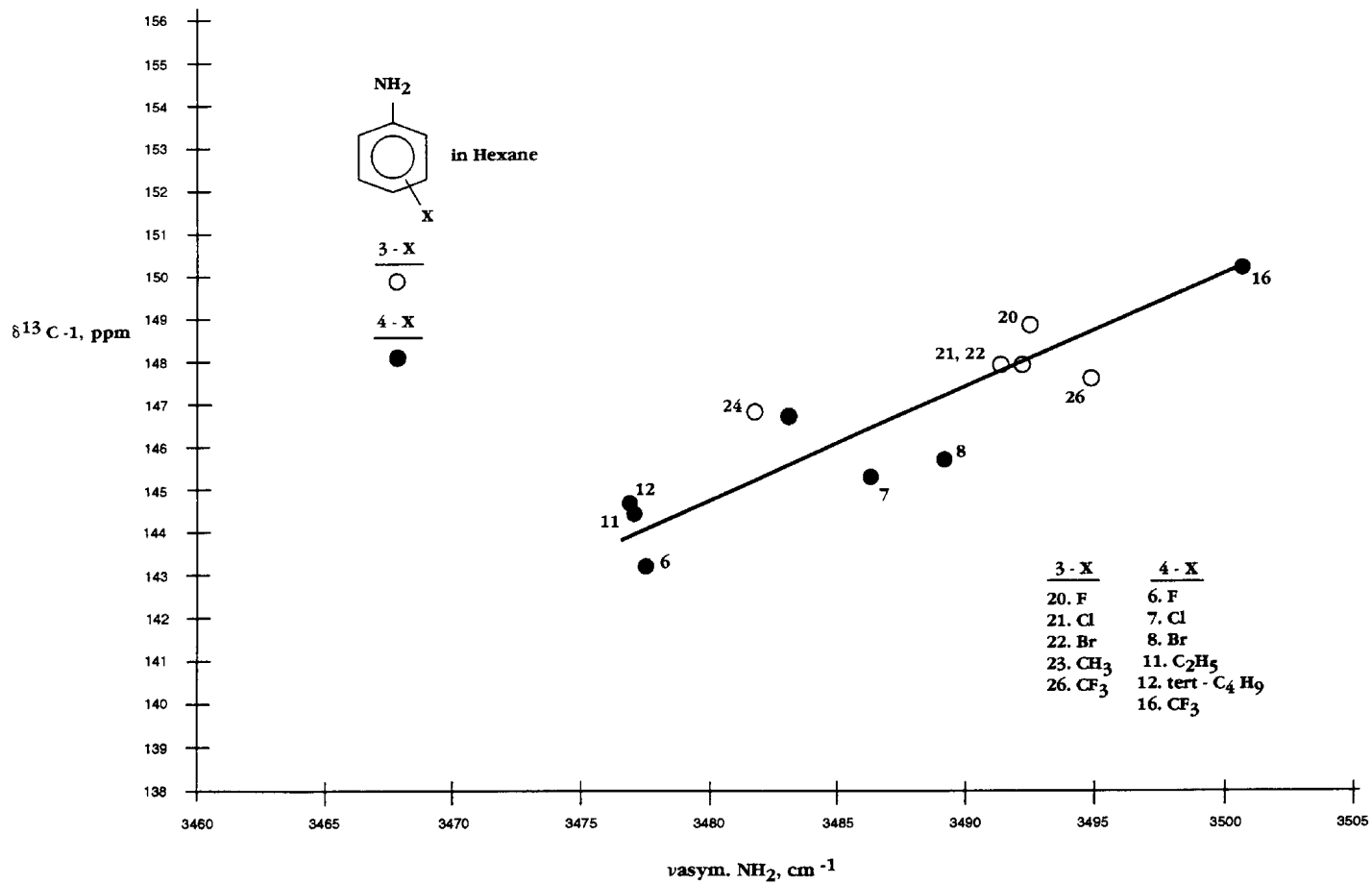


FIGURE 11.4 A plot of ν asym. NH₂ frequencies for 3-x- and 4-x-anilines in hexane solution vs $\delta^{13}\text{C-1}$ chemical shift data for 3-x- and 4-x-anilines in CHCl₃ solution.

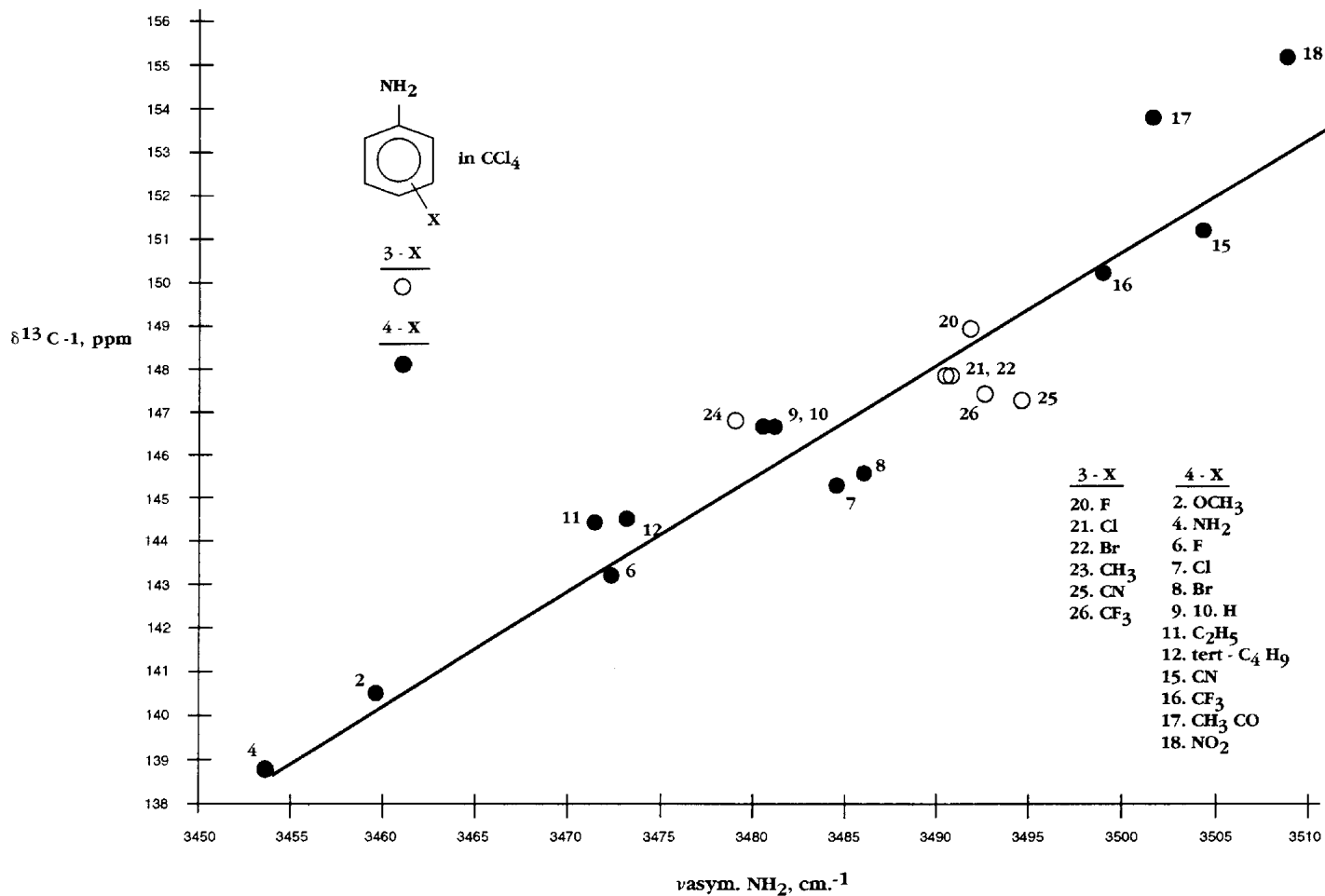


FIGURE 11.5 A plot of $\nu_{\text{asym. NH}_2}$ frequencies for 3-x- and 4-x-anilines in CCl_4 solution vs $\delta^{13}\text{C}-1$ chemical shift data for 3-x- and 4-x-anilines in CHCl_3 solution.

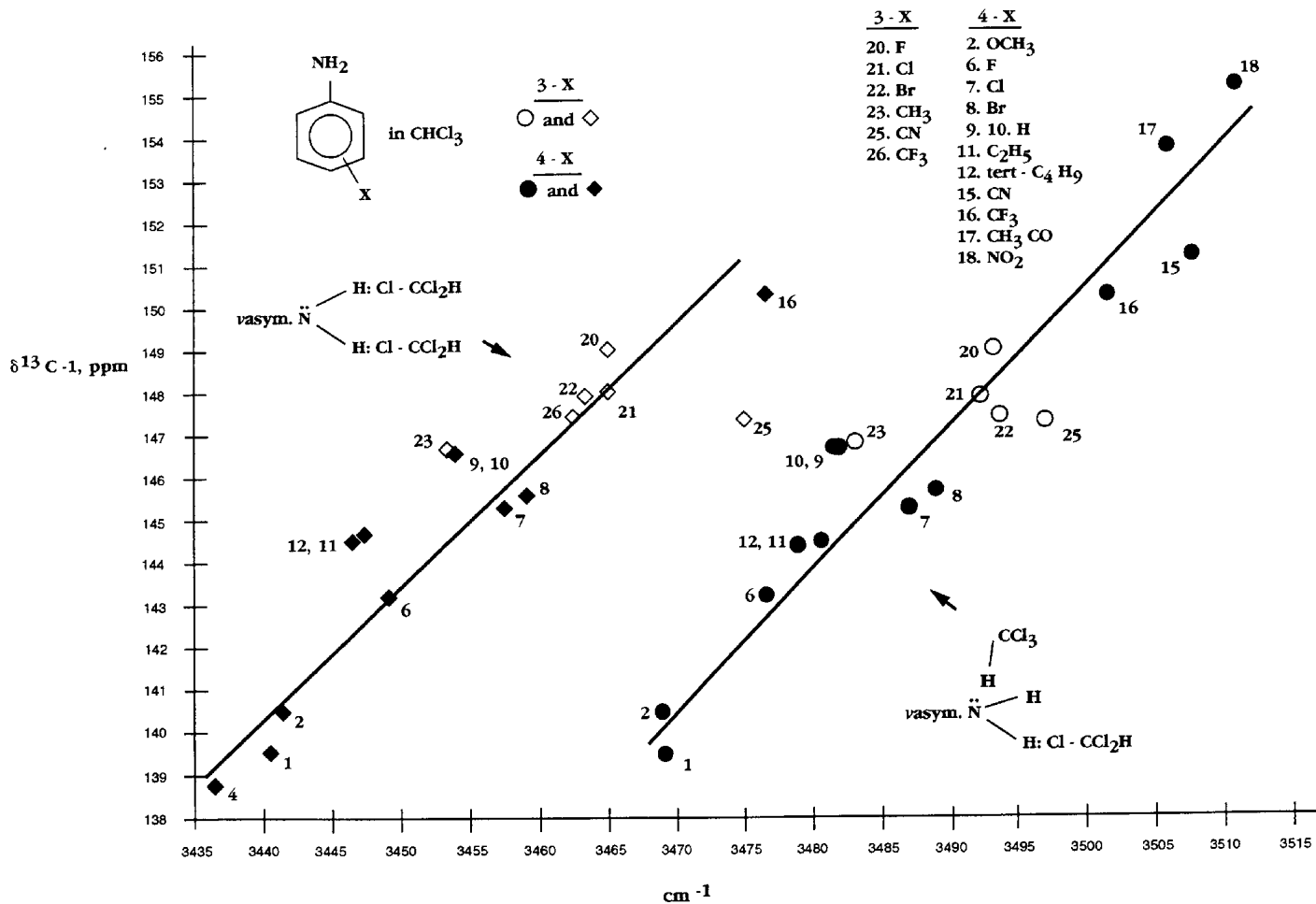


FIGURE 11.6 A plot of the ν asym. NH_2 frequencies for 3-x- and 4-x-anilines in CHCl_3 solution vs $\delta^{13}\text{C}-1$ chemical shift data for 3-x- and 4-x-anilines in CHCl_3 solution.

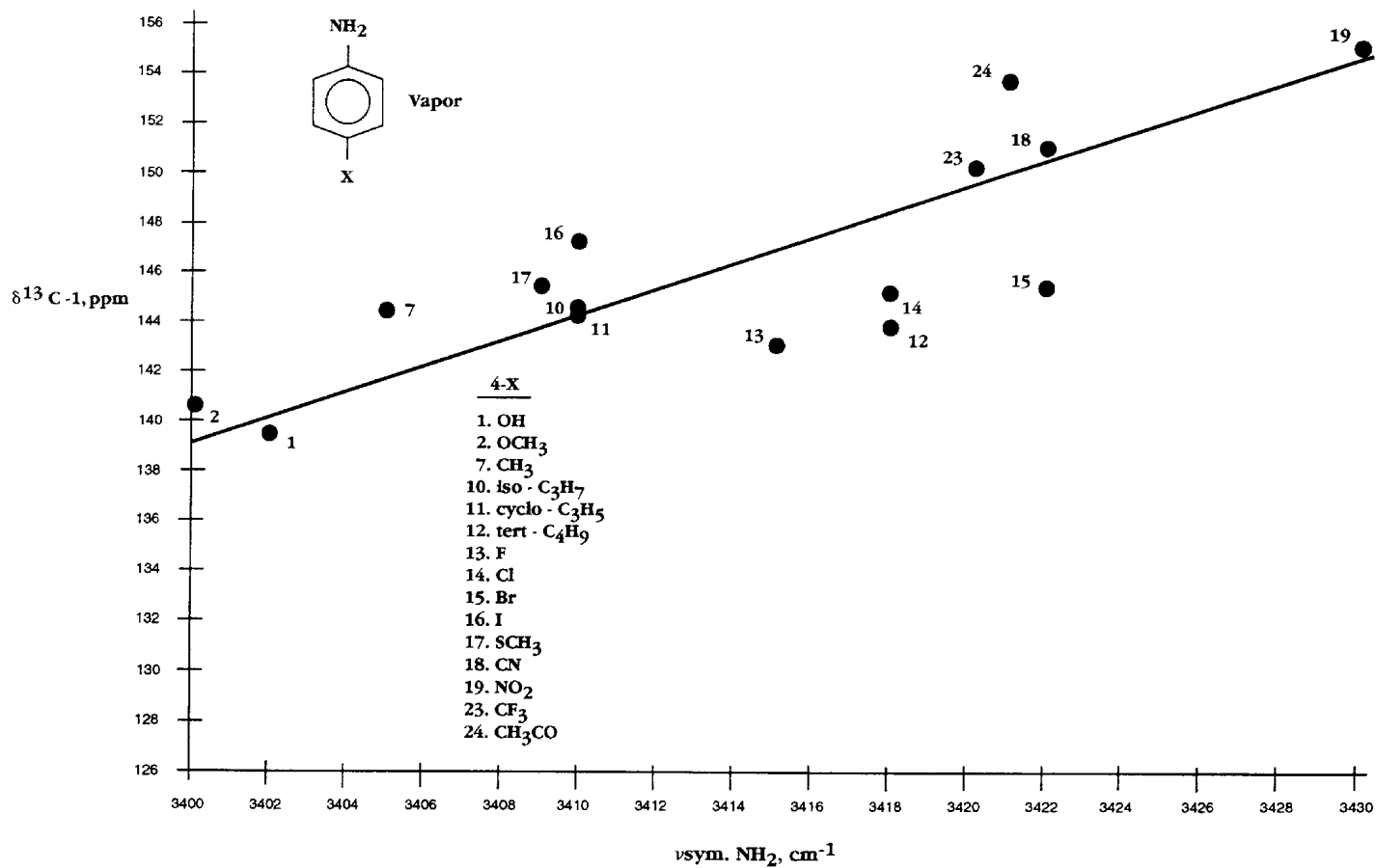


FIGURE 11.7 A plot of the $\nu_{\text{sym. NH}_2}$ frequencies for 4-x-anilines in the vapor phase vs $\delta^{13}\text{C}-1$ chemical shift data for 3-x- and 4-x-anilines.

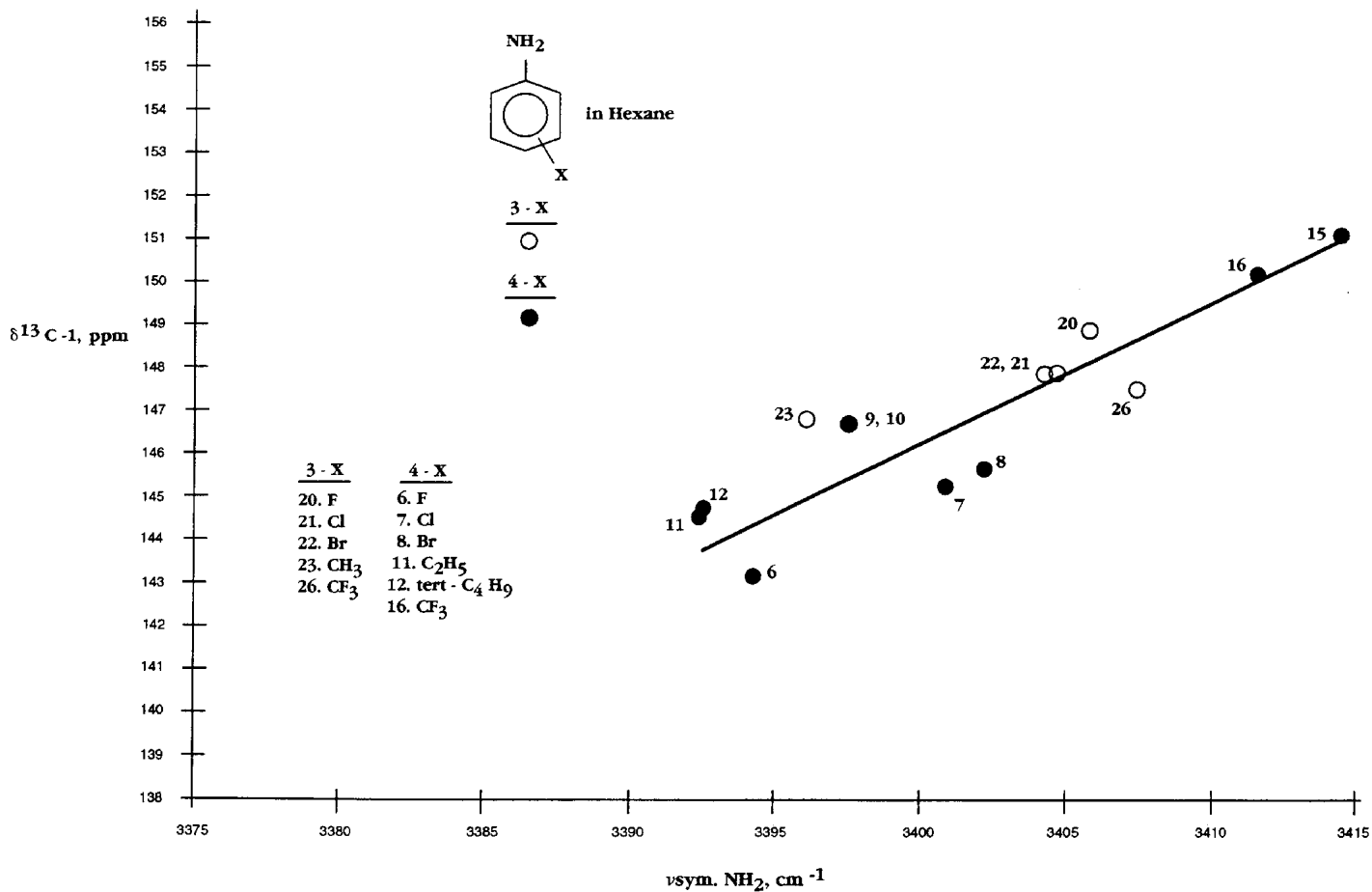


FIGURE 11.8 A plot of $\nu_{\text{sym. NH}_2}$ frequencies for 3-x- and 4-x-anilines in hexane solution vs $\delta^{13}\text{C-1}$ chemical shift data for 3-x- and 4-x-anilines in CHCl_3 solution.

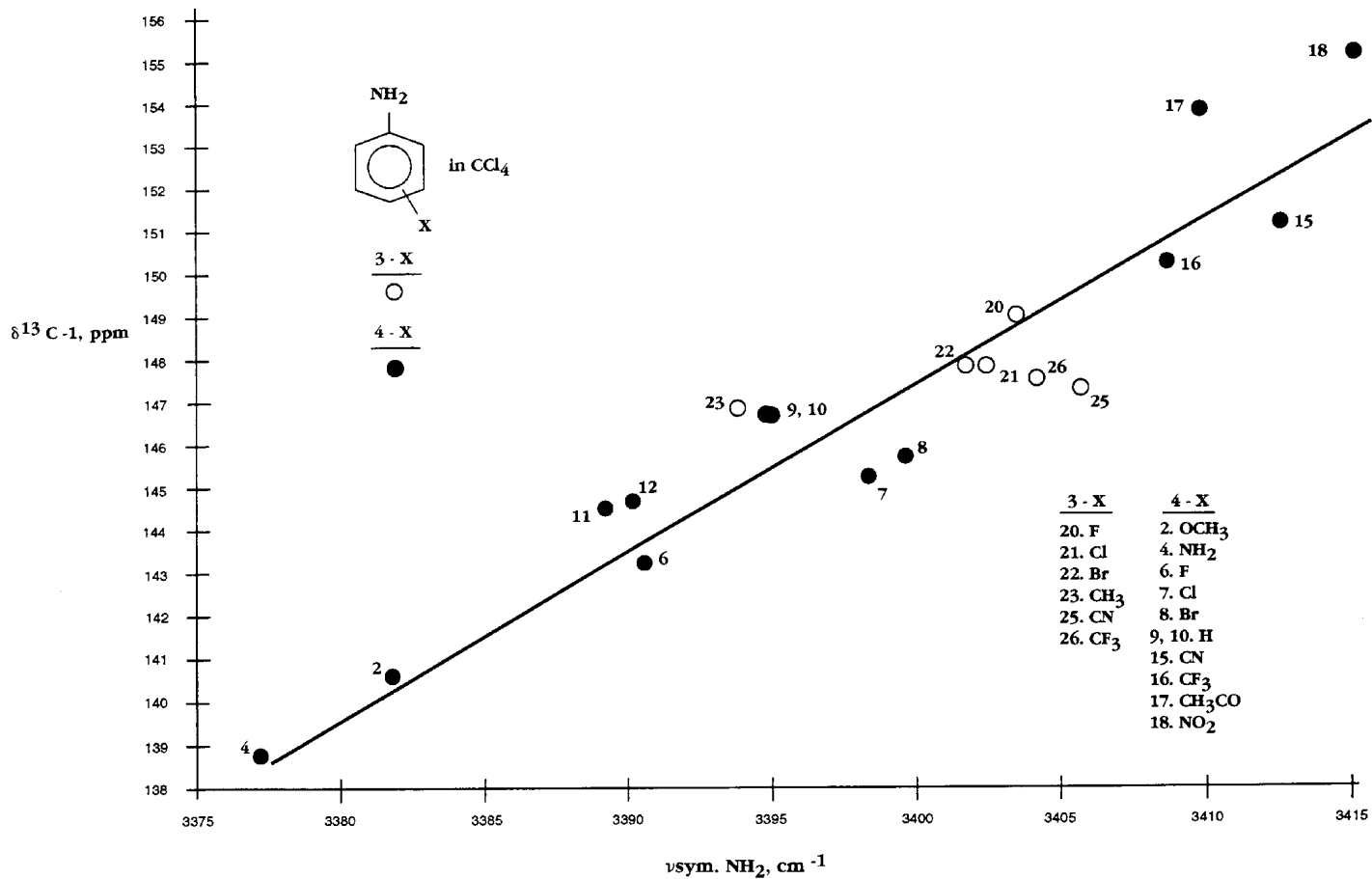


FIGURE 11.9 A plot of $\nu_{\text{sym. NH}_2}$ frequencies for 3-x- and 4-x-anilines in CCl_4 solution vs $\delta^{13}\text{C-1}$ chemical shift data for 3-x- and 4-x-anilines vs the $\delta^{13}\text{C-1}$ chemical shift data for 3-x- and 4-x-anilines in CHCl_3 solution.

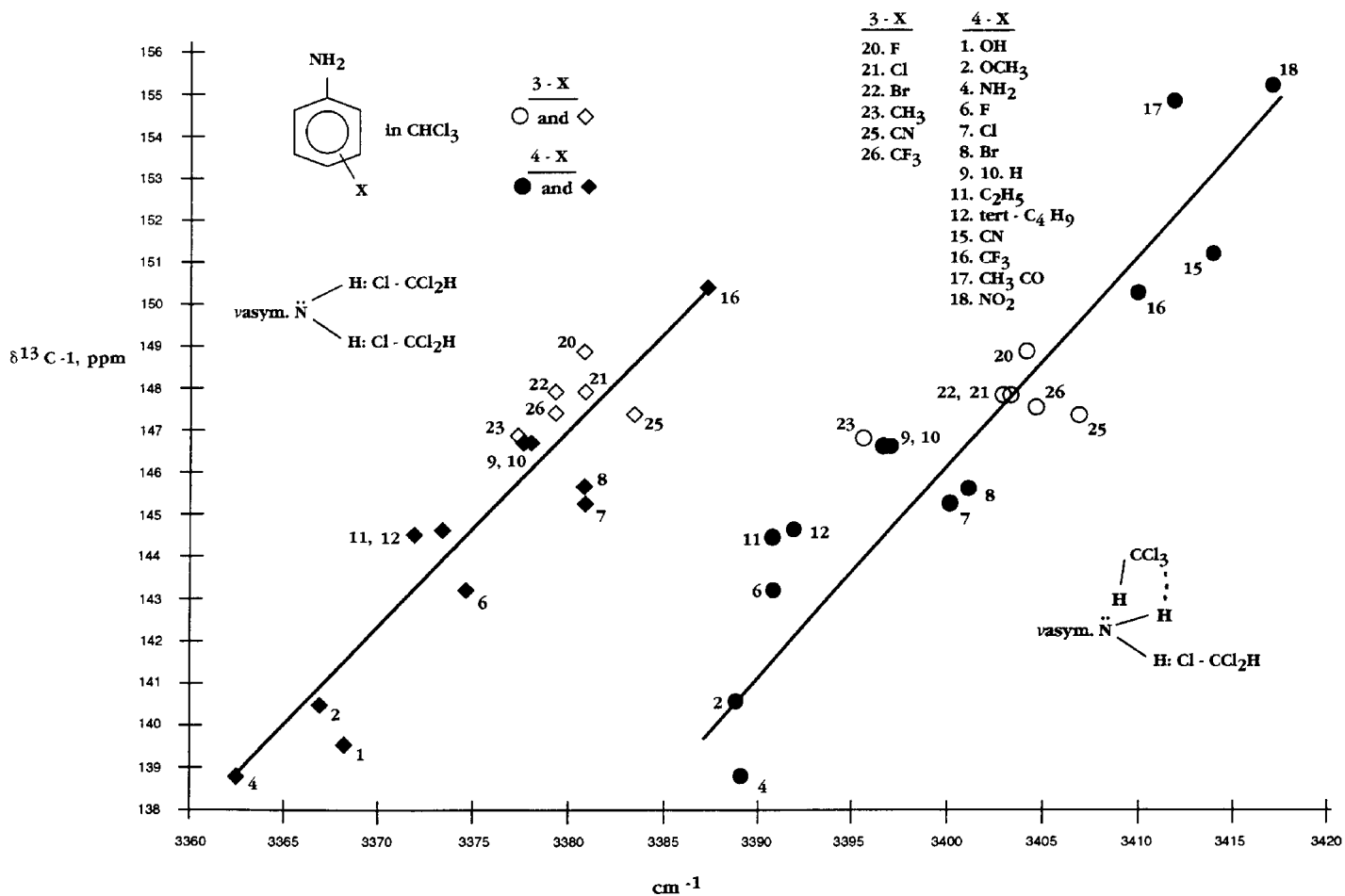


FIGURE 11.10 A plot of the ν sym. NH_2 frequencies for 3-x- and 4-x-anilines in CHCl_3 solution vs $\delta^{13}\text{C-1}$ chemical shift data for 3-x- and 4-x-anilines in CHCl_3 solution.

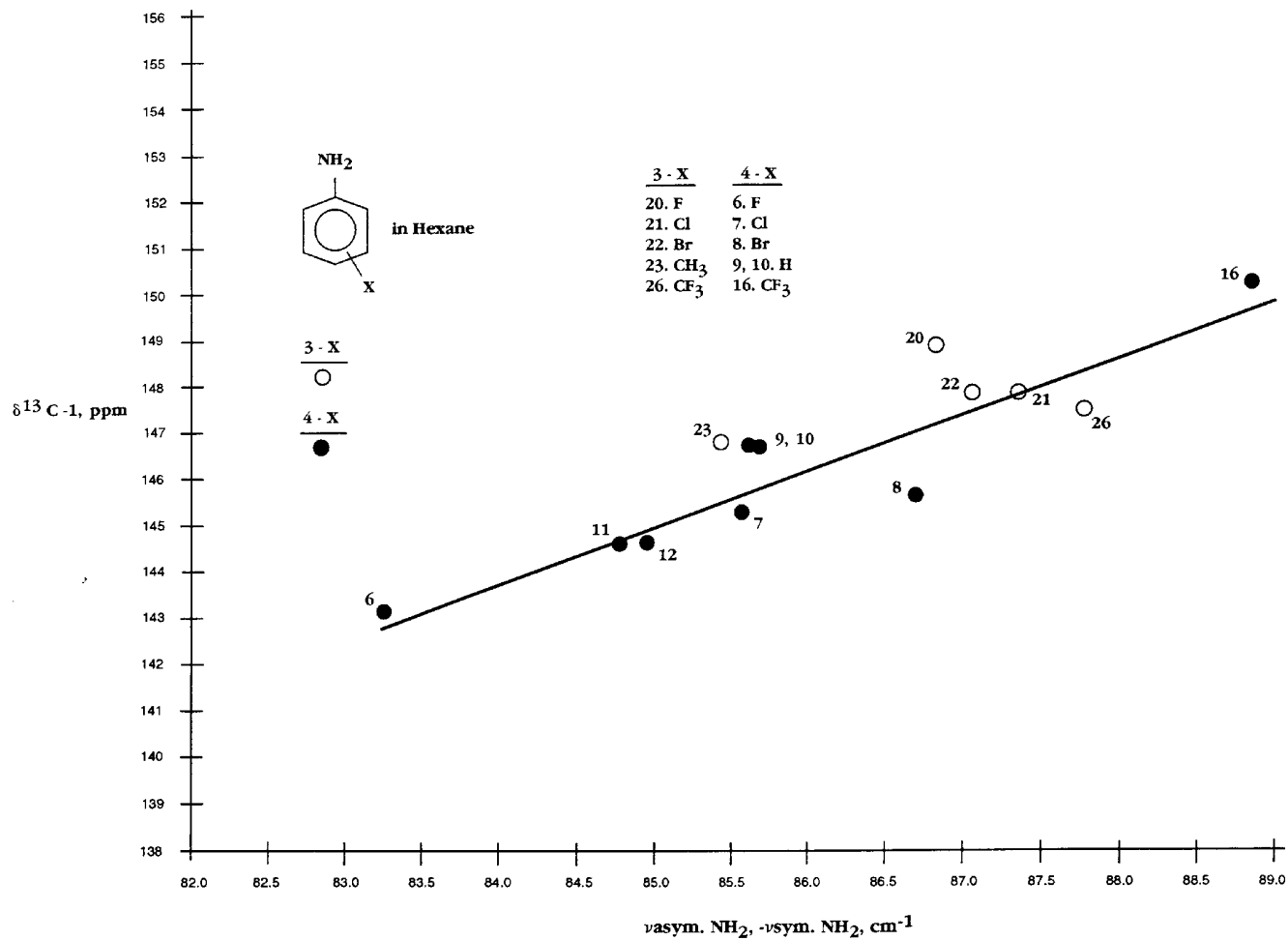


FIGURE 11.11 A plot of the frequency difference between $\nu_{\text{asym. NH}_2}$ and $\nu_{\text{sym. NH}_2}$ for 3-x- and 4-x-anilines in hexane solution vs $\delta^{13}\text{C-1}$ chemical shift data for 3-x- and 4-x-anilines in CHCl_3 solution.

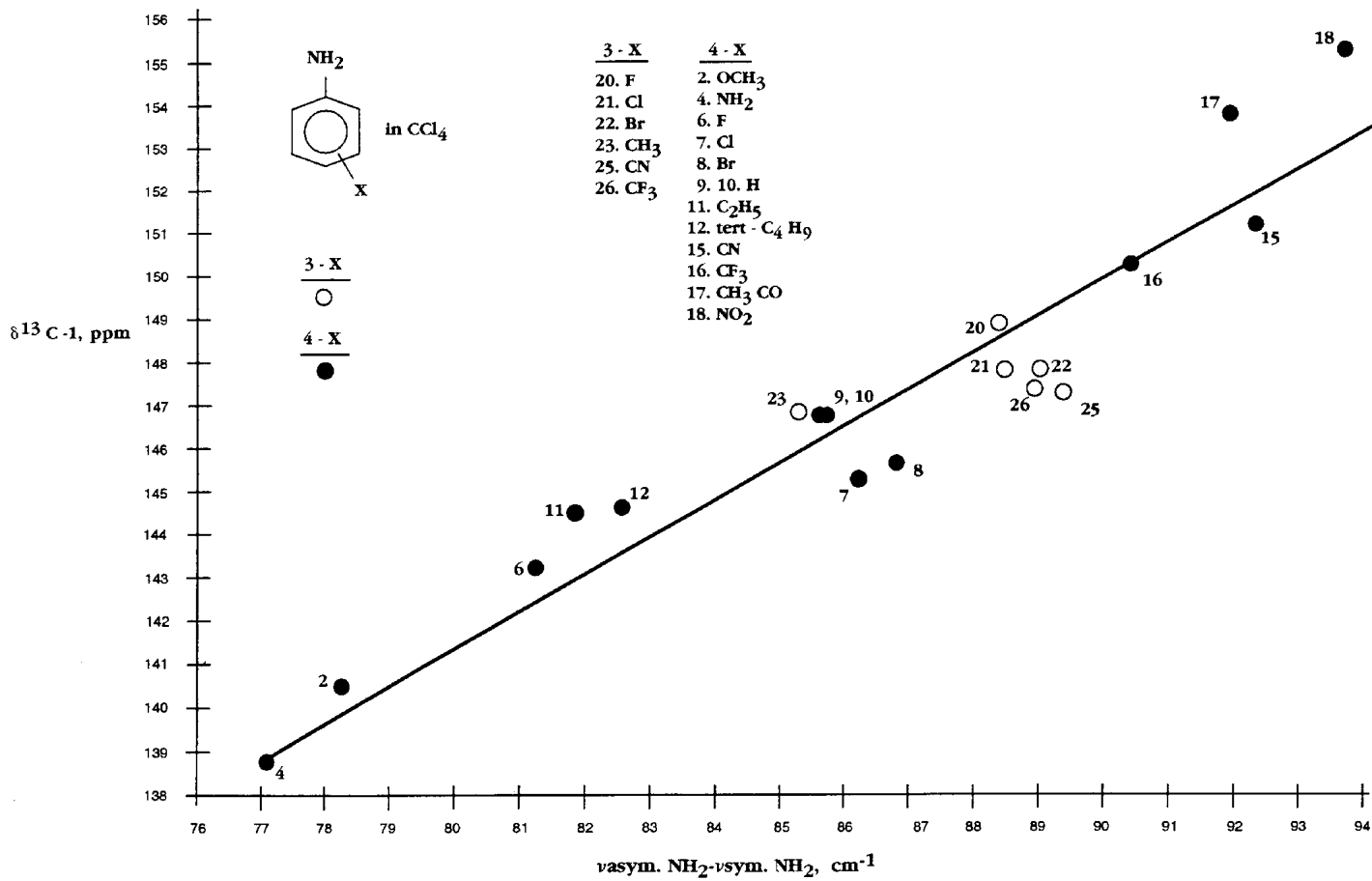


FIGURE 11.12 A plot of the frequency difference between $\nu_{\text{asym. NH}_2}$ and $\nu_{\text{sym. NH}_2}$ for 3-x- and 4-x-anilines in CCl_4 solution vs $\delta^{13}\text{C}-1$ chemical shift data for 3-x- and 4-x-anilines in CHCl_3 solution.

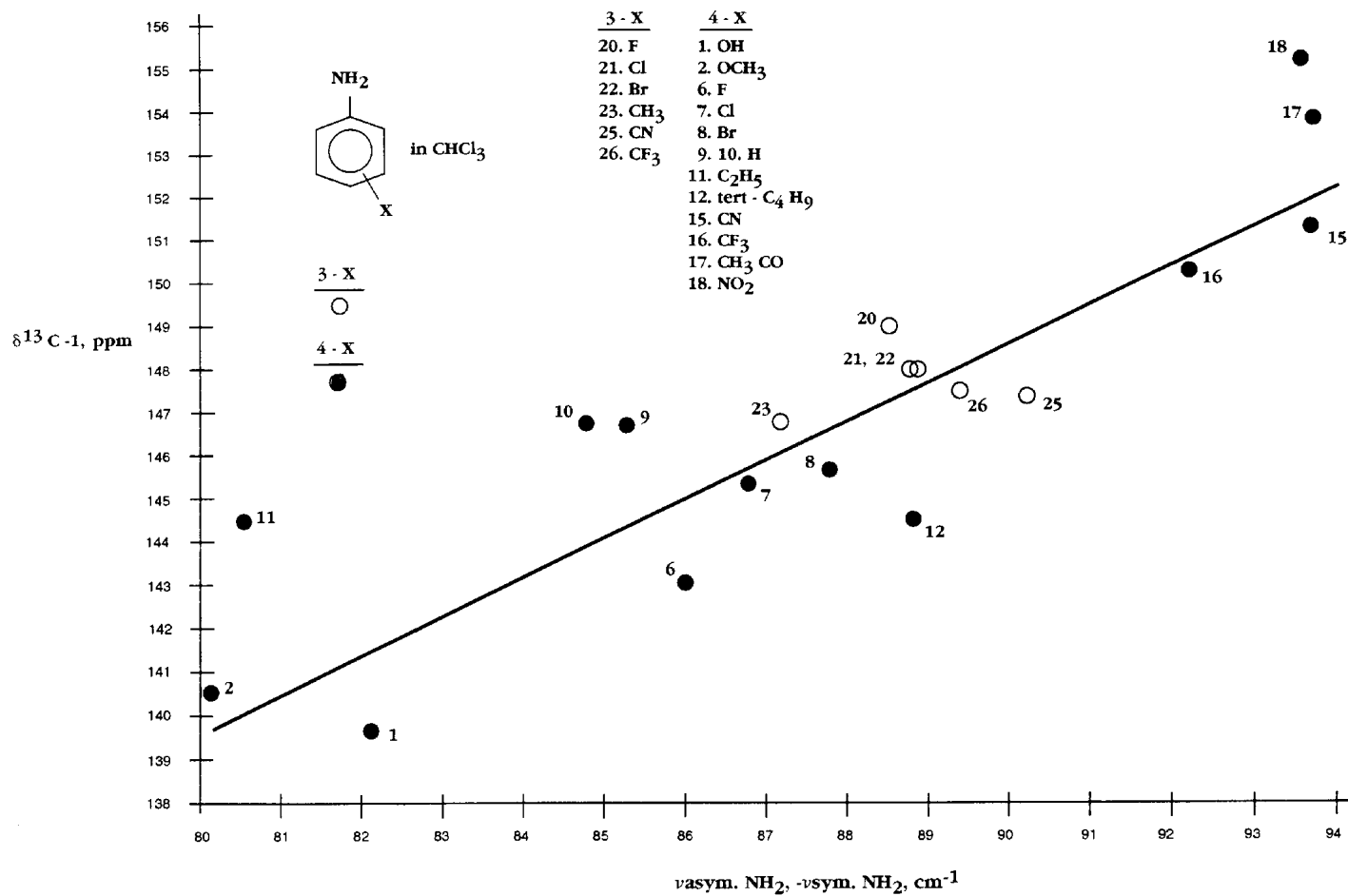


FIGURE 11.13 A plot of the frequency difference between $v_{\text{asym. NH}_2}$ and $v_{\text{sym. NH}_2}$ for 3-x- and 4-x-anilines in CHCl_4 solution vs $\delta^{13}\text{C-1}$ chemical shift data for 3-x- and 4-x-anilines in CHCl_3 solution.

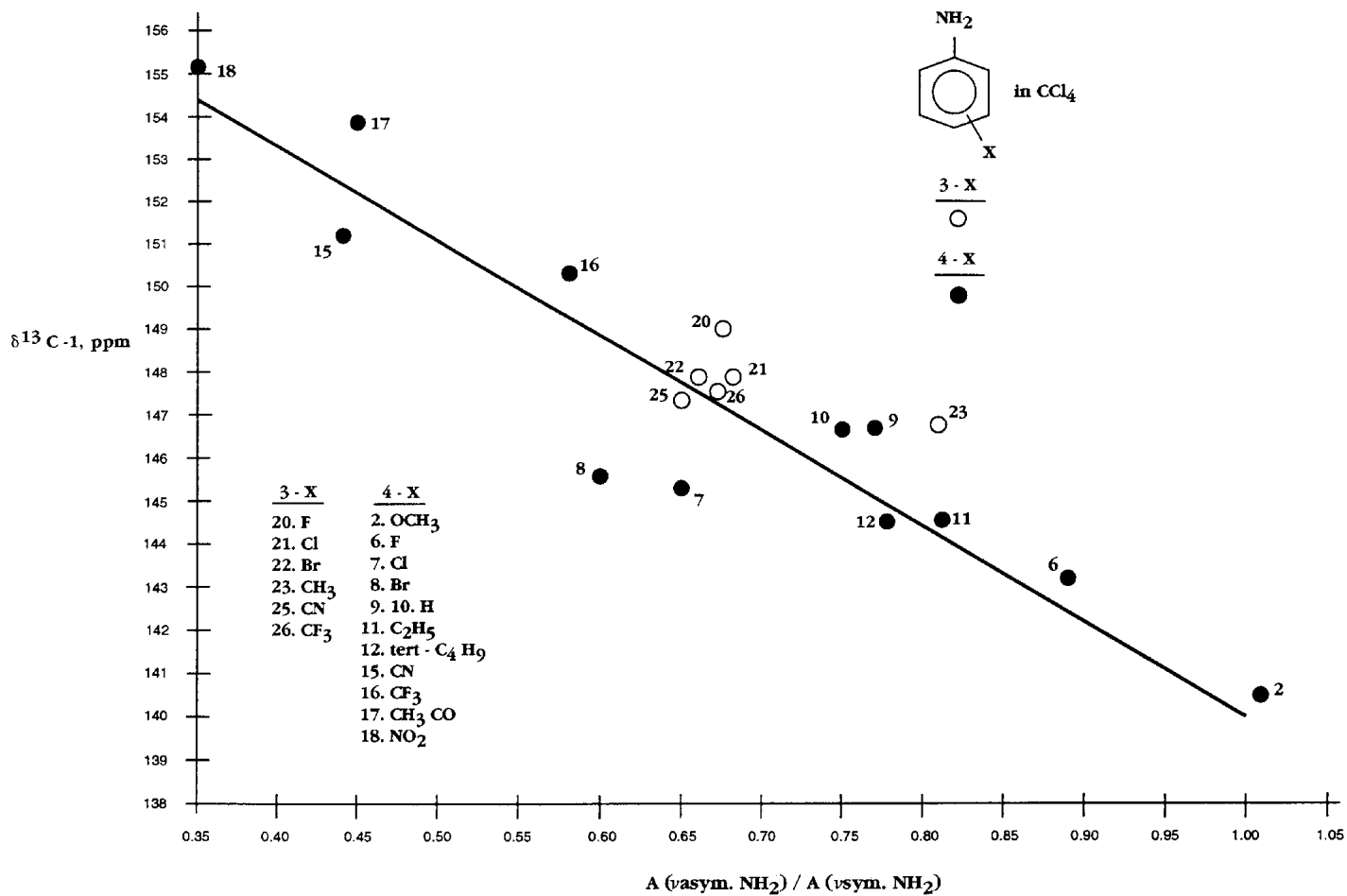


FIGURE 11.14 A plot of the absorbance ratio $A(\nu \text{ asym. NH}_2)/A(\nu \text{ sym. NH}_2)$ for 3-x- and 4-x-anilines in CCl_4 solution vs $\delta^{13}\text{C-1}$ chemical shift data for 3-x- and 4-x-anilines in CHCl_3 solution.

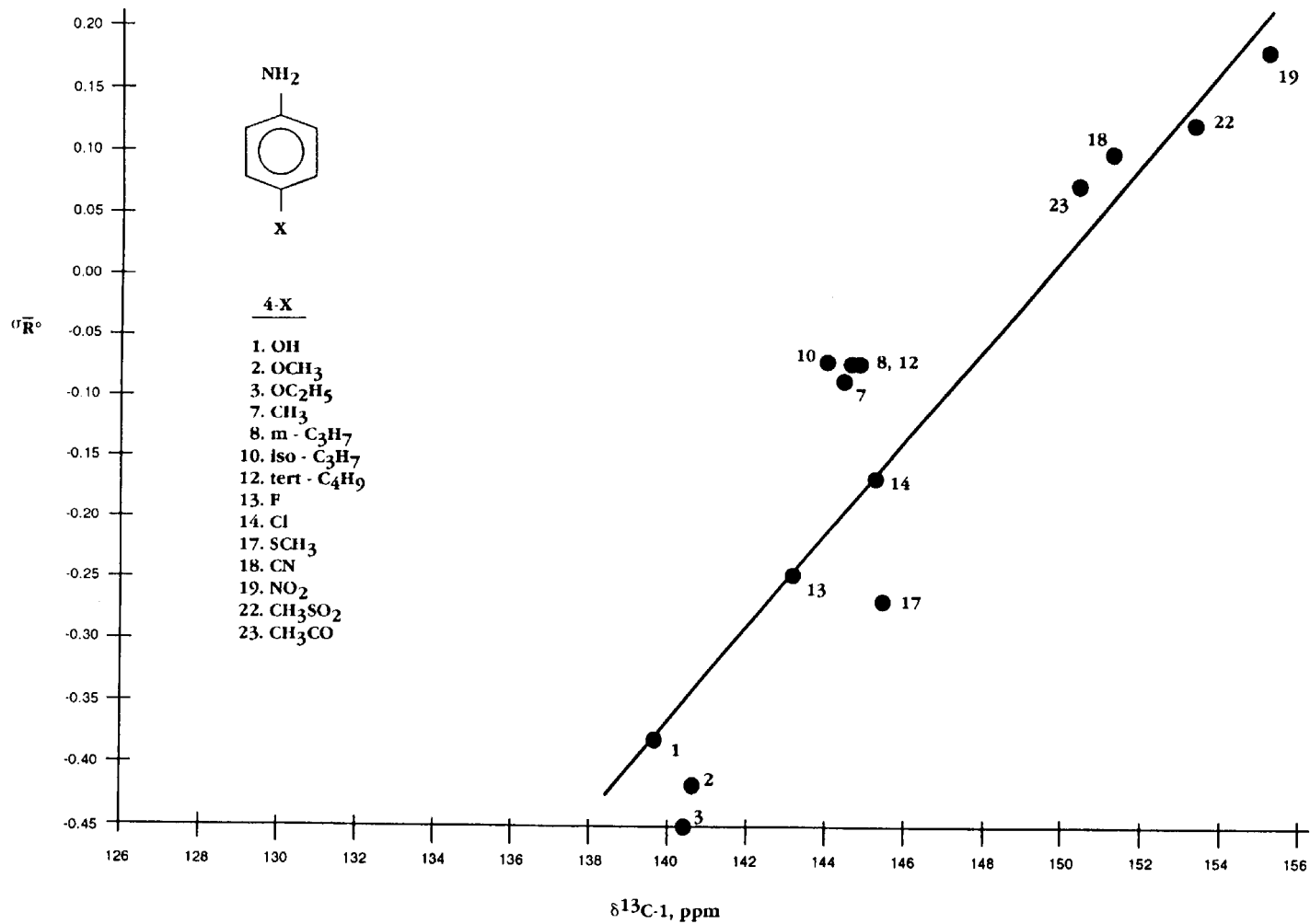


FIGURE 11.15 A plot of $\delta^{13}\text{C-1}$ chemical shift data for 4-x-anilines in CHCl_3 solution vs Taft σ_{R} values for the 4-x atom or group.

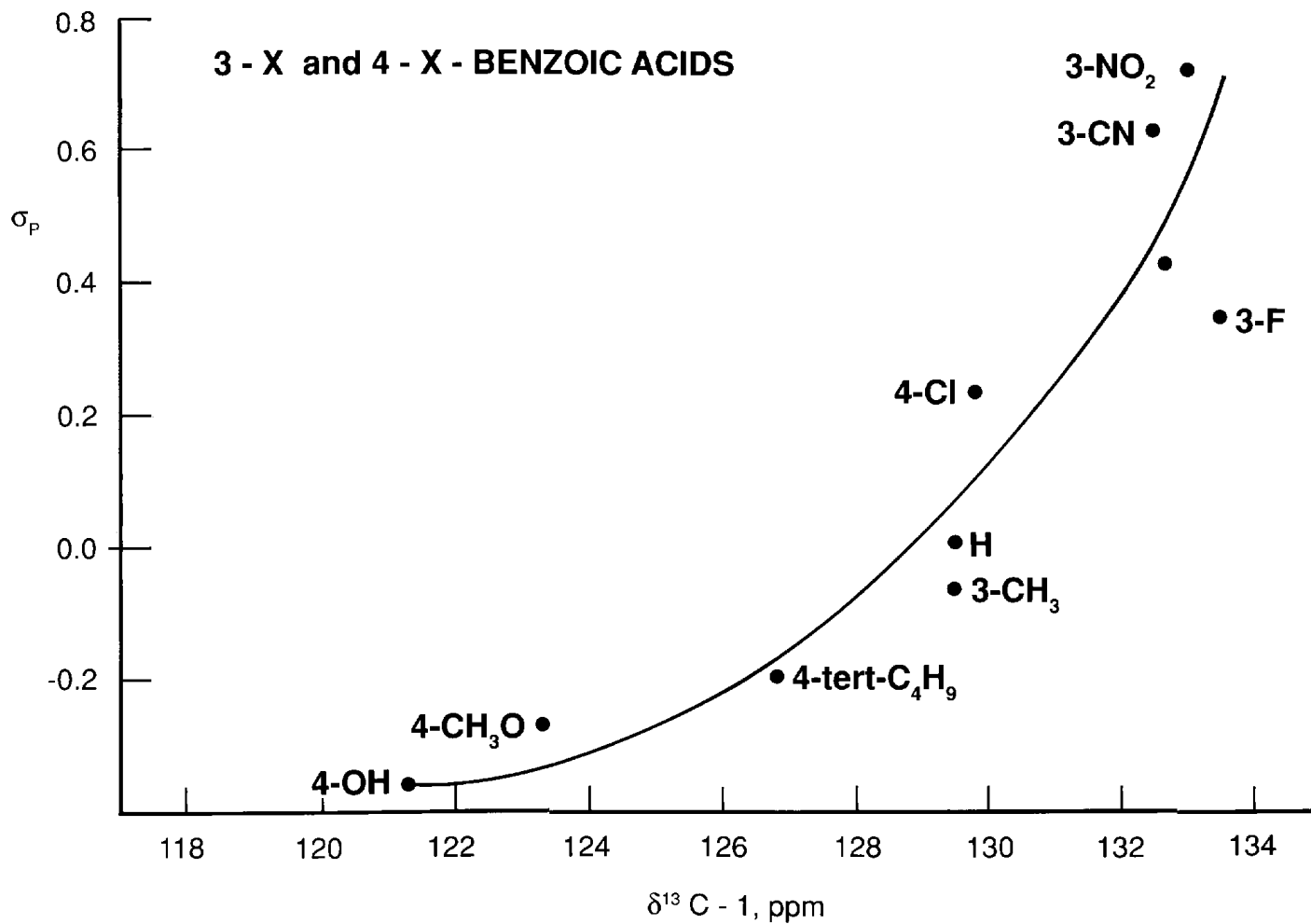


FIGURE 11.16 A plot of $\delta^{13}\text{C}-1$ for 3-x- and 4-x-benzoic acids vs Hammett σ values for the x atom or group.

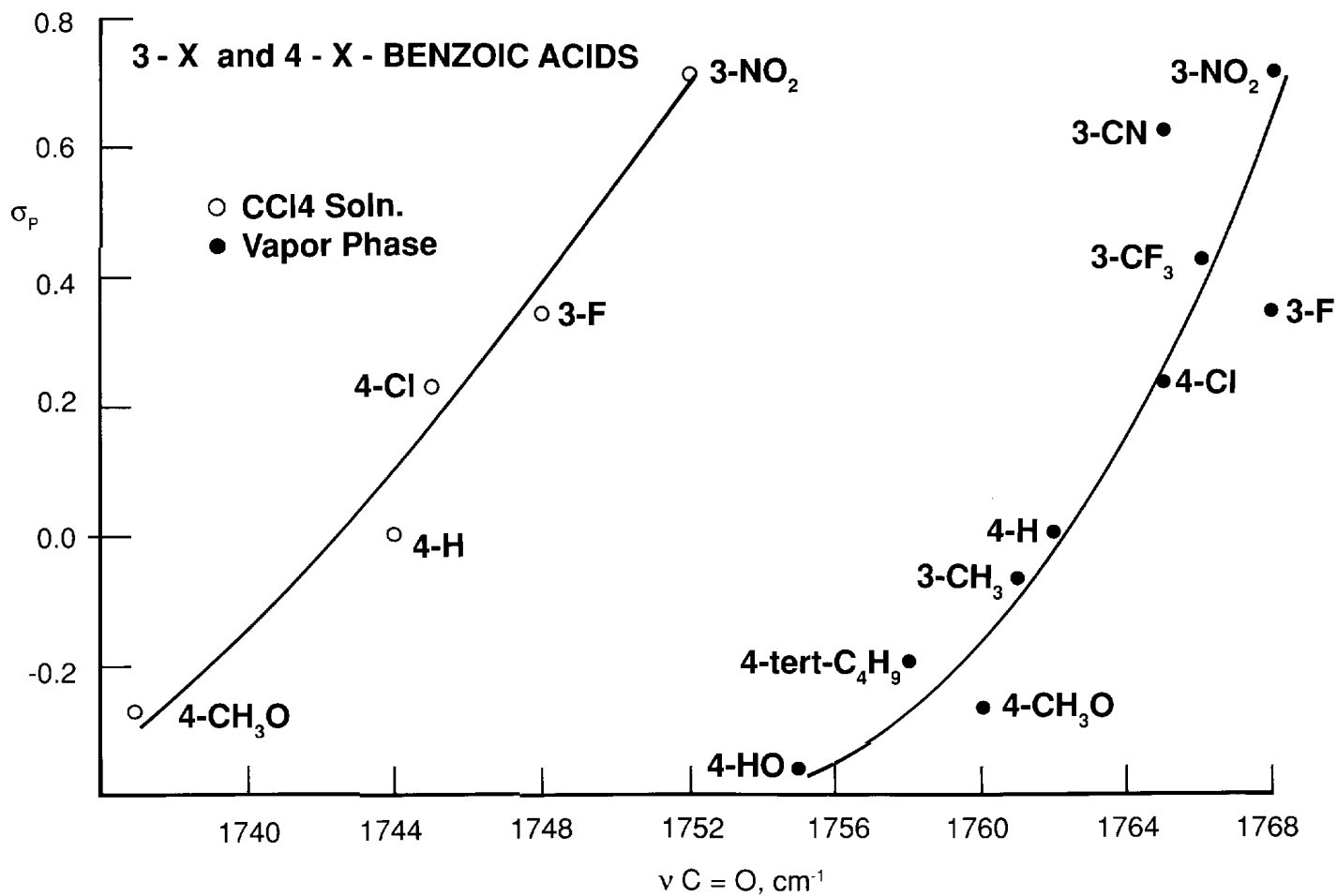


FIGURE 11.17 Plots of $\nu_{C=O}$ vs Hammett σ values of 3-x- and 4-x-benzoic acids. The solid circles are for IR data in the vapor phase. The open circles are for IR dilute solution data for unassociated 3-x- and 4-x-benzoic acids.

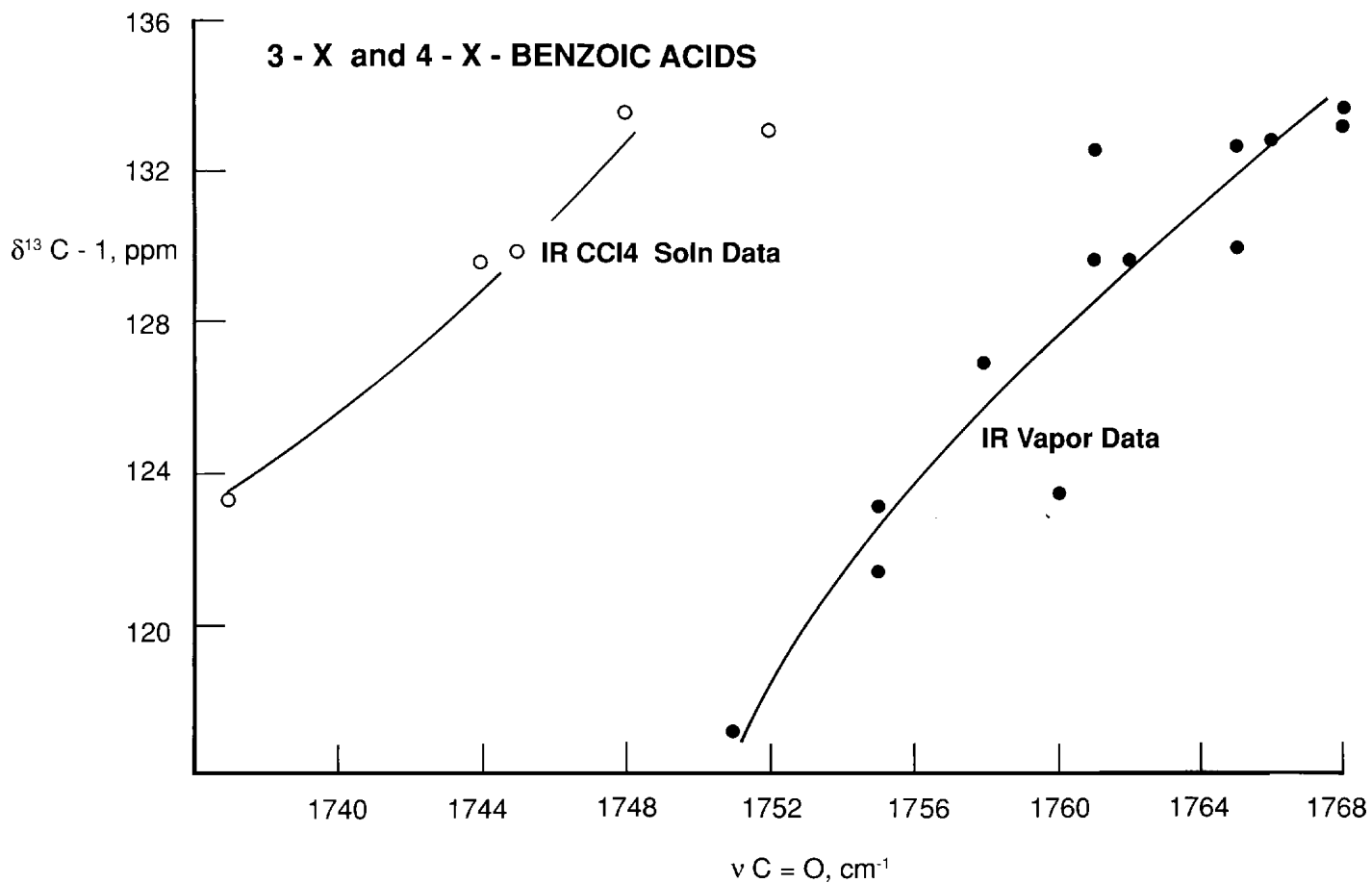


FIGURE 11.18 Plots of $\nu \text{C}=\text{O}$ vs $\delta^{13}\text{C}-1$ for 3-x- and 4-x-benzoic acids. The NMR data are for CDCl_3 solutions. The plot with closed circles includes vapor-phase IR data. The plot with open circles includes IR CCl_4 -solution data.

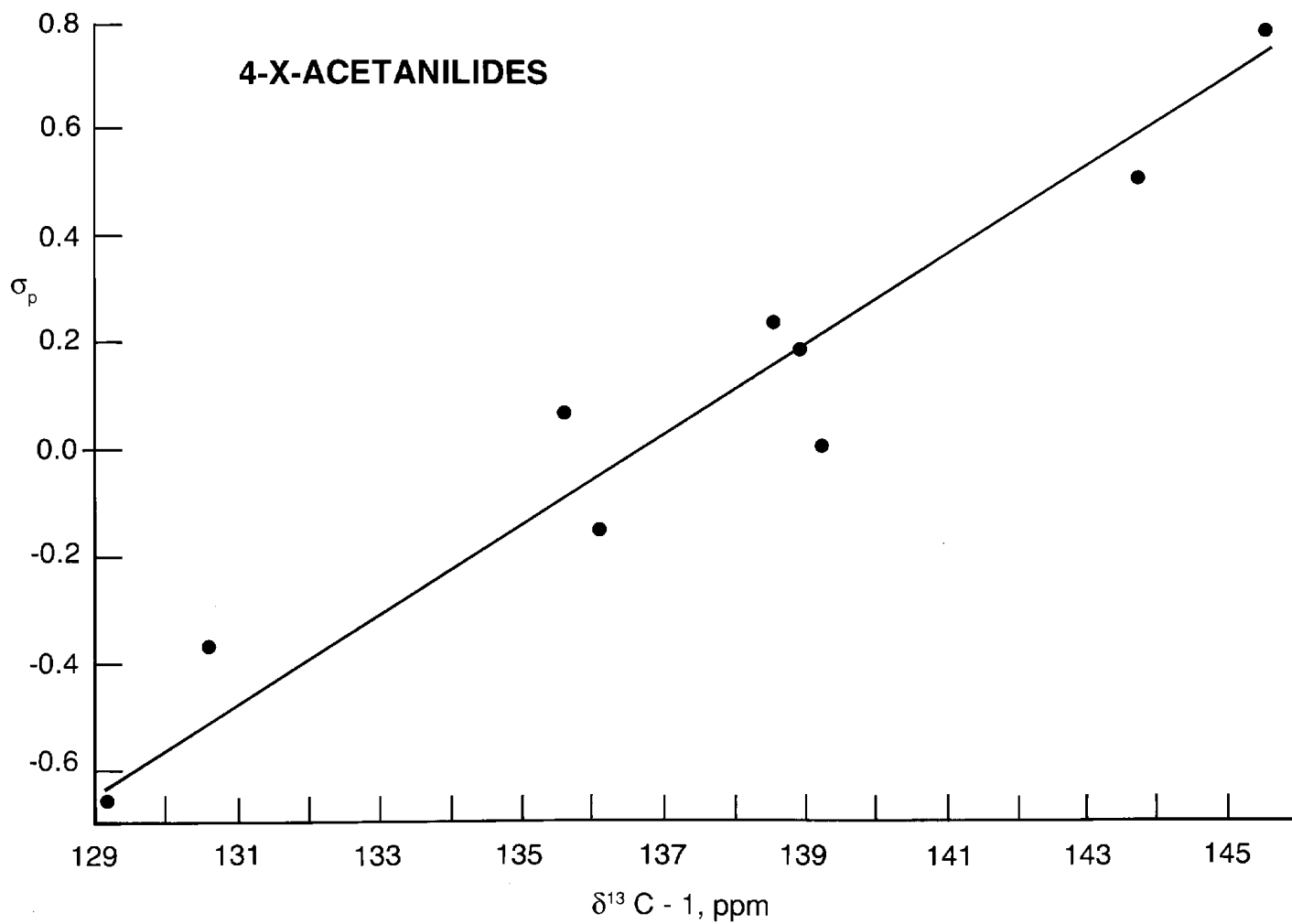


FIGURE 11.19 A plot of $\delta^{13}\text{C}-1$ for 4-x-acetanilides in CDCl_3 solution vs Hammett σ_p values for the x-atom or group.

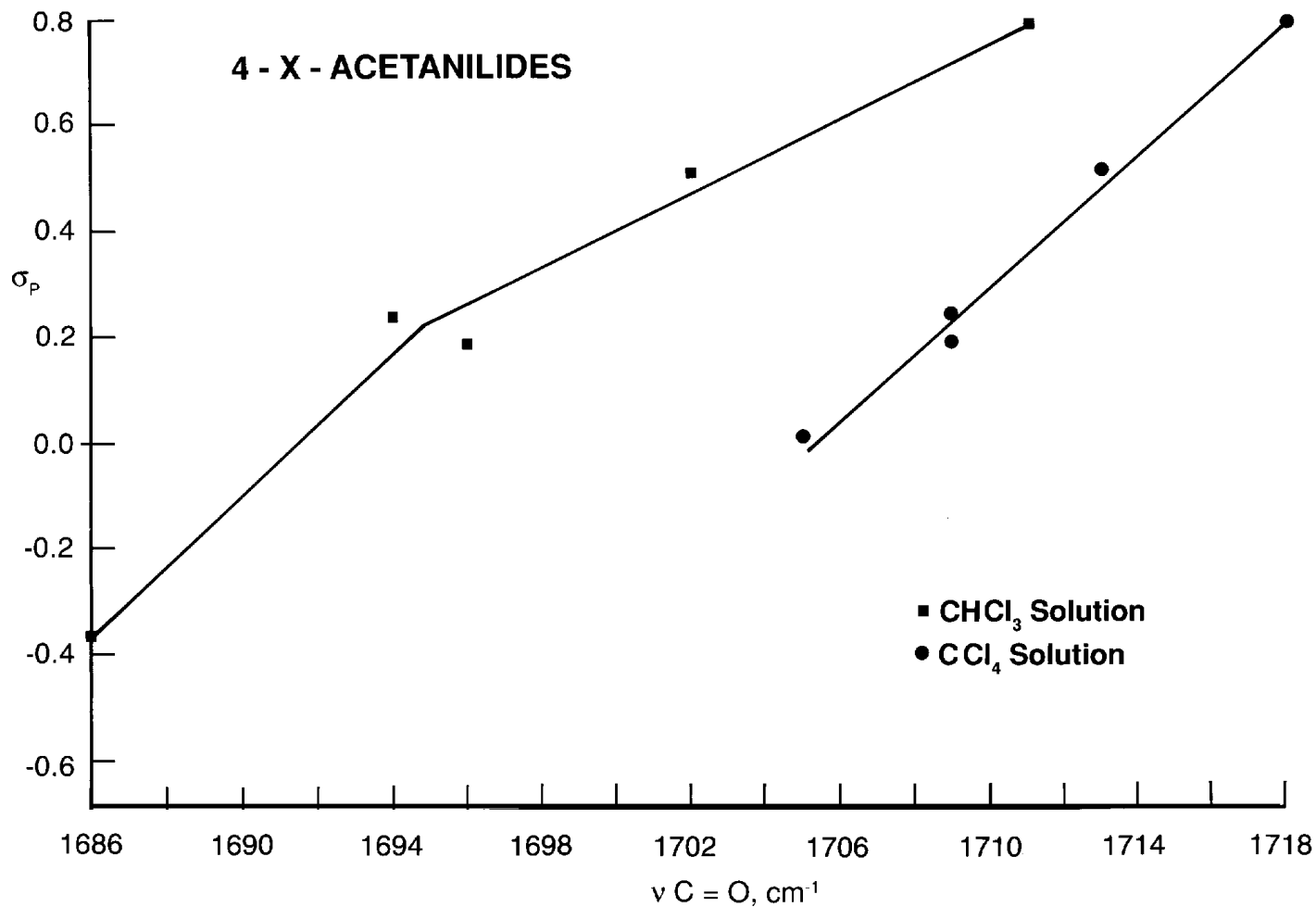


FIGURE 11.20 A plot of $\nu \text{ C}=\text{O}$ for 4-x-acetanilides vs Hammett σ_p values. The solid circles represent IR CCl_4 solution data and the solid squares represent IR CHCl_3 solution data.

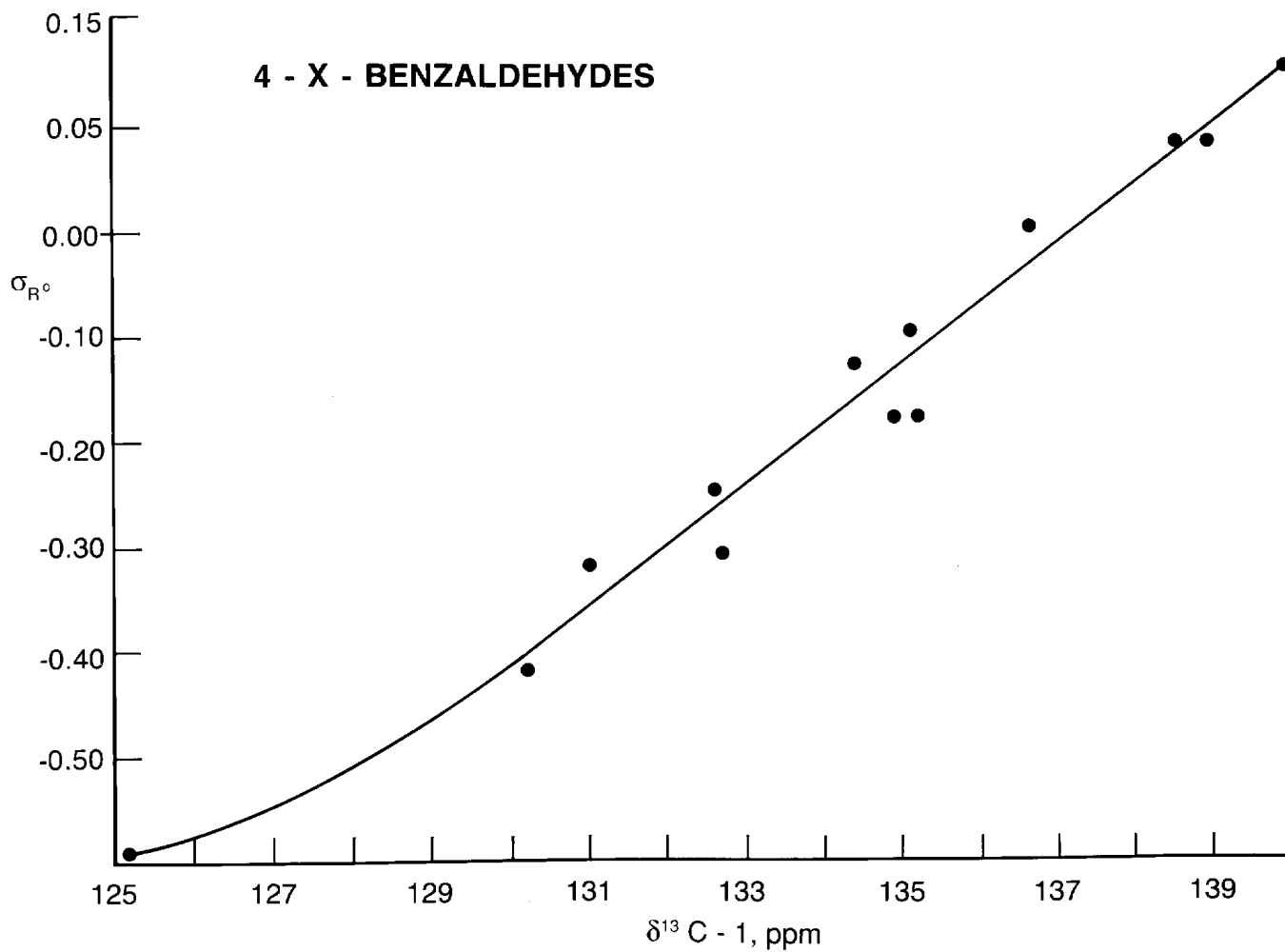


FIGURE 11.21 A plot of $\delta^{13}\text{C} - 1$ for 4-x-benzaldehydes vs Taft $\sigma_{\text{R}}^{\circ}$ values for the 4-x atom or group.

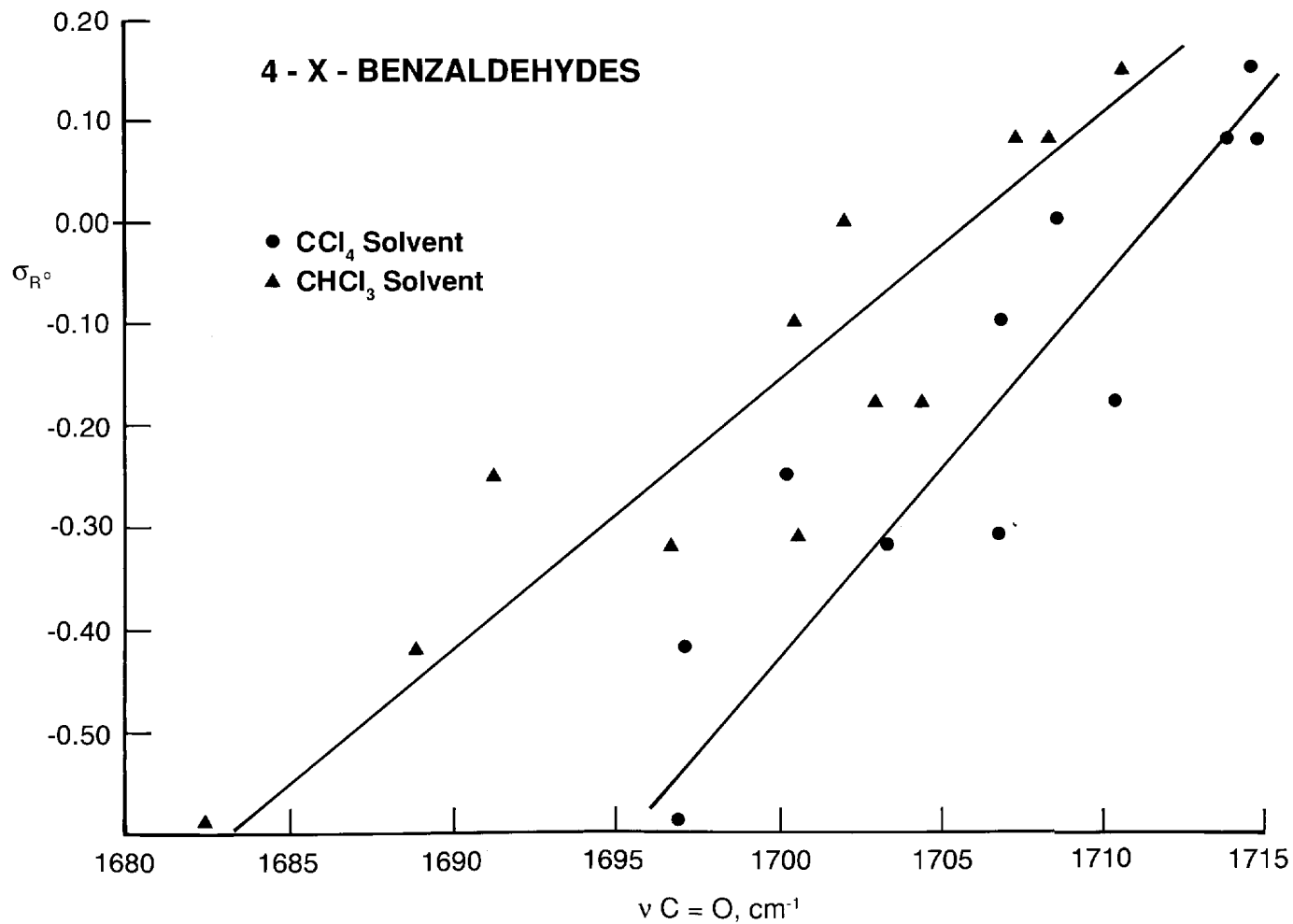


FIGURE 11.22 A plot of $\nu \text{ C}=\text{O}$ for 4-x-benzaldehydes vs Taft σ_{R° values for the 4-x atom or group. The solid circles represent IR data in CCl_4 solutions and the solid triangles represent IR data in CHCl_3 solutions.

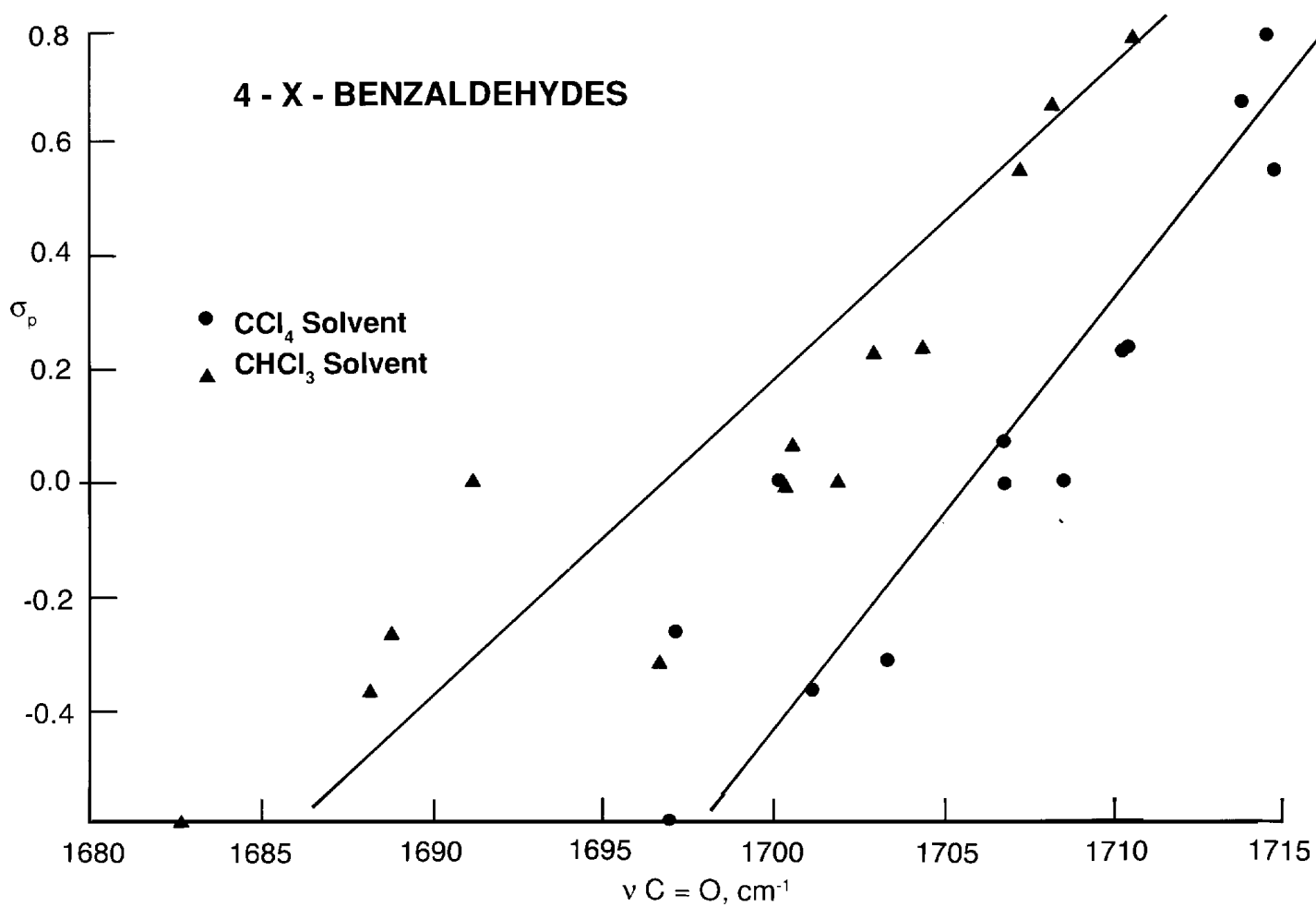


FIGURE 11.23 A plot of $\nu \text{ C}=\text{O}$ for 4-x-benzaldehydes vs Hammett σ_p values for the 4-x atom or group. The solid circles represent IR data in CCl_4 solution and the solid triangles represent IR data in CHCl_3 solutions.

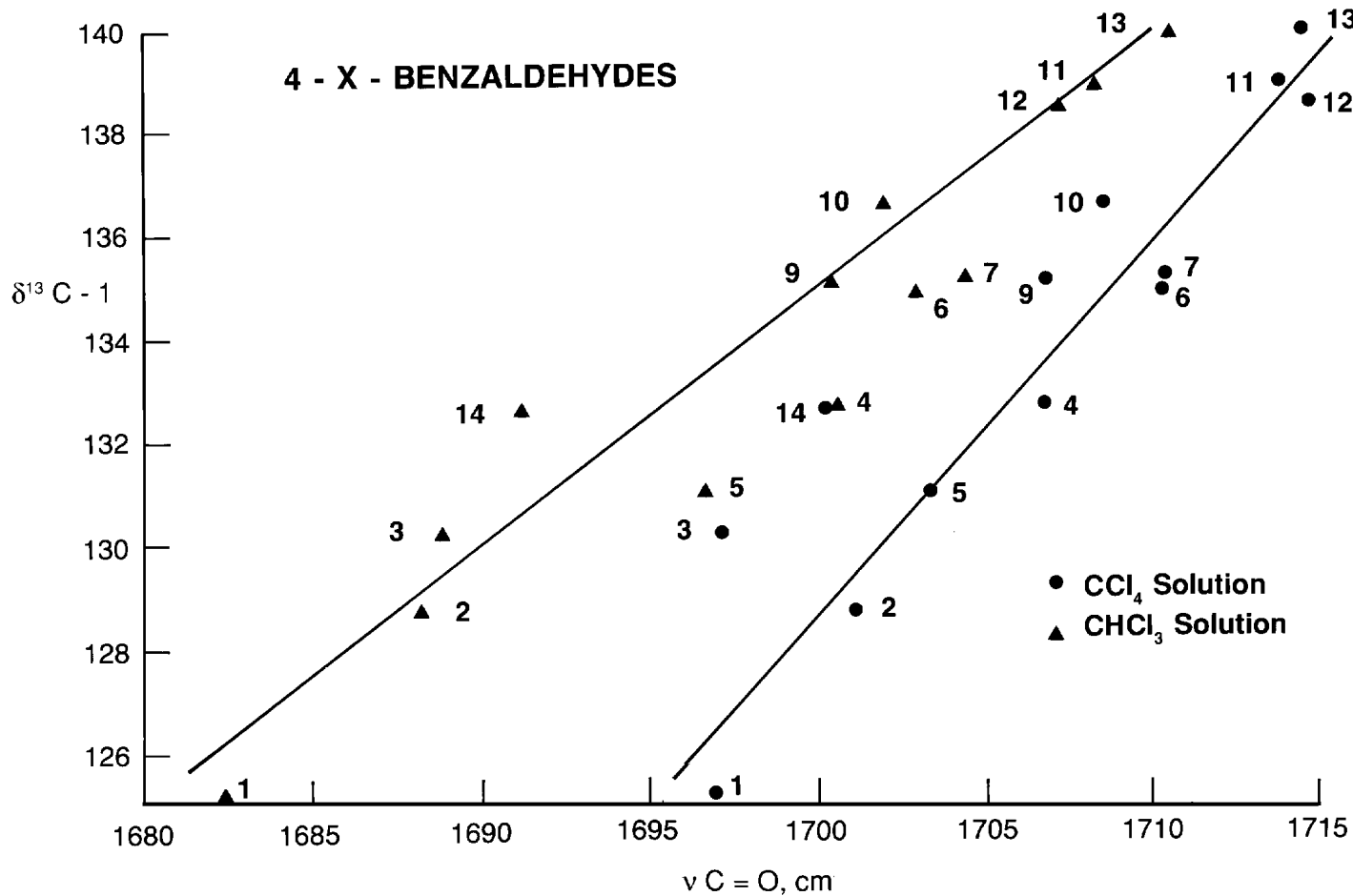


FIGURE 11.24 Plots of $\nu \text{C}=\text{O}$ vs $\delta^{13}\text{C}-1$ for 4-x-benzaldehydes. The $\delta^{13}\text{C}-1$ data are for CDCl_3 solutions. The plot with filled-in circles includes IR CCl_4 solution data and the plot with the filled-in triangles includes IR CHCl_3 solution data.

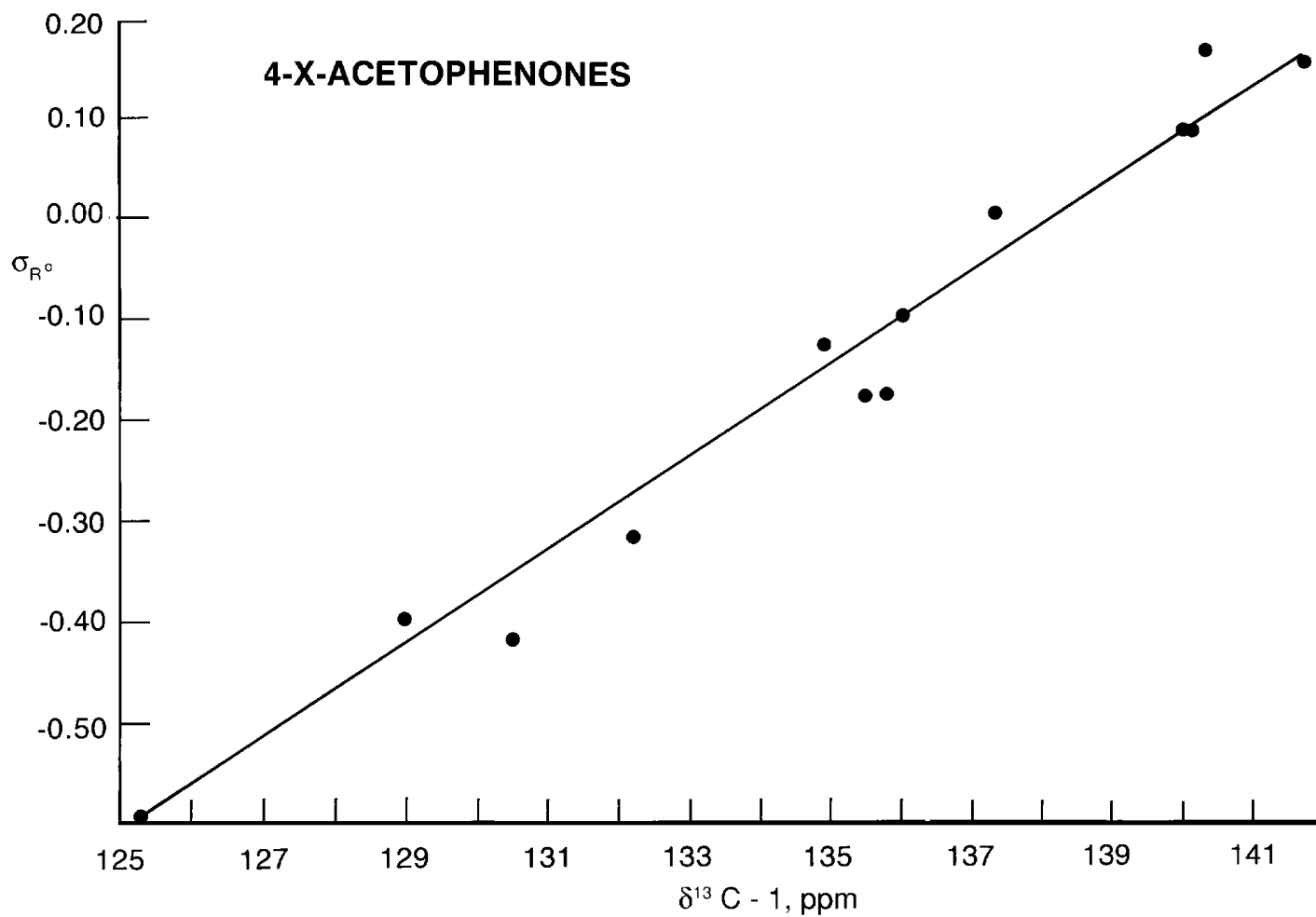


FIGURE 11.25 A plot of $\delta^{13}\text{C}-1$ for 4-x-acetophenones in CDCl_3 solutions vs Taft $\sigma_{R^{\circ}}$ values for the 4-x atom or groups.

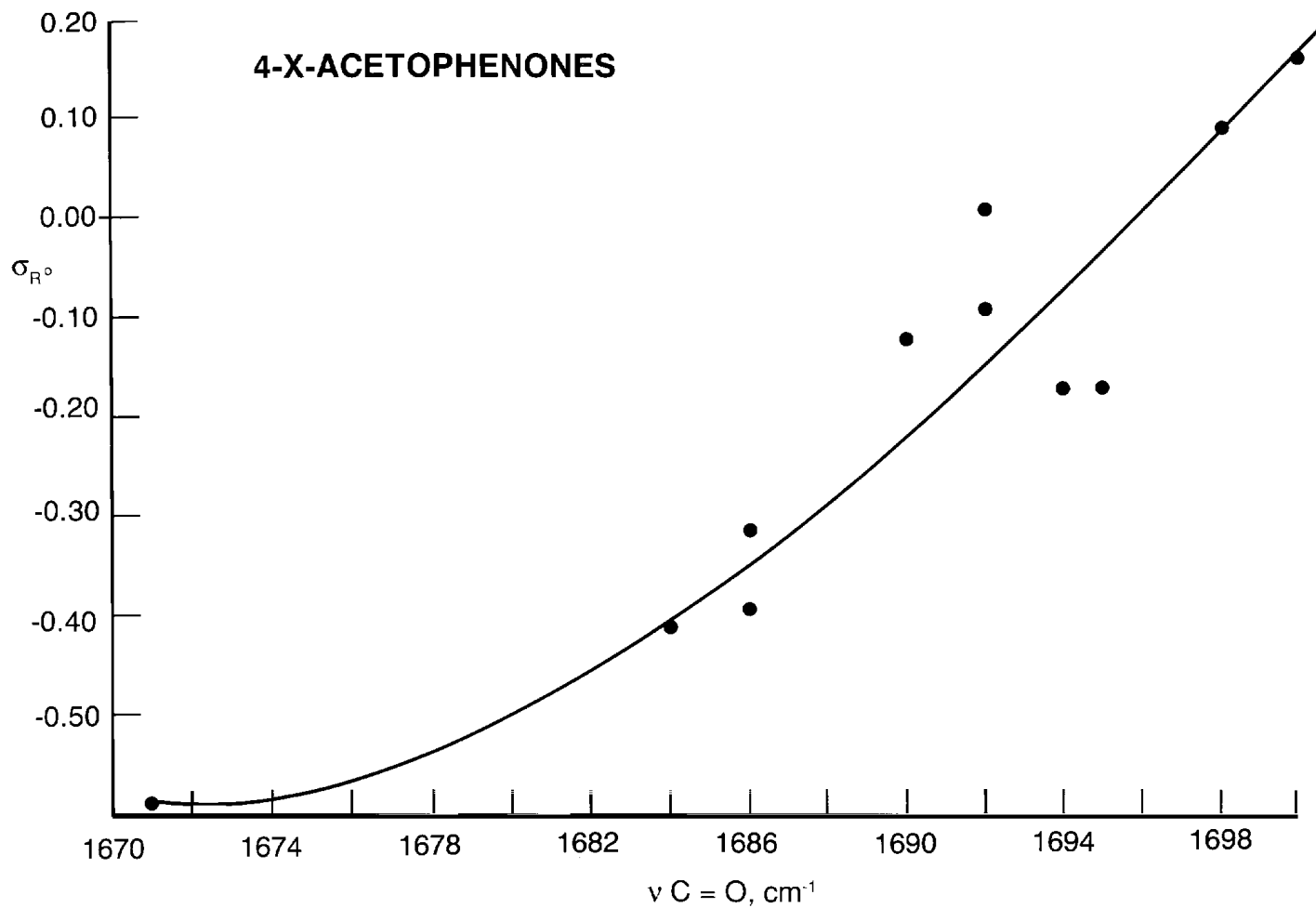


FIGURE 11.26 A plot of $\nu \text{ C}=\text{O}$ for 4-x-acetophenones vs Taft σ_{R^0} values for the 4-x atom or group. The IR data is that for the 4-x-acetophenones in CHCl_3 solution.

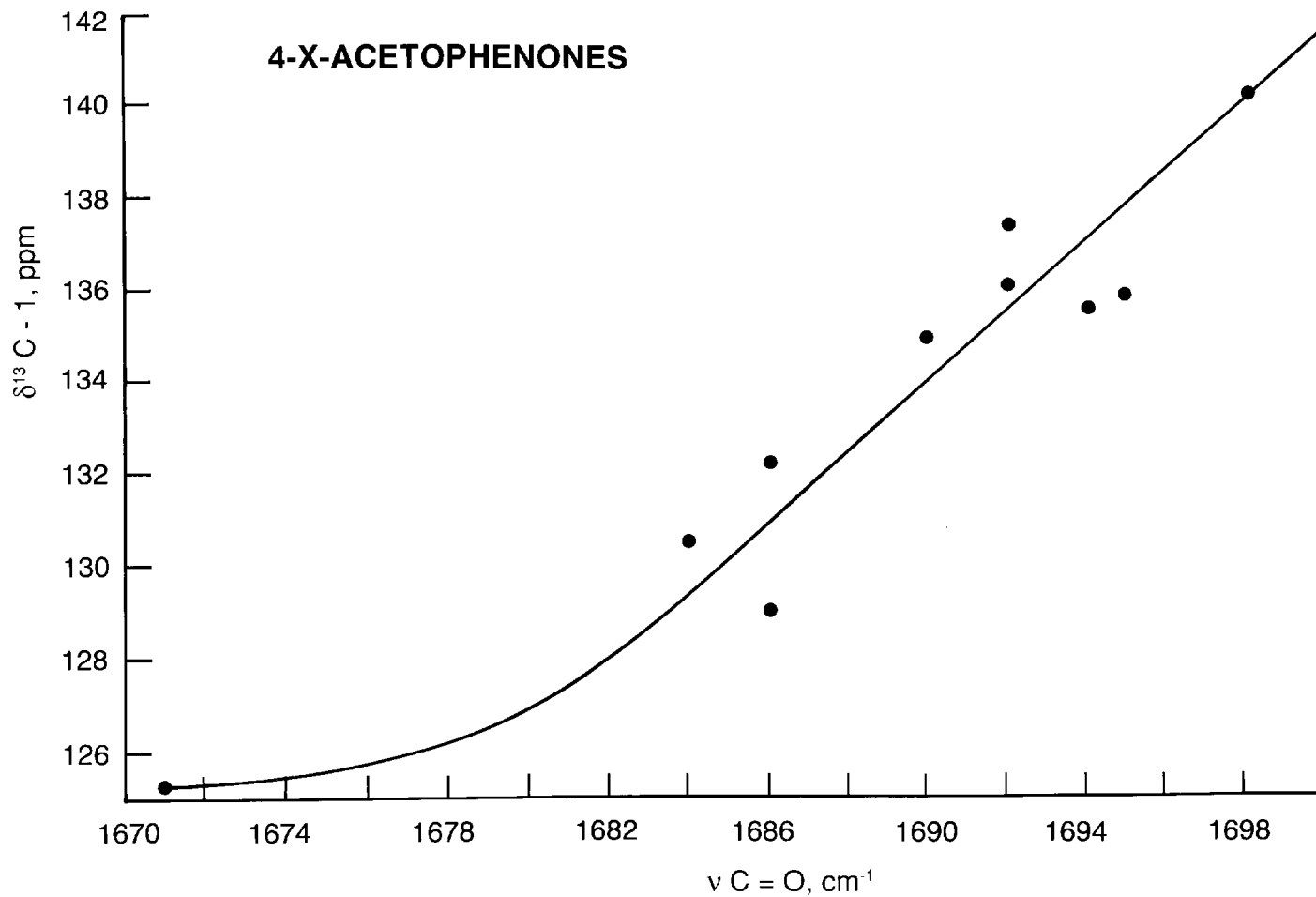


FIGURE 11.27 A plot of $\nu \text{ C}=\text{O}$ (CHCl_3 solution) vs $\delta^{13}\text{C}-1$ (CDCl_3 solution) for 4-x-acetophenones.

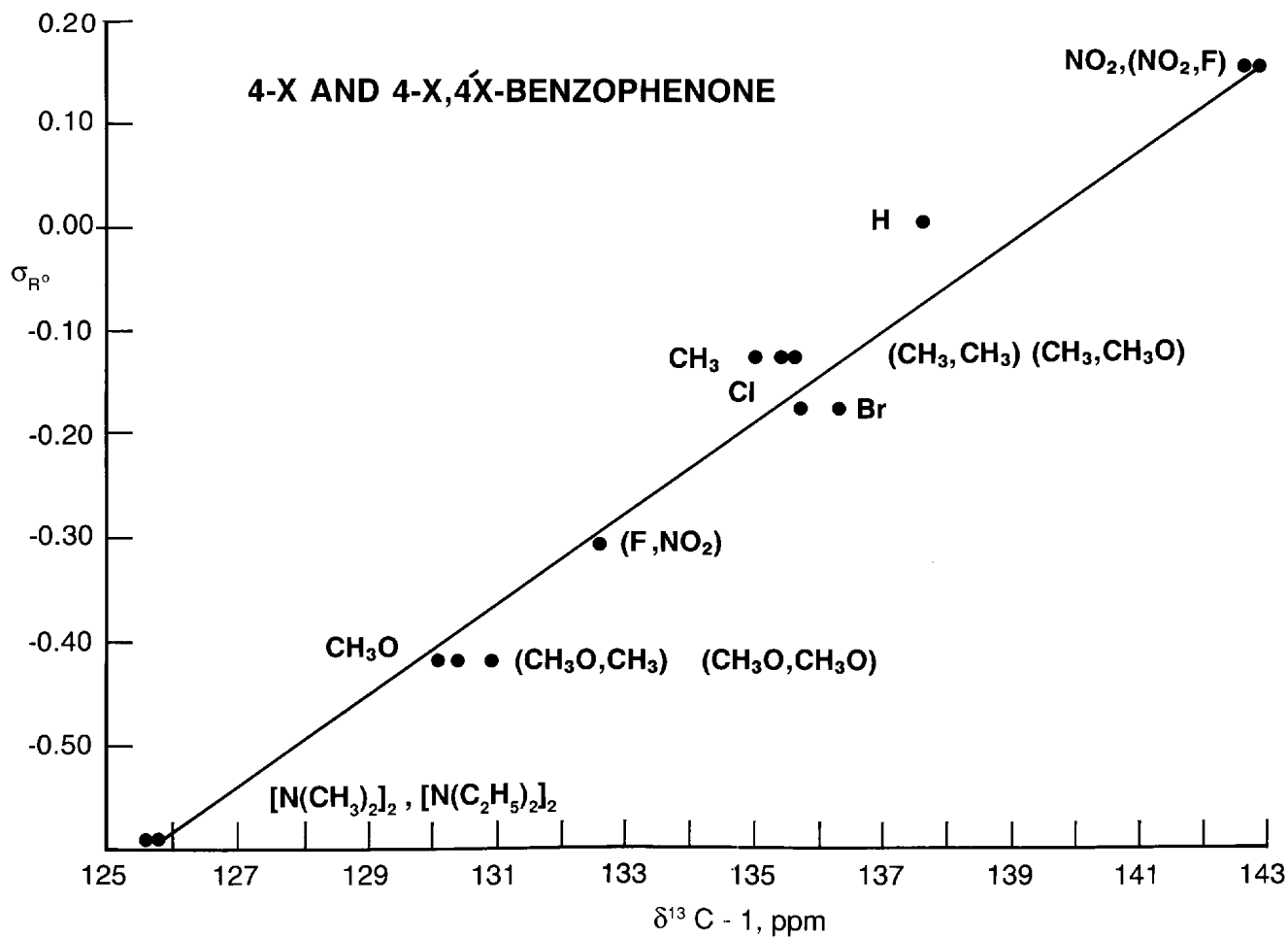


FIGURE 11.28 A plot of $\delta^{13}\text{C}-1$ vs Taft σ_{R} values for the 4-x and 4,4'-x,x atoms or groups for 4-x and 4,4'-x,x-benzophenones. These data are for CHCl_3 solutions.

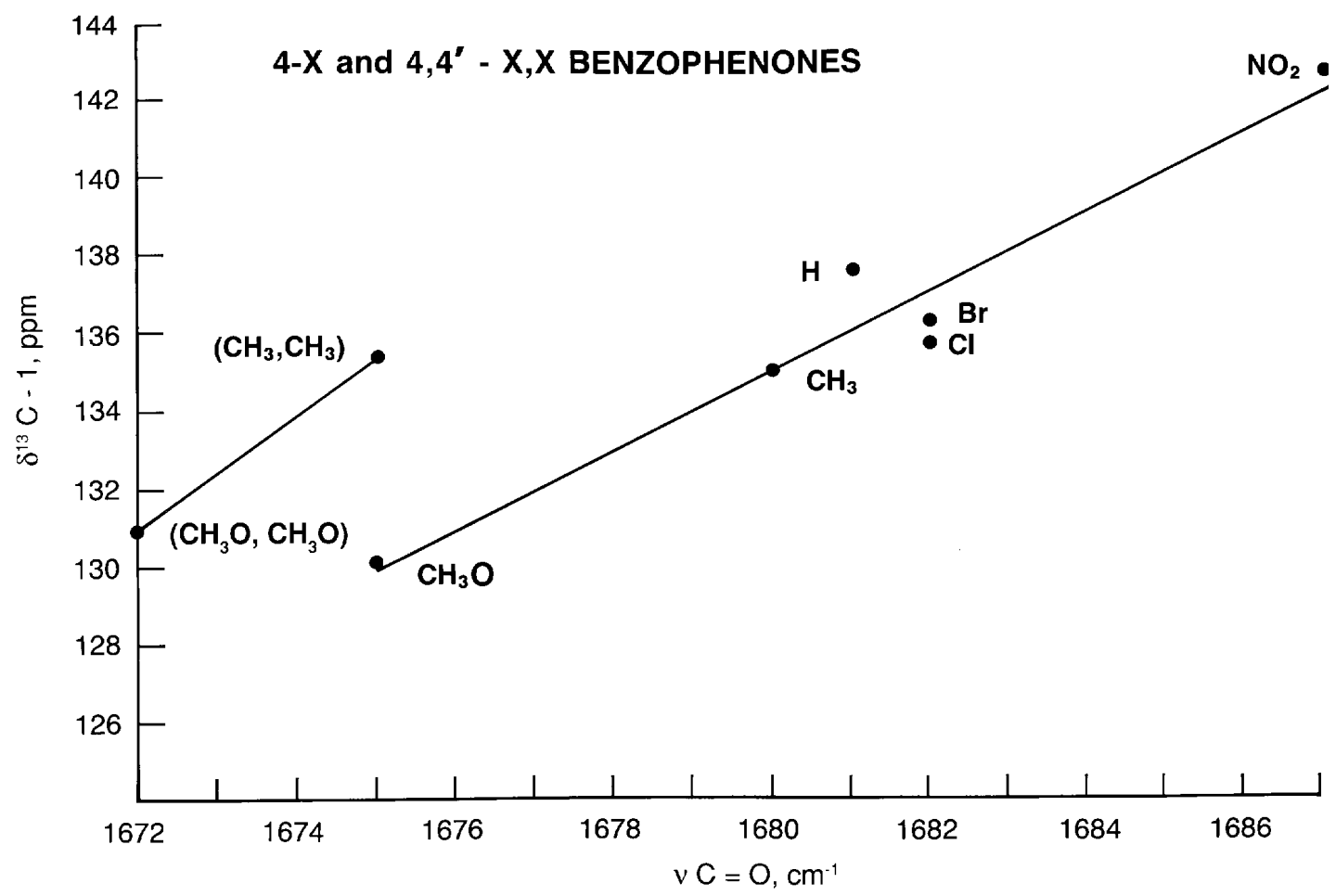


FIGURE 11.29 A plot of $\nu \text{ C}=\text{O}$ in the vapor phase vs $\delta^{13}\text{C}-1$ in CCl_3 solution for 4-x and 4,4'-x,x-benzophenones.

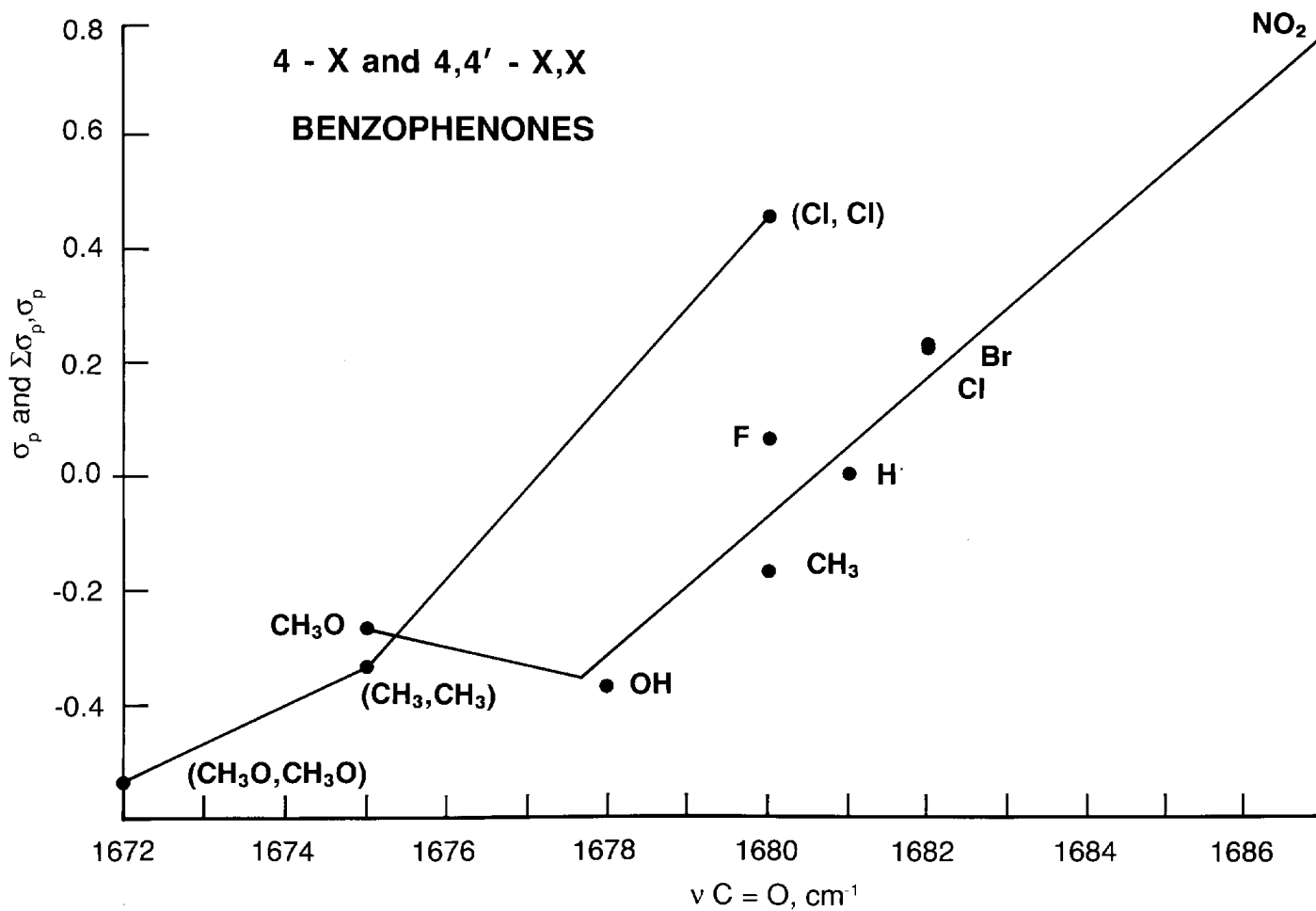


FIGURE 11.30 A plot of $\nu \text{C}=\text{O}$ in the vapor phase vs the sum of Hammett σ_p for the x-atom or group for 4-x- and 4,4'-x,x-benzophenones.

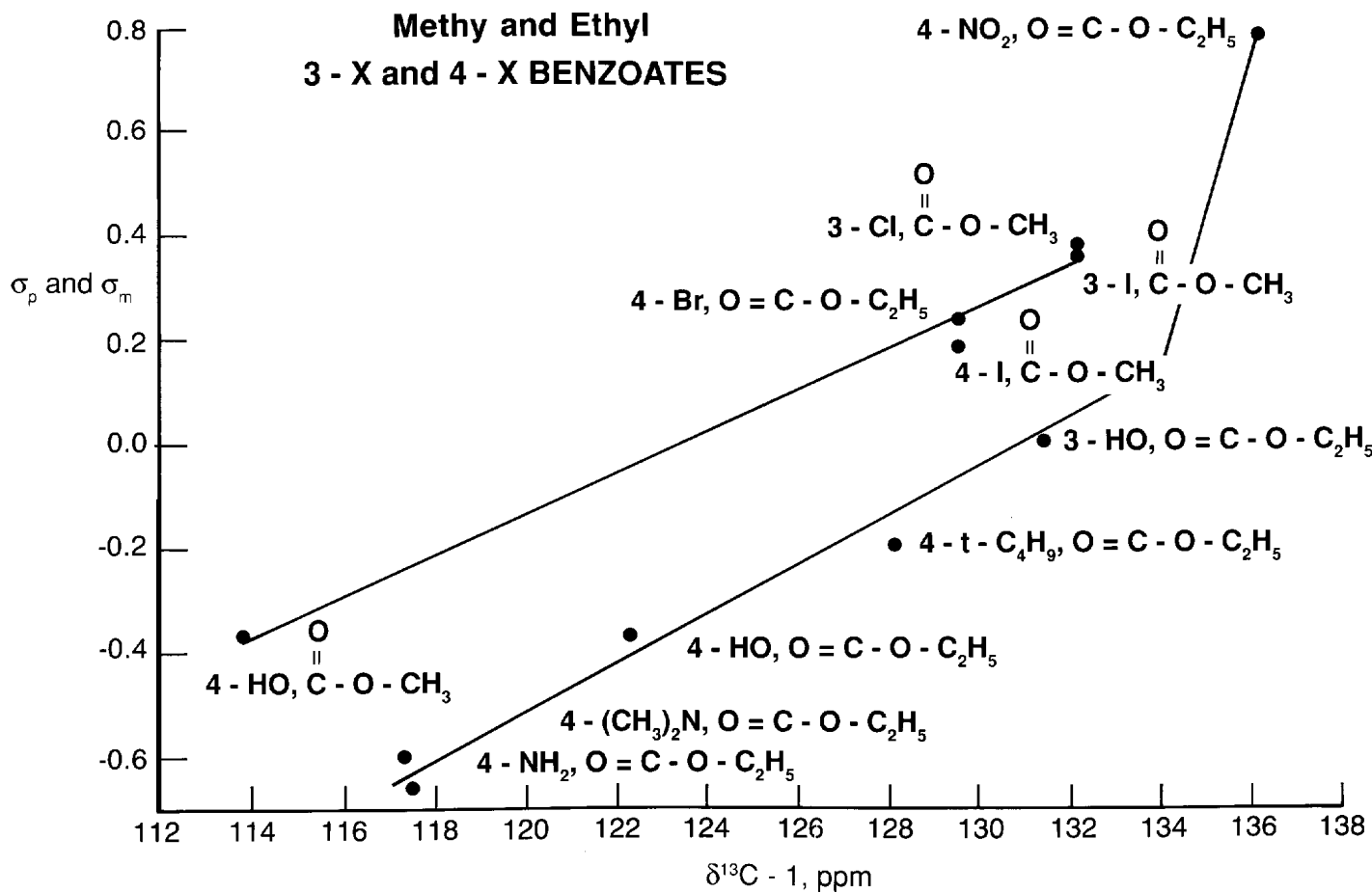


FIGURE 11.31 A plot of $\delta^{13}\text{C}-1$ in CHCl_3 solution vs Hammett σ values for the x atom or group for methyl and ethyl 3-x- and 4-x-benzoates.

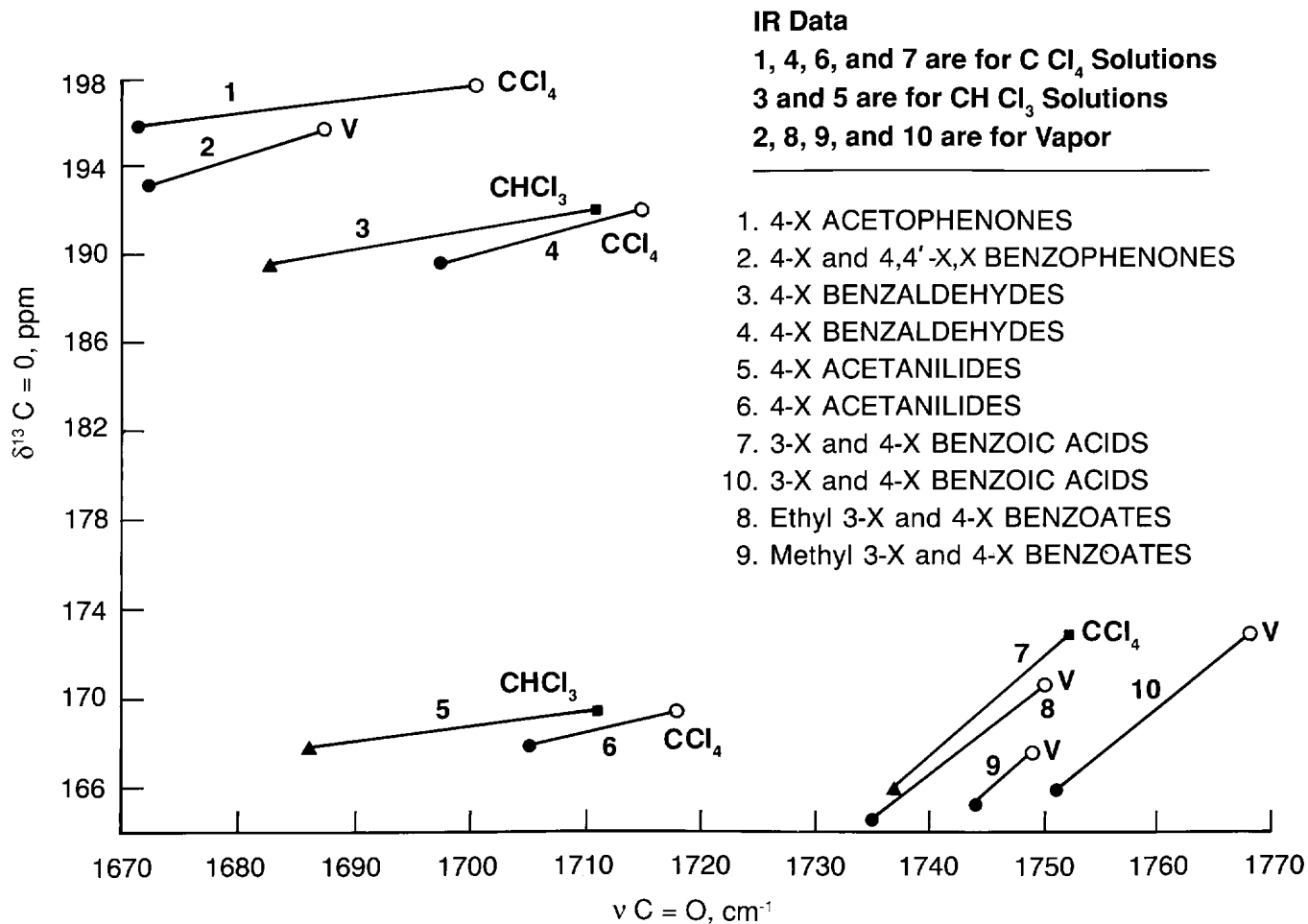


FIGURE 11.32 Plots of the range of $\nu \text{C}=\text{O}$ for the compounds studied in different physical phases vs the range of $\delta^{13}\text{C}=\text{O}$ for the compounds studied in CHCl_3 solutions.

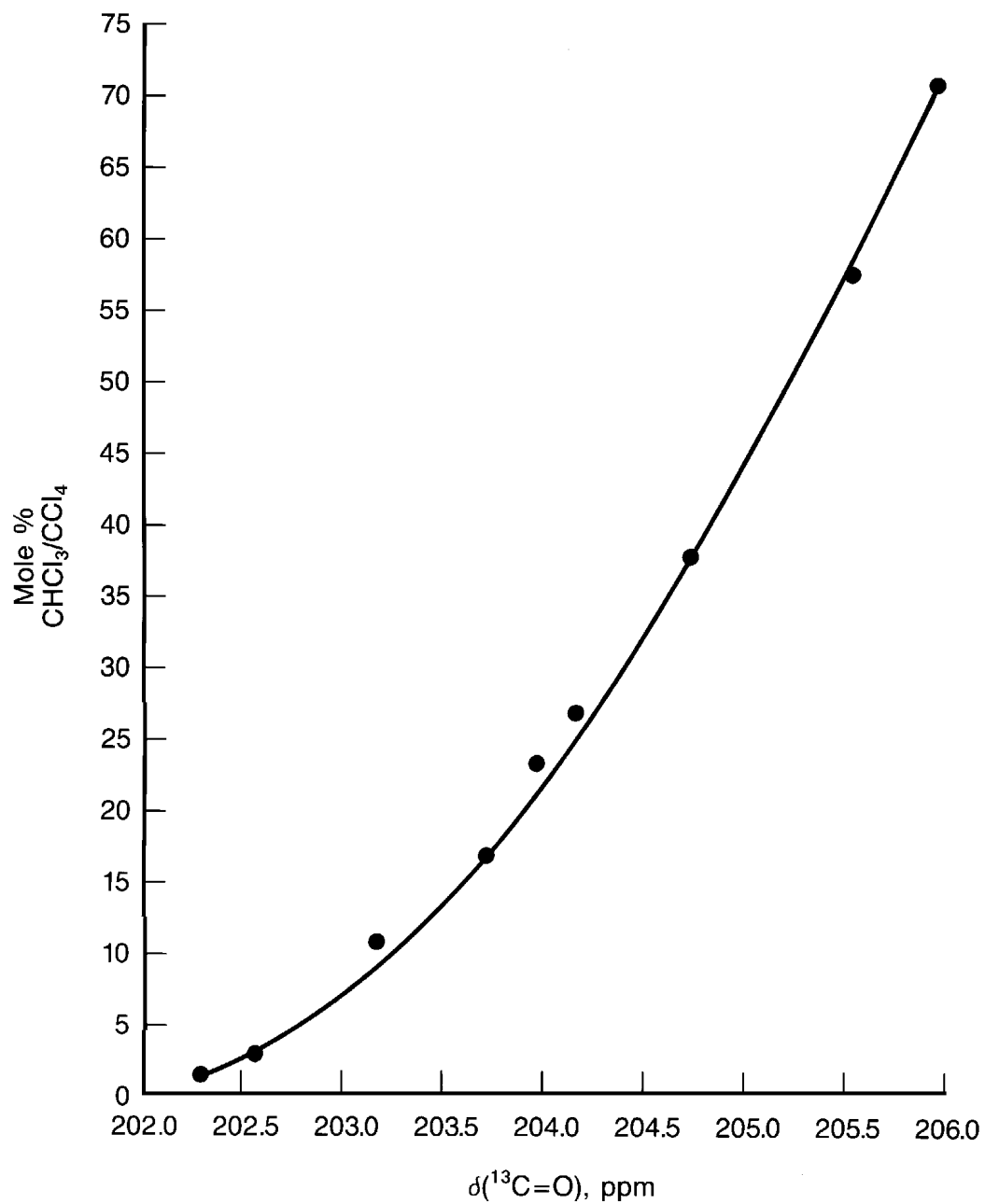
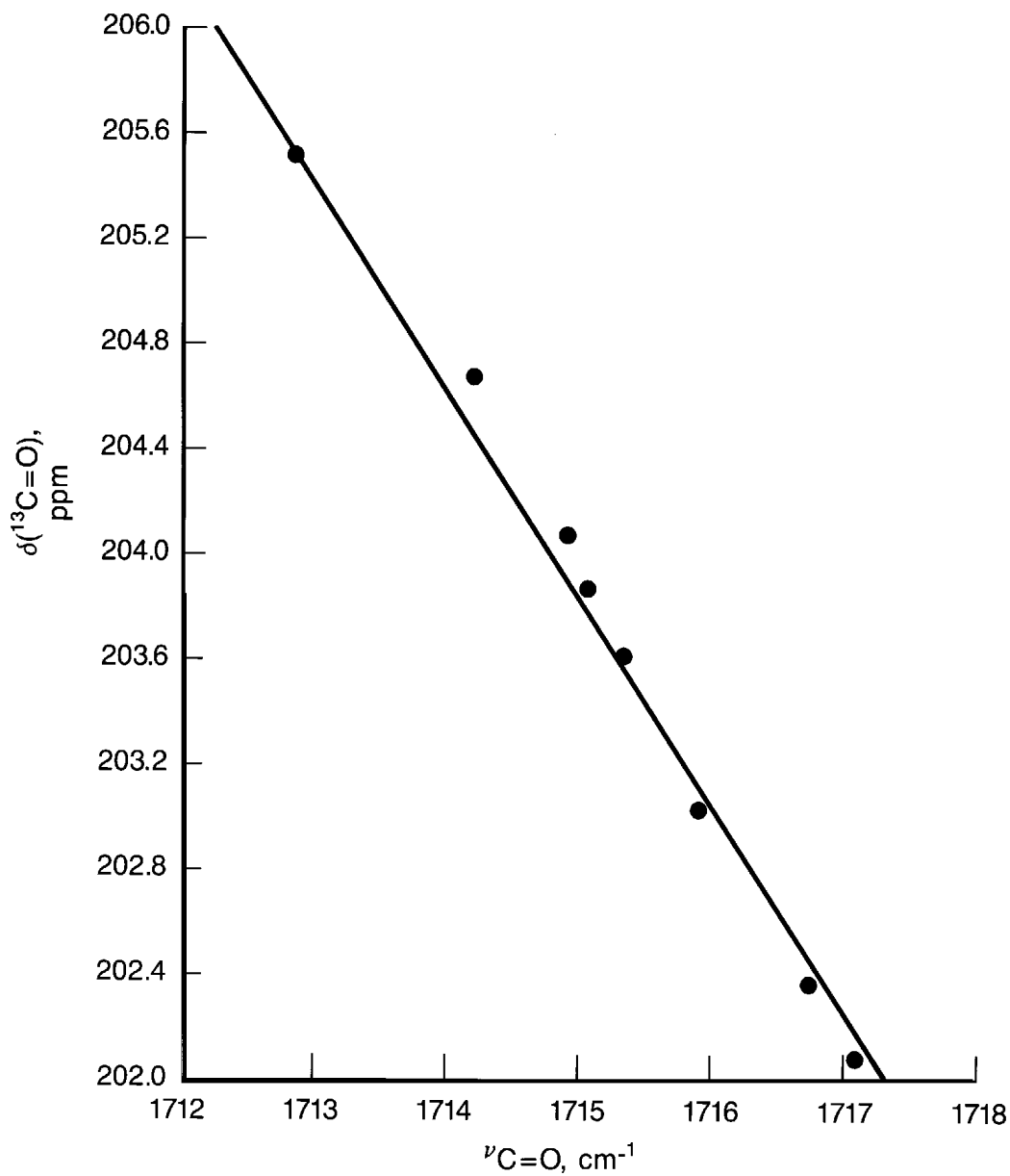


FIGURE 11.33 A plot of $\delta(^{13}\text{C}=\text{O})$ for acetone vs mole % $\text{CHCl}_3/\text{CCl}_4$ solutions.

FIGURE 11.34 A plot of $\nu_{\text{C=O}}$ vs $\delta^{13}\text{C=O}$ for acetone in mole % $\text{CHCl}_3/\text{CCl}_4$ solutions.

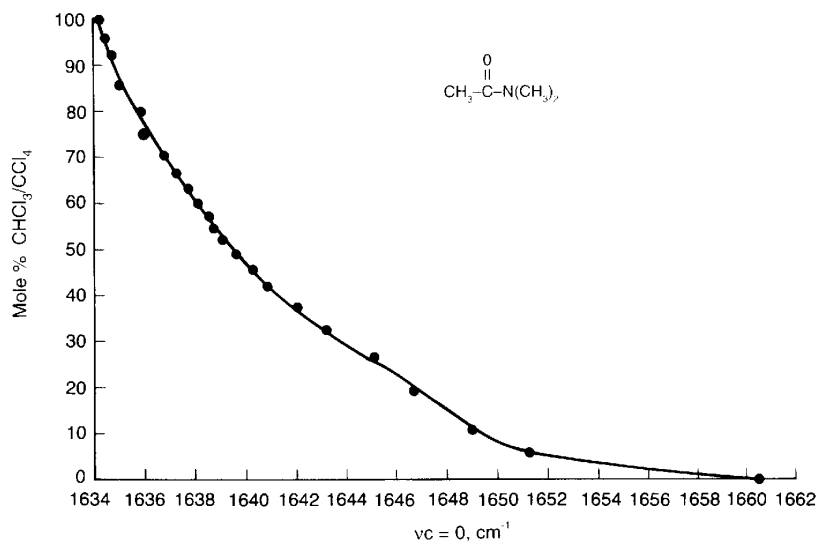


FIGURE 11.35 A plot of $\nu \text{C}=\text{O}$ for dimethylacetamide in CCl_4 and/or CHCl_3 solution vs mole % $\text{CHCl}_3/\text{CCl}_4$.

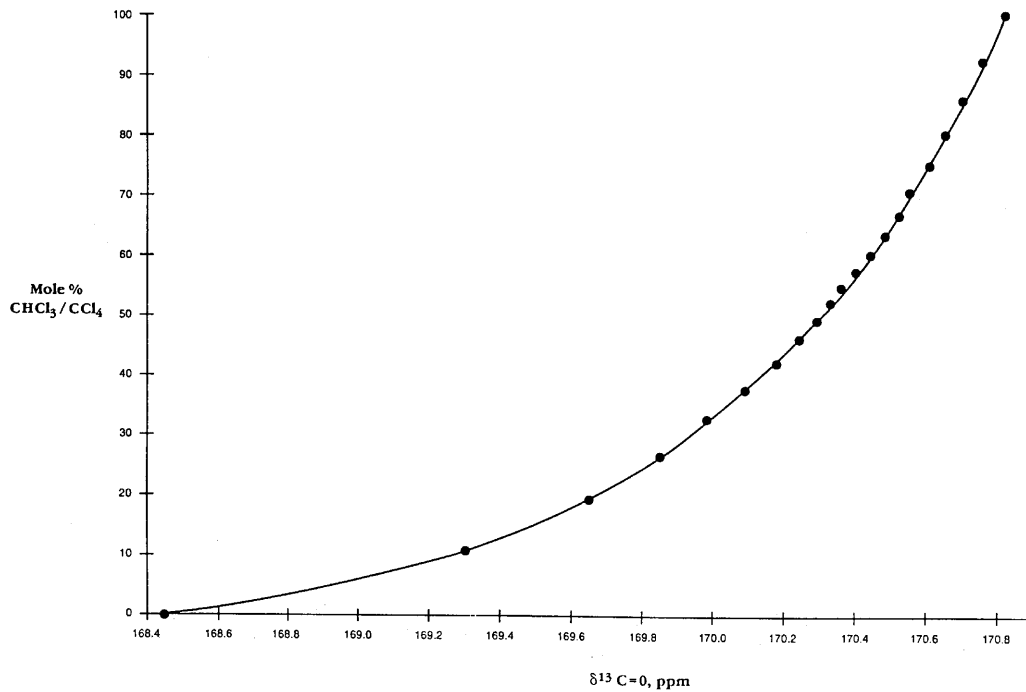


FIGURE 11.35a A plot of $\delta^{13}\text{C}=\text{O}$ for dimethylacetamide in CCl_4 and/or CHCl_3 solution vs mole % $\text{CHCl}_3/\text{CCl}_4$.

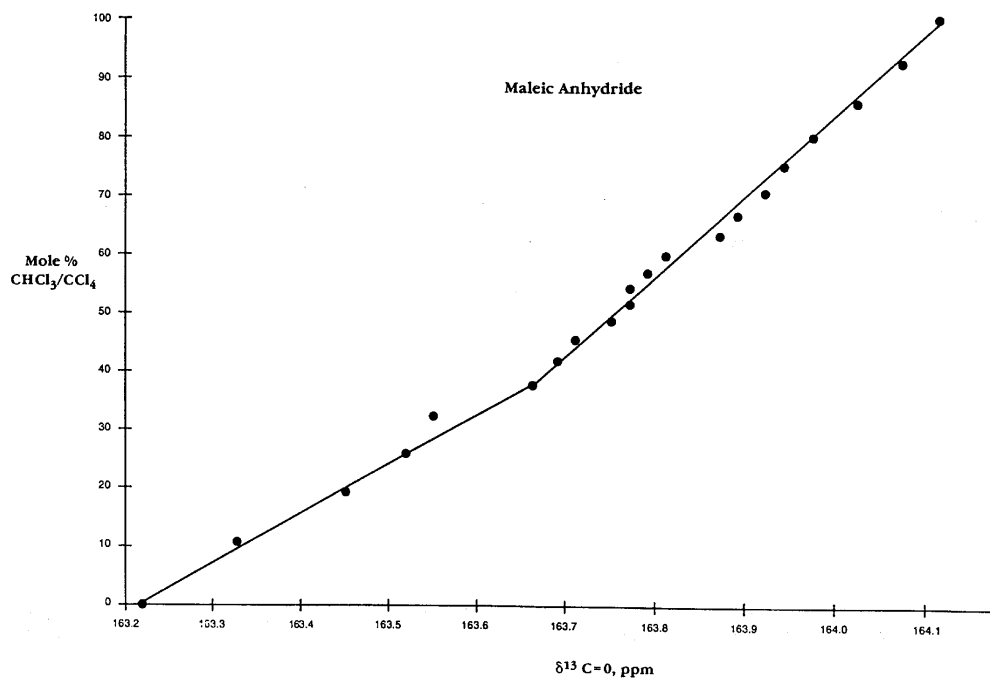


FIGURE 11.35b A plot of $\delta^{13}\text{C}=\text{O}$ for maleic anhydride vs mole % $\text{CHCl}_3/\text{CCl}_4$.

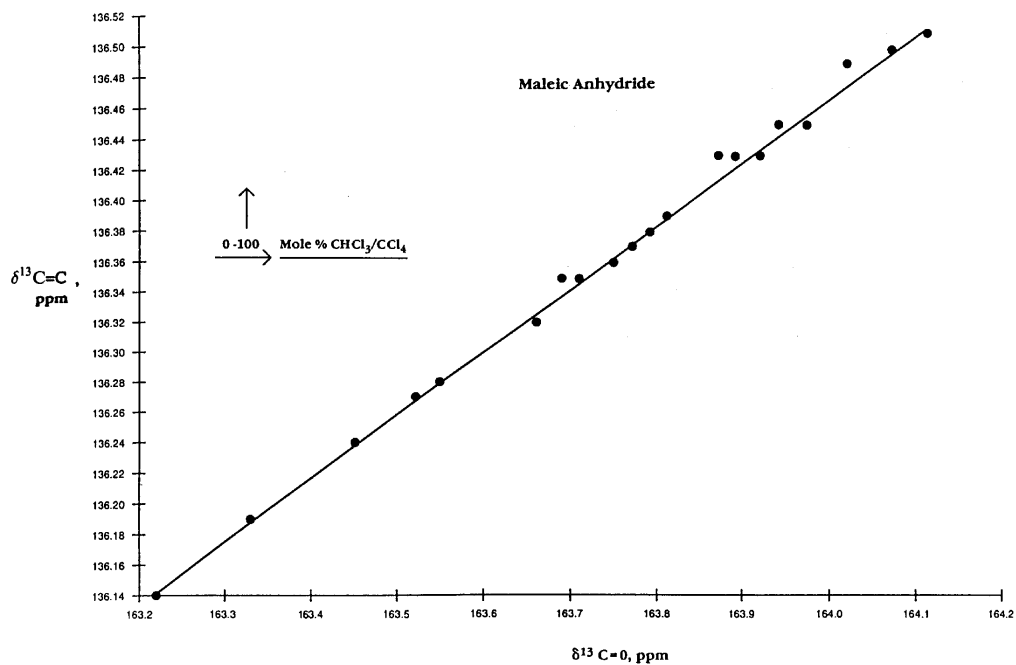


FIGURE 11.35c A plot of $\delta^{13}\text{C}=\text{O}$ vs $\delta^{13}\text{C}=\text{C}$ for maleic anhydride in 0 to 100 mol% $\text{CHCl}_3/\text{CCl}_4$ solutions.

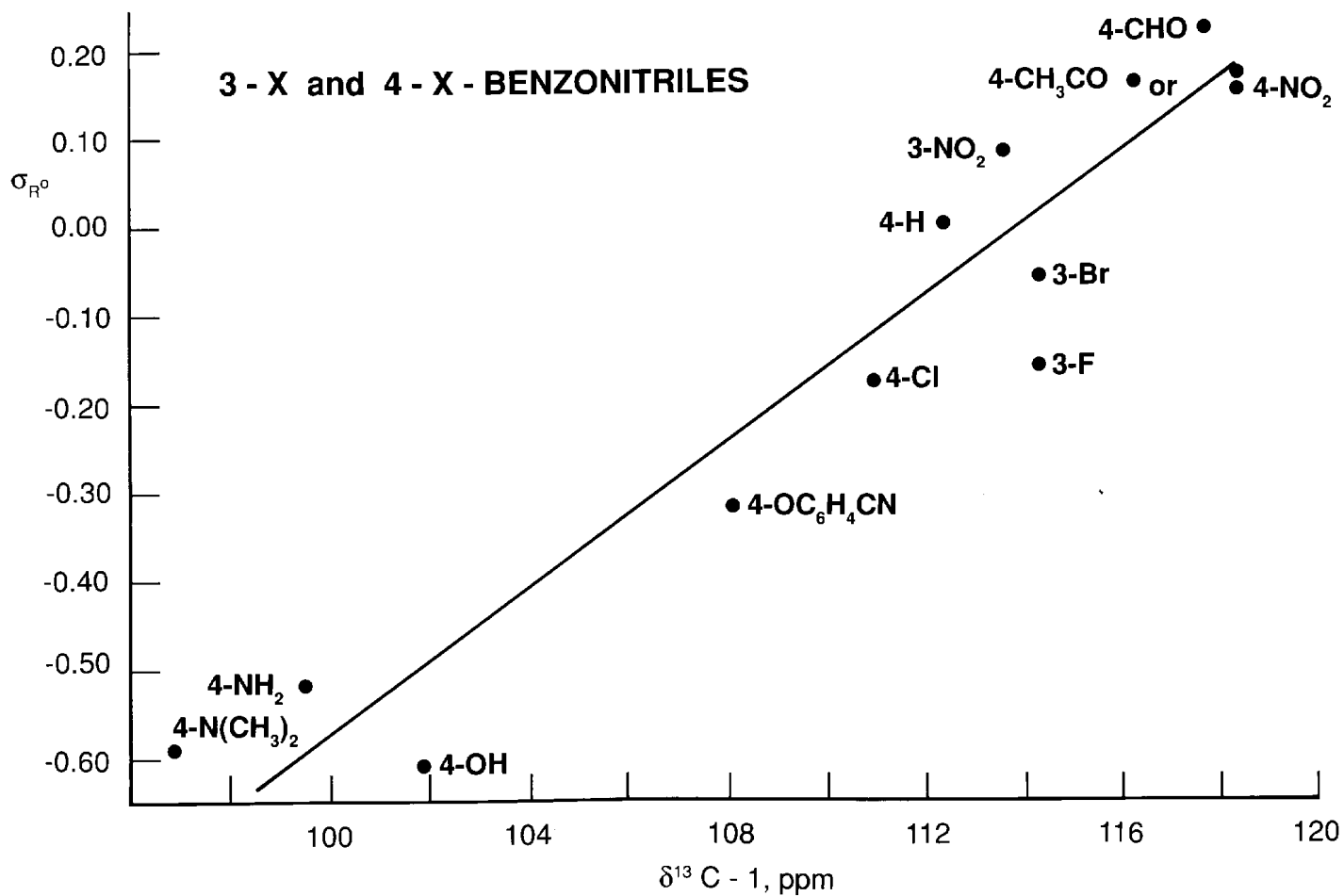


FIGURE 11.36 A plot of $\delta^{13}\text{C}-1$ vs Taft σ_{R^o} values for the 3-x and 4-x atom or group for 3-x- and 4-x-benzonitriles in CDCl_3 solution.

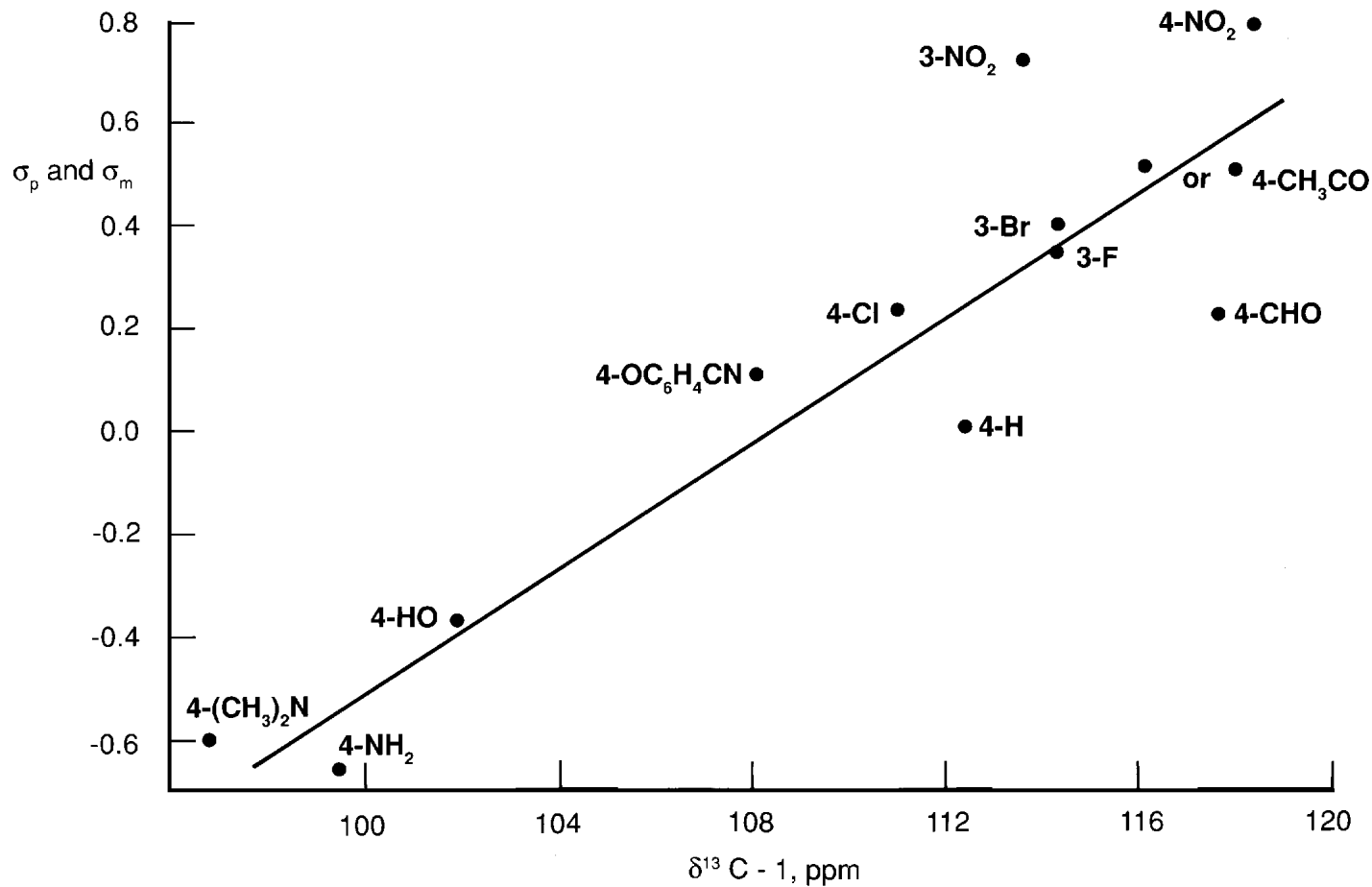


FIGURE 11.37 A plot of $\delta^{13}\text{C}-1$ vs Hammett σ values for the 3-x or 4-x atom or group for 3-x- and 4-x-benzonitriles in CHCl_3 solution.

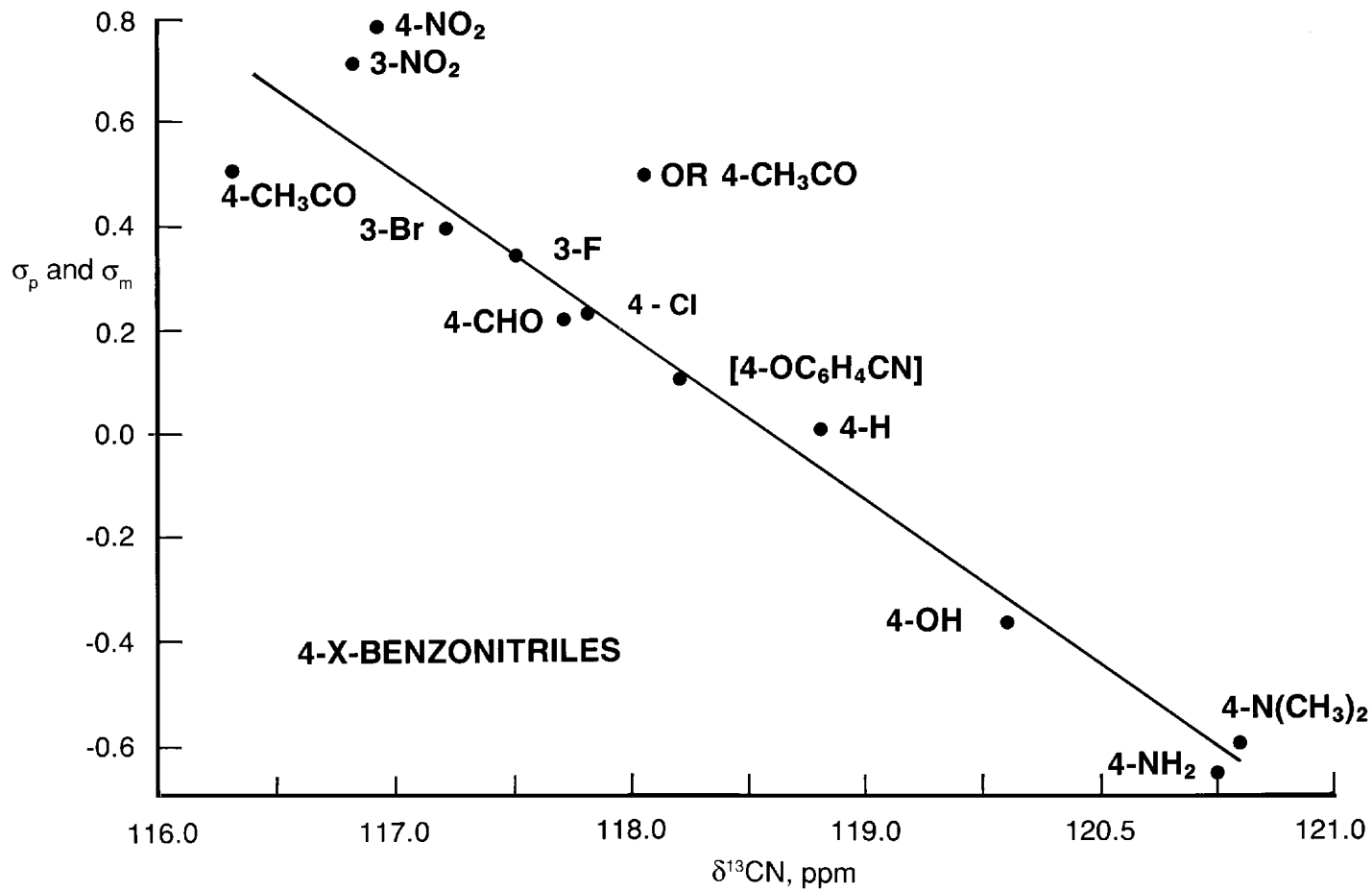


FIGURE 11.38 A plot of $\delta^{13}\text{CN}$ vs Hammett σ values for the 3-x or 4-x atom or group for 3-x- and 4-x-benzonitriles in CHCl_3 solution.

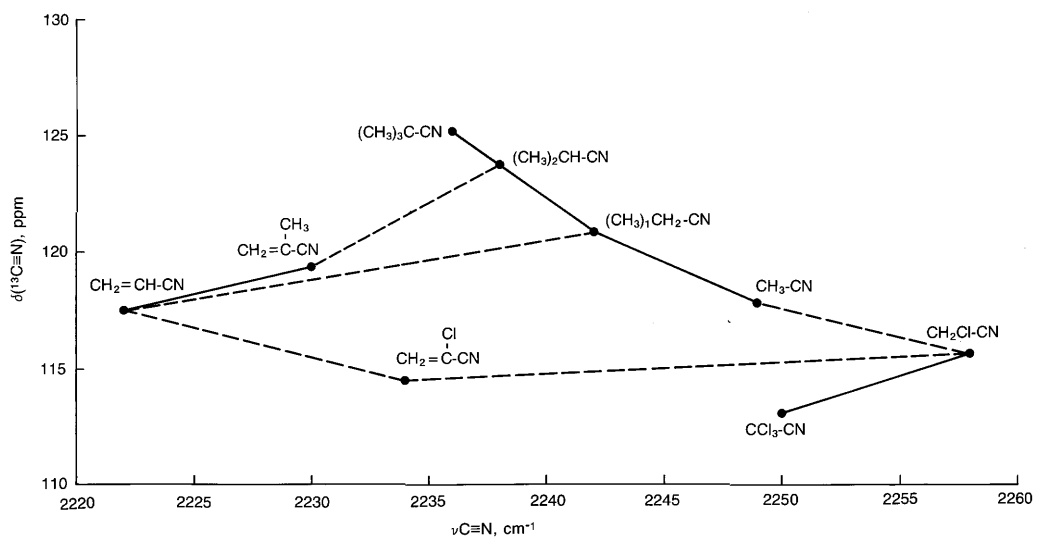


FIGURE 11.39 A plot of νCN vs $\delta^{13}\text{CN}$ for organonitriles.

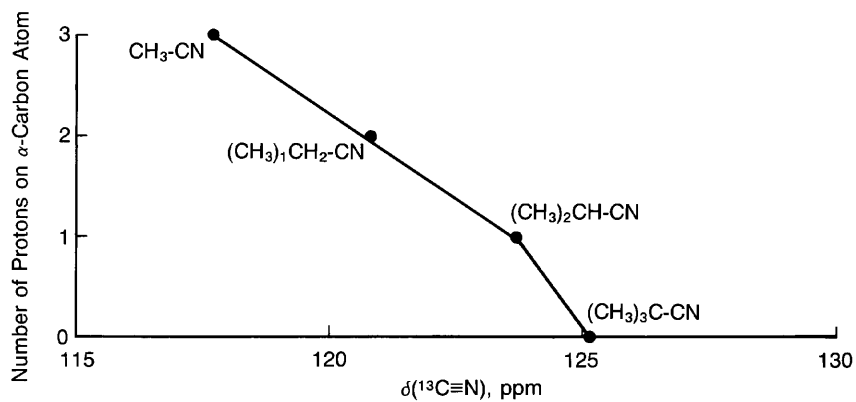
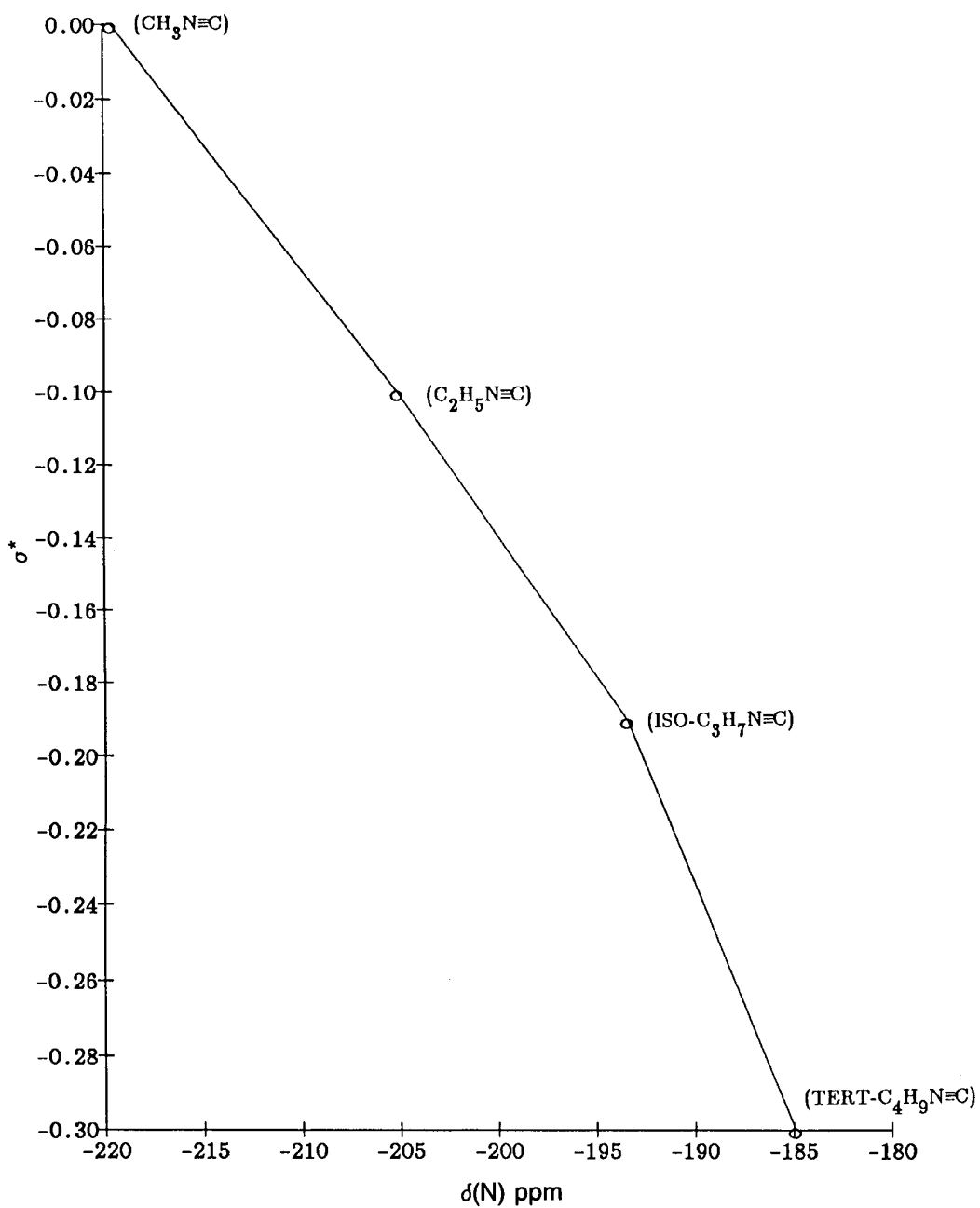
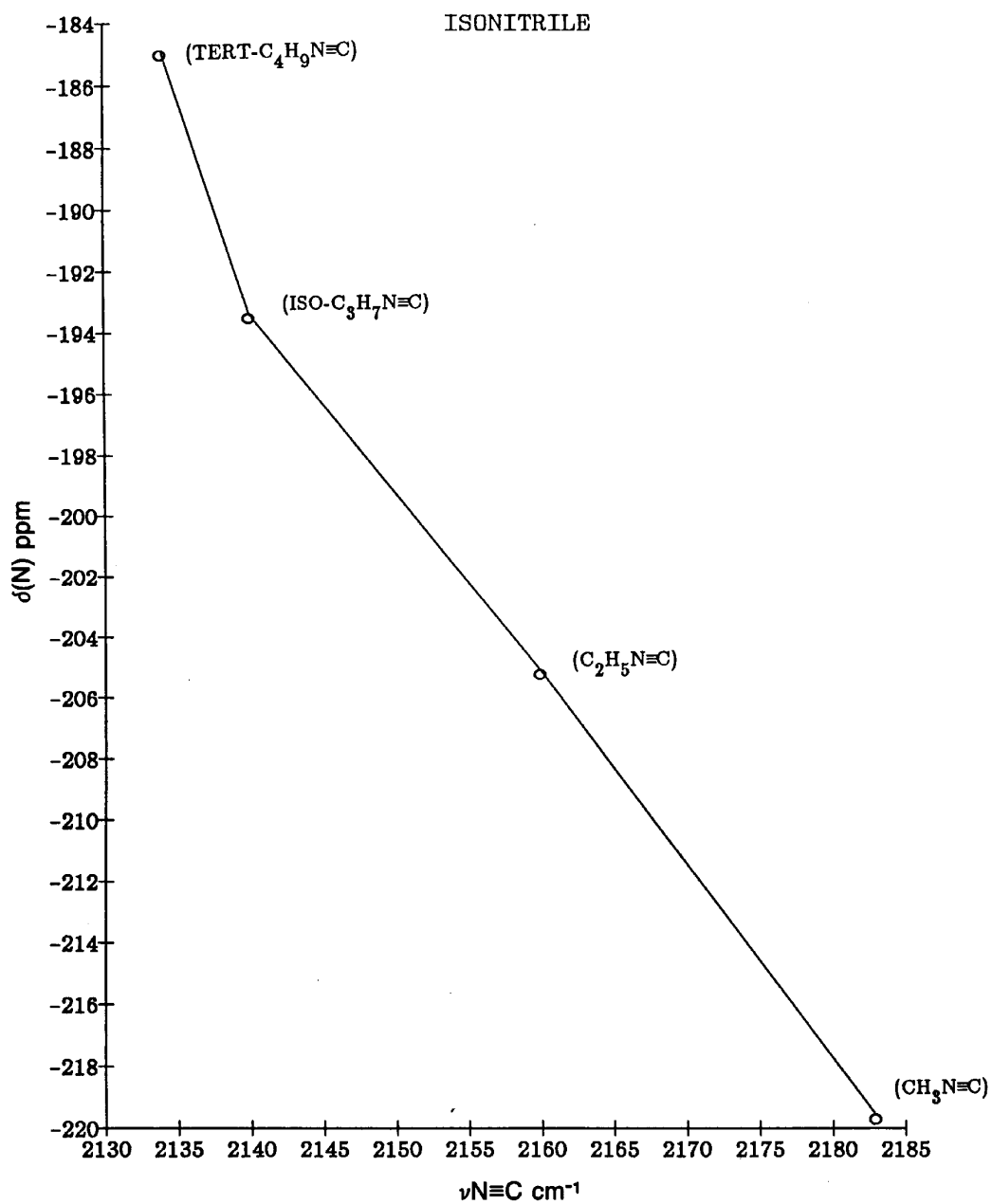


FIGURE 11.40 A plot of $\delta^{13}\text{CN}$ vs the number of protons on the α -carbon atom of alkyl nitriles.

ISONITRILE

FIGURE 11.41 A plot of Taft σ^* values for the alkyl group vs $\delta^{15}\text{N}$ for alkyl isonitriles.

FIGURE 11.42 A plot of $\delta^{15}\text{N}$ vs νNC for alkyl isonitriles.

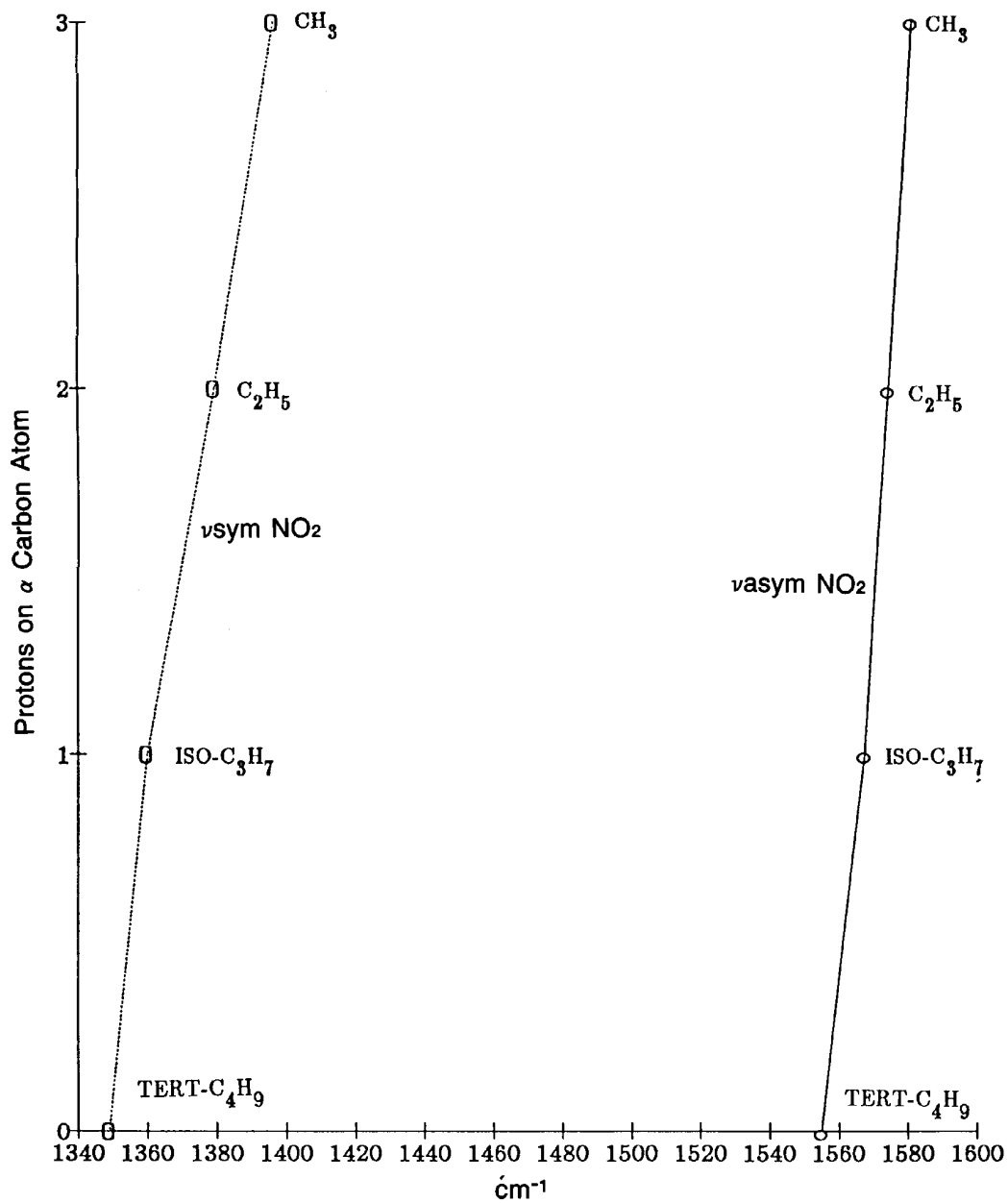
R-NO₂

FIGURE 11.43 Plots of the number of protons in the alkyl α -carbon atom vs $\nu_{\text{sym}} \text{NO}_2$ and $\nu_{\text{asym}} \text{NO}_2$ for nitroalkanes in the vapor phase.

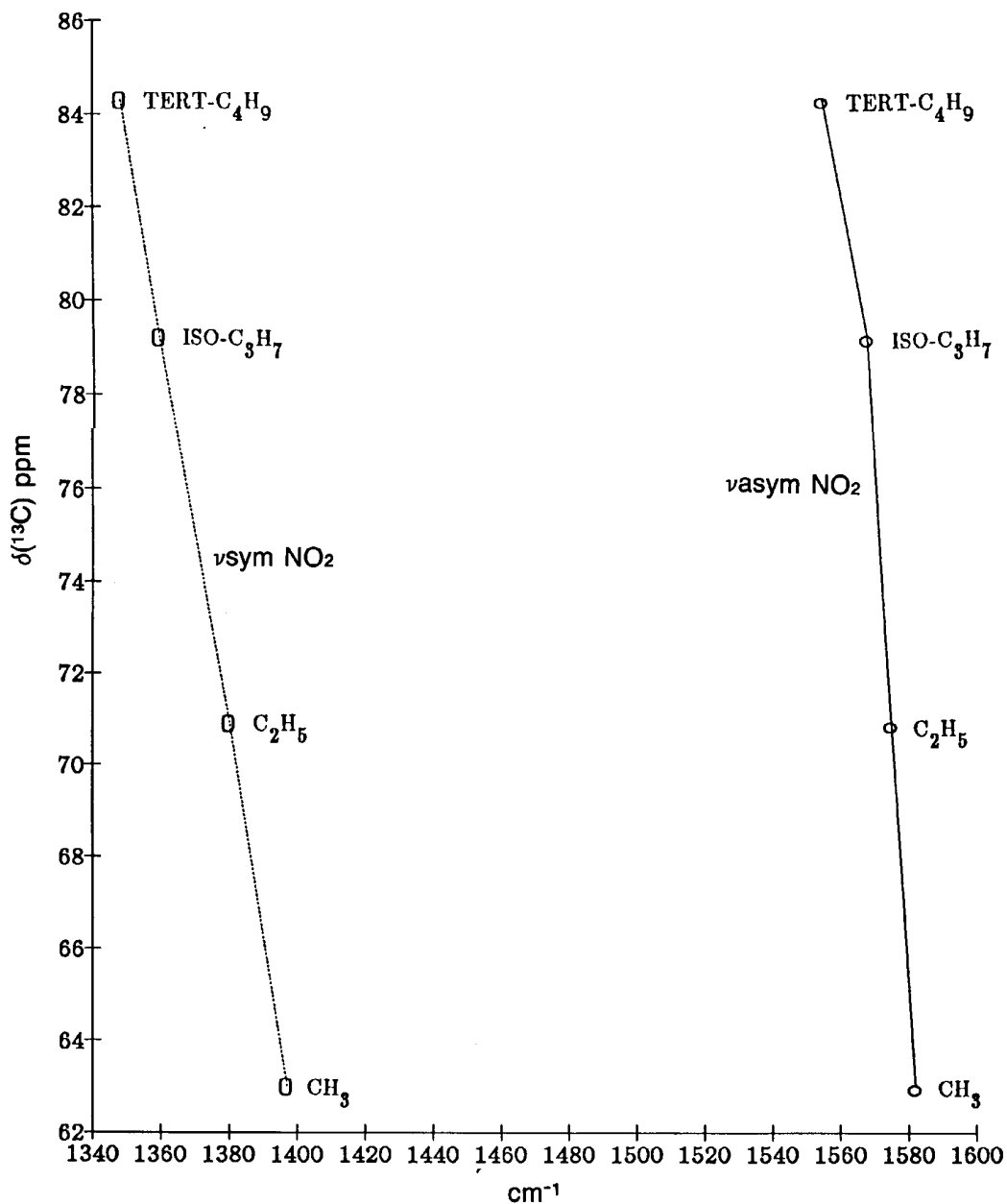
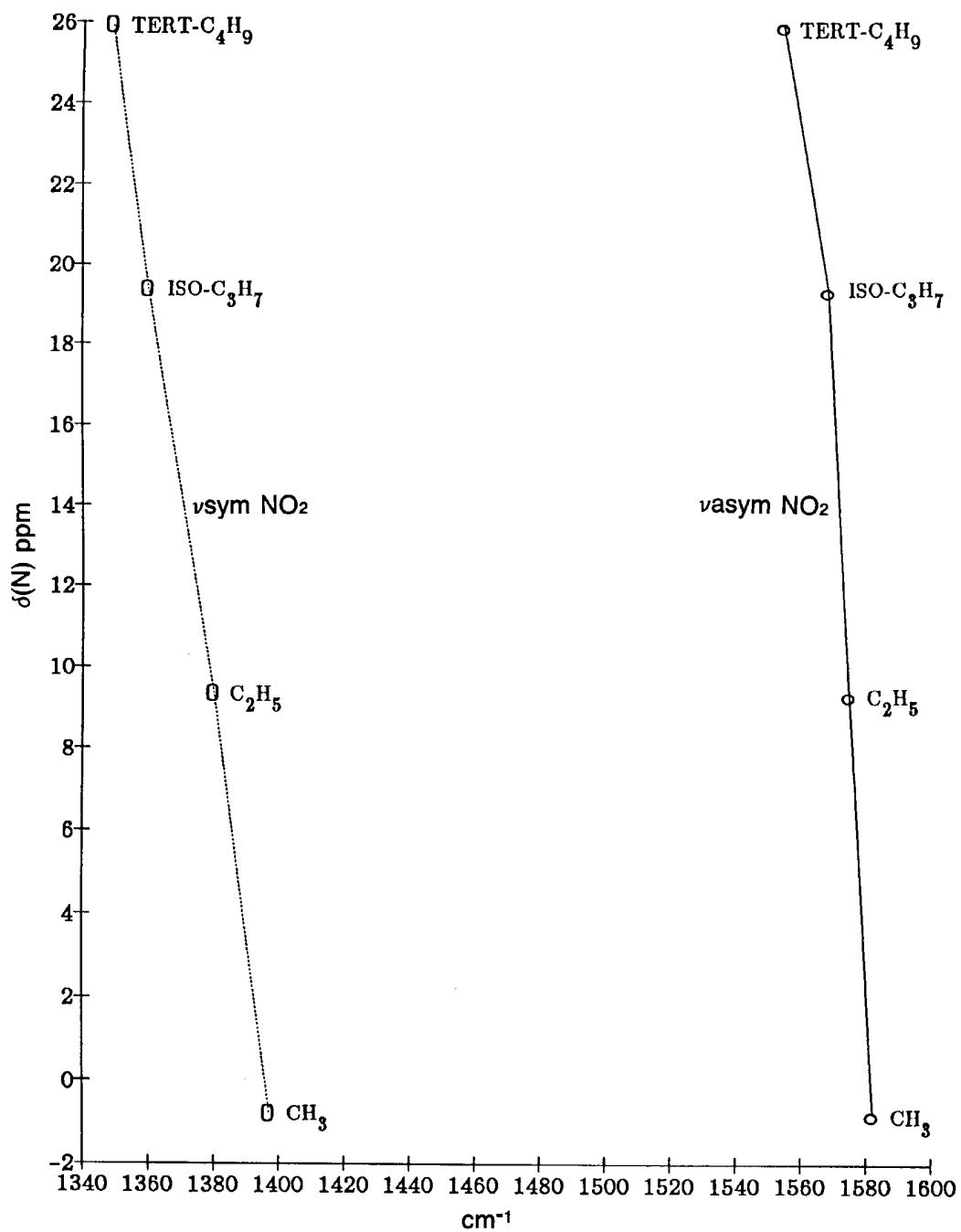
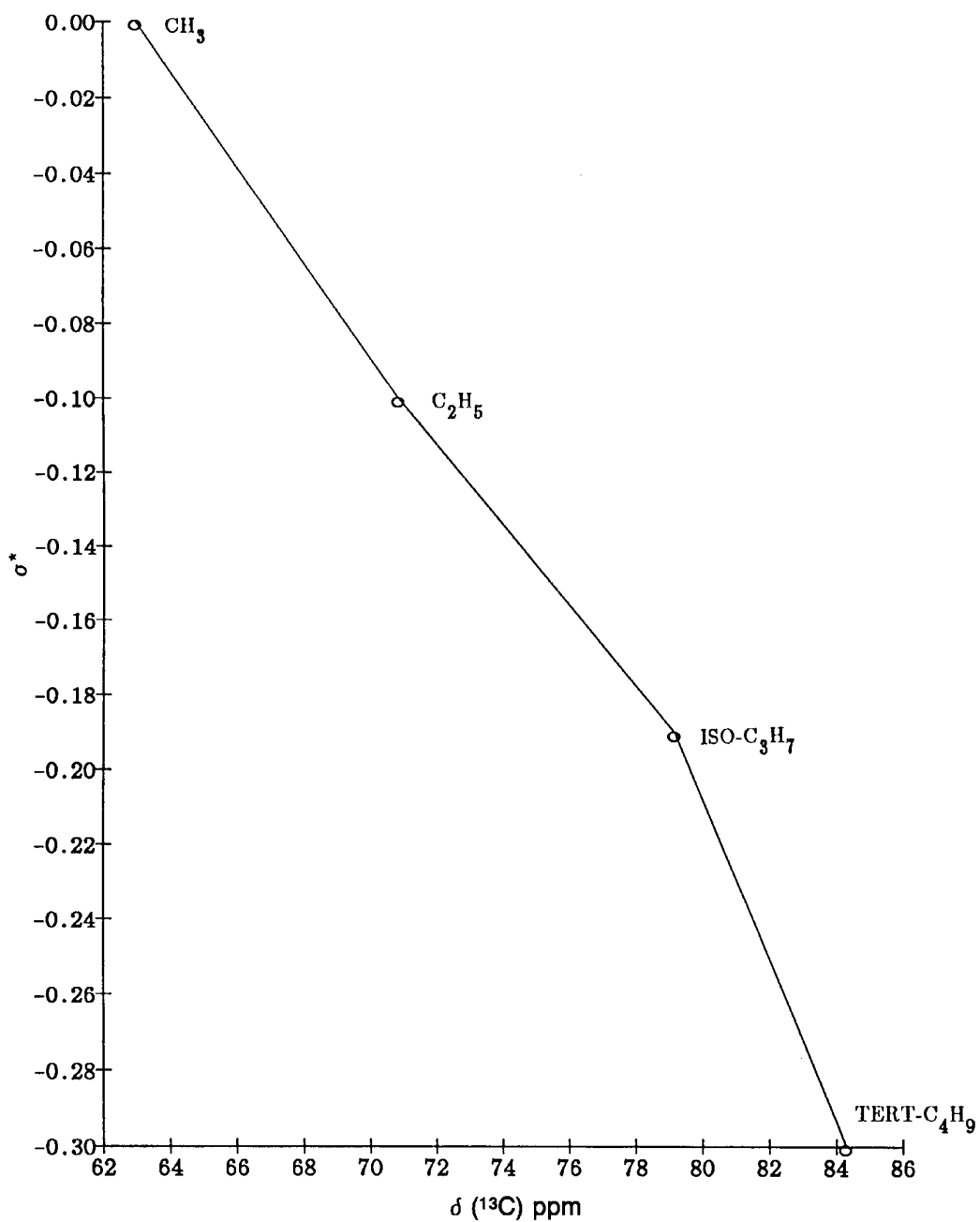
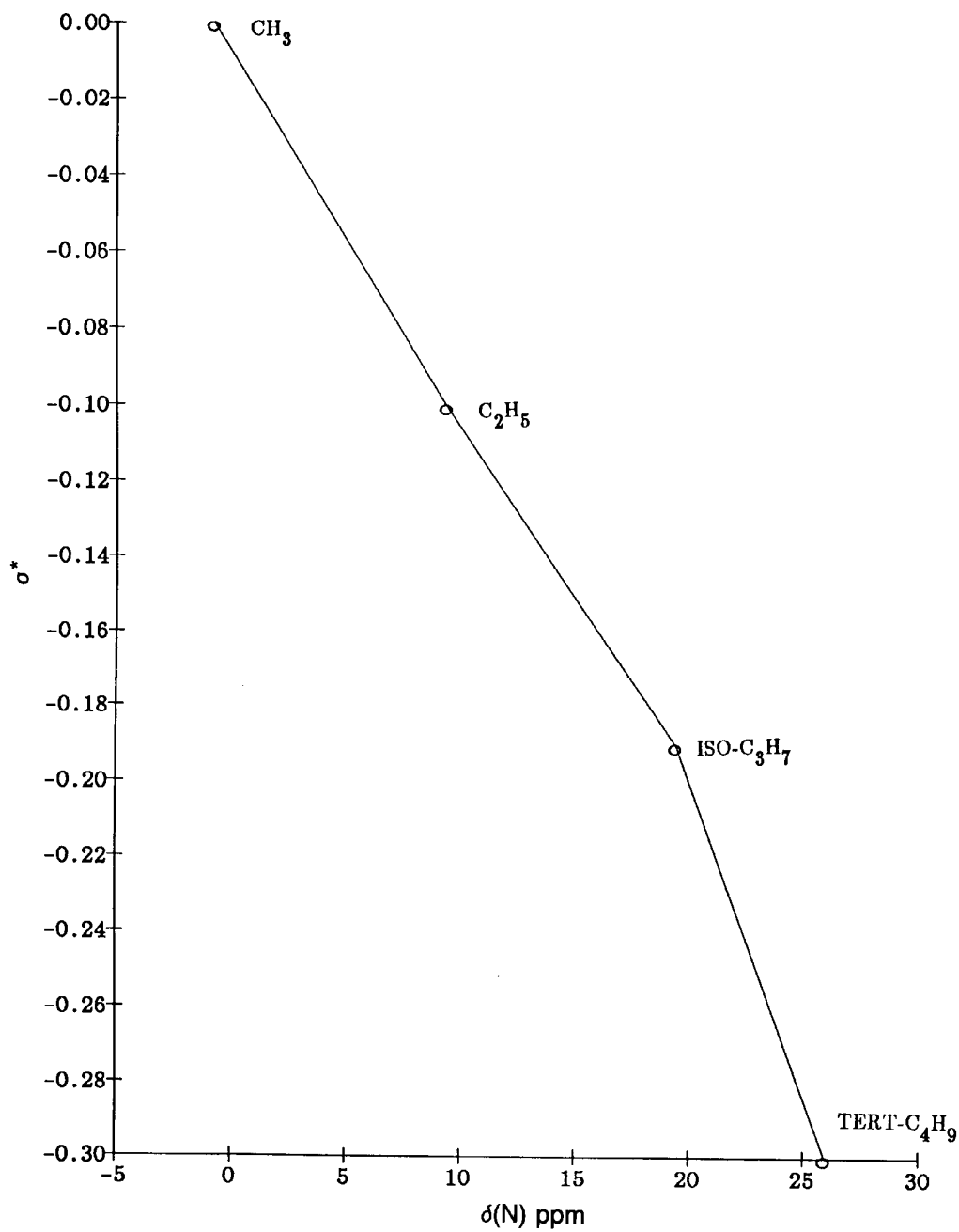
R-NO₂

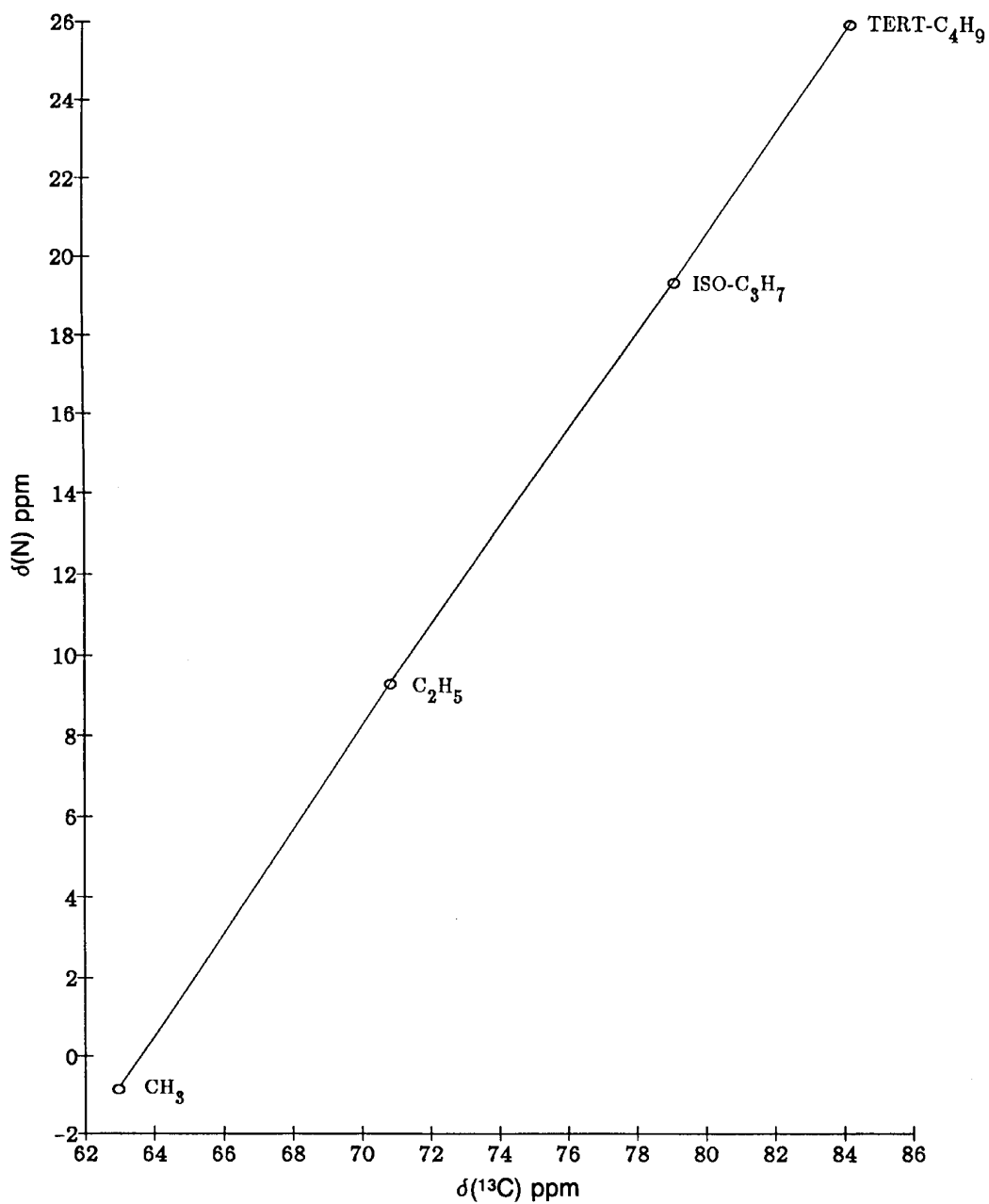
FIGURE 11.44 Plots of $\delta^{13}\text{C}$ (CHCl_3 solution) for the alkyl α -carbon atom vs $\nu_{\text{sym}} \text{NO}_2$ and $\nu_{\text{asym}} \text{NO}_2$ (vapor phase) for nitroalkanes.

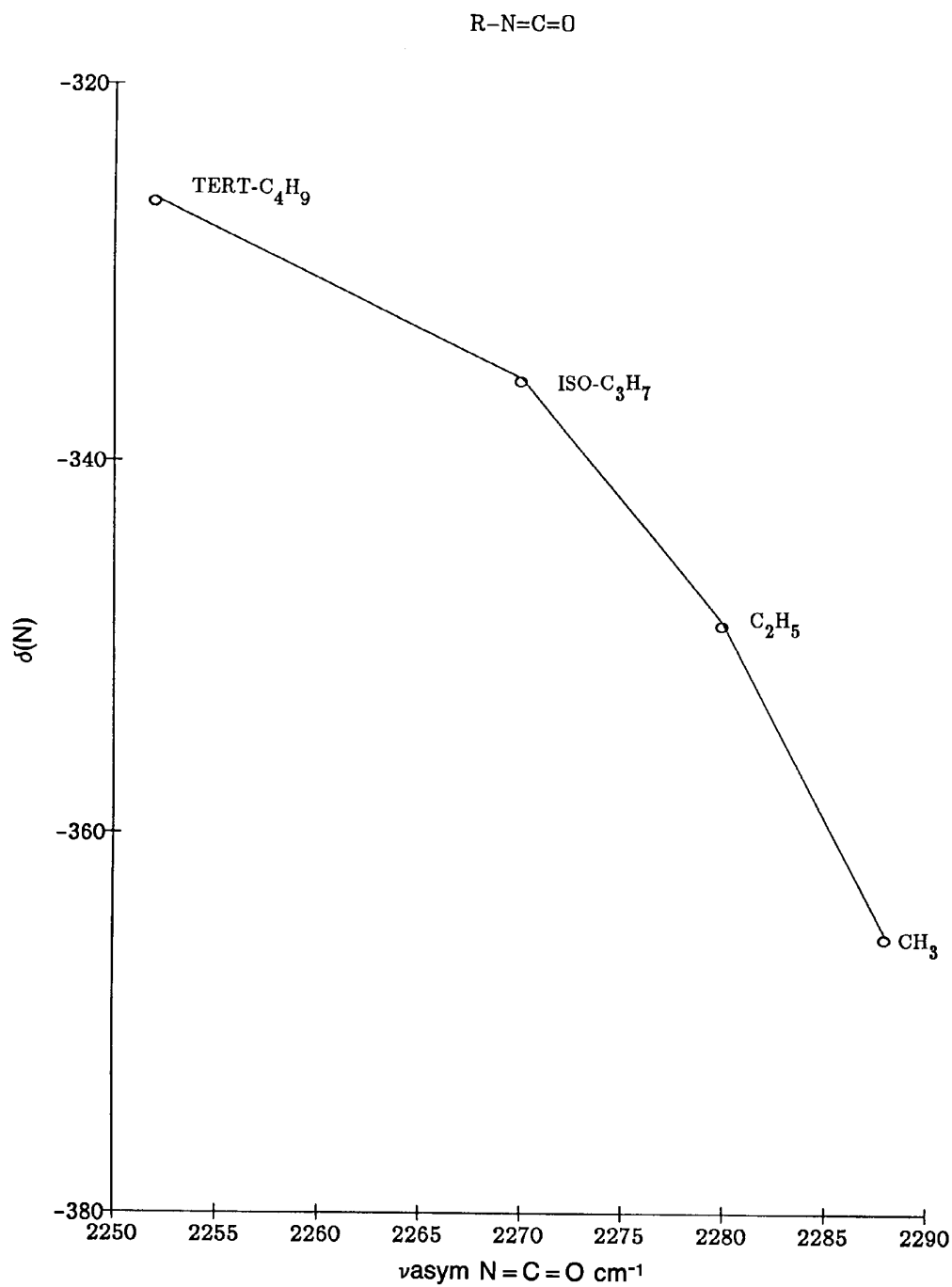
FIGURE 11.45 Plots of $\delta(^{15}\text{N})$ (in 0.3 M acetone) vs $\nu_{\text{sym}} \text{NO}_2$ and $\nu_{\text{asym}} \text{NO}_2$ (vapor phase) for nitroalkanes.

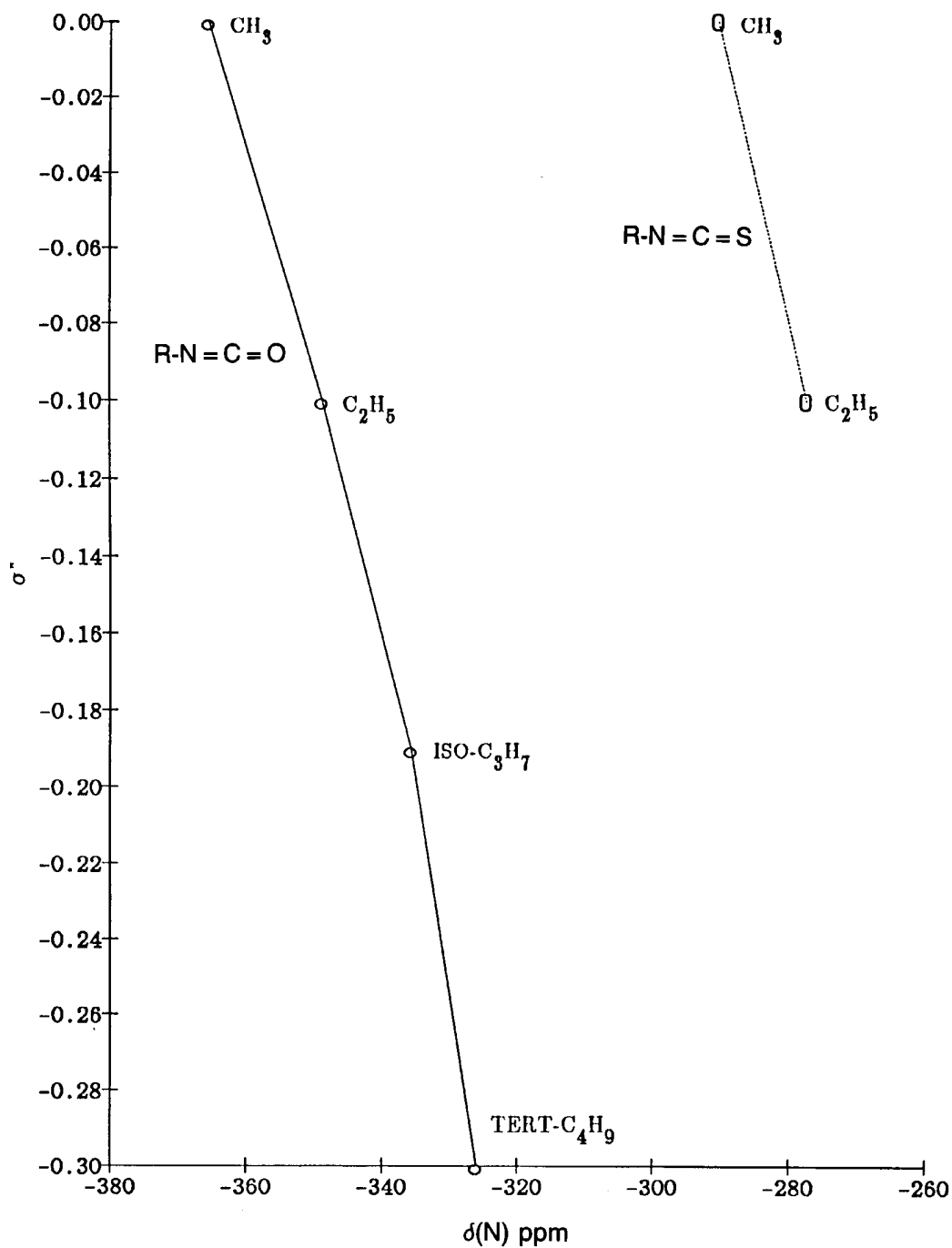
R-NO₂FIGURE 11.46 A plot of Taft σ^* values for the alkyl α -carbon atom group vs δ ^{13}C for nitroalkanes.

R-NO₂FIGURE 11.47 A plot of Taft σ^* values for the alkyl α -carbon atom vs $\delta^{15}\text{N}$ for nitroalkanes.

NITROGEN 15 VERSUS CARBON 13 SHIFTS

FIGURE 11.48 A plot of $\delta^{15}\text{N}$ vs $\delta^{13}\text{C}$ for the alkyl α -carbon atom for nitroalkanes.

FIGURE 11.49 A plot of $\delta^{15}N$ vs $\nu_{\text{asym}} N=C=O$ for alkyl isocyanates.

FIGURE 11.50 Plots of Taft σ^* values for the alkyl groups for alkyl isocyanates and alkyl isothiocyanates.

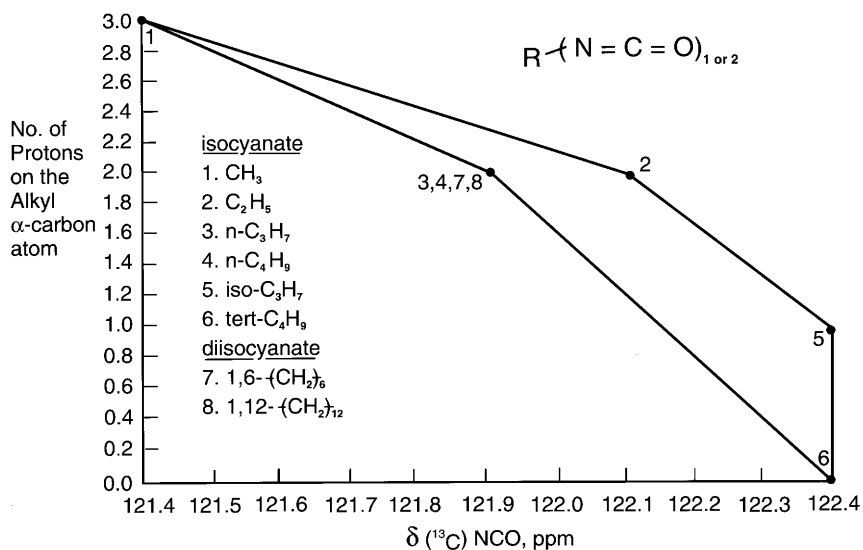


FIGURE 11.51 Plots of δ ^{13}C for the $\text{N}=\text{C}=\text{O}$ group vs the number of protons on the alkyl α -carbon atom for alkyl isocyanates and alkyl diisocyanates.

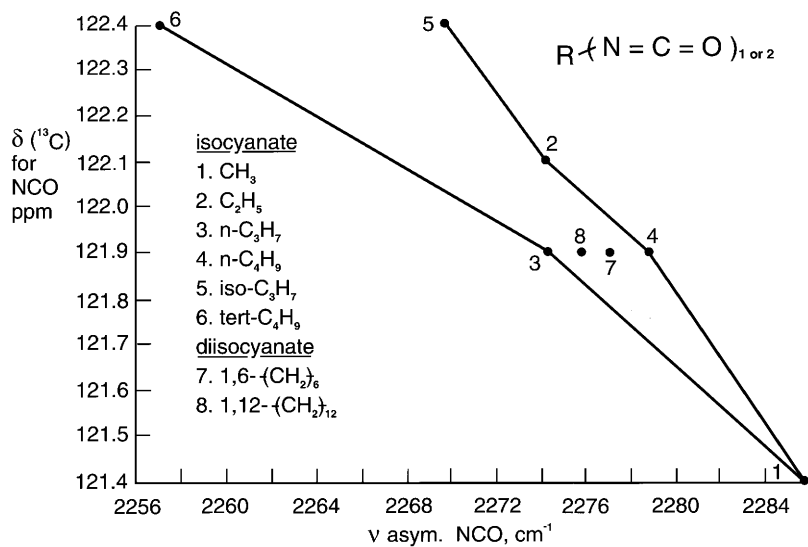
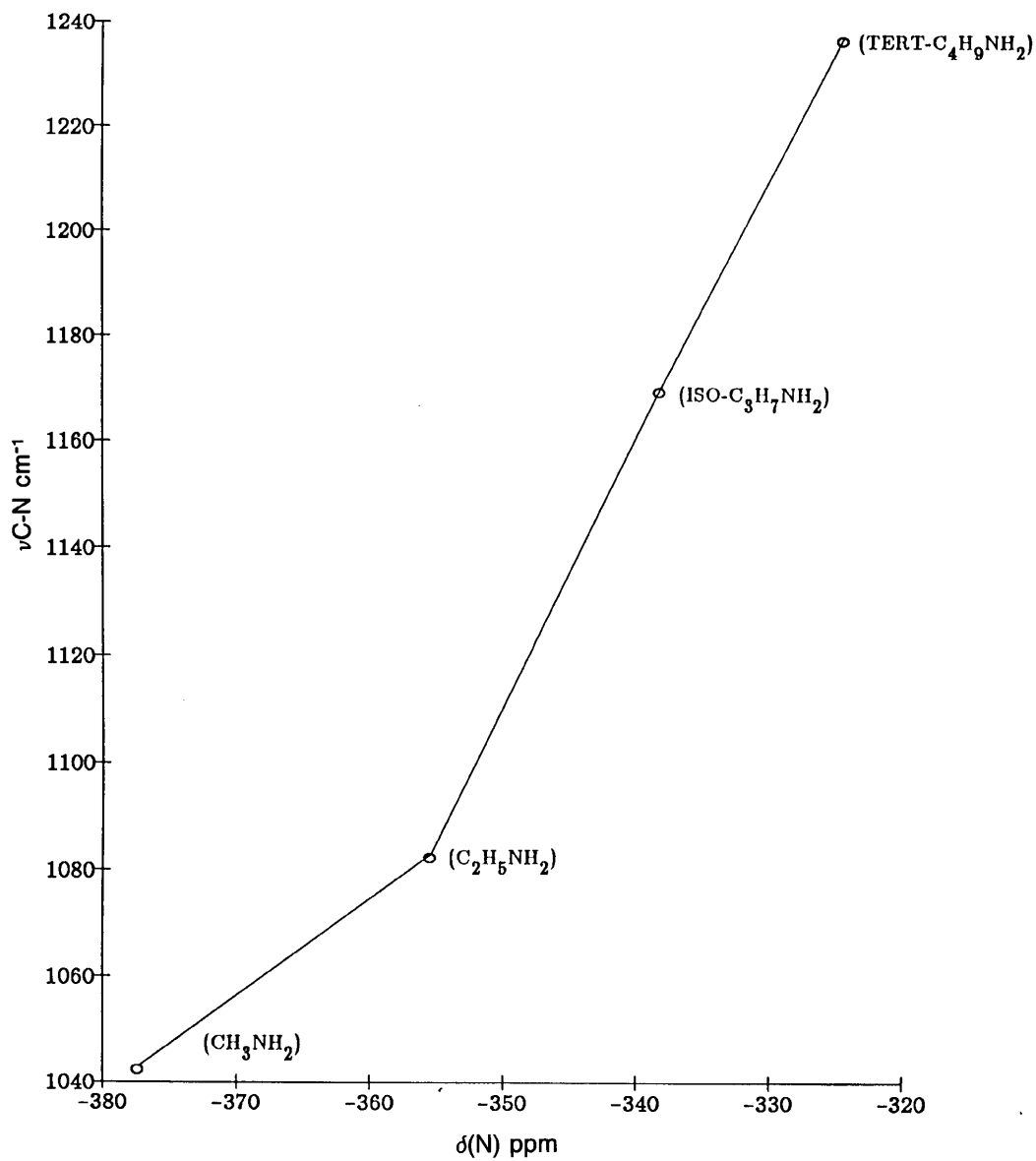
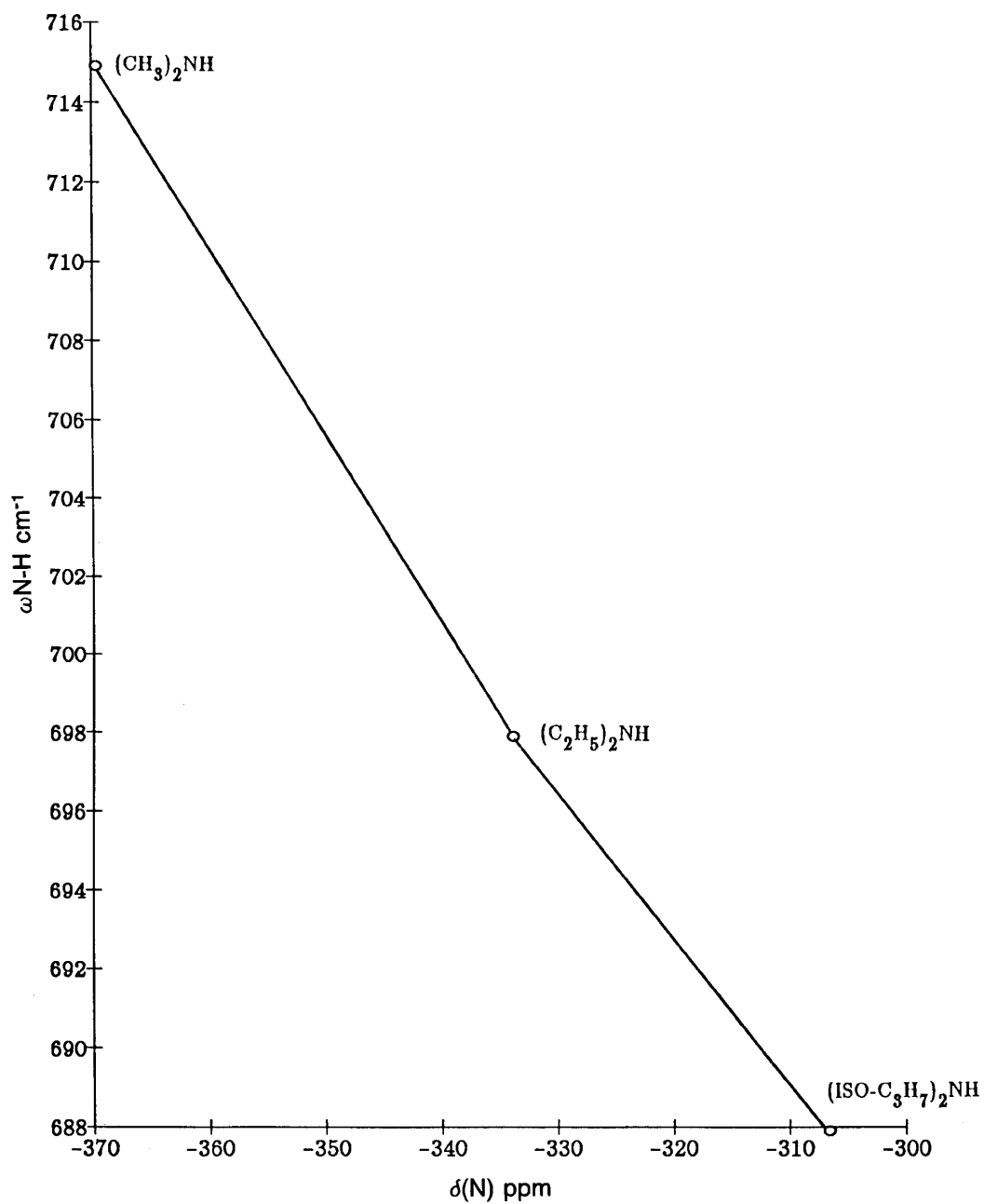


FIGURE 11.52 Plots of ν asym. $\text{N}=\text{C}=\text{O}$ vs δ ^{13}C for the $\text{N}=\text{C}=\text{O}$ group of alkyl isocyanates and alkyl diisocyanates.

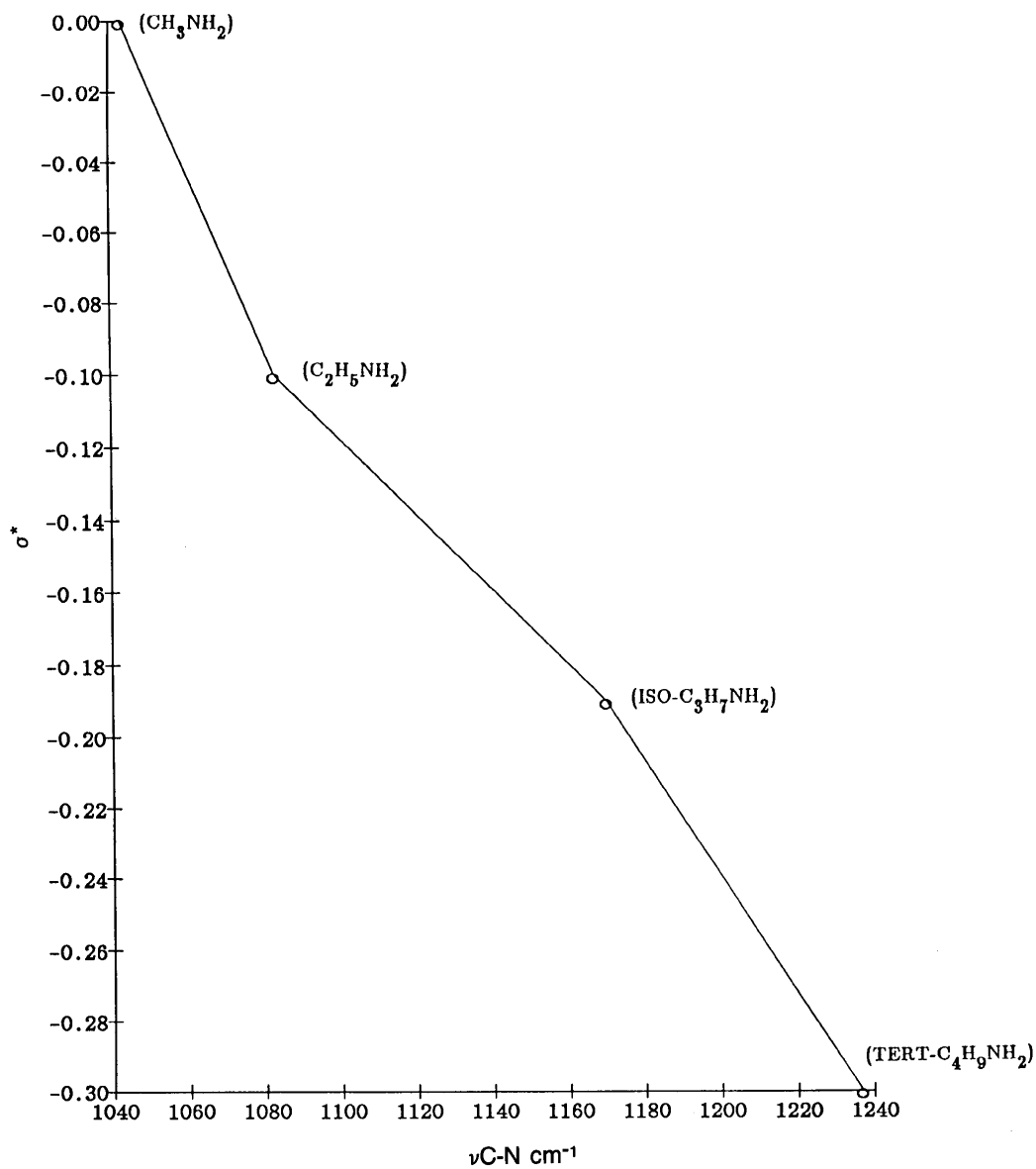
AMINE

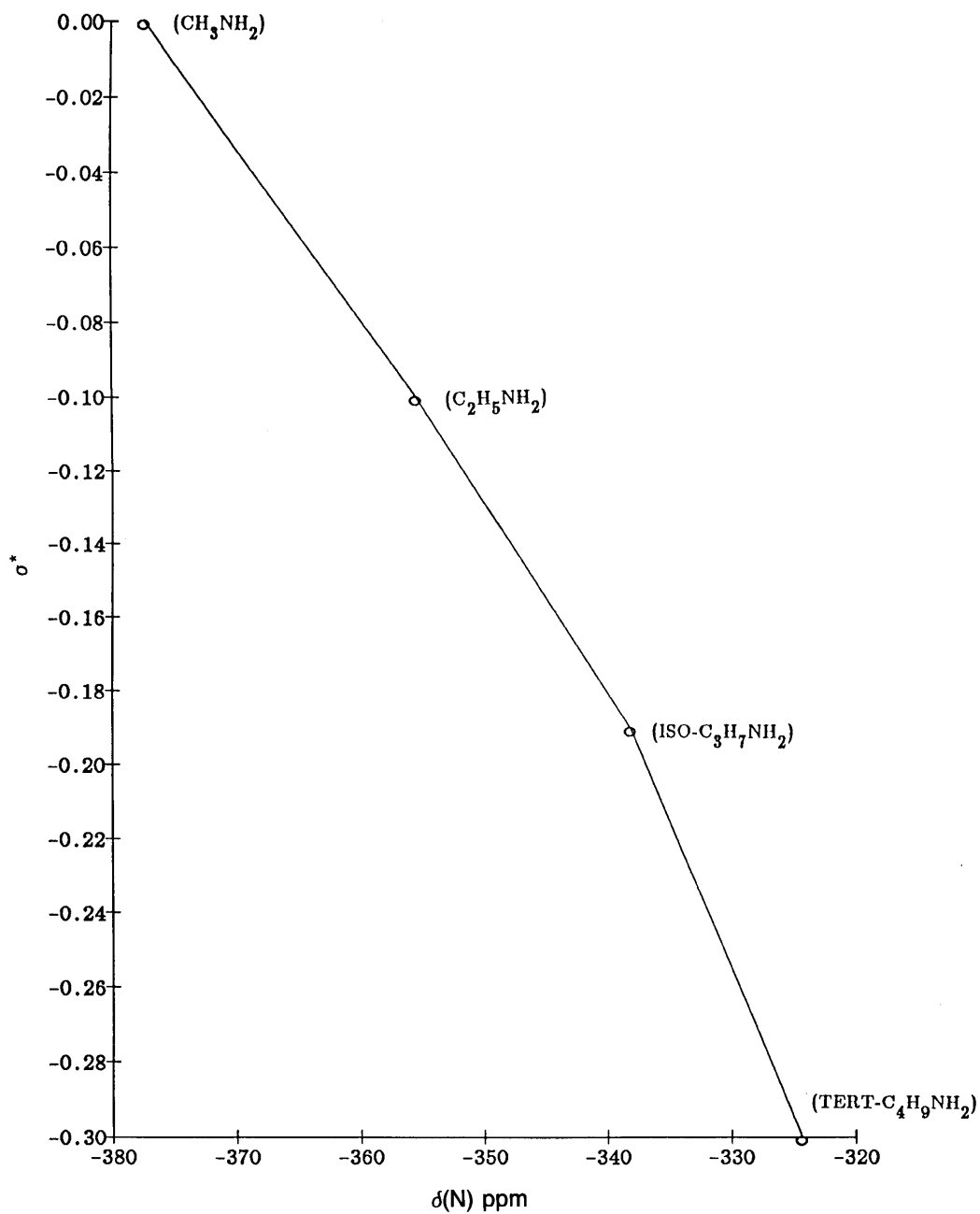
FIGURE 11.53 A plot of $\delta^{15}\text{N}$ vs $\nu\text{C-N}$ for primary alkylamines.

AMINE

FIGURE 11.54 A plot of $\delta^{15}\text{N}$ vs $\Omega_{\text{N-H}}$ for dialkylamines.

AMINE

FIGURE 11.55 A plot of $\nu_{\text{C-N}}$ vs Taft σ^* for the alkyl group of primary alkylamines.

FIGURE 11.56 A plot of $\delta^{15}\text{N}$ vs Taft σ^* for the alkyl group of primary alkylamines.

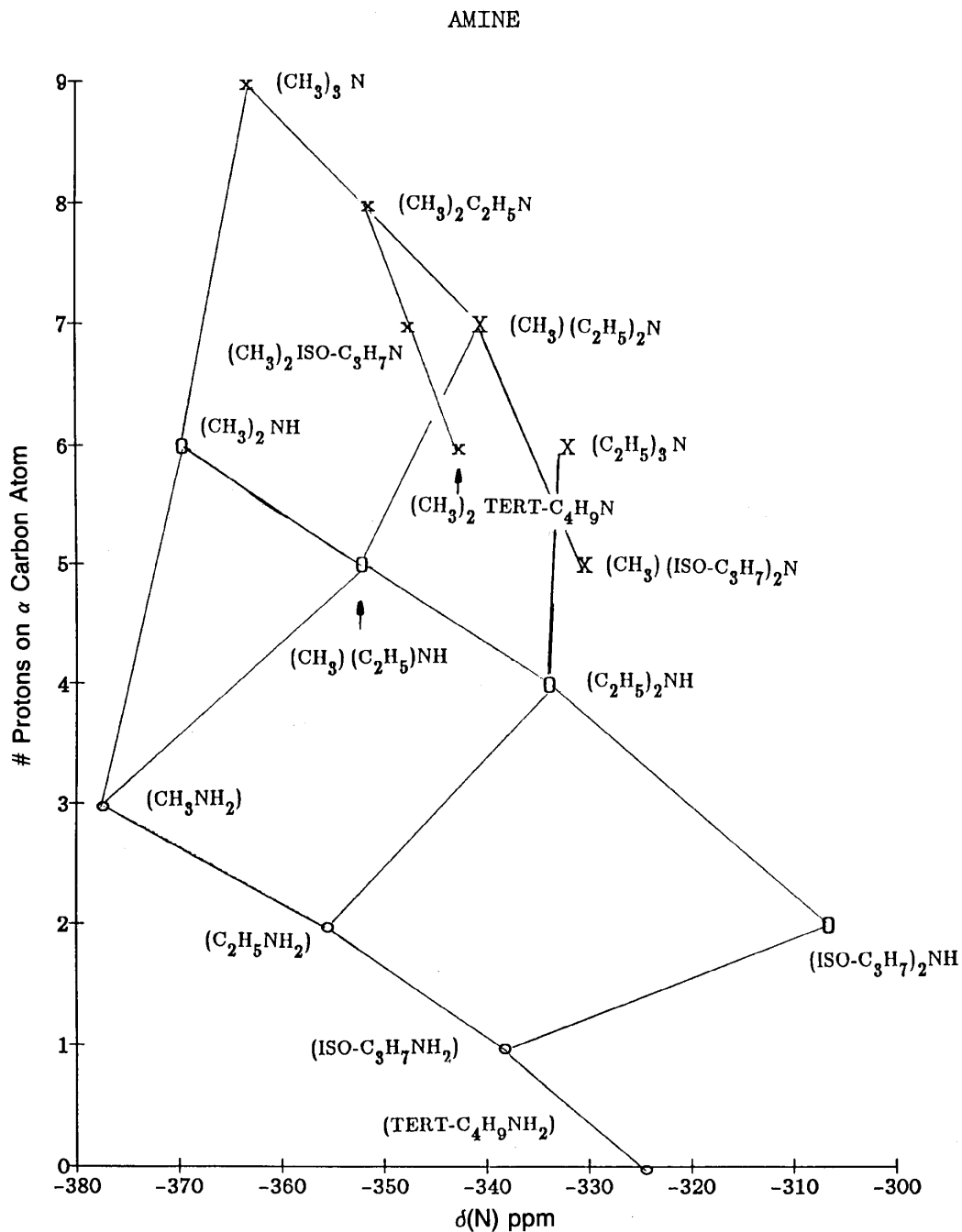


FIGURE 11.57 Plots of $\delta^{15}\text{N}$ vs the number of protons on the alkyl α -carbon atom(s) for mono-, di-, and trialkylamines.

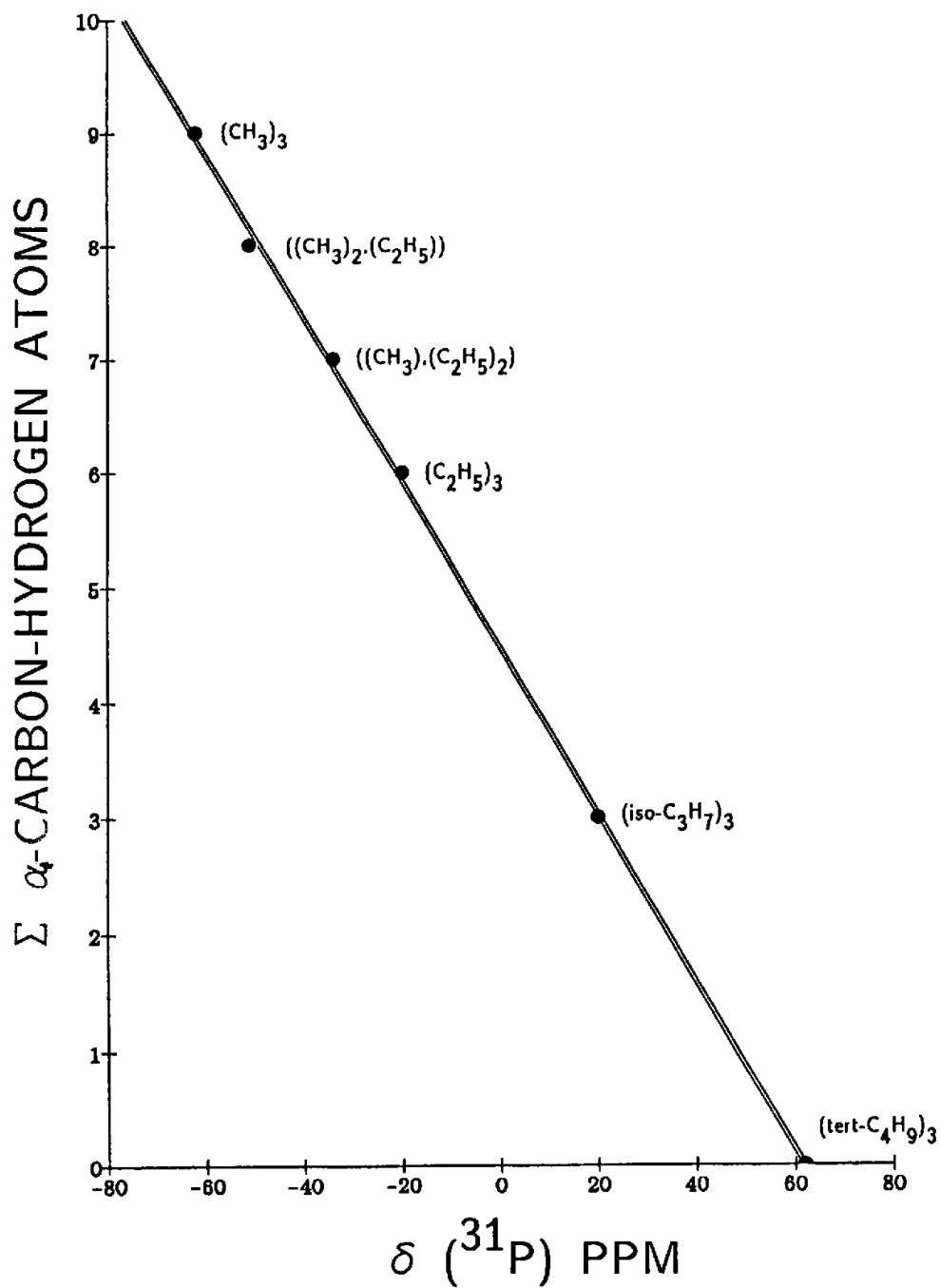


FIGURE 11.58 A plot of $\delta ^{31}\text{P}$ for trialkylphosphines vs the sum of the number of protons on the alkyl $\alpha\text{-C-P}$ carbon atoms.

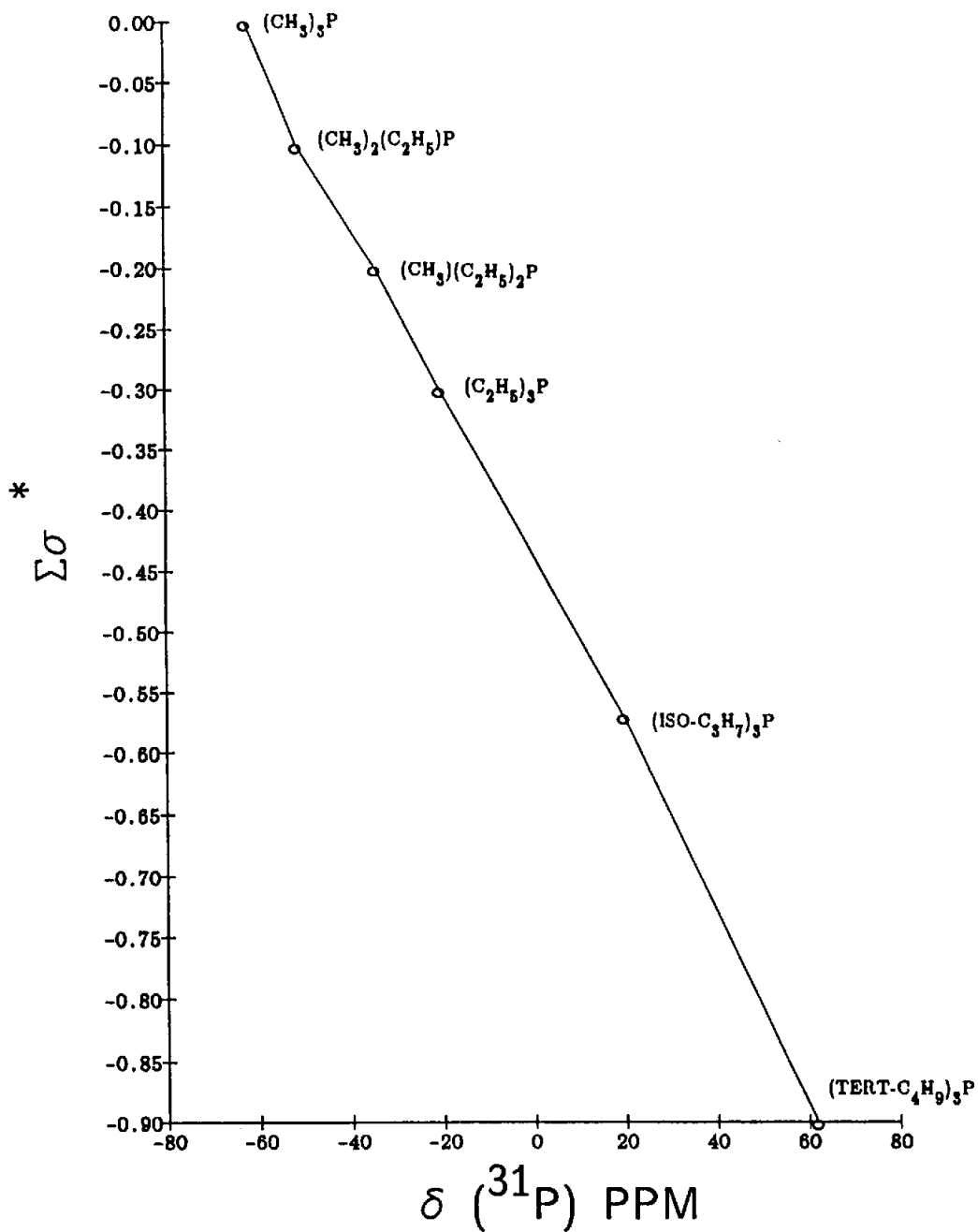


FIGURE 11.59 A plot of $\delta ^{31}\text{P}$ for trialkylphosphines vs Taft σ^* values for the alkyl groups.

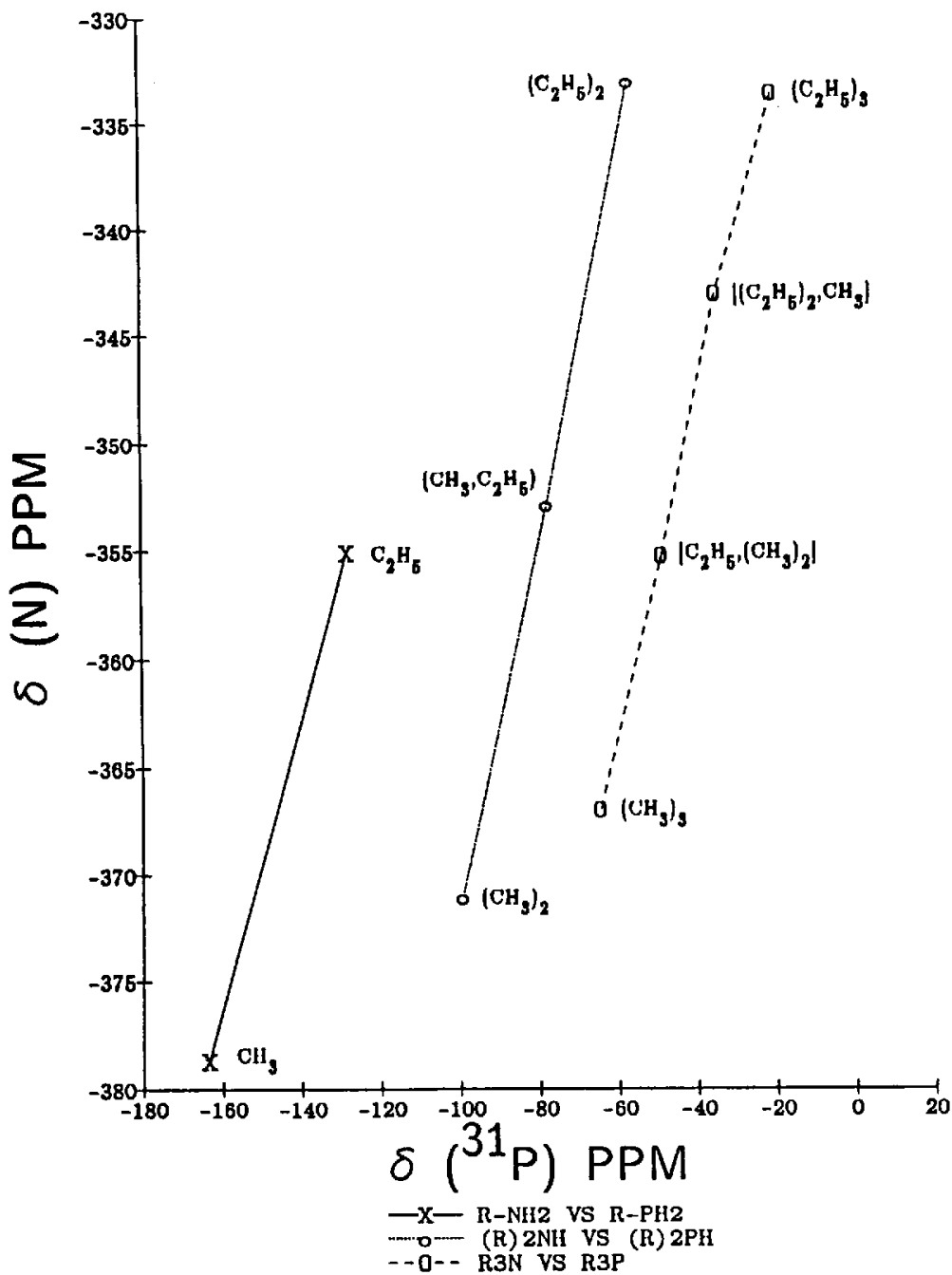


FIGURE 11.60 Plots of $\delta ^{31}\text{P}$ for R-PH₂ vs $\delta ^{15}\text{N}$ for R-NH₂, $\delta ^{31}\text{P}$ for (R-)₂PH vs $\delta ^{15}\text{N}$ for (R-)₂NH, and $\delta ^{31}\text{P}$ for (R-)₃P vs $\delta ^{15}\text{N}$ for (R-)₃N.

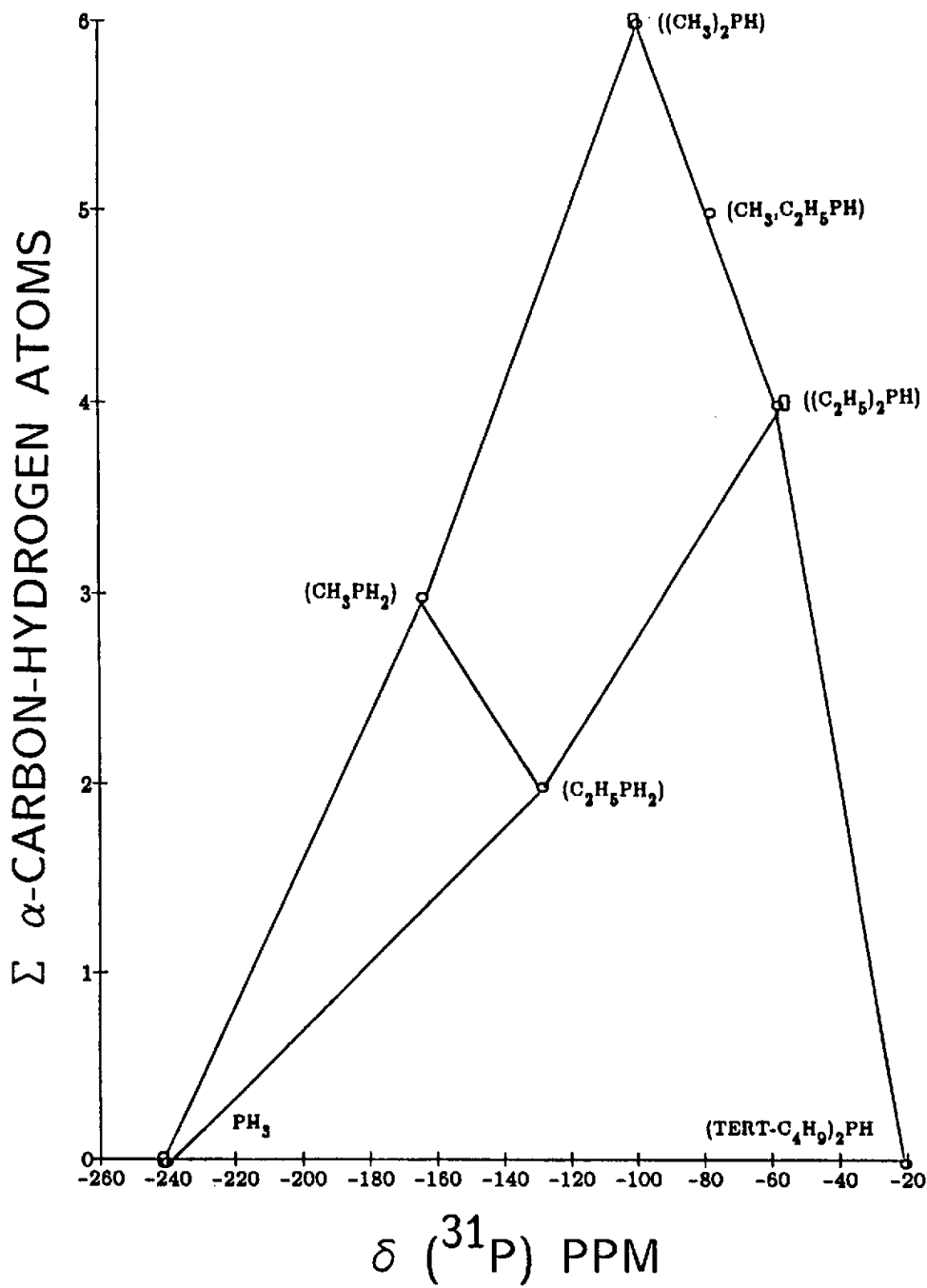
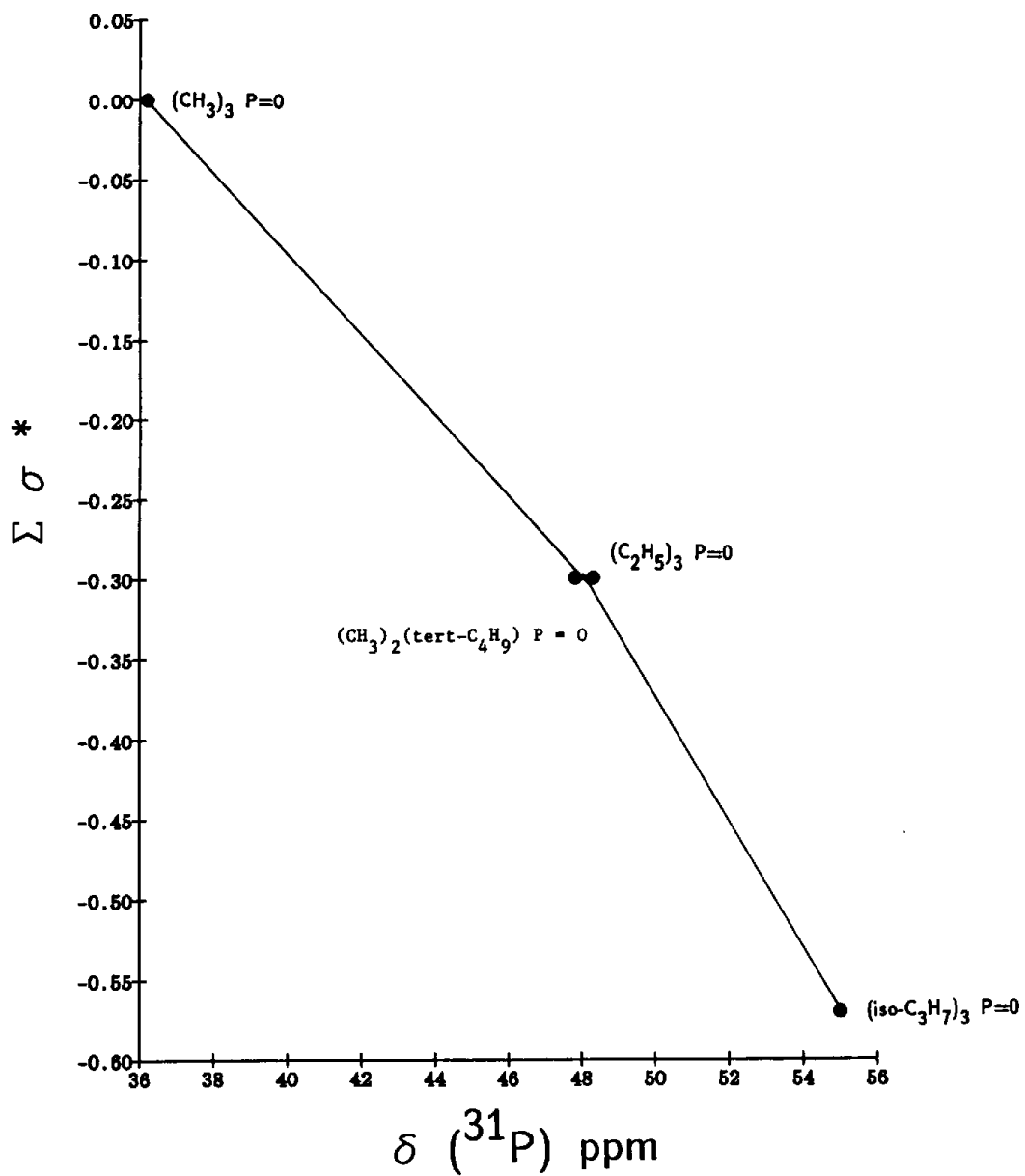


FIGURE 11.61 Plots of the number of protons on the α -C-P atom(s) vs $\delta ^{31}\text{P}$ for PH_3 , R-PH_2 , $(\text{R-})_2\text{PH}$.

FIGURE 11.62 A plot of the sum of Taft σ^* values $\delta ^{31}\text{P}$ for trialkylphosphine oxides.

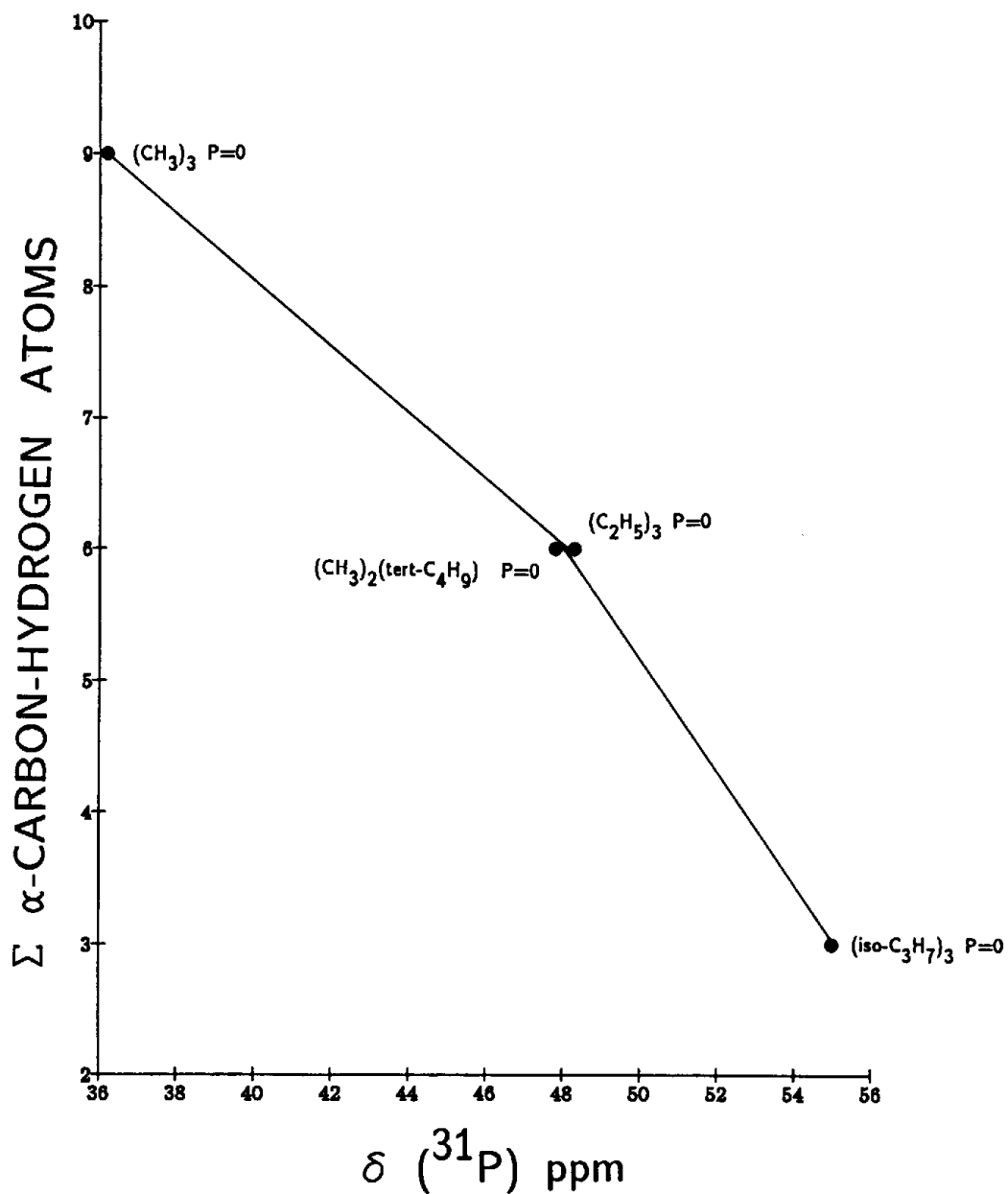


FIGURE 11.63 A plot of the sum of the number of protons on the $\alpha\text{-C-P}$ carbon atoms vs $\delta ^{31}\text{P}$ for trialkylphosphine oxides.

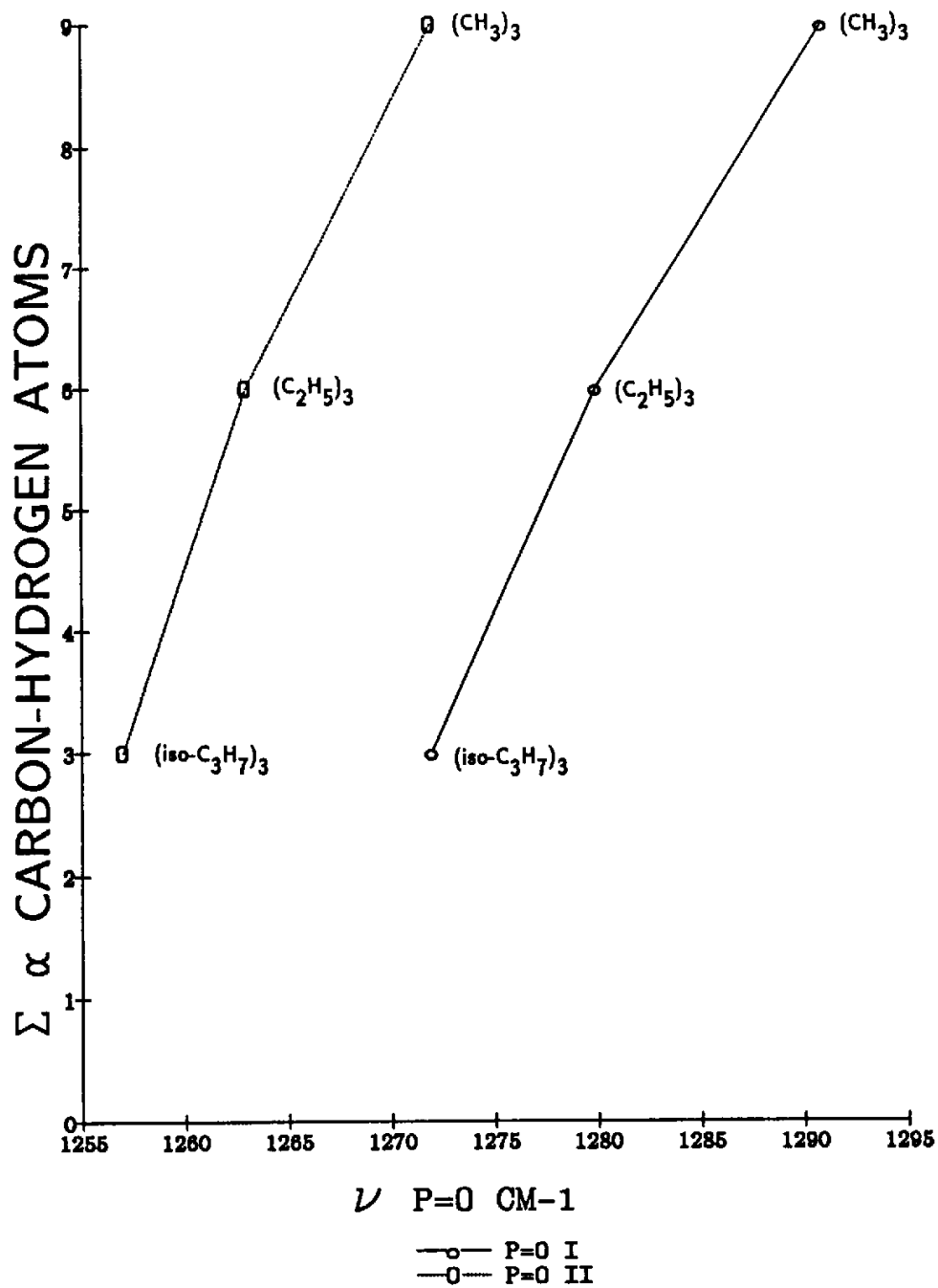


FIGURE 11.64 Plots of ν P=O rotational conformers vs the sum of the number of protons on the α -C-O-P carbon atoms for trialkyl phosphates.

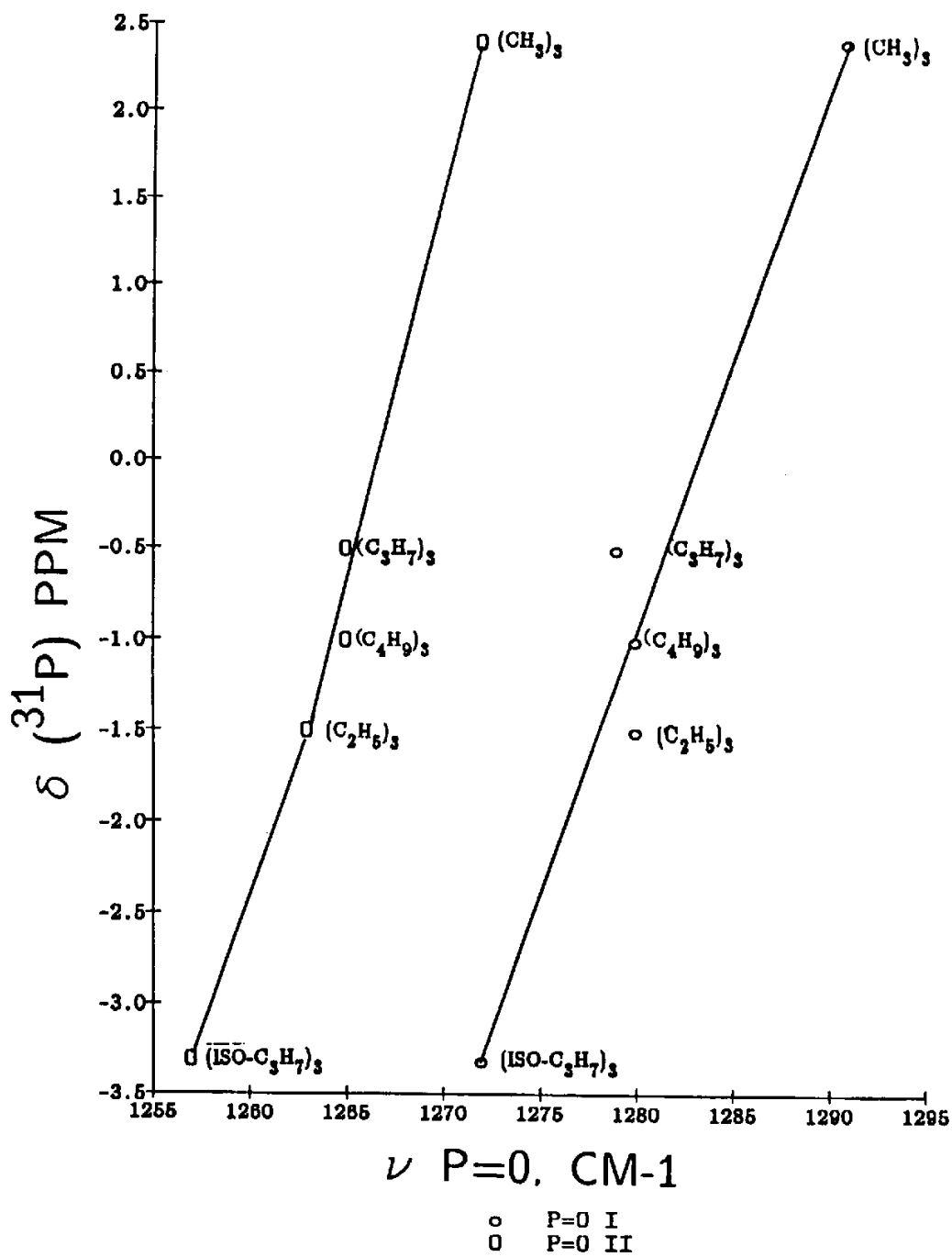


FIGURE 11.65 Plots of ν P=O rotational conformers vs δ ^{31}P for trialkyl phosphates.

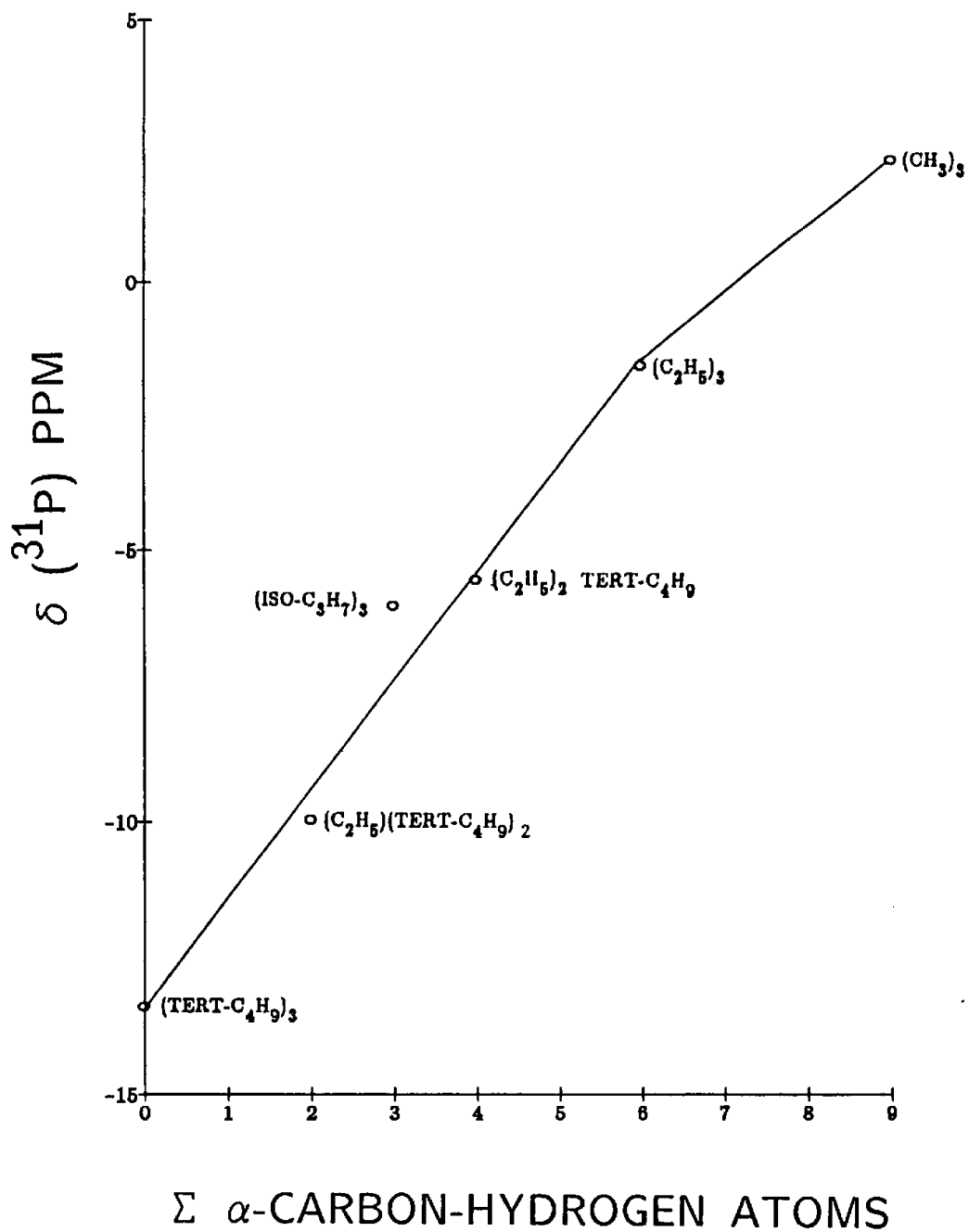


FIGURE 11.66 A plot of δ ^{31}P vs the sum of the number of protons on the α -C-O-P carbon atoms for trialkyl phosphates.

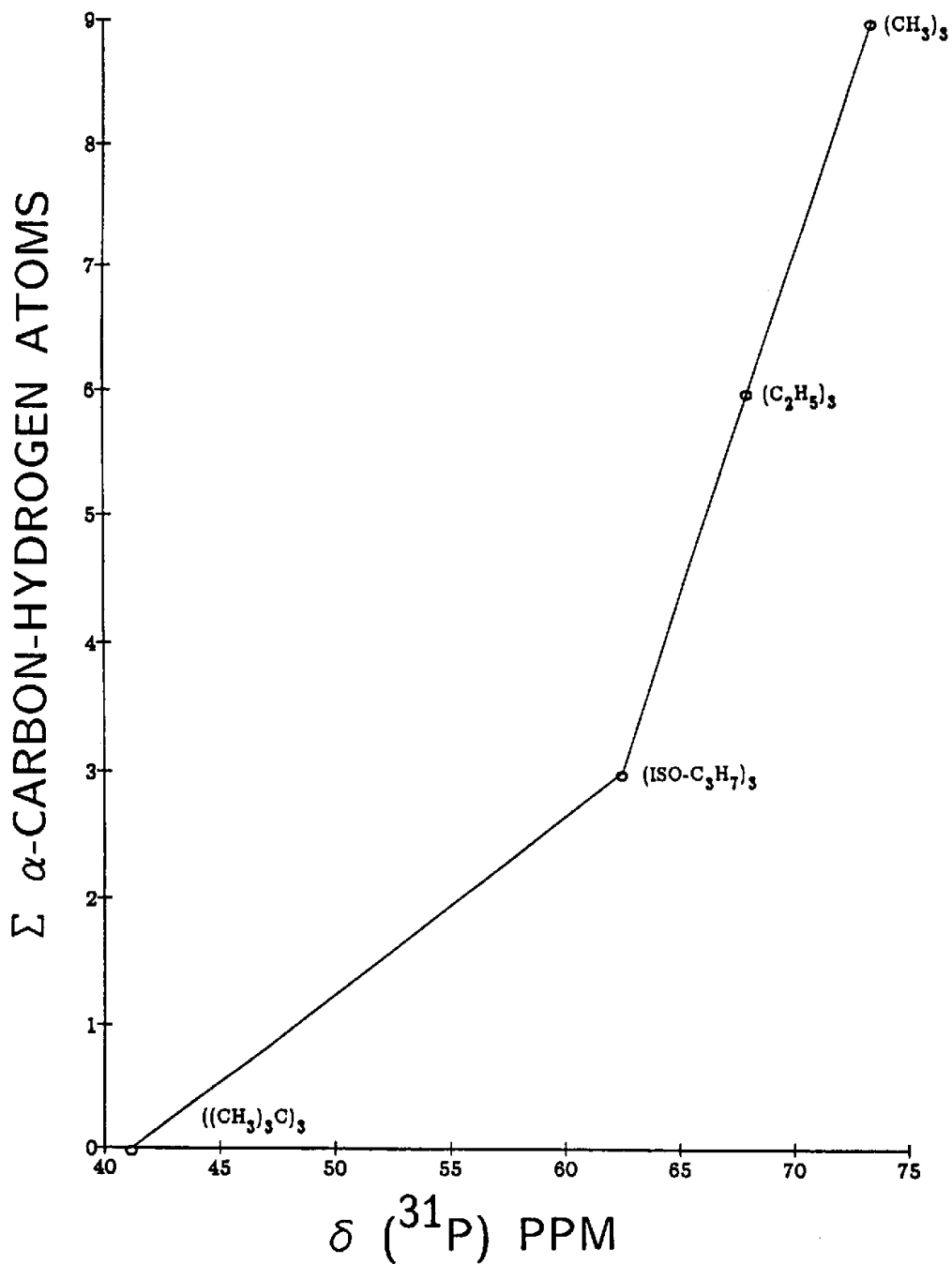


FIGURE 11.67 A plot of the sum of the protons on the $\alpha\text{-C-O-P}$ carbon atoms vs $\delta ^{31}\text{P}$ for O,O,O-trialkyl phosphorothioates.

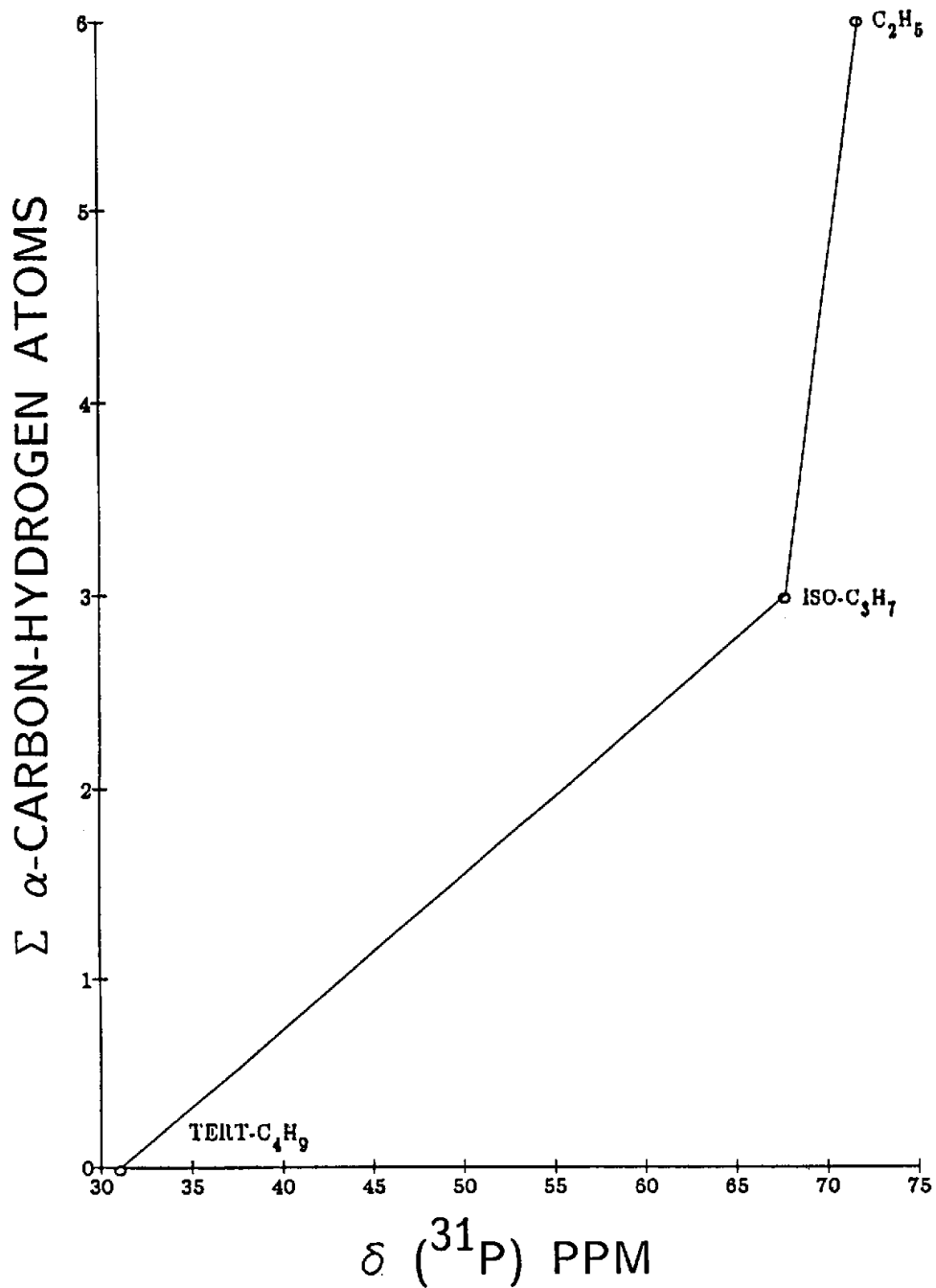


FIGURE 11.68 A plot of the sum of the number of protons on the $\alpha\text{-C-O-P}$ carbon atoms vs $\delta ^{31}\text{P}$ for O,O,O-trialkyl phosphoroselenates.

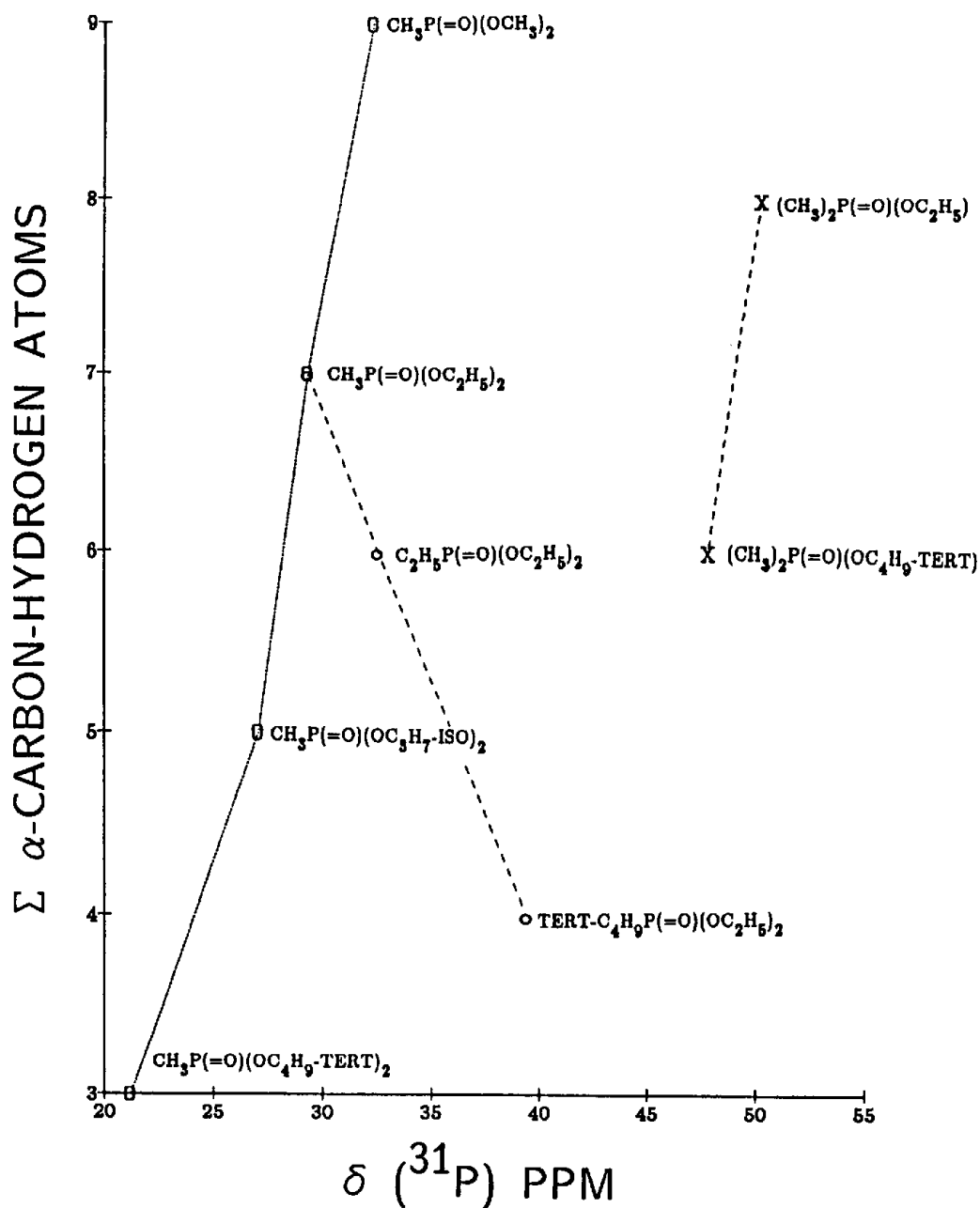


FIGURE 11.69 Plots of $\delta ^{31}\text{P}$ vs the sum of the number of protons on the $\alpha\text{-C-P}$ carbon atoms and the $\alpha\text{-C-O-P}$ carbon atoms for $\text{RP}(=\text{O})(\text{OC}_2\text{H}_5)_2$ and $(\text{R})_2\text{P}(=\text{O})(\text{OR})$.

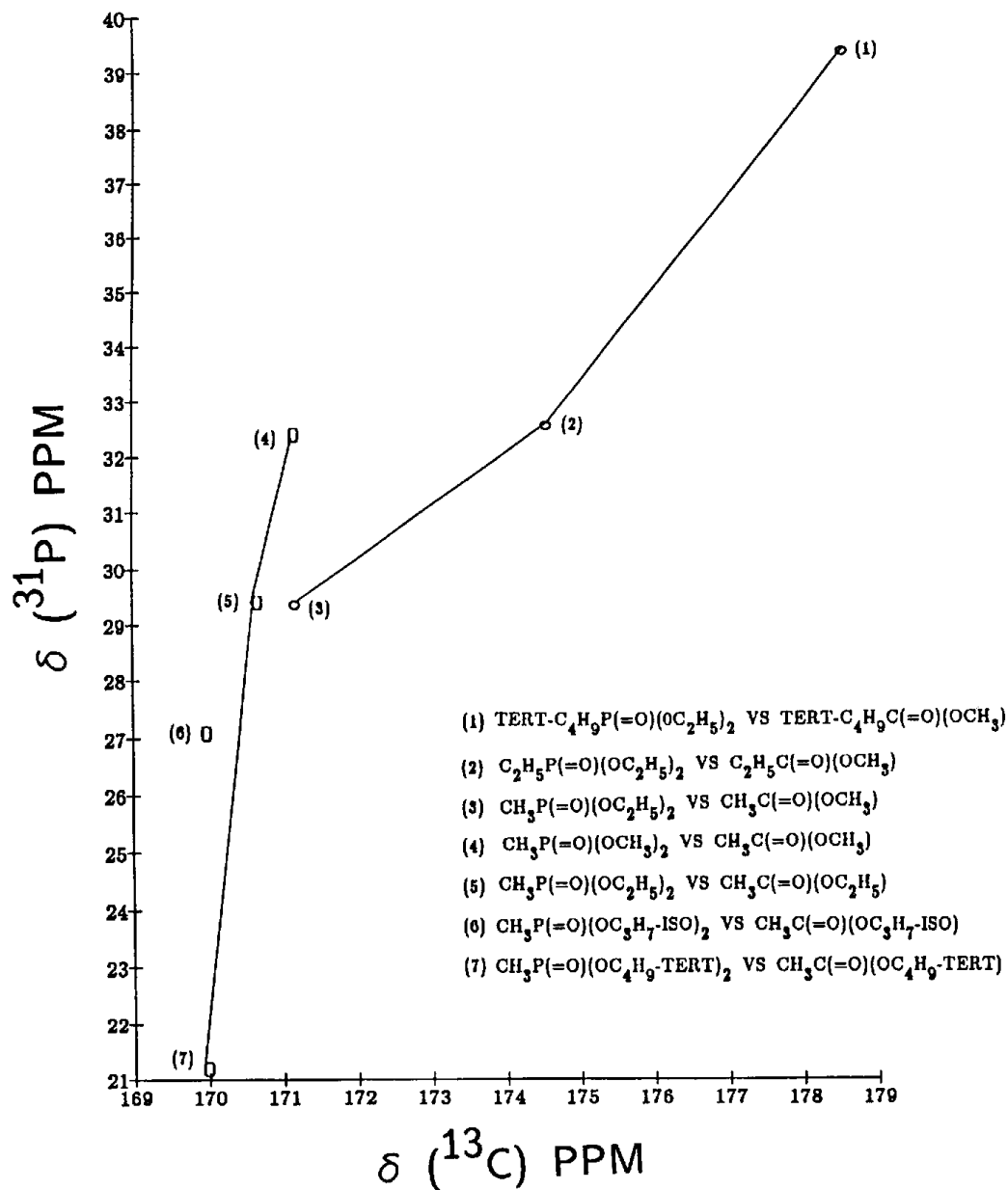


FIGURE 11.70 Plots of $\delta ^{31}\text{P}$ for $\text{RP}(=\text{O})(\text{OC}_2\text{H}_5)_2$ vs $\delta ^{13}\text{C}=\text{O}$ for $\text{RC}(=\text{O})(\text{OCH}_3)$ and $\delta ^{31}\text{P}$ for $\text{CH}_3\text{P}(=\text{O})(\text{OR})_2$ vs $\delta ^{13}\text{C}=\text{O}$ for $\text{CH}_3\text{C}(=\text{O})(\text{OR})$.

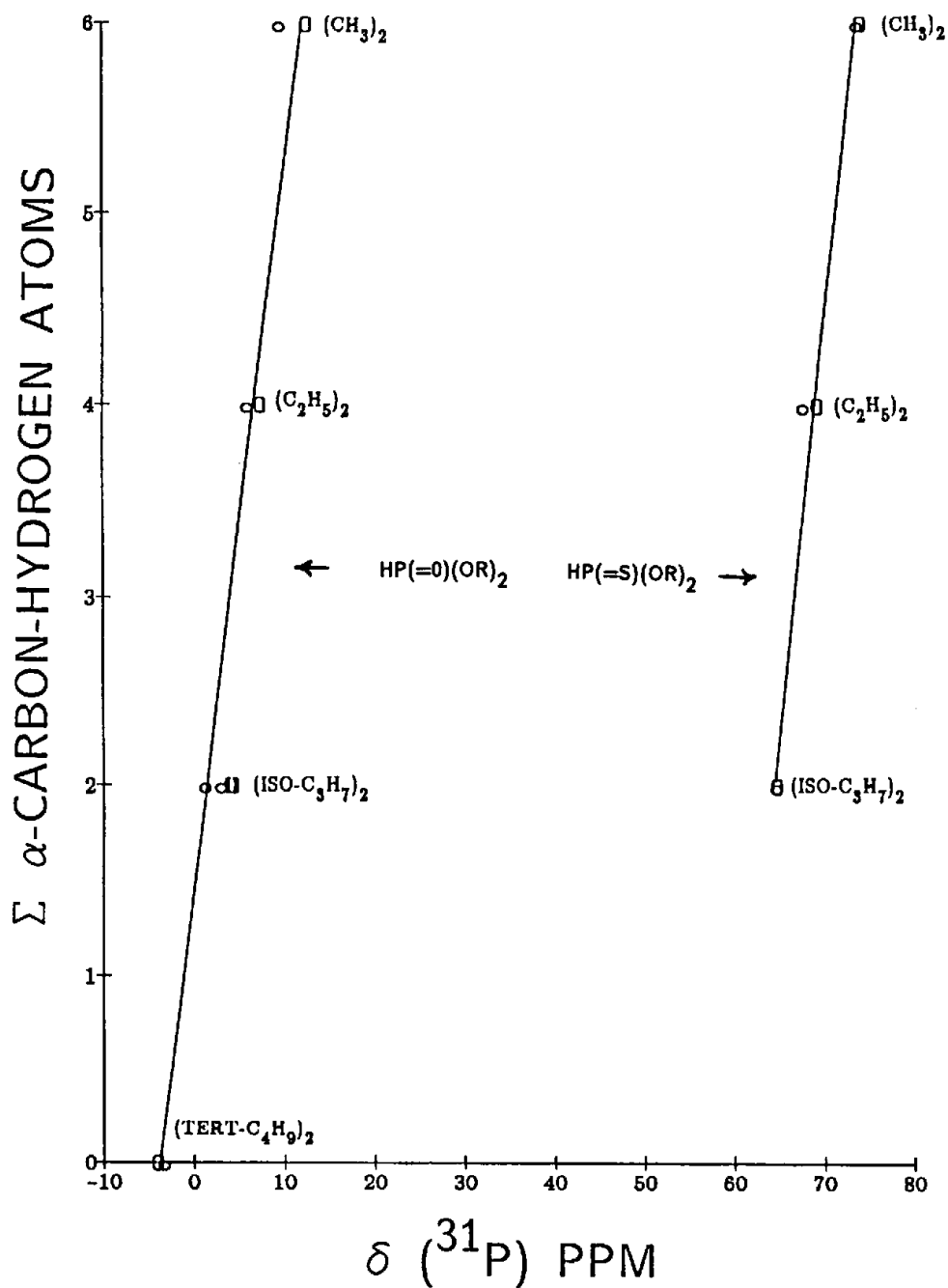
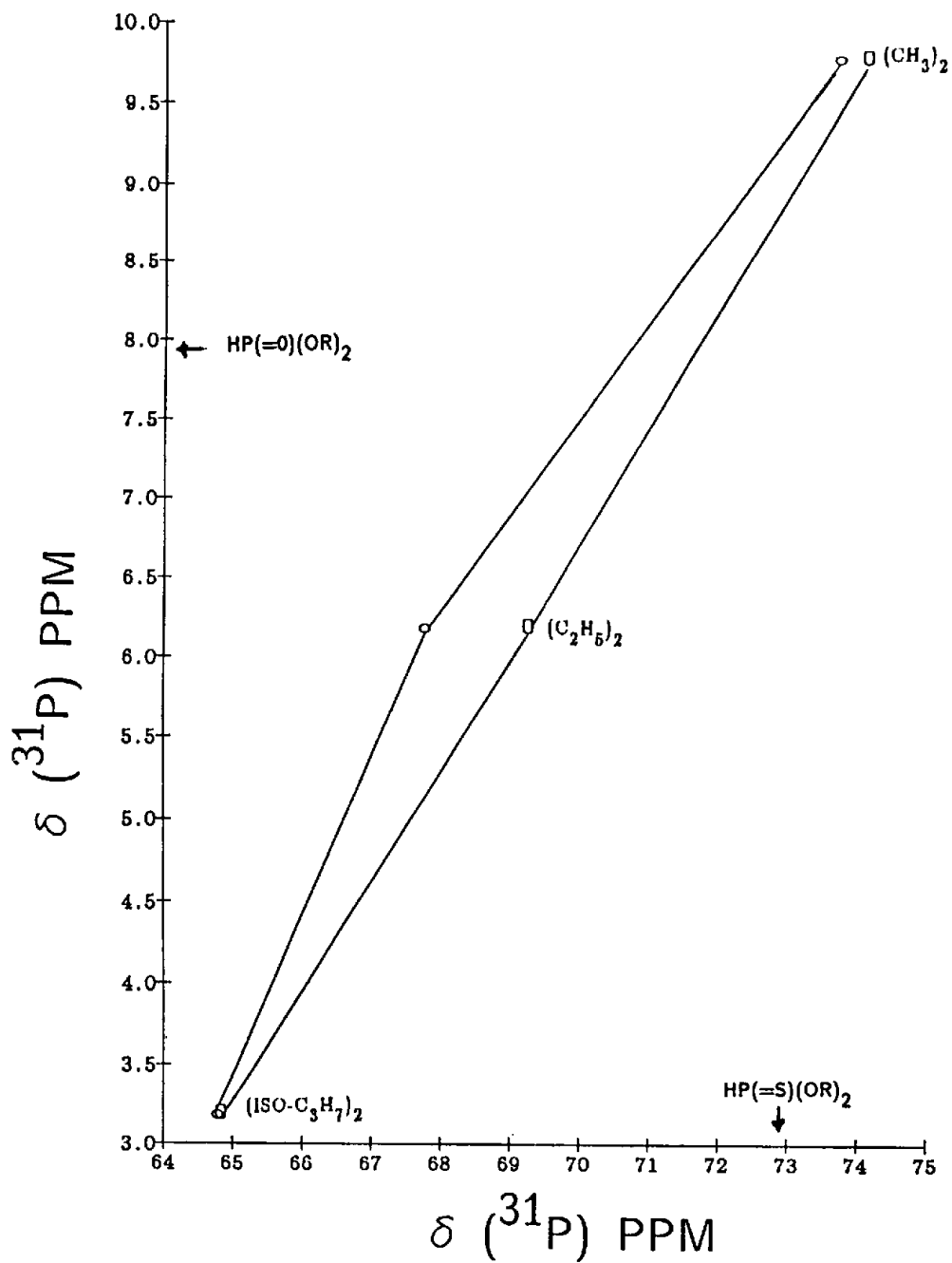
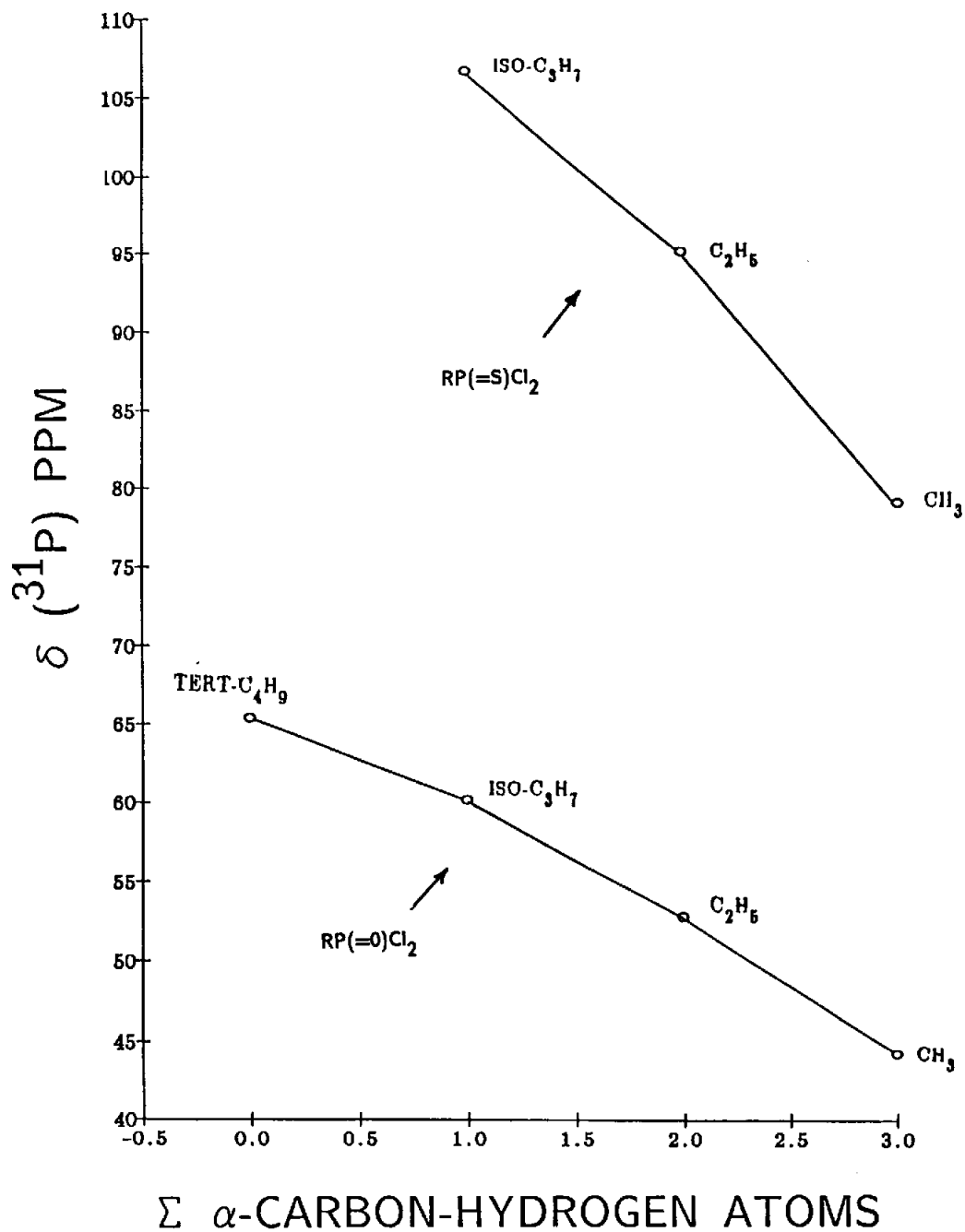
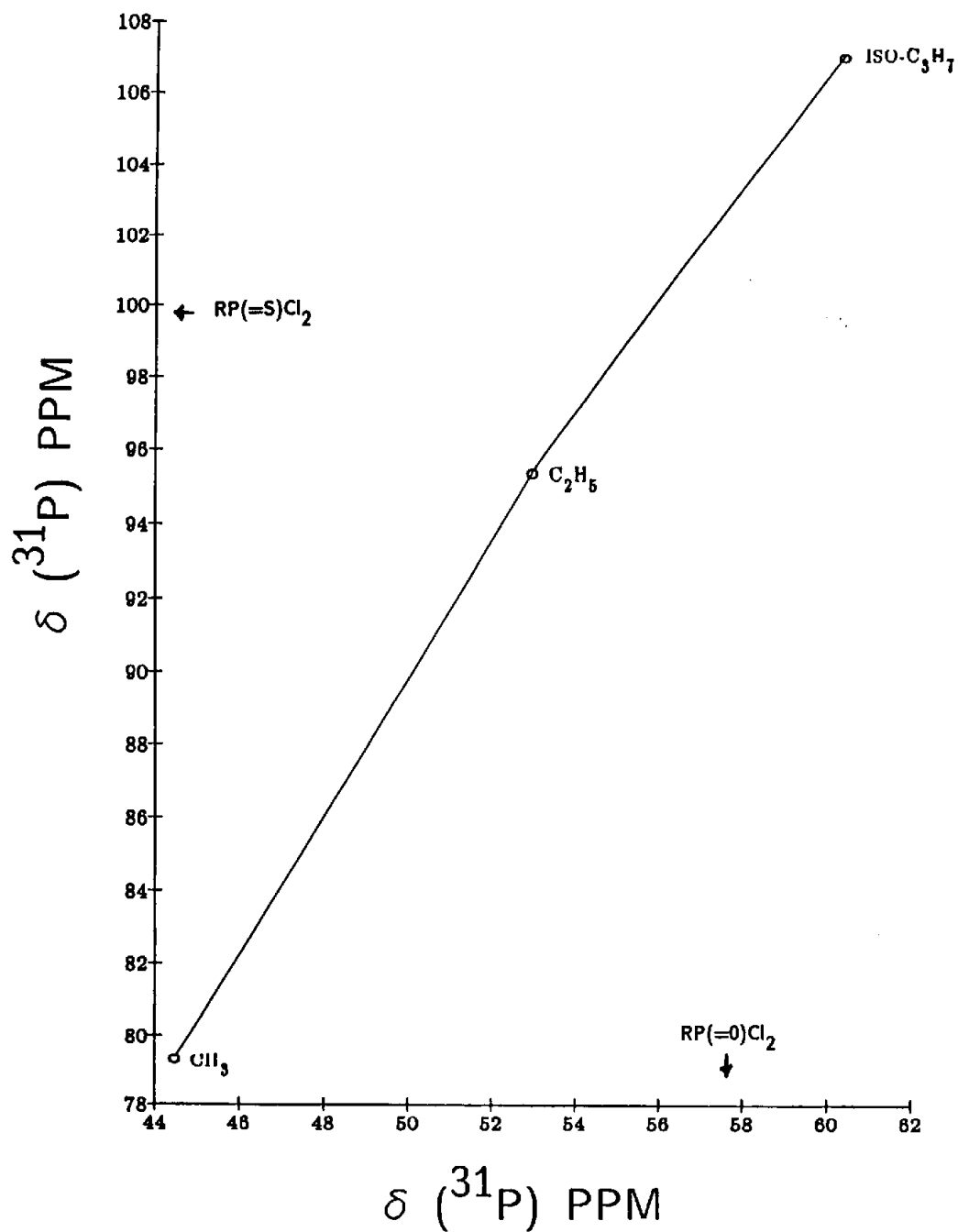
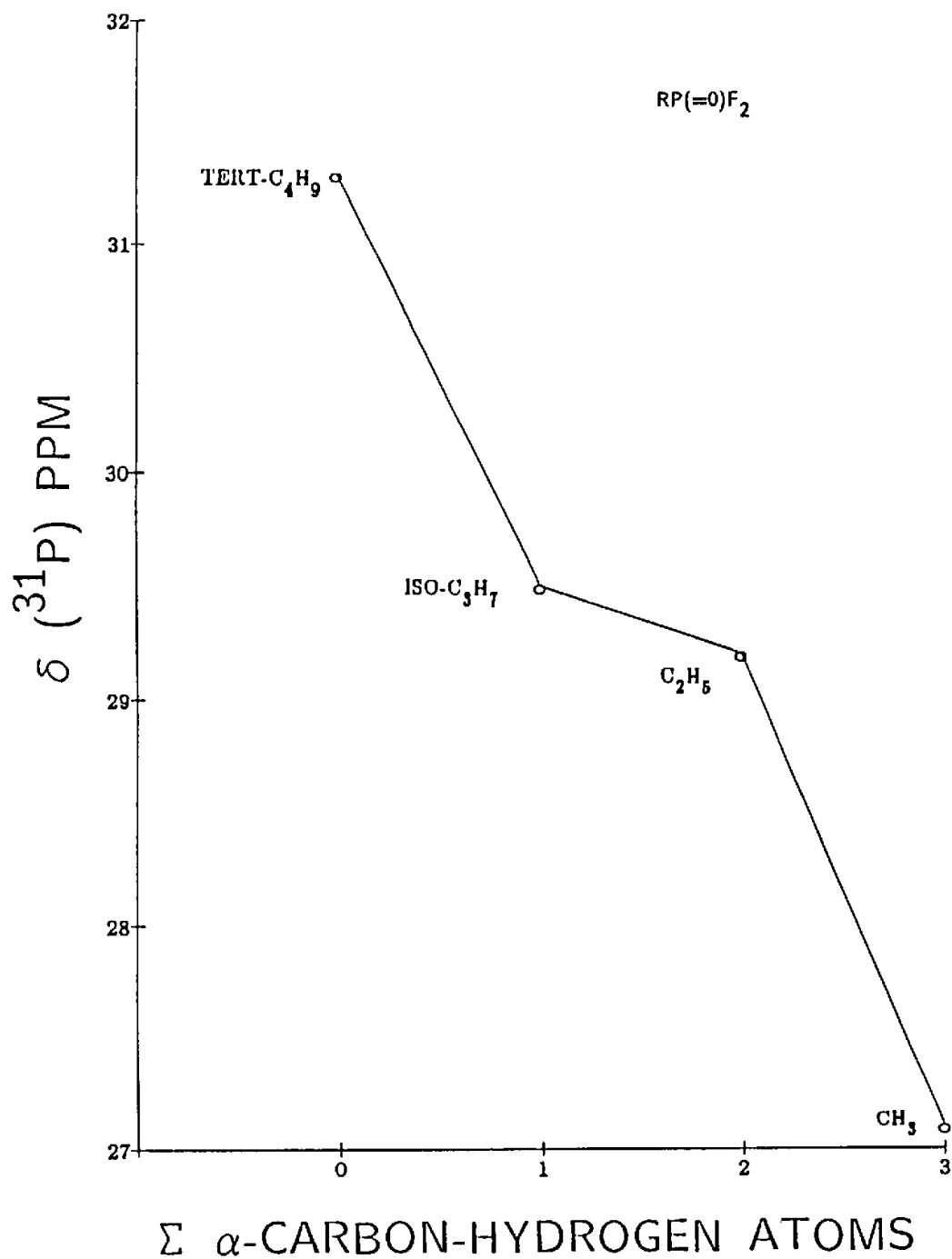


FIGURE 11.71 Plots of $\delta ^{31}\text{P}$ for $(\text{RO})_2\text{P}(=\text{O})\text{H}$ and for $(\text{RO})_2\text{P}(=\text{S})\text{H}$ vs the sum of the protons on the $\alpha\text{-C-O-P}$ carbon atoms.

FIGURE 11.72 A plot of $\delta^{31}\text{P}$ for $(\text{RO})_2\text{P}(=\text{O})\text{H}$ analogs vs $\delta^{31}\text{P}$ for the corresponding $(\text{RO})_2\text{P}(=\text{S})\text{H}$ alkyl analogs.

FIGURE 11.73 Plots of the number of protons on the α -CP carbon atoms vs $\delta ^{31}\text{P}$ for $\text{RP}(=\text{O})\text{Cl}_2$ and $\text{RP}(=\text{S})\text{Cl}_2$.

FIGURE 11.74 A plot of δ ^{31}P for $\text{RP}(=\text{S})\text{Cl}_2$ vs δ ^{31}P for $\text{RP}(=\text{O})\text{Cl}_2$.

FIGURE 11.75 A plot of δ ^{31}P vs the number of protons on the $\alpha\text{-C-P}$ carbon atom for $\text{RP}(=\text{O})\text{F}_2$.

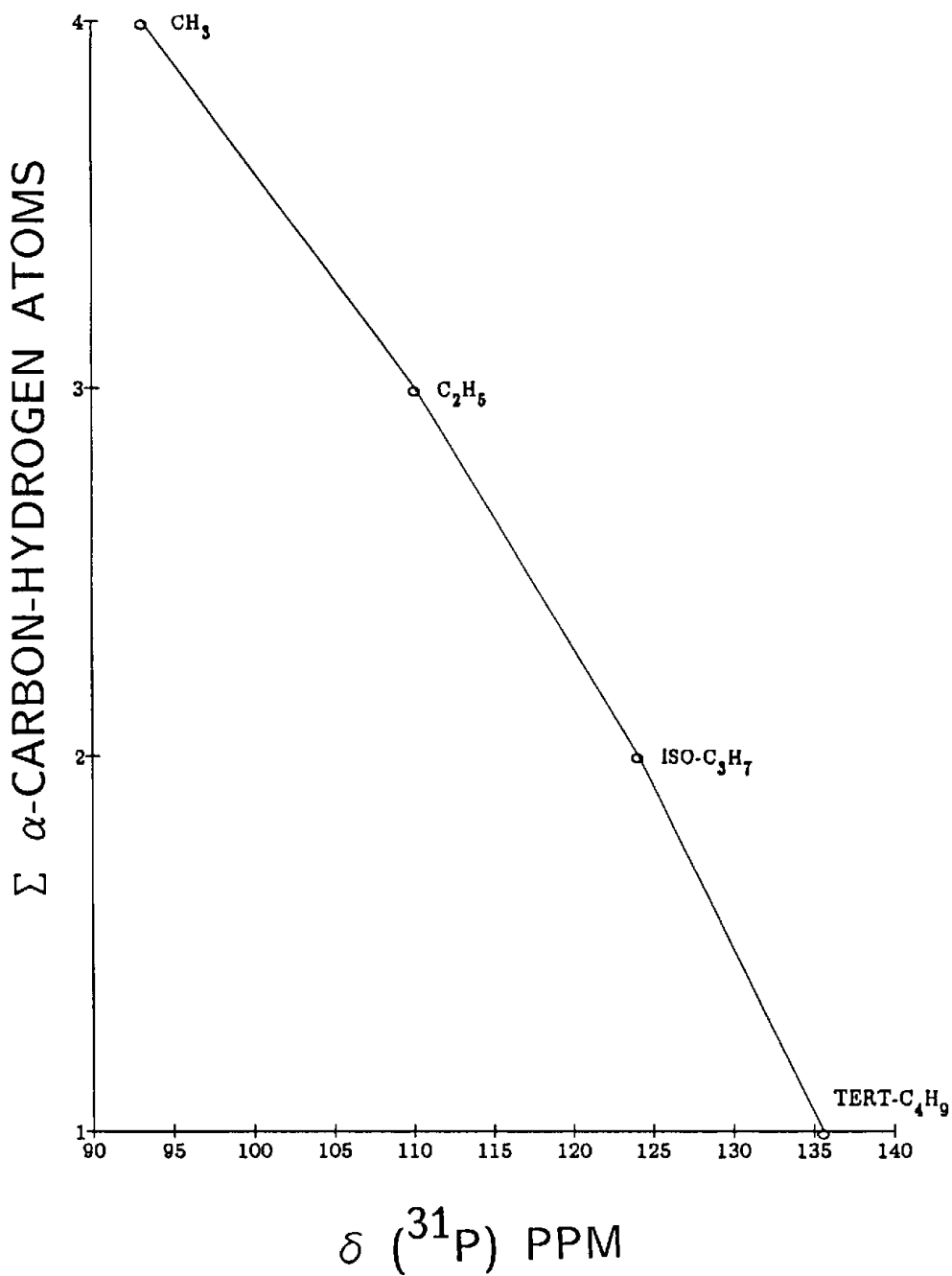


FIGURE 11.76 A plot of $\delta ^{31}\text{P}$ vs the sum of the number of protons on the $\alpha\text{-C-P}$ carbon atom and the number of protons on the $\alpha\text{-C-O-P}$ carbon atom for $\text{RP}(=\text{S})\text{Br}(\text{OC}_3\text{H}_7\text{-iso})$.

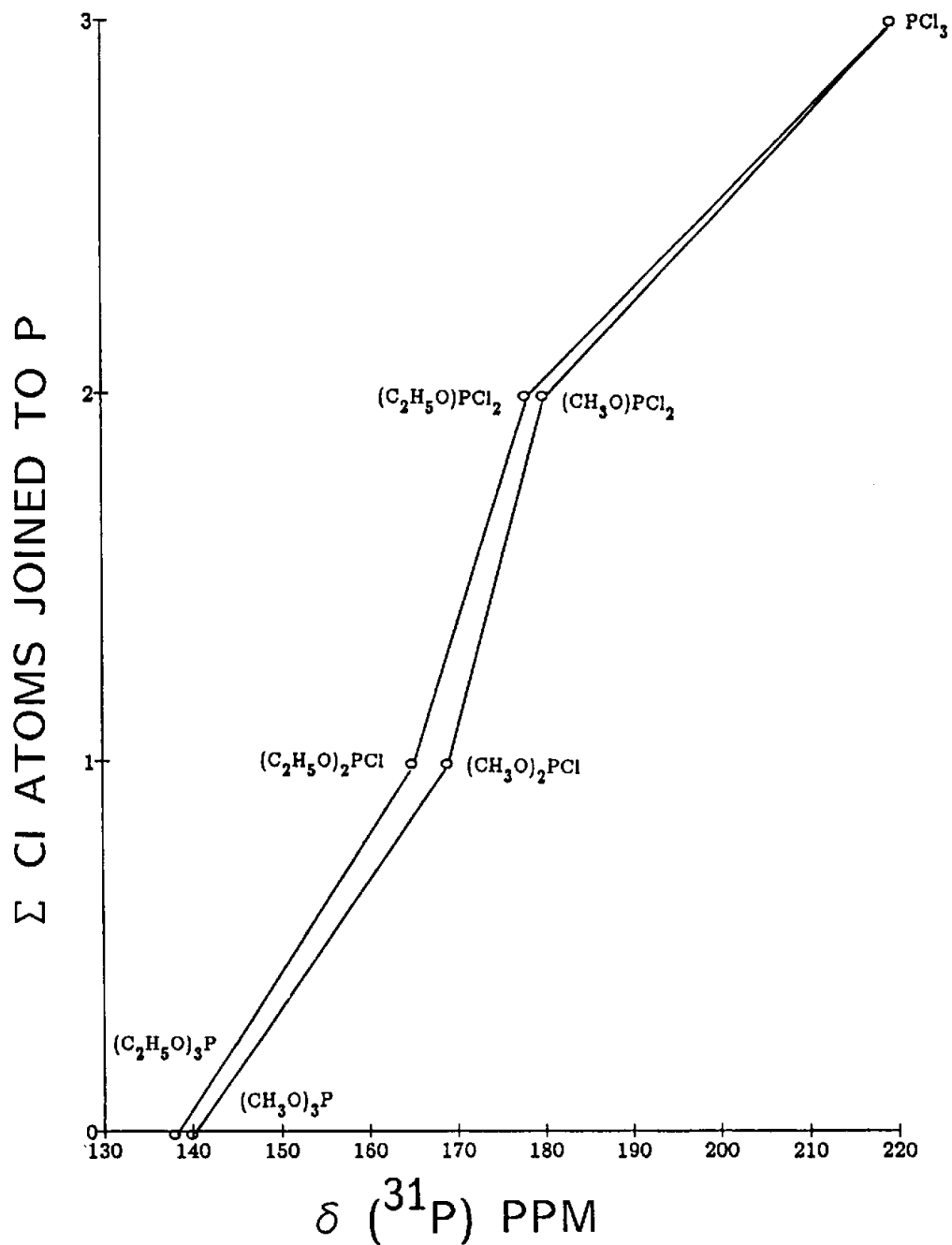
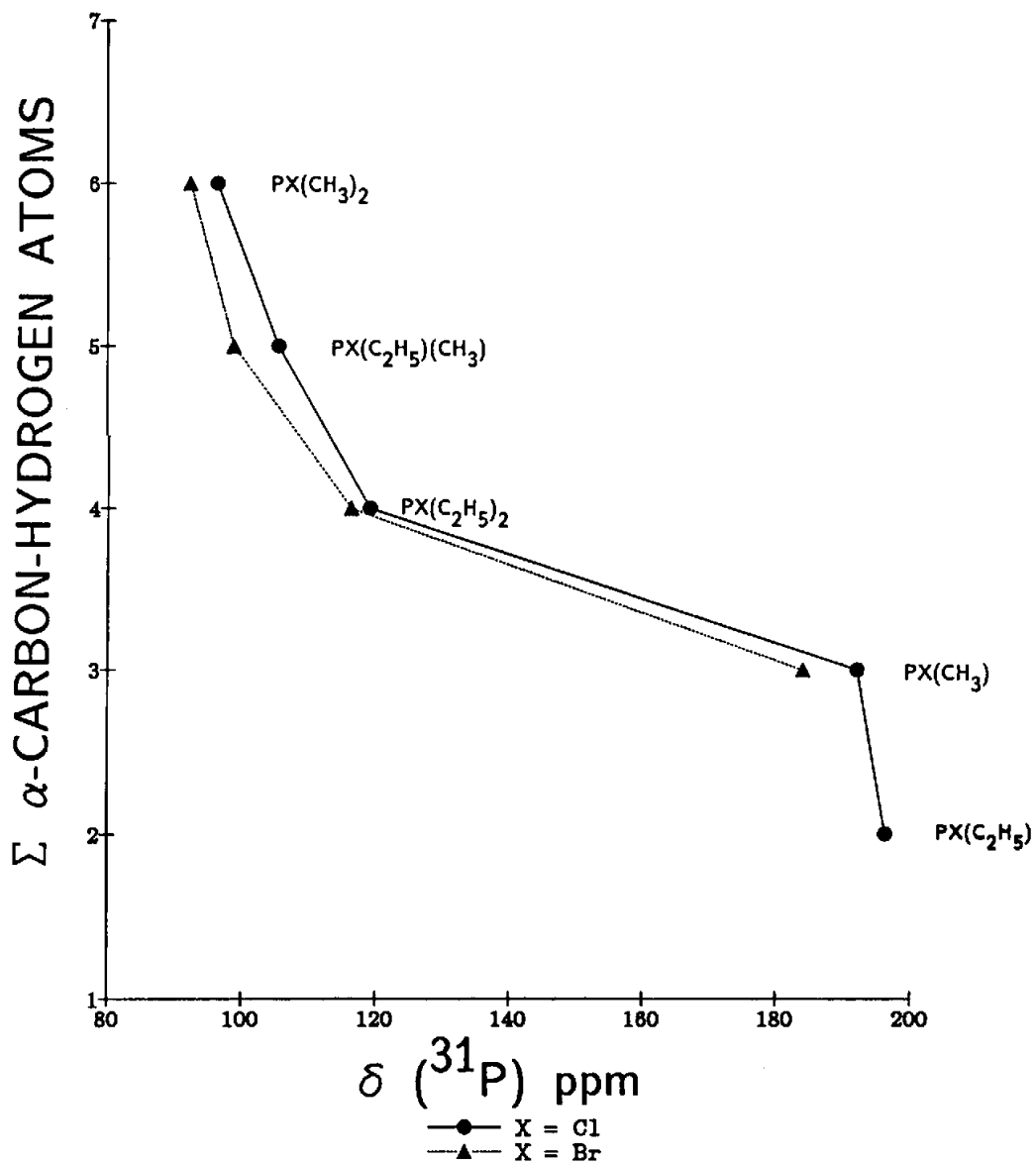


FIGURE 11.77 Plots of $\delta^{31}\text{P}$ vs the number of chlorine atoms joined to phosphorus for $\text{PCl}_{3-x}(\text{OR})_x$.

FIGURE 11.78 Plots of the sum of the number of protons on the α -C-P carbon atom(s) vs δ ^{31}P for $\text{PX}_{3-n}\text{R}_n$.

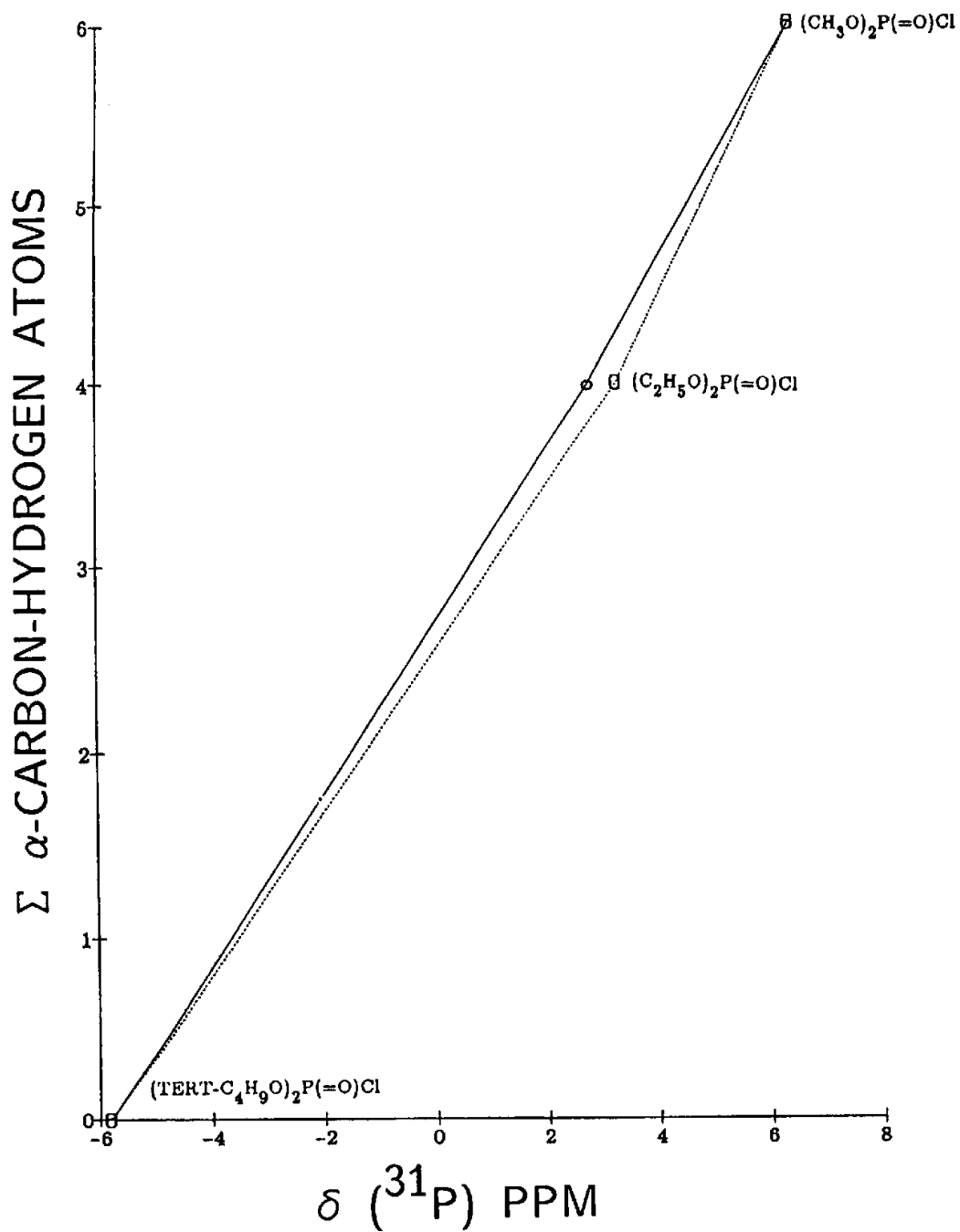


FIGURE 11.79 A plot of $\delta ^{31}\text{P}$ vs the number of protons on the $\alpha\text{-C-O-P}$ carbon atoms for $(\text{R})_2\text{P(=O)Cl}_2$.

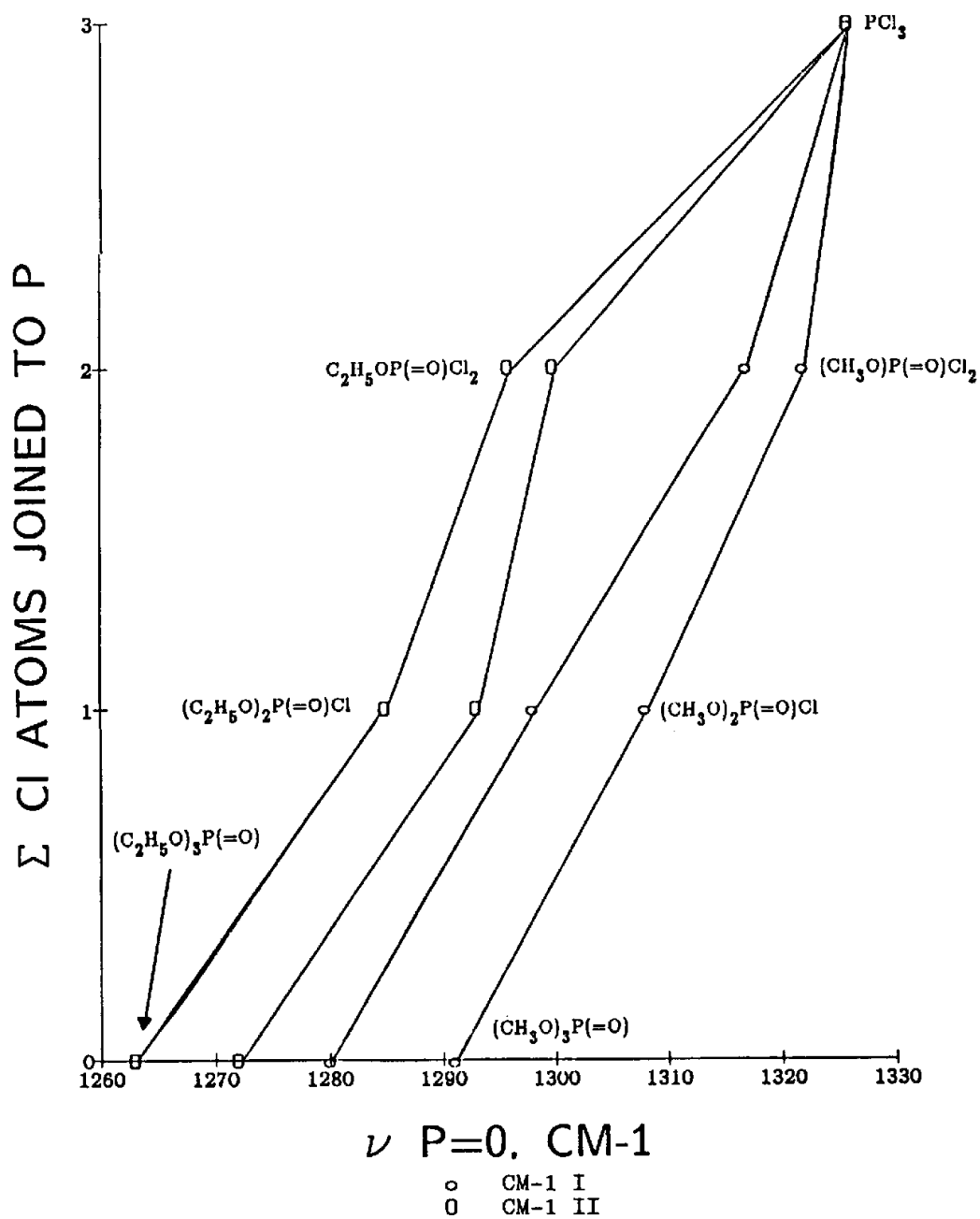


FIGURE 11.80 Plots of the number of Cl atoms joined to phosphorus vs ν P=O and ν P=O rotational conformers for $\text{P}(=\text{O})\text{Cl}_3$ through $\text{P}(=\text{O})\text{Cl}_{3-x}(\text{OR})_x$ where R is CH_3 or C_2H_5 .

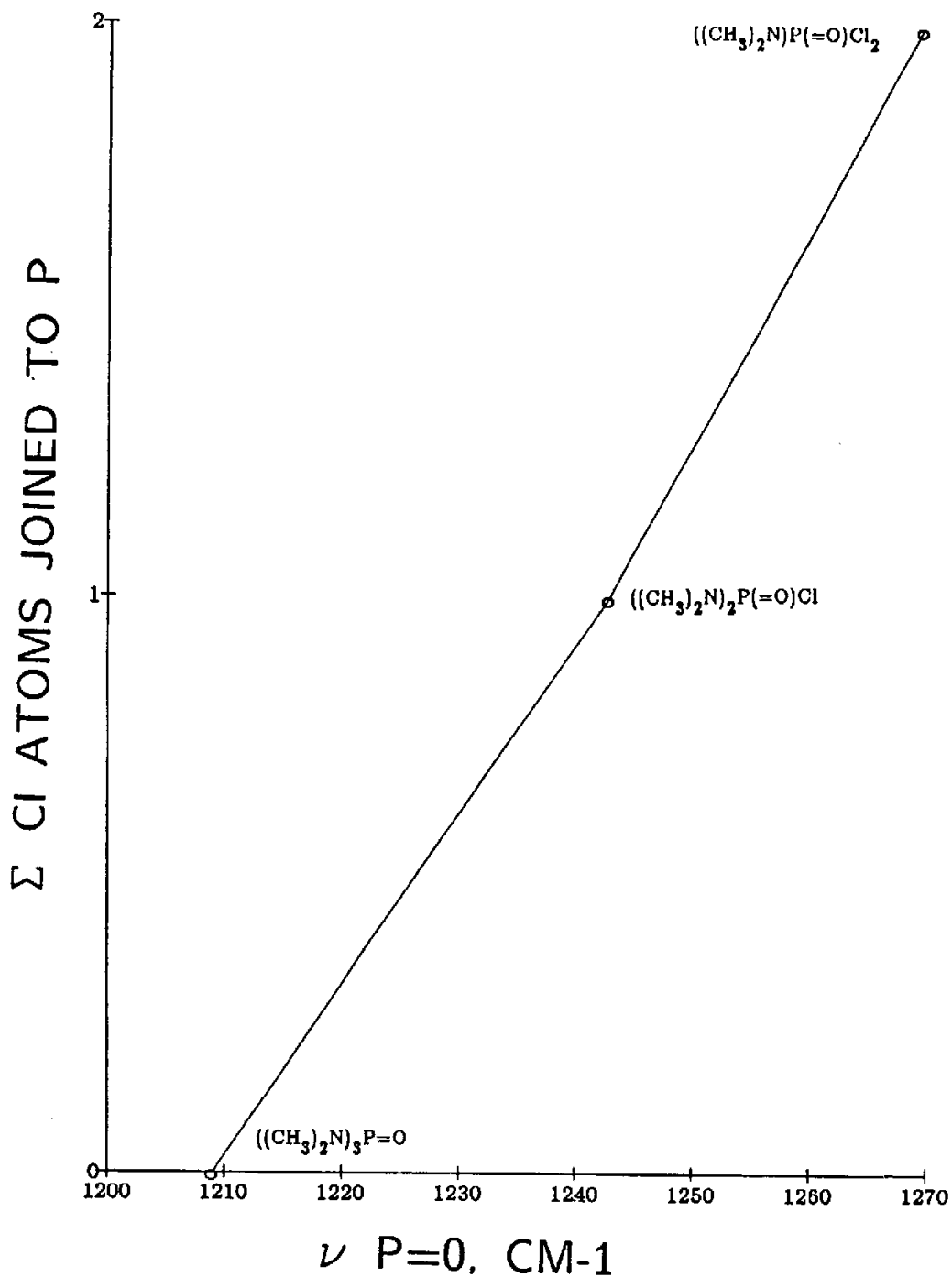
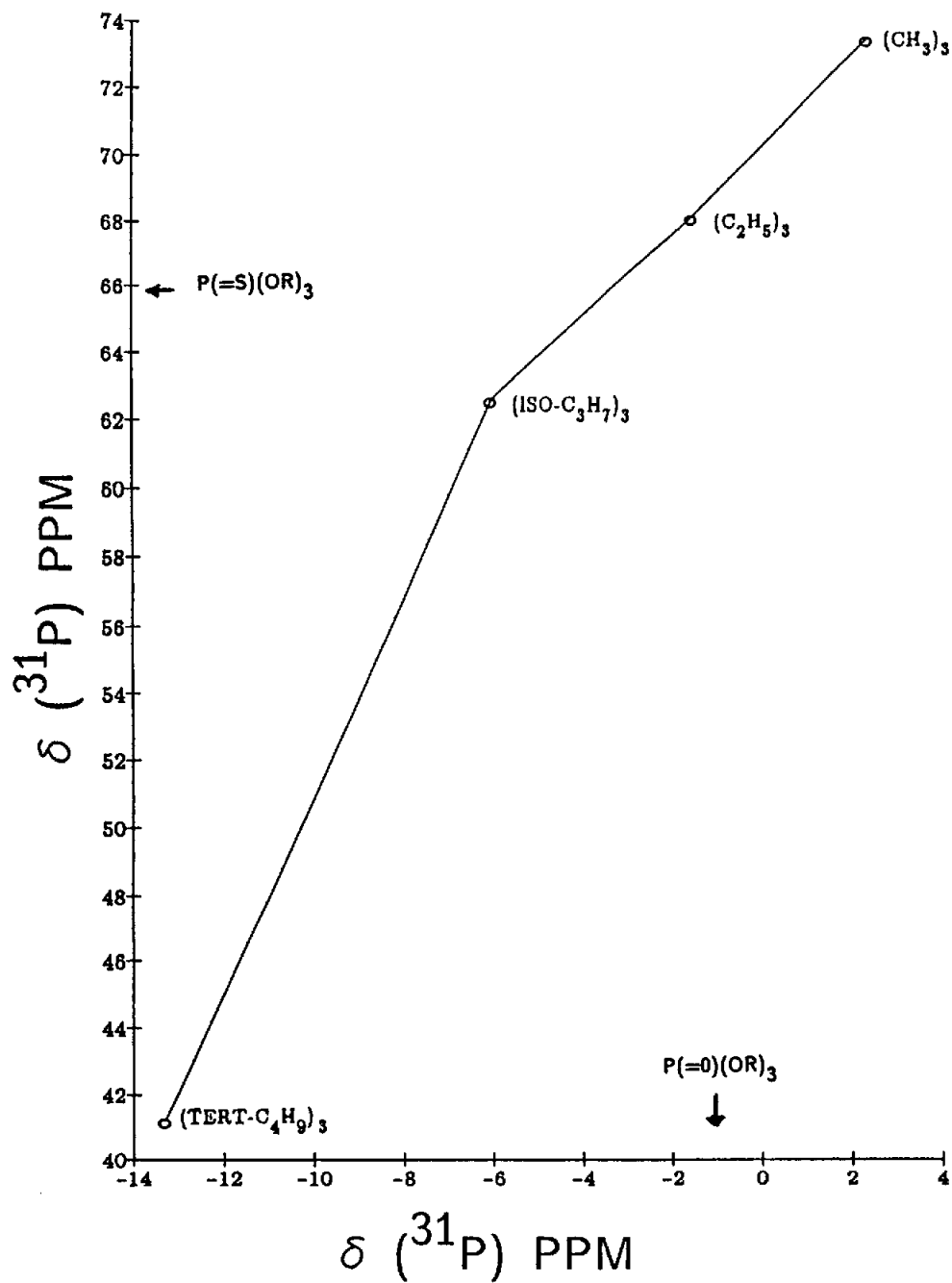


FIGURE 11.81 A plot of the number of Cl atoms joined to phosphorus vs ν P=O for $\text{P}(=\text{O})\text{Cl}_{3-x}[\text{N}(\text{CH}_3)_2]_x$.

FIGURE 11.82 A plot of $\delta ^{31}\text{P}$ for P(=S)(OR)_3 vs $\delta ^{31}\text{P}$ for the corresponding alkyl analogs of P(=O)(OR)_3 .

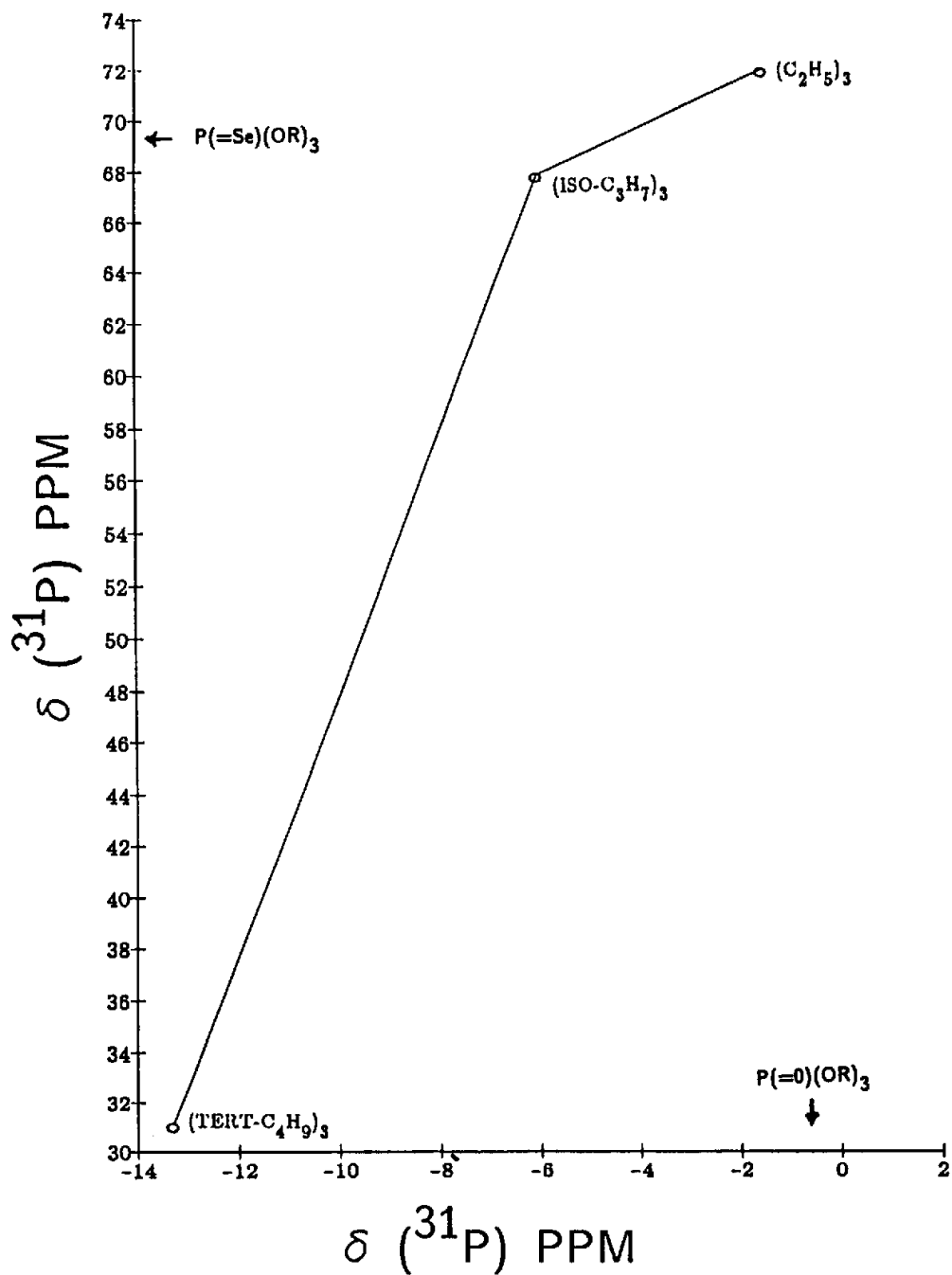


FIGURE 11.83 A plot of $\delta^{31}\text{P}$ for $\text{P}(=\text{Se})(\text{OR})_3$ vs $\delta^{31}\text{P}$ for corresponding alkyl analogs of $\text{P}(=\text{O})(\text{OR})_3$.

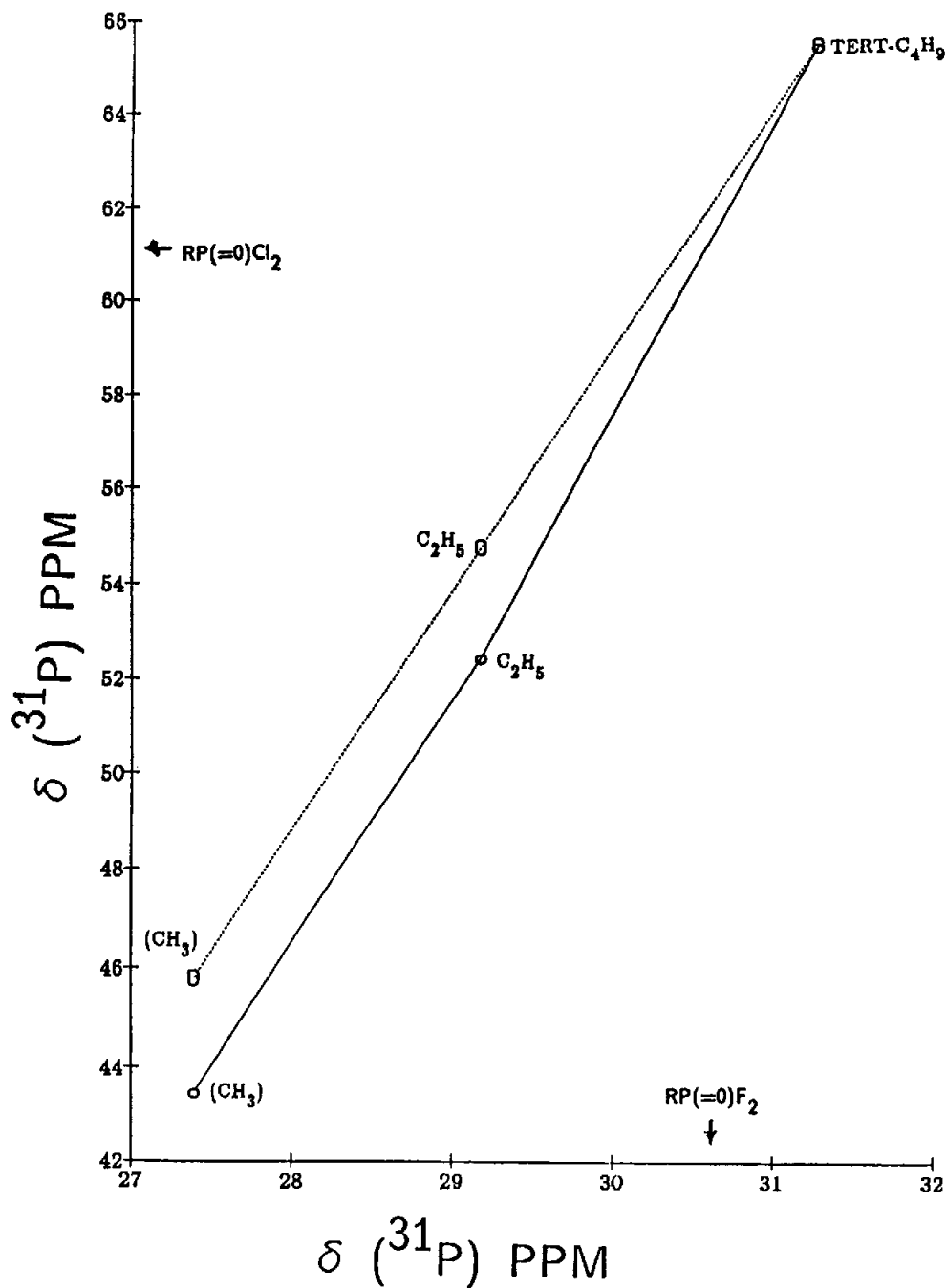
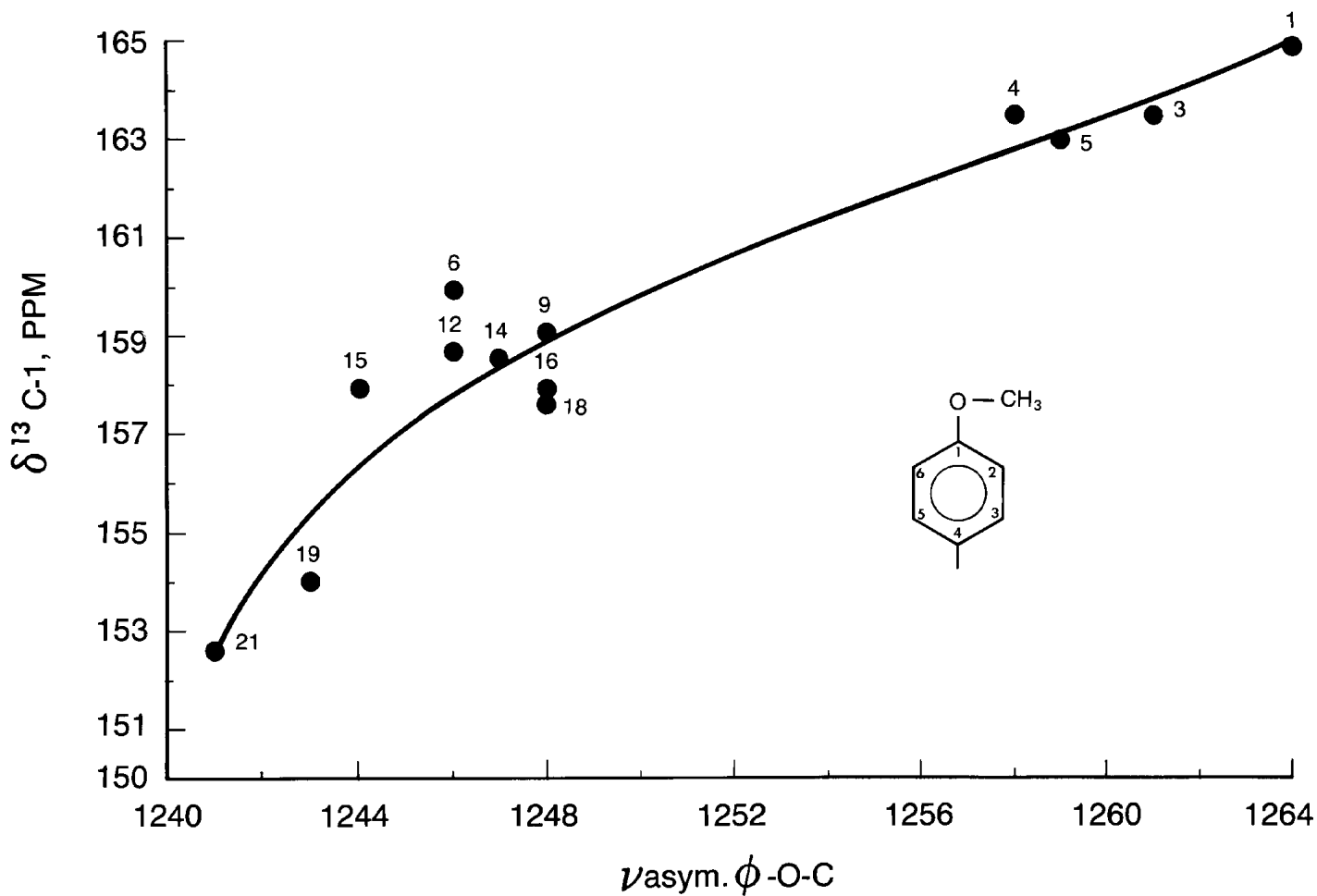
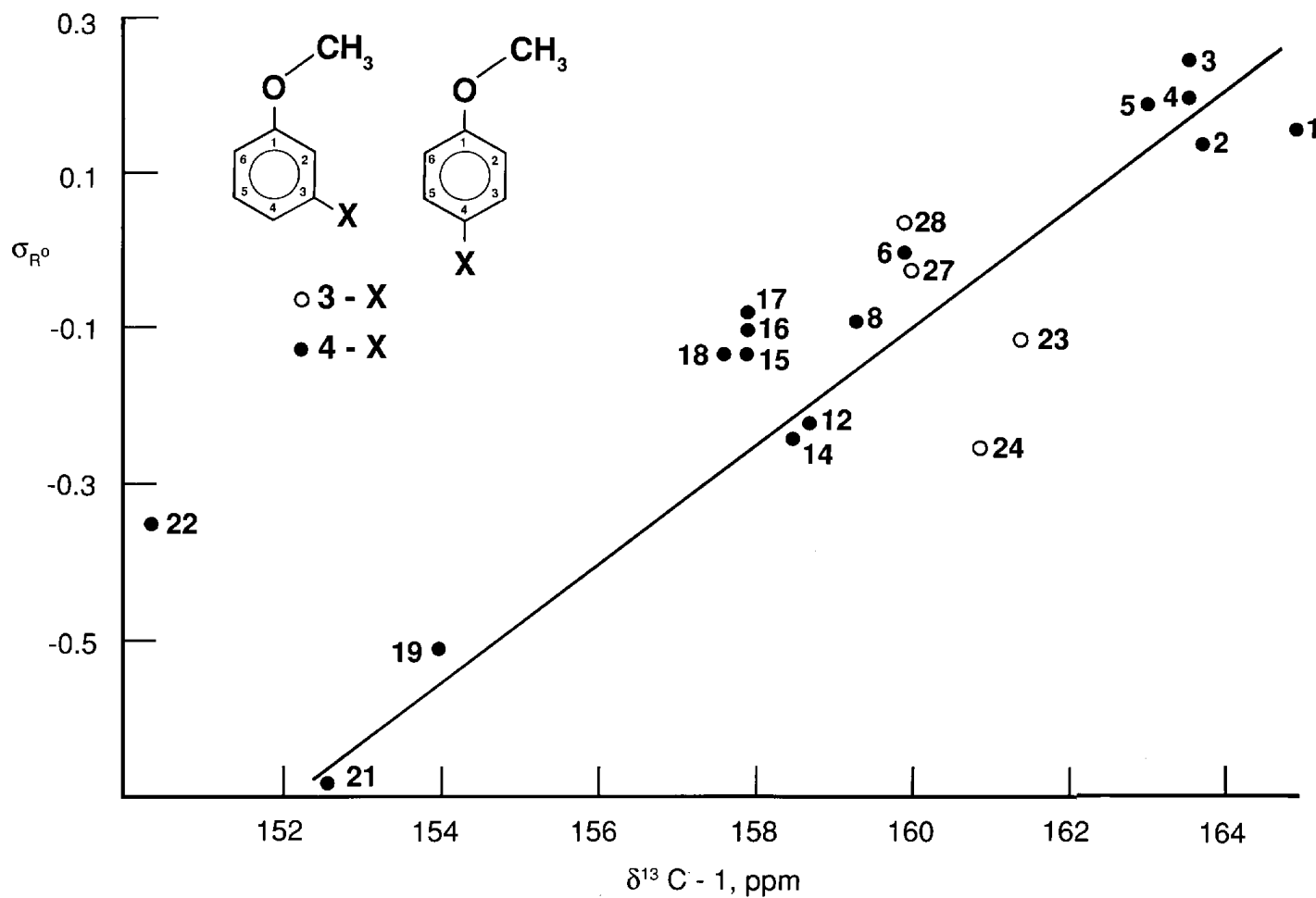
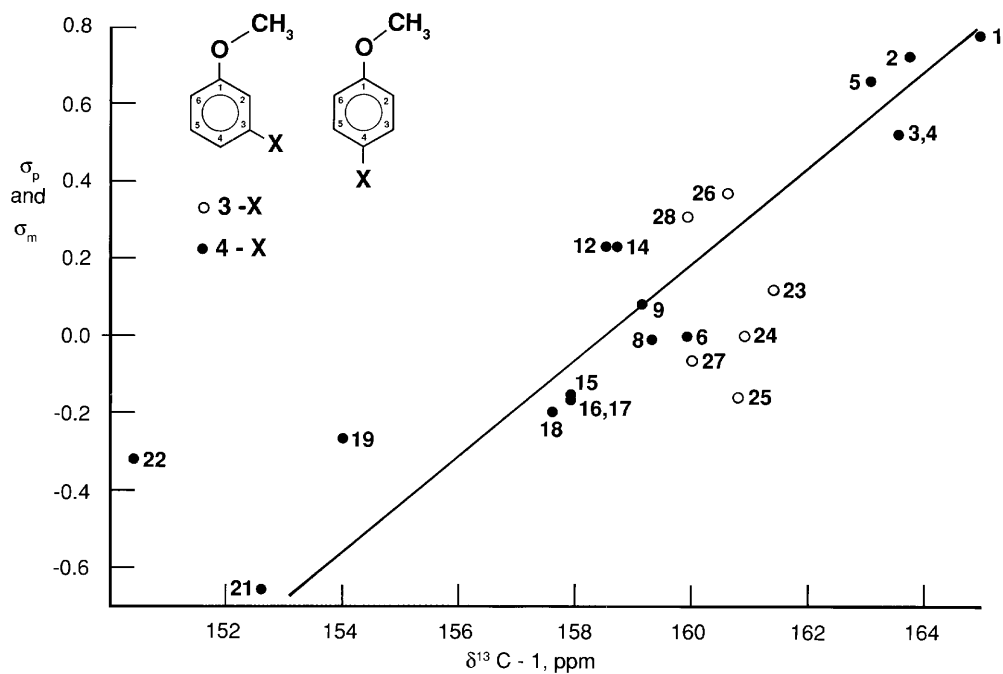
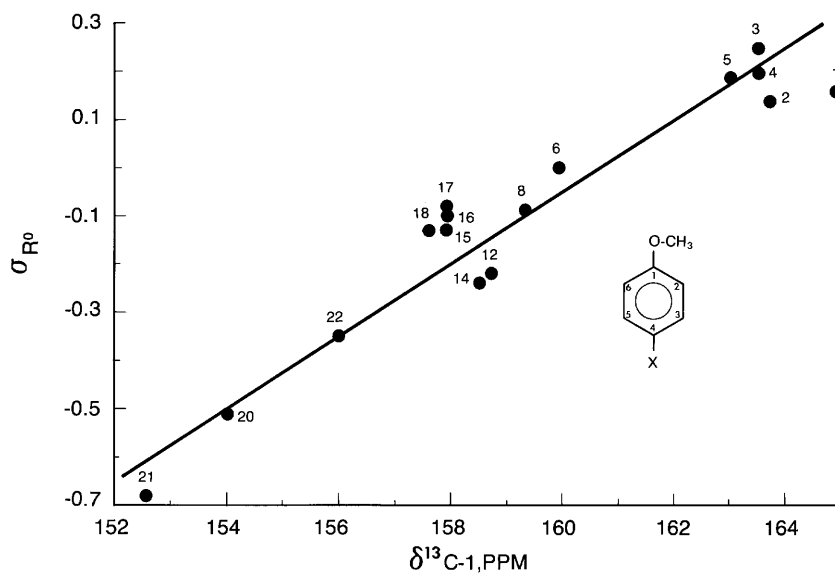


FIGURE 11.84 Plots of $\delta ^{31}\text{P}$ for $\text{RP}(=\text{O})\text{Cl}_2$ vs $\delta ^{31}\text{P}$ for corresponding alkyl analogs of $\text{RP}(=\text{O})\text{F}_2$. The double plot is the $\delta ^{31}\text{P}$ range given in the literature for the $\text{RP}(=\text{O})\text{Cl}_2$ analogs.

FIGURE 11.85 A plot of $\nu_{\text{asym. } \phi\text{-O-C}}$ vs $\delta^{13}\text{C-1}$ for 4-x-anisoles.

FIGURE 11.86 A plot of $\delta^{13}\text{C}-1$ vs Taft σ_{R^0} for 3-x- and 4-x-anisoles.

FIGURE 11.87 A plot of $\delta^{13}\text{C}-1$ vs Hammett σ values for 3-x^v- and 4-x-anisoles.FIGURE 11.88 A plot of Taft σ_{R^0} values vs $\sigma^{13}\text{C}-1$ for 4-x-anisoles.

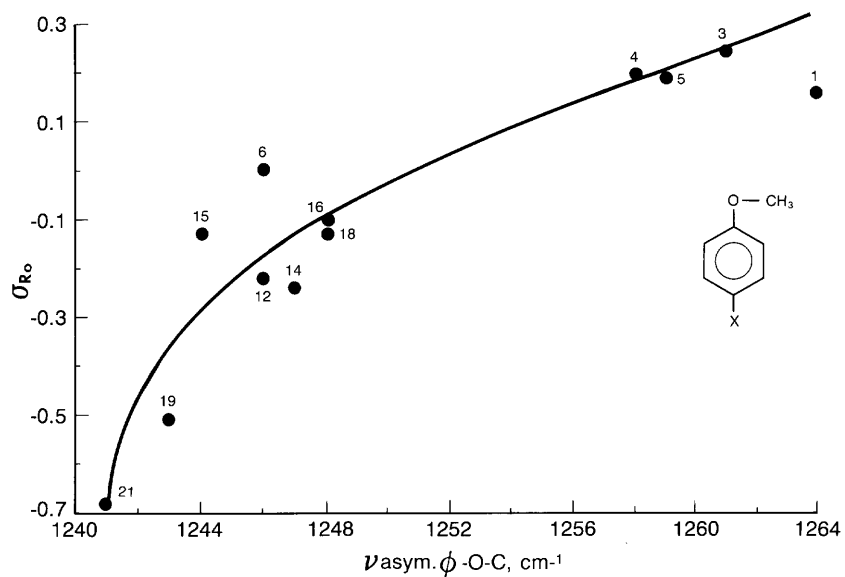


FIGURE 11.89 A plot of Taft σ_{R_o} values vs ν asym. ϕ -O-C for 4-x-anisoles.

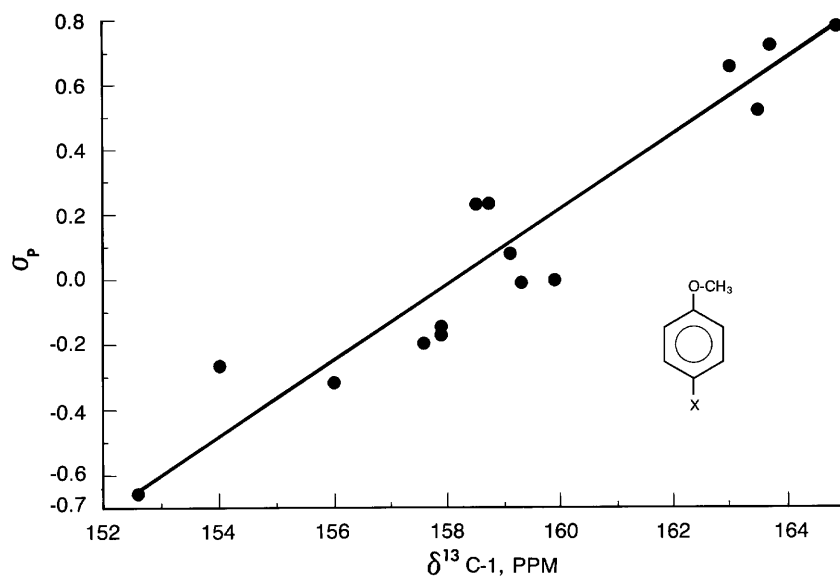
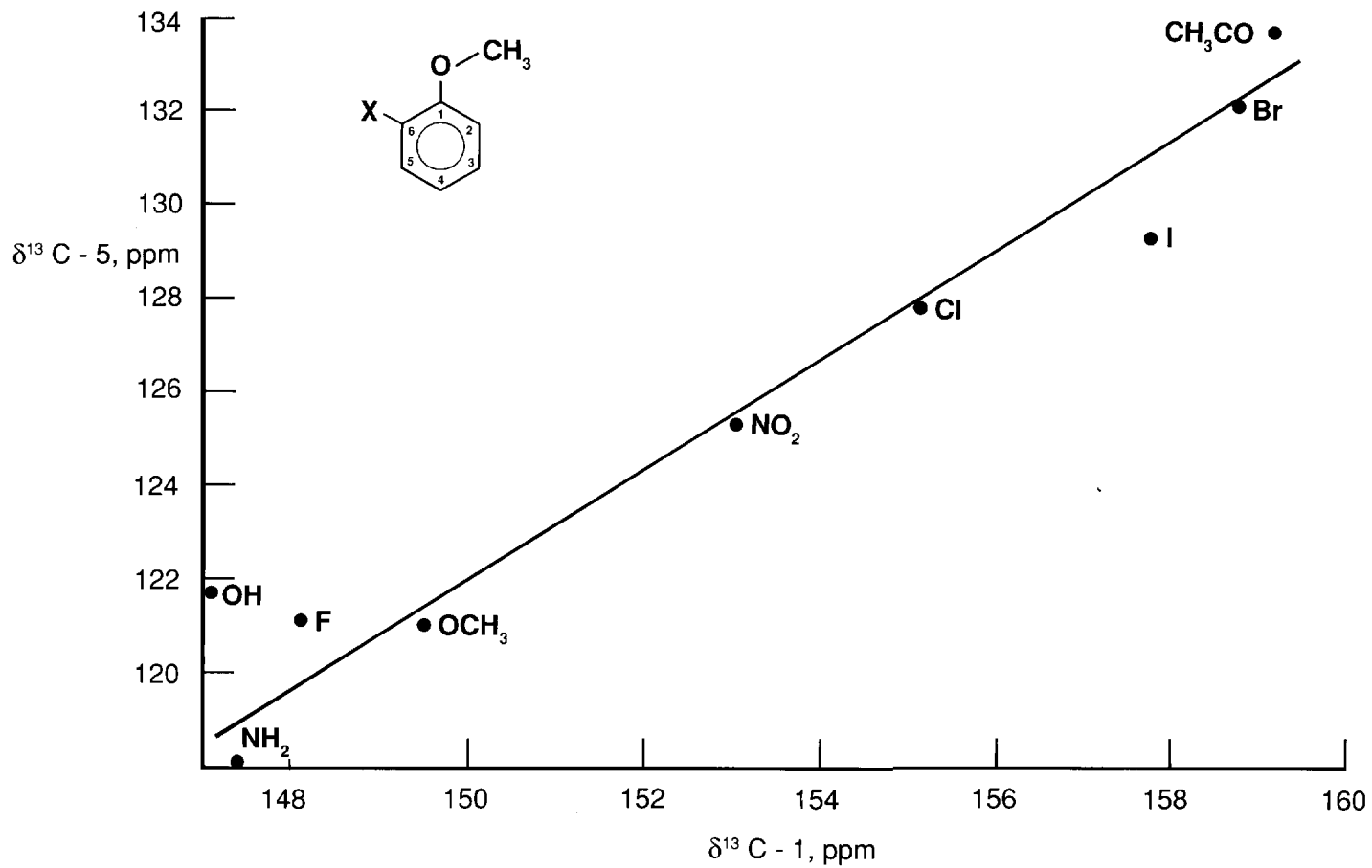
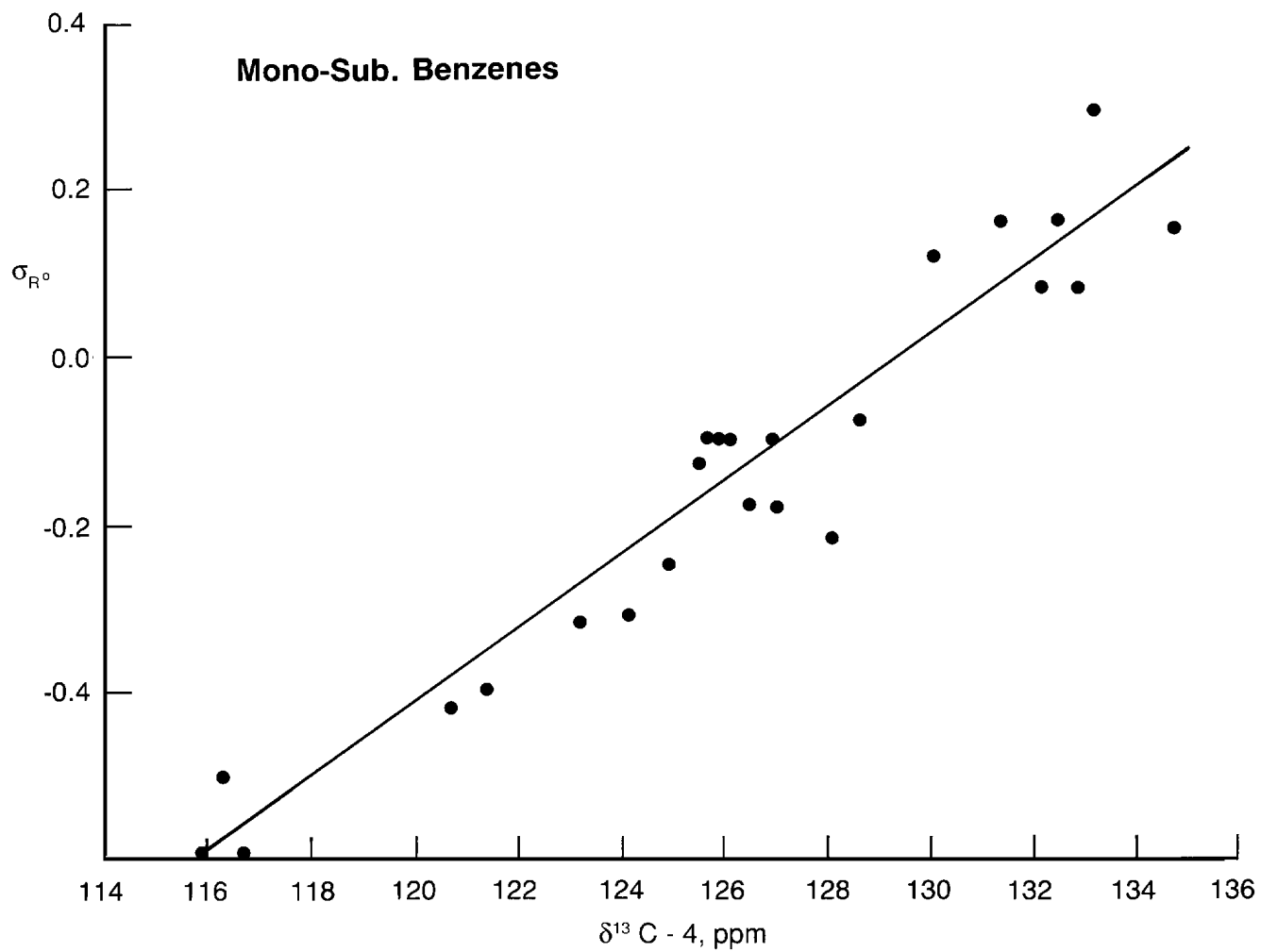
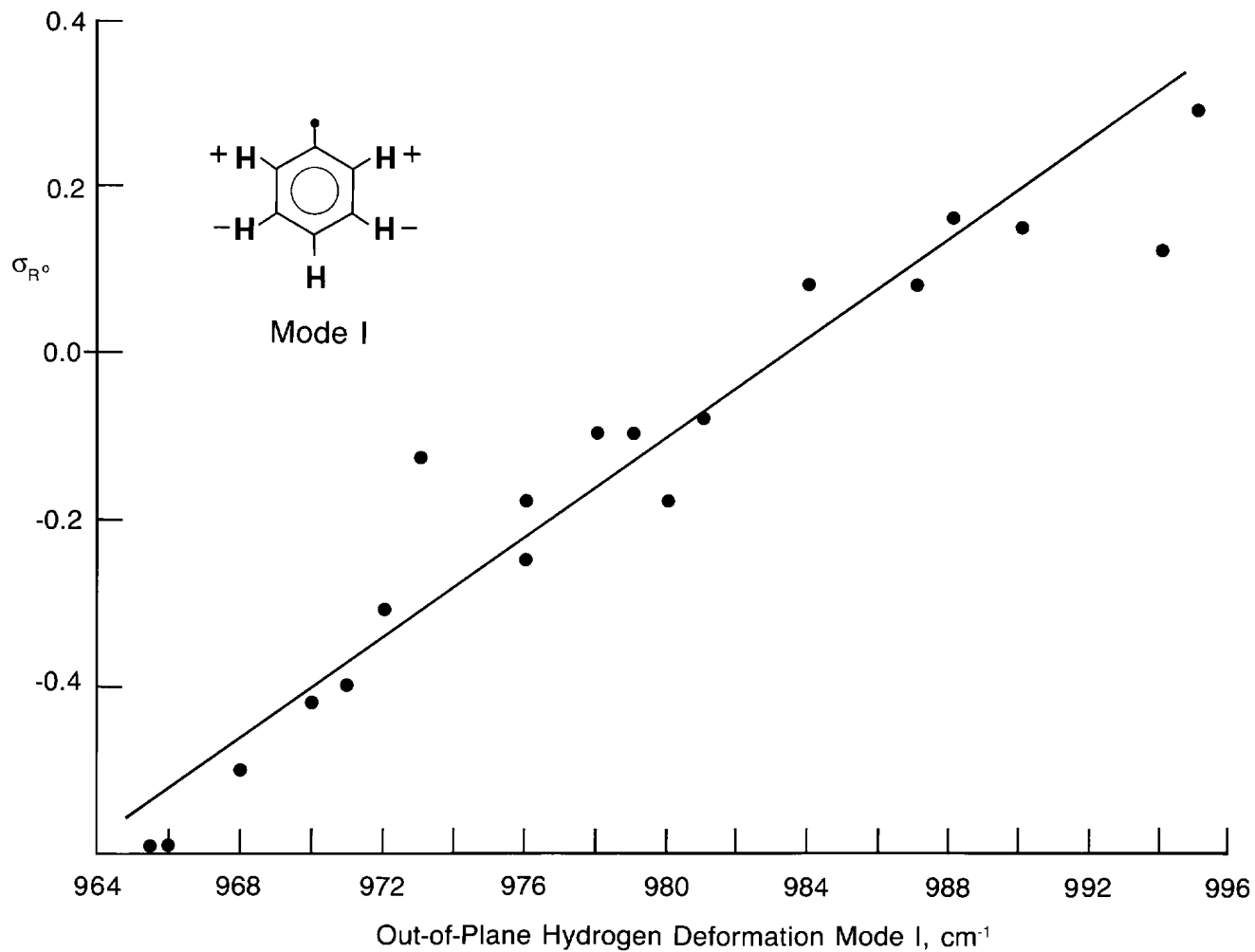
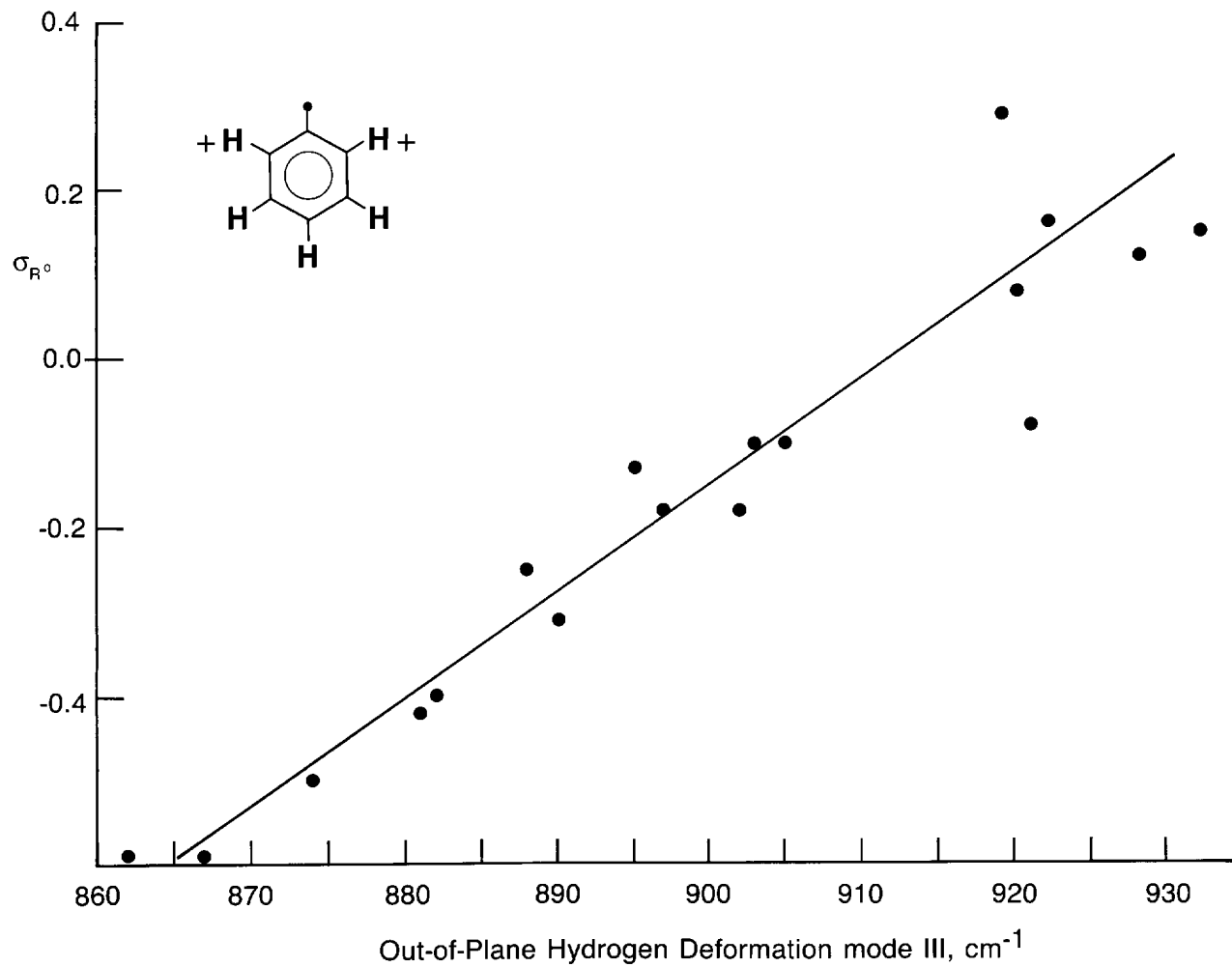


FIGURE 11.90 A plot of $\delta^{13}\text{C-1}$ vs Hammett σ_p values for 4-x-anisoles.

FIGURE 11.91 A plot of $\delta^{13}\text{C}-1$ vs $\delta^{13}\text{C}-5$ for 2-x-anisoles.

FIGURE 11.92 A plot of $\delta^{13}\text{C}-4$ for mono-substituted benzenes vs Taft $\sigma_{R^{\circ}}$ values.

FIGURE 11.93 A plot of the out-of-plane hydrogen deformation mode I for mono-substituted benzenes vs Taft σ_{R° values.

FIGURE 11.94 A plot of the out-of-plane hydrogen deformation mode III for mono-substituted benzenes vs Taft σ_{R^o} values.

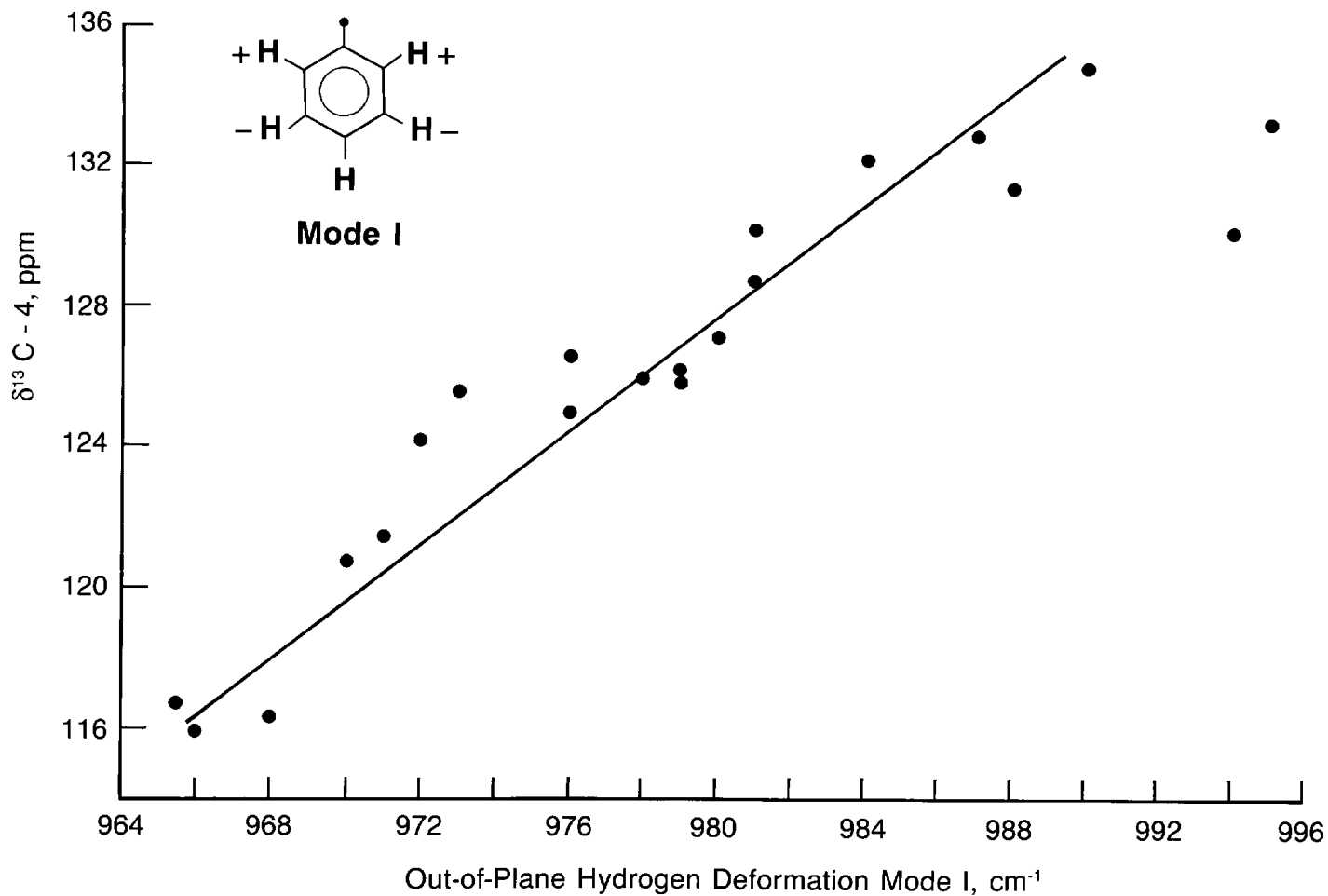
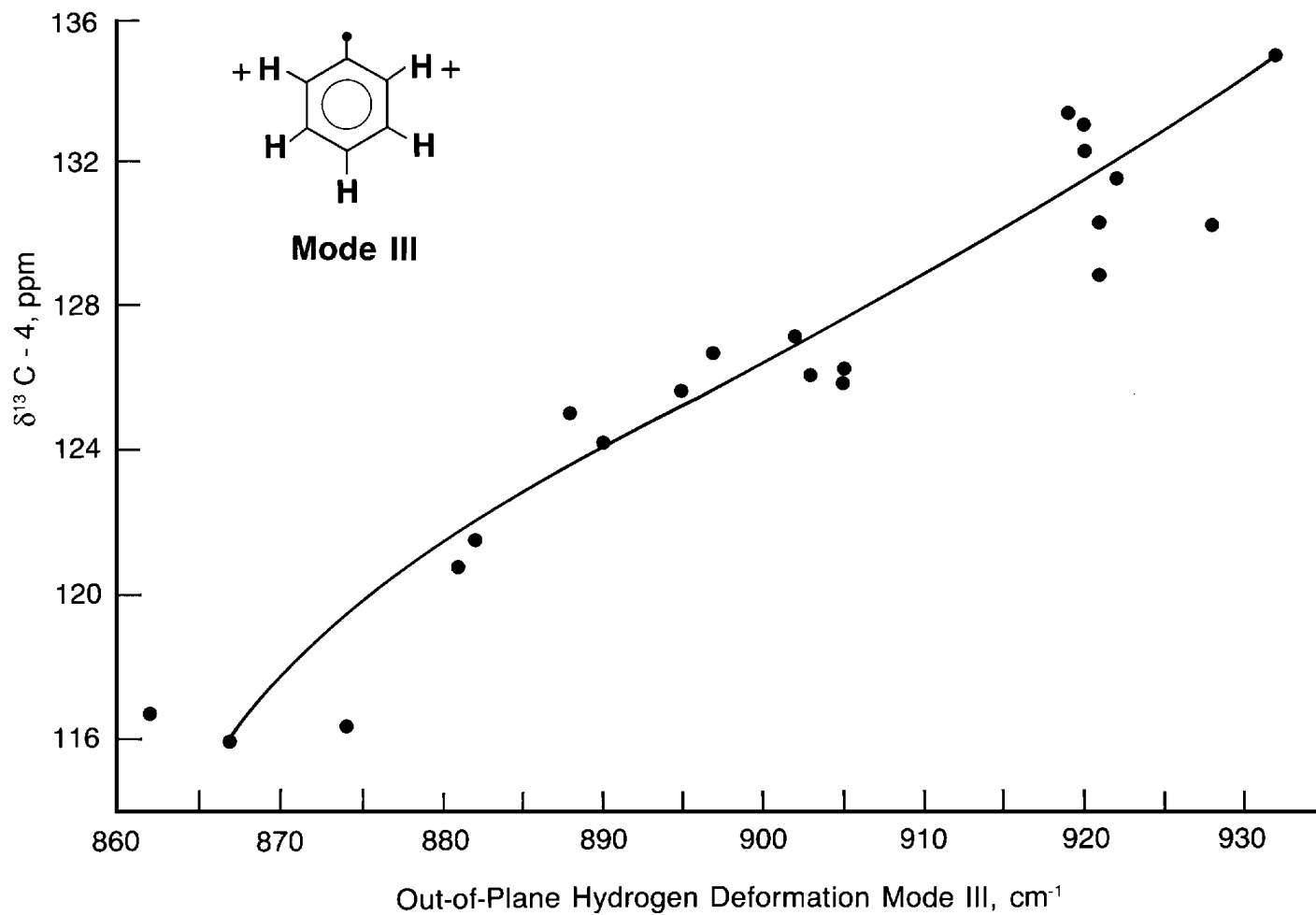


FIGURE 11.95 A plot of the out-of-plane hydrogen deformation mode I for mono-substituted benzenes vs $\delta^{13}\text{C}-4$ for mono-substituted benzenes.

FIGURE 11.96 A plot of the out-of-plane hydrogen deformation mode III vs $\delta^{13}\text{C}-4$ for mono-substituted benzenes.

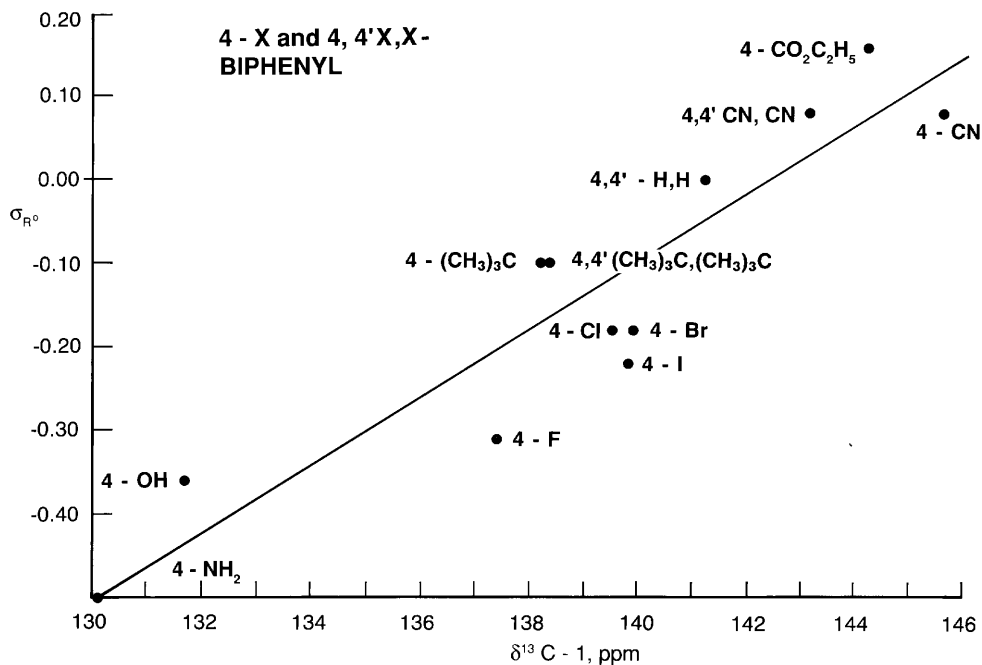


FIGURE 11.97 A plot of $\delta^{13}\text{C}-1$ vs Taft σ_{R° values for 4-x and 4,4'-x,x-biphenyls.

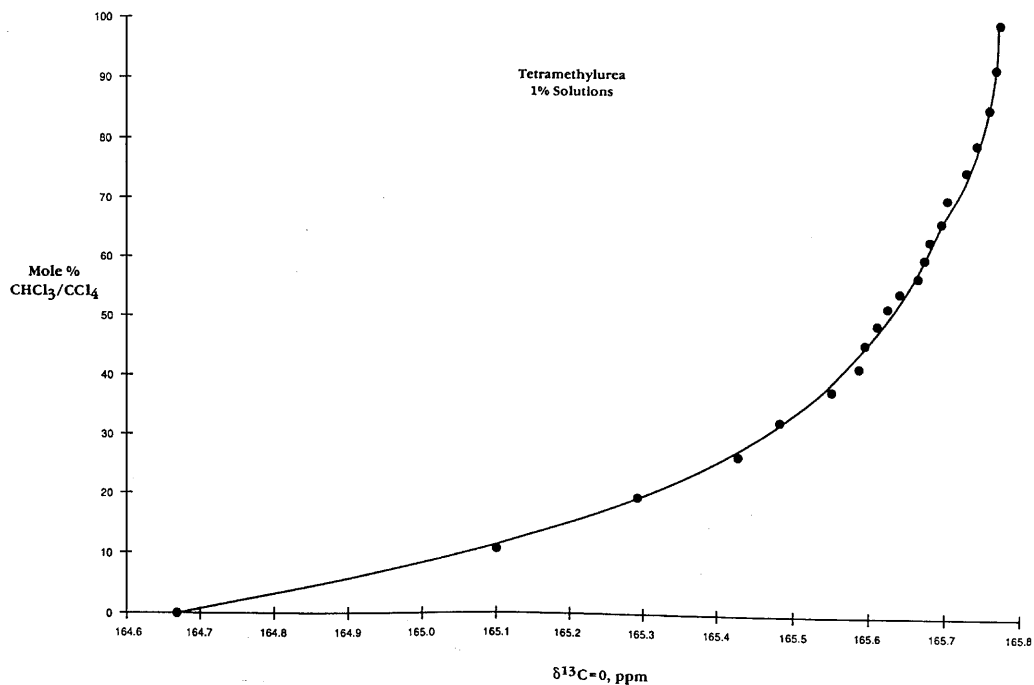
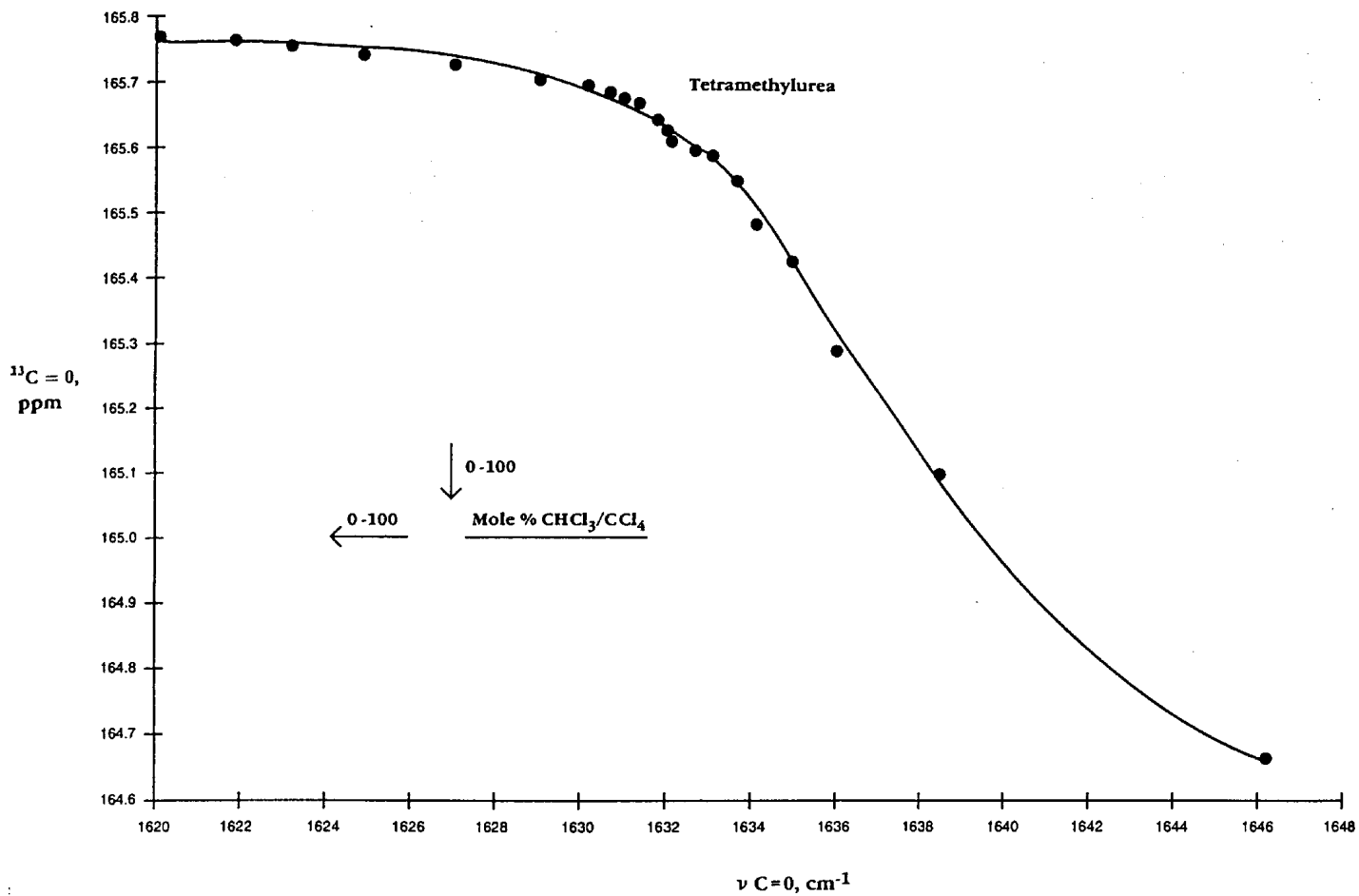
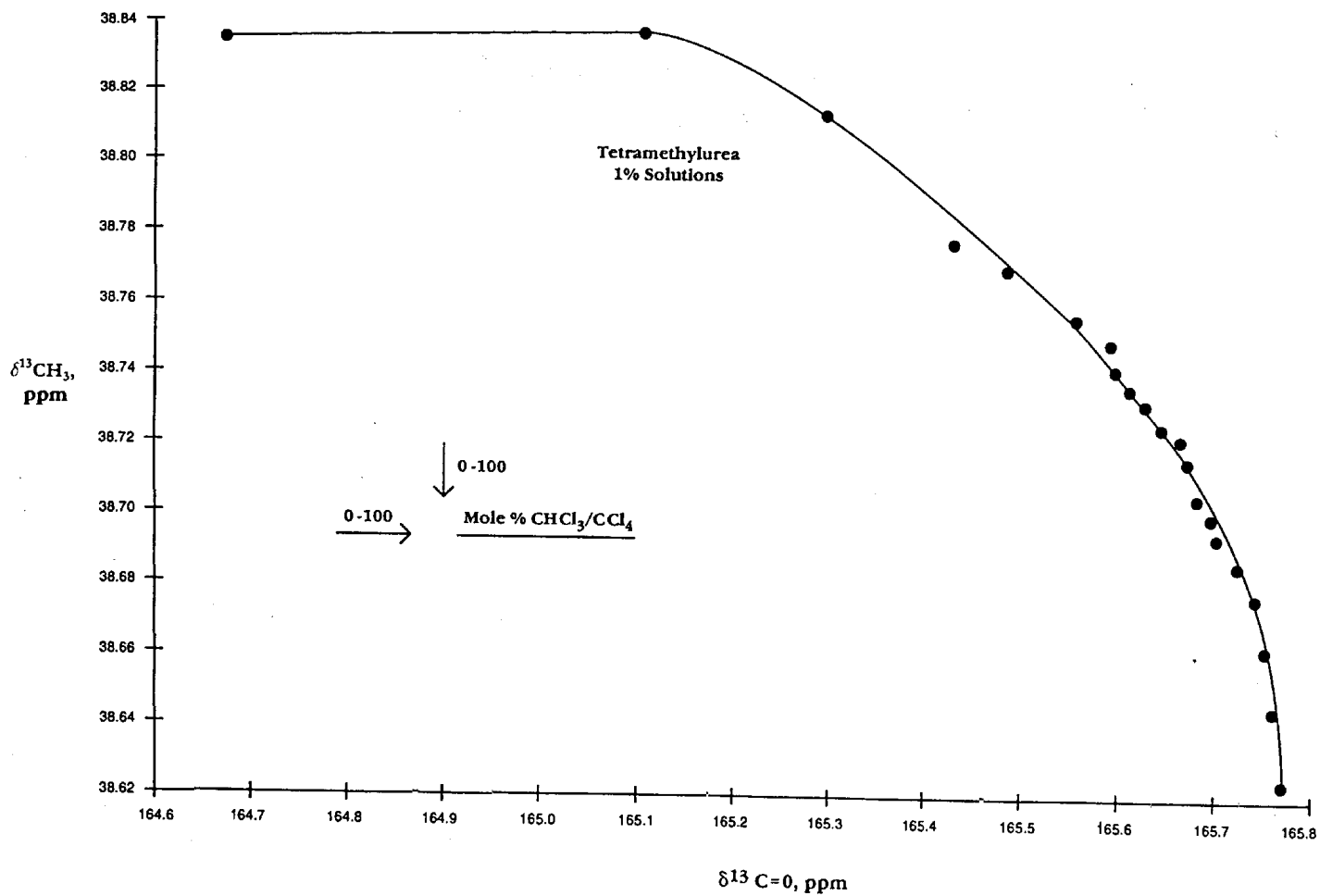
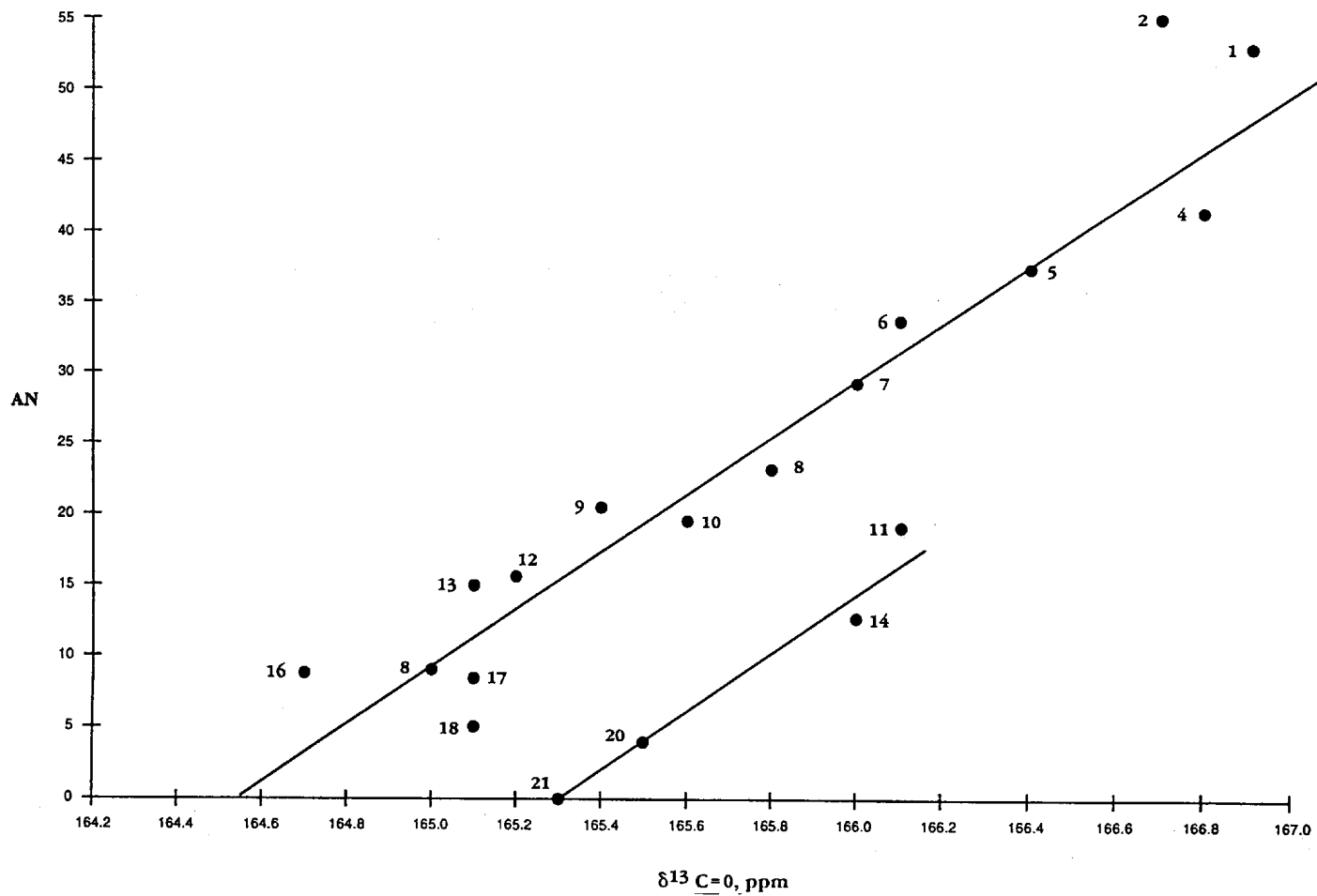


FIGURE 11.98 A plot of $\delta^{13}\text{C}=\text{O}$ for tetramethylurea (TMU) 1 wt./vol. % solutions vs mole % CHCl₃/CCl₄.

FIGURE 11.99 A plot of $\nu \text{ C}=\text{O}$ vs $\delta^{13}\text{C}=\text{O}$ for TMU 0-100 mol % $\text{CHCl}_3/\text{CCl}_4$ solutions.

FIGURE 11.100 A plot of $\delta^{13}\text{C}=\text{O}$ vs $\delta^{13}\text{CH}_3$ for TMU in 0–100 mol % $\text{CHCl}_3/\text{CCl}_4$ solutions.

FIGURE 11.101 A plot of $\delta^{13}\text{C}=\text{O}$ for TMU vs the solvent acceptor number (AN) for different solvents.

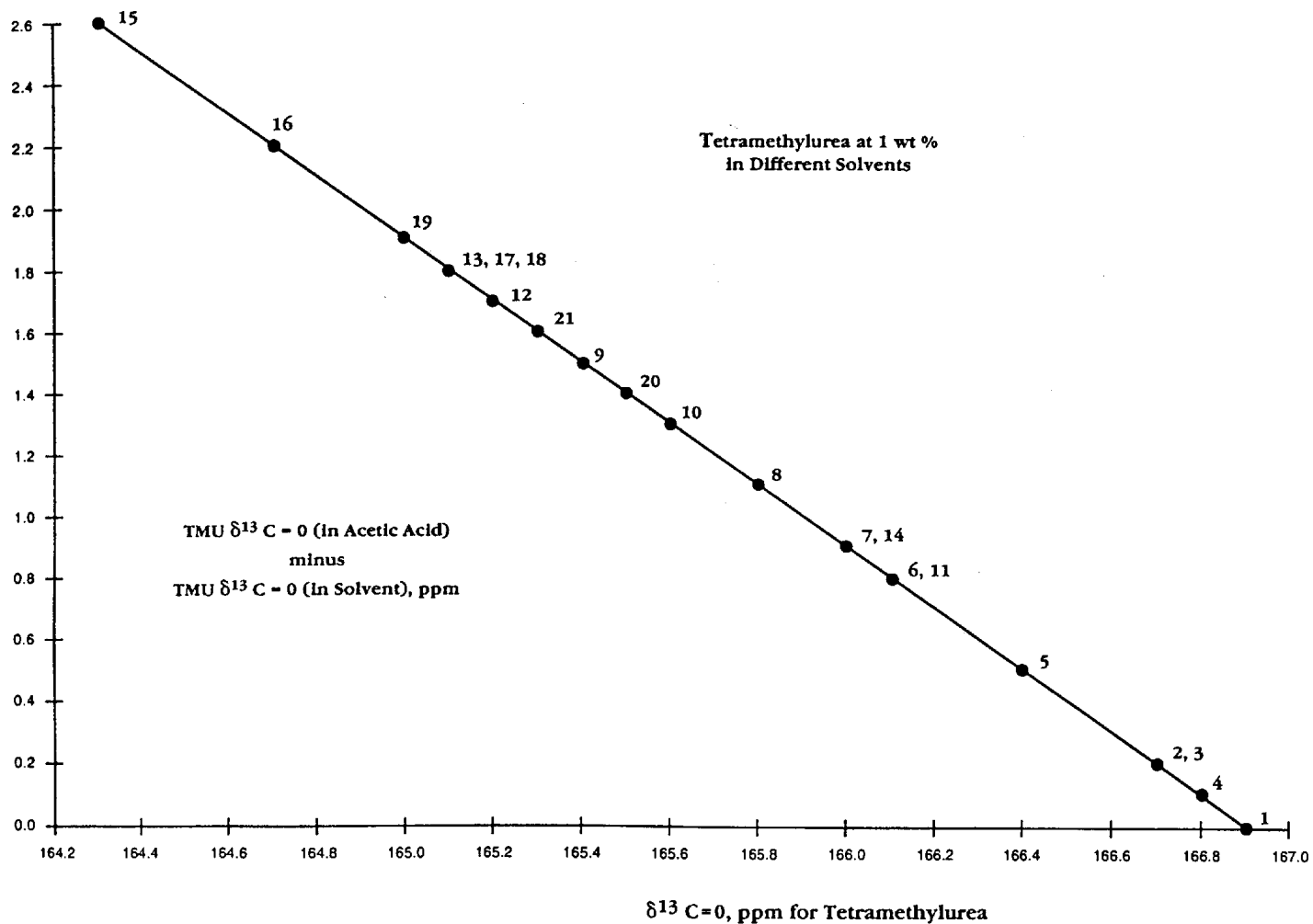
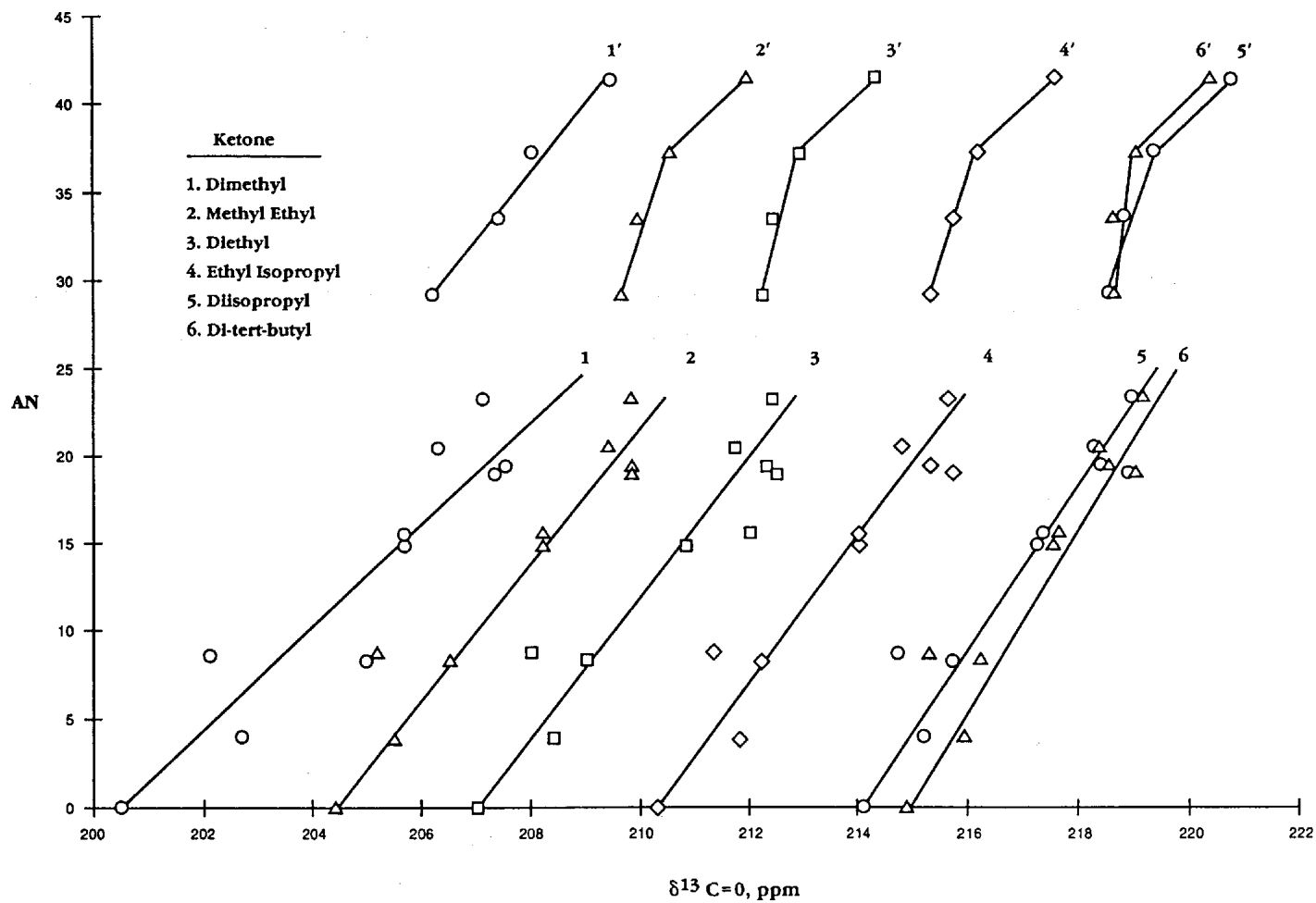


FIGURE 11.102 A plot of the $\delta^{13}\text{C}=\text{O}$ chemical shift difference between TMU in solution with acetic acid and in solution with each of the other solvents.

FIGURE 11.103 Plots of $\delta^{13}C=O$ for dialkylketones at 1 wt./vol. % in different solvents vs the AN for each solvent.

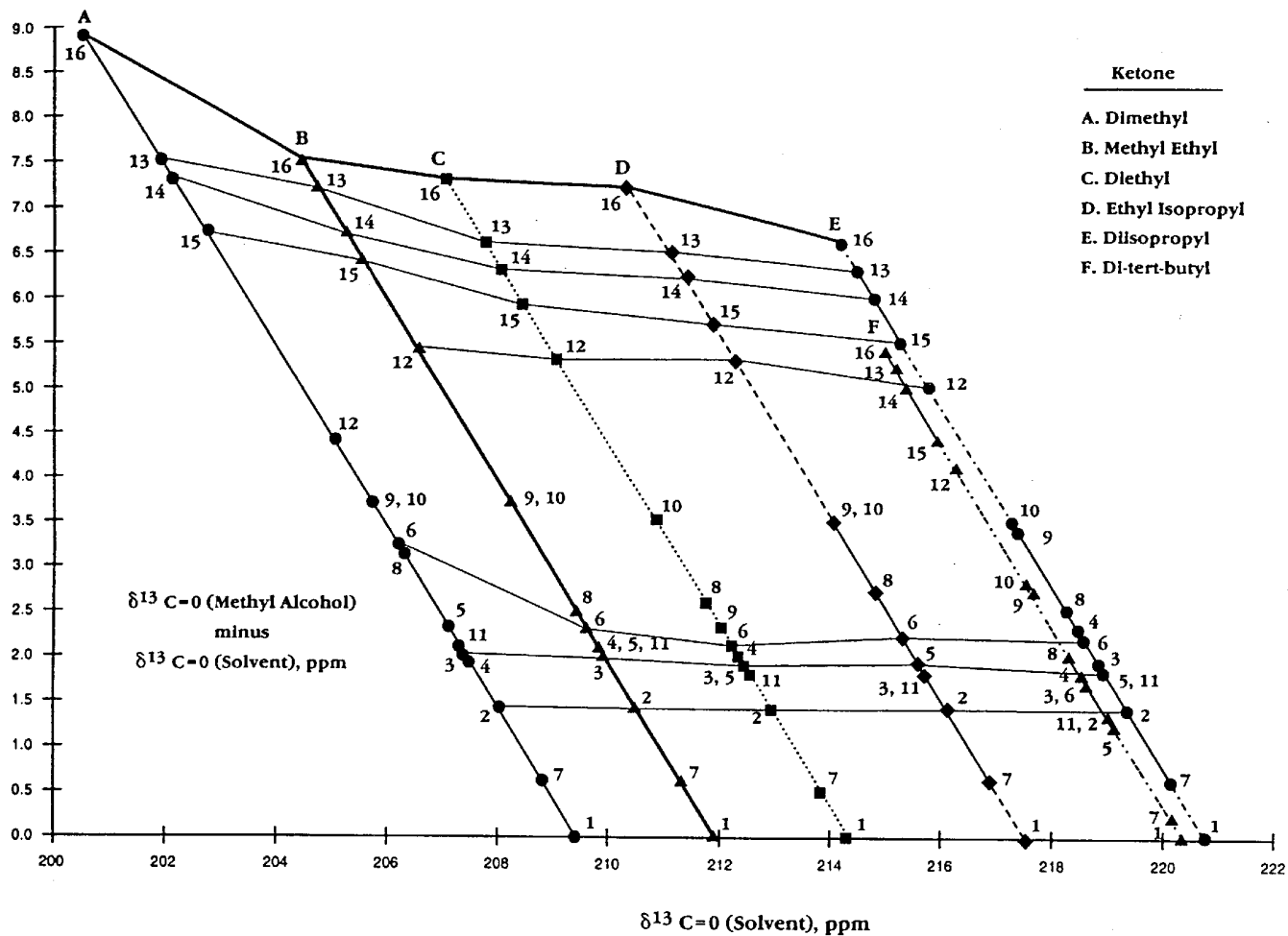


FIGURE 11.104 Plots of the $\delta^{13}\text{C}=\text{O}$ chemical shift difference between each dialkyl-ketone in methanol and the same dialkylketone in solution with each of the other solvents.

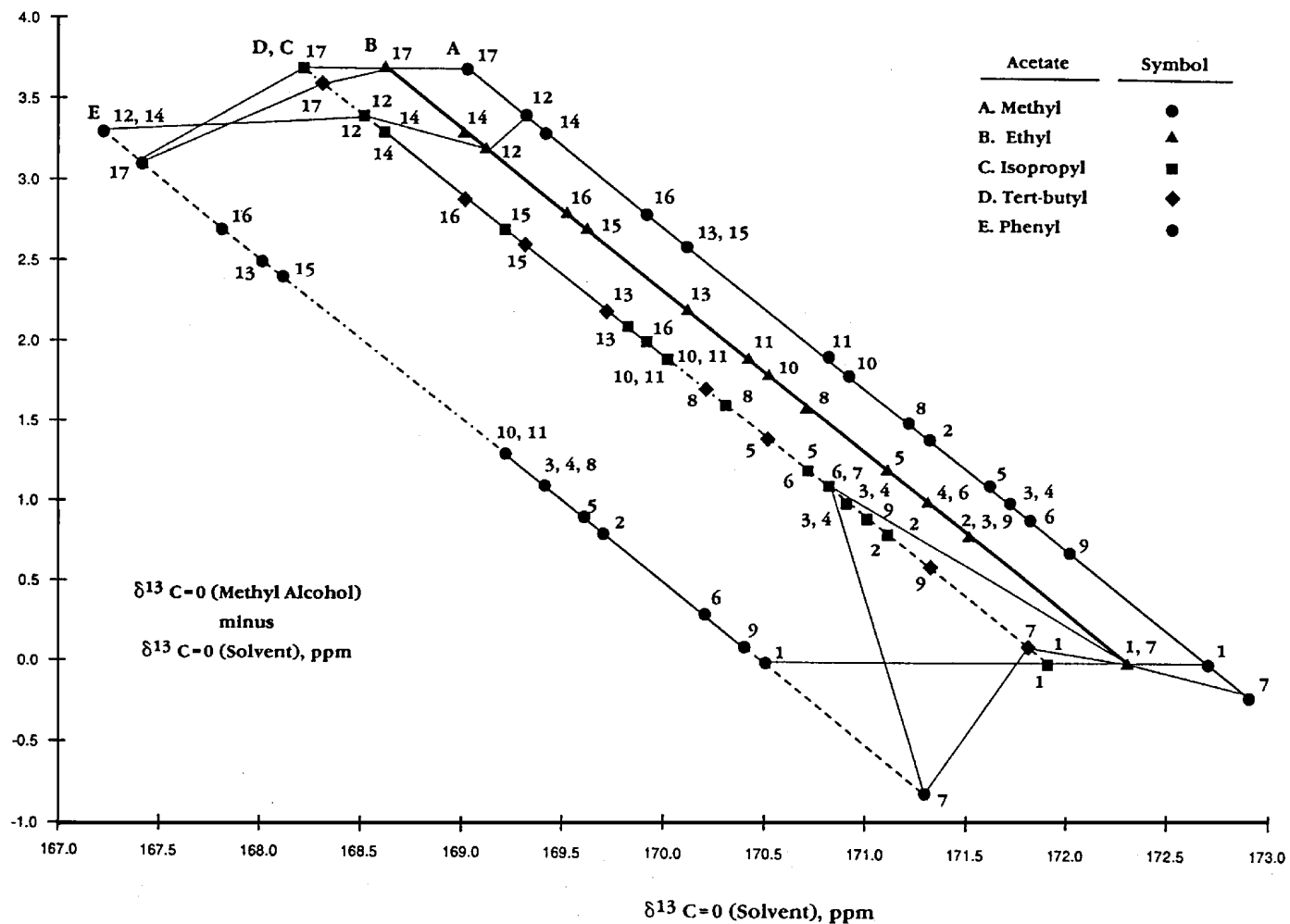


FIGURE 11.105 A plot of $\delta^{13}\text{C}=\text{O}$ for alkyl acetates and phenyl acetate vs the difference of $\delta^{13}\text{C}=\text{O}$ in methanol and $\delta^{13}\text{C}=\text{O}$ in each of the other solvents.

TABLE 11.1 The NMR ^{13}C solution-phase chemical shift data for 4-X-anilines

4-X-Aniline 4-X	Chemical shift $\delta^{13}\text{C-1}$ ppm	Chemical shift $\delta^{13}\text{C-2}$ ppm	Chemical shift $\delta^{13}\text{C-3}$ ppm	Chemical shift $\delta^{13}\text{C-4}$ ppm
NH ₂	138.8	116.1	116.1	138.8
OH	139.6	115.7	115.9	149.1
OCH ₃	140.5	116.3	114.9	152.6
OC ₂ H ₅	140.4	116.4	115.8	152
OC ₃ H ₇	140.5	116.4	115.8	152.1
OC ₄ H ₉	140.5	116.4	115.7	152.2
OC ₆ H ₁₃	140.3	116.3	115.7	152.2
CH ₃	144.3	115.2	129.7	127.2
n-C ₃ H ₇	144.5	115.3	129.2	132.4
n-C ₄ H ₉	144.4	115.3	129.1	132.7
iso-C ₃ H ₇	144.6	115.3	127	138.7
cyclo-C ₃ H ₅	144.3	115.3	126.8	133.4
t-C ₄ H ₉	143.9	114.9	125.8	140.9
F	143.1	116.1	115.7	156.4
Cl	145.2	116.3	129	122.8
Br	145.6	116.7	131.9	109.8
I	147.4	116.7	137.1	76.8
SCH ₃	145.4	115.6	130.8	125
CN	151.1	114.5	133.8	120.5
NO ₂	155.1	112.8	126.3	136.9
NO ₂ ,HCl	145.4	119.6	125.4	142.4
SO ₃ H	150.6	116.1	128	133.2
CH ₃ SO ₂	153.2	113.2	128.9	126.2
CF ₃	150.2	114.5	127	120.1
CH ₃ CO	153.8	113.9	131.4	168.8

TABLE 11.2 Infrared and NMR data for 3-x- and 4-x-benzoic acids

3-x or 4-x benzoic acid	σ m	Chemical shift $^{13}\text{C}=\text{O}$ ppm	Chemical shift $^{13}\text{C}-1$ ppm	Chemical shift $^{13}\text{CC}-2$ ppm	Chemical shift $^{13}\text{C}-3$ ppm	Chemical shift $^{13}\text{C}-4$ ppm	Chemical shift $^{13}\text{C}-5$ ppm	Chemical shift $^{13}\text{C}-6$ ppm	C=O str. vapor cm^{-1}	C=O str. CCl_4 soln. cm^{-1}	C=O str. [$\nu\text{-CCl}_4$ soln.] cm^{-1}
3-x											
F	0.34	167.3	133.5	116.5	162.6	119.8	130.3	125.7	1768	1748	20
CH_3	-0.07	172.9	129.5	128.4	138.3	134.5	130.8	127.5	1761		
NH_2		169.2	132.4	115.9	149.3	119.5	130	118.6	1761		
SO_2F		165.5	133.4	130.5	133.1	131.8	129.2	136.7			
CF_3	0.42	166.9	132.7	126.6	130.8	129.2	129.6	133.4	1766		
NO_2	0.71	166.1	133	127.1	148.2	127.1	129.9	135.5	1768	1752	16
CN	0.62	165.9	132.5	133	112.4	135.8	129.7	133.8	1765		
4-x											
	σ p										
OCH_3	-0.27	167.4	123.3	131.5	113.5	162.9			1760	1737	23
OH	-0.36	169.1	121.3	132.1	115.4	161.8			1755		
$\text{C}_4\text{H}_9\text{NH}$		168.1	117.1	131.2	110.7	152.7			1751		
OC_2H_5		167.4	123	131.4	113.9	162.4			1755		
$t\text{-C}_4\text{H}_9$	-0.2	172.7	126.8	130.2	125.4	157.6			1758		
OC_4H_9		167.5	123.1	131.5	114	162.7					
Cl	0.23	168.8	129.8	131.1	128.5	138.3			1765	1745	20
H	0	172.7	129.5	130.3	128.5	133.8			1762	1744	18
CO_2H		166.9	134.6	129.3							
Range		165.9–172.9	117.1–134.6	116.5–133	110.7–162.6	119.8–162.9	129.2–130.8	118.6–136.7	1751–1768	1737–1752	16–23

TABLE 11.3 Infrared and NMR data for 4-x-acetanilides in solution*

4-x-Acetanilides X	Chemical shift $^{13}\text{C}=\text{O}$ ppm	Chemical shift $^{13}\text{C}=1$ ppm	Chemical shift $^{13}\text{C}=2$ ppm	Chemical shift $^{13}\text{C}=3$ ppm	Chemical shift $^{13}\text{C}=4$ ppm	C=O str. [CHCl ₄] cm ⁻¹	C=O str. [CHCl ₃] cm ⁻¹	C=O str. [CCl ₄ -CHCl ₃] cm ⁻¹
NH ₂	167.8	129.2	121.5	114.4	144.1			
OH	168.6	130.6	121.8	115.2	153.6		1686	
H	168.7	139.2	119.7	128.5	123.3	1705		
F	168.5	135.6	121.2	115	158.4			
Br	168.4	138.5	121	114.8	131.2	1709	1694	15
I	168.9	138.9	137.3	137.3	86.2	1709	1696	13
iso-C ₃ H ₇	169.4	136.1	120.8	126.6	144.8			
CH ₃ C=O	168.9	143.7	118.4	129.2	131.6	1713	1702	11
NO ₂	169.3	145.5	118.6	124.6	142.3	1718	1711	7

*See References 3 and 6.

TABLE 11.4 Infrared and NMR data for 4-X-benzaldehydes in CCl₄ and/or CHCl₃ solutions

4-x-Benzaldehyde X	Chemical shift ¹³ CH ppm	Chemical shift ¹³ C=O ppm	Chemical shift C-1 ppm	C=O str. CCl ₄ soln. cm ⁻¹	C=O str. CHCl ₃ soln. cm ⁻¹	C=O str. [CCl ₄ -CHCl ₃] cm ⁻¹	σ_p	σ_l	σ_{R^e}
(CH ₃) ₂ N	9.66	189.5	125.2	1696.9	1682.5	14.4	-0.6	0.06	-0.59
OH	9.89	190.8	128.7	1701.1	1688.2	12.9	-0.37		-0.4
CH ₃ O	9.8	190.5	130.2	1697.1	1688.8	8.3	-0.268	0.27	-0.42
F	10	190.2	132.7	1706.7	1700.6	6.1	0.062	0.5	-0.31
C ₆ H ₅ O	9.92	190.3	131	1703.3	1696.6	6.7	-0.32	0.38	-0.32
Cl	9.91	190.5	134.9	1710.3	1702.9	7.4	0.226	0.46	-0.18
Br	9.97	190.6	135.2	1710.4	1704.3	6.1	0.232	0.44	-0.18
CH ₃	9.97	191.4	134.4	~1711			-0.17	-0.1	-0.13
C ₆ H ₅	10	191.9	135.1	1706.7	1700.3	6.4	-0.01	0.12	-0.1
H	9.94	192	136.6	1708.5	1701.9	6.6	0	0	0
CN	10.13	190.7	138.9	1713.7	1708.1	5.6	0.66	0.56	0.08
CF ₃	10.12	191	138.5	1714.6	1707.1	7.5	0.54	0.421	0.08
NO ₂	10.18	190.3	139.9	1714.4	1710.4	4.4	0.778	0.65	0.15
CH ₃ S		190.8	132.6	1700.2	1691.1	9.1	0		-0.25
Range	9.66-10.18	189.5-192	125.2-139.9	1699.9-1714.6	1682.5-1710.4	4.4-14.4			

TABLE 11.5 Infrared and NMR data for 4-x-acetophenones in CCl₄ and/or CHCl₃ solutions

4-x-Acetophenone X	Chemical shift ¹³ C=O ppm	Chemical shift ¹³ CH ₃ ppm	Chemical shift ¹³ C-1 ppm	Chemical shift ¹³ C-4 ppm	C=O str. CCl ₄ soln. cm ⁻¹	C=O str. CHCl ₃ soln. cm ⁻¹	C=O str. [CCl ₄ -CHCl ₃] cm ⁻¹
Cl	196.1	26.3	135.5	139.2	1705	1694	11
CH ₃	196.9	26.2	134.9	143.5	1701	1690	11
H	197.4	26.3	137.3	133	1709	1692	17
CH ₃ O	196	26	130.5	163.5		1684	
NO ₂	196.3	26.9	141.7	150.4	1710	1700	10
C ₆ H ₅ O	195.8	26.1	132.2	161.7		1686	
Br	196.3	26.3	135.8	128	1705	1695	10
CH ₃ CO	197.3	26.7	140.3	140.3			
C ₆ H ₅	197.5	26.5	136	145.7		1692	
CN	196.6	26.8	140	116.3		1697.5	
OH	196.6	26	129	162.2	1700	1686	14
CF ₃	97	26.8	140.1	134.6		1698	
N(CH ₃) ₂	196.4	26	125.3	153.3		1671	
Range	195.8–197.5	26.0–26.9	125.3–140.3	116.3–163.5		1671–1700	10–17

TABLE 11.6 Vapor-phase IR and NMR CHCl₃ solution-phase data for 4-x and 4,4'-x,x-benzophenones

4-x- or 4,4'-x,x- Benzophenone	Chemical shift ¹³ C=O ppm	Chemical shift ¹³ C-1 ppm	Chemical shift ¹³ C-2 ppm	Chemical shift ¹³ C-3 ppm	Chemical shift ¹³ C-4 ppm	Chemical shift ¹³ C'-1 ppm	Chemical shift ¹³ C'-2 ppm	Chemical shift ¹³ C'-3 ppm	Chemical shift ¹³ C'-4 ppm	C=O str. vapor cm ⁻¹
X										
H	196.1	137.6	129.8	128.2	132.2					1681
OCH ₃	194.6	130.1	132.4	113.6	163.3	138.4	129.6	128.2	131.8	1675
Cl	194.5	135.7	131.5	128.5	138.1	129.6	129.6	128.5	138.1	1682
Br	195.2	136.3	131.5	131.5	127.4	137.2	129.9	128.3	132.6	1682
CH ₃	195.6	135	128.9	130.1	142.9	138	129.7	1282.1	131.9	1680
NO ₂	194.3	142.6	130.5	123.4	136.1	136.1	129.8	128.9	133.3	1687
N(C ₂ H ₅) ₂ ,N(C ₂ H ₅) ₂	193.1	125.8	132.4	110	150.3					
N(CH ₃) ₂ ,N(CH ₃) ₂	192.4	125.6	131.5	110.5	152.5					
OCH ₃ ,OCH ₃	194.3	130.9	132.2	113.5	162.9					
CH ₃ ,OCH ₃	194.6	130.4	129.8	113.5	163					1672
CH ₃ ,CH ₃	195.4	135.4	130.1	128.9	142.6					1675
Cl,Cl										1680
F										1680
OH										1678
Range	193.1–195.6	125.6–142.8	128.8–132.9	110–132.3	127.4–163.3	129.6–138.4	129.6–129.9	128.1–128.9	131.8–138.1	1672–1687

TABLE 11.7 Infrared and NMR data for alkyl 3-x- and 4-x-benzoates

Alkyl 3-x or 4-x Benzoate	Chemical shift $^{13}\text{C}=\text{O}$ ppm	Chemical shift $^{13}\text{C}-1$ ppm	Chemical shift $^{13}\text{C}-2$ ppm	Chemical shift $^{13}\text{C}-3$ ppm	Chemical shift $^{13}\text{C}-4$ ppm	Chemical shift $^{13}\text{C}-5$ ppm	Chemical shift $^{13}\text{C}-6$ ppm	Chemical shift $^{13}\text{CH}_3\text{O}$ ppm	Chemical shift $^{13}\text{CH}_2$ ppm	Chemical shift $^{13}\text{CH}_3$ ppm	C=O str. vapor cm^{-1}
Methyl											
3-x											
NH ₂	167.4	131	115.7	147.1	119.3	129.3	119.3	51.9			1748
Cl	165.5	132.1	129.7	134.5	132.9	129.7	127.7	52.2			
I	165.2	132.1	138.4	93.8	141.6	129.9	128.7	52.2			1750
NO ₂											
4-x											
OH	170.6	113.8	131.3	117.2	167			50.9			1744
I	166	129.5	130.9	137.6	100.6			52			
Ethyl											
3-x											
OH	167.6	131.4	116.5	156.5	120.6	129.6	121.6		61.6	14.1	1741
NH ₂	167.2	131.6	115.7	147.5	119.2	129.2	119.2		61	14.3	
4-x											
OH	167.5	122.3	132	115.4	160.7				61.1	14.3	1738
NH ₂	166.6	117.5	131.5	113.3	153.3				60	14.4	1735
N(CH ₃) ₂	166.9	117.3	131.2	110.7	153.3				60	14.5	
t-C ₄ H ₉	166.2	128.1	129.6	125.2	156.2				60.5	14.4	1740
Br	165.4	129.5	131.1	131.6	127.8				61.1	14.4	1741
NO ₂	165.5	135.1	130.7	123.5	150.6				62	14.3	1749

TABLE 11.8 Summary of IR and NMR data for the C=O group

Compound type	Chemical shift ^{13}C -1 CHCl_3 soln. ppm	Chemical shift $^{13}\text{C}=\text{O}$ CHCl_3 soln. ppm	C=O str. cm^{-1}	Solvent or vapor	Solvent CHCl_3
4-x-Benzaldehyde	125.2–139.9	189.9–192.0	1696.9–1714.6	CCl_4	1682.5–1710.4
4-x-Acetophenone	125.3–140.3	195.8–197.5	1671–1700	CCl_4	
4-x-Acetanilide	129.2–145.5	167.8–169.4	1705–1718	CCl_4	1686–1711
4-x- and 4,4'-x,x'-Benzophenone	125.6–142.8	193.1–195.6	1672–1687	vapor	
3-x and 4-x-Benzoic acid	117.1–133.4	165.9–172.9	1751–1768	vapor	1737–1752
3-x- and 4-x-Methyl benzoate	113.8–132.1	165.2–170.6	1744–1750	vapor	
3-x- and 4-x-Ethyl benzoate	117.3–136.1	164.5–167.6	1735–1749	vapor	

TABLE 11.9 IR and NMR data for the C=O group of acetone in $\text{CHCl}_3/\text{CCl}_4$ solutions

$\text{CHCl}_3/\text{CCl}_4$	IR C=O str. cm^{-1}	NMR $\delta(^{13}\text{C}=\text{O})$ (ppm)
0	1717.5	
1.49	1717.1	202.29
3	1716.7	302.56
10.8	1716.1	
15.4	1715.9	203.27
16.9	1715.3	203.72
23.2	1715.1	203.97
26.7	1714.9	204.16
37.7	1714.2	204.74
42.1	1713.9	
45.9	1713.7	
49.2	1713.4	
52.2	1713.2	
55.7	1713.1	205.55
57.4	1712.9	
57.6	1712.8	
60.2	1712.7	
63.4	1712.6	
66.9	1712.3	
70.8	1712.1	205.96
75.2	1711.9	
80.2	1711.6	
85.8	1711.3	
92.4	1710.9	
100	1710.5	

TABLE 11.10 Infrared and NMR data for N,N'-dimethylacetamide in CHCl₃/CCl₄ solutions

Dimethylacetamide [1 wt./vol. %]	NMR ¹³ C=O ppm	NMR ¹³ CH ₃ , anti ppm	NMR ¹³ CH ₃ , syn ppm	NMR ¹³ CH ₃ ppm	IR C=O str. cm ⁻¹
Mole % CHCl ₃ /CCl ₄					
0	168.4	37.8	35.1	21.3	1660.5
10.74	169.3	37.9	35.2	21.4	1649
19.4	169.6	38	35.2	21.5	1646.7
26.54	169.9	38	35.2	21.5	1645.1
32.5	170	38	35.3	21.5	1645.2
37.58	170.1	38	35.3	21.5	1642
41.94	170.2	38.1	35.3	21.5	1640.8
45.73	170.2	38.1	35.3	21.5	1640.3
49.06	170.3	38.1	35.3	21.5	1639.6
52	170.3	38.1	35.3	21.6	1639.1
54.62	170.4	38.1	35.3	21.6	1638.7
57.21	170.4	38.1	35.3	21.6	1638.5
60.07	170.4	38.1	35.3	21.6	1638.1
63.23	170.5	38.1	35.3	21.6	1637.8
66.74	170.5	38.1	35.3	21.6	1637.3
70.65	170.6	38.1	35.3	21.6	1336.8
75.05	170.6	38.1	35.3	21.6	1636
80.05	170.6	38.1	35.3	21.6	1635.9
85.75	170.7	38.1	35.3	21.6	1635
92.33	170.8	38.1	35.3	21.6	1634.7
100	170.8	38.1	35.3	21.6	1634.2

TABLE 11.11 The NMR and IR data for maleic anhydride 1 wt./vol. % in CHCl₃/CCl₄ solutions

Maleic anhydride [1 wt./vol. %]	Chemical shift ¹³ C=O, ppm	Chemical shift ¹³ C=C, ppm	Out-of-phase (C=O) ₂ str. corrected for Fermi Res.(FR) cm ⁻¹	In-phase C=O) ₂ str. cm ⁻¹	B1 Combination tone corrected for FR cm ⁻¹
Mole % CHCl ₃ /CCl ₄					
0	163.2	136.1	1787.1	1851.7	1786.8
10.74	163.3	136.2	1786.8	1852	1787.6
19.4	163.4	136.2	1786.6	1852	1787
26.54	163.5	136.3	1786.5	1851.97	1788
32.5	163.6	136.3	1786.4	1851.97	1788.2
37.58	163.7	136.3	1786.35	1851.92	1788.3
41.94	163.7	136.3	1786.29	1851.93	1788.4
45.73	163.7	136.4	1786.26	1851.95	1788.5
49.06	163.8	136.4	1786.2	1851.96	1788.53
52	163.8	136.4	1786.16	1851.93	1788.58
54.62	163.8	136.4	1786.16	1851.9	1788.58
57.21	163.8	136.4	1786.14	1851.9	1788.59
60.07	163.8	136.4	1786.11	1851.87	1788.65
63.23	163.9	136.4	1786.09	1851.91	1788.68
66.74	163.9	136.4	1786.04	1851.88	1788.72
70.65	163.9	136.4	1785.64	1851.87	1788.64
75.05	163.9	136.4	1785.81	1851.85	1788.69
80.05	164	136.4	1785.72	1851.78	1788.77
85.75	164	136.5	1785.64	1851.75	1788.86
92.33	164.1	136.5	1785.4	1851.66	1789.09
100	164.1	136.5	1785.36	1851.68	1789.14
δ	0.9 ppm	0.4 ppm	[-1.75 cm ⁻¹]	[0.06 cm ⁻¹]	[2.38 cm ⁻¹]

TABLE 11.12 Infrared and NMR data for 3-x- and 4-x-benzonitriles

3-x or 4-x Benzonitrile	NMR Chemical shift ^{13}C N ppm	NMR Chemical shift ^{13}C -1 ppm	NMR Chemical shift ^{13}C -2 ppm	NMR Chemical shift ^{13}C -3 ppm	NMR Chemical shift ^{13}C -4 ppm	IR CN str. vapor cm^{-1}	IR CN str. neat cm^{-1}	σ m	σ_{R}
								σ m	σ_{R}
NH ₂	119.3	112.7			120.6		2212		
F	117.5	114.3				2241		0.34	-0.16
Br	117.2	114.3			136.1		2215	0.39	-0.06
	116.8	113.6			127.1			0.71	0.08
								σ p	
N(CH ₃) ₂	120.6	96.9	132.2	111.4	152.5			-0.6	-0.59
NH ₂	120.5	99.5	133.8	114.5	151.1			-0.66	-0.52
OH	119.6	101.9	134	116.5	161.4	2238		-0.37	-0.61
OC ₆ H ₄ CN	118.2	108.1	134.5	119.7	159.3			[0.100]*	-0.32
Cl	117.8	111	133.4	129.6	139.3		2220	0.226	-0.18
H	118.8	112.4	132.1	129.2	132.8		2211	0	0
	117.7	117.7	132.9	130	138.9			0.216	0.22
CH ₃ CO	116.3	117.9	132.6	128.8	140	2236		0.502	0.16
NO ₂	116.9	118.4	133.5	124.3	150.2	2240		0.778	0.15
Range	116.3–120.6	99.5–118.4	132.1–134.5	111.4–130	127.1–161.4				

* Estimated.

TABLE 11.13 Infrared, Raman and NMR data for organonitriles

Compound	Empirical structure	Raman data CN str., cm^{-1}	$\delta(^{13}\text{C})$ ppm	IR data[vapor] CN str., cm^{-1}	CN str. [v-neat] cm^{-1}
Acetonitrile	CH ₃ CN	2249	117.7	2280	31
Propionitrile	CH ₃ CH ₂ CN	2242	120.8		
Isobutyronitrile	(CH ₃) ₂ CHCN	2238	123.7	2255	17
Pivalonitrile	(CH ₃) ₃ CCN	2236	125.1		
Chloroacetonitrile	ClCH ₂ CN	2258	115.5		
Trichloroacetonitrile	Cl ₃ CCN	2250	113		
Acrylonitrile	CH ₂ =CHCN	2222	117.5		
Methacrylonitrile	CH ₂ =C(CH ₃)CN	2230	119.3		
Benzonitrile	COH ₅ CN	2230	118.7		
2-Chloroacrylonitrile	CH ₂ -C(Cl)CN	2234	114.5		

TABLE 11.14 A comparison of $\delta(\text{N})$ chemical shift data for primary, secondary and tertiary amines

Amine	$\delta(\text{N})$ ppm	No. protons on the α -carbon atom	C-N str. cm^{-1}	Sum Taft σ^*
Methyl	-377.3	3	1043	0
Ethyl	-355.4	2	1083	-0.1
Isopropyl	-338.1	1	1170	-0.19
Tert-butyl	-324.3	0	1237	-0.3
			wN-H cm^{-1}	
Dimethyl	-369.5	6	715	0
Ethyl methyl	-352	5	[—]	-0.1
Diethyl	-333.7	4	698	-0.2
Diisopropyl	-306.5	2	688	n-0.38
Trimethyl	363.1	9		0
Dimethyl ethyl	-351.3	8		-0.1
Dimethyl isopropyl	-340.5	7		-0.19
Dimethyl tert-butyl	-342.5	6		-0.3

TABLE 11.15 The NMR data for organophosphorus and organonitrogen compounds

Compound	[27,28] Chemical shift ^{31}P ppm	[23] Sum σ^*	[18,25] Chemical shift ^{15}N	Compound
$\text{P}(\text{CH}_3)_3$	-64	0	-366.9	$\text{N}(\text{CH}_3)_3$
$\text{P}(\text{CH}_3)_2(\text{C}_2\text{H}_5)$	-48	-0.1	-355.2	$\text{N}(\text{CH}_3)_2(\text{C}_2\text{H}_5)$
$\text{P}(\text{CH}_3)(\text{C}_2\text{H}_5)_2$	-34	-0.2	-343.1	$\text{N}(\text{CH}_3)(\text{C}_2\text{H}_5)_2$
$\text{P}(\text{C}_2\text{H}_5)_3$	-19.5	-0.3	-333.6	$\text{N}(\text{C}_2\text{H}_5)_3$
$\text{P}(\text{iso-C}_3\text{H}_7)_3$	19.4	-0.57		
$\text{P}(\text{tert-C}_4\text{H}_9)_3$	63	-0.9		
$\text{PH}_2(\text{CH}_3)$	-163.5		-378.7	$\text{NH}_2(\text{CH}_3)$
$\text{PH}_2(\text{C}_2\text{H}_5)$	-128		-355.1	$\text{NH}_2(\text{C}_2\text{H}_5)$
$\text{PH}(\text{CH}_3)_2$	-99		-371	$\text{NH}(\text{CH}_3)_2$
$\text{PH}(\text{CH}_3)(\text{C}_2\text{H}_5)$	-77		-352.8	$\text{NH}(\text{CH}_3)(\text{C}_2\text{H}_5)$
$\text{PH}(\text{C}_2\text{H}_5)_2$	-55		-333	$\text{NH}(\text{C}_2\text{H}_5)_2$

TABLE 11.16 Infrared and NMR data for organophosphorus compounds

Compound	[28] Chemical shift ^{31}P ppm	[31] P=O str. cm^{-1}	Compound	[28] Chemical shift ^{31}P ppm	[31] P=O str. cm^{-1} [CCl ₄]/[CHCl ₃]	Compound	[28] Chemical shift ^{31}P ppm	[31] P=O str. cm^{-1}
(CH ₃) ₃ P=O	36.2		(CH ₃)(Cl) ₂ P=O	44.5	1278.5/1268.9	(Cl) ₃ P	219.5	
(C ₂ H ₅) ₃ P=O	48.3		(C ₂ H ₅)(Cl) ₂ P=O	53		(CH ₃ O)(Cl) ₂ P	180	
(CH ₃) ₂ (tert-C ₄ H ₉)P=O	47.8		(iso-C ₃ H ₇)(Cl) ₂ P=O	60.4		(CH ₃ O) ₂ (Cl)P	169	
(iso-C ₃ H ₇) ₃ P=O	55		(tert-C ₄ H ₉)(Cl) ₂ P=O	65.6	1266.4/1255.7	(C ₂ H ₅ O)(Cl) ₂ P	178	
(CH ₃ O) ₃ P=O	2.4	1291/1272* ¹	(CH ₃)(Cl) ₂ P=S	79.4		(C ₂ H ₅ O) ₂ (Cl)P	165	
(C ₂ H ₅ O) ₃ P=O	-1.5	1280/1263* ¹	(C ₂ H ₅)(Cl) ₂ P=S	95.4		(CH ₃ O) ₃ P	140	
(C ₃ H ₇ O) ₃ P=O	-0.8	1279/1265* ¹	(iso-C ₃ H ₇)(Cl) ₂ P=S	107		(C ₂ H ₅ O) ₃ P	138	
(C ₄ H ₉ O) ₃ P=O	-1	1280/1265* ¹	(CH ₃)(F) ₂ P=O	27.1		(C ₂ H ₅)(Cl) ₂ P	196.3	
(iso-C ₃ H ₇ O) ₃ P=O	-6	1272/1257* ¹	(C ₂ H ₅)(F) ₂ P=O	29.2		(CH ₃)(Cl) ₂ P	192	
(tert-C ₄ H ₉ O) ₃ P=O	-13.3		(iso-C ₃ H ₇)(F) ₂ P=O	29.5		(C ₂ H ₅) ₂ (Cl)P	119	
(C ₂ H ₅ O) ₂ (tert-C ₄ H ₉ O)P=O	-5.5		(tert-C ₄ H ₉)(F) ₂ P=O	31.3		(CH ₃)(C ₂ H ₅) (Cl)P	105.2	
(C ₂ H ₅ O) (tert-C ₄ H ₉ O) ₂ P=O	-9.9					(CH ₃) ₂ (Cl)P	96	
		[P=S str.]	(iso-C ₃ H ₇ O)(Br) (CH ₃)P=S	93.2		(CH ₃)(Br) ₂ P	184	
(CH ₃ O) ₃ P=S	73.4	~605 VP	(iso-C ₃ H ₇ O)(Br) (C ₂ H ₅)P=S	110.2		(C ₂ H ₅) ₂ (Br)P	116.2	
(C ₂ H ₅ O) ₃ P=S	68	613 vp	(iso-C ₃ H ₇ O)(Br) (iso-C ₃ H ₇)P=S	124.1		(CH ₃)(C ₂ H ₅) (Br)P	98.5	
(iso-C ₃ H ₇ O) ₃ P=S	62.5		(iso-C ₃ H ₇ O)(Br) (tert-C ₄ H ₉)P=S	135.6		(CH ₃) ₂ (Br)P	92 or 87	
(tert-C ₄ H ₉ O) ₃ P=S	41.2					(CH ₃ O) ₃ P	140	
(CH ₃ O) ₃ P=Se		[P=Se]				(C ₂ H ₅ O) ₃ P	[137-139]	
(C ₂ H ₅ O) ₃ P=Se	72.1					(iso-C ₃ H ₇ O) ₃ P	137	
(iso-C ₃ H ₇ O) ₃ P=Se	67.9					(tert-C ₄ H ₉ O) ₃ P	138.2	
(tert-C ₄ H ₉ O) ₃ P=Se	31.3							

(continued)

TABLE 11.17 NMR data for 2-x-, 3-x- and 4-x-anisoles in CHCl₃ solutions

Anisole	¹³ C-1 ppm	¹³ C-2 ppm	¹³ C-3 ppm	¹³ C-4 ppm	¹³ C-5 ppm	¹³ C-6 ppm	¹³ CH ₃ O ppm	ES
4-x								
NO ₂	164.9	114.2	125.8	141.7			56.1	
CH ₃ SO ₂	163.7	114.6	129.5	132.4			55.8	
CH ₃ CO	163.5	113.8	130.5	130.5			55.3	
CO ₂ C ₂ H ₅	163.5	113.7	131.6	123.2			55.3	
CN	163	114.9	133.9	103.9			55.5	
H	159.9	114.1	129.5	120.7			54.8	
CH=CH ₂	159.7	114	127.4	130.5			54.9	
C ₆ H ₅	159.3	114.2	128	133.6			55	
CH ₂ OH	159.1	114	128.5	133.6			55.2	
iso-C ₃ H ₇	158.9	114	127	131.2			54.9	
2-ClC ₂ H ₄	158.8	114.1	129.8	130.3			55.1	
Br	158.7	115.7	132.1	112.7			55.1	
2-BrC ₂ H ₄	158.6	113.9	129.5	130.9			54.9	
Cl	158.5	115.3	129.3	125.5			55.3	
CH ₃	157.9	113.9	129.9	129.9			54.9	
C ₂ H ₅	157.9	113.9	128.8	136.4			55.1	
n-C ₃ H ₇	157.9	113.8	129.3	134.7			55	
t-C ₄ H ₉	157.6	113.5	126.1	143.1			54.8	
CH ₃ O	154	114.8	114.8	154			55.6	
C ₆ H ₅ CH ₂ O	154.1	114.7	115.9	153.1			55.5	
NH ₂	152.6	114.9	116.3	140.5			55.6	
C ₆ H ₅ O	156	115	120.7	150.4			55.4	
3-x								
CH ₃ O	161.4	100.8	161.4	106.4	130	106.4	55.1	
OH	160.9	102	157	108.5	130.5	106.9	55.3	
NH ₂	160.8	100.9	148.4	107.9	130.1	103.6	54.8	
Cl	160.6	114.6	135	120.9	130.3	112.6	55.3	
CH ₃	160	115	139.4	121.6	129.3	111.1	54.8	
CH ₃ CO	159.9	112.7	138.7	121	129.6	119.3	55.2	
3-BrC ₃ H ₆	159.8	114.3	142.1	120.8	129.4	111.4	55	
2-x								
CH ₃ CO	159.1	128.3	130.2	120.5	133.7	111.8	55.4	
Br	158.7	115.7	132.1	112.7	132	115.7	55.1	0
I	157.7	86	139.1	122.2	129.3	110.9	56.1	-0.2
Cl	155.1	122.4	130.2	121.2	127.8	112.2	55.8	0.18
NO ₂	153	140	134.4	120.4	125.3	114	56.5	-0.75
CH ₃ O	149.5	149.5	112	121	121	112	55.7	0.99
F	148.1	152.9	116.1	124.5	121.1	113.9	56	0.49
NH ₂	147.4	136.7	114.9	121.2	118.1	110.8	55.3	
OH	147.1	146.1	115	120.3	121.7	114.4	55.9	

TABLE 11.17A Infrared data for 3-x- and 4-x-substituted anisoles

Anisole	Phenyl-O-C asym. str. neat cm ⁻¹	Phenyl-O-C sym. Str. neat cm ⁻¹	Phenyl-O-C asym. str. CS ₂ soln. cm ⁻¹
4-x			
NO ₂	1262	1022	1264
CH ₃ SO ₂	1260	1021	[-]
CH ₃ CO	1249	1021	1261
CO ₂ C ₂ H ₅	1252	1028	1258
CN	1240	1024	1259
H	1248	1042	1246
CHCH ₂	1248	1040	[-]
C ₆ H ₅	1249	1032	[-]
CH ₂ OH	1245	1030	1248
CH ₃ CHCH ₂	1249	1037	[-]
2-ClC ₂ H ₄	1240	1031	[-]
Br	1240	1029	1246
2-C ₂ H ₄	1245	1031	[-]
Cl	1242	1032	1247
CH ₃	1242	1028	1244
C ₂ H ₅	1238	1035	1248
tert-C ₄ H ₉	1244	1038	[-]
CH ₃ O	1246	1029	1243
C ₆ H ₅ CH ₂ O	1230	1033	[-]
NH ₂	1238	1034	1241
C ₆ H ₅ O	1230	1039	[-]
3-x			
CH ₃ O	1211	1052	[-]
OH	1200	1043	[-]
NH ₂	1198	1029	[-]
Cl	1237	1029	[-]
CH ₃	1259	1042	[-]
CH ₃ CO	1270	1040	[-]
3-BrC ₃ H ₆	1250	1034	[-]

TABLE 11.18 Infrared and NMR data for mono-x-benzenes*

x-Benzene x	Chemical shift ^{13}C -1 ppm	Chemical shift ^{13}C -2 ppm	Chemical shift ^{13}C -3 ppm	Chemical shift ^{13}C -4 ppm	σ p	σ_{R}	Mode I cm^{-1}	Mode III cm^{-1}
H	128.5				0	0		
CH ₃	137.8	129.2	128.4	125.5	-0.17	-0.13	973	895
C ₂ H ₅	144.3	128.1	128.6	125.9	-0.15	-0.1	978	903
iso-C ₃ H ₇	148.8	126.6	128.6	126.1	-0.15	-0.1	979	905
tert-C ₄ H ₉	150.9	125.4	128.3	125.7	-0.2	-0.1	979	905
n-C ₄ H ₉	143.3	129	128.2	125.7	-0.15	-0.1		
s-C ₄ H ₉	148.4	127.9	129.3	126.8	-0.15			
iso-C ₄ H ₉	148.8	126.6	128.6	126.1	-0.15			
F	163.6	114.2	129.4	124.1	0.06	-0.31	972	890
Cl	134.9	128.7	129.5	126.5	0.23	-0.18	976	897
Br	122.6	131.5	130	127	0.23	-0.18	980	92
I	96.6	138.4	131.1	128.1	0.18	-0.22		
OH	155.1	115.7	130	121.4	-0.27	-0.4	971	882
OCH ₃	159.9	114.1	129.5	120.7	-0.66	-0.42	970	881
NH ₂	148.7	114.4	129.1	116.3		-0.5	968	874
NHCH ₃	150.4	112.1	129.1	115.9		-0.59	966	867
N(CH ₃) ₂	150.7	112.7	129	116.7		-0.59		
C ₆ H ₅	140.6	126.7	128.4	126.9	-0.01	-0.1		
C ₆ H ₅ O	157.7	119.1	129.9	123.2	0.32	-0.32		
CH ₂ Cl	137.9	128.9	128.8	128.6	0.18	-0.08	981	921
CN	112.8	132.1	129.2	132.8	0.66	0.08	987	920
CF ₃	131.5	125.5	129	132.1	0.54	0.08	984	920
CCl ₃	144.1	125.3	128.1	130.1	0.44		981	921
CO ₂ H	131.4	129.8	128.9	133.1	0.45	0.29	995	919
CO ₂ O ₂ H ₅	131	129.5	128	132.4	0.52	0.16		
COCH ₃	136.3	128.1	128.1	131.3	0.52	0.16	988	922
NO ₂	149.1	124.2	129.8	134.7	0.78	0.15	990	932
CH ₃ SO ₂	145.1	122.6	129.6	130	0.72	0.12	994	928
CH ₃ S	138.6	126.7	128.7	124.9	0	-0.25	976	888
Range	128.5-163.6	112.1-138.4	128.1-131.1	115.9-134.7			965-995	862-932

* See References 4 and 31.

TABLE 11.19 The NMR data for 4-x- and 4,4'-x,x-biphenyls in CHCl₃ solutions

Biphenyl 4-x or 4,4'-x,x	Chemical shift ¹³ C-1 ppm	Chemical shift ¹³ C-2 ppm	Chemical shift ¹³ C-3 ppm	Chemical shift ¹³ C-4 ppm	Chemical shift ¹³ C-1' ppm	Chemical shift ¹³ C-2' ppm	Chemical shift ¹³ C-3' ppm	Chemical shift ¹³ C-4' ppm
F	137.4	127	128.6	162.5	140.2	127	128.8	127.3
OH	131.7	127.8	115.9	157.2	140.7	126.2	128.6	126.2
t-C ₄ H ₉	138.3	125.6	126.9	150.1	150.1	126.9	138.3	126.9
t-C ₄ H ₉ ,t-C ₄ H ₉	138.2	126.6	125.5	149.7				
NH ₂ ,NH ₂	130.1	126.4	114.9	146				
C ₆ H ₅				135.1				
Cl	139.5	128.8	133.3	128.3	139.9	126.8	128.8	127.6
CO ₂ C ₂ H ₅ ,CO ₂ C ₂ H ₅	144.2	127.1	130.1	130.1				
H,H	141.2	127.1	128.7	127.1				
Br	139.9	128.5	131.7	121.5	139.9	126.7	128.7	127.5
CN,CN	143.1	127.9	132.7	111.8				
CN	145.6	129.1	132.5	111	139.1	127.7	128.7	127.2
I	139.8	128.8	137.7	93	140.5	126.7	128.8	127.5

TABLE 11.20 The NMR data for tetramethylurea in CHCl₃/CCl₄ solutions

Tetramethylurea [1 wt./vol. % solns.]	Chemical shift ¹³ C=O, ppm	Chemical shift ¹³ CH ₃ , ppm
Mole % CHCl ₃ /CCl ₄		
0	164.7	38.8
10.74	165.1	38.8
19.4	165.3	38.8
26.53	165.4	38.8
30.5	165.5	38.8
37.57	165.5	38.8
41.93	165.6	38.7
45.73	165.6	38.7
49.06	165.6	38.7
52	165.6	38.7
54.62	165.6	38.7
57.22	165.7	38.7
60.07	165.7	38.7
63.28	165.7	38.7
66.74	165.7	38.7
70.65	165.7	38.7
75.06	165.7	38.7
80.05	165.7	38.7
85.85	165.8	38.7
92.33	165.8	38.6
100	165.8	38.6
δ ppm	1.1	-0.2

TABLE 11.21 The NMR data for tetramethylurea 1 wt./vol. % in various solvents

Tetramethylurea [1 wt./vol. %]	Chemical shift $^{13}\text{C}=\text{O}$ ppm	Chemical shift $^{13}\text{CH}_3$ ppm	$^{13}\text{C}=\text{O}$ in acetic acid]- [$^{13}\text{C}=\text{O}$ in solvent] δ ppm	AN
Solvents				
Acetic acid	166.9	38.5	0	52.9
Water	166.7	38.1	0.2	54.8
Nitromethane	166.7	38.8	0.2	
Methyl alcohol	166.8	38.2	0.1	41.3
Ethyl alcohol	166.4	38.4	0.5	37.1
Isopropyl alcohol	166.1	38.7	0.8	33.5
t-Butyl alcohol	166	38.5	0.9	29.1
Chloroform	165.8	38.6	1.1	23.1
Methylene chloride	165.4	38.3	1.5	20.4
Dimethyl sulfoxide	165.6	38.3	1.3	19.3
Acetonitrile	166.1	38.7	0.8	18.9
Benzonitrile	165.2	38.4	1.7	15.5
Nitrobenzene	165.1	38.2	1.8	14.8
Acetone	166	38.9	0.9	12.5
Carbon disulfide	164.3	39	2.6	
Carbon tetrachloride	164.7	38.8	2.2	8.6
Benzene	165.1	38.1	1.8	8.2
Methyl t-butyl ether	165.1	38.5	1.8	5
Tetrahydrofuran	165	38.1	1.9	8.8
Diethyl ether	165.5	38.5	1.4	3.9
Hexane	165.3	38.5	1.6	0

TABLE 11.22 The NMR data for dialkylketones in various solvents at 1 wt./vol. % concentration

Solvent [1 wt./vol. %]	DMK $^{13}\text{C}=\text{O}$ ppm	MEK $^{13}\text{C}=\text{O}$ ppm	DEK $^{13}\text{C}=\text{O}$ ppm	EIK $^{13}\text{C}=\text{O}$ ppm	DIK $^{13}\text{C}=\text{O}$ ppm	DTBK $^{13}\text{C}=\text{O}$ ppm	AN
Methyl alcohol	209.4	211.9	214.3	217.5	220.7	220.3	41.3
Ethyl alcohol	208	210.5	212.9	216.1	219.3	219	37.1
Isopropyl alcohol	207.4	209.9	212.4	215.7	218.8	218.6	33.5
Dimethyl sulfoxide	207.5	209.8	212.3	215.3	218.4	218.5	19.3
Chloroform	207.1	209.8	212.4	215.6	218.9	219.1	23.1
t-Butyl alcohol	206.2	209.6	212.2	215.3	218.5	218.6	29.1
Nitromethane	208.8	211.3	213.8	216.9	220.1	220.1	
Methylene chloride	206.3	209.4	211.7	214.8	218.2	218.3	20.4
Benzonitrile	205.7	208.2	212	214	217.3	217.6	15.5
Nitrobenzene	205.3	208.2	210.8	214	217.2	217.5	14.8
Acetonitrile	207.1	209.8	212.5	215.7	218.9	219	18.9
benzene	205	206.5	209	212.2	215.7	216.2	8.2
Carbon disulfide	201.9	204.7	207.7	211	214.4	215.1	
Carbon tetrachloride	202.1	205.2	208	211.3	214.7	215.3	8.6
Diethyl ether	202.7	205.5	208.4	211.8	215.2	215.9	3.9
Hexane	200.5	204.4	207	210.3	214.1	214.9	0

TABLE 11.23 The NMR data for alkyl acetates and phenyl acetate 1 wt./vol. % in various solvents

Solvent [1 wt./vol. %]	Methyl acetate $^{13}\text{C}=\text{O}$ ppm	Ethyl acetate $^{13}\text{C}=\text{O}$ ppm	Isopropyl acetate $^{13}\text{C}=\text{O}$ ppm	t-Butyl acetate $^{13}\text{C}=\text{O}$ ppm	Phenyl acetate $^{13}\text{C}=\text{O}$ ppm
Methyl alcohol	172.7	172.3	171.9	171.9	170.5
Ethyl alcohol	171.3	171.5	171.1	171.1	169.7
Isopropyl alcohol	171.7	171.5	170.9	170.9	169.4
t-Butyl alcohol	171.7	171.3	170.9	170.9	169.4
Chloroform	171.6	171.1	170.7	170.5	169.6
Dimethyl sulfoxide	171.8	171.3	170.8	170.7	170.2
Nitromethane	172.9	172.3	170.8	171.8	171.3
Methylene chloride	171.2	170.7	170.3	170.2	169.4
Acetonitrile	172	171.5	171	171.3	170.4
Nitrobenzene	170.9	170.5	170	170	169.2
Benzonitrile	170.8	170.4	170	170	169.2
Carbon disulfide	169.3	169.1	168.5	168.5	167.2
Benzene	170.1	170.1	169.8	169.7	168
Carbon tetrachloride	169.4	169	168.6	168.6	167.2
Diethyl ether	170.1	169.6	169.2	169.3	168.1
Methyl t-butyl ether	169.9	169.5	169.9	169	167.8
Hexane	169	168.6	168.2	168.3	167.4

TABLE 11.24 Infrared and NMR data for alkyl acrylates and alkyl methacrylates

Chemical shift	Alkyl acrylates CCl_4 soln.	Alkyl acrylates CHCl_3 soln.	Alkyl methacrylate CCl_4 soln.	Alkyl methacrylate CHCl_3 soln.
δ $^{13}\text{C}=\text{O}$, ppm	164.2–165.2	165.7–166.7	165.6–166.7	167.1–167.8
δ $^{13}\text{CH}=\text{C}$, ppm	128.8–130.1	128.1–130.8		
δ $^{13}\text{CCH}_2=\text{C}$, ppm	129.6–130.7	130.4–131.4	136.2–136.9	135.9–136.8
δ $^{13}\text{CC}=\text{C}$, ppm			123.5–125.5	125.2–126.3
δ $^{13}\text{CCH}_3=\text{C}$, ppm			18.6–18.7	18.3–18.3
Group frequency				
$\text{C}=\text{O}$ str., cm^{-1}	1722.9–1734.1	1713.8–1724.5	1719.5–1726.0	1709–1718.0
$\text{C}=\text{C}$ str., s-trans, cm^{-1}	1635.3–1637.0	1635.3–1637.9		
$\text{C}=\text{C}$ str., s-cis, cm^{-1}	1619.2–1620.4	1618.5–1619.9		
$\text{C}=\text{C}$ str., cm^{-1}			1637.3–1638.0	1635.7–1637.3

List of Tables

CHAPTER 1

1.1	Vibrational assignments for ethylene oxide	15
1.2	Characteristic epoxy ring modes	16
1.2a	Vibrational assignments for 1-halo-1,2- epoxypropanes (or epihalohydrins)	17
1.2b	A comparison of IR data for epoxy ring modes and CH ₃ , (CH ₃) ₂ and (CH ₃) ₃ bending modes	18
1.3	Vibrational assignments for the CH ₂ X groups for 3-halo-1,2-epoxypropanes, 3-halopropynes, 3-halopropenes, and PCH ₂ X-containing compounds	19
1.4	Vapor-phase IR data for the oxirane ring vibrations of 1,2-epoxyalkenes	20
1.5	Correlations for the ring stretching vibrations for cyclic ethers	21
1.6	Infrared data for ethers	22
1.7	Infrared data for the a and s Aryl-O-R stretching vibrations for 3-X- and 4-X-anisoles in CS ₂ solution, vapor, and in the neat phase	23
1.8	Raman data and assignments for vinyl ethers	24
1.9	Vapor-phase IR data and assignments for the alkyl group of vinyl alkyl ethers	25

CHAPTER 2

2.1	Infrared data for nitriles and cyanogen halides in the vapor, neat or CCl ₄ solution phase	39
2.2	Infrared data for acetonitrile in various solvents	40
2.3	A comparison of the IR ν CN stretching frequencies for acetonitrile (corrected for Fermi resonance) with those for benzonitrile	40
2.4	The CN stretching frequency for 4-cyanobenzaldehyde in 0 to 100 mol % CHCl ₃ /CCl ₄ solutions (1% wt./vol. solutions)	41
2.5	Raman data for the C=N and C=C groups for some organonitriles in the neat phase	42
2.6	A comparison of infrared data for organonitriles vs organoisonitriles	42

- 2.7 A comparison of the infrared data for organothiocyanates in the vapor and neat phases 43

CHAPTER 3

- 3.1 Infrared and Raman data and assignments for the $(C=N-)_2$ antisymmetric and symmetric stretching vibrations for azines 57
- 3.2 The symmetric and/or asymmetric $N=C=O$ stretching frequencies for alkyl and aryl isocyanates in various physical phases 58
- 3.3 Infrared data for alkyl isocyanates in 0 to 100 mol % $CHCl_3/CCL_4$ in 0.5% wt./vol. solutions 59
- 3.4 Infrared data for the antisymmetrical $N=C=O$ stretching frequency and two combination tones for alkyl isocyanates in $CHCl_3$ and CCL_4 solutions 60
- 3.5 Infrared and Raman data for alkyl isocyanates 60
- 3.6 Infrared data for 1% wt./vol. alkyl isothiocyanates in 0 to 100 mol % $CHCl_3/CCL_4$ solutions [the ν asym. $N=C=S$ and the first overtone of ν $C-N$ frequencies are in Fermi resonance] 61
- 3.6a Vibrational data for organoisoisothiocyanates 62
- 3.7 Infrared vapor- and neat-phase data for dialkyl and diaryl carbodiimides 63

CHAPTER 4

- 4.1 Infrared and Raman data for alkanethiols and benzenethiols 74
- 4.1a Raman data for organic thiols 75
- 4.2 Vapor-phase infrared data for alkanethiols, alkane sulfides, and alkane disulfides 76
- 4.3 Infrared and Raman data for organic sulfides and disulfides 78
- 4.4 Vibrational assignments for 4-benzenethiol and 1,4-dichlorobenzene 79
- 4.5 The $P=S$, $P-S$, and $S-H$ stretching frequencies for O,O-dialkyl phosphorodithioate and O,O-bis-(aryl) phosphorodithioate 80
- 4.6 A comparison of alkyl group joined to sulfur, oxygen, or halogen 81

CHAPTER 5

- 5.1a A comparison of the $S=O$ stretching frequency for $S=O$ containing compounds 104
- 5.1b A comparison of asym. SO_2 and sym. SO_2 stretching frequencies in different physical phases, and asym. $N=S=O$ and sym. $N=S=O$ frequencies in CS_2 solution 105
- 5.1c Vapor-phase infrared data for dimethyl sulfoxide and dialkyl sulfones 107
- 5.1d Vapor- and solid-phase infrared data for dimethyl sulfoxide and dialkyl sulfones 108
- 5.2 Vapor- and solid-phase infrared data for diaryl sulfones 109
- 5.3 Infrared data for phenoxarsine derivatives containing the $AsS(SO_2)R$ and $AsO(SO_2)R$ groups in CS_2 solution 109

5.4	Infrared data for the SO ₂ stretching vibrations for compounds in CHCl ₃ and CCl ₄ solutions	110
5.5	Infrared data for dialkyl sulfites	111
5.6	Infrared data for primary sulfonamides in the vapor phase	111
5.6a	Infrared data for some NH and NH ₂ vibrations for compounds containing SO ₂ NH and SO ₂ NH ₂ groups in different physical phases	112
5.7	Infrared data for secondary and tertiary sulfonamides	112
5.8	Infrared data for organic sulfonates	113
5.9	Infrared data for organosulfonyl chlorides	114
5.9a	Infrared data for organosulfonyl fluorides	115
5.10	Infrared data for organosulfur compounds containing SO ₄ , SO ₃ , SO ₂ N, and SO ₂ X groups in different physical phases	116
5.11	Infrared data for sulfones and sulfoxides in different physical phases	117
5.12	Infrared data for N-sulfinyl-4-X-anilines and N,N'-disulfinyl- <i>p</i> -phenylenediamine	117

CHAPTER 6

6.1	Infrared and Raman data for the methylene halides	164
6.2	Raman and infrared data for trihalomethane and tetrahalomethane	164
6.2a	A comparison of CX, CX ₂ , CX ₃ and CX ₄ stretching frequencies	165
6.3	Vapor- and liquid-phase infrared data for 1- haloalkanes	166
6.4	Vapor- and liquid-phase infrared data for 2- halobutane and tert-butyl halide	167
6.5	Vapor and liquid-phase infrared and Raman liquid- phase data for 1-cyclohexanes	168
6.6	Vapor- and liquid-phase infrared data for primary, primary dialkanes	169
6.7	Raman data for methyl halides and IR and Raman data for tetrabromoalkanes	170
6.8	Carbon halogen stretching frequencies for ethylene propyne, 1,2-epoxypropane, and propadiene derivatives	171

CHAPTER 7

7.1	The ν asym. NO ₂ and ν sym. NO ₂ frequency shifts of substituted nitro compounds from those for nitromethane in the liquid phase	206
7.1a	Vapor-phase infrared data for nitroalkanes	207
7.2	Vapor-phase infrared data for nitroalkanes	208
7.3	Vapor- and liquid-phase infrared data for nitroalkanes	209
7.4	Vapor-phase infrared data for 4-X- nitrobenzenes	209
7.5	Infrared data for 4-X-nitrobenzenes in different phases	210
7.6	A comparison of the frequency differences between ν asym. NO ₂ and ν sym. NO ₂ in the vapor and CHCl ₃ solution and in the vapor and neat or solid phases	211
7.7	Infrared data for the ν asym. NO ₂ and ν sym. NO ₂ frequencies for 3-X and 4-X-nitrobenzenes in CCl ₄ and CHCl ₃ solutions	212
7.8	Infrared data for the ν asym. NO ₂ and ν sym. NO ₂ frequencies for 4-X-nitrobenzenes in the vapor, CCl ₄ , and CHCl ₃ solution phases	213

7.9	Infrared data for ν asym. NO_2 and ν sym. NO_2 frequencies of 4-nitrobenzaldehyde 1% wt./vol. in 0 to 100 mol % $\text{CHCl}_3/\text{CCl}_4$ solutions	214
7.10	A comparison of infrared data for nitromethane vs nitrobenzene in various solvents	215
7.11	Vapor-phase infrared data for 3-X-nitrobenzenes	216
7.12	Infrared data for 3-X-nitrobenzenes in different phases	216
7.13	A comparison of the frequency difference between ν asym. NO_2 and ν sym. NO_2 for 3-X-nitrobenzenes in the vapor and CHCl_3 solution and in the vapor, and solid or neat phases	217
7.14	Vapor-phase infrared data for 2-X-nitrobenzenes	218
7.15	Infrared data for 2-X-nitrobenzenes in different phases	218
7.16	A comparison of the frequency differences between ν asym. NO_2 and ν sym. NO_2 2-X-nitrobenzenes in the vapor and CHCl_3 solution and in the vapor, neat or solid phases	219
7.17	Infrared data for nitrobenzenes in the solid and CCl_4 solution phases	220
7.18	Vapor-phase infrared data for 2,5- and 2,6-X,Y-nitrobenzenes	221
7.19	A comparison of the frequency difference between ν asym. NO_2 and ν sym. NO_2 in the vapor, neat or solid phases	221
7.20	Vapor-phase infrared data for tri-X,Y,Z, WXWZ-tetra, and VWXYZ-penta-substituted nitrobenzenes	222
7.21	Infrared data for 4-X-nitrobenzenes in CCl_4 and CHCl_3 solutions (1% wt./vol. or less)	223
7.22	Infrared data and assignments for alkyl nitrates	224
7.23	Infrared data for alkyl nitrates in various phases	224
7.24	Infrared data for ethyl nitrate, nitroalkanes, and nitrobenzenes in CCl_4 and CHCl_3 solutions	225
7.25	Vapor-phase infrared data for alkyl nitrites	226
7.26	Vapor-phase infrared data of the characteristic vibrations of alkyl nitrites*	226
7.27	Raman data for organonitro compounds	227
7.28	Infrared and Raman data for nitroalkanes in different physical phases	227
7.29	Infrared and Raman data for nitrobenzenes in different physical phases	228
7.30	A comparison of the frequency separation between ν asym. NO_2 and ν sym. NO_2 [vapor-phase data minus CHCl_3 solution data] and [vapor-phase data minus neat-phase data] for nitrobenzenes	229
7.31	Infrared data for organonitro compounds in different physical phases	229
7.32	Infrared and Raman data for organonitrates, organonitrites, and organonitrosamines in different physical phases	230
7.33	The ν N=O frequency for nitrosamines in different physical phases	230

CHAPTER 8

8.1	Phosphorus halogen stretching frequencies for inorganic compounds	318
8.2	The PX_3 bending frequencies for compounds of forms PX_3 , PXY_2 , and XYZ	319
8.3	Vibrational data and assignments for PX_3 , P(=O)X_3 , and P(=S)X_3	320

8.4	The asym. and sym. PCl_2 stretching frequencies for XPCl_2 , XP(=O)Cl_2 , and XP(=S)Cl_2 groups	321
8.5	Vibrational assignments for $\text{F}_2\text{P(=S)Cl}$, $(\text{CH}_3\text{-O-})_2\text{P(=S)Cl}$, and $(\text{CD}_3\text{-O-})_2\text{P(=S)Cl}$	322
8.5a	The PCl_2 stretching frequencies for methyl phosphorodichloridate and O-methyl phosphorodichloridothioate	323
8.6	P-Cl stretching frequencies	323
8.7	Vibrational assignments for the CH_3 , CD_3 , C_2H_5 , CH_3CD_2 and CD_3CH_2 groups of R-O-R(=O)Cl_2 and R-O-P(=S)Cl_2 analogs	324
8.8	The P=O stretching frequencies for inorganic and organic phosphorus compounds	325
8.8a	A comparison of P=O stretching frequencies in different physical phases	326
8.9	Infrared data for the rotational conformer PO stretching frequencies of O,O-dimethyl O-(2-chloro-4-X-phenyl) phosphate	326
8.10	IR observed and calculated PO stretching compared*	327
8.11	The PO and PS stretching frequencies for phenoxarsine derivatives	327
8.12	The PO and PS stretching frequencies for P(O)X_3 - and P(S)X_3 -type compounds	328
8.13	The PS stretching frequencies for inorganic and organic phosphorus compounds	329
8.14	Vibrational assignments for the skeletal modes of S-methyl phosphorothiodichloridate, and P(O)Cl_3	331
8.15	Assignments of the P(C-O-)_3 skeletal vibrations for trimethyl phosphite and trimethyl phosphate	331
8.16	Vibrational assignments for the CH_3 groups of trimethyl phosphite	332
8.17	The PS , P-S and S-H stretching frequencies for O,O-dialkyl phosphorodithioate and O,O-diaryl phosphorodithioate	332
8.18	The PO , PH stretching, and PH bending vibrations for O,O-dialkyl hydrogenphosphonates*	333
8.19	The "C-O" and "P-O" stretching frequencies for the C-O-P group	334
8.20	The "C-O" and "P-O" stretching frequencies for compounds containing C-O-PO, C-O-PS, and C-O-PSe groups	336
8.21	The aryl-O stretching frequencies for O-methyl O-(X-phenyl) N-methylphosphoramidate	338
8.22	The C-P stretching frequencies for organophosphorus compounds	338
8.23	The trans and/or cis N-H stretching frequencies for compounds containing the P-NH-R group	339
8.24	The NH_2 , NHD , ND_2 , NH , and ND frequencies for O,O-dimethyl phosphoramidothioate and O,O-diethyl phosphoramidothioate, and N-methyl O, O-phosphoramidothioate.	340
8.25	The N-H and N-D stretching frequencies for O-methyl O-(2,4,5-trichlorophenyl) N-alkylphosphoramidate and the N-alkyl phosphoramidothioate analogs	341
8.26	The cis and trans NH stretching frequencies for compounds containing OP-NH-R or SP-NH-R groups*	342
8.27	Vibrational assignments for N-alkyl phosphoramidodichloridothioate and the CD_3NH , CD_3ND and CH_3ND analogs	343

8.28	Vibrational assignments for O,O- dimethyl O-(2,4,5-trichlorophenyl) phosphorothioate and its PO and (CD ₃ -O) ₂ analogs	344
8.29	Vibrational assignments for 1- fluoro-2,4,5-trichlorobenzene and the ring modes for O,O-dimethyl O-(2,4,5-trichlorophenyl) phosphorothioate and its PO and (CD ₃ -O-) ₂ analogs	345
8.30	Infrared data for O,O-dialkyl phosphorochloridothioate and O,O,O-trialkyl phosphorothioate in different physical phases	346
8.31	Infrared data for organophosphates and organohydrogenphosphorates in different physical phases	347
8.32	Infrared data for O-alkyl phosphorodichloridothioates and S-alkyl phosphorodichloridothioates in different physical phases	348
8.33	Infrared data for O,O-diethyl N- alkylphosphoramidates in different physical phases	349
8.34	Vibrational assignments for [CH ₃ -PO ₃] ²⁻ , [CD ₃ -PO ₃] ²⁻ , [HPO ₃] ²⁻ , and [PO ₄] ³⁻	349
8.35	Infrared data and assignments for the (CH ₃) ₂ PO ₂ ⁻ anion	350

CHAPTER 9

9.1	Vibrational data for chlorobenzene vs chlorinated biphenyls	403
9.2	Vibrational data for 1,2-dichlorobenzene vs chlorinated biphenyls	404
9.3	Vibrational data for 1,3-dichlorobenzene vs 2,3,3',5,6-pentachlorobiphenyl	405
9.4	Vibrational data for 1,4-dichlorobenzene vs chlorinated biphenyls	406
9.5	Vibrational data for 1,3,5-trichlorobenzene vs chlorinated biphenyls	407
9.6	Vibrational data for 1,2,3-trichlorobenzene vs 2,2',3-trichlorobiphenyl, 2,2',3',4,5-pentachlorobiphenyl, and 2,2',4,6,'-pentachlorobiphenyl	408
9.7	Vibrational data for 1,2,4-trichlorobenzene vs chlorinated biphenyls	409
9.8	Vibrational data for 1,2,4,5-tetrachlorobenzene vs chlorinated biphenyls	411
9.9	Vibrational data for 1,2,3,5-tetrachlorobenzene vs chlorinated biphenyls	413
9.10	Infrared data for 1,2,3,4-tetrachlorobenzene vs chlorinated biphenyls	414
9.11	Vibrational data for pentachlorobenzene vs 2,2',3,4,6-pentachloro-biphenyl, and 2,3,4,4',6-pentachlorobiphenyl	415
9.12	Vibrational data for 1,2,3,4,5,6-hexachlorobenzene vs 1,2,3,4,5-pentachloro-biphenyl	416
9.13	Raman data for monosubstituted benzenes	417
9.14	Infrared and Raman data for an A ₁ fundamental for mono-x-benzenes	418
9.15	Vibrational assignments for bromodichlorobenzenes	418
9.16	Raman data and assignments for some in-plane ring modes of 1,2-disubstituted benzenes	419
9.17	Raman data and assignments for some in-plane ring modes for 1,3-disubstituted benzenes	419
9.18	Raman data and assignments for some in-plane ring modes for 1,4-disubstituted benzenes	420

Factors Affecting Molecular Vibrations and Chemical Shifts	587
9.19 Raman data and tentative assignments for decabromobiphenyl and bis-(pentabromophenyl) ether	420
9.20 Vibrational assignments for benzene, benzene-d ₆ , benzyl alcohol, benzyl-2,3,4,5,6-d ₅ alcohol, pyridene, and pyridene-d ₅	421
9.21 Infrared data for the out-of-plane deformations for mono-x-benzenes	422
9.22 Summary of the out-of-plane hydrogen deformations for substituted benzenes, and the out-of-plane ring deformation for mono-substituted benzenes	422
9.23 Combination and overtones of the out-of-plane hydrogen deformations for substituted benzenes	423
9.24 Hexachlorobenzene vs 2,3,4,5,6-pentachlorobiphenyl	423
 CHAPTER 10	
10.1 Aliphatic hydrocarbons—the Nyquist Rule	432
10.2 Anilines—the Nyquist Rule	433
10.3 Anhydrides, imides, and 1,4- benzoquinones—the Nyquist Rule	434
10.4 Substituted hydantoin— the Nyquist Rule	435
10.5 1,4-Diphenylbutadiyne and 1-halopropadiene—the Nyquist Rule	435
10.6 3-Nitrobenzenes and 4-nitrobenzenes—the Nyquist Rule	436
10.7 Organic sulfate, sulfonate, sulfonyl chloride, and sulfones—the Nyquist Rule	437
 CHAPTER 11	
11.1 NMR ¹³ C solution- phase chemical shift data for 4-x-anilines	560
11.2 Infrared and NMR data for 3-x- and 4-x-benzoic acids	561
11.3 Infrared and NMR data for 4-x- acetanilides in solution	562
11.4 Infrared and NMR data for 4-x- benzaldehydes in CCl ₄ and/or CHCl ₃ solutions	563
11.5 Infrared and NMR data for 4-x- acetophenones in CCl ₄ and/or CHCl ₃ solutions	564
11.6 Vapor-phase IR and NMR CHCl ₃ solution-phase data for 4-x- and 4,4'-x,x-benzophenones	565
11.7 Infrared and NMR data for methyl and ethyl 3-x- and 4-x-benzoates	566
11.8 Summary of IR and NMR data for the CO group	567
11.9 Infrared and NMR data for acetone in CHCl ₃ /CCl ₄ solutions	567
11.10 Infrared and NMR data for N,N'-dimethylacetamide in CHCl ₃ /CCl ₄ solutions	568
11.11 Infrared and NMR data for 1 wt./vol. % maleic anhydride in CHCl ₃ /CCl ₄ solutions	569
11.12 Infrared and NMR data for 3-x- and 4-x-benzonitriles	570
11.13 Infrared, Raman, and NMR data for organonitriles	570
11.14 A comparison of $\delta^{15}\text{N}$ chemical shift data for primary, secondary and tertiary amines	571
11.15 The NMR data for organophosphorus and organonitrogen compounds	571

11.16	Infrared and NMR data for organophosphorus compounds	572
11.17	The NMR data for 2-x, 3-x, and 4-x-anisoles in CHCl_3 solutions	574
11.17a	Infrared data for 3-x- and 4-x-substituted anisoles	575
11.18	Infrared and NMR data for mono-x-benzenes	576
11.19	The NMR data for 4-x- and 4,4'-x,x'-biphenyls in CHCl_3 solutions	577
11.20	The NMR data for TMU in $\text{CHCl}_3/\text{CCl}_4$ solutions	577
11.21	The NMR data for TMU in various solvents	578
11.22	The NMR data for dialkylketones in various solvents at 1 wt./vol. % concentration	578
11.23	The NMR data for alkyl acetates and phenyl acetate in 1 wt./vol. % in various solvents	579
11.24	Infrared and NMR data for alkyl acrylates and alkyl methacrylates in CCl_4 and CHCl_3 solutions	579

List of Figures

CHAPTER 1

1.1	Vapor-phase IR spectrum of ethylene oxide.	8
1.2	Vapor-phase IR spectrum of propylene oxide.	9
1.3	A plot of the epoxy ring breathing mode frequency for styrene oxide vs the mole % CDCl ₃ /CCl ₄ (4).	10
1.4	A plot of the symmetric ring deformation frequency for styrene oxide vs mole % CDCl ₃ /CCl ₄ (4).	10
1.5	A plot of the antisymmetric ring deformation frequency for styrene oxide vs mole % CDCl ₃ /CCl ₄ (4).	11
1.6	Vapor-phase IR spectrum of trans-2,3-epoxybutane (or trans-1,2-dimethyl ethylene oxide).	12
1.7	A plot of the absorbance (A) for the oxirane ring breathing mode divided by (A) for the oxirane antisymmetric CH ₂ stretching mode vs the number of carbon atoms for the 1,2-epoxyalkanes (ethylene oxide is the exception).	13
1.8	A plot of (A) for oxirane antisymmetric CH ₂ stretching divided by (A) for antisymmetric CH ₂ stretching for the alkyl group vs the number of carbon atoms in the 1,2-epoxyalkanes.	13
1.9	Vapor-phase IR spectrum of tetrahydrofuran.	14

CHAPTER 2

2.1	A plot of $\nu_{\text{C}\equiv\text{N}}$ for alkanonitriles vs the number of protons on the α -carbon atom.	32
2.2	A plot of unperturbed $\nu_{\text{C}\equiv\text{N}}$, cm^{-1} (1% wt./vol.) vs AN (The solvent acceptor number).	32
2.3	Plots of $\nu_{\text{C}\equiv\text{N}}$, cm^{-1} for acetonitrile (1 wt./vol.%) vs ($\nu_{\text{C}\equiv\text{N}}$ in methyl alcohol minus ($\nu_{\text{C}\equiv\text{N}}$ in another solvent). The two plots represent perturbed and unperturbed $\nu_{\text{C}\equiv\text{N}}$.	33
2.4	A plot of $\nu_{\text{C}\equiv\text{N}}$ for 1 wt./vol. % vs $\nu_{\text{C}\equiv\text{N}}$ for 1% wt./vol. in 15 different solvents.	34
2.5	A plot of unperturbed $\nu_{\text{C}\equiv\text{N}}$ for acetonitrile vs $\nu_{\text{C}\equiv\text{N}}$ for benzonitrile. Both compounds were recorded at 1% wt./vol. separately in each of the 15 solvents.	35

- 2.6 A plot of $\nu\text{C}\equiv\text{N}$ for 4-cyanobenzaldehyde in cm^{-1} vs mole % $\text{CHCl}_3/\text{CCl}_4$. 36
- 2.7 A plot of the number of protons on the alkyl $\alpha\text{-C-N}\equiv$ atom vs $\nu\text{N}\equiv\text{C}$ for alkyl isonitriles. 37
- 2.8 A plot of Taft's σ^* vs $\nu\text{N}\equiv\text{C}$ for alkyl isonitriles. 38

CHAPTER 3

- 3.1 Plots of ν asym. $\text{N}=\text{C}=\text{O}$ and the combination tone $\nu(\text{C}_\alpha\text{-N}) + \nu$ sym. $\text{N}=\text{C}=\text{O}$ and $\nu(\text{C}_\alpha\text{-N}) + \delta$ sym. CH_3 for methyl isocyanate all corrected for Fermi resonance. 51
- 3.2 Plots of the three observed IR bands for methyl isocyanate occurring in the region 2250–2320 vs mole % $\text{CHCl}_3/\text{CCl}_4$. 51
- 3.3 Plots of the ν asym. $\text{N}=\text{C}=\text{O}$ frequencies for n-butyl, isopropyl and tert-butyl isocyanate and of the frequencies of the most intense IR band for ν asym. $\text{N}=\text{C}=\text{O}$ in FR (uncorrected for FR) for methyl, ethyl and n-propyl isocyanate vs mole% $\text{CHCl}_3/\text{CCl}_4$. 52
- 3.4 Plots of unperturbed ν asym. $\text{N}=\text{C}=\text{O}$ for the alkyl isocyanates vs mole % $\text{CHCl}_3/\text{CCl}_4$. 52
- 3.5 Plots of ν asym $\text{N}=\text{C}=\text{O}$ frequencies for alkyl isocyanates in CCl_4 solution and in CHCl_3 solution vs σ^* (The inductive release value of the alkyl group.) 53
- 3.6 Plots of ν asym. $\text{N}=\text{C}=\text{O}$ frequencies for alkyl isocyanates in CCl_4 solution and in CHCl_3 solution vs E_s (The stearic parameter of the alkyl group.) 53
- 3.7 Plots of ν asym. $\text{N}=\text{C}=\text{O}$ frequencies for alkyl isocyanates in CCl_4 solution and in CHCl_3 solution vs (E_s) (σ^*). 54
- 3.8 A plot of perturbed ν asym. $\text{N}=\text{C}=\text{S}$ (not corrected for FR) for five alkyl isothiocyanates vs mole % $\text{CHCl}_3/\text{CCl}_4$. 54
- 3.9 A plot of unperturbed ν asym. $\text{N}=\text{C}=\text{S}$ (corrected for FR) for four alkyl isothiocyanates vs mole % $\text{CHCl}_3/\text{CCl}_4$ and $\text{CDCl}_3/\text{CCl}_4$. 55
- 3.10 A plot of perturbed 2ν C-N and perturbed ν asym. $\text{N}=\text{C}=\text{S}$ and unperturbed 2ν C-N and unperturbed ν asym, $\text{N}=\text{C}=\text{S}$ vs mole % $\text{CHCl}_3/\text{CCl}_4$. 56
- 3.11 A plot of ν C-N for methyl isothiocyanate vs mole % $\text{CHCl}_3/\text{CCl}_4$. 56

CHAPTER 4

- 4.1 Infrared spectra of O,O-bis-(2,4,5-trichlorophenyl) phosphorodithioate in 5 wt./vol. in CS_2 solution ($2700\text{--}2400\text{ cm}^{-1}$) at temperatures ranging from 29 to -100°C . 71
- 4.2 Top: Liquid-phase IR spectrum of methyl (methylthio) mercury between KBr plates in the region $3800\text{--}450\text{ cm}^{-1}$. Bottom: Liquid-phase IR spectrum of methyl (methylthio) mercury between polyethylene plates in the region $600\text{--}45\text{ cm}^{-1}$. The IR band near 72 cm^{-1} is due to absorbance from poly (ethylene). 72
- 4.3 Top: Raman liquid-phase spectrum of methyl (methylthio) mercury in a glass capillary tube. The sample was positioned perpendicularly to both the laser beam

and the optical axis of the spectrometer. Bottom: Same as top except that the plane of polarization of the incident beam was rotated 90° . 73

CHAPTER 5

- 5.1 Plots of ν S=O and the mean average of (ν asym. SO₂ + ν sym. SO₂) vapor-phase frequencies for compounds containing the S=O or SO₂ group vs $\Sigma\sigma'$. 96
- 5.2 A plot of ν asym; SO₂ vs ν sym. SO₂ vapor-phase frequencies for a variety of compounds containing the SO₂ group. 97
- 5.3 Plots of ν asym. SO₂ vapor-phase frequencies for a variety of compounds containing a SO₂ group vs $\Sigma\sigma'$. 98
- 5.4 Plots of ν sym. SO₂ vapor-phase frequencies for a variety of compounds containing the SO₂ group vs $\Sigma\sigma'$. 99
- 5.5 Plots of ν asym. and ν sym. SO₂ for methyl phenyl sulfone in 10 wt./vol. solvent vs mole % CHCl₃/CCl₄. 100
- 5.6 A plot of ν asym. SO₂ vs ν sym. SO₂ for methyl phenyl sulfone in 1% wt./vol. solvent vs mole % CHCl₃/CCl₄. 101
- 5.7 Plots of ν asym. SO₂ and sym. SO₂ for dimethyl sulfate in 1% wt./vol. solvent vs mole % CDCl₃/CCl₄. 102
- 5.8 A plot of ν asym. SO₂ vs ν sym. SO₂ for dimethyl sulfate 1% wt./vol. solvent vs mole % CDCl₃/CCl₄. 103

CHAPTER 6

- 6.1* Methyl chloride (200-mm Hg sample) (27). 129
- 6.2* Methyl bromide (100-mm Hg sample) (27). 130
- 6.3* Methyl iodide (200-mm Hg sample) (27). 131
- 6.4* Methylene chloride (20- and 100-mm Hg sample) (27). 132
- 6.5* Methylene bromide (30-mm Hg sample) (27). 133
- 6.6* Trichloromethane (chloroform) (10- and 50-mm Hg sample) (27). 134
- 6.7 Tetrafluoromethane (freon 14) (2 and 100 Hg sample) (26) 135
- 6.8* Tetrachloromethane (carbon tetrachloride) (2- and 100-mm Hg sample) (27). 136
- 6.9* Chlorotrifluoromethane (10- and 50-mm Hg sample) (27). 137
- 6.10* Dichlorodifluoro methane (10- and 100-mm Hg sample) (27). 138
- 6.11* Trichlorofluoromethane (f and 40-mm Hg sample) (27). 139
- 6.12* Trichlorobromomethane (5- and 30-mm Hg sample) (27). 140
- 6.13* 1,2-Dichloroethane (ethylene dichloride) (50-mm Hg sample) (27). 141
- 6.14* Infrared spectra of 3-halopropenes (allyl halides) in CCl₄ solution (3800–1333 cm⁻¹) (133–400 cm⁻¹) (12). 142
- 6.15 Vapor-phase infrared spectra of 3-halopropenes (allyl halides) (12). 143
- 6.16a Vapor-phase IR spectrum of 3-fluoropropyne in a 5-cm KBr cell (50-mm Hg sample). 144

6.16b	Vapor-phase IR spectrum of 3-chloropropyne in a 5-cm KBr cell (vapor pressure at -10 and 25°C samples).	144
6.16c	Vapor-phase IR spectrum of 3-bromopropyne in a 5-cm KBr cell (vapor pressure at 0 and 25°C samples).	144
6.16d	Vapor-phase IR spectrum of 3-iodopropyne in a 15-cm KBr cell (~ 8 -mm Hg sample).	145
6.17a	Top: Liquid-phase IR spectrum of 3-chloropropyne-1-d in a 0.023-mm KBr cell. Bottom: Liquid-phase IR spectrum of 3-chloropropyne-1-d in a 0.1-mm polyethylene cell.	146
6.17b	Top: Vapor-phase IR spectrum of 3-chloropropyne-1-d in a 10-cm KBr cell (33- and 100-mm Hg sample); middle: 3-chloropropyne-1-d in a 10-cm polyethylene cell. Bottom: Solution-phase IR spectrum of 3-chloropropyne-1-d in 10% wt./vol. CCl_4 (3800 – 1333 cm^{-1}) and 10% wt./vol. in CS_2 (1333 – 400 cm^{-1}) using 0.1-mm KBr cells. Bands marked with X are due to 3-chloropropyne.	147
6.18	Top: A Raman liquid-phase spectrum of 3-chloropropyne-1-d. Bottom: A Raman polarized liquid-phase spectrum of 3-chloropropyne-1-d. Some 3-chloropropyne is present (15).	148
6.19	Top: Solution-phase IR spectrum of 3-bromopropyne-1-d in 10% wt./vol. in CCl_4 (3800 – 1333 cm^{-1}) and 10% wt./vol. in CS_2 (1333 – 450 cm^{-1}) using 0.1-mm KBr cells (16). Bottom: A vapor-phase IR spectrum of 3-bromopropyne-1-d in a 10-cm KBr cell (40-mm Hg sample). Infrared bands marked with X are due to the presence of 3-bromopropyne (16).	149
6.20	Top: Raman spectrum of 3-bromopropyne-1-d. Bottom: Polarized Raman spectrum of 3-bromopropyne-1-d. Infrared bands marked with X are due to the presence of 3-bromopropyne (16).	150
6.21	An IR spectrum of 1,3-dichloropropyne in 10% wt./vol. CCl_4 solution (3800 – 1333 cm^{-1}) and in CS_2 solution (1333 – 450 cm^{-1}) using 0.1-mm NaCl and KBr cells, respectively. Infrared bands at 1551 and 1580 cm^{-1} are due to CCl_4 and the IR band at 858 cm^{-1} is due to CS_2 (17).	151
6.22	Vapor-phase IR spectrum of 1,3-dichloropropyne (ambient mm Hg sample at 25°C in a 12.5-cm KBr cell) (17).	152
6.23	Solution-phase IR spectrum of 1,3-dibromopropyne in 10% wt./vol. in CCl_4 (3800 – 1333 cm^{-1}) and in CS_2 solution (1333 – 450 cm^{-1}) using 0.1-mm NaCl and KBr cells, respectively. Infrared bands at 1551 and 1580 cm^{-1} are due to CCl_4 and the IR band at 858 cm^{-1} to CS_2 (17).	153
6.24	Approximate normal modes for propyne, 3-halopropynes, and 1,3-dihalopropynes.	154
6.25	Vapor-phase IR spectrum for 1-bromopropyne in a 12.5-cm KBr cell. The weak IR band at 734 cm^{-1} is due to an impurity. The 1-bromopropyne decomposes rapidly in the atmosphere (25).	154
6.26	Infrared vapor spectrum for 1-iodopropyne in a 12.5-cm KBr cell (25).	155
6.27	Top: Vapor-phase IR spectrum of 1-bromo-1-chloroethylene using a 10-cm KBr cell (10-mm Hg sample). Bottom: Same as upper (100-mm Hg sample) (19).	155
6.28	Raman liquid-phase spectrum of 1-homo-1-chloroethylene. Top: Parallel polarization. Bottom: Perpendicular polarization.	156
6.29	Vapor-phase IR spectrum of 1-chloropropadiene in a 12.5-cm KBr cell (50- and 100-mm Hg sample) (23).	156

6.30	Vapor-phase IR spectrum of 1-bromopropadiene in a 12.5-cm KBr cell (50- and 100-mm Hg sample).	157
6.31	Vapor-phase IR spectrum of 1-iodopropadiene in a 5-cm KBr cell (vapor pressure at 25 °C). Bands at 1105 and 1775 cm^{-1} are due to the presence of an impurity.	157
6.32	Infrared spectrum of 1-iodopropadiene in 10% wt./vol. CCl_4 solution (3800–1333 cm^{-1}) and 10% wt./vol. CS_2 solution (1333–450 cm^{-1}) using NaCl and KBr cells, respectively.	157
6.33	Vapor-phase IR spectrum of 1-bromopropadiene-1-d in a 12.5-cm KBr cell (50- and 100-mm Hg sample) (16).	158
6.34	Solution-phase IR spectrum of 1-bromopropadiene-1-d 10% wt./vol. in CCl_4 (3800–1333 cm^{-1}) and in CS_2 solution using 0.1-mm KBr cells. Infrared bands marked with X are due to the presence of 1-bromopropadiene (16).	158
6.35	Top: Raman spectrum of 1-bromopropadiene-1-d using a capillary tube. Bottom: Polarized Raman spectrum of 1-bromopropadiene-1-d (16).	159
6.36*	Vapor-phase IR spectrum of tetrafluoroethylene (8- and 50-mm Hg samples) (27).	160
6.37*	Vapor-phase IR spectrum of tetrachloroethylene (13-mm Hg sample) (27).	161
6.38*	Vapor-phase IR spectrum of 1,1-dichloro-2,2-difluoroethylene (10- and 60-mm Hg samples) (26).	162
6.39*	Vapor-phase IR spectrum of trichloroethylene (10- and 50-mm Hg samples).	163

*Those vapor-phase infrared spectra figures for Chapter 6 with an asterisk following the figure number have a total vapor pressure of 600-mm Hg with nitrogen (N_2), in a 5-cm KBr cell. The mm Hg sample is indicated in each figure.

CHAPTER 7

7.1	A plot of the observed ν asym. NO_2 frequencies vs the calculated ν asym. NO_2 frequencies for nitroalkanes using the equation ν asym. $\text{NO}_2 = 1582 \text{ cm}^{-1} + \Sigma\Delta R$.	186
7.2	A plot of the observed ν sym. NO_2 frequencies vs the calculated ν sym. NO_2 frequencies using the equation ν sym. $\text{NO}_2 = 1397 \text{ cm}^{-1} + \Sigma\Delta R$.	187
7.3	Vapor-phase IR spectrum for nitromethane in a 5-cm KBr cell (5 and 20 mm Hg sample to 600 mm Hg with N_2).	188
7.4	Vapor-phase IR spectrum for 2-nitropropane in a 5-cm KBr cell (20 mm Hg sample to 600 mm Hg with N_2).	189
7.5	Plots of ν asym. NO_2 and ν C=O for 4-nitrobenzaldehyde vs mole % $\text{CHCl}_3/\text{CCl}_4$.	190
7.6	Plots of ν sym. NO_2 for 4-nitrobenzaldehyde vs mole % $\text{CHCl}_3/\text{CCl}_4$.	190
7.7	A plot of ν asym. NO_2 for 4-X-nitrobenzenes in CCl_4 solution vs ν asym. NO_2 in CHCl_3 solution.	191
7.8	A plot of ν asym. NO_2 for 4-X-nitrobenzenes in CCl_4 solution vs σ_p .	192
7.9	A plot of ν asym. NO_2 for 4-X-nitrobenzenes in CHCl_3 solution vs σ_p .	193
7.10	A plot of ν asym. NO_2 for 4-X-nitrobenzenes in CCl_4 solution vs σ_{R^+} .	194
7.11	A plot of ν asym. NO_2 for 4-X-nitrobenzenes in CHCl_3 solution vs σ_{R^+} .	195
7.12	A plot of ν asym. NO_2 for 4-X-nitrobenzenes in CCl_4 solution vs σ_R .	196
7.13	A plot of ν asym. NO_2 for 4-X-nitrobenzenes in CHCl_3 solution vs σ_R .	197
7.14	A plot of ν asym. NO_2 for 4-X-nitrobenzenes in CCl_4 solution vs σ_I .	198
7.15	A plot of ν asym. NO_2 for 4-X-nitrobenzenes in CHCl_3 solutions vs σ_I .	199

7.16	Vapor-phase IR spectrum for ethyl nitrate in a 5-cm KBr cell (5 and 30 mm Hg sample to 600 mm Hg with N ₂).	200
7.17	Vapor-phase IR spectrum for <i>n</i> -butyl nitrite in a 5-cm KBr cell (10 and 80 mm Hg sample to 600 mm Hg with N ₂).	201
7.18	Plots of <i>cis</i> ν N=O and <i>trans</i> ν N=O for alkyl nitrites vs σ^* .	202
7.19	A plot of <i>trans</i> ν N–O for alkyl nitrites vs σ^* .	203
7.20	A plot of <i>trans</i> ν N=O vs <i>trans</i> ν N–O for alkyl nitrites.	204
7.21	Plots of the absorbance ratio (A) <i>trans</i> ν N=O/(A) <i>cis</i> ν N=O vs σ^* .	205

CHAPTER 8

8.1	Top: Infrared spectrum of thiophosphoryl dichloride fluoride 10% wt./vol. in CCl ₄ solution (3800–1333 cm ⁻¹) and 10% wt./vol. in CS ₂ solution. Bottom: Vapor-phase spectrum of thiophosphoryl dichloride fluoride in the region 3800–450 cm ⁻¹ (9).	255
8.2	Top: Infrared spectrum of thiophosphoryl dichloride fluoride in hexane solution using polyethylene windows in the region 600–40 cm ⁻¹ . Bottom: Vapor-phase IR spectrum of thiophosphoryl dichloride fluoride using polyethylene windows in the region 600–150 cm ⁻¹ (9).	256
8.3	Top: Infrared spectrum of phosphoryl chloride in CCl ₄ solution (3800–1333 cm ⁻¹) and in CS ₂ solution (1333–45 cm ⁻¹). Bottom: Infrared spectrum of phosphoryl chloride in hexane solution (9).	257
8.4	A comparison of the approximate normal vibrations of thiophosphoryl dichloride fluoride vs those for phosphoryl chloride (9).	258
8.5	Top: Infrared spectrum of O-methyl phosphorodichloridothioate in 10 wt./vol. % in CCl ₄ solution (3800–1333 cm ⁻¹) and in 10 wt./vol. % in CS ₂ solution (1333–400 cm ⁻¹) using 0.1-mm KBr cells. The weak band at ~ 752 cm ⁻¹ is due to the presence of a trace amount of P(–S)Cl ₃ . The band at 659 cm ⁻¹ is due to the presence of $\sim 4\%$ O,O-dimethyl phosphorochloridothioate. Middle: Infrared spectrum of O-methyl-d ₃ phosphorodichloridothioate in 10 wt./vol. % in CCl ₄ solution (3800–1333 cm ⁻¹) and 10 + 2 wt./vol. % in CS ₂ solution (1333–400 cm ⁻¹) using 0.1-mm KBr cells. Bottom: Infrared spectrum of O-methyl phosphorodichloridate in 10 wt./vol. % in CCl ₄ solution (3800–1333 cm ⁻¹) and 10 wt./vol. % in CS ₂ solution (1333–450 cm ⁻¹) using 0.1-mm KBr cells (21).	259
8.6	Top: Infrared spectrum of O-methyl phosphorodichloridothioate in 10 wt./vol. % in hexane solution in a 1-mm polyethylene cell. Bottom: Infrared spectrum of O-methyl phosphorodichloridothioate in 25 wt./vol. % in hexane solution in a 2-mm polyethylene cell (25).	260
8.7	Top: Infrared spectrum of O-methyl-d ₃ phosphorodichloridothioate in 10 wt./vol. % hexane solution in a 1-mm polyethylene cell. Bottom: Infrared spectrum of O-methyl-d ₃ phosphorodichloridothioate in 25 wt./vol. % hexane solution in a 2-mm polyethylene cell and compensated with polyethylene (25).	261
8.8	Assumed normal vibrations of organophosphorus and inorganophosphorus compounds (25).	262

- 8.9 Top: Infrared spectrum of O-ethyl phosphorodichlorodithioate 10 wt./vol. % in CCl_4 solution ($3800\text{--}1333\text{ cm}^{-1}$) and 10 and 2 wt./vol. % in CS_2 solution ($1333\text{--}400\text{ cm}^{-1}$) in 0.1-mm KBr cells. The solvents were compensated. Bottom: Infrared spectrum of O-ethyl phosphorodichlorodithioate in 25 and 2 wt./vol. % in hexane solution ($600\text{--}45\text{ cm}^{-1}$) in a 1-mm polyethylene cell (22). 263
- 8.10 Top: Infrared spectrum of O-ethyl-1,1- d_2 phosphorodichlorodithioate in 10 wt./vol. % in CCl_4 solution ($3800\text{--}1333\text{ cm}^{-1}$) and 10 and 2.5 wt./vol. % in CS_2 solution ($1333\text{--}400\text{ cm}^{-1}$) in 0.1-mm KBr cells. The solvents are compensated. Bottom: Infrared spectrum of O-ethyl-1,1- d_2 phosphorodichlorodithioate in 10 wt./vol. hexane solution ($600\text{--}45\text{ cm}^{-1}$) in a 1-mm polyethylene cell (22). 264
- 8.11 Top: Infrared spectrum of O-ethyl-2,2,2- d_3 phosphorodichlorodithioate in 10 wt./vol. % CCl_4 solution ($3800\text{--}1333\text{ cm}^{-1}$) and 10 wt./vol. % CS_2 solution ($1333\text{--}400\text{ cm}^{-1}$) in 0.1-mm KBr cells. The solvents are not compensated. Bottom: Infrared spectrum of O-ethyl-2,2,2- d_3 phosphorodichlorodithioate in 10 wt./vol. hexane solution in a 1-mm polyethylene cell (22). 265
- 8.12 Top: Infrared spectrum of O,O-dimethyl phosphorochlorodithioate in 10 wt./vol. % in CCl_4 solution ($3800\text{--}1333\text{ cm}^{-1}$) and 10 and 2 wt./vol. % in CS_2 solution ($1333\text{--}450\text{ cm}^{-1}$) in 0.1-mm KBr cells. The solvents have not been compensated. Bottom: Liquid-phase IR spectrum of O,O-dimethyl phosphorochlorodithioate between KBr plates (27). 266
- 8.13 Top: Infrared spectrum of O,O-dimethyl- d_6 phosphorochlorodithioate in 10 wt./vol. % in CCl_4 solution ($3800\text{--}1333\text{ cm}^{-1}$) and 10 and 1 wt./vol. % in CS_2 solution ($1333\text{--}400\text{ cm}^{-1}$) in 0.1-mm KBr cells. Traces of toluene and methylene chloride are present. Bottom: Liquid-phase IR spectrum of O,O-dimethyl- d_6 phosphorochlorodithioate between KBr plates (27). 267
- 8.14 Top: Infrared spectrum of O,O-dimethyl phosphorochlorodithioate in 2-mm polyethylene cells. The polyethylene has been compensated. Bottom: Infrared spectrum of O,O-dimethyl- d_6 phosphorochlorodithioate in 10 wt./vol. % n-hexane in 1- and 2-mm polyethylene cells, respectively (27). 268
- 8.15 Top: Infrared spectrum of S-methyl phosphorodichlorodithioate in 10 wt./vol. % in CCl_4 solution ($3800\text{--}1333\text{ cm}^{-1}$) and in 10 and 2 wt./vol. % in CS_2 solution ($1333\text{--}400\text{ cm}^{-1}$) in 0.1-mm KBr cells. Bottom: Infrared liquid phase spectrum of S-methyl phosphorodichlorodithioate in 10 wt./vol. % hexane solution ($600\text{--}45\text{ cm}^{-1}$) in a 1-mm polyethylene cell (23). 269
- 8.16 Upper: Raman liquid-phase spectrum of S-methyl phosphorodichlorodithioate. Lower: Polarized Raman liquid-phase spectrum of S-methyl phosphorodichlorodithioate (23). Bottom: upper: Raman liquid-phase spectrum of phosphoryl chloride. Lower: Polarized Raman spectrum of phosphoryl chloride (23). 270
- 8.17 Top: Infrared spectrum of trimethyl phosphite 10 wt./vol. % ($1333\text{--}400\text{ cm}^{-1}$) and 10 wt./vol. % in CS_2 solution ($1333\text{--}400\text{ cm}^{-1}$) in 0.1-mm KBr cells. The solvents have not been compensated. Bottom: Infrared spectrum of trimethyl phosphite in 1 wt./vol. % CCl_4 solution ($3800\text{--}1333\text{ cm}^{-1}$) and in 1 wt./vol. % CS_2 solution ($1333\text{--}400\text{ cm}^{-1}$) using 0.1-mm KBr cells. The solvents have not been compensated (36). 271

- 8.18 Infrared spectrum of trimethyl phosphite in 10 wt./vol. % hexane solution in a 0.1-mm polyethylene cell. The IR band at $\sim 70 \text{ cm}^{-1}$ in a lattice mode for polyethylene (36). 272
- 8.19 Vapor-phase IR spectrum of trimethyl phosphite in a 10-cm KBr cell (36). 272
- 8.20 Top: Infrared spectrum of O,O-dimethyl phosphorodithioic acid in 10 wt./vol. % in CCl_4 solution ($3800\text{--}1333 \text{ cm}^{-1}$) and 10 and 2 wt./vol. % in CS_2 solution ($1333\text{--}450 \text{ cm}^{-1}$) in 0.1-mm KBr cells. Bottom: Infrared spectrum of O,O-dimethyl phosphorochlorodithioate in CCl_4 solution ($3800\text{--}1333 \text{ cm}^{-1}$) and 10 and 2 wt./vol. % in CS_2 solutions ($1333\text{--}450 \text{ cm}^{-1}$) in 0.1-mm KBr cells (32). 273
- 8.21 Top: Infrared spectrum of O,O-diethyl phosphorodithioic acid in 10 wt./vol. % in CCl_4 solution ($3800\text{--}1333 \text{ cm}^{-1}$) and 10 and 2 wt./vol. % in CS_2 solutions ($1333\text{--}400 \text{ cm}^{-1}$) in 0.1-mm KBr cells. The solvents have been compensated. Bottom: Infrared spectrum of O,O-diethyl phosphorochlorodithioate in 10 wt./vol. % in CCl_4 solution and in 10 and 2 wt./vol. % CS_2 solutions ($1333\text{--}450 \text{ cm}^{-1}$) in 0.1-mm KBr cells (32). 273
- 8.22 Top: Infrared spectrum of dimethyl hydrogenphosphonate in 10 wt./vol. % in CCl_4 solution ($3800\text{--}1333 \text{ cm}^{-1}$) and in 10 and 2 wt./vol. % CS_2 solutions in 0.1-mm KBr cells. The solvents have not been compensated. Bottom: Infrared spectrum of dimethyl deuterophosphonate in 10% wt./vol. CCl_4 solution ($3800\text{--}1333 \text{ cm}^{-1}$) and in 10 and 2 wt./vol. % solutions in CS_2 solution ($1333\text{--}400 \text{ cm}^{-1}$). The solvents have been compensated (32). 274
- 8.23 Top: Infrared spectrum of dimethyl hydrogenphosphonate saturated in hexane solution ($600\text{--}35 \text{ cm}^{-1}\text{--}1$) in a 2-mm polyethylene cell (32). 274
- 8.24 Top: Infrared spectrum of diethyl hydrogenphosphonate in 10 wt./vol. % in CCl_4 solution ($3800\text{--}1333 \text{ cm}^{-1}$) and in 10 and 2 wt./vol. % in CS_2 solutions ($1333\text{--}400 \text{ cm}^{-1}$) in 0.1-mm KBr cells. The solvents have not been compensated. Bottom: Infrared spectrum of diethyl deuterophosphonate in 10% wt./vol. % in CCl_4 solution ($3800\text{--}1333 \text{ cm}^{-1}$) and 10 and 2 wt./vol. % CS_2 solutions ($1333\text{--}400 \text{ cm}^{-1}$) in 0.1-mm KBr cells. The solvents have been compensated (32). 275
- 8.25 Top: Infrared spectrum for diethyl hydrogenphosphonate in 0.25 and 5 wt./vol. % hexane solutions ($600\text{--}35 \text{ cm}^{-1}$) in a 2-mm polyethylene cell. Bottom: Infrared spectrum for diethyl deuterophosphonate in 10 wt./vol. % hexane solution ($600\text{--}35 \text{ cm}^{-1}$) in a 1-mm polyethylene cell. 275
- 8.26 Top: Raman liquid-phase spectrum of dimethyl hydrogenphosphonate in a 2.5-ml multipass cell, gain 7, spectral slit-width 0.4 cm^{-1} . Bottom: Same as top but with the plane of polarization of the incident beam rotated through 90° (32). 276
- 8.27 Top: Infrared spectrum of (chloromethyl) phosphonic dichloride in 4 wt./vol. % CS_2 solution ($1500\text{--}400 \text{ cm}^{-1}$) at 0°C in a 0.1-mm KBr cell. Bottom: Same as above except at -75°C . 277
- 8.28 Top: Infrared spectrum of (chloromethyl) phosphonic dichloride in 10 wt./vol. % in CCl_4 solution ($3800\text{--}1333 \text{ cm}^{-1}$) and 10 wt./vol. % in CS_2 solution ($1333\text{--}400 \text{ cm}^{-1}$) in 0.1-mm KBr cells. Bottom: Infrared spectrum of (chloromethyl) phosphonic dichloride in 20 wt./vol. % hexane solution ($600\text{--}45 \text{ cm}^{-1}$) in a 1-mm polyethylene cell (17). 278

- 8.29 Top: Infrared spectrum of (chloromethyl) phosphonothioic dichloride in 10 wt./vol. % CCl_4 solution ($3800\text{--}1333\text{ cm}^{-1}$) and in 10 wt./vol. % CS_2 solution ($1333\text{--}400\text{ cm}^{-1}$) in 0.1-mm KBr cells. Bottom: Infrared spectrum of (chloromethyl) phosphonothioic dichloride in 20 wt./vol. % hexane solution ($600\text{--}45\text{ cm}^{-1}$) in a 1-mm polyethylene cell (17). 279
- 8.30 Infrared spectrum of (bromomethyl) phosphonic dibromide in 10 wt./vol. % CCl_4 solution ($3800\text{--}1333\text{ cm}^{-1}$) and 10 wt./vol. % in CS_2 solution ($1333\text{--}400\text{ cm}^{-1}$) in 0.1-mm KBr cells (17). 279
- 8.31 Top: Infrared spectrum of N-methyl phosphoramidodichloridothioate 10 wt./vol. % in CCl_4 solution ($3800\text{--}1333\text{ cm}^{-1}$) and 10 wt./vol. % in CS_2 solution ($1333\text{--}45\text{ cm}^{-1}$) in 0.1-mm KBr cells. The solvents have not been compensated. Bottom: Infrared spectrum of N-methyl phosphoramidodichloridothioate in 10 wt./vol. hexane solution ($600\text{--}45\text{ cm}^{-1}$) in a 1-mm polyethylene cell (24). 280
- 8.32 Top: Infrared spectrum of N-methyl- d_3 phosphoramidodichloridothioate in 10 wt./vol. % in CCl_4 ($3800\text{--}1333\text{ cm}^{-1}$) and 10 wt./vol. % in CS_2 solution ($1333\text{--}45\text{ cm}^{-1}$) in 0.1-mm KBr cells. Bottom: Infrared spectrum of N-methyl- d_3 phosphoramidodichloridothioate in 10 wt./vol. % in hexane solution ($600\text{--}45\text{ cm}^{-1}$) in a 1-mm polyethylene cell (24). 281
- 8.33 Top: Infrared spectrum of N-D, N-methyl phosphoramidodichloridothioate in 10 wt./vol. % CCl_4 solution ($3800\text{--}1333\text{ cm}^{-1}$) and in 10 wt./vol. % in CS_2 solution ($1333\text{--}45\text{ cm}^{-1}$) in 0.1-mm KBr cells. The solvents have been compensated. Bottom: Infrared spectrum of N-D, N-methyl phosphoramidodichloridothioate in 10 wt./vol. % hexane solution in a 1-mm polyethylene cell. Both samples contain N-methyl phosphoramidodichloridothioate as an impurity (24). 282
- 8.34 Top: Infrared spectrum for N-D, N-methyl- d_3 phosphoramidodichloridothioate in 10 wt./vol. % CCl_4 solution ($3800\text{--}1333\text{ cm}^{-1}$) and 10 and 2 wt./vol. % in CS_2 solutions ($1333\text{--}400\text{ cm}^{-1}$) in 0.1-mm KBr cells. The solvent bands are compensated. Bottom: Infrared spectrum of N-D, N-methyl- d_3 phosphoramidodichloridothioate in 10 wt./vol. % hexane solution in a 1-mm polyethylene cell. This sample contains N-methyl- d_3 phosphoramidodichloridothioate as an impurity (24). 283
- 8.35 Infrared spectrum 1 is for O-alkyl O-aryl N-methylphosphoramidate in 10 wt./vol. % CCl_4 solution ($3500\text{--}3000\text{ cm}^{-1}$) in a 0.1-mm NaCl cell. Infrared spectrum 2 is for O-alkyl O-aryl N-methylphosphoramidothioate in 10 wt./vol. % in CCl_4 solution ($3500\text{--}300\text{ cm}^{-1}$) in a 0.1-mm NaCl cell (42). 283
- 8.36 A plot of N-H stretching frequencies of O-alkyl O-aryl N-alkylphosphoramidates in the region $3450\text{--}3350\text{ cm}^{-1}$ vs an arbitrary assignment of one for each proton joined to the N- α -carbon atom (42). 284
- 8.37 Plots of cis and trans N-H stretching frequencies of O-alkyl O-aryl N-alkylphosphoramidothioates in the region $3450\text{--}3350\text{ cm}^{-1}$ vs an arbitrary assignment of one for every proton joined to the N- α -carbon atom (42). 284
- 8.38 Infrared spectra of the cis and trans N-H stretching absorption bands of O-alkyl O-aryl N-alkylphosphoramidothioates in 0.01 molar or less in CCl_4 solutions ($3450\text{--}3350\text{ cm}^{-1}$) in a 14-mm NaCl cell. The N-alkyl group for A is methyl, B is

- ethyl, C is n-propyl, D is isobutyl, E is n-butyl, F is isopropyl, G is sec-butyl, and H is tert-butyl. Spectra I and J are O,O-dialkyl N-methylphosphoramidothioate and O,O-dialkyl N-propylphosphoramidothioate, respectively (42). 285
- 8.39 Infrared spectra of the N–H stretching absorption bands of O-alkyl N,N'-dialkyl phosphorodiamidothioates. The N,N'-dialkyl group for A is dimethyl, B is diethyl, C is dipropyl, D is dibutyl, E is diisopropyl, F is di-sec-butyl, G is dibenzyl. The H and I are IR spectra for the N–H stretching bands of O-aryl N,N'-diisopropylphosphordiamidothioate and O-aryl N-isopropyl, N-methylphosphorodiamidothioate, respectively. Spectra A through J were recorded for 0.01 molar or less in CCl₄ solutions using 3-mm KBr cells. Spectra D and J are for O-aryl N,N'-dibutylphosphorodiamidothioate in 0.01 molar CCl₄ solution in a 3-mm cell and 10 wt./vol. % in CCl₄ solution in a 0.1-mm KBr cell (42). 285
- 8.40 Infrared spectrum R gives the N–H stretching absorption bands for O-alkyl O-aryl phosphoramidothioate in 0.01 molar CCl₄ solution in a 3-mm NaCl cell. Infrared spectrum S gives O,O-dialkyl phosphoramidothioate in 0.01 molar CCl₄ solution in a 3-mm NaCl cell (42). 286
- 8.41 Top: Infrared spectrum of O,O-diethyl methylphosphoramidothioate in 10 wt./vol. % CCl₄ solution (3800–1333 cm⁻¹) and 10 and 2 wt./vol. % CS₂ solutions (1333–400 cm⁻¹) in 0.1-mm KBr cells. Middle: Infrared spectrum of O,O-diethyl N-methyl, N-D-phosphoramidothioate in 2 wt./vol. % in CCl₄ solution (3800–1333 cm⁻¹) and in 2 wt./vol. % in CS₂ solution (1333–400 cm⁻¹) in 0.1-mm KBr cells. Bottom: Infrared spectrum of O,O-diethyl N-methyl, N-D-phosphoramidothioate 10 wt./vol. % in CCl₄ solution (3800–1333 cm⁻¹) and in 10 wt./vol. % CS₂ solution (1333–400 cm⁻¹) in 0.1-mm KBr cells (37). 287
- 8.42 Top: Infrared spectrum of O,O-diethyl phosphoramidothioate in 10 wt./vol. % in CCl₄ solution (3800–1333 cm⁻¹) and 2 and 10 wt./vol. % in CS₂ solutions (1333–400 cm⁻¹) in 0.1-mm KBr cells. Middle: Infrared spectrum of O,O-diethyl phosphoramidothioate-N-D₂ in 2 wt./vol. % in CCl₄ solution (3800–1333 cm⁻¹) and in 2 wt./vol. % CS₂ solution (1333–400 cm⁻¹) in 0.1-mm KBr cells. Bottom: Infrared spectrum of O,O-diethyl phosphoramidothioate-N-D₂ 10 wt./vol. % in CCl₄ solution (3800–1333 cm⁻¹) and 10 wt./vol. % in CS₂ solution (1333–400 cm⁻¹) in 0.1-mm KBr cells (37). 288
- 8.43 Top: Infrared spectrum of O,O-diethyl N-methylphosphoramidothioate 10 wt./vol. % in CCl₄ solution (3800–1333 cm⁻¹) and 10 and 2 wt./vol. % in CS₂ solutions (1333–400 cm⁻¹) in 0.1-mm KBr cells. Middle: Infrared spectrum of O,O-diethyl N-methyl, N-D phosphoramidothioate in 2 wt./vol. % in CS₂ solution (1333–400 cm⁻¹) in 0.1-mm KBr cells. Bottom: Infrared spectrum of O,O-diethyl N-methyl, N-D-phosphoramidothioate in 10 wt./vol. % CCl₄ solution (1333–400 cm⁻¹) in 0.1-mm KBr cells. The solvents are not compensated (37). 289
- 8.44 Infrared spectrum of O,O-dimethyl N-methylphosphoramidothioate in 10 wt./vol. % in CCl₄ solution (3800–1333 cm⁻¹) and 10 and 2 wt./vol. % in CS₂ solutions (1333–400 cm⁻¹) in 0.1-mm KBr cells (37). 290
- 8.45 Top: Infrared spectrum of O,O-dimethyl O-(2,4,5-trichlorophenyl) phosphorothioate 10 wt./vol. % in CCl₄ solution (3800–1333 cm⁻¹) and 10 and 2 wt./vol. % in CS₂ solutions (1333–400 cm⁻¹) in 0.1-mm KBr cells. Bottom: Infrared spectrum

- of O,O-dimethyl O-(2,4,5-trichlorophenyl) phosphate in 10 wt./vol. % in CCl₄ solution (3800–1333 cm⁻¹) in 0.1-mm KBr cells. The solvents are not compensated (43). 291
- 8.46 Top: Infrared spectrum for O,O-dimethyl-d₆ O-(2,4,5-trichlorophenyl) phosphorothioate in 10 wt./vol. % CCl₄ solution (3800–1333 cm⁻¹) and in 10 and 2 wt./vol. % CS₂ solution (1333–400 cm⁻¹) in 0.1-mm KBr cells. Bottom: Infrared spectrum for O,O-dimethyl-d₆ O-(2,4,5-trichlorophenyl) phosphate in 10 wt./vol. % CS₂ solutions (1333–450 cm⁻¹) in 0.1-mm KBr cells. The solvents have not been compensated. 292
- 8.47 Top: Infrared spectrum of disodium methanephosphonate. Bottom: Infrared spectrum of disodium methane-d₃-phosphonate. In fluorolube oil mull (3800–1333 cm⁻¹) and in Nujol oil mull (1333–400 cm⁻¹) (40). These mulls were placed between KBr plates. 293
- 8.48 Top: Infrared spectrum of disodium methanephosphonate in water solution between AgCl plates. Bottom: Infrared spectrum of disodium methane-d₃-phosphonate in water solution between AgCl plates (40). 294
- 8.49 Top: Infrared spectrum of disodium methanephosphonate. Middle: Infrared spectrum of disodium methane-d₃-phosphonate. Bottom: Infrared spectrum of dipotassium methanephosphonate. These spectra were recorded from samples prepared as Nujol mulls between polyethylene film (600–45 cm⁻¹) (40). 295
- 8.50 Infrared spectrum of disodium n-octadecanephosphonate prepared as a fluoroluble mull (3800–1333 cm⁻¹) prepared as a Nujol mull (1333–450 cm⁻¹) (40). 296
- 8.51 Top: Infrared spectrum of sodium dimethylphosphinate prepared as a fluoroluble mull (3800–1333 cm⁻¹) and prepared as a Nujol mull (1333–400 cm⁻¹) between KBr plates. Bottom: Infrared spectrum of sodium dimethylphosphinate saturated in water solution between AgCl plates (41). 297
- 8.52 Top: Infrared spectrum of sodium dimethylphosphinate prepared as Nujol mull between polyethylene film (600–45 cm⁻¹). Bottom: Infrared spectrum of potassium dimethylphosphinate prepared as a Nujol mull between polyethylene film (600–45 cm⁻¹) (41). 298
- 8.53 Top: Raman saturated water solution of sodium dimethylphosphinate using a 0.25-ml multipass cell, gain 13.4, spectral slit 10 cm⁻¹. Bottom: Same as above, except with the plane of polarization of the incident beam rotated 90° (41). 299
- 8.53a (Top): IR spectrum for sodium diheptylphosphinate. 300
- 8.53a (Bottom): IR spectrum for sodium dioctylphosphinate. 300
- 8.54 Plots of ν P=O for P(=O)Cl₃ vs mole % solvent system. The open triangles represent CCl₄/C₆H₁₄ as the solvent system. The open circles represent CHCl₃/C₆H₁₄ as the solvent system; and the open diamonds represent CHCl₃/CCl₄ as the solvent system (26). 301
- 8.55 A plot of ν P=O for CH₃P(=O)Cl₂ vs mole % CDCl₃/CCl₄ as represented by open circles, and plots of ν P=O for (CH₃)₃C P(db;O)Cl₂ vs mole % CHCl₃/CCl₄ (open triangles) and mole % (CDCl₃/CCl₄) (open diamonds) (26). 301
- 8.56 Plots of ν P–O rotational conformers 1 and 2 for CH₃O P(=O)Cl₂ (conformer 1, open circles; conformer 2, open squares), and for C₂H₅OP(=O)Cl₂ (conformer 1, open triangles; conformer 2, open diamonds) vs mole % CHCl₃/CCl₄ (26). 302

- 8.57 Plots of ν P=O rotational conformers 1 and 2 for $(\text{CH}_3\text{O})_3\text{P}=\text{O}$ vs mole % $\text{CHCl}_3/\text{CCl}_4$ (conformer 1, solid circles, and conformer 2, solid triangles) (55). 302
- 8.58 Plots of ν P=O rotational conformers 1 and 2 for $(\text{C}_2\text{H}_5\text{O})_3\text{P}=\text{O}$ vs mole % $\text{CDCl}_3/\text{CCl}_4$ (conformer 1, solid triangles, conformer 2, closed circles) (55). 303
- 8.59 Plots of ν P=O rotational conformers 1 and 2 for $(\text{C}_4\text{H}_9\text{O})_3\text{P}=\text{O}$ vs mole % $\text{CDCl}_3/\text{CCl}_4$ (conformer 1, solid circles, conformer 2, solid triangles) (55). 303
- 8.60 Plots of ν asym. PCL_3 for $\text{P}(=\text{O})\text{Cl}_3$ vs mole % solvent system. The open circles represent the $\text{CHCl}_3/\text{CCl}_4$ solvent system; the open triangles represent the $\text{CHCl}_3/\text{C}_6\text{H}_{14}$ solvent system; and the open diamonds represent the $\text{CCl}_4/\text{C}_6\text{H}_{14}$ solvent system (26). 304
- 8.61 Plots of ν asym. PCL_2 frequencies for $\text{CH}_3\text{P}(=\text{O})\text{Cl}_2$ (open circles) and for $(\text{CH}_3)_3\text{CP}(=\text{O})\text{Cl}_2$ (open triangle and open diamonds) vs mole % $\text{CDCl}_3/\text{CCl}_4$ and $\text{CHCl}_3/\text{CCl}_4$ (26). 304
- 8.62 Plots of ν asym. PCL_2 rotational conformers 1 and 2 frequencies for $\text{CH}_3\text{OP}(=\text{O})\text{Cl}_2$ (conformer 1, open circles; conformer 2, open squares) and for $\text{C}_2\text{H}_5\text{OP}(-\text{O})\text{Cl}_2$ (conformer 1, open triangles, conformer 2, open diamonds) frequencies vs mole % $\text{CHCl}_3/\text{CCl}_4$ (26). 305
- 8.63 Plots of ν sym. PCL_3 frequencies for $\text{P}(=\text{O})\text{Cl}_3$ vs mole % solvent system. The open circles represent $\text{CHCl}_3/\text{CCl}_4$ as the solvent system, the open triangles represent the $\text{CHCl}_3/\text{C}_6\text{H}_{14}$ solvent system, and the open diamonds represent the $\text{CCl}_4/\text{C}_6\text{H}_{14}$ solvent system. 305
- 8.64 A plot of ν sym. PCL_2 frequencies for $\text{CH}_3\text{P}(=\text{O})\text{Cl}_2$ vs mole % $\text{CDCl}_3/\text{CCl}_4$ (open circles) and plots of ν sym. PCL_2 frequencies for $(\text{CH}_3)_3\text{CP}(=\text{O})\text{Cl}_2$ vs mole % $\text{CHCl}_3/\text{CCl}_4$ (open triangles) and mole % $\text{CDCl}_3/\text{CCl}_4$ (open diamonds) (26). 306
- 8.65 Plots of ν sym. PCL_2 rotational conformers 1 and 2 vs mole % $\text{CHCl}_3/\text{CCl}_4$. The open circles and open squares are for $\text{CH}_3\text{OP}(=\text{O})\text{Cl}_2$ conformers 1 and 2, respectively. The open triangles and open diamonds are for $\text{C}_2\text{H}_5\text{OP}(=\text{O})\text{Cl}_2$ conformers 1 and 2, respectively (26). 306
- 8.66 Plots of ν asym. PCL_2 frequencies vs ν sym. PCL_2 frequencies for $\text{CH}_3\text{OP}(=\text{O})\text{Cl}_2$ (conformer 1, solid squares); $\text{CH}_3\text{OP}(=\text{O})\text{Cl}_2$ (conformer 2, open squares); $\text{C}_2\text{H}_5\text{OP}(=\text{O})\text{Cl}_2$ (conformer 1, solid triangles) $\text{C}_2\text{H}_5\text{OP}(=\text{O})\text{Cl}_2$ (conformer 2, open triangles); $(\text{CH}_3)_3\text{CP}(=\text{O})\text{Cl}_2$ (solid diamonds); and $\text{CH}_3\text{P}(=\text{O})\text{Cl}_2$ (solid circles) (26). 307
- 8.67 Plots of the absorbance (A) ratio of rotational conformer 1 and 2 band pairs for ν P=O (solid circles), ν COP (solid triangles), ν asym. PCL_2 (solid squares), and ν sym. PCL_2 (solid diamonds) for $\text{CH}_3\text{OP}(=\text{O})\text{Cl}_2$ vs mole % $\text{CHCl}_3/\text{CCl}_4$ (26). 307
- 8.68 Plots of the absorbance (A) ratio rational conformer 1 and 2 band pairs for ν P=O (solid circles), ν COP (solid triangles), ν asym. PCL_2 (solid squares), and ν sym. PCL_2 (solid diamonds) for $\text{C}_2\text{H}_5\text{OP}(=\text{O})\text{Cl}_2$ vs mole % $\text{CHCl}_3/\text{CCl}_4$ (26). 308
- 8.69 A plot of δ sym. CH_3 frequencies for $\text{CH}_3\text{P}(=\text{O})\text{Cl}_2$ vs mole % $\text{CHCl}_3/\text{CCl}_4$ (26). 308
- 8.70 A plot of ρCH_3 frequencies for $\text{CH}_3\text{P}(=\text{O})\text{Cl}_2$ vs mole % $\text{CHCl}_3/\text{CCl}_4$ (26). 309
- 8.71 Plots of the in-phase δ sym. $(\text{CH}_3)_3$ frequencies (open circles) and the out-of-phase δ sym. $(\text{CH}_3)_3$ frequencies (open triangles) vs mole % $\text{CHCl}_3/\text{CCl}_4$ (26). 309
- 8.72 Plots of the a' and a ρCH_3 frequencies for $\text{C}_{2\text{H}_5}\text{OP}(=\text{O})\text{Cl}_2$ vs mole % $\text{CHCl}_3/\text{CCl}_4$ (26). 310

8.73	Plots of the a' and a ρCH_3 modes of $(\text{C}_2\text{H}_5\text{O})_3\text{P}=\text{O}$ vs mole % $\text{CDCl}_3/\text{CCl}_4$ (55).	310
8.74	A plot of ν CC for $\text{C}_2\text{H}_5\text{OP}(=\text{O})\text{Cl}_2$ vs mole % $\text{CHCl}_3/\text{CCl}_4$ (26).	311
8.75	A plot of ν CC for $(\text{C}_2\text{H}_5\text{O})_3\text{P}=\text{O}$ vs mole % $\text{CDCl}_3/\text{CCl}_4$ (55).	311
8.76	Plots of ν COP rotational conformers 1 and 2 for $\text{CH}_3\text{O P}(=\text{O})\text{Cl}_2$ and $\text{C}_2\text{H}_5\text{OP}(=\text{O})\text{Cl}_2$ vs mole % $\text{CDCl}_3/\text{CCl}_4$ (26).	312
8.77	Plots of ν COP rotational conformers 1 and 2 frequencies for $(\text{CH}_3\text{O})_3\text{P}=\text{O}$ vs mole % $\text{CHCl}_3/\text{CCl}_4$. The solid triangles represent conformer 1 and the solid circles represent conformer 2 (55).	312
8.78	A plot of ν COP frequencies for $(\text{CH}_3\text{O})_3\text{P}=\text{O}$ vs mole percent; $\text{CHCl}_3/\text{CCl}_4$ (55).	313
8.79	A plot of ν (ϕOP), " $\nu\phi\text{-O}$ ", frequencies for triphenyl phosphate vs mole % $\text{CHCl}_3/\text{CCl}_4$ (55).	313
8.80	A plot of ν (ϕOP), " $\nu\text{P-O}$ ", frequencies for triphenyl phosphate vs mole % $\text{CHCl}_3/\text{CCl}_4$ (55).	314
8.81	A plot of the in-plane hydrogen deformation frequencies for the phenyl groups of triphenyl phosphate vs mole % $\text{CHCl}_3/\text{CCl}_4$ (55).	314
8.82	A plot of the out-of-plane ring deformation frequencies for the phenyl groups of triphenyl phosphate vs mole % $\text{CHCl}_3/\text{CCl}_4$ (55).	315
8.83	A plot of ν CD frequencies (for the solvent system $\text{CDCl}_3/\text{CCl}_4$) vs mole % $\text{CDCl}_3/\text{CCl}_4$ (55).	315
8.84	A plot of the ν CD frequencies for CDCl_3 vs mole % $\text{CDCl}_3/\text{CCl}_4$ for the $\text{CDCl}_3/\text{CCl}_4$ solvent system containing 1 wt./vol. % triphenylphosphate (55).	316
8.85	A plot of ν CD for CDCl_3 vs mole % $\text{CDCl}_3/\text{CCl}_4$.	316
8.86	A plot of ν CD for CDCl_3 vs mole % $\text{CDCl}_3/\text{CCl}_4$ containing 1% triethylphosphate.	317

CHAPTER 9

9.1	Infrared spectrum for 2,3,4,5,6-pentachlorobiphenyl.	368
9.2	Infrared spectrum for 2,2',3-trichlorobiphenyl.	368
9.3	Infrared spectrum for 2',3,4-trichlorobiphenyl.	369
9.4	Infrared spectrum for 2,2',3,4,6-pentachlorobiphenyl.	369
9.5	Infrared spectrum for 2,3,4,4',6-pentachlorobiphenyl.	370
9.6	Infrared spectrum for 2,3',4,5',6-pentachlorobiphenyl.	370
9.7	Infrared spectrum for 2,2',3',4,5-pentachlorobiphenyl.	371
9.8	Infrared spectrum for 2,2',4,6,6'-pentachlorobiphenyl.	371
9.9	Infrared spectrum for 2,3',4,4',6-pentachlorobiphenyl.	372
9.10	Infrared spectrum for 2,2',3,4',6-pentachlorobiphenyl.	372
9.11	Infrared spectrum for 2,2',3,5',6-pentachlorobiphenyl.	373
9.12	Infrared spectrum for 2,2',3,4',5-pentachlorobiphenyl.	373
9.13	Infrared spectrum for 2,2',3,5,5'-pentachlorobiphenyl.	374
9.14	Infrared spectrum for 2,2',4,4',5-pentachlorobiphenyl.	374
9.15	Infrared spectrum for 2,2',4,5,5'-pentachlorobiphenyl.	375
9.16	Infrared spectrum for 2,2',3,4,5'-pentachlorobiphenyl.	375
9.17	A plot of an A_1 fundamental for mono-substituted benzenes vs the number of protons on the ring α -carbon atom.	376

- 9.18 A plot of an A_1 fundamental for mono-substituted benzenes vs Tafts σ^* . 377
- 9.19 An IR spectrum for a uniaxially stretched syndiotactic polystyrene film (perpendicular polarization). 378
- 9.20 An IR spectrum for a uniaxially stretched syndiotactic polystyrene film (parallel polarization). 378
- 9.21 An IR spectrum of syndiotactic polystyrene film cast from boiling 1,2-dichlorobenzene onto a KBr plate. 379
- 9.22 An IR spectrum of the same film used to record the IR spectrum shown in Fig. 9.21 except that the film was heated to 290 °C then allowed to cool to ambient temperature before recording the IR spectrum of syndiotactic polystyrene. 380
- 9.23 An IR spectrum syndiotactic styrene (98%)-4-methylstyrene (2%) copolymer cast from boiling 1,2-dichlorobenzene onto a CsI plate. 381
- 9.24 An IR spectrum of a styrene (93%)-4-methylstyrene (7%) copolymer cast from boiling 1,2-dichlorobenzene onto a CsI plate. 382
- 9.25 A plot of the IR band intensity ratio $A(1511\text{ cm}^{-1})/A(900\text{--}904\text{ cm}^{-1})$ vs the weight % 4-methylstyrene in styrene-4-methylstyrene copolymers. 383
- 9.26 A plot of the IR band intensity ratio $A(815\text{--}817\text{ cm}^{-1})/A(900\text{--}904\text{ cm}^{-1})$ vs the weight % 4-methylstyrene in styrene-4-methylstyrene copolymers. 384
- 9.27 Top: Infrared spectrum of styrene (92%) -acrylic acid (8%) copolymer recorded at 35 °C. Bottom: Infrared spectrum of styrene (92%) -acrylic acid (8%) copolymer recorded at 300 °C. 385
- 9.28 Styrene (92%) -acrylic acid (8%) copolymer absorbance ratios at the indicated frequencies vs copolymer film temperatures in °C; R_1 , R_2 , and R_4 indicate an increase in CO_2H concentrations at temperatures > 150 °C; R_3 and R_5 indicate a decrease in $(CO_2H)_2$ concentrations at > 150 °C. Base line tangents were drawn from 1630–1780 cm^{-1} , 1560–1630 cm^{-1} and 720–800 cm^{-1} in order to measure the absorbance values at 1746 cm^{-1} and 1700 cm^{-1} , 1600 cm^{-1} and 752 cm^{-1} , respectively. 386
- 9.29 Top: Infrared spectrum of styrene-acrylamide copolymer recorded at 27 °C. Bottom: Infrared spectrum of styrene-acrylamide copolymer recorded at 275 °C. 387
- 9.30 An IR spectrum for a styrene-2-isopropenyl-2-oxazoline copolymer (SIPO) cast from methylene chloride onto a KBr plate. 388
- 9.31 A plot of the weight % IPO in the SIPO copolymer vs the absorbance ratio $(A)(1656\text{ cm}^{-1})/(A)(1600\text{ cm}^{-1})$. 388
- 9.32 Top: Vapor-phase IR spectrum of ethynylbenzene in a 4-m cell (vapor pressure is in an equilibrium with the liquid at 25 °C). Bottom: Vapor-phase IR spectrum of ethynylbenzene-d in a 4-m cell (vapor pressure is in an equilibrium with the liquid at 25 °C). 389
- 9.33 Top: An IR solution spectrum for ethynylbenzene (3800–1333 cm^{-1} in CCl_4 (0.5 M) solution in a 0.1 mm NaCl cell), (1333–450 cm^{-1} in CS_2 (0.5 M) solution in a 0.1 mm KBr cell), and in hexane (0.5 M) solution using a 2 mm cis I cell. The IR band at 1546 and 853 cm^{-1} is due to the solvents. Bottom: An IR solution spectrum for ethynylbenzene-d recorded under the same conditions used to record the top spectrum. 390

- 9.34 Top: Liquid-phase IR spectrum ethynylbenzene between KBr plates in the region 3800–450 cm^{-1} , and between C_6I plates in the region 450–300 cm^{-1} . Bottom: Liquid-phase IR spectrum of ethynylbenzene-d recorded under the same conditions as the top spectrum. 391
- 9.35 Top: Raman spectra for ethynylbenzene in the liquid phase. Bottom: Raman spectra for ethynylbenzene-d in the liquid phase. 392
- 9.36 A correlation chart for substituted benzenes in the region 5–6 μ (after Young, DuVall, and Wright). 393
- 9.37 Summary of out-of-plane hydrogen deformations and their combination and overtones for mono-substituted benzenes. 394
- 9.38 Summary of out-of-plane hydrogen deformations and their combination and overtones for 1,2-disubstituted benzenes. 395
- 9.39 Summary of out-of-plane hydrogen deformations and their combination and overtones for 1,3-disubstituted benzenes. 396
- 9.40 Summary of out-of-plane hydrogen deformations and their combination and overtones for 1,4-disubstituted benzenes. 397
- 9.41 Summary of out-of-plane hydrogen deformations and their combination and overtones for 1,3,5-trisubstituted benzenes. 398
- 9.42 Summary of out-of-plane hydrogen deformations and their combination and overtones for 1,2,3-trisubstituted benzenes. 399
- 9.43 Summary of out-of-plane hydrogen deformations and their combination and overtones for 1,2,4-trisubstituted benzenes. 399
- 9.44 Summary of out-of-plane hydrogen deformations and their combination and overtones for 1,2,3,4-tetrasubstituted benzenes. 400
- 9.45 Summary for out-of-plane hydrogen deformations and their combination and overtones for 1,2,3,5-tetrasubstituted benzenes. 400
- 9.46 Summary of out-of-plane hydrogen deformations and their combination and overtones for 1,2,4,5-tetrasubstituted benzenes. 401
- 9.47 Summary of out-of-plane hydrogen deformation and its first overtone for 1,2,3,4,5-pentasubstituted benzenes. 401
- 9.48 Infrared correlation chart for out-of-plane hydrogen deformations and their combination and overtones for substituted benzenes. 402

CHAPTER 11

- 11.1 A plot of the NMR δ ^{13}C -1 chemical shift data for 4-x-anilines in CHCl_3 solution vs Hammett σ_p values for the 4-x atom or group. 459
- 11.2 A plot of the NMR δ ^{13}C -1 chemical shift data for 4-x-anilines in CHCl_3 solution vs Taft σ_{R^e} values for the 4-x atom or group. 460
- 11.3 A plot of ν asym. NH_2 frequencies for 4-x-anilines in the vapor phase vs δ ^{13}C -1 chemical shift data for 4-x-anilines in CHCl_3 solution. 461
- 11.4 A plot of ν asym. NH_2 frequencies for 3-x- and 4-x-anilines in hexane solution vs δ ^{13}C -1 chemical shift data for 3-x- and 4-x-anilines in CHCl_3 solution. 462

- 11.5 A plot of ν asym. NH_2 frequencies for 3-x- and 4-x-anilines in CCl_4 solution vs $\delta^{13}\text{C}$ -1 chemical shift data for 3-x- and 4-x-anilines in CHCl_3 solution. 463
- 11.6 A plot of the ν asym. NH_2 frequencies for 3-x- and 4-x-anilines in CHCl_3 solution vs $\delta^{13}\text{C}$ -1 chemical shift data for 3-x- and 4-x-anilines in CHCl_3 solution. 464
- 11.7 A plot of the ν sym. NH_2 frequencies for 4-x-anilines in the vapor phase vs $\delta^{13}\text{C}$ -1 chemical shift data for 3-x- and 4-x-anilines. 465
- 11.8 A plot of ν sym. NH_2 frequencies for 3-x- and 4-x-anilines in hexane solution vs $\delta^{13}\text{C}$ -1 chemical shift data for 3-x- and 4-x-anilines in CHCl_3 solution. 466
- 11.9 A plot of ν sym. NH_2 frequencies for 3-x- and 4-x-anilines in CCl_4 solution vs $\delta^{13}\text{C}$ -1 chemical shift data for 3-x- and 4-x-anilines vs the $\delta^{13}\text{C}$ -1 chemical shift data for 3-x- and 4-x-anilines in CHCl_3 solution. 467
- 11.10 A plot of the ν sym. NH_2 frequencies for 3-x- and 4-x-anilines in CHCl_3 solution vs $\delta^{13}\text{C}$ -1 chemical shift data for 3-x- and 4-x-anilines in CHCl_3 solution. 468
- 11.11 A plot of the frequency difference between ν asym. NH_2 and ν sym. NH_2 for 3-x- and 4-x-anilines in hexane solution vs $\delta^{13}\text{C}$ -1 chemical shift data for 3-x- and 4-x-anilines in CHCl_3 solution. 469
- 11.12 A plot of the frequency difference between ν asym. NH_2 and ν sym. NH_2 for 3-x- and 4-x-anilines in CCl_4 solution vs $\delta^{13}\text{C}$ -1 chemical shift data for 3-x- and 4-x-anilines in CHCl_3 solution. 470
- 11.13 A plot of the frequency difference between ν asym. NH_2 and ν sym. NH_2 for 3-x- and 4-x-anilines in CHCl_4 solution vs $\delta^{13}\text{C}$ -1 chemical shift data for 3-x- and 4-x-anilines in CHCl_3 solution. 471
- 11.1.4 A plot of the absorbance ratio $A(\nu \text{ asym. } \text{NH}_2)/A(\nu \text{ sym. } \text{NH}_2)$ for 3-x- and 4-x-anilines in CCl_4 solution vs $\delta^{13}\text{C}$ -1 chemical shift data for 3-x- and 4-x-anilines in CHCl_3 solution. 472
- 11.1.5 A plot of $\delta^{13}\text{C}$ -1 chemical shift data for 4-x-anilines in CHCl_3 solution vs Taft σ_{R} values for the 4-x atom or group. 473
- 11.16 A plot of $\delta^{13}\text{C}$ -1 for 3-x- and 4-x-benzoic acids vs Hammett σ values for the x atom or group. 474
- 11.17 Plots of $\nu \text{ C=O}$ vs Hammett σ values of 3-x- and 4-x-benzoic acids. The solid circles are for IR data in the vapor phase. The open circles are for IR dilute solution data for unassociated 3-x- and 4-x-benzoic acids. 475
- 11.18 Plots of $\nu \text{ C=O}$ vs $\delta^{13}\text{C}$ -1 for 3-x- and 4-x-benzoic acids. The NMR data are for CDCl_3 solutions. The plot with closed circles includes vapor-phase IR data. The plot with open circles includes IR CCl_4 -solution data. 476
- 11.19 A plot of $\delta^{13}\text{C}$ -1 for 4-x-acetanilides in CDCl_3 solution vs Hammett σ_{p} values for the x-atom or group. 477
- 11.20 A plot of $\nu \text{ C=O}$ for 4-x-acetanilides vs Hammett σ_{p} values. The solid circles represent IR CCl_4 solution data and the solid squares IR CHCl_3 solution data. 478
- 11.21 A plot of $\delta^{13}\text{C}$ -1 for 4-x-benzaldehydes vs Taft σ_{R} values for the 4-x atom or group. 479
- 11.22 A plot of $\nu \text{ C=O}$ for 4-x-benzaldehydes vs Taft σ_{R} values for the 4-x atom or group. The solid circles represent IR data in CCl_4 solutions and the solid triangles represent IR data in CHCl_3 solutions. 480

- 11.23 A plot of ν C=O for 4-x-benzaldehydes vs Hammett σ_p values for the 4-x atom or group. The solid circles represent IR data in CCl_4 solution and the solid triangles IR data in CHCl_3 solutions. 481
- 11.24 Plots of ν C=O vs $\delta^{13}\text{C}-1$ for 4-x-benzaldehydes. The $\delta^{13}\text{C}-1$ data are for CDCl_3 solutions. The plot with filled-in circles includes IR CCl_4 solution data and the plot with the filled-in triangles includes IR CHCl_3 solution data. 482
- 11.25 A plot of $\delta^{13}\text{C}-1$ for 4-x-acetophenones in CDCl_3 solutions vs Taft σ_{R^o} values for the 4-x atom or groups. 483
- 11.26 A plot of ν C=O for 4-x-acetophenones vs Taft σ_{R^o} values for the 4-x atom or group. The IR data is that for the 4-x-acetophenones in CHCl_3 solution. 484
- 11.27 A plot of ν C=O (CHCl_3 solution) vs $\delta^{13}\text{C}-1$ (CDCl_3 solution) for 4-x-acetophenones. 485
- 11.28 A plot of $\delta^{13}\text{C}-1$ vs Taft σ_{R^o} values for the 4-x and 4,4'-x,x atoms or groups for 4-x and 4,4'-x,x-benophenones. These data are for CHCl_3 solutions. 486
- 11.29 A plot of ν C=O in the vapor phase vs $\delta^{13}\text{C}-1$ in CCl_3 solution for 4-x and 4,4'-x,x-benzophenones. 487
- 11.30 A plot of ν C=O in the vapor phase vs the sum of Hammett σ_p for the x-atom or group for 4-x- and 4,4'-x,x-benzophenones. 488
- 11.31 A plot of $\delta^{13}\text{C}-1$ in CHCl_3 solution vs Hammett σ values for the x atom or group for methyl and ethyl 3-x- and 4-x-benzoates. 489
- 11.32 Plots of the range of ν C=O for the compounds studied in different physical phases vs the range of $\delta^{13}\text{C}=\text{O}$ for the compounds studied in CHCl_3 solutions. 490
- 11.33 A plot of $\delta^{13}\text{C}=\text{O}$ for acetone vs mole % $\text{CHCl}_3/\text{CCl}_4$ solutions. 491
- 11.34 A plot of ν C=O vs $\delta^{13}\text{C}=\text{O}$ for acetone in mole % $\text{CHCl}_3/\text{CCl}_4$ solutions. 492
- 11.35 A plot of ν C=O for dimethylacetamide in CCl_4 and/or CHCl_3 solution vs mole % $\text{CHCl}_3/\text{CCl}_4$. 493
- 11.35a A plot of $\delta^{13}\text{C}=\text{O}$ for dimethylacetamide in CCl_4 and/or CHCl_3 solution vs mole % $\text{CHCl}_3/\text{CCl}_4$. 493
- 11.35b A plot of $\delta^{13}\text{C}=\text{O}$ for maleic anhydride vs mole % $\text{CHCl}_3/\text{CCl}_4$. 494
- 11.35c A plot of $\delta^{13}\text{C}=\text{O}$ vs $\delta^{13}\text{C}=\text{C}$ for maleic anhydride in 0 to 100 mole % $\text{CHCl}_3/\text{CCl}_4$ solutions. 494
- 11.36 A plot of $\delta^{13}\text{C}-1$ vs Taft σ_{R^o} values for the 3-x and 4-x atom or group for 3-x- and 4-x-benzonitriles in CDCl_3 solution. 495
- 11.37 A plot of $\delta^{13}\text{C}-1$ vs Hammett σ values for the 3-x or 4-x atom or group for 3-x- and 4-x-benzonitriles in CHCl_3 solution. 496
- 11.38 A plot of $\delta^{13}\text{CN}$ vs Hammett σ values for the 3-x or 4-x atom or group for 3-x- and 4-x-benzonitriles in CHCl_3 solution. 497
- 11.39 A plot of ν CN vs $\delta^{13}\text{CN}$ for organonitriles. 498
- 11.40 A plot of $\delta^{13}\text{CN}$ vs the number of protons on the -carbon atom of alkyl nitriles. 498
- 11.41 A plot of Taft σ^* values for the alkyl group vs $\delta^{15}\text{N}$ for alkyl isonitriles. 499
- 11.42 A plot of $\delta^{15}\text{N}$ vs ν NC for alkyl isonitriles. 500
- 11.43 Plots of the number of protons in the alkyl α -carbon atom vs ν sym. NO_2 and ν asym. NO_2 for nitroalkanes in the vapor phase. 501
- 11.44 Plots of $\delta^{13}\text{C}$ (CHCl_3 solution) for the alkyl α -carbon atom vs ν sym. NO_2 and ν asym. NO_2 (vapor phase) for nitroalkanes. 502

11.45	Plots of $\delta^{15}\text{N}$ (in 0.3 M acetone) vs ν sym. NO_2 and ν asym. NO_2 (vapor phase) for nitroalkanes.	503
11.46	A plot of Taft σ^* values for the alkyl α -carbon atom group vs $\delta^{13}\text{C}$ for nitroalkanes.	504
11.47	A plot of Taft σ^* values for the alkyl α -carbon atom vs $\delta^{15}\text{N}$ for nitroalkanes.	505
11.48	A plot of $\delta^{15}\text{N}$ vs $\delta^{13}\text{C}$ for the alkyl α -carbon atom for nitroalkanes.	506
11.49	A plot of $\delta^{15}\text{N}$ vs ν asym. $\text{N}=\text{C}=\text{O}$ for alkyl isocyanates.	507
11.50	Plots of Taft σ^* values for the alkyl groups for alkyl isocyanates and alkyl isothiocyanates.	508
11.51	Plots of $\delta^{13}\text{C}$ for the $\text{N}=\text{C}=\text{O}$ group vs the number of protons on the alkyl α -carbon atom for alkyl isocyanates and alkyl diisocyanates.	509
11.52	Plots of ν asym. $\text{N}=\text{C}=\text{O}$ vs $\delta^{13}\text{C}$ for the $\text{N}=\text{C}=\text{O}$ group of alkyl isocyanates and alkyl diisocyanates.	509
11.53	A plot of $\delta^{15}\text{N}$ vs ν $\text{C}-\text{N}$ for primary alkylamines.	510
11.54	A plot of $\delta^{15}\text{N}$ vs $\omega\text{N}-\text{H}$ for dialkylamines.	511
11.55	A plot of ν $\text{C}-\text{N}$ vs Taft σ^* for the alkyl group of primary alkylamines.	512
11.56	A plot of $\delta^{15}\text{N}$ vs Taft σ^* for the alkyl group of primary alkylamines.	513
11.57	Plots of $\delta^{15}\text{N}$ vs the number of protons on the alkyl α -carbon atom(s) for mono-, di-, and trialkylamines.	514
11.58	A plot of $\delta^{31}\text{P}$ for trialkylphosphines vs the sum of the number of protons on the alkyl α - $\text{C}-\text{P}$ carbon atoms.	515
11.59	A plot of $\delta^{31}\text{P}$ for trialkylphosphines vs Taft σ^* values for the alkyl groups.	516
11.60	Plots of $\delta^{31}\text{P}$ for $\text{R}-\text{PH}_2$ vs $\delta^{15}\text{N}$ for $\text{R}-\text{NH}_2$, $\delta^{31}\text{P}$ for $(\text{R}-)_2\text{PH}$ vs $\delta^{15}\text{N}$ for $(\text{R}-)_2\text{NH}$, and $\delta^{31}\text{P}$ for $(\text{R}-)_3\text{P}$ vs $\delta^{15}\text{N}$ for $(\text{R}-)_3\text{N}$.	517
11.61	Plots of the number of protons on the α - $\text{C}-\text{P}$ atom(s) vs $\delta^{31}\text{P}$ for PH_3 , $\text{R}-\text{PH}_2$, $(\text{R}-)_2\text{PH}$.	518
11.62	A plot of the sum of Taft σ^* values $\delta^{31}\text{P}$ for trialkylphosphine oxides.	519
11.63	A plot of the sum of the number of protons on the α $\text{C}-\text{P}$ carbon atoms vs $\delta^{31}\text{P}$ for trialkylphosphine oxides.	520
11.64	Plots of ν $\text{P}=\text{O}$ rotational conformers vs the sum of the number of protons on the α - $\text{C}-\text{O}-\text{P}$ carbon atoms for trialkyl phosphates.	521
11.65	Plots of ν $\text{P}=\text{O}$ rotational conformers vs $\delta^{31}\text{P}$ for trialkyl phosphates.	522
11.66	A plot of $\delta^{31}\text{P}$ vs the sum of the number of protons on the α - $\text{C}-\text{O}-\text{P}$ carbon atoms for trialkyl phosphates.	523
11.67	A plot of the sum of the protons on the α - $\text{C}-\text{O}-\text{P}$ carbon atoms vs $\delta^{31}\text{P}$ for O,O,O-trialkyl phosphorothioates.	524
11.68	A plot of the sum of the number of protons on the α - $\text{C}-\text{O}-\text{P}$ carbon atoms vs $\delta^{31}\text{P}$ for O,O,O-trialkyl phosphoroselenates.	525
11.69	Plots of $\delta^{31}\text{P}$ vs the sum of the number of protons on the α - $\text{C}-\text{P}$ carbon atoms and the α - $\text{C}-\text{O}-\text{P}$ carbon atoms for $\text{RP}(=\text{O})(\text{OC}_2\text{H}_5)_2$ and $(\text{R})_2\text{P}(=\text{O})(\text{OR})$.	526
11.70	Plots of $\delta^{31}\text{P}$ for $\text{RP}(=\text{O})(\text{OC}_2\text{H}_5)_2$ vs $\delta^{13}\text{C}=\text{O}$ for $\text{RC}(=\text{O})(\text{OCH}_3)$ and $\delta^{31}\text{P}$ for $\text{CH}_3\text{P}(=\text{O})(\text{OR})_2$ vs $\delta^{13}\text{C}=\text{O}$ for $\text{CH}_3\text{C}(=\text{O})(\text{OR})$.	527
11.71	Plots of $\delta^{31}\text{P}$ for $(\text{RO})_2\text{P}(=\text{O})\text{H}$ and for $(\text{RO})_2\text{P}(=\text{S})\text{H}$ vs the sum of the protons on the α - $\text{C}-\text{O}-\text{P}$ carbon atoms.	528

- 11.72 A plot of $\delta^{31}\text{P}$ for $(\text{RO})_2\text{P}(=\text{O})\text{H}$ analogs vs $\delta^{31}\text{P}$ for the corresponding $(\text{RO})_2\text{P}(=\text{S})\text{H}$ alkyl analogs. 529
- 11.73 Plots of the number of protons on the α -CP carbon atoms vs $\delta^{31}\text{P}$ for $\text{RP}(=\text{O})\text{Cl}_2$ and $\text{RP}(=\text{S})\text{Cl}_2$. 530
- 11.74 A plot of $\delta^{31}\text{P}$ for $\text{RP}(=\text{S})\text{Cl}_2$ vs $\delta^{31}\text{P}$ for $\text{RP}(=\text{O})\text{Cl}_2$. 531
- 11.75 A plot of $\delta^{31}\text{P}$ vs the number of protons on the α -C-P carbon atom for $\text{RP}(=\text{O})\text{F}_2$. 532
- 11.76 A plot of $\delta^{31}\text{P}$ vs the sum of the number of protons on the α -C-P carbon atom and the number of protons on the α -C-O-P carbon atom for $\text{RP}(=\text{S})\text{Br}(\text{OC}_3\text{H}_{7\text{-iso}})$. 533
- 11.77 Plots of $\delta^{31}\text{P}$ vs the number of chlorine atoms joined to phosphorus for $\text{PCl}_{3-x}(\text{OR})_x$. 534
- 11.78 Plots of the sum of the number of protons on the α -C-P carbon atom(s) vs $\delta^{31}\text{P}$ for $\text{PX}_{3-n}\text{R}_n$. 535
- 11.79 A plot of $\delta^{31}\text{P}$ vs the number of protons on the α -C-O-P carbon atoms for $(\text{R})_2\text{P}(=\text{O})\text{Cl}_2$. 536
- 11.80 Plots of the number of Cl atoms joined to phosphorus vs $\nu \text{P}=\text{O}$ and $\nu \text{P}=\text{O}$ rotational conformers for $\text{P}(=\text{O})\text{Cl}_3$ through $\text{P}(=\text{O})\text{Cl}_{3-x}(\text{OR})_x$ where R is CH_3 or C_2H_5 . 537
- 11.81 A plot of the number of Cl atoms joined to phosphorus vs $\nu \text{P}=\text{O}$ for $\text{P}(=\text{O})\text{Cl}_{3-x}[\text{N}(\text{CH}_3)_2]_x$. 538
- 11.82 A plot of $\delta^{31}\text{P}$ for $\text{P}(=\text{S})(\text{OR})_3$ vs $\delta^{31}\text{P}$ for the corresponding alkyl analogs of $\text{P}(=\text{O})(\text{OR})_3$. 539
- 11.83 A plot of $\delta^{31}\text{P}$ for $\text{P}(=\text{Se})(\text{OR})_3$ vs $\delta^{31}\text{P}$ for corresponding alkyl analogs of $\text{P}(=\text{O})(\text{OR})_3$. 540
- 11.84 Plots of $\delta^{31}\text{P}$ for $\text{RP}(=\text{O})\text{Cl}_2$ vs $\delta^{31}\text{P}$ for corresponding alkyl analogs of $\text{RP}(\text{O})\text{F}_2$. The double plot is the $\delta^{31}\text{P}$ range given in the literature for the $\text{RP}(=\text{O})\text{Cl}_2$ analogs. 541
- 11.85 A plot of ν asym. ϕ -O-C vs $\delta^{13}\text{C-1}$ for 4-x-anisoles. 542
- 11.86 A plot of $\delta^{13}\text{C-1}$ vs Taft σ_{R° for 3-x- and 4-x-anisoles. 543
- 11.87 A plot of $\delta^{13}\text{C-1}$ vs Hammett σ values for 3-x^v and 4-x-anisoles. 544
- 11.88 A plot of Taft σ_{R° values vs $\sigma^{13}\text{C-1}$ for 4-x-anisoles. 544
- 11.89 A plot of Taft σ_{R° values vs ν asym. ϕ -O-C for 4-x-anisoles. 545
- 11.90 A plot of $\delta^{13}\text{C-1}$ vs Hammett σ_{p} values for 4-x-anisoles. 545
- 11.91 A plot of $\delta^{13}\text{C-1}$ vs $\delta^{13}\text{C-5}$ for 2-x-anisoles. 546
- 11.92 A plot of $\delta^{13}\text{C-4}$ for mono-substituted benzenes vs Taft σ_{R° values. 547
- 11.93 A plot of the out-of-plane hydrogen deformation mode I for mono-substituted benzenes vs Taft σ_{R° values. 548
- 11.94 A plot of the out-of-plane hydrogen deformation mode III for mono-substituted benzenes vs Taft σ_{R° values. 549
- 11.95 A plot of the out-of-plane hydrogen deformation mode I for mono-substituted benzenes vs $\delta^{13}\text{C-4}$ for mono-substituted benzenes. 550
- 11.96 A plot of the out-of-plane hydrogen deformation mode III vs $\delta^{13}\text{C-4}$ for mono-substituted benzenes. 551
- 11.97 A plot of $\delta^{13}\text{C-1}$ vs Taft σ_{R° values for 4-x and 4,4'-x,x-biphenyls. 552

- 11.98 A plot of $\delta^{13}\text{C}=\text{O}$ for tetramethylurea (TMU) 1 wt./vol. % solutions vs mole % $\text{CHCl}_3/\text{CCl}_4$. 552
- 11.99 A plot of $\nu \text{C}=\text{O}$ vs $\delta^{13}\text{C}=\text{O}$ for TMU 0–100 mol % $\text{CHCl}_3/\text{CCl}_4$ solutions. 553
- 11.100 A plot of $\delta^{13}\text{C}=\text{O}$ vs $\delta^{13}\text{CH}_3$ for TMU in 0–100 mol % $\text{CHCl}_3/\text{CCl}_4$ solutions. 554
- 11.101 A plot of $\delta^{13}\text{C}=\text{O}$ for TMU vs the solvent acceptor number (AN) for different solvents. 555
- 11.102 A plot of the $\delta^{13}\text{C}-\text{O}$ chemical shift difference between TMU in solution with acetic acid and in solution with each of the other solvents. 556
- 11.103 Plots of $\delta^{13}\text{C}=\text{O}$ for dialkylketones at 1 wt./vol. % in different solvents vs the AN for each solvent. 557
- 11.104 Plots of the $\delta^{13}\text{C}=\text{O}$ chemical shift difference between each dialkyl-ketone in methanol and the same dialkylketone in solution with each of the other solvents. 558
- 11.105 A plot of $\delta^{13}\text{C}=\text{O}$ for alkyl acetates and phenyl acetate vs the difference of $\delta^{13}\text{C}=\text{O}$ in methanol and $\delta^{13}\text{C}=\text{O}$ in each of the other solvents. 559

Name index

B

Bellamy, L. J., 31n16, 94n3, 185nn5, 9, 14, 458n13
Bender, P., 94n12
Bentley, F. K., 50n1, 94n2
Berger, S., 457n5
Berry, R. J., 128n10
Bigorne, M., 254n53
Black, F., 253n18
Blair, E. H., 253nn37, 39
Blake, B. H., 128n26
Bouquet, M., 94n28
Bouquet, S., 254n53
Brame, E. G., Jr., 31n15
Braun, S., 457n5
Breitmaier, E., 458n35
Brown, H. C., 458n33
Brownlee, R.T.C., 185n11

C

Camiade, M., 128n9
Chassaing, G., 94n28
Chittenden, R. A., 253n30
Chrisman, R. W., 367nn17, 21
Clark, J. W., 253nn7, 11, 33
Clark, R.J.H., 95n42
Coburn, W. C., Jr., 50n10
Cole, K. C., 50n5
Colthup, N. B., xvnn3, 10, 31n4, 94n4, 128n1, 254n49
Corbridge, D.E.C., 254n46
Corset, J., 94n28
Craver, C. D., 254n48
Cross, P. C., xvn2
Crutchfield, M. M., 458n28

D

Daasch, L. W., 254n54
Daly, L. H., xvn3, 31n4
Deady, L., 458n15
Decius, J. C., xvn2
de Haseth, J. A., xvn8
Delwaulle, M. L., 253nn2, 8, 12, 13, 15, 34
Detoni, S., 94n16
Di Yorio, J., 253n19

Dollish, F. R., 50n1, 94n2
Dunbar, J. E., 94n36, 253n31
Dungan, C. H., 458n28
Durig, J. R., 128n7, 253nn7, 11, 18, 19, 33
Du Vall, R. B., 367n2

E

Ekejiuba, I.O.C., 128n8
Erley, D. S., 128n26
Eucken, A., 253nn5, 14
Evans, J. C., 7n8, 69nn4, 7, 9, 10, 128nn13, 23, 367nn4,
5, 20, 431n10

F

Fassel, V. A., 50n8, 458n22
Fateley, W. G., xvnn10, 50n1, 94nn2, 4, 128n1, 254n49
Favort, J., 94n28
Fawcett, A. H., 94n18
Fee, S., 94n18
Fiedler, S. L., 6n4, 431nn2, 7
Folt, V. L., 128n4
Forel, M., 128n9
Formeris, R., 94n14, 253n6
Fouchea, H. A., 50n17
Francois, F., 253nn2, 8, 12, 13, 15, 34

G

Gaufres, R., 95n42
Geisler, G., 94n15, 185n4
George, W. O., 128n5
Gerding, H., 253n10
Glockler, G., 128n19
Goldman, G. K., 458n30
Goodfield, J. E., 128n5
Grasselli, J. G., xvnn10, 31n15, 94n4, 128n1, 254n49
Griffiths, P. R., xvn8
Gutowwsky, H. S., 253n3

H

Hadzi, D., 94n16
Hallam, H. E., 128n8

Ham, N. S., 50n12
 Hanai, K., 94nn17, 30, 31, 34
 Hanschmann, G., 94n15
 Hasha, D. L., 50nn14, 17, 457n4, 458n9
 Hellwege, K. H., 253nn5, 14
 Herrail, F., 253n38
 Herzberg, G., xvnl, 7n14, 50n15, 128n25, 254n45
 Hirschmann, R. P., 50n8, 458n22
 Hoffman, G. A., 50n17
 Hoyer, H., 50n11

I

Igarashi, M., 6n5, 7n6

J

Jeschek, G., 458nn12, 36
 Jewett, G. L., 458n24
 Johnson, A. L., 128n16
 Joshi, M., 94n29
 Joshi, U. C., 94n29
 Joyner, P., 128n19

K

Kabachnik, M. I., 70n15
 Kagel, R. O., xvnl2, 7n18, 69n2, 254n51, 367n9
 Kalasinsky, V. J., 128n10
 Kalinowski, H. O., 457n5
 Kallos, G. J., 7nn9, 10, 128nn14, 15, 431n11
 Kanesaki, I., 94n35
 Karriker, J. M., 128n7
 Katritzky, A. R., 458n15
 Kawai, K., 94n35
 Kesler, G., 185n4
 Killingsworth, R. B., 50n3
 King, S. T., 50n6, 254n47
 Kirrman, A., 50n2
 Kitaev, Yu. P., 50n4
 Klæboe, P., 31n6, 94n7
 Kloster-Jensen, E., 31n6
 Kniseley, R. N., 50n8, 458n22
 Koster, D. F., 50n9
 Krimm, S., 128n4

L

Lagemann, R. T., 94n13
 Landolt-Bornstein, I., 253nn5, 14
 Lau, C. L., 367n10
 Lehman, H., 458n30

Leugers, M. A., xvnl1, 31n5, 94nn9, 19, 95n39, 254n51, 367n13
 Levin, J. W., 253n18
 Liehr, A. D., 253n3
 Limougi, J., 94n28
 Lin-Vien, D., xvnl0, 94n4, 128n1, 254n49
 Little, T. S., 128n10
 Lo, Y.-S., 128nn16, 23, 431n10
 Loy, B. R., 367nn17, 21
 Lunn, W. H., 185n2
 Luoma, D. A., 31nn13, 14, 50n13, 185n6, 431nn3, 8, 457n7, 458nn10, 37

M

Machida, K., 94nn17, 30, 31, 33
 Maddams, W. F., 128n5
 Malanga, M., 367n16
 Mann, J. R., 70n16
 Mark, V., 458n28
 Martz, D. E., 94n13
 Mavel, G., 458n27
 Mayants, L. S., 70n15
 McLachlan, R. D., 7n11, 128n11, 367n13
 Mitsch, R. A., 50n6
 Muelder, W. W., 69n10, 253nn21, 22, 24, 27, 35, 254n43, 367n5

N

Nakamoto, K., xvnn13, 14
 Neely, W. B., 253n39
 Newman, M. S., 31nn8, 9, 11
 Nielsen, J. R., 185n3
 Nivorozhkin, L. E., 50n4
 Nyquist, R. A., xvnn5-7, 11, 12, 6nn2-4, 7nn7-13, 15, 16, 18, 19, 31nn1, 2, 5, 7, 12-14, 17, 50nn7, 13, 14, 16-19, 69nn1, 2, 4, 7, 70nn12-14, 16, 94nn1, 5, 6, 9-11, 19-27, 36, 95nn37, 39, 40, 43, 128nn2, 11-18, 22-24, 185nn1, 6-8, 253nn9, 16, 17, 21-27, 31, 32, 35-37, 39-41, 254nn42, 43, 47, 48, 50-52, 55, 367nn6, 7, 9, 11, 13-21, 431nn1-12, 457nn1, 2, 4, 6, 7, 458nn8-12, 17, 18, 24, 26, 29, 31, 34, 36-39

O

Ogden, P. H., 50n6
 Ogilvie, J. F., 50n5
 Okamoto, Y. J., 458n33
 Okuda, T., 94nn30, 34
 Osborne, D. W., 253n37
 Overend, J., 50n6, 69n10, 128n21, 367n5
 Owen, N. L., 7n20

P

Paetzold, R., 94n8
Pan, C. Y., 185n3
Pauling, L., 458n32
Peters, T. L., 50n7
Peterson, D. P., 367n7
Platt, A. E., 367n18
Plegontov, S. A., 50n4
Polo, S. R., 253nn1, 4
Popov, E. M., 70n15
Potts, W. J., Jr., xvn4, 6n1, 254n50, 458n31
Priddy, D. B., 367n18
Puehl, C. W., 50n16, 253n26, 254n55, 431n3
Putzig, C. L., xvn11, 6n2, 7n7, 31n5, 50nn13, 14, 94nn9,
19, 95n39, 128n12, 254n51, 367nn7, 13, 17,
431nn8, 9, 458n9

R

Raevskii, O. A., 50n4
Rao, C.N.R., 458nn14, 30
Reder, T. L., 7nn9, 10, 128n14, 431n11
Reid, C., 50n15
Rey-Lafon, M., 128n9
Ronsch, E., 94n8
Rothschild, W. G., 128n6
Rouffi, C., 128n9

S

Saito, T., 458n16
Saito, Y., 94nn32, 33
Scherer, J. R., 69nn9–11, 128n21, 367nn3–5
Schrader, B., 128
Schuetz, J. E., 367n19
Settineri, S. E., 31nn13, 14, 185nn6, 8, 431n12, 457n7
Shanks, R. A., 458n15
Sheppard, N., 7n20, 69n5
Shipman, J. J., 128n4
Simons, W. W., 69n3
Singh, R. N., 94n29
Skelly, N. E., 7n7, 128n12
Sloane, H. J., 94n36, 253n31
Smith, D. C., 185n3, 254n54
Snyder, R. G., 367n10
Socrates, G., xvn9
Sportouch, S., 95n42
Stammreich, H., 94n14, 253n6
Steaniak, L., 458nn19, 21, 25
Stec, F. F., 7n10, 128n15, 431n11
Stephenson, C. V., 50n10
Stojilykovic, A., 69n8
Streck, R., 458nn12, 36, 39
Strycker, S. J., 94n36, 253n31
Stuckey, M., 94n18

T

Taft, R. W., Jr., 185n10, 253n29, 367nn12, 22, 458n23
Takasuka, M., 458n16
Tanka, Y., 94nn32, 33
Tarte, P., 185n12
Tavares, Y., 94n14, 253n6
Thill, B., 367n13
Thomas, L. C., 253n30
Thompson, J. W., 128n18
Titova, S. Z., 50n4
Topsom, R. D., 185n11, 458n15
Tsubio, M., 254n44

U

Unger, I., 253n39
Uno/Ubo, T., 94nn17, 30, 31

V

Van Wazer, J. R., 458n28
Varsanyi, G., 367n1
Venkataraghavan, R., 458n14
Voelter, W., 458n35

W

Walkden, P., 94n18
Ward, G. R., 7n9, 128n14
Wass, M. N., 253nn22, 24
Webb, G. A., 458nn19, 21, 25
Wertz, D. M., 128n7
West, W., 50n3
Westrick, R., 253n10
Whiffen, D. H., 69n8
Wiberley, S. E., xvn3, 31n4
Wilcox, W. S., 50n10
Willis, J. B., 50n12
Wilson, E. B., Jr., xvn2
Wilson, M. K., 253nn1, 4
Winter, F., 128n20
Witanowski, M., 458nn19, 21, 25
Wood, J. M., Jr., 94n12
Wright, N., 367n2
Wurrey, C. J., 128n10
Wyckoff, R., 31n10

Y

Yamakawa, M., 458n16
Yeh, Y. Y., 128n10
Young, C. W., 367n2

Subject index

A

Acetamide, dimethyl, 445, 493, 568
Acetanilides, 4-x, 443, 477, 478, 562
Acetates, 456, 559, 579
Acetone, 445, 491, 492, 567
Acetonitrile, 28, 29, 32, 33, 35, 40
Acetophenones, 4-x, 444, 483–485, 564
Acrylates
 glycidyl, 4
 spectra structure correlations, 456–457, 579
Acrylonitrile, 27
Aliphatic ethers, 5–6, 22, 23
Aliphatic hydrocarbons, 426–427, 432
Alkanedithiols, 66
Alkanes
 dihaloalkanes, 123–124, 169
 1-haloalkanes, 121–122, 166
 2-haloalkanes, 122, 167
 halocycloalkanes, 121, 123, 168
 nitro, 174–176, 186, 187, 206, 207, 208, 209,
 447–448, 501–506
 phosphonic bromide, O-isopropyl, 533
 phosphonic dichloride, 530, 531
 phosphonic difluoride, 532, 541
 phosphonothioic dichloride, 530, 531, 541
 tetrabromoalkanes, 125, 170
Alkanethiols
 C–S stretching, 66
 rotational conformers, 66
 S–S stretching, 65–66, 74, 76–77
Alkanonitriles, 32
Alkylamines, 448–449, 510–513, 571
Alkyl isocyanates, 448, 507–509
Alkyl isonitriles, 447, 499, 500
Alkyl group
 joined to sulfur, oxygen, or halogen, 68–69, 81–83
 vibrations and solvent effects, 250–251
Amides, styrene-acrylamide copolymer, 359, 387
Amines, alkyl, 448–449, 510–513, 571
Anhydrides, 428, 434
 maleic, 446, 494, 569
Anilines
 4-x-, 441–442, 459–473, 560
 Nyquist rule, 427–428, 433
 sulfinyl, 93, 117

Anisoles, 5–6, 23
 spectra structure correlations, 453–454, 542–546, 574,
 575
Antisymmetric ring deformation, 2, 3, 11
Aromatic ethers, 5–6, 22, 23
Aryl-O stretching, 241, 338
Azines
 aldehyde, 46
 benzaldehyde, 46, 57
 empirical structures, 45
 Fermi resonance, 46
 inductive effect, 46
 ketone, 46

B

Benzaldehydes
 azine, 46, 57
 4-x, 443, 479–482, 563
Benzene-d₆, 361, 421
Benzenes
 See also under type of
 correlation chart, 366
 hexachlorobenzene, 366, 423
 in- and out-of plane vibrations, 353
 infrared data and assignments, 361, 421
 isotactic polystyrene, 355
 mono-substituted, 362, 393, 394, 402, 422, 423
 mono-substituted, spectra structure correlations, 454,
 547–551, 576
 out-of-plane deformations, 362–366
 pentabromophenyl ether, 361, 420
 pentachlorobiphenyl, 366, 423
 potential energy distribution and ring modes,
 354
 potential energy distribution and toluene, 355
 quantitative analyses, use of, 356–358
 styrene-4-methylstyrene copolymer, 355–358, 381,
 382
 toluene, 353, 355
Benzenes, disubstituted (out-of-plane hydrogen
 deformations)
 1,2-, 363–364, 393, 395, 402, 423
 1,3-, 364, 393, 396, 402, 423
 1,4-, 364, 393, 397, 402, 423

Benzenes, disubstituted (Raman data and vibrations)
 1,2-, Raman data and vibrations, 360, 419
 1,3-, Raman data and vibrations, 361, 419
 1,4-, Raman data and vibrations, 361, 420
 Benzenes, pentasubstituted (out-of-plane hydrogen deformations), 366, 393, 401, 402, 423
 Benzenes, tetrasubstituted (out-of-plane hydrogen deformations)
 1,2,3,4-, 365, 393, 400, 402, 423
 1,2,3,5-, 365, 393, 400, 402, 423
 1,2,4,5-, 365, 393, 401, 402, 423
 Benzenes, trisubstituted (out-of-plane hydrogen deformations)
 1,2,3-, 364–365, 393, 399, 402, 423
 1,2,4-, 365, 393, 399, 402, 423
 1,3,5-, 364, 393, 398, 402, 423
 Benzenethiols, 66, 74, 79
 chlorobenzenethiol, 67–68, 79
 Benzoates, alkyl 3-x and 4-x, 444, 489, 566
 Benzoic acids, 3-x and 4-x, 442–443, 474–476, 561
 Benzonitriles, 27, 29, 34, 40
 3-x and 4-x, 446, 495–497, 570
 Benzophenones, 444, 486–488, 565
 Benzoquinones, 428, 434
 Benzyl alcohol, 361, 421
 Benzyl-2,3,4,5,6-d₅ alcohol, 361, 421
 Biphenyls
 chlorinated, spectra structure correlations, 454, 552, 577
 decabromo, 361, 420
 diffuse reflectance, 354
 polychloro, 353–355
 Bromodichlorobenzenes, 360, 418
 Butyl halides, tertiary, 122–125, 167

C
 Carbodiimides, dialkyl and diaryl, 50, 63
 Carboxylic acid, styrene-acrylic acid copolymer, 358–359, 385
 C–C mode for C₂H₅OP group, 251
 C–D mode for CDCl₃ and CCl₄ solutions, 252, 316, 317, 359–360
 CD₃–PO₃²⁻, 247–248, 349
 Chlorobenzenethiol, 67–68, 79
 C–H mode, 359–360
 C=O group, summary of, 444–445, 490, 567
 COP group, 251–252
 C–O–P stretching, 241, 334–337
 C–P stretching, vC–P, 241–242, 338
 C–S stretching, alkanethiols, 66
 Cyanamides, dialkyl, 31
 Cyanobenzaldehyde, 29–30, 36, 41
 Cyanogen halides, 28, 39

Cyclic ethers, 5, 21

D

Dialkyl cyanamides, 31
 Dialkylketones, 455–456, 557, 558, 578
 steric factor, 456
 Dielectric constants, 86
 Diffuse reflectance infrared Fourier transform. *See* DRIFT
 Dimethylacetamide, 445, 493, 568
 Dimethyl ether, 5
 Dimethyl sulfoxide, 29
 1,4-diphenylbutadiyne, 429–430, 435
 Dipolar interaction, 3, 28
 Disulfides
 alkane, 66–67, 76–77, 78
 dialkyl, aryl alkyl, and diaryl, 67
 DRIFT (diffuse reflectance infrared Fourier transform) technique, 353, 354

E

Epibromohydrin, 3
 Epichlorohydrin, 3
 Epihalohydrins, 3, 17
 Epoxides, 1–4
 Epoxyalkanes, 2, 4
 Epoxybutane, 3, 12
 Epoxypropane, 125–126, 171
 Ethers
 aliphatic and aromatic, 5–6, 22, 23
 cyclic, 5, 21
 glycidyl, 4
 pentabromophenyl, 361
 vinyl, 6, 24–26
 Ethylene oxide, 1–2, 8, 15
 tetrachloro, 3
 trans, 3, 12
 Ethylenes, 125–126, 171
 chloro- (vinyl chloride), 125, 126
 fluoro- (vinyl fluoride), 125
 tetrahalo-, 126
 trichloro-, 126
 Ethyl nitrates, 183, 225
 Ethynylbenzene, 359–360, 389, 390, 391
 out-of-plane hydrogen deformations, 363
 Ethynylbenzene-d, 359–360, 389, 390, 391

F

Fermi resonance
 acetonitrile, 29
 azines, 46

carbodiimides, 50
 isocyanates, 47, 51
 isothiocyanates, 49
 nitroalkanes, 174
 nitrobenzenes, 177, 182
 nitropropane, 175
 styrene-acrylic acid copolymer, 358

Field effects
 correction, 49
 N,N-dimethylacetamide, 445
 isocyanates, 47
 nitrile, 30
 out-of-plane ring deformations, 252
 solvent system and P=O stretching, 248–249

1-Fluoro-2,4,5-trichlorobenzene, 345

G

Glycidyl acrylate, 4
 Glycidyl ethers, 4

H

1-haloalkanes, 121–122, 166
 2-haloalkanes, 122, 167
 Halogen, alkyl groups joined to, 68–69, 81–83
 Halogenated hydrocarbons
 ethylene, propyne, epoxypropane, and propadiene,
 125–126, 171
 1-haloalkanes, 121–122, 166
 2-haloalkanes, 122, 167
 halopropadienes, 127
 methanes, 120–121, 127, 164
 tertiary butyl halides, 122–125, 167
 Halopropadienes, 127, 429–430, 435
 Hammett σ_p values, 182
 Hexachlorobenzene, 366, 423
 Hydantoins, 428–429, 435
 Hydrogen bonding, intermolecular
 alkanethiols, 65, 66
 anhydrides, 428
 anilines, 427–428
 benzoquinones, 428
 N,N-dimethylacetamide, 445
 1,4-diphenylbutadiyne, 429–430
 1-halopropadiene, 429–430, 435
 hydantoins, 429
 hydrogenphosphonate, dialkyl and diphenyl, 240–241
 imides, 428
 methyl phenyl sulfone, 92–93
 nitrobenzaldehyde, 178–179
 nitrobenzenes, 178, 181, 430
 O-alkyl O-aryl N-methylphosphor amidate and
 N-methylphosphor amidothioate, 244

phosphoramidates, 247
 P=O stretching, 249
 styrene-acrylic acid copolymer, 358–359
 sulfonamides, 89
 trimethyl phosphate, 249–250

Hydrogen bonding, intramolecular
 benzenethiols, 66
 nitrile, 30
 2-X-nitrobenzenes, 180
 phosphorodithioates, 68
 secondary sulfonamides, 90
 sulfonyl fluorides, 91–92, 115

Hydrogen phosphonate, 528–529
 dialkyl and diphenyl, 240–241, 333

Hydrogen phosphonothioate, 528, 529

I

Imides, 428, 434

Inductive effects
 alkyl nitriles, 28
 alkyl nitrites, 184
 azines, 46
 carbodiimides, 50
 cyanogen halides, 28
 isocyanates, 47
 isothiocyanates, 49
 nitroalkanes, 174
 P-NHR, 244
 sulfonamides, secondary, 90
 sulfoxides, 86

Infrared spectra
 1-bromo-1-chloroethylene, 155
 1-bromopropadiene, 157
 1-bromopropadiene-1-d, 158
 1-bromopropyne, 154
 3-bromopropyne, 144
 3-bromopropyne-1-d, 149
 bromotrichloromethane, 140
 n-butyl nitrite, 201
 carbon tetrachloride, 136
 1-chloropropadiene, 156
 3-chloropropyne, 144
 3-chloropropyne-1-d, 146, 147
 chlorotrifluoromethane (Freon-13), 137
 1,3-dibromopropyne, 153
 1,1-dichloro-2,2-difluoroethylene, 162
 dichlorodifluoromethane (Freon-12), 138
 1,2-dichloroethane (ethylene dichloride), 141
 1,3-dichloropropyne, 151, 152
 diethyl deuterophosphonate, 275
 diethyl hydrogenphosphonate, 275
 dimethyl deuterophosphonate, 274
 dimethyl hydrogenphosphonate, 274

Infrared spectra (*continued*)

disodium methane- d_3 -phosphonate, 293, 294, 295
 disodium methanephosphonate, 293, 294, 295
 disodium n-octadecanephosphonate, 296
 ethylene oxide, 1, 8
 ethyl nitrate, 200
 ethynylbenzene, 389, 390, 391
 ethynylbenzene- d , 389, 390, 391
 3-fluoropropyne, 144
 halopropenes, 142, 143
 1-iodopropadiene, 157
 1-iodopropyne, 155
 3-iodopropyne, 145
 methyl bromide, 130
 methyl chloride, 129
 methylene bromide, 133
 methylene chloride, 132
 methyl iodide, 131
 methyl (methylthio) mercury, 72
 nitromethane, 188
 2-nitropropane, 189
 N-D, N-methyl phosphoramidodi chloridothioate, 282, 283
 N-methyl- d_3 phosphoramidodichlorido thioate, 281
 N-methyl phosphoramidodichlorido thioate, 280
 O-alkyl N,N'-diaryl phosphordiamido thioate, 285
 O-alkyl O-aryl N-alkylphosphoramido thioate, 285
 O-alkyl O-aryl phosphoramidothioate, 286
 O-alkyl O-aryl N-methylphosphor amidate, 283
 O-alkyl O-aryl N-methylphosphoramido thioate, 283
 O-ethyl-1,1- d_2 phosphorodichlorido thioate, 236, 264
 O-ethyl-2,2,2- d_3 phosphorodichlorido thioate, 236, 265
 O-ethyl phosphorodichloridothioate, 236, 263
 O-methyl- d_3 phosphorodichlorido-thioate, 259, 261
 O-methyl phosphorodichloridothioate, 236, 259, 260
 O,O-dialkyl phosphoramidothioate, 286
 O,O-diethyl N-methyl phosphoramido thioate, 289
 O,O-diethyl N-methyl phosphoramido thioate N-d, 289
 O,O-diethyl phosphoramidothioate, 288
 O,O-diethyl phosphoramidothioate N- d_2 , 288
 O,O-diethyl phosphorodithioic acid, 273
 O,O-dimethyl- d_6 O-(2,4,5-trichlorophenyl) phosphate, 292
 O,O-dimethyl- d_6 O-(2,4,5-trichloro phenyl) phosphorothioate, 292
 O,O-dimethyl- d_6 phosphorochlorido thioate, 267, 268
 O,O-dimethyl methylphosphoramido thioate, 287
 O,O-dimethyl methylphosphoramido thioate N- d_2 , 287
 O,O-dimethyl N-methyl phosphoramido thioate, 290

O,O-dimethyl O-(2,4,5-trichlorophenyl) phosphate, 291
 O,O-dimethyl O-(2,4,5-trichlorophenyl) phosphorothioate, 291
 O,O-dimethyl phosphorochloridothioate, 236-237, 266, 268, 273
 O,O-dimethyl phosphorodithioic acid, 273
 2,2',3,4',5-pentachlorobiphenyl, 373
 2,2',3,4,5'-pentachlorobiphenyl, 375
 2,2',3',4,5-pentachlorobiphenyl, 371
 2,2',3,4,6-pentachlorobiphenyl, 369
 2,2',3,4',6-pentachlorobiphenyl, 372
 2,2',3,5,5'-pentachlorobiphenyl, 374
 2,2',3,5',6-pentachlorobiphenyl, 373
 2,2',4,4',5-pentachlorobiphenyl, 374
 2,2',4,5,5'-pentachlorobiphenyl, 375
 2,2',4,6,6'-pentachlorobiphenyl, 371
 2,3,4,4',6-pentachlorobiphenyl, 370
 2,3',4,4',6-pentachlorobiphenyl, 372
 2,3,4,5,6-pentachlorobiphenyl, 368
 2,3',4,5',6-pentachlorobiphenyl, 370
 phosphonic dibromide (bromomethyl), 279
 phosphonic dichloride (chloromethyl), 277, 278, 279
 phosphorodithioates, 68, 71
 phosphoryl chloride, 257
 potassium dimethylphosphinate, 298
 propylene oxide, 2, 9
 S-methyl phosphorodichloridothioate, 239, 269, 331
 sodium diheptylphosphinate, 300
 sodium dimethylphosphinate, 297, 298
 sodium dioctylphosphinate, 300
 styrene-acrylamide copolymer, 387
 styrene-acrylic acid copolymer, 385
 styrene-2-isopropenyl-2-oxazoline copolymer, 388
 styrene-4-methylstyrene copolymer, 381, 382
 syndiotactic polystyrene, 378, 379, 380
 tetrafluoroethylene, 160
 tetrafluoromethane, 135
 tetrahydrofuran, 5, 14
 thiophosphoryl dichloride fluoride, 255, 256
 trans-1,2-dimethyl ethylene oxide, 3, 12
 2,2',3-trichlorobiphenyl, 368
 2',3,4-trichlorobiphenyl, 369
 trichloroethylene, 161
 trichlorofluoromethane (Freon-11), 139
 trichloromethane, 134
 1,1,2-trichloro-1,2,2-trifluoroethane, 163
 trimethyl phosphite, 271, 272
 Infrared spectra structure correlations
 acetamide, dimethyl, 445, 493, 568
 acetanilides, 4-x, 443, 477, 478, 562
 acetone, 445, 491, 492, 567
 acetophenones, 4-x, 444, 483-485, 564
 acrylates, 456-457, 579

- amines, alkyl, 448–449, 510–513, 571
anisoles, 453–454, 542–546, 574, 575
benzaldehydes, 4-x, 443, 479–482, 563
benzenes, mono-substituted, 454, 547–551, 576
benzoates, alkyl 3-x and 4-x, 444, 489, 566
benzoic acids, 3-x and 4-x, 442–443, 474–476, 561
benzonitriles, 3-x and 4-x, 446, 495–497, 570
benzophenones, 444, 486–488, 565
isocyanates, 448, 507–509
maleic anhydride, 446, 494, 569
methacrylates, 456–457, 579
organonitriles, 446–447, 498, 570
phosphates, trialkyl, 521, 522, 523, 539, 572
phosphoramidates, 538
phosphorodichloridate, monoalkyl, 537
tetramethylurea (TMU), 454–455, 553
Isocyanates, alkyl and aryl, 46–49, 51, 52, 53, 54, 58, 59, 60, 448, 507–509
Isonitriles, 37, 38
 alkyl, 30, 447, 499, 500
Isothiocyanates, alkyl and aryl, 49–50, 54, 55, 56, 61–62
- K**
Ketones, dialkyl, 455–456, 557, 558, 578
 steric factor, 456
- M**
Maleic anhydride, 446, 494, 569
Methanes, 120–121, 127, 164
 tetra, 120, 164
 tri, 120, 164
Methyl halides, 120
Methyl (methylthio) mercury, 69, 72, 73
- N**
NH₂ stretching, 359
Nitrates
 alkyl, 182–183, 224
 ethyl, 183, 225
Nitriles, 27–30, 39
 acetonitrile, 28, 29, 32, 33, 35, 40
 benzonitrile, 27, 29, 34, 40, 446, 495–497, 570
 field effect, 30
 Hammett σ values, 30
 intramolecular hydrogen bonding, 30
 isonitriles, 30, 37, 38, 447, 499, 500
 organonitriles, 30, 42, 446–447, 498, 570
Nitrites, alkyl, 183–184, 226
Nitroalkanes, 174–176, 186, 187, 206–209
 empirical correlations, 174
 ethyl nitrates versus, 183, 225
 (NO₂)₄, 176–177
 Raman data for, 184, 227
 spectra-structure correlations, 447–448, 501–506
 trans and gauche conformers, 175
 vapor versus liquid-phase data, 176
Nitrobenzaldehyde, 178–179, 214
Nitrobenzenes, 177–178, 209–213, 215, 221–222
 band intensity ratios, 180
 ethyl nitrates versus, 183, 225
 Hammett σ_p values, 182
 intermolecular hydrogen bonding, 178, 430
 non-coplanar, 181
 Nyquist rule, 430, 436
 Raman data for, 184, 228
 solvent effects on NO₂, 181
 2-X-, 180–181, 218, 219
 3-X-, 179–180, 216, 217
 4-X-, 181–182, 220, 223
Nitrogen compounds, summary of correlations, 449–450
Nitrosamines, 185, 230
NMR spectra structure correlations
 acetamide, dimethyl, 445, 493, 568
 acetanilides, 4-x, 443, 477, 478, 562
 acetates, 456, 559, 579
 acetone, 445, 491, 492, 567
 acetophenones, 4-x, 444, 483–485, 564
 acrylates, 456–457, 579
 alkyl isonitriles, 447, 499, 500
 amines, alkyl, 448–449, 510–513, 571
 anilines, 3-x and 4-x, 441–442, 459–473, 560
 anisoles, 453–454, 542–546, 574, 575
 benzaldehydes, 4-x, 443, 479–482, 563
 benzenes, mono-substituted, 454, 547–551, 576
 benzoates, alkyl 3-x and 4-x, 444, 489, 566
 benzoic acids, 3-x and 4-x, 442–443, 474–476, 561
 benzonitriles, 3-x and 4-x, 446, 495–497, 570
 benzophenones, 444, 486–488, 565
 biphenyls, chlorinated, 454, 552, 577
 hydrogen phosphonates, 528–529
 isocyanates, 448, 507–509
 isonitriles, 447, 499, 500
 ketones, dialkyl, 455–456, 557, 558, 578
 maleic anhydride, 446, 494, 569
 methacrylates, 456–457, 579
 nitroalkanes, 447–448, 501–506
 organonitriles, 446–447, 498, 570
 phosphates, trialkyl, 521, 522, 523, 539, 572
 phosphine oxides, trialkyl, 519, 520, 572
 phosphines, dialkyl, 517, 518
 phosphines, monoalkyl, 518
 phosphines, trialkyl, 515, 516, 517, 518
 phosphonates, 526–529
 phosphonic bromide, alkane O-isopropyl, 533
 phosphonic dichloride, alkane, 530, 531

- NMR spectra structure correlations (*continued*)
 phosphonic difluoride, alkane, 532, 541
 phosphonothioic dichloride, alkane, 530, 531, 541
 phosphoroselenates, trialkyl, 525, 540, 572
 phosphorothioates, trialkyl, 524, 539, 540, 572
 tetramethylurea (TMU), 454–455, 552–556, 577, 578
 thiophosphonothioic dichloride, alkane, 530, 531, 541
 N=S=O, 93
 Nyquist Frequency, defined, 425
 Nyquist Vibrational Group Frequency Rule
 aliphatic hydrocarbons, 426–427, 432
 anhydrides, 428, 434
 anilines, 427–428, 433
 benzoquinones, 428, 434
 CH₂X₂, 120
 defined, 425–426
 1,4-diphenylbutadiyne, 429–430, 435
 1-halopropadiene, 429–430, 435
 hydantoins, 428–429, 435
 imides, 428, 434
 nitrobenzenes, 430, 436
 SO₂ vibrations 87, 88, 89, 92–93, 426
 sulfates, 430–431, 437
 sulfonates, 430–431, 437
 sulfones, 430–431, 437
 sulfonyl chloride, 430–431, 437
- O**
 Organoisothiocyanates, 62
 Organonitriles, 30, 42, 446–447, 498, 570
 Organophosphorus compounds, 450–452, 515, 516, 541, 571, 572–573
 Organophosphorus halides, phosphorus halogen stretching for, 235, 321
 Organothiocyanates, 31, 43
 Oxirane, 4, 13, 20
 Oxygen, alkyl groups joined to, 68–69, 81–83
- P**
 PCl₃ and PCl₂ vibrations, 250
 P–Cl stretching, 237, 323
 Pentabromophenyl ether, 361, 420
 Pentachlorobiphenyl, 366, 423
 Phenetole, 5
 Phenoxarsine derivatives
 P=O and P=S stretching for, 238–239, 327
 sulfate and thiosulfate, 88–89, 109, 110
 Phenylacetylene. *See* Ethynylbenzene
 Phosphates
 trialkyl, 521, 522, 523, 539, 572
 trimethyl, 240, 331
 Phosphinate
 potassium, 248, 350
 sodium dialkyl, 248, 350
 sodium dimethyl, 248, 350
 Phosphine oxides, trialkyl, 519, 520, 572
 Phosphines
 dialkyl, 517, 518
 monoalkyl, 518
 trialkyl, 515, 516, 517, 518
 Phosphites
 dialkyl chloro, 534, 535
 monoalkyl dichloro, 534
 trialkyl, 534
 trimethyl, 240, 271, 272, 331, 332
 Phosphonates, 526–529
 hydrogen, 528, 529
 Phosphonothioate, hydrogen, 528, 529
 Phosphoramidates
 O-alkyl O-aryl N-methyl, 243–244, 283
 O-methyl O-(2,4,5-trichlorophenyl) N-alkyl, 245, 341
 O,O-diethyl N-alkyl, 247, 349
 spectra structure correlations, 538
 Phosphoramidodichlorodithioate, N-alkyl, 245, 343
 Phosphoramidodithioates
 O-alkyl O-aryl N-methyl, 243–244, 283
 primary, P(=S)NH₂, 244, 245, 340
 Phosphorochlorodithioate, O,O-dialkyl, 246, 346
 Phosphorodichloridate, monoalkyl, 537
 Phosphorodichlorodithioate
 O-alkyl, 247, 348
 O-ethyl, 236, 263
 O-ethyl-1,1-d₂, 236, 264
 O-ethyl-2,2,2-d₃, 236, 265
 O-methyl, 236, 259, 260
 O,O-dimethyl, 236–237, 266, 268, 273
 S-alkyl, 247, 348
 S-methyl, 239, 269, 331
 Phosphorodithioates, 68, 71, 80
 Phosphoroselenates, trialkyl, 525, 540, 572
 Phosphorothioates
 O,O-dimethyl O-(2,4,5-trichlorophenyl), 245–246, 344, 345
 O,O,O-trialkyl, 246, 346, 524, 539, 540, 572
 Phosphorus compounds
 absorbance ratios, 250
 alkyl group vibrations, 250–251
 applications, 233
 C–C mode for C₂H₅OP group, 251
 C–D mode for CDCl₃ and CCl₄ solutions, 252
 CD₃–PO₃^{2–1}, 247–248, 349
 CH₃–PO₃^{2–1}, 247–248, 349
 (CH₃)₂–PO₂, 248, 297, 298, 350
 containing P–NH-R groups, 242–243, 339
 COP group, 251–252
 C–O–P stretching, 241, 334–337

- C–P stretching, ν_{C-P} , 241–242, 338
 halogen, 234–235, 318
 halogen stretching for organo phosphorus halides, 235, 321
 PCl_3 and PCl_2 vibrations, 250
 P–Cl stretching, 237, 323
 PNH₂ and PNH_2 , 245, 342
 P=O stretching, $\nu_{P=O}$, 237–238, 239, 240–241, 325, 326, 327
 $P(=S)NH_2$, 244, 245, 340
 P–S stretching, 240
 P=S stretching, $\nu_{P=S}$, 238–239, 240, 327, 329–330
 PX coupling, 234–235
 PX stretching, 234
 rotational conformers, 235–243, 246, 249–250, 251–252
 S–H stretching, 240
 solvent effects, 248–250, 301, 304–307
 summary of correlations, 452–453
 Phosphorus oxyhalides, analysis of, 239
 P–NH-R groups, 242–243, 339
 $P(-O-C)_3$, 240
 Polychlorobiphenyls, 353–355
 Polystyrene
 out-of-plane hydrogen deformations, 362–363
 styrene-acrylamide copolymer, 359, 387
 styrene-acrylic acid copolymer, 358–359, 385
 styrene/2-isopropenyl-2-oxazoline copolymer (SIPO), 359–360, 388
 styrene-4-methylstyrene copolymer, 355–358, 381, 382
 syndiotactic, 355, 362
 $P=O$ stretching, $\nu_{P=O}$
 in different physical phases, 237, 326
 for hydrogenphosphonate, dialkyl and diphenyl, 240–241, 333
 for O,O-dimethyl O-(2-chloro 4-X-phenyl) phosphate, 238, 326
 for phenoxarsine derivatives, 238–239, 327
 for phosphorus compounds, 237–238, 325, 326, 327
 predicting frequencies, 238, 327
 solvent effects, 248–250, 304–307
 versus P=S, 239, 328
 Propadiene analogs, 125–126, 171
 halo, 127
 Propenes, 4, 19
 Propylene oxide, 2, 9
 Propynes, 4, 19, 125–126, 171
 $P(=S)NH_2$, 244, 245, 340
 P–S stretching, 240
 P=S stretching, $\nu_{P=S}$, 240
 for phenoxarsine derivatives, 238–239, 327
 for phosphorus compounds, 239, 329–330
 versus P=O, 239, 328
- Q**
 Quantitative analyses, use of, 356–358
- R**
 Raman spectra
 1-bromo-1-chloroethylene, 156
 1-bromopropadiene-1-d, 159
 3-bromopropyne-1-d, 150
 3-chloropropyne-1-d, 148
 dimethyl hydrogenphosphonate, 276
 ethynylbenzene, 392
 ethynylbenzene-d, 392
 methyl (methylthio) mercury, 73
 S-methyl phosphorodichloridothioate, 270
 sodium dimethylphosphinate, 299
 Reaction field (RF), 3
 benzenes, 362
 defined, 86
 Reflectance, diffuse. *See* DRIFT (diffuse reflectance infrared Fourier transform)
 Refractive indices, 86
 Resonance. *See* Fermi resonance
 Ring breathing, 2–3, 10
 Ring formation, ethylene oxide, 1–2
 Rotational conformers
 alkanethiols, 66
 $ClCH_2P(=O)Cl_2$, 242
 dialkyl sulfides, 67
 1-haloalkanes, 121–122, 166
 2-haloalkanes, 122, 167
 phosphorodithioates, 68, 80
 phosphorus compounds, 235–243, 246, 249–250, 251–252
 P=O conformers for O-methyl phosphorodichloridate, 249, 302
 $(RO)_2P(=S)SH$, 240
- S**
 S–H stretching, 240
 alkanethiols, 65–66, 74, 76–77
 benzenethiols, 66, 74, 79
 phosphorodithioates, 68, 80
 Solvent effects, phosphorus compounds and, 248–250, 301, 304–307
 $S=O$ stretching
 frequencies, 86–87, 96, 104
 summary of, 92, 116–117
 SO_2 stretching
 calculated, 93
 correlations, 92
 frequencies, 87, 105–106
 summary of, 92, 116–117

- SO₂ stretching (*continued*)
 vibrations, 87, 88, 89, 92–93
- Spectra-structure correlations
- acetamide, dimethyl, 445, 493, 568
 - acetanilides, 4-x, 443, 477, 478, 562
 - acetates, 456, 559, 579
 - acetones, 445, 491, 492, 567
 - acetophenones, 4-x, 444, 483–485, 564
 - acrylates, 456–457, 579
 - alkane phosphonic bromide, O-isopropyl, 533
 - alkane phosphonic dichloride, 530, 531
 - alkane phosphonic difluoride, 532, 541
 - alkane phosphonothioic dichloride, 530, 531, 541
 - alkylamines, 448–449, 510–513, 571
 - alkyl isocyanates, 448, 507–509
 - alkyl isonitriles, 447, 499, 500
 - amines, 448–449, 510–513, 571
 - anilines, 3-x and 4-x, 441–442, 459–473, 560
 - anisoles, 453–454, 542–546, 574, 575
 - benzaldehydes, 4-x, 443, 479–482, 563
 - benzenes, mono-substituted, 454, 547–551, 576
 - benzoates, alkyl 3-x and 4-x, 444, 489, 566
 - benzoic acids, 3-x and 4-x, 442–443, 474–476, 561
 - benzonitriles, 3-x and 4-x, 446, 495–497, 570
 - benzophenones, 444, 486–488, 565
 - biphenyls, chlorinated, 454, 552, 577
 - C=O group, summary of, 444–445, 490, 567
 - dialkylketones, 455–456, 557, 558, 578
 - dimethylacetamide, 445, 493, 568
 - hydrogen phosphonates, 528, 529
 - hydrogen phosphonothioate, 528, 529
 - isocyanates, 448, 507–509
 - isonitriles, 447, 499, 500
 - maleic anhydride, 446, 494, 569
 - methacrylates, 456–457, 579
 - nitroalkanes, 447–448, 501–506
 - nitrogen compounds, summary of correlations, 449–450
 - organonitriles, 446–447, 498, 570
 - organophosphorus compounds, 450–452, 515, 516, 541, 571, 572–573
 - phosphates, trialkyl, 521, 522, 523, 539, 572
 - phosphine oxides, trialkyl, 519, 520, 572
 - phosphines, dialkyl, 517, 518
 - phosphines, monoalkyl, 518
 - phosphines, trialkyl, 515, 516, 517, 518
 - phosphites, dialkyl chloro, 534, 535
 - phosphites, monoalkyl dichloro, 534
 - phosphites, trialkyl, 534
 - phosphonates, 526–529
 - phosphonic bromide, alkane O-isopropyl, 533
 - phosphonic dichloride, alkane, 530, 531
 - phosphonic difluoride, alkane, 532, 541
 - phosphonothioic dichloride, alkane, 530, 531, 541
 - phosphoramidates, 538
 - phosphorodichloridate, monoalkyl, 537
 - phosphoroselenates, trialkyl, 525, 540, 572
 - phosphorothioates, trialkyl, 524, 539, 540, 572
 - phosphorus compounds summary of correlations, 452–453, 534
 - physical phases, 490
 - role of, 441
 - tetramethylurea (TMU), 454–455, 552–556, 577, 578
 - thiophosphonates, 528, 529
 - thiophosphonothioic dichloride, alkane, 530, 531, 541
- Steric factor
- alkanethiols, 66
 - alkyl nitriles, 28
 - alkyl nitrites, 183
 - cyanogen halides, 28
 - dialkyl sulfoxides, 86
 - isocyanates, 48
 - ketones, 456
 - P=O stretching, 249
 - sulfonamides, 89
- Styrene-acrylamide copolymer, 359, 387
- Styrene-acrylic acid copolymer, 358–359, 385
- Styrene/2-isopropenyl-2-oxazoline copolymer (SIPO), 359–360, 388
- Styrene-4-methylstyrene copolymer, 355–358, 381, 382
- Styrene oxide, 2–3, 10, 11
- dichloro-, 3
- Sulfates
- Nyquist rule, 430–431, 437
 - phenoxarsine derivatives, 88–89, 109, 110
- Sulfides
- alkane, 66–67, 76–77
 - dialkyl, 67, 78
- Sulfinyl anilines, 93, 117
- Sulfites, dialkyl, 89, 111
- Sulfonamides
- primary, 89–90, 111, 112
 - secondary and tertiary, 90, 112
- Sulfonates, organic, 91, 113
- Nyquist rule, 430–431, 437
- Sulfones
- dialkyl, 87–88, 107, 108
 - diaryl, 88, 109
 - Nyquist rule, 430–431, 437
- Sulfonyl chlorides, 91, 114
- Nyquist rule, 430–431, 437
- Sulfonyl fluorides, 91–92, 115
- Sulfoxides, dimethyl, 87–88, 107, 108
- reaction field, 86
- Sulfur, alkyl groups joined to, 68–69, 81–83
- Symmetric ring deformation, 2, 3, 10

T

Temperature effects

- chloromethyl phosphonic dichloride, 242
- isotactic polystyrene, 355
- O-methyl phosphorodichlorodithioate, 236
- phosphorodithioates, 68
- styrene-acrylamide copolymer, 359, 387
- styrene-acrylic acid copolymer, 358–359, 385

Tetrachloroethylene oxide, 3

Tetrahalomethane, 120, 164

Tetrahydrofuran, 5, 14

Tetramethylurea (TMU), 454–455, 552–556, 577, 578

Tetranitromethane, 176–177

Thiocyanates, 31

Thiols

See also Alkanethiols

benzenethiols, 66, 74, 79

chlorobenzenethiol, 67–68, 79

Thiosulfates, phenoxarsine derivatives, 88–89,
109, 110

Toluene, 353, 355

2,4,5-trichlorophenyl, 245–246, 344, 345

Trihalomethane, 120, 164

U

Urea, tetramethyl (TMU), 454–455, 552–556, 577, 578

V

Vinyl ethers, 6, 24–26